ORNL-6783

OAK RIDGE NATIONAL LABORATORY

MARTIN MARIETTA

PERFORMANCE ASSESSMENT FOR CONTINUING AND FUTURE OPERATIONS AT SOLID WASTE STORAGE AREA 6

Prepared for
ENERGY SYSTEMS WASTE
MANAGEMENT ORGANIZATION
MARTIN MARIETTA ENERGY SYSTEMS, INC.
Oak Ridge, Tennessee

MANAGED BY
MARTIN MARIETTA ENERGY SYSTEMS, INC.
FOR THE UNITED STATES
DEPARTMENT OF ENERGY

This report has been reproduced directly from the best available copy.

Available to DOE and DOE contractors from the Office of Scientific and Technical Information, P.O. Box 62, Oak Ridge, TN 37831; prices available from (615) 576-8401, FTS 626-8401.

Available to the public from the National Technical Information Service, U.S. Department of Commerce, 5285 Port Royal Rd., Springfield, VA 22161.

This report was prepared as an account of work sponsored by an agency of the United States Government. Neither the United States Government nor any agency thereof, nor any of their employees, makes any warranty, express or implied, or assumes any legal liability or responsibility for the accuracy, completeness, or usefulness of any information, apparatus, product, or process disclosed, or represents that its use would not infringe privately owned rights. Reference herein to any specific commercial product, process, or service by trade name, trademark, manufacturer, or otherwise, does not necessarily constitute or imply its endorsement, recommendation, or favoring by the United States Government or any agency thereof. The views and opinions of authors expressed herein do not necessarily state or reflect those of the United States Government or any agency thereof.

ORNL-6783

PERFORMANCE ASSESSMENT FOR CONTINUING AND FUTURE OPERATIONS AT SOLID WASTE STORAGE AREA 6

February 1994

Prepared for
ENERGY SYSTEMS WASTE MANAGEMENT ORGANIZATION
MARTIN MARIETTA ENERGY SYSTEMS, INC.
Oak Ridge, Tennessee

Prepared by
OAK RIDGE NATIONAL LABORATORY
Oak Ridge, Tennessee 37831
managed by
MARTIN MARIETTA ENERGY SYSTEMS, INC.
for the
U.S. DEPARTMENT OF ENERGY SYSTEMS, INC.
under Contract No. DE-AC05-84OR21400

TABLE OF CONTENTS

Page

LIST OF FIGURES vii
LIST OF TABLES xi
ABBREVIATIONS AND ACRONYMS xv
EXECUTIVE SUMMARY xix

1. INTRODUCTION 1-1

2. DISPOSAL FACILITY DESCRIPTION 2-1
2.1 SITE CHARACTERISTICS 2-1
2.1.1 Site Location and Topography 2-1
2.1.2 Geology and Soils 2-4
2.1.2.1 Geologic Setting 2-4
2.1.2.2 SWSA 6 Geology 2-10
2.1.2.3 Soils 2-10
2.1.3 Hydrogeology 2-14
2.1.4 Surface Water 2-19
2.1.5 Climate 2-20
2.2 WASTE CHARACTERISTICS 2-20
2.2.1 Low-Level Waste 2-20
2.2.2 Generic Description and Characteristics of Waste 2-20
2.2.3 Contact-Handled Low-Level Waste 2-21
2.2.3.1 Compactible Waste 2-21
2.2.3.2 Noncompactible Waste 2-23
2.2.4 Remotely Handled Low-Level Waste 2-25
2.2.4.1 High-Range Waste 2-25
2.2.4.2 Very High Range Waste 2-29
2.2.5 Fissile Waste 2-30
2.2.6 Biological Waste 2-31
2.2.7 Asbestos Waste 2-31
2.2.8 Suspect Waste 2-31
2.3 WASTE TREATMENT, CERTIFICATION, STORAGE, AND DISPOSAL 2-32
2.3.1 Waste Treatment Facilities 2-32
2.3.2 Low-Level Waste Characterization and Certification 2-32
2.3.2.1 Waste Characterization 2-32
2.3.2.2 Waste Certification 2-34
2.3.3 Interim Waste Storage Facilities 2-37
2.3.4 Solid Waste Storage Area 6 Disposal Facilities 2-37
2.3.5 Below-Grade Disposal 2-38
2.3.5.1 Low-Range and High-Range Silos 2-38
2.3.5.2 Asbestos Silos 2-43
2.3.5.3 High-Range Wells in Silos 2-45
2.3.5.4 High-Range Wells 2-48
2.3.5.5 Fissile Wells 2-48

Table of Contents (continued)

Page

2.3.5.6 Biological Trenches 2-50
2.3.5.7 Suspect Waste Landfill 2-50
2.3.6 Above-Grade Tumulus Disposal 2-51
2.3.6.1 Low-Level Waste Disposal Development and Demonstration Program 2-51
2.3.6.2 Tumulus I Disposal 2-51
2.3.6.3 Tumulus II Disposal 2-53
2.3.7 Interim Waste Management Facility 2-54

3. ANALYSIS OF PERFORMANCE 3-1
3.1 SOURCE TERMS 3-3
3.1.1 Mass Transport Models and Parameters 3-3
3.1.2 Radionuclide Screening Calculations 3-6
3.2 PATHWAYS AND SCENARIOS 3-10
3.2.1 Release from Disposal Units to Environmental Pathways 3-10
3.2.2 Transport Through the Environment 3-13
3.2.3 Closure Scenario 3-16
3.2.4 Human Exposure Scenarios 3-19
3.2.4.1 Operations and Institutional Control Periods (1988–2097) 3-19
3.2.4.2 Post-Institutional Control Period 3-20
3.3 ASSUMPTIONS 3-26
3.3.1 Source Terms 3-26
3.3.2 Site 3-26
3.3.2.1 Runoff-Recharge Factors 3-26
3.3.2.2 Aquifer Properties 3-30
3.3.2.3 Retardation 3-30
3.3.3 Wastes 3-31
3.4 PERFORMANCE ANALYSIS METHODOLOGY 3-31
3.4.1 Overview of Analysis 3-33
3.4.2 Site Hydrology 3-35
3.4.3 Facility Performance 3-35
3.4.4 Shallow Subsurface Transport 3-36
3.4.5 Transport in Groundwater 3-36
3.4.6 Transport to Surface Water 3-37
3.4.7 Dose Estimation 3-37
3.4.8 Verification and Validation of Methodology 3-38
3.4.8.1 Verification and Validation of UTM 3-38
3.4.8.2 Verification and Validation of SOURCE1 and SOURCE2 3-40
3.4.8.3 Verification and Validation of TUMSIM and WELSIM 3-40
3.4.8.4 Verification and Validation of USGS MOC 3-41

Table of Contents (continued)

	Page
4. RESULTS OF ANALYSIS	4-1
4.1 SOURCE TERMS	4-1
4.2 SHALLOW SUBSURFACE TRANSPORT	4-5
4.2.1 UTM Hydrologic Simulation Results	4-6
4.2.2 Nuclide Transport in Shallow Subsurface and to Groundwater	4-9
4.3 GROUNDWATER	4-9
4.3.1 Transport Simulations and Radionuclide Concentrations	4-18
4.3.2 Discussion	4-19
4.4 SURFACE WATER TRANSPORT	4-23
4.5 DOSE ANALYSIS	4-27
4.5.1 Analysis of Human Exposure Scenarios and Exposure Pathways	4-28
4.5.1.1 Protection of Groundwater and Surface Water Resources	4-28
4.5.1.2 Exposure Scenarios and Exposure Pathways for Off-Site Individuals	4-30
4.5.1.3 Exposure Scenarios and Exposure Pathways for Inadvertent Intruders	4-30
4.5.2 Discussion of Uncertainties in Exposure Pathways Analysis	4-40
4.5.3 Dose Analysis for Disposal Units in SWSA 6	4-42
4.5.3.1 Dose Analysis for Water Pathways	4-43
4.5.3.2 Dose Analysis for Direct Intrusion into Disposal Units	4-45
4.5.4 Comparison of Dose Estimates with Regulatory Requirements	4-61
4.5.4.1 Protection of Groundwater and Surface Water Resources	4-62
4.5.4.2 Protection of Off-Site Individuals	4-63
4.5.4.3 Protection of Inadvertent Intruders	4-63
4.6 SENSITIVITY AND UNCERTAINTY ANALYSIS	4-69
4.6.1 Analysis of Disposal System Performance	4-69
4.6.1.1 Sensitivity and Uncertainty of Leaching from Disposal Units	4-70
4.6.1.2 UTM and Shallow Subsurface Transport Sensitivity Analysis	4-80
4.6.1.3 Uncertainty of Shallow Subsurface Chemical Transport	4-80
4.6.1.4 Uncertainty of Groundwater Transport	4-88
4.6.1.5 Uncertainty of Surface Water Transport	4-98
4.6.1.6 Subjective Uncertainty	4-117
4.6.2 Analysis of Human Exposure Scenarios	4-122
4.6.2.1 Scenarios for Transport of Radionuclides in Water	4-122
4.6.2.2 Scenarios for Direct Intrusion into Disposal Units	4-125
4.7 INTERPRETATION OF RESULTS	4-126
4.7.1 Surface Water and Groundwater Pathways	4-126
4.7.1.1 Groundwater	4-127
4.7.1.2 Surface Water	4-130

Table of Contents (continued)

Page

4.7.2 Direct Intrusion Scenarios 4-132
4.7.2.1 Tumulus I 4-132
4.7.2.2 Tumulus II 4-133
4.7.2.3 IWMF 4-133
4.7.2.4 Low-Range Silos 4-133
4.7.2.5 High-Range Silos 4-134
4.7.2.6 High-Range Wells 4-135
4.7.2.7 Fissile Wells 4-136
4.7.2.8 Asbestos Silos 4-136
4.7.2.9 Biological Trenches 4-137
4.7.2.10 Summary 4-137
4.8 DESIGN CHANGES REQUIRED TO MEET PERFORMANCE OBJECTIVES 4-138
4.9 CONTINUED WORK 4-138
4.10 QUALITY ASSURANCE 4-139

5. PERFORMANCE EVALUATION 5-1
6. PREPARERS 6-1
7. REFERENCES 7-1

APPENDIX A: RADIONUCLIDE INVENTORY DATA AND EVALUATION OF UNCERTAINTY IN INVENTORY DATA IN SUPPORT OF THE U.S. DEPARTMENT OF ENERGY ORDER 5820.2A RADIOLOGICAL PERFORMANCE ASSESSMENT FOR CONTINUING OPERATIONS IN SOLID WASTE STORAGE AREA 6 . . . . . A-1
APPENDIX B: DESCRIPTION OF THE SOURCE1, SOURCE2, AND FLOWTHRU COMPUTER PROGRAMS B-1
APPENDIX C: WASTE PROPERTIES AND TRANSPORT PROPERTIES OF RADIONUCLIDES AT THE SOLID WASTE STORAGE AREA 6 DISPOSAL UNITS C-1
APPENDIX D: APPLICATION OF THE UNIFIED TRANSPORT MODEL, TUMSIM, AND WELSIM TO THE SOLID WASTE STORAGE AREA 6 PERFORMANCE ASSESSMENT D-1
APPENDIX E: THEORETICAL DESCRIPTION OF GROUNDWATER FLOW AND CONTAMINANT TRANSPORT: ASSUMPTIONS IN THE MATHEMATICAL MODEL OF RADIONUCLIDE TRANSPORT AT SOLID WASTE STORAGE AREA 6 . . . . . E-1

Table of Contents (continued)

		Page
APPENDIX F:	PREDICTED AMOUNTS OF VARIOUS RADIONUCLIDES LEACHED FROM DISPOSAL UNITS IN SOLID WASTE STORAGE AREA 6	F-1
APPENDIX G:	DOSE ANALYSIS FOR OFF-SITE INDIVIDUALS AND INADVERTENT INTRUDERS	G-1
APPENDIX H:	SENSITIVITY AND UNCERTAINTY ANALYSIS	H-1
APPENDIX I:	PERFORMANCE ASSESSMENT PEER REVIEW PANEL RECOMMENDATIONS	I-1

LIST OF FIGURES

		Page
2.1	Topographic map of Oak Ridge National Laboratory and the surrounding area	2-2
2.2	Location of Solid Waste Storage Area 6 in proximity to local surface waters, Highway 95, and White Oak Dam	2-3
2.3	Generalized geologic map of the Oak Ridge area	2-7
2.4	Geologic cross-section of the Oak Ridge area	2-8
2.5	Geologic map of Bethel Valley and Melton Valley	2-9
2.6	Generalized geologic map of Solid Waste Storage Area 6	2-11
2.7	Typical soil profiles observed at Solid Waste Storage Area 6	2-12
2.8	Soil map of Solid Waste Storage Area 6	2-13
2.9	Hydraulic conductivity vs depth at Solid Waste Storage Area 6	2-15
2.10	Solid Waste Storage Area 6 conductivity distribution	2-16
2.11	Average water table configuration in Solid Waste Storage Area 6	2-17
2.12	Segregation and disposition of solid radioactive waste at Oak Ridge National Laboratory	2-22
2.13	Certification process for solid low-level waste at Oak Ridge National Laboratory	2-36
2.14	Cross section of a concrete silo	2-40
2.15	Location of low-range silos, high-range silos, and fissile wells in Solid Waste Storage Area 6	2-41
2.16	Location of low-range silos and Tumulus in Solid Waste Storage Area 6	2-42
2.17	Location of asbestos silos and biological trenches in Solid Waste Storage Area 6	2-44
2.18	Cross section of a concrete silo with high-range wells	2-46
2.19	Location of high-range wells in Solid Waste Storage Area 6	2-47
2.20	Cross section of a high-range well	2-49
2.21	Generic concrete cask for tumulus disposal operations	2-52
2.22	Interim Waste Management Facility showing vaults of low-level waste, drain lines, and final cover	2-55
2.23	The Interim Waste Management Facility site in Solid Waste Storage Area 6	2-56
3.1	Schematic profile showing subsurface flow zones and intervals, general thickness ranges, estimated relative annual water flux, and change in water type with depth	3-15
3.2	Diagram of a disposal unit area (A) in relation to its upslope watershed area (B) and the soil volumes in the vertical path to groundwater and the lateral path to a receiving stream channel	3-28
3.3	Linkage of contaminant transport models for performance assessment of Solid Waste Storage Area 6	3-34
4.1	Numerical grid with observation points	4-14
4.2	Typical groundwater water table surface at Solid Waste Storage Area 6	4-16
4.3	Typical groundwater velocity vector field at Solid Waste Storage Area 6	4-17
4.4	Estimated areas outside of compliance boundaries with total nuclide activity > compliance limit (0 < T < 50 years)	4-20

List of Figures (continued)

Page

4.5 Estimated areas outside of compliance boundaries with total nuclide activity > compliance limit (50 < T < 100 years) 4-21
4.6 Estimated areas outside of compliance boundaries with total nuclide activity > compliance limit (T > 1000 years) 4-22
4.7 Chart illustrating the method for exchange of data sets between models used for sensitivity analysis 4-74
4.8 Relative frequency distribution of tritium leaching from the Interim Waste Management Facility at year 50 4-75
4.9 Relative frequency distribution of ^{238}U leaching from the low-range silos (south) at year 200 4-76
4.10 Relative frequency distribution of tritium leaching from the low-range silos (south) at year 50 4-77
4.11 Relative frequency distribution of ^{137}Cs leaching from the Interim Waste Management Facility at year 200 4-78
4.12 Relative frequency distribution of tritium transport to groundwater from the Interim Waste Management Facility at year 50 4-84
4.13 Relative frequency distribution of ^{238}U transport to groundwater from the low-range silos (south) at year 200 4-85
4.14 Relative frequency distribution of tritium transport in shallow subsurface flow to a stream channel from the low-range silos (south) at year 50 4-86
4.15 Relative frequency distribution of ^{137}Cs transport in shallow subsurface flow to a stream channel from the Interim Waste Management Facility at year 200 4-87
4.16 Latin hypercube sampled tritium surface water concentrations arising from shallow subsurface transport (middle curve) 4-91
4.17 Latin hypercube sampled ^{14}C surface water concentrations arising from shallow subsurface transport (middle curve) 4-92
4.18 Latin hypercube sampled ^{36}Cl surface water concentrations arising from shallow subsurface transport (middle curve) 4-93
4.19 Latin hypercube sampled ^{90}Sr surface water concentrations arising from shallow subsurface transport (middle curve) 4-94
4.20 Latin hypercube sampled ^{137}Cs surface water concentrations arising from shallow subsurface transport (middle curve) 4-95
4.21 Latin hypercube sampled ^{238}U surface water concentrations arising from shallow subsurface transport (middle curve) 4-96
4.22 Latin hypercube sampled tritium maximum groundwater concentrations at 100 m (328 ft), assumed to occur at node 168 (middle curve) 4-99
4.23 Latin hypercube sampled ^{14}C maximum groundwater concentrations at 100 m (328 ft), assumed to occur at node 168 (middle curve) 4-100
4.24 Latin hypercube sampled ^{36}Cl maximum groundwater concentrations at 100 m (328 ft), assumed to occur at node 168 (middle curve) 4-101
4.25 Latin hypercube sampled ^{90}Sr maximum groundwater concentrations at 100 m (328 ft), assumed to occur at node 168 (middle curve) 4-102

List of Figures (continued)

Page

4.26 Latin hypercube sampled ^{137}Cs maximum groundwater concentrations at 100 m (328 ft), assumed to occur at node 168 (middle curve) 4-103
4.27 Latin hypercube sampled ^{238}U maximum groundwater concentrations at 100 m (328 ft), assumed to occur at node 168 (middle curve) 4-104
4.28 Latin hypercube sampled tritium surface water concentrations arising from transport via groundwater (middle curve) 4-105
4.29 Latin hypercube sampled ^{14}C surface water concentrations arising from transport via groundwater (middle curve) 4-106
4.30 Latin hypercube sampled ^{36}Cl surface water concentrations arising from transport via groundwater (middle curve) 4-107
4.31 Latin hypercube sampled ^{90}Sr surface water concentrations arising from transport via groundwater (middle curve) 4-108
4.32 Latin hypercube sampled ^{137}Cs surface water concentrations arising from transport via groundwater (middle curve) 4-109
4.33 Latin hypercube sampled ^{238}U surface water concentrations arising from transport via groundwater (middle curve) 4-110
4.34 Total surface water concentration of tritium from Solid Waste Storage Area 6 disposal units 4-111
4.35 Total surface water concentration of ^{14}C from Solid Waste Storage Area 6 disposal units 4-112
4.36 Total surface water concentration of ^{36}Cl from Solid Waste Storage Area 6 disposal units 4-113
4.37 Total surface water concentration of ^{90}Sr from Solid Waste Storage Area 6 disposal units 4-114
4.38 Total surface water concentration of ^{137}Cs from Solid Waste Storage Area 6 disposal units 4-115
4.39 Total surface water concentration of ^{238}U from Solid Waste Storage Area 6 disposal units 4-116

LIST OF TABLES

		Page
1.1	Performance objectives for low-level radioactive waste disposal	1-1
2.1	Stratigraphic column of Cambro-Ordovician Rocks, White Oak Mountain Thrust Block, Oak Ridge, Tennessee	2-5
2.2	Current low-level waste (LLW) segregation categories	2-23
2.3	Waste descriptions	2-24
2.4	Solid Waste Storage Area 6 inventory data	2-25
2.5	Estimated total activity in low-range silos	2-26
2.6	Estimated total activity in high-range silos	2-26
2.7	Estimated total activity in asbestos silos	2-27
2.8	Estimated total activity in high-range wells	2-27
2.9	Estimated total activity in fissile wells	2-28
2.10	Estimated total activity in biological trenches	2-28
2.11	Estimated total activity in Tumulus I	2-28
2.12	Estimated total activity in Tumulus II	2-29
2.13	Estimated total activity in Interim Waste Management Facility	2-30
2.14	Disposal methods for waste disposed in Solid Waste Storage Area 6	2-39
3.1	Concentration limits in water for radionuclide screening	3-2
3.2	Input data summary for a high-range silo at Solid Waste Storage Area 6	3-7
3.3	SOURCE1 and SOURCE2 code inputs (nonradionuclide specific) for the uncertainty analysis	3-11
3.4	Mean radionuclide concentrations in air, 1991	3-12
3.5	Disposal units in Solid Waste Storage Area 6 showing starting and ending times of active use and the average distances of each site to groundwater and a receiving stream channel	3-17
3.6	Disposal units in Solid Waste Storage Area 6 showing number of units, containment area, and the upslope area draining directly into each site	3-29
3.7	Half-life, specific activity, and distribution coefficient (K_d) values of radionuclides simulated in the performance assessment of Solid Waste Storage Area 6	3-32
4.1	Abridged output summary for Solid Waste Storage Area 6 high-range silos	4-2
4.2	Groundwater recharge, shallow lateral subsurface flow, and surface runoff simulation results from the Unified Transport Model for three sets of weather conditions (dry, average, and wet) and for three time periods	4-7
4.3	Maximum annual nuclide flux and year of occurrence from Solid Waste Storage Area 6 disposal units into groundwater and to shallow subsurface waters during a 1000-year period with average weather conditions	4-10
4.4	Nuclides considered in Solid Waste Storage Area 6 groundwater transport analysis	4-18
4.5	Best estimates of groundwater concentrations for Solid Waste Storage Area 6 disposal sites with calculated concentration/allowable ratio $\geq$ 0.1 at 100-m (328-ft) compliance points	4-19

List of Tables (continued)

		Page
4.6	Combined maximum radionuclide release (mass, activity, and concentration basis) from all disposal units to surface waters from groundwater transport	4-24
4.7	Combined maximum radionuclide release (mass, activity, and concentration basis) from all disposal units to surface waters from shallow subsurface transport	4-25
4.8	Combined maximum radionuclide release (mass, activity, and concentration basis) from all disposal units to surface waters from groundwater and shallow subsurface transport	4-26
4.9	Annual effective dose equivalents from drinking water pathway per unit concentration of radionuclides in water	4-29
4.10	Annual effective dose equivalents to off-site individuals per unit concentration of radionuclides in water from all exposure pathways	4-31
4.11	Annual effective dose equivalents to inadvertent intruders per unit concentration of radionuclides in water from all exposure pathways	4-33
4.12	Annual effective dose equivalents to inadvertent intruders per unit concentration of radionuclides in disposal units from all exposure pathways for agriculture scenario	4-35
4.13	Annual effective dose equivalents to inadvertent intruders per unit concentration of radionuclides in disposal units for resident scenario	4-36
4.14	Effective dose equivalents to inadvertent intruders per unit concentration of radionuclides in disposal units for discovery scenario	4-37
4.15	Annual effective dose equivalents to inadvertent intruders per unit concentration of radionuclides in exhumed waste from all exposure pathways for postdrilling scenario	4-38
4.16	Results of dose analysis for off-site individuals from drinking water pathway due to releases to surface water	4-44
4.17	Results of dose analysis for off-site individuals from all exposure pathways due to releases to surface water	4-44
4.18	Results of dose analysis for drinking water pathway at disposal site due to releases to groundwater	4-46
4.19	Results of dose analysis for inadvertent intruders from all exposure pathways due to releases to groundwater	4-47
4.20	Upper-bound estimates of effective dose equivalents to inadvertent intruders for agriculture scenario	4-49
4.21	Upper-bound estimates of effective dose equivalents to inadvertent intruders for resident scenario	4-53
4.22	Upper-bound estimates of effective dose equivalents to inadvertent intruders for discovery scenario	4-55
4.23	Upper-bound estimates of effective dose equivalents to inadvertent intruders for postdrilling scenario	4-57
4.24	Summary of upper-bound estimates of effective dose equivalents to inadvertent intruders for assumed exposure scenarios	4-60
4.25	SOURCE1 and SOURCE2 variables examined in the sensitivity analysis	4-71

List of Tables (continued)

Page

4.26 SOURCE1 and SOURCE2 variables and values included in the uncertainty analysis 4-73
4.27 Mode and maximum nuclide leaching (g/year) from two disposal units under average and ± 50% (enhanced and reduced, respectively) water flow conditions at 50, 100, and 200 years 4-79
4.28 Attributes of the frequency distributions selected for chemical adsorption (K_d) that were used in Latin hypercube sampling 4-81
4.29 Attributes of the frequency distributions selected for disposal unit area that were used in Latin hypercube sampling 4-82
4.30 Attributes of the frequency distributions selected for distance to groundwater that were used in Latin hypercube sampling 4-82
4.31 Attributes of the frequency distributions selected for distance to a stream channel that were used in Latin hypercube sampling 4-83
4.32 Mode and maximum nuclide transport to groundwater (g/year) from two disposal units under average and ±50% (enhanced and reduced, respectively) water flow conditions at 50, 100, and 200 years 4-89
4.33 Mode and maximum nuclide transport in shallow subsurface flow to a stream channel (g/year) from two disposal units under average and ±50% (enhanced and reduced, respectively) water flow conditions at 50, 100, and 200 years 4-90
4.34 Description of subjective probability distributions for each segment of the composite transport model 4-119
4.35 Solid Waste Storage Area 6 probability of compliance (POC) and associated entropy-based uncertainty (U) at groundwater compliance node 166 4-121
4.36 Solid Waste Storage Area 6 probability of compliance (POC) and associated entropy-based uncertainty (U) in surface water 4-121
4.37 Resultant probability of compliance (POC) and associated entropy-based uncertainty (U) for radionuclides in groundwater at node 166 from convolution of subjective uncertainties associated with each segment of the composite transport model (CTM) with groundwater concentration distributions obtained from the parametric, Latin hypercube (LHC) analysis 4-123
4.38 Resultant probability of compliance (POC) and associated entropy-based uncertainty (U) for radionuclides in Solid Waste Storage Area 6 surface water from convolution of subjective uncertainties associated with each segment of the composite transport model (CTM) with surface water concentration distributions obtained from the parametric, Latin hypercube (LHC) analysis 4-124
5.1 Comparison of results with performance objectives 5-2

ABBREVIATIONS AND ACRONYMS

ANSI	American National Standards Institute
ARARs	Applicable or Relevant and Appropriate Requirements
A	disturbed area containing one disposal unit
A_o	Amount
Al	aluminum
Am	americium
Be	beryllium
B	average upslope area contributing lateral flow to one disposal unit
C	carbon
Cd	cadmium
CDF	cumulative distribution function
CERCLA	Comprehensive Environmental Response, Compensation, and Liability Act of 1980
Cf	californium
cfs	cubic feet per second
CH	contact-handled
CH-LLW	contact-handled low-level waste
Ci	curie
CIIDF	Class L-II Disposal Facility
Cl	chlorine
Cm	curium
C_{pw}	concentration of nuclide in pore water
Cs	cesium
C_s	solubility limit
C-S-H	calcium-silicate-hydrate (system)
CTM	composite transport model
D&D	decontamination and decommissioning
DOE	U.S. Department of Energy
DOE-ORO	U.S. Department of Energy, Oak Ridge Operations
D_c	retarded coefficient of diffusion through concrete
D_s	self-diffusion coefficient
D_w	retarded coefficient of diffusion through waste
EDE	effective dose equivalent
Energy Systems	Martin Marietta Energy Systems, Inc.
EPA	U.S. Environmental Protection Agency
ERWM	Environmental Restoration and Waste Management (Program)
ETF	Engineered Test Facility
Eu	europium
GCD	greater confinement disposal
GCO	Generator Certification Official
^3H	tritium
H	relative water saturation value
h	hour
HEPA	high-efficiency particulate air

HLW	high-level radioactive waste
ID	inside diameter
IWMF	Interim Waste Management Facility
K	potassium
K_d	distribution coefficient
LAI	leaf area index
LHC	Latin hypercube
LI	Line Item
LLLW	liquid low-level waste
LLW	low-level radioactive waste
LLWDDD	Low-Level Waste Disposal Development and Demonstration
MVST	Melton Valley storage tanks
NARM	naturally occurring and accelerator-produced radioactive material
Ni	nickel
Np	neptunium
NPDES	National Pollutant Discharge Elimination System
NRC	U.S. Nuclear Regulatory Commission
OD	outside diameter
ORGDP	Oak Ridge Gaseous Diffusion Plant (now Oak Ridge K-25 Site)
ORMWI	Oak Ridge Mixed Waste Incinerator
ORNL	Oak Ridge National Laboratory
ORR	Oak Ridge Reservation
Pa	protactinium
Pb	lead
POC	probability of compliance
psi	pounds per square inch
Pu	plutonium
PVC	polyvinylchloride
PWTP	Process Waste Treatment Plant
R	retardation factor
Ra	radon
RCRA	Resource Conservation and Recovery Act of 1976
RFI	Remedial Feasibility Investigation
RH	remotely handled
RH-LLW	remotely handled low-level waste
RSWO	Radioactive Solid Waste Operations
RTR	real-time radiography
SLLW	solid low-level waste
Sr	strontium
SWIMS	Solid Waste Information Management System
SWSA 6	Solid Waste Storage Area 6
TA	asbestos silo
TB	biological trench
Tc	technetium
TH	high-range well
Th	thorium
TL	low-range silo

TDDP	Tumulus Disposal Demonstration Project
TDEC	Tennessee Department of Environment and Conservation
TDHE	Tennessee Department of Health and Environment
THW	High-range wells/silos
TRU	transuranic
TSD	treatment, storage, and disposal
U	uranium
USGS MOC	U.S. Geological Survey Method of Characteristics
UTM	Unified Transport Model
VOC	volatile organic compound
VLA	very low activity
WAC	Waste Acceptance Criteria
WAG	Waste Area Grouping
WCR	water-cement ratio
WEAF	Waste Examination and Assay Facility
WF	fissile well
WH	double-walled pipe well
WHA	High-range wells

EXECUTIVE SUMMARY

This radiological performance assessment for the continued disposal operations at Solid Waste Storage Area 6 (SWSA 6) on the Oak Ridge Reservation (ORR) has been prepared to demonstrate compliance with the requirements of U.S. Department of Energy (DOE) Order 5820.2A. The performance assessment considers disposal operations conducted from the issue date of the order, September 26, 1988, through the projected operating lifetime of the facility. The performance objectives require that the facility be managed so as to accomplish the following:

1. Protect public health and safety in accordance with standards specified in Environmental Health Orders and other DOE Orders.
2. Assure that external exposure to the waste and concentrations of radioactive material which may be released into surface water, groundwater, soil, plants, and animals results in an effective dose equivalent (EDE) that does not exceed 25 mrem/year to a member of the public. Releases to the atmosphere shall meet the requirements of 40 CFR Pt. 61. Reasonable effort should be made to maintain releases of radioactivity in effluents to the general environment as low as reasonably achievable.
3. Assure that the committed EDEs received by individuals who inadvertently may intrude into the facility after the loss of active institutional control (100 years) will not exceed 100 mrem/year for continuous exposure or 500 mrem for a single acute exposure.
4. Protect groundwater resources, consistent with Federal, State and local requirements.

The performance assessment has been prepared in accordance with the guidance provided by the DOE Peer Review Panel that outlines the format and content for a radiological performance assessment. The consistency and technical quality of this performance assessment will be determined by the Peer Review Panel. The acceptability of the performance assessment will be determined by DOE Headquarters.

SWSA 6 is located about 3 km (1.9 miles) south of Oak Ridge National Laboratory (ORNL) on the DOE ORR. The facility is located on a 27.5 ha (68 acres) tract of land with rolling terrain. Approximately 12 ha (30 acres) of the site are suitable for disposal operations. The majority of the capacity was used before September 26, 1988. The facility is projected to continue operations until December 1997 when the available capacity will be exhausted. Those portions of the facility associated with historical disposal operations are presently subject to remediation under the Comprehensive Environmental Response, Compensation, and Liability Act of 1980 (CERCLA). Following the implementing

guidance for the order, the performance assessment has been prepared without the consideration of disposal operations performed before the issuance of the order. The performance assessment considers four different types of disposal units: concrete silos, tumulus units, concrete wells, and unlined trenches. Each disposal unit and the wastes expected to be emplaced therein are considered separately and then integrated for the performance assessment. In addition, the analysis of each disposal unit assumes normal or expected performance. Accidental releases or abnormal operations are considered in the safety documentation for the facility and are not part of the performance assessment.

Approximatley 2,000 m^3/year (75,000 ft^3/year) of low-level radioactive waste is managed at ORNL. The waste acceptable for disposal is disposed of in SWSA 6. The majority of the waste is contact-handled (CH) waste (<200 mrem/h dose rate at the surface). This type of waste includes debris from ORNL operations, research and development activities, environmental restoration, and decommissioning and demolition activities. Compactible and noncompactible waste are managed separately. CH waste is disposed of in concrete silos and in tumulus-type disposal units. Remotely-handled (RH) waste (>200 mrem/h dose rate at the surface) includes debris from reactors and hot cell operations. RH waste with <1 rem/h surface dose rate is disposed of in concrete silos, and RH waste with >1 rem/h surface dose rate is disposed of in concrete wells. Fissile waste, consisting of debris, is generated from research and development activities using enriched uranium and is disposed of separately in concrete wells. Biological waste consists of excrement and animal carcasses from biological research and is disposed of in unlined trenches. Asbestos waste consists of debris generated during maintenance and demolition of contaminated facilities and is disposed of in concrete silos. Continuing operations at SWSA 6 are conducted at the Interim Waste Management Facility (IWMF), which is a prototype tumulus disposal facility to be used at future disposal facilities on the ORR.

Wastes generated at ORNL are characterized and certified prior to disposal. Waste generators are responsible for providing the primary characterization data and for certifying that the waste meets the Waste Acceptance Criteria (WAC) for disposal units (ORNL 1993a). Waste certification accounts for the quality assurance and quality control procedures in data collection and manipulation, documentation and tracking systems, authority and responsibility, and other areas related to ensuring that characterization data of sufficient detail and quality are collected. Methods for characterizing wastes include process knowledge and controls, material accountability, direct or indirect measurements, and combinations of these elements. The characterization data are logged prior to storage, treatment, or disposal. Treatment processes include on-site waste compaction and the use of off-site vendors for supercompaction, incineration, and metal melting. Wastes are packaged in 30- and 55-gal drums, wood or metal boxes, 4-mil and 20-mil plastic bags, and 1-, 2-, 5-, 10-, and 20-gal metal cans prior to disposal.

The waste characteristics used for assessing the performance of SWSA 6 were defined using the existing data from the waste data management program and from an evaluation of the data and methods used for characterizing wastes. While the data from these records are imperfect and may not be accurate representations of future wastes generated at ORNL, they are the most reasonable representation of present and future wastes. An evaluation of the uncertainties in the waste data was performed as part of the performance assessment to provide an estimate of the likely characteristics of the wastes disposed of at SWSA 6. The best estimate inventory for each isotope at each disposal unit was derived from the evaluation of the uncertainties in the waste data and used in assessing the facility's performance. The isotopes considered in detail in the performance

assessment were determined by scoping analyses. The results of the scoping analyses defined the isotopes that were present in large quantities in the wastes generated or that had the potential to yield significant doses. For each isotope considered in detail, the release of contamination from the individual disposal units was estimated using the computer codes SOURCE1 and SOURCE2. These codes estimated the release rate of contamination by considering the wetting of waste by infiltration of water into the waste and the subsequent leaching and transport of radionuclides from the waste form by diffusion and advection. The complex forms of wastes, disposal units, and concrete barriers were approximated. The degradation and cracking of concrete over time were included in the analysis. The release of contamination was estimated for a period of 1000 years or until the maximum release had occurred.

Contamination released from the disposal units was analyzed for transport through the environment using the Unified Transport Model (UTM) and USGS MOC computer codes. Monitoring data from SWSA 6 over the past few decades suggest that emission of radionuclides directly to the atmosphere in gaseous form is not an important release mechanism on the ORR. Suspension of particulates by natural processes has not been identified as an important pathway for the transport of contamination and can be precluded as long as a minimal amount of overlying uncontaminated soil exists at a disposal facility. As a result, the pathways analyzed in detail for environmental transport were surface water, soils, and groundwater. The release of contamination from disposal units was assumed to occur primarily into the groundwater and surface water from shallow subsurface transport during storm events. Transport of contamination in surface water and groundwater took into account precipitation, storm hydrology, streamflow, infiltration, percolation, recharge, sorption, radioactive decay, and projected closure plans for SWSA 6. The computer codes used for analyzing environmental transport are well documented, verified, and validated to the extent that they provide reasonable representations of site performance. The results of these codes were used to estimate potential doses from waste disposal operations.

Doses to individuals and inadvertent intruders were estimated to determine the maximum potential doses attributable to disposal facility operations. For an individual residing outside the facility boundary, doses were estimated assuming direct ingestion of contaminated water, ingestion of milk and meat from dairy and beef cattle that drink contaminated water, and exposure from swimming in contaminated water released into White Oak Creek. Following the active institutional control period, the same exposure scenario is considered for an individual who inadvertently intrudes onto the facility. An inadvertent intruder is considered to ingest contaminated water from a well and to consume milk and meat from dairy and beef cattle that drink contaminated water. Additionally, an inadvertent intruder is assumed to engage in direct intrusion into disposal units according to one of four scenarios—the "agriculture," "discovery," "resident," and "postdrilling" scenarios. The discovery scenario is assumed to occur once in an individual's lifetime, whereas the other scenarios are continuous exposure scenarios. The agriculture scenario is assumed to occur at 300 years after facility closure for concrete disposal units and 100 years after facility closure for the biological trenches. The postdrilling, discovery, and resident scenarios are assumed to occur 100 years after facility closure for all disposal units. The dose analysis for the inadvertent intrusion scenarios assumed that no transport of contamination from the disposal units had occurred prior to intrusion. This conservative assumption was made because a reasonable, lower-bound estimate of the transport of

contamination from disposal units could not be made with the present state of knowledge of the long-term performance of engineered disposal technologies.

The analysis of SWSA 6 required the use of assumptions to supplement the available site data when the available data were incomplete for the purposes of analysis. Assumptions were made to define the partitioning of recharge to runoff from each disposal unit, the aquifer properties, the sorption characteristics of disposal units and the site, the geometry of waste configurations, and the degradation and cracking of concrete. These assumptions were selected to provide a reasonable yet conservative representation of facility performance and were based on the limited information available.

The methodology used to analyze the performance of SWSA 6 was based on the available data on the waste disposed of at SWSA 6, the disposal methods used at SWSA 6, and SWSA 6 site characteristics. In analyzing site performance, the results of the source-term modeling (which provide estimates of releases from disposal units) are used as input to the shallow subsurface model. The contamination released by the shallow subsurface model is diluted with upslope shallow subsurface drainage estimated to enter disposal units. The shallow subsurface model estimated the transport of contamination to surface water and the recharge to the saturated zone. The saturated zone model used the contaminated and uncontaminated recharge as input to estimate the transport of contamination to a well 100 m (328 ft) from the disposal unit and to determine the discharge of contaminated groundwater to surface water. The resulting concentrations in groundwater and surface water were used to estimate the dose from domestic use of water resources.

The results of the analysis indicate that all disposal units are in compliance with the performance objectives concerning the protection of off-site individuals. Compliance with the performance objective for the protection of groundwater resources is indicated for all disposal units except IWMF. Changes in operations that include improvements in the WAC along with continued work on the performance assessment are expected to result in a demonstration of compliance with the performance objective for protection of groundwater resources for IWMF. The analysis of inadvertent intruders showed that only the biological trenches complied with the performance objectives. The performance objectives were exceeded for seven of the remaining eight disposal units as a consequence of the disposal of uranium and the subsequent daughter formation of ^{222}Rn that yielded high doses at times distant in the future ($>10^6$ years). Doses arising from ^{222}Rn are the subject of a major issue facing waste management at SWSA 6. Doses from inadvertent intrusion into disposal units other than IWMF may be unreasonably conservative because of the assumption of no environmental transport of contamination and uncertain estimates of the waste inventory. These disposal units are the subject of CERCLA remediation and will be remediated to acceptable levels along with the disposal units closed before September 26, 1988. However, the estimated doses from inadvertent intrusion are certain to be overly conservative, as evidenced by the external dose estimated for the high-range wells that is significantly higher than the doses measured during waste disposal operations. For IWMF, changes in the WAC, along with continued work on the performance assessment, are expected to result in compliance with the performance objective for the protection of inadvertent intruders. Much of the difficulty in demonstrating compliance for the continuing operations at IWMF is the result of disposals of ^{36}Cl and ^{14}C. The disposal of ^{36}Cl is not a routine waste stream, and reductions in the WAC will reduce the potential doses dramatically. The ^{14}C inventory at IWMF is associated with several large disposals that, when curtailed, will reduce the potential doses significantly. Additionally, the ^{14}C

inventory is very uncertain, with divergences between reported disposals and the best estimate for disposals of up to a factor of 500 for IWMF.

The sensitivity and uncertainty of the results are important considerations in interpreting the results and evaluating the compliance of SWSA 6 with the performance objectives of DOE Order 5820.2A. Sensitivity analyses were used to evaluate the parameters in the models of site performance that were most influential on the results. The identified parameters were used in the uncertainty analysis to determine the confidence to be attributed to the results. The uncertainty analysis incorporated the subjective evaluation of the acceptability of each component of the modeling of site performance as well as the quantitative evaluation of model component uncertainty. The results of the uncertainty analysis indicated that the greatest source of uncertainty was associated with the waste inventory and that uncertainty in the calculated results increased as the time increased.

The results from the performance assessment indicate that several disposal units exceed the performance objectives, and changes in operations will be necessary. As of January 1, 1994, disposal operations in all disposal units other than IWMF will be discontinued. Additionally, the WAC will be revised in accordance with the results of the performance assessment. Future disposals in below-grade units will be considered only if all of the performance objectives can be demonstrated and approved prior to disposal. Continued work on the performance assessment is also warranted to address several elements of the SOURCE1 and SOURCE2 computer codes that are presently not verified or validated. While validation of these codes is not likely because validation data are not available and will not be available within a reasonable time frame, code verification is warranted. Additional work on estimating the waste inventory and the sorption characteristics of actinides in environmental transport will be performed. The results of the continued work and the changes in operations will be incorporated into a revision of the performance assessment for SWSA 6.

In conclusion, based on the results of this performance assessment, SWSA 6 does not presently meet the performance objectives of DOE Order 5820.2A. Changes in operations and continued work on the performance assessment are expected to demonstrate compliance with the performance objectives for continuing operations at IWMF. All other disposal operations in SWSA 6 are to be discontinued as of January 1, 1994. The disposal units at which disposal operations are discontinued will be subject to CERCLA remediation, which will result in acceptable protection of the public health and safety.

1. INTRODUCTION

Site-specific radiological performance assessments are required for the disposal of low-level radioactive waste at U.S. Department of Energy (DOE) facilities. The purpose of the performance assessment is to demonstrate compliance with the performance objectives for low-level waste (LLW) disposal stated in DOE Order 5820.2A, Chapter III, paragraph 3a (Table 1.1). Performance assessments are to be subjected to review by the Oversight and Peer Review Panel of DOE for technical quality and consistency across the DOE complex. Performance assessments are to include site-specific geohydrology and waste composition as part of the performance assessment methodology. This performance assessment has been prepared for the continued operations of LLW disposal at the Oak Ridge National Laboratory (ORNL).

The active LLW disposal facility at ORNL is identified as Solid Waste Storage Area (SWSA) 6. The facility began accepting waste in 1969 and became the sole waste disposal facility for ORNL in 1973 (Coobs and Gissel 1986). Prior to September 26, 1988, a variety of disposal methods were used. Many of these disposal methods are no longer practiced and are considered to be unacceptable by today's standards. As a result, a large

Table 1.1. Performance objectives for low-level radioactive waste disposal

1. Protect public health and safety in accordance with standards specified in EH Orders and other DOE Orders.
2. Assure that external exposure to the waste and concentrations of radioactive material which may be released into surface water, groundwater, soil, plants and animals results in an effective dose equivalent that does not exceed 25 mrem/yr to a member of the public. Releases to the atmosphere shall meet the requirements of 40 CFR Pt. 61. Reasonable effort should be made to maintain releases of radioactivity in effluents to the general environment as low as reasonably achievable.
3. Assure that the committed effective dose equivalents received by individuals who inadvertently may intrude into the facility after the loss of active institutional control (100 years) will not exceed 100 mrem/yr for continuous exposure or 500 mrem for a single acute exposure.
4. Protect groundwater resources, consistent with Federal, State and local requirements.

portion of SWSA 6 is now subject to remediation under the Comprehensive Environmental, Response, Compensation, and Liability Act of 1980 (CERCLA). Interim closure of many of the historical disposal units and a remediation investigation have been completed as RCRA actions prior to CERCLA remediation. In February 1993, the Deferred Action Alternative was selected in response to the Interim Proposed Plan for CERCLA remediation. The Deferred Action Alternative involves enhanced site monitoring and technology demonstration and development. Action will be deferred until the risks to public health and the environment warrant remedial action. A Letter of Agreement between the U.S. Environmental Protection Agency (EPA), the state (TDEC), and DOE that will outline the details of the Deferred Action Alternative is under development. Ultimately, the entire site will be remediated in accordance with the regulatory requirements of CERCLA. This performance assessment considers the portion of SWSA 6 in operation as of September 26, 1988, and all future disposal operations to be performed prior to the closure of the entire site. Following the guidance of T. Hindman, Assistant Secretary, DOE, the portions of the site used prior to September 26, 1988, have not been considered in evaluating the compliance of SWSA 6 with DOE Order 5820.2A.

The performance assessment for SWSA 6 has been prepared in accordance with the guidance provided by the DOE Peer Review Panel (DOE 1989) that describes the recommended format and content for DOE LLW disposal facility radiological performance assessment reports and is consistent with the guidance provided by the DOE Peer Review Panel for preparing performance assessments (DOE 1991). The performance assessment includes the disposal facility description, analysis of performance, results of the analysis, the performance evaluation, and design changes that are required to meet the performance objectives. The discussion of design changes and monitoring programs presented in this performance assessment represents those that have been identified in the course of this evaluation. Future work to be performed and incorporated in revisions to the performance assessment is identified.

SWSA 6 is located in a 28-ha (68-acre) tract of land with rolling terrain. The site includes two ephemeral streams. The site is adjacent to White Oak Lake on the south, a perennial stream on the east, a state highway on the west, and a ridge line on the north. Approximately 12 ha (30 acres) of the site is used for waste disposal with the majority of the site capacity used prior to September 28, 1988. A detailed description of the site and its characteristics is presented in Sect. 2.1. Current operations are performed using concrete silos and tumuli. A complete description of the waste disposal technologies is presented in Sect. 2.3. Future operations are planned to include a continuation of the present technologies. Waste is characterized, treated, and certified at facilities located outside SWSA 6.

The performance objectives for waste disposal in SWSA 6 are contained in DOE Order 5820.2A. The state of Tennessee has not issued regulations directly affecting waste disposal, nor has the state issued formal regulations protecting groundwater resources. The state of Tennessee, which is an agreement state, has issued implementing regulations for the Safe Drinking Water Act that limit the dose in drinking water for community water supplies to 4 mrem annual effective dose equivalent (EDE). In the present analysis, this regulatory limit has been regarded as the appropriate limit for the protection of groundwater resources. Compliance with the performance objective of groundwater resource protection usually has been interpreted as meaning that concentrations of

chemical and radioactive contaminants at any points of compliance should not exceed standards for public drinking water supplies established by the EPA. In this assessment, the point of compliance is at a location more than 100 m (328 ft) from any disposed waste at which the groundwater contaminant concentrations are the highest. The 100-m (328-ft) buffer zone is consistent with the guidance provided by the DOE Peer Review Panel (DOE 1991).

Because SWSA 6 is to be remediated under CERCLA, the use of the 4 mrem/year dose limit for groundwater protection is both conservative and reasonable. CERCLA has the intent of remediating sites to a useable condition without consideration of institutional control, and CERCLA specifically identifies drinking water standards as Applicable or Relevant and Appropriate Requirements (ARARs) for cleanup of groundwater at Superfund sites. Additionally, previous actions by the EPA in attempting to establish groundwater protection limits suggested the use of the 4 mrem/year limit. Future regulatory developments may resolve the appropriate limit for groundwater resource protection, but lacking this guidance, the 4 mrem/year limit has been adopted as the proper value for groundwater resource protection in this performance assessment.

White Oak Dam, which forms White Oak Lake, is located near the southwest corner of SWSA 6. The state of Tennessee has established National Pollutant Discharge Elimination System limits for discharges over White Oak Dam that do not include radioactivity. The discharges over White Oak Dam include releases from SWSA 6, previously closed disposal facilities, and all discharges from the ORNL plant area. SWSA 6 is a minor contributor to the discharge over White Oak Dam. Additional performance objectives for SWSA 6 will be defined as part of the CERCLA remediation of the facility. These limits are under development. For the purposes of this performance assessment, the 4 mrem annual EDE for protection of groundwater resources has been extended to surface water discharged over White Oak Dam. While this extension of the performance objectives is not explicitly required, the protection of surface water resources consistent with groundwater resources is expected to encompass any additional requirements on the protection of water resources by the CERCLA remediation of SWSA 6.

A scoping analysis of the performance of SWSA 6 was prepared as an initial assessment of the facility (Lee and Kocher 1990). Subsequently, a draft performance assessment was prepared and submitted to the DOE Peer Review Panel. The comments received from the Peer Review Panel have been addressed (Appendix I) and the document has been revised in response to these comments. The performance assessment has been reviewed by Rogers and Associates Engineering Corp. (1993) to further improve the technical presentation. The performance assessment identifies several areas of concern and the disposal units associated with doses that exceed the performance objectives. Many of these disposal units are included in the RFI prepared for SWSA 6. Remediation plans have not been formally implemented as a result of the selection of the Deferred Action Alternative. An Interim Corrective Measures program is under development to monitor historical disposal units and control any significant releases to the environment that may occur prior to CERCLA remediation of SWSA 6.

2. DISPOSAL FACILITY DESCRIPTION

2.1 SITE CHARACTERISTICS

Solid Waste Storage Area (SWSA) 6 has been used as a waste disposal facility since 1969 and continuously since 1974. The site has been investigated extensively, and much of the site description is based on these investigations. A summary of the detailed investigations of the site has been prepared (Bechtel 1991a).

2.1.1 Site Location and Topography

The SWSA 6 low-level radioactive waste (LLW) disposal site is located about 3 km (1.9 miles) south of Oak Ridge National Laboratory (ORNL) on the U.S. Department of Energy's Oak Ridge Reservation (ORR). The site lies in Melton Valley near the southwestern boundary of the ORR as shown on Fig. 2.1. Significant local features include White Oak Lake, south of SWSA 6, and the Clinch River, located about 1 km (0.6 mile) southwest of the site.

SWSA 6 has been used by ORNL for disposal of on-site generated solid LLW (SLLW) for approximately 20 years. Development of the 28-ha (68-acre) site was started in 1959, and the operational life is estimated to continue through 1997. Fewer than 12 ha (30 acres) of the total site are usable for LLW disposal because of land use constraints imposed by steep slopes, shallow water table, or proximity to streams.

Topography in and around Melton Valley is typical of that in the western portion of the Valley and Ridge Province of East Tennessee. The valley is about 2 km (1.2 miles) wide and trends northeast-southwest. Haw Ridge lies about 1 km (0.6 mile) northwest of Melton Valley with crest elevations of approximately 305 m (1000 ft). Melton Hill, with a high crest of 413 m (1356 ft) on Copper Ridge, lies about 1 km (0.6 mile) southeast of the axis of Melton Valley. A line of low knobs with crest elevations of about 260 m (850 ft) occurs near the center of Melton Valley. SWSA 6 is located on the southeast slope of such a knob. The lowest topography in the vicinity of SWSA 6 is at White Oak Lake [227 m (745 ft)], giving a total topographic relief in the site of about 30 m (98 ft). Slopes within SWSA 6 range from less than 5% to greater than 25%.

Most of Melton Valley, including SWSA 6, lies in the White Oak Creek watershed. White Oak Lake is impounded above an earthen dam located where Highway 95 crosses White Oak Creek. Surface runoff from SWSA 6 drains to three small ephemeral tributaries of White Oak Creek, which discharge into White Oak Creek and White Oak Lake. Two of these ephemeral streams originate within SWSA 6. Fig 2.2 shows the location of SWSA 6 in proximity to the local surface waters, Highway 95, and White Oak Dam. The caps identified in Fig. 2.2 represent interim closure of disposal units that were used prior to September 26, 1988, and are currently being addressed by the Comprehensive Environmental Response, Compensation, and Liability Act (CERCLA)

ORNL-DWG 90-12496

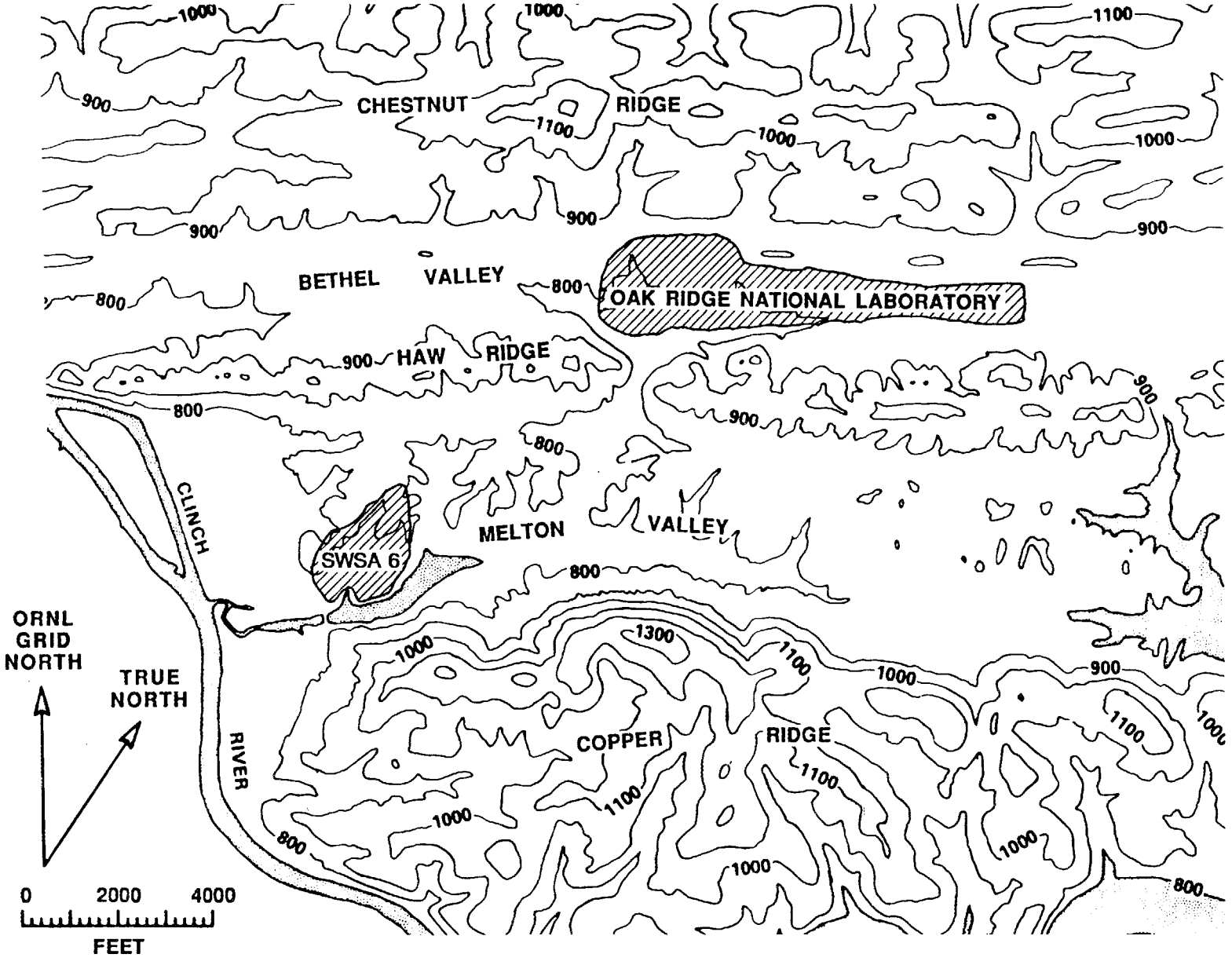

Fig. 2.1. Topographic map of Oak Ridge National Laboratory and the surrounding area.

ORNL-DWG 93M-8594R3

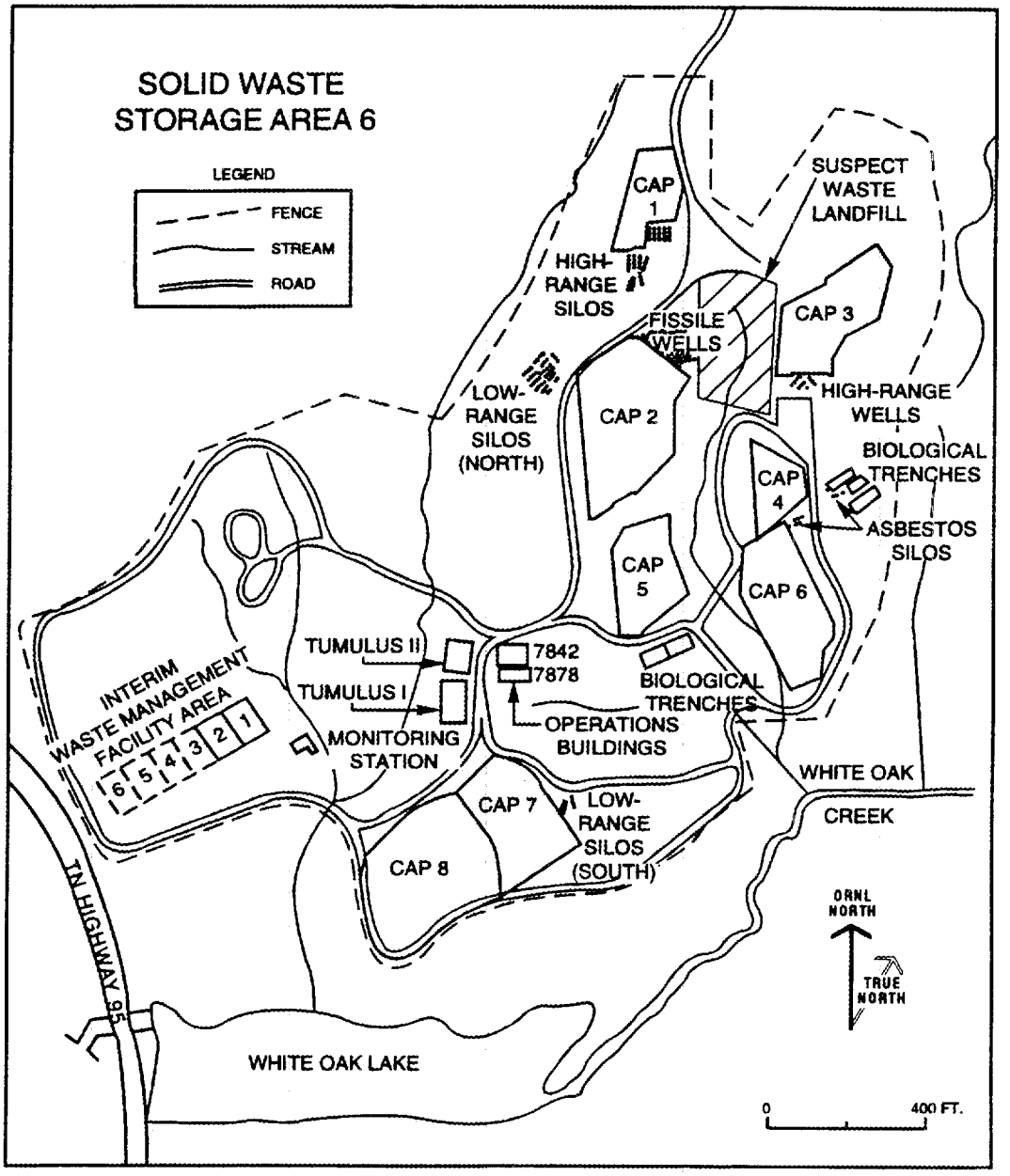

Fig. 2.2. Location of Solid Waste Storage Area 6 in proximity to local surface waters, Highway 95, and White Oak Dam.

process. The caps are plastic membranes to limit infiltration and cover approximately 4 ha (10 acres) of the total site area. Additionally, the disposal units considered in the performance assessment are identified.

2.1.2 Geology and Soils

2.1.2.1 Geologic Setting

The ORR is underlain by sedimentary bedrock of the Paleozoic Age that generally dips to the southeast in an imbricate pattern because of the regional geologic structure that formed during the Appalachian Orogeny some 300 million years ago. The stratigraphic column in Table 2.1 includes descriptions and local thicknesses of bedrock formations recognized on the ORR (Lee and Ketelle 1989). A geologic map of the ORR is shown in Fig. 2.3, and a geologic cross section through Haw Ridge and Melton Valley near SWSA 6 is shown in Fig. 2.4. Geologic structures present on the ORR include regional scale thrust faults, local faults having various orientations, local folds, and numerous sets of local joints and fractures. Bedrock fracturing is ubiquitous on the ORR with variation in the degree of fracturing based on local bedrock type and proximity to local or regional scale folds and faults. Two regionally important thrust faults cross the ORR in a northeast-southwest direction. These faults are the White Oak Mountain Fault Zone, which lies several miles northwest of the SWSA 6 site, and the Copper Creek Fault, which outcrops on the northwest slope of Haw Ridge about 1 km (0.6 mile) northwest of SWSA 6.

The Copper Creek Fault underlies the SWSA 6 site at a depth of about 300 m (1000 ft) below the land surface. Motion of bedrock above the Copper Creek Fault during the Appalachian Orogeny carried the Upper Rome Formation, the Conasauga Group, and the overlying Knox Group strata to their present orientation. At the end of the Paleozoic Age, the rocks that outcrop at the land surface were buried deeply beneath a mountainous deformation belt. The present regional terrain is the result of weathering and erosion of bedrock and soils over the millennia since the Appalachian Orogeny.

Variable resistance to weathering and erosion of the dipping strata causes the parallel alignment of ridges and valleys characteristic of the region. Locally, ridges are underlain by weathering- or erosion-resistant rock types, while valleys are underlain by the easily weathered or erodible rock types. A geologic map of the Melton Valley area is shown in Fig. 2.5. Haw Ridge, northwest of SWSA 6, is underlain by the hard sandstones of the Upper Rome Formation. Melton Valley is underlain by interbedded shale, calcareous siltstone, and limestone bedrock of the Cambrian Age Conasauga Group. The Conasauga Group is divided into six geologic formations on the ORR (Table 2.1). Conasauga bedrock is fairly weatherable because of the dominance of calcium-carbonate-cemented rock and the high silt content. Variations in the weathering and erosion patterns of the Conasauga formations result in the presence of a line of knobs underlain by the Maryville Limestone near the axis of Melton Valley.

Table 2.1. Stratigraphic column of Cambro-Ordovician Rocks, White Oak Mountain Thrust Block, Oak Ridge, Tennessee

Age	Group	Formation/ Unit	Description	Thickness (m)
Middle Ordovician	Chickamauga (Och)[b]	Unit H[a]	Thin interbedded limestone and calcareous siltstone. Gray, olive, buff, and maroon.	>82
		Unit G	Limestone and siltstone in thick beds. Limestone fine- to medium-grained, nodular.	88
		Unit F	Laminated to thin-bedded calcareous and shaley siltstone. Maroon and olive gray.	6
		Unit E	Limestone and siltstone in thick beds. Limestone fine- to medium-grained, nodular and amorphous. Siltstone dark gray with limestone laminae.	91
		Unit D	Limestone. Medium-grained and stylolitic. Nodular chert.	43
		Unit C	Limestone and siltstone in thick beds. Limestone nodular and micritic. Siltstone calcareous and dark gray. Nodular chert.	29
		Unit B	Siltstone. Massive maroon and gray with limestone in thin, even beds.	76
		Unit A	Limestone and siltstone in thick beds. Dark to light gray, purplish to maroon. Nodular and bedded chert.	91
Lower Ordovician	Knox (Oek)	Newala	Medium-bedded dolostones and limestones with variable chert content, scattered chert matrix limestones. Abundant maroon mottling.	274 (est)
		Longview	Dense, massive chert, bedded chert, and dolomoldic chert observed in residuum.	15–30 (est)
		Chepultepec	Dolostone, fine- to medium-grained, light to medium gray, medium to thick bedded, sandy near base.	150–300 (est)
Upper Cambrian		Copper Ridge	Dolostone, medium to thick bedded, fine to coarse crystalline, medium to dark gray. Chert varieties include massive, cryptopoan, and oolitic.	274–396 (est)

Table 2.1. (continued)

Age	Group	Formation/ Unit	Description	Thickness (m)
Middle Cambrian	Conasauga (εc)	Maynardville	**Upper** (Chances Branch Mbr.)—limestone and dolomitic limestone in thick massive beds.	43
			Lower (Low Hollow Mbr.)—dolomotic limestone in thick massive beds. Light gray to buff.	61
		Nolichucky	**Upper**—shale and limestone in thin to thick beds. Shale dark gray or maroon. Limestone light gray, oolitic, wavy-bedded, or massive.	18–43
			Lower—shale and limestone in medium to thick beds. Shale dark gray, olive gray, or maroon. Limestone light gray, oolitic, glauconitic, wavy-bedded, and intraclastic.	131–137
		Maryville	Limestone and shale or siltstone in medium beds. Limestone light gray, intraclastic, or wavy-bedded. Shale or siltstone dark gray.	98–125
		Rogersville	Shale and argillaceous limestone. Laminated to thin-bedded, maroon, dark gray, and light gray.	24–34
		Rutledge	Limestone and shale in thin beds. Limestone light to olive gray. Shale gray or maroon.	30–37
		Pumpkin Valley	**Upper**—shale and calcareous siltstone. Laminated to very thin-bedded. Shale reddish-brown, reddish-gray, or gray. Calcareous siltstone light gray or glauconitic.	40–46
			Lower—shale and siltstone or silty sandstone. Thin-bedded. Shale reddish-brown or gray to greenish-gray. Siltstone and silty sandstone light gray.	53
Lower Cambrian		Rome (εr)	Sandstone and thin shale interbeds. Sandstone fine-grained, light gray or pale maroon. Shale maroon or olive gray.	Unknown

[a]Chickamauga Group stratigraphic subdivisions reflect those identified at the Oak Ridge National Laboratory site. Other formation names are consistent with regional stratigraphic nomenclature.

[b]Group name abbreviations are those commonly used on geologic maps and cross sections in the region.

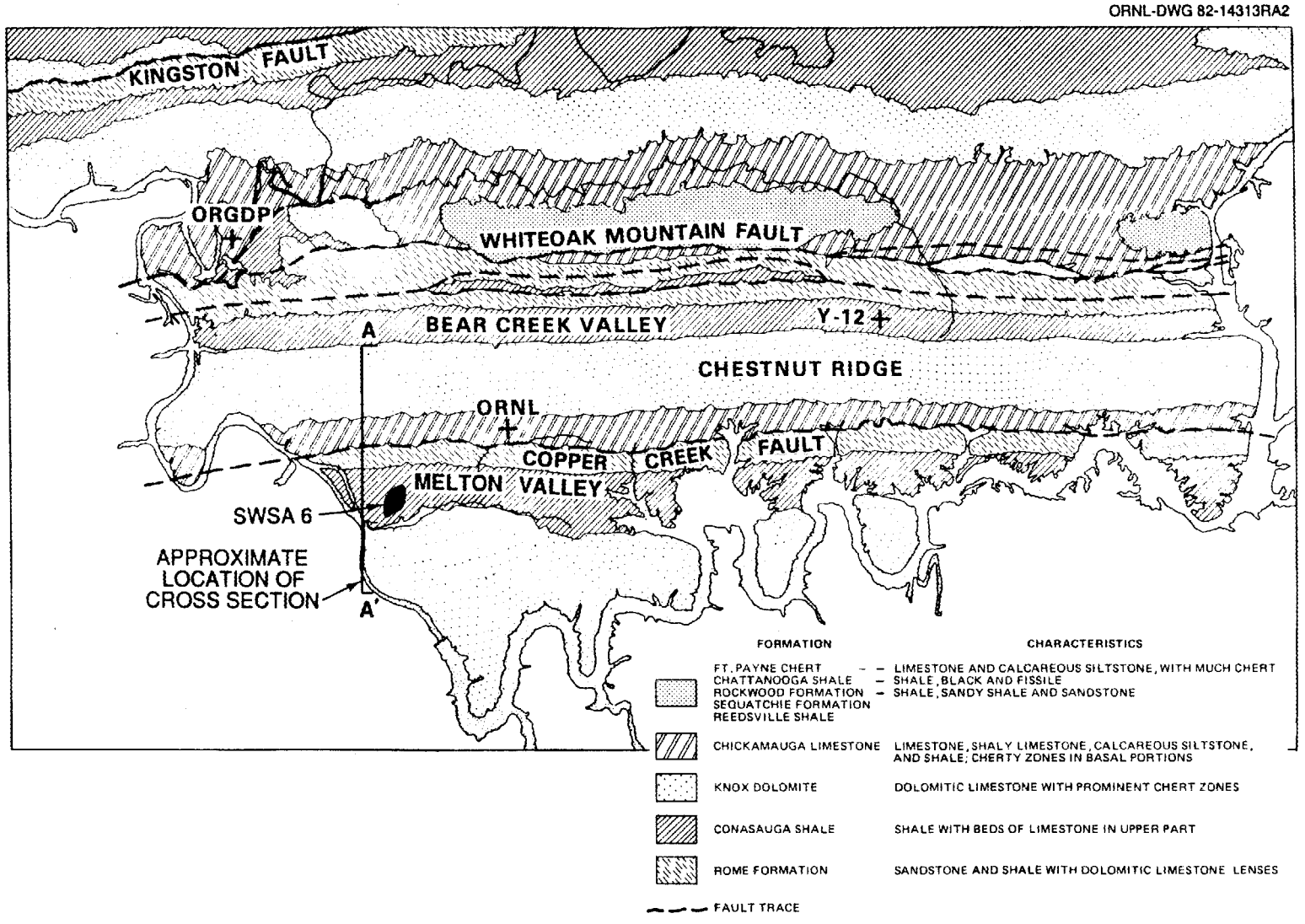

Fig. 2.3. Generalized geologic map of the Oak Ridge area. *Source:* modified from M. M. McMaster, *Geologic Map of the Oak Ridge Area, Tennessee.*

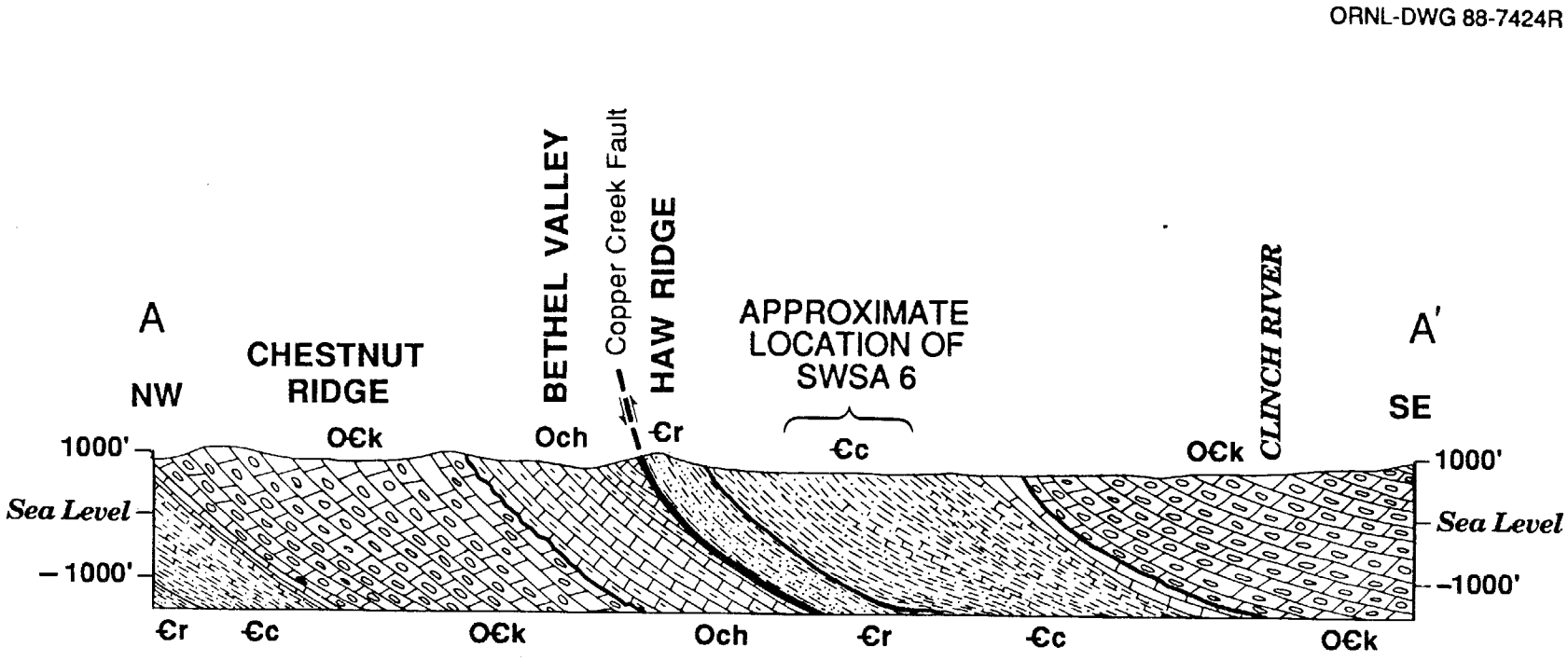

Fig. 2.4. Geologic cross-section of the Oak Ridge area. *Source:* modified from M. M. McMaster, *Geology of the Oak Ridge Area, Tennessee*, 1962.

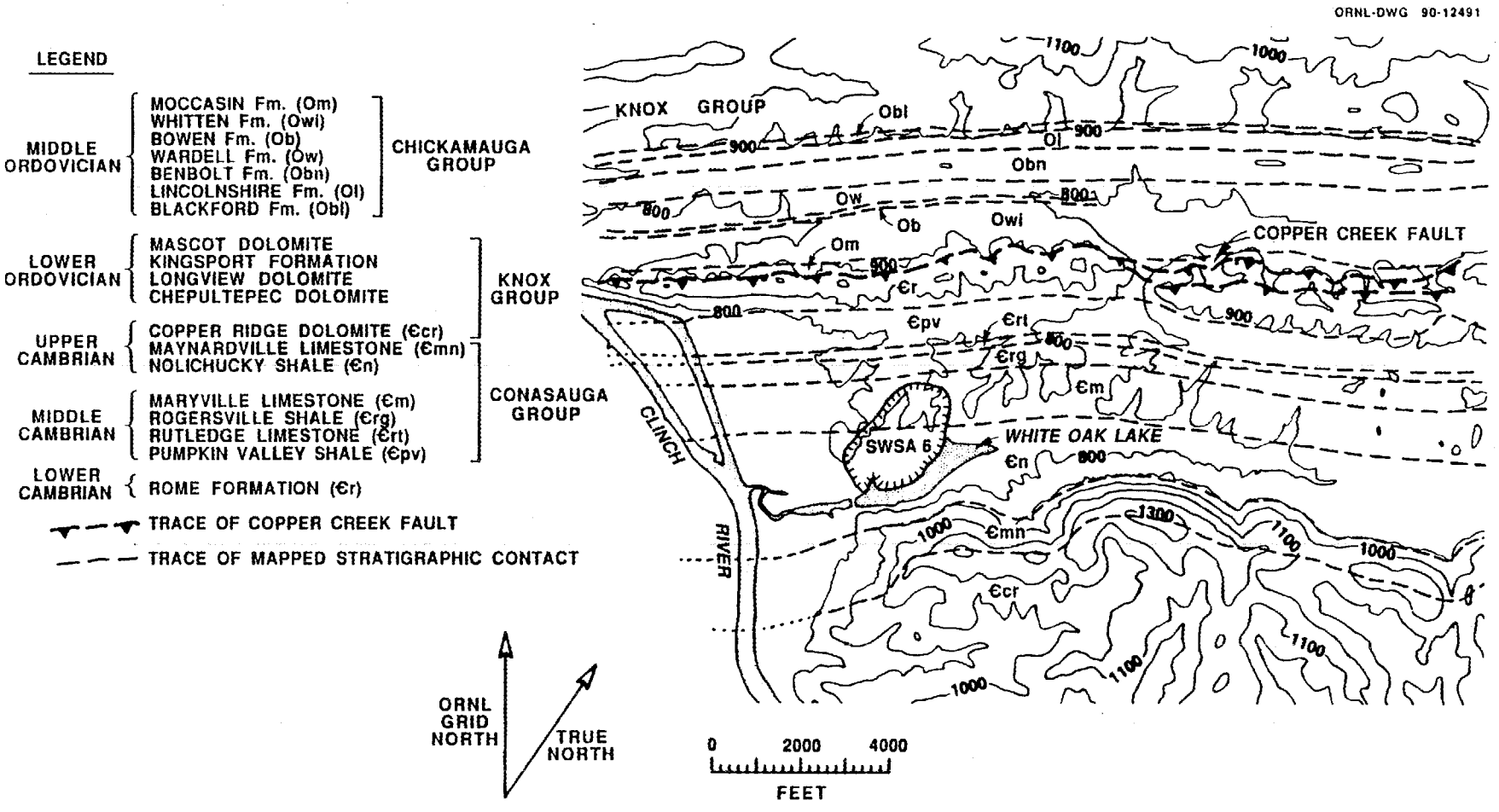

Fig. 2.5. Geologic map of Bethel Valley and Melton Valley. *Source:* Lemiszki, P. J., R. D. Hatcher, and R. H. Ketelle 1990. *Provisional Geologic Map of Oak Ridge Area,* Oak Ridge National Laboratory, Oak Ridge, Tenn. (May).

2.1.2.2 SWSA 6 Geology

SWSA 6 is underlain by two of the Conasauga Group formations. The Maryville Limestone underlies the northern half of the site, and the Nolichucky Shale underlies the southern half. The SWSA 6 geologic map (Fig. 2.6) shows the location of the stratigraphic contact between the Maryville Limestone and the Nolichucky Shale as well as other data related to geologic structure of SWSA 6. Overall, the bedrock in SWSA 6 dips to the southeast at an attitude of about 10–15°. However, at any specific location within the site, strike and dip of bedding are variable and are affected by local tight, plunging folds that are typically several meters wide and of undetermined length. Additionally, there is apparently a general rotation in geologic strike near the middle portion of the site, and localized faulting typical of the upper Maryville and lower Nolichucky occurs within the site.

2.1.2.3 Soils

Soils in most of the SWSA 6 area are residual products derived from weathering and leaching of the underlying bedrock. Soils, as discussed here, include the total thickness of weathered earth materials from the land surface to competent bedrock. The soil mass is an irregularly shaped volume, thinnest at creeks and thickest beneath upland terrain and topographic divides. This characteristic develops because streams have removed most weathered material beneath their beds and erosion carries soil to the site streams where it is carried to White Oak Creek as sediment.

Soils in SWSA 6 were investigated by Lee and Lietzke (1987). In most areas a relatively thin [<0.5 m (<1.5 ft)] soil column of residuum and/or colluvium overlies saprolite (weathered bedrock). Figure 2.7 shows typical soil profiles in hilltop, sideslope, and toeslope locations. The upper portion of saprolite (to depths of several meters) is typically leached by chemical weathering processes, is depleted of calcium carbonate, and has an acidic pH. Deeper saprolite zones typically have neutral pH, indicating the presence of free calcium carbonate. Below-grade waste disposal units in SWSA 6 are constructed in the saprolite zone.

Surficial soils and saprolite have been mapped in SWSA 6 as shown in Fig. 2.8. Residuum and saprolite derived from weathering of the major bedrock formations (Maryville Limestone and Nolichucky Shale) have been discriminated in the mapped soil units for the site. Several alluvial soils that mantle the underlying residuum have also been discriminated. Modern alluvium occurs along the site stream drainages, while old alluvial soils occur in the western portion of the site and are thought to have been deposited by the Clinch River during the Pleistocene.

Soils of the Maryville Limestone and Nolichucky Shale are discriminated in site mapping based on color and textural characteristics. Based on a review of soil test data (Lee and Lietzke 1987), the most obvious difference between the Maryville and Nolichucky soils is that the Maryville soils have soil-water retentions (i.e., differences in water content between field capacity and wilting point) of 10–20% while the Nolichucky soils tested have soil-water retentions of less than about 5%. Other physical and chemical properties of the Maryville and Nolichucky soils are quite similar. The soil hydraulic properties used for the analysis of SWSA 6 are given in Appendix D.

ORNL-DWG-93-12977

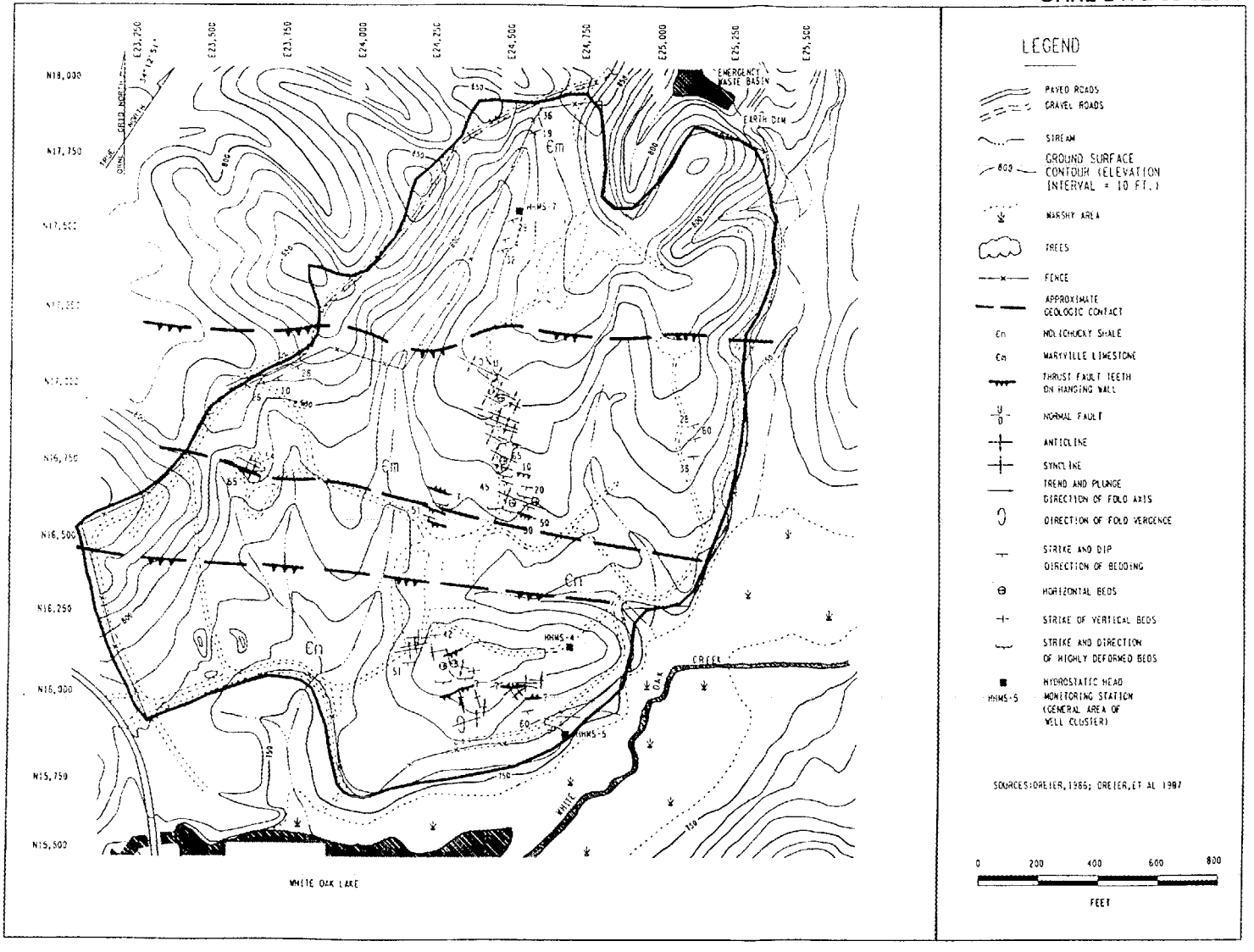

Fig. 2.6. Generalized geologic map of Solid Waste Storage Area 6.

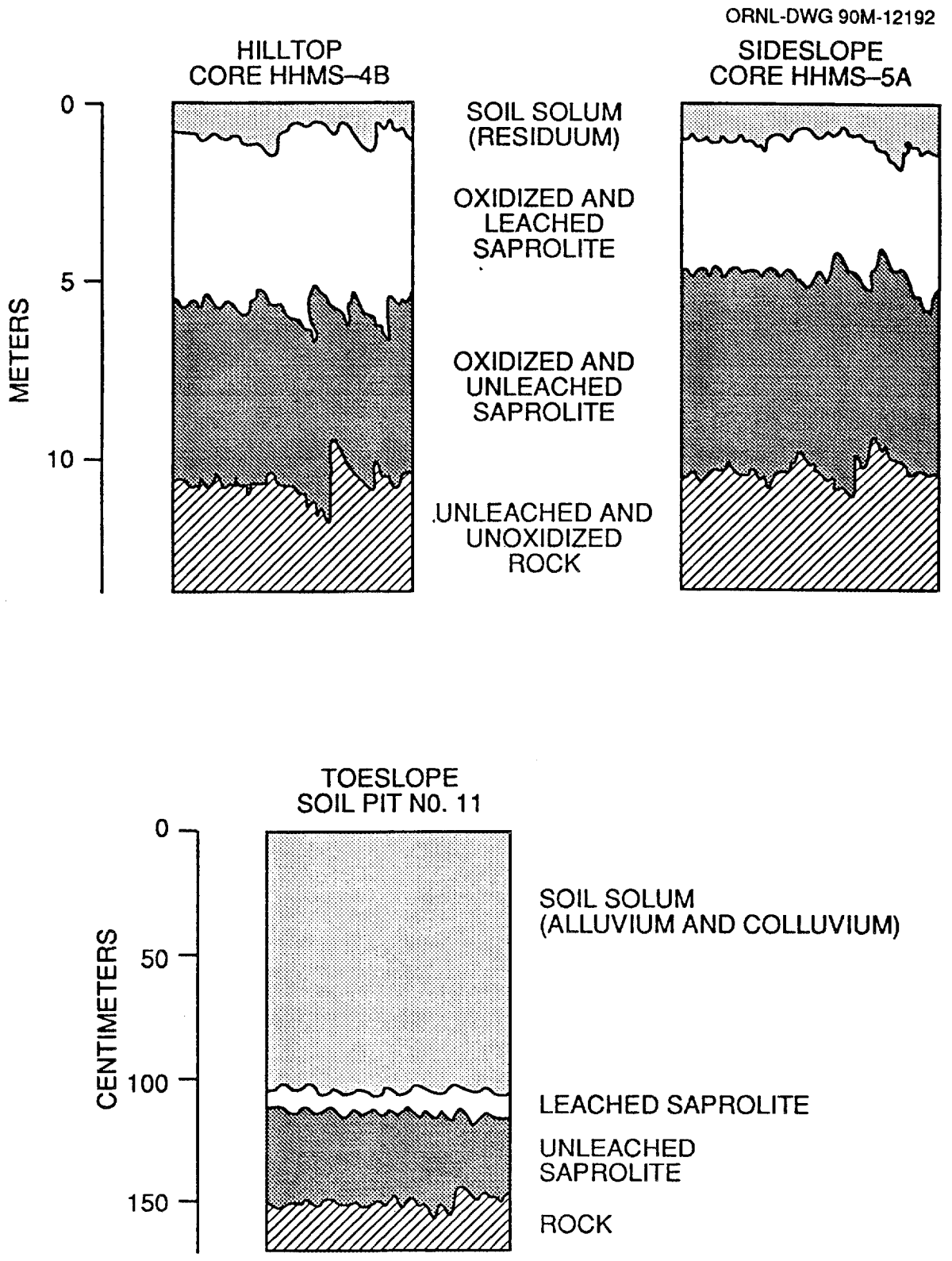

Fig. 2.7. Typical soil profiles observed at Solid Waste Storage Area 6.

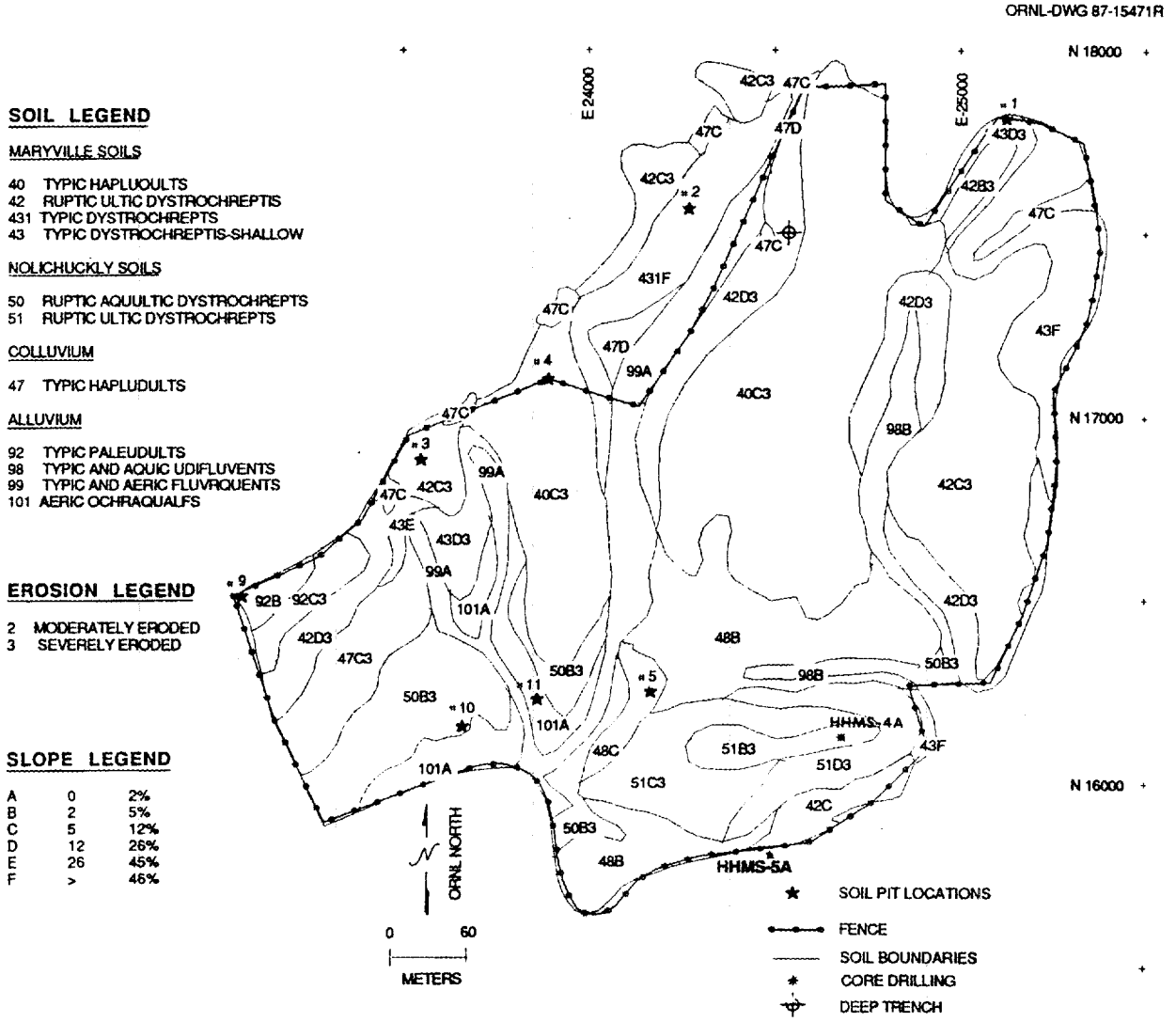

Fig. 2.8. Soil map of Solid Waste Storage Area 6.

The surface soil has been subject to a considerable amount of disturbance associated with waste management operations. These impacts have included road construction, surface gravel placement, compaction from vehicular traffic and hydraulic equipment, and maintenance of grass cover.

2.1.3 Hydrogeology

In areas underlain by the shales and silty limestones of the Conasauga Group, groundwater occurs in a continuous, unconfined, saturated zone. Most wells in the area cannot sustain pumping at rates greater than a few gallons per minute. Because the bedrock at Oak Ridge is lithified Paleozoic rock, the primary porosity is extremely low, and groundwater occurs and flows in fractures and weathered zones. The most prominent fracture orientations are parallel to local geologic strike and include bedding planes and strike-parallel fractures and joints. Less prominent and less penetrative fractures are perpendicular and oblique to local strike. Porosity of weathered and unweathered bedrock in the Conasauga Group is quite low (<5%). Additionally, groundwater storage is low because of this low porosity, and groundwater flow velocities are rapid through the fracture network [flow velocities >0.1 m/d (0.3 ft/d) have been documented] (Moore 1989). The combined influences of bedrock dip and fracture control of groundwater flow result in anisotropy of the aquifer hydraulic conductivity. Maximum hydraulic conductivity in this regime normally occurs parallel to local geologic strike.

Saturated hydraulic conductivity at the SWSA 6 site, as elsewhere in Conasauga terrain, generally decreases with increasing depth below the land surface (Fig. 2.9). At any discreet depth the conductivity may vary within two to three orders of magnitude. The decline in conductivity with depth is exponential, leading to some uncertainty as to the thickness of the active groundwater circulation zone. Fig. 2.10 shows the cumulative frequency distribution of hydraulic conductivity between depths of 1.5 and 10 m (5 and 35 ft) below ground surface at SWSA 6 determined by slug testing both piezometers and water quality monitoring wells. The heterogeneous character of the site aquifer is demonstrated by the four order of magnitude range in conductivity data and the high conductivities determined from five of the tests. The degree of anisotropy of hydraulic conductivity is variable and depends upon local conditions and the analytical method used in data interpretation. Anisotropy values determined from Conasauga Group aquifer pump tests on the ORR range from 3:1 to >30:1 with maximum conductivity parallel to strike. (Davis et al. 1984; Lozier, Spiers, and Pearson 1987; Lee et al. 1989).

The water table at SWSA 6, as in other areas on the ORR, is a subdued replica of the land surface. Historic water level data collection in SWSA 6 was performed by numerous investigators at different times and for different purposes. Historic data are plentiful; however, there are very few occasions in the historic data for which a large number of wells were measured in a short time interval. For this reason the water table configuration used in this analysis relies upon use of the average water elevation of all water table measurements for individual wells.

Figure 2.11 shows the approximate water table configuration at SWSA 6 based on average observed water table elevation. The water table contours shown are constrained by the ground surface elevations at streams and by the invert elevation for the french drain. In preparing this contour map, it was observed that in all cases use of these

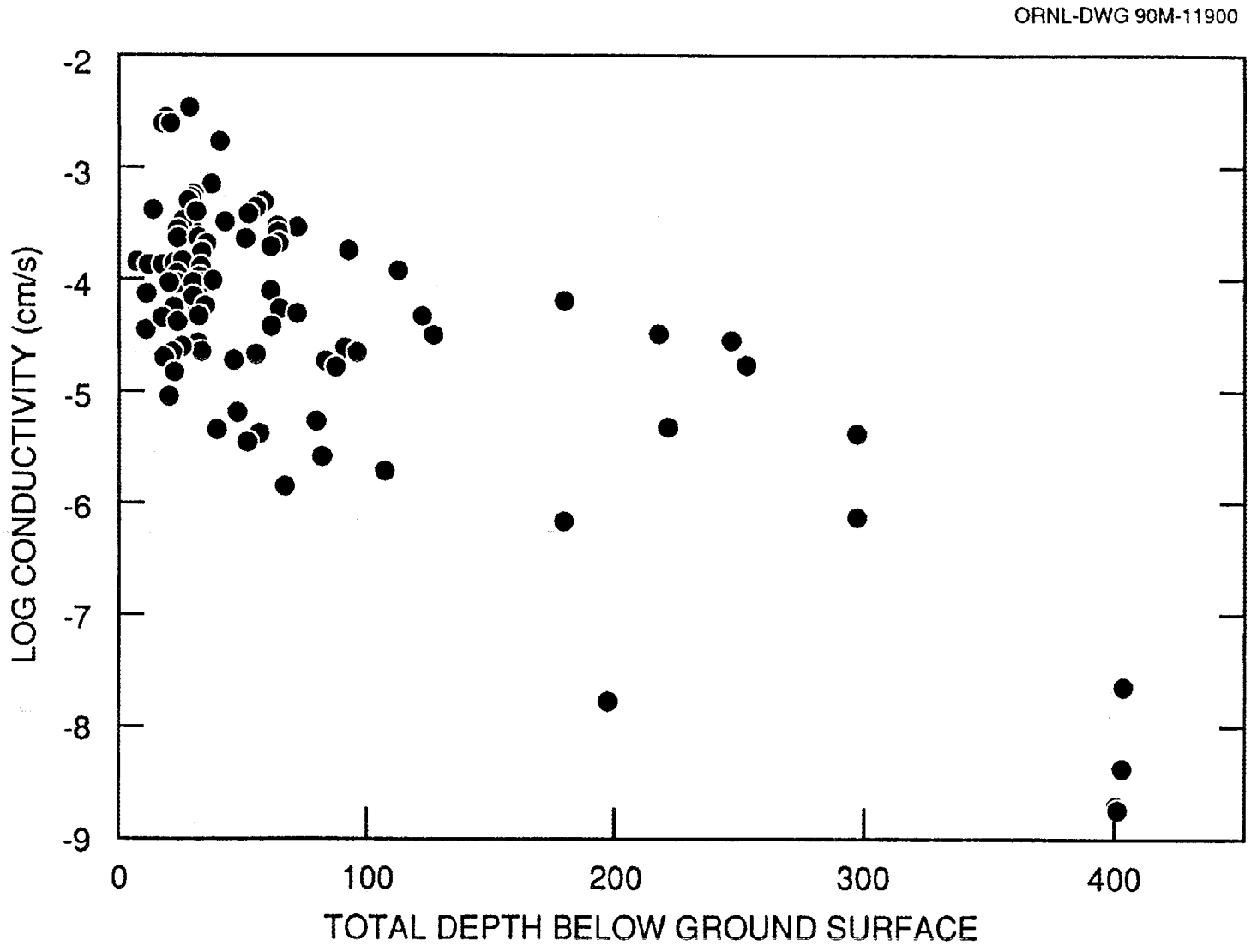

Fig. 2.9. Hydraulic conductivity vs depth at Solid Waste Storage Area 6.

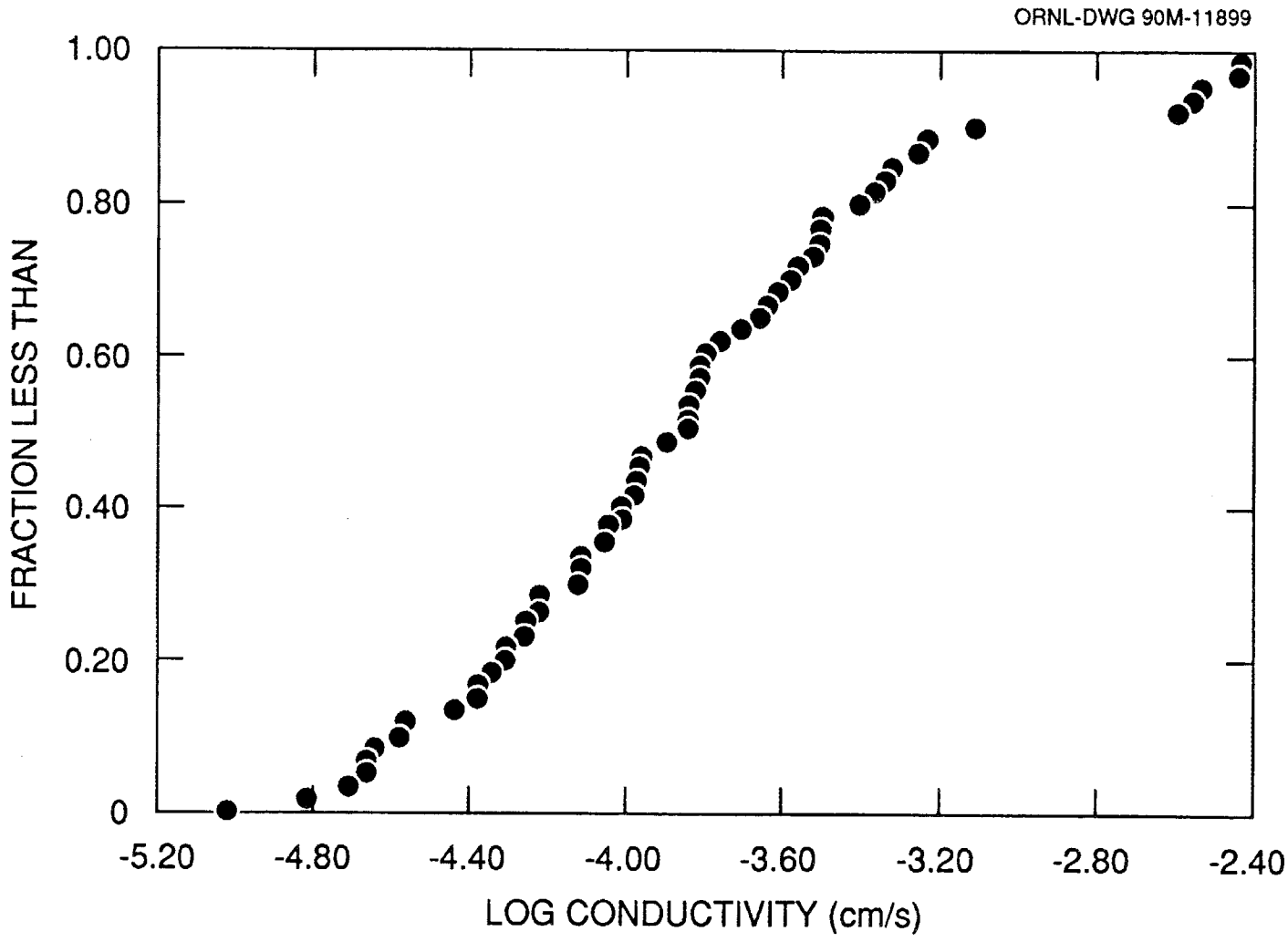

Fig. 2.10. Solid Waste Storage Area 6 conductivity distribution.

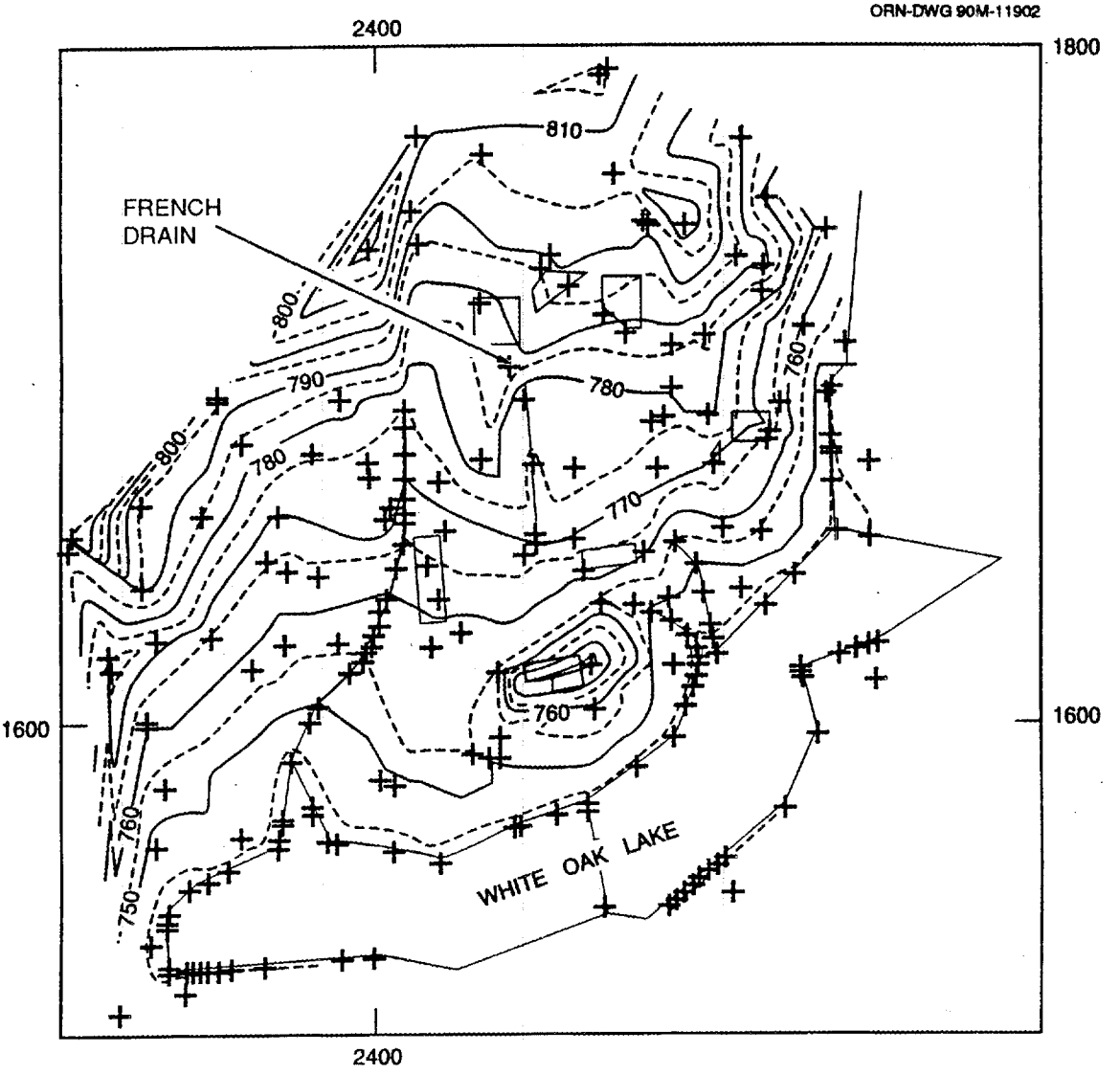

Fig. 2.11. Average water table configuration in Solid Waste Storage Area 6. Each crosshair (+) indicates the location of a monitoring well.

features as constraints on water table elevation resulted in lowering the water table elevation in those areas. This characteristic indicates that the average condition is for groundwater to discharge to the streams and the french drain. Well responses to seasonal variations in precipitation and evapotranspiration vary depending on well location and depth. Observed water level fluctuations in wells at SWSA 6 range from less than 1.5 m (5 ft) to more than 3 m (10 ft).

As previously mentioned, groundwater flow velocities tend to be relatively high in aquifers at ORR because flow occurs through fractures in otherwise low porosity rock. Solute transport in such systems can also be quite rapid depending on the ion exchange and adsorption characteristics of the soil or rock through which the solute migrates. Laboratory adsorption tests for various radionuclides have been performed on some soil and bedrock materials typical of those present at SWSA 6 (Friedman and Kelmers 1990). Most of these tests were performed under batch-type test conditions using materials with much higher surface area to volume ratios than are actually present along groundwater flow paths. For some radionuclides, the resulting distribution coefficients are substantially different than field measurements of contaminant movement at waste disposal facilities.

The presence of over 1000 previously constructed waste burial trenches and auger holes has undoubtedly affected the site geohydrology by increasing recharge to the site aquifer when disposal units were open to interception of shallow lateral groundwater flow. Capping of several disposal areas may temporarily reduce infiltration through previously constructed disposal units and reduce the total aquifer recharge in SWSA 6, but the longevity of caps and effectiveness in reducing infiltration is uncertain. The effect of existing groundwater contaminants on reduction of the aquifer retardation characteristics through occupation of available ion exchange sites or introduction of chelating agents into the aquifer is unknown.

Water quality of the upper subsurface is dominated by mixed cations and bicarbonate anions (Solomon et al. 1992). Water quality in the subsurface adjacent to the LLW silos, high-range wells, asbestos silos, and fissile wells is routinely sampled as part of the Active Sites Environmental Monitoring Program (Wickliff et al. 1991, Ashwood et al. 1991, Ashwood et al. 1992). Water quality in the drainage layers and in the subsurface of Tumulus I, Tumulus II, and the Interim Waste Management Facility (IWMF) is also routinely sampled. Monitoring program results suggest that contaminant releases from these units are currently low. Contaminant releases from silos used for disposal prior to September 26, 1988, have been recorded that indicate the release of ^{90}Sr. Low-level releases of ^{3}H have been associated with the underpad drainage layer of Tumulus I and a singular incident of a release of ^{3}H from Tumulus II has been recorded. Corrective action was taken to reduce future releases from Tumulus II. The cause for the low-level releases of ^{3}H in the underpad drainage layer of Tumulus I is currently under investigation, and corrective actions will be initiated once the cause is identified. Groundwater quality has been investigated extensively as part of the environmental surveillance activities for SWSA 6 (ORNL 1993). Groundwater quality has been adversely impacted from historical disposal operations. Volatile organic compounds (VOCs) and radionuclides have been identified in wells throughout the facility. VOC contamination is primarily along the eastern site boundary where data suggest that the VOCs are migrating towards the perennial creek to the east of the facility and concentrations are decreasing within the site. Extensive subsurface investigations have been performed as part of the CERCLA

remediation activities for SWSA 6 (Bechtel 1991b). Additional monitoring activities are performed as part of the Environmental Restoration and Waste Management (ERWM) Program to better define the extent of contamination within SWSA 6 and the effects of corrective measures (Clapp et al. 1992, Clapp 1992). Contamination of groundwater due to migration of plumes from previously used areas has occurred at the sites analyzed in this performance assessment, complicating the monitoring of the facilities analyzed in this assessment for performance verification or nonperformance detection. Additionally, the potential adsorption capacity of the site soils is unclear as a result of existing contaminant plumes.

2.1.4 Surface Water

As described in the location and topography section, surface water drainage from most of Melton Valley and all of SWSA 6 flows to White Oak Creek. The White Oak Creek watershed is 16.8 km^2 (6.5 $miles^2$) in area, and headwater flows originate on the southeast flank of Chestnut Ridge. White Oak Creek receives runoff and permitted wastewater discharges from ORNL and associated facilities in both Bethel and Melton valleys. The creek also receives discharges of contaminated groundwater from several former waste disposal sites associated with historic activities at ORNL. The average discharge of White Oak Creek at White Oak Dam is 3.9×10^7 L/d (15.9 cfs) (Kornegay 1992).

Precipitation has been measured at SWSA 6 using a continuous recording rain gauge since 1980. Data are maintained in the ORNL ERWM Data Base.

Surface runoff and groundwater discharges at SWSA 6 flow to three ephemeral tributaries of White Oak Creek, all of which discharge directly to White Oak Lake (Fig. 2.2). Discharges from some areas of SWSA 6 run off directly into White Oak Lake without convergence to a stream. Flows in the main stem of White Oak Creek and Melton Branch, its major upstream tributary, are gauged continuously at several flumes. Two small streams originate within SWSA 6, receiving surface runoff, stormflow discharges, and groundwater discharges. The third stream, which receives discharge from SWSA 6, lies east of the site and also receives runoff and groundwater discharges from a watershed of 0.65 km^2 (0.25 $mile^2$), which encompasses the southeast flank of Haw Ridge and a portion of the Pits and Trenches Waste Area Grouping 7. Long-term, continuous stream gauging has not been performed on the ephemeral tributaries originating in SWSA 6.

A limited data record for the ephemeral streams in SWSA 6 was obtained (Davis et al. 1987). These records indicate that site streams respond to rainfall events and generally go dry during summer and autumn. Discharge and water quality data for the ephemeral streams in SWSA 6 have been recorded to supplement the earlier data record (R. B. Clapp, ORNL, personal communication to D. W. Lee, ORNL, Oak Ridge, Tenn., June 29, 1993). These data have been collected using storm and grab samples from March 1992 to February 1993. Analysis of these data indicates that for over 90% of the time the discharge in the creeks is less than 1 L/s (0.04 cfs). Discharge events occur in response to precipitation events that occur infrequently throughout the year. Consequently, these ephemeral streams do not have sufficient discharge to support a drinking water supply for an individual and are not considered as possible drinking water resources in this performance assessment. Water quality data collected during this sampling period indicate

that ^{3}H is being released to surface water during storm events. Concentrations of 1–5 μCi/L are commonly reported in the surface water during and following a storm event. These releases of contamination are associated with historical disposal operations performed in SWSA 6 prior to September 26, 1988 are supported by the Active Sites Environmental Monitoring Program (Ashwood et al. 1992). Infrequent and low concentrations of ^{90}Sr and ^{137}Cs in surface water have also been reported in response to precipitation events (<30 pCi/L) (R. B. Clapp, ORNL, personal communication to D. W. Lee, ORNL, Oak Ridge, Tenn., June 29, 1993).

2.1.5 Climate

The climate of the ORR is moderated by the influence of the Cumberland Mountains to the west and the Great Smoky Mountains to the east. They divert the hot winds emanating from the Atlantic coast to produce warm, humid summers and cool winters. Extremes in precipitation, temperature, and winds are uncommon.

The mean annual temperature in Oak Ridge is 14.4°C (58°F). The coldest month is usually January, with temperatures averaging 3.3°C (38°F) and lows occasionally reaching −17°C (0°F). The warmest month is usually July, with temperatures averaging 25°C (77°F) and highs occasionally reaching 38°C (100°F). Daily temperature fluctuations are typically 12°C (20°F).

Prevailing winds are influenced by the topography and are either up-valley (northeasterly) or down-valley (southwesterly). Daytime winds are typically up-valley, and nighttime winds are typically down-valley. Tornadoes and high winds are rare.

Precipitation is highly variable within and between years. The 40-year annual average precipitation is 1.4 m (54 in.) with approximately 0.26 m (10.4 in.) of snowfall. Monthly precipitation is typically highest in January and February with storms of low intensity and long duration. Thunderstorms are common during the summer. October is typically lowest in precipitation.

2.2 WASTE CHARACTERISTICS

2.2.1 Low-Level Waste

LLW is radioactive waste not classified as high-level waste, transuranic (TRU) waste, spent nuclear fuel, or by-product material specified as uranium or thorium mill tailings and waste, as defined by DOE Order 5820.2A. Test specimens of fissionable material, irradiated for research and development only, may be classified as LLW, provided the concentration of TRU radionuclides is <100 nCi/g. Small volumes of waste containing naturally occurring and accelerator-produced radioactive material may also be managed as LLW in accordance with DOE Order 5820.2A, Chapter IV.

2.2.2 Generic Description and Characteristics of Waste

Approximately 2,000 m^3/year (75,000 ft^3/year) of LLW is routinely handled at ORNL. LLW is classified as either contact-handled (CH) or remotely handled (RH) based

on the radiation dose rate at the surface of the waste package. CH LLW accounts for 93% of the volume but only 1.5% of the activity. ORNL also manages some special categories of LLW such as fissile, asbestos, biological, and very low activity waste. The segregation and disposition of the various types of LLW are shown in Fig. 2.12. Table 2.2 lists the various categories of LLW at ORNL, and Table 2.3 provides a generic listing of LLW typically generated at ORNL. A complete listing of the reported and projected radionuclide inventories is presented in Appendix A. A summary of the projected radioactive wastes to be disposed of in SWSA 6 is shown in Table 2.4, which is based on the reported inventories in SWSA 6. Best estimates of inventories of each disposal unit are presented in Tables 2.5–2.13.

Radionuclide inventories and waste volumes for the disposal units listed in Table A.1 (Appendix A) were compiled using the results of data queries of the local Solid Waste Information Management Systems data base. The inventories listed in Table A.1 provide radionuclide activity and waste volume totals for LLW disposed of in these units during the period from September 26, 1988, through March 31, 1992. Table A.2 lists the actual number of disposal units used during this interval and provides projected estimates of additional disposal units required for disposal from April 1, 1992, through December 31, 1993. January 1, 1994, is the projected date when all disposal operations in SWSA 6 will cease, with the exception of the IWMF, which is projected to be operational through December 1997. Best estimates of the inventories in each disposal unit are presented in Tables A.13–A.21 based on the uncertainties in the projected inventories.

2.2.3 Contact-Handled Low-Level Waste

CH LLW (low-range) is waste that has a radiation dose rate at the package surface of $\leq$200 mrem/h. CH LLW consists of various contaminated items such as laboratory equipment, facility refurbishment waste, decontamination and decommissioning waste, personnel protective clothing, air filters, and bulk materials such as soil, sludge, and construction debris.

The physical form of the waste is the primary factor controlling the selection of treatment methods. ORNL segregates CH LLW into two categories, compactible and noncompactible, based on its physical characteristics.

2.2.3.1 Compactible Waste

Compactible waste consists of dry materials such as plastic bags, paper, personnel protective clothing, light-gauge metal, and glassware that can be compacted by conventional compaction equipment. Compactible waste is segregated from other LLW streams, double bagged in 4-mil-thick plastic bags, and stored in steel, double-door yellow dumpsters at the generator's facility. Compactible waste is treated at the ORNL

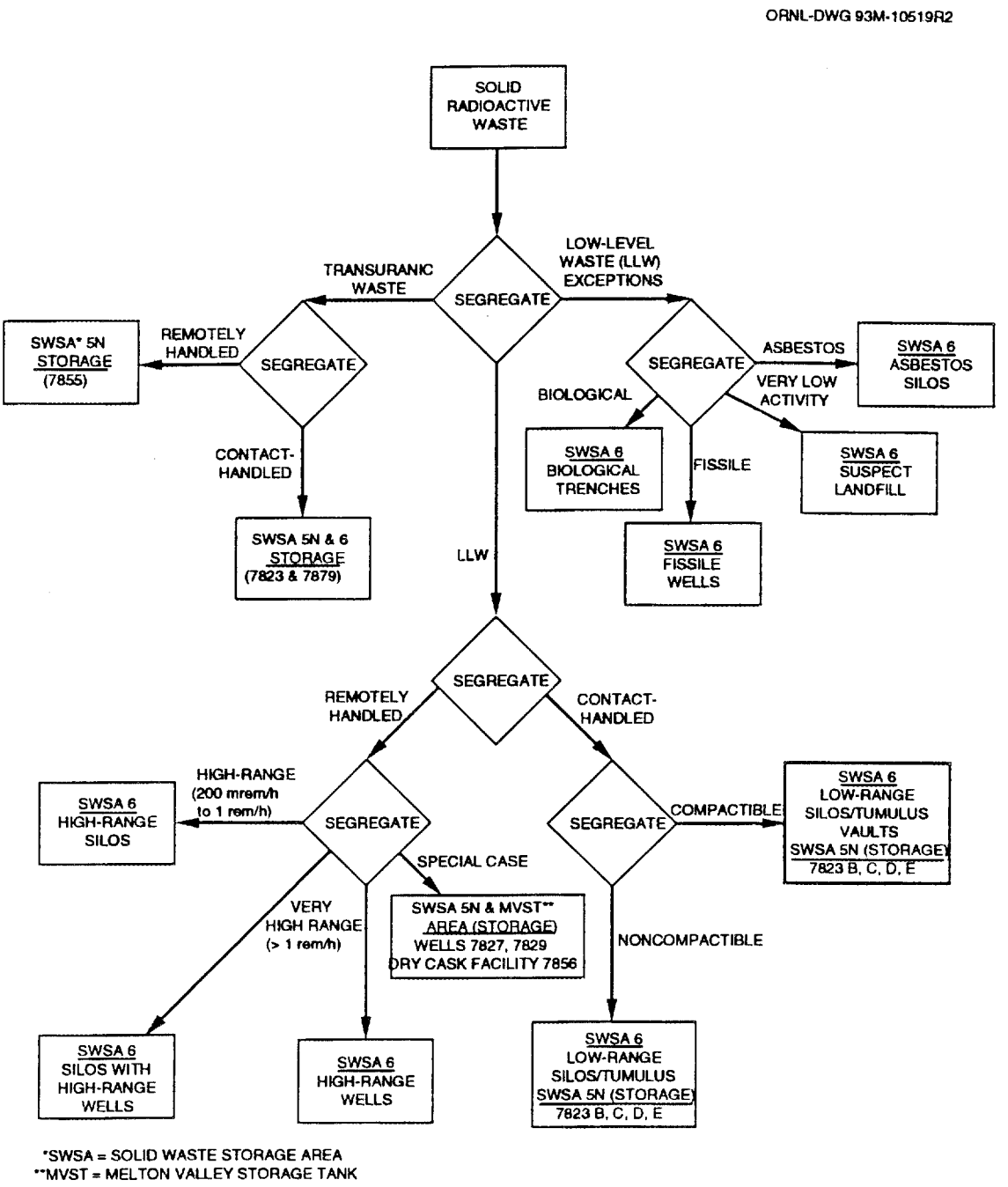

Fig. 2.12. Segregation and disposition of solid radioactive waste at the Oak Ridge National Laboratory.

Table 2.2. Current low-level waste (LLW) segregation categories

Waste type	Description
Contact-handled	LLW ≤200 mrem/h • compactible • noncompactible
Remotely handled	LLW >200 mrem/h • hot cell debris • irradiated hardware • solidified liquids • ion exchange resins • sealed sources
Fissile	LLW with a ^{235}U equivalent ≥1 g or ≥1 g/ft^3
Biological	Radioactively contaminated biological material
Asbestos	Radioactively contaminated asbestos material
Very low activity or suspect	Waste with no measurable external contamination but with the potential for inaccessible areas of internal contamination

compaction facility. In the future, waste may be incinerated or supercompacted at an off-site commercial treatment facility. The maximum unshielded surface dose rate of a bag of compactible waste is limited to ≤200 mrem/h. Most compactible waste packages have a surface dose rate of <10 mrem/h.

2.2.3.2 Noncompactible Waste

Noncompactible waste consists of large, heavy, or bulky items such as piping, equipment, instrumentation, heavy glass containers, wood, soil, concrete, and other debris that cannot be compacted at the ORNL compaction facility. Noncompactible waste is segregated from other waste streams, packaged in 4-mil-thick plastic bags, and placed in a 55-gal metal drum or 4 × 4 × 6-ft metal box. Bulk waste such as soil, gravel, concrete, asphalt, and other construction and demolition debris is generally packaged in plastic lined 4 × 4 × 6-ft metal boxes. Large items of noncompactible waste that will not fit in drum or box, such as large tanks or vessels, are accepted on a case-by-case basis. Some

Table 2.3. Waste descriptions

	Laboratory equipment	
Bench Equipment		
Glassware	Evaporating dishes	Gauges
Plastic bottles, tubing sheeting	Blotter paper	Clamps
	Electrodes	Ring stands
Wipes	Combustion boats	Wire
Crucibles	Mortars and pestles	Tongs
Processing equipment		
Bottles racks	Balances	Ultrasonic cleaners
Small furnaces	Band saws	Metal rods
Hydraulic presses	Glove boxes	Vacuum pumps
Welding equipment	Heat lamps	Sanders
Vacuum chambers	Grinders	Drill presses
Heat lamps	Small tanks	
	Personnel protective clothing and equipment	
Lab coats	Face masks	Rags
Coveralls	Paper suits	Buckets
Shoe covers	Mops	Tape
Rubber gloves	Brooms	Plastic bags
	Biological waste	
Reservation trees, shrubs, grass, etc.	Reservation deer, geese, ducks, fish, etc.	Research animal carcasses, tissues, etc.
	Asbestos	
Ovens	Floor tile	Insulation
Furnaces	Transite pipe	Gloves
	Facility refurbishment and decontamination and decommissioning	
Chemical hoods	Insulation	Wood
Choker Cables	Metal grating	Paper
Conduit	Miscellaneous furniture	Plastic
Cylinders	Sheet metal duct	Fans
Dry wall	Large tanks and vessels	Pumps
Tools	Vessels	Motors
Metal piping	Air filters	Valves
	Bulk waste	
Asphalt	Gravel	Sediment
Concrete	Plaster	Tar
Charcoal	Roofing	Sludge
Dirt	Sand	Resin

Table 2.4. Solid Waste Storage Area 6 inventory data

Disposal unit	Number of units	Volume (m^3)	Radioactivity (Ci)
Tumulus I vaults	197	535	29.4
Tumulus II vaults	220	601	26.9
Interim Waste Management Facility vaults	1980	5383	305
Low-range silos	113	895	35.6
High-range silos	50	433	130.6
Asbestos silos	17	167	0.168
High-range wells	54	15.6	6734
Fissile wells	1	0.6	42.5
Biological trenches	6	250	0.019
Suspect landfill	1	1756	0

noncompactible waste is transported to an off-site commercial treatment facility for incineration or supercompaction. The maximum surface dose rate of the outer container is limited to ≤200 mrem/h. Most noncompactible waste packages have a surface dose rate of <10 mrem/h.

2.2.4 Remotely Handled Low-Level Waste

RH LLW is waste that has a surface dose rate of >200 mrem/h and consists of debris from reactors and hot cell operations, ion exchange resins, and solidified supernatants from liquid LLW (LLLW) evaporation. RH LLW is subdivided into two categories for handling and long-term management: high range and very high range. High-range waste is RH LLW with a maximum contact reading ≤1 rem/h. Very high range waste is RH LLW with a contact intensity >1 rem/h.

2.2.4.1 High-Range Waste

High-range waste >200 mrem/h and <1 rem/h consists of the same types of compactible and noncompactible materials described in Sect. 2.2.3. High-range waste is generally double bagged in 4-mil plastic bags and placed inside an outer container. Large items that won't fit in a plastic bag may be double wrapped in plastic or placed in alternate containers. Approved outer containers are either 20-mil plastic bags, 1-20-gal metal cans, or 30- or 55-gal metal drums. High-range waste is not treated because a treatment facility for RH waste is not available and existing treatment facilities are not suitable for RH wastes.

Table 2.5. Estimated total activity in low-range silos

Radionuclide	Best estimate activity (Ci)
^{3}H	1.02×10^{1}
^{14}C	7.23×10^{1}
^{90}Sr	5.34×10^{0}
^{99}Tc	3.26×10^{0}
^{137}Cs	4.49×10^{0}
^{232}Th	1.08×10^{-3}
^{233}U	2.75×10^{-2}
^{238}U	1.37×10^{-1}
^{239}Pu	3.47×10^{-1}
^{241}Am	2.76×10^{-2}
^{243}Am	1.08×10^{-2}

Table 2.6. Estimated total activity in high-range silos

Radionuclide	Best estimate activity (Ci)
^{3}H	1.00×10^{1}
^{14}C	4.00×10^{-2}
^{63}Ni	2.74×10^{-2}
^{90}Sr	3.51×10^{2}
^{137}Cs	2.34×10^{1}
^{152}Eu	5.94×10^{-1}
^{232}Th	1.18×10^{-4}
^{238}U	1.10×10^{-2}
^{239}Pu	1.50×10^{-2}

Table 2.7. Estimated total activity in asbestos silos

Radionuclide	Best estimate activity (Ci)
^{3}H	5.00×10^{-2}
^{14}C	5.79×10^{-1}
^{90}Sr	4.71×10^{-2}
^{99}Tc	1.02×10^{-3}
^{137}Cs	5.65×10^{-2}
^{238}U	5.08×10^{-3}

Table 2.8. Estimated total activity in high-range wells

Radionuclide	Best estimate activity (Ci)
^{60}Co	5.59×10^{2}
^{90}Sr	7.00×10^{3}
^{99}Tc	4.00×10^{-1}
^{137}Cs	6.62×10^{3}
^{152}Eu	5.36×10^{2}
^{154}Eu	1.90×10^{2}
^{229}Th	7.50×10^{-3}
^{232}Th	3.70×10^{-5}

Table 2.9. Estimated total activity in fissile wells

Radionuclide	Best estimate activity (Ci)
^{137}Cs	3.85×10^{1}
^{235}U	8.75×10^{-4}
^{238}U	4.83×10^{-3}

Table 2.10. Estimated total activity in biological trenches

Radionuclide	Best estimate activity (Ci)
^{3}H	9.00×10^{-4}
^{90}Sr	1.81×10^{-1}
^{137}Cs	2.25×10^{-3}

Table 2.11. Estimated total activity in Tumulus I

Radionuclide	Best estimate activity (Ci)
^{3}H	2.70×10^{0}
^{14}C	9.76×10^{0}
^{63}Ni	9.68×10^{-2}
^{90}Sr	3.71×10^{0}
^{99}Tc	3.69×10^{-1}
^{137}Cs	9.96×10^{0}
^{152}Eu	1.66×10^{-1}
^{226}Ra	4.19×10^{-4}
^{232}Th	1.11×10^{-4}
^{233}U	9.81×10^{-2}
^{238}U	4.55×10^{-2}
^{239}Pu	9.03×10^{-2}
^{241}Am	8.27×10^{-2}
^{243}Am	1.86×10^{-3}

Table 2.12. Estimated total activity in Tumulus II

Radionuclide	Best estimate activity (Ci)
^{3}H	1.61×10^{0}
^{14}C	2.12×10^{0}
^{90}Sr	3.29×10^{0}
^{99}Tc	2.35×10^{-1}
^{137}Cs	5.20×10^{0}
^{152}Eu	7.08×10^{-2}
^{232}Th	3.97×10^{-4}
^{233}U	5.19×10^{-2}
^{238}U	7.33×10^{-3}
^{239}Pu	5.21×10^{-2}
^{241}Am	1.05×10^{-1}

2.2.4.2 Very High Range Waste

This waste consists primarily of obsolete equipment and materials contaminated with activation or fission products from reactors and from isotope production hot cells. Very high range wastes are packaged in an inner container, sealed, and placed in an outer container. The outer container is typically a 1–20-gal metal can or a 30- or 55-gal metal drum. This type of waste can have surface dose rates up to thousands of rem per hour and is handled as a special-case waste. Because of its very high radiation level, this waste must be transported in shielded waste carriers or shielded transport casks. Very high range wastes are not treated because a treatment facility for RH waste is not available and existing treatment facilities are not suitable for RH waste.

Very high range wet solid wastes are also generated during treatment of LLLW. Dewatered ion exchange resins from reactor facilities and solidified supernatants from the LLLW evaporator concentrate storage tanks produce a RH LLW >1 rem/h. These waste streams are packaged in large steel or high-density polyethylene containers.

Table 2.13. Estimated total activity in Interim Waste Management Facility

Radionuclide	Best estimate activity (Ci)
^{3}H	5.10×10^{0}
^{14}C	1.54×10^{1}
^{26}Al	1.66×10^{-4}
^{36}Cl	1.07×10^{0}
^{63}Ni	7.84×10^{-3}
^{90}Sr	3.13×10^{0}
^{99}Tc	1.47×10^{-1}
^{137}Cs	5.39×10^{0}
^{152}Eu	2.92×10^{-1}
^{232}Th	3.56×10^{-5}
^{233}U	9.26×10^{-2}
^{238}U	5.79×10^{-2}
^{239}Pu	4.65×10^{-2}
^{241}Am	6.67×10^{-3}
^{243}Am	2.61×10^{-3}

2.2.5 Fissile Waste

Waste that contains ^{233}U, ^{235}U, ^{238}Pu, ^{239}Pu, ^{241}Pu or the isotopes of neptunium, americium, curium, berkelium, and californium is managed as fissile waste, provided the concentration of the TRU radionuclides with half lives >20 years is <100 nCi/g. For criticality and security reasons, waste containing ≥ 1 g or ≥ 1 g/ft^3 of ^{235}U or its fissile mass equivalent is handled separately. All fissile wastes are packaged in containers that provide at least two containment barriers to prevent the inadvertent release of radioactive material during handling. The dose rate of fissile waste packages may be >1 rem/h. Fissile wastes are not treated because a treatment facility is not available for fissile waste and existing treatment facilities are not suitable for fissile wastes.

2.2.6 Biological Waste

Biological LLW consists of animal carcasses, tissues, excrements, and bedding that are generated when radionuclides are used in biological research. Also included are contaminated plants and animals from the ORR, including deer, ducks, geese, trees, grass, and plants. Sewage sludge from the Sanitary Wastewater Treatment Facility is also managed as biological LLW.

Radioactive animal carcasses and tissues are frozen and stored by the waste generator. Contaminated vegetation and sewage sludge is temporarily stored at an ORNL waste storage facility. When sufficient quantities of contaminated biological waste has accumulated, it is transported to an off-site commercial treatment facility for incineration. The treated waste is packaged in metal boxes and returned to ORNL for storage or disposal. The dose rate of biological LLW packages is usually much less than 10 mrem/h.

2.2.7 Asbestos Waste

Until the late 1970s, asbestos was used extensively at ORNL for the insulation of pipes. Asbestos waste is also found in floor tiles, ovens, and furnaces. Asbestos waste is generated during maintenance or demolition of contaminated facilities. Generally, asbestos waste is packaged in special, asbestos-labeled, 6-mil polyethylene bags, sealed with tape, and placed in a second asbestos-labeled polyethylene bag. Heavy materials such as asbestos tiles or bench tops are placed in fiber board drums. Asbestos waste is not treated because treatment facilities for asbestos waste are not available and existing treatment facilities are not suitable for asbestos waste. The maximum dose rate of packaged asbestos waste is limited to ≤ 1 rem/h. The typical dose rate of packaged asbestos waste is much less than 10 mrem/h.

2.2.8 Suspect Waste

Suspect waste consisted of debris that was generated during the decontamination and decommissioning or construction of facilities and other waste such as soil, air filters, wood, empty drums, laboratory equipment, and personal protective clothing listed in Table 2.2. Suspect waste was waste that had no measurable contamination but could not be certified by routine health physics surveys as free of internal contamination. Facilities that generate only alpha-emitting or beta-emitting radionuclides did not generate suspect waste. Facilities that generate beta- or gamma-emitting waste only generated suspect waste materials that had been individually surveyed, thus reducing the possibility that high concentrations of beta or gamma emitters were well shielded by uncontaminated material towards the outside of a waste package. Because of the history and location of these facilities, the waste was disposed of in a landfill in SWSA 6. This waste type is no longer classified as suspect. It is now classified as very low activity (VLA) waste or industrial waste.

VLA waste is segregated from other LLW and placed inside a 4 × 4 × 6-ft metal box. Large items that won't fit in a metal box are stored in a sea-land container. The packaged waste is stored at an ORNL storage facility until transported off-site for incineration or supercompaction at a commercial treatment facility. The treated waste is

packaged in metal boxes and returned to ORNL for storage or disposal. There are no external radiation readings on packages of VLA waste.

2.3 WASTE TREATMENT, CERTIFICATION, STORAGE, AND DISPOSAL

2.3.1 Waste Treatment Facilities

ORNL has one treatment facility for dry solid CH LLW. The ORNL waste compaction facility (Bldg. 7831) is located in SWSA 5N. Building 7831 is a metal Butler-type building approximately 12 × 13 m (40 × 42 ft) divided into a personnel area and compactor area 6 × 13 m (20 × 42 ft) each. The box compactor is used to reduce the volume of compactible CH LLW into 1.2 × 1.2 × 1.8-m (4 × 4 × 6-ft) metal boxes with a compressive force of 12 × 10^6 Pa (1750 psi). Off-site commercial treatment facilities are also used to reduce the volume of a portion of ORNL's CH LLW. Commercial services are available for supercompaction, incineration, and metal melting.

ORNL has one liquid treatment process that produces a solid CH LLW. Process wastewater is collected and treated at the Process Waste Treatment Plant (PWTP). The PWTP removes radionuclides by clarification, filtration, and ion exchange. The ferrous hydroxide sludge from the clarifier is passed through a filter press to reduce the liquid content and packaged in drums for on-site storage or disposal. Commercial vendors are used to treat ion exchange resins and solidify LLLW evaporator concentrates.

2.3.2 Low-Level Waste Characterization and Certification

The Martin Marietta Energy Systems, Inc. (Energy Systems) *Solid Waste Certification Program Plan* (Smith 1991) is based on the concept that site waste management organizations will establish waste acceptance criteria (WAC) against which waste handled at those facilities can be certified. In addition, DOE Order 5820.2A specifies the development of WAC for each radioactive waste treatment, storage, and disposal (TSD) facility that must be met by waste generators using these facilities. WAC establish not only the minimum acceptable amount of information that must be known about a waste, but also define certain acceptable waste characteristics. The purpose of the ORNL LLW Certification Program is to ensure that wastes generated are capable of being certified against WAC for the TSD facilities to which they are sent in a manner consistent with DOE Order 5820.2A and the Energy Systems Solid Waste Certification Program.

2.3.2.1 Waste Characterization

The waste generator is responsible for providing the primary characterization data and for certifying that the waste meets the WAC of the TSD facility. The following methods are considered acceptable for characterizing LLW:

- process knowledge and controls,
- materials accountability,

- direct or indirect measurements, or
- combinations of the above.

Documented process knowledge is the primary qualitative waste characterization method. Documenting the qualitative characteristics of a waste package relies heavily on the waste generator's understanding of the process whereby the waste is generated. Knowing the materials introduced into the process and the mechanism by which they are used can provide an indication of the probability that these materials will occur in the waste stream. The most appropriate method of determining those probabilities is through the use of a process flow chart.

Materials accountability, when used for characterizing waste, is a simplified version of process knowledge and control. Basically, this procedure uses a balance sheet, describing the input materials and their destination in the process. In the absence of a more sophisticated process model and control, this approach may provide some benefit, particularly in qualitative characterization. This method is particularly helpful in documenting the absence of particular chemical components. Knowledge of the identity and quantity of chemicals introduced into the process defines the chemicals that may be present in the waste. As with process knowledge, the materials accountability characterization data must be validated and verified through periodic independent assessments. The problems and attendant uncertainties in the waste inventory data have been investigated (Kenning and Yong 1993), and the findings have been included in Appendix A.

Quantitative waste characterization methods determine the quantity or concentration of the constituents and properties in a waste stream. This determination is usually made through some means of direct or indirect measurement, such as sampling and analytical methods, and requires a knowledge of the degree of uncertainty in the data.

Waste characterization data were recorded on two separate forms (Appendix A, Figs. A.1, A.2) until October 1993. These forms were replaced by the Oak Ridge Reservation Uniform Request for Disposal Package, Form UCN-2109, which contains the information gathered by the two previous forms that are described below. Form UCN-2822, "Request for Storage or Disposal of Radioactive Solid Waste or Special Materials" (Appendix A, Fig. A.1) is used to document the general characteristics of the waste and track the waste package from the point of generation to final disposal. A completed Form UCN-2822 must accompany each individual waste container. One section of the form is completed by the generator and documents the origin and provides a general description of the waste package (radionuclides present, quantities of those radionuclides, volume, weight, etc.), while a second section of the form is completed by a health physicist and provides radiological dose data for the waste package.

More specific waste characterization data were captured on the Form UCN-16114, "Log-In Data Sheet for Generators of LLW" (Appendix A, Fig. A.2). This form also accompanied each waste container of LLW. This form was filled out by the generator and reviewed by the Generator Certification Official (GCO) (Sect. 2.3.2.2) assigned to the generator area to determine that the characterization data provided is consistent with what would be considered representative of that waste stream. This form was used at the packet level (there may be several packets per waste package) to document such information as origin of the waste, radionuclides present, quantities of radionuclides present, chemical

form of the radionuclides, physical form of the waste, description of the waste matrix, and whether or not RCRA materials were also present. Completed copies of both forms are filed permanently in the Documentation Management Center of the Waste Management Operations Section.

2.3.2.2 Waste Certification

Waste certification is the process of verifying that the contents of an LLW package complies with the WAC for a specific waste TSD facility. Certification accounts for the quality assurance and quality control procedures in data collection and manipulation, documentation and tracking systems, authority and responsibility, and other areas related to ensuring that characterization data of sufficient detail and quality are collected. The ORNL LLW Certification Program applies to all operations that generate, ship, handle, treat, store, and dispose of LLW destined for ORNL TSD facilities.

In April 1986, LLW disposal operations in SWSA 6 at ORNL were halted by order of DOE Oak Ridge Operations (DOE-ORO). The order was issued because of concern that RCRA hazardous and mixed wastes were being disposed of in SWSA 6 in violation of the Resource Conservation and Recovery Act (RCRA). Insufficient administrative and process controls were in place to verify that RCRA materials were not being disposed of in SWSA 6. As a result of this action, ORNL initiated an LLW Certification Program to bring SWSA 6 back into active operation. The immediate goal of the program was to improve the segregation of RCRA materials from LLW and to better document the constituents of the waste. At that time the ORNL LLW Certification Program consisted of the following elements:

- establishment of an LLW training program that would focus on the requirements for packaging, proper documentation, acceptable characteristics, and excluded materials, with restrictions against untrained staff being allowed to package LLW;
- development of documentation to track the contents of individual waste packets being placed into the LLW container;
- reviews of generator LLW programs; and
- verification of CH LLW package contents by real-time radiography (RTR).

With the issuance of DOE Order 5820.2A, additional program elements needed addressing. One of the changes requiring that the ORNL LLW Certification Program be modified was the requirement to manage the disposal facility on the basis of the concentration of radionuclides in the waste rather than on the basis of the external radiation levels of the waste package. The management of LLW on a concentration basis is reflected in a need for a more definitive characterization of the waste (i.e., how much of which radionuclides are present). To incorporate this higher level of stringency required in the characterization of the waste, the scope of the ORNL LLW Certification Program is being expanded to include, in addition to the elements listed above, the following:

- establishment of a Waste Certification Group within the ORNL Waste Management and Remedial Action Division, but independent of the Waste Operations Section, with

the responsibility for the development, implementation, and oversight of the ORNL LLW Certification Program;

- development of WAC documents for the ORNL disposal facilities that mandate management of the LLW on a radionuclide concentration basis;
- establishment of a network of individuals (GCOs) within the generator organizations responsible for coordinating the implementation of the LLW program at the facility level;
- development of generator-level procedures that identify the individual LLW streams originating within the generator organization and the method(s) used by the generator for the characterization of the LLW; and
- more intensive monitoring of all LLW certification activities.

The ORNL LLW Certification Program is being phased in as described in the following paragraphs. The first steps have concentrated on developing and implementing the LLW Certification Program for wastes to be disposed of in the SWSA 6 IWMF. The *ORNL Certification Program Plan for Solid Low-Level Radioactive Waste* (Tull and Smith 1990) was issued in August 1990 and *Guidelines for Establishing Waste Certification Plans and Procedures at Waste Generator Facilities* (ORNL 1992) was issued in September 1992. The guidance document establishes specific criteria and acceptable methods for waste characterization consistent with the requirements of DOE Order 5820.2A.

The second step was to initiate a pilot certification program for IWMF wastes. A group of waste generators was selected to participate in the pilot program based on the highest waste volumes disposed of in the Tumulus I and II facilities and generation of radionuclides that have the greatest potential impact on the performance assessment source term for the IWMF. Pilot waste generators were interviewed to determine current practices in waste characterization and to assess the uncertainties associated with the certification process. The next phase of the pilot program was for the pilot waste generators to develop waste-stream-specific certification plans and procedures for waste characterization that would enable their waste to be certified against the IWMF WAC. The pilot program operated from January 1992 through January 1993.

The next phase of the ORNL LLW Certification Program is for the remainder of the ORNL waste generators to develop certification plans for characterizing their waste. These certification plans document the methods for determining radionuclides and curie content in specific waste streams. Approximately 90 waste certification plans will be developed by ORNL GCOs by January 1994. Following the development and approval of waste certification plans, ORNL Waste Management will implement concentration-based WAC. Concentration limits for each radionuclide with a half-life greater than 5 years are being developed based on the results of this performance assessment. The IWMF WAC will be revised to include concentration limits by April 1994. ORNL's LLW Certification Program will be fully compliant when the concentration-based WAC is fully implemented by September 1994.

Figure 2.13 schematically represents the LLW certification process at ORNL.

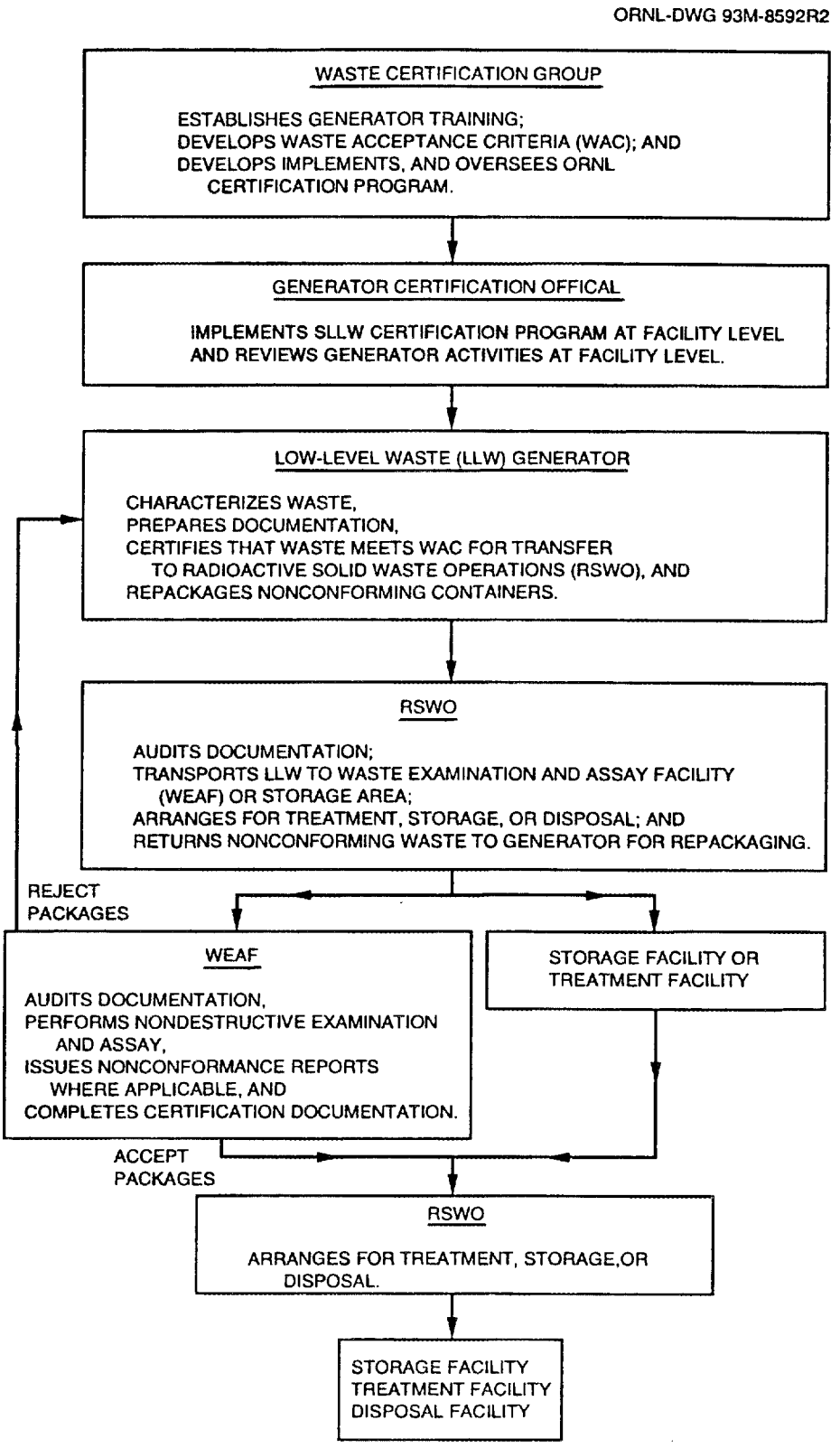

Fig. 2.13. Certification process for solid low-level waste at Oak Ridge National Laboratory.

2.3.3 Interim Waste Storage Facilities

In 1986, ORNL began interim storage of some CH LLW at the ORR K-25 Site because of limited disposal capacity remaining in SWSA 6. The K-25 Site uses surplus buildings for storage of CH LLW with a surface dose rate <50 mrem/h. The intention was to store this waste until a new disposal facility was developed at another site on the ORR. Storage of low-activity LLW at the K-25 Site was discontinued in 1991 because of limited existing storage space for RCRA waste. The K-25 Site is currently used to store only hazardous and mixed wastes generated on the ORR.

Due to the loss of the K-25 Site for storage of CH LLW, ORNL has constructed several above-grade storage facilities. The above-grade facilities currently used at ORNL include four portable Rubb structures (tents) in SWSA 5N. These facilities are used for interim storage of the low-activity waste streams such as contaminated soils, process wastewater sludge, biological waste, and VLA waste. ORNL plans to store these low-activity waste streams until new disposal facilities can be developed at other sites on the ORR or access is permitted at off-site DOE disposal facilities. Building 7842 in SWSA 6 is used as a temporary storage facility for CH LLW prior to disposal in the tumulus facility.

ORNL is also storing RH LLW that does not meet the WAC for ORNL disposal facilities. RH LLW is stored in above-grade and below-grade storage facilities. Above-grade concrete vault storage areas in SWSA 6 and near the former ORNL Hydrofracture Facility are used to store solidified supernatants from the LLW evaporator concentrate storage tanks. Below-grade storage wells in SWSA 5N and SWSA 6 are used to store irradiated fuel and fuel debris, irradiated hardware, sealed radiation sources, and other LLW that does not meet the WAC for SWSA 6 (ORNL 1993a). The cask storage area near the Hydrofracture Facility is also used to store irradiated hardware that is too large for the below-grade storage wells. These facilities have limited remaining storage capacity, so additional above-grade and below-grade storage facilities are planned at the ORNL SWSA 7 site. The plan is to store RH LLW at ORNL until suitable disposal facilities are available at off-site DOE disposal facilities.

2.3.4 Solid Waste Storage Area 6 Disposal Facilities

SWSA 6 is the only active LLW disposal area at ORNL. Until 1986 all LLW generated at ORNL, including low-level mixed waste, was disposed of by shallow land burial, generally in unlined trenches and auger holes. In 1984 the practice of shallow land disposal on the ORR came under closer scrutiny by federal and state regulators and DOE officials. As a result, major changes in the operation of SWSA 6 were initiated in 1986, including (1) the exclusion of all mixed waste from disposal in SWSA 6; (2) the use of greater confinement disposal (GCD) techniques for below-grade disposal such as concrete silos and pipe-lined auger holes; and (3) the storage of some low-activity LLW at the ORR K-25 Site and all mixed waste at ORNL. In addition to the GCD techniques for below-grade disposal, ORNL also developed plans in 1986 for demonstrating the above-grade tumulus disposal technology developed in France.

Because of the disposal practices prior to 1986, some areas in SWSA 6 were remediated under an RCRA interim status closure agreement with the Tennessee Department of Environment and Conservation (TDEC). The remediation activities were

coordinated with ongoing GCD waste operations. SWSA 6 will be remediated under CERCLA. A public meeting was held February 9, 1993 to discuss the proposed plan for remediation of SWSA 6. Comments from the public clearly indicated the preferred alternative of the Interim Proposed Plan was not supported, and new information indicates that CERCLA site priorities should be reordered. A "Response to Comments" from the public meeting and the overall strategy for investigation and remediation is currently being developed. The deferred action plan being developed will emphasize site monitoring and technology development and demonstration. Remediation under CERCLA will occur when risks from SWSA 6 warrant action. A Letter of Agreement between EPA, the state of Tennessee, and DOE is being developed that will outline the ultimate remedial action plan for SWSA 6 under CERCLA. The Letter of Agreement is expected to include a date for cessation of all waste disposal in SWSA 6. Prior to the public meeting, cessation of waste disposal except for IWMF operations was anticipated to be December 1993 with IWMF operations continuing until 1997. The performance assessment has been prepared using the schedule that was anticipated.

The disposal methods used for each type of waste disposed of in SWSA 6 since issuance of DOE Order 5820.2A on September 26, 1988, are presented in Table 2.14. Details on the design, waste handling, and waste disposal operations for each disposal unit are discussed in the text that follows. These descriptions of waste disposal operations do not address the cover system to be placed on the disposal units because of the uncertainties related to the CERCLA process. A scenario for the ultimate cover system is provided in Sect. 3.2.3 that may change significantly in the following years. Final remediation of SWSA 6 will be based on discussions at the national level concerning long-term land use, institutional control, and the benefit/cost ratio of remediation alternatives.

2.3.5 Below-Grade Disposal

Below-grade disposal methods that have been used in SWSA 6 include concrete silos, wells in concrete silos, pipe-lined auger hole wells, unlined trenches, and landfills. ORNL began phasing out some below-grade disposal operations in SWSA 6 in December 1992 at TDEC request because of concerns about shallow land disposal in the trenches and landfill and concerns that the below-grade wells would not meet the long-term performance objectives of DOE Order 5820.2A. Use of the wells in concrete silos and piped-lined auger hole wells for disposal was phased out in 1992, but they are still used for retrievable storage of very high range RH LLW. The landfill was also closed in 1992 for disposal of VLA waste. The unlined trenches were phased out for animal wastes in 1992 and for other biological wastes in early 1993. Only the concrete silos continue to be used for disposal of CH LLW and high-range RH LLW.

2.3.5.1 Low-Range and High-Range Silos

Concrete silos are used for disposal of low-range (CH LLW) and high-range (RH LLW <1 rem/h) waste. These concrete silos are located in separate areas of SWSA 6 but are identical in construction. Silos are constructed of two 14-gauge, 4.9-m (16-ft) long, corrugated steel pipes of 2.4- and 2.7-m (8- and 9-ft) diameters. A trench is dug

Table 2.14. Disposal methods for waste disposed in Solid Waste Storage Area 6

Waste type	Disposal unit
Contact-handled (CH) low-level waste (LLW) ($\leq$200 mrem/h)	Low-range silos, Tumulus vaults
Remotely handled (RH) LLW (>200 mrem/h and $\leq$1 rem/h)	High-range silos
RH LLW (>1 rem/h)	High-range wells and high-range wells in silos
Fissile waste	Fissile wells
Biological waste	Biological trenches
Asbestos waste	Asbestos silos
Very low activity waste	Landfill

approximately 12.2 m (40 ft) long by 4.6 m (15 ft) deep. The depth of the trench is always located and excavated with its lowest point a minimum of 0.6 m (2 ft) above the maximum water table elevation. Generally three or four silos are placed in the trench. The larger pipe is placed vertically in the trench with minimal space between the pipes and with the top of the pipe 15.2–30.5 cm (6–12 in.) above ground level. The smaller pipe is centered inside the larger pipe and extends approximately 15.2 cm (6 in.) above the top of the outer pipe.

A 6.1-m (20-ft) section of 7.6-cm (3-in.) diameter polyvinylchloride (PVC) pipe with slots cut in the bottom 0.6–0.9 m (2–3 ft) is used as a monitoring well in some of the silos. Another PVC pipe is placed outside the silos at the low point of the trench. The space around the silos is backfilled with dirt, leaving the tops of the outer pipes approximately 15.2 cm (6 in.) above finish grade. As the fill settles, more fill is added as required to provide surface water runoff away from the silo. A 0.3-m (1-ft) thick, steel-rod-reinforced concrete pad is poured in the bottom of each silo. The annular space between the two pipes is filled with concrete. Each silo is painted with a unique number [TL-XXX (trench/low-range) or TH-XXX (trench/high-range)] on the outside of the 2.4-m (8-ft) pipe that extends above the ground. A temporary cover is placed over the open silo when the silo is not being filled. A section view of a typical silo used for CH and RH LLW is shown in Fig. 2.14. Figures 2.15 and 2.16 show the locations of the low-range and high-range silos in proximity to other SWSA 6 disposal units, buildings, roads, ephemeral streams, and foliage. The shaded silos were evaluated for this performance assessment. The remaining silos were filled prior to September 26, 1988.

Generally, noncompactible bulky items, small boxes, 55-gal drums, or soil are disposed of in the low-range concrete silos. Waste packaged in 20-mil plastic bags containing doubled bagged waste or 1-, 2-, 5-, 10-, or 20-gal metal cans or 30- or 55-gal metal drums are disposed of in the high-range silos. The packaged (drums only) CH LLW

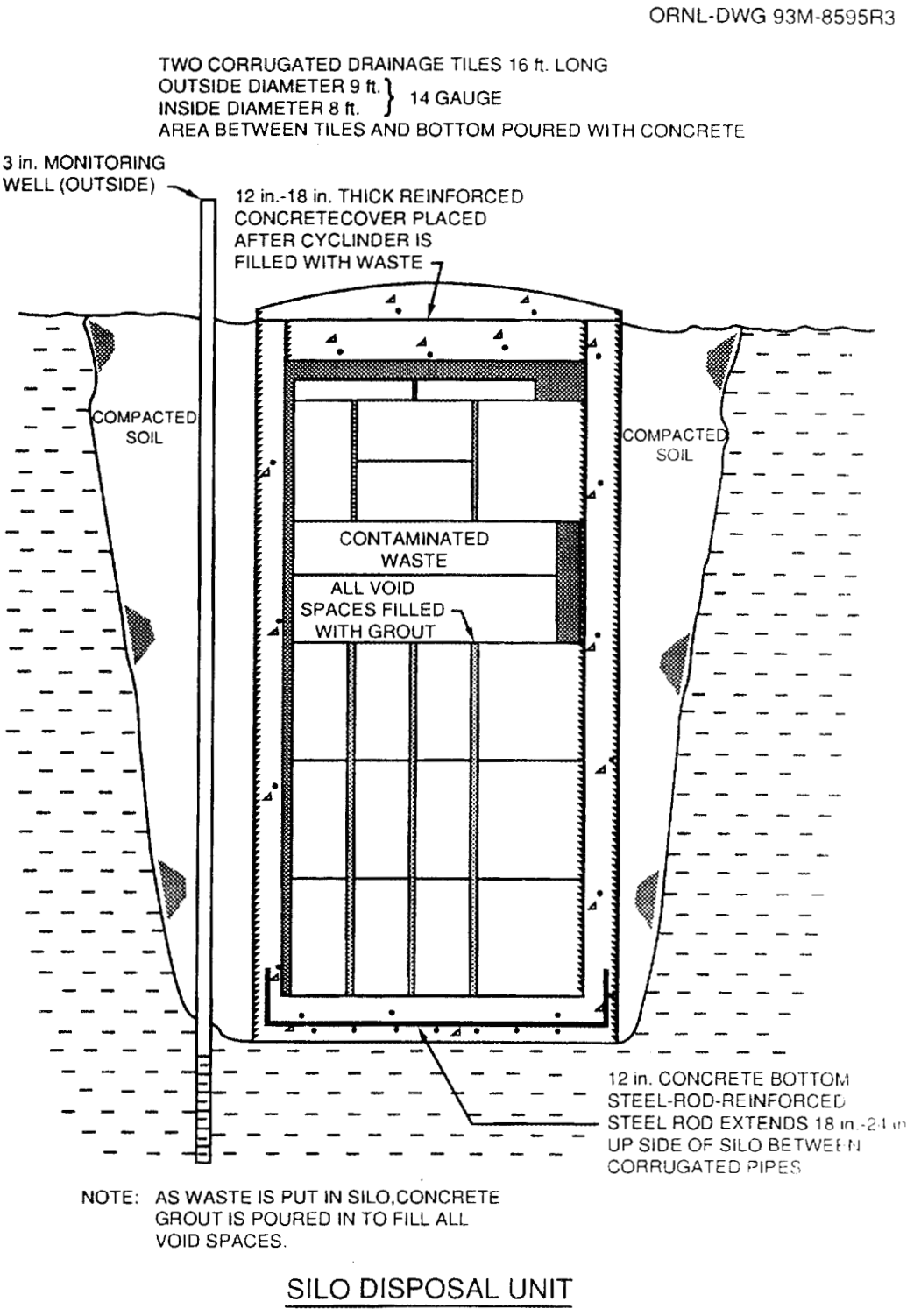

Fig. 2.14. Cross-section of a concrete silo.

ORNL-DWG 93M-11370R2

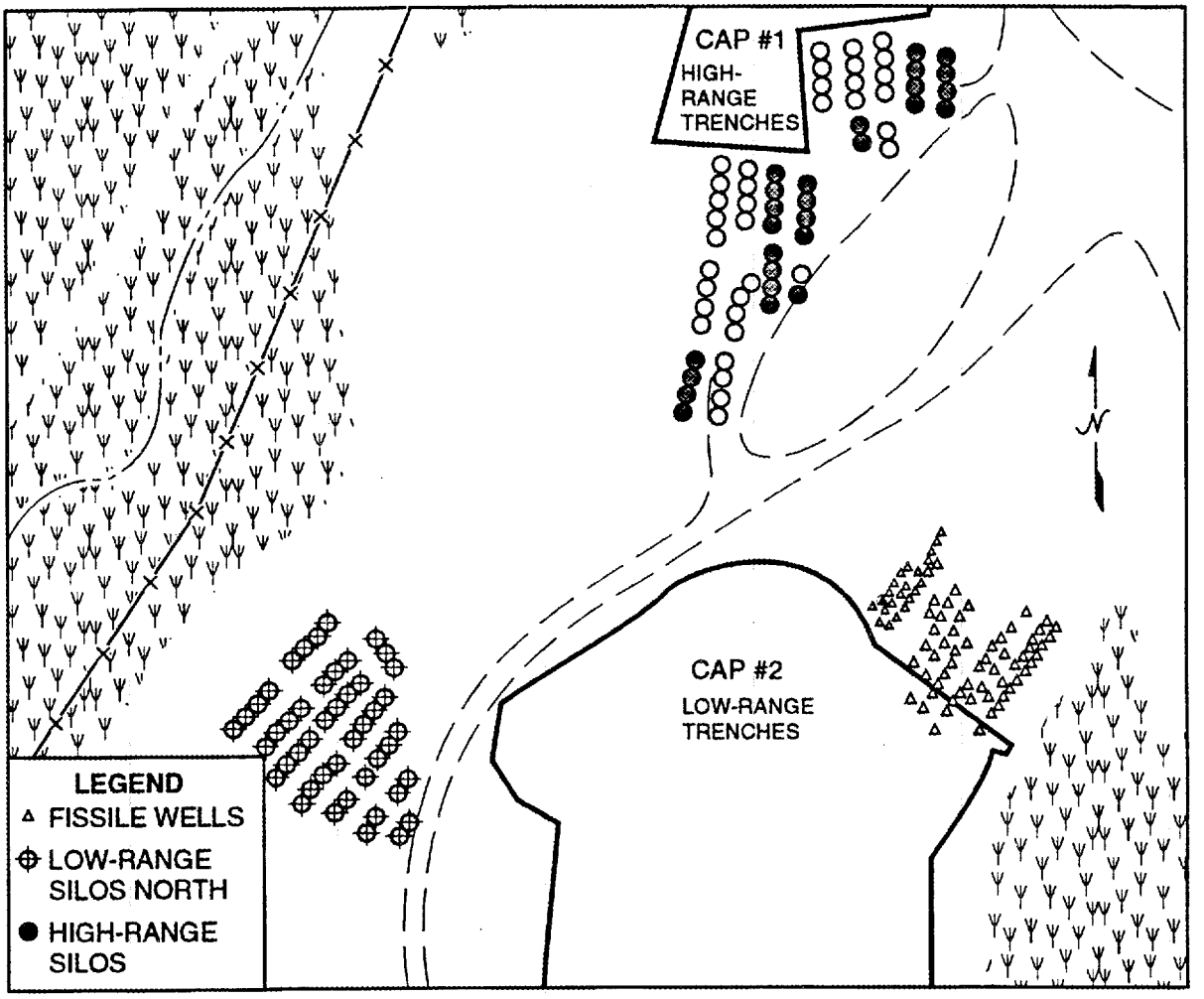

Fig. 2.15. Location of low-range silos, high-range silos, and fissile wells in Solid Waste Storage Area 6.

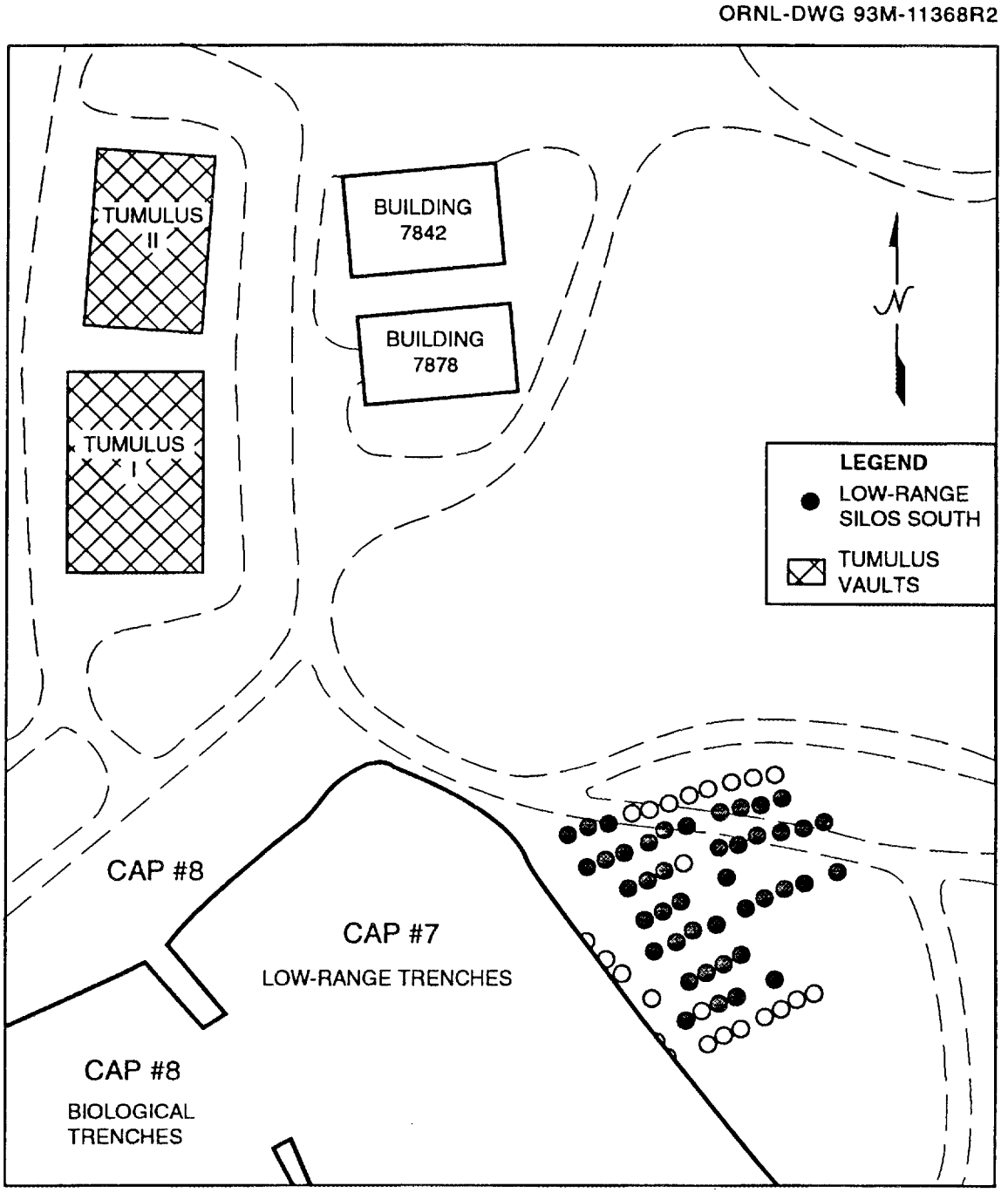

Fig. 2.16. Location of low-range silos and Tumulus in Solid Waste Storage Area 6.

is loaded on a transport vehicle and transported from the waste generator to the Waste Examination and Assay Facility (WEAF) for inspection by RTR. After successful inspection at the WEAF, the waste is transported to a temporary storage facility or a staging area at the disposal site. RH LLW is transported directly to the disposal site. A crane is used to remove the cover from the top of the silo and to lower the waste packages into the silo to prevent the packages from opening. Waste packages are placed as close to one another as practical to minimize the void space between containers. Waste is placed into the silo as long as the maximum radiation reading at the top of the silo does not exceed 200 mrem/h with the cap removed. If the dose rate is >200 mrem/h at the surface after waste is placed in an RH silo, the silo is roped off, and no additional waste is placed in the silo. The silo is then grouted until the dose rate at the surface is <200 mrem/h. After the silo is filled with waste, grout is poured between the waste packages to stabilize the waste. Waste placement and grouting is continued until the grout is within 0.3 m (1 ft) of the top of the silo. After the grout has hardened, the silo is covered with a minimum 0.3 m (1 ft) thick, steel-rod-reinforced concrete cap. Prior to the concrete cap hardening, a stenciled bolt with the silo identification number is placed in the soft concrete cap. After closure and capping of the silo, the radiation reading over the top of the silo is <2.5 mrem/h. The best estimates of the total activity to be disposed of in the low-range and high-range silos are presented in Tables 2.5 and 2.6.

The current management plan is to cease disposal of CH LLW and RH LLW in silos by January 1, 1994. Thereafter, the waste will be disposed of in the above-grade tumulus facility (IWMF) or stored on-site in above-grade concrete storage containers until new disposal facilities are constructed at other sites on the ORR or access to an off-site DOE disposal facility is available.

2.3.5.2 Asbestos Silos

Contaminated asbestos waste is disposed of in dedicated concrete silos. The asbestos concrete silos are located in separate areas of SWSA 6 but are identical in construction to the concrete silos described previously in Sect. 2.3.5.1. Figure 2.17 shows the location of the asbestos silos in proximity to other SWSA 6 disposal units, roads, ephemeral streams, and foliage. The legend indicates the silos evaluated in this performance assessment. The other silos were filled prior to September 26, 1988. Generally, asbestos waste is packaged in special, asbestos-labeled, 6-mil polyethylene bags, sealed with tape, and placed in a second asbestos-labeled polyethylene bag. Asbestos waste is transported from the generator's facility directly to the disposal site in dumpsters in a closed transport vehicle. Waste disposal and silo closure is to be implemented in the same manner as is described in Sect. 2.3.5.1. The best estimate of the total activity to be disposed of in the asbestos silos is presented in Table 2.7.

The current management plan is to cease disposal of asbestos waste in silos by January 1, 1994. Thereafter, the waste will be disposed of in the above-grade tumulus (IWMF) vaults or stored on-site in above-grade concrete storage containers until new disposal facilities are constructed at other sites on the ORR or access to an off-site DOE disposal facility is available.

ORNL-DWG 93M-11367R2

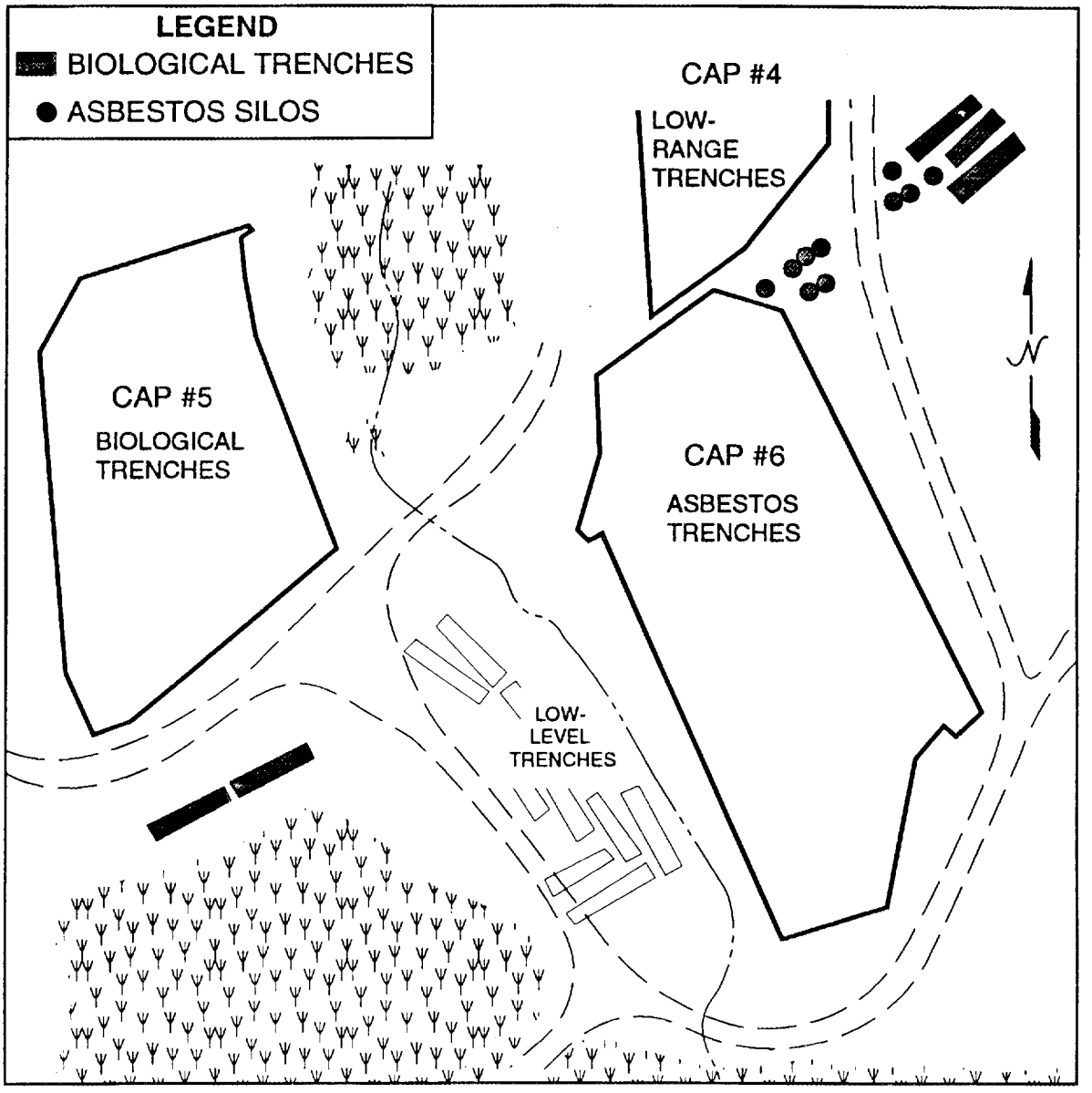

Fig. 2.17. Location of asbestos silos and biological trenches in Solid Waste Storage Area 6.

2.3.5.3 High-Range Wells in Silos

A modified version of the previously described concrete silo was used for the disposal of very high range waste (RH LLW >1 rem/h). A trench was dug approximately 12.2 m (40 ft) long by 4.6 m (15 ft) deep. The depth of the trench was always located and excavated with its lowest point a minimum of 0.6 m (2 ft) above the maximum water table elevation. Three or four concrete silos constructed of one 16-gauge, 4.9-m (16-ft) long, 2.7-m (9-ft) diameter, corrugated steel pipe were placed in each trench with minimal space between the silos and with the top of the silo 15.2 to 30.5 cm (6 to 12 in.) above ground level. The space around the silos was backfilled with dirt leaving the top of the silo approximately 15.2 cm (6 in.) above finish grade. As the fill settled, more fill was added as required to provide surface water runoff away from the silo. A 0.3-m (1-ft) thick, steel-rod-reinforced concrete pad was poured in the bottom of each silo. A 6.1-m (20-ft) section of 7.6-cm (3-in.) diameter PVC pipe with slots cut in the bottom 0.6–0.9 m (2–3 ft) was used as a monitoring well. The PVC pipe was placed inside each silo with the bottom resting on the concrete pad.

Seven wells were placed in a geometric array inside each silo. The wells were constructed of 2-cm (0.75-in.) thick steel pipes, 5-m (16-ft) long with an inside diameter of 51 cm (20 in.). The annular space between the outside surface of the pipes and the inside surface of the silo was filled with concrete to approximately 1.3 cm (0.5 in.) below the top of the pipes. A bolt stenciled with the well identification number was placed in the concrete at the top of each of the seven wells. Each well is identified by a unique number [WH-XXX (well/high-range)]. A temporary cover was placed over the open wells when they were not being filled. A typical section view of a concrete silo with high-range wells used for waste with an unshielded container dose rate >1 rem/h is shown in Fig. 2.18. Figure 2.19 shows the location of the high-range wells in silos in proximity to other SWSA 6 disposal units, roads, ephemeral streams, and foliage. The legend indicates the high-range wells in silos evaluated in this performance assessment. The remaining units were filled prior to September 26, 1988.

The waste disposed of in concrete silos with high-range wells was packaged in 1-, 2-, 5-, 10-, or 20-gal metal cans or 30-gal metal drums and transported to the disposal site in a lead-shielded, bottom-discharge carrier. Using a crane, the carrier was placed over the well, the bottom carrier drawer was opened, and the waste was lowered into the well. Prefabricated concrete plugs were placed in the well on top of the waste to reduce the radiation reading at the top of the well to <200 mrem/h. When a well in the silo was filled, the well was capped with a minimum 0.3-m (1-ft) steel-rod-reinforced concrete cap. Prior to the concrete cap hardening, a stenciled bolt with the well identification number was placed in the soft concrete cap. The radiation reading over the top of a closed well was <2.5 mrem/h. The total estimated activity disposed of in the high-range wells and high-range wells in silos is presented in Table 2.8.

Very high range wastes are no longer disposed of in high-range wells in concrete silos. This waste is managed as a special-case waste and is transported to ORNL retrievable storage wells in shielded waste carriers. The current waste management plan for very high range LLW is to store the waste on-site until access to an off-site DOE disposal facility is available.

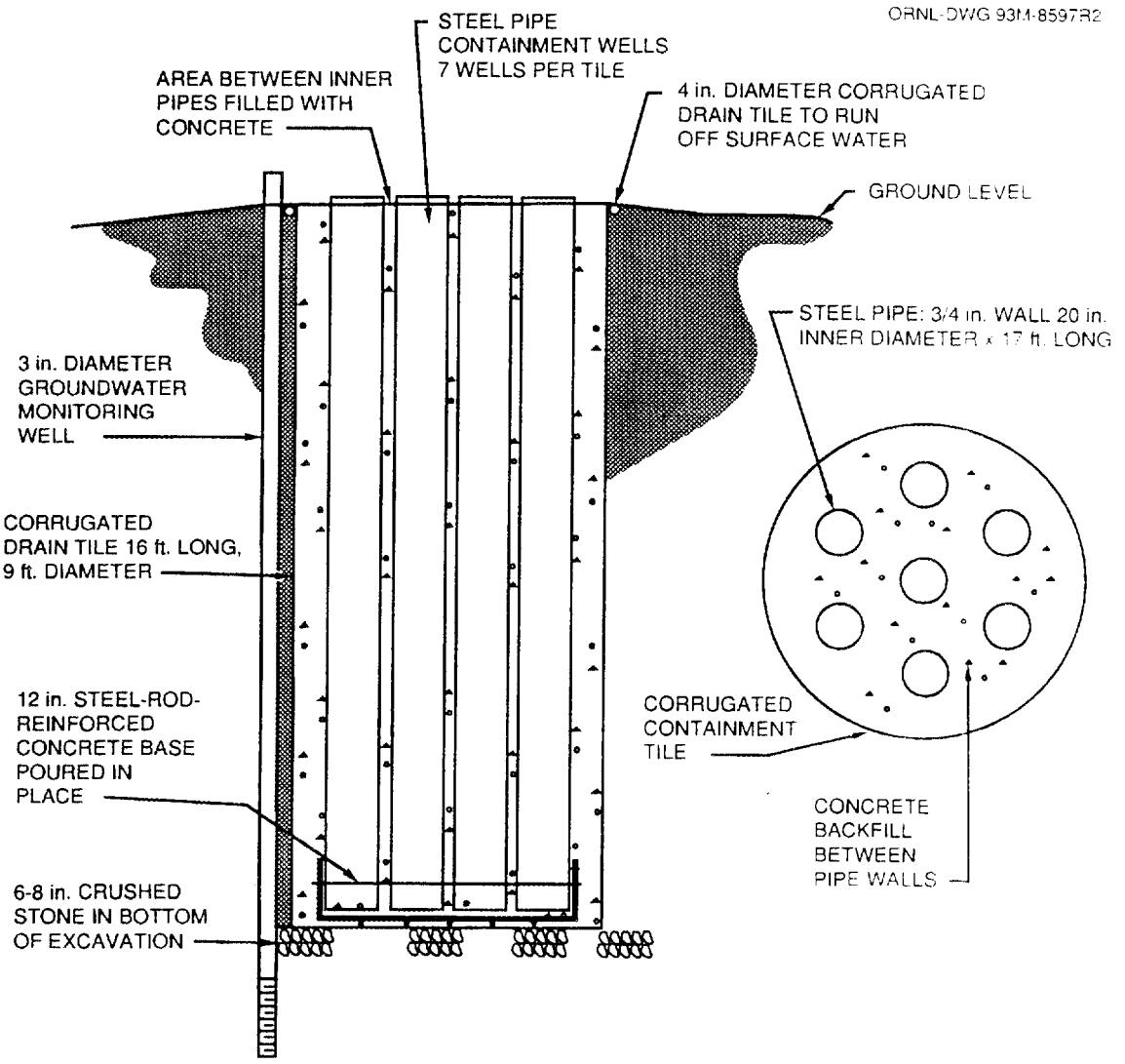

NOTE: WHEN FILLED WITH WASTE, THE INDIVIDUAL WELLS ARE CAPPED WITH A 12 in.-THICK STEEL-ROD-REINFORCED CONCRETE CAP

MULTIPLE WELL DISPOSAL UNIT

Fig. 2.18. Cross section of a concrete silo with high-range wells.

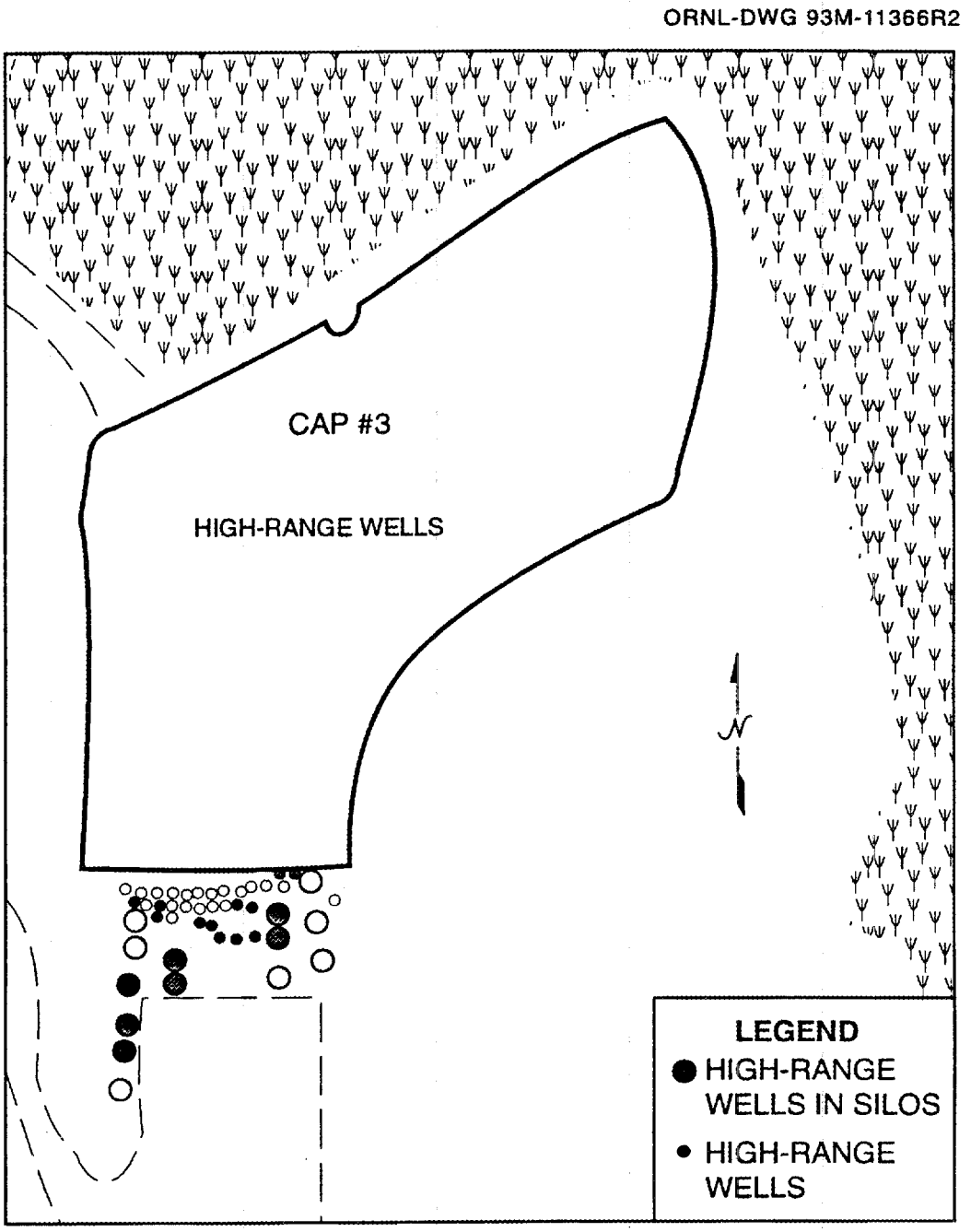

Fig. 2.19. Location of high-range wells in Solid Waste Storage Area 6.

2.3.5.4 High-Range Wells

Heavy-wall steel pipe wells were also used to dispose of very high range waste (RH LLW >1 rem/h). These wells were constructed of 2-cm (0.75-in.) thick steel pipe vertically centered in a drilled auger hole with the top of the well approximately 15.2 cm (6 in.) above ground level. The surrounding space was backfilled with dirt. The pipes were generally 5 m (16 ft) long with an inside diameter of 76.2 cm (30 in.). A 0.3-m (1-ft) thick concrete plug was poured in the bottom of the well.

A monitoring well, made from a 7.6-cm (3-in.) diameter PVC pipe with a bottom cap and slotted 0.3 m (1 ft) from the bottom, was placed outside the well to allow collection of liquids for sampling and quarterly monitoring of the hydrological isolation of the well. The top of each well is painted with a unique identification number [WH-XXX (well/high-range)]. A typical section view of a high-range well used for RH LLW with an unshielded container dose rate >1 rem/h is shown in Fig. 2.20. Figure 2.19 shows the location of the high-range wells in proximity to other SWSA 6 disposal units, roads, ephemeral streams, and foliage. The legend indicates which high-range wells are evaluated in this performance assessment. The remaining wells were filled prior to September 26, 1988.

Generally, only waste packaged in 55-gal metal drums was disposed of in high-range wells. The waste was transported to the burial site and disposed of in the same manner as the high-range wells in silos. After the well was filled, the well was capped with a minimum 0.3-m (1-ft) thick, steel-rod-reinforced concrete cap. Prior to the concrete cap hardening, a stenciled bolt with the well identification number was placed in the soft concrete cap. After well closure and capping, the radiation reading over the top of the well was <2.5 mrem/h. The estimated total activity in the high-range wells and high-range wells in silos is presented in Table 2.8.

Very high range wastes are no longer disposed of in high-range wells. This waste is managed as a special-case waste and is transported to ORNL retrievable storage wells in shielded waste carriers. The current waste management plan for very high range LLW is to store the waste on-site until access to an off-site DOE disposal facility is available.

2.3.5.5 Fissile Wells

Fissile waste was disposed of in dedicated fissile wells. The fissile wells were constructed in the same manner as the high-range wells described in Sect. 2.3.5.4. Fissile wells were spaced so that a minimum of 0.9 m (3 ft) of earth separates the sides of adjacent wells. Fissile wells are numbered WF-XXX (well/fissile). Fissile waste was packaged in 1-, 2-, 5-, 10-, or 20-gal cans or 30- or 55-gal drums, transported to the burial site in a shielded waste carrier, and disposed of in the same manner as waste in the high-range wells (Sect. 2.3.5.4). The well was capped in the same manner as the high-range wells. Figure 2.15 shows the location of the fissile wells in proximity to other SWSA 6 disposal units, roads, ephemeral streams, and foliage. The legend indicates the fissile well evaluated in this performance assessment. The remaining wells were filled prior to September 26, 1988. The best estimate of the total activity disposed of in the fissile wells is presented in Table 2.9.

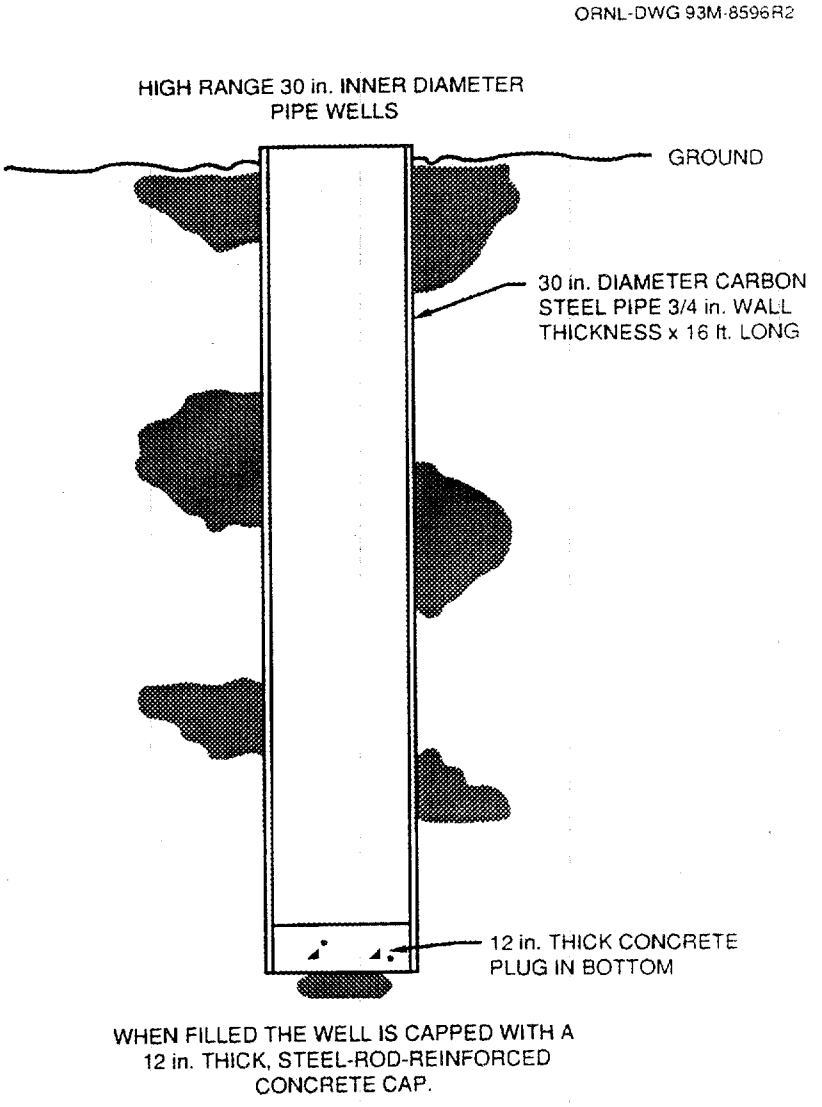

Fig. 2.20. Cross section of a high-range well.

Fissile waste is no longer disposed of in fissile wells. This waste is also managed as a special-case waste and is transported to ORNL retrievable storage wells in shielded waste carriers. The current waste management plan for fissile waste is to store the waste on-site until access to an off-site DOE disposal facility is available.

2.3.5.6 Biological Trenches

Biological waste was disposed of in trenches that were approximately 3–15 m (10–50 ft) long and 3 m (10 ft) wide. The depth of the trenches varied depending upon the water table elevation. The lowest point in the trench was at least 0.6 m (2 ft) above the known maximum water table elevation, and spacing between adjacent trenches is at least 1.5 m (5 ft). The trench was graded to slope to one end at a rate of approximately 4 cm/m (0.5 in./ft). Trenches were separately located from other waste disposal sites. Each trench is identified by a unique number [TB-XXX (trench/biological)]. Surface water drainage is controlled by separate ditching around the trench that conforms to existing topographic conditions. The ditching is compatible with the overall drainage network of the waste area regardless of whether the trench is on standby, in use, or closed.

The trenches were located and oriented for the most efficient and practical land usage. The trenches were sized and sectioned by removable steel plates to improve efficiency of land usage and prevent trench sidewall collapse. In the event that unforeseen fluctuations in the water table caused the excavation to fall below the water table, the trench was backfilled with Conasauga shale to a depth of at least 0.6 m (2 ft) above the maximum water table. After biological waste was placed in the trench, it was covered with at least 0.9 m (3 ft) of dirt. When the trench was filled, the surface of the closed trench was planted with grass, mowed, and kept free of trees.

Figure 2.17 shows the location of the biological trenches in proximity to other SWSA 6 disposal units, roads, ephemeral streams, and foliage. The legend indicates which biological trenches were evaluated for the performance assessment. The remaining trenches were filled prior to September 26, 1988. The best estimate of the total activity disposed of in the biological trenches is presented in Table 2.10.

Biological waste is no longer disposed of in the SWSA 6 biological trenches. The current waste management plan is to incinerate the waste at an off-site commercial treatment facility. The treated waste will be returned to ORNL for storage or disposal in the above-grade tumulus facility (IWMF).

2.3.5.7 Suspect Waste Landfill

Suspect waste was disposed of in an open landfill in the northeast area of SWSA 6 until December 1992. The landfill covered less than 0.4 ha (1 acre). After disposal the waste was covered with at least 0.3 m (1 ft) of soil. Suspect waste is no longer disposed of in the landfill. Waste previously classified as suspect waste is now classified as VLA waste or nonradioactively contaminated waste handled in other facilities.

VLA waste is segregated from clean material and other LLW and placed inside a 4 × 4 × 6-ft metal box. Large items that will not fit in a metal box are stored inside a large cargo container (sea/land). The packaged VLA waste is stored at an ORNL storage facility until transported off-site for treatment by incineration or supercompaction. The

treated waste is packaged in metal boxes and returned to ORNL for storage or disposal in the IWMF vaults or low-range silos.

2.3.6 Above-Grade Tumulus Disposal

Above-grade tumulus is the preferred method for disposal of CH LLW on the ORR. Tumuli I and II were used for the disposal of CH LLW from April 1988 through March 1992. The IWMF began operation in December 1991 and will provide disposal for CH LLW until the proposed Class L-II Disposal Facility (CIIDF) is constructed. The CIIDF is outside the scope of this performance assessment.

2.3.6.1 Low-Level Waste Disposal Development and Demonstration Program

In July 1987, Energy Systems issued the Low-Level Waste Disposal Development and Demonstration (LLWDDD) Program strategy for managing LLW on the ORR. The LLWDDD strategy established four classes of LLW based on the specific types and quantities of radionuclides in the waste. Class L-I was low activity waste suitable for disposal in an industrial type landfill. Class L-II was waste primarily containing radionuclides with half lives <30 years that required disposal in engineered facilities designed to isolate the waste from the environment for several hundred years. During this period, the short-lived radionuclides would decay to acceptable levels. Class L-II waste may also contain low concentrations of long-lived radionuclides. Class L-III was waste with half-lives >30 years that was to be disposed of in facilities that provide intruder protection and groundwater protection by treatment of wastes prior to disposal. Class L-IV was high activity waste not suitable for disposal on the ORR. In implementing the LLWDDD strategy, a site-specific pathways analysis was going to establish the specific waste concentration limits for the various waste disposal technologies. Although the formal LLWDDD Program was phased out in 1989, the new LLW disposal facilities that were to be designed, constructed, and operated as part of the LLWDDD program continue to be developed.

2.3.6.2 Tumulus I Disposal

Tumulus I was originally referred to as the Tumulus Disposal Demonstration Project (TDDP), which was developed and implemented as part of the LLWDDD Program. The purpose of the TDDP was to demonstrate the ability of an above-grade disposal facility to contain the release of LLW to the environment. Tumulus disposal involves packaging LLW in steel boxes, placing the steel boxes inside concrete vaults (Fig. 2.21), stacking the vaults on a curbed concrete pad, and capping with natural materials. Figure 2.16 shows the location of Tumulus I in proximity to other SWSA 6 disposal units, buildings, and roads.

ORNL-DWG 93M-8593R3

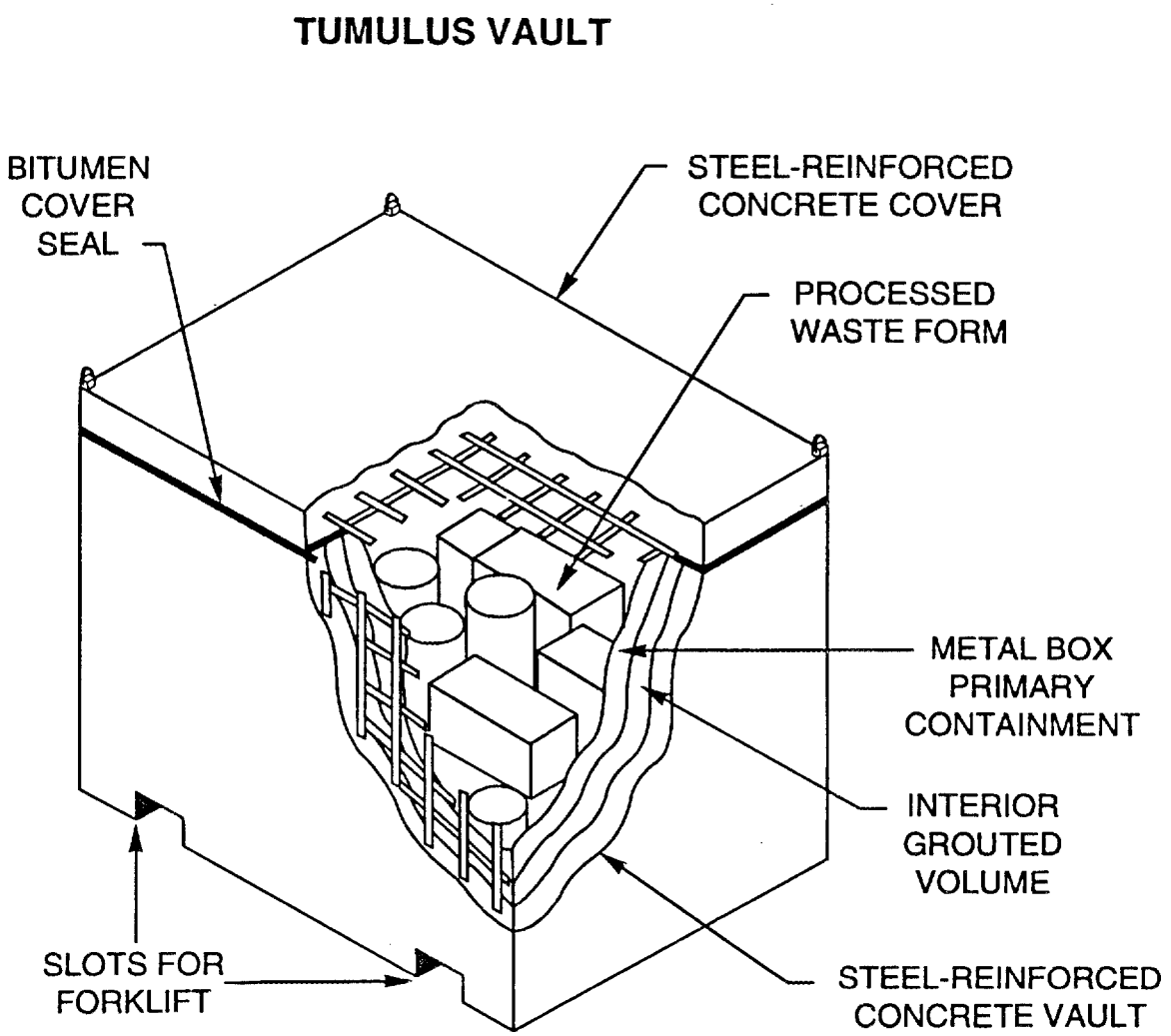

BASIC VAULT DIMENSIONS: 6 ft TALL x 8 ft LONG x 6 ft WIDE
INTERIOR WASTE VOLUME: 100 ft^3
MAXIMUM LOADED WEIGHT: 15 TONS

Fig. 2.21. Generic concrete cask for tumulus disposal operations.

The first tumulus pad (Tumulus I) was constructed in SWSA 6 during early 1987. Actual loading of concrete vaults onto the pad began in April 1988. The Tumulus I pad was filled to capacity in June 1990, and a tent was installed over the entire facility after Tumulus II was filled to capacity. A total of 290 vaults [approximately 788 m^3 (27,840 ft^3)] were placed on the Tumulus I pad.

The Tumulus I pad is located on an approximately 0.60-ha (1.5-acre) site in the south area of SWSA 6 (Fig. 2.16). The Tumulus I pad is approximately 19.8 × 32 m (65 × 105 ft). The pad was constructed using high-strength (6000 psi) concrete and reinforced using epoxy-coated rebar. The concrete pad varies in thickness from 20.3 cm (8 in.) at the center to 40.6 cm (16 in.) along the perimeter of the pad. The pad has a concrete curb 15.2 cm (6 in.) high along the entire perimeter. The concrete pad was designed to serve as the primary leachate collection system for any leachate generated during operations and after closure. Surface drainage channels were constructed north, east, and south of the pad to divert surface runoff away from the pad.

The concrete vaults that were loaded and doubled stacked on the concrete pad are designed to be used as structurally stable overpacks for containerized LLW. The concrete vaults are approximately 0.2 m (8 in.) thick and are 1.6 m (5.4 ft) high, 1.7 m (5.6 ft) wide, and 2.4 m (7.8 ft) long. An inner cavity is sized to receive a 1.2 × 1.2 × 1.8-m (4 × 4 × 6-ft) metal box with a 10.2-cm (4-in.) annular space. After the containerized SLLW is placed in the vault, the annular space is filled with concrete, and a 0.2-m (8-in.) thick precast concrete lid is placed on the vault and sealed with bitumen. The loaded and sealed concrete vaults are subsequently placed and stacked on the tumulus pad in rows abutting each other. The best estimate of the total activity disposed of in Tumulus I is presented in Table 2.11.

2.3.6.3 Tumulus II Disposal

The Tumulus II facility was operated after the Tumulus I pad was filled and preceded the operation of the IWMF. The Tumulus II pad began operation in October 1990 and was filled to capacity in March 1992 using vaults identical to those used for Tumulus I. A tent was installed over the entire facility. A total of 220 vaults [approximately 598 m^3 (21,120 ft^3)] were placed on the Tumulus II pad. The best estimate of the total activity disposed of in Tumulus II is presented in Table 2.12.

The Tumulus II pad is located on an approximately 0.40-ha (1-acre) site just north of the Tumulus I pad (Fig. 2.16). The tumulus pad is approximately 18.2 × 27.4 m (60 × 90 ft) and 30.5 cm (12 in.) thick. The pad was constructed of high-density concrete and reinforced with epoxy-coated steel. The pad has concrete curbs 0.30 m (1 ft) high on the south, east, and west sides. The north side does not have a curb and was used for vehicle access during vault loading operations. The loading area was adjacent to the north side of the pad and was constructed of crushed stone. Surface drainage channels are constructed north and east of the pad. These channels are connected to the existing surface drainage channels for Tumulus I.

One of the principal features of tumulus disposal is the inherent capability for monitoring ground and surface water for contamination. The sealed concrete pad is the primary barrier from the groundwater. The pad is sloped 1% to one side where a curb and gutter collects all surface pad runoff and drains the water to a monitoring station. A liner

below the pad provides a secondary barrier from the groundwater and collects any water that may have penetrated the pad. Any water collected in the secondary barrier is also diverted to the monitoring station. The monitoring station is equipped for receiving, monitoring, and collecting samples from flows received from both the surface pad drain and underpad liner drain systems.

2.3.7 Interim Waste Management Facility

The IWMF is the only active above-grade tumulus disposal facility in SWSA 6. The IWMF occupies an area of approximately 3.8 ha (9.5 acres) in the southwest portion of SWSA 6 (Fig. 2.23). Each tumulus pad will be approximately 18.2 × 27.4 m (60 × 90 ft) and 30.5 cm (12 in.) thick. The pads are constructed using high-density concrete and reinforced with epoxy-coated steel. The pad has concrete curbs 0.30 m (1 ft) high on the north, south, and west sides. The east side does not have a curb and is used for vehicle access during vault loading operations. Each pad provides disposal for approximately 330 vaults [approximately 897 m^3 (31,680 ft^3)] stacked three high. IWMF uses vaults identical to those used for Tumulus I and Tumulus II.

The IWMF has been designed to divert water into three sumps. The sumps are located in a monitoring station adjacent to the tumulus pads. The monitoring station is equipped for receiving, monitoring, and collecting samples from flows received from the storm water, underpad, and infiltration drain systems. The underpad sump is designed to allow monitoring of any groundwater that may accumulate under the pads. The storm-water sump collects water from the pad that is in operation. The infiltration sump is used to collect water from the pads that have been filled with vaults. An illustration showing vaults stacked on the curbed concrete pad, drain lines, and the proposed tumulus cap is shown in Fig. 2.22.

The original facility was designed for six tumulus pads. The disposal capacity of the first six IWMF pads is anticipated to be filled by December 1997. Figure 2.23 shows the IWMF in proximity to the monitoring station, roads, ephemeral streams, and foliage.

Construction of the first two IWMF pads was completed in 1992. The first IWMF pad was operated from December 21, 1991 to March 31, 1993. The second IWMF pad began operation on April 7, 1993. Construction of the remaining pads will continue over the period of operation. The first phase of construction included two tumulus pads, a loading area, surface drainage channels, the underpad drain system, the monitoring/transfer station, and the required utilities. When the disposal capacity of the first pad was depleted, planning of the third pad was initiated. This process will continue until six pads have been constructed.

Generally, compactible and noncompactible CH LLW packaged in metal boxes or drums is disposed of on the tumulus pads. The packaged waste is loaded on a transfer vehicle and transported from the waste generator or compactor to a staging area at the disposal site. A crane is used to remove the lid from the concrete vault and place the packaged waste into the vault. The vault is filled with grout and the lid is sealed with bitumen. A unique LLW number (LL-XXXX) is stenciled on all four sides of the vault. A crane is used to load the vault onto a transfer vehicle to transport the waste to the pad. The vault is placed on the pad so that the side having the highest surface dose rate is

ORNL-DWG 93M-8591

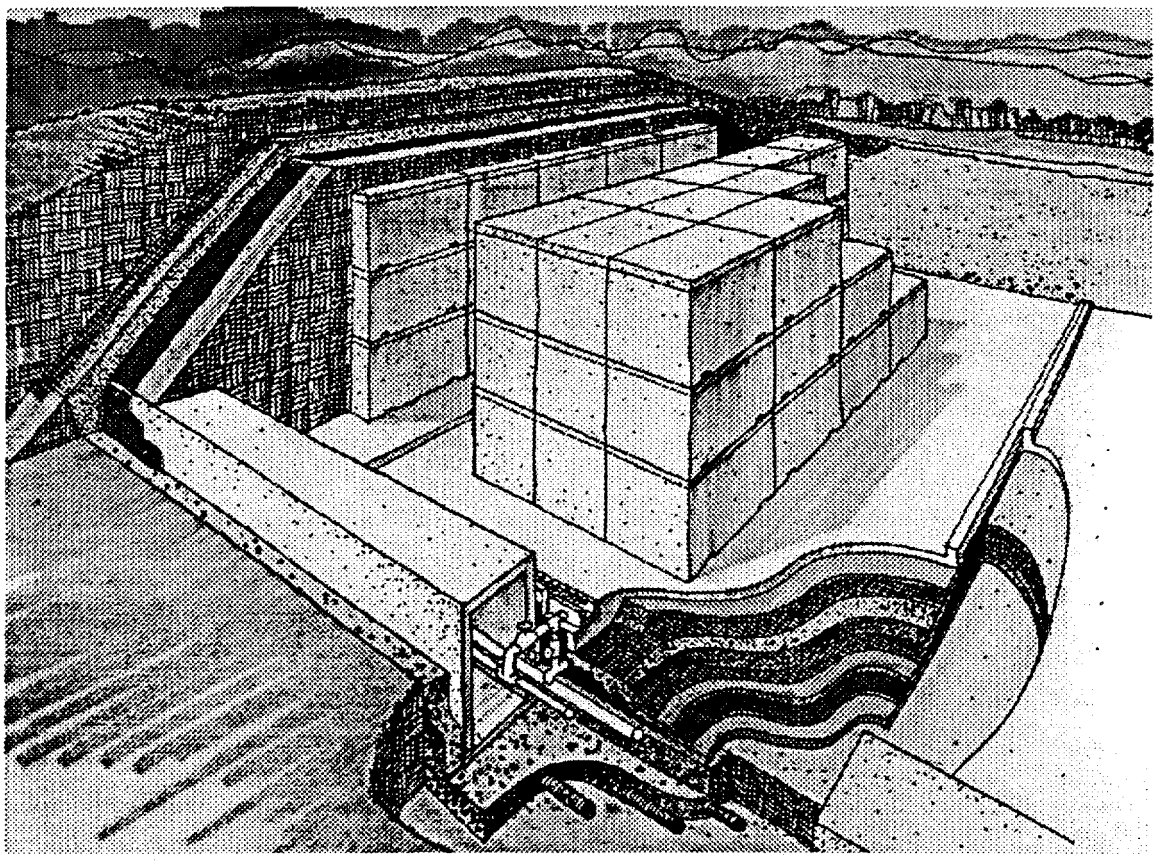

Fig. 2.22. Interim Waste Management Facility showing vaults of low-level waste, drain lines, and final cover.

ORNL-DWG 93M-11369R2

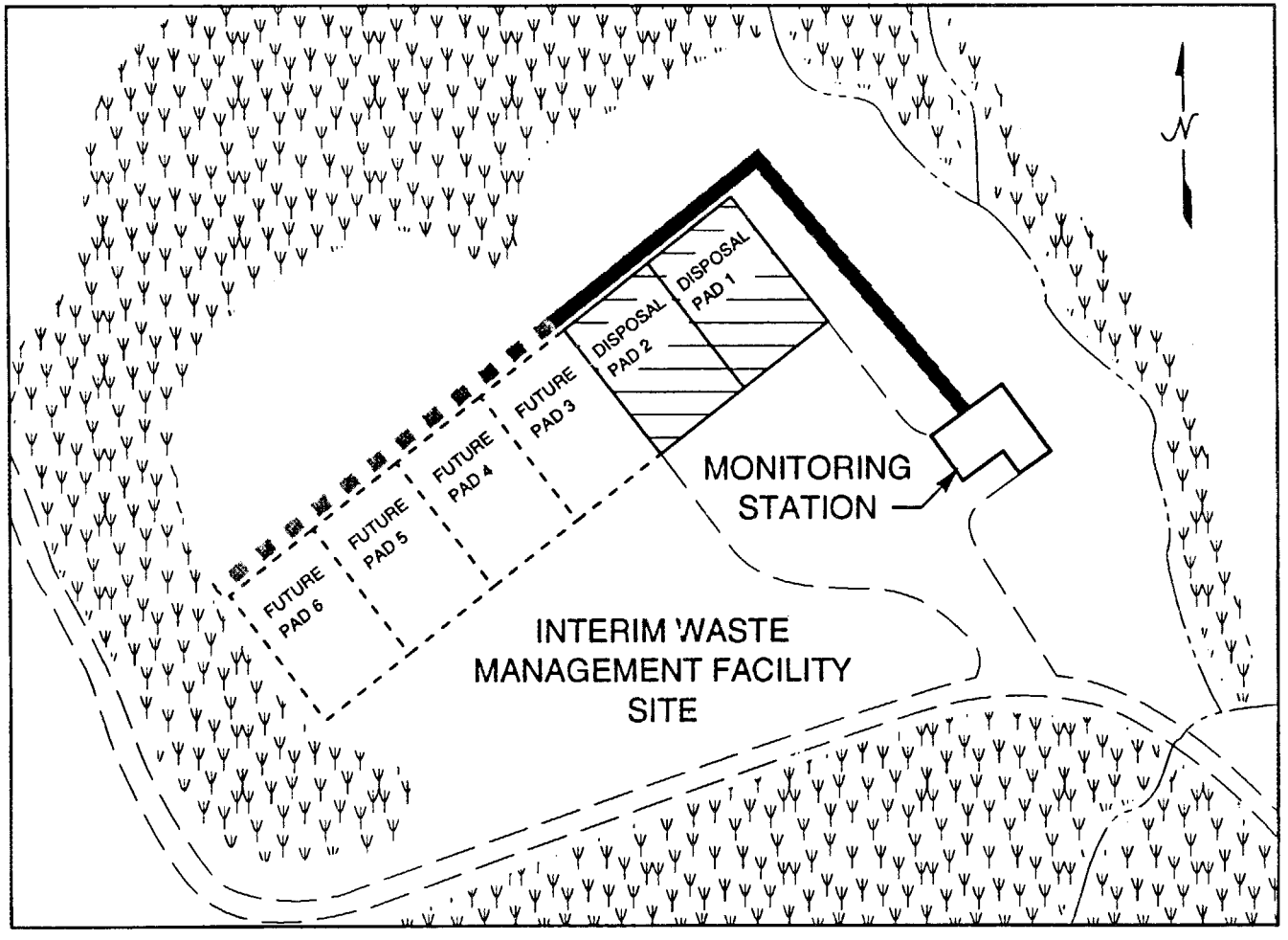

Fig. 2.23. The Interim Waste Management Facility site in Solid Waste Storage Area 6.

facing inward. Vaults are placed and stacked on the pad in rows abutting each other with minimal space between each vault. The maximum surface dose rate of a vault is not to exceed 200 mrem/h. The best estimate of the total activity to be disposed of in the IWMF is presented in Table 2.13.

The current waste management plan is to continue disposal of CH LLW that meets the IWMF WAC. Revised WAC incorporating concentration limits for radionuclides will be implemented by April 1994 to bring the operation of the IWMF into compliance with the performance objectives.

3. ANALYSIS OF PERFORMANCE

This section describes the methods used to analyze the performance of Solid Waste Storage Area (SWSA) 6 and provides an overview of the data used in the analysis. As discussed in Sect. 2.2, the wastes disposed of in SWSA 6 include a broad range of radionuclides (see Appendix A). The transport of radionuclides in the environment was analyzed using a series of site-specific computer models. In order for the analysis of the transport of contamination to be focused but comprehensive, a screening technique was applied. The screening technique used the performance objective of 4 mrem/year effective dose equivalent (EDE) for the protection of groundwater resources and converted the dose objective to concentrations in water for radionuclides with half-lives greater than 5 years for an individual consuming 2 L (0.5 gal) of contaminated water per day. The calculations were performed using the dose equivalents presented in Sect. 4.5.1 (Tables 4.9–4.15). Radionuclides with half-lives less than 5 years were eliminated from consideration because the performance of engineered barriers in conjunction with radionuclide travel times in the environment ensures these radionuclides will decay to innocuous levels before transport to a compliance point. The concentration limits used for screening are presented in Table 3.1. In the screening analysis, when the calculated concentrations using the SOURCE1 and SOURCE2 codes (Sect. 3.1) were less than the concentrations in Table 3.1 (which corresponds to the 4 mrem/year EDE), the radionuclide was eliminated from further consideration because dilution of any release in the 100-m (328-ft) buffer zone around the disposal unit would ensure that potential doses would be substantially less than the performance objective. (The input data for the SOURCE1 and SOURCE2 screening calculations are presented in Appendix C, Tables C.1–C.10.) In the analysis described in Sects. 3.2–3.4, when calculated concentrations of individual radionuclides were less than 10% of the concentration limit defined by the 4 mrem/year dose objective, the radionuclide was dropped from further consideration in the analysis of the environmental transport of contamination. This additional factor of safety for screening radionuclides in the calculations of environmental transport was applied to ensure that only significant radionuclides were considered in detail in the analysis.

Seventy radionuclides are included in the reported inventory of wastes presented in Appendix A, Tables A.3–A.11. The screening method reduced the list to 17 radionuclides. The screening method has an embedded assumption that sufficient reductions in concentration will occur during environmental transport to justify eliminating a radionuclide from further consideration. For the radionuclides considered in detail and with the results presented in Sect. 4, the validity of the assumptions used for screening can be examined. For the tumulus disposal units, concentration reductions ranged from 2.2×10^4 for ^{238}U to 1.2×10^{24} for ^{137}Cs. For the Interim Waste Management Facility (IWMF), concentration reductions ranged from 4.4×10^2 for ^{99}Tc to 3.7×10^{22} for ^{137}Cs.

Table 3.1. Concentration limits in water for radionuclide screening

Nuclide	Limit[a]	Nuclide	Limit[a]
^{3}H	8.7×10^{-2}	^{232}Th	2.0×10^{-6}
^{10}Be	1.3×10^{-3}	^{232}U	4.2×10^{-6}
^{14}C	2.7×10^{-3}	^{233}U	2.0×10^{-5}
^{26}Al	4.2×10^{-4}	^{234}U	2.1×10^{-5}
^{36}Cl	1.8×10^{-3}	^{235}U	2.2×10^{-5}
^{40}K	2.9×10^{-4}	^{236}U	2.2×10^{-5}
^{60}Co	2.1×10^{-4}	^{238}U	2.4×10^{-5}
^{63}Ni	1.0×10^{-2}	^{237}Np	1.4×10^{-6}
^{90}Sr	4.0×10^{-5}	^{238}Pu	1.4×10^{-6}
^{99}Tc	4.2×10^{-3}	^{239}Pu	1.3×10^{-6}
^{113m}Cd	3.6×10^{-4}		
^{137}Cs	1.1×10^{-4}	^{240}Pu	1.3×10^{-6}
^{152}Eu	9.1×10^{-4}	^{242}Pu	1.3×10^{-6}
^{154}Eu	6.1×10^{-4}	^{241}Am	1.2×10^{-6}
^{155}Eu	4.2×10^{-3}	^{243}Am	1.2×10^{-6}
^{210}Pb	1.1×10^{-6}	^{243}Cm	1.9×10^{-6}
^{226}Ra	5.0×10^{-6}	^{244}Cm	2.4×10^{-6}
^{229}Th	1.5×10^{-6}	^{249}Cf	1.2×10^{-6}
^{230}Th	1.0×10^{-5}		

[a]Concentration limits in water for each radionuclide are given in units of μCi/L, and are based on an effective dose equivalent of 4 mrem/year (see Appendix G).

For the remaining disposal units, the smallest concentration reduction was 3.0×10^{2} for ^{3}H at the biological trenches. The results of the detailed analysis support the assumptions used in the screening method.

This screening technique is considered justified in that the primary pathway for the transport of contamination from wastes to human exposure at SWSA 6 is by the hydrologic pathways (see Sect. 3.2). For the purposes of the analysis of inadvertent intrusion, this screening technique was not applied and all radionuclides with half-lives greater than 5 years were considered. The application of the screening technique reduced

the number of radionuclides considered in detail to a meaningful and comprehensive list that is presented in the results of the analysis (Sect. 4).

3.1 SOURCE TERMS

The release of radionuclides with time from the SWSA 6 disposal units was calculated to provide source terms for the hydrogeological modeling using the SOURCE1 and SOURCE2 codes (Appendix B). The amounts of several key radionuclides expected to permeate (by advection and diffusion) the waste and concrete as a function of time were determined to evaluate units described in Sects. 2.3.5 and 2.3.6. The initial average concentration in each disposal unit was calculated using the data in Tables A.13–A.21 in Appendix A. The results are presented in Tables C.13–C.22 in Appendix C. The SOURCE1 and SOURCE2 codes use these average values as input for each unit listed in Table A.2 of Appendix A. The application of these averages is reasonable for routine operations but may be misleading for nonroutine operations or one-time operations. The performance assessment modeling is based on release of contamination as a function of time from the following disposal units at SWSA 6: Tumulus I, Tumulus II, IWMF, asbestos silos, biological trenches, high-range silos, low-range silos, fissile wells, and high-range wells.

3.1.1 Mass Transport Models and Parameters

The key radionuclides contained in their respective disposal units at SWSA 6 were assessed using the SOURCE1 and SOURCE2 computer codes (Appendix B). These computer programs were developed to analyze the release of contamination from a waste disposal unit in which advective (pressure-driven) and diffusive (concentration-driven) transport plus the degradation of engineered barriers (as they affect flow) were taken into account. The calculated total release resulting from advection and diffusion is compared with the solubility limit of the nuclide in water. If this limit is exceeded by the calculated release, the release is reduced to the solubility limit. Each radioisotope is modeled independently without consideration of the effects of other isotopes of the same nuclide. For nuclides with several radioisotopes, this results in an overestimate of radionuclide transport, as reflected in the results of Sect. 4. Continued work towards addressing this conservatism is discussed in Sect. 4.9, and the effect of this conservatism on the interpretation of the results is presented in Sect. 4.7.1.

The modeling methodology used in simulating the long-term performance of disposal units at SWSA 6 has been incorporated into two separate computer codes. The SOURCE1 code models the performance of the tumulus disposal technology employed in the Tumulus I and II facilities and IWMF. The SOURCE2 computer code models the performance of the asbestos, high-range, and low-range silos; fissile wells; biological trenches; and high-range wells. The SOURCE1 and SOURCE2 computer codes were developed to provide a mechanism for modeling radionuclide release rates from the disposal units employed at SWSA 6.

The disposal units incorporate a variety of engineered barriers in an attempt to better isolate the waste from the environment. Consequently, projecting patterns and rates

of radionuclide release requires an understanding of the manner in which these engineered barriers perform over extended periods of time. Radionuclide release rates from the tumulus, silo, and well disposal units are largely a function of the integrity of the engineered barriers used in the construction of each. When intact, these barriers minimize contact of water with the waste, thereby minimizing releases of radionuclides from the disposal unit. Over time, as the barriers deteriorate and fail, water can more readily contact the waste, thereby accelerating releases to the environment. Changes in the material properties of the barriers due to chemical and physical attack are modeled (e.g., sulfate attack, loss of calcium hydroxide, and corrosion of steel). The projected material properties are considered in structural and cracking analyses of the disposal units, performed to assess the ability of the disposal units to bear the loads placed upon them. As the ability to bear design loads is compromised, the structures fail, and rates of percolation of water through the waste are increased. Rates of water percolation through the waste are used to calculate release rates due to advection. Releases due to diffusion are also calculated by the SOURCE1 and SOURCE2 computer codes. Releases from the disposal units are partitioned into the quantity of contamination that migrates with the lateral flow component of unsaturated flow at the site and the quantity that is transported to, and discharged into, the site aquifer.

In this analysis, the waste and concrete are considered to be unconsolidated and consolidated porous media, respectively. The transport of various radionuclides through such media can usually be analyzed and explained in terms of advection and diffusion.

The release of radionuclides due to advection (see Sect. B.1, Appendix B) is modeled as a zero-order leaching process accounting for both sorption and decay. Advective leaching is proportional to the amount of water contacting the waste and concrete and the degree to which the radionuclides are retained by the waste and concrete matrices. For this model, the radionuclide inventory is assumed to be homogeneously mixed within a finite waste volume that is contacted by water, and the water infiltration rates vary on a monthly basis. Infiltration values were obtained from Unified Transport Model (UTM) calculations described in Sect. 3.4. The inventory is assumed constant during a given time period and is updated at the end of the time period to reflect leaching and decay losses (Shuman, Chau, and Jennrich 1992). If these assumptions are applied, the advective release rate can be quantified as:

$$\lambda_a = \left[\frac{Q_a}{h_w(H_w + K_d \rho_w)} \sum_{i=1}^{12} I_i \right] \exp\left[-\left(\ln 2/t_{1/2}\right) t_a \right] , \tag{3.1}$$

where

λ_a = radionuclide release rate due to advection in year a (g/year),

Q_a = radionuclide inventory available for leaching at the beginning of year a (g),

I_i = water percolation rate through the waste during month i (cm/month),

h_w = waste thickness (cm),

H_w = relative saturation of waste (H_2O volume/waste volume),
K_d = radionuclide distribution coefficient (mL/g),
ρ_w = density of waste (g/cm^3),
$t_{1/2}$ = half-life of radionuclide (years), and
t_a = duration of leaching interval (1 year).

The release of radionuclides due to diffusion (and decay) is modeled as a two-slab system. The inner slab, representing the grouted waste, is initially contaminated; the outer slab, representing the concrete components of the vaults, silos, and wells, is initially uncontaminated (see Sect. B.2, Appendix B). The inner slab of half-thickness (a) contains an initial contaminant concentration of C_0 and decay constant λ. The outer slab of thickness $b - a$ is initially uncontaminated. The concentrations in the inner slab and outer slab are C_1 and C_2, respectively. The diffusion equations for the contaminant are

$$D_1 \frac{\partial^2 C_1}{\partial x^2} - \lambda C_1 = \frac{\partial C_1}{\partial t} \tag{3.2}$$

and

$$D_2 \frac{\partial^2 C_2}{\partial x^2} - \lambda C_2 = \frac{\partial C_2}{\partial t} \quad , \tag{3.3}$$

with initial conditions

$$C_1 (x, 0) = C_0, \quad 0 \le x < a \tag{3.4}$$

and

$$C_2 (x, 0) = 0, \quad a \le x < b \tag{3.5}$$

and boundary conditions

$$C_2 (b, t) = 0 \quad , \tag{3.6}$$

$$\left(\frac{\partial C_1}{\partial x}\right)_{x=0} = 0 \quad , \tag{3.7}$$

$$C_1\ (a,\ t) = C_2\ (a,\ t) \quad , \tag{3.8}$$

and

$$D_1 \left(\frac{\partial C_1}{\partial x}\right)_{x=a} = D_2 \left(\frac{\partial C_2}{\partial x}\right)_{x=a} \quad . \tag{3.9}$$

The methodology for solving Eqs. (3.2)-(3.8) is detailed in Appendix B, Sect. B.2.

The biological trenches were modeled with the SOURCE2 code by replacing the hydraulic properties of concrete with the hydraulic properties for soil. The steel included in the SOURCE2 code was neglected. The results from the use of SOURCE2 for the biological trenches are comparable to those used in the draft performance assessment for SWSA 6.

The chemical properties, nuclear properties, and transport properties of the radionuclides considered in the assessment of the SWSA 6 disposal units are presented in Appendix C. This information was used to construct a worksheet for each radionuclide considered in each disposal unit. An example of such a worksheet for the high-range silo is presented in Table 3.2. Examples of the worksheets generated for the tumulus, silo, well, and biological-trench disposal concepts are presented in Appendix F. The input requirements for the computer programs include retarded diffusion coefficients representing diffusion through the waste (D_w) and diffusion through the concrete (D_c). The theoretical formulation of the methodology for evaluating diffusion properties is presented in Appendix C.

The SOURCE1 and SOURCE2 program standard outputs give the decayed amount of each nuclide leached in yearly intervals for 1000 years (other time spans and intervals are possible).

3.1.2 Radionuclide Screening Calculations

A preliminary analysis for screening radionuclides released from disposal units was made using the SOURCE1 and SOURCE2 codes (Appendix B). If the maximum concentration of a radionuclide (Tables A.3-A.11, Appendix A) or the concentrations resulting from the SOURCE1 and SOURCE2 calculations were less than 10% of the limit in Table 3.1, the radionuclide was eliminated from further consideration. (Tables A.3-A.11 exclude isotopes with half-lives less than 5 years.) Those radionuclides with concentrations

Table 3.2. Input data summary for a high-range silo at Solid Waste Storage Area 6[a]

Groundwater properties

Groundwater entering trench (cm/month)

January:	9.58×10^{0}	February:	8.56×10^{0}	March:	8.30×10^{0}
April:	5.77×10^{0}	May:	7.43×10^{0}	June:	6.70×10^{-1}
July:	2.00×10^{-1}	August:	2.50×10^{-1}	September:	1.60×10^{-1}
October:	1.00×10^{-1}	November:	7.00×10^{-2}	December:	6.86×10^{0}

Waste trench area	1.00×10^{1} m^2
Total dissolved solids	3.49×10^{2} mg/L
Groundwater temperature	1.50×10^{1} °C
Groundwater pH	6.75×10^{0}
Saturated hydraulic conductivity	
Recharge	5.80×10^{-7} cm/s
Soil backfill	3.50×10^{-3} cm/s
Concrete	1.00×10^{-10} cm/s
Groundwater constituent concentrations	
Ca^{2+}	2.10×10^{-3} mol/L
Cl^{-}	2.04×10^{-4} mol/L
CO_3^{2-}	1.00×10^{-3} mol/L
Mg^{2+}	5.21×10^{-4} mol/L
SO_4^{2-} (inside)	2.62×10^{-4} mol/L
SO_4^{2-} (outside)	2.62×10^{-4} mol/L
O_2	1.63×10^{-4} mol/L
Constituent solubilities	
$Ca(OH)_2$	2.00×10^{-2} mol/L
CO_3^{2-}	1.20×10^{-3} mol/L
Mg^{2+}	1.20×10^{-3} mol/L

Properties of concrete

Concrete constituent concentrations	
Calcium concentration in C-S-H system	1.75×10^{0} mol/L
Calcium concentration in pore fluid	2.00×10^{-2} mol/L
CaO content in cement	2.11×10^{0} mol/L
Free Cl^{-}	1.00×10^{-2} mol/L
Silica concentration in C-S-H system	7.10×10^{-1} mol/L

Table 3.2. (continued)

Concrete design specifications	
Compressive strength at 28 days	3.52×10^{2} kg/cm^2
Poisson's ratio of concrete	1.50×10^{-1}
Modulus of elasticity of steel	2.04×10^{6} kg/cm^2
Yield strength of steel	4.22×10^{3} kg/cm^2
Modulus of subgrade reaction	2.11×10^{1} kg/cm^2
Young's modulus of elasticity	2.04×10^{5} kg/cm^2
Concrete water/cement ratio	4.00×10^{-1}
Concrete density	2.40×10^{0} g/cm^3
Concrete porosity	1.50×10^{-1}
Cement content	3.85×10^{2} kg/m^3
Initial pH	1.26×10^{1}
Diffusion coefficients in concrete	
NaOH, KOH	2.12×10^{-11} m^2/s
$Ca(OH)_2$	1.82×10^{-11} m^2/s
Cl^-	5.08×10^{-11} m^2/s
CO_2	1.92×10^{-10} m^2/s
O_2	2.10×10^{-10} m^2/s
SO_4^{2-}	1.06×10^{-11} m^2/s
Silo design specifications	
Silo dimensions	
Silo radius	1.30×10^{0} m
Silo height	6.10×10^{0} m
Concrete member thickness	
Roof	3.05×10^{1} cm
Walls	1.52×10^{1} cm
Floor	3.05×10^{1} cm
Steel reinforcement radius	
Roof	4.76×10^{-1} cm
Walls	0.00×10^{0} cm
Floor	4.76×10^{-1} cm
Spacing of steel reinforcement	
Roof	1.52×10^{1} cm
Walls	0.00×10^{0} cm
Floor	1.52×10^{1} cm
Corrugated steel thickness	
Compression face	1.52×10^{-1} cm
Tension face	1.52×10^{-1} cm

Table 3.2. (continued)

Concrete cover thickness on tension face	
Roof	
X-direction	1.48×10^{1} cm
Y-direction	1.48×10^{1} cm
Walls	
Horizontal direction	0.00×10^{0} cm
Vertical direction	0.00×10^{0} cm
Floor	
X-direction	1.48×10^{1} cm
Y-direction	1.48×10^{1} cm
Static load	3.95×10^{-1} kg/cm^2
Soil and waste properties	
Earthen cover thickness	1.83×10^{0} m
Earthen cover density	1.76×10^{0} g/cm^3
Friction angle of waste backfill	4.00×10^{1} deg
Friction angle of soil backfill	3.00×10^{1} deg
Density of waste backfill	1.76×10^{0} g/cm^3
Density of soil backfill	1.76×10^{0} g/cm^3
Waste density	1.76×10^{0} g/cm^3
Average moisture content of waste	9.90×10^{-1}
Concrete and steel failure rates	
Epoxy coating	
Start of failure	0.00×10^{0} years
Time to complete failure	2.00×10^{1} years
Steel liner	
Start of failure	0.00×10^{0} years
Time to complete failure	5.00×10^{1} years
Nuclide-specific parameters	
Nuclide	^{137}Cs
Half-life	3.00×10^{1} years
Solubility	1.60×10^{1} mol/L
Waste K_d	1.99×10^{1} ml/g
Diffusion coefficient	
Waste	6.80×10^{-12} m^2/s
Concrete	5.12×10^{-13} m^2/s
Initial inventory	8.15×10^{-3} g

[a]1000-year simulation length, 50-year output edit frequency.

greater than the screening limit are used in the environmental transport of contamination and are listed in Appendix C (Tables C.13–C.22). The screening analysis was performed without the consideration of parameter uncertainties. The uncertainty analysis (see Sect. 4.6) of the performance assessment for SWSA 6 requires low, high, and probable values for the waste inventory as well as for other key input parameters to the codes. (Key input parameters are those that impact the leaching results significantly.) The key input parameters were identified through a sensitivity analysis and are listed in Table 3.3 and Tables C.13–C.22 in Appendix C.

3.2 PATHWAYS AND SCENARIOS

Radionuclides released to the environment from the SWSA 6 disposal units are subject to transport and can lead to human exposures. This section describes the potential pathways for the transport of radionuclides in the environment and the scenarios for human exposure. Pathways and scenarios addressed in detail are identified and the justification for not considering some pathways and scenarios in detail is presented. Each of the disposal units discussed in Sects. 2.3.5–2.3.7 were modeled separately. The releases to the environment were analyzed separately, and the resulting releases to surface water were added, consistent with the time of arrival. In the analysis, overlapping plumes from the various types of disposal units did not occur.

3.2.1 Release from Disposal Units to Environmental Pathways

At SWSA 6, several types of disposal units are situated above and below ground. The below-ground units include the low-range silos, high-range silos, high-range wells, fissile wells, asbestos silos, and biological trenches. The above-ground units include Tumulus I, Tumulus II, and the IWMF. Detailed descriptions of these units are given in Sects. 2.3.5–2.3.7.

The durability of concrete and bulk movement of water through concrete are significant elements in the performance model for the release of contamination from the various types of wells, silos, and tumuli, all of which rely on concrete for waste isolation. Leachate generated after water reaches the waste in the disposal units may be released through leaks in containment and by advection and diffusion through the concrete in the wells, silos, and tumuli. In this analysis, diffusion of contaminants through concrete is assumed to be the primary mechanism of release during the period of time that the concrete remains intact. When the concrete degrades and cracks are assumed to form, advection becomes the primary mechanism for release of radionuclides. The performance of concrete in the various disposal units and the assumptions used in modeling are discussed in Sects. 3.1 and 3.3.2 and Appendixes B and C.

Based on existing data (Lee and Kocher 1990), releases of radionuclides from the disposal units to surface water and groundwater are assumed to be the primary pathways for the transport of radionuclides in the environment. Observations at existing disposal facilities over the last few decades suggest that emission of radionuclides directly to the atmosphere in gaseous form is not an important release mechanism at Oak Ridge National Laboratory (ORNL) (Bechtel 1991b). Although routine monitoring of gaseous emissions

Table 3.3. SOURCE1 and SOURCE2 code inputs (nonradionuclide specific) for the uncertainty analysis[a,b]

Description	Probable	Low	High
Earthen cover and waste properties			
Density, earthen cover (g/cm^3)	1.76×10^0	1.60×10^0	2.20×10^0
Density, waste (g/cm^3)	1.76×10^0	1.00×10^0	2.60×10^0
Moisture content, waste (cm^3/cm^3)	9.90×10^{-1}	1.50×10^{-1}	1.00×10^0
Groundwater concentrations			
Calcium (mol/L)	2.10×10^{-3}	1.78×10^{-3}	2.41×10^{-3}
Chloride (mol/L)	2.04×10^{-4}	1.81×10^{-4}	2.27×10^{-4}
Magnesium (mol/L)	5.21×10^{-4}	4.02×10^{-4}	6.40×10^{-4}
Oxygen (mol/L)	1.63×10^{-4}	5.00×10^{-5}	3.20×10^{-4}
Sulfate (inside the cask) (mol/L)	2.62×10^{-4}	1.89×10^{-4}	3.34×10^{-4}
Sulfate (outside the cask) (mol/L)	2.62×10^{-4}	1.89×10^{-4}	3.34×10^{-4}
Effective diffusivity in concrete			
Alkalis (m^2/s)	2.12×10^{-11}	2.12×10^{-12}	2.86×10^{-10}
Calcium hydroxide (m^2/s)	1.82×10^{-11}	1.82×10^{-12}	1.82×10^{-10}
Chloride (m^2/s)	5.08×10^{-11}	2.03×10^{-12}	2.03×10^{-10}
Carbon dioxide (m^2/s)	1.92×10^{-10}	1.92×10^{-11}	3.84×10^{-10}
Oxygen (m^2/s)	2.10×10^{-10}	2.10×10^{-10}	4.20×10^{-10}
Sulfate (m^2/s)	1.06×10^{-11}	1.06×10^{-12}	1.06×10^{-10}
Groundwater parameters			
Groundwater pH	6.75×10^0	4.85×10^0	8.10×10^0
Total dissolved solids in groundwater (mg/L)	3.49×10^2	2.82×10^2	4.17×10^2
Groundwater temperature (°C)	1.50×10^1	1.20×10^1	1.85×10^1
Container corrosion			
Time for complete corrosion of vaults (years)	6.00×10^1	2.50×10^1	1.00×10^2
Time for complete epoxy failure (years)	2.00×10^1	1.00×10^1	5.00×10^1
Concrete parameters			
Saturated hydraulic conductivity of concrete (cm/s)	1.00×10^{-10}	1.00×10^{-11}	1.00×10^{-9}
Soil parameters			
Saturated hydraulic conductivity of soil beneath disposal unit (cm/s)	5.8×10^{-7}	2.31×10^{-11}	1.16×10^{-3}
Container corrosion			
Steel liner corrosion (years)	5.00×10^1	2.00×10^1	1.00×10^2
Container corrosion			
Iron pipe corrosion (years)	7.50×10^1	2.50×10^1	1.25×10^2

[a]*Source*: Based on experience and engineering judgment.
[b]Radionuclide-specific parameters shown in Tables C.13–C.22.

at SWSA 6 is not performed, an ambient air monitoring station is located at White Oak Dam, just to the south of SWSA 6. The air monitoring station takes biweekly samples of both airborne particulates and gases. Remote air monitoring stations in Philadelphia, Tennessee, and Knoxville, Tennessee, collect the same data. Table 3.4 summarizes the data collected for 1991. The comparatively elevated concentrations of ^{137}Cs and ^{90}Sr observed at White Oak Dam are consistent with all other air monitoring stations located on the Oak Ridge Reservation (ORR) and, therefore, do not reflect emissions from SWSA 6. The slightly elevated gross alpha concentration is attributable to isotopes that occur naturally in soil and are suspended during waste operations at SWSA 6 and nearby activities (Kornegay et al. 1992).

Assuming all the airborne activity measured at the White Oak Dam Monitoring Station were indicative of releases from SWSA 6, the annual effective dose to an individual would be less than 0.04 mrem. In reality, these data represent activity from all operations at ORNL, the Y-12 Plant, and the K-25 Site, including stack releases and releases from 50 years of historical operations. Over this period of historical operations in Oak Ridge, millions of curies have been disposed of in nearby disposal facilities or discharged to surface water. The data in Table 3.4 suggest that the release of radioactivity as gases and particulate matter in the atmosphere is not significant. Consequently, airborne releases of contamination are not considered in detail in this performance assessment.

Table 3.4. Mean radionuclide concentrations in air, 1991

Nuclide	Concentration (10^{-15} μCi/mL)	
	White Oak Dam	Remote network
Gross alpha	2.3	1.8
Gross beta	20	19
^{60}Co	0.018	0.031
^{137}Cs	0.023	0.0034
^{238}Pu	0.001	0.0018
^{239}Pu	−0.00022[a]	−0.0011[a]
^{228}Th	0.0023	0.0037
^{230}Th	0.0019	0.003
^{232}Th	0.0021	0.0037
Total Sr	0.12	0.037
^{234}U	−0.0095[a]	0.0079
^{235}U	0.0028	0.00028
^{238}U	0.0042	0.0053

[a]Concentrations are determined by subtracting background readings from measured readings. For some isotopes, this results in apparent negative concentrations.

Source: Kornegay, F. C., et al. 1992. *Oak Ridge Reservation Environmental Report for 1991*, ES/ESH-22/V1, Martin Marietta Energy Systems, Inc., Oak Ridge, Tenn.

Suspension of particulates by natural processes has not been identified as an important pathway for the transport of contamination and can be excluded as long as a minimal amount of uncontaminated soil or other similar cover material exists at a disposal unit. Even if some waste should become exposed due to natural erosion at the site, the amount of waste that could be suspended into the atmosphere by natural processes would be small. Observations in Oak Ridge and nearby areas clearly show that extensive vegetative ground cover is quickly established on any cleared lands and that reforestation of unattended lands occurs within a few decades. Extensive vegetation and forestation at the disposal units, combined with the high annual rainfall and low average wind speeds in Oak Ridge, provide conditions that minimize the suspension of radionuclides in particulate form by natural processes.

ORNL is in full compliance with the requirements of 40 CFR 61. Total EDEs for 1992 have been determined for the ORR (including ORNL) and are well below the 10 mrem National Emission Standards for Hazardous Air Pollutants limit (Kornegay et al. 1993). For SWSA 6 to exceed the 40 CFR 61 limit, atmospheric releases from SWSA 6 would need to increase by more than two orders of magnitude. With ongoing waste disposal operations and environmental restoration activities occurring, such an increase in emissions is not plausible, and reasonable scenarios for analysis are difficult to construct. Consequently, atmospheric releases from SWSA 6 are given no further consideration in this performance assessment.

Release of radionuclides from the above-ground (tumulus) disposal units is assumed to occur primarily to surface water or to the soil surface. Leachate moves out of the vaults by diffusion or through cracks in the concrete. Most of the leachate is expected to run off the concrete pad to surface soil and surface water with some leachate transported to groundwater. Some leachate may pass through the pad by diffusion or through cracks to shallow subsurface soil and then to groundwater or surface water. At SWSA 6, where the water table may be only a few feet below the surface, the lack or failure of a groundwater suppression system may allow mixing of the leachate with the groundwater beneath the pad.

Radionuclides released from below-ground silos and wells are assumed to enter soils and groundwater. Leachate moves out of the units by diffusion or through cracks in the concrete to the saturated or unsaturated zones. The models for transport of radionuclides from the various disposal units are discussed further in Sects. 3.1.1 and 3.4 and in Appendix B.

Releases of radionuclides from the biological trenches also occur mostly to groundwater and soils. These units do not include engineered barriers to inhibit flow and transport. Leachate is generated following precipitation events and is transported to surface water after being discharged through the shallow subsurface or groundwater.

3.2.2 Transport Through the Environment

As discussed elsewhere (Stevens 1990), the environmental transport pathways for radionuclides that could result in exposures of off-site individuals or inadvertent intruders include transport in air, surface water, groundwater (in the saturated and unsaturated zones), and biota. Available data for facilities on the ORR (Lee and Kocher 1989) indicate that transport in surface water and groundwater are the most important pathways

that could result in doses to off-site members of the public. Based on data (Sect. 3.2.1), air transport to off-site locations is not expected to be significant due to the topography, low average wind speed, and high average rainfall in the area and the dispersion and deposition of airborne contaminants that would occur between source and receptor locations.

The hydrologic framework for the ORR has been described by Solomon et al. (1992) in terms of the following four zones (Fig. 3.1):

- *A stormflow zone* is composed of the upper 1-2 m (3-7 ft) of the soil profile, in which precipitation-driven lateral flow generates about 90% of streamflow. This zone is a major pathway for transporting contaminants from the subsurface to surface waters. All silos, wells, and trenches intersect this flow zone.
- *A vadose zone* is predominantly unsaturated and consists of weathered saprolite of 1-15 m (3-49 ft) thickness with a fluctuating water table as the lower boundary. This zone has (exponentially) decreasing hydraulic conductivity with depth.
- *A groundwater zone* contributes the remaining 10% of streamflow, which occurs through a permeable saprolite layer called the water table interval. This flow zone has a thickness of 1-5 m (3-16 ft) (Clapp 1992, p. 123-126). Intermediate and deep intervals of the aquifer have thicknesses of up to 100 m (328 ft), and contribute very little to streamflow due to low hydraulic conductivity and disconnected fractures.
- *An aquiclude* at depths beyond 200 m (656 ft) has extremely slow water flow rates that are estimated to change on geological time scales.

These four zones occur in SWSA 6 and occupy the upper 30 m (100 ft) or less of the landscape. These hydrologically active features are responsible for essentially all radionuclide transport from the disposal units.

Solomon et al. (1992) conclude that groundwater flow volumes decrease and solute residence times increase sharply with depth. They further estimate that the chemical transport rate in the stormflow zone is on the order of meters per hour, decreasing exponentially with depth to flow rates of a few centimeters per year. Their review showed no evidence for contaminant migration along deep subsurface flow paths of the intermediate and deep intervals of the groundwater (Fig. 3.1). The residence times for solutes in the water table interval are in the range from a few days to a few years. Deeper flow rates of solutes have been estimated from ^{14}C measurements to be in the order of hundreds to tens of thousands of years (Solomon et al. 1992). Chemical adsorption and matrix diffusion have been identified as important geochemical processes that retard chemical transport in facility soils, creating secondary contaminant sources that may persist for many decades.

The model for transport of radionuclides in surface water and the unsaturated zone takes into account precipitation, storm hydrology, streamflow, infiltration, and percolation. The model also takes into account the effects and performance of caps installed at SWSA 6 as part of the Resource Conservation and Recovery Act (RCRA) facility closure activities. Discharges from the shallow subsurface provide the flow in ephemeral creeks at SWSA 6 and contribute to the flow in perennial streams. The model includes dilution in the surface streams during transport. The model also predicts flow of water through the

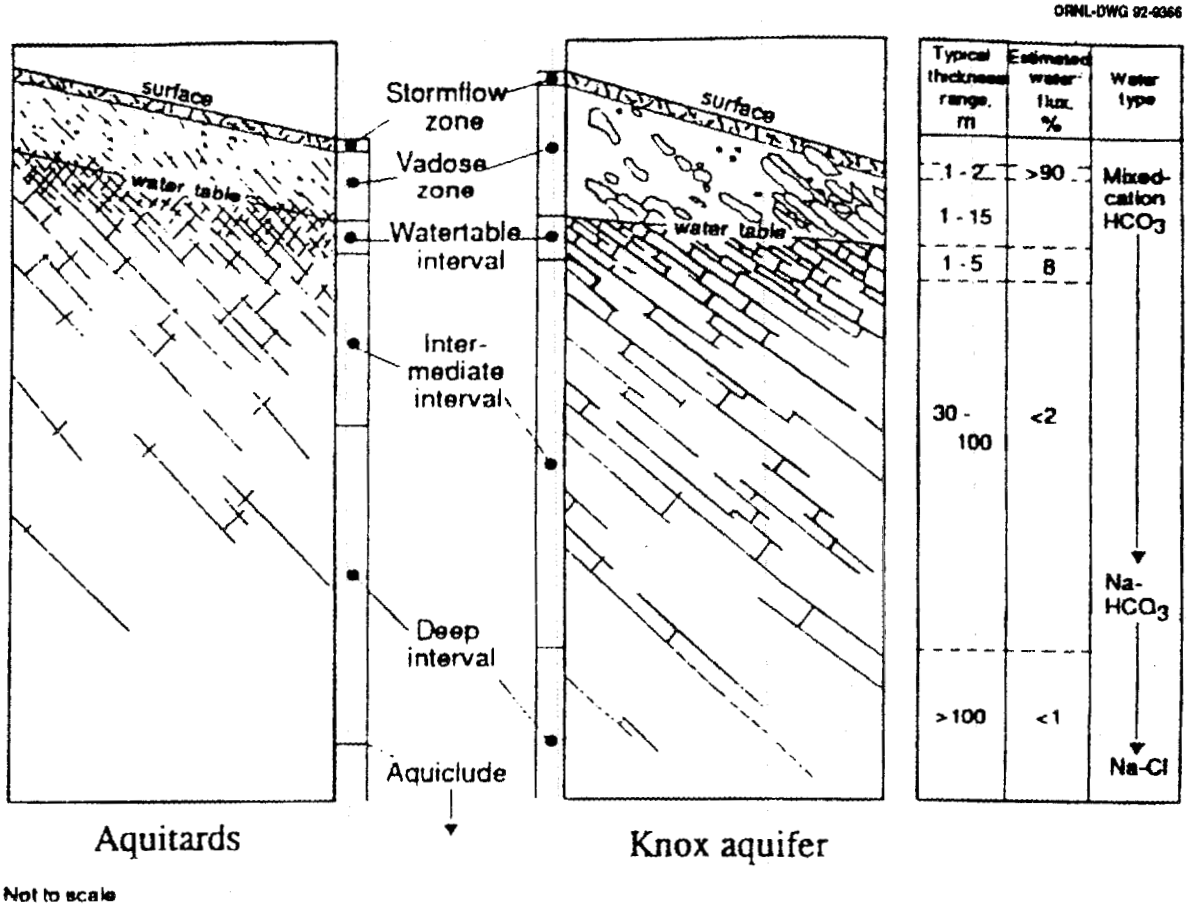

Fig. 3.1. Schematic profile showing subsurface flow zones and intervals, general thickness ranges, estimated relative annual water flux, and change in water type with depth.

unsaturated zone to surface water, recharge to the saturated zone, concentration and flux of leachate to surface water, and concentration and flux of leachate to the saturated zone.

The model for transport of radionuclides in the saturated zone includes recharge, advection, some diffusion, adsorption, and some dilution in groundwater. The model predicts flow of water in the saturated zone, concentration and flux of leachate in the groundwater, and concentration and arrival time of radionuclides at compliance points within SWSA 6 and at the boundary of SWSA 6. For protection of groundwater resources, the compliance points within SWSA 6 are taken to be any locations outside the 100-m (328-ft) buffer zone around any disposal units. The model for groundwater transport includes radioactive decay from the time the contaminant enters the groundwater and a conservative estimate of radionuclide retardation during transport.

Transport of contamination through biological uptake has occurred with the resulting contamination of deer, waterfowl, and fish on the ORR. Contamination of biota is primarily the result of historical discharges of contaminated water or existing discharges from historical disposal operations. Wildlife is routinely monitored, and the results are reported (Kornegay et al. 1992). The maximum annual dose attributable to the consumption of fish contaminated as a result of ORNL operations past and present is less than 0.8 mrem. The maximum annual dose attributable to the consumption of 310 L (82 gal) of contaminated milk is reported to be 0.2 mrem. The maximum annual dose from the consumption of two contaminated deer is reported to be 1 mrem. The maximum annual dose from the consumption of a contaminated goose and a contaminated duck was reported to be 1 mrem. These reported doses are associated with releases of radioactivity significantly exceeding the potential releases from SWSA 6. Additionally, less than 2% of the deer killed in 1991 were contaminated. As a result, the transport of contamination through biota to humans from SWSA 6 can reasonably be concluded to be less than those reported in Kornegay et al. (1992). Because the doses from consuming contaminated biota are much less than the performance objectives for LLW disposal, and the potential releases from SWSA 6 are certain to be less than those releases that have already occurred and are occurring, the transport of contamination by biota has not been considered in this performance assessment. The remaining pathway for biotic transport of contamination could occur from root uptake of contamination by plants, resulting in the potential exposure to contamination by individuals (Sect. 3.2.4). Exposure to contaminated soils and ingestion of contaminated vegetation is incorporated into the analysis of direct intrusion (Sect. 3.2.4). Because contaminated vegetation is not transported off-site by natural processes and the exposure to contaminated vegetation is incorporated into the performance assessment, the transport of contamination by biotic processes is not considered in the performance assessment in the analysis of transport through the environment.

3.2.3 Closure Scenario

The schedule for waste disposal operations, site closure, institutional control period, and post-institutional control period for SWSA 6 were selected based on the best information available at the time that simulations were initiated (Sect. 2.3.4). The following time sequence of events was used in this performance assessment.

Active Operations (September 1988 to December 1997). Within this period, disposal units are being filled and new ones constructed. The time taken to fill a particular type of disposal unit was estimated by Energy Systems Waste Management Organization staff (Table 3.5) and used in the calculations, which assumed a uniform rate of disposal-unit filling.

Exposed Geomembrane Cover (1998 to 2027). This cover was designed to provide temporary hydrologic isolation of the disposal units by (1) diversion of shallow subsurface flow through the use of french drains and (2) diversion of surface water by large geomembrane covers that extend over the disposal units and most of the upslope drainage area. Arbitrarily, 99% credit was given to the hydrologic isolation for the 30-year period due to the high level of maintenance and planned 10-year replacement interval for the

Table 3.5. Disposal units in Solid Waste Storage Area 6 showing starting and ending times of active use and the average distances of each site to groundwater and a receiving stream channel

Disposal unit	Starting month	Ending month	Distance to groundwater (m)	Distance to stream (m)
Low-range silos–north (TLN)	10/1988	12/1993	1	87
Low-range silos–south (TLS)	10/1988	12/1993	5	293
High-range silos (TH)	10/1988	12/1993	1	152
Asbestos silos (TA)	10/1988	12/1993	1	135
Tumulus I (TUM1)	10/1988	6/1990	2	43
Tumulus II (TUM2)	7/1990	3/1992	1	43
IWMF (IWM1)	10/1991	12/1997	2	239
High-range wells/silos (THW)	10/1988	12/1993	6	185
High-range wells (WHA)	10/1988	12/1993	6	185
Fissile wells (WF)	10/1988	12/1993	3	120
Biological trenches (TB)	10/1988	12/1993	1	130

membrane. Since making the assessment calculations, the proposed remediation of SWSA 6 under the Comprehensive Environmental Response Compensation and Liability Act (CERCLA), which included a geomembrane cover, has been abandoned (Sect. 2.3.4), and no alternative has been decided upon. An assessment of the hydrologic consequences of changes in chemical transport as a result of the ongoing CERCLA remediation of SWSA 6 will be made in future revisions of the performance assessment (see Sect. 4.9).

CERCLA Cap (2028 to 2097). A multilayer cap with the following layer structure has been proposed for construction over the tumulus units, IWMF, and other disposal units:

- grass vegetation on surface,
- 45 cm (18 in.) of topsoil,
- a drainage layer,

- a flexible membrane, and
- 60 cm (24 in.) of compacted clay.

Leveling fill would be used as needed. This description was provided in internal correspondence dated December 28, 1992 [B. L. Kimmel, ORNL, letter to L. E. McNeese, ORNL, Oak Ridge, Tenn.]; however, the UTM hydrologic simulations were performed using a cap with the following layers:

- mown grass vegetation (leaf area index of 4.9),
- 60 cm (24 in.) of topsoil,
- a flexible membrane, and
- 60 cm (24 in.) of compacted clay.

The compacted clay was assigned a saturated hydraulic conductivity of 0.2 mm/day (2.3×10^{-9} m/s) [0.008 in./day (8×10^{-9} ft/s)]. This value is somewhat higher than the 1×10^{-9} m/s (3×10^{-9} ft/s) specified by the U.S. Environmental Protection Agency (EPA); however, it is very difficult to compact soil to defined specifications in the field (Goldman et al. 1988), and the higher conductivity is a conservative assumption. During the first 10 years after installation, the flexible membrane liner was considered to control the overall effectiveness of the cap, and an arbitrary drainage rate of 1% of precipitation was chosen. This effectiveness value was also used for the exposed geomembrane cover. Differential settling and inadequately sealed seams between adjacent geomembrane sheets can eventually lead to hydrologic failure of the flexible membrane liner (Bass et al. 1985). The CERCLA cap was assigned an effective life of 10 years (2028–2037) with a low drainage rate. During the following 10 years (2038–2047), percolation through the cap was allowed to linearly ramp up to values simulated for a leaking cap with macropores. The integrity of the flexible membrane was expected to diminish during this period, and root penetration into the compacted layer was also expected to occur. These developments would lead to shrinkage and swelling of clay materials and the gradual formation of cracks and channels that would allow drainage to bypass much of the compacted clay matrix (Suter et al. 1993). For the 50-year period from 2048 to 2097, the burial ground was simulated with a mown grass cover and a leaking cap. The 100-year period of institutional control following initiation of site closure ends in 2097. The cap simulation used in the analysis is functionally equivalent to the cap proposed for field construction but provides enhanced infiltration by neglecting the performance of the proposed drainage layer. The enhanced infiltration, over the period of time that the drainage layer would be functional, is a conservative representation of the site's performance.

Forest Cover (2098+). The site is considered to revert to forest vegetation through species succession after the grass cover is no longer actively maintained. Natural succession proceeds by invasion of early succession tree species such as eastern red cedar, short-leaf pine, and sweetgum; these are followed by oak-hickory forest species at a later stage (Suter et al. 1993). The hydrologic consequence of these temporal changes in species was not considered significant, and one set of hydrologic simulation results was used for the period following termination of institutional control.

Each time period was modeled separately with appropriate soil and vegetation variables and parameters. Results from the end of one time period were used as inputs for the following time period.

3.2.4 Human Exposure Scenarios

3.2.4.1 Operations and Institutional Control Periods (1988–2097)

For existing operating procedures at SWSA 6, monitoring data indicate that releases of radionuclides beyond the site boundary result in radiation doses to members of the general public that are far less than the limit on annual EDE of 25 mrem, which is the performance objective for off-site individuals. Furthermore, concentrations of radionuclides at inlets to public drinking water systems on the Clinch River downstream from ORNL are less than the applicable limits in the EPA's interim standards for radioactivity in community drinking water systems (40 CFR Part 141), which include a limit on annual dose equivalent of 4 mrem to whole body or any organ from all beta/gamma-emitting radionuclides. During both the operations and institutional control periods, a facility monitoring program will be used to evaluate compliance with standards for off-site releases and protection of groundwater.

The dose analysis for off-site members of the general public considers only doses to maximally exposed individuals who reside near the boundary of the disposal units. Estimates of collective dose in the exposed population beyond the site boundary are not considered. At the present time, most of the off-site population that could be exposed to releases from SWSA 6 is located a considerable distance from the disposal units. The only credible pathway for exposure of off-site populations is transport of radionuclides in the Clinch River. Because the normal flow in the Clinch River provides a large dilution factor for releases into the river from SWSA 6, the dose received by individuals in population groups downstream of the disposal units is expected to be far less than the dose to a hypothetical individual at the site boundary.

During the operations and institutional control periods, only off-site members of the general public could receive radiation exposures from waste disposal in SWSA 6. As described previously, radionuclides released from disposal units are assumed to be transported primarily by surface water and groundwater. Existing monitoring data at SWSA 6 clearly indicate that off-site transport of contamination occurs more rapidly by surface water and that contaminated groundwater on the site discharges to surface water within the present site boundary (see Sect. 3.4). Thus, there are no indications that contaminated groundwater will occur beyond the site boundary in the future. All surface water from SWSA 6 discharges to White Oak Lake and from there to the Clinch River. Consequently, an off-site individual is assumed to be exposed to contaminated surface water released into the Clinch River from the present location of White Oak Dam.

The maximally exposed off-site individual is assumed to use contaminated water released into the Clinch River from White Oak Creek for domestic and recreational purposes, and the following exposure pathways are assumed to occur:

- direct ingestion of contaminated water;
- ingestion of milk and meat from dairy and beef cattle that drink contaminated water; and
- external exposure while swimming in contaminated water.

An off-site individual also could use contaminated water for irrigation of food crops consumed by the individual or irrigation of pasture land used for grazing by dairy and beef cattle. However, consumption of contaminated foodstuffs resulting from irrigation with contaminated water is not considered in the dose analysis because irrigation is rarely practiced in the Oak Ridge area at the present time, due to the usually abundant rainfall.

3.2.4.2 Post-Institutional Control Period

As in the operational and institutional control periods, estimates of collective dose in the off-site population are not considered in the dose analysis for the post-institutional control period because it is not expected that new population centers will be developed along the Clinch River near the present boundary of the ORR. Therefore, the analysis again considers only doses to maximally exposed individuals beyond the site boundary near the location of White Oak Dam. Exposures are assumed to result from the discharge of contaminated water into White Oak Creek, and the exposure pathways for off-site individuals are assumed to be the same as those listed above for exposures during the operational and institutional control periods.

Following loss of active institutional control over SWSA 6 at 100 years after facility closure, inadvertent intruders are assumed to come onto the site and establish permanent homesteads, including on-site sources of water and foodstuffs. Furthermore, intruders are assumed to have no prior knowledge of waste disposal activities at the site. Inadvertent intruders are assumed to receive radiation exposures from use of contaminated water obtained from a well, which is assumed to be located a distance of 100 m (328 ft) from any disposal unit and in the direction of maximum contaminant flow from disposal units at the point of maximum concentration, and from direct intrusion into disposal units. Each type of below-ground and above-ground disposal unit is treated separately in the dose analysis for inadvertent intruders.

For inadvertent intruders, the following exposure pathways involving use of contaminated water from a well are assumed to occur:

- direct ingestion of contaminated water; and
- ingestion of milk and meat from cattle that drink contaminated water.

These pathways are the same as two of the exposure pathways for off-site individuals listed previously, but the pathway involving external exposure while swimming is not considered in the dose analysis for inadvertent intruders. At the present time, White Oak Lake is the only surface water within 100 m (328 ft) of disposal units in SWSA 6 that could be used for swimming, and no suitable streams exist on the site itself. Exclusion of this exposure pathway from the dose analysis is based on the assumption that White Oak Lake will be drained prior to loss of institutional control over the site. As in the dose analysis for off-site individuals, irrigation of food crops and pasture land with contaminated water is not

considered in the dose analysis for inadvertent intruders. Use of contaminated well water by an intruder is assumed to occur in conjunction with any of the scenarios for direct intrusion into disposal units discussed in the following paragraphs.

Exposures of inadvertent intruders resulting from direct intrusion into disposal units are assumed to occur according to one of four scenarios—the agriculture, resident, discovery, and post-drilling scenarios. The following paragraphs provide a brief description of these scenarios.

The agriculture scenario is assumed to occur continuously over an intruder's lifetime. In this scenario, an intruder is assumed to construct a home directly on top of disposal units, with the foundation extending into the waste itself. Waste is assumed to be exhumed during construction of the foundation, and all waste remaining in the disposal units at the time the foundation is dug is assumed to be indistinguishable from native soil. Some of the exhumed waste is assumed to be mixed with native soil in the intruder's vegetable garden, and the following exposure pathways are assumed to occur:

- ingestion of vegetables grown in the contaminated garden soil;
- direct ingestion of contaminated soil from the garden in conjunction with vegetable intakes;
- external exposure to contaminated soil while working in the garden or residing in the home on top of the disposal facility; and
- inhalation of radionuclides suspended into air from contaminated soil while working in the garden or while residing in the home.

The resident scenario also is assumed to occur continuously over an intruder's lifetime. As in the agriculture scenario described above, the resident scenario assumes that an intruder excavates a foundation for a home on top of disposal units. During excavation, however, the intruder is assumed to encounter an intact engineered barrier (e.g., reinforced concrete roof) on top of the disposal units that cannot be penetrated by the types of excavation equipment normally used on the ORR. The intruder then is assumed to construct a home directly on top of the intact engineered barrier. Because the engineered barriers are assumed not to be penetrated during excavation, the only exposure pathway of concern for the resident scenario is external exposure to photon-emitting radionuclides in the waste during the time the intruder resides in the home on top of the disposal units. The presence of intact engineered barriers would preclude any ingestion or inhalation exposures.

The external exposure pathway of concern for the resident scenario is similar to one of the exposure pathways assumed for the agriculture scenario. Because the resident scenario assumes the presence of an intact engineered barrier between the waste and the receptor location but the agriculture scenario does not, the dose per unit concentration of radionuclides clearly will be considerably less for the resident scenario than for the agriculture scenario. However, the agriculture scenario presumably cannot occur for a substantial period of time after the resident scenario, because the agriculture scenario requires that the engineered barriers are physically degraded and can be penetrated by normal excavation procedures. Therefore, the resident scenario is potentially important (i.e., could result in doses comparable to or greater than the doses for the agriculture scenario) if the inventory of photon-emitting radionuclides in disposal units is depleted

significantly over time prior to failure of the engineered barriers, either by radioactive decay or by mobilization and transport in infiltrating water. For radionuclides that are relatively long-lived or immobile, the resident scenario should result in considerably lower estimates of dose than the agriculture scenario.

The discovery scenario is assumed to occur only once over an intruder's lifetime. In this scenario, an intruder attempts to excavate a foundation for a home at the location of disposal units, as in the agriculture scenario described previously, but is assumed to encounter an intact and impenetrable engineered barrier (e.g., reinforced concrete) used in constructing the disposal units. Thus, the discovery scenario involves the same assumption about the engineered barriers as the resident scenario described above but differs from the resident scenario in two respects. First, shortly after encountering the intact engineered barrier, the intruder decides to abandon digging at the location of disposal units and moves elsewhere, thus resulting in a short-term acute exposure rather than a long-term chronic exposure as in the resident scenario. Second, it is assumed that the excavation could encounter an engineered barrier at the side of disposal units, rather than just at the top of disposal units as in the resident scenario. This difference is potentially important because several types of disposal units in SWSA 6 are engineered with walls that are thinner than the cap, and the external dose rate per unit concentration of radionuclides in the waste thus could be significantly higher for the discovery scenario than for the resident scenario. As for the resident scenario, the only exposure pathway of concern for the discovery scenario is external exposure to photon-emitting radionuclides in the waste during the time the intruder excavates at the site, and the presence of intact barriers precludes any ingestion or inhalation exposures.

From their definitions, the resident and discovery scenarios would occur at the same time. Furthermore, the exposure pathway of concern—namely, external exposure to photon-emitting radionuclides in the waste—essentially is the same for the two scenarios. Thus, the dose analyses for these scenarios depend only on (1) the assumed exposure time, which presumably would be considerably less for the discovery scenario involving a short-term acute exposure than for the resident scenario involving a long-term chronic exposure, (2) the amount of shielding provided by the engineered barriers in disposal units, and (3) the shielding factor during indoor residence, which applies only to the resident scenario and reduces the external dose rate per unit concentration of radionuclides in the waste compared with the external dose rate outdoors in the discovery scenario. The shielding factor for a home should be no more than a factor of two.

From the descriptions of the resident and discovery scenarios given above, the dose per unit concentration of radionuclides clearly would be considerably greater for the resident scenario than for the discovery scenario when the thickness of the engineered barriers encountered during excavation would be the same in the two scenarios. However, since the resident scenario assumes that an intruder attempts to excavate into disposal units only from above, and the intruder's home sits on top of the engineered barriers above the waste, but the discovery scenario takes into account that an excavation also could encounter an engineered barrier at the side of disposal units, the dose for the discovery scenario could be comparable to or greater than the dose for the resident scenario if the thickness of the engineered barriers at the side of disposal units is considerably less than the thickness of the barriers at the top of disposal units. Considerably different thicknesses of engineered barriers on the top and sides of disposal

units occur with some of the units in SWSA 6, so the discovery scenario is considered in addition to the resident scenario in these cases, in spite of the considerably shorter exposure time that presumably occurs for the discovery scenario. On the other hand, the discovery scenario clearly can be neglected compared with the resident scenario for disposal units in which the thickness of the engineered barriers at the side of the units is the same as the thickness of the barriers at the top of the units.

The post-drilling scenario is assumed to occur continuously over an intruder's lifetime. In this scenario, direct intrusion into disposal units during construction of a home on the site, as in the agriculture scenario described previously, is assumed not to occur. However, an intruder is assumed to access solid waste by drilling through a disposal unit (e.g., for the purpose of constructing a well for the intruder's domestic water supply). The contaminated drilling waste that is brought to the surface is assumed to be indistinguishable from native soil, and all of the drilling waste is assumed to be mixed with native soil in the intruder's vegetable garden. The following exposure pathways are assumed to occur:

- ingestion of vegetables grown in contaminated garden soil;
- direct ingestion of contaminated soil from the garden in conjunction with vegetable intakes;
- external exposure to contaminated soil while working in the garden; and
- inhalation of radionuclides suspended into air from contaminated soil while working in the garden.

These exposure pathways are conceptually the same as some of the pathways assumed for the agriculture scenario. However, in the post-drilling scenario, external and inhalation exposures while residing in the home on the disposal site are not relevant because all waste exhumed by drilling is assumed to be mixed with native soil in the garden and the intruder's home is assumed not to be located directly on top of disposal units or contaminated soil.

For the four exposure scenarios involving direct intrusion into waste disposal units considered in this analysis, a potentially important assumption is the time after disposal at which the scenarios first could occur, because the dose from many radionuclides is reduced significantly over time due to radioactive decay and mobilization and transport from disposal units into the environment. The earliest time after disposal at which the scenarios reasonably can occur depends on the time period for active institutional control over the disposal site and the length of time the engineered barriers in many types of disposal units are assumed to maintain their integrity and preclude direct intrusion into waste, either by excavation or by drilling.

The agriculture scenario is based on the assumption that a waste disposal unit must be penetrable by normal excavation procedures used in digging a foundation for a home. Therefore, for all disposal units that are constructed using concrete walls and caps (i.e., all disposal units except the biological trenches), this scenario cannot reasonably occur until the concrete barriers have lost essentially all of their structural and physical integrity because normal excavation procedures used in digging a foundation for a home cannot readily penetrate an intact concrete barrier. The extent of barrier degradation that would

permit normal excavation presumably is more severe than the type of cracking degradation that results in increased infiltration of water (as discussed in Sect. 3.1.1).

A detailed analysis of the physical degradation of concrete barriers to an extent sufficient to permit normal excavation has not been performed in this assessment. Rather, the presence of concrete barriers in all disposal units except the biological trenches is assumed to preclude the agriculture scenario for 300 years after disposal. Although the expected lifetime of the concrete barriers is not known, this assumption is intended to be somewhat pessimistic (i.e., the concrete barriers could maintain their integrity and preclude intrusion by excavation for longer than 300 years, but a technical justification for a longer time period cannot be provided). The effect of longer barrier lifetimes on predicted doses for the agriculture scenario is also investigated in this analysis. For disposal in unlined biological trenches, the agriculture scenario is assumed to occur immediately upon loss of active institutional control at 100 years after disposal.

The resident and discovery scenarios are based on the assumption that a disposal unit is impenetrable by normal excavation procedures used in digging a foundation for a home. Therefore, for all units constructed with engineered barriers, these scenarios are assumed to occur immediately upon loss of active institutional control at 100 years after disposal. These scenarios are not relevant for the biological trenches, which are constructed without engineered barriers and can be penetrated by normal excavation procedures. The resident scenario is considered for all disposal units except the biological trenches, but the discovery scenario is potentially important only for disposal units in which the thickness of the engineered barriers at the sides of the units is considerably less than the thickness of the engineered barriers at the top of the units, due to the shorter exposure time for the discovery scenario than for the resident scenario. The disposal units for which the discovery scenario is considered thus include the low-range silos, high-range silos, high-range wells, and asbestos silos; the discovery scenario need not be considered for Tumulus I, Tumulus II, the IWMF, and the fissile wells.

The post-drilling scenario is based on the assumption that a disposal unit can be penetrated by normal well-drilling procedures, even in the presence of intact engineered barriers, because drilling through hard rock is commonplace near the ORR. Furthermore, all drilling waste is assumed to be indistinguishable from native soil. Therefore, the post-drilling scenario is assumed to occur at 100 years after disposal for all units, including those constructed with engineered barriers.

In summary, the following four scenarios are assumed in the dose analysis for inadvertent intruders into the different disposal units at SWSA 6:

- an agriculture scenario involving direct intrusion into disposal units by excavation, which is assumed to occur at any time beyond 300 years after disposal for units constructed with engineered barriers and at any time beyond 100 years after disposal for the biological trenches;
- a resident scenario involving exposure during residence in a home on top of intact engineered barriers above disposal units, which is assumed to occur at 100 years after disposal and is applied to all disposal units except the biological trenches;
- a discovery scenario involving exposure while excavating at a disposal site in the presence of intact engineered barriers, which is assumed to occur at 100 years after disposal for all disposal units except the biological trenches but is applied only to those

disposal units in which the thickness of the engineered barriers at the sides of the units is considerably less than the thickness of the engineered barriers at the top of the units; and

- a post-drilling scenario involving direct intrusion into disposal units by drilling, which is assumed to occur at 100 years after disposal for all disposal units.

Two other scenarios also were considered but not included in the dose analysis for inadvertent intruders—the so-called construction and drilling scenarios. These scenarios and the justification for not including them in the dose analysis are described as follows.

The construction scenario involves short-term, acute exposure and considers doses that would be received while excavating a foundation for a home on the disposal site that extends into the waste itself. The construction scenario thus can be thought of as the precursor of the chronic agriculture scenario, which considers exposures that might be received after construction of the home is completed. The potential importance of the construction scenario arises primarily from the assumption that excavation activities could result in airborne concentrations of radionuclides that are substantially higher than those resulting from normal residence on exposed waste, as in the agriculture scenario. Ingestion exposure presumably is unimportant during normal excavation activities, and the dose from external exposure to radionuclides in the waste during excavation should be considerably less than the dose from external exposure while residing in the home after construction is completed, due to the lower exposure time involved.

The construction scenario clearly would occur at the same time as the agriculture scenario, so the dose analysis for the two scenarios would be based on the same concentrations of radionuclides. Previous calculations (Kennedy and Peloquin 1988) provide a direct comparison of doses for the two scenarios. For a few radionuclides, the dose per unit concentration could be slightly higher for the construction scenario, but for most radionuclides the dose per unit concentration is expected to be greater for the agriculture scenario. This result assumes a reasonable exposure time for the construction scenario and the use of reasonably consistent assumptions for the exposure pathways for the two scenarios. Therefore, since the dose limit for the acute construction scenario is five times higher than the dose limit for the chronic agriculture scenario, the construction scenario can be neglected in the dose analysis for inadvertent intruders.

The drilling scenario also involves a short-term, acute exposure and considers doses that would be received while drilling through waste and constructing a well. The drilling scenario thus can be thought of as the precursor of the chronic post-drilling scenario, which considers exposures that might be received after well drilling is completed. The potential importance of the drilling scenario arises primarily from the assumption that an intruder could be located near an unshielded pile of drilling waste for a substantial period of time and, thus, receive a significant external exposure. Ingestion exposure presumably is unimportant during normal drilling activities. Although some radionuclides in the drilling waste could be suspended into air and inhaled during well drilling and construction, inhalation exposures are expected to be relatively unimportant due to such factors as the initial water content of the drilling waste, the small volume of drilling waste produced, and the absence of direct mechanical disturbance of the waste pile.

The drilling scenario clearly would occur at the same time as the post-drilling scenario, and the dose analysis for the two scenarios would be based on the same

concentrations of radionuclides. Previous calculations (Kennedy and Peloquin 1988) again provide a direct comparison of doses for the two scenarios. For all radionuclides, the dose per unit concentration for the drilling scenario is expected to be at least an order of magnitude less than the dose per unit concentration for the post-drilling scenario, provided that a reasonable exposure time for the drilling scenario and reasonably consistent assumptions for the exposure pathways for the two scenarios are assumed. Therefore, the drilling scenario can be neglected in the dose analysis for inadvertent intruders.

3.3 ASSUMPTIONS

In the approach to this performance assessment (described in Sects. 3.1 and 3.2), many assumptions are required to provide a complete model for calculating quantitative results. Those assumptions that are considered important to the quantitative results presented in Sect. 4 and the method described in Sect. 3.4 are discussed in this section.

3.3.1 Source Terms

The basic assumptions used in the modeling of the source terms are as follows:

(1) The radionuclide leaching from wastes and concrete barriers is by advective and diffusive mass transport;
(2) The complex forms of the wastes and concrete barriers can be approximated sufficiently as simpler forms (e.g., slabs);
(3) The diffusion coefficients needed in the mass transport models (Appendix B) can be appropriately represented as retarded diffusion coefficients;
(4) The bulk chemical and physical properties of the concrete barriers deteriorate—over the time span of interest—to an extent that they significantly affect the values of the advective flow;
(5) The release of radionuclides due to advection is modeled as a zero-order leaching process accounting for sorption (retardation) and decay;
(6) The degradation (cracking and failure) of concrete is caused by sulfate attack, loss of calcium hydroxide, and corrosion of reinforcing steel; and
(7) The concentration of a radioisotope in leachate cannot exceed the solubility limit of the isotope.
(8) The effect of concrete cracking on the leaching of radionuclides is delayed until structural degradation of the disposal unit occurs.

3.3.2 Site

3.3.2.1 Runoff-Recharge Factors

The disposal units were assumed to operate within miniwatersheds in which inflow from the immediate upslope surroundings interacts with nuclides leaking from disposal units. This same process was assumed to be maintained at various stages of disposal unit

operation and closure. Terrain modification during closure may differ from that assumed in the assessment; however, little can be done to anticipate specific changes that may occur in the future. The general topography present during filling of the disposal units was assumed to be preserved throughout the life of the facility.

The total monthly water flow contacting disposal units was adjusted for the local landscape attributes. The average upslope area contributing lateral flow (B) to a disposal unit (Fig. 3.2) was determined from an AUTOCAD map of SWSA 6, and the ratio of this area to the disturbed area containing the disposal unit (A) was calculated (B/A values given in Table 3.6). The vertical recharge at a disposal unit site plus B/A times the sum of lateral flow and surface runoff entering the site from upslope sources was multiplied by the number of units for each site to give the water volume in contact with chemicals released from the disposal units at a given point in time. In all cases the disposal units at each site were considered to be influenced by a bathtub effect. Davis et al. (1989) have demonstrated with piezometer monitoring wells that the backfill around disposal units in a trench excavation becomes saturated from the bottom of the trench back to the surface during seepage events. The nuclides leaching from the disposal units are dissolved in this water volume and the solution partitioned into groundwater recharge and lateral flow components. Groundwater was preferentially recharged with the nuclide solution formed with the trench water using Darcy's Law to calculate recharge. This calculation used the saturated hydraulic conductivity of the aquifer and a unit hydraulic gradient. The remainder of the nuclide solution, if any, was removed each month from the site as shallow subsurface flow by subtracting the total nuclide solution volume from the recharge volume (see Appendix B.1.5.4.2). This treatment of hydrologic processes at a disposal unit site favors the preferential recharge to groundwater of the lateral drainage from the upslope mini-watersheds associated with a disposal unit site (Fig. 3.1). Monthly water level monitoring in disposal trenches has shown that water does not accumulate in trenches (Davis, Francis, and Luxmoore 1989), and the removal of the bathtub water on a monthly basis is considered appropriate.

Chemical transport from each disposal unit passed through the soils of the stormflow and vadose zones, and chemical adsorption was determined during transport with an equilibrium K_d calculation. The soil volume in the recharge pathway to groundwater was determined as the disposal unit site area multiplied by the depth to groundwater, which was determined from water table maps of SWSA 6 (Davis et al. 1987). In the case of lateral flow, the path length from the disposal units to the nearest stream channel (Table 3.5) was multiplied by one quarter of the site area to give the soil volume interacting with chemicals moving in shallow subsurface flow (Fig. 3.2). This quantity is an arbitrary estimate of the relevant soil volume for lateral flow. The number of filled units was adjusted annually during the active-use period as a linear function of time from the starting year (Table 3.5). This adjustment resulted in units having different ages, which was accounted for in the chemical transport calculations. Hydrologic transport from three disposal units (Tumulus I, Tumulus II, and IWMF) was simulated on a per pad basis and not on a per vault basis. Each pad was loaded with several hundred vaults (see Sect. 2.3.6).

The calculations of lateral subsurface transport through the stormflow zone did not specifically account for the effects of matrix diffusion. This effect can cause a difference between the time of first arrival of chemical during a transport event and the time of peak

ORNL-DWG 90M-11250

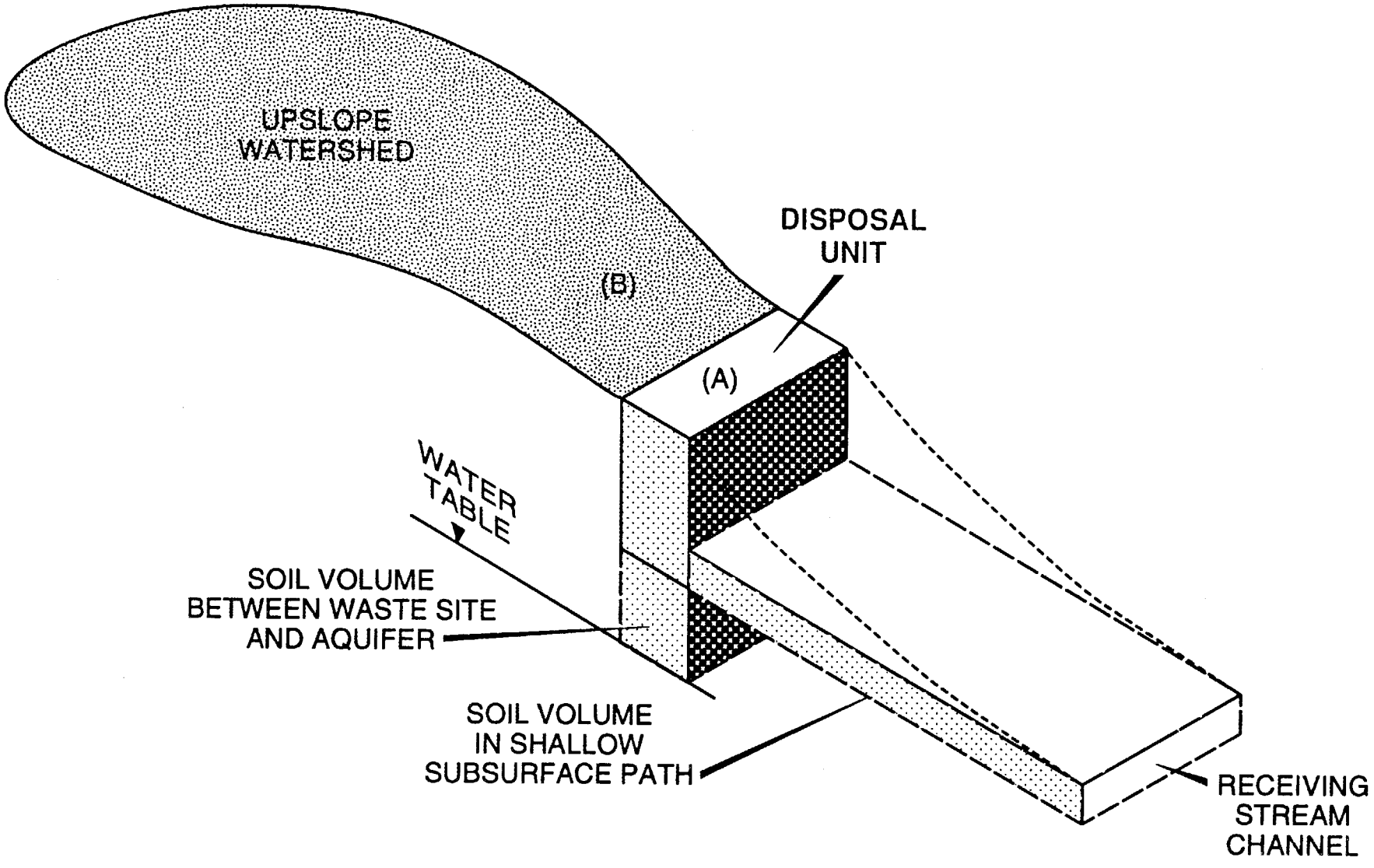

Fig. 3.2. Diagram of a disposal unit area (A) in relation to its upslope watershed area (B) and the soil volumes in the vertical path to groundwater and the lateral path to a receiving stream channel.

Table 3.6. Disposal units in Solid Waste Storage Area 6 showing number of units, containment area, and the upslope area draining directly into each site[a]

Waste site	Number of units	(*A*) Containment area per unit (m^2)	(*B*) Upslope area per unit (m^2)	*B/A*
Low-range silos–north (TLN)	23	10	26	2.6
Low-range silos–south (TLS)	90	10	30	3.0
High-range silos (TH)	50	10	37	3.7
Asbestos silos (TA)	17	10	70	7.0
Tumulus I (TUM1)	1	466	559	1.2
Tumulus II (TUM2)	1	356	1388	3.9
Interim Waste Management Facility (IWM1)	1	356	1566	4.4
High-range wells/silos (THW)	6	10	0	0.0
High-range wells (WHA)	12	1	0	0.0
Fissile wells (WF)	1	1	20	20.0
Biological trenches (TB)	6	47	329	7.0

[a]The ratio *B/A* was used to calculate the quantity of upslope subsurface flow entering a disposal unit site.

concentration in the flow paths (Solomon et al. 1992). Matrix diffusion acts as a buffer that "smears out" the transport of chemicals by diffusive uptake of solutes from flow paths into the microporosity of the matrix. Solutes are later released as a secondary source from the matrix after the chemical concentration from the primary source (e.g., leaking silo) declines. Annual time steps were adopted for chemical transport in the stormflow zone, and a quasimatrix diffusion effect was provided by mixing the new input of chemical in a given year with the soil solution that was retained by capillary forces in the flow path (field capacity) in previous time steps. There was no allowance for any bypass (macropore) flow in the transport of chemical to groundwater or to surface water through the

stormflow zone, which resulted in all of the soil being effective in chemical adsorption. These approximations avoided the need for the application of a three-dimensional finite-element transport model for each disposal unit, which was viewed as unjustified given the uncertainties in both the nuclide inventory estimates and the parameter values used in waste containment degradation.

Recharge to groundwater has been estimated from water budget and modeling methods that provided values in the range of 1–7 cm/year (0.4–3 in./year) (Tucci 1986, Bailey and Lee 1990, Solomon et al. 1992). These estimates were used as a guide for comparison with simulations obtained with the UTM hydrologic model. The extensive disturbance from trench excavation and well drilling has very likely increased recharge at the facility (see Sect. 2.1.3).

3.3.2.2 Aquifer Properties

For purposes of performance assessment groundwater modeling, the following assumptions were made concerning the aquifer:

- **Water table.** The water table is variable within a nominal thickness of 4 m (12 ft) to 5 m (15 ft). This thickness is consistent with published data and enabled calibration of the flow model to the water table norm (above) under recharge constraints.
- **2% porosity.** This value was determined in tests at the Engineered Test Facility (ETF) and was used in aquifer simulations for ETF.
- **Homogeneous hydraulic conductivity.** A value of 1.2×10^{-4} cm/s (3.9×10^{-6} ft/s) was used. This value was obtained from computer simulations in which calculated head values were calibrated to measured heads (see Sect. 4.3). While higher than the mean value reported for the Consauga Group in Melton Valley (Solomon 1992), it is the value that produced the closest agreement between measured and calculated head surfaces. The aquifer is heterogeneous; however, the geographic distribution of data at the site does not permit deterministically prescribing heterogeneous conductivity at a scale consistent with realistic variations or with the scale of modeling performed.
- **Anisotropy.** Anisotropy of 3:1 parallel to strike was used. This ratio is consistent with the observed drawdown pattern from a pump test performed at the ETF site and results in flow vectors consistent with the observed movement of solute at SWSA 6.

3.3.2.3 Retardation

Values for distribution coefficients (K_d) of nuclides on the soils of SWSA 6 were obtained or estimated from published research; values are given in Table 3.7.

The K_d value of zero was selected for H, C, Cl, and Tc because the soluble anion forms of these nuclides were not expected to adsorb onto soil. The K_d for Cd was obtained from Turner and Steele (1988), and the value for Ni was obtained from Swanson (1983). The K_d values for the remainder of the nuclides were based on the recommendations of Friedman and Kelmers (1990). In all cases the K_d values were obtained with equilibrium methods using soil material from the facility or from the same soil type.

These K_d values were used in transport calculations through the stormflow zone to surface water and in the transport of nuclides into the groundwater through the vadose zone. The K_d values were applied to a soil volume estimated to occur between the individual disposal units and the nearest stream channel or water table as appropriate for lateral flow and recharge calculations (Table 3.5). Jardine et al. (1993) have shown that K_d values obtained by equilibrium methods apply well for representing adsorption during unsaturated flow for many radionuclides, even if the flow is close to saturation.

The retardation characteristics of the bedrock in SWSA 6 were estimated by Friedman and Kelmers (1990). These data (Table 3.7) were taken as a basis for a distribution of possible values of K_d, assuming it is a random variable. The distribution of values for K_d for each isotope was, then, based on laboratory data. For many of the radionuclides in Table 3.7, the values used in the analysis are substantially less than values measured in the field (Sheppard and Thibault 1990; Trabalka and Garten 1983).

Retardation factors have a major influence on all components of the transport analysis. For the groundwater component, larger values of K_d effectively slowed the advective transport so that diffusion was an important factor for very large values for time. Extreme values, as used in the uncertainty analysis (Sect. 4.6), resulted in very large transport times, probably well beyond any range of validity for the modeling.

3.3.3 Wastes

The release of radionuclides is influenced by the water saturation of a disposal unit (i.e., the waste and concrete containment). In this study, the relative saturation of waste (volume of H_2O/volume of waste), or H_w [as given in Eq. (C.1)] is taken to be equal to the void fraction of the waste. In other words, the pores in the waste are full of water or saturated. Further, the fraction of pore capacity to hold liquid that is filled, or H [as given in Eq. (C.3)], is assumed to be unity. In other words, the pores in the concrete (and waste) are saturated with water. The assumption that a disposal unit (waste and concrete containment) is saturated represents conservatism in that it gives the largest release by advection and diffusion with all other parameters being fixed.

Each disposal unit was assumed to be a uniform composition (i.e., homogeneously heterogeneous in a engineering sense). The waste was taken to have an average open-pore void fraction of 0.27, and the concrete, of 0.15. The shapes and dimensions of the disposal units are given in Sects. 2.3.5 and 2.3.6.

The radionuclides were assumed to be transported through the disposal units (i.e., waste and concrete) by advection and diffusion. The transport properties are presented in Appendix C.

3.4 PERFORMANCE ANALYSIS METHODOLOGY

This section presents the method for analyzing the transport and exposures to radionuclides disposed of in SWSA 6. The method utilizes models of the site and the transport of radionuclides in the environment. The methods for calculating doses for exposures to radionuclides from transport in the environment and from direct intrusion

Table 3.7. Half-life, specific activity, and distribution coefficient (K_d) values of radionuclides simulated in the performance assessment of Solid Waste Storage Area 6

Nuclide	Half-life (years)	Specific activity (Ci/g)	K_d (mL/g)
^{3}H	12.3	9650	0
^{14}C	5730	4.46	0
^{26}Al	720000	0.0191	3000
^{36}Cl	301000	0.033	0
^{60}Co	5.27	1130	3000
^{63}Ni	100	61.7	2000
^{90}Sr	28.5	136	30
^{99}Tc	213000	0.017	0
^{113m}Cd	13.7	217	200
^{137}Cs	30	87	3000
^{152}Eu	13.3	173	3000
^{154}Eu	8.8	270	3000
^{155}Eu	4.96	465	3000
^{226}Ra	1600	0.989	3000
^{229}Th	7340	0.213	40
^{230}Th	75400	0.0211	40
^{232}Th	14100000000	0.00000011	40
^{232}U	68.9	21.4	40
^{233}U	159000	0.00968	40
^{234}U	245000	0.00625	40
^{235}U	704000000	0.00000216	40
^{236}U	23400000	0.0000647	40
^{237}Np	2140000	0.000705	40
^{238}U	4470000000	0.000000336	40
^{238}Pu	87.7	17.1	40
^{239}Pu	24100	0.0622	40
^{240}Pu	6560	0.228	40
^{242}Pu	376000	0.00382	40
^{241}Am	433	3.43	40
^{243}Am	7380	0.199	40
^{243}Cm	28.5	51.6	40
^{244}Cm	18.1	80.9	40
^{249}Cf	35.1	4.1	40

are discussed. Verification and validation of models used in the performance assessment are also described.

3.4.1 Overview of Analysis

The performance analysis was based on data available on the waste disposed of at SWSA 6, the disposal methods used at SWSA 6, and SWSA 6 site characteristics. Assumptions were made when data needed were unavailable. All assumptions were conservative and representative of the ORR. These assumptions are discussed in Sect. 3.3.

The analysis is based on the determination that surface water and groundwater are the significant pathways for transport of radionuclides from disposal units. The pathways for exposure—either of off-site individuals and inadvertent intruders due to radionuclides in contaminated water or of inadvertent intruders resulting from direct intrusion into disposal units—are discussed in Sect. 3.2.4.

Simulations of the release of radionuclides from disposal units and subsequent transport in water were carried out using six computer codes—UTM, SOURCE1, SOURCE2, WELSIM, TUMSIM, and U.S. Geological Survey Method of Characteristics (USGS MOC). All codes are written in standard Fortran and run on Digital Equipment Corporation VAX (UTM only) or Hewlett-Packard HP9000 computer hardware. The relationship between the codes is shown schematically in Fig. 3.3.

Both UTM, a hydrologic transport model, and USGS MOC, a model for solute transport and dispersion in a saturated porous medium, are approved by the U.S. Department of Energy code center. The SOURCE1 and SOURCE2 codes were developed for estimating the release of radionuclides from porous waste forms using advection and diffusion models and are described in Appendix B. The TUMSIM code describes lateral subsurface nuclide transport through the stormflow zone and transport to groundwater through recharge from the tumulus or IWMF disposal units. These units consist of concrete pads loaded with concrete vaults containing nuclide wastes. Shallow subsurface transport and nuclide flux to groundwater from all other sites (wells, silos, and trenches) was simulated with WELSIM. The TUMSIM and WELSIM codes use annual time-step simulations of nuclide transport and account for nuclide-adsorption on the subsurface soil materials and radioactive decay of nuclides (Appendix D.2).

Each code had specific uses in SWSA 6 modeling. The UTM code was used to model the site water budget. SOURCE1 and SOURCE2 were used to compute leachate generation and movement from the disposal units and to predict contaminant release from the units over time. The TUMSIM and WELSIM codes predict transport and retention of nuclides in the shallow subsurface in both the stormflow zone and in recharge to the aquifer. The USGS MOC program was used to simulate flows in the saturated zone and to predict contaminant transport in groundwater. The discharge of nuclides from the shallow subsurface, calculated by TUMSIM and WELSIM, and from groundwater, calculated by USGS MOC, were combined to give the total transport to surface water. The surface transport values were used in dose assessment calculations.

ORNL-DWG 93-16528

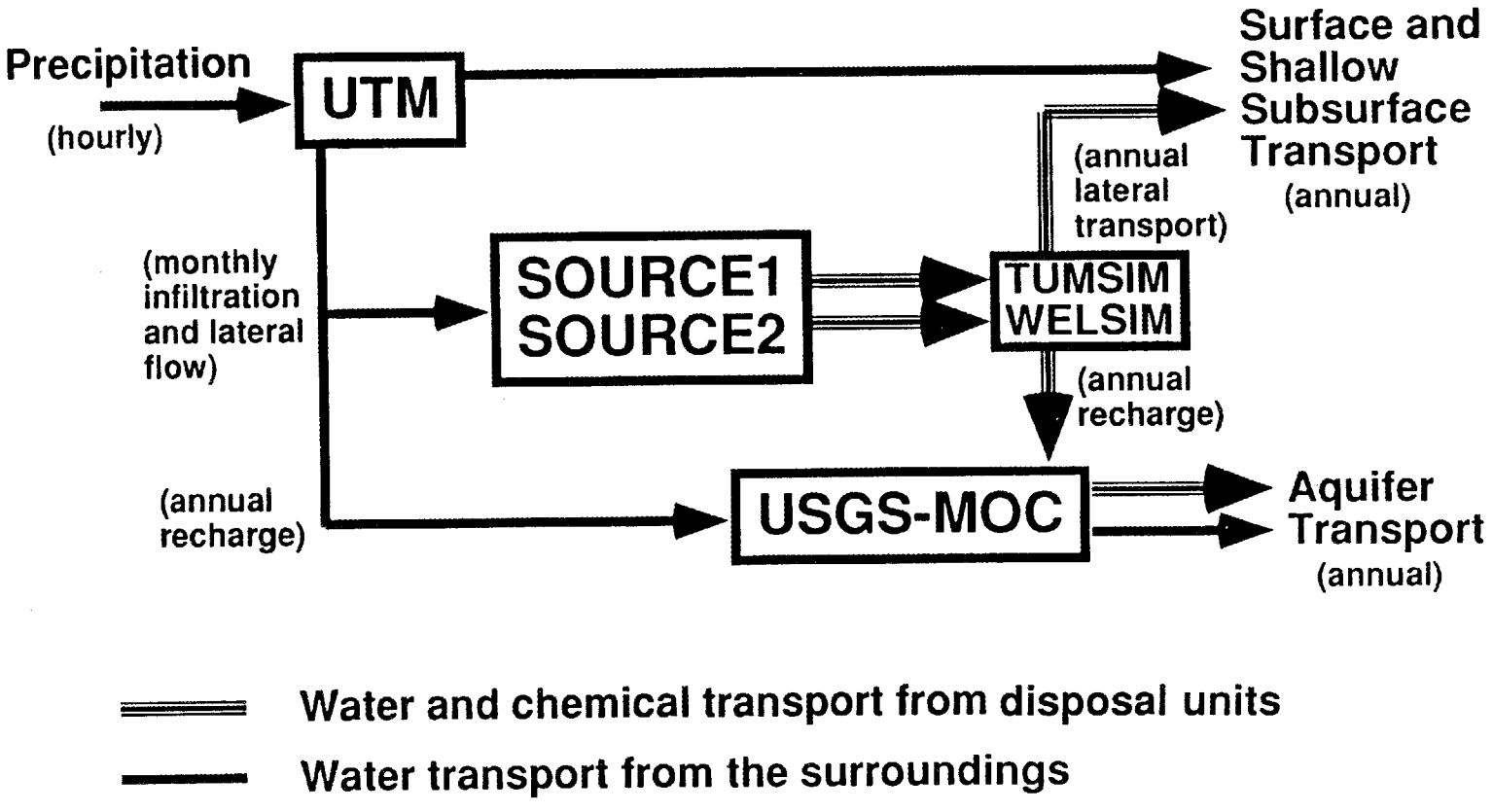

Fig. 3.3. Linkage of contaminant transport models for performance assessment of Solid Waste Storage Area 6.

3.4.2 Site Hydrology

Historical precipitation records for the Oak Ridge area were reviewed, and data representative of dry, average, and wet years were selected. Water budget simulations were run for these three contrasting climate years to examine a range of climatic phenomena. For the dose assessment the average climate conditions were used.

Characteristics of vegetation and soil conditions were input to UTM to represent the site during all phases of the closure scenario (Sect. 3.2.3 and Appendix D.1). Soil, during the active operations period, was modeled as disturbed and uncovered, during institutional control, as covered by mown grass or other shallow-rooted vegetation, and during post-institutional control, as forested. The UTM simulation included variations in the integrity of compacted soil caps during institutional control, and the site was modeled with both functional and leaking caps (see Sect. 3.2.3 and Appendix D.1).

The UTM simulations predicted total annual surface and shallow subsurface water flow in each disposal site for dry, wet, and average years during the time periods of interest. In addition, recharge for each disposal unit in the same time periods was predicted. The climate conditions used by UTM included the effects of storms (hourly precipitation) for dry, wet, and average years.

3.4.3 Facility Performance

The source term for pathways analysis at SWSA 6 was based on the volume and characteristics of the waste disposed of at the facility. The characteristics of the waste include an inventory of specific radionuclides, their chemical form, and total curies by type of disposal unit. Total water per month available at each disposal unit was predicted by the UTM code using soil and vegetation characteristics that were adjusted for the changing conditions of the closure scenario. In the current analysis, values for an average precipitation year were used for nuclide transport. The influence of variation in hydrologic flows on nuclide transport is addressed in the section dealing with uncertainty.

The SOURCE1 and SOURCE2 codes were used to predict radionuclide release over time from individual disposal units. Input for disposal units included initial conditions and dimensions of each unit type—silo, well, and tumulus (Appendix B). The model included radioactive decay, advection, and diffusion through concrete for each radionuclide in the waste. The solubility of each radionuclide in the unit was based on its chemical form. Retardation contributed by other waste materials in the unit was not included in the analysis. For each unit type considered, the simulations predicted cumulative leached amounts as a function of time for each radionuclide in the unit. For the tumulus and IWMF disposal units, no credit was taken in the analysis for the pad drain collection systems. The pad drain collection system has been shown to be effective in removing leachate from these disposal units during active use and prior to facility closure, as discussed in Sect. 2.1.3. The advective release of contamination from disposal vaults occurs after structural failure of the vaults. This failure is considered to occur after the drainage system becomes clogged and ineffective. The existing french drain system in SWSA 6 has been shown to be less effective over time. Therefore, the omission of the pad drain collection system from the analysis of performance is not considered to have a significant effect on the results presented in Sect. 4.

3.4.4 Shallow Subsurface Transport

Hydrologic and water budget simulations were conducted with UTM to provide surface runoff, drainage, and lateral flow of water in response to hourly inputs of precipitation. The model accounted for the nonlinear flow dynamics using variable time steps as needed (the smallest was 0.5 min and the longest was 60 min). These flow values were summed to give monthly values that were used in the simulation of chemical leaching from disposal units with the SOURCE1 and SOURCE2 models and in the groundwater simulations with USGS MOC (Fig. 3.3).

The soil and vegetation characteristics used in the hydrologic simulations were based on input data available from the site or from sources with similar soil and plant attributes. More specific aspects of the water budget modeling are outlined in Sect. 3.4.7.

Nuclide leaching from the disposal units predicted by the SOURCE1 and SOURCE2 models is taken as input to the TUMSIM and WELSIM codes for simulation of nuclide transport through the lateral shallow subsurface (stormflow) path and the drainage into the groundwater (recharge). The TUMSIM and WELSIM codes account for the position of the disposal units in the landscape and the distances from the disposal units to the nearest receiving stream channels for subsurface discharge and to the water table. These aspects have been described in Sect. 3.3.2.1 and summarized in Fig. 3.1 and Tables 3.5 and 3.6. Fluctuations in water table elevation due to seasonal changes in water budgets and anticipated effects of changing land covers for the closure scenario (Sect. 3.2.3) were not considered in calculations performed in this performance assessment. The uncertainty due to fluctuating water tables is considered in the uncertainty analysis (Sect. 4.6.1.3). The calculated results and the results of the uncertainty analysis are used in the interpretation of results (Sect. 4.7). The TUMSIM and WELSIM codes account for nuclide adsorption (see Sect. 3.3.2.3, Table 3.7) and radioactive decay during transport. Further descriptions of these models are given in Sect. 3.4.8.3.

3.4.5 Transport in Groundwater

Groundwater flow in the saturated zone at SWSA 6 was modeled with the USGS MOC code. The flow values were combined with recharge and chemical transport values from TUMSIM and WELSIM to predict direction and concentration of contaminant flow in the groundwater at SWSA 6.

Input to the MOC code was site-specific. Historical water elevation data from wells in the SWSA 6 area were integrated to produce an average water table, which was used as the initial condition for hydraulic head in the simulations as well as a norm for hydraulic parameter determination. Groundwater recharge values at a disposal unit were those predicted from the UTM, TUMSIM, and WELSIM codes. Diffuse recharge over the entire area was adjusted to conserve mass and to match the data-derived hydraulic head surface. Hydraulic conductivity parameters were derived from recent measurements at SWSA 6 (Bechtel 1989); other parameters were based on measurements or derived from modeling and tracer test results in similar geological materials at Bear Creek Valley (Lee and Ketelle 1989).

To enhance the site specificity of the simulation, the flow equation in the MOC code included driving terms to match conditions at SWSA 6. The flow equation in the MOC code was adjusted to reflect the integrated head surface constructed from the historical data, keeping intact important hydrological sinks, sources, and barriers known from site data. Furthermore, to more realistically simulate the monitored closure and postclosure scenarios described in Sect. 3.2.3, the MOC code was modified to allow input of time-dependent boundary and recharge conditions (see Appendix E).

Transport in the groundwater was modeled principally as advective flow, with small dispersivity added to allow for heterogeneities in the system. A best estimate of retardation in the saturated zone was included in the simulation (Sect. 3.3.2.3). The modeling methods followed those used successfully in the contaminant transport model validation study at Bear Creek Valley (Lee and Ketelle 1989), and the resultant flow field was consistent with those results.

Contaminant plumes, updated every simulation year, were tracked assuming continuous source terms supplied from the TUMSIM and WELSIM recharge simulations and the UTM surface and shallow subsurface transport simulations. The MOC code predicted transport in the groundwater for each radionuclide, including concentration-arrival times at given points within SWSA 6 and at the SWSA 6 boundary outflows. For ^{238}U, having extremely long release times, an analytic element was used in place of MOC. The analytic code also was used for sensitivity analysis of ^{232}Th. (Details are described in Appendix E.)

3.4.6 Transport to Surface Water

The chemical outflows to surface water calculated from the shallow subsurface (TUMSIM, WELSIM) and groundwater (USGS MOC) modeling were combined to give the total chemical flux from SWSA 6 on an annual basis. The mean annual concentration of nuclides released from SWSA 6 was calculated as the ratio of the annual chemical flux and the annual surface water flux from SWSA 6. The UTM hydrologic simulations provided estimates of the annual surface water fluxes for a range of precipitation conditions (dry, average, and wet). Summary information on the annual nuclide fluxes and mean annual nuclide concentration was used in the dose assessment calculations.

3.4.7 Dose Estimation

Results from the models used to estimate release of radionuclides from disposal units and transport in the environment provide estimates of radionuclide concentrations in surface water and groundwater as a function of time after disposal. These concentrations provide input to the exposure pathway models for estimating (1) dose to off-site individuals and inadvertent intruders from all exposure pathways involving use of contaminated water and (2) dose from consumption of contaminated groundwater or surface water by the drinking water pathway only.

Results from the models for estimating the release of radionuclides could be used to estimate radionuclide concentrations in disposal units as a function of time. These concentrations could provide input to models for estimating doses to inadvertent intruders. However, for reasons described in Sect. 4.5.3.2, the eventual depletion of radionuclide

inventories in disposal units by leaching of wastes has not been included in the dose analysis for inadvertent intruders. The models for estimating dose per unit concentration of radionuclides in water or in solid waste in disposal units are described in detail in Appendix G.

Exposure of members of the public beyond the site boundary can occur at any time during the operations, institutional control, and post-institutional control periods. Maximum annual EDEs to off-site individuals resulting from use of contaminated surface water at the site boundary were estimated on the basis of the predicted maximum concentrations of radionuclides in surface water. Maximum annual effective equivalents from direct consumption of contaminated groundwater are based on the predicted maximum concentrations of radionuclides in groundwater at any locations more than 100 m (328 ft) from any disposal unit at any time after disposal. Although active institutional controls are assumed to exclude individuals from the disposal site for 100 years after disposal, the requirement for groundwater resource protection outside the 100-m (328-ft) buffer zone is assumed to apply at any time after disposal. Predicted concentrations of radionuclides remaining in disposal units after loss of active institutional control at 100 years after disposal were used to estimate maximum EDEs to inadvertent intruders resulting from direct intrusion into each type of disposal unit. As described in Sect. 3.2.4, direct intrusion is assumed to occur at 100 or 300 years after disposal, depending on the particular exposure scenario and design of the disposal units. An intruder dose analysis is performed separately for each type of disposal unit.

3.4.8 Verification and Validation of Methodology

Verification and validation of the codes used in the performance assessment for SWSA 6 are necessary to assure that the results presented are meaningful. To the extent reasonable, the codes used in this performance assessment have been verified and validated and are discussed in this section. Verification is considered to mean that the codes are correct in a mathematical and numerical sense and that the theory incorporated into the codes is correct. Validation is considered to mean that the application of the code to the SWSA 6 facility is a reasonable representation of the site. The verification and validation efforts to date are not complete; however, providing unequivocal assurance that the codes used for this performance assessment are verified and validated is not reasonable because data characterizing the long-term performance of the engineered disposal technologies in SWSA 6 are not available.

SWSA 6 has been used as a disposal facility for many years, and (as noted in Sect. 2.1) small amounts of contamination are being released to surface water from disposal units used prior to September 26, 1988. Validating the model of site performance using current monitoring data was considered but abandoned because the data describing the inventory of the disposed wastes is of limited value in developing a representative source term.

3.4.8.1 Verification and Validation of UTM

UTM has been under development for over two decades and has been applied in a range of locations, including North Carolina, Missouri, Oklahoma, and Tennessee. Water

budget simulations involve algorithms for various components of the hydrologic cycle (Appendix D). These algorithms are based on well established physical and physiological relationships. UTM is used in the performance assessment for simulation of water budgets for various conditions of the SWSA 6 site during operation and closure and after closure. The paragraphs that follow outline the components of water budget calculations in UTM.

Interception. A defined volume for water caught in the canopy and litter that varies for the winter and summer seasons and is filled with rainfall before throughfall enters the soil. Water in this storage has priority in evaporation calculations. The storage volumes were adjusted for deciduous forests so that simulated interception matched the empirical observations of Helvey and Patrick (1965). This model development and testing is described on pages 17–20 of Huff et al. (1977). Input values for simulations with grass cover were obtained from a previous application (Luxmoore and Sharma 1980).

Infiltration. The time-compression method of Reeves and Miller (1977) has been implemented in UTM to partition throughfall into infiltration and surface runoff at the soil surface. Reeves and Miller describe the algorithm and have tested the method. This algorithm is not often invoked in forest simulations due to the high infiltration rates of forest soils. Runoff in forested watersheds is generally the result of exfiltration of subsurface flow in lower slope positions. Huff et al. (1977) describe the method on pages 20–23 of the documentation report for the UTM hydrologic module.

Evapotranspiration. The complex of evaporative surfaces (foliage, litter, and soil) in a vegetated landscape is viewed as one surface in a "big leaf" approach for which the Penman-Monteith equation determines evapotranspiration. Sinclair et al. (1976) demonstrated the utility of this approach for calculation of evapotranspiration. A number of meteorological variables (air temperature, vapor pressure, solar radiation, and wind speed) are needed along with an empirical surface resistance to vapor loss from the surface. This resistance was obtained from experimental observations for the vegetation of interest (Luxmoore et al. 1978, Luxmoore and Sharma 1980). The algorithms are described on pages 24–26 of Huff et al. (1977). Luxmoore and Huff (1989) showed that the calculations of forest evapotranspiration are in agreement with independent estimates for the Oak Ridge area.

Recharge and Subsurface Lateral Flow. The Darcy flow equation was used in soil water-flow calculations to estimate water movement between soil layers. (The parameters for the layers of soil in question are specified by the user.) The equation uses a hydraulic gradient and hydraulic conductivity that are determined from soil hydraulic properties. These properties (water pressure–water content and hydraulic conductivity–water content relationships) are based on input values chosen by the user for the site of interest. Pages 26–33 of Huff et al. (1977) describe the flow equations and the use of soil hydraulic properties. The calculation of recharge to groundwater uses a hydraulic gradient of unity and a hydraulic conductivity appropriate to the water content of the lowest layer of the soil profile being simulated. Lateral flow is calculated as the excess of soil water above the saturation value flowing into a soil layer from above. Algorithms for bypass flow, due to macropores, are an option in the soil water-flow calculations. The basis for the macropore flow option is described on pages 25–31 of Hetrick et al. (1982).

Simulation of Water Budgets for Soil-Plant Systems. UTM has been applied to a range of sites, and reasonable agreement has been obtained for the components of the water budgets at the sites as follows:

Grassland watersheds in Oklahoma. Results are published in open literature in Sharma and Luxmoore (1979), Luxmoore and Sharma (1980), and Luxmoore (1983a). These results show the utility of UTM for grassland conditions, which are part of the SWSA 6 closure scenario.
Forested watershed on the ORR. Open literature publications of UTM applications to forest stands of the ORR are given in Luxmoore et al. (1978), Luxmoore et al. (1981), and Luxmoore (1983b).
Scenarios of Landfill Barrier Designs. A report discusses the hydrologic behavior of four alternative cap designs simulated with UTM (Luxmoore and Tharp 1993).
Forested watershed in southeastern Missouri. Simulation of water budgets and heavy metal transport in a watershed adjacent to a lead mining and smelter operation was reported in Luxmoore and Begovich (1979).

The experience gained from these studies provides a sound basis for simulation of water budgets for SWSA 6 operation and closure scenarios. Several sensitivity analysis reports have also been prepared, and these have given a thorough appreciation for the important vegetation and soil variables in water budget simulation. These reports are Luxmoore et al. (1976), Begovich and Luxmoore (1979), Luxmoore et al. (1981), and Sharma et al. (1987).

3.4.8.2 Verification and Validation of SOURCE1 and SOURCE2

The description of the SOURCE1 and SOURCE2 codes is provided in Appendix B. These codes were developed for application to SWSA 6 and have not been subjected to comprehensive verification and validation exercises. At this stage of development, the codes are research codes for a unique application and warrant additional development prior to being considered verified and validated for application to SWSA 6. The development of these codes was deemed necessary to provide a reasonable representation of the performance of the disposal units at SWSA 6 that could not be represented by existing codes that have been subjected to more extensive development. A primary impediment to the validation of these codes is the absence of performance data for the disposal units considered in the performance assessment. Future revisions of the SWSA 6 performance assessment will address the efforts to verify and validate the SOURCE1 and SOURCE2 codes for application to SWSA 6.

3.4.8.3 Verification and Validation of TUMSIM and WELSIM

TUMSIM and WELSIM are custom-written FORTRAN codes prepared for this performance assessment. The codes describe radionuclide retardation (K_d) and radionuclide decay in annual time-step calculations of subsurface radionuclide transport from waste sites (Fig. 3.2). Radionuclide migration from each disposal unit was represented in relation to its position in the landscape using topographic characteristics to estimate transport distances between disposal units and groundwater and the nearest surface water drainage as outlined in Sect. 3.3.2.1 (Fig. 3.1, Table 3.5). TUMSIM was used to simulate transport from Tumulus I, Tumulus II, and the IWMF; and WELSIM,

transport from the other disposal facilities (wells, silos, and trenches), for which the numbers of units varied over time during the active-sites period (Appendix D.2).

There are only two mechanistic equations in each of these two codes. One is for chemical adsorption onto soil; the other is for half-life decay calculations. Jardine et al. (1993) have demonstrated that the chemical adsorption calculations with K_d are an appropriate representation of adsorption in unsaturated flow systems. The radionuclide decay calculations were based on the well-accepted half-life equation and the well-known half-life values for the various nuclides (Table 3.7).

3.4.8.4 Verification and Validation of USGS MOC

The USGS MOC code was developed initially in 1974 and has been subjected to extensive development since its first release. The code has been used for numerous applications and has been verified mathematically, numerically, and experimentally throughout the period of development. The application of the USGS MOC code to a complex heterogeneous setting such as SWSA 6 involved the careful construction of a conceptual model for SWSA 6 and its application to the site using the available site data. The approach taken has not been validated directly to the SWSA 6 site but has been the subject of a validation study on the ORR at a site with a nearly identical hydrogeologic setting in Bear Creek Valley (Lee and Ketelle 1988, Lee et al. 1989, Lee et al. 1991). The validation study involved the modeling of a tracer placed at the water table. The investigation demonstrated that the flow, direction, and concentrations of the tracer could be reasonably modeled using an application of the USGS MOC code. The results from the validation study in Bear Creek Valley provide justification that the application of the USGS MOC code to SWSA 6 is valid.

4. RESULTS OF ANALYSIS

This section presents (1) the results of the analysis performed using the methodology presented in Sect. 3, (2) the sensitivity and uncertainty of these results, and (3) the interpretation of the results for compliance with the performance objectives of U.S. Department of Energy (DOE) Order 5820.2A. Changes in waste management operations to meet the performance objectives and continued work on this performance assessment also are presented. The inventory used in the analysis presented in this section is presented in Appendix A, Tables A.13–A.21. The most probable or best estimate values were used in preparing the results presented in Sects. 4.1–4.5. The maximum and minimum values were used in the uncertainty analysis presented in Sect. 4.6.

4.1 SOURCE TERMS

The source terms calculated using the SOURCE1 and SOURCE2 programs provide the decayed amount of each nuclide leached as a function of time for each of the disposal units. These units include a tumulus vault [representative of a vault at the Tumulus I and Tumulus II facilities and the Interim Waste Management Facility (IWMF)], asbestos silos, low-range silos, high-range silos, biological trenches, fissile wells, and high-range wells. Table 4.1 provides an abridged illustration of an output file. Similar tables that illustrate abridged output files for Tumulus I, Tumulus II, high-range silos, high-range wells in silos, and biological trench are given in Tables F.1–F.5 in Appendix F. These amounts are the source terms used in shallow subsurface transport and groundwater models for Solid Waste Storage Area (SWSA) 6. Table 4.1 also presents the amounts of the selected radionuclide estimated to be in the specified storage unit at the end of each year. The program calculates this running inventory by difference [i.e., leached amount subtracted from original amount (corrected for decay)]. Figures F.1–F.17 in Appendix F illustrate the flux of radionuclides released from the various disposal units over time using the SOURCE1 and SOURCE2 codes. The figures illustrate the period of advection and diffusion in the absence of structural cracking that occurs over a period of approximately 50–250 years. Following this period, structural cracking occurs with an associated increase in advection-controlled releases. These releases are sustained until the inventory is exhausted. Releases by advection and diffusion are affected by the solubility limits of the radionuclides subject to transport. Release rates are reduced until the distribution coefficient (K_d) controlled release rate (see Sect. 4.7.1.1) is less than or equal to the solubility limit. The radionuclides presented in Appendix F include all those that were considered in detail in the transport of radioactivity in the environment.

Table 4.1. Abridged[a] output summary for Solid Waste Storage Area 6 high-range silos[b]

Year	Inventory (g)	Annual amount leached (g/year)		
		Advection	Diffusion	Total
1	7.96×10^{-3}	1.14×10^{-10}	0.00×10^{0}	1.14×10^{-10}
10	6.47×10^{-3}	9.30×10^{-10}	7.77×10^{-23}	9.30×10^{-10}
20	5.13×10^{-3}	1.48×10^{-9}	1.39×10^{-14}	1.48×10^{-9}
30	4.07×10^{-3}	1.76×10^{-9}	6.77×10^{-12}	1.76×10^{-9}
40	3.23×10^{-3}	1.86×10^{-9}	1.35×10^{-10}	1.99×10^{-9}
50	2.57×10^{-3}	1.84×10^{-9}	7.49×10^{-10}	2.59×10^{-9}
60	2.04×10^{-3}	1.46×10^{-9}	1.84×10^{-9}	3.30×10^{-9}
70	1.62×10^{-3}	1.16×10^{-9}	3.22×10^{-9}	4.38×10^{-9}
80	1.28×10^{-3}	9.22×10^{-10}	4.57×10^{-9}	5.50×10^{-9}
90	1.02×10^{-3}	7.32×10^{-10}	5.67×10^{-9}	6.40×10^{-9}
100	8.08×10^{-4}	5.81×10^{-10}	6.39×10^{-9}	6.97×10^{-9}
110	6.42×10^{-4}	4.61×10^{-10}	6.72×10^{-9}	7.18×10^{-9}
120	5.09×10^{-4}	3.66×10^{-10}	6.72×10^{-9}	7.09×10^{-9}
130	4.04×10^{-4}	2.90×10^{-10}	6.46×10^{-9}	6.75×10^{-9}
140	3.21×10^{-4}	2.30×10^{-10}	6.03×10^{-9}	6.26×10^{-9}
150	2.54×10^{-4}	1.83×10^{-10}	5.49×10^{-9}	5.67×10^{-9}
160	2.02×10^{-4}	1.45×10^{-10}	4.90×10^{-9}	5.05×10^{-9}
170	1.60×10^{-4}	1.15×10^{-10}	4.31×10^{-9}	4.43×10^{-9}
180	1.27×10^{-4}	9.14×10^{-11}	3.74×10^{-9}	3.83×10^{-9}
190	1.01×10^{-4}	7.25×10^{-11}	3.21×10^{-9}	3.28×10^{-9}
200	8.00×10^{-5}	5.75×10^{-11}	2.73×10^{-9}	2.79×10^{-9}
210	6.35×10^{-5}	4.56×10^{-11}	2.30×10^{-9}	2.35×10^{-9}
220	5.04×10^{-5}	3.62×10^{-11}	1.93×10^{-9}	1.97×10^{-9}
230	4.00×10^{-5}	2.87×10^{-11}	1.61×10^{-9}	1.64×10^{-9}
240	2.85×10^{-5}	1.58×10^{-6}	1.26×10^{-9}	1.58×10^{-6}
250	1.32×10^{-5}	7.33×10^{-7}	6.11×10^{-10}	7.34×10^{-7}
260	6.14×10^{-6}	3.40×10^{-7}	2.94×10^{-10}	3.40×10^{-7}
270	2.85×10^{-6}	1.58×10^{-7}	1.41×10^{-10}	1.58×10^{-7}
280	1.32×10^{-6}	7.33×10^{-8}	6.74×10^{-11}	7.34×10^{-8}
290	6.14×10^{-7}	3.40×10^{-8}	3.21×10^{-11}	3.41×10^{-8}
300	2.85×10^{-7}	1.58×10^{-8}	1.53×10^{-11}	1.58×10^{-8}
310	1.32×10^{-7}	7.33×10^{-9}	7.25×10^{-12}	7.34×10^{-9}

Table 4.1 (continued)

Year	Inventory (g)	Annual amount leached (g/year)		
		Advection	Diffusion	Total
320	6.14×10^{-8}	3.40×10^{-9}	3.44×10^{-12}	3.41×10^{-9}
330	2.85×10^{-8}	1.58×10^{-9}	1.62×10^{-12}	1.58×10^{-9}
340	1.32×10^{-8}	7.33×10^{-10}	7.67×10^{-13}	7.34×10^{-10}
350	6.14×10^{-9}	3.40×10^{-10}	3.62×10^{-13}	3.41×10^{-10}
360	2.85×10^{-9}	1.58×10^{-10}	1.70×10^{-13}	1.58×10^{-10}
370	1.32×10^{-9}	7.33×10^{-11}	8.01×10^{-14}	7.34×10^{-11}
380	6.14×10^{-10}	3.40×10^{-11}	3.77×10^{-14}	3.41×10^{-11}
390	2.85×10^{-10}	1.58×10^{-11}	1.77×10^{-14}	1.58×10^{-11}
400	1.32×10^{-10}	7.33×10^{-12}	8.29×10^{-15}	7.34×10^{-12}
410	6.14×10^{-11}	3.40×10^{-12}	3.89×10^{-15}	3.40×10^{-12}
420	2.85×10^{-11}	1.58×10^{-12}	1.82×10^{-15}	1.58×10^{-12}
430	1.32×10^{-11}	7.33×10^{-13}	8.51×10^{-16}	7.33×10^{-13}
440	6.13×10^{-12}	3.40×10^{-13}	3.98×10^{-16}	3.40×10^{-13}
450	2.85×10^{-12}	1.58×10^{-13}	1.86×10^{-16}	1.58×10^{-13}
460	1.32×10^{-12}	7.32×10^{-14}	8.69×10^{-17}	7.33×10^{-14}
470	6.13×10^{-13}	3.40×10^{-14}	4.06×10^{-17}	3.40×10^{-14}
480	2.85×10^{-13}	1.58×10^{-14}	1.89×10^{-17}	1.58×10^{-14}
490	1.32×10^{-13}	7.32×10^{-15}	8.84×10^{-18}	7.33×10^{-15}
500	6.13×10^{-14}	3.40×10^{-15}	4.12×10^{-18}	3.40×10^{-15}
510	2.85×10^{-14}	1.58×10^{-15}	1.92×10^{-18}	1.58×10^{-15}
520	1.32×10^{-14}	7.32×10^{-16}	8.95×10^{-19}	7.33×10^{-16}
530	6.13×10^{-15}	3.40×10^{-16}	4.17×10^{-19}	3.40×10^{-16}
540	2.84×10^{-15}	1.58×10^{-16}	1.94×10^{-19}	1.58×10^{-16}
550	1.32×10^{-15}	7.32×10^{-17}	9.04×10^{-20}	7.32×10^{-17}
560	6.13×10^{-16}	3.39×10^{-17}	4.21×10^{-20}	3.40×10^{-17}
570	2.84×10^{-16}	1.58×10^{-17}	1.96×10^{-20}	1.58×10^{-17}
580	1.32×10^{-16}	7.31×10^{-18}	9.12×10^{-21}	7.32×10^{-18}
590	6.12×10^{-17}	3.39×10^{-18}	4.24×10^{-21}	3.40×10^{-18}
600	2.84×10^{-17}	1.57×10^{-18}	1.97×10^{-21}	1.58×10^{-18}
610	1.32×10^{-17}	7.31×10^{-19}	9.17×10^{-22}	7.32×10^{-19}
620	6.12×10^{-18}	3.39×10^{-19}	4.26×10^{-22}	3.40×10^{-19}
630	2.84×10^{-18}	1.57×10^{-19}	1.98×10^{-22}	1.58×10^{-19}

Table 4.1 (continued)

Year	Inventory (g)	Annual amount leached (g/year)		
		Advection	Diffusion	Total
640	1.32×10^{-18}	7.31×10^{-20}	9.21×10^{-23}	7.31×10^{-20}
650	6.12×10^{-19}	3.39×10^{-20}	4.28×10^{-23}	3.39×10^{-20}
660	2.84×10^{-19}	1.57×10^{-20}	1.99×10^{-23}	1.58×10^{-20}
670	1.32×10^{-19}	7.30×10^{-21}	9.24×10^{-24}	7.31×10^{-21}
680	6.11×10^{-20}	3.39×10^{-21}	4.29×10^{-24}	3.39×10^{-21}
690	2.84×10^{-20}	1.57×10^{-21}	1.99×10^{-24}	1.57×10^{-21}
700	1.32×10^{-20}	7.30×10^{-22}	9.26×10^{-25}	7.31×10^{-22}
710	6.11×10^{-21}	3.39×10^{-22}	4.30×10^{-25}	3.39×10^{-22}
720	2.84×10^{-21}	1.57×10^{-22}	2.00×10^{-25}	1.57×10^{-22}
730	1.32×10^{-21}	7.30×10^{-23}	9.27×10^{-26}	7.30×10^{-23}
740	6.11×10^{-22}	3.39×10^{-23}	4.31×10^{-26}	3.39×10^{-23}
750	2.84×10^{-22}	1.57×10^{-23}	2.00×10^{-26}	1.57×10^{-23}
760	1.32×10^{-22}	7.29×10^{-24}	9.28×10^{-27}	7.30×10^{-24}
770	6.11×10^{-23}	3.38×10^{-24}	4.31×10^{-27}	3.39×10^{-24}
780	2.83×10^{-23}	1.57×10^{-24}	2.00×10^{-27}	1.57×10^{-24}
790	1.32×10^{-23}	7.29×10^{-25}	9.28×10^{-28}	7.30×10^{-25}
800	6.10×10^{-24}	3.38×10^{-25}	4.31×10^{-28}	3.39×10^{-25}
810	2.83×10^{-24}	1.57×10^{-25}	2.00×10^{-28}	1.57×10^{-25}
820	1.31×10^{-24}	7.29×10^{-26}	9.28×10^{-29}	7.29×10^{-26}
830	6.10×10^{-25}	3.38×10^{-26}	4.31×10^{-29}	3.39×10^{-26}
840	2.83×10^{-25}	1.57×10^{-26}	2.00×10^{-29}	1.57×10^{-26}
850	1.31×10^{-25}	7.28×10^{-27}	9.27×10^{-30}	7.29×10^{-27}
860	6.10×10^{-26}	3.38×10^{-27}	4.30×10^{-30}	3.38×10^{-27}
870	2.83×10^{-26}	1.57×10^{-27}	2.00×10^{-30}	1.57×10^{-27}
880	1.31×10^{-26}	7.28×10^{-28}	9.26×10^{-31}	7.29×10^{-28}
890	6.09×10^{-27}	3.38×10^{-28}	4.30×10^{-31}	3.38×10^{-28}
900	2.83×10^{-27}	1.57×10^{-28}	1.99×10^{-31}	1.57×10^{-28}
910	1.31×10^{-27}	7.27×10^{-29}	9.25×10^{-32}	7.28×10^{-29}
920	6.09×10^{-28}	3.38×10^{-29}	4.29×10^{-32}	3.38×10^{-29}
930	2.83×10^{-28}	1.57×10^{-29}	1.99×10^{-32}	1.57×10^{-29}
940	1.31×10^{-28}	7.27×10^{-30}	9.23×10^{-33}	7.28×10^{-30}
950	6.09×10^{-29}	3.37×10^{-30}	4.28×10^{-33}	3.38×10^{-30}

Table 4.1 (continued)

Year	Inventory (g)	Annual amount leached (g/year)		
		Advection	Diffusion	Total
960	2.83×10^{-29}	1.57×10^{-30}	1.99×10^{-33}	1.57×10^{-30}
970	1.31×10^{-29}	7.27×10^{-31}	9.22×10^{-34}	7.28×10^{-31}
980	6.09×10^{-30}	3.37×10^{-31}	4.28×10^{-34}	3.38×10^{-31}
990	2.82×10^{-30}	1.57×10^{-31}	1.98×10^{-34}	1.57×10^{-31}
1000	1.31×10^{-30}	7.26×10^{-32}	9.20×10^{-35}	7.27×10^{-32}
The solubility constraints were not exceeded.				

[a]Abridged means that the results are shown at 10-year intervals instead of the normal 1-year interval.
[b]Nuclide-specific parameters (^{137}C): half-life 3.00×10^{1} years; solubility 1.60×10^{1} mol/L; waste K_d 1.99×10^{1} mL/g; diffusion coefficient of waste 6.80×10^{-12} m²/s; diffusion coefficient of concrete, 5.12×10^{-13} m²/s; initial inventory 8.15×10^{-3} g.

4.2 SHALLOW SUBSURFACE TRANSPORT

The Unified Transport Model (UTM) provided water budget simulations of surface runoff, shallow subsurface flow, and groundwater recharge using inputs of hourly precipitation and daily weather conditions for three selected years. Data from the Oak Ridge Reservation (ORR) for 3 years having high [189.5 cm (74.6 in.)] average [137.2 cm (54 in.)] and low [93.3 cm (36.7 in.)] annual precipitation were used to compare a wide range of simulated hydrologic conditions.

The performance assessment was conducted for a 1000-year duration, divided into three main time periods: an "active use" period (1988–1997), a 100-year "monitored closure" period (1998–2097), and a long "postclosure" period from 2098 to 2989. The vegetation variables for these three periods were adjusted to represent the anticipated changes from disturbed grass surface [leaf area index (LAI) = 2.0] or disturbed gravel surface (LAI = 0.001) during the active-use period, to mown grass (LAI = 4.9) for the 100-year monitored closure period, to forest vegetation (LAI = 4.9) for the postclosure period. Similarly, infiltration properties for the various soil surfaces were modified for the three time periods. Cumulative infiltration for the disturbed surface for the 1988–1997 period was taken as a linear time function increasing from the origin to an infiltration value of 1 mm (0.004 in.) at 16 min, and extrapolated linearly for longer times. This represented a highly impacted soil surface with surface runoff generation during high rainfall periods. The grass and forest of the two later periods were given high infiltration rates, and no surface runoff was calculated in these periods. The attributes of geomembrane caps covering waste sites for 30 years (1998–2027) during the 100-year closure period were described earlier in Sect. 3.2.3.

4.2.1 UTM Hydrologic Simulation Results

The monthly sums of surface runoff, lateral flow, and recharge obtained from the UTM simulations for the dry, average, and wet weather conditions showed seasonal differences. For example, the results for the 1988–1997 period with grass cover showed reduced recharge and lateral flow in the July–November period (Table 4.2) when evapotranspiration was high. This pattern differed for the gravel surface simulation, which had somewhat greater recharge and much greater lateral flow than the grass surface due to reduced evapotranspiration. Surface runoff was simulated only for the active use period (1988–1997) as a result of the low infiltration property selected for this period. Lateral flow exceeded recharge in the quantity of water transported on an annual basis, and the proportion of lateral flow increased as annual precipitation increased from a dry to a wet year.

Recharge was greatly reduced by the geomembrane cap (1998–2027 period) compared to the earlier period, with no lateral flow being generated below the cap and a small amount of recharge being simulated. The values for surface runoff presented in Table 4.2 for the period following 1997 are zero because no infiltrating water interacted with the disposal unit, as was the case prior to 1998 (the upslope watershed was isolated from the disposal unit as shown in Fig. 3.2). The water budget simulations for the period with a geomembrane cap resulted in large lateral flows of drainage water that are not presented in Table 4.2. The geotextile membrane was assumed to allow a small amount of leakage. This temporary cover was followed by a permanent Comprehensive Environmental Response, Compensation, and Liability Act (CERCLA) cap, and the same recharge and lateral flow values were used for a 10-year period in which drainage was controlled by the small amount of seepage through a flexible geomembrane within the cap. In the next 10 years (2038–2047), a linear ramp function was used to estimate the recharge and lateral flow values as explained in Sect. 3.2.3. In the remaining 50 years of the monitored closure period, recharge and shallow subsurface flow increased as a result of complete failure of the cap represented by the macropore flow algorithms of the UTM. The simulation results for the period 2048–2097 (CERCLA cap failure) and for the postclosure period (forest) were the same (Table 4.2), and strong seasonality was shown with high lateral flow in the late winter and spring months.

The monthly water flow values in Table 4.2 are shown on a per unit area basis (mm^3/mm^2) and these values were modified for the landscape position of each disposal unit within SWSA 6—as explained in Sect. 3.3.2.1—to give the estimated water quantity interacting with the chemicals leaking from the disposal units. Monthly values of water entering a disposal unit site were used to simulate the monthly values for radionuclide leakage with the SOURCE1 and SOURCE2 models. These SOURCE1 and SOURCE2 calculations were conducted on the basis of a single disposal unit for the sites with silos, wells, and trenches. The WELSIM code accounted for the changing number of disposal units and their filling schedule. The simulations for Tumulus I and II and the IWMF were conducted on a per pad basis and not on an individual vault basis. The SOURCE1 and SOURCE2 simulations provided monthly nuclide leakage for the various types of disposal units. The SOURCE1 and SOURCE2 codes partitioned the monthly leachate values into groundwater recharge and lateral flow components. Groundwater recharge received all of the chemical leachate up to a maximum recharge rate determined by the product of the

Table 4.2. Groundwater recharge, shallow lateral subsurface flow, and surface runoff simulation results from the Unified Transport Model for three sets of weather conditions (dry, average, and wet) and for three time periods
Each column of simulation results shows twelve monthly values, beginning with January

Time period	Recharge (mm/month)			Lateral flow (mm/month)			Runoff (mm/month)		
	Dry	Average	Wet	Dry	Average	Wet	Dry	Average	Wet
Active use, 1988–1997 (LAI[a] = 2.0, disturbed vegetation)	2.8	15.5	15.5	42.3	70.3	99.5	0.0	18.3	15.1
	14.1	14.0	14.0	19.9	72.8	78.7	1.0	23.9	15.7
	15.5	15.5	15.5	25.0	75.8	125.9	9.7	24.9	90.6
	15.0	15.0	15.0	70.3	52.8	65.3	13.1	37.3	20.7
	15.5	15.5	15.5	28.2	58.2	58.0	8.5	51.0	118.7
	15.0	15.0	15.0	4.2	7.6	40.0	46.0	20.9	58.3
	13.3	12.0	15.3	0.0	0.0	3.3	15.3	87.3	67.1
	7.0	6.6	10.4	0.0	0.0	0.0	18.9	27.7	7.0
	4.5	5.1	5.5	0.0	0.0	0.0	7.5	15.7	20.6
	3.6	4.8	4.4	0.0	0.0	0.0	3.4	17.9	22.6
	2.7	3.9	3.4	0.0	0.0	0.0	7.3	2.8	149.3
	2.4	5.9	8.5	0.0	28.2	82.5	15.2	32.6	85.8
Active use, 1988–1997 (LAI = 0.001, gravel surface)	15.5	15.5	15.5	110.1	71.8	101.8	0.0	18.4	15.3
	14.5	14.0	14.0	22.3	73.9	81.2	1.0	24.2	15.7
	15.5	15.5	15.5	26.6	77.7	128.8	9.9	25.4	90.8
	15.0	15.0	15.0	72.7	54.5	68.7	13.6	37.3	20.9
	15.5	15.5	15.5	47.6	86.5	109.9	8.9	51.5	120.3
	15.0	15.0	15.0	51.6	31.1	76.9	48.5	22.8	60.2
	15.5	15.5	15.5	19.0	57.0	31.1	16.0	90.4	69.7
	15.5	15.5	15.5	9.5	70.5	43.5	20.7	29.7	7.5
	15.0	15.0	15.0	3.1	9.0	10.6	8.3	16.2	21.9
	15.5	15.5	15.5	14.6	30.0	19.9	3.4	18.1	22.7
	15.0	15.0	15.0	16.6	17.7	65.7	7.3	2.8	149.3
	15.5	15.5	15.5	40.8	82.6	121.8	15.4	33.0	86.0

Table 4.2 (continued)

Time period	Recharge (mm/month)			Lateral flow (mm/month)			Runoff (mm/month)		
	Dry	Average	Wet	Dry	Average	Wet	Dry	Average	Wet
Monitored closure, 1998–2027 (exposed geomembrane caps)	0.1	0.5	0.1	0.0	0.0	0.0	0.0	0.0	0.0
	0.1	1.0	0.3	0.0	0.0	0.0	0.0	0.0	0.0
	0.1	4.0	6.3	0.0	0.0	0.0	0.0	0.0	0.0
	0.1	7.9	9.1	0.0	0.0	0.0	0.0	0.0	0.0
	0.2	5.9	6.9	0.0	0.0	0.0	0.0	0.0	0.0
Monitored closure, 2028–2037 (CERCLA[b] caps)	0.3	3.9	4.5	0.0	0.0	0.0	0.0	0.0	0.0
	0.4	2.2	3.6	0.0	0.0	0.0	0.0	0.0	0.0
	0.3	1.4	2.6	0.0	0.0	0.0	0.0	0.0	0.0
	0.3	1.0	1.7	0.0	0.0	0.0	0.0	0.0	0.0
	0.2	0.7	1.0	0.0	0.0	0.0	0.0	0.0	0.0
	0.2	0.6	0.7	0.0	0.0	0.0	0.0	0.0	0.0
	0.1	0.5	0.6	0.0	0.0	0.0	0.0	0.0	0.0
Monitored closure, 2038–2047 (10-year linear ramp for cap failure)									
Monitored closure, 2048–2097 (grass and leaking cap)	3.3	15.5	15.5	0.0	81.9	84.0	0.0	0.0	0.0
	13.3	14.0	14.0	0.0	84.5	94.5	0.0	0.0	0.0
	15.5	15.5	15.5	24.9	97.0	215.6	0.0	0.0	0.0
	15.0	15.0	15.0	73.1	60.9	84.7	0.0	0.0	0.0
	15.5	15.5	15.5	24.9	108.9	139.4	0.0	0.0	0.0
2098+ (forest)	15.0	15.0	15.0	5.6	17.1	35.1	0.0	0.0	0.0
	15.5	15.5	15.5	0.0	0.3	12.5	0.0	0.0	0.0
	14.7	15.5	15.5	0.0	1.6	0.0	0.0	0.0	0.0
	6.3	15.0	15.0	0.0	1.5	0.0	0.0	0.0	0.0
	4.6	15.5	15.5	0.0	0.0	0.0	0.0	0.0	0.0
	3.8	13.6	9.6	0.0	0.0	105.2	0.0	0.0	0.0
	3.4	8.5	15.5	0.0	0.0	166.7	0.0	0.0	0.0

[a]LAI = Leaf Area Index.
[b]CERCLA = Comprehensive Environmental Response, Compensation, and Liability Act.

saturated hydraulic conductivity of the aquifer and a unit hydraulic gradient. The lateral subsurface flow component accounted for any remaining leachate. The monthly values of chemical leaching to groundwater and lateral flow were summed to give annual totals, which were used in WELSIM and TUMSIM calculations.

4.2.2 Nuclide Transport in Shallow Subsurface and to Groundwater

Extensive sets of annual computer results were obtained with WELSIM and TUMSIM for the 87 combinations of nuclides and disposal unit sites that were each simulated for 1000 years. The 1000-year results for chemical transport to groundwater and in lateral flow were each scanned, and the maximum chemical flux in each of the two flow paths along with the years of occurrence were recorded. These values (Table 4.3) show that nuclide transport in the lateral path was approximately an order of magnitude larger than transport to groundwater. Tritium, with a relatively short half-life and no chemical adsorption, showed peak transport rates much earlier than the other nuclides. Very few nuclides showed peak transport rates before the end of the monitored closure period in 2097. The year of peak transport rate was often similar for both groundwater recharge and lateral flow paths. Uranium-238 did not show a peak transport rate during the 1000-year simulation period for the low-range silos (two locations) or the fissile wells.

The simulations showed results that have qualitative agreement with field observations from other disposal facilities on the ORR currently subject to remediation under CERCLA. For example, Wickliff et al. (1989) showed ^{137}Cs, ^{90}Sr, and ^{3}H releases from bathtubbing trenches in SWSA 5 during storm events. Tritium and ^{90}Sr were detected in local streams, whereas ^{137}Cs was strongly adsorbed by soil. Some transport of ^{137}Cs adsorbed on migrating clay colloids is expected. Some of the highest simulated release rates are identified with the low-range silos (south), Tumulus I, and the high-range wells.

4.3 GROUNDWATER

An assessment of potential dose attributable to groundwater contamination requires careful consideration of radionuclides in saturated porous media from disposal units to potential points of exposure. Additionally, groundwater may eventually discharge to surface water along a complex route by which contaminated water may ultimately be drawn from the surface rather than from a well. Thus, the analysis accounts for solute concentrations as well as flow patterns and rates. Such analyses are conducted by modeling the groundwater flow and the resultant transport of dissolved contaminants. In this regard, use was made of a standard numerical computer code for which input quantities were adjusted and shaped specifically for the hydrogeology and radionuclide sources at SWSA 6. Most probable concentrations at compliance points were computed based on best estimates for inputs and sources. Potential uncertainties are discussed in Sect. 4.6.

Figure 4.1 depicts the SWSA 6 area overlain by the grid used in the mathematical simulation for radionuclide concentrations in the groundwater. Included in Fig. 4.1 are the modeled locations of disposal units, proposed CERCLA caps, and observation points. The numbered observation points are of particular concern because they are either located

Table 4.3. Maximum annual nuclide flux and year of occurrence from Solid Waste Storage Area 6 disposal units into groundwater and to shallow subsurface waters during a 1000-year period with average weather conditions

Nuclide	Recharge to groundwater		Subsurface water	
	Maximum rate (g/year)	Year of occurrence	Maximum rate (g/year)	Year of occurrence
	Low-range silos (north)			
^{3}H	3.51×10^{-7}	17	1.06×10^{-6}	8
^{14}C	7.25×10^{-2}	241	6.96×10^{-1}	241
^{90}Sr	9.29×10^{-9}	91	6.93×10^{-8}	255
^{99}Tc	8.34×10^{-1}	241	8.01×10^{0}	241
^{137}Cs	9.28×10^{-11}	263	8.99×10^{-10}	264
^{232}Th	4.41×10^{-1}	614	4.27×10^{0}	611
^{233}U	1.62×10^{-4}	370	1.59×10^{-3}	370
^{238}U	1.16×10^{1}	1000[c]	1.10×10^{2}	1000[c]
^{239}Pu	3.12×10^{-5}	375	3.07×10^{-4}	370
^{241}Am	2.55×10^{-7}	374	2.53×10^{-6}	345
^{243}Am	2.96×10^{-6}	372	2.91×10^{-5}	369
	Low-range silos (south)			
^{3}H	4.44×10^{-7}	20	2.33×10^{-6}	8
^{14}C	1.09×10^{-1}[a]	244	1.15×10^{0}[b]	244
^{90}Sr	8.71×10^{-9}	96	6.46×10^{-8}	256
^{99}Tc	1.31×10^{0}[a]	244	1.38×10^{1}[b]	244
^{137}Cs	7.81×10^{-11}	264	8.17×10^{-10}	264
^{232}Th	5.70×10^{-1}[a]	652	6.13×10^{0}[b]	649
^{233}U	1.72×10^{-4}	449	1.85×10^{-3}	450
^{238}U	2.13×10^{1}[a]	1000[c]	2.28×10^{2}[b]	1000[c]
^{239}Pu	3.33×10^{-5}	452	3.58×10^{-4}	450
^{241}Am	2.57×10^{-7}	348	2.75×10^{-6}	374
^{243}Am	3.15×10^{-6}	442	3.39×10^{-5}	443

Table 4.3 (continued)

Nuclide	Recharge to groundwater: Maximum rate (g/year)	Recharge to groundwater: Year of occurrence	Subsurface water: Maximum rate (g/year)	Subsurface water: Year of occurrence
		High-range silos		
^{3}H	1.78×10^{-6}	18	5.85×10^{-6}	8
^{14}C	1.57×10^{-4}	243	1.50×10^{-3}	243
^{90}Sr	3.20×10^{-6}	92	1.45×10^{-5}	254
^{137}Cs	2.36×10^{-9}	262	1.51×10^{-8}	263
^{232}Th	2.78×10^{-1}	358	2.08×10^{0}	385
^{238}U	8.25×10^{0}	381	6.22×10^{1}	405
^{239}Pu	6.09×10^{-5}	355	4.56×10^{-4}	382
		Asbestos silos		
^{3}H	9.20×10^{-9}	18	2.99×10^{-8}	8
^{14}C	1.59×10^{-3}	243	3.11×10^{-2}	243
^{90}Sr	4.11×10^{-10}	90	3.67×10^{-9}	251
^{99}Tc	7.11×10^{-4}	243	1.39×10^{-2}	243
^{238}U	2.57×10^{0}	358	4.61×10^{1}	361
		Tumulus I		
^{3}H	1.11×10^{-5}	17	7.79×10^{-6}	5
^{14}C	3.06×10^{-2}	106	1.78×10^{-1}	106
^{90}Sr	3.31×10^{-7}	127	2.32×10^{-6}	127
^{99}Tc	3.07×10^{-1}	107	1.88×10^{0}	107
^{137}Cs	7.58×10^{-9}	137	4.64×10^{-8}	137
^{226}Ra	1.70×10^{-9}[a]	312	1.03×10^{-8}[b]	322
^{232}Th	2.37×10^{-1}	387	1.42×10^{0}	382
^{233}U	2.35×10^{-3}[a]	393	1.41×10^{-2}	386
^{238}U	1.20×10^{1}	512[c]	7.15×10^{1}	502[c]
^{239}Pu	3.31×10^{-4}[a]	395	1.98×10^{-3}[b]	387
^{241}Am	3.19×10^{-6}[a]	314	1.92×10^{-5}	312
^{243}Am	2.07×10^{-6}	387	1.24×10^{-5}	384

Table 4.3 (continued)

Nuclide	Recharge to groundwater: Maximum rate (g/year)	Recharge to groundwater: Year of occurrence	Subsurface water: Maximum rate (g/year)	Subsurface water: Year of occurrence
		Tumulus II		
^{3}H	6.50×10^{-6}	17	3.33×10^{-6}	5
^{14}C	4.63×10^{-3}	104	6.38×10^{-2}	103
^{90}Sr	2.81×10^{-7}	121	4.80×10^{-6}	121
^{99}Tc	1.30×10^{-1}	104	1.82×10^{0}	104
^{137}Cs	4.56×10^{-9}	131	7.40×10^{-8}	131
^{232}Th	3.99×10^{-1}	278	6.00×10^{0}	268
^{233}U	8.22×10^{-4}	261	1.24×10^{-2}	254
^{238}U	3.34×10^{0}	262	5.05×10^{1}	250
^{239}Pu	1.27×10^{-4}	267	1.91×10^{-3}	255
^{241}Am	3.12×10^{-6}	240	4.77×10^{-5}[b]	234
		Interim Waste Management Facility		
^{3}H	2.23×10^{-4}[a]	18	6.84×10^{-5}	51
^{14}C	2.51×10^{-1}	54	3.46×10^{0}	54
^{36}Cl	9.78×10^{0}[a]	18	6.12×10^{1}[b]	52
^{90}Sr	4.49×10^{-6}	75	6.18×10^{-5}	75
^{99}Tc	5.93×10^{-1}	54	8.22×10^{0}	54
^{137}Cs	7.86×10^{-8}	83	1.07×10^{-6}	83
^{232}Th	3.79×10^{-1}	252	5.22×10^{0}	255
^{233}U	1.11×10^{-2}	258	1.53×10^{-1}[b]	259
^{238}U	4.35×10^{1}	341	5.99×10^{2}	342
^{239}Pu	8.58×10^{-4}	262	1.18×10^{-3}	263
^{241}Am	1.54×10^{-6}	221	2.12×10^{-5}	224
^{243}Am	1.48×10^{-5}	259	2.03×10^{-4}[b]	258
		High-range wells and silos		
^{90}Sr	1.20×10^{-3}	88	1.94×10^{-4}	88
^{99}Tc	4.57×10^{-1}	78	8.07×10^{-2}	79
^{137}Cs	1.47×10^{-5}	96	2.37×10^{-6}	96
^{152}Eu	9.62×10^{-8}	81	1.55×10^{-8}	81
^{154}Eu	2.64×10^{-9}	80	4.26×10^{-10}	80
^{229}Th	5.26×10^{-6}	225	8.72×10^{-7}	238
^{232}Th	5.14×10^{-2}	234	8.54×10^{-3}	251

Table 4.3 (continued)

Nuclide	Recharge to groundwater: Maximum rate (g/year)	Recharge to groundwater: Year of occurrence	Subsurface water: Maximum rate (g/year)	Subsurface water: Year of occurrence
		High-range wells		
^{90}Sr	2.45×10^{-3}[a]	87	3.97×10^{-4}[b]	87
^{99}Tc	9.13×10^{-1}	77	1.61×10^{-1}	78
^{137}Cs	3.00×10^{-5}[a]	95	$4.85E \times 10^{-6}$	94
^{152}Eu	2.03×10^{-7}[a]	80	3.27×10^{-8}[b]	80
^{154}Eu	5.71×10^{-9}[a]	79	9.21×10^{-10}[b]	79
^{229}Th	1.05×10^{-5}[a]	226	1.74×10^{-6}[b]	243
^{232}Th	9.36×10^{-2}	656	1.61×10^{-2}	682
		Fissile wells		
^{137}Cs	1.93×10^{-8}	78	9.81×10^{-6}[b]	78
^{235}U	7.25×10^{-3}[a]	200	2.27×10^{0}[b]	194
^{238}U	3.81×10^{-2}	1000[c]	3.31×10^{0}	1000[c]
		Biological trenches		
^{3}H	7.28×10^{-9}	5	2.22×10^{-7}	5
^{90}Sr	8.03×10^{-8}	8	4.23×10^{-9}	8

[a]Highest nuclide transport rate to groundwater.
[b]Highest nuclide transport rate in lateral path.
[c]Maximum release rate controlled by the solubility limit of uranium.

100 m (328 ft) downgradient from a disposal unit or at points where groundwater discharges to the surface. The concentration of each radionuclide was computed at these observation points for the purpose of conversion to dose estimates. Also, mass and volumetric flux entering the surface water were computed on an annual basis (see Sect. 4.4).

Using the water table attributes discussed in Sect. 2.1.3, elevations presented in Fig. 2.11, and available data for site-specific hydrological parameters—such as hydraulic conductivity—a dynamic, groundwater flow application was constructed that responded to variations in recharge from the scenarios of monitored closure and postclosure described in Sect. 4.2.1. These variations included CERCLA capping plans for SWSA 6 and included cap deterioration. Independently modeled water tables and velocity fields (EBASCO 1992) served as a target for this evolving groundwater flow system. Actual model calibration was

ORNL-DWG 93-16529

CONTAMINANT SOURCES AND COMPLIANCE NODES USED IN THE SWSA6 PA GROUNDWATER ANALYSIS

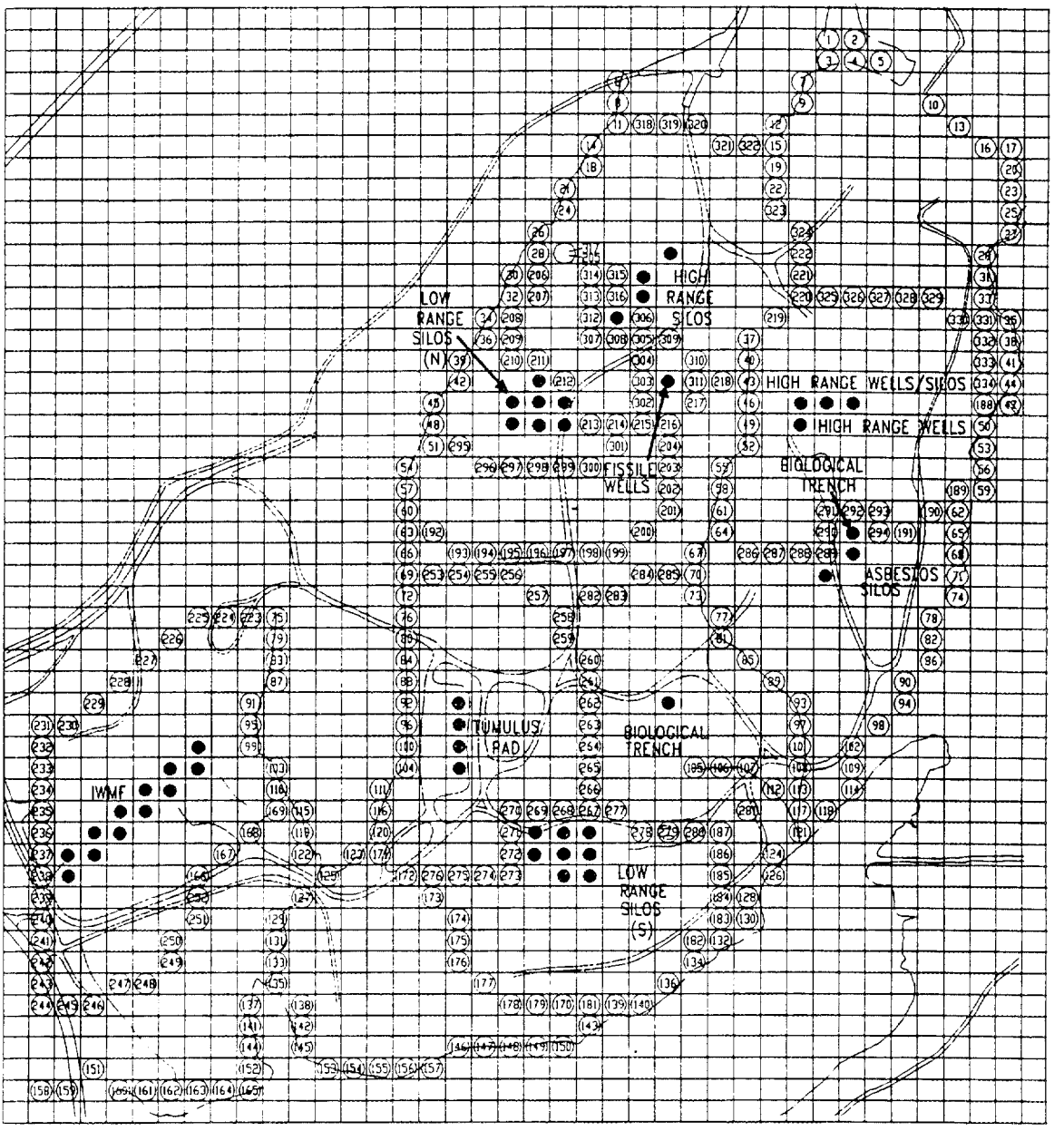

LEGEND

- (33) COMPLIANCE NODE
- ● SOURCE LOCATION
- STREAM
- ROAD

SWSA6 DISPOSAL SITES

- IWMF (IWMF)
- TUMULUS I (TUM1)
- TUMULUS II (TUM2)
- LOW RANGE SILOS-N (TLN)
- LOW RANGE SILOS-S (TLS)
- BIOLOGICAL TRENCH (TB)
- HIGH RANGE WELLS/SILOS (THW)
- ASBESTOS SILOS (TA)
- HIGH RANGE SILOS (TH)
- HIGH RANGE WELLS (WHA)
- FISSILE WELLS (WF)

Fig. 4.1. Numerical grid with observation points.

accomplished via numerous runs in which various hydraulic variables (i.e., hydraulic conductivity, recharge, etc.) were adjusted until resultant head distributions and velocity fields similar to the EBASCO results were obtained. Once calibrated, the model was used to determine groundwater velocity profiles on a yearly basis for a total of 1000 years starting at year 1988. These velocity fields differed significantly during the period of approximately 1988–2088 due to the previously described effects of variable recharge and deteriorating caps. However, after about 100 years, calculated groundwater flow fields for the SWSA 6 site were essentially steady state. A typical calculated water table surface and corresponding velocity field for $T = 1$ year can be seen in Figs. 4.2 and 4.3, respectively.

Technically, the deterministic modeling of the flow of groundwater is separate from calculation of the groundwater concentrations of a dissolved radionuclide. The latter are found only after velocity fields have been determined. This is done using standard methods (Schiedeggor 1960) in which contaminant concentrations are functions of these groundwater velocities and parameters used to quantify dispersion effects. The methodology used in determining groundwater contaminant concentrations followed that of a tracer calibration test performed at Bear Creek Valley on the ORR using the same numerical code (Lee et al. 1989). Because the movement of radionuclides in SWSA 6 groundwater was presumed to be driven by processes similar to those in Bear Creek, the major transport process was taken to be advective flow with retardation due to adsorption. Effects of radioactive decay and dispersion were also included. Appendix E lists the basic assumptions used in the transport modeling at SWSA 6. These assumptions augment those listed in the description of site characteristics in Sect. 3.3.2.

Due to the lack of reliable, site-wide data from the same time period, it was not possible to adjust transport parameters at SWSA 6 so that predicted concentrations matched those measured for any existing source-plume combination. Furthermore, plumes present from waste disposal operations prior to September 26, 1988, are confounded in field data with plumes from post 1988 sources. Consequently, important model parameters, such as those relating to retardation effects, were estimated as discussed in Sect. 3.3.2.3. Values for all parameters used in the groundwater transport analysis are listed in Appendix E.

Transport simulations were performed until a maximum concentration was reached at each observation point. Independent simulations were performed for each of the 17 radionuclides considered in the analysis (Table 4.4). All sites where the given nuclide was present were modeled as contaminant sources with recharge and mass flux supplied by the UTM code as described in Sect. 4.2.2.

The numerical model was not used in instances where the contaminant flux to groundwater (calculated using the TUMSIM and WELSIM codes) did not reach a maximum value. This was most evident in the case of ^{238}U. As shown in Table 4.3, peak calculated fluxes of ^{238}U to groundwater occurred at 1000 years for a number of sites [low-range silos (north), low-range silos (south), and fissile wells]. The flux of contaminant to groundwater at 1000 years for these sites was actually increasing by a very small, linear rate. Additional transport simulations were made for these sites with time periods as long as 5000 years. However, all computer simulations showed the same, gradual rise in flux rate of contaminant to groundwater. Furthermore, because of the extremely long half-life of ^{238}U (4.4×10^9 years), model simulations on the order of 10^9–10^{10} years were needed to determine peak groundwater concentrations. Even with the available state-of-the-art

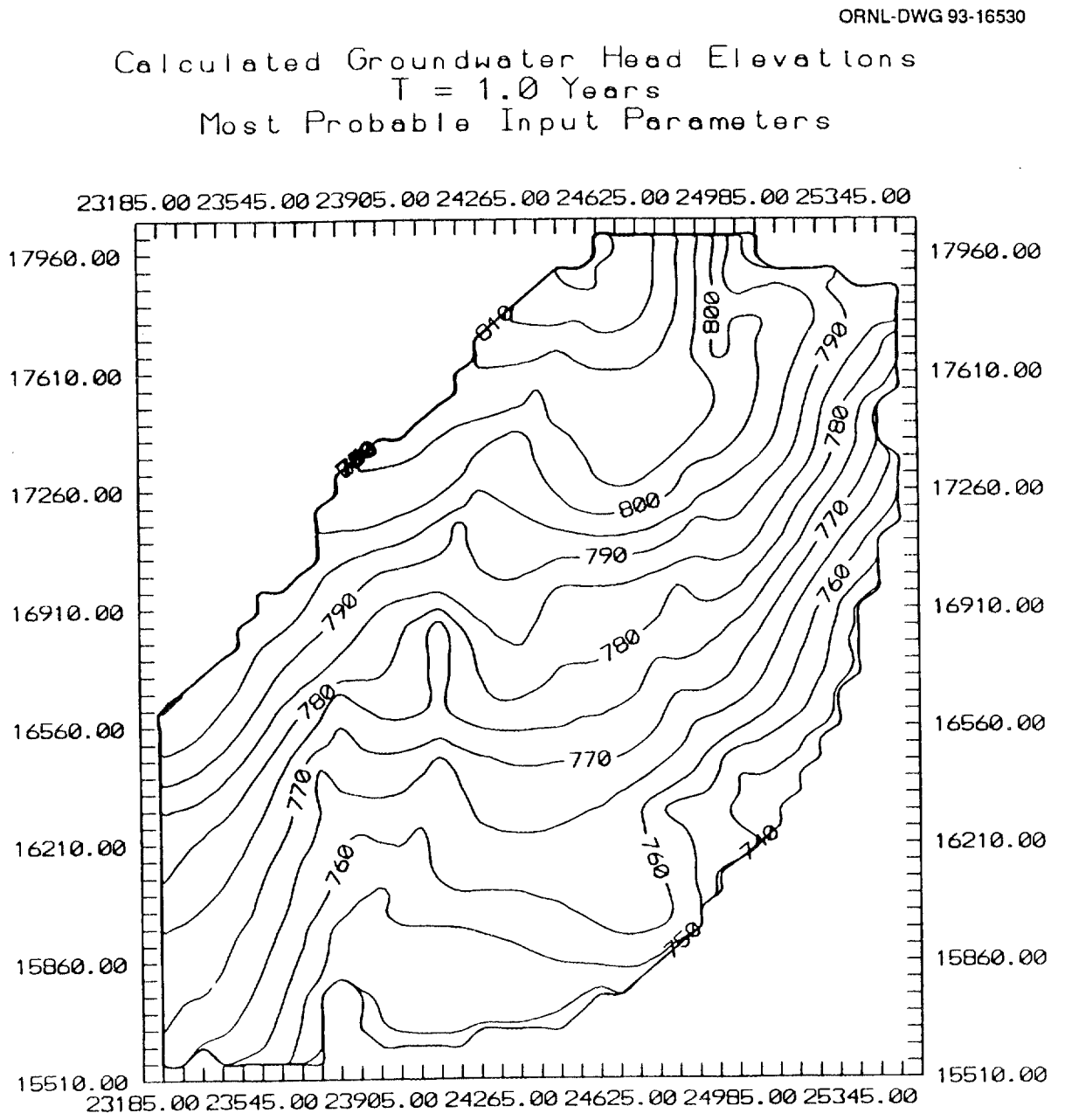

Fig. 4.2. Typical groundwater water table surface at Solid Waste Storage Area 6.

ORNL-DWG 93-16531

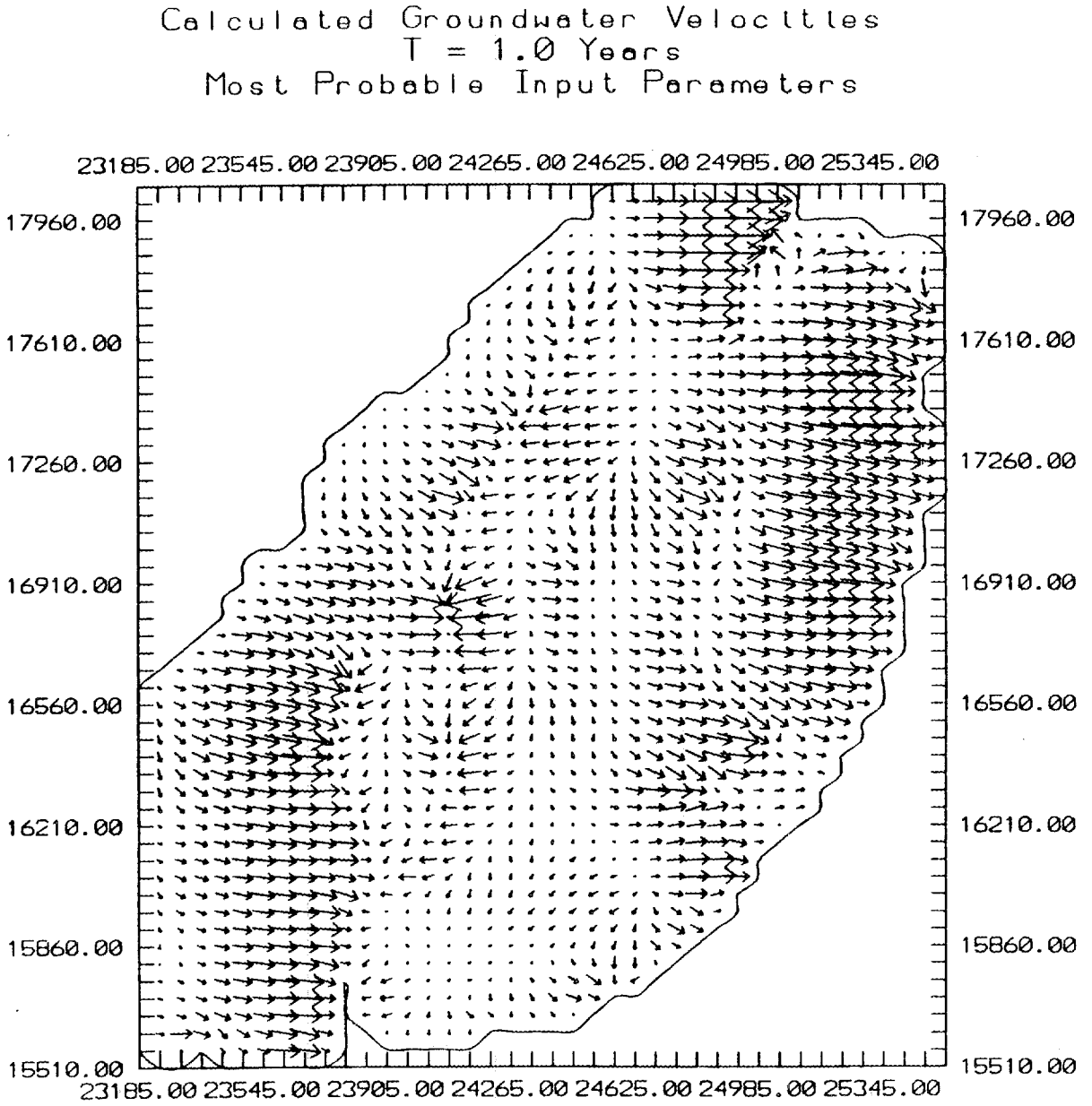

Fig. 4.3. Typical groundwater velocity vector field at Solid Waste Storage Area 6.

Table 4.4. Nuclides considered in Solid Waste Storage Area 6 groundwater transport analysis

^{3}H	^{229}Th
^{14}C	^{232}Th
^{36}Cl	^{233}U
^{90}Sr	^{235}U
^{99}Tc	^{238}U
^{137}Cs	^{239}Pu
^{152}Eu	^{241}Am
^{154}Eu	^{243}Am
^{226}Ra	

computing power, the real time needed to perform such simulations was not practical. Because of these difficulties, groundwater concentrations of ^{238}U were calculated with an analytic model (see Appendix E). This code was capable of both performing simulations covering 10^9–10^{10} years or more and estimating flux into groundwater based on initial site inventory and contaminant flux rate at 1000 years.

4.3.1 Transport Simulations and Radionuclide Concentrations

Results of the SWSA 6 groundwater transport analysis are summarized in Table 4.5. The best estimate concentrations (activity/volume) and corresponding times of occurrence for nuclides that exceed 10% of allowable limits at 100-m (328-ft) compliance points are presented. In addition, for those isotopes in which this value occurs during the 100-year period of institutional control (monitored closure), corresponding concentrations at 100 years are also shown. Dose estimates for groundwater (Sect. 4.5.3.1) were based on these values. Tables E.4–E.20 in Appendix E list the maximum concentration and time of occurrence for all radionuclides at each compliance point. Figures 4.4–4.6 show the approximate regions outside the compliance boundaries around each disposal unit where the sum of activity from all nuclides exceeds compliance limits. The approximate areas represented by the shaded regions in Figs. 4.4–4.6 are 2,930, 4,040, and 1,250 m^2 (31,500, 43,500, and 13,500 ft^2), respectively. The compliance boundaries shown are defined either by points 100 m (328 ft) from the disposal unit or by surface water bodies. The latter are assumed to intercept contaminant plumes as little underflow of groundwater beneath surface water outlets is believed possible.

Table 4.5. Best estimates of groundwater concentrations for Solid Waste Storage Area 6 disposal sites with calculated concentration/allowable ratio ≥ 0.1 at 100-m (328-ft) compliance points

Nuclide	Concentration C [μCi/L]	Ratio $C/C_{Allowable}$	Year of occurrence	Source
^{3}H	1.9×10^{-1}	2.1×10^{0}	30	Interim Waste Management Facility (IWMF)
^{3}H	2.1×10^{-7}	2.2×10^{-6}	100[a]	IWMF
^{14}C	1.4×10^{-1}	5.4×10^{1}	67	IWMF
^{14}C	4.4×10^{-3}	1.7×10^{0}	100[a]	IWMF
^{14}C	1.2×10^{-3}	4.5×10^{-1}	270	Low-range silo (south)
^{14}C	2.9×10^{-4}	1.1×10^{-1}	270	Low-range silo (north)
^{36}Cl	6.8×10^{-2}	3.8×10^{1}	34	IWMF
^{36}Cl	1.4×10^{-5}	7.8×10^{-3}	100[a]	IWMF
^{99}Tc	1.6×10^{-3}	3.7×10^{-1}	67	IWMF
^{99}Tc	1.0×10^{-4}	2.5×10^{-2}	180	High-range silo
^{233}U	8.9×10^{-6}	4.5×10^{-1}	2400	IWMF
^{239}Pu	4.2×10^{-6}	3.3×10^{0}	2400	IWMF
^{239}Pu	1.4×10^{-7}	1.1×10^{-1}	2800	High-range silo
^{243}Am	2.1×10^{-7}	1.7×10^{-1}	2400	IWMF

[a]100 years = time for loss of institutional control.

4.3.2 Discussion

The results presented in Table 4.5 indicate that calculated concentrations for 7 of the 17 nuclides considered in SWSA 6 groundwater analysis were near or exceeded allowable limits at 100-m (328-ft) compliance points. However, with the exception of ^{14}C and ^{239}Pu, these concentrations drop below allowable limits by the end of the 100-year instutitonal control period. While the concentration values reported in Table 4.5 can be attributed to a number of different disposal units, most are associated with releases from the IWMF facility. Futhermore, the highest calculated groundwater concentrations at SWSA 6 are also due primarily to releases from the IWMF.

ORNL-DWG 93-16532

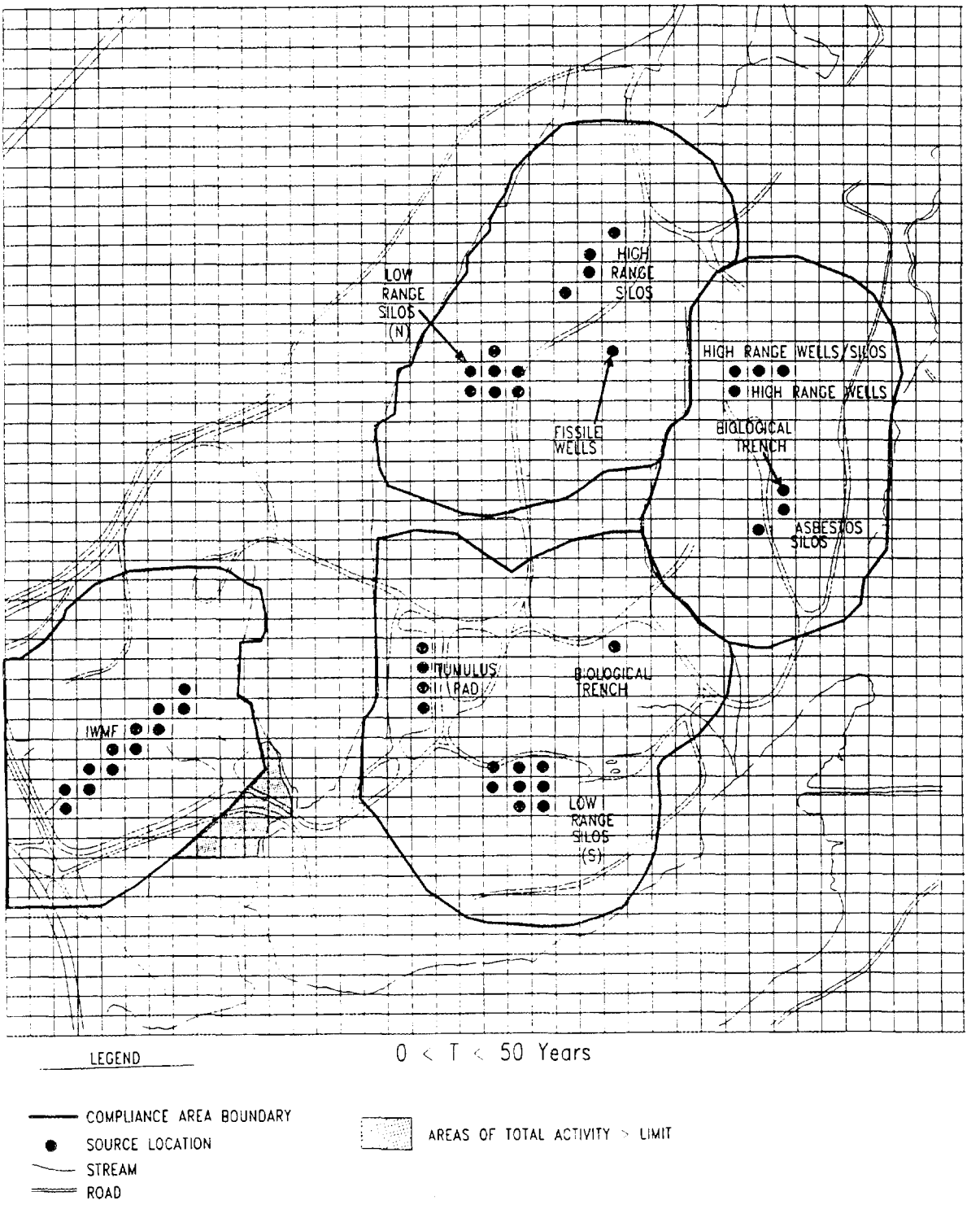

Fig. 4.4. Estimated areas outside of compliance boundaries with total nuclide activity > compliance limit (0 < T < 50 years).

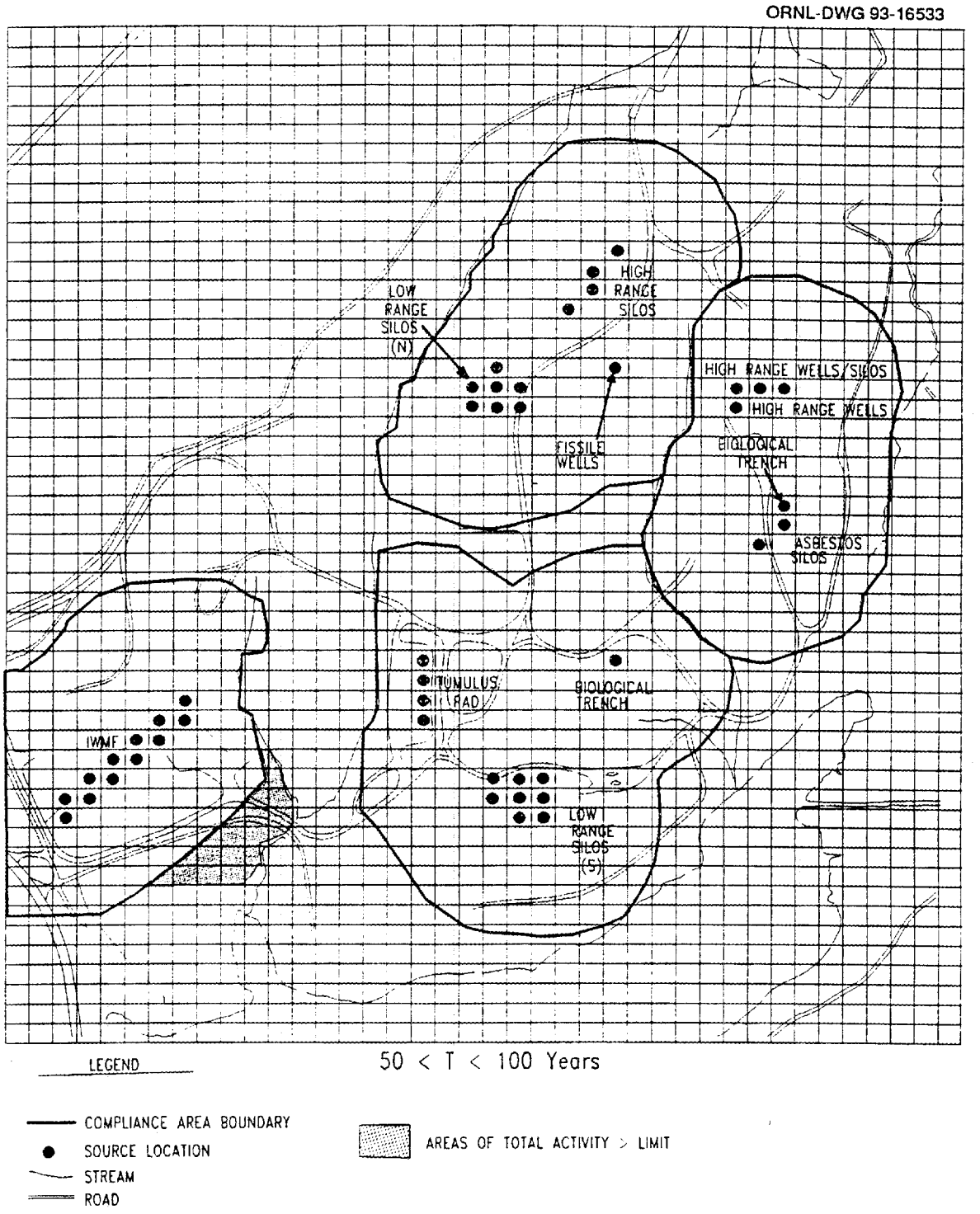

Fig. 4.5. Estimated areas outside of compliance boundaries with total nuclide activity > compliance limit (50 < T < 100 years).

ORNL-DWG 93-16534

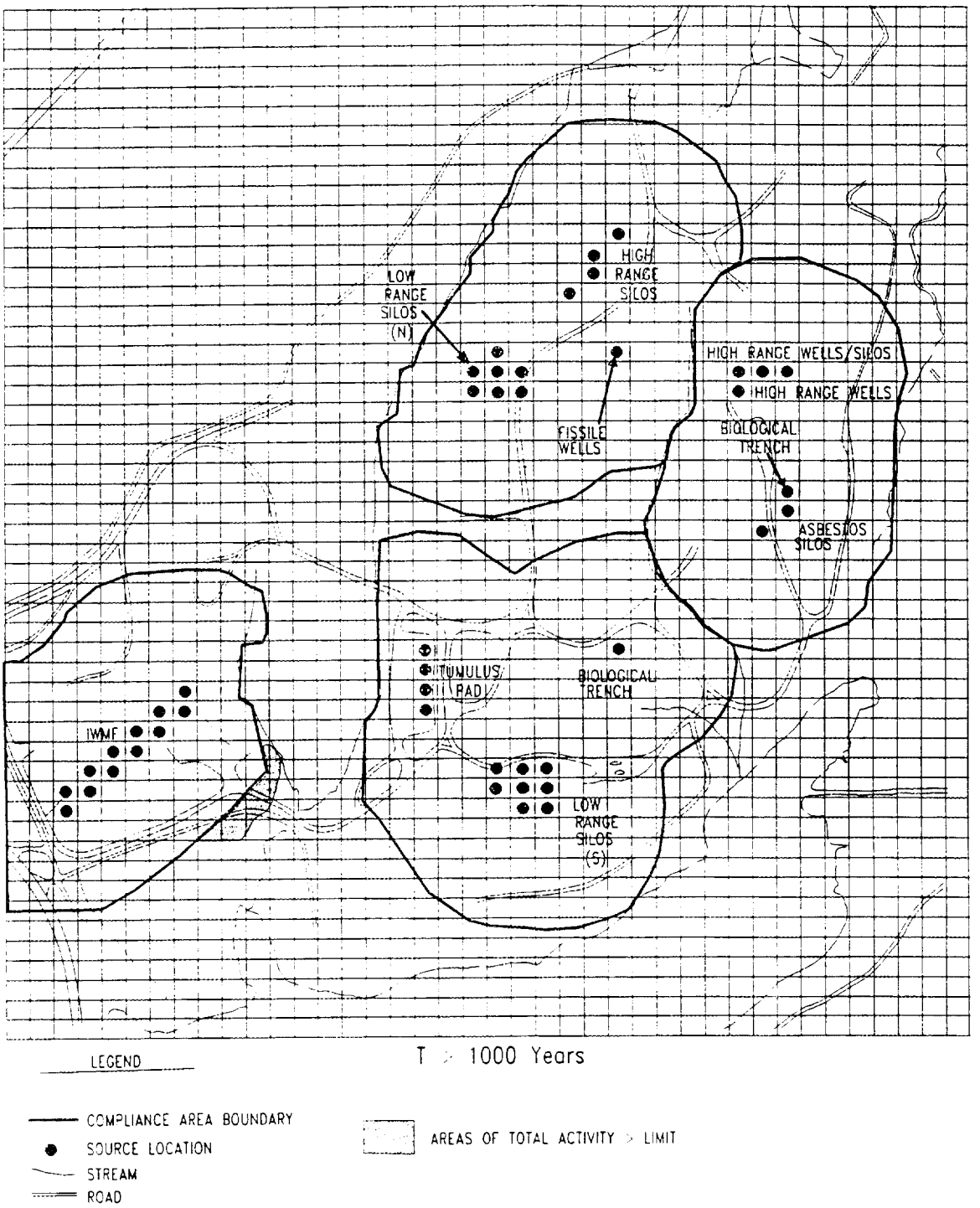

Fig. 4.6. Estimated areas outside of compliance boundaries with total nuclide activity > compliance limit (T > 1000 years).

Figures 4.4–4.6 illustrate another important point. These figures show areas outside the 100-m (328-ft) compliance boundaries where the calculated sum of activity from all radionuclides in groundwater exceeds the 4 mrem dose limit. It should be stressed that while contaminant concentrations may exceed allowable limits at points within 100 m (328 ft) of each site, Figs. 4.4–4.6 show that only a small portion of the total SWSA 6 area outside of these compliance boundaries is contaminated above allowable limits. This area is confined to a small region located near the IWMF. Activities above allowable levels occur in this area between 0 and 100 years and then again at times greater than 1000 years. Contamination in this area during the 0–100 year time period is due primarily to the presence of ^{3}H, ^{14}C, and ^{36}Cl, while contamination occuring after 1000 years is due to the presence of ^{239}Pu, ^{243}Am, and ^{233}U.

As noted in Sect. 4.3.1, Table 4.5 does not include radionuclides that were less than 10% of the allowable limit. For the IWMF, low-range silos (north), low-range silos (south), and high-range wells, the sum of the ratios of the contaminant concentration to the allowable concentration for each isotope not listed in Table 4.5 was less than 0.024, 0.013, 0.011, and 0.091, respectively. For the remaining disposal units, the sum of the ratios for all isotopes was less than 0.091.

The entries in Table 4.5 represent the best estimates of the maximum radionuclide concentrations in groundwater. A crucial assumption in the groundwater transport model is that the mechanism controlling chemical adsorption allows for unlimited adsorption. This property, characterized by a linear isotherm for the definition of the distribution coefficient, may result in very small transport velocities and may be invalid for some isotopes. Conversely, the model includes dispersion effects so that solute can be transported a nontrivial distance [$\geq$ 100 m (328 ft)] over a very long time without significant advection. These effects can be seen in the uncertainty simulations based on Latin hypercube (LHC) sampling (Sect. 4.6.).

4.4 SURFACE WATER TRANSPORT

Studies undertaken for this assessment involved the simulation of radionuclide transport to surface waters through two pathways. Groundwater discharged into stream channels at SWSA 6 carries with it nuclides that have leached from units through the vadose zone and the saturated media of the aquifer system. The other source of nuclides transported into surface water is from lateral subsurface flow through the stormflow zone. Nuclide transport from each of these paths is shown separately in Tables 4.6 and 4.7, and the total amounts of radionuclides transported to surface water are given in Table 4.8. Concentrations in Tables 4.6–4.8 include dilution by 175,780 m^3 (6,207,600 ft^3) of surface runoff predicted by UTM for an average year. The results for groundwater transport (Table 4.6) are summarized from the groundwater simulations described in Sect. 4.3. In these simulations, ^{14}C showed the highest annual activity released from groundwater into surface water. Three nuclides, ^{3}H, ^{14}C, and ^{36}Cl, showed relatively high levels of activity released into surface water. Several nuclides with high K_d values (^{137}Cs, ^{152}Eu, ^{154}Eu, ^{226}Ra) showed very low release rates. The largest peak material flux predicted from groundwater simulations was 5.1 g/year for ^{238}U. However, this peak did not account for the highest level of activity (Table 4.6).

Table 4.6. Combined maximum radionuclide release (mass, activity, and concentration basis) from all disposal units to surface waters from groundwater transport
(Time-range of peak transport rate occurrences is also shown.[a])

Radionuclide	Transport to surface water (g/year)	Range of occurrences (year)	Activity (Ci/year)	Concentration (Ci/m^3)
^{3}H	6.54×10^{-6}	8–160	6.31×10^{-2}	3.59×10^{-7}
^{14}C	1.45×10^{-2}	57–1000	6.45×10^{-2}[b]	3.67×10^{-7}
^{36}Cl	5.24×10^{-1}	23–4000	1.73×10^{-2}	9.83×10^{-8}
^{90}Sr	5.90×10^{-11}	80–1960	8.02×10^{-9}	4.56×10^{-14}
^{99}Tc	6.47×10^{-2}	54–2000	1.10×10^{-3}	6.25×10^{-9}
^{137}Cs	1.05×10^{-19}	10–500	9.12×10^{-18}	5.19×10^{-23}
^{152}Eu	4.12×10^{-23}	10–190	7.13×10^{-21}	4.06×10^{-26}
^{154}Eu	1.30×10^{-25}	58–160	3.51×10^{-23}	2.00×10^{-28}
^{226}Ra	3.15×10^{-17}	5000–50000	3.12×10^{-17}	1.77×10^{-22}
^{229}Th	2.65×10^{-8}	10–3000	5.63×10^{-9}	3.21×10^{-14}
^{232}Th	3.26×10^{-2}	96–20000	4.40×10^{-9}	2.50×10^{-14}
^{233}U	4.37×10^{-4}	830–5000	4.23×10^{-6}	2.41×10^{-11}
^{235}U	1.29×10^{-3}	640–4000	2.79×10^{-9}	1.59×10^{-14}
^{238}U	5.10×10^{0}	580–64000	1.71×10^{-6}	9.74×10^{-12}
^{239}Pu	4.00×10^{-5}	110–3000	2.49×10^{-6}	1.42×10^{-11}
^{241}Am	5.55×10^{-8}	52–2000	1.90×10^{-7}	1.08×10^{-12}
^{243}Am	4.56×10^{-7}	52–5000	9.07×10^{-8}	5.16×10^{-13}

[a]Concentration was calculated on the basis of 175780 m^3 (6,207,600 ft^3) of surface runoff in an average year (runoff is 40% lower in a dry year and 78% higher in a wet year).

[b]Highest activity.

Table 4.7. Combined maximum radionuclide release (mass, activity, and concentration basis) from all disposal units to surface waters from shallow subsurface transport
(Time-range of occurrences is also shown.[a])

Radionuclide	Transport to surface water (g/year)	Range of occurrences (year)	Activity (Ci/year)	Concentration (Ci/m^3)
^{3}H	8.90×10^{-5}	5–50	8.59×10^{-1}	4.89×10^{-6}
^{14}C	5.59×10^{0}	54–240	2.49×10^{1}[b]	1.42×10^{-4}
^{36}Cl	6.10×10^{1}	52	2.01×10^{0}	1.15×10^{-5}
^{90}Sr	6.75×10^{-4}	8–260	9.18×10^{-2}	5.22×10^{-7}
^{99}Tc	3.41×10^{1}	54–240	5.80×10^{-1}	3.30×10^{-6}
^{137}Cs	1.82×10^{-5}	78–260	1.58×10^{-3}	9.01×10^{-9}
^{152}Eu	4.83×10^{-8}	80–81	8.35×10^{-6}	4.75×10^{-11}
^{154}Eu	1.35×10^{-9}	79–80	3.63×10^{-6}	2.07×10^{-11}
^{226}Ra	1.03×10^{-8}	320	1.02×10^{-8}	5.80×10^{-14}
^{229}Th	2.62×10^{-6}	238–243	5.57×10^{-7}	3.17×10^{-12}
^{232}Th	2.52×10^{1}	250–680	2.77×10^{-6}	1.58×10^{-11}
^{233}U	1.83×10^{-1}	250	1.06×10^{-3}	6.06×10^{-9}
^{235}U	2.27×10^{0}	190	4.90×10^{-6}	2.79×10^{-11}
^{238}U	1.13×10^{3}	250–1000	3.80×10^{-4}	2.16×10^{-9}
^{239}Pu	1.68×10^{-2}	250–450	1.04×10^{-3}	5.94×10^{-9}
^{241}Am	9.34×10^{-5}	220–370	3.20×10^{-4}	1.82×10^{-9}
^{243}Am	3.27×10^{-4}	260–440	6.51×10^{-5}	3.70×10^{-10}

[a]Concentration was calculated on the basis of 175,780 m^3 (6,207,600 ft^3) of surface runoff in an average year (runoff is 40% lower in a dry year and 78% higher in a wet year).
[b]Highest activity.

Table 4.8. Combined maximum radionuclide release (mass, activity, and concentration basis) from all disposal units to surface waters from groundwater and shallow subsurface transport
(Time-range of peak transport rate occurrences is also shown.[a])

Radionuclide	Transport to surface water (g/year)	Range of occurrences (year)	Activity (Ci/year)	Concentration (Ci/m^3)
^{3}H	9.55×10^{-5}	5–160	9.22×10^{-1}	5.24×10^{-6}
^{14}C	5.60×10^{0}	54–1000	2.50×10^{1}[b]	1.42×10^{-4}
^{36}Cl	6.15×10^{1}	23–4000	2.03×10^{0}	1.15×10^{-5}
^{90}Sr	6.75×10^{-4}	8–2000	9.18×10^{-2}	5.22×10^{-7}
^{99}Tc	3.41×10^{1}	54–2000	5.80×10^{-1}	3.30×10^{-6}
^{137}Cs	1.82×10^{-5}	10–500	1.58×10^{-3}	9.01×10^{-9}
^{152}Eu	4.83×10^{-8}	10–190	8.35×10^{-6}	4.75×10^{-11}
^{154}Eu	1.35×10^{-9}	60–160	3.63×10^{-7}	2.07×10^{-12}
^{226}Ra	1.03×10^{-8}	320–5000	1.02×10^{-8}	5.80×10^{-14}
^{229}Th	2.64×10^{-6}	10–3000	5.63×10^{-7}	3.20×10^{-12}
^{232}Th	2.52×10^{1}	96–20000	2.77×10^{-6}	1.58×10^{-11}
^{233}U	1.83×10^{-1}	250–5000	1.77×10^{-3}	1.01×10^{-8}
^{235}U	2.27×10^{0}	190–4000	4.90×10^{-6}	2.79×10^{-11}
^{238}U	1.13×10^{3}	250–64000	3.80×10^{-4}	2.16×10^{-9}
^{239}Pu	1.68×10^{-2}	110–3000	1.04×10^{-3}	5.94×10^{-9}
^{241}Am	9.34×10^{-5}	52–2000	3.20×10^{-4}	1.82×10^{-9}
^{243}Am	3.27×10^{-4}	52–5000	6.51×10^{-5}	3.70×10^{-10}

[a]Concentration was calculated on the basis of 175,780 m^3 (6,207,600 ft^3) of surface runoff in an average year (runoff is 40% lower in a dry year and 78% higher in a wet year). Time-range of occurrence of peak fluxes from the various disposal units is not shown.

[b]Highest activity.

The peak nuclide transport rates from the eleven different disposal units via the groundwater, lateral flow path, and combined surface water release were summed for each nuclide without regard for the year of occurrence (a conservative assumption) to show the maximum annual release predicted. The range of occurrences indicates the time interval over which the peak nuclide transport rates were calculated. Therefore, the concentrations in Tables 4.6, 4.7, and 4.8 provide conservative overestimates of the maximum concentrations in any year because the predicted peak values due to releases from different disposal units do not occur at the same time. Carbon-14, chiefly associated with the low-range silos (south), gave the highest annual activity release (Table 4.7). Comparison of Tables 4.6 and 4.7 shows that predicted radionuclide flux through the lateral flow path was often 10 or more times higher than that for the groundwater path.

In all cases, the total nuclide flux was dominated by transport in the lateral flow path. The results for the total annual radionuclide transport to surface water (Table 4.8) were made available for the surface water dose calculations (Section 4.5.3.1).

4.5 DOSE ANALYSIS

This section presents the results of the analysis of radiation doses resulting from disposal of low-level radioactive waste (LLW) in the different types of disposal units in the SWSA 6 facility. The dose analysis considers two critical groups of exposed individuals:

- off-site individuals (i.e., members of the public who reside outside the boundary of the disposal facility) and
- inadvertent intruders onto the disposal site following loss of active institutional controls (during the postclosure period).

Off-site individuals may receive exposures from radionuclides that are transported beyond the facility boundary at any time after disposal, but exposures of inadvertent intruders are assumed to be precluded by active institutional controls until a minimum of 100 years after disposal.

As indicated in Sects. 4.2–4.4, the performance assessment for disposal units in SWSA 6 considers the transport in shallow subsurface water and groundwater as the principal mechanism for removal of radionuclides from the disposal unit into the environment. Therefore, off-site individuals are assumed to receive radiation doses primarily as a result of exposure to contaminated water beyond the facility boundary.

The dose analysis for inadvertent intruders considers two general types of exposure scenarios. The first, which is similar to the assumed exposure scenario for off-site individuals, involves exposure to contaminated water obtained from a source within the facility boundary. The second type of scenario involves direct intrusion into disposal units, and four different scenarios for exposures from direct intrusion are evaluated.

The inputs to the dose analyses for off-site individuals and inadvertent intruders from exposure to contaminated water are provided by (1) the estimated maximum concentrations of radionuclides in surface water at locations beyond the facility boundary at any time after disposal and (2) the estimated maximum concentrations of radionuclides in groundwater within the facility boundary at any time after loss of active institutional

control, as presented in Sects. 4.3 and 4.4. The inputs to the dose analyses for inadvertent intruders from direct intrusion into disposal units according to the different exposure scenarios are provided by the estimated concentrations of radionuclides in disposal units at various times after loss of active institutional controls.

Disposal of LLW at DOE sites also must protect groundwater resources consistent with federal, state, and local requirements (DOE 1988). In this performance assessment, the requirement for protection of groundwater resources has been interpreted as a limit on annual effective dose equivalent (EDE) of 4 mrem from consumption of 2 L/day (0.5 gal/day) of drinking water from affected sources at any location beyond the 100-m (328-ft) buffer zone around any of the disposal units in SWSA 6. Therefore, doses from the drinking water pathway only also are evaluated. The dose estimates use as input the estimated maximum concentrations of radionuclides in groundwater at any location beyond the buffer zone and at any time after disposal. Thus, the dose limit of 4 mrem per year is interpreted as a requirement for resource protection regardless of whether the groundwater could actually be used (e.g., during the institutional control period). The drinking water standards described above also are applied to any potentially potable surface waters beyond the buffer zone and at any time.

4.5.1 Analysis of Human Exposure Scenarios and Exposure Pathways

This section describes the exposure scenarios and exposure pathways assumed in the dose analyses for off-site individuals and inadvertent intruders. The results of the dose analyses for each group of individuals and its associated exposure scenarios, which can be thought of as scenario dose conversion factors, are given in summary tables. For the scenarios involving exposure to contaminated water, the scenario dose conversion factors are given in the form of EDEs per unit concentration of radionuclides in water. For the scenarios involving direct intrusion into disposal units, the scenario dose conversion factors are given in the form of EDEs per unit concentration of radionuclides in disposal units at the time intrusion is assumed to occur. For protection of groundwater and surface water resources, results for the drinking water pathway only are given in the form of EDEs per unit concentration of radionuclides in water. The models and parameter values used in obtaining the results in the summary tables are described in Appendix G.

4.5.1.1 Protection of Groundwater and Surface Water Resources

As described above, this performance assessment assumes that disposal of LLW must protect groundwater and surface water resources beyond the 100-m (328-ft) buffer zone around any disposal units in SWSA 6 such that the annual EDE from direct consumption of 2 L/day (0.5 gal/day) of drinking water from the affected sources would not exceed 4 mrem. The annual EDEs from the drinking water pathway per unit concentration of radionuclides in water are given in Table 4.9. The results in this table were obtained from Table G.7 of Appendix G. In Sect. 4.5.3.1, the scenario dose conversion factors in Table 4.9 are combined with the estimated maximum concentrations of radionuclides in groundwater or surface water to obtain the dose estimates for the drinking water pathway.

Table 4.9. Annual effective dose equivalents from drinking water pathway per unit concentration of radionuclides in water[a]

Nuclide[b]	Annual dose (rem/year per μCi/L)	Nuclide[b]	Annual dose (rem/year per μCi/L)
^{3}H	4.6×10^{-2}	$^{232}Th + d$	3.4×10^{3}
^{14}C	1.5	$^{232}U + d$	1.5×10^{3}
^{26}Al	9.5	^{233}U	2.0×10^{2}
^{36}Cl	2.2	^{234}U	1.9×10^{2}
^{40}K	1.4×10^{1}	^{235}U	1.8×10^{2}
^{60}Co	1.9×10^{1}	^{236}U	1.8×10^{2}
^{63}Ni	3.9×10^{-1}	$^{238}U + d$	1.8×10^{2}
$^{90}Sr + d$	1.0×10^{2}	^{237}Np	2.8×10^{3}
^{99}Tc	9.5×10^{-1}	^{238}Pu	2.8×10^{3}
^{113m}Cd	1.1×10^{2}	^{239}Pu	3.1×10^{3}
^{137}Cs	3.7×10^{1}	^{240}Pu	3.1×10^{3}
^{152}Eu	4.4	^{242}Pu	3.0×10^{3}
^{154}Eu	6.6	^{241}Am	3.3×10^{3}
^{155}Eu	9.5×10^{-1}	^{243}Am	3.3×10^{3}
$^{210}Pb + d$	4.9×10^{3}	^{243}Cm	2.1×10^{3}
$^{226}Ra + d$[c]	5.7×10^{3}	^{244}Cm	1.7×10^{3}
$^{229}Th + d$	2.9×10^{3}	^{249}Cf	3.4×10^{3}
^{230}Th	3.9×10^{2}		

[a]Results are obtained from Table G.7 of Appendix G.

[b]"d" denotes short-lived radioactive decay products that are assumed to be in secular equilibrium with the parent.

[c]Decay products include ^{210}Pb and its decay product, which are assumed to be in secular equilibrium with the parent.

4.5.1.2 Exposure Scenarios and Exposure Pathways for Off-Site Individuals

Exposures of off-site individuals beyond the facility boundary are assumed to result primarily from the use of contaminated surface water, because all groundwater on the disposal site discharges to the surface within the facility boundary (see Sect. 4.2). The following pathways involving exposure to contaminated water are assumed to occur:

- direct ingestion of contaminated water;
- ingestion of milk and meat from dairy and beef cattle that drink contaminated water; and
- external exposure while swimming in contaminated water.

Use of contaminated water by off-site individuals (as well as inadvertent intruders) for irrigation of food crops or pasture land is not considered in the dose analysis because irrigation is not commonly practiced near Oak Ridge.

The scenario dose conversion factors for exposure of off-site individuals from exposure to contaminated water, as obtained from Table G.13 of Appendix G, are given in Table 4.10. This table gives annual EDEs per unit concentration of radionuclides in contaminated water. For all radionuclides, the dose from direct ingestion of drinking water is greater than the dose from all the other exposure pathways; for most radionuclides, the dose from all pathways is determined almost entirely by the dose from the drinking water pathway alone. In Sect. 4.5.3.1, the results in this table are combined with the estimated maximum concentrations of radionuclides in surface water to obtain the dose estimates for all exposure pathways.

4.5.1.3 Exposure Scenarios and Exposure Pathways for Inadvertent Intruders

An inadvertent intruder is assumed to establish a permanent homestead on the disposal site, including on-site sources of foodstuffs, at any time after the end of active institutional controls at 100 years after disposal. Furthermore, an intruder is assumed to have no prior knowledge of waste disposal activities at the site. Inadvertent intruders are assumed to receive radiation exposures from use of contaminated water obtained from a source within the facility boundary and from direct intrusion into disposal units.

4.5.1.3.1 Use of contaminated water

Exposure of inadvertent intruders to radionuclides in contaminated water obtained from a source within the facility boundary is assumed to occur in conjunction with any of the exposure scenarios involving direct intrusion into disposal units described below. The following exposure pathways involving use of contaminated water are assumed to occur:

- direct ingestion of contaminated water; and
- ingestion of milk and meat from dairy and beef cattle that drink contaminated water.

Thus, inadvertent intruders are assumed to use contaminated water for domestic purposes only, and the assumed exposure pathways listed above are the same as the corresponding

Table 4.10. Annual effective dose equivalents to off-site individuals per unit concentration of radionuclides in water from all exposure pathways[a]

Nuclide[b]	Annual dose (rem/year per μCi/L)	Nuclide[b]	Annual dose (rem/year per μCi/L)
^{3}H	5.5×10^{-2}	$^{232}Th + d$	3.4×10^{3}
^{14}C	2.0	$^{232}U + d$	1.5×10^{3}
^{26}Al	9.9	^{233}U	2.0×10^{2}
^{36}Cl	3.6	^{234}U	1.9×10^{2}
^{40}K	1.7×10^{1}	^{235}U	1.8×10^{2}
^{60}Co	2.2×10^{1}	^{236}U	1.8×10^{2}
^{63}Ni	4.1×10^{-1}	$^{238}U + d$	1.8×10^{2}
$^{90}Sr + d$	1.0×10^{2}	^{237}Np	2.8×10^{3}
^{99}Tc	1.1	^{238}Pu	2.8×10^{3}
^{113m}Cd	1.1×10^{2}	^{239}Pu	3.1×10^{3}
$^{137}Cs + d$	4.4×10^{1}	^{240}Pu	3.1×10^{3}
^{152}Eu	4.7	^{242}Pu	3.0×10^{3}
^{154}Eu	6.9	^{241}Am	3.3×10^{3}
^{155}Eu	9.9×10^{-1}	^{243}Am	3.3×10^{3}
$^{210}Pb + d$	4.9×10^{3}	^{243}Cm	2.1×10^{3}
$^{226}Ra + d$[c]	5.7×10^{3}	^{244}Cm	1.7×10^{3}
$^{229}Th + d$	2.9×10^{3}	^{249}Cf	3.4×10^{3}
^{230}Th	3.9×10^{2}		

[a]Results are obtained from Table G.13 of Appendix G.

[b]"d" denotes short-lived radioactive decay products that are assumed to be in secular equilibrium with the parent.

[c]Decay products include ^{210}Pb and its decay product, which are assumed to be in secular equilibrium with the parent.

pathways for off-site individuals. However, the pathway involving external exposure while swimming in contaminated water, which is included in the dose analysis for off-site individuals, is not considered for inadvertent intruders because surface waters suitable for swimming do not occur within the boundaries of SWSA 6.

The scenario dose conversion factors for exposure of inadvertent intruders to contaminated water, as obtained from Table G.14 of Appendix G, are given in Table 4.11. The table gives annual EDEs per unit concentration of radionuclides in contaminated water. For most radionuclides, the results in Table 4.11 are the same as the results in Table 4.10 for off-site individuals because the dose from external exposure while swimming in contaminated surface water is relatively unimportant for off-site individuals. For all radionuclides, the dose from the drinking water pathway is again the principal contributor to the dose from all exposure pathways. In Sect. 4.5.3.1, the results in this table are combined with the estimated maximum concentrations of radionuclides in groundwater to obtain the dose estimates for all exposure pathways.

4.5.1.3.2 Direct intrusion into disposal units

Exposures of inadvertent intruders resulting from direct intrusion into disposal units after loss of active institutional controls are assumed to occur according to one of four different scenarios, called the agriculture, resident, discovery, and postdrilling scenarios. These scenarios are based in large part on those used by the U.S. Nuclear Regulatory Commission (NRC) in developing licensing criteria for near-surface land disposal of commercial radioactive wastes (NRC 1982, Oztunali and Roles 1986). Descriptions of these scenarios and their associated exposure pathways and the scenario dose conversion factors for each scenario are given below. Additional scenarios developed by the NRC (NRC 1982, Oztunali and Roles 1986) that were considered but not included in this analysis, called the construction and drilling scenarios, are discussed in Sect 3.2.4.2. The agriculture, resident, discovery, and postdrilling scenarios for direct intrusion into disposal units do not include doses from exposure to contaminated groundwater. The scenario for exposure to contaminated groundwater is described in the previous subsection.

The agriculture scenario is assumed to involve continuous lifetime exposure. In this scenario, an inadvertent intruder is assumed to construct a home directly on top of disposal units, with the foundation extending into the disposed waste. Waste is assumed to be exhumed during construction of the foundation, and all waste remaining in the disposal units at the time intrusion occurs is assumed to be indistinguishable from native soil. Some of the exhumed waste is assumed to be mixed with native soil in the intruder's vegetable garden, and the following exposure pathways are assumed to occur:

- ingestion of vegetables grown in the contaminated garden soil;
- direct ingestion of contaminated soil from the garden in conjunction with vegetable intakes;
- external exposure to contaminated soil while working in the garden or residing in the home on top of the disposal units; and
- inhalation of radionuclides suspended into air from contaminated soil while working in the garden or while residing in the home.

Table 4.11. Annual effective dose equivalents to inadvertent intruders per unit concentration of radionuclides in water from all exposure pathways[a]

Nuclide[b]	Annual dose (rem/year per μCi/L)	Nuclide[b]	Annual dose (rem/year per μCi/L)
^{3}H	5.5×10^{-2}	$^{232}Th + d$	3.4×10^{3}
^{14}C	2.0	$^{232}U + d$	1.5×10^{3}
^{26}Al	9.6	^{233}U	2.0×10^{2}
^{36}Cl	3.6	^{234}U	1.9×10^{2}
^{40}K	1.7×10^{1}	^{235}U	1.8×10^{2}
^{60}Co	2.2×10^{1}	^{236}U	1.8×10^{2}
^{63}Ni	4.1×10^{-1}	$^{238}U + d$	1.8×10^{2}
$^{90}Sr + d$	1.0×10^{2}	^{237}Np	2.8×10^{3}
^{99}Tc	1.1	^{238}Pu	2.8×10^{3}
^{113m}Cd	1.1×10^{2}	^{239}Pu	3.1×10^{3}
^{137}Cs	4.4×10^{1}	^{240}Pu	3.1×10^{3}
^{152}Eu	4.5	^{242}Pu	3.0×10^{3}
^{154}Eu	6.8	^{241}Am	3.3×10^{3}
^{155}Eu	9.8×10^{-1}	^{243}Am	3.3×10^{3}
$^{210}Pb + d$	4.9×10^{3}	^{243}Cm	2.1×10^{3}
$^{226}Ra + d$[c]	5.7×10^{3}	^{244}Cm	1.7×10^{3}
$^{229}Th + d$	2.9×10^{3}	^{249}Cf	3.4×10^{3}
^{230}Th	3.9×10^{2}		

[a]Results are obtained from Table G.14 of Appendix G.

[b]"d" denotes short-lived radioactive decay products that are assumed to be in secular equilibrium with the parent.

[c]Decay products include ^{210}Pb and its decay product, which are assumed to be in secular equilibrium with the parent.

The scenario dose conversion factors for the agriculture scenario for inadvertent intruders, as obtained from Table G.22 of Appendix G, are given in Table 4.12. The table gives annual EDEs per unit concentration of radionuclides in disposal units at the time intrusion is assumed to occur. The most important exposure pathways depend on the particular radionuclide. For the fission and activation products and ^{210}Pb, the vegetable pathway is the most important, unless the radionuclide is a photon emitter in which case external exposure while residing in the home is the most important pathway. For ^{226}Ra, ^{232}Th, and ^{232}U, inhalation of radon and its short-lived decay products while residing in the home is the most important pathway. However, if the inhalation dose from radon were excluded (see Sect. 4.5.4), external exposure while residing in the home would be the most important pathway for ^{226}Ra and the actinide radioelements when the isotope is a high-energy photon emitter, but the vegetable and soil ingestion pathways and inhalation exposure while residing in the home usually would be significant contributors to the total dose when the isotope is not a high-energy photon emitter. For many of the actinides, the soil ingestion pathway is more important than the vegetable pathway, due to the low plant-to-soil concentration ratios in vegetables assumed for most of these elements.

The resident scenario also is assumed to involve continuous lifetime exposure. As in the agriculture scenario, this scenario assumes that an intruder excavates a foundation for a home on top of disposal units. However, in excavating at the site, the intruder is assumed to encounter an intact engineered barrier (e.g., reinforced concrete roof) on top of the disposal units that cannot be penetrated by the types of excavation equipment normally used on the ORR. Thus, the intruder is assumed to construct a home directly above the intact engineered barrier. Since the engineered barrier is assumed not to be penetrated during excavation, the only exposure pathway of concern for the resident scenario is external exposure to photon-emitting radionuclides in the waste during indoor residence in the home on top of the disposal units. The presence of an intact engineered barrier would preclude any ingestion exposures or inhalation of radionuclides in particulate form. The thickness of intact engineered barriers on top of disposal units (about 30 cm or 12 in., see Sects. 2.3.5–2.3.7) also is presumed sufficient to mitigate significant inhalation exposures to radon and its short-lived decay products. Although some exposures to radon presumably would occur even in the presence of an intact barrier (e.g., due to the formation of small cracks), the exposures would be much less than those that would occur at later times when excavation into the waste becomes credible and the agriculture scenario is assumed to occur. That is, radon exposures that are ignored in the resident scenario essentially are captured in the agriculture scenario.

The scenario dose conversion factors for the resident scenario for inadvertent intruders, as obtained from Table G.23 of Appendix G, are given in Table 4.13. The table gives annual EDEs per unit concentration of radionuclides in disposal units at the time intrusion is assumed to occur. In the dose analysis for the resident scenario, the impenetrable engineered barrier on top of disposal units is assumed to provide shielding equivalent to 30 cm (12 in.) of soil.

The discovery scenario is assumed to involve a single, acute exposure during an individual's lifetime. This scenario assumes that an intruder attempts to excavate at the location of disposal units in constructing a foundation for a home, as in the agriculture and resident scenarios, but encounters an intact and impenetrable engineered barrier used in constructing the disposal units, as in the resident scenario. However, the intruder is

Table 4.12. Annual effective dose equivalents to inadvertent intruders per unit concentration of radionuclides in disposal units from all exposure pathways for agriculture scenario[a]

Nuclide[b]	Annual dose (rem/year per μCi/m^3)	Nuclide[b]	Annual dose (rem/year per μCi/m^3)
^{3}H	3.9×10^{-6}	^{232}Th + d[d]	4.3×10^{-3}
^{14}C	1.5×10^{-5}	^{220}Rn	1.0×10^{-2}[e]
^{26}Al	4.9×10^{-3}	^{232}U + d[d]	2.7×10^{-3}
^{36}Cl	1.2×10^{-3}	^{220}Rn	1.0×10^{-2}[e]
^{40}K	3.4×10^{-4}	^{233}U	1.1×10^{-5}
^{60}Co	4.6×10^{-3}	^{234}U	1.1×10^{-5}
^{63}Ni	1.8×10^{-7}	^{235}U + d	1.9×10^{-4}
^{90}Sr + d	1.8×10^{-4}	^{236}U	1.0×10^{-5}
^{99}Tc	1.1×10^{-5}	^{238}U + d	4.0×10^{-5}
^{113m}Cd	1.3×10^{-4}	^{237}Np + d	5.8×10^{-4}
^{137}Cs + d	1.0×10^{-3}	^{238}Pu	3.4×10^{-5}
^{152}Eu	2.0×10^{-3}	^{239}Pu	4.0×10^{-5}
^{154}Eu	2.2×10^{-3}	^{240}Pu	4.0×10^{-5}
^{155}Eu	3.9×10^{-5}	^{242}Pu	3.8×10^{-5}
^{210}Pb + d	3.0×10^{-4}	^{241}Am	5.6×10^{-5}
^{226}Ra + d[c,d]	3.4×10^{-3}	^{243}Am + d	2.7×10^{-4}
^{222}Rn	1.2×10^{-1}[e]	^{243}Cm	1.7×10^{-4}
^{229}Th + d	5.2×10^{-4}	^{244}Cm	2.0×10^{-5}
^{230}Th	1.1×10^{-5}	^{249}Cf	5.7×10^{-4}

[a]Results are obtained from Table G.22 of Appendix G and apply only to the assumed scenario for direct intrusion into disposal units.

[b]"d" denotes short-lived radioactive decay products that are assumed to be in secular equilibrium with the parent.

[c]Decay products include ^{210}Pb and its decay product.

[d]Dose from radon decay product is listed separately.

[e]Value is normalized to unit concentration of parent radionuclide.

Table 4.13. Annual effective dose equivalents to inadvertent intruders per unit concentration of radionuclides in disposal units for resident scenario[a]

Nuclide[b]	Annual dose (rem/year per μCi/m^3)	Nuclide[b]	Annual dose (rem/year per μCi/m^3)
^{26}Al	3.3×10^{-4}	^{232}Th + d	3.0×10^{-4}
^{40}K	2.1×10^{-5}	^{232}U + d	2.3×10^{-4}
^{60}Co	2.9×10^{-4}	^{235}U + d	5.6×10^{-7}
^{137}Cs + d	3.2×10^{-5}	^{238}U + d	1.2×10^{-6}
^{152}Eu	9.8×10^{-5}	^{237}Np + d	3.5×10^{-6}
^{154}Eu	1.1×10^{-4}	^{243}Am + d	1.1×10^{-6}
^{155}Eu	2.0×10^{-8}	^{243}Cm	7.7×10^{-7}
^{226}Ra + d	1.9×10^{-4}	^{249}Cf	8.1×10^{-6}
^{229}Th + d	1.0×10^{-5}		

[a]Results are obtained from Table G.23 of Appendix G and apply only to assumed scenario for direct intrusion into disposal units.

[b]"d" denotes short-lived radioactive decay products that are assumed to be in secular equilibrium with the parent.

assumed to access disposal units from the side during excavation, rather than from the top as in the agriculture and resident scenarios. This distinction is potentially important when several types of disposal units in SWSA 6 contain engineered barriers that are thinner at the sides than at the top and provide less shielding from external exposure when approached from the side. Then, shortly after encountering the intact and impenetrable engineered barrier, the scenario assumes that the intruder decides to abandon excavating at that location and moves elsewhere. As in the resident scenario, the only exposure pathway of concern for the discovery scenario is external exposure to photon-emitting radionuclides in the waste during the time the intruder excavates at the site.

The scenario dose conversion factors for the discovery scenario for inadvertent intruders, as obtained from Table G.24 of Appendix G, are given in Table 4.14. The table gives EDEs per unit concentration of radionuclides in disposal units at the time intrusion is assumed to occur. In the dose analysis for the discovery scenario, the impenetrable engineered barrier at the side of disposal units is assumed to provide shielding equivalent to 15 cm (6 in.) of soil. In addition, the exposure time for this scenario is assumed to be 1% of the time during a year (i.e., about 100 h). Since the external dose per unit concentration of radionuclides is directly proportional to the assumed exposure time, the results in Table 4.14 easily can be modified if a different exposure time is assumed.

The postdrilling scenario is assumed to involve continuous lifetime exposure. In this scenario, an inadvertent intruder is assumed to drill directly through a disposal unit (e.g., for the purpose of constructing a well for the intruder's domestic water supply), and the

Table 4.14. Effective dose equivalents to inadvertent intruders per unit concentration of radionuclides in disposal units for discovery scenario[a]

Nuclide[b]	Dose (rem per μCi/m^3)	Nuclide[b]	Dose (rem per μCi/m^3)
^{26}Al	3.0×10^{-5}	^{232}Th + d	2.7×10^{-5}
^{40}K	1.9×10^{-6}	^{232}U + d	1.8×10^{-5}
^{60}Co	2.9×10^{-5}	^{235}U + d	2.5×10^{-7}
^{137}Cs + d	4.5×10^{-6}	^{238}U + d	1.4×10^{-7}
^{152}Eu	1.1×10^{-5}	^{237}Np + d	8.1×10^{-7}
^{154}Eu	1.2×10^{-5}	^{241}Am	3.6×10^{-10}
^{155}Eu	2.0×10^{-8}	^{243}Am + d	3.4×10^{-7}
^{226}Ra + d	1.8×10^{-5}	^{243}Cm	7.7×10^{-7}
^{229}Th + d	1.5×10^{-6}	^{249}Cf	1.7×10^{-6}

[a]Results are obtained from Table G.24 of Appendix G and apply only to assumed scenario for direct intrusion into disposal units.

[b]"d" denotes short-lived radioactive decay products that are assumed to be in secular equilibrium with the parent.

contaminated drilling waste brought to the surface is assumed to be indistinguishable from native soil. All of the drilling waste is assumed to be mixed with native soil in the intruder's vegetable garden, and the following exposure pathways are assumed to occur:

- ingestion of vegetables grown in contaminated garden soil,
- direct ingestion of contaminated soil from the garden in conjunction with vegetable intakes,
- external exposure to contaminated soil while working in the garden, and
- inhalation of radionuclides suspended into air from contaminated soil while working in the garden.

These exposure pathways essentially are the same as the corresponding pathways assumed for the agriculture scenario. In the postdrilling scenario, however, external and inhalation exposures while residing in the home are not considered because all of the waste exhumed by drilling is assumed to be mixed with native soil in the intruder's vegetable garden and the intruder's home is assumed not to be located on top of disposal units or other contaminated soil.

The scenario dose conversion factors for the postdrilling scenario for inadvertent intruders, as obtained from Table G.25 of Appendix G, are given in Table 4.15. The table gives annual EDEs per unit concentration of radionuclides in disposal units at the time intrusion is assumed to occur. For each exposure pathway in this scenario, the dose per

Table 4.15. Annual effective dose equivalents to inadvertent intruders per unit concentration of radionuclides in exhumed waste from all exposure pathways for postdrilling scenario[a]

Nuclide[b]	Annual dose (rem/year per μCi/m^3)	Nuclide[b]	Annual dose (rem/year per μCi/m^3)
^{3}H	3.9×10^{-7}	^{232}Th + d[e]	6.2×10^{-6}
^{14}C	1.5×10^{-6}	^{220}Rn	2.1×10^{-6}[e]
^{26}Al	2.2×10^{-6}	^{232}U + d[e]	5.7×10^{-6}
^{36}Cl	1.2×10^{-4}	^{220}Rn	2.1×10^{-6}
^{40}K	6.0×10^{-6}	^{233}U	7.5×10^{-7}
^{60}Co	2.1×10^{-6}	^{234}U	7.3×10^{-7}
^{63}Ni	1.8×10^{-8}	^{235}U + d	7.9×10^{-7}
^{90}Sr + d	1.8×10^{-5}	^{236}U	6.9×10^{-7}
^{99}Tc	1.1×10^{-6}	^{238}U + d	6.6×10^{-7}
^{113m}Cd	1.3×10^{-5}	^{237}Np + d	2.4×10^{-5}
^{137}Cs + d	1.3×10^{-6}	^{238}Pu	2.1×10^{-6}
^{152}Eu	9.4×10^{-7}	^{239}Pu	2.5×10^{-6}
^{154}Eu	1.0×10^{-6}	^{240}Pu	2.5×10^{-6}
^{155}Eu	2.6×10^{-8}	^{242}Pu	2.4×10^{-6}
^{210}Pb + d	3.0×10^{-5}	^{241}Am	3.1×10^{-6}
^{226}Ra + d[c,d]	3.3×10^{-5}	^{243}Am + d	3.2×10^{-6}
^{222}Rn	1.3×10^{-5}[e]	^{243}Cm	1.6×10^{-6}
^{229}Th + d	3.0×10^{-6}	^{244}Cm	1.3×10^{-6}
^{230}Th	3.4×10^{-7}	^{249}Cf	2.8×10^{-6}

[a]Results are obtained from Table G.25 of Appendix G and apply only to assumed scenario for direct intrusion into disposal units.

[b]"d" denotes short-lived radioactive decay products that are assumed to be in secular equilibrium with the parent.

[c]Decay products include ^{210}Pb and its decay product.

[d]Dose from radon decay product is listed separately.

[e]Value is normalized to unit concentration of parent radionuclide.

unit concentration differs from the corresponding value for the agriculture scenario only as a result of the difference in the assumed dilution factor for mixing of waste exhumed from a disposal unit with native soil in the vegetable garden. In this analysis, the dilution factor for the postdrilling scenario is assumed to be one-tenth of the value for the agriculture scenario (see Appendix G).

The scenario dose conversion factors for the agriculture, resident, discovery, and postdrilling scenarios for inadvertent intruders can be compared using the results summarized in Tables 4.12, 4.13, 4.14, and 4.15, respectively. Such a comparison indicates, for example, that the agriculture scenario yields considerably higher estimates of dose than any of the other scenarios when all scenarios are assumed to occur at the same time. However, comparisons of doses for the different scenarios based only on the results in the summary tables do not take into account two important factors that must be considered in the intruder dose analysis.

First, the use of engineered barriers in constructing most of the disposal units in SWSA 6 presumably would preclude the agriculture scenario for some period of time after loss of active institutional controls (i.e., the engineered barriers presumably will maintain their integrity and be impenetrable by normal excavation techniques for considerably longer than 100 years). Therefore, for relatively short-lived radionuclides (e.g., ^{90}Sr and ^{137}Cs), the estimated dose for the resident, discovery, or postdrilling scenarios could be higher than the dose for the agriculture scenario if the former scenarios reasonably can occur immediately after loss of active institutional controls but the latter scenario is precluded for hundreds of years after disposal by intact engineered barriers.

Second, the radionuclide concentrations that should be used as input to the dose analysis for inadvertent intruders are not the same for the different exposure scenarios. From the descriptions of the agriculture, resident, and discovery scenarios, the appropriate radionuclide concentrations for use in the dose analysis are the values averaged over the entire volume of the region encompassed by the disposal units, rather than the average concentrations in disposed waste within individual disposal units. That is, the dose analysis for these scenarios should take into account the uncontaminated regions between disposal units and the region occupied by any engineered barriers because the size of an excavation in constructing a foundation for a home would be considerably larger than the size of individual disposal units. Therefore, for the agriculture, resident, and discovery scenarios, a dose reduction factor, called the geometrical reduction factor, should be applied to the average radionuclide concentrations in disposed waste to give the concentrations averaged over the region encompassed by the disposal units. This factor, which is the ratio of the contaminated volume of disposed waste to the total volume in the region encompassed by particular disposal units, is discussed further when the results of the dose analyses are presented in Sect. 4.5.3.2. On the other hand, the postdrilling scenario assumes that drilling through a single disposal unit occurs. Therefore, the appropriate radionuclide concentrations for this scenario are the average values in disposed waste in individual disposal units, and the geometrical reduction factor described above does not apply. In Sect. 4.5.3.2, the scenario dose conversion factors in Tables 4.12–4.15 are combined with the estimated concentrations of radionuclides in disposal units at various times after disposal to obtain dose estimates for inadvertent intruders for the different assumed exposure scenarios.

4.5.2 Discussion of Uncertainties in Exposure Pathways Analysis

The estimates of dose per unit concentration of radionuclides in water given in Tables 4.9–4.11 and the estimates of dose per unit concentration of radionuclides in disposal units given in Tables 4.12–4.15 are single values based on the models and parameter values presented in Appendix G. This section discusses uncertainties in these scenario dose conversion factors. These uncertainties are independent of uncertainties in predicting radionuclide concentrations in water and in disposal units at any time after disposal. For further discussion of uncertainties in the various exposure pathway models, see Sect. 4.6.2.

In implementing the models for the various exposure pathways in Appendix G, data specific to the ORR generally were not available for such important parameters as the elemental plant-to-soil concentration ratios in vegetables and the airborne concentrations of suspended radionuclides. Therefore, generic parameter values obtained from the literature were used in all exposure pathway models.

The parameter values used in the models for the different exposure pathways were usually intended to represent average conditions that might be experienced by off-site individuals or inadvertent intruders, as opposed to the maximum possible conditions that would yield the highest estimates of dose. This approach normally was used in selecting parameter values related to human activities such as the annual consumption of foodstuffs, breathing rate, and exposure times, and parameter values describing transport of radionuclides through environmental pathways to man (e.g., the plant-to-soil concentration ratios and atmospheric mass loading of activity suspended from soil). The two exceptions are (1) the assumption of a consumption rate of contaminated drinking water by exposed individuals of 2 L/day (0.5 gal/day), as often assumed by the U.S. Environmental Protection Agency (EPA 1989), and (2) the assumption of an exposure time for the discovery scenario of about 100 h. Both of these assumptions probably tend to overestimate exposure conditions that would be experienced by average individuals in critical population groups.

For some important parameters in the models developed in Appendix G, data available in the literature can be used to provide crude estimates of uncertainty. Two of the most important parameters in estimating dose for the agriculture and postdrilling scenarios are the elemental plant-to-soil concentration ratios in the model for the vegetable pathway and the atmospheric mass loadings of suspended activity from soil in the model for the inhalation pathways. Data available in the literature, which often were obtained under conditions that may not be representative of the ORR, indicate that these parameters could be uncertain by two to three orders of magnitude or more (Ng, Colsher, and Thompson 1982; Petersen 1983; Anspaugh et al. 1975; Healy 1980). When external exposure is not an important pathway for a particular radionuclide, uncertainties in the dose estimates for the agriculture and postdrilling scenarios would be about the same magnitude as the uncertainties in the plant-to-soil concentration ratio and the atmospheric mass loading of suspended activity from soil. Similarly, for the resident and discovery scenarios, data given in Table G.6 and calculations in the literature (Kocher and Sjoreen 1985) indicate that the estimates of external dose could be uncertain by an order of magnitude or more if the assumed thickness of shielding between the source and receptor locations is in error by a few tens of centimeters.

For other important parameters in the exposure pathway models, however, it is difficult to quantify the uncertainty, even on the basis of available generic data. An example of an essentially unquantifiable uncertainty is provided by the assumed dilution factor for mixing of wastes exhumed from disposal units with native soil in a vegetable garden [i.e., the parameter f_s first introduced in Eq. (G.8) of Appendix G, not to be confused with the geometrical reduction factor for different disposal units introduced at the end of Sect. 4.5.1.3 and described further in Sect. 4.5.3.2]. The dose from several exposure pathways in the agriculture scenario and from all exposure pathways in the postdrilling scenario is directly proportional to this dilution factor. An analysis of the uncertainty in this parameter could be based on estimated uncertainties in (1) the volume of waste material exhumed from disposal units, (2) the fraction of exhumed waste that is mixed with soil in a vegetable garden, and (3) the size of the garden. But, except for the assumed size of the garden, there are no data that could be used to support such an uncertainty analysis. The uncertainty in this dilution factor is probably an order of magnitude or more. However, it also seems likely that the values chosen for the present analysis (see Appendix G) tend to overestimate the average concentrations of radionuclides that would be found in contaminated soil in a vegetable garden. The dilution factor of 0.2 for mixing of exhumed waste with native soil in a vegetable garden assumed in the agriculture scenario (i.e., the assumption that garden soil would be 20% waste material from the location of disposal units and 80% native soil at the garden site) is believed to be reasonably conservative because exhumed waste presumably would not be fertile material and, thus, soil containing a significantly larger fraction of waste would not support plant growth. The dilution factor of 0.02 for mixing of exhumed waste with native soil in a vegetable garden used in the postdrilling scenario is based on reasonable assumptions for the volume of drilling waste and the size of the vegetable garden. The assumption that all drilling waste is mixed with native soil in the garden clearly is conservative.

The most important source of uncertainty in the estimates of dose per unit concentration of radionuclides for off-site individuals or inadvertent intruders presented in Appendix G probably is the definitions of the different exposure scenarios themselves, notwithstanding any parameter uncertainty analyses that could be performed and regardless of whether the results would reasonably represent the variability in doses that could be experienced on the ORR. That is, the dose analyses are based on assumptions that the scenarios will occur as postulated, but many of the explicit or implicit assumptions used in defining the exposure scenarios are open to question and are likely to be conservative.

In defining exposure scenarios, it seems reasonable to assume that (1) off-site individuals and inadvertent intruders will use water obtained from local sources and (2) an inadvertent intruder will establish a homestead within the boundary of the disposal facility at some time after loss of active institutional controls because these activities commonly occurred on the ORR prior to 1942. However, several of the assumptions used in developing the particular exposure scenarios for this analysis are less certain and probably pessimistic. For example, all scenarios assume that individuals will have no knowledge of prior waste disposal activities at the site at any time after loss of active institutional controls, but this assumption seems unreasonable at times immediately after loss of institutional controls. Furthermore, even if knowledge of the disposal facility were lost, all

exposure scenarios assume that (1) off-site individuals and inadvertent intruders will obtain essentially all of their water from the particular locations at which the highest concentrations of radionuclides are predicted to occur, (2) inadvertent intruders will build a home or drill a well at the location of disposal units, rather than in uncontaminated areas, and (3) exhumed waste will be mixed with uncontaminated soil in a vegetable garden. All of these assumptions clearly are pessimistic.

By their very definitions, the exposure scenarios for off-site individuals and inadvertent intruders assume conditions that probably tend to produce estimates of dose far greater than doses that reasonably could be received by most individuals in the two population groups. Therefore, it is not really the purpose of a dose analysis, particularly in the case of inadvertent intruders, to provide best estimates of dose that likely would be received. Rather, the primary purpose of the analysis is to indicate whether certain disposal practices would be adequately protective of public health for the assumed conditions of exposure. That is, the analysis is used primarily to establish criteria for the construction and performance of disposal units and the acceptability of wastes for disposal. Furthermore, quantitative estimates of uncertainties in calculated doses based on parameter uncertainty analyses may not be meaningful because the results are conditional on the occurrence of assumed exposure scenarios. This is a particularly relevant concern for the postdrilling scenario because, for some of the disposal units in the form of wells or silos (e.g., the fissile wells), drilling directly through disposal units clearly would occur only with a relatively low probability.

4.5.3 Dose Analysis for Disposal Units in SWSA 6

This section presents the estimated doses to off-site individuals and inadvertent intruders resulting from disposal of LLW in the various types of disposal units in SWSA 6. Doses to off-site individuals are assumed to result entirely from releases of radionuclides to surface waters, and the estimated annual EDEs from direct consumption of contaminated water and from all exposure pathways are obtained from (1) the estimated maximum concentrations of radionuclides transported to surface waters given in Sect. 4.4 and (2) the annual doses per unit concentration of radionuclides summarized in Tables 4.9 and 4.10. Inadvertent intruders are assumed to be exposed to contaminated groundwater, and the estimated annual EDEs from direct consumption of contaminated water and from all exposure pathways are obtained from (1) the estimated maximum concentrations of radionuclides in groundwater outside the 100-m (328-ft) buffer zone around any disposal units given in Sect. 4.3.1 and (2) the annual doses per unit concentration of radionuclides summarized in Tables 4.9 and 4.11. Finally, estimated EDEs to inadvertent intruders resulting from direct intrusion into disposal units are based on (1) estimated concentrations of radionuclides in disposal units at the time intrusion is assumed to occur and (2) the doses per unit concentration of radionuclides in disposal units for the four assumed exposure scenarios summarized in Tables 4.12, 4.13, 4.14, and 4.15.

The results of the dose analysis for direct intrusion into disposal units are presented separately for each type of disposal unit in SWSA 6. However, in the dose analyses for off-site individuals and inadvertent intruders for the water pathways, the results for each radionuclide represent the dose resulting from releases from all disposal units in SWSA 6. In addition, in the dose analyses for contaminated groundwater, the particular disposal

units that produce most of the contamination are identified. In general, results are presented only for those radionuclides that contribute the highest doses.

4.5.3.1 Dose Analysis for Water Pathways

4.5.3.1.1 Off-site individuals

Doses to off-site individuals are assumed to result entirely from use of contaminated surface water discharged from the present location of White Oak Dam. Because all contaminated groundwater in SWSA 6 is assumed to discharge to the surface within the facility boundary, off-site individuals would not be exposed to contaminated groundwater obtained from a well.

The estimated maximum concentrations of radionuclides in surface water are obtained from (1) the maximum concentrations of radionuclides discharged into surface water near the location of White Oak Dam due to releases from all disposal units, as given in Sect. 4.4, (2) an assumed water discharge of 1.8×10^8 L/year (4.8×10^7 gal/year) from SWSA 6, and (3) an assumed flow rate of water at the point of use in White Oak Creek of 0.38 m^3/s (13 cfs), or 1.2×10^{10} L/year (3.2×10^9 gal/year). Thus, the estimated maximum concentrations of radionuclides in μCi/L at the point of use are given by the maximum concentrations in surface discharges multiplied by the ratio of the discharge rate from SWSA 6 to the flow rate at the point of use, or 0.015. Discharges of radionuclides beyond the facility boundary take into account the contributions from contaminated groundwater that discharges to the surface within the facility boundary as well as the contributions from shallow subsurface discharges to the surface.

The results of the dose analysis for off-site individuals from the surface water pathway, based on the maximum radionuclide concentrations in surface water near the facility boundary obtained as described above from results in Table 4.8, and the annual doses per unit concentration of radionuclides in Tables 4.9 and 4.10, are summarized in Tables 4.16 and 4.17. These tables give the estimated doses for the drinking water pathway only and for all exposure pathways, respectively. As described in Sect. 4.4, these results are obtained from the sum of the peak releases from all disposal units, regardless of when they occur. Therefore, the estimated doses are conservative, and it is not meaningful to give a single time at which the peak dose occurs.

4.5.3.1.2 Inadvertent intruders

Doses to inadvertent intruders resulting from transport of radionuclides in water are assumed to result entirely from use of contaminated groundwater obtained from a well within the boundary of the disposal facility. The surface water pathway can be neglected for inadvertent intruders because the flow rate of surface streams within the boundary of SWSA 6 is insufficient to provide a domestic water supply for an individual.

The maximum concentrations of radionuclides in groundwater near the different disposal units in SWSA 6 are summarized in Table 4.5. The well used by an intruder is assumed to be located at a distance of 100 m (328 ft) from any disposal unit [the point of maximum contaminant concentration outside the 100-m (328-ft) buffer zone].

Table 4.16. Results of dose analysis for off-site individuals from drinking water pathway due to releases to surface water[a]

Nuclide	Concentration (μCi/L)[b]	Annual dose (rem/year)
^{14}C	2.1×10^{-3}	3.2×10^{-3}
^{36}Cl	1.7×10^{-4}	3.8×10^{-4}
^{90}Sr	7.8×10^{-6}	7.8×10^{-4}
^{239}Pu	8.9×10^{-8}	2.8×10^{-4}
Others		$<1.0 \times 10^{-4}$

[a]Dose estimates include contributions from all disposal units and take into account releases to surface water, subsurface water, and groundwater on the SWSA 6 site. Annual dose per unit concentration of radionuclides in water is given in Table 4.9.

[b]Maximum concentrations of radionuclides in off-site surface water at any time after disposal, based on maximum concentrations in discharges from SWSA 6 given in Table 4.8 and dilution factor for release to off-site surface water at point of use of 0.015. Ranges of time over which peak concentrations are predicted to occur are described in Sect. 4.4 and Table 4.8.

Table 4.17. Results of dose analysis for off-site individuals from all exposure pathways due to releases to surface water[a]

Nuclide	Concentration (μCi/L)[b]	Annual dose (rem/year)
^{14}C	2.1×10^{-3}	4.3×10^{-3}
^{36}Cl	1.7×10^{-4}	6.2×10^{-4}
^{90}Sr	7.8×10^{-6}	7.8×10^{-4}
^{239}Pu	8.9×10^{-8}	2.8×10^{-4}
Others		$<1.0 \times 10^{-4}$

[a]Dose estimates include contributions from all disposal units and take into account releases to surface water, subsurface water, and groundwater on the SWSA 6 site. Annual dose per unit concentration of radionuclides in water is given in Table 4.10.

[b]Maximum concentrations of radionuclides in off-site surface water at any time after disposal, based on maximum concentrations in discharges from SWSA 6 given in Table 4.8 and dilution factor for release to off-site surface water at point of use of 0.015. Ranges of time over which peak concentrations are predicted to occur are described in Sect. 4.4 and Table 4.8.

The results of the dose analysis for inadvertent intruders from the groundwater pathway, based on the maximum radionuclide concentrations in groundwater and the annual doses per unit concentration of radionuclides in Tables 4.9 and 4.11, are summarized in Tables 4.18 and 4.19. Again, dose estimates are given for the drinking water pathway only and for all exposure pathways.

For some radionuclides, the maximum concentrations in groundwater are predicted to occur prior to loss of active institutional controls at 100 years after disposal (the monitored closure period), and exposures of inadvertent intruders at that time presumably would be precluded. However, the requirement for protection of groundwater resources consistent with standards for radioactivity in drinking water is assumed to apply at any time after disposal, regardless of whether exposure to contaminated groundwater actually could occur. Thus, results are given in Table 4.18 for the times of maximum concentration. In Table 4.19, however, results are given only for the maximum concentrations in groundwater at any time after loss of active institutional controls, because the results apply to exposures of inadvertent intruders from all pathways involving use of contaminated groundwater and the dose estimates apply only at times when the exposures are credible.

4.5.3.2 Dose Analysis for Direct Intrusion into Disposal Units

Direct intrusion into disposal units presumably can occur at any time after loss of active institutional controls at 100 years after closure. However, the particular exposure scenarios that are assumed to be credible depend on the time after disposal, because the engineered barriers in most of the disposal units are assumed to preclude the agriculture scenario for some period of time after loss of institutional controls.

4.5.3.2.1 Agriculture scenario

The agriculture scenario is based on the assumption that an inadvertent intruder would excavate into disposal units at some time after loss of active institutional controls and, furthermore, that all solid waste in the disposal units would be indistinguishable from native soil. However, the agriculture scenario is assumed to be precluded for as long as any engineered barriers used in constructing disposal units maintained their integrity.

As described in Sect. 2.3.5, most of the below-grade disposal units in SWSA 6 are constructed using a thick concrete cap. The one exception is the trenches for biological waste, which include only an earthen cover. In addition, the above-grade tumuli described in Sect. 2.3.6 are constructed using vaults with a thick concrete cap.

In the present analysis, the use of thick concrete caps or vaults in all disposal units except the biological trenches is assumed to preclude the agriculture scenario for 300 years after disposal. Although the expected lifetime of the concrete barriers is not known, the assumed lifetime of 300 years is believed to be pessimistic and may result in conservative estimates of dose for shorter-lived radionuclides. Thus, the agriculture scenario is assumed to occur beginning at 300 years after disposal for all disposal units, except the scenario is assumed to occur at 100 years after disposal for the biological trenches, which do not include engineered barriers that would prevent access to the waste during excavation.

Table 4.18. Results of dose analysis for drinking water pathway at disposal site due to releases to groundwater[a]

Nuclide	Time (year)[b]	Concentration (μCi/L)[c]	Disposal units[d]	Annual dose (rem/year)
^{3}H	30	1.9×10^{-1}	Interim Waste Management Facility (IWMF)	8.7×10^{-3}
^{14}C	67	1.4×10^{-1}	IWMF	2.1×10^{-1}
^{36}Cl	34	6.8×10^{-2}	IWMF	1.5×10^{-1}
^{99}Tc	67	1.6×10^{-3}	IWMF	1.5×10^{-3}
^{233}U	2400	8.9×10^{-6}	IWMF	1.8×10^{-3}
^{239}Pu	2400	4.2×10^{-6}	IWMF	1.3×10^{-2}
^{243}Am	2400	2.1×10^{-7}	IWMF	6.9×10^{-4}
Others				$<4.0 \times 10^{-4}$

[a]Dose estimates include contributions from all disposal units. Annual dose per unit concentration of radionuclides in water is given in Table 4.9.

[b]Time after disposal at which maximum concentration in groundwater occurs. For times less than 100 years, use of contaminated groundwater is precluded by active institutional controls, but requirement for protection of groundwater resources is assumed to apply when groundwater would not be used.

[c]Maximum concentrations of radionuclides in groundwater beyond 100-m (328-ft) buffer zone around any disposal units at any time after disposal, as obtained from Table 4.5.

[d]Units primarily responsible for maximum concentrations in groundwater.

For all disposal units constructed with engineered barriers, the agriculture scenario can occur at any time after the barriers have lost their integrity; for the biological trenches, the scenario can occur at any time after loss of active institutional controls. For most radionuclides, the dose for the agriculture scenario has its maximum value at the earliest time the scenario can occur because the concentrations in disposal units decrease monotonically with time. However, a potentially important exception occurs with ^{238}U. This radionuclide decays to other radionuclides, principally ^{226}Ra and its short-lived decay products, for which the dose per unit concentration in the agriculture scenario is much higher than the value for the parent radionuclide (see Table 4.12). However, the activities of the important decay products are insignificant before about 10^4 years and reach secular equilibrium with the activity of ^{238}U only after about 10^6 years. Therefore, in addition to estimating doses at the time the agriculture scenario first could occur, doses are estimated at times beyond 10^6 years for ^{238}U and its decay products. The dose estimates at far future times also take into account potentially significant contributions from other radionuclides with half-lives greater than about 10^6 years, but the contributions from all other radionuclides at these times would be insignificant. Consideration of potential doses at far

Table 4.19 Results of dose analysis for inadvertent intruders from all exposure pathways due to releases to groundwater[a]

Nuclide	Time (year)[b]	Concentration (μCi/L)[c]	Disposal units[d]	Annual dose (rem/year)
^{3}H	100	2.1×10^{-7}	Interim Waste Management Facility (IWMF)	1.2×10^{-8}
^{14}C	100	4.4×10^{-3}	IWMF	8.8×10^{-3}
^{36}Cl	100	1.4×10^{-5}	IWMF	5.0×10^{-5}
^{99}Tc	180	1.0×10^{-4}	High-range wells	1.1×10^{-4}
^{233}U	2400	8.9×10^{-6}	IWMF	1.8×10^{-3}
^{239}Pu	2400	4.2×10^{-6}	IWMF	1.3×10^{-2}
^{243}Am	2400	2.1×10^{-7}	IWMF	6.9×10^{-4}
Others				$<4.0 \times 10^{-4}$

[a]Dose estimates include contributions from all disposal units. Annual dose per unit concentration of radionuclides in water is given in Table 4.11.

[b]Time after disposal at which maximum concentration in groundwater occurs, except exposures are not credible during 100-year active institutional control period. If maximum concentration occurs within 100 years after disposal, maximum concentration at 100 years or beyond is used in dose analysis.

[c]Maximum concentrations of radionuclides in groundwater beyond 100-m (328-ft) buffer zone around any disposal units at any time after loss of active institutional controls at 100 years after disposal, as obtained from Table 4.5.

[d]Units primarily responsible for maximum concentrations in groundwater.

future times is needed because there presently is no time limit for evaluating compliance with the performance objective for protection of inadvertent intruders.

For the agriculture scenario, the concentrations of radionuclides used as input to the dose analysis for each type of disposal unit were obtained from (1) the estimated inventories of radionuclides in the disposal units at the time of disposal and the volume of disposed waste, as given in Appendix A, (2) the assumption that the initial radionuclide concentrations are reduced over time only by radioactive decay, and (3) the geometrical reduction factor described at the end of Sect. 4.5.1.3, which is the fraction of the total volume encompassed by each type of disposal unit that contains waste and which converts the average concentrations of radionuclides in disposed waste to the concentrations averaged over the region that would be accessed by an excavation for a home. The assumption that radionuclide concentrations in the disposal units are reduced over time only by radioactive decay clearly is conservative, especially at far future times when the

doses from buildup of the important ^{238}U decay products are estimated, because it does not take into account reductions in concentrations over time due to release and transport by infiltrating water. Therefore, the calculations described above provide upper-bound estimates of dose. Removal of radionuclides from disposal units by infiltrating water has not been taken into account in the intruder dose analysis because the models for release and transport are believed to overestimate releases that might occur. Use of a release model that overestimates releases could result in significant underestimates of potential doses to future inadvertent intruders.

The geometrical reduction factor for a particular type of disposal unit depends on the design and spacing of individual units. For Tumulus I, Tumulus II, and the IWMF, the geometrical reduction factor is estimated to be 0.4 on the basis of the dimensions of individual waste vaults, the volume of each vault occupied by waste, and the close packing of vaults in the disposal units. For the low-range silos, high-range silos, asbestos silos, and biological trenches, the geometrical reduction factor is estimated to be 0.25 on the basis of the dimensions and spacing of individual disposal units. The high-range wells have approximately the same size and spacing as the three types of silos listed above, but the geometrical reduction factor for the high-range wells is estimated to be 0.075 because waste in these units is placed in cast iron pipes that occupy only about 30% of the interior area of the wells. Finally, the fissile wells, which have approximately the same size and spacing as the various silos, require special consideration because only a single such well has received waste since DOE Order 5820.2A went into effect on September 26, 1988, and thus is of concern to this performance assessment (Appendix A, Table A.2). The geometrical reduction factor for the single fissile well is given by the ratio of the area occupied by waste in the well to area of a typical excavation in building a home. The area of the waste in a fissile well is 0.45 m^2 (4.8 ft^2), and the area of a typical excavation is about 300 m^2 (3200 ft^2) (NRC 1982). Therefore, the geometrical reduction factor for the fissile well is estimated to be 0.0015.

The results of the dose analysis for the agriculture scenario, based on the average radionuclide concentrations at disposal units at the time intrusion is assumed to occur as described above and the annual doses per unit concentration of radionuclides in Table 4.12, are summarized in Table 4.20. These results again are upper-bound estimates of dose, because removal of radionuclides from disposal units by infiltrating water has not been taken into account. As described previously, dose estimates for the agriculture scenario are given at two different times. The first results apply at the time the scenario first occurs, which is either 100 or 300 years after disposal, and the second results apply at times beyond about 10^6 years, when only very long-lived radionuclides and their decay products could be of concern. In addition, for these two different times, two dose estimates are given, one including the contributions from isotopes of radon and the other excluding these contributions. At the present time, the performance objective for protection of inadvertent intruders does not exclude the dose from radon.

4.5.3.2.2 Resident scenario

The resident scenario is based on the assumption that an inadvertent intruder attempts to excavate into disposal units from above but encounters an intact and impenetrable engineered barrier on top of the waste. The intruder then constructs a home

Table 4.20. Upper-bound estimates of effective dose equivalents to inadvertent intruders for agriculture scenario[a]

Disposal unit	Nuclide	Concentration (μCi/m^3)[b]	Annual dose (rem/year)
Tumulus I	^{14}C	1.8×10^4	0.10
	^{99}Tc	6.9×10^2	0.003
	^{137}Cs	1.9×10^4	0.008
	^{226}Ra[c]	7.8×10^{-1}	–
	^{222}Rn	–	0.033
	^{238}U[d]	8.5×10^1	0.001
	^{226}Ra[c]		0.12
	^{222}Rn		4.1
	^{239}Pu	1.7×10^2	0.003
	^{241}Am	1.5×10^2	0.002
	Others		<0.001
	Sum[e]		0.15 (0.12)[f]
	Sum[g]		4.2 (0.12)[f]
Tumulus II	^{14}C	3.5×10^3	0.020
	^{99}Tc	3.9×10^2	0.002
	^{137}Cs	8.7×10^3	0.004
	^{232}Th[c]	6.6×10^{-1}	0.001
	^{220}Rn	–	0.003
	^{238}U[d]	1.2×10^1	–
	^{226}Ra[c]		0.016
	^{222}Rn		0.58
	^{239}Pu	8.7×10^1	0.001
	^{241}Am	1.8×10^2	0.002
	Others		<0.001
	Sum[e]		0.033 (0.030)[f]
	Sum[g]		0.60 (0.017)[f]
Interim Waste Management Facility	^{14}C	4.1×10^4	0.24
	^{36}Cl	2.8×10^3	1.3
	^{99}Tc	3.9×10^2	0.002
	^{137}Cs	1.4×10^4	0.006
	^{233}U	2.4×10^2	0.001
	^{238}U[d]	1.5×10^2	0.002
	^{226}Ra[c]		0.20
	^{222}Rn		7.2
	^{239}Pu	1.2×10^2	0.002
	Others		<0.001
	Sum[e]		1.6
	Sum[g]		7.4 (0.20)[f]

Table 4.20 (continued)

Disposal unit	Nuclide	Concentration (μCi/m^3)[b]	Annual dose (rem/year)
Low-range silo	^{14}C	1.2×10^5	0.45
	^{99}Tc	5.5×10^3	0.015
	^{137}Cs	7.6×10^3	0.002
	^{226}Ra[c]	1.1×10^1	0.008
	^{222}Rn		0.29
	^{232}Th[c]	1.8	0.002
	^{220}Rn		0.005
	^{238}U[d]	2.3×10^2	0.002
	^{226}Ra[c]		0.20
	^{222}Rn		6.9
	^{243}Am	1.8×10^1	0.001
	Others		<0.001
	Sum[e]		0.78 (0.48)[f]
	Sum[g]		7.1 (0.20)[f]
High-range silo	^{90}Sr	1.2×10^6	0.037
	^{137}Cs	8.2×10^4	0.021
	^{232}Th[c]	4.1×10^{-1}	–
	^{220}Rn		0.001
	^{238}U[d]	3.8×10^1	–
	^{226}Ra[c]		0.032
	^{222}Ra		1.1
	Others		<0.001
	Sum[e]		0.059 (0.058)[f]
	Sum[g]		1.1 (0.033)[f]
High-range well[h]	^{90}Sr	4.5×10^8	4.2
	^{99}Tc	2.6×10^4	0.021
	^{137}Cs	4.2×10^8	32
	^{152}Eu	3.4×10^7	0.001
	^{229}Th	4.8×10^2	0.018
	^{232}Th[c]	2.4	–
	^{220}Rn		0.002
	^{238}U[d]	2.6×10^{-1}	–
	^{226}Ra[c]		–
	^{222}Rn		0.002
	Others		<0.001
	Sum[e]		36 (36)[f]
	Sum[g]		0.004 (<0.001)[f]

Table 4.20 (continued)

Disposal unit	Nuclide	Concentration (μCi/m^3)[b]	Annual dose (rem/year)
Fissile well	^{137}Cs	6.8×10^7	0.10
	^{238}U[d]	8.5×10^3	–
	^{226}Ra[c]		0.043
	^{222}Rn		1.5
	Others		<0.001
	Sum[e]		0.10
	Sum[g]		1.5 (0.043)[f]
Asbestos silo	^{14}C	5.4×10^3	0.020
	^{232}Th[c]	4.0×10^{-1}	–
	^{220}Rn		0.001
	^{238}U[d]	4.7×10^1	–
	^{226}Ra[c]		0.040
	^{222}Ra		1.4
	Others		<0.001
	Sum[e]		0.021 (0.020)[f]
	Sum[g]		1.4 (0.041)[f]
Biological trench[i]	^{90}Sr	8.7×10^2	0.003
	Others		<0.001
	Sum		0.003

[a]Scenario is assumed to occur at 300 years after disposal for all disposal units, except as noted.

[b]Radionuclide concentrations in waste at time of disposal. Concentrations are assumed to be reduced over time by radioactive decay, but removal of activity from disposal units by infiltrating water is not taken into account.

[c]Dose estimate for radon decay product is listed separately.

[d]Dose estimates for long-lived decay products, which reach secular equilibrium with ^{238}U only after about 10^6 years, are listed separately.

[e]Dose estimate at 300 years after disposal.

[f]Dose estimate in parentheses excludes contributions from radon.

[g]Dose estimate at times beyond 10^6 years after disposal when only very long-lived radionuclides could be present.

[h]Dose estimates for these units probably are unreasonably high (see Sect. 4.5.4.3).

[i]Scenario is assumed to occur at 100 years after disposal.

immediately on top of the engineered barriers and takes up residence at the site. The intent of this scenario is to represent exposures that might occur immediately after loss of active institutional controls at 100 years after disposal when permanent residence on the disposal site presumably is credible but before excavation into waste in most types of disposal units would be credible.

The resident scenario is assumed to occur beginning at 100 years after disposal for all disposal units constructed with engineered barriers. This scenario is not relevant for the biological trenches, because these units were constructed without engineered barriers and

the agriculture scenario would apply at any time after 100 years. In addition, the resident scenario need not be considered at times far in the future, when ingrowth of ^{226}Ra from the decay of ^{238}U could become significant, because the engineered barriers are assumed to maintain their integrity for only a relatively short time after disposal and the agriculture scenario would apply at any time after the barriers have failed. Therefore, because the concentrations of all potentially important radionuclides decrease monotonically with time during the period that the engineered barriers are expected to remain intact, the resident scenario is applied only at 100 years after disposal when the doses would be the highest.

As described in Sect. 4.5.1.3 and Appendix G, the estimates of external dose for the resident scenario are based on the assumption that the intact engineered barriers on top of all disposal units provide shielding equivalent to 30 cm (12 in.) of soil. This is a good approximation for those disposal units constructed with a 30-cm-thick (12-in.-thick) concrete cap (see Sects. 2.3.5 and 2.3.6) because a given thickness of soil and concrete provide about the same shielding. However, for the high-range wells described in Sects. 2.3.5.3 and 2.3.5.4, some of the disposal units were constructed with a 100-cm-thick (39-in.-thick) concrete cap. Therefore, the dose estimates for the resident scenario would be quite conservative for such units. However, since data on radionuclide concentrations in the distinct types of high-range wells with different cap thicknesses are not available, the assumption of 30 cm (12 in.) of shielding was applied to all high-range wells. This approach provides worst-case estimates of dose for these units.

The radionuclide concentrations used as input to the dose analysis for the resident scenario were obtained as described above for the agriculture scenario. The geometrical reduction factor for each type of disposal unit is included.

The results of the dose analysis for the resident scenario, based on the average radionuclide concentrations at disposal sites at 100 years after disposal (obtained as described above) and the annual doses per unit concentration of radionuclides in Table 4.13, are summarized in Table 4.21. These results are upper-bound estimates of dose because removal of radionuclides from disposal units by infiltrating water has not been taken into account.

4.5.3.2.3 Discovery scenario

The discovery scenario is based on the assumption that an inadvertent intruder attempts to excavate into disposal units from the side but encounters an intact and impenetrable engineered barrier beside the waste. Then, rather than taking up residence at the site, the intruder soon abandons that location and moves elsewhere. The intent of this scenario is to represent acute exposures that might occur immediately after loss of active institutional controls at 100 years after disposal when excavation through intact barriers could be attempted but might be abandoned, in distinction from the resident scenario. If the engineered barriers at the side of all disposal units were the same thickness as at the top, then the resident scenario would always give higher doses, and the discovery scenario would not need to be considered.

The discovery scenario is assumed to occur beginning at 100 years after disposal for all disposal units constructed with engineered barriers. However, the discovery scenario is considered only if the shielding provided by the engineered barriers at the sides of disposal units is significantly less than the shielding provided by the barriers at the top of the units.

Table 4.21. Upper-bound estimates of effective dose equivalents to inadvertent intruders for resident scenario[a]

Disposal unit[b]	Nuclide	Concentration (μCi/m^3)[c]	Annual dose (rem/year)
Tumulus I	^{137}Cs	1.9×10^4	0.024
	Others		<0.001
	Sum		0.024
Tumulus II	^{137}Cs	8.7×10^3	0.011
	Others		<0.001
	Sum		0.011
Interim Waste Management Facility	^{137}Cs	1.4×10^4	0.018
	Others		<0.001
	Sum		0.018
Low-range silo	^{137}Cs	7.6×10^3	0.006
	Others		<0.001
	Sum		0.006
High-range silo	^{137}Cs	8.2×10^4	0.066
	Others		<0.001
	Sum		0.066
High-range well[d]	^{60}Co	3.6×10^7	0.002
	^{137}Cs	4.2×10^8	100
	^{152}Eu	3.4×10^7	1.5
	^{154}Eu	1.2×10^7	0.037
	Others		<0.001
	Sum		100
Fissile well	^{137}Cs	6.8×10^7	0.33
	Others		<0.001
	Sum		0.33
Asbestos silo	All		<0.001

[a]Scenario is assumed to occur at 100 years after disposal.

[b]Scenario applies only to disposal units listed. Scenario is not relevant for biological trenches, which are constructed without engineered barriers.

[c]Radionuclide concentrations in waste at time of disposal. Concentrations are assumed to be reduced over time only by radioactive decay, but removal of activity from disposal units by infiltrating water is not taken into account.

[d]Dose estimates for these units probably are unreasonably high (see Sect. 4.5.4.3).

If the thickness of the barriers is the same at the top and sides of disposal units, then the resident scenario will always yield higher estimates of dose, due to the longer exposure time assumed, and the discovery scenario can be neglected. Doses for the discovery scenario thus are estimated only for the low-range silos, high-range silos, high-range wells, and asbestos silos. As with the resident scenario, the discovery scenario is not relevant for the biological trenches, and the scenario is applied only at 100 years after disposal when the doses would be the highest.

As described in Sect. 4.5.1.3 and Appendix G, the estimates of external dose of the discovery scenario are based on the assumption that the intact engineered barriers at the sides of the disposal units provide shielding equivalent to 15 cm (6 in.) of soil. This is a somewhat conservative approximation for the low-range silos, high-range silos, and asbestos silos, because the assumed shielding takes into account the 15-cm (6-in.) thickness of concrete at the sides of the silos but does not take into account the presence of thin-walled steel pipes containing the concrete. However, for the high-range wells described in Sects. 2.3.5.3 and 2.3.5.4, some of the disposal units were constructed with 2-cm-thick (0.8-in.-thick) steel pipes inside the silos, in addition to the concrete and steel pipe at the sides, and other disposal units were constructed using only 2-cm-thick (0.8-in.-thick) steel pipe. For the case of steel pipes inside silos, the dose estimates for the discovery scenario would be quite conservative. For the case of wells with steel pipes only, since the shielding provided by any material is roughly proportional to the square of the average atomic number, the 2-cm (0.8-in.) thickness of steel pipe provides approximately the same shielding as 15 cm (6 in.) of concrete, and the dose estimates should be appropriate. However, as for the resident scenario, since data on radionuclide concentrations in the distinct types of high-range wells with different amounts of shielding are not available, the assumption of 15 cm (6 in.) of shielding was applied to all high-range wells. This approach provides worst-case estimates of dose for these units.

The radionuclide concentrations used as input to the dose analysis for the discovery scenario were obtained as described above for the agriculture scenario. The geometrical correction factor for each type of disposal unit is included.

The results of the dose analysis for the discovery scenario, based on the average radionuclide concentrations at disposal sites at 100 years after disposal and the annual doses per unit concentration of radionuclides in Table 4.14, are summarized in Table 4.22. These results are upper-bound estimates of dose because removal of radionuclides from disposal units by infiltrating water has not been taken into account.

4.5.3.2.4 Postdrilling scenario

The postdrilling scenario is based on the assumption that an inadvertent intruder exhumes a small volume of waste while drilling through a disposal unit and that the exhumed waste is indistinguishable from native soil. In addition, the assumption is made that a drilling technology appropriate for penetrating hard rock formations would be used, so that none of the engineered barriers used in constructing some of the disposal units would preclude drilling through waste.

Table 4.22. Upper-bound estimates of effective dose equivalents to inadvertent intruders for discovery scenario[a]

Disposal unit[b]	Nuclide	Concentration (μCi/m^3)[c]	Dose (rem)
Low-range silo	All		<0.001
High-range silo	^{137}Cs	8.2×10^4	0.009
	Others		<0.001
	Sum		0.009
High-range well[d]	^{137}Cs	4.2×10^8	14
	^{152}Eu	3.4×10^7	0.19
	^{154}Eu	1.2×10^7	0.004
	Others		<0.001
	Sum		14
Asbestos silo	All		<0.001

[a]Scenario is assumed to occur at 100 years after disposal.

[b]Scenario applies only to disposal units listed. For Tumulus I, Tumulus II, Interim Waste Management Facility, and fissile wells, dose estimates for resident scenario in Table 4.28 will always be higher, and discovery scenario is not relevant for biological trenches, which are constructed without engineered barriers.

[c]Radionuclide concentrations in waste at time of disposal. Concentrations are assumed to be reduced over time only by radioactive decay, but removal of activity from disposal units by infiltrating water is not taken into account.

[d]Dose estimates for these units probably are unreasonably high (see Sect. 4.5.4.3).

Because of the assumption that engineered barriers would not be effective in precluding drilling through disposal units, the postdrilling scenario is assumed to occur beginning at 100 years after disposal for all types of disposal units. As with the other scenarios, the dose from most radionuclides would have its highest value at the time the postdrilling scenario could first occur, and doses thus are estimated at 100 years after disposal. However, as in the agriculture scenario, the postdrilling scenario can occur in the absence of engineered barriers. Therefore, doses also are estimated at times beyond 10^6 years after disposal, in order to take into account potentially significant doses due to the buildup of ^{226}Ra produced in the decay of ^{238}U.

The radionuclide concentrations used as input to the dose analysis for the postdrilling scenario were obtained from the data on radionuclide inventories in the disposal units at the time of disposal and the volume of the disposal units, corrected for radioactive decay over time prior to occurrence of the scenario. However, the geometrical correction factor used in estimating radionuclide concentrations averaged over the disposal site in the agriculture, resident, and discovery scenarios is not used in the postdrilling scenario, because drilling is assumed to occur through the waste itself and the uncontaminated regions encompassed by the disposal units are not relevant. The presence

of uncontaminated material in the drilling waste is taken into account implicitly in the assumed dilution factor for mixing of drilling waste with native soil in the intruder's vegetable garden.

The results of the dose analysis for the postdrilling scenario, based on the average radionuclide concentrations in disposal units at the time intrusion is assumed to occur and the annual doses per unit concentration of radionuclides in Table 4.15, are summarized in Table 4.23. These results are upper-bound estimates of dose because removal of radionuclides from disposal units by infiltrating water has not been taken into account. As described previously, dose estimates for the postdrilling scenario are given at two different times. The first results apply at 100 years after disposal, which is the time that the scenario first could occur, and the second results given for some units apply at times beyond 10^6 years, when only very long-lived radionuclides and their decay products could be of concern. In addition, for these two different times, two dose estimates are given for some units, one including the contributions from radon and the other excluding these contributions. Again, the present performance objective for protection of inadvertent intruders does not exclude the dose from radon.

4.5.3.2.5 Summary of dose analysis for direct intrusion

For any of the scenarios for direct intrusion into waste disposal units assumed in this analysis, the total dose is the sum of the contributions from all radionuclides in the disposal units at the time intrusion is assumed to occur. For each of the disposal units, the upper-bound estimates of total doses for the four intrusion scenarios, as obtained from the results in Tables 4.20, 4.21, 4.22, and 4.23, are summarized in Table 4.24. For the agriculture and postdrilling scenarios, dose estimates again are given at the time the scenario first can occur (i.e., either at 100 or 300 years after disposal) and at far future times beyond 10^6 years when only very long-lived radionuclides and their decay products could be of concern. In addition, for each of these times, dose estimates are given both including and excluding contributions from radon and its short-lived decay products.

The results of the intruder dose analyses presented in Tables 4.20–4.23 and summarized in Table 4.24 are discussed in detail in Sect. 4.5.4. However, a few general comments can be made on the basis of the results in Table 4.24.

First, the estimated doses for the discovery scenario are always less than the estimated doses for the resident scenario. As discussed previously, the discovery scenario is considered only for disposal units in which the thickness of the engineered barriers at the sides of disposal units is significantly less than the thickness of the barriers on top of the units. The lesser importance of the discovery scenario for all disposal units to which the scenario is applied then results from the assumed exposure times, which are 50% of the time during the year for the resident scenario and about 1% of the time during a year for the discovery scenario. The dose from the discovery scenario would be comparable to the dose from the resident scenario only if the exposure time for the discovery scenario were increased considerably, which probably is unreasonable, or if the assumed thicknesses of the engineered barriers in disposal units are incorrect and the thickness of the barriers on top of the units is considerably higher relative to the thickness of the barriers at the sides.

Second, the dose for the resident scenario is not necessarily less than the dose for the agriculture scenario, even though (1) the one exposure pathway in the resident

Table 4.23. Upper-bound estimates of effective dose equivalents to inadvertent intruders for postdrilling scenario[a]

Disposal unit	Nuclide	Concentration (μCi/m^3)[b]	Annual dose (rem/year)
Tumulus I	^{14}C	1.8×10^4	0.027
	^{90}Sr	6.9×10^3	0.011
	^{137}Cs	1.9×10^4	0.002
	^{238}U[c]	8.5×10^1	–
	^{226}Ra[d]		0.003
	^{222}Rn		0.001
	Others		<0.001
	Sum[e]		0.040
	Sum[f]		0.004 (0.003)[g]
Tumulus II	^{14}C	3.5×10^3	0.005
	^{90}Sr	5.5×10^3	0.009
	^{137}Cs	8.7×10^3	0.001
	Others		<0.001
	Sum		0.015
Interim Waste Management Facility	^{14}C	4.1×10^4	0.062
	^{36}Cl	2.8×10^3	0.34
	^{90}Sr	8.2×10^3	0.013
	^{137}Cs	1.4×10^4	0.002
	^{238}U[c]	1.5×10^2	–
	^{226}Ra[d]		0.005
	^{222}Rn		0.002
	Others		<0.001
	Sum[e]		0.42
	Sum[f]		0.007 (0.005)[g]
Low-range silo	^{14}C	1.2×10^5	0.18
	^{90}Sr	9.0×10^3	0.014
	^{99}Tc	5.5×10^3	0.006
	^{137}Cs	7.6×10^3	0.001
	^{238}U[c]	2.3×10^2	–
	^{226}Ra[d]		0.008
	^{222}Rn		0.003
	Others		<0.001
	Sum[e]		0.20
	Sum[f]		0.011 (0.008)[g]

Table 4.23 (continued)

Disposal unit	Nuclide	Concentration (μCi/m^3)[b]	Annual dose (rem/year)
High-range silo	^{90}Sr	1.2×10^6	2.0
	^{137}Cs	8.2×10^4	0.011
	^{238}U[c]	3.8×10^1	–
	^{226}Ra[d]		0.001
	^{222}Rn		–
	Others		<0.001
	Sum[e]		2.0
	Sum[f]		0.001 (0.001)[g]
High-range well[h]	^{90}Sr	4.5×10^8	720
	^{99}Tc	2.6×10^4	0.029
	^{113m}Cd	8.3×10^5	0.069
	^{137}Cs	4.2×10^8	55
	^{152}Eu	3.4×10^7	0.20
	^{154}Eu	1.2×10^7	0.005
	^{229}Th	4.8×10^2	0.001
	Others		<0.001
	Sum		780
Fissile well[h]	^{137}Cs	6.8×10^7	8.8
	^{235}U	1.5×10^3	0.001
	^{238}U[c]	8.5×10^3	0.006
	^{226}Ra[d]		0.28
	^{222}Rn		0.11
	Sum[e]		8.8
	Sum[f]		0.39 (0.28)[g]
Asbestos silo	^{14}C	5.4×10^3	0.008
	^{238}U[c]	4.7×10^1	–
	^{226}Ra[d]		0.002
	^{222}Rn		–
	Others		<0.001
	Sum[e]		0.008
	Sum[f]		0.002 (0.002)[g]

Table 4.23 (continued)

Disposal unit	Nuclide	Concentration (μCi/m^3)[b]	Annual dose (rem/year)
Biological trench	^{90}Sr	8.7×10^2	0.001
	Others		<0.001
	Sum		0.001

[a]Scenario is assumed to occur at 100 years after disposal for all disposal units, except as noted.

[b]Radionuclide concentrations in waste at time of disposal. Concentrations are assumed to be reduced over time only by radioactive decay; removal of activity from disposal units by infiltrating water is not taken into account.

[c]Dose estimates for long-lived decay products, which reach secular equilibrium with ^{238}U only after about 10^6 years, are listed separately.

[d]Dose estimate for radon decay product is listed separately.

[e]Dose estimate at 100 years after disposal.

[f]Dose estimate at times beyond 10^6 years after disposal when only very long-lived radionuclides could be present.

[g]Dose estimate in parentheses excludes contributions from radon.

[h]Scenario probably is not credible for these units (see Sect. 4.5.4.3).

scenario also occurs in the agriculture scenario and the dose per unit concentration of radionuclides for this pathway is substantially less for the resident scenario than for the agriculture scenario due to the presence of shielding between the waste and receptor locations in the resident scenario and (2) additional exposure pathways are included in the agriculture scenario that do not occur in the resident scenario. Higher doses for the resident scenario can result from the assumptions that this scenario occurs at 100 years after disposal but that the agriculture scenario cannot occur until 300 years after disposal, particularly when such relatively short-lived, photon-emitting radionuclides as ^{137}Cs are significant contributors to the total dose for either scenario.

Third, the dose for the postdrilling scenario is not necessarily less than the dose for the agriculture scenario, even though (1) the exposure pathways in the postdrilling scenario also occur in the agriculture scenario and the doses per unit concentration of radionuclides for these pathways are substantially less for the postdrilling scenario than for the agriculture scenario due to the lower dilution factor for mixing of exhumed waste with native soil in the intruder's vegetable garden assumed in the postdrilling scenario, and (2) additional exposure pathways are included in the agriculture scenario that do not occur in the postdrilling scenario. Higher doses for the postdrilling scenario can result from two factors. The first is the use of the geometrical reduction factor in the dose analysis for the agriculture scenario, which takes into account excavation of uncontaminated material in the vicinity of disposed waste and which reduces the average concentration of radionuclides in exhumed waste by more than an order of magnitude for some disposal units. The geometrical reduction factor is not included in the dose analysis for the postdrilling scenario because drilling is assumed to occur directly through disposed waste.

Table 4.24. Summary of upper-bound estimates of effective dose equivalents to inadvertent intruders for assumed exposure scenarios[a]

Disposal unit	Agriculture (rem/year)[b]	Resident (rem/year)[c]	Discovery (rem)[d]	Postdrilling (rem/year)[e]
Tumulus I	0.15 (0.12)[f] 4.2 (0.12)[f]	0.024	–	0.040 0.004 (0.003)[f]
Tumulus II	0.033 (0.030)[f] 0.60 (0.017)[f]	0.011	–	0.015
Interim Waste Management Facility	1.6 7.4 (0.20)[f]	0.018	–	0.42 0.007 (0.005)[f]
Low-range silo	0.78 (0.48)[f] 7.1 (0.20)[f]	0.006	<0.001	0.20 0.011 (0.008)[f]
High-range silo	0.059 (0.058)[f] 1.1 (0.033)[f]	0.066	0.009	2.0 0.001 (0.001)[f]
High-range well[g,h]	36 (36)[f] 0.004 (<0.001)[f]	100	14	780
Fissile well[h]	0.10 1.5 (0.043)[f]	0.33	–	8.8 0.39 (0.28)[f]
Asbestos silo	0.021 (0.020)[f] 1.4 (0.041)[f]	<0.001	<0.001	0.008 0.002 (0.002)[f]
Biological trench	0.003	–	–	0.001

[a]Total doses from all radionuclides for agriculture, resident, discovery, and postdrilling scenarios are obtained from Tables 4.13, 4.14, 4.15, and 4.16, respectively.

[b]Scenario is assumed to occur beginning at 300 years after disposal, except at 100 years after disposal for biological trenches. Second set of dose estimates for some disposal units applies at times beyond 10^6 years after disposal when only very long-lived radionuclides could be present.

[c]Scenario is assumed to occur at 100 years after disposal, except scenario is not relevant for biological trenches.

[d]Scenario is assumed to occur at 100 years after disposal, except scenario is not relevant for biological trenches and scenario need not be considered for Tumulus I, Tumulus II, the Interim Waste Management Facility, and the fissile wells because resident scenario always yields higher estimates of dose.

[e]Scenario is assumed to occur beginning at 100 years after disposal. Second set of dose estimates for some disposal units applies at times beyond 10^6 years after disposal when only very long-lived radionuclides could be present.

[f]Dose estimate in parentheses excludes contributions from radon.

[g]Dose estimates for agriculture, resident, and discovery scenarios probably are unreasonably high for these units (see Sect. 4.5.4.3).

[h]Postdrilling scenario probably is not credible for these units (see Sect. 4.5.4.3).

The second is the assumptions that the postdrilling scenario can occur at 100 years after disposal but that the agriculture scenario cannot occur until 300 years after disposal for most units. This difference is particularly important when such relatively short-lived radionuclides as ^{90}Sr and ^{137}Cs are significant contributors to the total dose for each scenario.

Finally, the potential for high doses at times far into the future (due to the buildup of ^{226}Ra and its decay products produced in the decay of ^{238}U) is always more important for the agriculture scenario than for the postdrilling scenario, primarily because the dose from radon during indoor residence, which is considered in the agriculture scenario but is not relevant in the postdrilling scenario, is substantially higher than the dose from radon while working in the vegetable garden, which is considered in both scenarios. For the agriculture scenario, the potential doses at far future times can be higher than the doses at the time the scenario first can occur, depending on the concentration of ^{238}U in the waste relative to the concentrations of other important constituents. For the postdrilling scenario, however, the potential doses at far future times always are substantially less than the doses at the time the scenario first can occur.

4.5.4 Comparison of Dose Estimates with Regulatory Requirements

DOE has established performance objectives for limitation of dose that might be received by off-site individuals and inadvertent intruders at DOE LLW disposal sites (DOE 1988). DOE also requires protection of groundwater resources, and a dose limit consistent with current standards for radioactivity in public drinking water supplies is assumed in this analysis to apply to protection of groundwater near disposal units. The same dose limit used for protection of groundwater resources also is applied to protection of surface water resources near the disposal units.

The performance objectives for new LLW disposal facilities in SWSA 6 may be stated as follows:

- for off-site individuals at any time after disposal, a limit on annual EDE from all exposure pathways of 0.025 rem (25 mrem);
- for inadvertent intruders after loss of active institutional controls at 100 years after disposal, limits on EDE from all exposure pathways of 0.1 rem (100 mrem) per year for scenarios involving continuous exposure and 0.5 rem (500 mrem) for scenarios involving a single, acute exposure; and
- at any time after disposal, a limit on annual EDE from consumption of drinking water from contaminated groundwater or surface water of 0.004 rem (4 mrem).

With regard to the performance objective for inadvertent intruders, the agriculture, resident, and postdrilling scenarios assumed in this analysis represent continuous exposure scenarios for which the dose limit is 0.1 rem per year, whereas the discovery scenario represents an acute exposure scenario for which the dose limit is 0.5 rem.

As indicated in Tables 4.20 and 4.23, exposures of inadvertent intruders to isotopes of radon are the most important contributors to the total dose from all radionuclides for some of the assumed exposure scenarios. The performance objective for inadvertent intruders given above does not explicitly exclude potential doses from radon, so exposure

to radon presumably must be taken into account in demonstrating compliance with the performance objective. However, the performance objective for inadvertent intruders is patterned after current radiation protection standards for the public, and such standards exclude contributions from radon. Furthermore, exposures of the public to radon from either naturally occurring or technologically enhanced sources generally are not regulated by means of dose limits in the same manner as exposures to other radionuclides. Therefore, in anticipation of the possibility that the performance objective for inadvertent intruders may be revised to exclude exposures to radon, doses from radon are reported separately in this analysis. This approach permits the dose from all other radionuclides to be compared with the performance objective.

In the remainder of this section, the dose estimates presented in Sect. 4.5.3 are compared with the different performance objectives stated above.

4.5.4.1 Protection of Groundwater and Surface Water Resources

The limit on annual EDE of 4 mrem from consumption of drinking water obtained from a source of contaminated groundwater or surface water is assumed to apply at any time after disposal. In particular, the performance objective applies to protection of groundwater resources at the facility site even during the institutional control period, when use of contaminated groundwater would be precluded, because the performance objective is directed at groundwater resource protection.

The results of the dose analysis for direct consumption of drinking water obtained from contaminated surface waters beyond the boundary of the SWSA 6 site are given in Table 4.16. The maximum annual dose from any radionuclide is about 3 mrem (^{14}C), and the total dose from all radionuclides is about 5 mrem. However, the maximum concentrations of all radionuclides in off-site surface waters would not occur at the same time. As discussed in Sect. 4.4, the transport of radionuclides to surface water presented in Table 4.8 is the peak nuclide transport rates from the eleven different disposal units without regard to the year of occurrence. The range of time over which these peak transport rates occur is large, extending over 60,000 years for some isotopes. As shown in Appendix F, Figs. F.1–F.17, the release of contamination from disposal units extends over long periods of time with large ranges in contaminant concentrations. The dose analysis is based on maximum concentrations that would exceed the peak value in any year. Thus, the analysis indicates that releases of radionuclides to surface waters are not likely to result in annual doses from the drinking water pathway that exceed the performance objective for protection of surface waters at any time after disposal.

The results of the dose analysis for direct consumption of drinking water obtained from contaminated groundwater on the facility are given in Table 4.18. The maximum annual doses from ^{3}H (9 mrem), ^{14}C (210 mrem), ^{36}Cl (150 mrem), and ^{239}Pu (13 mrem) each exceed the performance objective, but the doses from all other radionuclides are less than the performance objective. The maximum doses from ^{3}H, ^{14}C, and ^{36}Cl occur during the institutional control period when exposures would be precluded. Again, the performance objective is directed towards resource protection regardless of whether or not exposures could occur.

4.5.4.2 Protection of Off-Site Individuals

Doses to off-site individuals are assumed to result entirely from the use of contaminated surface water near the facility boundary. The results of the dose analysis for off-site individuals are given in Table 4.17. For all radionuclides, the dose from all exposure pathways differs from the dose from the drinking water pathway only, as given in Table 4.16, by less than a factor of two; and, for most radionuclides, the drinking water pathway contributes essentially all of the dose. The maximum annual dose from any radionuclide (^{14}C) is about 4 mrem, and the total dose from all radionuclides would only be about 6 mrem, even if the maximum concentrations of all radionuclides in off-site surface waters occurred at the same time. Therefore, the maximum dose to off-site individuals is considerably less than the performance objective of 25 mrem.

4.5.4.3 Protection of Inadvertent Intruders

Exposures of inadvertent intruders are assumed to result from the use of contaminated groundwater obtained from a well located outside the 100-m (328-ft) buffer zone around any of the disposal units and from direct intrusion into the disposal units according to the agriculture, resident, discovery, and postdrilling scenarios.

4.5.4.3.1 Groundwater pathway

Use of contaminated groundwater by inadvertent intruders is assumed to result in continuous exposure. Therefore, doses from the groundwater pathway are considered in conjunction with doses from the agriculture, resident, and postdrilling scenarios, which also involve continuous exposure, in evaluating compliance with the limit on annual EDE of 0.1 rem for continuous exposure in the performance objective for inadvertent intruders.

The results of the dose analysis for inadvertent intruders from use of contaminated groundwater are given in Table 4.19. The dose estimates take into account releases from all disposal units, and the disposal units that contribute most of the dose are given in the table. For the radionuclides listed, the drinking water pathway again contributes most of the dose from all pathways. For ^{3}H, ^{14}C, ^{36}Cl, and ^{99}Tc, the maximum concentrations in groundwater occur during the institutional control period (see Table 4.18), but only the maximum concentrations after the institutional control period are relevant to the dose analysis for inadvertent intruders from all exposure pathways. The results presented in Sect. 4.3 (Fig. 4.6) clearly illustrate that a very small tract of land along strike from IWMF is the only location where an inadvertent intruder could consume contaminated groundwater and receive doses from ^{14}C, ^{36}Cl, ^{233}U, ^{239}Pu, and ^{243}Am. For all other locations within SWSA 6, the largest annual dose would be less than 2 mrem. The largest annual dose from the groundwater pathway occurs for ^{239}Pu (13 mrem), and the annual doses from all other radionuclides are less than 10 mrem. Therefore, doses to inadvertent intruders from exposure to contaminanted groundwater do not appear to be significant in regard to meeting the performance objective of 0.1 rem for all exposure pathways, including the pathways from direct intrusion into disposal units discussed below.

4.5.4.3.2 Direct intrusion scenarios

The estimated doses for the agriculture, resident, discovery, and postdrilling scenarios are given in Table 4.20, 4.21, 4.22, and 4.23, respectively, and are summarized in Table 4.24. For each type of disposal unit, the total dose at any time is the sum of the doses from all radionuclides remaining in the units at that time.

As described previously, the limits on EDE in the performance objective for protection of inadvertent intruders are 0.1 rem/year for the agriculture, resident, and postdrilling scenarios and 0.5 rem for the discovery scenario. These limits include the doses from the groundwater pathway, which, as described above, are not expected to be significant on the basis of the present analysis.

The results for each type of disposal unit are treated separately in regard to evaluating compliance with the performance objective for protection of inadvertent intruders. The results for each disposal unit are discussed in the following paragraphs. These discussions focus on the dose estimates at the earliest time the different intrusion scenarios are assumed to occur, which is either 100 or 300 years after disposal. For the agriculture and postdrilling scenarios, doses also were estimated at times beyond 10^6 years after disposal, when only very long-lived radionuclides, principally ^{238}U and its decay products, could be present in the waste in significant quantities. As shown in Table 4.24, the upper-bound estimates of dose at far future times are well above the performance objective of 0.1 rem/year for several disposal units for the agriculture scenario and for the fissile wells for the postdrilling scenario. However, these results clearly are unreasonable when mobilization and transport of radionuclides away from disposal units over the very long time period between disposal and exposure has not been taken into account. Therefore, the primary purpose of the dose estimates at far future times is not to compare the results with the performance objective; rather, it is to indicate the importance of taking into account the depletion of radionuclide inventories due to mobilization and transport.

Tumulus I. The estimated dose for the agriculture scenario at 300 years after disposal exceeds the performance objective of 0.1 rem/year by about 50%, but the estimated doses for the resident and postdrilling scenarios at 100 years after disposal are less than this performance objective.

The most important radionuclide in the agriculture scenario is ^{14}C. Since ^{14}C may be mobilized and transported in infiltrating water relatively easily, consideration of this effect is potentially important for the intruder dose analysis. Reduction of the inventory of ^{14}C in these disposal units by a factor of two or more in the first 300 years after disposal would result in a dose estimate for the agriculture scenario that is less than the performance objective.

Tumulus II. The estimated doses for the agriculture scenario at 300 years after disposal and for the resident and postdrilling scenarios at 100 years after disposal all are less than the performance objective of 0.1 rem/year, even without taking into account mobilization and transport of radionuclides in infiltrating water. Tumulus II differs from Tumulus I in having substantially lower inventories of the most important radionuclides.

IWMF. The estimated doses for the agriculture scenario at 300 years after disposal and for the postdrilling scenario at 100 years after disposal exceed the performance

objective of 0.1 rem/year by factors of 16 and 4, respectively, but the estimated dose for the resident scenario at 100 years after disposal is less than this performance objective.

The most important radionuclides in the agriculture and postdrilling scenarios are ^{14}C and ^{36}Cl. Both of these radionuclides, especially the more important ^{36}Cl, may be mobilized and transported in infiltrating water relatively easily. Therefore, consideration of this effect is potentially important in the dose analysis.

Low-range silos. The estimated doses for the agriculture scenario at 300 years after disposal and for the postdrilling scenario at 100 years after disposal exceed the performance objective of 0.1 rem/year by factors of eight and two, respectively, but the estimated doses for the resident and discovery scenarios at 100 years after disposal are less than their respective performance objectives of 0.1 rem/year and 0.5 rem.

The most important radionuclide in the agriculture and postdrilling scenarios is ^{14}Cl; ^{222}Rn produced in the decay of ^{226}Ra in the waste is also a significant contributor to the total dose in the agriculture scenario. For ^{14}C, taking into account mobilization and transport in infiltrating water again is a potentially important consideration in the dose analysis. This effect also should be considered, but may be less important, for ^{226}Ra.

High-range silos. The estimated dose for the postdrilling scenario at 100 years after disposal exceeds the performance objective of 0.1 rem/year by a factor of 20, but the estimated doses for the agriculture scenario at 300 years after disposal and for the resident scenario at 100 years after disposal are less than the performance objective of 0.1 rem/year by 30–40%. The estimated dose for the discovery scenario at 100 years after disposal is far less than the performance objective of 0.5 rem.

The most important radionuclide in the postdrilling scenario is ^{90}Sr. Although taking into account mobilization and transport of ^{90}Sr in infiltrating water is a potentially important consideration in the dose analysis, it is doubtful that the inventory would be reduced by more than an order of magnitude within the first 100 years.

High-range wells. The estimated dose for the agriculture scenario at 300 years after disposal exceeds the performance objective of 0.1 rem/year by a factor of nearly 400, the estimated dose for the resident scenario at 100 years after disposal exceeds the performance objective of 0.1 rem/year by a factor of 1000, the estimated dose for the discovery scenario at 100 years after disposal exceeds the performance objective of 0.5 rem by a factor of nearly 30, and the estimated dose for the postdrilling scenario at 100 years after disposal exceeds the performance objective of 0.1 rem/year by a factor of nearly 8000. Therefore, all scenarios result in upper-bound estimates of dose that exceed the performance objective by large amounts. However, for reasons discussed below, none of these dose esimates are likely to be credible.

The most important radionuclides in the agriculture scenario are ^{90}Sr and ^{137}Cs. All other radionuclides result in doses that are substantially less than the performance objective. There are several factors not yet taken into account in the dose analysis that could significantly reduce the estimated doses from ^{90}Sr and ^{137}Cs. First, as with all other disposal units, consideration of mobilization and transport of these radionuclides in infiltrating water for 300 years after disposal could substantially reduce the inventories at the time the agriculture scenario is assumed to occur. Second, as indicated by the discussion of the resident scenario below, most of the waste may have been placed near the bottom of wells, with very little near the top, in order to meet a requirement that the external dose rate at the ground surface after disposal be less than 2.5 mrem/h (see

Sect. 2.3.5.3). If this were the case, the activity of the exhumed waste mixed with native soil in the intruder's vegetable garden may have been overestimated, which is important for ^{90}Sr since consumption of contaminated vegetables is the dominant exposure pathway for this radionuclide. In addition, the shielding provided by the source region in the absence of engineered barriers may have been underestimated, which is important for ^{137}Cs since external exposure while residing in a home on top of exposed waste is the dominant exposure pathway for this radionuclide. Finally, if the engineered barriers above the waste would remain intact for longer than 300 years, as assumed in this analysis, the dose from ^{90}Sr and ^{137}Cs would be reduced by about a factor of 10 for every additional 100 years that the barriers would remain intact and preclude excavation into the waste.

The most important radionuclides in the resident scenario are ^{137}Cs and ^{152}Eu. The estimated annual EDE for this scenario at 100 years after disposal is about 100 rem, but this estimate appears to be unreasonably pessimistic. The only exposure pathway in this scenario is external exposure while residing in a home immediately on top of intact engineered barriers. As mentioned previously, following emplacement of waste in the high-range wells and construction of the caps on top of the wells, the external dose rate at the ground surface must be less than 2.5 mrem/h. Therefore, for residence in a home on top of intact engineered barriers immediately following construction of the cap, the annual dose equivalent corresponding to the maximum allowable dose rate would be about 8 rem, assuming a residence time of 50% and a shielding factor during indoor residence of 0.7 as in the resident scenario. Furthermore, the resident scenario cannot occur until 100 years after facility closure, and the inventory of ^{137}Cs, which contributes most of the dose for the resident scenario, would be a factor of 10 less at 100 years than at the time of facility closure. Therefore, the annual EDE for the resident scenario could not exceed about 0.8 rem. This estimate is also an upper bound because it does not take into account reduction of radionuclide inventories due to mobilization and transport by infiltrating water and it does not take into account that the dose from ^{152}Eu would be reduced by substantially more than a factor of 10 at 100 years after disposal due only to radioactive decay.

Thus, the dose estimate for the resident scenario for the high-range wells apparently exceeds the maximum possible dose, based on a criterion for waste emplacement and cap construction, by more than a factor of 100. If the estimated inventories of ^{137}Cs and ^{152}Eu in the high-range wells are reasonably accurate, then the considerable overestimation of dose in this analysis presumably results from an improper accounting of waste emplacement in the wells and the thickness of the engineered caps above the waste. For example, if the average thickness of the caps above the waste were about 100 cm (39 in.), instead of 30 cm (12 in.) as assumed in this analysis, then the estimated annual dose for the resident scenario would be reduced to about 0.3 rem, even if the radionuclides were uniformly distributed throughout the depth of the wells below the caps.

The most important radionuclides in the discovery scenario also are ^{137}Cs and ^{152}Eu. The estimated annual EDE for this scenario at 100 years after disposal is about 14 rem, but this estimate may be somewhat pessimistic. The only exposure pathway in this scenario is external exposure while working at the side of the disposal units, with the engineered barriers uncovered but intact. In the dose analysis for the discovery scenario, the thickness of the engineered barriers at the sides of the high-range wells was assumed to be 15 cm (6 in.) for all such units. However, for some of the high-range wells, the placement of pipe

wells within concrete silos (see Sect. 2.3.5.3) would result in a thickness of the engineered barriers at the sides of the units equivalent to about 30 cm (12 in.) of soil. In this case, the dose for the discovery scenario at 100 years after disposal would be reduced to about 3 rem. This estimate still may be an upper bound because it does not take into account reduction of radionuclide inventories due to mobilization and transport by infiltrating water.

The most important radionuclides in the postdrilling scenario are ^{90}Sr and ^{137}Cs, and ^{152}Eu is also of concern. The dose estimate of 780 rem/year for the high-range wells is very high. The considerations of the thickness of the engineered barriers that apparently are important in reducing the dose estimates for the resident and discovery scenarios are not relevant for the postdrilling scenario because the scenario assumes that the presence of engineered barriers of any thickness would not preclude drilling through the waste. In addition, if drilling through the high-range wells is assumed to be credible, then the relatively few number of wells and placement of waste mostly in the bottom of the wells, as mentioned above in the discussion of the dose estimate for the agriculture scenario, would not be relevant for the postdrilling scenario. Finally, mobilization and transport of the important radionuclides is not likely to reduce the dose at 100 years after disposal by a large amount. Perhaps the most important factor to be considered for the postdrilling scenario is the relatively small area occupied by the high-range wells. From information given in Sects. 2.3.5.3 and 2.3.5.4 and Appendix A, the area occupied by all high-range wells is only about 14 m^2 (150 ft^2). With the assumption that an individual would drill at random locations on the SWSA 6 site, it may be reasonable to argue that drilling through any of the high-range wells would be relatively unlikely and, thus, that the postdrilling scenario is not credible for these units.

In summary, for the high-range wells, the post-drilling scenario may not be credible, and the estimated doses for the agriculture, resident, and discovery scenarios appear to be unreasonably pessimistic. For the latter scenarios, however, there is not sufficient information to provide more realistic estimates of dose. For the resident scenario, the operating criterion for external dose rate can be used to bound the estimated intruder doses.

Fissile wells. The estimated dose for the agriculture scenario at 300 years after disposal is equal to the performance objective of 0.1 rem/year, and the estimated doses for the resident and postdrilling scenarios at 100 years after disposal exceed the performance objective of 0.1 rem/year by factors of about 3 and 90, respectively. As discussed with the agriculture scenario in Sect. 4.5.3.2.1, the dose estimates for the agriculture and resident scenarios are influenced by the fact that only a single fissile well is included in this performance assessment. If additional units were included, the dose for the two scenarios would increase in proportion to the number of units.

The only important radionuclide in the agriculture, resident, and postdrilling scenarios is ^{137}Cs. The dose for the agriculture scenario probably would be reduced below the performance objective if mobilization and transport of ^{137}Cs in infiltrating water in the first 300 years after disposal were taken into account, and mobilization and transport in the first 100 years may be an important consideration for the resident scenario. However, it seems unlikely that mobilization and transport of ^{137}Cs in the first 100 years after disposal could reduce the dose for the postdrilling scenario by nearly two orders of magnitude. The most important mitigating factor for the postdrilling scenario probably is

the fact that the single fissile well of concern to this analysis occupies an area of only about 0.45 m^2 (4.8 ft^2) (see Sect. 2.3.5.5). Therefore, the probability that an individual drilling at random locations on the SWSA 6 site would drill through the fissile well is clearly very low, and the postdrilling scenario probably is not credible for this disposal unit.

Asbestos silos. The estimated dose for the agriculture scenario at 300 years after disposal is about 20% of the performance objective of 0.1 rem/year, the estimated dose for the postdrilling scenario at 100 years after disposal is less than 10% of the performance objective of 0.1 rem/year, and the estimated doses for the resident and discovery scenarios at 100 years after disposal are far less than their respective performance objectives of 0.1 rem/year and 0.5 rem. Taking into account mobilization and transport of radionuclides in infiltrating water would reduce the dose estimates even farther below the performance objectives. The asbestos silos have lower concentrations of radionuclides than any other disposal units except the biological trenches.

Biological trenches. The estimated doses for the agriculture and postdrilling scenarios at 100 years after disposal are at most a few percent of the performance objective of 0.1 rem/year for each scenario, even without taking into account mobilization and transport of radionuclides in infiltrating water. The biological trenches have the lowest concentrations of radionuclides of any disposal units in SWSA 6.

Summary. The analysis summarized in Table 4.24 indicates that several of the disposal units in SWSA 6 may not be in compliance with the performance objective for protection of inadvertent intruders. The particular disposal units and the assumed exposure scenarios for inadvertent intruders that resulted in upper-bound estimates of dose that exceeded the performance objective are as follows:

- Tumulus I (agriculture scenario);
- IWMF (agriculture and postdrilling scenarios);
- low-range silos (agriculture and postdrilling scenarios);
- high-range silos (postdrilling scenario);
- high-range wells (agriculture, resident, discovery, and postdrilling scenarios); and
- fissile wells (resident and postdrilling scenarios).

This section also discusses a number of factors not yet accounted for in the dose analysis for inadvertent intruders that might result in significant reductions in dose for the various disposal units and exposure scenarios of concern.

First, for all disposal units, reductions in radionuclide inventories over time due to mobilization and transport in infiltrating water have not been taken into account. This effect presumably would result in significant reductions in dose for ^{14}C and ^{36}Cl, which are the most important radionuclides in some disposal units and are expected to be relatively mobile, and may also be significant for other important radionuclides in some disposal units such as ^{90}Sr and ^{137}Cs. Mobilization and transport in water also should be important for the very long-lived radionuclide ^{238}U over time periods of 10^6 years and beyond, when the upper-bound estimates of dose for the agriculture scenario exceed the performance objective for several disposal units, if this effect is not taken into account.

Second, for the high-range wells, the thickness of the engineered barriers at the top and sides of the wells and the selective placement of waste near the bottom of the wells apparently have not been properly taken into account in the dose analyses for the

agriculture, resident, and discovery scenarios. It is evident, for example, on the basis of current requirements for limiting the external dose rate above the wells following closure that a proper accounting of the thickness of the engineered caps on top of the high-range wells would greatly reduce the dose for the resident scenario. However, for the resident scenario, the dose can be bounded on the basis of the requirement that the external dose rate above grade after the units are capped should not exceed 2.5 mrem/h.

Finally, for the high-range wells and fissile wells, the postdrilling scenario results in the highest estimates of dose. This scenario is based on the assumption that drilling directly through a disposal unit is a credible (likely) occurrence. However, drilling directly through the single fissile well of very small cross-sectional area clearly would be highly unlikely, and drilling directly through any of the high-range wells also may not be credible due to the small total cross-sectional area for these units.

4.6 SENSITIVITY AND UNCERTAINTY ANALYSIS

The sensitivity of the models used to analyze the performance of SWSA 6 and the uncertainty of the results presented in Sects. 4.1–4.4 are important considerations in evaluating compliance of SWSA 6 with the performance objectives in DOE Order 5820.2A. For purposes of this discussion, the models and data bases related to waste disposals, the performance of engineered systems, and release and transport of radionuclides through the environment to assumed human receptor locations are treated separately from the models for estimating dose per unit concentration of radionuclides at assumed receptor locations. This separation of the treatment of uncertainties can be justified on the grounds that predictions of radionuclide concentrations in the environment at assumed human receptor locations are based on analyses of physical systems, whereas the analysis of doses per unit concentration of radionuclides in the environment is based on largely hypothetical constructs that do not depend on the physical disposal system.

The uncertainties associated with the inventory used in the analysis are evaluated in detail in Appendix A. The evaluation considers the reported inventory in Tables A.3–A.11 for radionuclides identified in the screening analysis and the standard waste characterization methods and potential sources of error in characterization. Deterministic and probabilistic methods were used to calculate the most probable, maximum, and minimum estimates of activity in wastes. For many isotopes in several disposal units, the best estimate of the inventory differed significantly from the reported values in Appendix A, Tables A.3–A.11. The most probable or best estimates were used in the analysis presented in Sects. 4.1–4.5 and are presented with the 95% confidence level maximum and minimum activity values in Appendix A, Tables A.13–A.21. The uncertainty in the inventory data in the analysis of environmental transport is addressed in the following sections.

4.6.1 Analysis of Disposal System Performance

The LHC sampling method was used to analyze the effects of input variable uncertainties on the simulation models used in this study. LHC sampling (Iman and Helton 1985) has been shown to require fewer model iterations to approximate the

desired variable distribution than the simple Monte Carlo method. The LHC method ensures that the entire range of each input variable to a model is sampled, and that the distribution of each variable will be represented with fewer samples. PRISM (Gardner, Röjder, and Berström 1983) was the program used to implement the LHC sampling technique for sensitivity and uncertainty analyses of the model predictions. Input data sets were generated from specified distributions for input variables for a selected number (50) of equal probability class intervals, and these data sets served as input to the simulation models. A statistical summary of the model results produced indices of sensitivity and uncertainty that related the effects of heterogeneity of input variables to model predictions.

4.6.1.1 Sensitivity and Uncertainty of Leaching from Disposal Units

An initial sensitivity analysis of the SOURCE1 and SOURCE2 models was conducted to summarize the relative influence of input variables on model results. Three representative cases, ^{3}H from the IWMF, ^{137}Cs from high-range silos, and ^{90}Sr from low-range silos (south) were selected for this analysis, and 48 input variables (Table 4.25) were examined. The predicted output result of interest from the SOURCE1 and SOURCE2 models was the annual release of radionuclides (g/year) from the disposal units. This release was partitioned into lateral and vertical (recharge) components, and these two components along with their corresponding water flow values were the model output functions used in the sensitivity and uncertainty analyses.

In the sensitivity analysis, input variables were varied $\pm 1\%$ of the best estimate input values (Table 3.3 and Tables C.13–C.22 in Appendix C), and the variation in model outputs was compared. The statistical summary of the model results for the three cases identified 13 input variables (Table 4.26) having the most influence on model predictions. The sensitivity analysis did not consider variables that exhibit a wide range in the field environment that could have an effect on results similar to a sensitive variable. For example, the 1% variation in groundwater pH had little effect on the output, but if the groundwater pH were to vary from pH 5 to pH 8, leaching could be affected. In general, the variables examined in the sensitivity analysis (Table 4.25) that were included in the uncertainty analysis (Table 4.26) are not expected to show wide variations in the field such that leaching of nuclides from the disposal units would be affected significantly. For simulations of ^{90}Sr in low-range silos (south), and ^{137}Cs in high-range silos, the first 10–15 years of model results were most influenced by saturated hydraulic conductivity of concrete; time required for complete corrosion of corrugated steel liners; radionuclide inventory in vault, silo, or well; density of waste; and radionuclide distribution coefficient. Each parameter contributed approximately 20% of the variation in model predictions. After 20 years, the concrete diffusion coefficient dominated output variations with values ranging from 70 to 90%; radionuclide inventory and the corrosion time for steel liners followed in ranking, with values ranging from 10 to 20% and 2 to 10%, respectively. The simulation for ^{3}H at the IWMF showed that radionuclide inventory in vault, silo, or well was most influential in the initial years, accounting for approximately 75% of the variation in model predictions. After 20 years, the waste container corrosion time dominated output variations with values ranging from 75 to 98%; radionuclide values accounted for 1–12% of the output variation. Only variables that contributed at least 5% of the variability in the

Table 4.25. SOURCE1 and SOURCE2 variables examined in the sensitivity analysis

SLDNS	Density of soil backfill around tumulus or silo or well (g/cm^3)
CVRDNS	Density of earthen cover (g/cm^3)
WSTDNS	Density of waste (g/cm^3)
WSTHT	Moisture content of waste
CAGW	Concentration of calcium in groundwater (mole/L)
CL	Concentration of chloride in groundwater (mole/L)
CO2	Concentration of carbon dioxide outside tumulus or silo or well (mole/L)
CO3	Concentration of carbonate in groundwater (mole/L)
XMG2	Concentration of magnesium in groundwater (mole/L)
O2	Concentration of oxygen at tumulus or silo or well surface (mole/L)
SO4I	Concentration of sulfate inside vault (mole/L)
SO4O	Concentration of sulfate outside vault (mole/L)
DFALK	Effective diffusivity of alkalis in concrete (m^2/s)
DFCAOH	Effective diffusivity of calcium hydroxide in concrete (m^2/s)
DFCL	Effective diffusivity of chloride in concrete (m^2/s)
DFCO2	Effective diffusivity of carbon dioxide in concrete (m^2/s)
DFO2	Effective diffusivity of oxygen in concrete (m^2/s)
DFSO4	Effective diffusivity of sulfate in concrete (m^2/s)
PHGW	Groundwater pH
TDS	Total dissolved solids in groundwater (ppm)
TEMP	Groundwater temperature (°C)
CFT1	Time at which waste containers begin to corrode (year)
DCFT	Time required for complete corrosion of waste containers (year)
EFT1	Time at which epoxy-coating begins to fail (year)
DEFT	Time required for complete failure of epoxy-coating (year)
DWFT	Time required for complete corrosion of the cast iron pipe (year)
XLFT1	Time at which corrugated steel liners begin to corrode (year)
DLFT	Time required for complete corrosion of corrugated steel liners (year)
SITARA	Upslope drainage area (m^2)
SLKR	Saturated hydraulic conductivity of recharge component (cm/s)
SLK	Saturated hydraulic conductivity of soil backfill around tumulus, well, or silo (cm/s)
CCK	Saturated hydraulic conductivity of intact concrete (cm/s)
WATER(1)	Disposal 'trench' percolation rate for first month of year (cm)
WATER(2)	Disposal 'trench' percolation rate for second month of year (cm)
WATER(3)	Disposal 'trench' percolation rate for third month of year (cm)
WATER(4)	Disposal 'trench' percolation rate for fourth month of year (cm)
WATER(5)	Disposal 'trench' percolation rate for fifth month of year (cm)
WATER(6)	Disposal 'trench' percolation rate for sixth month of year (cm)
WATER(7)	Disposal 'trench' percolation rate for seventh month of year (cm)
WATER(8)	Disposal 'trench' percolation rate for eighth month of year (cm)
WATER(9)	Disposal 'trench' percolation rate for ninth month of year (cm)
WATER(10)	Disposal 'trench' percolation rate for tenth month of year (cm)

Table 4.25 (continued)

WATER(11)	Disposal 'trench' percolation rate for eleventh month of year (cm)
WATER(12)	Disposal 'trench' percolation rate for twelfth month of year (cm)
XKD	Radionuclide distribution coefficient (mL/g)
QSW	Radionuclide inventory in vault or silo or well (g)
DFWST	Waste diffusion coefficient (m^2/s)
DFCON	Concrete diffusion coefficient (m^2/s)

SOURCE1 and SOURCE2 output at some period during the simulation were included in the uncertainty analysis.

The 13 most influential input variables (Table 4.26) were used to determine the uncertainty for predicted annual leaching with the SOURCE1 and SOURCE2 models. A triangular input distribution was assumed and used to describe the univariate distribution of all variables with the exception of the hydraulic conductivity that controls the rate of recharge, which was described by a lognormal distribution (Luxmoore, Spalding, and Munro 1981). The number of equal probability classes (model iterations) needed to reasonably approximate these univariate distributions was determined by comparing output results from uncertainty analyses for a representative case implemented with 50, 100, and 200 equal probability classes. The variances were calculated for the annual leach rates for each case and compared. The variances were not significantly reduced by increasing the number of model iterations above 50, and 50 iterations were considered sufficient to approximate the frequency distributions of input variables.

Uncertainty analyses of the SOURCE1 and SOURCE2 models were conducted for 43 combinations of nuclides and disposal units (Table 4.3). Each analysis of the model consisted of 50 iterations, and each iteration was executed for at least 1000 years. The method for the exchange of data sets between the models used in the performance assessment for the uncertainty analyses is presented in Fig. 4.7. These uncertainty runs were conducted with average water flow conditions from UTM. The output data sets from simulations provided annual lateral and vertical chemical releases and corresponding water flow values that served as input frequency distribution data sets to the TUMSIM and WELSIM models (Fig. 4.7). Additional SOURCE1 and SOURCE2 simulations were made for two disposal units [IWMF and low-range silo (south)] and three nuclides (^{3}H, ^{238}U, ^{137}Cs) with modified water flow conditions. These selected nuclides represented the range of K_d and half-life values used in this study. Water flow into and around the disposal units was modified to simulate dry conditions by reducing the average water flow rate by 50%, and enhanced water flow conditions were simulated by increasing average water flow values by 50%.

Frequency distributions were compiled for these simulations, and comparisons of leaching rates for reduced, average, and enhanced leaching conditions were made. Figures 4.8–4.11 illustrate the relative frequency distributions generated from the uncertainty analyses of these representative cases at selected times under average water flow conditions. The relative frequency distribution for tritium leaching from the IWMF at year 50 was highly skewed (Fig. 4.8). The majority (94%) of occurrences had a mean

Table 4.26. SOURCE1 and SOURCE2 variables and values included in the uncertainty analysis

Parameter[a]	SOURCE1	SOURCE2	Mean	Standard deviation	Minimum	Maximum
CVRDNS	yes	yes	1.76		1.60	2.20
WSTDNS	yes	yes	1.76		1.00	2.60
WSTHT	yes	yes	0.99		0.15	1.00
DFSO4	yes	yes	1.06×10^{-11}		1.06×10^{-12}	1.06×10^{-10}
DCFT	yes	no	60.00		25.00	100.00
DEFT	yes	yes	20.00		10.00	50.00
DLFT	no	yes	50.00		20.00	100.00
DWFT	no	yes	75.00		25.00	125.00
SLKR	yes	yes	5.8×10^{-7}	2.31×10^{-6}	2.31×10^{-11}	1.16×10^{-3}
CCK	yes	yes	1.00×10^{-10}		1.00×10^{-11}	1.00×10^{-9}
XKD	yes	yes	*b*		*b*	*b*
QSW	yes	yes	*b*		*b*	*b*
DFCON	yes	yes	*b*		*b*	*b*

[a]Parameter definitions are provided in Table 4.25.

[b]These parameters are nuclide- and facility-specific. Tables C.13–C.22 in Appendix C provide the probable, minimum, and maximum values for each nuclide at each facility used in the uncertainty analysis.

tritium leaching rate of 2.75×10^{-7} g/year. A contrasting pattern was obtained for ^{238}U leaching from the low-range silo (south) with the maximum transport rate being also the most frequent class (Fig. 4.9). A strongly skewed frequency distribution of tritium leaching from a low-range silo (south) was obtained at year 50 (Fig. 4.10). There was a small probability (2%) of higher leaching rates with the maximum leaching rate being 19 times higher than the modal rate. The uncertainty analysis of ^{137}Cs leaching from the IWMF at year 200 showed the maximum leaching rate to be 19 times greater than the rate for the most frequent class (Fig. 4.11). These four examples of relative frequency distributions show that skewed distributions are a common outcome in the uncertainty analyses with the SOURCE1 and SOURCE2 models. In a few cases, distributions with an approximately normal distribution were obtained.

Table 4.27 provides a summary of the output frequency distributions for four disposal units, listing the most frequent and maximum total chemical release along with relative frequencies from the SOURCE1 and SOURCE2 models with reduced, average, and enhanced water flow conditions described previously. Under the average water flow conditions, the maximum leaching rates were 20–40 times higher than modal rates. Increase in water flow conditions caused an initial more rapid leaching of nuclides from disposal units [e.g., ^{238}U from low-range silos (south) at year 50]; however, at longer times (e.g., ^{137}Cs from the IWMF at year 200) greater release was predicted under dryer conditions due to the higher inventory remaining in the disposal unit.

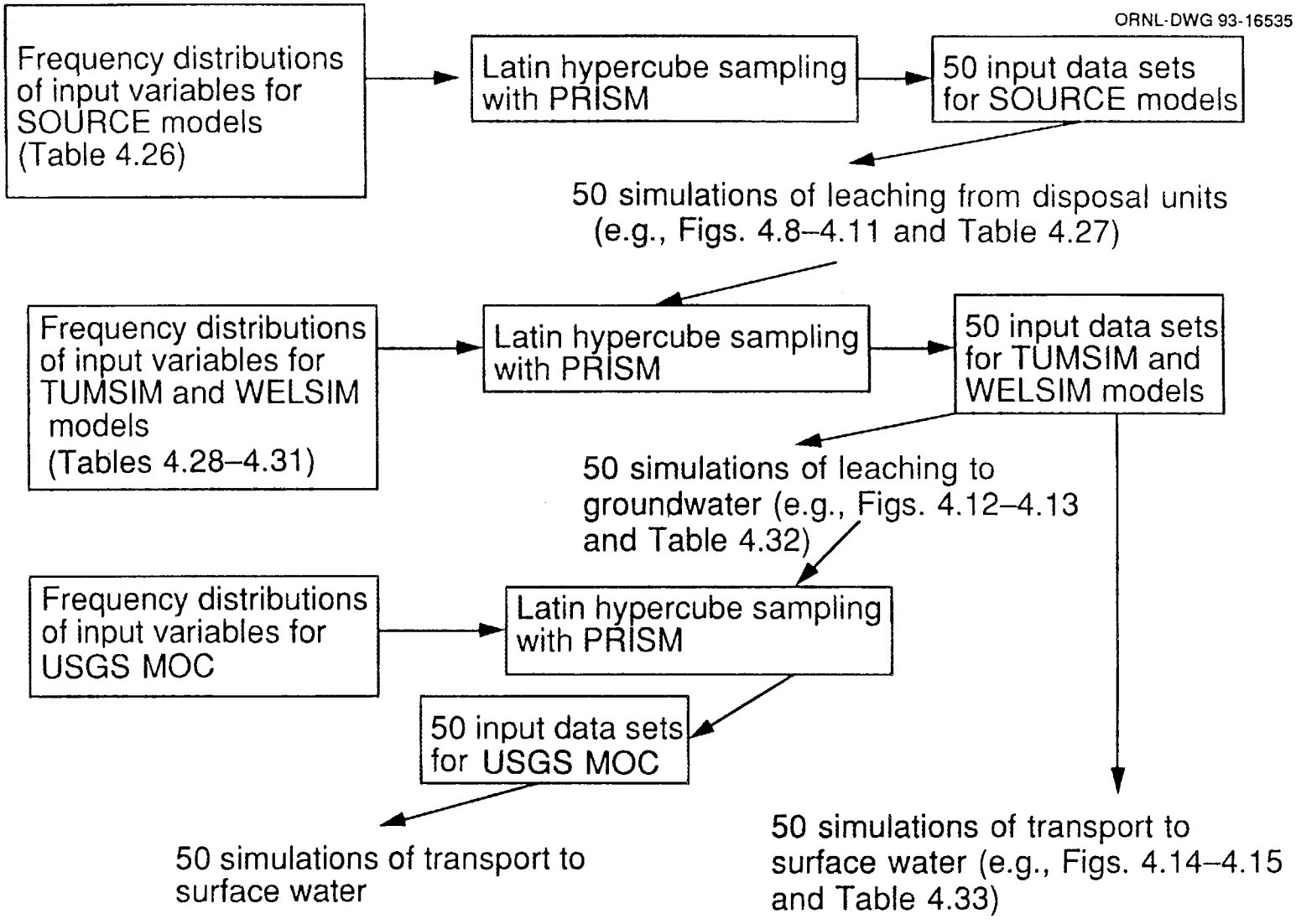

Fig 4.7. Chart illustrating the method for exchange of data sets between models used for sensitivity analysis.

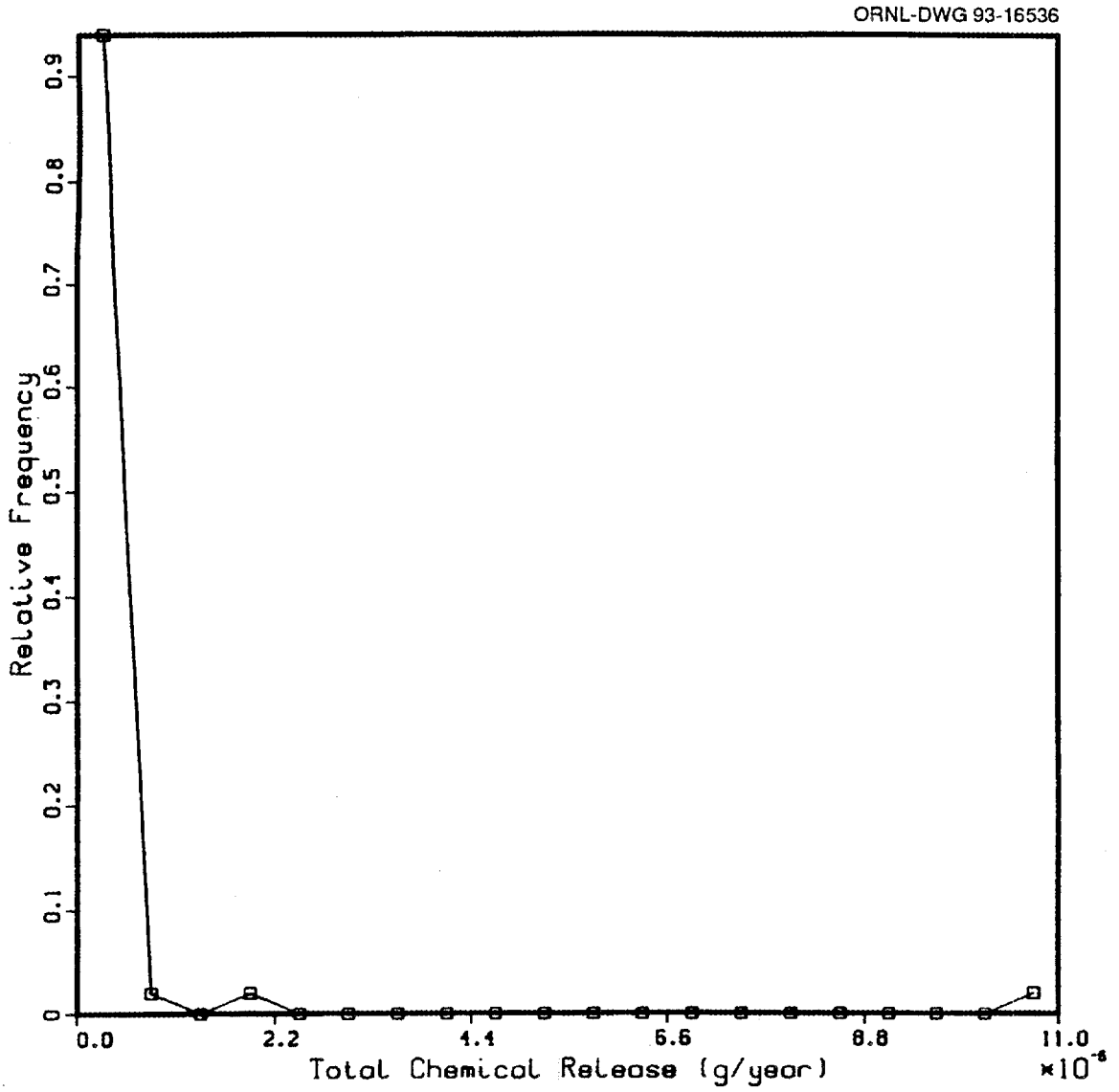

Fig. 4.8. Relative frequency distribution of tritium leaching from the Interim Waste Management Facility at year 50.

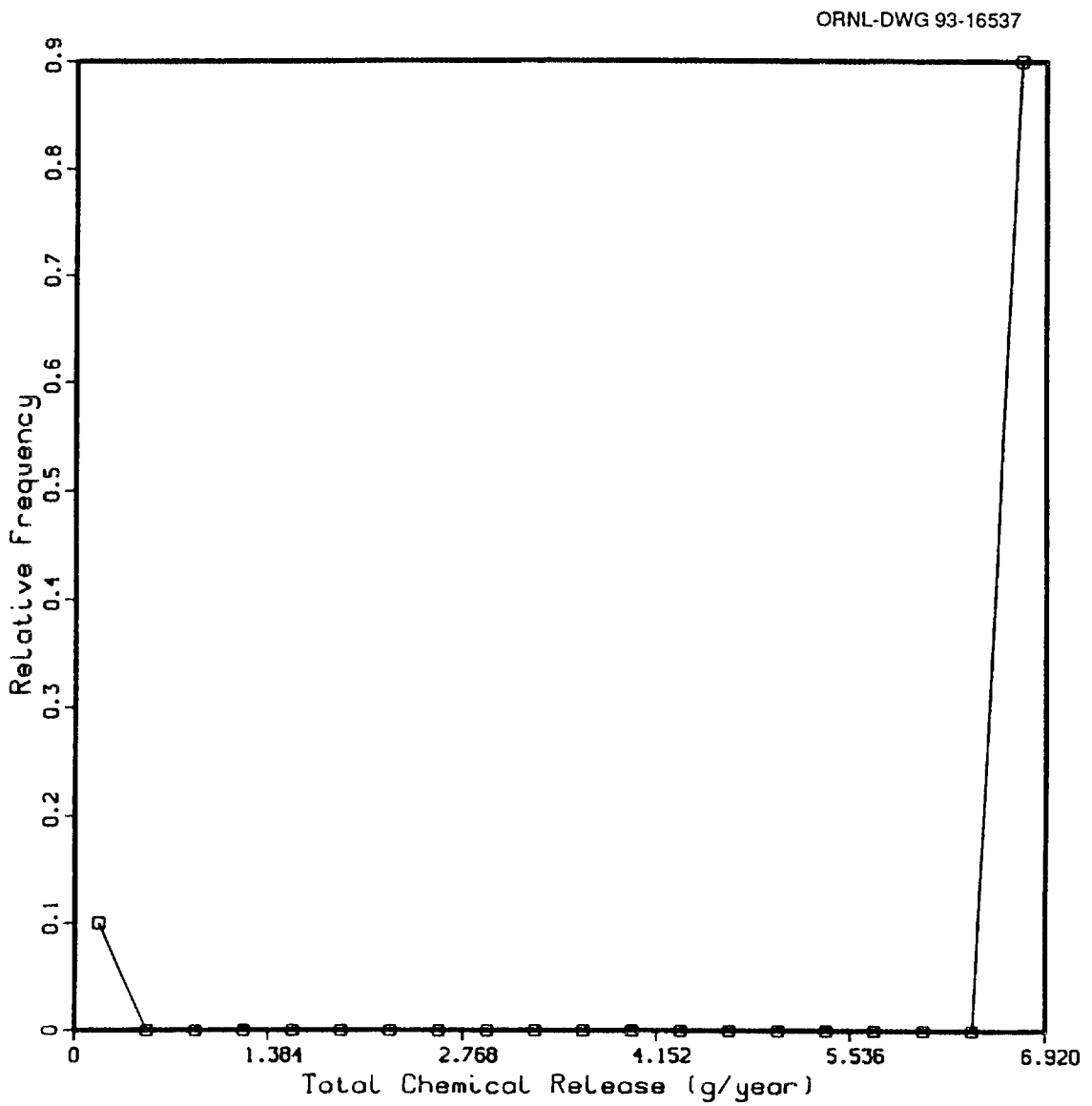

Fig. 4.9. Relative frequency distribution of ^{238}U leaching from the low-range silos (south) at year 200.

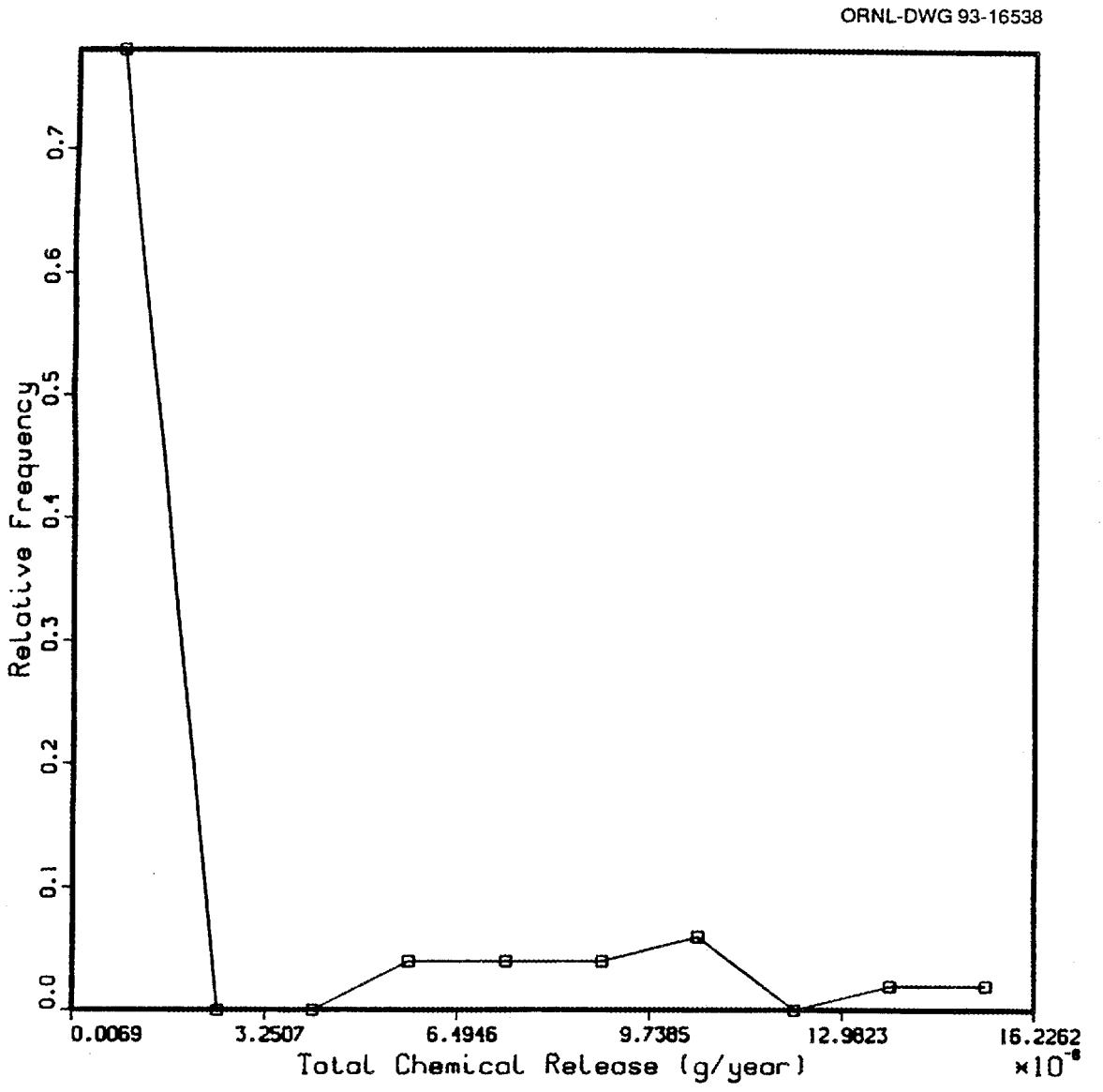

Fig. 4.10 Relative frequency distribution of tritium leaching from the low-range silos (south) at year 50.

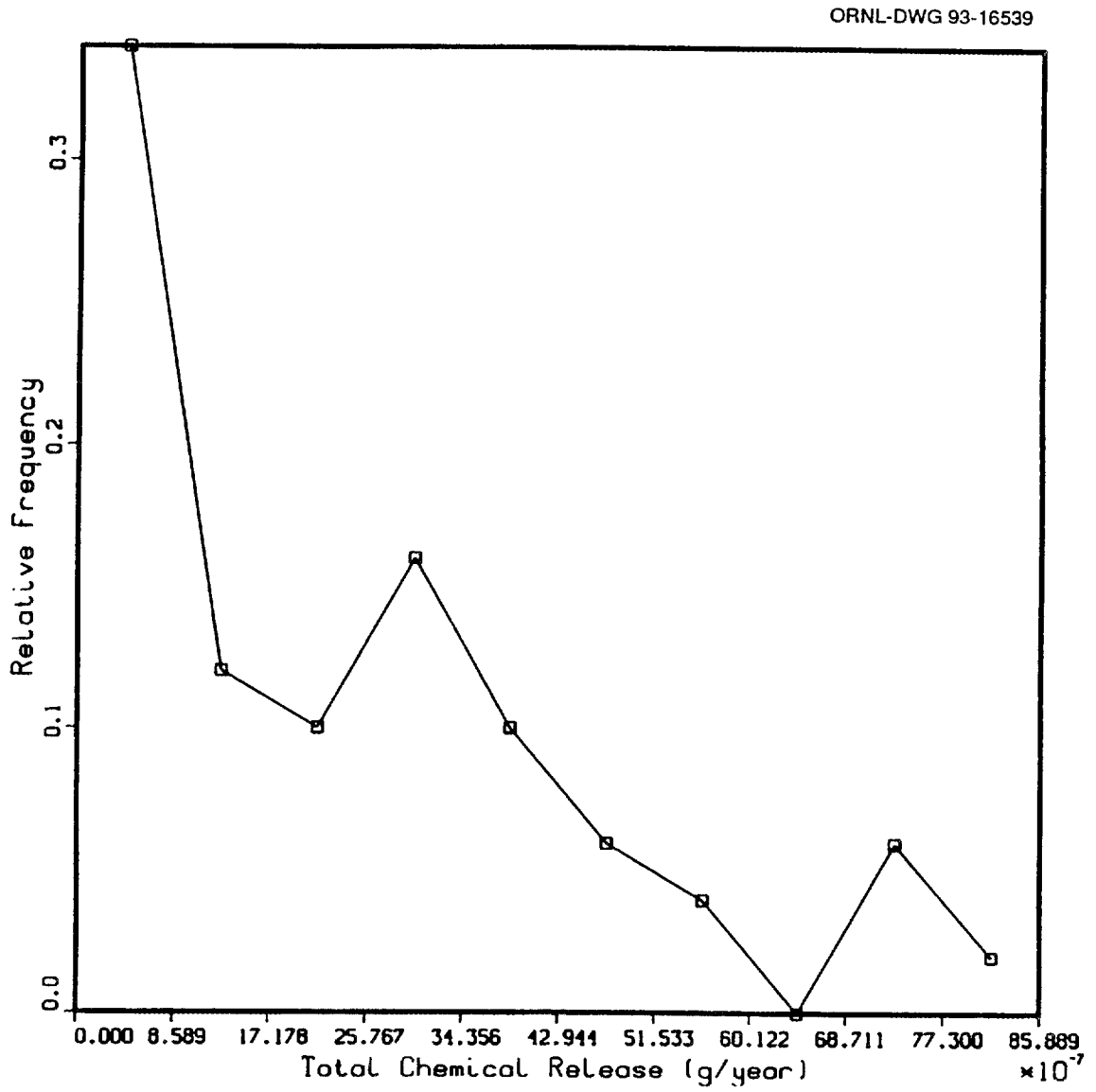

Fig. 4.11. Relative frequency distribution of ^{137}Cs leaching from the Interim Waste Management Facility at year 200.

Table 4.27. Mode and maximum nuclide leaching (g/year) from two disposal units under average and ± 50% (enhanced and reduced, respectively) water flow conditions at 50, 100, and 200 years
(Relative frequencies of occurrence are shown in parentheses.)

Year	Reduced mode	Reduced maximum	Average mode	Average maxium	Enhanced mode	Enhanced maximum
			^{3}H from low-range silo (south)			
50	3.98×10^{-9}(.82)	7.55×10^{-8}(.02)	8.18×10^{-9}(.78)	1.54×10^{-7}(.02)	1.00×10^{-8}(.82)	1.90×10^{-7}(.02)
100	1.10×10^{-9}(.96)	2.09×10^{-8}(.02)	4.13×10^{-13}(.72)	7.85×10^{-12}(.04)	3.30×10^{-9}(.98)	6.27×10^{-8}(.02)
200	1.30×10^{-14}(.96)	5.07×10^{-13}(.02)	1.01×10^{-12}(.96)	3.93×10^{-11}(.02)	6.50×10^{-16}(.84)	2.54×10^{-14}(.02)
			^{3}H from Interim Waste Management Facility			
50	5.50×10^{-7}(.88)	2.15×10^{-5}(0.2)	2.75×10^{-7}(.94)	1.07×10^{-5}(.02)	8.00×10^{-7}(.96)	3.12×10^{-5}(.02)
100	1.05×10^{-8}(.98)	4.10×10^{-7}(.02)	4.14×10^{-11}(.98)	1.62×10^{-9}(.02)	1.00×10^{-9}(.98)	3.90×10^{-8}(.02)
200	5.00×10^{-16}(.98)	1.95×10^{-14}(.02)	1.66×10^{-21}(.98)	6.46×10^{-20}(.02)	6.50×10^{-23}(.98)	2.54×10^{-22}(.02)
			^{137}Cs from Interim Waste Management Facility			
50	5.50×10^{-5}(.32)	1.05×10^{-3}(.02)	1.35×10^{-4}(.14)	8.55×10^{-4}(.08)	3.00×10^{-4}(.22)	1.14×10^{-3}(.02)
100	7.70×10^{-5}(.22)	1.33×10^{-4}(.02)	6.75×10^{-5}(.34)	1.43×10^{-4}(.02)	9.00×10^{-5}(.28)	1.90×10^{-4}(.02)
200	2.97×10^{-6}(.16)	7.07×10^{-6}(.08)	4.29×10^{-7}(.34)	8.16×10^{-6}(.02)	4.94×10^{-7}(.50)	9.40×10^{-6}(.02)
			^{238}U from low-range silo (south)			
50	1.75×10^{-2}(.82)	6.83×10^{-1}(.18)	3.38×10^{-2}(.78)	1.32×10^{0}(.22)	5.25×10^{-2}(.82)	2.05×10^{0}(.18)
100	3.41×10^{1}(.58)	3.41×10^{1}(.58)	6.75×10^{0}(.64)	6.75×10^{0}(.64)	1.01×10^{1}(.58)	1.01×10^{1}(.58)
200	3.41×10^{1}(.84)	3.41×10^{1}(.84)	6.75×10^{0}(.90)	6.75×10^{0}(.90)	1.01×10^{1}(.84)	1.01×10^{1}(.84)

4.6.1.2 UTM and Shallow Subsurface Transport Sensitivity Analysis

A number of sensitivity simulations were conducted with UTM during model development (Luxmoore, Stolzy, and Holdeman 1976, Begovich and Luxmoore 1979, Sharma and Luxmoore 1979) to evaluate the response of water budget components of soil-plant systems to variation of input variables. The heterogeneity of plant physiological variables and of soil physical properties have complex interacting effects that did not need to be re-evaluated for this performance assessment. Such heterogeneity causes the quantity of water interacting with disposal units to vary. This effect was represented by directly varying the water interacting with disposal units by multiplying the water flux value used in each simulation by the SOURCE1 and SOURCE2 models by $\pm$ 50%. In addition, the sensitivity of chemical leaching to water flux in the SOURCE1 and SOURCE2 models was combined with the uncertainty analysis of subsurface chemical transport as calculated with the TUMSIM and WELSIM codes. Output from the SOURCE1 and SOURCE2 models was used for three cases called reduced, average, and enhanced [not the same as the results for three sets of weather conditions (dry, average, and wet) shown earlier in Table 4.2] as outlined above (Sect. 4.6.1.1), and these three cases were run with the uncertainty analysis of shallow subsurface transport as explained in the next section.

4.6.1.3 Uncertainty of Shallow Subsurface Chemical Transport

Five variables used in the TUMSIM and WELSIM codes were selected for uncertainty analysis as follows:

- bulk density of soil
- chemical adsorption (K_d)
- disposal unit area
- distance from the disposal unit to groundwater, and
- distance from the disposal unit to nearest stream channel.

The saprolite of the transport pathway to groundwater and in the lateral flow path were given the same mean bulk density of 1.35 g/cm^3 measurements (Luxmoore 1982). A normal frequency distribution was assumed for bulk density with a standard deviation of 0.15, and the maximum and minimum values for the distribution were set at 1.8 and 0.9, respectively. The frequency distributions for the nuclide K_d values (Table 4.28) were normal for all K_d values that were greater than 10; otherwise they were lognormal. The frequency distributions for the area and distance variables of the disposal units were all assumed normal (Tables 4.29–4.31). Variation in the distance variables reflects tortuosity of flow in porous media. The distance to groundwater also represents variability in mean annual water table elevation.

The LHC sampling resulted in 50 input data sets, each containing randomly assigned values for the five variables listed above. The TUMSIM and WELSIM codes were run, as appropriate, for the 4350 (87 $\times$ 50) simulations. Each simulation was conducted for 1000 years, and a vast amount of computer output was generated. All of these runs were conducted for the average precipitation and water flow conditions.

Table 4.28. Attributes of the frequency distributions selected for chemical adsorption (K_d) that were used in Latin hypercube sampling

Nuclide	K_d (mL/g)	Standard deviation	Distribution	Maximum	Minimum
^{3}H	0.2	0.2	lognormal	10	0
^{14}C	0.2	0.2	lognormal	10	0
^{26}Al	3000	600	normal	5000	1000
^{36}Cl	0.2	0.2	lognormal	10	0
^{60}Co	3000	600	normal	5000	1000
^{63}Ni	2000	400	normal	3500	500
^{90}Sr	30	6	normal	54	8
^{99}Tc	0.2	0.2	lognormal	10	0
^{113m}Cd	200	40	normal	350	50
^{137}Cs	3000	600	normal	5000	1000
^{152}Eu	3000	600	normal	5000	1000
^{154}Eu	3000	600	normal	5000	1000
^{155}Eu	3000	600	normal	5000	1000
^{226}Ra	3000	600	normal	5000	1000
^{229}Th	40	8	normal	70	10
^{230}Th	40	8	normal	70	10
^{232}Th	40	8	normal	70	10
^{232}U	40	8	normal	70	10
^{233}U	40	8	normal	70	10
^{234}U	40	8	normal	70	10
^{235}U	40	8	normal	70	10
^{236}U	40	8	normal	70	10
^{237}Np	40	8	normal	70	10
^{238}U	40	8	normal	70	10
^{238}Pu	40	8	normal	70	10
^{239}Pu	40	8	normal	70	10
^{240}Pu	40	8	normal	70	10
^{242}Pu	40	8	normal	70	10
^{241}Am	40	8	normal	70	10
^{243}Am	40	8	normal	70	10
^{243}Cm	40	8	normal	70	10
^{244}Cm	40	8	normal	70	10
^{249}Cf	40	8	normal	70	10

Table 4.29. Attributes of the frequency distributions selected for disposal unit area that were used in Latin hypercube sampling

Disposal unit	Disposal unit area: Mean (m^2)	Disposal unit area: Standard deviation	Maximum	Minimum
Tumulus I	466	23	535	397
Tumulus II	356	18	410	302
Interim Waste Management Facility	356	18	410	303
Low-range silos (north)	10	0.5	11.5	8.5
Low-range silos (south)	10	0.5	11.5	8.5
High-range silos	10	0.5	11.5	8.5
High-range wells	1	0.05	1.15	0.85
High-range wells and silos	10	0.5	11.5	8.5
Fissile well	1	0.05	1.15	0.85
Asbestos silos	10	0.5	11.5	8.5
Biological trenches	47	2.4	54.2	39.8

Table 4.30. Attributes of the frequency distributions selected for distance to groundwater that were used in Latin hypercube sampling

Disposal unit	Distance to water table: Mean (m)	Distance to water table: Standard deviation	Maximum	Minimum
Tumulus I	2	0.4	4	0
Tumulus II	1	0.2	2	0
Interim Waste Management Facility	2	0.4	4	0
Low-range silos (north)	1	0.2	2	0
Low-range silos (south)	5	1	10	0
High-range silos	1	0.2	2	0
High-range wells	6	1.2	12	0
High-range wells and silos	6	1.2	12	0
Fissile well	3	0.6	5	0
Asbestos silos	1	0.2	2	0
Biological trenches	1	0.2	2	0

Table 4.31. Attributes of the frequency distributions selected for distance to a stream channel that were used in Latin hypercube sampling

Disposal unit	Distance to stream: Mean (m)	Distance to stream: Standard deviation	Maximum	Minimum
Tumulus I	43	8.6	68.8	17.2
Tumulus II	40	8	64	18
Interim Waste Management Facility	115	23	184	46
Low-range silos (north)	35	7	56	14
Low-range silos (south)	200	40	320	80
High-range silos	90	18	144	36
High-range wells	100	20	160	40
High-range wells and silos	100	20	160	40
Fissile well	70	14	112	28
Asbestos silos	100	20	160	40
Biological trenches	65	13	104	26

The flux of tritium to groundwater from IWMF at year 50 (Fig 4.12) showed a skewed frequency distribution. The majority of transport occurred at low rates ($< 8 \times 10^{-7}$ g/year), and a small amount of flow occurred at a much higher rate. The transport of ^{238}U to groundwater from the low-range silos (south) at year 200 (Fig. 4.13) showed a much more skewed distribution than shown for tritium. A high proportion of transport was at a level < 7 g/year, which was about 10-fold less than the maximum simulated flux. In the lateral transport path, tritium from the low-range silos (south) at year 50 was skewed to the left with a factor of 10 between the mode and maximum transport rates (Fig. 4.14). In a fourth example, ^{137}Cs transport from IWMF at year 200 in the shallow lateral flow path to a stream channel displayed a frequency distribution that may be normal (Fig. 4.15).

Some additional simulations were made for reduced (−50%) and enhanced (+50%) water flow into the disposal units to provide a sensitivity analysis in combination with the uncertainty analysis as outlined in Sect. 4.6.1.1. Results are compared for a nuclide with low K_d and short half-life (^{3}H) from two disposal units with shorter or longer transport path lengths [IWMF and low-range silos (south), respectively]; for a nuclide with a moderate K_d and long half-life (^{238}U) from the low-range silos (south); and lastly for a

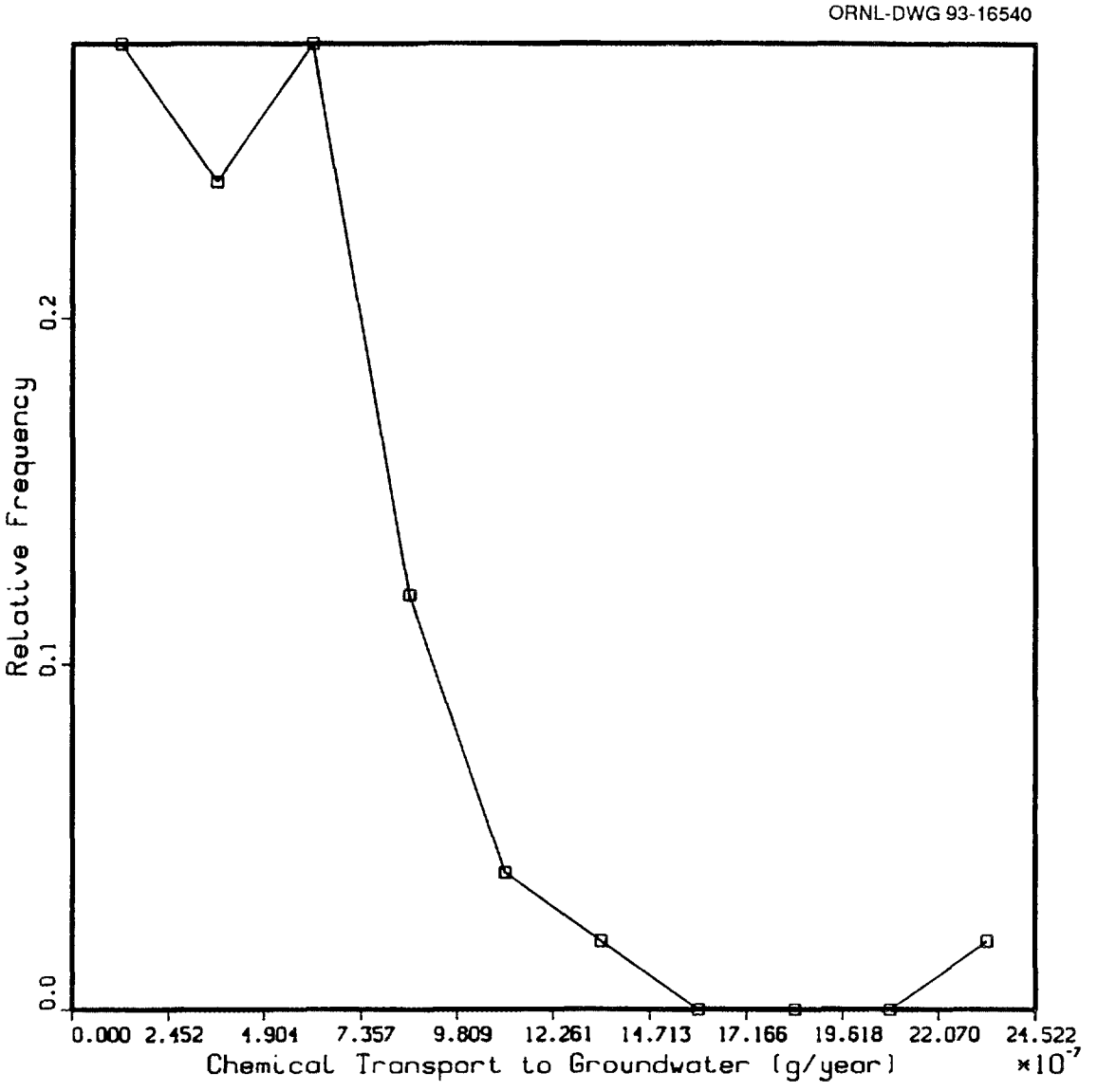

Fig. 4.12. Relative frequency distribution of tritium transport to groundwater from the Interim Waste Management Facility at year 50.

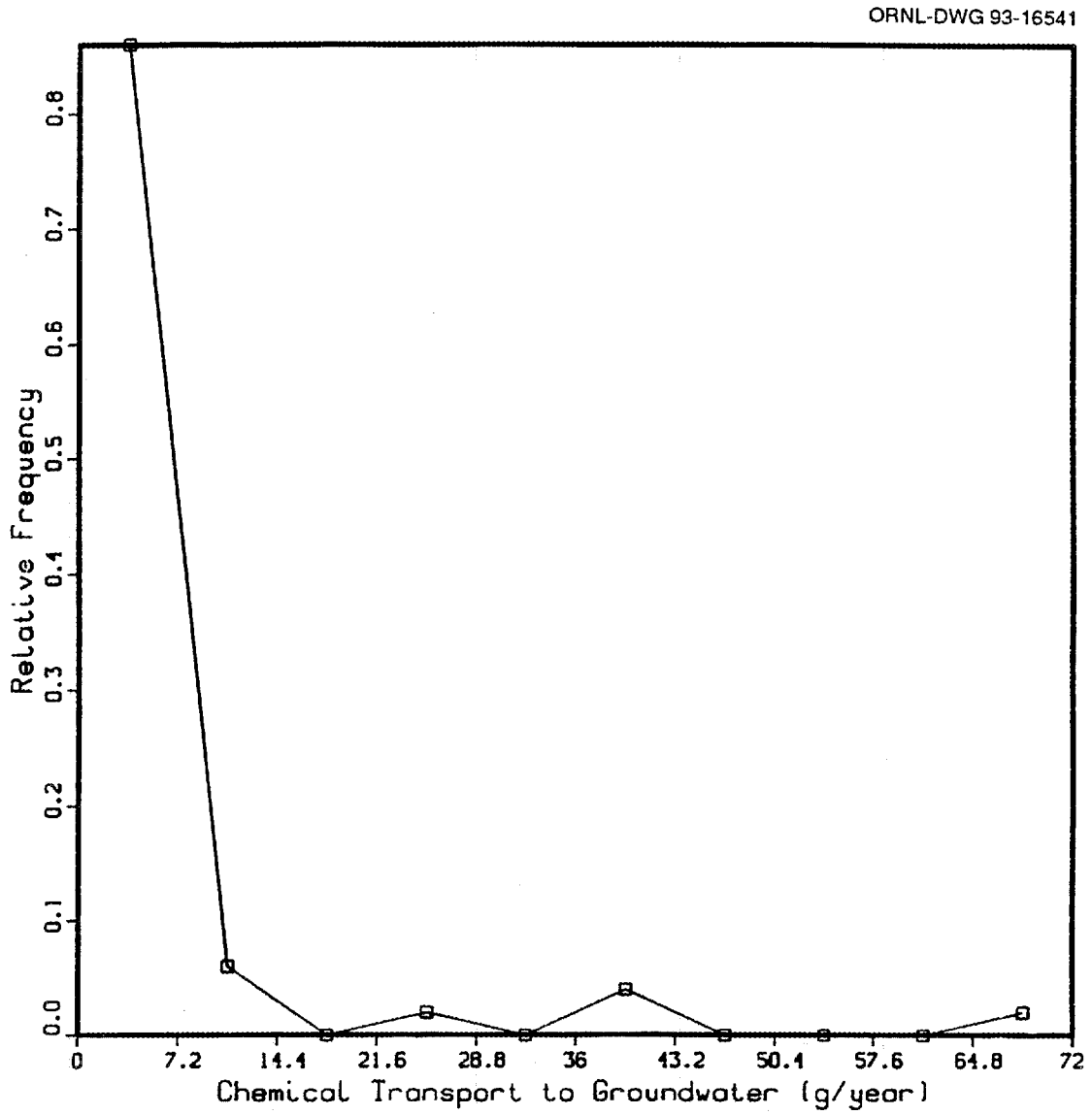

Fig. 4.13. Relative frequency distribution of ^{238}U transport to groundwater from the low-range silos (south) at year 200.

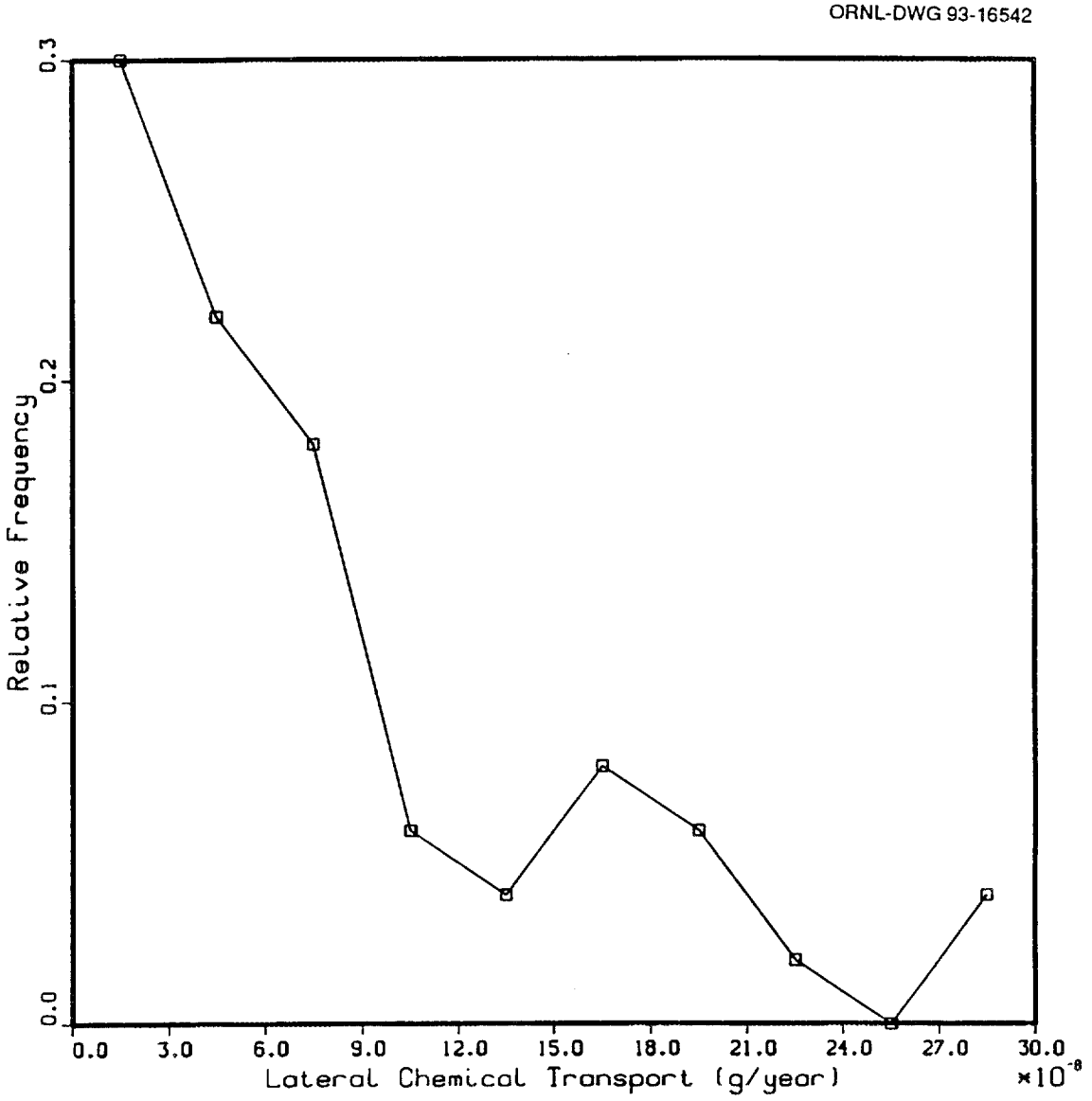

Fig. 4.14. Relative frequency distribution of tritium transport in shallow subsurface flow to a stream channel from the low-range silos (south) at year 50.

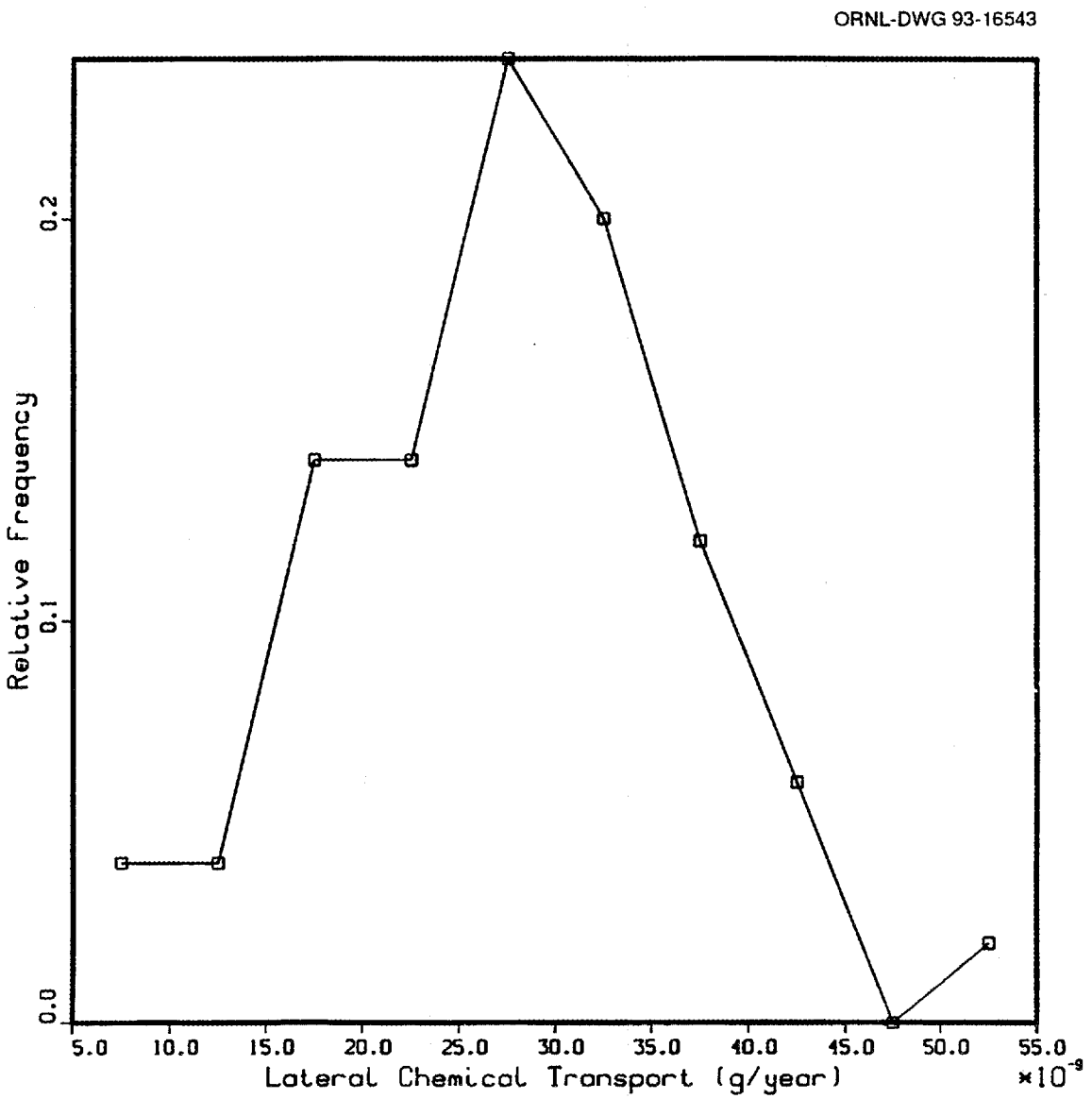

Fig. 4.15. Relative frequency distribution of ^{137}Cs transport in shallow subsurface flow to a stream channel from the Interim Waste Management Facility at year 200.

nuclide with a high K_d and moderate half-life (^{137}Cs) from the IWMF. This provided a combination of four runs that were conducted for the average water flow and $\pm$ 50% change in flow for a total of 12 combinations.

Similar figures to the above were prepared for the cases with $\pm$ 50% of water flow, and the results have been summarized in tables showing the most frequent class (mode) and the maximum transport rates in recharge to groundwater and in lateral flow to surface water (Tables 4.32 and 4.33). Under average water flow conditions, nuclide transport in recharge to groundwater for the most frequent class (mode) was often about 20 times smaller than the maximum transport rate. This ratio was preserved at different times during transport. The relative frequency of the maximum transport rate was from 2 to 10% of the distribution, whereas the major proportion of the transport was dominated by the modal class (24–90% of the distribution, Table 4.32). There was very little effect of differing water flow conditions (reduced, average, enhanced) on transport to groundwater. The leachate concentration was higher as the quantity of water declined, and this largely caused transport in recharge to be insensitive to water flow conditions.

In contrast to the results for recharge, shallow subsurface transport was often higher with increases in water flow, and the maximum transport rate was up to 20–40 times higher than the modal case (Table 4.33). The implication of this uncertainty analysis to the surface water dose analysis is that there is a small possibility (usually in the 2–4 % range) of transport being higher by a factor of 20–40. This maximum transport is a result of heterogeneity in factors controlling leaching and shallow subsurface transport.

The uncertainty in shallow subsurface chemical transport can also be represented as cumulative distribution functions (CDFs) to illustrate the probability that the concentration in shallow subsurface water is less than the compliance limit of 4 mrem/year for drinking water. This probability is related to the uncertainty in the model as discussed in Sect. 4.6.1.4. The CDFs for ^{3}H, ^{14}C, ^{36}Cl, ^{90}Sr, ^{137}Cs, and ^{238}U are presented in Figs. 4.16–4.21. These figures are for total concentrations in surface water as a result of shallow subsurface water transport. Comparison of Figs. 4.16–4.21 with the CDFs for groundwater (Sect. 4.6.1.4) and surface water (Sect. 4.6.1.5) provides insight into the evolution of uncertainty in environmental transport.

4.6.1.4 Uncertainty of Groundwater Transport

The effects of parametric uncertainty on groundwater transport were evaluated in a manner consistent with methods used to quantify uncertainties associated with leaching from disposal units and transport through the shallow subsurface. In addition to the 50 calculated groundwater flux time profiles for each disposal unit described in Sect. 4.6.1.3, model input for which signifigant uncertainties were assumed to exist included the four additional variables used by the USGS MOC code:

- saprolite bulk density
- hydraulic conductivity
- chemical adsorption
- saprolite porosity

Table 4.32. Mode and maximum nuclide transport to groundwater (g/year) from two disposal units under average and ±50% (enhanced and reduced, respectively) water flow conditions at 50, 100, and 200 years
(Relative frequencies of occurrence are shown in parentheses.)

Year	Reduced mode	Reduced maximum	Average mode	Average maximum	Enhanced mode	Enhanced maximum
			Tritium from the low-range silos (south)			
50	3.6×10^{-8} (.38)	67.5×10^{-8} (.04)	9.2×10^{-8} (.64)	17.5×10^{-7} (.02)	4.5×10^{-8} (.52)	85.5×10^{-8} (.02)
100	1.5×10^{9} (.52)	28.3×10^{-9} (.02)	9.3×10^{-10} (.46)	17.8×10^{-9} (.04)	9.5×10^{-10} (.50)	18.0×10^{-9} (.04)
200	3.1×10^{-12} (.82)	12.2×10^{-11} (.02)	4.8×10^{-13} (.40)	90.5×10^{-13} (.04)	2.2×10^{-12} (.86)	85.1×10^{-12} (.02)
			Tritium from the Interim Waste Management Facility			
50	2.9×10^{-7} (.52)	54.8×10^{-7} (.02)	3.7×10^{-7} (.24)	23.0×10^{-7} (.02)	8.9×10^{-8} (.26)	16.9×10^{-7} (.02)
100	1.7×10^{-9} (.44)	32.7×10^{-9} (.02)	1.1×10^{-9} (.40)	20.5×10^{-9} (.10)	1.0×10^{-9} (.40)	19.4×10^{-9} (.04)
220	2.1×10^{-12} (.64)	39.0×10^{-12} (.02)	2.2×10^{-12} (.66)	40.9×10^{-12} (.02)	1.5×10^{-12} (.64)	28.5×10^{-12} (.04)
			Cesium-137 from the Interim Waste Management Facility			
50	4.1×10^{-9} (.78)	78.8×10^{-9} (.02)	0.5×10^{-8} (.78)	11.5×10^{-8} (.02)	6.1×10^{-9} (.82)	11.6×10^{-8} (.02)
100	3.6×10^{-9} (.76)	67.6×10^{-9} (.04)	4.8×10^{-9} (.78)	91.7×10^{-9} (.02)	4.5×10^{-9} (.78)	86.9×10^{-9} (.02)
200	1.4×10^{-9} (.80)	26.0×10^{-9} (.02)	1.6×10^{-9} (.82)	29.9×10^{-9} (.02)	1.5×10^{-9} (.84)	27.8×10^{-9} (.02)
			Uranium-238 from the low-range silos (south)			
50	1.0×10^{-3} (.84)	19.0×10^{-3} (.02)	5.0×10^{-3} (.84)	95.0×10^{-3} (.02)	3.1×10^{-3} (.90)	58.9×10^{-3} (.02)
100	1.0×10^{0} (.94)	19.0×10^{0} (.02)	1.3×10^{0} (.90)	24.7×10^{0} (.02)	1.5×10^{0} (.92)	28.5×10^{0} (.02)
200	2.8×10^{0} (.88)	52.3×10^{0} (.02)	3.6×10^{0} (.86)	68.4×10^{0} (.02)	4.1×10^{0} (.86)	77.9×10^{0} (.02)

Table 4.33. Mode and maximum nuclide transport in shallow subsurface flow to a stream channel (g/year) from two disposal units under average and ±50% (enhanced and reduced, respectively) water flow conditions at 50, 100, and 200 years
(Relative frequencies of occurrence are shown in parentheses.)

Year	Reduced mode	Reduced maximum	Average mode	Average maximum	Enhanced mode	Enhanced maximum
			Tritium from low-range silos (south)			
50	5.5×10^{-9} (.32)	10.5×10^{-8} (.04)	1.5×10^{-8} (.30)	28.5×10^{-8} (.04)	2.3×10^{-8} (.26)	44.0×10^{-8} (.04)
100	4.1×10^{-9} (.46)	$160. \times 10^{-9}$ (.02)	1.1×10^{-8} (.68)	19.1×10^{-8} (.04)	1.0×10^{-8} (.72)	40.0×10^{-8} (.02)
200	9.1×10^{-12} (.64)	35.4×10^{-11} (.02)	2.8×10^{-11} (.90)	52.3×10^{-11} (.02)	2.6×10^{-11} (.90)	99.8×10^{-11} (.02)
			Tritium from the Interim Waste Management Facility			
50	9.3×10^{-7} (.40)	58.9×10^{-7} (.06)	3.6×10^{-7} (.80)	68.9×10^{-7} (.02)	3.5×10^{-7} (.84)	67.3×10^{-7} (.02)
100	1.1×10^{-8} (.86)	4.1×10^{-7} (.02)	4.5×10^{-9} (.96)	1.8×10^{-7} (.02)	1.2×10^{-8} (.98)	48.6×10^{-8} (.02)
200	2.9×10^{-12} (.98)	11.3×10^{-11} (.02)	4.7×10^{-14} (.98)	1.8×10^{-12} (.02)	1.5×10^{-14} (.98)	58.1×10^{-14} (.02)
			Cesium-137 from the Interim Waste Management Facility			
50	1.0×10^{-8} (.32)	19.6×10^{-8} (.40)	10.0×10^{-8} (.20)	63.7×10^{-8} (.04)	6.4×10^{-8} (.22)	12.2×10^{-7} (.02)
100	3.8×10^{-8} (.16)	14.5×10^{-8} (.08)	20.3×10^{-8} (.18)	42.8×10^{-8} (.02)	26.1×10^{-8} (.20)	70.8×10^{-8} (.02)
200	11.5×10^{-9} (.24)	24.2×10^{-9} (.02)	27.5×10^{-9} (.24)	52.5×10^{-9} (.02)	58.3×10^{-9} (.22)	77.8×10^{-9} (.02)
			Uranium-238 from low-range silos (south)			
50	1.2×10^{-4} (.84)	21.9×10^{-4} (.02)	0.8×10^{-3} (.80)	15.2×10^{-3} (.02)	1.7×10^{-3} (.82)	31.4×10^{-3} (.02)
100	3.0×10^{-1} (.46)	5.7×10^{0} (.02)	1.4×10^{0} (.42)	25.7×10^{0} (.06)	3.0×10^{0} (.48)	57.0×10^{0} (.06)
200	1.0×10^{0} (.20)	19.0×10^{0} (.08)	4.2×10^{0} (.16)	79.8×10^{0} (.08)	9.0×10^{0} (.18)	1.71×10^{2} (.10)

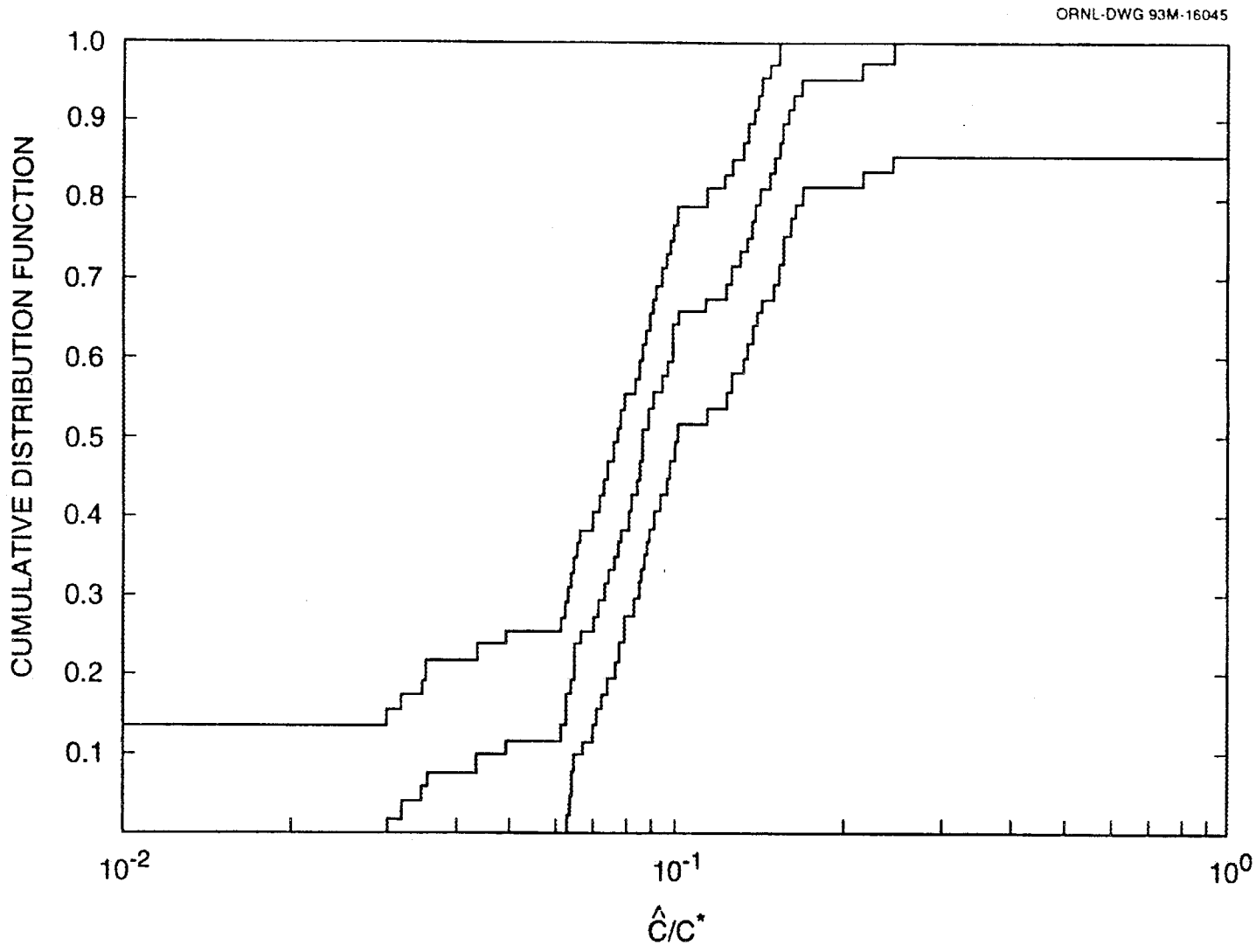

Fig. 4.16. Latin hypercube sampled tritium surface water concentrations arising from shallow subsurface transport (middle curve). Values are expressed relative to the compliance limit. Curves on either side are Kolmogorov quantiles for a $\pm 68\%$ confidence interval.

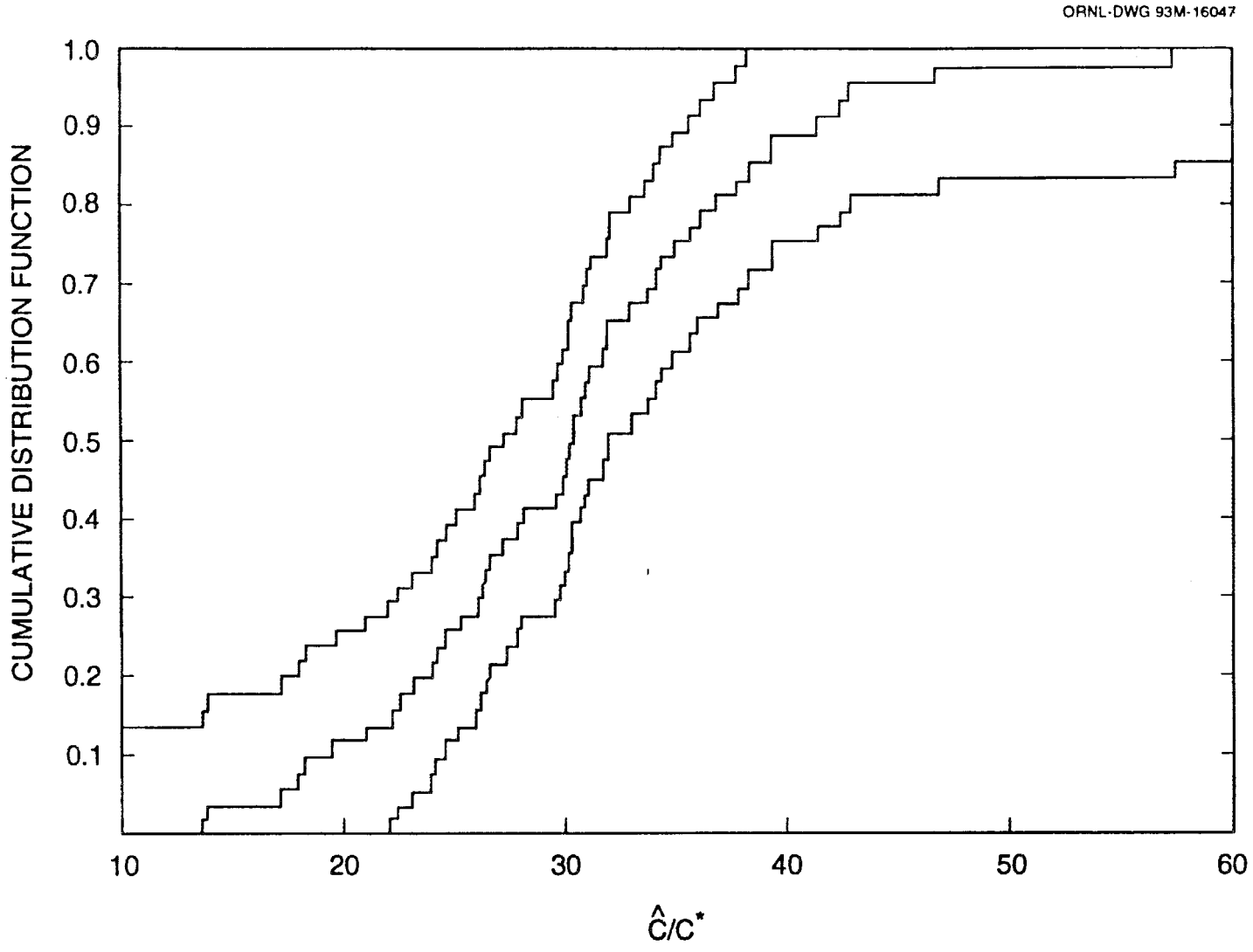

Fig. 4.17. Latin hypercube sampled ^{14}C surface water concentrations arising from shallow subsurface transport (middle curve). Values are expressed relative to the compliance limit. Curves on either side are Kolmogorov quantiles for a $\pm 68\%$ confidence interval.

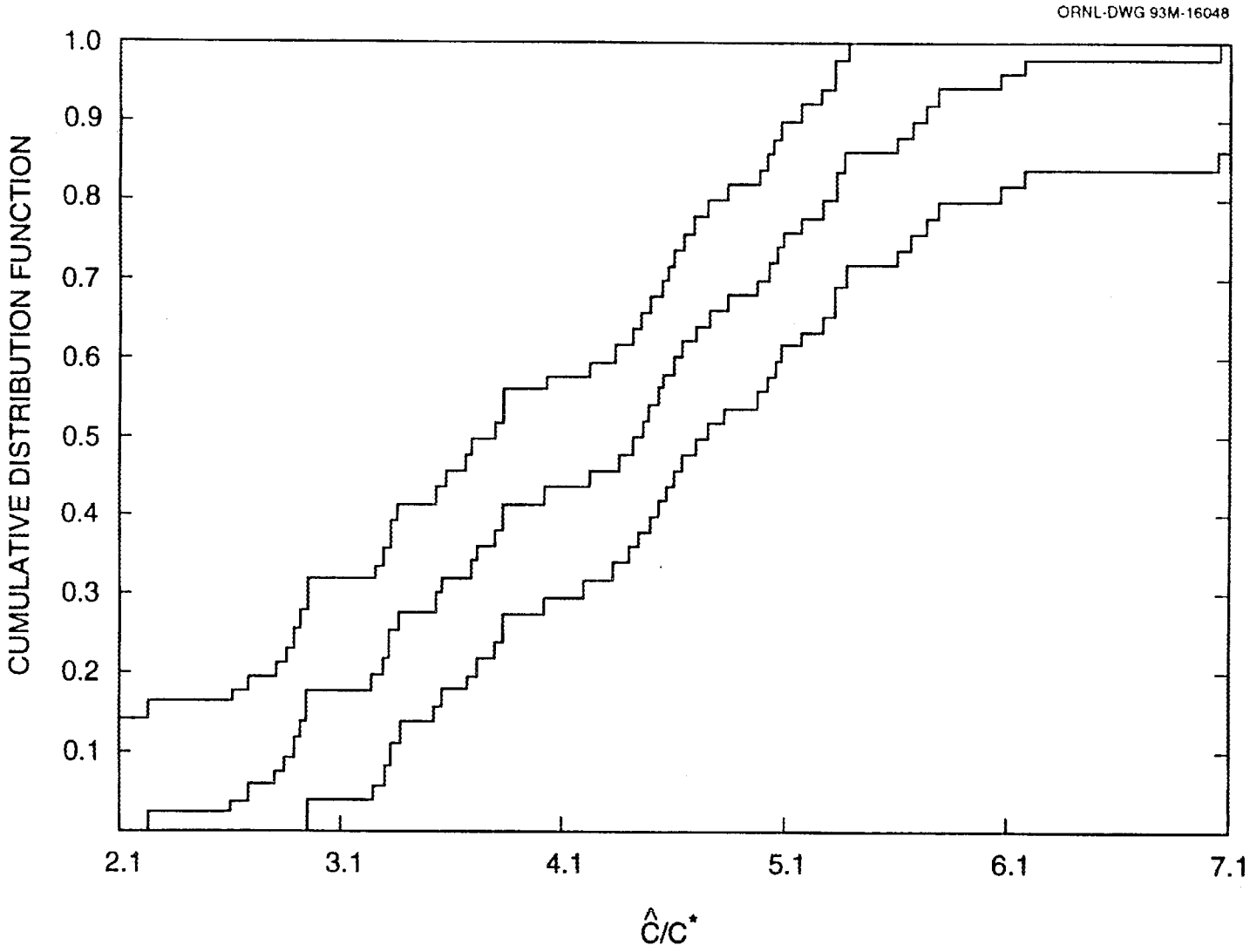

Fig. 4.18. Latin hypercube sampled ^{36}Cl surface water concentrations arising from shallow subsurface transport (middle curve). Values are expressed relative to the compliance limit. Curves on either side are Kolmogorov quantiles for a ±68% confidence interval.

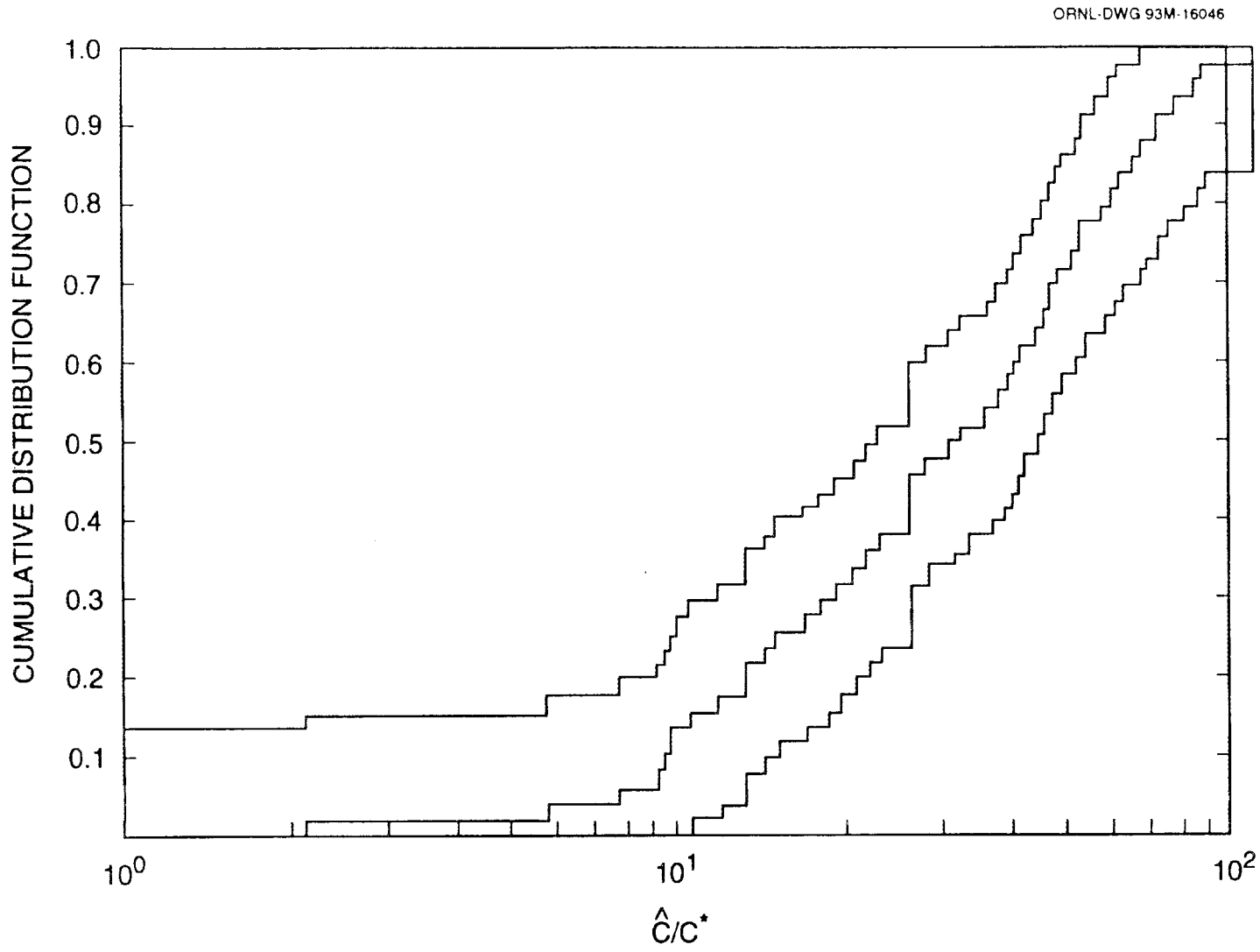

Fig. 4.19. Latin hypercube sampled ^{90}Sr surface water concentrations arising from shallow subsurface transport (middle curve). Values are expressed relative to the compliance limit. Curves on either side are Kolmogorov quantiles for a $\pm 68\%$ confidence interval.

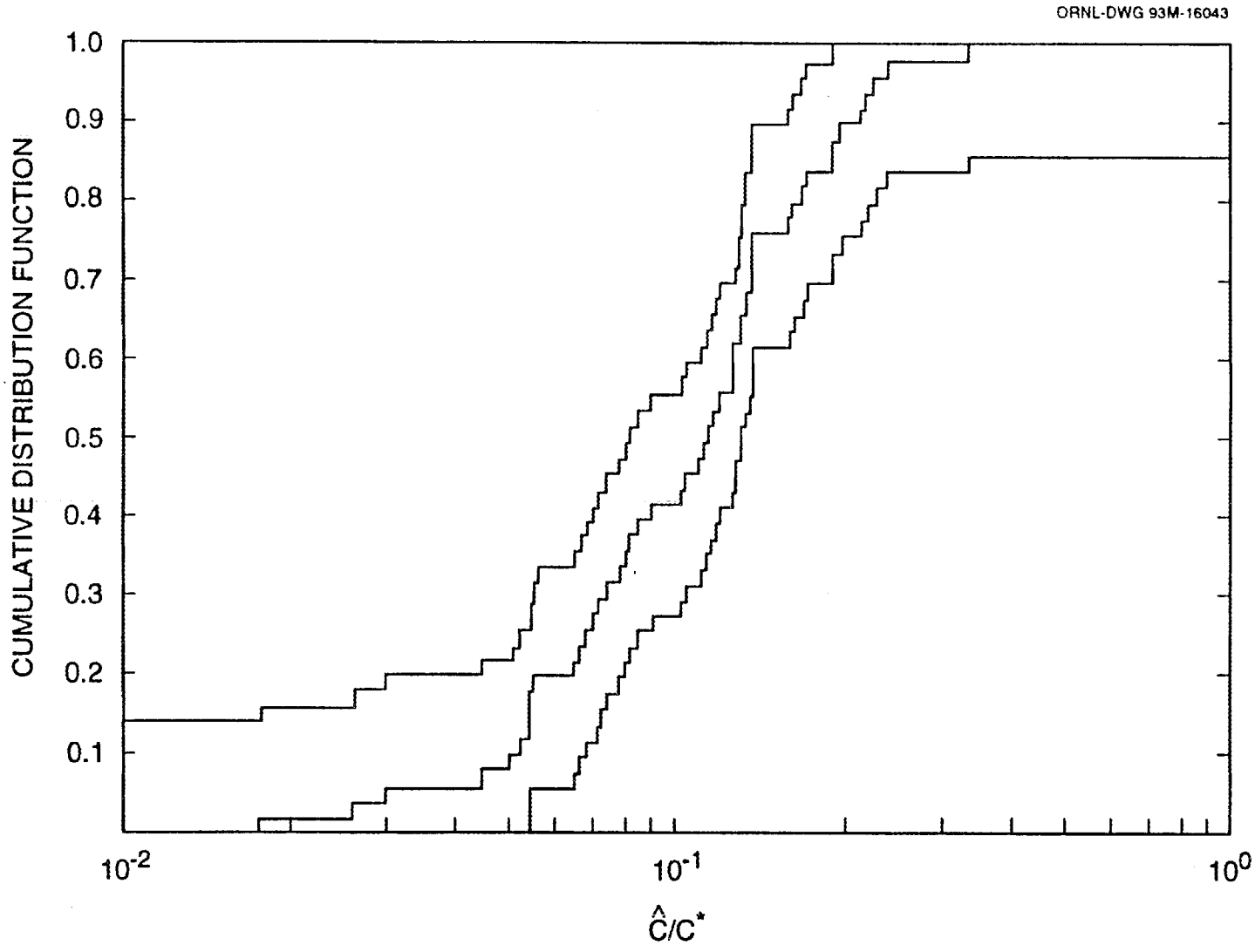

Fig. 4.20. Latin hypercube sampled ^{137}Cs surface water concentrations arising from shallow subsurface transport (middle curve). Values are expressed relative to the compliance limit. Curves on either side are Kolmogorov quantiles for a $\pm 68\%$ confidence interval.

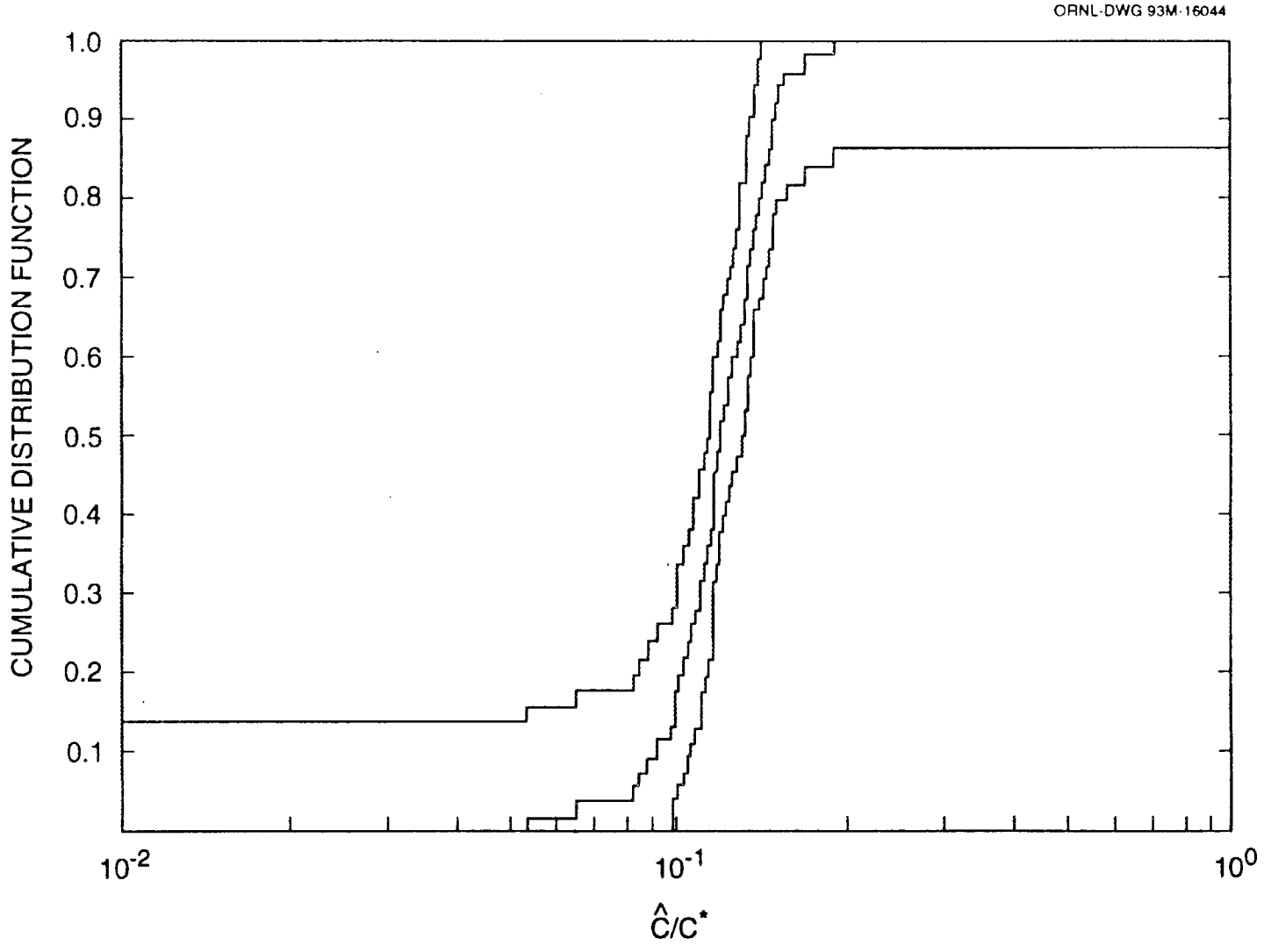

Fig. 4.21. Latin hypercube sampled ^{238}U surface water concentrations arising from shallow subsurface transport (middle curve). Values are expressed relative to the compliance limit. Curves on either side are Kolmogorov quantiles for a $\pm 68\%$ confidence interval.

Consistent with Sect. 4.6.1.1, saprolite bulk density was assumed to be normally distributed with a mean of 1.35 g/cm^3, standard deviation of 0.15, and a minimum and maximum of 0.9 and 1.8, respectively. Hydraulic conductivities were assumed to be lognormally distributed with a geometric mean of 1.20×10^{-6} m/s (3.94×10^{-6} ft/s) and standard deviation of 2.4. The range of hydraulic conductivities was selected to represent the uncertainty associated with using a porous-medium model for a heterogeneous fractured medium. The representation of the site as an effective porous medium is justified by the model validation work of Lee (1991); however, local variations in conductivity are to be expected. This concern is reflected in the subjective uncertainty analysis (Sect. 4.6.1.6). Distributions for K_d values were identical to those given in Table 4.28. Porosity was assumed to be uniformly distributed between 0.02 and 0.05.

Using distributions for the parameters identified in the previous section, LHC sampling was performed using the PRISM (Gardner, Röjder, and Berström 1983) computer code to construct 50 random data sets per nuclide. With the exception of ^{232}Th and ^{238}U, these data were then used as input for nuclide-specific simulations performed using the USGS MOC model. Unlike the previous uncertainty analyses conducted on the SOURCE1, SOURCE2, TUMSIM, or WELSIM codes, in which seperate simulations were performed for each disposal unit, all units associated with a given nuclide were analyzed simultaneously in each of the 50 MOC runs.

Due to the extremely long simulation times required to obtain "peak" concentration values, use of the MOC computer code was deemed impractical for use in analyzing ^{232}Th and ^{238}U. For these nuclides, uncertainty analyses were performed using the analytical model described in Appendix E. Unlike the MOC runs, individual analyses were made for each disposal unit where these nuclides were present.

The results of the groundwater transport uncertainty analysis yielded distributions of 50 values of maximum groundwater concentration per nuclide at each of the 334 modeled observation points. Distributions of total contaminant fluxes to surface water for each nuclide were also generated. Of all the distributions generated, special attention was paid to ^{14}C, ^{36}Cl, ^{3}H, ^{90}Sr, ^{137}Cs, and ^{238}U at compliance points adjacent to IWMF. Nuclides ^{14}C, ^{36}Cl, and ^{3}H are of interest based on results from the deterministic analysis outlined in Sect. 4.3, which indicated "best estimate" groundwater concentrations predicted near the IWMF site exceeded compliance limits. Cesium-137 and ^{90}Sr are of concern due to high initial inventories, while calculated ^{238}U concentrations are of special interest because they were obtained using the analytical model outlined in Appendix E. CDFs showing calculated groundwater concentrations relative to compliance limits for the following representative nuclides, ^{14}C, ^{3}H, ^{36}Cl, ^{90}Sr, ^{137}Cs, and ^{238}U, were generated and are presented in Figs. 4.22–4.27. Additional CDFs showing the contributions from groundwater flux to total surface water concentration for the above nuclides are also shown in Figs. 4.28–4.33.

The results in Sect. 4.3.1 show calculated groundwater concentrations at observation points based on the best-case values of input parameters. However, with the inclusion of uncertainties associated with available input information, corresponding uncertainties associated with the calculated groundwater contaminant concentrations are introduced. One method of quantifying these uncertainties is to equate uncertainty with the amount of scatter associated with predicted groundwater concentrations. The CDFs shown in Figs. 4.22–4.27 can be used to illustrate this point. While the best case results presented in

Table 4.5 indicate that the maximum groundwater concentrations for three nuclides, ^{3}H, ^{14}C, and ^{36}Cl, exceeded compliance limits during the 100-year insitutional control period, Figs. 4.22–4.24 show potential groundwater concentrations for these contaminants range from 0.0002 to 5.0 times the values reported in Table 4.5. The range of potential values is even greater for the nuclides ^{90}Sr and ^{137}Cs, the potential values of which span 10 and 8 orders of magnitude, respectively.

Associated with the CDFs in Figs. 4.22–4.27 are the corresponding probabilities that groundwater contaminant concentration at a given observation point complies with the 4 mrem/year drinking water limit. These probabilities range from 0.19 for ^{36}Cl; 0.3 for ^{14}C; 0.7 for ^{3}H; and 1.0 for ^{90}Sr, ^{137}Cs, and ^{238}U. Using these compliance probabilities, an alternate method for quantifying uncertainty by viewing it as entropy (see Appendix H) can be used to assign an actual value to the uncertainty associated with the modeled predictions. If a probability of compliance (POC) is 0.5, then no confident conclusion can be drawn as to whether a predicted concentration is less than the limit, or whether there is an even chance of compliance. If the POC is 0 or 1, then a strong statement can be made concerning compliance or the lack of compliance. A quantitative measure of this confidence is expressed by the uncertainty (U), which is maximized ($U = 1.0$) when $P_c = 0.5$. In this entropy-based formula for uncertainty, U is given by:

$$U = -[P_c \log_2(P_c) + (1 - P_c)\log_2(1 - P_c)] \quad , \tag{4.1}$$

where

P_c = probability that contaminant concentration is less than the allowable limit.

In this case, the corresponding uncertainties are 0.88 for ^{14}C and ^{3}H; 0.68 for ^{36}Cl; and 0.0 for ^{90}Sr, ^{137}Cs, and ^{238}U.

4.6.1.5 Uncertainty of Surface Water Transport

The effects of parametric uncertainty on surface water transport were determined using the results of the uncertainty analysis for groundwater and shallow subsurface water. Each of these analyses provided cumulative distribution functions of the transport of contamination from the respective models that were combined for the CDFs for surface water transport. The resulting CDFs for surface water are presented in Figs. 4.34–4.39 for the isotopes ^{3}H, ^{14}C, ^{36}Cl, ^{90}Sr, ^{137}Cs, and ^{238}U. The figures show the CDFs for combined discharge to White Oak Creek from the ephemeral creeks. Consequently, they provide insight into the concentrations of radionuclides in the ephemeral creeks in SWSA 6 that are not suitable for use as a surface water resource by an individual or a community. The CDFs for the combined shallow subsurface water and groundwater contaminant discharges provide a relative estimate of the uncertainty in the results presented in Sect. 4.4, Table 4.8. Figures 4.34–4.39 indicate that the ephemeral creeks within SWSA 6 are likely to exceed the 4 mrem/year drinking water concentration limit prior to discharge to White Oak Creek for the nuclides ^{14}C, ^{36}Cl, and ^{90}Sr. Similarly, the uncertainty results indicate that the concentrations in surface water for ^{3}H, ^{137}Cs, and ^{238}U are not likely to exceed the

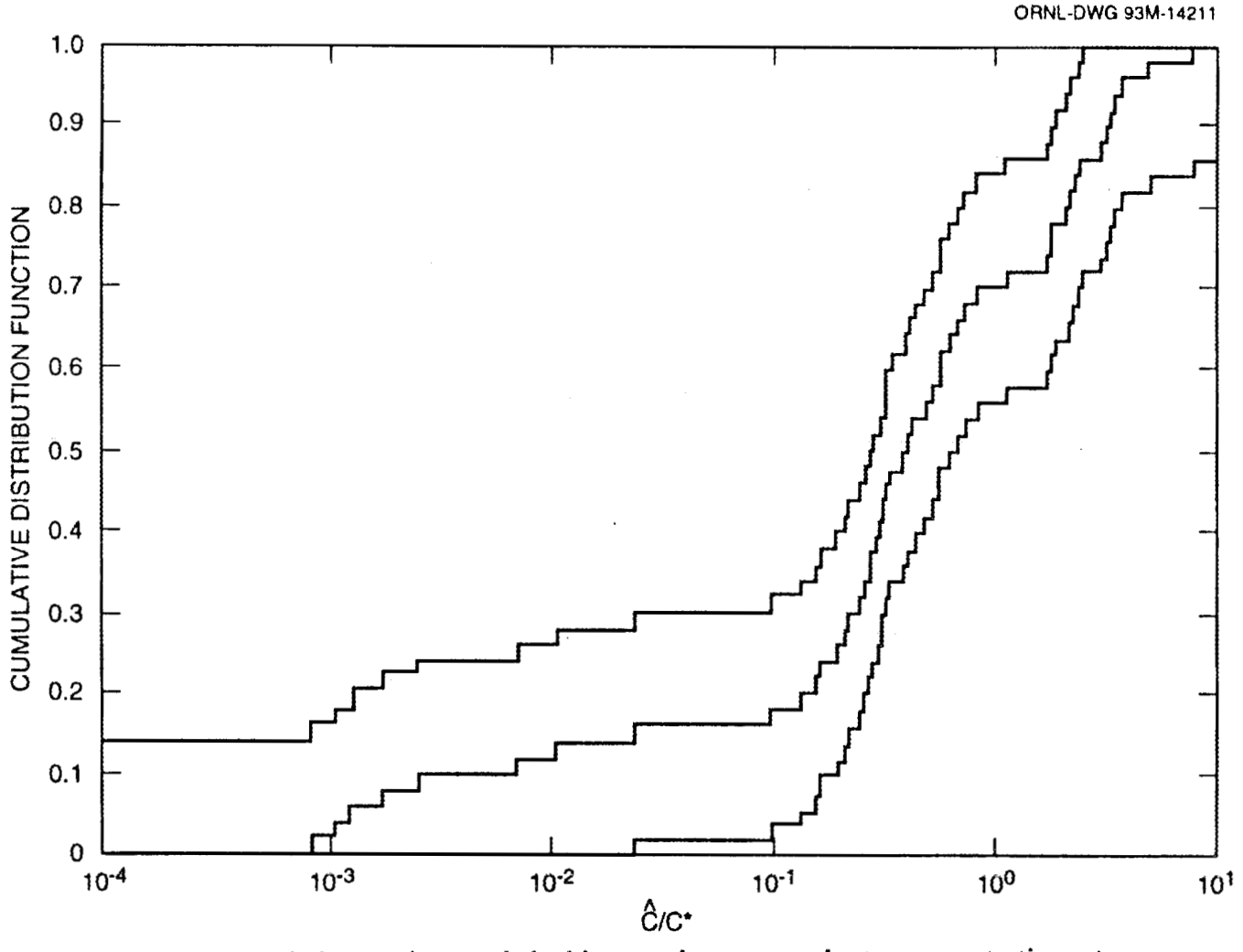

Fig. 4.22. Latin hypercube sampled tritium maximum groundwater concentrations at 100 m (328 ft), assumed to occur at node 168 (middle curve). Values are expressed relative to the compliance limit. Curves on either side are Kolmogorov quantiles for a ±68% confidence interval.

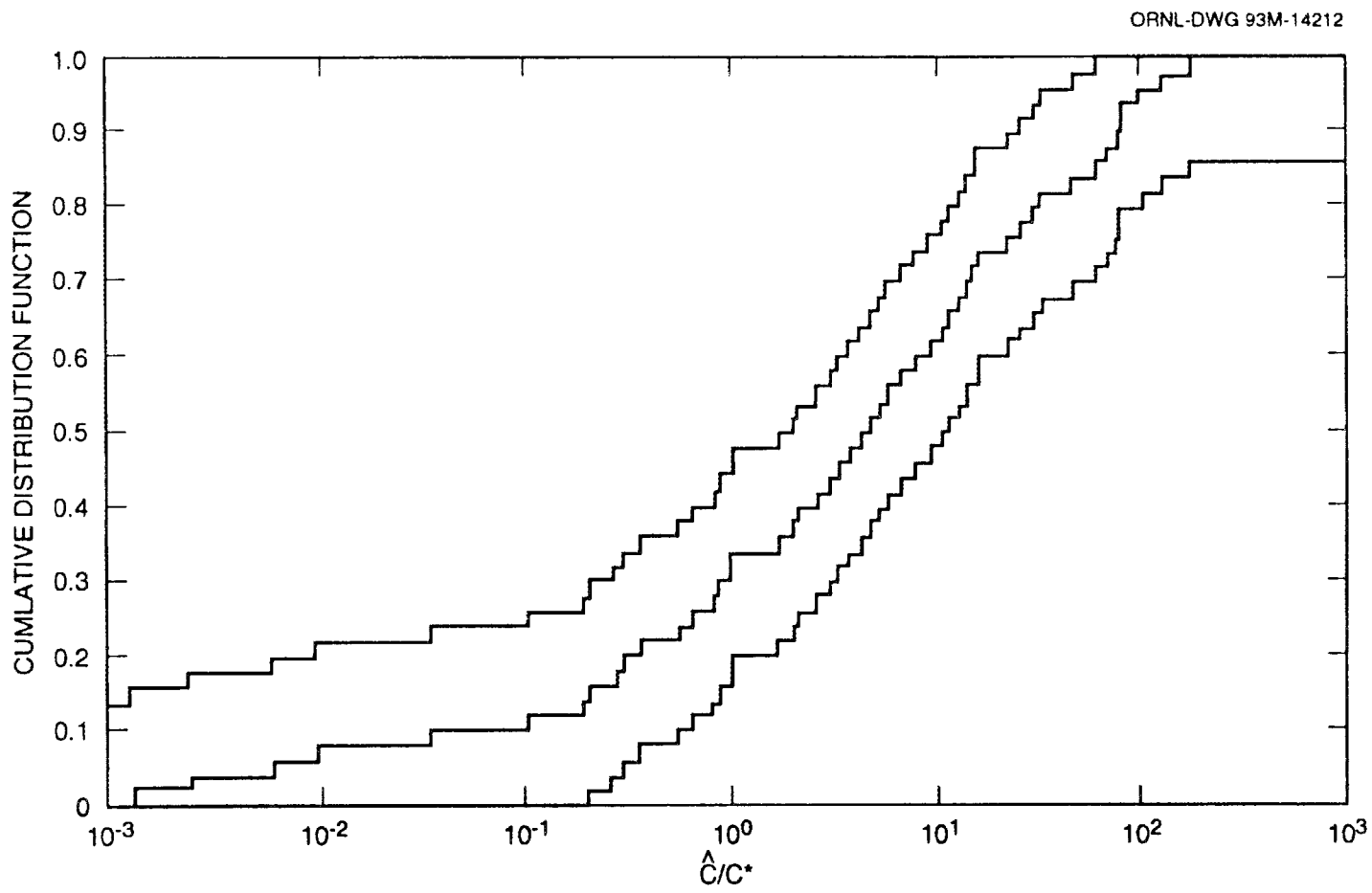

Fig. 4.23. Latin hypercube sampled ^{14}C maximum groundwater concentrations at 100 m (328 ft), assumed to occur at node 168 (middle curve). Values are expressed relative to the compliance limit. Curves on either side are Kolmogorov quantiles for a $\pm 68\%$ confidence interval.

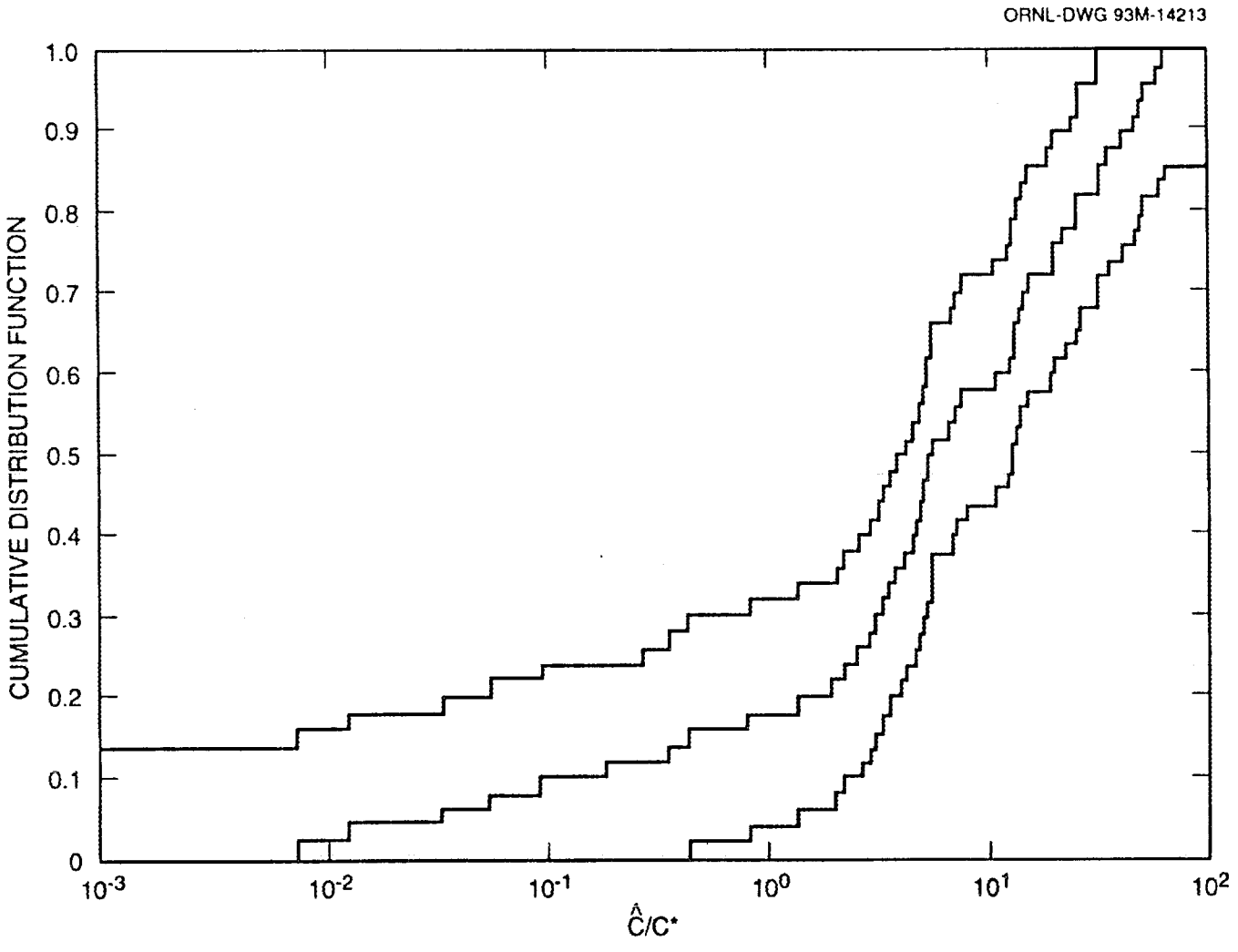

Fig. 4.24. Latin hypercube sampled ^{36}Cl maximum groundwater concentrations at 100 m (328 ft), assumed to occur at node 168 (middle curve). Values are expressed relative to the compliance limit. Curves on either side are Kolmogorov quantiles for a ±68% confidence interval.

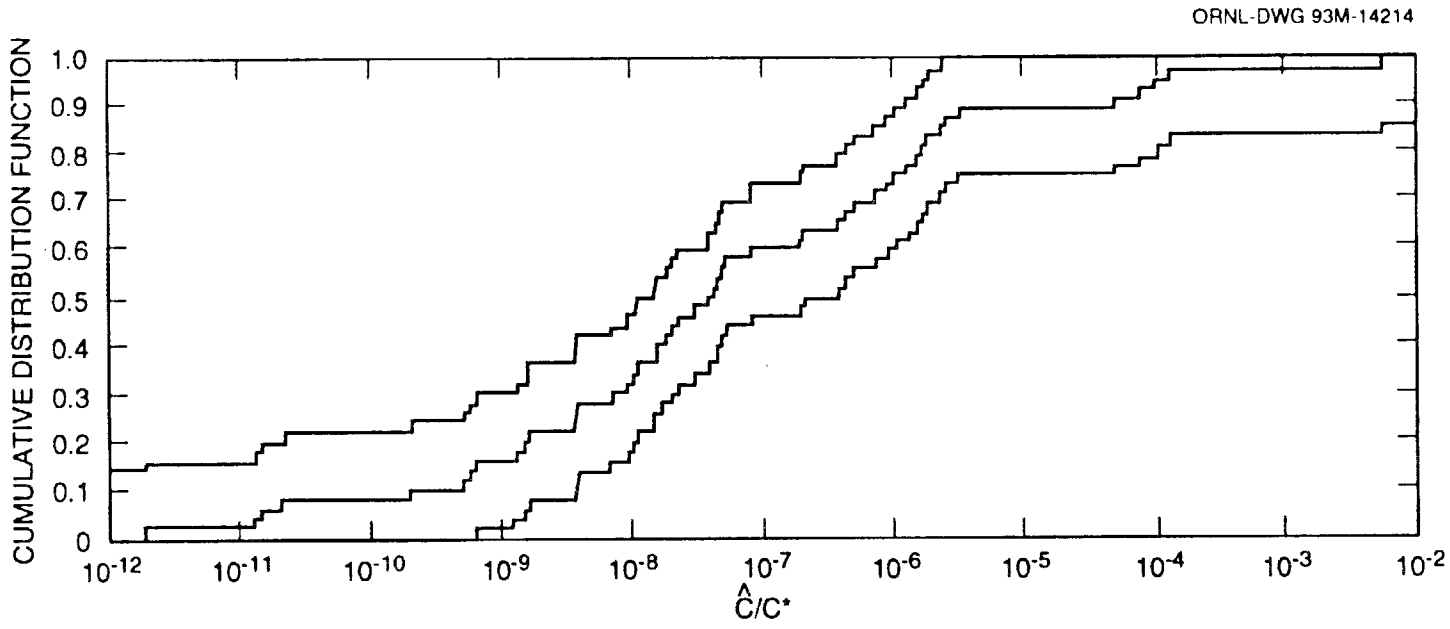

Fig. 4.25. Latin hypercube sampled ^{90}Sr maximum groundwater concentrations at 100 m (328 ft), assumed to occur at node 168 (middle curve). Values are expressed relative to the compliance limit. Curves on either side are Kolmogorov quantiles for a ±68% confidence interval.

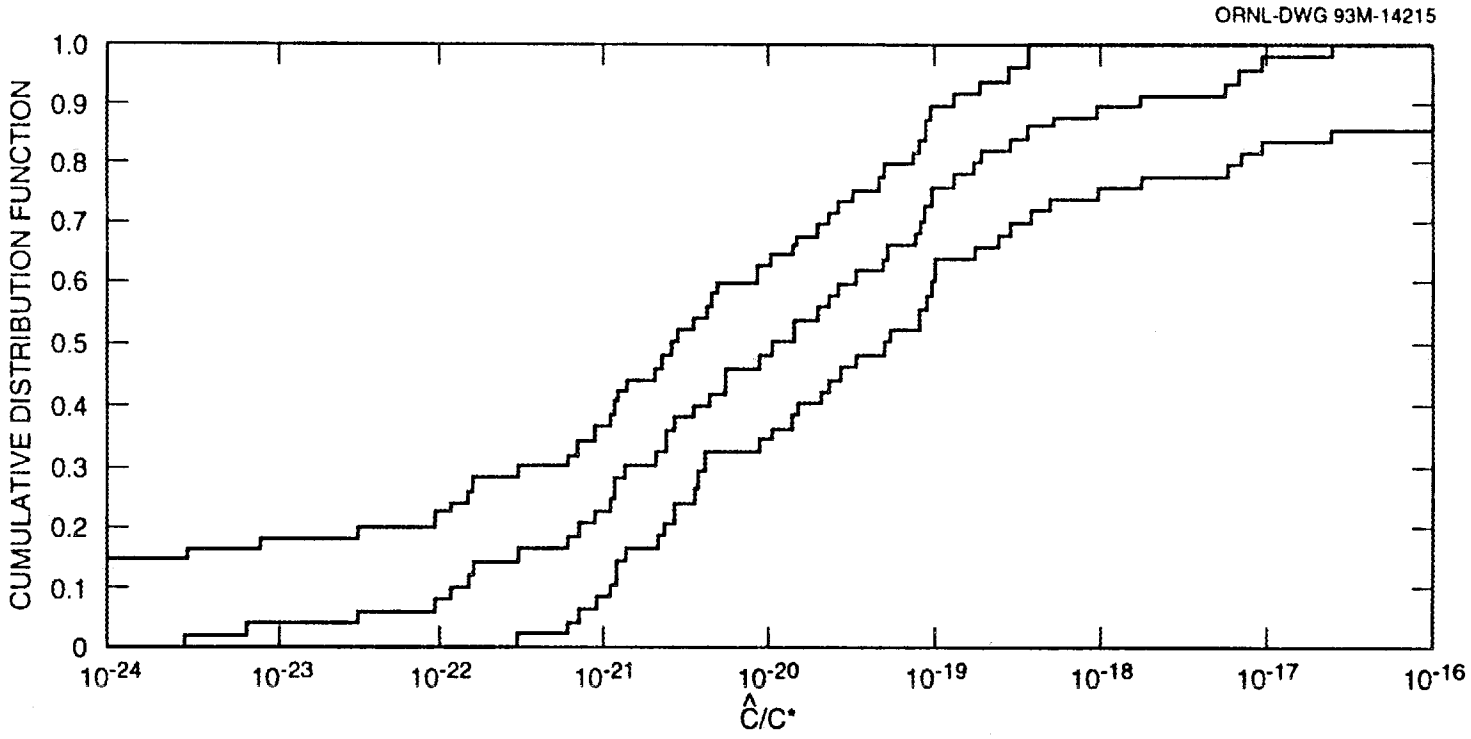

Fig. 4.26. Latin hypercube sampled ^{137}Cs maximum groundwater concentrations at 100 m (328 ft), assumed to occur at node 168 (middle curve). Values are expressed relative to the compliance limit. Curves on either side are Kolmogorov quantiles for a ±68% confidence interval.

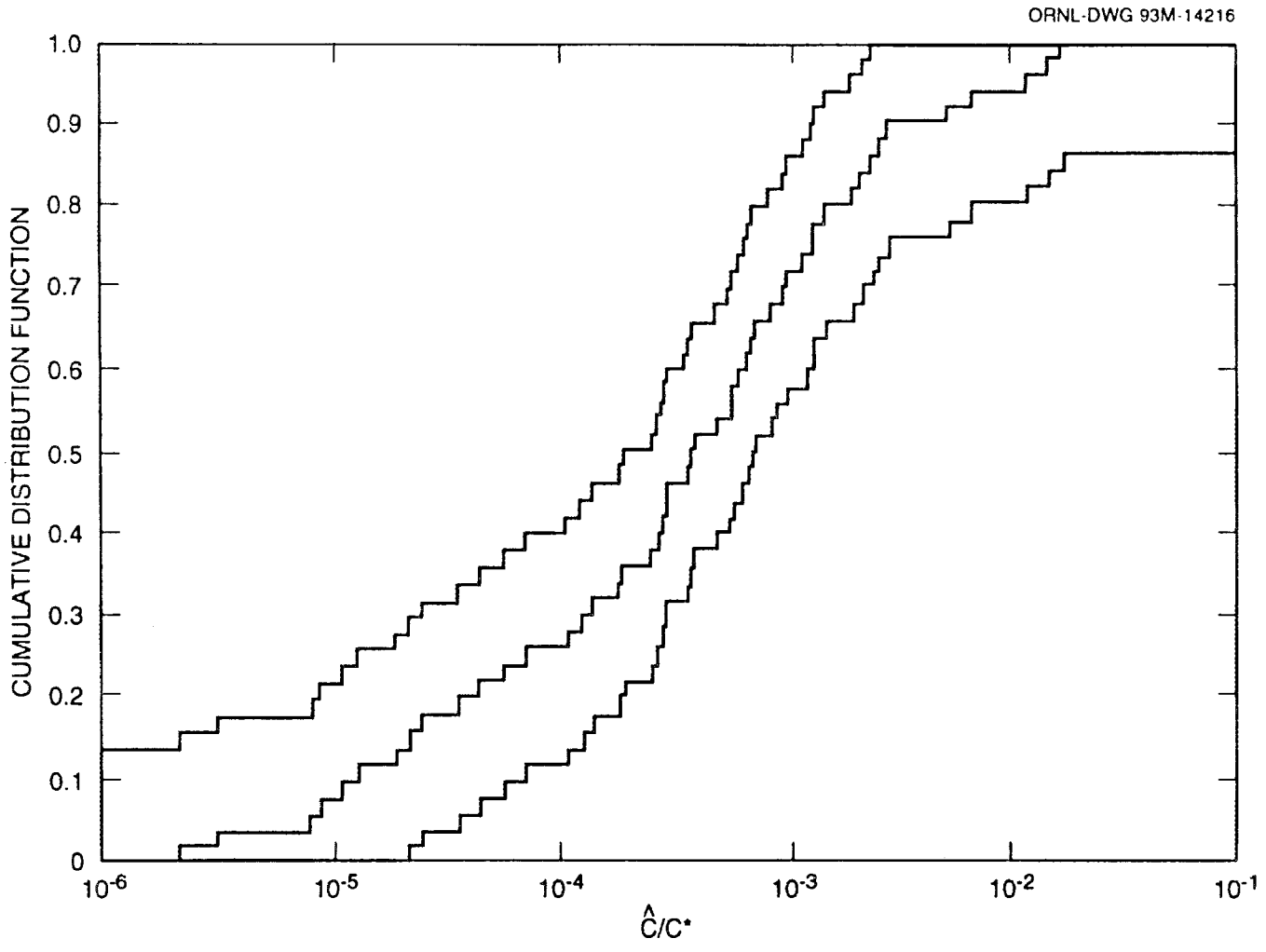

Fig. 4.27. Latin hypercube sampled ^{238}U maximum groundwater concentrations at 100 m (328 ft), assumed to occur at node 168 (middle curve). Values are expressed relative to the compliance limit. Curves on either side are Kolmogorov quantiles for a ±68% confidence interval.

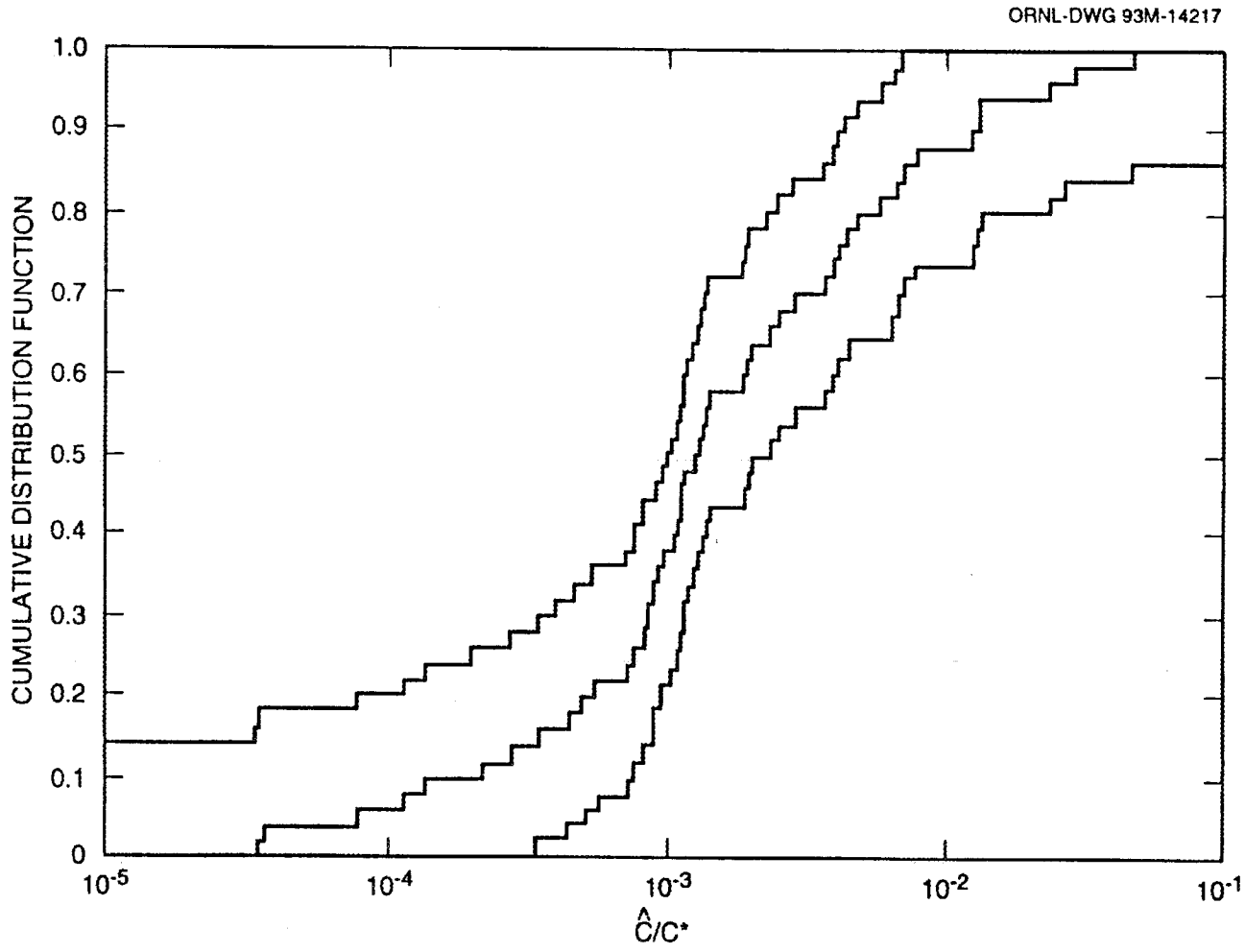

Fig. 4.28. Latin hypercube sampled tritium surface water concentrations arising from transport via groundwater (middle curve). Values are expressed relative to the compliance limit. Curves on either side are Kolmogorov quantiles for a ±68% confidence interval.

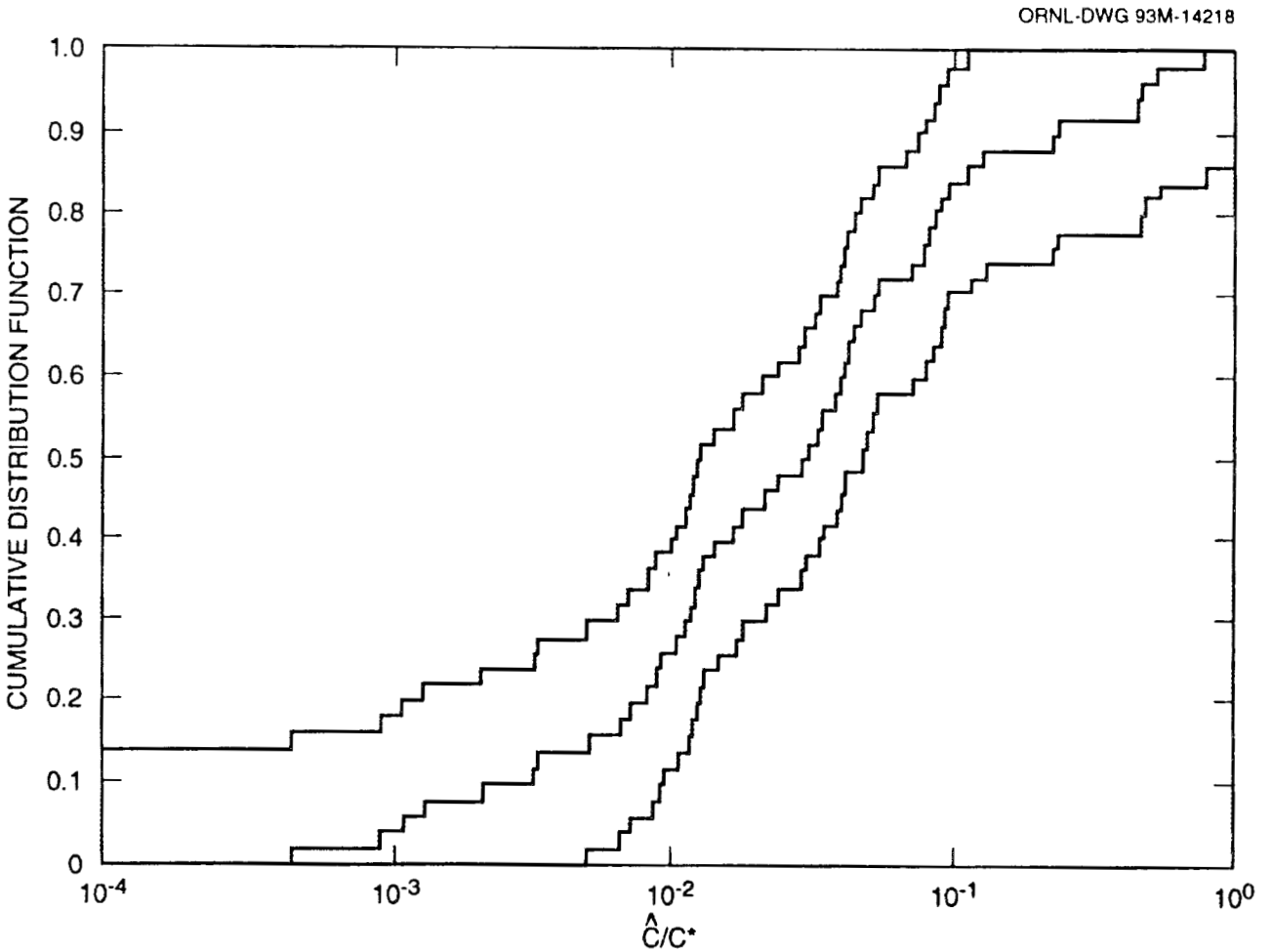

Fig. 4.29. Latin hypercube sampled ^{14}C surface water concentrations arising from transport via groundwater (middle curve). Values are expressed relative to the compliance limit. Curves on either side are Kolmogorov quantiles for a $\pm 68\%$ confidence interval.

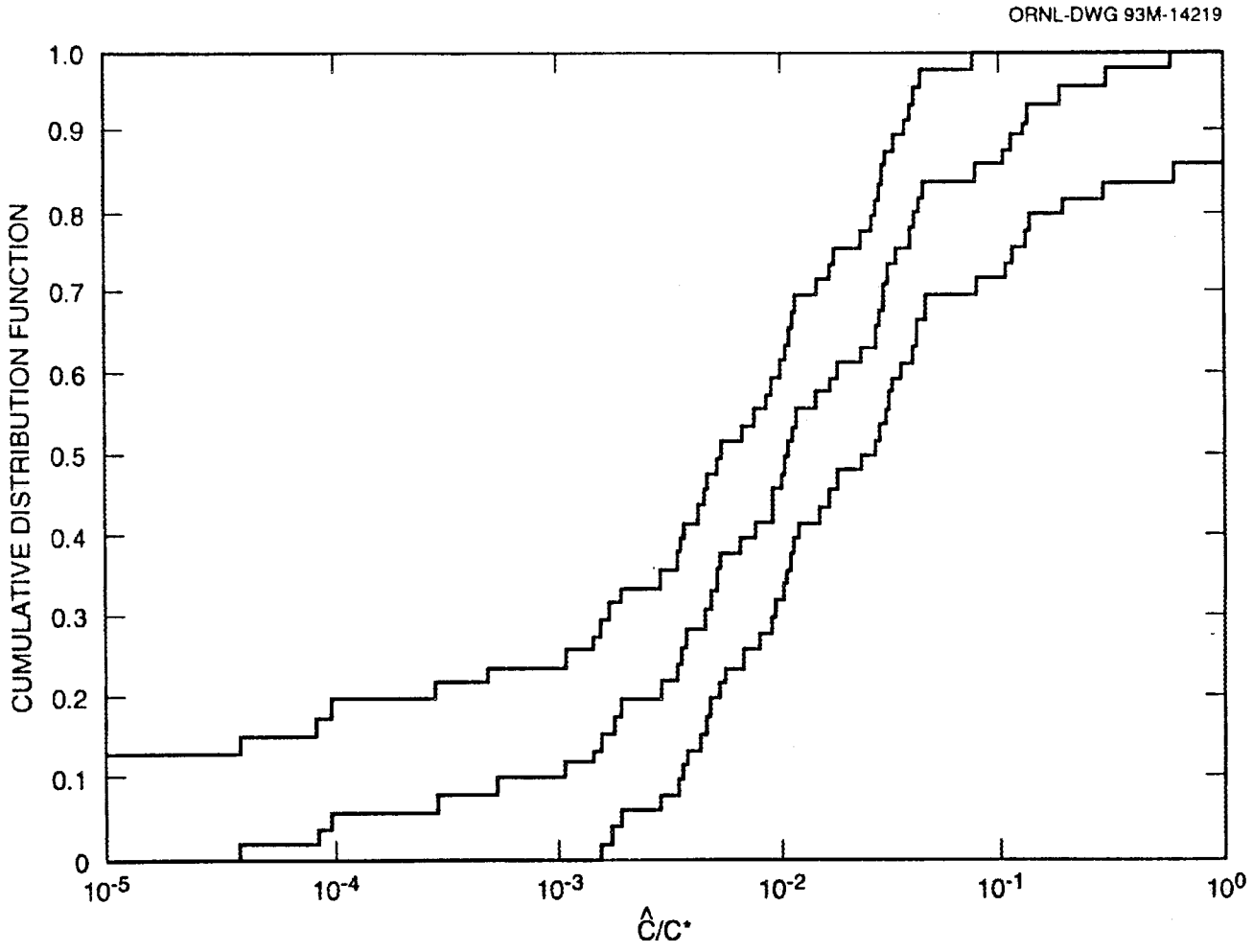

Fig. 4.30. Latin hypercube sampled ^{36}Cl surface water concentrations arising from transport via groundwater (middle curve). Values are expressed relative to the compliance limit. Curves on either side are Kolmogorov quantiles for a $\pm 68\%$ confidence interval.

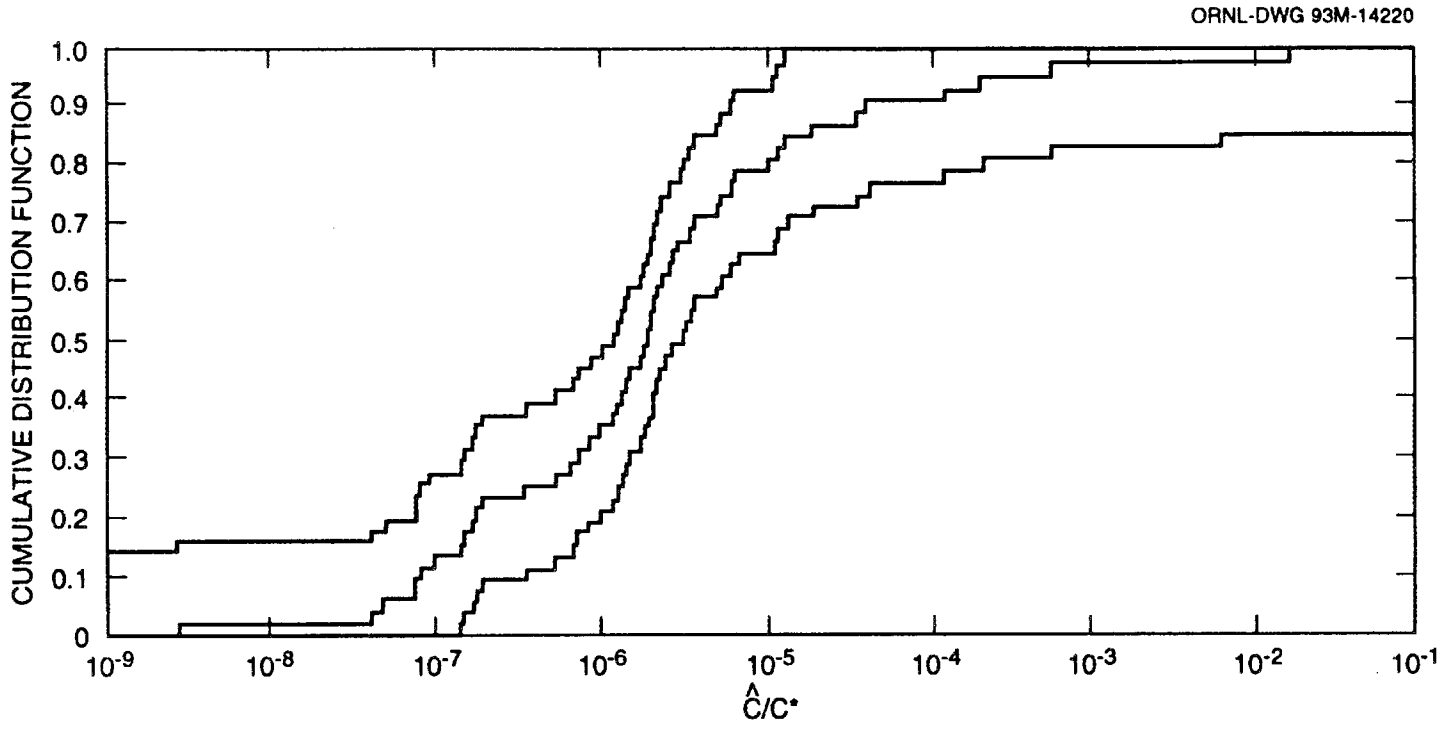

Fig. 4.31. Latin hypercube sampled ^{90}Sr surface water concentrations arising from transport via groundwater (middle curve). Values are expressed relative to the compliance limit. Curves on either side are Kolmogorov quantiles for a $\pm 68\%$ confidence interval.

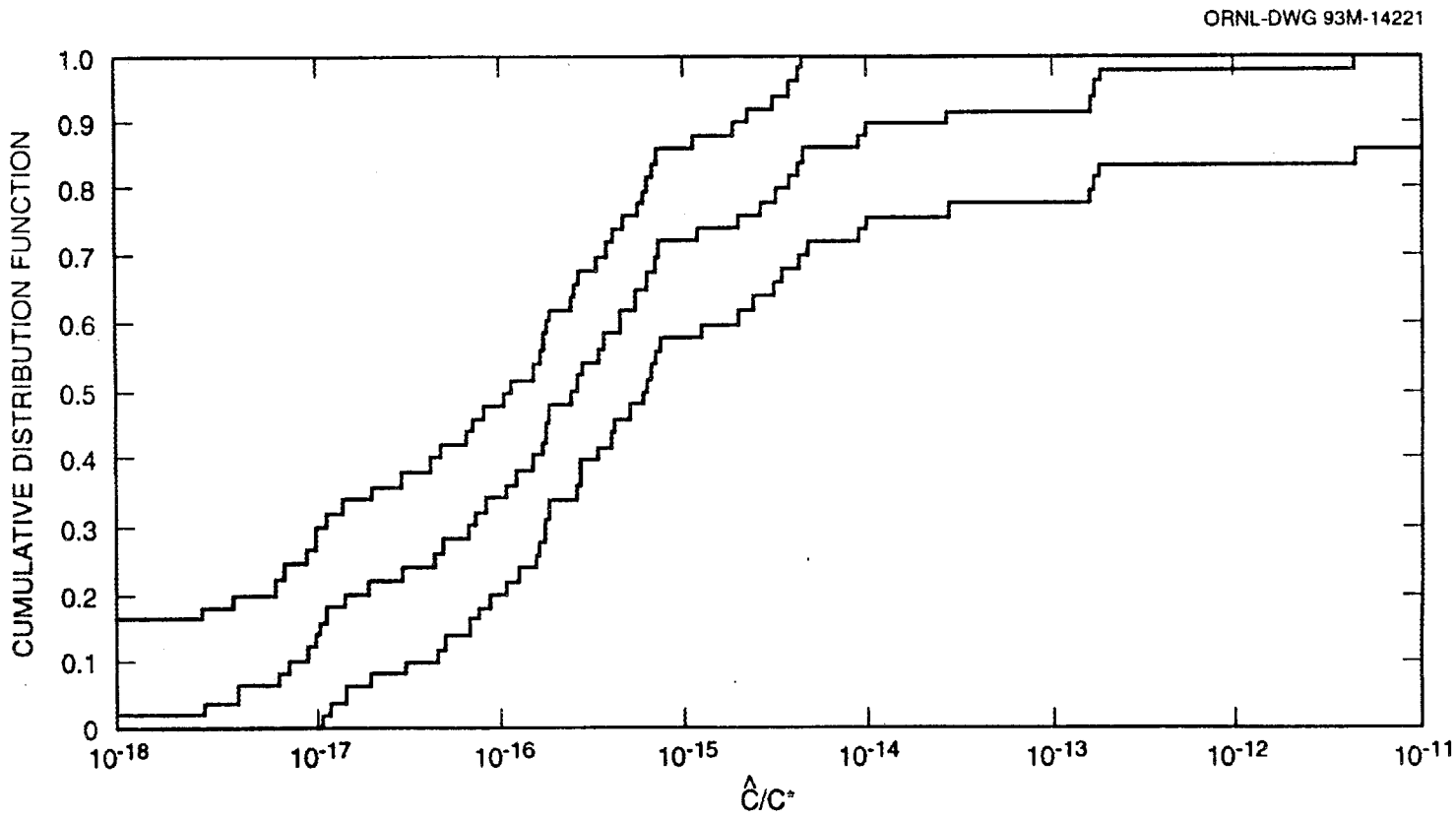

Fig. 4.32. Latin hypercube sampled ^{137}Cs surface water concentrations arising from transport via groundwater (middle curve). Values are expressed relative to the compliance limit. Curves on either side are Kolmogorov quantiles for a $\pm 68\%$ confidence interval.

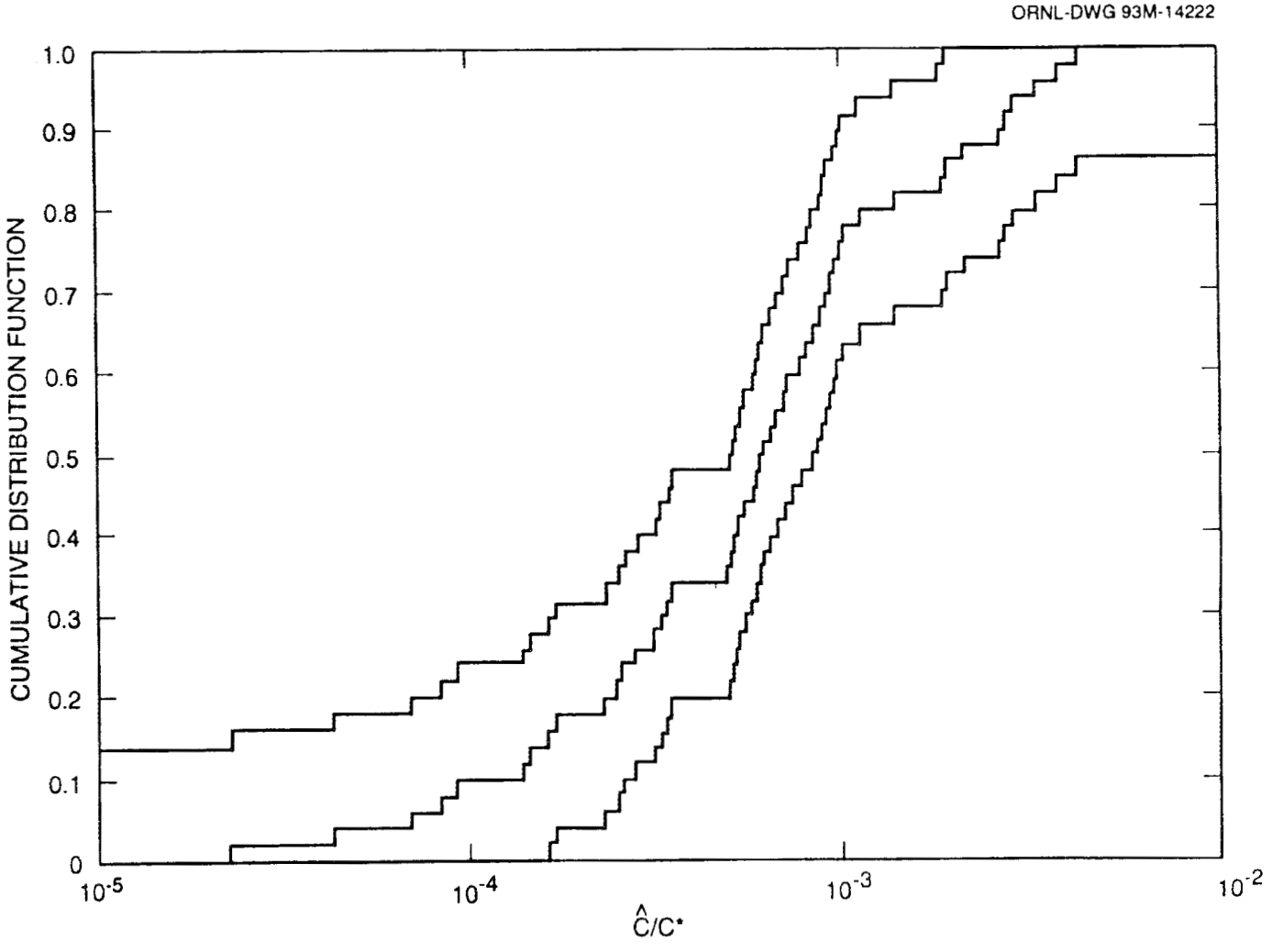

Fig. 4.33. Latin hypercube sampled ^{238}U surface water concentrations arising from transport via groundwater (middle curve). Values are expressed relative to the compliance limit. Curves on either side are Kolmogorov quantiles for a $\pm 68\%$ confidence interval.

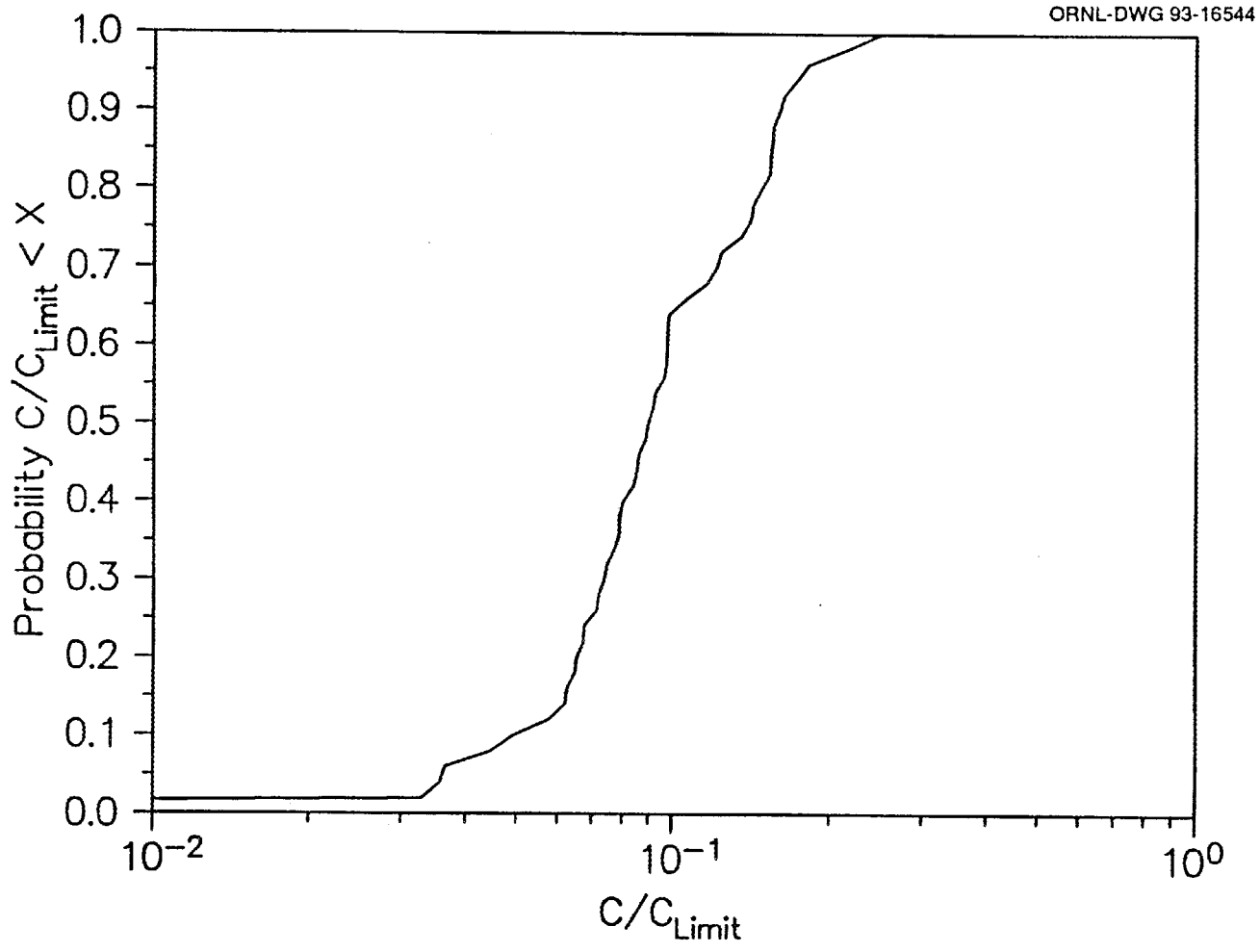

Fig. 4.34. Total surface water concentration of tritium from Solid Waste Storage Area 6 disposal units.

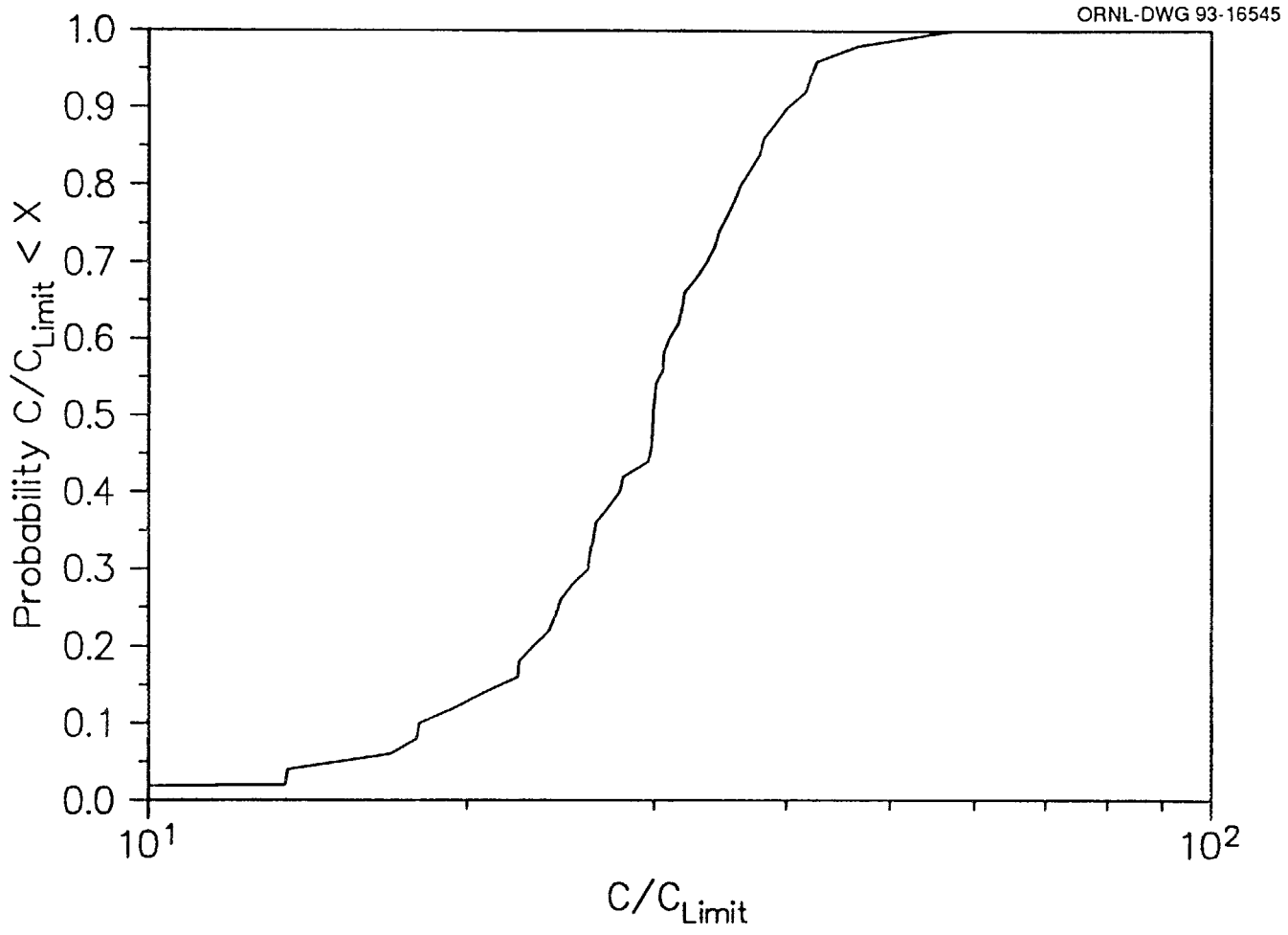

Fig. 4.35. Total surface water concentration of ^{14}C from Solid Waste Storage Area 6 disposal units.

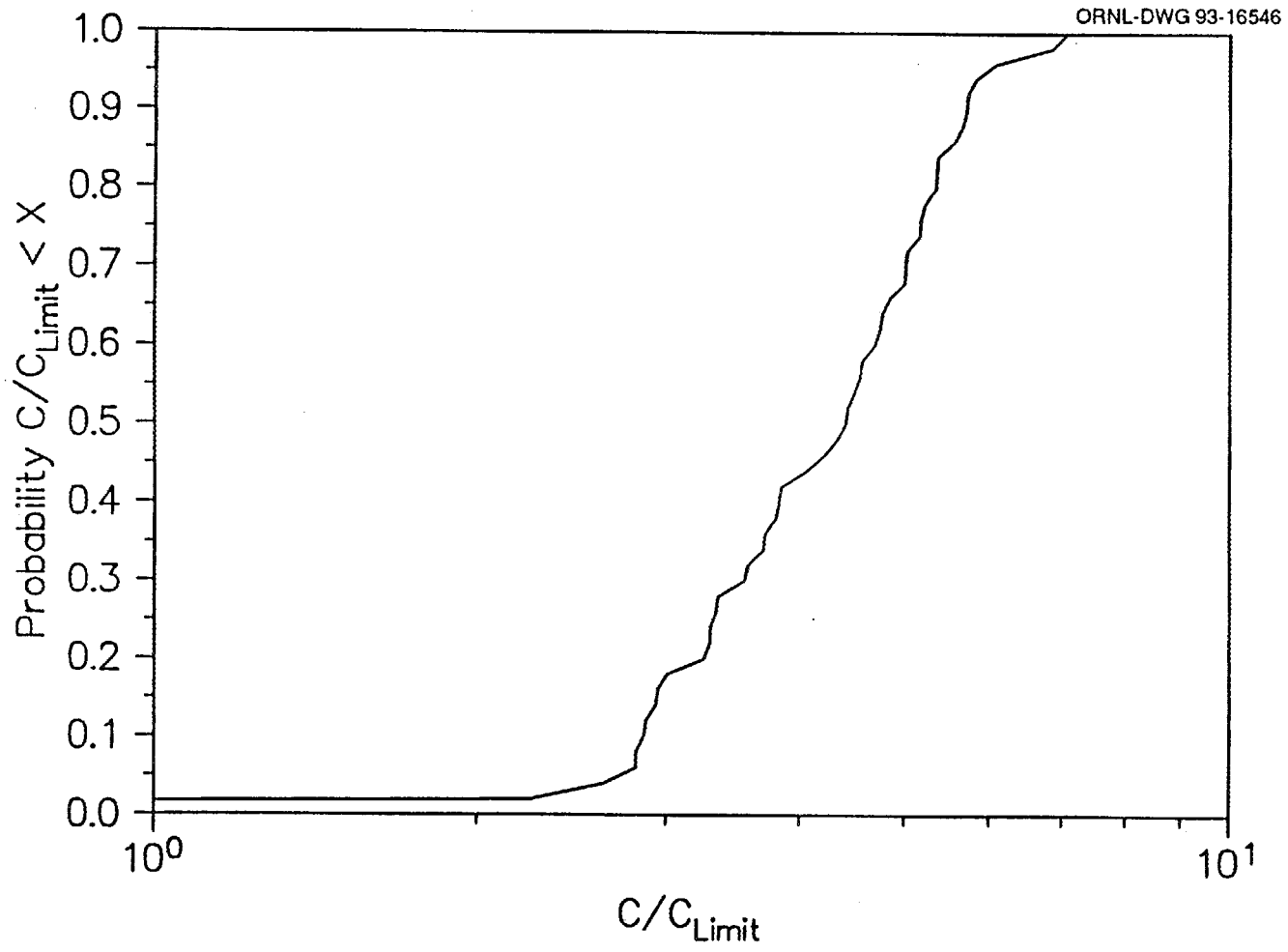

Fig. 4.36. Total surface water concentration of ^{36}Cl from Solid Waste Storage Area 6 disposal units.

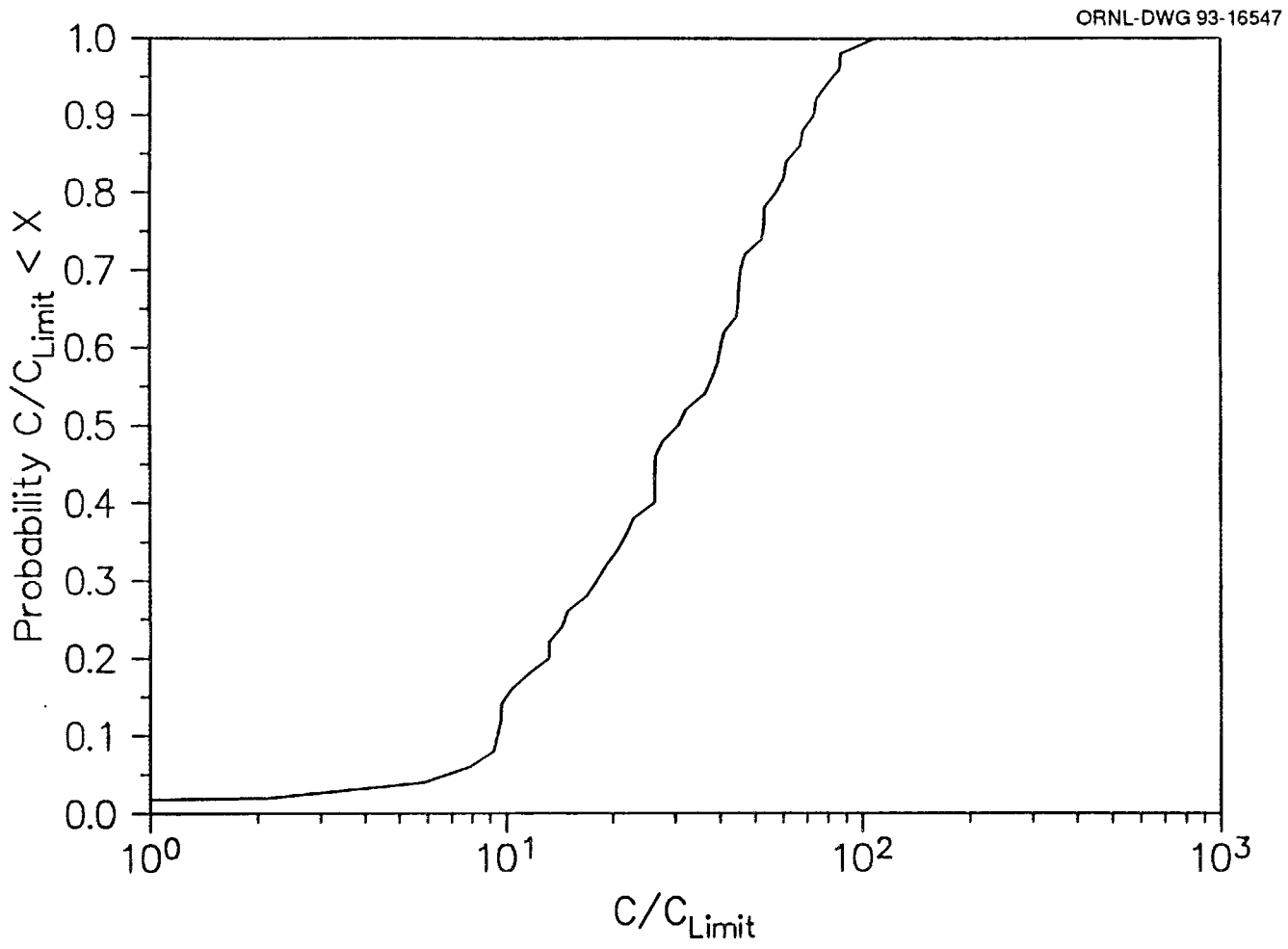

Fig. 4.37. Total surface water concentration of ^{90}Sr from Solid Waste Storage Area 6 disposal units.

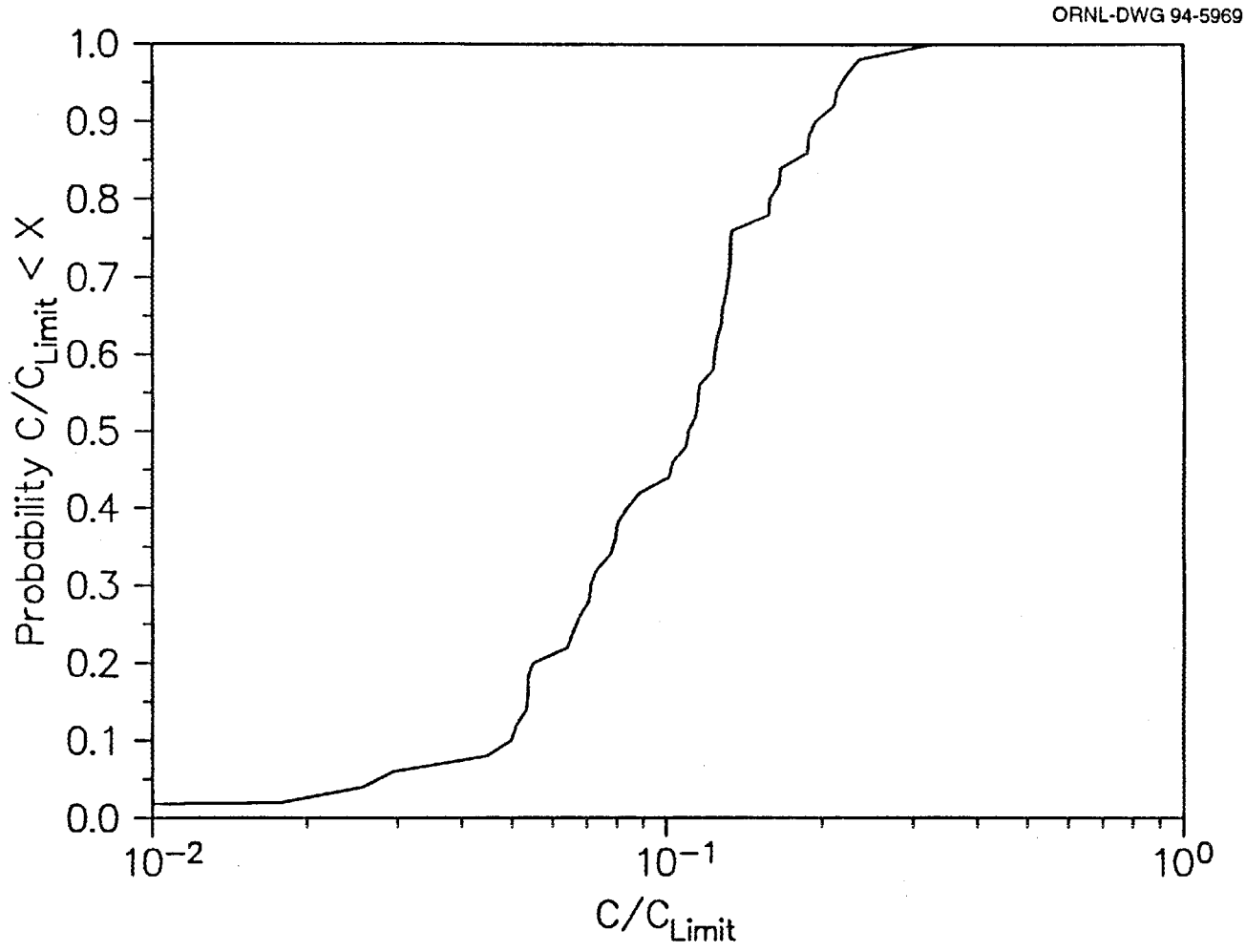

Fig. 4.38. Total surface water concentration of ^{137}Cs from Solid Waste Storage Area 6 disposal units.

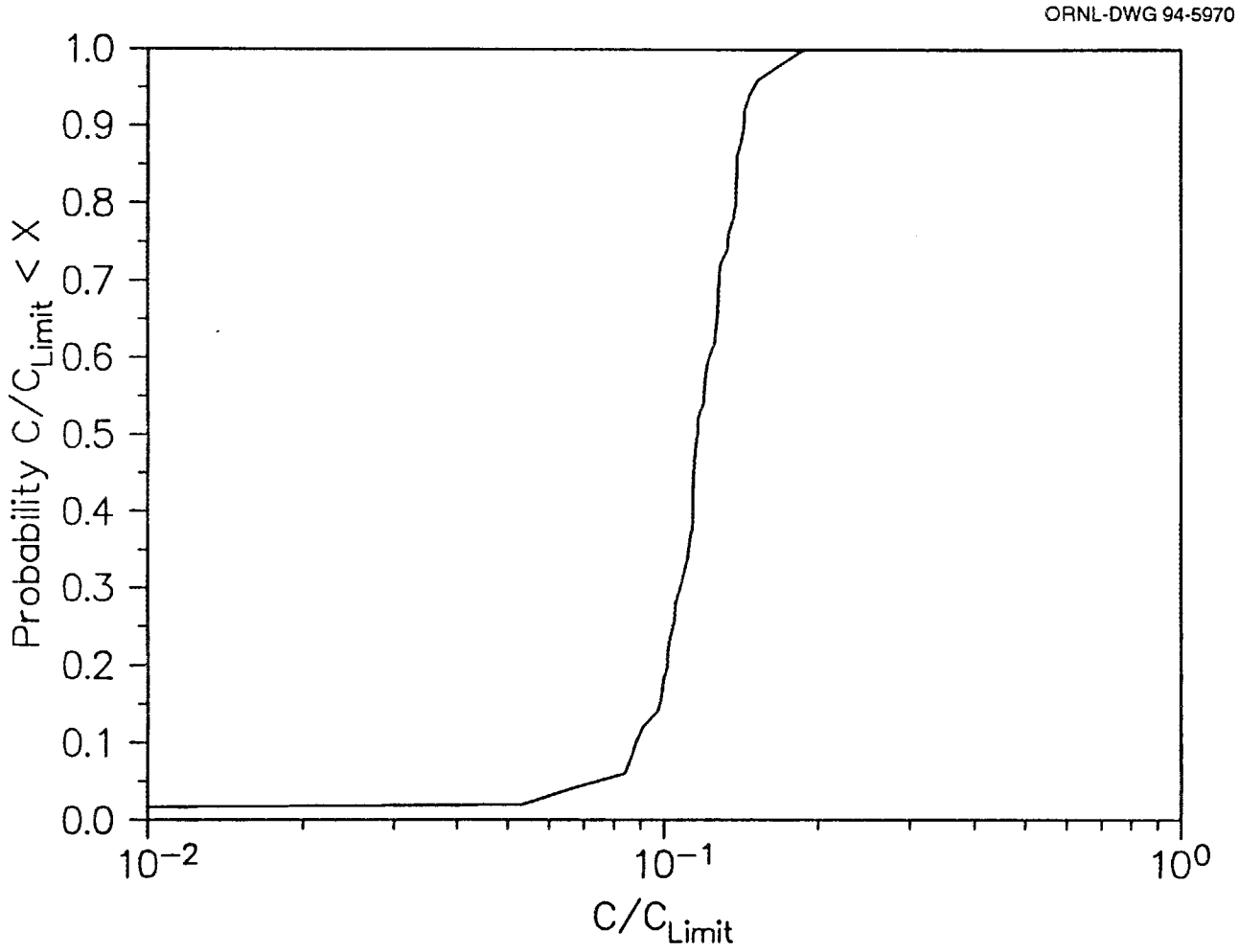

Fig. 4.39. Total surface water concentration of ^{238}U from Solid Waste Storage Area 6 disposal units.

4 mrem/year drinking water concentration limit. The overall acceptability of these results is considered in the following section, in which subjective estimates of the acceptability of the overall transport model using expert opinion is addressed.

4.6.1.6 Subjective Uncertainty

Sections 4.6.1.1–4.6.1.6 describe how the effects of input parameter uncertainties can be propagated through a series of environmental transport models, hereafter referred to as the composite transport model (CTM), to form distributions of total flux to surface water or groundwater concentrations at observation points. From these distributions, the probability that the groundwater or surface water concentration at a given point complies with allowable limits can be estimated using the following equation:

$$P(C < C^*) = P(\hat{C} < C^*) \quad , \tag{4.2}$$

where

$P()$	=	probability of event (),
C	=	actual concentration of contaminant,
$\hat{C}$	=	modeled concentration of contaminant,
C^*	=	limiting concentration corresponding to the 4 mrem/year drinking water standard.

However, the uncertainty due to parameter variance is only one component of the total uncertainty associated with the transport modeling of contaminants at SWSA 6. The methodology detailed in Appendix H suggests that additional uncertainties exist because the models and assumptions used in such analyses are only approximations of an actual system. Quantitative values for these uncertainties are not explicitly calculated or measured but rather subjectively estimated by experts (i.e. those individuals who have extensive knowledge of the modeling process). By including the effects of this subjective uncertainty, the modified equation for the total probability that a predicted groundwater or surface water concentration complies with allowable limits becomes:

$$P(C < C^*) = P(\hat{C} < C^*/A)P(A) + P(\hat{C} < C^*/\tilde{A})P(\tilde{A}) \quad , \tag{4.3}$$

where

C	=	actual concentration of contaminant,
$\hat{C}$	=	modeled concentration of contaminant,
C^*	=	limiting concentration corresponding to the 4 mrem/year drinking water standard,
$P()$	=	probability of event (),
A	=	the event that the model is valid,
$\tilde{A}$	=	the event that the model is not valid.

Note that in most conventional uncertainty analyses, the subjective probability that the model or modeling process may not accurately represent the physical scenario, $P(\bar{A})$, is arbitrarily set equal to 0, and the subjective probability that the model is valid, $P(A)$, is correspondingly set to 1.0 [i.e., there is no subjective uncertainty; Eq. (4.3) reduces to Eq. (4.2)].

The methods detailed in Appendix H were used to incorporate the effects of the subjective uncertainty associated with each segment of CTM into the analysis, which required that experts on each component estimate the distribution of actual values relative to a predicted concentration (or flux) of value C. The nature of these distributions is summarized in Table 4.34. Using the computer code described in Appendix H, the subjective distributions associated with contaminant inventory, UTM model, SOURCE1 and SOURCE2 models, and the TUMSIM and WELSIM models were convoluted with the output distributions obtained from the parametric uncertainty analysis (Sect. 4.6.1.3) to obtain modified distributions of total concentration in surface water due to flux from the shallow subsurface. Similarly, using the above subjective distributions plus those associated with the USGS MOC model, modified distributions, which reflected both subjective and parametric uncertainties, for contaminant concentration in groundwater and total contaminant concentration in surface water bodies due to flux from groundwater were also obtained. Finally, distributions for total concentration in surface water bodies were generated by convoluting the modified distributions of flux from shallow subsurface and groundwater described above. For the purposes of the uncertainty analysis, the surface waters evaluated were the ephemeral streams within SWSA 6 prior to dilution in White Oak Creek.

The inclusion of subjective uncertainty has a significant effect on the POCs (i.e., the probabilities that predicted contaminant concentrations in groundwater or surface water at SWSA 6 are less than allowable compliance limits). This effect is evident by the results given in Table 4.35, which lists POCs for six radionuclides in groundwater at node 166 (see Fig. 4.3) determined by the parametric LHC uncertainty analysis and the corresponding POCs, which reflect the incorporation of subjective uncertainties. Similarly, Table 4.36 lists POCs for the six nuclides in surface waters within SWSA 6 for both the parametric and parametric plus subjective uncertainty analyses. In addition, Tables 4.35 and 4.36 also list the entropy-based uncertainty values [see Eq. (4.3)] corresponding to each POC.

Results in Tables 4.35 and 4.36 indicate that the convolution of subjective opinion with LHC results tends to drive the POC towards 0.5. Hence, from Eq. (4.1), the uncertainty associated with predicted concentrations increases. Furthermore, the effect of time on the uncertainty associated with model predictions is demonstrated by the changes in uncertainty shown in column 5 of Table 4.35. The calculated radionuclide concentrations that experience the greatest increase in uncertainty with the inclusion of subjective opinion are those that occur at large time values. For example, ^{14}C, ^{3}H, and ^{36}Cl groundwater concentrations reach maximum values within 50–100 years and experience only a small increase in uncertainty. This implies that CTM may be used to estimate groundwater concentrations within this time frame with a reasonable amount of confidence that the calculated values reflect the actual nuclide concentration. For ^{90}Sr and ^{137}Cs, which reach peak groundwater concentrations at 200–300 years, the increase in uncertainty is significantly greater; therefore, the confidence that groundwater

Table 4.34. Description of subjective probability distributions for each segment of the composite transport model

Nuclide	Approximate type of distribution	Comments
		Inventory
^{3}H	Uniform	50% of actual values within ± 50% of predicted value
^{14}C	Uniform	20% of actual values within ± 50% of predicted value
^{36}Cl	Uniform	40% of actual values within approximately 30% of predicted value
^{137}Cs	Uniform	80% of actual values within approximately ± 25% of predicted value
^{90}Sr	Uniform	60% of actual values within ± 100% of predicted value
^{238}U	Uniform	40% of actual values within ± 35% of predicted value
		Recharge calculations using UTM[a]
All	Uniform	90% of actual values within ± 20% of predicted value
		SOURCE1 and SOURCE2 calculations
^{14}C, ^{3}H, ^{36}Cl, ^{137}Cs, ^{90}Sr	Lognormal	Mean of $\hat{C}^{b}$, and standard deviation of 0.9
^{238}U	Lognormal	Mean of $\hat{C}$, and standard deviation of 1.5

Table 4.34. (continued)

Nuclide	Approximate type of distribution	Comments
		TUMSIM and WELSIM calculations
^{14}C, ^{3}H, ^{36}Cl, ^{137}Cs, ^{90}Sr	Uniform	90% of values within ± 1 order of magnitude of predicted value
^{238}U	Uniform	90% of values within ± 2 orders of magnitude of predicted values
		USGS MOC calculations
^{14}C, ^{3}H, ^{36}Cl	Lognormal	90% of values within ± 1 order of magnitude of predicted value
^{137}Cs, ^{90}Sr	Lognormal	90% of values within ± 2 orders of magnitude of predicted value
^{238}U	Loguniform	Loguniform over ± 5 orders of magnitude of predicted value

[a]UTM = Unified Transport Model.
[b]$\hat{C}$ = Modeled concentration of contaminant; see Eq. (4.2).

concentrations predicted during this time period are representative of actual values is considerably lower. Finally, for U^{238}, which reaches maximum concentration in groundwater at times of 1,000–10,000,000 years, the uncertainty is nearly 1.0; therefore, while CTM can be used to predict groundwater contaminant concentrations on a geologic time scale, little confidence exists that the predicted concentrations are representative of the actual groundwater concentrations that would occur.

To a degree, the observation that uncertainty increases as the period of analysis is extended in time is to be expected because of the subjective probability distributions presented in Table 4.34 that show large distributions for isotopes with extended times for transport. The results presented in Table 4.35 quantify the uncertainty associated with these subjective probability distributions and provide insight as to when the uncertainties approach 1.0.

The use of subjective uncertainty may also be used to identify the segments of CTM that are the chief contributors to the total uncertainty in predicted values, thereby identifying areas of CTM that would benefit most from further research. For example,

Table 4.35. Solid Waste Storage Area 6 probability of compliance (POC) and associated entropy-based uncertainty (*U*) at groundwater compliance node 166

	Parametric[a]		Parametric+subjective[b]		
Nuclide	(1) POC	(2) *U*	(3) POC	(4) *U*	(5) *U*[c]
^{3}H	.70	.88	.53	.99	+.11
^{14}C	.30	.88	.46	.99	+.11
^{36}Cl	.19	.68	.44	.99	+.31
^{90}Sr	1.00	.00	.710	.87	+.87
^{137}Cs	1.00	.00	.82	.68	+.68
^{238}U	1.00	.00	.62	.96	+.96

[a]Probabilities and uncertainties based on parametric uncertainty analyses.
[b]Probabilities and uncertainties based on parametric+subjective uncertainty analyses.
[c] (4) − (2).

Table 4.36. Solid Waste Storage Area 6 probability of compliance (POC) and associated entropy-based uncertainty (*U*) in surface water

	Parametric[a]		Parametric+subjective[b]		
Nuclide	(1) POC	(2) *U*	(3) POC	(4) *U*	(5) *U*[c]
^{3}H	1.00	0.00	.44	.99	+.99
^{14}C	0.00	0.00	.24	.79	+.79
^{36}Cl	0.00	0.00	.24	.77	+.77
^{90}Sr	0.00	0.00	.22	.75	+.75
^{137}Cs	1.00	0.00	.62	.96	+.96
^{238}U	1.00	0.00	.35	.93	+.93

[a]Probabilities and uncertainties based on parametric uncertainty analyses.
[b]Probabilities and uncertainties based on parametric+subjective uncertainty analyses.
[c](4) − (2).

consider the change in the POC (and, therefore, the change in overall uncertainty) that occurs when the subjective uncertainties associated with each segment of CTM are individually convoluted with initial parametric uncertainties associated with the concentration distributions obtained from the LHC analysis. The results presented in Tables 4.37 (groundwater) and 4.38 (surface water) show that the CTM segment used to determine radionuclide inventory contributed to the greatest overall increase in uncertainty associated with predicted radionuclide concentrations (in both groundwater and surface water) resulting from subjective uncertainty. This is consistent with data given in Appendix A that indicate that reported inventories for the six radionuclides identified above differed from the best-case values used in the LHC analysis by as much as three orders of magnitude. Therefore, the logical first step to reduce the overall uncertainty associated with radionuclide concentrations predicted by CTM would be to develop a more reliable method for estimating the inventory of disposed radioactive material.

4.6.2 Analysis of Human Exposure Scenarios

This section discusses the sensitivity and uncertainty analysis for the models used to estimate dose to off-site individuals or inadvertent intruders per unit concentration of radionuclides in the appropriate environmental medium (i.e., water for off-site individuals and water or disposed waste for inadvertent intruders). Some aspects of uncertainty in the dose assessment models have been discussed previously in Sect. 4.5.2.

In this analysis, uncertainties in the dose assessment models are evaluated only in a semi-quantitative fashion. This approach is justified on the grounds that these uncertainties undoubtedly are far less than the uncertainties in predicting concentrations of radionuclides in water or disposed waste at times far into the future; therefore, a rigorous, quantitative uncertainty analysis of the dose assessment models is not needed.

4.6.2.1 Scenarios for Transport of Radionuclides in Water

In this analysis, radionuclides are assumed to be transported from disposal units into the environment primarily by the groundwater and surface water pathways. For off-site individuals and inadvertent intruders, doses were estimated for the drinking water pathway only (in order to evaluate compliance with the performance objective for protection of groundwater and surface water resources) and for all exposure pathways involving use of contaminated water (in order to evaluate compliance with the performance objectives for off-site individuals and inadvertent intruders).

As shown in Eq. G.1 of Appendix G, the dose from the drinking water pathway per unit concentration of a radionuclide in groundwater or surface water depends only on the assumed intake of contaminated water and the ingestion dose conversion factor for the radionuclide. Although both of these parameters would be variable quantities in any exposed population, they are assumed in this analysis to be fixed values with no uncertainty that are prescribed by regulatory authorities and radiation protection experts. Therefore, the dose from the drinking water pathway, given estimated concentrations of radionuclides in water, essentially has no uncertainty.

Table 4.37. Resultant probability of compliance (POC) and associated entropy-based uncertainty (*U*) for radionuclides in groundwater at node 166 from convolution of subjective uncertainties associated with each segment of the composite transport model (CTM) with groundwater concentration distributions obtained from the parametric, Latin hypercube (LHC) analysis

	Parametric[a]		Parametric+ Inventory[b]		Parametric+ UTM[c]		Parametric+ SOURCE[d]		Parametric+ WELSIM[e]		Parametric+ MOC[f]	
Nuclide	POC	*U*	POC	*U*[g]	POC	*U*	POC	*U*	POC	*U*	POC	*U*
^{3}H	0.70	0.88	0.59	0.98	0.68	0.90	0.68	0.90	0.63	0.95	0.65	0.93
^{14}C	0.30	0.88	0.45	0.99	0.32	0.90	0.31	0.89	0.34	0.92	0.33	0.91
^{36}Cl	0.19	0.70	0.37	0.95	0.21	0.74	0.20	0.72	0.27	0.84	0.33	0.91
^{90}Sr	1.00	0.00	0.47	1.00	0.95	0.29	1.00	0.00	0.93	0.37	0.97	0.19
^{137}Cs	1.00	0.00	0.79	0.74	0.95	0.29	1.00	0.00	0.95	0.29	1.00	0.0
^{238}U	1.00	0.00	0.69	0.89	0.95	0.29	1.00	0.00	0.93	0.37	0.97	0.19

[a]POC and *U* based on parametric uncertainties only.
[b]POC and *U* for LHC results convoluted with subjective uncertainties associated with Inventory model segment.
[c]POC and *U* for LHC results convoluted with subjective uncertainties associated with UTM model segment.
[d]POC and *U* for LHC results convoluted with subjective uncertainties associated with SOURCE1 and SOURCE2 model segment.
[e]POC and *U* for LHC results convoluted with subjective uncertainties associated with WELSIM and TUMSIM model segments.
[f]POC and *U* for LHC results convoluted with subjective uncertainties associated with MOC model segments.
[g]CTM model segment whose subjective uncertainty results in the greatest change in total POC.

Table 4.38. Resultant probability of compliance (POC) and associated entropy-based uncertainty (*U*) for radionuclides in Solid Waste Storage Area 6 surface water from convolution of subjective uncertainties associated with each segment of the composite transport model (CTM) with surface water concentration distributions obtained from the parametric, Latin hypercube (LHC) analysis

	Parametric[a]		Parametric+ inventory[b]		Parametric+ UTM[c]		Parametric+ SOURCE[d]		Parametric+ WELSIM[e]		Parametric+ MOC[f]	
Nuclide	POC	*U*	POC	*U*[g]	POC	*U*	POC	*U*	POC	*U*	POC	*U*
^{3}H	1.00	0.00	0.66	0.92	0.90	0.47	0.99	0.09	0.84	0.63	1.00	0.00
^{14}C	0.00	0.00	0.20	0.72	0.01	0.04	0.01	0.04	0.01	0.04	0.00	0.00
^{36}Cl	0.00	0.00	0.21	0.74	0.01	0.04	0.11	0.51	0.11	0.51	0.00	0.00
^{90}Sr	0.00	0.00	0.17	0.66	0.01	0.04	0.00	0.00	0.01	0.04	0.00	0.00
^{137}Cs	1.00	0.00	0.80	0.72	0.85	0.61	0.99	0.11	0.85	0.62	1.00	0.00
^{238}U	1.00	0.00	0.47	1.00	0.90	0.48	0.96	0.27	0.66	0.93	0.97	0.21

[a]POC and *U* based on parametric uncertainties only.
[b]POC and *U* for LHC results convoluted with subjective uncertainties associated with Inventory model segment.
[c]POC and *U* for LHC results convoluted with subjective uncertainties associated with UTM model segment.
[d]POC and *U* for LHC results convoluted with subjective uncertainties associated with SOURCE1 and SOURCE2 model segment.
[e]POC and *U* for LHC results convoluted with subjective uncertainties associated with WELSIM and TUMSIM model segments.
[f]POC and *U* for LHC results convoluted with subjective uncertainties associated with MOC model segments.
[g]CTM model segment whose subjective uncertainty results in the greatest change in total POC.

For releases to groundwater or surface water, the dose from all exposure pathways includes contributions from the milk and meat pathways and, for off-site individuals, from external exposure while swimming in contaminated water. However, the results in Tables 4.9, 4.10, and 4.11 show that, for most radionuclides, the dose from all exposure pathways is due almost entirely to the dose from the drinking water pathway only. The other exposure pathways are significant only for ^{36}Cl, in which case the dose from the milk and meat pathways contributes about 40% of the dose from all pathways. External exposure while swimming is not significant for any radionuclides. Therefore, for most radionuclides, there is essentially no uncertainty in the dose per unit concentration in water from all exposure pathways, regardless of the uncertainty in the dose per unit concentration for the pathways other than drinking water. For ^{36}Cl, there is little information available to evaluate the uncertainty in the dose from the milk and meat pathways, which depends primarily on the intake-to-milk and intake-to-meat transfer coefficients for dairy and beef cattle, respectively [see Eqs. (G.2)-(G.5) of Appendix G]. However, the uncertainties in these parameters would not be significant unless they were quite large (i.e., well in excess of an order of magnitude) because the performance objective for the drinking water pathway of 4 mrem/year is considerably more restrictive than the performance objectives for all exposure pathways of 25 mrem/year for off-site individuals and 100 mrem/year for inadvertent intruders. Therefore, allowable releases of radionuclides to groundwater or surface water will be determined almost entirely by the dose from the drinking water pathway alone, and the dose from the other exposure pathways involving use of contaminated water should not be important in determining compliance with the performance objectives.

4.6.2.2 Scenarios for Direct Intrusion into Disposal Units

The results of the dose analysis for direct intrusion into disposal units according to the agriculture, resident, discovery, and postdrilling scenarios are discussed in Sect. 4.5.3.2. As indicated by these discussions, only two exposure pathways contribute essentially all of the dose for any of the assumed scenarios: (1) external exposure to photon-emitting radionuclides and (2) ingestion of contaminated vegetables. In considering an uncertainty analysis for these pathways, it should also be emphasized that the definitions of the different intruder scenarios are intended to provide reasonably conservative estimates of dose to individuals who might actually intrude onto the facility.

The dose from external exposure per unit concentration of radionuclides in the environment depends on the exposure time, the external dose-rate conversion factor, and, for the agriculture scenario, the shielding factor during indoor residence [e.g., see Eq. (G.13) of Appendix G]. The external dose-rate conversion factor is treated as a fixed parameter with no uncertainty. The exposure time is subject to uncertainty, but the values selected for use in this analysis are intended to be reasonably conservative. In particular, the assumed exposure time during indoor residence for the agriculture scenario of 50% is reasonable for an average site occupant and cannot underestimate the actual value by more than a factor of two. The uncertainty in the shielding factor during indoor residence should be no more than about 50% for typical homes in the Oak Ridge area.

For the vegetable pathway, the important parameters in the model for estimating dose are the plant-to-soil concentration ratios of radionuclides and the intake of

contaminated vegetables [see Eqs. (G.7) and (G.8) of Appendix G]. The latter parameter was selected to be somewhat conservative but could be uncertain by as much as a factor of two. Data obtained from sources listed in Table G.15 of Appendix G indicate that the plant-to-soil concentration ratio may be uncertain by an order of magnitude or more for some important radionuclides (e.g., ^{36}Cl), but the uncertainty may only be about a factor of four for other important radionuclides (e.g., ^{90}Sr). It should also be emphasized that the uncertainty estimates for the plant-to-soil concentration ratio are based on generic data for a variety of vegetation and soil types. Therefore, these estimates may not be meaningful for application to the ORR (i.e., they may not be representative of the variability in plant-to-soil concentration ratios that would be observed in different types of vegetation at the facility).

4.7 INTERPRETATION OF RESULTS

The results presented in Sects. 4.1–4.5 provide insight into the performance of the different types of disposal units in SWSA 6. However, the results have a significant degree of uncertainty, and this uncertainty is important in interpreting the results. The uncertainties in the inventories of radionuclides in disposed waste and the long-term performance of disposal units and the facility are not likely to be totally resolved in the near future. Continued work, discussed in Sect. 4.9, is directed towards reducing uncertainties; but the need for interpretation of results in the face of considerable and, in some cases, essentially unresolvable uncertainty will remain an important aspect of the performance assessment for SWSA 6.

4.7.1 Surface Water and Groundwater Pathways

In the present analysis, the results presented in Sects. 4.1–4.5 and the uncertainty analysis presented in Sect. 4.6 provide a complicated view of the performance of SWSA 6. In addition to the results presented, the underlying assumptions used in the analysis, discussed in Sect. 3.3, further complicate the interpretation of the results. A simple reliance on the numerical results presented in Sect. 4.5 does not provide a reasonable means for formulating conclusions or assessing the performance of the facility. The remainder of this section addresses the results presented and provides interpretation of these results for evaluating the performance of the facility.

Table 4.18 shows that the groundwater performance objective established in Sect. 1 is not satisfied at SWSA 6 outside the 100-m (328-ft) buffer zone around the IWMF. All other disposal units in SWSA 6 satisfy the groundwater performance objective. Tables 4.16 and 4.17 show that the performance objectives related to surface water are satisfied for SWSA 6. These results are dependent on the assumptions invoked, the application of the performance objectives, and the uncertainties in the modeling methodology. Each of these factors needs to be considered for groundwater and surface water before evaluating the performance of SWSA 6.

4.7.1.1 Groundwater

The concentrations of radionuclides in groundwater are dependent on the assumed inventory, the assumptions in the source term, subsurface transport, and groundwater models. As discussed in Sect. 4.6.1, the uncertainties associated with the inventory are large and dominate the uncertainties related to the modeling of contaminant transport. Appendix A includes the reported inventories of radionuclides in waste as well as the evaluation of the likely range of radionuclides in wastes. These inventories are extrapolated throughout the operating life of the facility. Assuming that the inventories of the past are representative of the future is the most reasonable assumption that can be made, but it is not well supported by historical trends in wastes generated at ORNL. One of the isotopes shown to exceed the groundwater performance objective is ^{36}Cl, which is associated with only one disposal event. Future disposals of ^{36}Cl are not anticipated. ^{14}C is another isotope associated with exceeding the performance objective for groundwater and is pervasive in ORNL waste streams. However, the difference between the reported inventories in Appendix A and the mean value in the analysis of the distribution of the radionuclides disposed of in SWSA 6 is a factor of 500. The mean value was used as the best case for developing Table 4.18. While this difference in the inventory estimate underscores the uncertainties in the waste inventories, it also suggests that the forecasted doses for ^{14}C may not be accurate. ^{239}Pu was commonly disposed of in the period from 1988 to 1991 but is no longer typical of ORNL wastes streams; therefore, extrapolating historical disposals throughout the operating life of the IWMF may not be appropriate for ^{239}Pu.

The performance of SWSA 6 was assessed with the presumed presence of a geomembrane installed over the facility in 1998. This cover was given substantial credit from 1998–2027 in hydrologically isolating the wastes. The plans for installing the geomembrane over SWSA 6 are currently being revised, and the likelihood of a geomembrane installed in 1998 is reduced. The effect of the geomembrane on the results has not been quantified; however, the lack of a geomembrane could hasten the transport of contamination. The consequences of quicker releases of contamination on the doses to inadvertent intruders and off-site individuals is uncertain. Once revised plans are formulated for the CERCLA remediation of SWSA 6, the need to revise the performance assessment will be assessed. The absence of a geomembrane may not be significant because the head and velocity profiles presented in Sect. 4.3 were not significantly affected by the presence of the geomembrane and the geomembrane was not planned to extend as a cover over IWMF. Additionally, the large increase in advective releases of contaminants from disposal units from concrete degradation (Table F.2) occurs after credit for the geomembrane is removed. Consequently, the presence or absence of the geomembrane is not anticipated to have a significant effect on the results of the performance assessment.

The SOURCE1 code used for analyzing the IWMF characterizes large increases in advection occurring in the IWMF after degradation of concrete has reduced the structural strength of the IWMF vaults. This assumed modeling sequence is reasonable but has the effect of estimating rapid releases from the IWMF at a relatively short time after closure. As shown in the release curves presented in Appendix F, the onset of advection results in a dramatic release rate that is especially pronounced for ^{3}H. This modeling assumption has not been validated and cannot be validated with the existing data for vault performance.

While there is reason for concern that releases may be overly conservative, monitoring being performed as part of the Environmental Restoration Program has recorded the tritium releases from SWSA 5, which was the disposal facility used prior to SWSA 6. Over a 5-year time period, the monitoring data reveal an exponential reduction in the release rate of tritium. The elimination half-life of the release of tritium from SWSA 5 is approximately 3 years. The computational results in Appendix F show an elimination half-life for tritium at SWSA 6 of 4 to 5 years. This slight increase can be attributed to the engineered features present in SWSA 6 tumulus technology. The comparison of release data does not verify the SOURCE1 results but provides evidence that the results are reasonable and not unrealistically conservative representations of disposal unit performance.

The following programming steps in the SOURCE1 and SOURCE2 codes were identified that require modification or rewriting:

- In the SOURCE1 code, after cracking occurs, the inventory is not accounted for correctly in the cracked vaults. The inventory in intact vaults is adjusted properly at all times. However, when a vault is cracked, the current inventory is in essence reset erroneously to the original (zero leaching time) value. As a result, the inventory available for leaching after cracking occurs is too large. This leads to predicted leach rates that are larger than they should be. The effect is particularly pronounced for short-lived, very soluble nuclides (e.g., tritium).
- In the SOURCE1 code, the inventory is not updated correctly if the amount predicted to be leached by advection plus diffusion exceeds the solubility limit of a nuclide. In this case, the amount leached should be set equal to the solubility-limit value. However, the code incorrectly uses the higher advection-plus-diffusion value to update the inventory. For a sparingly soluble nuclide (e.g., Th, U, and Pu) in particular, this situation causes the inventory to be depleted at a rate much greater than it should be.
- For multiple isotopes of a given nuclide, the SOURCE1 and SOURCE2 codes take only the isotope of concern into account in the evaluation of a solubility-limit value. If the nuclide (e.g., Pu) is present as several isotopes (e.g., ^{239}Pu, ^{240}Pu, etc.) in several oxidation states (e.g., Pu^{3+}, Pu^{4+}, etc.), a consideration of the solubility-limit value to assign becomes very complex. Rather detailed information on pore-water chemistry (e.g., pH, Eh, redox potential, etc.) is needed. Such information is generally not readily available and is not amenable to extrapolation in the SOURCE1 and SOURCE2 codes without considerable effort.
- In the case of tritium, the SOURCE1 and SOURCE2 codes do not properly handle tritium concentration. The codes consider only the amount of tritium in a disposal unit to calculate a concentration for use in predicting its leach rate. The correct concentration of tritium with respect to leaching should be a concentration that also accounts for hydrogen (H) in the pore water. In other words, the tritium should be isotopically diluted with natural water present. Generally, when applied to disposal units saturated with water, this dilution will lower the leach rate for tritium by several thousand.

The assumptions of critical concern to the analysis of groundwater concentrations relate to the partitioning of infiltrating water between the shallow subsurface transport

zone and recharge to groundwater (Sect. 3.3.2.1). Best efforts towards correctly establishing the partitioning have been made but are complicated by the multitude of excavations that have occurred at SWSA 6 over its operational lifetime. The effect of excavations on site performance cannot be rigorously determined with the available data and could lead to significant changes in arrival times of contaminants. While the effect of excavations cannot be quantified, some observations of site behavior influence many potential concerns. Most of the excavations considered in the performance assessment are in upper landscape positions, which are less likely to be inundated by rising water tables. The singular exception is the biological trenches, where inundation is possible in extreme conditions. Inundation could result in an increase in transport rates. However, increased recharge accompanying increased transport rates would tend to increase dilution. As a result, a slower buildup of the concentration peak with a broader but lower maximum is a likely result. The approach to modeling SWSA 6 taken in this performance assessment does not have sufficient resolution in time to quantitatively evaluate individual storm-related events and provide a meaningful estimate of long-term performance.

The effect of retardation on the transport of radionuclides is significant to the accuracy of the calculated results, which are proportional to the distribution coefficient (K_d). Distribution coefficients for this analysis were selected using the recommendations of Friedman and Kelmers (1990). The suggested value for uranium was extended to Th, Np, Pu, Am, Cm, and Cf as a conservative representation of retardation. This selection is overly conservative for Th, Pu, Am, and Cm by a factor of 50 to 200. As a result, the transport calculations for these isotopes are at substantially higher velocities and concentrations than would result with more reasonable selections of K_d. Consequently, the calculated concentration of ^{239}Pu at IWMF is certain to be too high and the arrival time too soon. Continued work in assessing the performance of IWMF is warranted (Sect. 4.9), and the calculated results for Pu and Am presented in Sect. 4.5.3.1 need to be appreciated as extreme upper bounds.

Groundwater modeling assumptions of interest in interpreting the results are discussed in Sect. 3. The effect of these assumptions on the accuracy of the results is captured in the uncertainty analysis; they tend to broaden the range of uncertainty but not to the extent that significant changes in the results could be attributed to them alone.

The performance objective of 4 mrem/year for groundwater resource protection is not established as a federal, state, or local requirement. While 4 mrem/year has been used in this performance assessment, regulatory developments are ongoing that could increase or decrease the limit. In addition to the lack of a promulgated requirement, the application of the 4 mrem/year limit has been applied at the edge of a 100-m (328-ft) buffer zone around each disposal unit. As a result of the hydrogeologic behavior of SWSA 6, where contaminants are released to ephemeral surface waters and do not underflow surface water outlets, the resulting areas of groundwater contamination are very small (Figs. 4.4–4.6). The zone of contaminated water is largest during the period of active institutional control when ^{3}H, ^{14}C, and ^{36}Cl contaminant plumes exceed the 4 mrem/year limit by a factor of 50. At the end of active institutional control, the contaminant plumes are less than the 4 mrem/year limit for ^{3}H and ^{36}Cl, and ^{14}C exceeds the limit by a factor of 1.7. The ^{14}C plume diminishes after 250 years to less than the 4 mrem/year limit. The development of the ^{239}Pu zone of contamination occurs over 2000 years later, is somewhat smaller than the other contaminant plumes, and exceeds the 4 mrem/year limit by a factor

of about 3. For the purposes of groundwater resource protection, the zone of contamination is shown to exist but is small and not persistent over time. This conclusion is also subject to the uncertainties presented in Sect. 4.6.

The uncertainties in the modeling of groundwater transport are significant. The inventory estimates overshadow all modeling uncertainties. Figures 4.22–4.24 show that there is a POC of 0.7 for ^{3}H, 0.3 for ^{14}C, and 0.19 for ^{36}Cl. The ranges in concentrations for these three isotopes are over 4–5 orders of magnitudes. When expert opinion on the acceptability of the models is considered, the POC is increased for ^{3}H and ^{36}Cl but is decreased for ^{14}C. The uncertainty in the calculations is increased for all isotopes. The consideration of uncertainties suggests that the values presented in Table 4.18 are very uncertain and may not actually occur.

The modeling and inventory data have been developed for this performance assessment using a very conservative approach while attempting to remain as reasonable as possible. In the absence of confirmatory data, conservative assumptions and interpretations have been used. Owing to the substantial uncertainties, the lack of promulgated regulations on groundwater resource protection, and the limited understanding of the existing and future inventory disposed of in SWSA 6, the contamination of the groundwater resource presented in Table 4.18 should be viewed with caution and not as a clear violation of the performance objectives for the protection of groundwater resources. Changes in operations (Sect. 4.8) and continued work on the performance assessment (Sect. 4.9) can reasonably be expected to resolve the apparent lack of compliance presented in this performance assessment for the protection of groundwater resources.

4.7.1.2 Surface Water

The concentrations of radionuclides in surface water are dependent on the assumed inventory of wastes, the assumptions in the source term, and subsurface and groundwater transport models. In addition, the uncertainties in the analysis are large. As noted in Sect. 4.6.1, the uncertainties in the inventory dominate the uncertainties in the modeling of the facility. Tables 4.16 and 4.17 note that the doses estimated for the best case for an off-site individual are less than the performance objectives. These doses are determined for the use of surface waters for an off-site individual using the discharge at White Oak Dam as a water supply. Doses from surface waters within the disposal facility would be larger, but the limited discharge of surface waters within the facility precludes them from being used as a water source by an individual. If the surface waters within SWSA 6 were subjected to a dose analysis, independent of the availability of the surface waters being suitable as a supply, the doses would exceed the performance objectives for ^{14}C, ^{36}Cl, ^{90}Sr, and ^{239}Pu. The interpretation of results related to the inventories and models presented in Sect. 4.7.1.1 are also applicable to surface water. However, the uncertainties in surface water could result in exceeding the performance objectives for model parameters more conservative than those used to calculate the best estimate.

The results from the surface water analysis are related to the time of arrival of contaminants to the surface water bodies. In Sect. 4.5.4.1 and 4.4, the time of arrival of surface water contamination is discussed. The calculated maximum transport rate to surface water is the sum of the peak transport rates from the eleven different disposal units without regard for the year of occurrence. The peak transport rates for radionuclides

of interest span 64,000 years such that the doses presented in Tables 4.16 and 4.17 are unquestionably conservative. When summed together, the total dose slightly exceeds 4 mrem/year but is substantially less than the 25 mrem/year performance objective for off-site individuals. Given the conservative nature of the results presented, there is reasonable assurance that the doses in surface water will be less than 4 mrem/year at any time in the future. As noted in Table 4.38, the subjective uncertainties related to the UTM, WELSIM, and TUMSIM calculations are significant for isotopes with early arrival times (^{3}H, ^{14}C, and ^{36}Cl). This uncertainty could result in a change in estimated concentrations in surface waters located within the site boundary. Earlier arrivals would be at higher concentrations than estimated. Later arrivals would be at lower concentrations with additional reductions in concentrations from decay. In either case, doses in surface water at White Oak Dam for an off-site individual are not expected to exceed the performance objectives.

The partitioning of precipitation between shallow subsurface water and groundwater has an additional effect on surface water concentrations. The results presented in the performance assessment are predicated on the partition of 90% of precipitation to shallow subsurface water and the remainder to recharge of groundwater. The shallow subsurface waters are transported to surface water relatively quickly in comparison to groundwater. For the heavily disturbed environment of SWSA 6, the validation of the partitioning of precipitation is difficult. As a result, there is substantial uncertainty attached to the analysis. More than likely, the effect of the extensive excavations over time in SWSA 6 would tend to increase groundwater recharge. However, the cumulative effect in terms of the overall performance of SWSA 6 is not easily quantified. Longer transport times to surface water via the groundwater pathway will lead to lower concentrations in surface water as a result of decay and additional adsorption on soils. Shorter transport times via shallow subsurface waters will tend to elevate the estimated radionuclide concentrations in surface waters.

The dynamics of the shallow subsurface can have a significant effect on the concentrations of radionuclides in surface waters. Transport of isotopes during significant storm events is quicker, and the isotopes are subjected to much larger dilution during runoff. The performance assessment results capture the effects of storms by using short time steps in UTM calculations that are integrated over long times for estimating the concentrations in surface waters. Small changes in climate that would alter the water budget or the fluxes of water transported in the shallow subsurface could result in changes in the estimated concentrations. The likelihood of changes in climate that would result in changes in the fluxes of shallow subsurface water over time is uncertain and is not amenable to analysis but is captured in the uncertainty analysis in Sect. 4.6.1.3 and Figs. 4.16–4.21. However, the potential effects need to be considered as part of evaluating the results of the performance assessment.

In summary, the analysis of surface waters has been prepared using a conservative approach that is as reasonable a representation of site performance as the available data permit. Conservative assumptions and interpretations have been used throughout the analysis. The results indicate that estimated releases of contamination from SWSA 6 as a result of facility operations are in compliance with the performance objectives of DOE Order 5820.2A. Substantial uncertainties are associated with the analysis, but the

uncertainties that have been identified are expected to provide for compliance with the performance objectives in surface water.

4.7.2 Direct Intrusion Scenarios

In the present analysis, the assumptions regarding direct intrusion into disposal units result in estimated doses that exceed the performance objective for inadvertent intruders for Tumulus I, the IWMF, the low-range silos, high-range silos, high-range wells, and fissile wells. For Tumulus II, the performance objective for inadvertent intruders would be exceeded only if the calculations are carried out for about 10^6 years in the future, but the dose estimates in this case probably are highly conservative because mobilization and transport of uranium has not been taken into account. For the asbestos silos and biological trenches, the estimated doses are less than the performance objective.

As emphasized in the discussion of uncertainties in Sect. 4.5.2, the results of the dose analyses for inadvertent intruders depend significantly on the assumptions used in defining the different exposure scenarios. In particular, the estimated doses depend on the assumption that particular scenarios will occur as postulated and, in many cases, on the particular times after disposal at which the scenarios are assumed to occur.

The following paragraphs briefly discuss the results of the intruder dose analyses for each of the different types of disposal units in SWSA 6. The discussion, which focuses on the dose estimates at the times the various exposure scenarios are first assumed to occur, emphasizes whether the results are likely to be realistic and important factors that could significantly alter the results of the analysis. The dose estimates at far future times are not discussed further because mobilization and transport of uranium is the single most important factor in reducing the dose in all cases.

4.7.2.1 Tumulus I

For Tumulus I, the agriculture scenario is the only exposure scenario of concern in regard to meeting the performance objective for protection of inadvertent intruders, but the performance objective is exceeded by only about 50%. The most important factor that could reduce the estimated dose below the performance objective is a proper accounting of mobilization and transport of ^{14}C in infiltrating water over the first 300 years after disposal. On the other hand, the dose for the agriculture scenario could be underestimated, but only if ^{14}C were not transported from the disposal units in significant quantities prior to 300 years after disposal and if the plant-to-soil concentration ratio for this radionuclide were underestimated. The vegetable pathway is the only important exposure pathway for ^{14}C, and the plant-to-soil concentration ratio is the most important parameter in the model for estimating dose from the vegetable pathway.

The dose estimates for the resident and postdrilling scenario are less than the performance objective by factors of about 2–4. For the resident scenario, the dose depends primarily on the exposure time, which is assumed to be 50% in this analysis. Thus, the dose cannot be underestimated by more than a factor of two, and the performance objective cannot reasonably be exceeded. As in the case of the agriculture scenario, the dose for the postdrilling scenario could be underestimated, but only if ^{14}C and ^{90}Sr were not transported from the disposal units in significant quantities prior to

100 years after disposal and if the plant-to-soil concentration ratios for these radionuclides were underestimated by substantial amounts.

4.7.2.2 Tumulus II

For Tumulus II, none of the exposure scenarios result in dose estimates that exceed the performance objective for protection of inadvertent intruders, although the estimates in all cases are within factors of 3–10 of the performance objective.

For the agriculture scenario, the most important radionuclide is ^{14}C. The dose for this scenario could be underestimated assuming that the inventory at disposal is correct, but only if ^{14}C were not transported from the disposal units in significant quantities prior to 300 years after disposal and if the plant-to-soil concentration ratio for this radionuclide were underestimated by a substantial amount.

For the resident scenario, the only important radionuclide is ^{137}Cs. From the definition of this scenario, it is not possible that the dose could be increased by a factor of nearly 10, as would be required to give a dose exceeding the performance objective.

For the postdrilling scenario, the most important radionuclides are ^{14}C and ^{90}Sr. The performance objective could be exceeded for this scenario, but only if mobilization and transport of these radionuclides for 100 years after disposal were unimportant and if the plant-to-soil concentration ratios for these radionuclides were underestimated by an order of magnitude or more.

4.7.2.3 IWMF

For the IWMF, both the agriculture and postdrilling scenarios are of concern in regard to meeting the performance objective for protection of inadvertent intruders, and the performance objective is exceeded by factors of 16 for the agriculture scenario and 4 for the postdrilling scenario. The most important radionuclides for both scenarios are ^{14}C and ^{36}Cl. For these presumably mobile radionuclides, the most important factor that could reduce the estimated dose below the performance objective is a proper accounting of mobilization and transport in infiltrating water over the first 100 or 300 years after disposal. The doses for these scenarios could be underestimated, but only if ^{14}C and ^{36}Cl were not transported from the disposal units in significant quantities within the first 100 or 300 years after disposal and if the plant-to-soil concentration ratios for these radionuclides were underestimated.

For the resident scenario, the most important radionuclide is ^{137}Cs. From the definition of this scenario, it is not possible that the dose could be increased by a factor of nearly 6, as would be required to give a dose exceeding the performance objective.

4.7.2.4 Low-Range Silos

For the low-range silos, both the agriculture and postdrilling scenarios are of concern in regard to meeting the performance objective for protection of inadvertent intruders, and the performance objective is exceeded by factors of 8 for the agriculture scenario and 2 for the postdrilling scenario. The most important radionuclide for both scenarios is ^{14}C, and ^{226}Ra also is an important radionuclide for the agriculture scenario.

For ^{14}C, the most important factor that could reduce the estimated dose below the performance objective is a proper accounting of mobilization and transport in infiltrating water over the first 100 or 300 years after disposal. This factor also could be important in reducing the dose from ^{226}Ra at 300 years after disposal. The doses for these scenarios could be underestimated, but only if ^{14}C were not transported from the disposal units in significant quantities within the first 100 or 300 years after disposal and if the plant-to-soil concentration ratio for this radionuclide were underestimated. The natural-analog model for estimating inhalation dose from ^{222}Rn during indoor residence on top of exposed waste, which is the most important exposure pathway for ^{226}Ra in the agriculture scenario, probably does not underestimate the dose by a significant amount.

For the resident scenario, the most important radionuclide is ^{137}Cs. From the definition of this scenario, it is not possible that the dose could be increased by a factor of nearly 20, as would be required to give a dose exceeding the performance objective.

4.7.2.5 High-Range Silos

For the high-range silos, the postdrilling scenario is the only exposure scenario of concern in regard to meeting the performance objective for protection of inadvertent intruders, and the performance objective is exceeded by a factor of 20. The only important radionuclide for the postdrilling scenario is ^{90}Sr. Consideration of mobilization and transport of this radionuclide for the first 100 years after disposal could reduce the estimated dose, but it seems unlikely that the resulting dose would be less than the performance objective. On the other hand, the dose for the postdrilling scenario could be underestimated, but only if ^{90}Sr were not transported from the disposal units in significant amounts prior to 100 years after disposal and if the plant-to-soil concentration ratio for this radionuclide were underestimated.

The dose estimates for the agriculture, resident, and discovery scenarios are less than the performance objective by factors of less than 2 for the agriculture and resident scenarios and about 60 for the discovery scenario.

The dose for the agriculture scenario could be underestimated, but only if transport of ^{90}Sr and ^{137}Cs from the disposal units during the first 300 years after disposal were insignificant and if the plant-to-soil concentration ratio for ^{90}Sr were underestimated. External exposure during indoor residence is the only important pathway for ^{137}Cs, and the dose from this radionuclide in the agriculture scenario cannot be underestimated by more than a factor of 2, which would not increase the total dose from all radionuclides by a significant amount.

The dose for the resident scenario could be increased above the performance objective, but only if a residence time in the home at the disposal unit site of about 75% or greater is assumed. Such an exposure time is unlikely for an average resident at the disposal unit site. Similarly, the dose for the discovery scenario could be increased if the exposure time were increased, but the dose would be far less than the performance objective for any reasonable exposure time.

4.7.2.6 High-Range Wells

For the high-range wells, all four scenarios result in doses that exceed the performance objective for protection of inadvertent intruders. Furthermore, the performance objective is exceeded by large amounts, ranging from a factor of about 30 for the discovery scenario to a factor of nearly 8000 for the postdrilling scenario. The most important radionuclides are ^{90}Sr and ^{137}Cs for the agriculture and postdrilling scenarios and ^{137}Cs and ^{152}Eu for the resident and discovery scenarios. However, the dose estimates for the agriculture, resident, and discovery scenarios appear to be unreasonably pessimistic, and the postdrilling scenario may not be credible for these units.

Mobilization and transport of radionuclides from disposal units prior to the time the various intrusion scenarios are assumed to occur could be important in reducing estimated doses for all scenarios, but it seems unlikely that the reductions would result in doses that are less than the performance objective for any scenario. However, there also are other factors that should reduce the dose for some scenarios by substantial amounts.

For the resident scenario, the dose estimate of 100 rem/year clearly is unreasonably pessimistic because disposal in the high-level wells is subject to the constraint that the dose rate at the ground surface following closure of a unit cannot exceed 2.5 mrem/h. Thus, the dose for the resident scenario at 100 years after disposal cannot exceed about 0.8 rem/year and may be substantially less. The higher dose estimate obtained in this analysis clearly has not properly taken into account the thickness of engineered caps above the waste and, possibly, the distribution of activity with depth in the wells.

For the discovery scenario, the dose estimate of 14 rem also is likely to be unreasonably pessimistic because many of the high-level wells have shielding at the sides of the units that is about twice as thick as assumed in this analysis, in which case the dose would be reduced to about 3 rem. However, because the proper distribution of activity between the wells in concrete silos, which provide the increased shielding, and the wells in auger holes, which provide the amount of shielding assumed in this analysis, is not known, the lower dose estimate cannot be supported for all wells, and the most conservative value is given.

For the agriculture scenario, an additional factor that has not been taken into account that could substantially reduce the dose is the possibility that most of the activity is located near the bottom of the wells. This possibility is suggested by the unreasonably pessimistic dose estimate for the resident scenario, compared with the operating constraint on external dose rate, discussed above. If this were the case, the amount of waste exhumed during excavation at the site would be overestimated in this analysis, resulting in a corresponding overestimate of the dose from ^{90}Sr due to the vegetable pathway and the external dose from ^{137}Cs during indoor residence. The magnitude of the reduction in doses from these two radionuclides is difficult to estimate; however, it does not seem reasonable that the dose for the agriculture scenario could be reduced by a factor of 360, as would be required in order to meet the performance objective. The only other possibility for reducing the dose would be if the engineered barriers could be shown to maintain their integrity and prevent excavation into the waste for more than 300 years. The dose reduction in this case would be a factor of 10 for every additional 100 years that the barriers remained intact.

For the postdrilling scenario, which results in a very high estimate of dose for the high-range wells, none of the factors discussed above that could reduce the dose for the agriculture, resident, or discovery scenarios would be relevant, except for mobilization and transport over the first 100 years after disposal. However, the high-range wells occupy only a relatively small area in SWSA 6 [about 14 m^2 (150 ft^2)]. Therefore, it should be relatively unlikely that drilling through any of the high-range wells could occur, particularly during the first few hundred years after loss of active institutional controls when the estimated doses exceed the performance objective, and the postdrilling scenario may not be credible for these disposal units.

4.7.2.7 Fissile Wells

For the fissile wells, all three relevant exposure scenarios are of concern in regard to meeting the performance objective for protection of inadvertent intruders. The estimated dose for the agriculture scenario is the same as the performance objective, the estimated dose for the resident scenario exceeds the performance objective by a factor of 3, and the estimated dose for the postdrilling scenario exceeds the performance objective by nearly a factor of 100. The only important radionuclide for these scenarios is ^{137}Cs.

For the agriculture and resident scenarios, external exposure during indoor residence is the only important pathway. Therefore, the dose for these scenarios cannot be overestimated by more than a few tens of percent and perhaps would be reduced if mobilization and transport from disposal units prior to the time the scenarios are assumed to occur were taken into account. The dose for the agriculture scenario would be reduced below the performance objective if the engineered barriers maintained their integrity for longer than 300 years.

For the postdrilling scenario, the dose would be underestimated only if mobilization and transport from disposal units for 100 years after disposal were insignificant and the plant-to-soil concentration ratio for ^{137}Cs were underestimated. On the other hand, it seems unlikely that the dose has been overestimated by as much as a factor of 100, as would be required to meet the performance objective. However, the fissile wells occupy only a very small area in SWSA 6 [about 0.45 m^2 (4.8 ft^2)]. Therefore, it is clearly quite unlikely that drilling through the single fissile well of concern to this performance assessment could occur, particularly during the first few hundred years after loss of active institutional controls when the estimated doses exceed the performance objective, and the postdrilling scenario probably is not credible for this disposal unit.

4.7.2.8 Asbestos Silos

For the asbestos silos, none of the exposure scenarios result in dose estimates that exceed the performance objective for protection of inadvertent intruders. The dose estimate is within a factor of 5 of the performance objective for the agriculture scenario and slightly more than a factor of 10 for the postdrilling scenario, but the dose estimates for the resident and discovery scenarios are far below the performance objective.

For the agriculture and postdrilling scenarios, the only important radionuclide is ^{14}C. The estimated dose for the agriculture scenario could exceed the performance objective only if mobilization and transport of ^{14}C from the disposal units prior to occurrence of the

scenario were insignificant and if the plant-to-soil concentration ratio for this radionuclide were underestimated by a factor of 5. Similar considerations apply to the postdrilling scenario, except the plant-to-soil concentration ratio would need to be underestimated by more than a factor of 10.

4.7.2.9 Biological Trenches

For the biological trenches, neither the agriculture nor the postdrilling scenario results in dose estimates that exceed the performance objective for protection of inadvertent intruders, and the resident and discovery scenarios are not relevant for these disposal units. The dose estimate is less than the performance objective by about a factor of 30 for the agriculture scenario and a factor of 100 for the postdrilling scenario.

For the agriculture and postdrilling scenarios, the only important radionuclide is ^{90}Sr. The estimated dose for the agriculture scenario could exceed the performance objective only if mobilization and transport of ^{90}Sr from the disposal units prior to occurrence of the scenario were insignificant and if the plant-to-soil concentration ratio for this radionuclide were underestimated by a factor of 30. Similar considerations apply to the postdrilling scenario, except the plant-to-soil concentration ratio would need to be underestimated by a factor of 100.

4.7.2.10 Summary

Although the dose analyses for the direct intrusion scenarios for the different types of disposal units in SWSA 6 depend greatly on the assumptions used in defining the scenarios, thereby resulting in some uncertainty in the dose estimates, the results described above indicate the problematic nature of some of the present disposal practices in SWSA 6 in regard to protection of future inadvertent intruders.

The most important problem area is disposal of high concentrations of ^{90}Sr, ^{137}Cs, and ^{152}Eu in the high-range wells. Although the calculations used in this analysis do not yet provide reasonably realistic estimates of dose for the agriculture, resident, and discovery scenarios, it appears unlikely that refined dose estimates would be less than the performance objective. In addition, the dose estimates for the postdrilling scenario probably can be dismissed only if the scenario is judged not to be credible, due to the relatively small area occupied by these disposal units.

Disposal of high concentrations of ^{14}C in Tumulus I, ^{14}C and ^{36}Cl in the IWMF, ^{14}C and ^{226}Ra in the low-range silos, ^{90}Sr in the high-range silos, and ^{137}Cs in the fissile wells also may be problematic. However, further refinements to the analysis may result in substantial reductions in dose estimates in some cases. In particular, consideration of mobilization and transport of ^{14}C and ^{36}Cl from disposal units prior to occurrence of the exposure scenarios should be important for these presumably mobile radionuclides, and such considerations may be important for the other radionuclides as well. In addition, the dose from ^{226}Ra in the low-range silos would be insignificant if the dose from ^{222}Rn were excluded from the performance objective.

4.8 DESIGN CHANGES REQUIRED TO MEET PERFORMANCE OBJECTIVES

The results presented in Sects. 4.1–4.5 indicate that SWSA 6 as a whole will not be in compliance with the performance objectives of DOE Order 5820.2A if operations continue as currently conducted. January 1, 1994, has been established as the date of cessation of all below-grade disposal in SWSA 6. IWMF will continue to operate; however, concentration-based Waste Acceptance Criteria (WAC) will be imposed to bring the technology into compliance with the performance objectives of DOE Order 5820.2A. The approach to be employed for all waste management planning in SWSA 6 will be to re-evaluate those disposal technologies that did not meet the performance objectives; analyze the impact of restricted disposal while addressing limitation or exclusion of radionuclides that were responsible for noncompliance; and determine whether, under those constraints, the technology can perform within the objectives. Those technologies that can be demonstrated to do so will then have revised WAC imposed upon them for future operation. Technologies that cannot be made to meet the performance objectives will be permanently discontinued.

4.9 CONTINUED WORK

The present performance assessment provides a comprehensive analysis of the performance of SWSA 6 from disposal of wastes from September 26, 1988, to the projected close of the facility in December 1997. The analysis examines the many uncertainties associated with the results. Recognizing the development of the performance assessment as a process, further improvements are expected and appropriate for reducing uncertainty and improving the accuracy of the assessment.

The performance assessment was prepared with the best available estimates of the inventory of wastes disposed of in SWSA 6. Large discrepancies exist between the reported disposals and the estimates of the range of concentrations disposed of. These large differences contribute to the uncertainties associated with the performance assessment, and continued work is warranted to reduce these differences to the maximum extent possible. The WAC (ORNL 1993a) and Waste Certification Program (Smith 1991) currently being implemented will contribute towards reducing uncertainties in the future. A more rigorous attempt to provide reasonable forecasts of future disposals will be undertaken to remove the inherent weaknesses associated with a simple extrapolation into the future.

In Sect. 4.7.1.1, several shortcomings of the SOURCE1 and SOURCE2 codes were identified that relate to the accounting within the code for the inventory after cracking, the inventory accounting for solubility-limited isotopes, the leaching of multiple isotopes of a solubility-limited radionuclide, and the leaching of tritium. Improvements will be made to remove these weaknesses and improve the code's accuracy. Additionally, the formal documentation and quality assurance procedures necessary to achieve acceptance of the code will be completed.

The verification of the SOURCE1 and SOURCE2 codes used in this analysis will be undertaken. In addition to verifying the numerical accuracy of the models, efforts will be made to better characterize the nature of concrete degradation in environments similar to

those of SWSA 6. An improved understanding of the durability of concrete will allow for a reduction in the number of assumptions incorporated into the SOURCE1 and SOURCE2 codes. At present, the codes model the onset of advection as a zero-order process. A more sophisticated approach to the onset of advection is warranted that considers the time dependence of advection. Additionally, the time dependence of diffusion of contaminants will be addressed in upgrading the SOURCE1 and SOURCE2 codes.

Additional analysis is warranted to address the apparent noncompliance of SWSA 6 operations with the protection of groundwater resources. Further analysis of the transport of Th, Pu, Am, and Cm, with more realistic selections for the distribution coefficient, will be undertaken. Distribution coefficients for these radionuclides will be based on Sheppard and Thibault (1990) and are expected to significantly reduce the calculated results below the performance objective for groundwater resource protection.

An evaluation of the effect of changes in the closure scenario for SWSA 6 will be undertaken. The present concept of closure is being reconsidered in response to the originally proposed remediation plan that was criticized in the public review of planned environmental restoration activities at SWSA 6. An initial evaluation of the revised plan for monitoring the facility and developing a better understanding of releases from the facility showed an increase in tritium transport rates prior to the initiation of remediation activities. The revised plan for site remediation is not expected to have an adverse effect on other less mobile radionuclides whose transport is associated with the degradation of concrete. Further coordination with the Environmental Restoration Program will be undertaken to reduce the uncertainties in the likely future of SWSA 6 after disposal operations are completed.

4.10 QUALITY ASSURANCE

This performance assessment has been prepared in accordance with the Quality Assurance Program of ORNL (ORNL 1993b). The program is based on the requirements set forward in the ANSI/ASME NQA-1 program requirements. Software developed for this performance assessment has been prepared in accordance with Martin Marietta Energy Systems, Policy, Standards, and Procedures for software quality assurance (Mynatt 1992). The requirements set forward in software quality assurance have been adhered to; however, full documentation requirements specified for software have not been completed because some software development is associated with the continuing work discussed in Sect. 4.9.

5. PERFORMANCE EVALUATION

The purpose of this site-specific performance assessment for Solid Waste Storage Area (SWSA) 6 is to provide the technical basis for demonstrating compliance of the facility with the performance objectives for low-level radioactive waste (LLW) disposal in U.S. Department of Energy (DOE) Order 5820.2A. This section presents the overall evaluation of the facility and its compliance with the performance objectives.

The performance assessment for the continued and future operations of SWSA 6 provides a comprehensive, site-specific analysis of the effects of LLW disposal over an extended period of time. The comparison of the results of this analysis with the performance objectives is presented in Table 5.1. The results, representing the best estimates presently available, are presented with respect to each type of disposal unit, although the protection of groundwater resources applies to the entire facility. The results provide direct comparisons with the performance objectives for off-site individuals and inadvertent intruders. For a meaningful evaluation of the facility, the quantitative results require interpretation with respect to the uncertainties involved in the analysis, the assumptions incorporated into the analysis, and actions taken in response to the analysis.

The performance assessment of SWSA 6, as summarized in Table 5.1, indicates that the facility is not presently in compliance with the performance objectives of DOE Order 5820.2A for all disposal operations. Modifications to the existing Waste Acceptance Criteria (WAC) for continuing operations at the Interim Waste Management Facility (IWMF) are necessary and will be implemented to reduce potential exposures from inadvertent intrusion into the wastes and potential contamination of groundwater resources. In addition, continued development and refinement of the performance assessment are expected to reduce estimated doses to inadvertent intruders and potential contamination of groundwater resources. The protection of surface waters to the same performance objective as groundwater also is expected to result from continued refinement of the performance assessment. Continuing disposal operations at IWMF have been shown to be in compliance with the performance objective for protecting any member of the public from exposures greater than 25 mrem/year. Consequently, with modifications to operations as discussed above, continuing disposal operations at the IWMF at SWSA 6 are expected to be performed in a manner that will demonstrate compliance with the performance objectives of DOE Order 5820.2A. This performance assessment will be revised when these improvements are completed to document compliance with the performance objectives.

Disposal operations in all disposal units in SWSA 6 other than the IWMF will be terminated as of January 1, 1994. All of these disposal units have been shown to comply with the performance objectives for protection of any member of the public and of groundwater. Environmental releases from these disposal units contribute to the potential contamination of surface water but to a lesser extent than the IWMF. Disposal operations performed at IWMF, Tumulus I, the low-range silos, high-range silos, high-range wells,

Table 5.1. Comparison of results with performance objectives

Receptor	Performance objective	Maximum dose for disposal unit								
Public (off-site) (mrem/year)	25	6								
		Low-range silos	High-range silos	High-range wells	Fissile well	Asbestos silo	Biological trenches	Tumulus I	Tumulus II	IWMF
Inadvertent intrusion										
Chronic (mrem/year)	100	780	2000	780,000[c]	100[d]	21	3	150	33	1600
Chronic (>10^6 years)[b] (mrem/year)	100	7100	1100	4[c]	1500	1400	—	4200	600	7400
Acute (mrem)	500	<1	9	14,000[c]	—	<1	—	—	—	—
Groundwater										
During active institutional control (mrem/year)	4	*e*	*e*	*e*	*e*	*e*	*e*	*e*	*e*	370
After active institutional control (mrem/year)	4	2[a]	0.4[a]	*e*	*e*	*e*	*e*	*e*	*e*	15

[a]See Table 4.5.
[b]Results are conservative because transport of uranium from disposal units over long periods of time has not been taken into account.
[c]Based on operational requirement that external dose rate above disposal units following waste emplacement not exceed 2.5 mrem/h, result is known to be conservative.
[d]Result based on agriculture scenario; postdrilling scenario not regarded as credible.
[e]<0.4 mrem/year.

and the fissile well have been shown to exceed the performance objective for continuous exposure from inadvertent intrusion. The performance objective for a single acute exposure from inadvertent intrusion has been shown to be exceeded at the high-range wells. The asbestos silos and Tumulus II are shown to be in compliance with the performance objectives of DOE Order 5820.2A with the exception of doses attributable to radon (^{222}Rn) at long times ($>10^6$ years). The biological trenches have been shown to be in compliance with all of the performance objectives of DOE Order 5820.2A.

The estimated doses from inadvertent intrusion at all disposal units have been obtained using the best estimates of the radionuclide inventories in the wastes. Substantial uncertainties are associated with the estimated inventories used in preparing the performance assessment. Waste disposal records have been investigated to remove errors in data entry, and waste characterization and certification methods have been examined. The remaining uncertainties are large and cannot be reasonably expected to be resolved entirely by further analysis. The inventory estimates used in the analysis are probably conservative for most cases, as evidenced by the estimated external exposures at the high-range wells that significantly exceed measured doses resulting from waste disposal operations.

The effect of the uncertainties in waste inventories on the dose estimates for inadvertent intrusion is especially significant for ^{14}C, which is a major dose contributor for the IWMF, low-range silos, and Tumulus I. The divergence between the best estimate and the reported value on waste manifests is a factor of 500 for the IWMF and Tumulus I and a factor of 1000 for the low-range silos. Additionally, the estimated doses from inadvertent intrusion have been obtained using the assumption that the entire inventory of wastes remains in the disposal units. This assumption implies that no environmental releases of radionuclides occur after disposal, which is not supported by the analysis of environmental transport for this performance assessment or the available monitoring data at SWSA 6. This assumption was invoked for the analysis of inadvertent intrusion because reasonable, lower-bound estimates of environmental releases from the disposal units cannot be determined with the present state of knowledge regarding the long-term performance of engineered disposal units. Consequently, the estimated noncompliance with the performance objectives for inadvertent intrusion presented in Table 5.1 is likely to be an artifact of the assumptions invoked for most disposal units.

Doses to an inadvertent intruder at long times ($>10^6$ years) arise from the presence of uranium in the wastes disposed of in SWSA 6. At long times, ^{222}Rn is produced as daughter buildup occurs in uranium-contaminated wastes, yielding the high dose estimates. The performance objectives for DOE Order 5820.2A do not exclude ^{222}Rn, although other regulatory agencies have acted to exclude ^{222}Rn from dose limits for the management of radioactive materials. The effect of environmental transport of uranium over long times may be incorporated into the remediation of SWSA 6 under the Comprehensive Environmental Response, Compensation, and Liability Act (CERCLA) or the closure plans for the operating disposal units in SWSA 6; however, CERCLA remediation plans are currently being reconsidered, and current closure concepts do not provide a sufficient basis for excluding ^{222}Rn from the potential doses to an inadvertent intruder. Future closure and remediation plans may reduce potential exposures from ^{222}Rn, or revisions to DOE Order 5820.2A may exclude ^{222}Rn from the dose-based performance objectives for waste disposal. Additionally, any environmental transport of uranium and its daughters will

reduce the potential dose from ^{222}Rn to an inadvertent intruder at far future times. The estimated doses to inadvertent intruders that exceed the performance objectives because of ^{222}Rn are not considered clear violations of the performance objectives of DOE Order 5820.2A but constitute one of the important issues facing waste management for SWSA 6.

The combined effects of the uncertainties in waste inventories, the assumption of no environmental release of contamination for estimating doses to inadvertent intruders, and the long-term release of ^{222}Rn from uranium disposals lead to high dose estimates from inadvertent intrusion at the IWMF, Tumulus I, low-range silos, high-range silos, high-range wells, and the fissile wells. The degree of conservatism incorporated into the estimated doses from inadvertent intrusion cannot be defined with the current analysis; however, reasonable representations of these three major areas of conservatism could reduce potential doses to values more consistent with the performance objectives for several different disposal units. All of the disposal units in SWSA 6 except the IWMF are to be included in the CERCLA remediation of SWSA 6. Consequently, the long-term risks to the public from disposal units to be addressed by CERCLA ultimately will be reduced to acceptable levels. At the conclusion of CERCLA remediation, the policy presented in DOE Order 5820.2A for protecting the public health and safety, preserving the environment, and ensuring no legacy requiring remedial action should be realized. Additional analysis effort towards reducing the uncertainty and estimated doses from inadvertent intrusion in this performance assessment will be incorporated into the CERCLA remediation of SWSA 6.

For the continuing disposal operations at the IWMF, potential doses from inadvertent intrusion are largely attributed to ^{36}Cl and ^{14}C. Both of these radionuclides will be restricted by changes in the current WAC to reduce potential doses. Chlorine-36 is not associated with routine waste disposals so that changes in the WAC will be effective in reducing potential doses. Carbon-14 is more commonly included in routine wastes, but much of the current inventory of ^{14}C in wastes is associated with a few disposals with large inventories. Consequently, restrictions in the WAC are expected to be effective in reducing potential doses. Consideration of environmental transport of these radionuclides will further reduce the potential doses to an inadvertent intruder. This performance assessment also indicates that disposal of ^{14}C and ^{36}Cl in the IWMF results in doses exceeding the performance objective for groundwater protection. Regulations prescribing the limits for groundwater protection are not promulgated, but a limit of 4 mrem/year outside a 100-m (328-ft) buffer zone has been used for the purposes of this performance assessment. The limited area (less than 1 acre) of the groundwater resource shown to exceed the 4 mrem/year performance objective is due to ^{14}C, ^{36}Cl, and to a minor extent ^{99}Tc during and immediately following the period of active institutional control. Restrictions on disposals of these isotopes in the WAC will reduce the potential doses to less than the performance objective. Doses from the consumption of groundwater exceed the performance objective 2400 years after site closure from the combined effects of ^{233}U, ^{239}Pu, and ^{243}Am in a similarly sized small area of the groundwater resource. Improvements in the analysis, including additional credit for retardation during transport, are expected to reduce the estimated doses to less than 4 mrem/year. Ongoing monitoring activities by the Active Sites Monitoring Program at SWSA 6 and the Environmental Restoration Program at SWSA 6 and other historical disposal facilities are anticipated to provide data to support the improvements in the analysis.

The performance assessment for SWSA 6 does not yet provide reasonable assurance that the facility is in full compliance with the performance objectives specified in DOE Order 5820.2A. This performance assessment demonstrates compliance with the performance objective for protecting public health and safety in accordance with standards specified in Environmental Health orders and other DOE orders. Compliance with the performance objective for the protection of any member of the public has been demonstrated. Reasonable assurance has been provided to demonstrate compliance with the performance objective for the protection of groundwater resources for all disposal units, except continuing operations at the IWMF. Changes in operations at the IWMF and improvements in the analysis are expected to demonstrate compliance with the groundwater protection requirement. Compliance with the performance objective for protection of inadvertent intruders for disposal operations performed prior to January 1, 1994, has not been demonstrated. Discontinuing disposal operations and remediating these disposal units under the provisions of CERCLA support the policy of DOE Order 5820.2A for these disposal units. Compliance with the performance objective for protection of inadvertent intruders for continuing operations at the IWMF has not been demonstrated, but improvements in the performance assessment and restrictions on future waste disposals are expected to demonstrate compliance with the performance objectives of DOE Order 5820.2A.

6. PREPARERS

The following individuals were responsible for the preparation of this performance assessment for Solid Waste Storage Area 6. All of these individuals are associated with Oak Ridge National Laboratory.

John M. Bownds; Ph.D., Applied Mathematics; Groundwater Analysis and Uncertainty Analysis

J. Robert Forgy, Jr.; M.S., Radiological Health; Waste Characteristics, Treatment, and Certification

Herschel W. Godbee; Ph.D., Chemical Engineering; Source Term Analysis

Alan S. Icenhour; B.S., Nuclear Engineering; Source Term Analysis

Richard H. Ketelle; M.S., Geology; Site Characteristics and Groundwater Analysis

David C. Kocher; Ph.D., Nuclear Physics; Dose Analysis

Donald W. Lee; Ph.D., Applied Mechanics; Task Group Leader

Robert J. Luxmoore; Ph.D., Soil Science; Shallow Subsurface and Surface Water Analysis

Richard E. Maerker; Ph.D., Physics; Sensitivity and Uncertainty Analysis

James W. Nehls, Jr.; B.S., Chemical Engineering; Source Term Analysis

C. William Nestor, Jr.; Ph.D., Physics; Source Term Analysis

Steven J. Norton; Ph.D., Physics; Sensitivity and Uncertainty Analysis

Joe N. Stone; M.A., English; Lead Editor

M. Lynn Tharp; M.S., Computer Science; Sensitivity and Uncertainty Analysis

Mark W. Yambert; B.S., Engineering Mechanics; Groundwater Analysis and Uncertainty Analysis

7. REFERENCES

Anspaugh, L. R., et al. 1975. "Resuspension and Redistribution of Plutonium in Soils," *Health Physics* **29**, 571.

Ashwood, T. L., et al. 1990. *Active Sites Environmental Monitoring Program, Program Plan Revision O,* Oak Ridge National Laboratory, Oak Ridge, Tenn., April.

Ashwood, T. L., D. S. Wickliff, and C. M. Morrissey 1991. *Active Sites Environmental Monitoring Program: Mid-FY 1991 Report*, ORNL/M-1442, Martin Marietta Energy Systems, Inc., Oak Ridge, Tenn.

Ashwood, T. L., D. S. Hicks, and C. M. Morrissey 1992. *Active Sites Environmental Monitoring Program: FY 1991 Report*, ORNL/M-1792, Martin Marietta Energy Systems, Inc., Oak Ridge, Tenn.

Bailey, Z. C., and R. W. Lee 1991. *Hydrogeology and Geochemistry in Bear Creek and Union Valleys near Oak Ridge, Tennessee*, Water Resources Investigation Report 90-4088, U.S. Geological Survey, Nashville, Tenn.

Bass, J. M., W. J. Lyman, and J. P. Trantnyek 1985. *Assessment of Synthetic Membrane Successes and Failures at Waste Storage and Disposal Sites*, EPA/S2-85/100, U.S. Environmental Protection Agency, Washington, D.C.

Bechtel (Bechtel National, Inc.) 1989. *Draft Site Characterization Summary Report for ORNL Waste Area Grouping 6,* ORNL/RAP/Sub-87/99053/XXX, Oak Ridge National Laboratory, Oak Ridge, Tenn.

Bechtel (Bechtel National, Inc.) 1991a. *RCRA Facility Investigation Report for Waste Area Grouping 6 at Oak Ridge National Laboratory, Oak Ridge, Tennessee*, Vol. 3, ES/ER-22/V3 & D1, ORNL/ER/Sub-87/99053/5/V3, Oak Ridge, Tenn.

Bechtel (Bechtel National, Inc.) 1991b. *RCRA Facility Investigation Report for Waste Area Grouping 6 at Oak Ridge National Laboratory, Oak Ridge, Tennessee*, Vol. 1, ES/ER-22/V1 & D1 ORNL/ER/Sub-87/99053/5/V1, Oak Ridge, Tenn.

Begovich, C. L., and R. J. Luxmoore 1979. *Some Sensitivity Studies of Chemical Transport Simulated in Models of the Soil-Plant-Litter System*, ORNL/TM-6791, Oak Ridge National Laboratory, Oak Ridge, Tenn.

Clapp, R. B., 1992. *Annual Report of the Environmental Restoration Monitoring and Assessment Program at Oak Ridge National Laboratory for FY 1992*, ORNL/ER-124, Martin Marietta Energy Systems, Inc., Oak Ridge, Tenn.

Clapp, R. B., and D. S. Marshall 1992. *SWSA 6 Interim Corrective Measures Environmental Monitoring: FY 1991 Results*, ORNL/ER-87, Martin Marietta Energy Systems, Inc., Oak Ridge, Tenn.

Coobs, J. H., and J. R. Gissel 1986. *History of Disposal of Radioactive Wastes into the Ground at Oak Ridge National Laboratory,* ORNL/TM-10269, Oak Ridge National Laboratory, Oak Ridge, Tenn.

Davis, E. C., et al. 1984. *Site Characterization Techniques Used at a Low-Level Waste Shallow Land Burial Field Demonstration Facility,* ORNL/TM-9146, Oak Ridge National Laboratory, Oak Ridge, Tenn.

Davis, E. C., et al. 1987. *Summary of Environmental Characterization Activities at the Oak Ridge National Laboratory Solid Waste Storage Area Six, FY 1986 through 1987,* ORNL/RAP/LTR-87/68, Oak Ridge National Laboratory, Oak Ridge, Tenn.

Davis, E. C., C. W. Francis, and R. J. Luxmoore 1989. *An Evaluation of Water Leakage into Concrete Low-Level Radioactive Waste Disposal Silos at ORNL's Solid Waste Storage Area Six,* ORNL/TM-11164, Oak Ridge National Laboratory, Oak Ridge, Tenn.

DOE (U.S. Department of Energy) 1988. "Management of Low-Level Waste," in *Radioactive Waste Management*, DOE Order 5820.2A, Washington, D.C.

DOE (U.S. Department of Energy) 1989. *Recommended Format and Content for DOE Low-Level Waste Disposal Facility Radiological Performance Assessment Reports,* DOE/LLW-81, Washington D.C.

DOE (U.S. Department of Energy) 1991. *Performance Assessment Review Guide for DOE Low-Level Radioactive Waste Disposal Facilities*, DOE/LLW-93, Washington, D.C.

EBASCO (EBASCO Services, Inc.) 1992. *OR-ERWM Program Design Criteria Studies: Results of 3DFEMWATER Modeling*, ER/W6.01-002, Rev. 0, Environmental Consulting Engineers, Inc., Knoxville, Tenn., November 23.

EPA (U.S. Environmental Protection Agency) 1989. *Human Health Evaluation Manual (Part A)*, Vol. 1 (of *Risk Assessment Guidance for Superfund*), EPA/540/1-89/002, Washington, D.C.

Francis, C. W., 1990. *Leachate Characteristics of Oak Ridge Low-Level Wastes,* Letter Report, Oak Ridge National Laboratory, Oak Ridge, Tenn., January 9.

Friedman, H. A., and A. D. Kelmers, 1990. *Laboratory Measurement of Radionuclide Sorption in Solid Waste Storage Area 6 Soil/Groundwater Systems,* ORNL/TM-10561, Oak Ridge National Laboratory, Oak Ridge, Tenn.

Gardner, R. H., B. Röjder, and U. Berström 1983. *PRISM, A Systematic Method for Determining the Effect of Parameter Uncertainties on Model Predictions*, Report NW-83-555, Studsvik Energiteknik AB, Nykoping, Sweden.

Goldman, L. J., L. I. Greenfield, A. S. Damie, G. L. Kingsbury, C. M. Northeim, and R. S. Truesdale 1988. "Design, Construction, and Evaluation of Clay Liners for Waste Management Facilities," EPA/530-SW-86-007-F, Risk Reduction Engineering Laboratory, U.S. Environmental Protection Agency, Cincinnati.

Healy, J. W. 1980. "Review of Resuspension Models," in *Transuranic Elements in the Environment,* ed. W. C. Hanson, DOE/TIC-22800, U.S. Department of Energy, Washington, D.C.

Helvey, J. D., and J. H. Patrick 1965. "Canopy and Litter Interception of Rainfall by Hardwoods of Eastern United States," *Water Resources Research* 1, 193–206.

Hetrick, D. M., J. T. Holdeman, and R. J. Luxmoore 1982. *AGTEHM: Documentation of Modifications to the Terrestrial Ecosystem Hydrology Model (TEHM) for Agricultural Applications*, ORNL/TM-7856. Oak Ridge National Laboratory, Oak Ridge, Tenn.

Horwedel, J. E. 1990. *A GRESS/ADGEN Sample Problem,* ORNL/TM-1121, Oak Ridge National Laboratory, Oak Ridge, Tenn.

Huff, D. D., et al. 1977a. "The Application of Analytic and Mechanistic Hydrologic Models to the Study of Walker Branch Watershed," pp.741-63 in *Watershed Research in Eastern North America*, ed. D. L. Correll, Chesapeake Bay Center for Environmental Studies, Smithsonian Institution, Edgewater, Md.

Huff, D. D., et al. 1977b. *TEHM: A Terrestrial Ecosystem Hydrology Model*, ORNL/NSF/EATC-27, Oak Ridge National Laboratory, Oak Ridge, Tenn.

Hydzik, R. J., and M. A. Smith 1992. *Guidelines for Establishing Waste Certification Plans and Procedures at Waste Generator Facilities*, Martin Marietta Energy Systems, Inc., Oak Ridge National Laboratory, Oak Ridge, Tenn., September.

Iman, R. L., and J. C. Helton 1985. *A Comparison of Uncertainty and Sensitivity Analysis Techniques for Computer Models*, NUREG/CR-3904, SAND/84-1461, Sandia National Laboratory, Albuquerque, N.M.

Jardine, P. M., G. V. Wilson, and R. J. Luxmoore 1988. "Modeling the Transport of Inorganic Ions Through Undistributed Soil Columns from Two Contrasting Watersheds," *Soil Science Society of America Journal* 52, 1252-59.

Jardine, P. M., G. K. Jacobs, and G. V. Wilson (1993). "Unsaturated Transport Processes in Undisturbed Heterogeneous Media," I. Inorganic contaminants. *Soil Science Society of America Journal.*

Kennedy, W. E. Jr., and R. A. Peloquin 1988. *Intruder Scenarios for Site-Specific Low-Level Waste Classification*, DOE/LLW-71T, U.S. Department of Energy, Idaho Operations Office, Idaho Falls, Idaho.

Kenning and Yong 1993. *Evaluation of Uncertainty in the SWSA 6 Inventory Data.* Prepared for Martin Marietta Energy Systems by Atlan-Tech, Inc., Roswell, Ga. (February).

Kocher, D. C., and A. L. Sjoreen 1985. "Dose-Rate Conversion Factors for External Exposure to Photon Emitters in Soil," *Health Physics* **48**, 193.

Kornegay, F. C., et al. 1991. *Oak Ridge Reservation Environmental Report for 1990*, Martin Marietta Energy Systems, Inc., Oak Ridge, Tenn.

Kornegay, F. C., et al. 1992. *Oak Ridge Reservation Environmental Report for 1991*, ES/ESH-22/V1, Martin Marietta Energy Systems, Inc., Oak Ridge, Tenn.

Kornegay, F. C., et al. 1993. *Oak Ridge Reservation Environmental Report for 1992*, ES/ESH-31/V1, Martin Marietta Energy Systems, Inc., Oak Ridge, Tenn.

Lee, D. W., and D. C. Kocher 1989. *Scoping Analysis for the Performance Assessment for SWSA 6,* ORNL/CF-90/67, Oak Ridge National Laboratory, Oak Ridge, Tenn.

Lee, R. R., et al. 1989. *Calibration of a Groundwater Flow and Contaminant Transport Model: Progress Toward Model Validation,* ORNL/TM-11294, Oak Ridge National Laboratory, Oak Ridge, Tenn.

Lee, R. R., R. H. Ketelle 1988. *Contaminant Transport Model Validation: The Oak Ridge Reservation*, ORNL/TM-10972, Martin Marietta Energy Systems, Inc., Oak Ridge, Tenn.

Lee, R. R., and R. H. Ketelle 1989. *Geology of the West Bear Creek Valley Site,* ORNL/TM-10887, Oak Ridge National Laboratory, Oak Ridge, Tenn.

Lee, R. R., et al. 1991. "Aquifier Analysis and Modeling in a Fractured Heterogeneous Medium" *Ground Water* **30**(4), 589-97.

Lee, S. Y., and D. A. Lietzke 1987. "Soils of SWSA 6," in *Summary of Environmental Characterization Activity at the Oak Ridge National Laboratory Solid Waste Storage Area Six FY 1986 through 1987,* ed. E. C. Davis, ORNL/RAP/LTR-87/68, Oak Ridge National Laboratory, Oak Ridge, Tenn.

Luxmoore, R. J. 1982. *Physical Characteristics of Soils of the Southern Region,* ORNL-5868. Oak Ridge National Laboratory, Oak Ridge, Tenn.

Luxmoore, R. J. 1983a. "Infiltration and Runoff Predictions for a Grassland Watershed," *Journal of Hydrology* **65**, 271–78.

Luxmoore, R. J. 1983b. "Water Budget of an Eastern Deciduous Forest Stand," *Soil Science Society of America Journal* **47**, 785–91.

Luxmoore, R. J., and C. L. Begovich 1979. "Simulated Heavy Metal Fluxes in Tree Microcosms and a Deciduous Forest," *International Society of Ecological Modeling Journal* **1**, 48–60.

Luxmoore, R. J., and M. L. Sharma 1980. "Runoff Responses to Soil Heterogeneity: Experimental and Simulation Comparisons for Two Contrasting Watersheds," *Water Resources Research* **16**, 675–84.

Luxmoore, R. J., B. P. Spalding, and I. M. Munro 1981. "Areal Variation and Chemical Modification of Weathered Shale Infiltration Characteristics," *Soil Science Society of America Journal* **45**, 687–91.

Luxmoore, R. J., and D. D. Huff 1989. "Water," in *Analysis of Biogeochemical Cycling Processes in Walker Branch Watershed,* eds. D. W. Johnson and R. I. Van Hook, Springer-Verlag, New York.

Luxmoore, R. J., and M. L. Tharp 1993. *Simulation of Barrier Heterogeneity and Preferential Flow Effects on the Performance of Shallow Land Burial Facilities,* ORNL/TM-12058, Oak Ridge National Laboratory, Oak Ridge, Tenn.

Luxmoore, R. J., et al. 1978. "Some Measured and Simulated Plant Water Relations of Yellow Poplar," *Forest Science* **24**, 327–41.

Luxmoore, R. J., J. L. Stolzy, and J. T. Holdeman 1976. *Some Sensitivity Analyses of an Hourly Soil-Plant-Water Relations Model,* ORNL/TM-5343, Oak Ridge National Laboratory, Oak Ridge, Tenn.

Luxmoore, R. J., J. L. Stolzy, and J. T. Holdeman 1981. "Sensitivity of a Soil-Plant-Atmosphere Model to Changes in Air Temperature, Dewpoint Temperature, and Solar Radiation," *Agricultural Meteorology* **23**, 115–29.

Moore, G. K. 1988. *Concepts of Groundwater Occurrence and Flow near Oak Ridge National Laboratory, Tennessee,* ORNL/TM-10969. Oak Ridge National Laboratory, Oak Ridge, Tenn.

Moore, G. K. 1989. *Groundwater Parameters and Flow Systems Near Oak Ridge National Laboratory,* ORNL/TM-11368, Oak Ridge National Laboratory, Oak Ridge, Tenn.

Moore, G. K., and L. E. Toran 1992. *Supplement to a Hydrologic Framework for the Oak Ridge Reservation, Oak Ridge, Tennessee,* ORNL/TM-12191, Oak Ridge National Laboratory, Oak Ridge, Tenn.

Mynatt, F. R. 1992. "Software Quality Assurance," ESS-QA-19.0, Martin Marietta Energy Systems, Inc., Policy, Standards, and Procedures, Oak Ridge, Tenn.

Ng, Y. C., C. S. Colsher, and S. E. Thompson 1982. *Soil-to-Plant Concentration Factors for Radiological Assessments,* NUREG/CR-4370, UCID-19463, Lawrence Livermore National Laboratory, Livermore, Calif.

NRC (U.S. Nuclear Regulatory Commission) 1982. *Final Environmental Impact Statement on 10 CFR Part 61 "Licensing Requirements for Land Disposal of Radioactive Waste,"* Vol. 1, NUREG-0945, Washington, D.C.

ORNL (Oak Ridge National Laboratory) 1992. *Guidelines for Establishing Waste Certification Plans and Procedures at Waste Generator Facilities*, WMRA-WMPC-CGD-001, Martin Marietta Energy Systems, Inc., Oak Ridge, Tenn., September.

ORNL (Oak Ridge National Laboratory) 1993. *Groundwater Quality Assessment Report for the Solid Waste Storage Area 6 at the Oak Ridge National Laboratory 1992*, Martin Marietta Energy Systems, Inc., Oak Ridge, Tenn.

ORNL (Oak Ridge National Laboratory) 1993a. *Waste Acceptance Criteria for Radioactive Solid Waste Disposal at SWSA 6*, WMRA-WMCP-204, Martin Marietta Energy Systems, Inc., Oak Ridge, Tenn., April.

ORNL (Oak Ridge National Laboratory) 1993b. *Quality Assurance Manual*, current edition, Oak Ridge National Laboratory, Oak Ridge, Tenn., November.

Oztunali, O. I., and G. W. Roles 1986. *Update of Part 61 Impacts Analysis Methodology—Methodology Report,* Vol. 1, NUREG/CR-4370, U.S. Nuclear Regulatory Commission, Washington, D.C.

Patterson, M. R., et al. 1974. *A User's Manual for the Fortran IV Version of the Wisconsin Hydrologic Transport Model*, ORNL-NSF-EATC-7, Oak Ridge National Laboratory, Oak Ridge, Tenn.

Peterson, H. T. Jr. 1983. "Terrestrial and Aquatic Food Chain Pathways," in *Radiological Assessment,* ed. J. E. Till and R. H. Meyer, NUREG/CR-3332, ORNL-5968, U.S. Nuclear Regulatory Commission and Oak Ridge National Laboratory, Oak Ridge, Tenn.

Reeves, M., and E. E. Miller 1975. "Estimating Infiltration for Erratic Rainfall," *Water Resources Research* **11**, 102–10.

Rogers and Associates Engineering Corporation 1989. *The BARRIER Code: A Tool for Estimating the Long-Term Performance of Low-Level Radioactive Waste Disposal Facilities, User's Manual,* NP-6218-CCML, Electric Power Research Institute, Palo Alto, Calif.

Rogers and Associates Engineering Corporation 1993. Correspondence from Rob Shuman, Rogers and Associates, to L. E. McNeese, Oak Ridge National Laboratory.

Rogers et al. 1987. *Oak Ridge Reservation Environmental Monitoring Report for 1986,* ES/ESH-1/V1, Oak Ridge National Laboratory, Oak Ridge, Tenn.

Rogers et al. 1988. *Oak Ridge Reservation Environmental Monitoring Report for 1987,* ES/ESH-4/V1, Oak Ridge National Laboratory, Oak Ridge, Tenn.

Rogers et al. 1989. *Oak Ridge Reservation Environmental Monitoring Report for 1988,* ES/ESH-8/V1,V2, Oak Ridge National Laboratory, Oak Ridge, Tenn.

Rothschild, E. R., et al. 1984. *Characterization of Soils at Proposed Solid Waste Storage Area (SWSA) 7,* ORNL/TM-9326, Oak Ridge National Laboratory, Oak Ridge, Tenn.

Scheidegger, A. E. 1960. *Physics of Flow through Porous Media*, 2nd ed., Macmillan, New York.

Sharma, M. L., and R. J. Luxmoore 1979. "Soil Spatial Variability and its Consequence on Simulated Water Balance," *Water Resources Research* **15**, 1567–573.

Sharma, M. L., et al. 1987. "Subsurface Water Flow Simulated for Hillslopes with Spatially Dependent Soil Hydraulic Characteristics," *Water Resources Research* **23**, 1523–30.

Sheppard, M. E., and D. E. Thibault 1990. "Default Soil Solid/Liquid Partition Coefficients, K_dS for Four Major Soil Types: A Compendium," *Health Physics* **59**(4), 471–82.

Shuman, R., N. Chau, and E. A. Jennrich 1992. *The SOURCE Computer Codes: Models for Evaluating the Long-Term Performance of SWSA 6 Disposal Units, Version 1.0: User's Manual*, RAE-9005/8-1, Rogers and Associates Engineering Corporation, Salt Lake City, April.

Sinclair, T. R., C. E. Murphy, Jr., and K. R. Knoerr 1976. "Development and Evaluation of Simplified Models for Simulating Canopy Photosynthesis and Transpiration," *Journal of Applied Ecology* **13**, 813–29.

Smith, M. A. 1991. *Martin Marietta Energy Systems, Inc. Solid Waste Certification Program Plan*, Martin Marietta Energy Systems, Inc., K/WM-14, Central Waste Management Division, Oak Ridge, Tenn., January.

Solomon, D. K., et al. 1992. "Status Report: A Hydrologic Framework for the Oak Ridge Reservation," ORNL/TM-12026, Oak Ridge National Laboratory, Oak Ridge, Tenn.

Stevens, M. M. 1990. *Conceptual Model for Radiological Performance Assessment of Low-Level-Radioactive-Waste Disposal Facility,* ORNL/TM-11495, Oak Ridge National Laboratory, Oak Ridge, Tenn.

Suter, G. W., R. J. Luxmoore, and E. D. Smith 1993. "Compacted Soil Barriers at Abandoned Landfill Sites are Likely to Fail in the Long Term," *Journal of Environmental Quality* **22** (in press).

Swanson, J. L. 1983. *Mobility of Organic Complexes of Nickel and Cobalt in Soils*, PNL/4796, Pacific Northwest Laboratory, Richland, Wash.

Trabalka, J. R., and C. T. Garten, Jr. 1983. "Behavior of the Long-Lived Synthetic Elements and Their Natural Analogs in Food Chains," pp. 39–103 in *Advances in Radiation Biology*, V. K. Ehman and A. B. Cox eds., Academic Press, New York.

Tucci, P. 1986. *Groundwater Flow in Melton Valley, Oak Ridge Reservation, Roane County, Tennessee—Preliminary Model Analysis*, Water Resources Investigation Report 85-4221, U.S. Geological Survey, Nashville, Tenn.

Tull, M. W., and M. A. Smith 1990. *Oak Ridge National Laboratory Certification Program Plan for Solid Low-Level Radioactive Waste*, ORNL/TM-11600, Martin Marietta Energy Systems, Inc., Oak Ridge National Laboratory, Oak Ridge, Tenn., August.

Turner, R. R., and K. F. Steele 1988. "Cadmium and Manganese Sorption by Soil Macropore Linings and Fillings," *Soil Science* **145**, 79–86.

USGS MOC 1990. Computer code, with instructions in L. F. Knoikow and J. D. Bredehoeft, "Computer Model of Two-Dimensional Solute Transport and Dispersion in Ground Water," Chap. C2, Book 7 of *Geological Survey Techniques of Water-Resources Investigations of the United States Geological Survey*, U.S. Department of the Interior, Washington, D.C., 1978.

Wickliff, D. S., et al. 1989. *Contaminant Transport During Storms near Solid Waste Areas 4 and 5,* ORNL/RAP/LTR-89/20, Oak Ridge National Laboratory, Oak Ridge, Tenn.

Wickliff, D. S., et al. 1990. *Environmental Monitoring Program: Mid-FY 1990 Summary Report,* Draft ORNL/TM, Oak Ridge National Laboratory, Oak Ridge, Tenn.

Wickliff, D. S., C. M. Morrissey, and T. L. Ashwood 1991. *Active Sites Environmental Monitoring Program: FY 1990 Report*, ORNL/M-1327, Martin Marietta Energy Systems, Inc., Oak Ridge, Tenn.

Wilson, G. V., and R. J. Luxmoore 1988. "Infiltration, Macroporosity, and Mesoporosity Distributions on Two Forested Watersheds," *Soil Science Society of America Journal* 52, 329–35.

Wilson, G. V., J. M. Alfonsi, and P. M. Jardine 1989. "Spatial Variability of Saturated Hydraulic Conductivity of the Subsoil of Two Forested Watersheds," *Soil Science Society of America Journal* 53, 679–85.

APPENDIX A

RADIONUCLIDE INVENTORY DATA AND EVALUATION OF UNCERTAINTY IN INVENTORY DATA IN SUPPORT OF THE U.S. DEPARTMENT OF ENERGY ORDER 5820.2A RADIOLOGICAL PERFORMANCE ASSESSMENT FOR CONTINUING OPERATIONS IN SOLID WASTE STORAGE AREA 6

September 1988 to December 1997

J. R. Forgy, Jr.

A.1 RADIONUCLIDE INVENTORY DATA FOR SOLID WASTE STORAGE AREA 6

INSTRUCTIONS FOR COMPLETING THE UCN-2822 FORM
"REQUEST FOR STORAGE OR DISPOSAL OF RADIOACTIVE SOLID WASTE OR SPECIAL MATERIALS"

The following information is to assist you in the proper completion of the UCN-2822 Form. The form must be completed in ink.

Date: Date waste is being sent to burial ground.

Origin of Waste: Building where waste was generated. Always use a building or area number. Comment section may be used to further describe the origin of waste.

G.C.O. Signature: Legible signature of Generator Certification Official. Also include G.C.O. Badge Number, Division Code, Phone Number, and Mailing Address. Must be Martin Marietta employee.

Total Volume: Total volume of waste including the outer package in cubic feet.

Combustible Volume: Amount in cubic feet of the total volume that is combustible.

Weight: Total weight of waste and container in pounds.

UCN 2681 No.: Only applicable if waste has a UCN-2681, *ORNL Nuclear Materials Intra-Laboratory Transfer.*

Charge/Work Order No.: Active charge or work order number.

Waste Class Code: Choose only one of the following codes that best describes the waste:

Code		Code Description
1	-	Contact Handled TRU or U-233 >100nCi/gram.
2	-	Uranium/Thorium
3	-	Fission Product.
4	-	Induced Activity
5	-	Tritium
6	-	Remote Handled TRU or U-233 >100nCi/gram.
7	-	TRU or U-233 <100nCi/gram.
9	-	Landfill/Suspect
A	-	Asbestos, contaminated and suspect/brown tag.
P	-	Resource lead

Waste Type Code: Choose only one of the following codes that best describes the waste:

Code		Code Description
BW	-	Biological Waste
CE	-	Contaminated Equipment
DD	-	Decontamination Debris
DS	-	Dry Solids
SS	-	Solidified Sludge

UCN-2822 Instruction Sheet (Front)

Fig. A.1. Form UCN-2822, "Request for Storage or Disposal of Solid Radioactive Waste or Special Materials" and instructions.

RCRA Present? (Y/N): Indicate presence/absence of RCRA materials (TRU waste packages only).

Asbestos: For radioactively contaminated asbestos material. Enter preassigned number from the form UCN-13386, *Request for the Disposal of Asbestos or Material Containing Asbestos.*

Package Type Code: Choose one code each that best describes the inner and outer packages. If the containers listed do not provide adequate size or shielding, other containers may be used subject to the approval of Radioactive Solid Waste Operations supervisor:

Code		Code Description
1	-	55 Gallon Stainless Steel Drum (volume 7.5 ft^3, max. weight 400 lbs)
4	-	6 inch Concrete Cask (58 ft^3 volume)
5	-	12 inch Concrete Cask (23 ft^3 volume)
6	-	55 Gallon 17H drum (volume 7.5 ft^3, max. weight 400 lbs)
8	-	Wooden box: Provide dimensions in comment section.
9	-	Other: Provide description in comment section.
11	-	Plastic
12	-	Dumpster: Provide dumpster number.
13	-	None
14	-	Lead Shielded Carrier
15	-	Metal box: Provide dimensions in the comment section. Sizes other than 4'x 4'x 6', (96 ft^3) require RSWO approval.

Principal Isotopes Contributing More Than 5% Total Package Activity: List the principal isotopes and their quantity in Curies and/or grams in the appropriate columns as in the following examples: Cs-137 or Sr-90, etc. 1.0E-4 or $1x10^{-4}$

List the quantity of Fissile isotopes and Uranium/Thorium in grams, all other quantities in curies. Totals for the isotopes from the accompanying log-in data sheets (TX-5352 or UCN-16114) should be represented in the appropriate column. Log-in data sheet(s) must be complete, approved, and attached to the UCN-2822.

General Waste Description/Comments: Provide a brief description or general comments, as appropriate.

Radiation Protection Section: This section must be completed by Radiation Protection before the waste will be accepted by RSWO. Transferable contamination and dose rate data is for the exterior of the outer package. Dose rate for both the surface, and at one meter, must be provided for the exterior of the outer package. Provide survey instrument serial number(s).

Radioactive Solid Waste Operations: Approval of RSWO Field Representative. Required before waste can be accepted. G.C.O. section (including Principle Isotopes) and Radiation Protection Section of the UCN-2822 must be complete.

REQUEST FOR STORAGE OR DISPOSAL OF RADIOACTIVE SOLID WASTE OR SPECIAL MATERIALS

Number 83053

GCO Section

(GCO and Radiation Protection Sections Must Be Complete Before Arranging Material Transfer

Date	Origin of Waste	G.C.O. Signature (Legible)	Badge No.	Div. Code	Phone No.

Mailing Address (Bldg/MS)	Total Volume (ft^3)	Comb. Volume (ft^3)	Weight (lbs)	UCN 2681 No.

Charge/Work Order No.	Waste Class Code	Waste Type Code	PACKAGE TYPE CODES		
RCRA Present (Y/N)	Asbestos - UCN 13386 No.		Inner	Outer	Dumpster No.

Principle Isotopes Contributing More Than 5% Total Package Activity

(Report Fissile, Uranium/Thorium in Grams)

Identity	Curies	Grams	Identity	Curies	Grams
1.			8.		
2.			9.		
3.			10.		
4.			11.		
5.			12.		
6.			13.		
7.			14.		

General Waste Description/Comments:

RADIATION PROTECTION

EXTERIOR TRANSFERABLE CONTAMINATION:

Alpha _____ dpm/100 cm^2 Beta/Gamma _____ dpm/100 cm^2

DOSE RATE: Beta/Gamma: Surface _____ mrem/hr @ one meter _____ mrem/hr

Neutron: Surface _____ mrem/hr @ one meter _____ mrem/hr

Survey Instrument Serial Number:

Radiation Protection Signature	Badge No.	Date

RADIOACTIVE SOLID WASTE OPERATIONS

RSWO Signature	Badge No.	Date
Basic Description (DOT)	Cost Symbol	Adjustment

Comments

LLN	WSR Number:			ATN

UCN-2822 (3 9-92)

DISTRIBUTION: WHITE - SWSA FOREMAN FORWARDS TO DMC
BLUE - RETAINED BY SWSA FOREMAN
CANARY - RETAINED BY GENERATOR

GENERATOR INSTRUCTIONS FOR FILLING OUT THE "LOG-IN DATA SHEET FOR GENERATORS OF SLLW"

LLW No.	Enter the bar-coded number affixed to the container (box, drum, other).
Column 1	PACKET NUMBER: Enter packet number. The first packet placed in each container should be labeled number one and each subsequent packet labeled and numbered sequentially thereafter. Each article placed in the container (box, drum, other) must be bagged or sealed.
Column 2	DATE: Enter the date that each packet is placed in the container.
Column 3	WEIGHT (LBS): Estimate (within 10% accuracy) the weight of the packet in pounds.
Column 4	PKT. ORIGIN BLDG./ROOM NO: Enter the building, room number, or other information which identifies the location from which the waste originated.
Column 5	DOSE RATE MREM/H: Monitor each packet for alpha, beta and/or gamma radiation using a survey instrument per RP requirements and enter the result. If appropriate, monitor for neutrons using a BF_3 counter, fast neutron survey meter, or a comparable instrument and enter the result.
Columns 6-11	ISOTOPES: **List only 1 isotope per column.** List all radionuclides present in packet that account for 5% of activity, starting with the dominant radionuclides first. Include radionuclides that process knowledge indicates are present but are undetectable at the detection limit of the analysis instrument.
	CURIES OR GRAMS: Use the procedure identified in your waste management plan for estimating curies. Report in curies or grams as appropriate. Report fissile materials in grams.
Column 12	PHYSICAL DESCRIPTION: Describe the physical form of the contaminated material (plastic, paper, glass, metal, soil, wood, rubber, cloth, etc.).
Column 13	CHEMICAL FORM (radionuclide): Describe the chemical form of the isotopes. Acceptable entries for chemical form include: oxide, chloride, nitrate, metal oxide, elemental, inorganic salt, general chemical description, etc.
Column 14	RCRA (YES/NO): Enter either YES or NO if waste packet contains RCRA regulated materials.
Column 15	GENERATOR'S SIGNATURE: The person placing each sealed or bagged article in the container certifies that the waste was packaged in accordance with the Waste Acceptance Criteria, SLLW QA Plan, and the ORNL Certification Program Plan (initials are NOT acceptable). This person must be current in Waste Generator Training for SLLW (TMIS# 1365).
Column 16	BADGE NO.: Enter badge number of person signing in column 15.

RSWOG PERSONNEL INSTRUCTIONS FOR CHECKING AND COMPLETING THE "LOG-IN DATA SHEET FOR GENERATORS OF SLLW"

1. Check to see that a LLW No. and UCN-2822 Doc. No. are entered and that Columns 1 through 16 and Notes 1 through 3 are filled out completely and legibly.

2. The RSWO representative must sign at the bottom of the page prior to waste transfer to the SWSA.

Fig. A.2. Form UCN-16114, "Log-in Data Sheet for Generators of Solid Low-Level Radioactive Waste" and instructions.

UCN-16114 Log-In Data Sheet for Generators of SLLW

Page 1 of

LLW Container Bar Code Number:	UCN-2822 Doc. No

Pkt No.	Date	Weight (lbs)	Pkt. Origin Bldg/Room No.	Dose Rate mRem/hr	Isotope	Isotope	Isotope	Isotope	Isotope	Isotope	Physical Desc. (glass, paper, etc)	Chemical Form	RCRA (Yes/ No)	Generator's Signature	Badge No.
					Ci or Gms	Ci or Gms	Ci or Gms	Ci or Gms	Ci or Gms	Ci or Gms					

1. Drum closure: If waste is packaged in a 55-Gal drum, the gasket has been put in place and the closure ring bolt tightened to 45 ft-lbs. (Signature of individual who tightened closure ring) _____

2. Are TRU wastes generated in the areas of waste generation listed on these forms? (GCO sign) ___ Yes ___ No _____

3. GCO Signature - Certifies that the waste was packaged in accordance with the Waste Acceptance Criteria, ORNL SLLW Certification Program Plan, and SLLW QA Plan requirements. (GCO must be MMES employee) Badge: _____ _____

Radioactive Solid Waste Operations

RSWO AUTHORIZED SIGNATURE	BADGE NO.	Date

UCN-16114 Rev. 04
1-14-93

DISTRIBUTION:
WHITE - SWSA FOREMAN FORWARDS TO DMC
BLUE - RETAINED BY SWSA FOREMAN
CANARY - RETAINED BY GENERATOR

UCN-16114a Log-In Data Sheet for Generators of SLLW (Continuation)

Page of

LLW Container
Bar Code Number:

UCN-2822 Doc. No

Pkt No.	Date	Weight Lbs	Pkt. Origin Bldg/Room No.	Dose Rate mRem/hr	Isotope	Isotope	Isotope	Isotope	Isotope	Isotope	Physical Desc. (glass, paper, etc)	Chemical Form	RCRA (Yes/No)	Generator's Signature	Badge
					Ci or Gms	Ci or Gms	Ci or Gms	Ci or Gms	Ci or Gms	Ci or Gms					

Radioactive Solid Waste Operations

RSWO AUTHORIZED SIGNATURE	BADGE NO.	Date

UCN-16114A Rev. 04
1-14-93

DISTRIBUTION:
WHITE - SWSA FOREMAN FORWARDS TO DMC
BLUE - RETAINED BY SWSA FOREMAN
CANARY - RETAINED BY GENERATOR

Table A.1. Solid Waste Storage Area Waste 6 inventory data (9/88–3/92)

Disposal Unit	Number of Units	Volume (m^3)	Radioactivity (Ci)
Tumulus I vaults	197	535	29.4
Tumulus II vaults	220	601	26.9
Interim Waste Management Facility vaults[a]	140	381	21.6
Low-range silos	75	594	23.6
High-range silos	33	286	86.2
Asbestos silos	11	108	0.109
High-range wells	54	15.6	6734
Fissile wells	1	0.6	42.5
Biological trenches	5	208	0.016
Suspect waste landfill	1	1756	0

[a]Interim Waste Management Facility data includes waste disposed of from December 1991 through June 1992.

Table A.2. Solid Waste Storage Area 6 disposal units

Disposal unit	Current number (9/88–3/92)	Projected number (4/92–12/97)	Total
Tumulus I vaults	197	0	197
Tumulus II vaults	220	0	220
Interim Waste Management Facility (IWMF) vaults	140[a]	1840[b]	1980
Low-range silos (north)	23	0	23
Low-range silos (south)	52	38	90
High-range silos	33	17	50
Asbestos silos	11	6	17
High-range wells	12	0	12
High-range wells in silos[c]	42	0	42
Fissile wells	1	0	1
Biological trenches	5	1	6
Suspect landfill	1	0	1

[a]IWMF disposal from December 1991 through June 1992.
[b]IWMF projected disposal from July 1992 through December 1997.
[c]There are a total of six silos, each containing seven high-range wells.

Table A.3. Reported radionuclide inventory for Tumulus I[a]

Nuclide	Half-life (days)	Radioactivity (Ci)	Specific activity (Ci/g)	Mass (g)
^{3}H	4.50×10^{3}	2.70×10^{0}	9.65×10^{3}	2.80×10^{-4}
^{14}C	2.09×10^{6}	1.95×10^{-2}	4.46×10^{0}	4.38×10^{-3}
^{22}Na	9.50×10^{2}	1.70×10^{-2}	6.25×10^{3}	2.72×10^{-6}
^{35}S	8.75×10^{1}	2.67×10^{-4}	4.26×10^{4}	6.26×10^{-9}
^{39}Ar	9.83×10^{4}	1.30×10^{-3}	3.41×10^{1}	3.81×10^{-5}
^{43}K	9.29×10^{-1}	8.30×10^{-4}	3.27×10^{6}	2.54×10^{-10}
^{51}Cr	2.77×10^{1}	1.50×10^{-2}	9.24×10^{4}	1.62×10^{-7}
^{54}Mn	3.12×10^{2}	1.50×10^{-2}	7.74×10^{3}	1.94×10^{-6}
^{55}Fe	9.97×10^{2}	5.00×10^{-2}	2.50×10^{3}	2.00×10^{-5}
^{59}Fe	4.45×10^{1}	1.00×10^{-2}	4.92×10^{4}	2.03×10^{-7}
^{57}Co	2.72×10^{2}	1.10×10^{-2}	8.46×10^{3}	1.30×10^{-6}
^{60}Co	1.93×10^{3}	3.92×10^{0}	1.13×10^{3}	3.47×10^{-3}
^{63}Ni	3.66×10^{4}	2.02×10^{-1}	6.17×10^{1}	3.27×10^{-3}
^{64}Cu	5.29×10^{-1}	9.03×10^{-3}	3.86×10^{6}	2.34×10^{-9}
^{68}Ge	2.71×10^{2}	5.86×10^{-2}	7.09×10^{3}	8.27×10^{-6}
^{85}Kr	3.92×10^{3}	2.36×10^{-2}	3.92×10^{2}	6.02×10^{-5}
^{85}Sr	6.48×10^{1}	3.00×10^{-3}	2.37×10^{4}	1.27×10^{-7}
^{90}Sr	1.04×10^{4}	3.31×10^{0}	1.36×10^{2}	2.43×10^{-2}
^{90}Y	2.67×10^{0}	3.91×10^{-2}	5.44×10^{5}	7.19×10^{-8}
^{95}Zr	6.40×10^{1}	5.50×10^{-5}	2.15×10^{4}	2.56×10^{-9}
^{99}Tc	7.78×10^{7}	2.34×10^{-3}	1.70×10^{-2}	1.38×10^{-1}
^{106}Ru	3.73×10^{2}	1.70×10^{-4}	3.35×10^{3}	5.08×10^{-8}
^{103}Pd	1.70×10^{1}	1.25×10^{-3}	7.47×10^{4}	1.67×10^{-8}
^{119m}Sn	2.93×10^{2}	3.50×10^{-2}	4.48×10^{3}	7.82×10^{-6}
^{125}I	6.01×10^{1}	7.09×10^{-2}	1.74×10^{4}	4.08×10^{-6}
^{131}I	8.04×10^{0}	2.95×10^{-2}	1.24×10^{5}	2.38×10^{-7}

Table A.3. (continued)

Nuclide	Half-life (days)	Radioactivity (Ci)	Specific activity (Ci/g)	Mass (g)
^{134}Cs	7.53×10^{2}	6.36×10^{-1}	1.29×10^{3}	4.91×10^{-4}
^{137}Cs	1.10×10^{4}	1.40×10^{1}	8.70×10^{1}	1.61×10^{-1}
^{147}Pm	9.58×10^{2}	4.50×10^{-1}	9.27×10^{2}	4.85×10^{-4}
^{152}Eu	4.87×10^{3}	4.85×10^{-1}	1.73×10^{2}	2.81×10^{-3}
^{154}Eu	3.21×10^{3}	7.89×10^{-1}	2.70×10^{2}	2.92×10^{-3}
^{153}Gd	2.42×10^{2}	6.97×10^{-1}	3.53×10^{3}	1.98×10^{-4}
^{182}Ta	1.15×10^{2}	1.53×10^{-3}	6.25×10^{3}	2.45×10^{-7}
^{188}W	6.94×10^{1}	1.70×10^{-3}	1.00×10^{4}	1.70×10^{-7}
^{191}Os	1.54×10^{1}	6.44×10^{-2}	4.44×10^{4}	1.45×10^{-6}
^{192}Ir	7.38×10^{1}	1.57×10^{0}	9.21×10^{3}	1.70×10^{-4}
^{204}Tl	1.38×10^{3}	5.00×10^{-2}	4.64×10^{2}	1.08×10^{-4}
^{210}Pb	8.15×10^{3}	1.71×10^{-2}	7.64×10^{1}	2.24×10^{-4}
^{226}Ra	5.84×10^{5}	1.70×10^{-3}	9.89×10^{-1}	1.72×10^{-3}
^{228}Th	6.99×10^{2}	9.01×10^{-4}	8.20×10^{2}	1.10×10^{-6}
^{232}Th	5.13×10^{12}	1.66×10^{-4}	1.10×10^{-7}	1.51×10^{3}
^{232}U	2.52×10^{4}	1.60×10^{-5}	2.14×10^{1}	7.48×10^{-7}
^{233}U	5.81×10^{7}	1.02×10^{-2}	9.68×10^{-3}	1.05×10^{0}
^{235}U	2.57×10^{11}	1.51×10^{-4}	2.16×10^{-6}	6.99×10^{1}
^{238}U	1.63×10^{12}	2.28×10^{-3}	3.36×10^{-7}	6.78×10^{3}
^{238}Pu	3.20×10^{4}	5.10×10^{-4}	1.71×10^{1}	2.98×10^{-5}
^{239}Pu	8.81×10^{6}	1.17×10^{-2}	6.22×10^{-2}	1.88×10^{-1}
^{240}Pu	2.40×10^{6}	6.80×10^{-3}	2.28×10^{-1}	2.98×10^{-2}
^{241}Am	1.58×10^{5}	2.23×10^{-2}	3.43×10^{0}	6.50×10^{-3}
^{243}Am	2.70×10^{6}	2.21×10^{-3}	1.99×10^{-1}	1.11×10^{-2}
^{243}Cm	1.04×10^{4}	1.10×10^{-5}	5.16×10^{1}	2.13×10^{-7}
^{244}Cm	6.61×10^{3}	2.45×10^{-2}	8.09×10^{1}	3.03×10^{-4}
^{249}Cf	1.28×10^{5}	1.11×10^{-4}	4.10×10^{0}	2.71×10^{-5}
^{252}Cf	9.66×10^{2}	3.00×10^{-5}	5.38×10^{2}	5.58×10^{-8}

[a]Inventory based on 197 vaults.

Table A.4. Reported radionuclide inventory for Tumulus II[a]

Nuclide	Half-life (days)	Radioactivity (Ci)	Specific activity (Ci/g)	Mass (g)
^{3}H	4.50×10^{3}	1.51×10^{0}	9.65×10^{3}	1.56×10^{-4}
^{14}C	2.09×10^{6}	4.24×10^{-3}	4.46×10^{0}	9.51×10^{-4}
^{22}Na	9.50×10^{2}	1.10×10^{-3}	6.25×10^{3}	1.76×10^{-7}
^{35}S	8.75×10^{1}	7.00×10^{-4}	4.26×10^{4}	1.64×10^{-8}
^{55}Fe	9.97×10^{2}	4.00×10^{-3}	2.50×10^{3}	1.60×10^{-6}
^{60}Co	1.93×10^{3}	3.60×10^{0}	1.13×10^{3}	3.18×10^{-3}
^{68}Ge	2.71×10^{2}	2.80×10^{-3}	7.09×10^{3}	3.95×10^{-7}
^{90}Sr	1.04×10^{4}	7.96×10^{0}	1.36×10^{2}	5.84×10^{-2}
^{90}Y	2.67×10^{0}	2.68×10^{-2}	5.44×10^{5}	4.93×10^{-8}
^{95m}Tc	6.10×10^{1}	1.00×10^{-4}	2.25×10^{4}	4.44×10^{-9}
^{99}Tc	7.78×10^{7}	1.62×10^{-2}	1.70×10^{-2}	9.56×10^{-1}
^{103}Pd	1.70×10^{1}	1.70×10^{-4}	7.47×10^{4}	2.28×10^{-9}
^{125}I	6.01×10^{1}	1.24×10^{-2}	1.74×10^{4}	7.14×10^{-7}
^{137}Cs	1.10×10^{4}	1.29×10^{1}	8.70×10^{1}	1.48×10^{-1}
^{152}Eu	4.87×10^{3}	2.08×10^{-1}	1.73×10^{2}	1.20×10^{-3}
^{154}Eu	3.21×10^{3}	1.08×10^{-1}	2.70×10^{2}	4.00×10^{-4}
^{153}Gd	2.42×10^{2}	1.41×10^{-1}	3.53×10^{3}	4.00×10^{-5}
^{179}Ta	6.54×10^{2}	3.40×10^{-3}	1.12×10^{3}	3.05×10^{-6}
^{191}Os	1.54×10^{1}	6.84×10^{-2}	4.44×10^{4}	1.54×10^{-6}
^{194}Os	2.19×10^{3}	9.52×10^{-2}	3.07×10^{2}	3.10×10^{-4}
^{192}Ir	7.38×10^{1}	5.58×10^{-2}	9.21×10^{3}	6.06×10^{-6}
^{210}Po	1.38×10^{2}	4.47×10^{-2}	4.49×10^{3}	9.95×10^{-6}
^{232}Th	5.13×10^{12}	5.02×10^{-4}	1.10×10^{-7}	4.58×10^{3}
^{232}U	2.52×10^{4}	1.00×10^{-6}	2.14×10^{1}	4.67×10^{-8}
^{233}U	5.81×10^{7}	4.15×10^{-2}	9.68×10^{-3}	4.29×10^{0}
^{235}U	2.57×10^{11}	7.00×10^{-6}	2.16×10^{-6}	3.24×10^{0}
^{238}U	1.63×10^{12}	1.14×10^{-3}	3.36×10^{-7}	3.39×10^{3}
^{238}Pu	3.20×10^{4}	5.77×10^{-4}	1.71×10^{1}	3.37×10^{-5}
^{239}Pu	8.81×10^{6}	1.06×10^{-2}	6.22×10^{-2}	1.71×10^{-1}
^{241}Am	1.58×10^{5}	1.25×10^{-2}	3.43×10^{0}	3.64×10^{-3}
^{244}Am	4.21×10^{-1}	6.10×10^{-4}	1.27×10^{6}	4.79×10^{-10}
^{244}Cm	6.61×10^{3}	1.94×10^{-2}	8.09×10^{1}	2.40×10^{-4}

[a]Inventory based on 220 vaults.

Table A.5. Reported radionuclide inventory for Interim Waste Managment Facility[a]

Nuclide	Half-life (days)	Radioactivity (Ci)	Specific activity (Ci/g)	Mass (g)
^{3}H	4.50×10^{3}	4.10×10^{-2}	9.65×10^{3}	4.25×10^{-6}
^{14}C	2.09×10^{6}	3.10×10^{-2}	4.46×10^{0}	6.96×10^{-3}
^{26}Al	2.63×10^{8}	1.00×10^{-3}	1.91×10^{-2}	5.24×10^{-2}
^{32}P	1.43×10^{1}	1.60×10^{-3}	2.85×10^{5}	5.61×10^{-9}
^{33}P	2.53×10^{1}	1.50×10^{-3}	1.56×10^{5}	9.61×10^{-9}
^{36}Cl	1.10×10^{8}	8.50×10^{-3}	3.30×10^{-2}	2.58×10^{-1}
^{40}K	4.66×10^{11}	6.60×10^{-4}	5.65×10^{-6}	1.17×10^{2}
^{51}Cr	2.77×10^{1}	8.30×10^{-2}	9.24×10^{4}	8.98×10^{-7}
^{55}Fe	9.97×10^{2}	1.83×10^{-3}	2.50×10^{3}	7.32×10^{-7}
^{60}Co	1.93×10^{3}	9.90×10^{-1}	1.13×10^{3}	8.75×10^{-4}
^{63}Ni	3.66×10^{4}	1.70×10^{-2}	6.17×10^{1}	2.76×10^{-4}
^{64}Cu	5.29×10^{-1}	1.40×10^{-3}	3.86×10^{6}	3.63×10^{-10}
^{85}Kr	3.92×10^{3}	4.03×10^{-3}	3.92×10^{2}	1.03×10^{-5}
^{90}Sr	1.04×10^{4}	3.50×10^{0}	1.36×10^{2}	2.57×10^{-2}
^{90}Y	2.67×10^{0}	9.70×10^{-5}	5.44×10^{5}	1.78×10^{-10}
^{99}Tc	7.78×10^{7}	3.40×10^{-4}	1.70×10^{-2}	2.01×10^{-2}
^{125}I	6.01×10^{1}	4.98×10^{-3}	1.74×10^{4}	2.87×10^{-7}
^{131}I	8.04×10^{0}	1.88×10^{-3}	1.24×10^{5}	1.52×10^{-8}
^{134}Cs	7.53×10^{2}	5.79×10^{-3}	1.29×10^{3}	4.47×10^{-6}
^{137}Cs	1.10×10^{4}	8.50×10^{0}	8.70×10^{1}	9.77×10^{-2}
^{147}Pm	9.58×10^{2}	2.19×10^{0}	9.27×10^{2}	2.36×10^{-3}
^{152}Eu	4.87×10^{3}	8.60×10^{-1}	1.73×10^{2}	4.97×10^{-3}
^{154}Eu	3.21×10^{3}	3.90×10^{-3}	2.70×10^{2}	1.44×10^{-5}
^{153}Gd	2.42×10^{2}	4.49×10^{-2}	3.53×10^{3}	1.27×10^{-5}
^{182}Ta	1.15×10^{2}	5.06×10^{-3}	6.25×10^{3}	8.09×10^{-7}
^{188}W	6.94×10^{1}	1.71×10^{-1}	1.00×10^{4}	1.71×10^{-5}
^{191}Os	1.54×10^{1}	3.23×10^{-3}	4.44×10^{4}	7.28×10^{-8}

Table A.5. (continued)

Nuclide	Half-life (days)	Radioactivity (Ci)	Specific activity (Ci/g)	Mass (g)
^{192}Ir	7.38×10^{1}	2.08×10^{-3}	9.21×10^{3}	2.26×10^{-7}
^{210}Pb	8.15×10^{3}	4.00×10^{-4}	7.64×10^{1}	5.24×10^{-6}
^{232}Th	5.13×10^{12}	6.00×10^{-5}	1.10×10^{-7}	5.47×10^{2}
^{233}U	5.81×10^{7}	1.10×10^{-3}	9.68×10^{-3}	1.14×10^{-1}
^{235}U	2.57×10^{11}	3.60×10^{-5}	2.16×10^{-6}	1.67×10^{1}
^{238}U	1.63×10^{12}	2.70×10^{-3}	3.36×10^{-7}	8.03×10^{3}
^{239}Pu	8.81×10^{6}	6.00×10^{-4}	6.22×10^{-2}	9.65×10^{-3}
^{242}Pu	1.37×10^{8}	1.00×10^{-6}	3.82×10^{-3}	2.62×10^{-4}
^{241}Am	1.58×10^{5}	2.20×10^{-4}	3.43×10^{0}	6.41×10^{-5}
^{243}Am	2.70×10^{6}	1.50×10^{-4}	1.99×10^{-1}	7.53×10^{-4}
^{244}Cm	6.61×10^{3}	2.40×10^{-2}	8.09×10^{1}	2.97×10^{-4}

[a]Inventory based on 140 vaults.

Table A.6. Reported radionuclide inventory for low-range silos[a]

Nuclide	Atomic number	Half-life (days)	Radioactivity (Ci)	Specific activity (Ci/g)	Mass (g)
^{3}H	1	4.50×10^{3}	1.02×10^{1}	9.65×10^{3}	1.06×10^{-3}
^{14}C	6	2.09×10^{6}	7.23×10^{-2}	4.46×10^{0}	1.62×10^{-2}
^{22}Na	11	9.50×10^{2}	1.70×10^{-4}	6.25×10^{3}	2.72×10^{-8}
^{40}K	19	4.66×10^{11}	1.76×10^{-4}	5.65×10^{-6}	3.12×10^{1}
^{59}Fe	26	4.45×10^{1}	1.37×10^{-3}	4.92×10^{4}	2.79×10^{-8}
^{60}Co	27	1.93×10^{3}	1.03×10^{0}	1.13×10^{3}	9.11×10^{-4}
^{90}Sr	38	1.04×10^{4}	2.67×10^{0}	1.36×10^{2}	1.96×10^{-2}
^{90}Y	39	2.67×10^{0}	4.59×10^{0}	5.44×10^{5}	8.44×10^{-6}
^{99}Tc	43	7.78×10^{7}	7.59×10^{-3}	1.70×10^{-2}	4.48×10^{-1}
^{125}I	53	6.01×10^{1}	1.74×10^{-4}	1.74×10^{4}	1.00×10^{-8}
^{131}I	53	8.04×10^{0}	1.05×10^{0}	1.24×10^{5}	8.47×10^{-6}

Table A.6. (continued)

Nuclide	Atomic number	Half-life (days)	Radioactivity (Ci)	Specific activity (Ci/g)	Mass (g)
^{137}Cs	55	1.10×10^{4}	3.23×10^{0}	8.70×10^{1}	3.71×10^{-2}
^{147}Pm	61	9.58×10^{2}	4.24×10^{-2}	9.27×10^{2}	4.57×10^{-5}
^{152}Eu	63	4.87×10^{3}	1.38×10^{-3}	1.73×10^{2}	7.98×10^{-6}
^{154}Eu	63	3.21×10^{3}	5.10×10^{-4}	2.70×10^{2}	1.89×10^{-6}
^{153}Gd	64	2.42×10^{2}	7.82×10^{-3}	3.53×10^{3}	2.22×10^{-6}
^{179}Ta	73	6.54×10^{2}	1.70×10^{-3}	1.12×10^{3}	1.52×10^{-6}
^{191}Os	76	1.54×10^{1}	1.70×10^{-5}	4.44×10^{4}	3.83×10^{-10}
^{192}Ir	77	7.38×10^{1}	1.91×10^{-1}	9.21×10^{3}	2.07×10^{-5}
^{197}Pt	78	7.63×10^{-1}	1.70×10^{-4}	8.69×10^{5}	1.96×10^{-10}
^{226}Ra	88	5.84×10^{5}	6.40×10^{-3}	9.89×10^{-1}	6.48×10^{-3}
^{228}Th	90	6.99×10^{2}	6.00×10^{-6}	8.20×10^{2}	7.32×10^{-9}
^{229}Th	90	2.68×10^{6}	1.70×10^{-4}	2.13×10^{-1}	7.99×10^{-4}
^{230}Th	90	2.75×10^{7}	1.17×10^{-3}	2.11×10^{-2}	5.55×10^{-2}
^{232}Th	90	5.13×10^{12}	1.14×10^{-3}	1.10×10^{-7}	1.04×10^{4}
^{233}U	92	5.81×10^{7}	6.71×10^{-2}	9.68×10^{-3}	6.93×10^{0}
^{234}U	92	8.96×10^{7}	1.21×10^{-4}	6.25×10^{-3}	1.94×10^{-2}
^{235}U	92	2.57×10^{11}	1.90×10^{-5}	2.16×10^{-6}	8.79×10^{0}
^{236}U	92	8.55×10^{9}	6.60×10^{-5}	6.47×10^{-5}	1.02×10^{0}
^{238}U	92	1.63×10^{12}	1.12×10^{-2}	3.36×10^{-7}	3.33×10^{4}
^{237}Np	93	7.82×10^{8}	1.70×10^{-4}	7.05×10^{-4}	2.41×10^{-1}
^{238}Pu	94	3.20×10^{4}	9.81×10^{-4}	1.71×10^{1}	5.73×10^{-5}
^{239}Pu	94	8.81×10^{6}	9.00×10^{-4}	6.22×10^{-2}	1.45×10^{-2}
^{241}Am	95	1.58×10^{5}	7.84×10^{-3}	3.43×10^{0}	2.28×10^{-3}
^{243}Am	95	2.70×10^{6}	6.21×10^{-3}	1.99×10^{-1}	3.12×10^{-2}
^{244}Cm	96	6.61×10^{3}	2.70×10^{-2}	8.09×10^{1}	3.34×10^{-4}
^{249}Cf	98	1.28×10^{5}	1.10×10^{-4}	4.10×10^{0}	2.68×10^{-5}
^{252}Cf	98	9.66×10^{2}	6.80×10^{-3}	5.38×10^{2}	1.26×10^{-5}

[a]Inventory based on 75 silos.

Table A.7. Reported radionuclide inventory for high-range silos[a]

Nuclide	Half-life (days)	Radioactivity (Ci)	Specific activity (Ci/g)	Mass (g)
^{3}H	4.50×10^{3}	1.00×10^{1}	9.65×10^{3}	1.04×10^{-3}
^{14}C	2.09×10^{6}	4.11×10^{-2}	4.46×10^{0}	9.22×10^{-3}
^{22}Na	9.50×10^{2}	2.30×10^{-4}	6.25×10^{3}	3.68×10^{-8}
^{32}P	1.43×10^{1}	8.50×10^{-5}	2.85×10^{5}	2.98×10^{-10}
^{40}K	4.66×10^{11}	1.70×10^{-3}	5.65×10^{-6}	3.01×10^{2}
^{54}Mn	3.12×10^{2}	2.21×10^{-2}	7.74×10^{3}	2.86×10^{-6}
^{55}Fe	9.97×10^{2}	1.70×10^{-3}	2.50×10^{3}	6.80×10^{-7}
^{59}Fe	4.45×10^{1}	5.03×10^{-1}	4.92×10^{4}	1.02×10^{-5}
^{60}Co	1.93×10^{3}	1.31×10^{1}	1.13×10^{3}	1.16×10^{-2}
^{63}Ni	3.66×10^{4}	8.30×10^{-2}	6.17×10^{1}	1.35×10^{-3}
^{64}Cu	5.29×10^{-1}	6.65×10^{-2}	3.86×10^{6}	1.72×10^{-8}
^{90}Sr	1.04×10^{4}	2.31×10^{1}	1.36×10^{2}	1.69×10^{-1}
^{90}Y	2.67×10^{0}	2.18×10^{0}	5.44×10^{5}	4.01×10^{-6}
^{103}Pd	1.70×10^{1}	2.86×10^{0}	7.47×10^{4}	3.83×10^{-5}
^{111m}Ag	7.50×10^{-4}	1.00×10^{-1}	1.56×10^{9}	6.39×10^{-11}
^{137}Cs	1.10×10^{4}	2.57×10^{1}	8.70×10^{1}	2.95×10^{-1}
^{147}Pm	9.58×10^{2}	2.38×10^{-4}	9.27×10^{2}	2.57×10^{-7}
^{152}Eu	4.87×10^{3}	1.24×10^{0}	1.73×10^{2}	7.17×10^{-3}
^{154}Eu	3.21×10^{3}	5.55×10^{-2}	2.70×10^{2}	2.06×10^{-4}
^{155}Eu	1.81×10^{3}	2.90×10^{-2}	4.65×10^{2}	6.24×10^{-5}
^{153}Gd	2.42×10^{2}	7.87×10^{-1}	3.53×10^{3}	2.23×10^{-4}
^{179}Ta	6.54×10^{2}	8.30×10^{-2}	1.12×10^{3}	7.44×10^{-5}
^{182}Ta	1.15×10^{2}	2.11×10^{0}	6.25×10^{3}	3.37×10^{-4}
^{191}Os	1.54×10^{1}	5.25×10^{-2}	4.44×10^{4}	1.18×10^{-6}
^{192}Ir	7.38×10^{1}	3.43×10^{0}	9.21×10^{3}	3.72×10^{-4}
^{230}Th	2.75×10^{7}	1.00×10^{-6}	2.11×10^{-2}	4.74×10^{-5}
^{232}Th	5.13×10^{12}	1.36×10^{-4}	1.10×10^{-7}	1.24×10^{3}
^{235}U	2.57×10^{11}	1.00×10^{-6}	2.16×10^{-6}	4.63×10^{-1}
^{238}U	1.63×10^{12}	9.96×10^{-3}	3.36×10^{-7}	2.96×10^{4}
^{239}Pu	8.81×10^{6}	1.01×10^{-3}	6.22×10^{-2}	1.62×10^{-2}
^{244}Cm	6.61×10^{3}	5.11×10^{-1}	8.09×10^{1}	6.32×10^{-3}

[a]Inventory based on 33 silos.

Table A.8. Reported radionuclide inventory for asbestos silos[a]

Nuclide	Half-life (days)	Radioactivity (Ci)	Specific activity (Ci/g)	Mass (g)
^{3}H	4.50×10^{3}	1.00×10^{-3}	9.65×10^{3}	1.04×10^{-7}
^{14}C	2.09×10^{6}	5.79×10^{-4}	4.46×10^{0}	1.30×10^{-4}
^{60}Co	1.93×10^{3}	4.98×10^{-3}	1.13×10^{3}	4.40×10^{-6}
^{90}Sr	1.04×10^{4}	4.24×10^{-2}	1.36×10^{2}	3.11×10^{-4}
^{99}Tc	7.78×10^{7}	1.20×10^{-3}	1.70×10^{-2}	7.08×10^{-2}
^{137}Cs	1.10×10^{4}	5.67×10^{-2}	8.70×10^{1}	6.52×10^{-4}
^{152}Eu	4.87×10^{3}	1.00×10^{-3}	1.73×10^{2}	5.78×10^{-6}
^{154}Eu	3.21×10^{3}	1.00×10^{-5}	2.70×10^{2}	3.71×10^{-8}
^{192}Ir	7.38×10^{1}	2.60×10^{-4}	9.21×10^{3}	2.82×10^{-8}
^{232}Th	5.13×10^{12}	4.30×10^{-5}	1.10×10^{-7}	3.92×10^{2}
^{233}U	5.81×10^{7}	1.02×10^{-4}	9.68×10^{-3}	1.05×10^{-2}
^{238}U	1.63×10^{12}	2.71×10^{-4}	3.36×10^{-7}	8.06×10^{2}
^{244}Cm	6.61×10^{3}	3.20×10^{-5}	8.09×10^{1}	3.96×10^{-7}

[a]Inventory based on 11 silos.

Table A.9. Reported radionuclide inventory for high-range wells[a]

Nuclide	Half-life (days)	Radioactivity (Ci)	Specific activity (Ci/g)	Mass (g)
^{14}C	2.09×10^{6}	1.00×10^{-6}	4.46×10^{0}	2.24×10^{-7}
^{54}Mn	3.12×10^{2}	3.32×10^{1}	7.74×10^{3}	4.29×10^{-3}
^{59}Fe	4.45×10^{1}	2.80×10^{1}	4.92×10^{4}	5.69×10^{-4}
^{58}Co	7.09×10^{1}	3.80×10^{1}	3.18×10^{4}	1.19×10^{-3}
^{60}Co	1.93×10^{3}	2.15×10^{3}	1.13×10^{3}	1.90×10^{0}
^{68}Ge	2.71×10^{2}	5.00×10^{-3}	7.09×10^{3}	7.05×10^{-7}
^{90}Sr	1.04×10^{4}	1.36×10^{3}	1.36×10^{2}	9.97×10^{0}
^{99}Tc	7.78×10^{7}	4.00×10^{-1}	1.70×10^{-2}	2.36×10^{1}
^{113m}Cd	5.00×10^{3}	1.30×10^{1}	2.17×10^{2}	6.00×10^{-2}
^{134}Cs	7.53×10^{2}	1.22×10^{0}	1.29×10^{3}	9.43×10^{-4}
^{137}Cs	1.10×10^{4}	1.40×10^{3}	8.70×10^{1}	1.61×10^{1}
^{152}Eu	4.87×10^{3}	1.12×10^{3}	1.73×10^{2}	6.48×10^{0}
^{154}Eu	3.21×10^{3}	5.81×10^{2}	2.70×10^{2}	2.15×10^{0}
^{182}Ta	1.15×10^{2}	3.60×10^{0}	6.25×10^{3}	5.76×10^{-4}

Table A.9 (continued)

Nuclide	Half-life (days)	Radioactivity (Ci)	Specific activity (Ci/g)	Mass (g)
^{192}Ir	7.38×10^{1}	2.39×10^{1}	9.21×10^{3}	2.59×10^{-3}
^{229}Th	2.68×10^{6}	7.50×10^{-3}	2.13×10^{-1}	3.53×10^{-2}
^{232}Th	5.13×10^{12}	3.70×10^{-5}	1.10×10^{-7}	3.37×10^{2}
^{235}U	2.57×10^{11}	1.00×10^{-6}	2.16×10^{-6}	4.63×10^{-1}
^{238}U	1.63×10^{12}	4.00×10^{-6}	3.36×10^{-7}	1.19×10^{1}

[a]Inventory based on 54 wells.

Table A.10. Reported radionuclide inventory for fissile waste[a]

Nuclide	Half-life (days)	Radioactivity (Ci)	Specific activity (Ci/g)	Mass (g)
^{137}Cs	1.10×10^{4}	4.25×10^{1}	8.70×10^{1}	4.89×10^{-1}
^{235}U	2.57×10^{11}	8.75×10^{-4}	2.16×10^{-6}	4.05×10^{2}
^{238}U	1.63×10^{12}	4.83×10^{-3}	3.36×10^{-7}	1.44×10^{4}

[a]Inventory based on 1 well.

Table A.11. Reported radionuclide inventory for biological trenches[a]

Nuclide	Half-life (days)	Radioactivity (Ci)	Specific activity (Ci/g)	Mass (g)
^{3}H	4.50×10^{3}	1.80×10^{-4}	9.65×10^{3}	1.87×10^{-8}
^{14}C	2.09×10^{6}	1.70×10^{-4}	4.46×10^{0}	3.81×10^{-5}
^{60}Co	1.93×10^{3}	2.20×10^{-5}	1.13×10^{3}	1.95×10^{-8}
^{90}Sr	1.04×10^{4}	1.04×10^{-2}	1.36×10^{2}	7.62×10^{-5}
^{125}I	6.01×10^{1}	2.37×10^{-3}	1.74×10^{4}	1.36×10^{-7}
^{131}I	8.04×10^{0}	6.90×10^{-4}	1.24×10^{5}	5.56×10^{-9}
^{137}Cs	1.10×10^{4}	2.25×10^{-3}	8.70×10^{1}	2.59×10^{-5}

[a]Inventory based on 5 trenches.

A.2 EVALUATION OF UNCERTAINTY IN THE INVENTORY DATA FOR SOLID WASTE STORAGE AREA 6

A.2.1 Purpose

The purpose of this task is to provide technical assistance to Oak Ridge National Laboratory's (ORNL's) Waste Management and Remedial Action Division in evaluating uncertainties in the radioactive inventory of low level radioactive waste (LLW) disposed of after September 26, 1988, in Solid Waste Storage Area (SWSA) 6. The results of this task have been used in the overall uncertainty analysis of the SWSA 6 radiological performance assessment.

A.2.2 Background

U.S. Department of Energy (DOE) Order 5820.2A, "Management of Low-Level Radioactive Waste," Chapter III, requires field organizations with LLW disposal sites to prepare a site-specific performance assessment to demonstrate disposal site compliance with the performance objectives stated in the order.

ORNL submitted a draft performance assessment in September 1990 to DOE for review. In March 1991, DOE-Headquarters' LLW Peer Review Panel completed their preliminary review. Their comments and recommendations for the final performance assessment were issued to DOE-Headquarters in April 1991. One recommendation of the Peer Review Panel was to determine the potential radiological dose impact due to uncertainty in the SWSA 6 transport and dose models. The radionuclide inventory is one of seven major model components evaluated in the SWSA 6 performance assessment uncertainty analysis.

The results of the draft performance assessment raised concerns regarding the concentration of several radionuclides disposed of at five of the seven SWSA 6 disposal units. Draft radionuclide concentration limits, developed in January 1991, were based upon the results of the draft performance assessment, which considers waste disposed of from September 1, 1988, until October 4, 1989, for estimating waste inventories over the projected period of facility operation. Based upon the total activity, volume, and concentration limit, key radionuclides were identified for which the concentration is of significance relative to its concentration limit. The final performance assessment considers waste disposed of from September 26, 1988, to December 31, 1997, for estimating waste inventories over the projected period of facility operation. The start date was revised from September 1 to September 26 to reflect the effective date of DOE Order 5820.2A. Some of the key radionuclides identified in the draft performance assessment were found to be relatively insignificant in the final performance assessment (e.g., ^{232}Th in low-range silos and ^{232}Th, ^{233}U, and ^{237}Np in tumulus vaults). This difference is due to errors found in the original inventory data for ^{232}Th in low-range silos and tumulus vaults and lower average concentrations due to increases in total waste volume versus small or no increase in activity. Nevertheless, other key radionuclides are still of concern because of the large inventory in disposal. The key radionuclides for the performance assessment are ^{90}Sr, ^{99}Tc, ^{137}Cs, and ^{152}Eu in high-range wells, ^{137}Cs, ^{235}U, ^{238}U in fissile wells, and ^{90}Sr in high-range

silos, low-range silos, tumulus vaults, and the Interim Waste Management Facility (IWMF).

The list of key radionuclides was expanded further for the purpose of this uncertainty analysis to include any radionuclide of interest that represented even a small fraction (>0.1%) of the concentration limit developed in the draft performance assessment (September 1990). This small fraction was chosen to ensure that a radionuclide reported with an apparently insignificant activity would not result in a significant dose impact due to a large error or uncertainty in this reported activity. This report will provide most probable values and associated uncertainty for all radionuclides of interest for each disposal unit. The radionuclides of interest are indicated in Table A.12. The disposal units include the asbestos silos, biological trenches, fissile wells, high-range silos, high-range wells, IWMF, low-range silos, Tumulus I, and Tumulus II.

A.2.3 Waste Generator Reporting Practices

Inspection of the available data recorded on form UCN-16114, "Log-In Data Sheet for Generators of LLW" and form UCN-2822, "Request for Disposal or Storage of Radioactive Solid Waste or Special Materials" reveals several pieces of information related to radionuclide activity. This information, its validity, and its usefulness in terms of activity estimation are discussed below.

A.2.3.1 Principal Isotopes

For most facilities, facility operations personnel inferred the listed isotopes based upon their knowledge of the facility operation or the material being processed. In general, it cannot be said with certainty that any specific package contained the specific radionuclide(s) reported. It also cannot be stated that a package did not contain additional radionuclides (other than the one(s) reported). On rare occasions, the waste was sampled and appropriate analyses were performed to specifically identify the radionuclides present. The identification of the principal isotope was straightforward for certain facilities that handled only specific isotopes and where the waste represented process waste. For many facilities, however, the waste form was contaminated components or irradiated materials that probably contained several different radionuclides. In these cases, the principal isotope identified in each waste package was the isotope or isotopes that were considered by the generator to be the most significant. This significance was typically based on an isotope's activity and radiological half-life. For example, the irradiated metal waste from Building 3525 (stainless-steel cladding hulls) contained a variety of activation products shortly after irradiation; but ^{60}Co was reported as the only principal isotope because it was the most significant in terms of activity, half-life, and radiation energy. In the case of Building 3517, the principal isotopes were listed as ^{137}Cs and ^{90}Sr. Operations personnel based this listing on the general operating history of the facility. Even though source production processes were operating in different hot cells, all packages of waste from the facility were considered to be composed of equal activities of ^{137}Cs and ^{90}Sr.

Table A.12. Significant radionuclides listed by disposal unit

Asbestos silos	Biological trench	Fissile wells	High-range silos	High-range wells	Interim Waste Management Facility	Low-range silos	Tumulus
^{3}H	^{3}H		^{3}H		^{3}H	^{3}H	^{3}H
						^{10}Be	
^{14}C			^{14}C		^{14}C	^{14}C	^{14}C
					^{26}Al		
					^{36}Cl		
				^{60}Co			
			^{63}Ni		^{63}Ni		^{63}Ni
^{90}Sr	^{90}Sr		^{90}Sr	^{90}Sr	^{90}Sr	^{90}Sr	^{90}Sr
^{99}Tc				^{99}Tc	^{99}Tc	^{99}Tc	^{99}Tc
^{137}Cs	^{137}Cs	^{137}Cs	^{137}Cs	^{137}Cs	^{137}Cs	^{137}Cs	^{137}Cs
			^{152}Eu	^{152}Eu	^{152}Eu		^{152}Eu
				^{154}Eu			
							^{226}Ra
				^{229}Th			

Table A.12 (continued)

Asbestos silos	Biological trench	Fissile wells	High-range silos	High-range wells	Interim Waste Management Facility	Low-range silos	Tumulus
						^{230}Th	
			^{232}Th	^{232}Th	^{232}Th	^{232}Th	^{232}Th
					^{233}U	^{233}U	^{233}U
		^{235}U					
^{238}U		^{238}U			^{238}U	^{238}U	^{238}U
			^{239}Pu		^{239}Pu	^{239}Pu	^{239}Pu
					^{241}Am	^{241}Am	^{241}Am
					^{243}Am	^{243}Am	^{243}Am

A.2.3.2 Radiation Survey Data for Waste Packages

Radiation survey data were obtained on waste packages using either in-cell probes or portable ion chambers. For the highly radioactive packages, in-cell probes were typically used whenever available. These measurements were made by facility operators and were normally taken in close proximity to the waste package. The distance was typically within 0.3 m (1 ft) from the surface of the package, but in the case of the 5-gal metal can—normally used by most isotope facilities for highly radioactive in-cell waste—this distance was within 0.3 m (1 ft) from the center of the can. It should be noted that the in-cell probes have not been calibrated since installation, and most have been in place for many years. The portable survey meters are calibrated semi-annually by Radiation Standards and Calibration Laboratory staff to an accuracy of $\pm 10\%$.

Some facilities did not have in-cell probes and were forced to rely on methods by which portable ion chambers were used in the measurement of large activity packages. In these cases, each facility used a method unique to that facility to obtain the measurements. Due to limitations imposed by the facility design and the range of the available portable instruments, measurements were taken at distances typically ranging from 1 to 3 m (3 to 10 ft). The distance to the container within the package was also somewhat uncertain. In these cases, however, facility personnel corrected the dose rate to a 0.3 m (1 ft) reading using an inverse square relationship (based upon the assumed distance from the dose point to the surface of the package) prior to multiplying by the conversion factor to determine the curie content.

For the low activity waste packages, most measurements were made by Radiation Protection staff using portable ion chambers. In the majority of these cases, dose rates were taken on small plastic bags of contaminated materials in very close proximity to (if not in contact with) the package surface. Particularly in these cases, the measurement was taken at several locations along the periphery of the bag, and the value recorded was the highest dose rate observed, not the average dose rate.

A.2.3.3 Quantity of the Principal Isotope

Most ORNL waste generators estimated the quantity of radioactive material in waste packages by multiplying the beta-gamma dose rate (as discussed above) for each waste packet by the conversion factors listed in the instructions for completing form UCN-16114, "Log-In Data Sheet for Generators of SLLW." If the waste was considered to be composed of a single radionuclide, the activity so calculated would be assigned to the principal radionuclide. If the generator considered multiple radionuclides to be present (as discussed above), the activity was equally divided among the radionuclides. Facilities such as Building 3517 split the total activity equally between ^{137}Cs and ^{90}Sr. As a general rule, facilities that reported both ^{137}Cs and ^{90}Sr assigned half of the total activity to each.

The 1 MeV photon dose rate to curie conversion factor was typically used in assigning activity to packages thought to contain radionuclides that emit only alpha or beta particles or very low energy gamma or x-rays (e.g., ^{3}H, ^{14}C, ^{63}Ni, ^{90}Sr, ^{99}Tc, ^{233}U, ^{238}U, ^{239}Pu, ^{241}Am, and ^{243}Am). In certain cases, however (typically those involving disposal of fissile material), the activity values were based upon those found on form UCN-2681, "ORNL Nuclear Materials Intra-Laboratory Transfer."

A.2.3.4 Radiation Survey Data for Waste Carriers

Initially, radiation survey data for waste carriers were considered a tool to verify the estimated package activities, but the manner in which surveys were taken and recorded varied considerably from package to package and facility to facility. Radiation Protection staff typically located and recorded the "hot spot" dose rate on the carrier, even though the survey was not always identified as such. The hot spot was usually a streaming pathway of some sort, associated with a joint or seam in the transport cask. For these reasons, calculating source activity in a package from the carrier dose rates was judged to be of doubtful value, and this approach was not used in the uncertainty analysis.

A.2.3.5 Package Weight

The weight of each package is also required on form UCN-16114, and the total weight is required for form UCN-2822. Facilities typically do not weigh each package of waste; instead, the package weight is usually estimated by facility personnel based on their knowledge of the package contents.

A.2.4 Shortcomings of the ORNL Dose Rate to Curie Conversion Factors

The table of conversion factors listed on the back of form UCN-16114 are provided to facilitate determination of the package activity based upon the measured dose rate. This dose rate to curie conversion factor was calculated at a distance of 0.3 m (1 ft) for a 1-Ci point source emitting a single 1 MeV photon per disintegration. This is the familiar $6\,C\,E\,n$ formula, with E = 1-MeV per photon and n = 1 photon per disintegration. Thus, the dose rate at 0.3 m (1 ft) from a 1-Ci point source is approximately 6 R/h. Conversely, a dose rate of approximately 1 R/h at 0.3 m (1 ft) is attributed to a 0.17 Ci point source. Thus, to determine the activity (in curies) of a point source, a conversion factor of 0.17 Ci/R/h (as used on form UCN-16114) is multiplied by the dose rate, in R/h, measured at 0.3 m (1 ft).

Using this conversion factor creates many potential sources of error. Some typical errors that could occur are provided in the following list.

- The radionuclide emits a gamma ray with an energy other than 1 MeV (E).
- The radionuclide emits a gamma ray with an abundance other than 1.0 (n).
- The exposure rate measurement was not taken at 0.3 m (1 ft).
- The waste package was not a point source.
- The radionuclide only emits alpha or beta particles or soft x-rays.

The first two factors are evident when considering the gamma factors or common radionuclides as listed in the *Radiological Health Handbook* (BRH 1970). The following table shows the dose rates at 0.3 m (1 ft) for a 1 Ci point source of each of the specified radionuclides.

Radionuclide	Dose Rate (R/hr)
^{137}Cs	3.55
^{60}Co	14.21
^{152}Eu	6.24
^{154}Eu	6.67
^{192}Ir	5.17

The ORNL conversion factor is based upon a dose rate of 6 R/h. The above table indicates, for example, that a 1 Ci ^{60}Co point source gives a dose rate that is a factor of 2.4 times greater than would be estimated from the ORNL factor. On the other hand, 3.55 R/h would be observed for a 1 Ci source of ^{137}Cs. This dose rate is only 59% of the 6 R/h used to calculate the ORNL conversion factor. The inverse of the factors in the table above would be used to determine the curie content of the specific radionuclide associated with a measured dose rate [at 0.3 m (1 ft)]. Using the ORNL conversion factor (0.17 Ci/R/hr), the ^{60}Co activity would be *overestimated* by a factor of 2.4, while the ^{137}Cs activity would be *underestimated* by a factor of 1.7. Activities of ^{152}Eu, ^{154}Eu, and ^{192}Ir would be more accurately represented (within 15%) using the ORNL conversion factor.

The above factors are, as indicated, for a distance of 0.3 m (1 ft) from a *point* source. For a point source, measurements taken at other distances, if not corrected to a 0.3-m (1-ft) reading, could introduce significant errors in the activity estimates, particularly for surveys taken in close proximity to the source. Measurements taken at distances less than 0.3 m (1 ft) from the source would lead to overestimates of source activity, while measurements at distances greater than 0.3 m (1 ft) would give an underestimate. These errors are in addition to those mentioned above for specific radionuclides.

Unfortunately, true point sources are rarely encountered in the field. High-activity radioactive materials are often disposed of in 5-gal metal cans. The cans are normally wrapped in several layers of plastic to avoid contamination of the carrier; consequently, measurements can be taken from no closer than a few inches from the wall of the can. Therefore, while the dose rate from a source such as the metal can will begin to approach that from a point source as the distance from the source increases, the use of a point source response dictates calculation of the dose rate using the distance to the *center* of the can, not the wall of the can. In the case of the metal can, measurements made with in-cell probes are typically made with the can near the detector, perhaps several inches from the surface of the can. With the can radius of 13 cm (5 in.), the probe could be placed perhaps 8-13 cm (3-5 in.) from the *wall* of the can, which would be 20-25 cm (8-10 in.) from the *center* of the can. This would result in a higher dose rate than would be

measured at 0.3 m (1 ft), which, for a point source, would overestimate the activity by factors ranging from 1.4 to 2.3.

For those cases in which the dose rate to curie conversion factor was applied to a survey measurement taken at a distance of 0.3 m (1 ft) from the *surface* of the can instead of the center of the can, the resulting activity would be underestimated. In the case of a measurement at 0.3 m (1 ft) from the surface of a metal can, the resulting activity would be underestimated by a factor of 2.0 because the distance to the center of the can would be 43 cm (17 in.). For larger waste containers, such as the 55-gal drum, this underestimation would be larger, depending on the particulars of the specific situation. For a 55-gal drum measured at 0.3 m (1 ft) from the drum surface, the curie content would be underestimated by a factor of 3.8.

At small distances, waste containers do not behave like point sources; furthermore, the definition of "small" depends upon the size of the particular container. A small distance for the metal can would be approximately 0.5 m (1.5 ft) measured from the *center* of the can. Surveys taken at points closer than this distance would result in higher dose rates per unit activity than would be observed for a point source at the same distance. At 20 cm (8 in.) from the center of the can [8 cm (3 in.) from the wall], the effects due to geometry give a dose rate higher than that for a point source by a factor of 1.2. In this case, the geometry effect would result in an *underestimation* of the curie content by this factor.

Another impact of the non-point source geometry is that of self absorption of the source and attenuation by the walls of the container. These effects cause an *underestimation* of the package activity, the significance of which is dependent upon the density and material composition of the waste, the size of the package, and the energy of the photon. Most waste packages have a fairly low density, typically in the range of 0.2–1.0 g/cm^3. The impact is greater with increasing density and size and decreasing photon energy. For ^{137}Cs in a metal can, for example, the underestimation varies from a factor of 1.1 to 1.3 as the density increases from 0.2 to 1.0 g/cm^3. For the 55-gal drum, the activity would be underestimated by a factor of 1.3–2.1. For lower energy photon emitters (including both low-energy gamma and x-rays) as well as bremsstrahlung photons, the degree of underestimation would be even greater.

In most cases, the inventory of alpha-emitting radionuclides was determined by applying the 1 MeV photon conversion factor. Depending upon a number of factors, the extent of underestimation of the activity may be quite significant. In some cases, the alpha emitter may also emit gamma rays of relatively high energy. In other cases, low energy gamma rays, x-rays, or beta particles are emitted. In most cases, the alpha-emitting radionuclides have radioactive daughters that may in turn decay by emission of measurable radiation. There is some level of uncertainty in the degree of equilibrium that exists. If it can be assumed that a sufficient period of time has elapsed since production of the source to establish some degree of equilibrium, the daughter's photon emissions can be used to estimate the source activity of the parent. If the daughter decays by beta emission, the ensuing bremsstrahlung photons can also be used. A significant limiting factor for the alpha emitters is the sensitivity of the portable survey instruments used to make the measurements as well as the background radiation present in many of the ORNL facilities. The typical ion chamber has a sensitivity of 0.1 mR/h. However, using this value along with the radionuclide's true dose rate to curie conversion factor may result in calculated

quantities of the radionuclide that are far from insignificant, given their relatively low concentration limits. In addition, the radiation background at many facilities is at the very least a few tenths of a millirad per hour, if not higher. At these values any waste package surveys taken within a facility may represent background levels, in which case there is not activity present in the package being surveyed. It is also quite possible that any low-level radiation measurements are not caused by the alpha emitter in the waste package but the insignificant levels of photon-emitting contaminants in the package. For all of these reasons, the actual activity of the alpha-emitting material calculated for this uncertainty analysis could then be significantly lower. The calculated most probable value assumes that the dose rate reported for the package is entirely due to the alpha-emitting radionuclide; thus, the activity is quite conservative.

Consideration of the significance of disposal of the calculated quantity of the radionuclide may also permit the application of some "reasonableness" criterion to estimate the uncertainty of the calculated activity. The total activity of a transuranic (TRU) radionuclide calculated using its specific dose conversion factor may lead to an unreasonable activity (i.e., one that is not physically possible). For the case of the TRU radionuclides, a limiting factor (i.e., upper bound) was applied to the package such that, based upon the weight of the package contents, the total activity would not exceed 10 nCi/g. This value is 10% of the limit of 100 nCi/g, above which waste must be classified as TRU waste and may not be disposed of in SWSA 6. The value of 10% was chosen instead of the limit itself because an evaluation of all wastes disposed of in SWSA 6 showed that essentially all waste packages were well under the 100 nCi/g limit. In fact, almost all were under 10 nCi/g. The evaluation of wastes with TRU radionuclides disposed of after September 26, 1988, was performed using the data on forms UCN-2822 and UCN-16114 to calculate average concentrations of TRU radionuclides in waste packages containing TRU waste. All 32 waste packages containing TRU waste disposed of in IWMF were less than 10 nCi/g and only one package exceeded 1 nCi/g. All 50 waste packages disposed of in Tumulus I and Tumulus II were less than 10 nCi/g with 10 exceeding 1 nCi/g. All 14 waste packages disposed of in the high-range silos were less than 10 nCi/g with 2 exceeding 1 nCi/g. Five of 81 packages in the low-range silos had TRU waste concentrations over 10 nCi/g with 64 packages less than 1 nCi/g. The use of 10 nCi/g, then, is considered to be a conservative upper bound for TRU activities in ORNL LLW.

For those cases in which the disposal activity of fissile materials is determined from form UCN-2681 the uncertainty would be rather low, especially relative to the other methods outlined above. In these cases, levels of activity are determined either directly or indirectly from analytical measurements of the source material and are known to be within the uncertainty of the measurement.

Strontium-90 (and its daughter ^{90}Y) is a significant contributor to the SWSA 6 inventory. This radionuclide emits only beta particles. However, the same 1 MeV photon conversion factor is used to determine its activity in waste packages, which significantly underestimates the activity of ^{90}Sr. Fortuitously, ^{90}Sr (and its daughter ^{90}Y) does emit relatively high-energy beta particles so that enough bremsstrahlung photons are produced in many waste packages to allow a measurable dose rate from a package of pure ^{90}Sr. For the case of components contaminated with ^{90}Sr, the fraction of the incident beta energy converted into photons is only 2%. For other materials, the production of bremsstrahlung

photons in that material varies with the energy of the beta particle and the atomic number of the absorber. The bremsstrahlung photons from ^{90}Sr will exhibit a continuous spectrum with the peak energy flux occurring around 0.15 MeV. A similar distribution but with a lower energy peak is produced for bremsstrahlung photons from radionuclides with lower energy beta particles. The dose rate significance will vary as a function of the same parameters as mentioned in previous paragraphs with source and package playing an even greater role. Relative to a photon emitter such as ^{137}Cs, the conversion factor for ^{90}Sr in a metal can is 40 times lower, but it is some 50 times lower for ^{90}Sr in a 55-gal drum. Compared to the 1 MeV photon emitter upon which the ORNL conversion factor is based, the ^{90}Sr activity would be underestimated by even greater factors. A situation normally encountered is that in which the facility considers both ^{137}Cs and ^{90}Sr as the principal radionuclides and believes that each is present in equal quantities. Upon determining the curie content using the ORNL conversion factor, half of the total is assigned to each radionuclide. The error in this approach is that essentially all of the measured dose rate is due to the ^{137}Cs, while little is due to the ^{90}Sr. The total activity calculated via the conversion factor should be attributed to ^{137}Cs, but by dividing this activity in half, the facility introduces a factor of two underestimation in both the ^{137}Cs and ^{90}Sr activities. A fortuitous aspect of this assumption is that by assuming that ^{90}Sr is present in equal quantities with ^{137}Cs (as is assumed in almost all cases), the error in the ^{90}Sr activity is still much less than if ^{90}Sr alone were present.

In most cases, waste generators estimated the activity of certain very low energy, pure beta emitters (^{3}H and ^{14}C) by some means that they considered to be appropriate to the specific situation at hand (i.e., they did not use the 1 MeV point source conversion factor). These estimates were taken as accurate but with some significant level of uncertainty. In some cases, however, activity for these radionuclides was calculated using the measured dose rates and the standard ORNL conversion factor. With the very low energy of the beta particle emitted, an appreciable quantity of the radionuclide is required to give any detectable dose rate due to bremsstrahlung. The degree of underestimation of the reported activity is certainly quite significant, but it is difficult to quantify. In these cases, the most probable value for the activity in this uncertainty analysis was estimated to be 50–1000 times greater than that reported. This order of magnitude correction was somewhat arbitrarily chosen but was empirically based upon the data available for the above-mentioned activities estimated for ^{3}H and ^{14}C.

A.2.5 Uncertainty Calculations for Activity Estimates

A.2.5.1 Deterministic Model Calculations

Calculations were performed using a deterministic model to compute the source activity and values for the low and high activity estimates. The results from the calculations were then used to check the reasonableness of the probabilistic model calculations, which are discussed in Sect. A.2.5.2. The deterministic model is based upon the following equation:

$$A = (D/R) \times C \ , \qquad \text{(A.1)}$$

where:

A is the estimated source activity,
D is the measured dose rate at distance x from the source,
R is the expected dose rate per curie conversion factor for a material of density ρ at distance x from the source, and
C is the distance correction factor for the error in the source-to-detector distance x.

The parameter D is nothing more than the actual value of the dose rate measurement. R is the dose rate to curie conversion factor and is the most complex aspect of the calculation. It is radionuclide dependent and is a function of the type of radiation emitted in the decay; the source geometry, composition, and density; and the distance from the source to the point of the dose rate measurement. These dose rate to curie conversion factors have been used for all radionuclides of interest, including those that emit high or low energy gamma rays, x-rays, or beta particles (with the ensuing bremsstrahlung photons). This includes any radionuclides that have radioactive daughters that may emit such radiation, which is particularly important for some of the transuranics. The parameter C is one that has been added to account for the effect on the dose rate caused by an error in the source-to-detector distance.

To describe the methodology used, a simple example calculation is provided. The basis for the assumptions made are pointed out as they appear in the calculation. The example calculation consists of a waste package (the 5-gal metal can) from Building 3525. The principal isotope is ^{60}Co. Although the dose rate used in the activity determination was 648 R/h, the actual measured dose rate was 72 R/h, taken at approximately 1 m (3 ft) using a portable ion chamber. Facility personnel used an inverse square relationship to derive a 0.3-m (1-ft) dose rate of 648 R/h, which was used in the activity calculation with the standard 1 MeV photon conversion factor. Uncertainties are associated with the measured dose rate due to calibration tolerances and the energy dependence of the instrument response. The response of the standard ORNL ion chamber is fairly linear over a wide range of energies, hence the overall uncertainty attributed to the measured dose rate was assumed to be $\pm 10\%$.

For this example, shielding calculations were performed using a cylindrical source (for the metal can) of ^{60}Co with dimensions of 25 × 36 cm [10 × 14 in. (diameter × height)]. An iron shield of 0.06-cm (0.02-in.) thickness was included in the calculations to approximate the attenuation effects of the steel metal can wall. The source material density was varied from 0.5 g/cm^3 to 2.0 g/cm^3 in increments of 0.5 g/cm^3. Since the density of iron is 7.86 g/cm^3, a metal can filled completely with 2.0 g/cm^3 density material corresponds to a metal can with 25% steel (iron) and 75% void space (this void space might contain a very small volume of low density material such as paper and plastic waste). The weight of such a can would be approximately 37 kg (100 lb). Since the reported weight for the waste packages ranged from 8 to 37 kg (20 to 100 lb), the use of 2.0 g/cm^3 as the upper bound for the average waste material density is appropriate. The lower bound for density of the waste material was 0.5 g/cm^3, which translates to an 8-kg (20-lb) metal can completely filled with this material. This value is deemed to be reasonable in terms of a lower bound. The dose rate at a distance of 1 m (3 ft) was calculated for a 1 Ci source of ^{60}Co, which represents a dose rate to curie conversion factor for this distance as

a function of source density and geometry. At 1 m (3 ft), the dose rate for material densities of 0.5 g/cm^3 and 2.0 g/cm^3 ranged from approximately 1.4 to 1.0 R/h per curie, respectively.

Dose rates as a function of distance were also calculated for the cylindrical source used above with a density of 1.0 g/cm^3. This calculation was done to examine the effect on the dose rate because of the uncertainty associated with the distance at which the measurement was obtained. For this example, an uncertainty of ± 0.3 m (1 ft) was considered to be reasonable, taking into consideration the manner in which the measurement was made. The calculations showed that the dose rate at a source-to-detector distance of 0.6 m (2 ft) was 2.5 times greater than the response obtained at 1 m (3 ft). Conversely, the dose rate response at 1.2 m (4 ft) was 0.6 times that obtained at 1 m (3 ft). At these distances, the metal can approximates a point source reasonably well.

While in the above example the dose rate was obtained with a portable ion chamber, many facilities use in-cell probes to obtain measurements of waste package dose rates. The uncertainty associated with these detectors is undoubtedly greater than that for the portable ion chamber, perhaps in the range of $\pm 25\%$.

A.2.5.1.1 Source Activity Estimate

In the example above, a dose rate of 72 R/h was measured at a distance of 1 m (3 ft). The source activity estimate is determined as follows:

$$A = (72/1.2) = 60 \text{ Ci} \quad ,$$

where:

72 R/h is the measured dose rate at 1 m (3 ft), and
1.2 R/h/Ci is the average dose rate per curie (for $\rho = 0.5$ and 2.0 g/cm^3).

Because the source activity estimate is based upon the measurement at 1 m (3 ft), there is no distance correction factor (i.e., $C = 1.0$).

A.2.5.1.2 Low Activity Estimate

In order to estimate the lower bound of the activity, the values of D and C should be minimized, while the activity should be maximized. Substituting into the above equation gives

$$A = (64.8/1.4) \times 0.6 = 27.8 \approx 28 \text{ Ci} \quad ,$$

where:

64.8 R/h is the lower bound of the measured dose rate at 1 m (3 ft) (72 − 10%),
1.4 R/h/Ci is the dose rate per curie for $\rho = 0.5$ g/cm^3, and
0.6 is the distance correction factor for $x = 1.2$ m (4 ft).

A.2.5.1.3 High Activity Estimate

In order to estimate the upper bound of the activity, the values of D and C should be maximized, while the activity should be minimized. Substituting into the above equation gives:

$$A = (79.2/1.0) \times 2.5 = 198 \approx 200 \text{ Ci} ,$$

where:

79.2 R/h is the upper bound of the measured dose rate at 1 m (3 ft) (72 + 10%),
1.0 R/h/Ci is the dose rate per curie for $\rho = 2.0$ g/cm^3, and
2.5 is the distance correction factor for $x = 0.6$ m (2 ft).

A.2.5.1.4 Deterministic Model Conclusions

As can be seen, this deterministic model gives an estimated activity of 60 Ci for ^{60}Co in the waste package, with a range of 28–200 Ci. The activity as determined on form UCN-16114 for this package (using the ORNL 1 MeV photon conversion factor) was 110 Ci. The activity estimate using the 6 $C\ E\ n$ formula for ^{60}Co (with a dose rate of 648 R/h at 0.3 m (4 ft), 1.25 MeV energy and 2 photons per disintegration) is 43 Ci.

The deterministic values for the calculated source activity provide the estimated source activity and range but do not allow for the independent variability of the uncertainties associated with the input parameters (e.g., the ion chamber dose rate response, the dose rate conversion factor associated with the waste material density, and the distance at which the measurement was taken). This approach gives the range of source activities that are *possible*, but does not tell what is *probable*.

A.2.5.2 Probabilistic Model Calculations

The most probable source activity and its associated uncertainty for each radionuclide were calculated using Crystal Ball[1] by propagating the uncertain parameters through a model of the joint distribution to produce a distribution of activity predictions. Latin Hypercube Sampling was used as the numerical method for propagation. Normally, Crystal Ball uses Monte Carlo sampling, generating random numbers for a probability distribution over the entire range of possible values for that distribution. For this reason, a large number of trials is required to obtain results that approximate the true shape of the distribution. With Latin Hypercube sampling, an assumption's probability distribution is divided into intervals of equal probability. Crystal Ball then generates an assumption value for each interval according to the interval's probability distribution. Compared with conventional Monte Carlo sampling, Latin Hypercube sampling is more precise because the entire range of the distribution is sampled in a more even, consistent manner.

[1]Decisioneering, Inc., Boulder, Colo.

To account for the uncertainties in the input parameters, a numerical method using Latin Hypercube Sampling was used to determine a probability distribution for the source activity. For the Building 3525 ^{60}Co example, three input parameters [the measured dose rate at 1 m (3 ft), the dose rate per curie response at 1 m (3 ft), and the distance correction factor] were used. The uncertainties associated with these parameters were propagated. A normal distribution with a mean of 72 R/h and a standard deviation of 2.4 R/h was used to describe the probability distribution for the measured dose rate. A uniform probability distribution with a range of 1.0–1.4 R/h/Ci was used for the dose rate per curie response. The distance probability distribution was described using a distance correction factor that was distributed normally with a mean of 0.914 m (3.00 ft) and a standard deviation of 0.10 m (0.34 ft).

A run with 1000 iterations was made for this example. This calculation allows for the determination of a ^{60}Co activity probability distribution with a most probable activity and an upper and lower bound value, each with an associated confidence interval. The most probable activity (i.e., the mode of the calculated activity probability distribution) was 54.4 Ci, with a range minimum at 95% confidence of 31.9 Ci and a range maximum at 95% confidence of 92.1 Ci. The $\pm$95% confidence interval represents $\pm$1.96 standard deviations about the mean of the calculated activity probability distribution. The deterministic model gave an estimated activity of ^{60}Co in the waste of 60 Ci with a range of 28–200 Ci. The activity as determined on form UCN-16114 for this package (using the ORNL 1 MeV photon conversion factor) was 110 Ci.

Similar uncertainty analyses were performed for other radionuclides and source geometries. An additional uncertainty distribution was introduced into the calculation whenever it was assumed that a package contained equal quantities of two or more radionuclides. In most cases, this assumption was made for packages containing ^{137}Cs and ^{90}Sr. The uncertainty represents the extent to which the radionuclides are present in equal quantities. For most cases, the fraction of the total represented by ^{137}Cs was set equal to 0.5, and was represented by a uniform probability fraction. The addition of this uncertainty results in a larger range in activity (from the minimum to the maximum activity estimates) than would be observed for each individual radionuclide.

This probabilistic approach facilitates the estimation of source activity for packages of waste based upon the principal radionuclide(s) identified, the measured dose rate at the specified distance, the instrument used for the measurement, the dose rate per curie response for the specified distance (a function of source density and geometry), and, if present, the mixture of multiple radionuclides in a package.

A.2.6 Shielding Calculations

The dose rate response calculations were performed using MICROSHLD[1], a personal computer (PC) version of the ISOSHLD[2] shielding code. The latter program uses point-kernel integration (with buildup) to calculate the radiation dose rate at a detector point for bremsstrahlung and decay gamma rays emitted by radioisotope sources.

[1]Atlan-Tech, Inc., Roswell, Ga.
[2]Radiation Shielding Information Center, CCC-79, Oak Ridge, Tenn.

For each waste package type considered, ISOSHLD uses information about the geometry of the problem, radioisotopes in the source, and the material composition of the source and shield regions to calculate the dose rate. The ISOSHLD code libraries contain the information used to calculate the dose rate and radiation spectra (i.e., attenuation coefficients, gamma ray decay energies and probabilities, maximum beta energies and probabilities, and buildup factor data). All the shielding calculations that were performed to determine the detector response to the waste packages in which the waste material was placed for disposal used a cylindrical source and, if appropriate, a cylindrical shield to account for the wall of the waste package. For the low activity waste, which was typically disposed of in small plastic bags, there would be no shield.

A.2.7 Results

Tables A.13–A.21 present the calculated radionuclide uncertainties for the asbestos silos, biological trenches, fissile wells, high-range silos, high-range wells, IWMF, low-range silos, Tumulus I, and Tumulus II, respectively. These tables indicate the radionuclide of interest, inventory reported in the Solid Waste Information Management System (SWIMS) data base, most probable activity, minimum activity at the 95% confidence level, maximum activity at the 95% confidence level, and an uncertainty weight. Information in Sect. A.2.8 is provided in order to supply information concerning particular details of the results of this uncertainty analysis for specific radionuclides in each disposal unit, including the basis for significant differences between the inventory reported in the SWIMS data base and the most probable activity.

The uncertainty weight has been assigned to the most probable activity for each radionuclide of interest in each disposal unit. It represents an overall, subjective opinion that the "true" activity falls within the minimum and maximum activity values specified. A value near 1.0 indicates a high level of confidence, while a value near 0.0 represents a low level of confidence. This uncertainty weight has no statistical relationship to the actual uncertainty estimates provided in the table; as stated previously, the minimum and maximum activities are based upon an interval of ± 1.96 standard deviations about the mean of the calculated activity probability distribution and thus represent a $\pm 95\%$ confidence interval. The general criteria used to assign the uncertainty weights are as follows. For those radionuclides whose most probable activities are generally derived from an actual waste assay (e.g., fissile material accompanied by form UCN-2681) a weight of 0.9 has been assigned. A weight of 0.8 has been allocated to those radionuclides that decay with emission of high energy gamma rays. For those radionuclides whose decay produces high energy beta particles or those whose dose rate to curie conversion factors are based upon a radioactive daughter that emits high energy gamma rays, a weight of 0.6 is given. A weight of 0.4 has been allocated to those radionuclides that decay with emission of intermediate energy beta particles or those whose dose rate to curie conversion factors are based upon a radioactive daughter that emits low energy gamma rays or beta particles. Lastly, those radionuclides that emit very low energy beta particles have been given an uncertainty weight of 0.2.

Table A.13. Radionuclide uncertainty for asbestos silos

Radionuclide	Inventory reported in Table A.8 (Ci)	Most probable activity (Ci)	Minimum activity 95% confidence limit (Ci)	Maximum activity 95% confidence limit (Ci)	Uncertainty weight ω_1
^{3}H	1.00×10^{-3}	5.00×10^{-2}	5.00×10^{-2}	5.00×10^{-1}	0.2
^{14}C	5.79×10^{-4}	5.79×10^{-1}	2.90×10^{-1}	8.69×10^{-1}	0.2
^{90}Sr	4.24×10^{-2}	4.71×10^{-2}	1.25×10^{-2}	1.03×10^{-1}	0.6
^{99}Tc	1.20×10^{-3}	1.02×10^{-3}	5.50×10^{-5}	2.74×10^{-3}	0.6
^{137}Cs	5.67×10^{-2}	5.65×10^{-2}	4.49×10^{-2}	7.50×10^{-2}	0.8
^{238}U	2.71×10^{-4}	5.08×10^{-3}	3.78×10^{-3}	6.99×10^{-3}	0.4

Table A.14. Radionuclide uncertainty for biological trenches

Radionuclide	Inventory reported in Table A.11 (Ci)	Most probable activity (Ci)	Minimum activity 95% confidence limit (Ci)	Maximum activity 95% confidence limit (Ci)	Uncertainty weight ω_1
^{3}H	1.80×10^{-4}	9.00×10^{-3}	9.00×10^{-4}	9.00×10^{-2}	0.2
^{90}Sr	1.04×10^{-2}	1.81×10^{-1}	1.31×10^{-1}	2.32×10^{-1}	0.6
^{137}Cs	2.25×10^{-3}	2.25×10^{-3}	1.78×10^{-3}	2.98×10^{-3}	0.8

Table A.15. Radionuclide uncertainty for fissile wells

Radionuclide	Inventory reported in Table A.10 (Ci)	Most probable activity (Ci)	Minimum activity 95% confidence limit (Ci)	Maximum activity 95% confidence limit (Ci)	Uncertainty weight $\omega 1$
^{137}Cs	4.25×10^{1}	3.85×10^{1}	2.34×10^{1}	5.38×10^{1}	0.8
^{235}U	8.75×10^{-4}	8.75×10^{-4}	7.88×10^{-4}	9.63×10^{-4}	0.9
^{238}U	4.83×10^{-3}	4.83×10^{-3}	4.35×10^{-3}	5.31×10^{-3}	0.9

Table A.16. Radionuclide uncertainty for high-range silos

Radionuclide	Inventory reported in Table A.7 (Ci)	Most probable activity (Ci)	Minimum activity 95% confidence limit (Ci)	Maximum activity 95% confidence limit (Ci)	Uncertainty weight ω1
^{3}H	1.00×10^{1}	1.00×10^{1}	5.00×10^{0}	1.50×10^{1}	0.2
^{14}C	4.11×10^{-2}	4.00×10^{-2}	2.00×10^{-2}	6.00×10^{-2}	0.2
^{63}Ni	8.30×10^{-2}	2.74×10^{-2}	2.63×10^{-3}	5.64×10^{-2}	0.6
^{90}Sr	2.31×10^{1}	3.51×10^{2}	2.28×10^{2}	6.03×10^{2}	0.6
^{137}Cs	2.57×10^{1}	2.34×10^{1}	1.42×10^{1}	3.27×10^{1}	0.8
^{152}Eu	1.24×10^{0}	5.94×10^{-1}	3.73×10^{-1}	8.78×10^{-1}	0.8
^{232}Th	1.36×10^{-4}	1.18×10^{-4}	1.01×10^{-4}	1.31×10^{-4}	0.6
^{238}U	9.96×10^{-3}	1.10×10^{-2}	9.71×10^{-3}	1.24×10^{-2}	0.4
^{239}Pu	1.01×10^{-3}	1.50×10^{-2}	1.50×10^{-3}	6.57×10^{-2}	0.4

Table A.17. Radionuclide uncertainty for high-range wells

Radionuclide	Inventory reported in Table A.9 (Ci)	Most probable activity (Ci)	Minimum activity 95% confidence limit (Ci)	Maximum activity 95% confidence limit (Ci)	Uncertainty weight $\omega 1$
^{60}Co	2.15×10^{3}	5.59×10^{2}	4.45×10^{2}	7.41×10^{2}	0.8
^{90}Sr	1.36×10^{3}	7.00×10^{3}	4.73×10^{3}	9.32×10^{3}	0.6
^{99}Tc	4.00×10^{-1}	4.00×10^{-1}	3.80×10^{-1}	4.20×10^{-1}	0.9
^{137}Cs	1.40×10^{3}	6.62×10^{3}	6.03×10^{3}	7.63×10^{3}	0.8
^{152}Eu	1.12×10^{3}	5.36×10^{2}	3.37×10^{2}	7.92×10^{2}	0.8
^{154}Eu	5.81×10^{2}	1.90×10^{2}	1.19×10^{2}	2.80×10^{2}	0.8
^{229}Th	7.50×10^{-3}	7.50×10^{-3}	6.75×10^{-3}	8.25×10^{-3}	0.6
^{232}Th	3.70×10^{-5}	3.70×10^{-5}	3.33×10^{-5}	4.07×10^{-5}	0.6

Table A.18. Radionuclide uncertainty for the Interim Waste Management Facility

Radionuclide	Inventory reported in Table A.5 (Ci)	Most probable activity (Ci)	Minimum activity 95% confidence limit (Ci)	Maximum activity 95% confidence limit (Ci)	Uncertainty weight ω1
^{3}H	5.10×10^{0}	5.10×10^{0}	2.55×10^{0}	7.65×10^{0}	0.5
^{14}C	3.07×10^{-2}	1.54×10^{1}	7.68×10^{0}	2.30×10^{1}	0.2
^{26}Al	1.00×10^{-3}	1.66×10^{-4}	1.28×10^{-4}	2.15×10^{-4}	0.8
^{36}Cl	8.50×10^{-3}	1.07×10^{0}	8.25×10^{-1}	1.41×10^{0}	0.4
^{63}Ni	1.70×10^{-2}	7.84×10^{-3}	7.50×10^{-4}	1.61×10^{-2}	0.4
^{90}Sr	3.48×10^{0}	3.13×10^{0}	8.28×10^{-1}	6.82×10^{0}	0.6
^{99}Tc	3.40×10^{-4}	1.47×10^{-1}	1.04×10^{-1}	1.98×10^{-1}	0.4
^{137}Cs	8.52×10^{0}	5.39×10^{0}	4.28×10^{0}	7.16×10^{0}	0.8
^{152}Eu	8.59×10^{-1}	2.92×10^{-1}	2.32×10^{-1}	3.84×10^{-1}	0.8
^{232}Th	6.00×10^{-5}	3.56×10^{-5}	2.50×10^{-5}	4.13×10^{-5}	0.6
^{233}U	1.07×10^{-3}	9.26×10^{-2}	9.26×10^{-3}	9.26×10^{-1}	0.2
^{238}U	2.71×10^{-3}	5.79×10^{-2}	4.30×10^{-2}	7.95×10^{-2}	0.4
^{239}Pu	5.98×10^{-4}	4.65×10^{-2}	4.65×10^{-3}	7.35×10^{-2}	0.4
^{241}Am	2.21×10^{-4}	6.67×10^{-3}	3.25×10^{-3}	2.48×10^{-2}	0.4
^{243}Am	1.50×10^{-4}	2.61×10^{-3}	7.87×10^{-4}	6.95×10^{-3}	0.4

Table A.19. Radionuclide uncertainty for low-range silos

Radionuclide	Inventory reported in Table A.6 (Ci)	Most probable activity (Ci)	Minimum activity 95% confidence limit (Ci)	Maximum activity 95% confidence limit (Ci)	Uncertainty weight $\omega 1$
^{3}H	1.02×10^{1}	1.02×10^{1}	5.68×10^{0}	1.46×10^{1}	0.2
^{10}Be	3.20×10^{-3}	0	0	0	0
^{14}C	7.23×10^{-2}	7.23×10^{1}	3.62×10^{1}	1.08×10^{2}	0.2
^{90}Sr	2.67×10^{0}	5.34×10^{0}	1.10×10^{0}	1.30×10^{1}	0.6
^{99}Tc	7.59×10^{-3}	3.26×10^{0}	2.32×10^{0}	4.39×10^{0}	0.4
^{137}Cs	3.23×10^{0}	4.49×10^{0}	2.73×10^{0}	6.27×10^{0}	0.8
^{230}Th	1.17×10^{-3}	0	0	0	0
^{232}Th	1.14×10^{-3}	1.08×10^{-3}	9.49×10^{-4}	1.19×10^{-3}	0.6
^{233}U	6.71×10^{-2}	2.75×10^{-2}	2.75×10^{-3}	2.75×10^{-1}	0.2
^{238}U	1.12×10^{-2}	1.37×10^{-1}	1.03×10^{-1}	1.87×10^{-1}	0.4
^{239}Pu	9.00×10^{-4}	3.47×10^{-1}	3.47×10^{-3}	7.38×10^{-2}	0.4
^{241}Am	7.84×10^{-3}	2.76×10^{-2}	4.20×10^{-3}	8.70×10^{-2}	0.4
^{243}Am	6.21×10^{-3}	1.08×10^{-2}	1.08×10^{-3}	8.28×10^{-2}	0.4

Table A.20. Radionuclide uncertainty for Tumulus I

Radionuclide	Inventory reported in Table A.3 (Ci)	Most probable activity (Ci)	Minimum activity 95% confidence limit (Ci)	Maximum activity 95% confidence limit (Ci)	Uncertainty weight $\omega 1$
^{3}H	2.70×10^{0}	2.70×10^{0}	1.35×10^{0}	4.05×10^{0}	0.2
^{14}C	1.95×10^{-2}	9.76×10^{0}	4.88×10^{0}	1.46×10^{1}	0.2
^{63}Ni	2.02×10^{-1}	9.68×10^{-2}	9.26×10^{-3}	1.99×10^{-1}	0.6
^{90}Sr	3.31×10^{0}	3.71×10^{0}	9.82×10^{-1}	8.09×10^{0}	0.6
^{99}Tc	2.34×10^{-3}	3.69×10^{-1}	2.61×10^{-1}	5.00×10^{-1}	0.6
^{137}Cs	1.40×10^{1}	9.96×10^{0}	7.90×10^{0}	1.32×10^{1}	0.7
^{152}Eu	4.85×10^{-1}	1.66×10^{-1}	1.32×10^{-1}	2.18×10^{-1}	0.9
^{226}Ra	1.70×10^{-3}	4.19×10^{-4}	3.28×10^{-4}	5.57×10^{-4}	0.6
^{232}Th	1.66×10^{-4}	1.11×10^{-4}	7.16×10^{-5}	1.39×10^{-4}	0.6
^{233}U	1.02×10^{-2}	9.81×10^{-2}	9.81×10^{-3}	9.81×10^{-1}	0.2
^{238}U	2.28×10^{-3}	4.55×10^{-2}	3.38×10^{-2}	6.25×10^{-2}	0.4
^{239}Pu	1.17×10^{-2}	9.03×10^{-2}	9.03×10^{-3}	8.70×10^{-1}	0.3
^{240}Pu	6.80×10^{-3}	0	0	0	0
^{241}Am	2.23×10^{-2}	8.27×10^{-2}	8.27×10^{-3}	8.27×10^{-1}	0.5
^{243}Am	2.21×10^{-3}	1.86×10^{-3}	2.36×10^{-4}	1.01×10^{-2}	0.5

Table A.21. Radionuclide uncertainty for Tumulus II

Radionuclide	Inventory reported in Table A.4 (Ci)	Most probable activity (Ci)	Minimum activity 95% confidence limit (Ci)	Maximum activity 95% confidence limit (Ci)	Uncertainty weight ω1
^{3}H	1.51×10^{0}	1.61×10^{0}	8.04×10^{-1}	2.41×10^{0}	0.2
^{14}C	4.24×10^{-3}	2.12×10^{0}	1.06×10^{0}	3.18×10^{0}	0.2
^{90}Sr	7.96×10^{0}	3.29×10^{0}	8.71×10^{-1}	7.17×10^{0}	0.6
^{99}Tc	1.62×10^{-2}	2.35×10^{-1}	1.67×10^{-1}	3.17×10^{-1}	0.4
^{137}Cs	1.29×10^{1}	5.20×10^{0}	4.12×10^{0}	6.89×10^{0}	0.8
^{152}Eu	2.08×10^{-1}	7.08×10^{-2}	5.62×10^{-2}	9.30×10^{-2}	0.7
^{232}Th	5.02×10^{-4}	3.97×10^{-4}	2.78×10^{-4}	4.60×10^{-4}	0.6
^{233}U	4.15×10^{-2}	5.19×10^{-2}	5.19×10^{-3}	5.19×10^{-1}	0.2
^{238}U	1.14×10^{-3}	7.33×10^{-3}	5.56×10^{-3}	9.90×10^{-3}	0.4
^{239}Pu	1.06×10^{-2}	5.21×10^{-2}	5.21×10^{-3}	5.21×10^{-1}	0.4
^{241}Am	1.25×10^{-2}	1.05×10^{-1}	1.05×10^{-2}	1.05×10^{0}	0.4

A.2.8 Radionuclide Uncertainty Details

For each radionuclide of interest in each disposal unit, the general methodology used to determine the total most probable activity and associated uncertainty involved a two-phased approach. The first consisted of evaluating the source inventory of each disposal unit and selecting records for a sufficient number of waste packages to comprise a relatively large percentage of the total activity for each radionuclide of interest. Interviews with waste generators and evaluation of the data sheets (forms UCN-2822 and 16114) for these significant packages were conducted to ascertain (1) the method used by the generator to determine the activity for the package (e.g., 6 *C E n*, estimation, calculation, assay, etc.); (2) the physical form of the *packets* within the package (e.g., 5-gal metal cans, small plastic bags, 55-gal drums, etc.); (3) the instrument used to perform the survey (portable ion chamber or in-cell probe); (4) the dose rate measured for the packets within the package; (5) the distance from the instrument to the packet; and (6) the generator's assumptions concerning packet contents (i.e., whether or not the packet contained multiple radionuclides). Based upon the above information, the activity probability distribution was calculated and the most probable activity and associated minimum and maximum activity (at the 95% confidence interval) were determined for each radionuclide of interest in these significant packages.

For those packages for which the waste generators used the standard ORNL dose rate to curie conversion factor to estimate the activity of the principal isotope, the proper conversion factor was multiplied by the dose rate for the package to determine the most probable activity. The proper conversion factor is dependent upon items (2), (3), (5), and (6) and is obviously a function of the specific radionuclide. The conversion factors were normally calculated for a unit dose rate (1 R/h), and this had units of curies/(R/h). Similar factors were determined for the minimum and maximum activities so that, once the dose rate was ascertained, the three activity values were readily calculated. It should be noted that in the case of multiple radionuclides in the same packet, the dose factor of each was considered in the determination of the most probable activity. For the case of the significant radionuclides ^{137}Cs and ^{90}Sr, the dose rate measured for the package is essentially due only to the ^{137}Cs. The ^{90}Sr activity is then given by multiplying the measured dose rate by the ^{137}Cs conversion factor. The same situation was also encountered for ^{192}Ir and ^{99}Tc, ^{192}Ir and ^{63}Ni, and ^{137}Cs and ^{99}Tc. In each of these cases, the conversion factor for the gamma emitter was used to estimate the activity of the beta emitters. In the case of high-range waste from Building 3517 (all ^{137}Cs and ^{90}Sr), the dose factors were calculated specifically for each waste package because the 55-gal drums were surveyed at varying distances. In general, high-range waste was handled (and surveyed) in 5-gal metal cans while low-range waste was placed in small plastic bags.

For the case of TRU waste for which the standard ORNL dose factor had been used to calculate the activity, an upper limit was set to the package activity based upon the specific activity limit of 10 nCi/g for TRU waste in the disposal units. The calculation was made for each package based upon the net weight of the waste. Activity in the package was calculated using both the specific activity limit and the proper dose factor. The lower of the two calculated values was considered to be the most probable activity. In the specific activity calculation, minimum and maximum activities were calculated using values of 1 and 100 nCi/g, respectively. The upper bound of 100 nCi/g represents a quite

acceptable value for the maximum activity of a package. However, 1 nCi/g represents a conservative lower bound and was used primarily for expediency. It is quite likely that a large fraction (much greater than 5%) of the TRU waste packages contain less activity than this value.

In most cases in which the generator assigned the package activity by some type of estimation other than the standard dose rate to curie conversion, the activity estimated by the generator was assumed to be the most probable activity and the minimum and maximum activities were calculated as $\pm 50\%$ of the most probable activity. In most cases in which the ORNL conversion factor had been used to calculate the activity of ^{3}H or ^{14}C, a significant correction was applied to estimate the most probable activity of these very low energy beta emitters. These correction values ranged from 50 to 500 depending upon the particular circumstances. In these cases, the minimum and maximum activity were again calculated as $\pm 50\%$ of the most probable activity. If the activity reported by the generator was based upon an assay, the activity calculated by the generator was assumed to be the most probable activity with a minimum and maximum activity calculated at $\pm 10\%$ of the most probable activity.

The end result for the first phase was the calculation of most probable activity and associated minimum and maximum activity for each package evaluated. The second phase to the approach accounted for the remaining activity. The total radionuclide activity *reported* in the packages that were evaluated in the first phase was subtracted from the total activity reported for the radionuclide in the disposal unit, giving the portion of the total reported activity yet unevaluated. For those radionuclides whose activity determination by the waste generator was likely to have been based upon the standard ORNL dose rate to curie conversion factor, the dose rate that was used in the calculation of activity was estimated by dividing the unevaluated activity by the standard dose rate to curie conversion factor. The resulting dose rate was then multiplied by the proper conversion factors for the radionuclide to determine the most probable activity, minimum activity, and maximum activity. An additional adjustment to the dose rate determination was necessary in those cases in which the generator assumed that multiple radionuclides were present in the package. This additional adjustment is an important consideration, particularly for the significant radionuclides ^{137}Cs and ^{90}Sr. If the generator assumed that equal quantities of both radionuclides were present, he or she would have divided the total activity (as determined by multiplying the measured dose rate by the ORNL dose rate to curie conversion factor) in half, assigning 50% to each radionuclide. To account for this practice, the dose rate calculated by dividing the unevaluated activity by the standard dose rate to curie conversion factor was normally multiplied by a factor of 2. This correction was modified slightly in the case of the ^{137}Cs activity. Based upon review of the reported disposal activities, ^{90}Sr was normally reported together with ^{137}Cs. However, the converse was not true. ^{137}Cs was just as likely to have been reported alone as it was together with ^{90}Sr. Therefore, for ^{137}Cs, the activity reported with ^{90}Sr and without ^{90}Sr were both determined. The additional correction factor of 2 was applied for that fraction of the ^{137}Cs activity that was reported with ^{90}Sr. No *additional* correction factor was used for that fraction of the ^{137}Cs activity that was not reported without ^{90}Sr. As an example of this correction, consider the case of the low-range silos. Here, 45% of the ^{137}Cs activity is reported in conjunction with ^{90}Sr, while 55% is not. The dose rate to be used in the

calculation of the most probable activity for the radionuclide in question in "other packages" is then given by the following:

$$\text{Dose Rate} = \{\text{Total Activity} - \text{Activity in Packages}\} \times \{0.45 \times 2 + 0.55 \times 1\}/\{0.17\} .$$

The determination of the proper methodology to be used in the most probable activity calculation (6 *C E n*, estimation, calculation, assay, etc.) was based upon that assumed to be appropriate for the unevaluated activity, as inferred through interviews with waste generators and the review of selected data sheets. This determination was specific to each radionuclide in each disposal unit. The methodology used for the remaining activity was, in some cases, different than that used in the calculation for the significant package(s). Once the proper method was selected, the assignment of uncertainties used to determine the minimum and maximum activity was identical to those used for the selected packages in phase one.

The total activity for each radionuclide in the disposal unit is given by the sum of the most probable activities for the significant package(s) and the remaining activity. A similar summation gives the minimum and maximum activity for each radionuclide in each disposal unit.

Table A.22 provides specific information concerning the differences between the radionuclide inventory reported in Tables A.3–A.11 and the calculated most probable activity, including the basis for significant differences.

A.3 REFERENCES

BRH (Bureau of Radiological Health) 1970. *Radiological Health Handbook*, U.S. Department of Health Education, and Welfare; Rockville, Md., January.

Table A.22. Information concerning the differences between the reported radionuclide inventory and the calculated most probable activity

Nuclide	Pertinent information
	Tumulus I
^{3}H	Assumed correct. Original activity had been estimated.
^{14}C	Very significant error. Original activity was calculated with standard conversion factor.
^{63}Ni	Good results. Although the nuclide is a beta emitter, it was assumed to be present with ^{192}Ir.
^{90}Sr	Good results. Although the nuclide is a beta emitter, it was assumed to be present with ^{137}Cs.
^{99}Tc	Significant error. Original activity was calculated with standard conversion factor. Proper conversion factor is high because the nuclide is a low energy beta emitter.
^{137}Cs	Good results. Most ^{137}Cs activity was reported without ^{90}Sr.
^{152}Eu	Original results overestimated activity. Nuclide is a high energy gamma emitter.
^{226}Ra	Original results overestimated activity. Nuclide is a high energy gamma emitter.
^{232}Th	Original results slightly overestimated activity. Daughters are high energy gamma emitters.
^{233}U	Original results underestimated activity. Relatively minimal beta/gamma emission by daughters. Activity is bounded by 10 nCi/g.
^{238}U	Original results underestimated activity. Relatively minimal beta/gamma emission by daughters.
^{239}Pu	Original results underestimated activity. Low yield photon emission. Activity is bounded by 10 nCi/g.
^{240}Pu	Activity in package 64624 was originally reported as ^{240}Pu. Actual nuclide is assumed to be ^{239}Pu; activity is included in that radionuclide's totals.
^{241}Am	Original results underestimated activity. Low yield photon emission. Activity is bounded by 10 nCi/g.
^{243}Am	Original results overestimated activity due to bounding by 10 nCi/g. (Note: The mass of ^{241}Am waste is much greater than that of ^{243}Am.)

Table A.22 (continued)

Nuclide	Pertinent information
	Tumulus II
^{3}H	Original activity had been estimated and is assumed to be correct.
^{14}C	Very significant error. Original activity was calculated with standard conversion factor.
^{90}Sr	Good results. Although the nuclide is a beta emitter, it is assumed to be present with ^{137}Cs. Package 900092 erroneously reported 5.00 Ci.
^{99}Tc	Significant error. Original activity was calculated with standard conversion factor. Proper conversion factor is high because the nuclide is a low energy beta emitter.
^{137}Cs	Good results. Most ^{137}Cs was reported without ^{90}Sr. Package 900092 erroneously reported 5.10 Ci.
^{152}Eu	Original results overestimated activity. Nuclide is a high energy gamma emitter.
^{226}Ra	Original results overestimated activity. Nuclide is a high energy gamma emitter.
^{232}Th	Original results slightly overestimated activity. Daughters are high energy gamma emitters.
^{233}U	Original results underestimated activity. Relatively minimal beta/gamma emission by daughters. Activity is bounded by 10 nCi/g.
^{238}U	Original results underestimated activity. Relatively minimal beta/gamma emission by daughters.
^{239}Pu	Original results underestimated activity. Low yield photon emission. Activity is bounded by 10 nCi/g.
^{241}Am	Original results underestimated activity. Low yield photon emission. Activity is bounded by 10 nCi/g.
	Interim Waste Management Facility
^{3}H	Original activity had been estimated and is assumed to be correct.
^{14}C	Very significant error. Original was activity calculated with standard conversion factor.
^{26}Al	Original results overestimated activity. Nuclide is a high energy gamma emitter.
^{36}Cl	Large error. Original activity calculated with standard conversion factor. Proper conversion factor is high because the nuclide is a pure beta (medium energy) emitter.
^{63}Ni	Good results. Although the nuclide is a beta emitter, it is assumed to be present with ^{192}Ir.

Table A.22 (continued)

Nuclide	Pertinent information
^{90}Sr	Good results. Although the nuclide is a beta emitter, it is assumed to be present with ^{137}Cs.
^{99}Tc	Significant error. Original activity was calculated with standard conversion factor. Proper conversion factor is high because the nuclide is low energy beta emitter.
^{137}Cs	Good results. Most ^{137}Cs reported without ^{90}Sr.
^{152}Eu	Original results overestimated activity. Nuclide is a high energy gamma emitter.
^{232}Th	Original results slightly overestimated activity. Daughters are high energy gamma emitters.
^{233}U	Original results underestimated activity. Relatively minimal beta/gamma emission by daughters. Activity is bounded by 10 nCi/g.
^{238}U	Original results underestimated activity. Relatively minimal beta/gamma emission by daughters.
^{239}Pu	Original results underestimated activity. Low yield photon emission. Activity is bounded by 10 nCi/g.
^{241}Am	Original results underestimated activity. Low yield photon emission.
^{243}Am	Original results overestimated activity. Low yield photon emission.
	Asbestos silos
^{3}H	Very significant error. Original activity was calculated with standard conversion factor.
^{14}C	Very significant error. Original activity was calculated with standard conversion factor.
^{90}Sr	Good results. Although the nuclide is a beta emitter, it is assumed to be present with ^{137}Cs.
^{99}Tc	Good results. Although the nuclide is a beta emitter, it is assumed to be present with ^{137}Cs.
^{137}Cs	Good results. Most ^{137}Cs was reported without ^{90}Sr.
^{238}U	Original results underestimated activity. Relatively minimal beta/gamma emission by daughters.
	Biological trenches
^{3}H	Very significant error. Original activity was calculated with standard conversion factor.
^{90}Sr	Significant error. Original activity was calculated with standard conversion factor. ^{90}Sr was reported alone, not with ^{137}Cs.
^{137}Cs	Excellent results. Most ^{137}Cs was reported with ^{90}Sr.

Table A.22 (continued)

Nuclide	Pertinent information
	Fissile wells
^{137}Cs	Good results. All ^{137}Cs was reported without ^{90}Sr.
^{235}U	Original activity had been assayed and is assumed to be correct.
^{238}U	Original activity had been assayed and is assumed to be correct.
	High-range silos
^{3}H	Original activity had been estimated and is assumed to be correct.
^{14}C	Original activity had been estimated and is assumed to be correct.
^{63}Ni	Good results. Although the nuclide is a beta emitter, it is assumed to be present with ^{192}Ir.
^{90}Sr	Significant error. Original activity was calculated with standard conversion factor. A large fraction of ^{90}Sr was reported alone, not with ^{137}Cs.
^{137}Cs	Good results.
^{152}Eu	Original results overestimated activity. Nuclide is a high energy gamma emitter.
^{232}Th	Original results slightly overestimated activity. Daughters are high energy gamma emitters.
^{233}U	Original results slightly underestimated activity. Relatively minimal beta/gamma emission by daughters.
^{238}Pu	Original results slightly underestimated activity. Relatively minimal beta/gamma emission by daughters.
^{239}Pu	Original results underestimated activity. Low yield photon emission. Activity is bounded by 10 nCi/g.
	High-range wells
^{60}Co	Original results overestimated activity. Nuclide is a high energy gamma emitter.
^{90}Sr	Original results underestimated activity. Almost all waste came from Building 3517 and was surveyed in 55-gal drums. Although the nuclide is a beta emitter, it is assumed to be present with ^{137}Cs.
^{99}Tc	Original activity had been assayed and is assumed to be correct.
^{137}Cs	Original results underestimated activity. Almost all waste came from Building 3517 and was surveyed in 55-gal drums. Activity was split 50:50 with ^{90}Sr.
^{152}Eu	Original results overestimated activity. Nuclide is a high energy gamma emitter.
^{154}Eu	Original results overestimated activity. Nuclide is a high energy gamma emitter.

Table A.22 (continued)

Nuclide	Pertinent information
^{229}Th	Original activity had been assayed and is assumed to be correct.
^{232}Th	Original activity had been assayed and is assumed to be correct.
	Low-range silos
^{3}H	Original activity had been estimated and is assumed to be correct.
^{10}Be	Error. Package 65288 contained a Ra-Be neutron source, which is composed of stable ^{9}Be, not radioactive ^{10}Be.
^{14}C	Very significant error. Original activity was calculated with standard conversion factor.
^{90}Sr	Good results. Although the nuclide is a beta emitter, it is assumed to be present with ^{137}Cs.
^{99}Tc	Significant error. Original activity was calculated with standard conversion factor. Proper conversion factor is high because the nuclide is a low energy beta emitter.
^{137}Cs	Good results.
^{230}Th	Package 76028 contained natural thorium-contaminated soil. ^{230}Th is a uranium series daughter. Nuclide is assumed to be ^{232}Th.
^{232}Th	Most of the original activity had been assayed and is assumed to be correct. Remaining results slightly overestimated activity. Daughters are high energy gamma emitters.
^{233}U	Fortuitously good results due to bounding by 10 nCi/g.
^{238}U	Original results underestimated activity. Relatively minimal beta/gamma emission by daughters.
^{239}Pu	Original results underestimated activity. Low yield photon emission. Activity is bounded by 10 nCi/g.
^{241}Am	Original results underestimated activity. Low yield photon emission.
^{243}Am	Original results underestimated activity. Low yield photon emission. Activity is bounded by 10 nCi/g.

APPENDIX B

DESCRIPTION OF THE SOURCE1, SOURCE2, AND FLOWTHRU COMPUTER PROGRAMS

Rob Shuman
Nam Chau
Bill Nestor, Jr.
Herschel Godbee
Alan Icenhour

June 1993

B. DESCRIPTION OF THE SOURCE1, SOURCE2, AND FLOWTHRU COMPUTER PROGRAMS

B.1 SOURCE1 AND SOURCE2

The modeling methodology used in simulating the long-term performance of disposal units at SWSA 6 has been incorporated into two separate computer codes (Shuman, Chau, and Jennrich 1992). The SOURCE1 code models the performance of the tumulus disposal technology employed in the Tumulus I and II facilities and the Interim Waste Management Facility. The SOURCE2 computer code models the performance of disposal silos, wells, multiple containment wells, and biological trenches.

B.1.1 Code Objectives

The objective of developing the SOURCE computer codes is to provide a mechanism for modeling radionuclide release rates from the disposal units employed at the SWSA 6 low-level waste disposal facility. The disposal units incorporate a variety of engineered barriers in an attempt to better isolate the waste from the environment. Consequently, projecting patterns and rates of radionuclide release requires an understanding of the manner in which these engineered barriers perform over extended periods of time.

B.1.2 Code Summary

Radionuclide release rates from the tumulus, silo, and well disposal units are largely a function of the integrity of the engineered barriers used in the construction of each. When intact, these barriers minimize contact of water with the waste, thereby minimizing releases of radionuclides from the disposal unit. As the barriers deteriorate over time and fail, water can more readily contact the waste, thereby accelerating releases to the environment.

The SOURCE computer codes model the long-term performance of the engineered barriers used in the tumulus, silo, and well disposal units. Changes in the material properties of the barriers due to chemical and physical attack are modeled. The projected material properties are considered in structural and cracking analyses of the disposal units, performed to assess the ability of the disposal units to bear the loads placed upon them. As the ability to bear design loads is compromised and the structures fail, rates of percolation of water through the waste are adjusted.

Rates of percolation of water through the waste are used to calculate release rates due to advection. Releases due to diffusion are also calculated by the SOURCE computer codes using the FLOWTHRU computer code (see Appendix B.2). Releases from the disposal units are partitioned into the quantity of contamination that migrates with the

lateral flow component of unsaturated flow at the site and that which is transported to, and discharged into, the site aquifer.

B.1.3 System Requirements

The SOURCE computer codes were written using the Microsoft FORTRAN Version 5.0 compiler. This software conforms to the American National Standard Programming Language FORTRAN 77, as described in the American National Standards Institute (ANSI) X3.9-1978 standard.

Separate codes were developed for the tumulus technology and those employing disposal silos and wells to maximize flexibility while minimizing computing equipment requirements. Each code is designed to be used on an IBM-compatible personal computer. It is recommended that the codes be used on an 80386-grade computer equipped with a math coprocessor.

B.1.4 Computer Code Design

Each SOURCE computer code consists of the main program, 17 to 19 subroutines, and three functions. The code hierarchy of the SOURCE1 and SOURCE2 code is illustrated in Figs. B.1 and B.2, respectively. A brief description of the function(s) performed by the program modules is provided in Table B.1. The logic flow of the two computer codes is similar and is summarized in Fig. B.3. Input data describing the disposal site and features of the disposal unit under consideration are read in and used to calculate additional quantities necessary to conduct a simulation. A structural analysis of the disposal unit is conducted to establish the moments and forces placed on the various structural components.

Following the structural analysis, the computer codes enter an annual loop in which chemical and physical deterioration of the concrete and steel barriers used in the disposal unit are modeled. Properties of the structural members of the facility are updated to reflect this degradation and are used in cracking analyses of the roof, wall(s), and floor of the disposal unit to assess the structure's ability to bear the loads placed upon it. As the engineered structure is weakened by chemical and physical attack, a point is reached at which the structure is no longer able to bear the loads placed upon it. Under these conditions, the engineered barriers will crack or otherwise fail. As failure occurs, the amount of water contacting the wastes, and leaching radionuclides from these wastes, increases. Rates of water percolation through the waste and increased rates of release are updated to reflect this phenomenon.

Rates of concrete deterioration are provided at user-specified intervals during the simulation. Rates of corrosion of metal engineered components are provided at the same user-specified intervals for disposal units incorporating these barriers. Crack characteristics of the concrete structural components are provided as these components deteriorate and fail with time. Separate output files containing annual radionuclide release rates are generated for the lateral and vertical components of unsaturated flow. A detailed illustration of the logic flow used in the SOURCE computer codes to model the degradation of engineered barriers and their eventual failure is provided in Fig. B.4. The simulation begins with the structural analysis of the disposal unit. Shear forces, bending

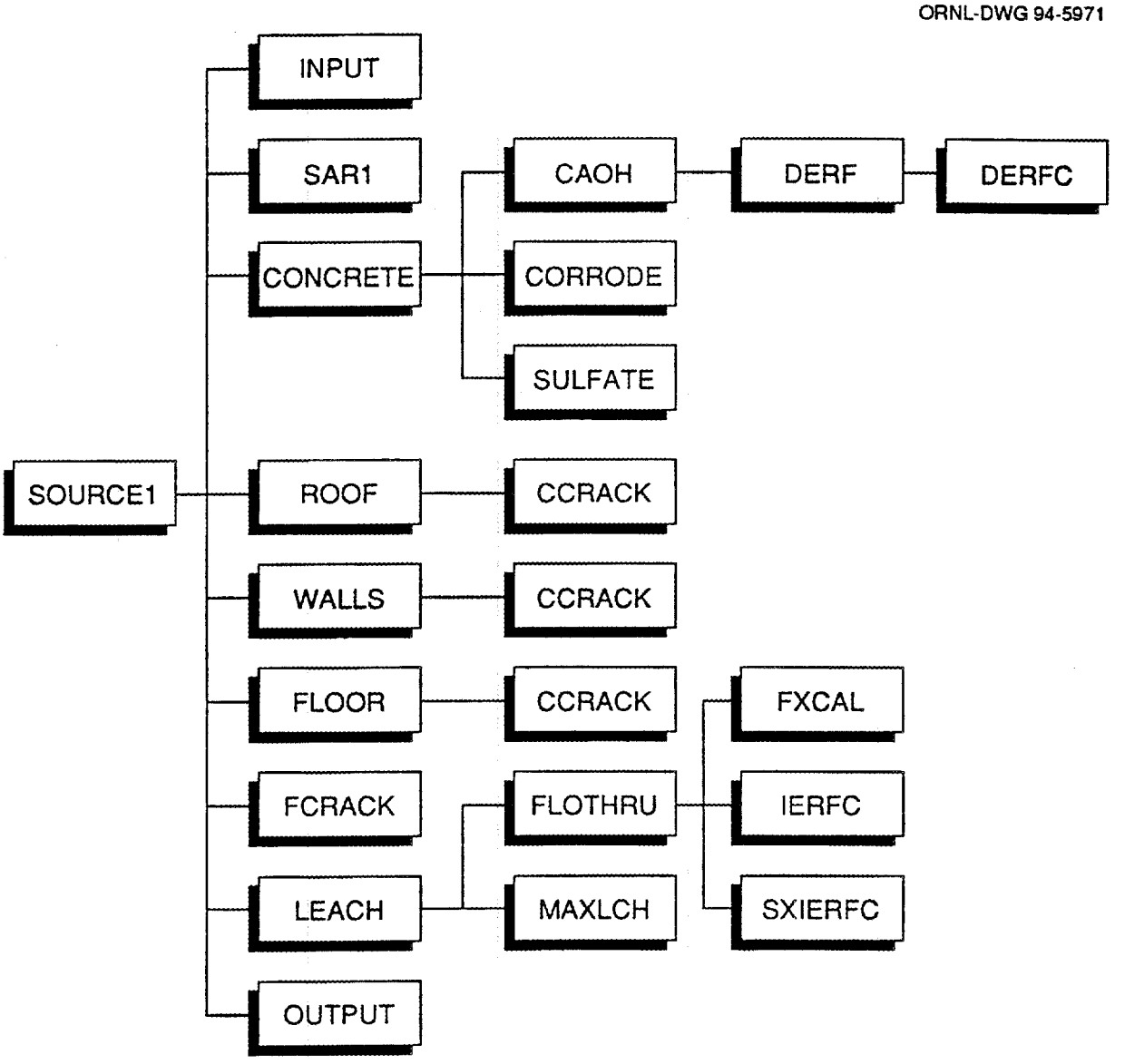

Fig. B.1. SOURCE1 code hierarchy for modeling tumulus disposal units.

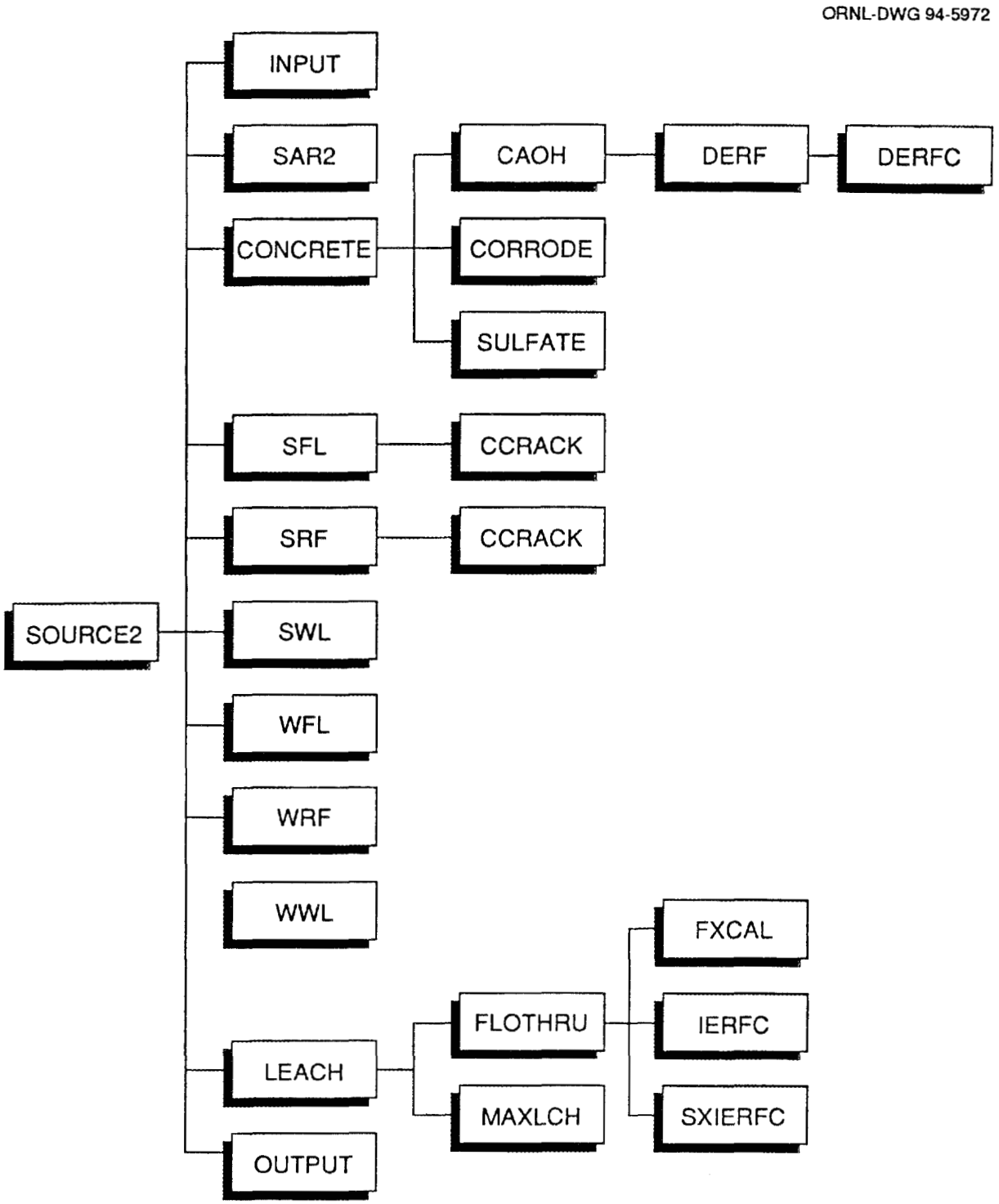

Fig. B.2. SOURCE2 code hierarchy for modeling disposal silos and wells.

Table B.1. SOURCE program module description

Module	Purpose
SOURCE	Main program; coordinates subroutine calls
CAOH	Calculates changes in concrete member strength and pH due to leaching of calcium hydroxide
CONCRETE	Coordinates calls to concrete degradation subroutines
CORRODE	Calculates initiation and propagation of corrosion of steel reinforcement
CCRACK	Performs cracking analysis for cracking due to corrosion
INPUT	Reads input data file and performs preliminary calculations
FCRACK	Calculates number of casks that have undergone cracking
FLOOR	Performs cracking analysis for cask floor
FLOTHRU	Calculates radionuclide releases due to diffusion
LEACH	Coordinates leaching calculations and calculates radionuclide releases due to advection
MAXLCH	Calculates solubility limits on radionuclide leaching
OUTPUT	Prints summary of concrete degradation and cracking analyses and radionuclide release rates
ROOF	Performs cracking analysis for cask roof
SAR1	Performs structural analysis for cask roof, walls, and floor
SAR2	Performs structural analysis for silo and well roof, wall, and floor
SFL	Performs cracking analysis for silo floor
SRF	Performs cracking analysis for silo roof
SULFATE	Calculates change in concrete member thickness due to sulfate attack
SWL	Performs cracking analysis for silo wall
WALL	Performs cracking analysis for cask walls
WFL	Performs cracking analysis for well floor
WRF	Performs cracking analysis for well roof
WWL	Performs cracking analysis for well wall

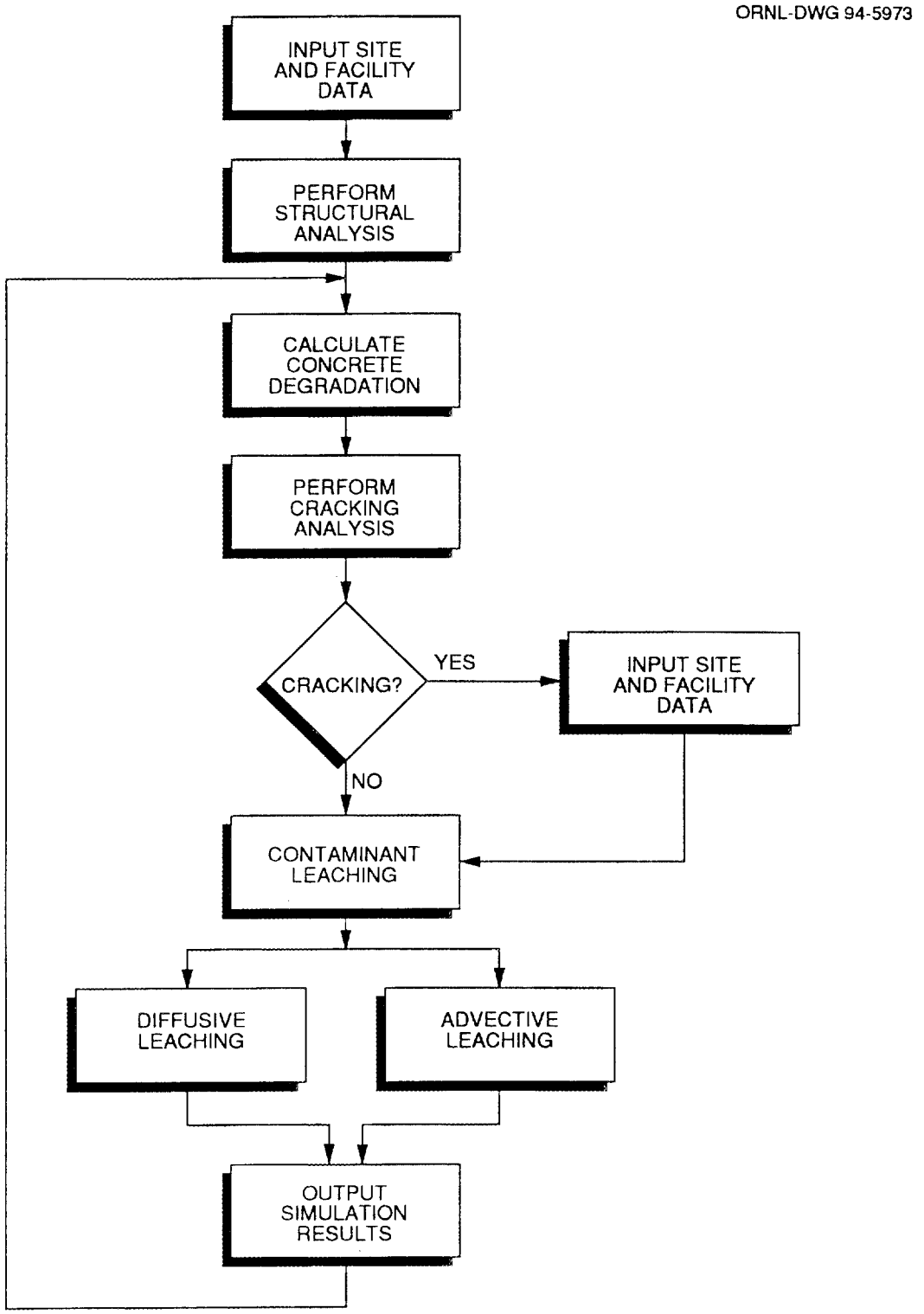

Fig. B.3. Logic flow in the SOURCE computer codes.

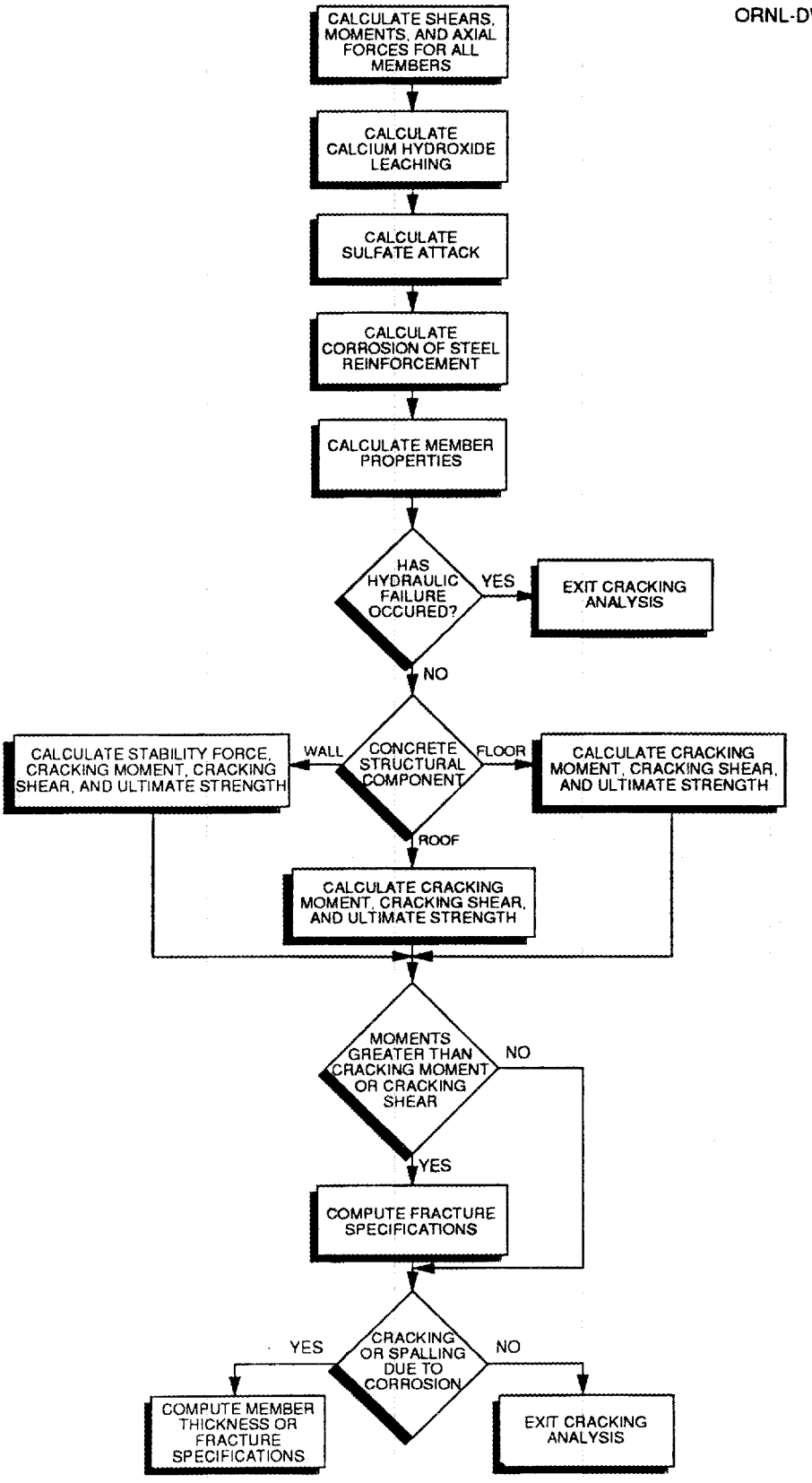

Fig. B.4. Logic flow in concrete degradation and cracking subroutines.

moments, axial forces, and compressive forces are calculated, as appropriate, for each structural component of the disposal unit.

The deterioration of the concrete barriers is modeled with respect to the removal of calcium hydroxide from the cement matrix, surface attack from sulfate ions, and corrosion of steel reinforcement. Concrete component properties—including strength, thickness, and pH—are updated to reflect projected rates of deterioration by these mechanisms. Failure rates of iron and steel liners and boxes are determined as appropriate.

The cracking analysis is performed if hydraulic failure of the disposal unit has not occurred. The cracking moment, cracking shear, ultimate strength, and stability force are calculated for the roof, wall(s), and floor and compared to the moments and forces calculated in the structural analysis. If the calculated moments and shears exceed the cracking moments and shear forces, the structural member is projected to crack. Fracture characteristics—including depth, spacing, and width—are calculated with the onset of cracking. Cracking or spalling of concrete members of the disposal unit may result because of corrosion of the steel reinforcement. In the event of cracking, fracture characteristics are calculated. In the event that spalling of the concrete surface occurs, concrete member thicknesses are updated.

The concrete deterioration analysis is performed for each year of the simulation, while the cracking analysis is conducted until the disposal unit has failed. Failure is judged in terms of the disposal unit's ability to isolate the waste from water percolating through the disposal site. When the disposal unit is no longer hydraulically intact, the engineered barriers are assumed to confer no benefit.

B.1.5 Conceptual and Mathematical Modeling Methodology

The conceptual and mathematical modeling methodology used in the SOURCE computer codes is discussed below. This discussion considers the approaches taken in (1) modeling concrete degradation, (2) performing the structural and cracking analyses for the disposal units, (3) partitioning water through the disposal facility, and (4) modeling advective and diffusive releases of waste radionuclides.

B.1.5.1 Concrete Degradation Modeling

Modes of concrete degradation are considered in terms of surface and bulk attack mechanisms. Surface attack mechanisms are initiated at the surface of the concrete component and progress inward over time. Bulk attack mechanisms modify the properties of the entire concrete component uniformly. Sulfate attack is generally considered the most significant surface attack mechanism in the context of waste repositories (Atkinson and Hearne 1984). In areas characterized by cold winters, freeze-thaw cycling may also represent a serious threat to concrete in disposal facilities. In terms of bulk attack processes, the most notable degradation processes are likely to be calcium hydroxide leaching and alkali-aggregate attack. Corrosion of reinforced steel may also undermine the ability of engineered disposal units to isolate waste therein from the environment. This process differs from the surface and bulk attack processes noted above in that it does not directly alter the properties of the concrete. The models used in simulating the degradation of concrete due to chemical and physical attack are discussed below. The

deterioration processes considered in the SOURCE computer codes include sulfate attack, calcium hydroxide leaching, and corrosion of steel reinforcement.

B.1.5.1.1 Sulfate Attack

Sulfate attack generally manifests itself in the form of expansion and, ultimately, cracking of concrete. It may also result in a progressive loss of strength and mass due to deterioration in the cohesiveness of the cement hydration products.

Three steps are recognized in the deterioration of concrete due to sulfate attack (Atkinson and Hearne 1990):

1. Sulfate ions from the environment penetrate the concrete, usually by diffusion.
2. Sulfate ions react expansively with certain aluminum-containing phases in the concrete.
3. The resulting internal expansion causes stress, cracking, and exfoliation of the concrete surface.

These aspects of the degradation process are incorporated into the sulfate attack model used in the SOURCE computer codes.

The sulfate attack model is based on the work of Atkinson and Hearne (1990). In this model, the reaction zone is assumed to spall out when it reaches a critical thickness, given by

$$X_{spall} = \frac{2\alpha\gamma\,(1-\mu_c)}{E\,(\beta C_e)^2} \quad , \qquad \textbf{(B.1)}$$

where

X_{spall}	=	reaction zone thickness at which spalling occurs (m),
α	=	roughness factor for fracture path,
γ	=	fracture surface energy of concrete (J/m^2),
μ_c	=	Poisson's ratio for concrete,
E	=	Young's modulus (Pa),
β	=	linear strain caused by a mole of sulfate reacted in 1 m^3,
C_e	=	concentration of sulfate as ettringite (mol/m^3).

This critical thickness is achieved at a time

$$t_{spall} = \frac{X_{spall}^2 \, C_e}{2D_i c_o} \quad , \tag{B.2}$$

where

t_{spall}	=	time at which spalling occurs (s),
D_i	=	intrinsic diffusivity (m^2/s),
c_o	=	groundwater sulfate concentration (mol/m^3).

Based on Eqs. (B.1) and (B.2), the rate of degradation is defined as

$$R = \frac{E\beta^2 \, c_o \, C_e \, D_i}{\alpha\gamma \left(1-\mu_c\right)} \quad , \tag{B.3}$$

where R is the degradation rate (m/s). As sulfate attack progresses into the concrete member, it is assumed that the affected layers spall off, effectively reducing the thickness of the concrete member.

It is necessary to use an iterative method to determine the concentration of sulfate as ettringite, C_e, and the degradation rate due to sulfate attack. The starting approximation for C_e is calculated assuming complete reaction in the reacted zone (Atkinson and Hearne 1990). Zero-order values of the X_{spall}, t_{spall}, and R are calculated on this basis; and t_{spall} is compared to the time required for the reaction to go to completion. If t_{spall} is not great enough to permit complete reaction, t_{spall} and C_e are iterated to self-consistency.

B.1.5.1.2 Calcium Hydroxide Leaching

Leaching of calcium hydroxide [$Ca(OH)_2$] results in a loss of strength in the concrete as well as a lowering of the pH of the material. A loss of strength will affect the ability of the concrete structure to withstand the loads placed upon it. Declines in the pH of the concrete may lead to depassivation of the steel reinforcement, thereby promoting corrosion of the steel.

$Ca(OH)_2$ may be leached from the concrete through diffusion and advection. The loss of $Ca(OH)_2$ from concrete members due to diffusion is calculated by solving the following equation:

$$\frac{\partial f_t}{\partial t} = -D\frac{\partial^2 f_t}{\partial^2 y^2} \quad , \tag{B.4}$$

where

f_t	=	fraction of $Ca(OH)_2$ remaining in concrete member,
t	=	time (s),
D_y	=	effective diffusivity of $Ca(OH)_2$ in concrete (m^2/s),
y	=	distance to edge of concrete member from centerline (m).

The boundary conditions that apply are

$$\begin{aligned} f_t\,(y,\ t = 0) &= 1 \text{ for } |y| < \frac{W}{2} \\ &= 0 \text{ for } |y| > \frac{W}{2} \quad , \end{aligned} \tag{B.5}$$

where W is the width in meters of the concrete member.

The equation for f_t is given by

$$f_t = 0.5 \text{ erf } \frac{(y + W/2)R_f}{2(D_y\ t)^{0.5}} - 0.5 \text{ erf } \frac{(y - W/2)R_f}{2(D_y\ t)^{0.5}} \quad , \tag{B.6}$$

where R_f is the retardation factor.

The potential for leaching of $Ca(OH)_2$ through advective mechanisms will depend upon the nature of the groundwater. If the groundwater is saturated or supersaturated with calcium carbonate, no dissolution of $Ca(OH)_2$ will occur. Groundwater that is not saturated with calcium carbonate may leach $Ca(OH)_2$ as it passes through the concrete.

Langelier (1936) has developed the calcium carbonate saturation, or Langelier, index as a means of characterizing the degree of calcium carbonate saturation of groundwater. The index takes into account the effect of temperature, total dissolved solids, total alkalinity, pH, and calcium content on the saturation characteristics of the groundwater. A negative value for the Langelier index denotes a groundwater that is not saturated with calcium carbonate [i.e., one capable of leaching $Ca(OH)_2$ from concrete]. Index values equal to or greater than zero indicate calcium carbonate saturation.

Data taken from Langelier (1936) are used in a regression to estimate the saturation index as a function of the total dissolved solids and temperature of the groundwater. When predicted values of the index are positive, losses of $Ca(OH)_2$ are modeled to occur as a result of diffusion alone. When the groundwater is not saturated with calcium carbonate (i.e., the Langelier index is negative), advective leaching of $Ca(OH)_2$ is calculated using the following formula based on Atkinson (1985):

$$Ca_l = I \frac{Ca_p}{C_t Ca_c} , \qquad \textbf{(B.7)}$$

where

Ca_l	=	groundwater release rate of $Ca(OH)_2$ ($year^{-1}$),
I	=	percolation rate through cask (m/year),
Ca_p	=	$Ca(OH)_2$ concentration in concrete pore solution (mol/L),
C_t	=	concrete member thickness (m),
Ca_c	=	$Ca(OH)_2$ concentration in concrete (mol/L).

The presence of other ions in the groundwater may influence the rate at which $Ca(OH)_2$ is leached from the concrete. Atkinson (1985) reports that magnesium and carbonate are among the species most likely to speed the loss of $Ca(OH)_2$. The effect of these species is modeled using Eq. (B.7), replacing the pore solution concentration of $Ca(OH)_2$, Ca_p, with the sum of this concentration and the groundwater concentrations of magnesium and carbonates.

The quantities of $Ca(OH)_2$ lost from the concrete member due to diffusion and advection are summed to determine the total amount of the constituent leached from the concrete. The concentration of $Ca(OH)_2$ in the concrete is adjusted downward to reflect these losses. All $Ca(OH)_2$ leached from the concrete is assumed to be drawn from the calcium-silicate-hydrate (C-S-H) system of the concrete. The calcium incorporated into the relatively less soluble phases of the concrete is not considered.

Changes in the pH of concrete as a result of the loss of $Ca(OH)_2$ have been well documented (Atkinson 1985). The pH of the concrete is maintained at levels greater than approximately 12.5 in the presence of alkalis, NaOH and KOH. As these highly soluble species are lost due to leaching, the pH declines until it reaches 12.5, at which point the pH of the concrete is controlled primarily by the $Ca(OH)_2$ content of the concrete.

Changes in the pH of the concrete are modeled as alkalis and $Ca(OH)_2$ are leached from the concrete. Based on the data of Greenberg and Chang (1965), the pH is modeled to decline linearly from the initial pH of the concrete, as specified by the user, to 12.5 in direct proportion to the reduction in NaOH and KOH in the concrete. The rates of loss

of these species due to leaching by diffusion and advection are calculated using Eqs. (B.6) and (B.7), respectively.

Following the complete loss of NaOH and KOH from the concrete, changes in the pH of the concrete are modeled as a function of the $Ca(OH)_2$ content. Using data from the work of Greenberg and Chang (1965), concrete pH was regressed on the Ca:Si ratio of the material. As $Ca(OH)_2$ is leached from the concrete, the Ca:Si ratio is updated, and the pH of the concrete is estimated using this regression.

In addition to the pH effects noted, the loss of $Ca(OH)_2$ will also result in a reduction in the strength of the concrete. The loss in strength has been estimated to be approximately 1.5% for every 1.0% of the $Ca(OH)_2$ leached from the concrete (Lea 1970). On the basis of this relationship, the compressive strengths of the concrete members are updated to reflect losses of $Ca(OH)_2$.

B.1.5.1.3 Corrosion of Steel Reinforcement

The damage to concrete resulting from the corrosion of steel reinforcement manifests itself in expansion, cracking, and spalling of the concrete member. The reinforced concrete member may suffer structural damage due to loss of the bond between the steel and concrete, as well as the loss of reinforcement cross-sectional area.

Steel reinforcement is generally made passive because of the alkalinity of the liquid phase in the concrete pores and, hence, does not undergo corrosion. This passive layer may be destroyed through a direct lowering of the pH of the concrete via carbonation or chloride ion penetration to the steel. Both mechanisms of depassivation are considered in the SOURCE computer codes.

Carbonation of the concrete occurs because of the diffusion of carbon dioxide into the material. The depth of carbonation is given by

$$X = k\, t^{0.5} \quad , \tag{B.8}$$

where

X	=	depth of carbonation (m),
k	=	carbonation coefficient (m^2/s),
t	=	time (s).

Upon solving for k, the depth of penetration of the carbonation front into the concrete can be determined for any specified time.

The carbonation coefficient is calculated using the following formula based on Tuutti (1982):

$$\frac{C_x - C_1}{g\left[\frac{k}{2} D_{CO2}^{0.5}\right]} + C_x - C_2 = 0 \quad , \tag{B.9}$$

where

C_x	=	concentration of CO_2 bound in concrete (mol/L),
C_1	=	CO_2 concentration at surface of concrete (mol/L),
C_2	=	CO_2 concentration ahead of carbonation front (mol/L),
D_{CO2}	=	diffusion coefficient of CO_2 in concrete (m^2/s),
$g\left[\frac{k}{2} D_{CO2}^{0.5}\right]$	=	function.

The function $g\left[\frac{k}{2} D_{CO2}^{0.5}\right]$ is given by

$$g\left[\frac{k}{2} D_{CO2}^{0.5}\right] = \pi^{0.5} \frac{k}{2D_{CO2}^{0.5}} \exp\left[\frac{k^2}{4D_{CO2}^2}\right] \operatorname{erfc}\left[\frac{k}{2D_{CO2}^{0.5}}\right] \quad . \tag{B.10}$$

Eqs. (B.9) and (B.10) are combined to arrive at a solution for k, the carbonation coefficient. If it is assumed that the concentration of carbon dioxide ahead of the carbonation front is zero, this solution can be simplified to yield

$$k^2 = \frac{4D_{CO2}\, C_1}{(C_x - 1)\, \pi^{0.5}} \quad . \tag{B.11}$$

A portion of the carbon dioxide diffusing into the concrete is bound by concrete constituents and does not penetrate to the steel reinforcement. This bound carbon dioxide plays no role in depassivation. The amount of carbon dioxide bound in the concrete is set equal to amount of hydrated lime in the concrete (Tuutti 1982). The quantity of hydrated lime is calculated as the product of the CaO content in the concrete and the degree of hydration. The degree of hydration, estimated on the basis of the water-cement ratio for Portland cements (Tuutti 1982), is given by

$$H_f = 0.4 + 0.5WCR \quad , \tag{B.12}$$

where H_f is the fraction of hydrated CaO and WCR is the water-cement ratio.

Given the carbonation coefficient, k, the depth of carbonation is calculated using Eq. (B.8). This solution assumes that the carbonation front is discontinuous. At that time when the front has penetrated to the depth of the steel reinforcement, depassivation of the steel is assumed to occur, and corrosion is initiated.

Steel reinforcement may also be depassivated as a result of the penetration of chloride ions to the steel surface. Using a standard solution to Fick's first law of diffusion, the chloride ion concentration at the steel is calculated as

$$CL_s = CL_i + \left(CL_{gw} - CL_i\right)\left[1 - \mathrm{erf}\frac{C_c}{2(D_{Cl}t)^{0.5}}\right] \quad , \tag{B.13}$$

where

CL_s	=	chloride ion concentration at steel reinforcement (mol/L),
CL_i	=	initial chloride ion concentration in concrete (mol/L),
CL_{gw}	=	chloride ion concentration in groundwater (mol/L),
C_c	=	concrete cover thickness (m),
D_{Cl}	=	effective diffusivity of chloride in concrete (m^2/s),
t	=	time (s).

The concentration of chloride ions at the steel reinforcement required to depassivate the steel has been considered by numerous investigators. Hausmann (1967) found that the pH of the concrete had an effect on the level of chloride ions required to initiate corrosion. In studies carried out using NaOH and $Ca(OH)_2$ solutions, it was found that a chloride ion to hydroxide ion concentration ratio of 0.61 was sufficient to depassivate the steel.

Using the results of Hausmann, a chloride ion to hydroxide ion ratio of 0.61 is assumed to result in depassivation of the steel. The hydroxide ion concentration used in calculating this ratio is determined using the modeled concrete pH. As discussed in Sect. B.1.5.1.2, the pH of the concrete changes with time as NaOH, KOH, and $Ca(OH)_2$ are leached from the material.

Upon depassivation of the steel reinforcement by either carbonation or chloride penetration, corrosion is modeled to occur at a rate determined by the rate of diffusion of

oxygen to the steel. The molar flow of oxygen to the surface of the steel reinforcement is modeled using Fick's first law of diffusion,

$$J_o = -D_o A \frac{d[O_2]}{dx} \quad , \tag{B.14}$$

where

J_o = oxygen flux at the steel reinforcement (g/s),

D_o = effective diffusivity of oxygen through concrete (cm^2/s),

A = surface area over which oxygen diffuses to the reinforcement (cm^2),

$\frac{d[O_2]}{dx}$ = dissolved oxygen concentration gradient (g/cm^4).

The rate of oxygen consumption by the corrosion reaction is assumed to be greater than the rate of oxygen diffusion to the reaction surface. Under these conditions, the corrosion rate is limited by the flux of oxygen at the steel reinforcement.

The use of epoxy-coated steel reinforcement may delay the onset of corrosion by isolating the steel from aggressive ions and oxygen. The coating is not assumed to delay the time of depassivation of the reinforcement. Upon depassivation, however, the coating is assumed to prevent corrosion as long as it remains intact. The effectiveness of epoxy coating on steel reinforcement is modeled using a linear failure function. Using the time at which failure of the coating begins and the time required for all epoxy coating to fail, a fraction of the reinforcement coating that has failed is calculated. This failure fraction is used to adjust the projected rate of corrosion downward.

Corrosion of components other than steel reinforcement will also affect the long-term performance of the disposal units at SWSA 6. Specifically, the metal boxes placed inside disposal casks, the corrugated steel liners used in the construction of disposal silos, and the cast iron pipes used in well construction will all eventually fail due to corrosion. Corrosion of steel and iron barriers used in the tumulus, silo, and well disposal technologies is considered in the SOURCE computer codes. Failure rates of these barriers are modeled using linear failure functions. The user specifies the time at which corrosion of the metal component begins and the number of years required, following this time, for the member to fail completely. Using these data, a failure fraction is calculated for each year of the simulation.

B.1.5.2 Concrete Structural and Cracking Analyses

The structural and cracking analyses serve two distinct purposes in modeling the long-term performance of the SWSA 6 disposal units. The structural analysis considers the

loads placed on the disposal unit to determine the bending moments, shears, axial tensions, and compressive forces placed on the various structural components. Because these loads vary with the structural component under consideration, this analysis is carried out for the roof, wall(s), and floor of each disposal unit.

The cracking analysis is concerned with the ability of the disposal unit to bear the loads placed upon it. Bending moments, shears, axial tensions, and compressive forces calculated as part of the structural analysis are compared to loads and forces at which structural failure will occur to determine the structural integrity of the disposal unit. The cracking analysis must account for the changes in concrete properties projected to occur due to physical and chemical attack. Therefore, it is conducted for each year of the simulation or until hydraulic failure of the disposal unit is complete.

The structural and cracking analyses must address the structural features of each disposal unit. While the disposal silos and wells share a number of common features, both of these technologies differ significantly from the tumulus technology. Consequently, the following discussion considers the tumulus technology separately from that of silos and wells.

The models used in the structural and cracking analyses are generally applicable to performance analysis of concrete, steel, and iron structural components. However, the manner in which some of these models are applied is specific to the disposal technologies in use at SWSA 6. Consequently, general application of the SOURCE computer codes to other disposal configurations requires extreme caution.

B.1.5.2.1 Tumulus Technology

The long-term performance of the tumulus disposal unit is a function of the performance of the individual casks of which it is composed. The structural and cracking analyses performed to model the behavior of these casks are discussed in Sects. B.1.5.2.1.1 and B.1.5.2.1.2, respectively.

B.1.5.2.1.1 Structural analysis

Each structural component of the casks has unique loading conditions placed upon it. Thus, separate structural analyses are conducted for the roof or lid, walls, and floor of the casks. These analyses are described below.

Cask roof. The roof is analyzed structurally as a simply supported, or hinged, slab. The uniform load on the roof of a cask in layer i of the tumulus disposal unit is calculated as

$$q_r = s\rho_s + ih_r\rho_c + (i-1)\left(h_w\rho_w + h_f\rho_c\right) \quad , \tag{B.15}$$

where

q_r = uniform load on cask roof in layer i (lb/in.^{2}),

s	=	soil cover thickness over tumulus (in.),
ρ_s	=	density of soil cover (lb/in.^{3}),
h_r	=	roof thickness (in.),
ρ_c	=	density of reinforced concrete (lb/in.^{3}),
h_w	=	waste thickness (in.),
ρ_w	=	density of waste (lb/in.^{3}),
h_f	=	floor thickness (in.).

Thermal loads on the casks are not considered because the insulating properties of the cover material minimize thermal gradients across the concrete structural components.

The deflection of the simply supported rectangular roof due to the uniform load is given by

$$W(x,y) = \frac{16\, q_r w_r}{\pi^6 D_r} \sum_{m=1}^{\infty} \sum_{n=1}^{\infty} \frac{\sin(m\pi x/a)\, \sin(n\pi y/b)}{mn\left[(m^2/a^2) + (n^2/b^2)\right]^2} , \qquad \textbf{(B.16)}$$

where

$W(x,y)$	=	deflection of roof at location (x,y) (in.),
a	=	width of waste cell (in.),
b	=	length of waste cell (in.),
m, n	=	1, 3, 5, . . . ,
D_r	=	flexural rigidity of the roof (lb-in.^{2}),
w_r	=	width of roof in (x,y) direction (in.).

The flexural rigidity of the roof is calculated using

$$D_r = \frac{E_c h_r^3 w_r}{12\left(1-\mu_c^2\right)} \quad , \tag{B.17}$$

where E_c is the modulus of elasticity of concrete (lb/in.^{2}) and μ_c is Poisson's ratio of concrete. Based on Eqs. (B.16) and (B.17), the bending moments due to uniform loading as a function of location on the roof are calculated as

$$M_x = q_r a^2 \left\{ \frac{16}{\pi^4} \sum_{m=1}^{\infty} \sum_{n=1}^{\infty} \frac{\sin(m\pi x/a)\ \sin(n\pi y/b)}{n/m \left[m^2 + \frac{n^2}{(b/a)^2} \right]^2} + \mu_c \frac{\sin(m\pi x/a)\ \sin(n\pi y/b)}{(b/a)^2\ (m/n) \left[m^2 + \frac{n^2}{(b/a)^2} \right]^2} \right\} \tag{B.18}$$

$$M_y = q_r b^2 \left\{ \frac{16}{\pi^4} \sum_{m=1}^{\infty} \sum_{n=1}^{\infty} \frac{\sin(m\pi x/a)\ \sin(n\pi y/b)}{(m/n) \left[\frac{m^2}{(a/b)^2} + n^2 \right]^2} + \mu_c \frac{\sin(m\pi x/a)\ \sin(n\pi y/b)}{(a/b)^2\ (n/m) \left[\frac{m^2}{(a/b)^2} + n^2 \right]^2} \right\} \tag{B.19}$$

where

M_x = bending moment due to uniform loading in the x direction parallel to width of roof (lb-in./in.),

M_y = bending moment due to uniform loading in the y direction parallel to length of roof (lb-in./in.).

Uniform loads on the cask roof result in shear forces upon that component as well. These forces are calculated as

$$Q_x = q_r a \left[16/\pi^3 \sum_{m=1}^{\infty} \sum_{n=1}^{\infty} \cos(m\pi x/a) \cdot \sin(n\pi y/b) \left\{ \frac{m^2}{n\left[m^2+n^2(a/b)^2\right]^2} + \frac{n}{\left[m^2(b/a) + n^2(a/b)\right]^2} \right\} \right] \tag{B.20}$$

$$Q_y = q_r b \left[16/\pi^3 \sum_{m=1}^{\infty} \sum_{n=1} \sin(m\pi x/a) \cdot \cos(n\pi y/b) \left\{ \frac{m}{\left[m^2(b/a)+n^2(a/b)\right]^2} + \frac{n^2}{m\left[m^2(b/a)^2+n^2\right]^2} \right\} \right] , \tag{B.21}$$

where Q_x and Q_y represent the shear force due to uniform loading in the x and y direction, respectively (lb/in.).

Cask walls. The cask walls are subject to vertical, or uniform, loads and hydrostatic pressures. The uniform loads are due to the weight of the roof and walls and are calculated for a cask in layer i of the tumulus disposal unit using

$$q_w = \rho_s \left[(h_r/2)\, i + (h_f + h_w)\,(i-1) + s\right] \left(1 - \sin f_s\right) , \tag{B.22}$$

where q_w is the uniform load on the cask wall in layer i (lb/in.^{2}) and f_s is the friction angle of soil backfill around tumulus (deg.).

Hydrostatic pressures on the cask walls result from lateral soil pressures from the soil backfill and the waste or grout inside the cask. This load is calculated as

$$P = \rho_s \left[h_w + \frac{h_r + h_f}{2} \right] \left(1 - \sin f_s\right) - \rho_w \left[h_w + \frac{h_r + h_f}{2} \right] \left(1 - \sin f_w\right) , \tag{B.23}$$

where P is the maximum hydrostatic pressure (lb/in.^{2}) and f_w is the friction angle of waste (deg.).

Bending moment calculations for the cask walls must account for the uniform loads and hydrostatic pressures on the structural components. Bending moments due to the uniform load are calculated using Eqs. (B.18) and (B.19), substituting the uniform load on the wall for the uniform load on the roof and changing roof dimensions to those of the wall. Bending moments due to hydrostatic pressures are calculated using

$$M_x = Pa^2 \sum_{m=1}^{\infty} (m\pi)^2 \left\{ \frac{2(-1)^{m+1}}{\pi^5 m^5} + \left[(1-\mu_c)A_m - 2\mu_c B_m\right] \cosh\left[\frac{m\pi y}{a}\right] + (1-\mu_c)B_m \left[\frac{m\pi}{a}\right] y \sinh\left[\frac{m\pi y}{a}\right] \right\} \sin\left[\frac{m\pi x}{a}\right] \tag{B.24}$$

$$M_y = Pa^2 \sum_{m=1}^{\infty} (m\pi)^2 \left\{ \frac{2(-1)^{m+1}}{\pi^5 m^5}\mu_c + \left[(\mu_c-1)A_m - 2B_m\right] \cosh\left[\frac{m\pi y}{a}\right] + (\mu_c-1)B_m \left[\frac{m\pi}{a}\right] y \sinh\left[\frac{m\pi y}{a}\right] \right\} \sin\left[\frac{m\pi x}{a}\right] . \tag{B.25}$$

The quantities A_m and B_m are given by

$$A_m = -\frac{(2 + \alpha_m \tanh \alpha_m)(-1)^{m+1}}{\pi^5 m^5 \cosh \alpha_m} \tag{B.26}$$

$$B_m = \frac{(-1)^{m+1}}{\pi^5 m^5 \cosh \alpha_m} , \tag{B.27}$$

where $\alpha_m = (m\pi b/2a)$.

Bending moments calculated for the uniform load and hydrostatic pressure on the wall are summed to arrive at the final bending moments for the wall as a function of location. The calculations of the bending moments are repeated for each wall geometry comprising the disposal cask.

Shear forces due to hydrostatic pressures on the cask walls are calculated as

$$Q_x = 2Pa \sum_{m=1}^{\infty} (m\pi)^3 \left[\frac{(-1)^{m+1}}{\pi^5 m^5} - B_m \cosh\left[\frac{m\pi y}{a}\right]\right] \cos\left[\frac{m\pi x}{a}\right] \tag{B.28}$$

$$Q_y = -2Pa \sum_{m=1}^{\infty} (m\pi y)^3 B_m \sinh\left[\frac{m\pi y}{a}\right] \sin\left[\frac{m\pi x}{a}\right] . \tag{B.29}$$

Shear forces due to uniform and hydrostatic loads are summed for each wall location. Calculations of shear forces are performed for each wall geometry comprising the cask.

The walls of the casks are subject to compressive forces due to the roof reaction and the weight of the walls. This force, calculated as a function of height on the wall, is given by

$$F_w = R_{ry} + h_{wl} z \rho_c \quad , \tag{B.30}$$

where

F_w	=	compressive force on cask wall at height z (lb/in.),
R_{ry}	=	roof reaction in y direction at height z (lb/in.),
h_{wl}	=	thickness of wall (in.).

Cask floor. The floor of a given cask must bear loads from the walls, including the wall weight and loads transmitted to the walls from the roof, and loads from the waste within the cask. Based on the floor geometry illustrated in Fig. B.5, the bending moments in the region x (or y) $\leq a$ of the beam subjected to a concentrated force and moment are calculated as

$$M_x = \frac{P_x I_{1px}}{2\lambda_x\left[\sinh^2(\lambda_x w_f) - \sin^2(\lambda_x w_f)\right]} \tag{B.31}$$

$$M_y = \frac{P_y I_{1py}}{2\lambda_y\left[\sinh^2(\lambda_y l_f) - \sin^2(\lambda_y l_f)\right]} \quad , \tag{B.32}$$

where

M_x	=	bending moment in x direction parallel to width of floor (lb-in./in.),
P_x	=	applied concentrated load due to wall in x direction (lb/in.),
I_{1px}	=	trigonometric function,
λ_x	=	$(kl_f/4D_{fx})^{0.25}$ (in.$^{-1}$),
k	=	modulus of the subgrade reaction (lb/in.^{3}),
w_f	=	width of floor (in.),

D_{fx} = flexural rigidity of floor (lb-in.^{2}),

M_y = bending moment in y direction parallel to length of floor (lb-in./in.),

P_y = applied concentrated load due to wall in y direction (lb),

I_{1py} = trigonometric function,

λ_y = $(kw_f/4D_{fy})^{0.25}$ (in.$^{-1}$),

l_f = length of floor (in.).

Applied moments due to the wall are not considered in the bending moment calculations, as the assumption is that the floor and walls are hinged.

ORNL-DWG 94-5975

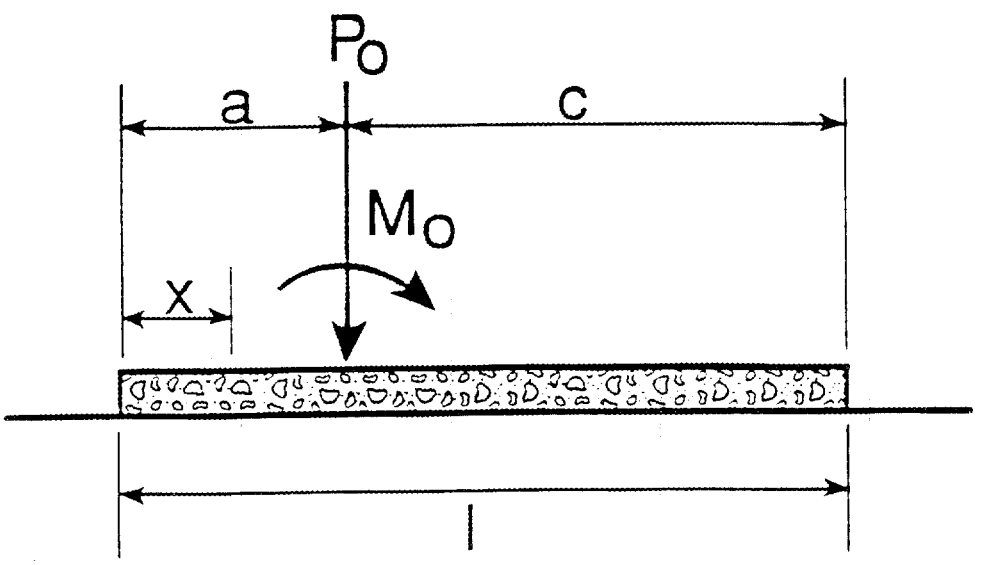

Fig. B.5. Schematic diagram of floor geometry used in the calculation of bending moments.

The concentrated load on the floor, P_x or P_y, is calculated as a function of location using

$$P_x = R_{rx} + h_{wl}\left[h_w + \frac{h_r + h_f}{2}\right]\left(\rho_c - \rho_w\right) \tag{B.33}$$

$$P_y = R_{ry} + h_{wl} + \left[h_w + \frac{h_r + h_f}{2}\right]\left(\rho_c - \rho_w\right) \ . \tag{B.34}$$

The flexural rigidity of the floor is calculated using Eq. (B.17). To calculate the quantity D_{fx}, the thickness and width of the floor are substituted for h_r and w_r, respectively. The thickness and length of the floor are substituted for h_r and w_r, respectively, to calculate D_{fy}.

The parameters I_{1py} are complex trigonometric functions of λ_x, λ_y, and the geometry of the structural member. They are given by

$$\begin{aligned} I_{1px} = {} & 2\sinh(\lambda_x x)\sin(\lambda_x x)\,[\sinh(\lambda_x w_f)\cos(\lambda_x a)\cosh(\lambda_x c) \\ & - \sin(\lambda_x w_f)\cosh(\lambda_x a)\cos(\lambda_x c)] - [\sinh(\lambda_x x)\cos(\lambda_x x) \\ & - \cosh(\lambda_x x)\sin(\lambda_x x)]\,\{\sinh(\lambda_x w_f)\,[\sin(\lambda_x a)\cosh(\lambda_x c) \\ & - \cos(\lambda_x a)\sinh(\lambda_x c)] + \sin(\lambda_x w_f)\,[\sinh(\lambda_x a)\cos(\lambda_x c) \\ & - \cosh(\lambda_x a)\sin(\lambda_x c)]\} \end{aligned} \tag{B.35}$$

$$\begin{aligned} I_{1py} = {} & 2\sinh(\lambda_y y)\sin(\lambda_y y)\,[\sinh(\lambda_y l_f)\cos(\lambda_y a)\cosh(\lambda_y c) \\ & - \sin(\lambda_y l_f)\cosh(\lambda_y a)\cos(\lambda_y c)] - [\sinh(\lambda_y y)\cos(\lambda_y y) \\ & - \cosh(\lambda_y y)\sin(\lambda_y y)]\,\{\sinh(\lambda_y l_f)\,[\sin(\lambda_y a)\cosh(\lambda_y c) \\ & - \cos(\lambda_y a)\sinh(\lambda_y c)] + \sin(\lambda_y l_f)\,[\sinh(\lambda_y a)\cos(\lambda_y c) \\ & - \cosh(\lambda_y a)\sin(\lambda_y c)]\} \ , \end{aligned} \tag{B.36}$$

where the parameters a and c are indicated in Fig. B.5.

Shear forces on the floor of the cask are calculated as a function of location using

$$Q_x = \frac{P_x I_{2px}}{\left[\sinh^2(\lambda_x w_f) - \sin^2(\lambda_x w_f)\right]} \tag{B.37}$$

$$Q_y = \frac{P_y I_{2py}}{\left[\sinh^2(\lambda_y l_f) - \sin^2(\lambda_y l_f)\right]} \quad . \tag{B.38}$$

The parameters I_{2px} and I_{2py} are functions of λ_x, λ_y, and the geometry of the structural member, and are given by

$$\begin{aligned} I_{2px} = {} & [\cosh(\lambda_x x)\ \sin(\lambda_x x) + \sinh(\lambda_x x)\ \cos(\lambda_x x)]\ [\sinh(\lambda_x w_f) \\ & \cos(\lambda_x a)\ \cosh(\lambda_x c) - \sin(\lambda_x w_f)\cosh(\lambda_x a)\ \cos(\lambda_x c)] \\ & + \sinh(\lambda_x x)\ \sin(\lambda_x x)\ \{\sinh(\lambda_x w_f)\ [\sin(\lambda_x a)\ \cosh(\lambda_x c) \\ & - \cos(\lambda_x a)\ \sinh(\lambda_x c)] + \sin(\lambda_x w_f)[\sinh(\lambda_x a)\ \cos\ (\lambda_x c) \\ & - \cosh(\lambda_x a)\ \sin(\lambda_x c)]\} \quad . \end{aligned} \tag{B.39}$$

$$\begin{aligned} I_{2py} = {} & [\cosh(\lambda_y y)\ \sin(\lambda_y y) + \sinh(\lambda_y y)\ \cos(\lambda_y y)]\ [\sinh(\lambda_y l_f) \\ & \cos(\lambda_y a)\ \cosh(\lambda_y c) - \sin(\lambda_y l_f)\ \cosh(\lambda_y a)\ \cos(\lambda_y c)] \\ & + \sinh(\lambda_y y)\ \sin(\lambda_y y)\ \{\sinh(\lambda_y l_f)\ [\sin(\lambda_y a)\ \cosh(\lambda_y c) \\ & - \cos(\lambda_y a)\ \sinh(\lambda_y c)] + \sin(\lambda_y l_f)\ [\sinh(\lambda_y a)\cos\ (\lambda_y c) \\ & - \cosh(\lambda_y a)\ \sin(\lambda_y c)]\} \quad . \end{aligned} \tag{B.40}$$

B.1.5.2.1.2 Cracking analysis

The cracking analysis is performed to assess the ability of the structural components of each cask to bear the loads placed upon it. In the event that the roof, wall(s), or floor of a cask cannot bear these loads, cracking will occur. Cracking of these components may occur as a result of shear forces or bending; cracking of the cask walls may also result from compressive loads on the structure. The manner in which these modes of cracking are modeled is discussed below.

Shear cracking will occur if the shear force on a concrete member exceeds the cracking shear of the member. The cracking shears for the roof, floor, and wall in the horizontal direction are calculated as the minimum of

$$V_{cr} = d_t \left(1.9 C_{str}^{0.5} + 2500 s_{tn} \, Q_x / M_x\right) \tag{B.41}$$

$$V_{cr} = 3.5 C_{str}^{0.5} \, d_t \quad , \tag{B.42}$$

where

V_{cr}	=	shear force at which cracking occurs (lb/in.),
d_t	=	distance from steel reinforcement in tension to compression face of concrete (in.),
S_{tn}	=	area of steel reinforcement in tension per unit width (in.^{2}/in.),
C_{str}	=	compressive strength of concrete (lb/in.^{2}).

The cracking shear for the wall in the vertical direction is the minimum of Eqs. (B.41) and (B.43) where Eq. (B.43) is

$$V_{cr} = 3.5 C_{str}^{0.5} h_{wl} \left[1.0 + F_w \, / \left(500 \, h_{wl}\right)\right]^{0.5} \quad . \tag{B.43}$$

In the event of cracking due to shear failure, crack characteristics are determined. The depth of the single crack is the thickness of the concrete member, and the crack width is 0.013 in.

Cracking due to bending will be initiated if the bending moments calculated for a given concrete member exceed the cracking moment for that structural component. The cracking moment is given by

$$M_{cr} = \frac{I_g f_r}{y_t} \quad , \tag{B.44}$$

where

M_{cr}	=	cracking moment for unit width (lb-in.),
I_g	=	moment of inertia of concrete section (in.^{4}),

y_t = distance from the centroidal axis to the tensile face of the concrete (in.),

f_r = modulus of rupture (lb/in.^{2}).

For a rectangular slab

$$I_g = \frac{a_u h_m^3}{12} , \tag{B.45}$$

where

a_u = unit width of concrete member (in.),

h_m = concrete member thickness (in.),

$$y_t = \frac{h_m}{2} . \tag{B.46}$$

Axial compression force is conservatively neglected in the roof and floor.

If the bending moments exceed the cracking moment but do not exceed the ultimate strength of the concrete member, cracks will not propagate through the entire member. If, however, the bending moments exceed the ultimate strength of the structural component, cracks will span the thickness of the member. The usable flexural strength of a member without compressive steel is approximated using

$$M_u = \phi S_m f_y \left[d_t - \frac{C_d}{2} \right] , \tag{B.47}$$

where

M_u = ultimate flexural strength (lb-in./in.),

ϕ = strength reduction factor,

f_y = yield strength of steel reinforcement (lb/in.^{2}),

C_d = depth of the compression block (in.).

The depth of the compression block is calculated using

$$C_d = \frac{S_{tn} f_y}{0.85 C_{str}} \quad . \tag{B.48}$$

In the case where all reinforcement has been lost due to corrosion, the ultimate strength is equal to the cracking moment.

Crack characteristics are calculated as fractures due to loading form and propagate through a given structural component. The depth of cracking due to bending is calculated as the distance from the surface of the concrete to the neutral axis. Crack depth is computed using the strain compatibility relation, wherein the tensile crack depth is given by

$$d_{cr} = \frac{d_t}{(St_n/E_s) + (St_m/E_c)} \left[(S_{tn}/E_s) + \epsilon_{sh}\right] + d_c \quad , \tag{B.49}$$

where

d_{cr}	=	crack depth (in.),
ϵ_{sh}	=	shrinkage strain of concrete (in./in.),
d_c	=	concrete cover thickness on tension face (in.),
St_n	=	tensile stress in steel reinforcement (lb/in.^{2}),
St_m	=	maximum concrete compressive stress (lb/in.^{2}),
E_s	=	modulus of elasticity of steel reinforcement (lb/in.^{2}).

In modeling the water flow characteristics of failed concrete, it is assumed that cracks achieving a depth equal to three-fourths of the remaining slab thickness functionally penetrate the slab. Prior to this, flow through the concrete is the same as that through intact concrete. If the bending moment exceeds the ultimate strength of the concrete slab, cracks penetrate immediately through the slab.

Numerous equations have been proposed for the prediction of crack spacing and width in flexural members. Nawy (1966) developed a formula for calculating mean crack spacing for a two-way concrete slab,

$$S_{m1} = 0.5 K_n \left[\frac{S_{d1}\, S_{p2}}{Q_d}\right]^{0.5} \quad , \tag{B.50}$$

where

S_{m1} = mean crack spacing in direction 1 (in.),

S_{d1} = diameter of steel reinforcement in direction 1 closest to concrete outer tension face (in.),

S_{p2} = spacing of steel reinforcement in direction 2, perpendicular to direction 1 (in.).

The variables K_n and Q_d are given by

$$K_n = \left[1.6 + 2.4\left[\frac{a}{b} - 0.5\right]\right] 0.29 \tag{B.51}$$

$$Q_d = \frac{S_{tn}}{24 d_c} \quad . \tag{B.52}$$

If the bending moment exceeds the cracking moment but not the ultimate strength of the concrete member, the mean crack width is given by

$$W_m = S_m \left[\beta_r \frac{St_n}{E_s} + \epsilon_{sh}\right] \quad , \tag{B.53}$$

where W_m is the mean crack width (in.) and S_m is the mean crack spacing (in.).

The quantity β_r is given by

$$\beta_r = \frac{d_{cr}}{d_{cr} - d_c} \quad . \tag{B.54}$$

If the bending moment exceeds the ultimate strength of the concrete member, the crack width is calculated as

$$W_m = S_m \left[\frac{f_y}{E_s} + \epsilon_{sh}\right] \quad . \tag{B.55}$$

If the compressive forces on the wall exceed the ultimate strength of the wall in compression, cracking will occur. The ultimate strength of the wall in compression is calculated as

$$M_{uc} = 0.39 h_{wl} C_{str} \left[1.0 - \left[\frac{h_c}{32\, h_{wl}} \right]^2 \right] , \tag{B.56}$$

where h_c is the height of cask wall (in.). Cracking due to compression results in a single crack extending through the concrete member; the crack width is one-tenth the height of the wall section under consideration.

Cracking of a reinforced concrete member may also occur because of corrosion of the steel reinforcement. Since the concrete surrounding the reinforcement prevents free expansion, the products of steel corrosion will exert pressure within the concrete. Based on the elasticity theory (Saada 1974), the magnitude of this internal pressure is approximated using

$$P_i = \frac{\Delta}{r_o} \frac{1}{\left\{1-\mu_r / E_r + [(1-\mu_c) r_o^2 + (1+\mu_c) d_{cv}^2 / E_c (d_{cv}^2 - r_o^2)]\right\}} , \tag{B.57}$$

where

P_i	=	internal pressure due to corrosion (lb/in.^{2}),
d_{cv}	=	distance from concrete face to center of steel reinforcement (in.),
r_o	=	original radius of steel reinforcement (in.),
Δ	=	thickness of the free expansion layer (in.),
μ_r	=	Poisson's ratio of corrosion product,
E_r	=	modulus of elasticity of corrosion product (lb/in.^{2}).

The thickness of the free expansion layer is given by

$$\Delta = r_e + C_t - r_o , \tag{B.58}$$

where r_e is the radius of remaining steel reinforcement (in.) and C_t is the thickness of the corrosion layer under conditions of free expansion (in.).

A general series form of stress function in bipolar coordinates was given by Jeffrey (1920). This function has been applied to the situation of a semi-infinite region with a

circular hole under a uniform radius pressure (Fig. B.6). Based on this work, the stress on the surface of the concrete is given by

$$\sigma_x = -4P_i \frac{r_o^2\left(x^2 - d_{cv}^2 + r_o^2\right)}{\left(x^2 + d_{cv}^2 + r_o^2\right)^2} \quad , \tag{B.59}$$

where σ_x is the stress at the surface of concrete (lb/in.^{2}), and x is the distance from point A (Fig. B.6) along the surface of the concrete (in.). The point of maximum stress occurs at point A (Fig. B.6), where $x = 0$,

$$\sigma_{xA} = \frac{4P_i\, r_o^2}{\left(d_{cv}^2 - r_o^2\right)} \quad . \tag{B.60}$$

The tangent stress at any point, Q or Q', around the circular hole is given by

$$\sigma_{\theta Q} = P_i\,(1 + 2\tan^2\phi) \quad , \tag{B.61}$$

where $\sigma_{\theta Q}$ is the tangent stress at point Q (lb/in.^{2}). This relationship exhibits a maximum tangent stress at point E and is calculated using

$$\sigma_{\theta E} = P_i \frac{d_{cv}^2 + r_o^2}{d_{cv}^2 - r_o^2} \quad , \tag{B.62}$$

where $\sigma_{\theta E}$ is the maximum tangent stress (lb/in.^{2}).

The magnitude of the maximum stress around the circular hole is a function of the ratio of the concrete cover thickness and the radius of the remaining steel reinforcement. The following dependencies are noted:

if $d_{cv} < 1.73r$	$\sigma_{xA} > \sigma_{\theta E} > 2P_i$
if $d_{cv} = 1.73r$	$\sigma_{xA} = \sigma_{\theta E} = 2P_i$
if $d_{cv} > 1.73r$	$\sigma_{xA} < \sigma_{\theta E} < 2P_i$

These relationships provide a simple method for determining where cracking due to corrosion will begin.

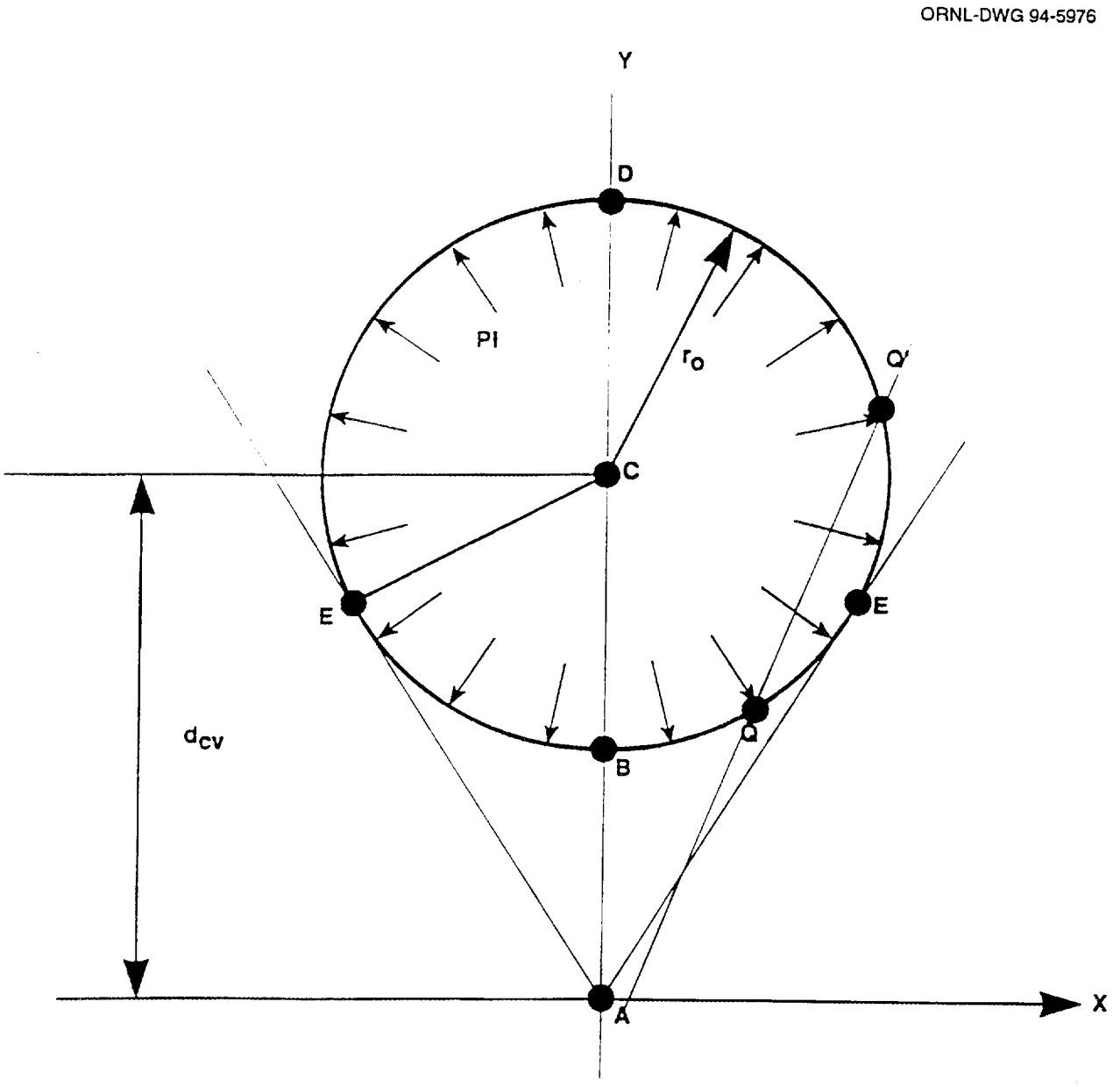

Fig. B.6. Schematic diagram of steel/concrete geometry used in calculating stresses due to corrosion of steel reinforcing.

When the concrete cover thickness is greater than three times the diameter of the reinforcing steel, the tensile stresses around the circular boundary will approach the applied pressure P_i. Plain concrete has minimal tensile strength to resist these stresses, with only 6 to 8% of the specified compressive strength of concrete. Consequently, the maximum tension stress can readily exceed the tensile strength of concrete, at which point cracking begins.

Cracking due to corrosion is typically initiated internally, along the circular boundary, as the ratio of concrete cover thickness to the original radius of the steel is usually greater than 1.73 (Crank 1979). As corrosion progresses, accompanied by the deterioration of the concrete cover, cracking will propagate towards the surface of the concrete slab. When the tension stress at the concrete surface equals or exceeds the tensile strength of the concrete, the cracking will penetrate the concrete cover. This cracking will occur along the length of the steel reinforcement.

Spalling out of the concrete will occur if the concrete cover over the steel reinforcement is small ($d_{cv} \leq 1.73r_o$). Under these conditions, the stresses at the concrete surface exceed both the stresses at the steel surface and the tensile strength of concrete, and spalling along the reinforcement occurs.

B.1.5.2.2 Disposal Silo and Well Technology

The structural and cracking analyses of the disposal silos, wells, and multiple containment wells (wells placed within a silo) are discussed below. While these analyses are similar in many respects to the analyses conducted for the tumulus disposal technology, features unique to these disposal units require additional modeling considerations.

B.1.5.2.2.1 Structural analysis

The structural analysis of the silo and well disposal technologies considers the three structural components of each, loosely referred to as the roof, wall, and floor. These analyses differ depending upon whether the silo or well configuration is being considered. In the event of the multiple containment wells, structural analyses of both the silo and well are performed.

Silo or well roof. A polar coordinate system is used in the structural analysis of the roof of the silo or well disposal unit. The roof is modeled as a simply supported circular plate under uniform loading. The load upon the roof is calculated as

$$q_r = h_r \rho_c + s\rho_s \quad , \tag{B.63}$$

where q_r is the uniform load on the silo or well roof (lb/in.^{2}).

The final bending moments on the roof due to the uniform load consist of radial and tangential components, which are given by

$$M_r = \frac{q_r}{16}\left(3 + \mu_c\right)\left(R_d^2 - r^2\right) \tag{B.64}$$

$$M_t = \frac{q_r}{16}\left[R_d^2\left(3 + \mu_c\right) - r^2\left(1 + 3\mu_c\right)\right] \quad , \tag{B.65}$$

where

M_r = radial component of bending moment (lb-in./in.),

M_t = tangential component of bending moment (lb-in./in.),

R_d = radius of silo or well (in.),

r = distance from center of silo or well roof (in.).

These components are summed to arrive at the total bending moment at location (θ, r):

$$M_x = M_r \cos^2\theta + M_t \sin^2\theta \tag{B.66}$$

$$M_y = M_r \sin^2\theta + M_t \cos^2\theta \quad . \tag{B.67}$$

The shear force on the roof at distance d_t from the interior face of the wall is calculated using

$$Q = \frac{q_r \left[R_d - \frac{h_{wl}}{2} - d_t \right]}{2} \quad . \tag{B.68}$$

Silo or well wall. The wall of the silo or well is subject to uniform and hydrostatic pressures. Setting the origin of the coordinate system at the midheight of the wall, the uniform pressure or load is calculated as

$$q_w = \rho_s \left[s + \frac{h_r}{2} + \frac{h_s}{2} \right] \left(1 - \sin f_s\right) - \frac{h_s}{2} \rho_w \left(1 - \sin f_w\right) \quad , \tag{B.69}$$

where

q_w = uniform load on silo or well wall (lb/in.^{2}),

h_s = silo or well height (in.),

f_s = friction angle of soil backfill around silo or well (deg),

f_w = friction angle of waste inside silo or well (deg).

The corresponding maximum antisymmetrical hydrostatic pressure on the wall is calculated using

$$P = \frac{h_s}{2}\left[\rho_s\left(1-\sin f_s\right) - \rho_w\left(1-\sin f_w\right)\right] \quad . \tag{B.70}$$

Bending moments and shear forces due to uniform pressure are calculated for the silo or well wall using

$$M_y = \frac{q_w\, h_s^2}{4\alpha^2}\left[\frac{\sin\alpha\,\sinh\alpha}{\cos 2\alpha + \cosh 2\alpha}\cos\beta y\,\cosh\beta y - \frac{\cos\alpha\,\cosh\alpha}{\cos 2\alpha + \cosh 2\alpha}\sin\beta y\,\sinh\beta y\right] \tag{B.71}$$

$$Q_y = \frac{q_w h_s}{2\alpha}\left[\frac{\sin\alpha\,\sinh\alpha}{\cos 2\alpha + \cosh 2\alpha}\left(\cos\beta y\,\sinh\beta y - \sin\beta y\,\cosh\beta y\right) - \frac{\cos\alpha\,\cosh\alpha}{\cos 2\alpha + \cosh 2\alpha}\left(\cos\beta y\,\sinh\beta y + \sin\beta y\,\cosh\beta y\right)\right] \quad , \tag{B.72}$$

where

M_y = bending moment due to uniform loading (lb-in./in.),

Q_y = shear force due to uniform loading (lb/in.).

The quantities α and β are given by

$$\alpha = \frac{\beta\, h}{2} \tag{B.73}$$

$$\beta = \left[\frac{3\left(1-\mu_c^2\right)}{R_d^2\, h_{wl}^2}\right]^{0.25} \quad . \tag{B.74}$$

The silo and well walls are also subject to axial and ring compression forces. The axial compressive force on the silo wall is calculated using Eq. (B.30). This same equation is used for the well wall calculation by substituting the density of the cast iron for ρ_C, the density of concrete. The ring compression force due to a uniform load is calculated as

$$N_\theta = q_w R_d \left[1 - \frac{2 \sin \alpha \sinh \alpha}{\cos 2\alpha + \cosh 2\alpha} \sin \beta y \sinh \beta y - \frac{2 \cos \alpha \cosh \alpha}{\cos 2\alpha + \cosh 2\alpha} \cos \beta y \cosh \beta y\right] . \tag{B.75}$$

The bending moments and shear forces due to antisymmetrical hydrostatic pressure are calculated using

$$M_y = \frac{Ph_s^2}{4\alpha^2} \left[\frac{\sin\alpha \cosh\alpha}{\cosh 2\alpha - \cos 2\alpha} \cos\beta y \sinh\beta y - \frac{\cos\alpha \sinh\alpha}{\cosh 2\alpha - \cos 2\alpha} \sin\beta y \cosh\beta y\right] \tag{B.76}$$

$$Q_y = \frac{Ph_s}{2\alpha} \frac{\sin\alpha \cosh\alpha}{\sinh 2\alpha - \cos 2\alpha} (\cos\beta y \cosh\beta y - \sin\beta y \sinh\beta y) - \frac{\cos\alpha \sinh\alpha}{\cosh 2\alpha - \cos 2\alpha} (\cos\beta y \cosh\beta y + \sin\beta y \sinh\beta y) . \tag{B.77}$$

The ring compression force due to hydrostatic pressure is calculated using

$$N_\theta = 2PR_d \left[\frac{y}{h_s} - \frac{\sin \alpha \cosh \alpha}{\cosh 2\alpha - \cos 2\alpha} \sin \beta y \cosh \beta y - \frac{\cos \alpha \sinh \alpha}{\cosh 2\alpha - \cos 2\alpha} \cos \beta y \sinh \beta y\right] . \tag{B.78}$$

Bending moments, shear forces, and ring compression forces calculated for the uniform and antisymmetrical hydrostatic pressures are summed at each location on the wall to arrive at the final values.

Silo or well floor. The circular floor plate is subjected to a distributed line load, or concentrated force, along its perimeter. This concentrated force is calculated as

$$F_c = R_r + h_{wl} h_s (\rho_c - \rho_w) . \tag{B.79}$$

The radial and tangential components of the bending moments for the circular floor are given by

$$M_r = -\frac{D}{l^2}\left[C_1 Z_{2r} - C_2 Z_{1r} - \frac{l}{r}(1-\mu_c)\left(C_1 Z'_{1r} + C_2 Z'_{2r}\right)\right] \tag{B.80}$$

$$M_t = -\frac{D}{l^2}\left[\mu_c\left(C_1 Z_{2r} - C_2 Z_{1r}\right) + \frac{l}{r}(1-\mu_c)\left(C_1 Z'_{1r} + C_2 Z'_{2r}\right)\right] \quad . \tag{B.81}$$

The final bending moments are calculated using Eqs. (B.66) and (B.67).

The maximum shear force on the floor is calculated using

$$Q_r = -\frac{D}{l^3}\left[C_l Z'_{2r} - C_2 Z'_{1r})\right] \quad . \tag{B.82}$$

The quantities D, C_1, C_2, and l are calculated as

$$D = \frac{E_c\, h_f^3}{12(1-\mu^2)} \tag{B.83}$$

$$C_1 = -\frac{F_c}{kl\psi}\left[Z_{1r} + \frac{l}{R_d}(1 - \mu_c)Z'_{2r}\right] \tag{B.84}$$

$$C_2 = -\frac{F_c}{kl\psi}\left[Z_{2r} - \frac{l}{R_d}(1 - \mu_c)Z'_{1r}\right] \tag{B.85}$$

$$l = \left[\frac{D}{k}\right]^{0.25} \quad . \tag{B.86}$$

The quantities Z_{1r}, Z_{2r}, Z_{1r}', and Z_{2r}' are calculated using the following equations:

$$Z_{1r} = 1 + \sum_{n=1}^{\infty} (-1)^n \frac{\left[\frac{r/l}{2}\right]^{4n}}{[(2n)!]^2} \tag{B.87}$$

$$Z_{2r} = \sum_{n=1}^{\infty} (-1)^n \frac{\left[\frac{r/l}{2}\right]^{4n-2}}{[(2n-1)!]^2} \tag{B.88}$$

$$Z'_{1r} = \sum_{n}^{\infty} (-1)^n \frac{2n \left[\frac{r/l}{2}\right]^{4n-1}}{[(2n)!]^2} \tag{B.89}$$

$$Z'_{2r} = \sum_{n}^{\infty} (-1)^n \frac{(2n-1) \left[\frac{r/l}{2}\right]^{4n-3}}{[(2n-1)!]^2} \tag{B.90}$$

where n is 1, 2, 3 . . . The variable ψ, used in Eqs. (B.84) and (B.85), is calculated as

$$\psi = Z_{1R}Z'_{2R} - Z'_{1R}Z_{2R} + \frac{l}{R_d}(1-\mu_c)\,(Z'^2_{1R} + Z'^2_{2R}) \quad . \tag{B.91}$$

The quantities Z_{1R}, Z_{2R}, Z_{1R}', and Z_{2R}' are calculated using Eqs. (B.87) through (B.90), substituting the silo or well radius, R_d, for the parameter r.

B.1.5.2.2.2 Cracking analysis

Cracking or failure of the disposal silos, wells, and multiple containment wells will occur at that point when the structural components can no longer bear the loads placed upon them. Cracking of the roof, wall, and floor of the silo or well may occur as a result of shear forces or bending; the wall may also crack because of compressive forces on the structure.

The cracking analysis for the disposal silos is similar to that performed for the tumulus in that it models the initiation and propagation of cracks in concrete barriers and calculates fracture characteristics. By contrast, the cracking analysis for the wells simply determines when the roof, wall, or floor will undergo initial failure and does not calculate fracture characteristics.

Shear cracking of a silo or a well will occur if the shear force on the structural member exceeds the cracking shear of the member. The cracking shears for the roof and floor in the silo and the well are calculated using Eqs. (B.41) and (B.42).

The cracking shear for the silo wall in the vertical direction is the minimum of

$$V_{cr} = h_{wl}\left(1.9C_{str}^{0.5} + 2500S_{tn}\,Q_x/M_{my}\right) \tag{B.92}$$

$$V_{cr} = 3.5C_{str}^{0.5}h_{wl}\left[1.0 + F_w / \left(500h_{wl}\right)\right]^{0.5} \quad . \tag{B.93}$$

The modified moment, M_{my}, is given by

$$M_{my} = M_y - 0.38F_{wh_{wl}} \quad . \tag{B.94}$$

A single fracture will extend through the entire concrete member due to shear cracking. The width of the fracture is 0.013 in. The shear force at which failure of the cast iron wall of the well occurs is given by

$$V_f = 0.7h_{wl}f_{ws} \quad , \tag{B.95}$$

where f_{ws} is the yield strength of cast iron (lb/in.^{2}).

The roof and floor of the silos and wells will crack if the bending moment at a given location exceeds the cracking moment. The cracking moment is calculated using Eq. (B.44). Cracks will not extend through the entire member unless the bending moments exceed the ultimate strength of the member. The usable flexural strength of the roof and floor is calculated using Eq. (B.47). The ultimate strength for the silo wall is calculated using

$$M_u = \phi \left[S_{tn}f_y\left[d_t - \frac{C_d}{2}\right] + L_{tn}f_y\left[h_{wl} + \frac{L_{tn}}{2} - \frac{C_d}{2}\right] + L_{cm}f_y\left[\frac{C_d}{2} + \frac{L_{cm}}{2}\right]\right] \quad , \tag{B.96}$$

where L_{tn} and L_{cm} are the thickness (in.) of the corrugated steel liner on the tension face and compression face, respectively. The depth of the compression block is given by

$$C_d = \frac{f_y\left(S_{tn} + L_{tn} - L_{cm}\right)}{-0.85C_{str}} \quad . \tag{B.97}$$

Fracture depth, spacing, and width are calculated as cracks initiate and propagate in concrete members comprising the silos and wells. These characteristics are calculated using the approach discussed for the tumulus (Sect. B.1.5.2.1.2).

The wall of the silo or well may fail due to axial or ring compression. In terms of axial compression, the silo wall will crack if the axial compression force on the member

exceeds the ultimate strength of the wall in compression or critical buckling strength. The strength of the wall in axial compression is calculated as the minimum of

$$N_{ac} = 0.39 h_{wt} C_{str} \tag{B.98}$$

$$N_{ac} = \frac{D_w}{h_s^2} m^2 \pi^2 + E_{ch_w} \frac{h_s^2}{R_d^2} m^2 \pi^2 \quad , \tag{B.99}$$

where

N_{ac}	=	ultimate strength or critical buckling strength under axial compression (lb/in.),
D_w	=	flexural rigidity of wall (lb-in.^{2}),
m	=	1, 2, 3 . . .

The flexural rigidity of the wall is calculated using Eq. (B.17), substituting the thickness and unit width of the wall for h_r and w_r, respectively.

If the ring compression force on the silo exceeds the ultimate or buckling strength of the disposal unit, cracking will occur. The strength of the wall subject to ring compression is given by the minimum value, calculated using

$$N_{rc} = \frac{D_w}{R_d^2} \left[n^2 - 1 + \frac{2n^2 - 1 - \mu_c}{1 + A} \right] + \frac{E h_s}{(n^2 - 1)(1 + A)^2} \quad , \tag{B.100}$$

where N_{rc} is the ultimate strength or critical buckling strength under ring compression (lb/in.), and n is 2, 3, 4 . . . The parameter A is calculated using

$$A = \left[\frac{n h_s}{\pi R_d} \right]^2 . \tag{B.101}$$

Compressive forces and bending moments on the wall of the disposal well may result in failure of that unit. If the combined stresses on the wall exceed the yield strength of the cast iron, failure will occur. The combined stresses are calculated as

$$N_{ac} = \frac{F_w}{h_{wl}} + \frac{6M_y}{h_{wl}^2} \quad . \tag{B.102}$$

The wall will also fail if the ring compression force on the well wall exceeds the buckling strength of the wall. The ultimate strength of the wall subject to ring compression is the minimum of

$$N_{rc} = 2h_{wl} \left[2 \times 10^6 \frac{h_{wl}}{R_d} \right] \mid \left[1 - 33.3 \frac{h_{wl}}{R_d} \right] \mid \tag{B.103}$$

$$N_{rc} = 3 \times 10^4 \, h_{wl} \quad . \tag{B.104}$$

Cracking of reinforced concrete due to the corrosion of the steel reinforcement is modeled by the same methodology developed for the tumulus disposal unit. This portion of the cracking analysis is performed for the roof and floor of the disposal silo only. The walls of the silo and the roof and floor of the well lack steel reinforcement.

B.1.5.3 Flow Partitioning

A benefit of the concrete engineered barriers used in the tumulus, silo, and well disposal units is the low hydraulic conductivity of the material. When intact, concrete will usually prevent water in the disposal trenches from contact with the disposed waste. As the concrete members deteriorate with time, however, cracks will form, and greater amounts of water may seep into the waste. Eventually, the conductivity of the concrete will be no better than that of the soil backfill around the disposal units.

In order to calculate radionuclide releases due to advection, one must estimate the amount of water percolating through the waste. The water entering a disposal trench is divided into two components, a component which flows around the disposal unit(s) and a component which contacts the waste.

The flow partitioning scheme used in the SOURCE computer codes is based on the assumption of a saturated steady-state system under a unit hydraulic gradient. Under these conditions, the amount of water percolating through the intact casks, silos, and wells is equal to the saturated hydraulic conductivity of the concrete. As the concrete members deteriorate and crack, preferential flow of water through the fractures occurs at much greater rates.

Preliminary analyses conducted with the SOURCE computer codes have indicated that much of a disposal unit's ability to exclude water is lost when fractures penetrate through one or more concrete members. Based on these observations, the amount of water percolating through the waste is set equal to the amount of water entering the disposal trench when fractures first penetrate the disposal unit. From this point on, the amount of water contacting the waste is solely a function of the hydraulic characteristics of the site soils and soil backfill.

B.1.5.4 Radionuclide Release Modeling

The SOURCE computer codes consider two mechanisms through which waste radionuclides are released to the environment, diffusive leaching and advective leaching. Rates of release from disposal facilities that have not undergone structural failure will generally be low and largely the result of diffusive processes. As the facility deteriorates and undergoes cracking, water may more easily percolate through the waste. Under these conditions, leaching of radionuclides due to advection will be accelerated and tend to overshadow rates of release due to diffusion.

B.1.5.4.1 Leaching Due to Diffusion

Leaching of radionuclides from the disposal units due to diffusion is modeled using the FLOWTHRU computer code (see Sect. B.2). This code represents the diffusion of contamination from grouted waste materials to the outside surface of the disposal unit. The disposal unit is modeled as a two-slab system. The inner slab, representing the grouted waste, is initially contaminated; the outer slab—representing the concrete components of the casks, silos, and wells—is initially uncontaminated.

The steel boxes placed within the casks will play a role in determining the rates of release of waste radionuclides. When the boxes are intact, no releases are considered possible. As failure of the steel boxes due to corrosion becomes more prevalent, greater rates of release are possible. As discussed in Sect. B.1.5.1, a container failure fraction is calculated for the steel boxes for each year of the simulation. This failure fraction is multiplied by the total tumulus inventory to determine the portion of the inventory that is subject to diffusive and advective leaching.

All waste placed in disposal silos or wells is assumed to be subject to diffusive and advective leaching. Neither of these disposal units is equipped with steel barriers to completely isolate the waste from the environment when the barriers are intact.

B.1.5.4.2 Leaching Due to Advection

Leaching of radionuclides due to advection will be proportional to the amount of water contacting the waste and the degree to which radionuclides are sorbed by the waste matrix. Under these conditions, releases can be quantified using

$$\lambda_a = \left[\frac{Q_a}{h_w(H_w + K_d \rho_w)} \sum_{i=1}^{12} I_i \right] \exp\left[-(ln2/t_{1/2})t_a \right] , \qquad \text{(B.105)}$$

where

λ_a = radionuclide release rate due to advection in year a (g/year),

Q_a = radionuclide inventory available for leaching at beginning of year a (g),

I_i = water percolation rate through the waste during month i (cm/month),

h_w = waste thickness (m),

H_w = relative saturation of waste (H_2O volume/waste volume),

K_d = radionuclide distribution coefficient (mL/g),

$t_{1/2}$ = half-life of radionuclide (years),

ρ_w = density of waste (g/cm^3),

t_a = duration of leaching interval (1 year).

The radionuclide inventory available for leaching in the tumulus is the product of the total tumulus inventory and the container failure fraction for the steel boxes. All waste in the disposal silos and wells is assumed to be available for leaching.

Advective leach rates are calculated for each year of the simulation. Radionuclides leached from the waste are assumed to be immediately available for transport away from the disposal unit with the infiltrating groundwater. Rates of release due to advection and diffusion are summed to arrive at the total radionuclide release.

Radionuclides leached from the waste will be transported away from the disposal unit with the water percolating through the disposal "trench." Two flow components are observed at SWSA 6. A vertical component represents recharge to the underlying aquifer at the site, while a lateral subsurface component discharges to surface waters.

Radionuclide releases from the disposal units at SWSA 6 are partitioned between the recharge and lateral flow components in proportion to the vertical and lateral fluxes. The amount of water flowing vertically to the aquifer is calculated as the minimum of the amount of water percolating through the waste trench and the saturated hydraulic conductivity of the soils on the site. Water in excess of the saturated hydraulic conductivity is modeled as lateral subsurface flow.

Assuming that radionuclide concentrations are equal in each flow component, the amount of material entering the recharge component in a given month is given by

$$Q_r = Q_t \frac{I_r}{I} \tag{B.106}$$

where

Q_r = radionuclide release entering recharge flow component (g/month),

Q_t = total radionuclide release from disposal unit (g/month),

I_r = vertical water percolation rate (mm/month),

I = total water percolation rate (mm/month).

The mass of material entering the lateral flow component is simply the difference of the total release and the mass of material transported to the aquifer. Annual releases for each flow component are calculated by summing the monthly releases.

B.2. THE FLOWTHRU COMPUTER PROGRAM

This code represents the diffusion of contamination from grouted waste materials to the outside surface of the disposal unit. The disposal unit is modeled as a two-slab system. The inner slab, representing the grouted waste, is initially contaminated; the outer slab—representing the concrete components of the casks, silos, and wells—is initially uncontaminated.

Assume that we have a two-layer slab with the inner layer of half-thickness a, initially containing a contaminant with concentration C_0 and decay constant λ, and with the outer layer of thickness $b - a$, initially uncontaminated. We will write C_1 for the concentration in the inner layer, and C_2 for the concentration in the outer layer. The diffusion equations for the contaminant are then

$$D_1 \frac{\partial^2 C_1}{\partial x^2} - \lambda C_1 = \frac{\partial C_1}{\partial t} \tag{B.107}$$

and

$$D_2 \frac{\partial^2 C_2}{\partial x^2} - \lambda C_2 = \frac{\partial C_2}{\partial t} \quad , \tag{B.108}$$

with initial conditions

$$C_1 (x, 0) = C_0, \quad 0 \le x < a \tag{B.109}$$

and

$$C_2 (x, 0) = 0, \quad a \le x < b \tag{B.110}$$

and boundary conditions

$$C_2 (b, t) = 0 \quad , \tag{B.111}$$

$$\left(\frac{\partial C_1}{\partial x}\right)_{x=0} = 0 \quad , \tag{B.112}$$

$$C_1\ (a,\ t) = C_2\ (a,\ t) \quad , \tag{B.113}$$

$$D_1 \left(\frac{\partial C_1}{\partial x}\right)_{x=a} = D_2 \left(\frac{\partial C_2}{\partial x}\right)_{x=a} \quad . \tag{B.114}$$

Taking the Laplace transform of the differential equations, we obtain

$$D_1 \frac{d^2\overline{C_1}}{dx^2} - \lambda\overline{C_1} = s\overline{C_1} - C_0 \tag{B.115}$$

and

$$D_2 \frac{d^2\overline{C_2}}{dx^2} - \lambda\overline{C_2} = s\overline{C_2} \quad . \tag{B.116}$$

Solutions to the ordinary differential equations are

$$\overline{C_1}\ (x) = A_1(s)\ \cosh\left(x\sqrt{\frac{s+\lambda}{D_1}}\right) + \frac{C_0}{s+\lambda} \tag{B.117}$$

and

$$\overline{C_2}\ (x) = A_2(s)\ \sinh\left[(b-x)\sqrt{\frac{s+\lambda}{D_2}}\right] \quad . \tag{B.118}$$

Note that these solutions satisfy the transformed boundary conditions

$$\left(\frac{d\overline{C_1}}{dx}\right)_{x=0} = 0 \tag{B.119}$$

and

$$\overline{C_2}\ (b) = 0 \quad . \tag{B.120}$$

Applying the transformed boundary conditions at $x = a$, we obtain

$$\frac{C_0}{s + \lambda} + A_1(s) \cosh\left(a \sqrt{\frac{s + \lambda}{D_1}}\right) = A_2(s) \sinh\left[(b - a)\sqrt{\frac{s + \lambda}{D_2}}\right] \tag{B.121}$$

$$D_1 A_1(s) \sqrt{\frac{s + \lambda}{D_1}} \sinh\left(a \sqrt{\frac{s + \lambda}{D_1}}\right) = -D_2 A_2(s) \sqrt{\frac{s + \lambda}{D_2}} \cosh\left[(b - a)\sqrt{\frac{s + \lambda}{D_2}}\right] . \tag{B.122}$$

Since we wish to find the transform of the release rate at $x = b$, we solve the second equation for $A_1(s)$ in terms of $A_2(s)$, and substitute the result in the first equation to solve for $A_2(s)$. Let

$$p_1 = \sqrt{\frac{s + \lambda}{D_1}} \tag{B.123}$$

and

$$p_2 = \sqrt{\frac{s + \lambda}{D_2}} . \tag{B.124}$$

We obtain

$$A_2(s) = \frac{C_0}{s + \lambda} \frac{\sinh ap_1}{\sinh[(b - a)p_2] \sinh ap_1 + \sqrt{D_2/D_1} \cosh[(b - a)p_2] \cosh ap_1} . \tag{B.125}$$

The transformed release rate at $x = b$ is

$$\bar{q}(s) = -D_2 \left(\frac{d\bar{c}_2}{dx}\right)_{x=b} = D_2 \sqrt{\frac{s + \lambda}{D_2}} A_2(s) \tag{B.126}$$

or

$$\bar{q}(s) = \frac{C_0}{p_2} \frac{\sinh ap_1}{\sinh[(b - a)p_2] \sinh(ap_1) + \sqrt{D_2/D_1} \cosh[(b - a)p_2] \cosh(ap_1)} , \tag{B.127}$$

so that

$$q(t) = C_0 \, e^{-\lambda t} \, g(t) \tag{B.128}$$

with

$$\bar{g}(s) = \frac{\sinh a\sqrt{s/D_1} \,/\, \sqrt{s/D_2}}{\sinh[(b-a)\sqrt{s/D_2}]\,\sinh(a\sqrt{s/D_1}) + \kappa\cosh[(b-a)\sqrt{s/D_2}]\,\cosh(a\sqrt{s/D_1})} \quad , \tag{B.129}$$

where $\kappa = \sqrt{D_2/D_1}$.

The zeroes of the denominator are all on the imaginary axis; we write

$$a\sqrt{s_n \,/\, D_1} = ix_n \quad , \tag{B.130}$$

$$(b-a)\sqrt{s_n \,/\, D_2} = i\alpha x_n \quad , \tag{B.131}$$

so that

$$\alpha = \frac{b-a}{\kappa a} \quad . \tag{B.132}$$

We then need to solve the transcendental equation

$$f(x) = \kappa\cos(x)\cos(\alpha x) - \sin(x)\sin(\alpha x) = 0 \quad . \tag{B.133}$$

The derivatives of $f(x)$ are

$$f'(x) = -(\kappa + \alpha)\sin(x)\cos(\alpha x) - (1 + \kappa\alpha)\cos(x)\sin(\alpha x) \quad , \tag{B.134}$$

$$f''(x) = (\alpha^2 + \alpha\kappa + 1)\sin(x)\sin(\alpha x) - [(\alpha^2 + 1)\kappa + 2\alpha]\cos(x)\cos(\alpha x) \tag{B.135}$$

$$f'''(x) = C_1\cos(x)\sin(\alpha x) + C_2\sin(x)\cos(\alpha x) \quad , \tag{B.136}$$

where

$$C_1 = \alpha^3\kappa + 3\alpha^2 + 3\alpha\kappa + 1 \tag{B.137}$$

and

$$C_2 = \alpha^3 + 2\alpha^2\kappa + 3\alpha + \kappa \ . \tag{B.138}$$

We have plotted $f(x)$ for a few values of a, b, D_1, and D_2 in Figs. B.7. through B.9. We note that the first part of the curves is similar to a cosine curve; we approximate

$$f(x) \approx \kappa \cos \gamma x \ , \tag{B.139}$$

$$f''(x) \approx -\gamma^2 \kappa \cos \gamma x \ , \tag{B.140}$$

$$\gamma = \sqrt{\frac{-f''(0)}{f(0)}} = \sqrt{\frac{(\alpha^2 + 1)\kappa + 2\alpha}{\kappa}} \ , \tag{B.141}$$

and, for a starting estimate for the first root, we use $x_1 = \pi/2\gamma$. We show a few values of the first root and the number of Newton-Raphson iterations needed to reduce the relative error to 5×10^{-9} in Table B.2. Between successive higher roots, the curves resemble sine curves. We approximate

$$f(x) \approx A \sin \gamma x \ , \tag{B.142}$$

$$f'(x) \approx \gamma A \cos \gamma x \ , \tag{B.143}$$

and

$$f'''(x) \approx -\gamma^3 A \cos \gamma x \ . \tag{B.144}$$

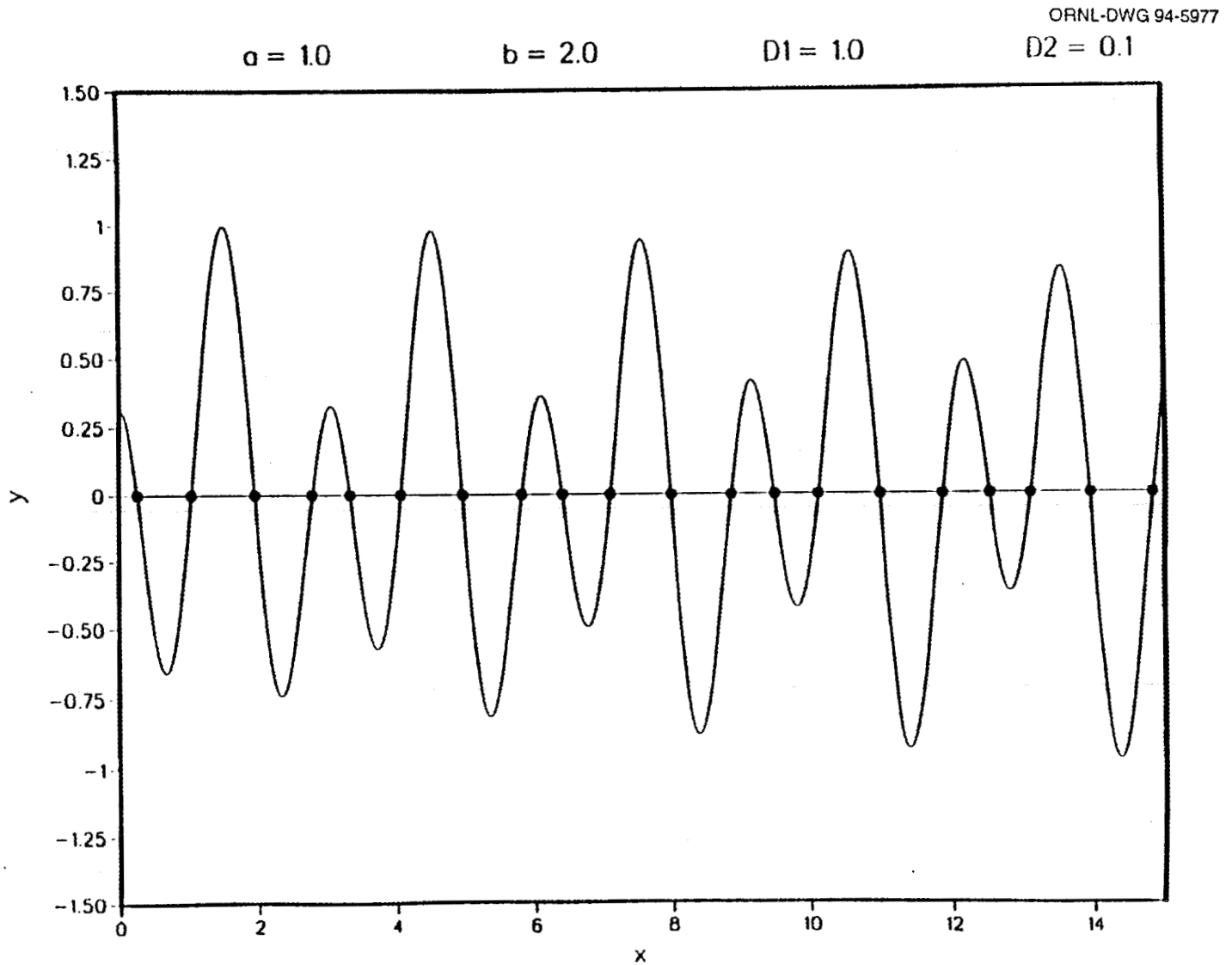

Fig. B.7. Roots of the transcendental equation (dots) for $D_2/D_1 = 0.1$.

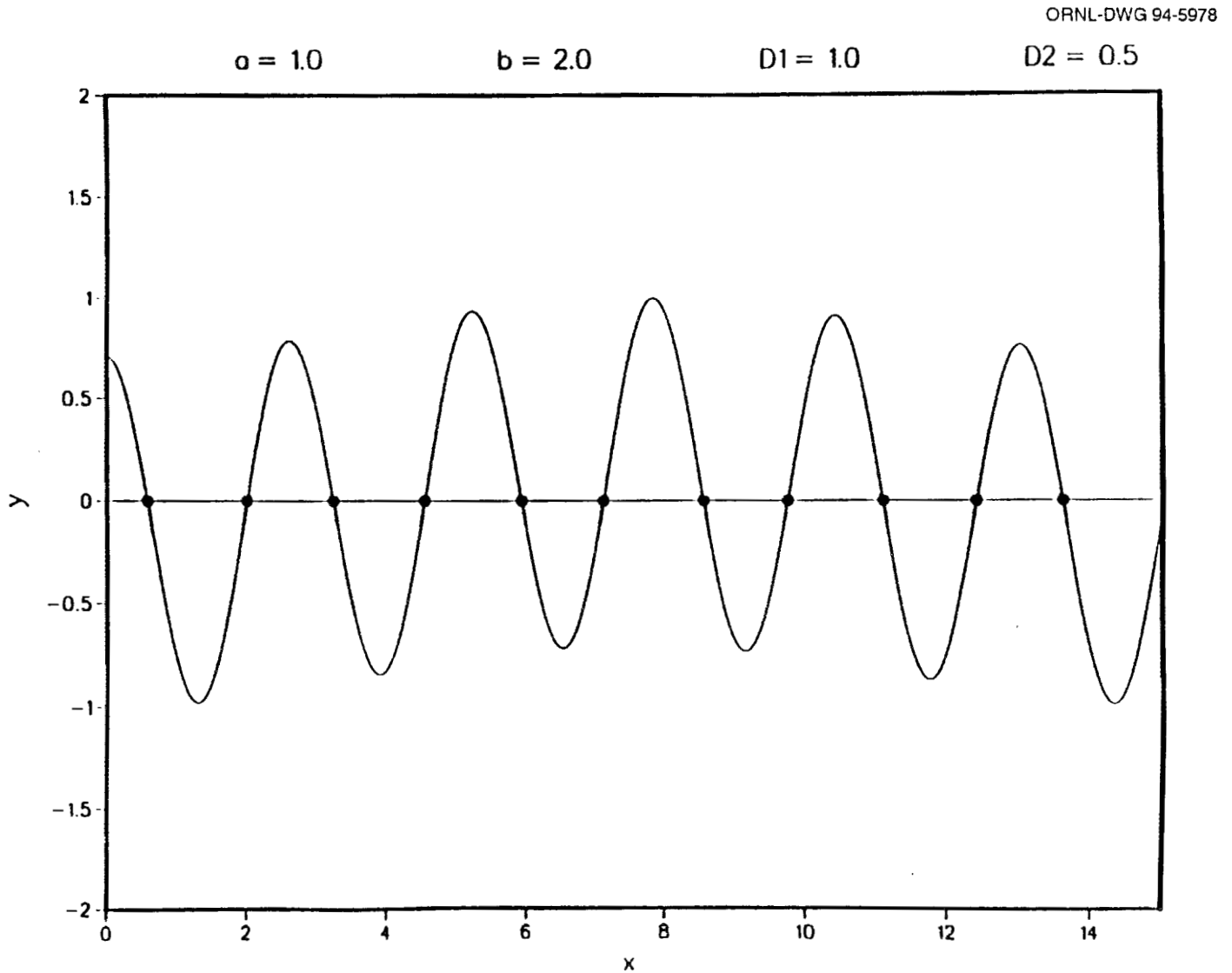

Fig. B.8. Roots of the transcendental equation (dots) for $D_2/D_1 = 0.5$.

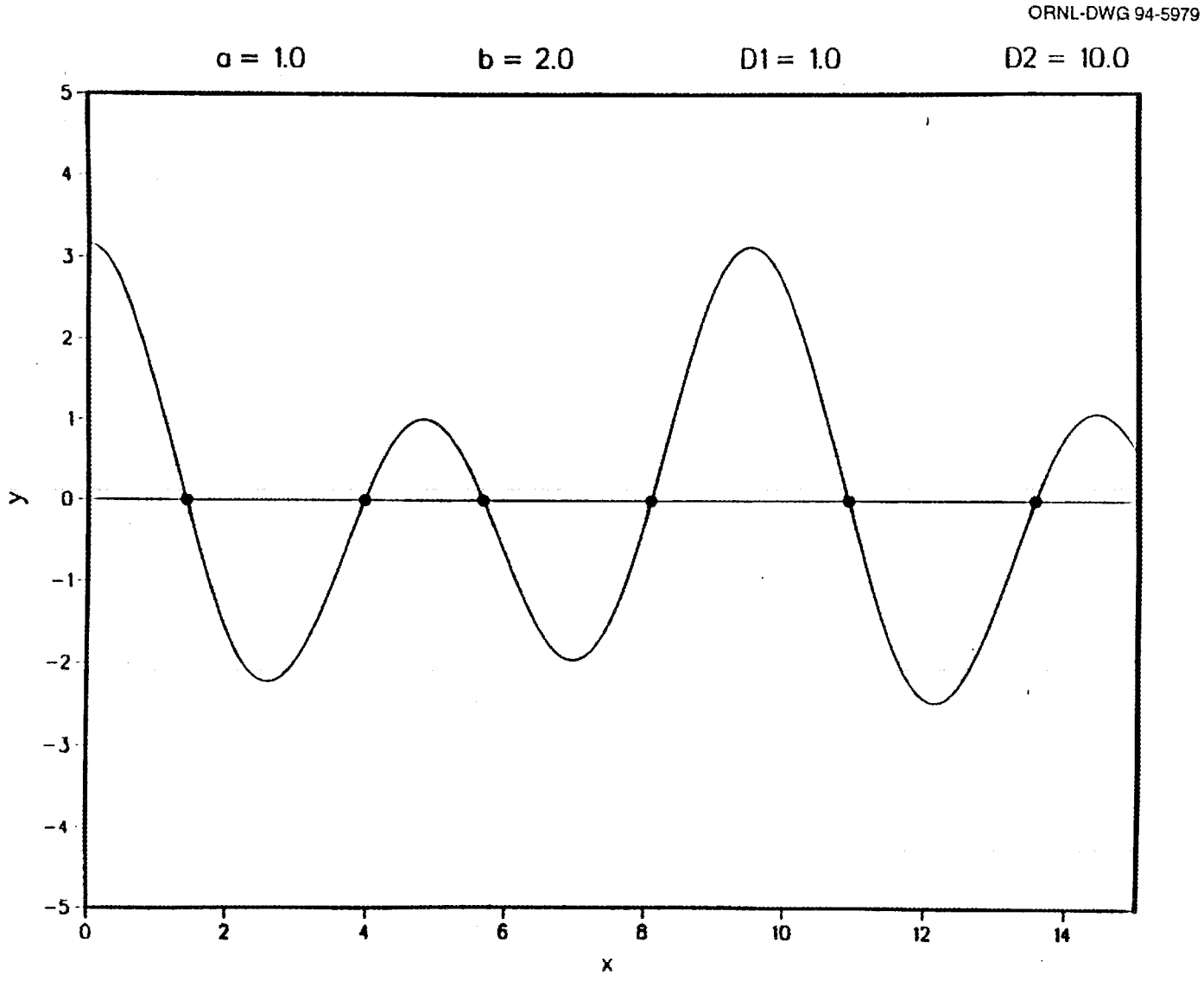

Fig. B.9. Roots of the transcendental equation (dots) for $D_2/D_1 = 10$.

Table B.2. First root of $\kappa \cos x \cos \alpha x \sin \alpha x$[a]

α	.05		.10		.15		.20	
κ								
.1	1.076583	3	.859559	4	.734800	4	.651694	4
.2	1.264279	3	1.075710	3	.949012	4	.857237	4
.5	1.428653	3	1.312642	3	1.217087	3	1.137256	3
1.0	1.495997	1	1.427997	1	1.365910	1	1.308997	1
2.0	1.532429	2	1.495596	3	1.459970	3	1.425310	3
5.0	1.555214	3	1.539765	3	1.524287	3	1.508631	3
10.0	1.562966	3	1.555120	3	1.547167	3	1.539016	3

[a]The integer to the right of each root entry is the number of Newton-Raphson iterations required.

If x_n is a root, we evaluate

$$\gamma = \sqrt{\frac{-f'''(x_n)}{f'(x_n)}} \quad , \tag{B.145}$$

and for a starting estimate of the next root, we use

$$x_{n+1} = x_n + \frac{\pi}{\gamma} \quad . \tag{B.146}$$

Typically, three or four Newton-Raphson iterations are sufficient to obtain convergence to a relative error of 10^{-8}.

The function $\bar{g}(s)$ is of the form

$$\bar{g}(s) = \frac{P(s)}{Q(s)} \tag{B.147}$$

with

$$P(s) = \frac{\sinh a\sqrt{s/D_1}}{\sqrt{s/D_2}} \tag{B.148}$$

and

$$Q(s) = \sinh\left[(b-a)\sqrt{s/D_2}\right]\sinh\left(a\sqrt{s/D_1}\right) + \kappa\cosh\left[(b-a)\sqrt{s/D_2}\right]\cosh\left(a\sqrt{s/D_1}\right) . \tag{B.149}$$

The inverse transform is then

$$g(t) = \sum_{n=1}^{\infty} \frac{P(s_n)}{Q'(s_n)} e^{-s_n t} . \tag{B.150}$$

Carrying out the differentiation of $Q(s)$ and substituting the values for s_n, we obtain

$$g(t) = 2D_1\kappa a \sum_{n=1}^{\infty} \frac{\sin x_n \, e^{-D_1 x_n^2 t/a^2}}{\left[\frac{a(b-a)}{\kappa} + \kappa a^2\right] \cos(\alpha x_n)\sin(x_n) + ab\sin(\alpha x_n)\cos(x_n)} . \tag{B.151}$$

The cumulative amount released remaining at time t is

$$R(t) = \int_0^t q(\tau)\, e^{-\lambda(t-\tau)} d\tau \; ; \tag{B.152}$$

since $q(\tau) = C_0\, e^{-\lambda\tau} g(\tau)$,

$$R(t) = 2\kappa a C_0 e^{-\lambda t} \sum_{n=1}^{\infty} \frac{(1 - e^{-D_1 x_n^2 t/a^2}) \sin x_n}{x_n^2\left[(\alpha + \kappa)\cos \alpha x_n \sin(x_n) = \frac{b}{a}\sin(\alpha x_n)\cos x_n\right]} . \tag{B.153}$$

When $\lambda = 0$, $\lim_{t\to\infty} \frac{R(t)}{aC_0} = 1$, so that

$$\sum_{n=1}^{\infty} \frac{\sin x_n}{x_n^2\left[(\alpha + \kappa)\cos(\alpha x_n)\sin(x_n) + \frac{b}{a}\sin(\alpha x_n)\cos(x_n)\right]} = \frac{1}{2\kappa} \quad ; \tag{B.154}$$

$$\frac{R(t)}{aC_0} = e^{-\lambda t}\left[1 - 2\kappa \sum_{n=1}^{\infty} \frac{e^{-D_1 x_n^2 t/a^2}\sin x_n}{x_n^2\left[(\alpha + \kappa)\cos(\alpha x_n)\sin(x_n) + \frac{b}{a}\sin(\alpha x_n)\cos x_n\right]}\right] . \tag{B.155}$$

At small t, the above expression has two serious computational defects. The series is slowly convergent, and the sum is nearly equal to $1/(2\kappa)$, so that serious loss of significant figures will occur in the subtraction. To develop an alternative expression for small time, we note that

$$\bar{R}(s) = \frac{\bar{q}(s)}{s + \lambda} \tag{B.156}$$

and

$$R(t) = C_0 e^{-\lambda t} h(t) \tag{B.157}$$

where

$$\bar{h}(s) = \frac{\sqrt{D_2}\sinh a\sqrt{s/D_1}}{s^{3/2}\{\sinh[(b-a)\sqrt{s/D_2}]\ \sinh(a\sqrt{s/D_1}) + \kappa\ \cosh[(b-a)\sqrt{s/D_2}]\ \cosh(a\sqrt{s/D_1})\}} . \tag{B.158}$$

If we express all hyperbolic functions in terms of exponential and multiply numerator and denominator by

$$\exp(-a\sqrt{s/D_1})\,\exp\left[-(b-a)\sqrt{s/D_2}\right] , \tag{B.159}$$

we obtain, to first order,

$$\bar{h}(s) \approx \frac{2\sqrt{D_2}}{1+\kappa}\,\frac{e^{-(b-a)\sqrt{s/D_2}}}{s^{3/2}} , \tag{B.160}$$

so that

$$\frac{R(t)}{aC_0} \approx \frac{4}{a(1+\kappa)}\sqrt{D_2 t}\ \mathrm{ierfc}\left(\frac{b-a}{2\sqrt{D_2 t}}\right) \tag{B.161}$$

where ierfc x is the integrated complementary error function (Crank 1979). To compare the two solutions, we show in Table B.3 the first 19 roots of the transcendental equation with the calculated values of $f(x)$ and $f'(x)$; the column headed IT shows the number of Newton-Raphson iterations required. In the second part of the table, we have listed the sum of the first 19 terms of the series at $t = 0$, which should have the value $1/(2\kappa)$. The time T makes the argument of the integrated complementary error function equal to unity.

In some cases, we will need more than the first term. Assuming that we can neglect the terms involving D_1, the series is of the form

$$\bar{h}(s) \approx \frac{2\sqrt{D_2}}{(1+\kappa)s^{3/2}}\sum_{n=0}^{\infty} e^{-(2n+1)(b-a)\sqrt{s/D_2}}\left(\frac{1-\kappa}{1+\kappa}\right)^n , \tag{B.162}$$

so that

$$h(t) \approx \frac{4\sqrt{D_2 t}}{1+\kappa}\sum_{n=0}^{\infty}\left(\frac{1-\kappa}{1+\kappa}\right)^n \mathrm{ierfc}\left[\frac{(2n+1)(b-a)}{2\sqrt{D_2 t}}\right] . \tag{B.163}$$

Since ierfc(10) $\approx 10^{-44}$, we sum the series until the relative error is 5×10^{-9}, or until the argument of the integrated complementary error function is greater than 10. If more than three terms are required, we use the Aitken delta-squared process to accelerate the convergence.

Table B.3. Comparison of series and alternate solutions

a = 121.92 cm, b − a = 15.24 cm, D1 = D2 = 1.(10**−6)

N	*IT*	*x*(*N*)	*f*(*x*)	*f'*(*x*)
1	2	4.18879×10^{0}	2.47794×10^{-16}	1.12500×10^{0}
2	2	6.98132×10^{0}	-5.54298×10^{-16}	-1.12500×10^{0}
3	2	9.77384×10^{0}	6.49762×10^{-16}	1.12500×10^{0}
4	1	1.25664×10^{1}	2.74089×10^{-9}	-1.12500×10^{0}
5	0	1.53589×10^{1}	-2.74089×10^{-9}	1.12500×10^{0}
6	1	1.81514×10^{1}	2.74088×10^{-9}	-1.12500×10^{0}
7	1	2.09440×10^{1}	-1.21669×10^{-7}	1.12500×10^{0}
8	2	2.37365×10^{1}	1.36664×10^{-16}	-1.12500×10^{0}
9	2	2.65290×10^{1}	1.63999×10^{-16}	1.12500×10^{0}
10	2	2.93215×10^{1}	-4.80844×10^{-17}	-1.12500×10^{0}
11	2	3.21141×10^{1}	3.93766×10^{-15}	1.12500×10^{0}
12	1	3.49066×10^{1}	1.21669×10^{-7}	-1.12500×10^{0}
13	1	3.76991×10^{1}	-2.74040×10^{-9}	1.12500×10^{0}
14	0	4.04916×10^{1}	2.74040×10^{-9}	-1.12500×10^{0}
15	1	4.32842×10^{1}	-2.74088×10^{-9}	1.12500×10^{0}
16	1	4.60767×10^{1}	1.21669×10^{-7}	-1.12500×10^{0}
17	2	4.88692×10^{1}	-2.13521×10^{-15}	1.12500×10^{0}
18	2	5.16617×10^{1}	-2.18182×10^{-15}	-1.12500×10^{0}
19	2	5.44543×10^{1}	-2.33385×10^{-15}	1.12500×10^{0}

Sum of series at t = 0:	5.00330×10^{-1}
1/(2*kappa) :	5.00000×10^{-1}
Sum of series at t = T:	4.96859×10^{-1}
Last term retained:	2.42018×10^{-9}
Release (series):	6.28182×10^{-3}
Release (ierfc):	6.28182×10^{-3}

T = (b × a) **2/(4.*D2).

B.3. REFERENCES

Atkinson A., and J. A. Hearne 1984. *An Assessment of the Long-Term Durability of Concrete in Radioactive Waste Repositories*, AERE Harwell, AERE-R11465, October.

Atkinson, A. 1985. *The Time Dependence of pH Within a Repository for Radioactive Waste Disposal*, Harwell Laboratory, AERE-R11777, April.

Atkinson A., and J. A. Hearne 1990. "Mechanistic Model for the Durability of Concrete Barriers Exposed to Sulphate-Bearing Groundwaters," *Mat. Res. Soc. Symp. Proc.* **176**, 149–56.

Crank, J. 1979. *The Mathematics of Diffusion*, Clarendon Press, Oxford, England.

Greenburg, S. A., and T. N. Chang 1965. "Investigation of the Colloidal Hydrated Calcium Silicates. II. Solubility Relationships in the Calcium Oxide-Silica-Water System at 25 D," *J. Phys. Chem.* **69**, 182.

Hausmann, D. A. 1967. "Steel Corrosion in Concrete," *Materials Protection*, November 19–23.

Jeffrey, G. B. 1920. "Plane Stress and Plane Strain in Bipolar Coordinates," pp. 265–293 in *Transactions of the Royal Society of London*, Vol. 221, Harrison & Sons Ltd., March.

Langelier, W. F. 1936. "The Analytical Control of Anti-Corrosion Water Treatment," *J. Amer. Water Works Assoc.* **28**(10), 1500–21.

Lea, F. M. 1970. *The Chemistry of Cement and Concrete*, 3d ed., Edward Arnold, Ltd., London.

Nawy, E. D. 1966. "Crack Width Control in Welded Fabric Reinforced Centrally Loaded Two-Way Concrete Slabs," presentation at the 62nd ACI Annual Convention, Philadelphia, March.

Saada, A. S. 1974. *Elasticity Theory and Application*, Pergamon Press, Inc., New York.

Shuman, R., N. Chau, and E. A. Jennrich 1992. *The Source Computer Codes: Models for Evaluating the Long-Term Performance of SWSA 6 Disposal Units, Version 1.0: User's Manual*, RAE-9005/8-1, Rogers and Associates Engineering Corporation, Salt Lake City, Utah, April.

Tuutti, K. 1982. *Corrosion of Steel in Concrete*, Swedish Cement and Concrete Research Institute, Stockholm.

APPENDIX C

WASTE PROPERTIES AND TRANSPORT PROPERTIES OF RADIONUCLIDES AT THE SOLID WASTE STORAGE AREA 6 DISPOSAL UNITS

H. W. Godbee
J. W. Nehls, Jr.
A. S. Icenhour

June 1993

C. WASTE PROPERTIES AND TRANSPORT PROPERTIES OF RADIONUCLIDES AT THE SOLID WASTE STORAGE AREA 6 DISPOSAL UNITS

C.1 WASTE PROPERTIES

The solubilities in water for various compounds, oxides, and metals of the identified key nuclides used for screening in the Solid Waste Storage Area (SWSA) 6 disposal units (as described in Sect. 3) are presented in Tables C.1 through C-10. The solubilities of the radionuclides determine whether pore water concentrations exceed solubility limits. If the pore water concentration of a species exceeds the solubility limit concentration in the pores, the transport process is said to have a solubility-limit constraint. If the pore water concentration of a species is less than the solubility limit concentration in the pores, the process is taken to have a partition or distribution coefficient (K or K_d) constraint. Values for these coefficients are given in Table C.11. The inventory of nuclides reported to be in the SWSA 6 disposal units are presented in Tables A.3 through A.11 of Appendix A.

Depletion of the source in this study occurs in three ways: (1) bulk or mass flow under a hydraulic gradient (i.e., advection), (2) flow under a concentration gradient (i.e., diffusion), and (3) radioactive decay of the source. The input data to SOURCE1 and SOURCE2 for key nuclides used for screening are listed in Tables C.1 through C.10.

C.2 WASTE TRANSPORT PROPERTIES

In this analysis the waste and concrete are considered to be unconsolidated and consolidated porous media, respectively. The transport of various species through such media can usually be analyzed and explained in terms of advection and diffusion.

Release of radionuclides due to advection can be modeled as a zero-order leaching process accounting for both sorption and decay. Advective leaching is proportional to the amount of water contacting the waste and concrete, and is inversely proportional to the degree to which the radionuclides are retained by the waste and concrete matrices. For this model, the radionuclide inventory is assumed to be homogeneously mixed within a finite waste volume that is contacted by a constant infiltration rate of water. The inventory is assumed constant during a given time period and is updated at the end of the time period to reflect losses (see Ref. 1 in App. B). If these assumptions are applied, the advective release rate can be quantified as

$$\lambda_a = \left[\frac{Q_a}{h_w(H_w + K_d \rho_w)} \sum_{i=1}^{12} I_i \right] \exp\left[-(\ln 2/t_{1/2})t_a\right] , \qquad \text{(C.1)}$$

where

λ_a	=	radionuclide release rate due to advection in year a, g/year;
Q_a	=	radionuclide inventory available for leaching at the beginning of year a, g;
I_i	=	water percolation rate through the waste during month i, cm/month;
h_w	=	waste thickness, cm;
H_w	=	relative saturation of waste, volume H_2O/volume waste;
K_d	=	radionuclide distribution coefficient, mL/g;
ρ_w	=	density of waste, g/cm^3;
$t_{1/2}$	=	half-life of radionuclide, year; and
t_a	=	duration of leaching interval, 1 year.

The release of radionuclides due to diffusion can be modeled as a two-slab system. The inner slab, representing the grouted waste, is initially contaminated; the outer slab, representing the concrete components of the vaults, silos, and wells, is initially uncontaminated (see Sect. B.2 in App. B). The diffusion coefficient for a given species can be expressed as

$$D = \frac{D_s}{R} , \qquad \text{(C.2)}$$

where

D	=	apparent (effective) diffusion coefficient for the species in the porous body [e.g., concrete (D_c), waste (D_w), etc.], cm^2/s;
D_s	=	self-diffusion coefficient of the species in an infinite or free volume of pore liquid, cm^2/s; and
R	=	retardation factor, dimensionless.

As generally treated, the evaluation of R depends upon the concentration of a species in the pore liquid. If the pore liquid concentration (C_{pw}) of a species is below its solubility limit concentration (C_s), R is expressed as

$$R = G(1 + K)(H^{-1}) \quad , \tag{C.3}$$

where

G	=	geometry or matrix factor, dimensionless;
K	=	partition coefficient, dimensionless; and
H	=	fraction of pore capacity to hold liquid that is filled, dimensionless.

Thus, for the case where $C_{pw} < C_s$, the apparent (effective or retarded) diffusion coefficient is given by

$$D = \frac{D_s}{G(1 + K)(H^{-1})} \quad . \tag{C.4}$$

The geometry factor, G, is defined as τ^2/γ, where τ is tortuosity and γ is constrictivity. Tortuosity is a measure of the diffusion path length in a porous body, and constricitivity is a measure of the choking effect of the pores. Both factors have sound physical meaning, and independent methods to determine them are available. Tortuosity (like porosity) is a parameter characterizing the pore space, while constrictivity depends on the types of transport phenomena taking place. Thus, G generally represents a physical containment or retardation factor of the matrix. The expression $(1 + K)$ can account for phenomena such as sorption/desorption and ion exchange; thus, it represents a chemical containment or retardation factor. The relationship of the dimensionless partition coefficient K to other commonly measured partition or distribution coefficients is shown in the following table.

Type of partition coefficient	Units of partition coefficient	Relationship to K
Mixed, K_{MP}	$\frac{\text{amount of species/mass of pore-free solid}}{\text{amount of species/volume of liquid}}$	$K = \rho_p\left(\frac{1-e}{e}\right)K_{MP}$
Mixed, K_{MB}	$\frac{\text{amount of species/volume of porous body}}{\text{amount of species/volume of liquid}}$	$K = \rho_b\left(\frac{1}{e}\right)K_{MB}$

Volume, K_{vv}

$$\frac{\text{amount of species/volume of pore-free solid}}{\text{amount of species/volume of liquid}} \qquad K = \left(\frac{1-\epsilon}{\epsilon}\right)K_{vv}$$

Geometry, K_{GV}

$$\frac{\text{amount of species/volume of porous body}}{\text{amount of species/volume of liquid}} \qquad K = \left(\frac{1}{\epsilon}\right)K_{GV}$$

In the relationship equations, ρ_p is the density of the pore-free solid (i.e., mass of pore-free solid/volume of pore-free solid), ϵ is the void fraction (i.e., volume of pores/volume of porous body), and ρ_b is the density of the porous body (mass of porous body/volume of porous body).

If there is a solubility constraint for a species—that is, the pore liquid is saturated—the leachate concentration is set equal to the solubility limit. In other words, the program compares C_{pw} (concentration due to advection plus diffusion) to C_s (concentration at the solubility limit), and if C_{pw} exceeds C_s, the leachate concentration is set at C_s.

The self-diffusion coefficients (D_s) needed to estimate retarded diffusion coefficients (D) were taken from available literature values or estimated by interpolation or extrapolation of known values for other ions (of the same oxidation state) in the same chemical family (e.g., actinides). The self-diffusion coefficients and the retarded diffusion coefficients are presented in Table C.12.

The geometry factors (G) needed were taken from available literature values or estimated from a known value using the relationship

$$G_2 = G_1\left(\frac{r_2}{r_1}\right)^2 , \qquad \text{(C.5)}$$

where G and r are the geometry factor and hydrated ionic radius, respectively. Values of hydrated ionic radii are listed in standard chemical handbooks. The values of G used in this study are given in Table C.12.

The distribution coefficients, K, were taken from available literature values or estimated from a known value using a relationship of the form

$$K_2 = K_1\left(\frac{Z_2}{Z_1}\right) , \tag{C.6}$$

where K and Z are the distribution coefficient and atomic number, respectively. The values of K used are presented in Table C.12.

The diffusion coefficients calculated for waste (D_w) and concrete (D_c) using Eq. (C.4) are listed in Table C.12.

C.3 SCREENING CALCULATIONS

As described in Sect. 3, the SOURCE1 and SOURCE2 models were used to screen the radionuclides disposed of in SWSA 6 for the purposes of limiting the scope of the transport of contamination in the environment. The reduced list of radionuclides used in the environmental transport of contamination is presented in Tables C.13–C.22. These tables also provide low and high estimates of the modeling parameters that were used in the uncertainty analysis presented in Sect. 4.6.

Table C.1. Input data to SOURCE1 for key nuclides in Tumulus I

Nuclide	Half-life[a] (year)	Formula	Formula weight	Solubility[b] (mol/L)	Waste K_d[c] (mL/g)	Inventory (g/vault)	Diffusion coefficient[d] (m^2/s)	
							Waste	Concrete
^{3}H	1.23×10^{1}	T_2O	22	1.11×10^{2}	1.99×10^{-1}	1.42×10^{-6}	3.88×10^{-9}	1.86×10^{-9}
^{14}C	5.73×10^{3}	$BaCO_3$	199	1.11×10^{-4}	1.09×10^{0}	2.22×10^{-5}	1.44×10^{-11}	2.18×10^{-12}
^{60}Co	5.27×10^{0}	Co	60	3.46×10^{0}	3.97×10^{6}	1.76×10^{-5}	1.66×10^{-17}	6.77×10^{-13}
^{63}Ni	1.00×10^{2}	$NiCO_3$	123	7.83×10^{-4}	6.36×10^{0}	1.66×10^{-5}	1.01×10^{-11}	1.21×10^{-12}
^{90}Sr	2.85×10^{1}	$SrCO_3$	150	7.45×10^{-5}	8.74×10^{0}	1.23×10^{-4}	1.17×10^{-11}	1.34×10^{-12}
^{99}Tc	2.13×10^{5}	NH_4TcO_4	181	9.11×10^{-2}	1.29×10^{0}	7.01×10^{-4}	1.25×10^{-11}	1.82×10^{-12}
^{137}Cs	3.00×10^{1}	Cs_2CO_3	334	1.60×10^{1}	1.99×10^{1}	8.17×10^{-4}	6.80×10^{-12}	5.12×10^{-13}
^{152}Eu	1.33×10^{1}	Eu_2O_3	352	2.84×10^{-6}	3.78×10^{0}	1.42×10^{-5}	7.95×10^{-13}	9.17×10^{-14}
^{154}Eu	8.80×10^{0}	Eu_2O_3	356	2.84×10^{-6}	3.78×10^{0}	1.48×10^{-5}	7.95×10^{-13}	9.17×10^{-14}
^{226}Ra	1.60×10^{3}	$RaSO_4$	322	6.21×10^{-8}	1.99×10^{1}	8.73×10^{-6}	4.10×10^{-13}	4.74×10^{-14}
^{232}Th	1.41×10^{10}	ThO_2	264	7.57×10^{-8}	5.36×10^{1}	7.68×10^{0}	3.24×10^{-14}	3.73×10^{-15}
^{232}U	6.89×10^{1}	UO_2	264	1.46×10^{-6}	5.56×10^{1}	3.80×10^{-9}	3.11×10^{-14}	3.50×10^{-15}
^{233}U	1.59×10^{5}	UO_2	265	1.46×10^{-6}	5.56×10^{1}	5.35×10^{-3}	3.11×10^{-14}	3.50×10^{-15}
^{235}U	7.04×10^{8}	UO_2	267	1.46×10^{-6}	5.56×10^{1}	3.55×10^{-1}	3.11×10^{-14}	3.50×10^{-15}
^{238}U	4.47×10^{9}	UO_2	270	1.46×10^{-6}	5.56×10^{1}	3.44×10^{1}	3.11×10^{-14}	3.50×10^{-15}
^{238}Pu	8.77×10^{1}	PuO_2	270	1.71×10^{-8}	5.76×10^{1}	1.51×10^{-7}	3.00×10^{-14}	3.41×10^{-15}

Table C.1 (continued)

Nuclide	Half-life[a] (year)	Formula	Formula weight	Solubility[b] (mol/L)	Waste K_d[c] (mL/g)	Inventory (g/vault)	Diffusion coefficient[d] (m^2/s)	
							Waste	Concrete
^{239}Pu	2.41×10^4	PuO_2	271	1.71×10^{-8}	5.76×10^1	9.55×10^{-4}	3.00×10^{-14}	3.41×10^{-15}
^{240}Pu	6.56×10^3	PuO_2	272	1.71×10^{-8}	5.76×10^1	1.51×10^{-4}	3.00×10^{-14}	3.41×10^{-15}
^{241}Am	4.33×10^2	Am_2O_3	530	3.27×10^{-6}	5.76×10^1	3.30×10^{-5}	5.46×10^{-14}	6.26×10^{-15}
^{243}Am	7.38×10^3	Am_2O_3	534	3.27×10^{-6}	5.76×10^1	5.63×10^{-5}	5.46×10^{-14}	6.26×10^{-15}
^{243}Cm	2.85×10^1	Cm_2O_3	534	2.84×10^{-6}	5.76×10^1	1.08×10^{-9}	5.46×10^{-14}	6.26×10^{-15}
^{244}Cm	1.81×10^1	Cm_2O_3	536	2.84×10^{-6}	5.76×10^1	1.54×10^{-6}	5.46×10^{-14}	6.26×10^{-15}
^{249}Cf	3.51×10^2	$Cf(NO_3)_3$	435	3.49×10^0	5.96×10^1	1.37×10^{-7}	5.28×10^{-14}	6.10×10^{-15}

Note: Inventory based on 197 vaults and the inventories for these radionuclides given in Table A.3 of Appendix A.

[a]*Sources:* General Electric Company, *Chart of the Nuclides*, Knolls Atomic Power Laboratory, Schenectady, N.Y., 1983; E. Browne and R. B. Firestone, *Table of Radioactive Isotopes*, ed. V. S. Shirley, John Wiley and Sons, Inc., New York, 1986.

[b]*Sources:* D. R. Lide, ed., *CRC Handbook of Chemistry and Physics*, 73rd ed., 1992; Freie Universität Berlin and Institut für Anorganische und Analytische Chemie, *Solubility and Speciation of Actinides in Salt Solutions and Migration Experiments of Intermediate Level Waste in Salt Formations*, FUB/FI 53132-415/85, 1986; M. Schweingruber, *Actinide Solubility in Deep Groundwaters—Estimates for Upper Limits Based on Chemical Equilibrium Calculations*, EIR-Bericht Nr. 507, December 1983; Agence Internationale de l'Energie Atomique, *Seminaire sur les Techniques d'Etude et les Methodes d'Evaluation des Sites en vue du Stockage Definitif Souterrain des Dechets Radioactifs*, IAEA-SR-104, February 1984.

[c]*Sources:* H. A. Friedman and A. D. Kelmers, *Laboratory Measurement of Radionuclide Sorption in Solid Waste Storage Area 6 Soil/Groundwater Systems*, ORNL-TM-10561, Martin Marietta Energy Systems, Inc., Oak Ridge Natl. Lab., June 1990; I. Neretnieks, "Diffusivities of Some Constituents in Compacted Wet Bentonite Clay and the Impact on Radionuclide Migration in the Buffer," *Nucl. Tech.* 71, 458–70 (1985).

[d]The apparent (effective or retarded) diffusion coefficient, D, is calculated using the self-diffusion coefficient, D_s, and the relationship $D = D_s/R$ where the retardation factor $R = G(1+K)(H^{-1})$. The G factor represents physical retardation effects. The factor K is a partition coefficient. The factor H represents the fraction of water saturation.

Table C.2. Input data to SOURCE1 for key nuclides in Tumulus II

Nuclide	Half-life (year)	Formula	Formula weight	Solubility (mol/L)	Waste K_d (mL/g)	Inventory (g/vault)	Diffusion coefficient (m^2/s)[a]	
							Waste	Concrete
^{3}H	1.23×10^{1}	T_2O	22	1.11×10^{2}	1.99×10^{-1}	7.11×10^{-7}	3.88×10^{-9}	1.86×10^{-9}
^{14}C	5.73×10^{3}	$BaCO_3$	199	1.11×10^{-4}	1.09×10^{0}	4.32×10^{-6}	1.44×10^{-11}	2.18×10^{-12}
^{60}Co	5.27×10^{0}	Co	60	3.46×10^{0}	3.97×10^{6}	1.45×10^{-5}	1.66×10^{-17}	6.77×10^{-13}
^{90}Sr	2.85×10^{1}	$SrCO_3$	150	7.45×10^{-5}	8.74×10^{0}	2.65×10^{-4}	1.17×10^{-11}	1.34×10^{-12}
^{99}Tc	2.13×10^{5}	NH_4TcO_4	181	9.11×10^{-2}	1.29×10^{0}	4.34×10^{-3}	1.25×10^{-11}	1.82×10^{-12}
^{137}Cs	3.00×10^{1}	Cs_2CO_3	334	1.60×10^{1}	1.99×10^{1}	6.74×10^{-4}	6.80×10^{-12}	5.12×10^{-13}
^{152}Eu	1.33×10^{1}	Eu_2O_3	352	2.84×10^{-6}	3.78×10^{0}	5.47×10^{-6}	7.95×10^{-13}	9.17×10^{-14}
^{154}Eu	8.80×10^{0}	Eu_2O_3	356	2.84×10^{-6}	3.78×10^{0}	1.82×10^{-6}	7.95×10^{-13}	9.17×10^{-14}
^{232}Th	1.41×10^{10}	ThO_2	264	7.57×10^{-8}	5.36×10^{1}	2.08×10^{1}	3.24×10^{-14}	3.73×10^{-15}
^{232}U	6.89×10^{1}	UO_2	264	1.46×10^{-6}	5.56×10^{1}	2.12×10^{-10}	3.11×10^{-14}	3.50×10^{-15}
^{233}U	1.59×10^{5}	UO_2	265	1.46×10^{-6}	5.56×10^{1}	1.95×10^{-2}	3.11×10^{-14}	3.50×10^{-15}
^{235}U	7.04×10^{8}	UO_2	267	1.46×10^{-6}	5.56×10^{1}	1.47×10^{-2}	3.11×10^{-14}	3.50×10^{-15}
^{238}U	4.47×10^{9}	UO_2	270	1.46×10^{-6}	5.56×10^{1}	1.54×10^{1}	3.11×10^{-14}	3.50×10^{-15}
^{238}Pu	8.77×10^{1}	PuO_2	270	1.71×10^{-8}	5.76×10^{1}	1.53×10^{-7}	3.00×10^{-14}	3.41×10^{-15}
^{239}Pu	2.41×10^{4}	PuO_2	271	1.71×10^{-8}	5.76×10^{1}	7.75×10^{-4}	3.00×10^{-14}	3.41×10^{-15}
^{241}Am	4.33×10^{2}	Am_2O_3	530	3.27×10^{-6}	5.76×10^{1}	1.66×10^{-5}	5.46×10^{-14}	6.26×10^{-15}
^{244}Cm	1.81×10^{1}	Cm_2O_3	536	2.84×10^{-6}	5.76×10^{1}	1.09×10^{-6}	5.46×10^{-14}	6.26×10^{-15}

Note: Inventory based on 220 vaults and the inventories for these radionuclides given in Table A.4 of Appendix A.
For sources, see notes a–c, Table C.1.
[a]See note d, Table C.1.

Table C.3. Input data to SOURCE1 for key nuclides in the Intermediate Waste Management Facility

Nuclide	Half-life (year)	Formula	Formula weight	Solubility (mol/L)	Waste K_d (mL/g)	Inventory (g/vault)	Diffusion coefficient (m^2/s)[a]	
							Waste	Concrete
^{3}H	1.23×10^{1}	T_2O	22	1.11×10^{2}	1.99×10^{-1}	3.03×10^{-8}	3.88×10^{-9}	1.86×10^{-9}
^{14}C	5.73×10^{3}	$BaCO_3$	199	1.11×10^{-4}	1.09×10^{0}	4.97×10^{-5}	1.44×10^{-11}	2.18×10^{-12}
^{26}Al	7.20×10^{5}	Al	26	5.24×10^{0}	1.99×10^{5}	3.74×10^{-4}	1.24×10^{-16}	7.23×10^{-13}
^{36}Cl	3.01×10^{5}	KCl	75	4.61×10^{0}	1.99×10^{-1}	1.84×10^{-3}	3.38×10^{-10}	5.08×10^{-11}
^{40}K	1.28×10^{9}	KCl	75	4.61×10^{0}	3.98×10^{0}	8.36×10^{-1}	1.26×10^{-11}	9.66×10^{-13}
^{60}Co	5.27×10^{0}	Co	60	3.46×10^{0}	3.97×10^{6}	6.25×10^{-6}	1.66×10^{-17}	6.77×10^{-13}
^{63}Ni	1.00×10^{2}	$NiCO_3$	123	7.83×10^{-4}	6.36×10^{0}	1.97×10^{-6}	1.01×10^{-11}	1.21×10^{-12}
^{90}Sr	2.85×10^{1}	$SrCO_3$	150	7.45×10^{-5}	8.74×10^{0}	1.83×10^{-4}	1.17×10^{-11}	1.34×10^{-12}
^{99}Tc	2.13×10^{5}	NH_4TcO_4	181	9.11×10^{-2}	1.29×10^{0}	1.43×10^{-4}	1.25×10^{-11}	1.82×10^{-12}
^{137}Cs	3.00×10^{1}	Cs_2CO_3	334	1.60×10^{1}	1.99×10^{1}	6.98×10^{-4}	6.80×10^{-12}	5.12×10^{-13}
^{152}Eu	1.33×10^{1}	Eu_2O_3	352	2.84×10^{-6}	3.78×10^{0}	3.55×10^{-5}	7.95×10^{-13}	9.17×10^{-14}
^{154}Eu	8.80×10^{0}	Eu_2O_3	356	2.84×10^{-6}	3.78×10^{0}	1.03×10^{-7}	7.95×10^{-13}	9.17×10^{-14}
^{232}Th	1.41×10^{10}	ThO_2	264	7.57×10^{-8}	5.36×10^{1}	3.91×10^{0}	3.24×10^{-14}	3.73×10^{-15}
^{233}U	1.59×10^{5}	UO_2	265	1.46×10^{-6}	5.56×10^{1}	8.12×10^{-4}	3.11×10^{-14}	3.50×10^{-15}
^{235}U	7.04×10^{8}	UO_2	267	1.46×10^{-6}	5.56×10^{1}	1.19×10^{-1}	3.11×10^{-14}	3.50×10^{-15}
^{238}U	4.47×10^{9}	UO_2	270	1.46×10^{-6}	5.56×10^{1}	5.74×10^{1}	3.11×10^{-14}	3.50×10^{-15}
^{239}Pu	2.41×10^{4}	PuO_2	271	1.71×10^{-8}	5.76×10^{1}	6.89×10^{-5}	3.00×10^{-14}	3.41×10^{-15}
^{242}Pu	3.76×10^{5}	PuO_2	274	1.71×10^{-8}	5.76×10^{1}	1.87×10^{-6}	3.00×10^{-14}	3.41×10^{-15}
^{241}Am	4.33×10^{2}	Am_2O_3	530	3.27×10^{-6}	5.76×10^{1}	4.58×10^{-7}	5.46×10^{-14}	6.26×10^{-15}
^{243}Am	7.38×10^{3}	Am_2O_3	534	3.27×10^{-6}	5.76×10^{1}	5.38×10^{-6}	5.46×10^{-14}	6.26×10^{-15}
^{244}Cm	1.81×10^{1}	Cm_2O_3	536	2.84×10^{-6}	5.76×10^{1}	2.12×10^{-6}	5.46×10^{-14}	6.26×10^{-15}

Note: Inventory based on 140 vaults and the inventories for these radionuclides given in Table A.5 of Appendix A.
For sources, see notes a–c, Table C.1.
[a]See note d, Table C.1.

Table C.4. Input data to SOURCE2 for key nuclides in low-range silos

Nuclide	Half-life (year)	Formula	Formula weight	Solubility (mol/L)	Waste K_d (mL/g)	Inventory (g/unit)	Diffusion coefficient (m^2/s)[a]	
							Waste	Concrete
^{3}H	1.23×10^{1}	T_2O	22	1.11×10^{2}	1.99×10^{-1}	1.41×10^{-5}	3.88×10^{-9}	1.86×10^{-9}
^{14}C	5.73×10^{3}	$BaCO_3$	199	1.11×10^{-4}	1.09×10^{-4}	2.16×10^{-4}	1.44×10^{-11}	2.18×10^{-12}
^{40}K	1.28×10^{9}	KCl	75	4.61×10^{0}	3.98×10^{0}	4.16×10^{-1}	1.26×10^{-11}	9.66×10^{-13}
^{60}Co	5.27×10^{0}	Co	60	3.46×10^{0}	3.97×10^{6}	1.21×10^{-5}	1.66×10^{-17}	6.77×10^{-13}
^{90}Sr	2.85×10^{1}	$SrCO_3$	150	7.45×10^{-5}	8.74×10^{0}	2.61×10^{-4}	1.17×10^{-11}	1.34×10^{-12}
^{99}Tc	2.13×10^{5}	NH_4TcO_4	181	9.11×10^{-2}	1.29×10^{0}	5.97×10^{-3}	1.25×10^{-11}	1.82×10^{-12}
^{137}Cs	3.00×10^{1}	Cs_2CO_3	334	1.60×10^{1}	1.99×10^{1}	4.95×10^{-4}	6.80×10^{-12}	5.12×10^{-13}
^{152}Eu	1.33×10^{1}	Eu_2O_3	352	2.84×10^{-6}	3.78×10^{0}	1.06×10^{-7}	7.95×10^{-13}	9.17×10^{-14}
^{154}Eu	8.80×10^{0}	Eu_2O_3	356	2.84×10^{-6}	3.78×10^{0}	2.52×10^{-8}	7.95×10^{-13}	9.17×10^{-14}
^{226}Ra	1.60×10^{3}	$RaSO_4$	322	6.21×10^{-8}	1.99×10^{1}	8.64×10^{-5}	4.10×10^{-13}	4.74×10^{-14}
^{229}Th	7.34×10^{3}	ThO_2	261	7.57×10^{-8}	5.36×10^{1}	1.07×10^{-5}	3.24×10^{-14}	3.73×10^{-15}
^{230}Th	7.54×10^{4}	ThO_2	262	7.57×10^{-8}	5.36×10^{1}	7.40×10^{-4}	3.24×10^{-14}	3.73×10^{-15}
^{232}Th	1.41E+10	ThO_2	264	7.57×10^{-8}	5.36×10^{1}	1.39×10^{2}	3.24×10^{-14}	3.73×10^{-15}
^{233}U	1.59×10^{5}	UO_2	265	1.46×10^{-6}	5.56×10^{1}	9.24×10^{-2}	3.11×10^{-14}	3.50×10^{-15}
^{234}U	2.45×10^{5}	UO_2	266	1.46×10^{-6}	5.56×10^{1}	2.58×10^{-4}	3.11×10^{-14}	3.50×10^{-15}
^{235}U	7.04×10^{8}	UO_2	267	1.46×10^{-6}	5.56×10^{1}	1.17×10^{-1}	3.11×10^{-14}	3.50×10^{-15}
^{236}U	2.34×10^{7}	UO_2	268	1.46×10^{-6}	5.56×10^{1}	1.36×10^{-2}	3.11×10^{-14}	3.50×10^{-15}

Table C.4 (continued)

Nuclide	Half-life (year)	Formula	Formula weight	Solubility (mol/L)	Waste K_d (mL/g)	Inventory (g/unit)	Diffusion coefficient (m^2/s)[a]	
							Waste	Concrete
^{238}U	4.47×10^{9}	UO_2	270	1.46×10^{-6}	5.56×10^{1}	4.44×10^{2}	3.11×10^{-14}	3.50×10^{-15}
^{237}Np	2.14×10^{6}	Np_2O_3	522	4.05×10^{-5}	5.56×10^{1}	3.22×10^{-3}	3.11×10^{-14}	3.50×10^{-15}
^{238}Pu	8.77×10^{1}	PuO_2	270	1.71×10^{-8}	5.76×10^{1}	7.64×10^{-7}	3.00×10^{-14}	3.41×10^{-15}
^{239}Pu	2.41×10^{4}	PuO_2	271	1.71×10^{-8}	5.76×10^{1}	1.93×10^{-4}	3.00×10^{-14}	3.41×10^{-15}
^{241}Am	4.33×10^{2}	Am_2O_3	530	3.27×10^{-6}	5.76×10^{1}	3.05×10^{-5}	5.46×10^{-14}	6.26×10^{-15}
^{243}Am	7.38×10^{3}	Am_2O_3	534	3.27×10^{-6}	5.76×10^{1}	4.15×10^{-4}	5.46×10^{-14}	6.26×10^{-15}
^{244}Cm	1.81×10^{1}	Cm_2O_3	536	2.84×10^{-6}	5.76×10^{1}	4.45×10^{-6}	5.46×10^{-14}	6.26×10^{-15}
^{249}Cf	3.51×10^{2}	$Cf(NO_3)_3$	435	3.49×10^{0}	5.96×10^{1}	3.58×10^{-7}	5.28×10^{-14}	6.10×10^{-15}

Note: Inventory based on 75 silos and the inventories for these radionuclides given in Table A.6 of Appendix A.
For sources, see notes a–c, Table C.1.
[a]See note d, Table C.1.

Table C.5. Input data to SOURCE2 for key nuclides in high-range silos

Nuclide	Half-life (year)	Formula	Formula weight	Solubility (mol/L)	Waste K_d (mL/g)	Inventory (g/unit)	Diffusion coefficient (m^2/s)[a]	
							Waste	Concrete
^{3}H	1.23×10^{1}	T_2O	22	1.11×10^{2}	1.99×10^{-1}	3.14×10^{-5}	3.88×10^{-9}	1.86×10^{-9}
^{14}C	5.73×10^{3}	$BaCO_3$	199	1.11×10^{-4}	1.09×10^{0}	2.79×10^{-4}	1.44×10^{-11}	2.18×10^{-12}
^{40}K	1.28×10^{9}	KCl	75	4.61×10^{0}	3.98×10^{0}	2.74×10^{1}	1.26×10^{-11}	9.66×10^{-13}
^{60}Co	5.27×10^{0}	Co	60	3.46×10^{0}	3.97×10^{6}	3.51×10^{-4}	1.66×10^{-17}	6.77×10^{-13}
^{63}Ni	1.00×10^{2}	$NiCO_3$	123	7.83×10^{-4}	6.36×10^{0}	4.08×10^{-5}	1.01×10^{-11}	1.21×10^{-12}
^{90}Sr	2.85×10^{1}	$SrCO_3$	150	7.45×10^{-5}	8.74×10^{0}	5.13×10^{-3}	1.17×10^{-11}	1.34×10^{-12}
^{137}Cs	3.00×10^{1}	Cs_2CO_3	334	1.60×10^{1}	1.99×10^{1}	8.95×10^{-3}	6.80×10^{-12}	5.12×10^{-13}
^{152}Eu	1.33×10^{1}	Eu_2O_3	352	2.84×10^{-6}	3.78×10^{0}	2.17×10^{-4}	7.95×10^{-13}	9.17×10^{-14}
^{154}Eu	8.80×10^{0}	Eu_2O_3	356	2.84×10^{-6}	3.78×10^{0}	6.23×10^{-6}	7.95×10^{-13}	9.17×10^{-14}
^{155}Eu	4.96×10^{0}	Eu_2O_3	358	2.84×10^{-6}	3.78×10^{0}	1.89×10^{-6}	7.95×10^{-13}	9.17×10^{-14}
^{230}Th	7.54×10^{4}	ThO_2	262	7.57×10^{-8}	5.36×10^{1}	1.44×10^{-6}	3.24×10^{-14}	3.73×10^{-15}
^{232}Th	1.41×10^{10}	ThO_2	264	7.57×10^{-8}	5.36×10^{1}	3.76×10^{1}	3.24×10^{-14}	3.73×10^{-15}
^{235}U	7.04×10^{8}	UO_2	267	1.46×10^{-6}	5.56×10^{1}	1.40×10^{-2}	3.11×10^{-14}	3.50×10^{-15}
^{238}U	4.47×10^{9}	UO_2	270	1.46×10^{-6}	5.56×10^{1}	8.98×10^{2}	3.11×10^{-14}	3.50×10^{-15}
^{239}Pu	2.41×10^{4}	PuO_2	271	1.71×10^{-8}	5.76×10^{1}	4.92×10^{-4}	3.00×10^{-14}	3.41×10^{-15}
^{244}Cm	1.81×10^{1}	Cm_2O_3	536	2.84×10^{-6}	5.76×10^{1}	1.91×10^{-4}	5.46×10^{-14}	6.26×10^{-15}

Note: Inventory based on 33 silos and the inventories for these radionuclides given in Table A.7 of Appendix A.
For sources, see notes a–c, Table C.1.
[a]See note d, Table C.1.

Table C.6. Input data to SOURCE2 for key nuclides in high-range wells in auger holes

Nuclide	Half-life (year)	Formula	Formula weight	Solubility (mol/L)	Waste K_d (mL/g)	Inventory (g/unit)	Diffusion coefficient (m^2/s)[a]	
							Waste	Concrete
^{14}C	5.73×10^{3}	$BaCO_3$	199	1.11×10^{-4}	1.09×10^{0}	4.15×10^{-9}	1.44×10^{-11}	2.18×10^{-12}
^{60}Co	5.27×10^{0}	Co	60	3.46×10^{0}	3.97×10^{6}	3.52×10^{-2}	1.66×10^{-17}	6.77×10^{-13}
^{90}Sr	2.85×10^{1}	$SrCO_3$	150	7.45×10^{-5}	8.74×10^{0}	1.85×10^{-1}	1.17×10^{-11}	1.34×10^{-12}
^{99}Tc	2.13×10^{5}	NH_4TcO_4	181	9.11×10^{-2}	1.29×10^{0}	4.37×10^{-1}	1.25×10^{-11}	1.82×10^{-12}
^{113m}Cd	1.37×10^{1}	Cd	113	7.64×10^{0}	3.97×10^{5}	1.11×10^{-3}	2.33×10^{-16}	9.09×10^{-13}
^{137}Cs	3.00×10^{1}	Cs_2CO_3	334	1.60×10^{1}	1.99×10^{1}	2.98×10^{-1}	6.80×10^{-12}	5.12×10^{-13}
^{152}Eu	1.33×10^{1}	Eu_2O_3	352	2.84×10^{-6}	3.78×10^{0}	1.20×10^{-1}	7.95×10^{-13}	9.17×10^{-14}
^{154}Eu	8.80×10^{0}	Eu_2O_3	356	2.84×10^{-6}	3.78×10^{0}	3.99×10^{-2}	7.95×10^{-13}	9.17×10^{-14}
^{229}Th	7.34×10^{3}	ThO_2	261	7.57×10^{-8}	5.36×10^{1}	6.53×10^{-4}	3.24×10^{-14}	3.73×10^{-15}
^{232}Th	1.41×10^{10}	ThO_2	264	7.57×10^{-8}	5.36×10^{1}	6.25×10^{0}	3.24×10^{-14}	3.73×10^{-15}
^{235}U	7.04×10^{8}	UO_2	267	1.46×10^{-6}	5.56×10^{1}	8.57×10^{-3}	3.11×10^{-14}	3.50×10^{-15}
^{238}U	4.47×10^{9}	UO_2	270	1.46×10^{-6}	5.56×10^{1}	2.20×10^{-1}	3.11×10^{-14}	3.50×10^{-15}

Note: Inventory based on 12 wells and the total inventory for these radionuclides given in Table A.9 of Appendix A.
For sources, see notes a–c, Table C.1.
[a]See note d, Table C.1.

Table C.7. Input data to SOURCE2 for key nuclides in high-range wells in silos

Nuclide	Half-life (year)	Formula	Formula weight	Solubility (mol/L)	Waste K_d (mL/g)	Inventory (g/unit)	Diffusion coefficient (m^2/s)[a]	
							Waste	Concrete
^{14}C	5.73×10^{3}	$BaCO_3$	199	1.11×10^{-4}	1.09×10^{0}	2.91×10^{-8}	1.44×10^{-11}	2.18×10^{-12}
^{60}Co	5.27×10^{0}	Co	60	3.46×10^{0}	3.97×10^{6}	2.46×10^{-1}	1.66×10^{-17}	6.77×10^{-13}
^{90}Sr	2.85×10^{1}	$SrCO_3$	150	7.45×10^{-5}	8.74×10^{0}	1.29×10^{0}	1.17×10^{-11}	1.34×10^{-12}
^{99}Tc	2.13×10^{5}	NH_4TcO_4	181	9.11×10^{-2}	1.29×10^{0}	3.06×10^{0}	1.25×10^{-11}	1.82×10^{-12}
^{113m}Cd	1.37×10^{1}	Cd	113	7.64×10^{0}	3.97×10^{5}	7.77×10^{-3}	2.33×10^{-16}	9.09×10^{-13}
^{137}Cs	3.00×10^{1}	Cs_2CO_3	334	1.60×10^{1}	1.99×10^{1}	2.09×10^{0}	6.80×10^{-12}	5.12×10^{-13}
^{152}Eu	1.33×10^{1}	Eu_2O_3	352	2.84×10^{-6}	3.78×10^{0}	8.40×10^{-1}	7.95×10^{-13}	9.17×10^{-14}
^{154}Eu	8.80×10^{0}	Eu_2O_3	356	2.84×10^{-6}	3.78×10^{0}	2.79×10^{-1}	7.95×10^{-13}	9.17×10^{-14}
^{229}Th	7.34×10^{3}	ThO_2	261	7.57×10^{-8}	5.36×10^{1}	4.57×10^{-3}	3.24×10^{-14}	3.73×10^{-15}
^{232}Th	1.41×10^{10}	ThO_2	264	7.57×10^{-8}	5.36×10^{1}	4.37×10^{1}	3.24×10^{-14}	3.73×10^{-15}
^{235}U	7.04×10^{8}	UO_2	267	1.46×10^{-6}	5.56×10^{1}	6.00×10^{-2}	3.11×10^{-14}	3.50×10^{-15}
^{238}U	4.47×10^{9}	UO_2	270	1.46×10^{-6}	5.56×10^{1}	1.54×10^{0}	3.11×10^{-14}	3.50×10^{-15}

Note: Inventory based on 6 silos with 7 wells in each silo for a total of 42 wells, and the total inventory for these radionuclides (54 wells) given in Table A.9 of Appendix A.

For sources, see notes a–c, Table C.1.

[a]See note d, Table C.1.

Table C.8. Input data to SOURCE2 for key nuclides in fissile wells

Nuclide	Half-life (year)	Formula	Formula weight	Solubility (mol/L)	Waste K_d (mL/g)	Inventory (g/unit)	Diffusion coefficient (m^2/s)[a]	
							Waste	Concrete
^{137}Cs	3.00×10^{1}	Cs_2CO_3	334	1.60×10^{1}	1.99×10^{1}	4.89×10^{-1}	6.80×10^{-12}	5.12×10^{-13}
^{235}U	7.04×10^{8}	UO_2	267	1.46×10^{-6}	5.56×10^{1}	4.05×10^{2}	3.11×10^{-14}	3.50×10^{-15}
^{238}U	4.47×10^{9}	UO_2	270	1.46×10^{-6}	5.56×10^{1}	1.44×10^{4}	3.11×10^{-14}	3.50×10^{-15}

Note: Inventory based on one well and the total inventory for these radionuclides given in Table A.10 of Appendix A.
For sources, see notes a–c, Table C.1.
[a]See note d, Table C.1.

Table C.9. Input data to SOURCE2 for key nuclides in asbestos silos

Nuclide	Half-life (year)	Formula	Formula weight	Solubility (mol/L)	Waste K_d (mL/g)	Inventory (g/unit)	Diffusion coefficient (m^2/s)[a]	
							Waste	Concrete
^{3}H	1.23×10^{1}	T_2O	22	1.11×10^{2}	1.99×10^{-1}	9.42×10^{-9}	3.88×10^{-9}	1.86×10^{-9}
^{14}C	5.73×10^{3}	$BaCO_3$	199	1.11×10^{-4}	1.09×10^{0}	1.18×10^{-5}	1.44×10^{-11}	2.18×10^{-12}
^{60}Co	5.27×10^{0}	Co	60	3.46×10^{0}	3.97×10^{6}	4.00×10^{-7}	1.66×10^{-17}	6.77×10^{-13}
^{90}Sr	2.85×10^{1}	$SrCO_3$	150	7.45×10^{-5}	8.74×10^{0}	2.83×10^{-5}	1.17×10^{-11}	1.34×10^{-12}
^{99}Tc	2.13×10^{5}	NH_4TcO_4	181	9.11×10^{-2}	1.29×10^{0}	6.44×10^{-3}	1.25×10^{-11}	1.82×10^{-12}
^{137}Cs	3.00×10^{1}	Cs_2CO_3	334	1.60×10^{1}	1.99×10^{1}	5.93×10^{-5}	6.80×10^{-12}	5.12×10^{-13}
^{152}Eu	1.33×10^{1}	Eu_2O_3	352	2.84×10^{-6}	3.78×10^{0}	5.26×10^{-7}	7.95×10^{-13}	9.17×10^{-14}
^{154}Eu	8.80×10^{0}	Eu_2O_3	356	2.84×10^{-6}	3.78×10^{0}	3.37×10^{-9}	7.95×10^{-13}	9.17×10^{-14}
^{232}Th	1.41×10^{10}	ThO_2	264	7.57×10^{-8}	5.36×10^{1}	3.56×10^{1}	3.24×10^{-14}	3.73×10^{-15}
^{233}U	1.59×10^{5}	UO_2	265	1.46×10^{-6}	5.56×10^{1}	9.58×10^{-4}	3.11×10^{-14}	3.50×10^{-15}
^{238}U	4.47×10^{9}	UO_2	270	1.46×10^{-6}	5.56×10^{1}	7.33×10^{1}	3.11×10^{-14}	3.50×10^{-15}
^{244}Cm	1.81×10^{1}	Cm_2O_3	536	2.84×10^{-6}	5.76×10^{1}	3.60×10^{-8}	5.46×10^{-14}	6.26×10^{-15}

Note: Inventory based on 11 silos and the inventories for these radionuclides given in Table A.8 of Appendix A.
For sources, see notes a–c, Table C.1.
[a]See note d, Table C.1.

Table C.10. Input data to SOURCE2 for key nuclides in biological trenches

Nuclide	Half-life (year)	Formula	Formula weight	Solubility (mol/L)	Waste K_d (mL/g)	Inventory (g/unit)	Diffusion coefficient (m^2/s)[a]	
							Waste	Concrete[b]
^{3}H	1.23×10^{1}	T_2O	22	1.11×10^{2}	1.99×10^{-7}	3.73×10^{-9}	3.88×10^{-9}	NA
^{14}C	5.73×10^{3}	$BaCO_3$	199	1.11×10^{-4}	1.09×10^{0}	7.63×10^{-6}	1.44×10^{-11}	NA
^{60}Co	5.27×10^{0}	Co	60	3.46×10^{0}	3.97×10^{6}	3.89×10^{-9}	1.66×10^{-17}	NA
^{90}Sr	2.85×10^{1}	$SrCO_3$	150	7.45×10^{-5}	8.74×10^{0}	1.52×10^{-5}	1.17×10^{-11}	NA
^{137}Cs	3.00×10^{1}	Cs_2CO_3	334	1.60×10^{1}	1.99×10^{1}	5.17×10^{-6}	6.80×10^{-12}	NA

Note: Inventory based on 5 trenches and the inventories for these radionuclides given in Table A.11 of Appendix A.
For sources, see notes a–c, Table C.1.
[a]See note d, Table C.1.
[b]NA = not applicable. Biological trenches are not lined.

Table C.11. Distribution coefficients and solubility limits of key nuclides in SWSA 6

Nuclide	Formula	Solubility[a] (mol/L)	Waste distribution coefficient[b]		Concrete distribution coefficient[b]	
			K (dimensionless)	K_d (mL/g)	K (dimensionless)	K_d (mL/g)
^{3}H	T_2O	1.11×10^{2}	1.00×10^{0}	1.99×10^{-1}	1.00×10^{0}	6.51×10^{-2}
^{14}C	$BaCO_3$	1.11×10^{-4}	5.50×10^{0}	1.09×10^{0}	5.50×10^{0}	3.58×10^{-1}
^{26}Al	Al	5.24×10^{0}	1.00×10^{6}	1.99×10^{5}	2.50×10^{1}	1.63×10^{0}
^{36}Cl	KCl	4.61×10^{0}	1.00×10^{0}	1.99×10^{-1}	1.00×10^{0}	6.51×10^{-2}
^{40}K	KCl	4.61×10^{0}	3.50×10^{1}	3.98×10^{0}	6.90×10^{1}	5.07×10^{0}
^{60}Co	Co	3.46×10^{0}	2.00×10^{7}	3.97×10^{6}	7.60×10^{1}	4.95×10^{0}
^{63}Ni	$NiCO_3$	7.83×10^{-4}	3.20×10^{1}	6.36×10^{0}	4.20×10^{1}	2.73×10^{0}
^{79}Se	$NaSeO_4$	2.88×10^{0}	1.00×10^{0}	1.99×10^{-1}	1.00×10^{0}	6.51×10^{-2}
^{90}Sr	$SrCO_3$	7.45×10^{-5}	4.40×10^{1}	8.74×10^{0}	5.80×10^{1}	3.78×10^{0}
^{94}Nb	$NbOF_3$-2KF	2.60×10^{-1}	1.20×10^{2}	2.38×10^{1}	1.60×10^{2}	1.04×10^{1}
^{99}Tc	NH_4TcO_4	9.11×10^{-2}	6.50×10^{0}	1.29×10^{0}	6.50×10^{0}	4.23×10^{-1}
^{113m}Cd	Cd	7.64×10^{0}	2.00×10^{6}	3.97×10^{5}	7.60×10^{1}	4.95×10^{0}
^{121m}Sn	$SnCl_2$	1.37×10^{1}	5.80×10^{1}	1.15×10^{1}	7.60×10^{1}	4.95×10^{0}
^{126}Sn	$SnCl_2$	1.37×10^{1}	5.80×10^{1}	1.15×10^{1}	7.60×10^{1}	4.95×10^{0}
^{129}I	KI	7.68×10^{0}	1.00×10^{0}	1.99×10^{-1}	1.00×10^{0}	6.51×10^{-2}

Table C.11 (continued)

Nuclide	Formula	Solubility[a] (mol/L)	Waste distribution coefficient[b]		Concrete distribution coefficient[b]	
			K (dimensionless)	K_d (mL/g)	K (dimensionless)	K_d (mL/g)
^{137}Cs	Cs_2CO_3	1.60×10^{1}	1.00×10^{2}	1.99×10^{1}	2.00×10^{2}	1.30×10^{1}
^{151}Sm	$Sm(C_2O_4)$	7.25×10^{-7}	1.90×10^{1}	3.78×10^{0}	2.50×10^{1}	1.63×10^{0}
^{152}Eu	Eu_2O_3	2.84×10^{-6}	1.90×10^{1}	3.78×10^{0}	2.50×10^{1}	1.63×10^{0}
^{154}Eu	Eu_2O_3	2.84×10^{-6}	1.90×10^{1}	3.78×10^{0}	2.50×10^{1}	1.63×10^{0}
^{155}Eu	Eu_2O_3	2.84×10^{-6}	1.90×10^{1}	3.78×10^{0}	2.50×10^{1}	1.63×10^{0}
^{226}Ra	$RaSO_4$	6.21×10^{-8}	1.00×10^{2}	1.99×10^{1}	1.30×10^{2}	8.47×10^{0}
^{229}Th	ThO_2	7.57×10^{-8}	2.70×10^{2}	5.36×10^{1}	3.50×10^{2}	2.28×10^{1}
^{230}Th	ThO_2	7.57×10^{-8}	2.70×10^{2}	5.36×10^{1}	3.50×10^{2}	2.28×10^{1}
^{232}Th	ThO_2	7.57×10^{-8}	2.70×10^{2}	5.36×10^{1}	3.50×10^{2}	2.28×10^{1}
^{232}U	UO_2	1.46×10^{-6}	2.80×10^{2}	5.56×10^{1}	3.70×10^{2}	2.41×10^{1}
^{233}U	UO_2	1.46×10^{-6}	2.80×10^{2}	5.56×10^{1}	3.70×10^{2}	2.41×10^{1}
^{234}U	UO_2	1.46×10^{-6}	2.80×10^{2}	5.56×10^{1}	3.70×10^{2}	2.41×10^{1}
^{235}U	UO_2	1.46×10^{-6}	2.80×10^{2}	5.56×10^{1}	3.70×10^{2}	2.41×10^{1}
^{236}U	UO_2	1.46×10^{-6}	2.80×10^{2}	5.56×10^{1}	3.70×10^{2}	2.41×10^{1}
^{238}U	UO_2	1.46×10^{-6}	2.80×10^{2}	5.56×10^{1}	3.70×10^{2}	2.41×10^{1}

Table C.11 (continued)

Nuclide	Formula	Solubility[a] (mol/L)	Waste distribution coefficient[b]		Concrete distribution coefficient[b]	
			K (dimensionless)	K_d (mL/g)	K (dimensionless)	K_d (mL/g)
^{237}Np	Np_2O_3	4.05×10^{-5}	2.80×10^{2}	5.56×10^{1}	3.70×10^{2}	2.41×10^{1}
^{238}Pu	PuO_2	1.71×10^{-8}	2.90×10^{2}	5.76×10^{1}	3.80×10^{2}	2.47×10^{1}
^{239}Pu	PuO_2	1.71×10^{-8}	2.90×10^{2}	5.76×10^{1}	3.80×10^{2}	2.47×10^{1}
^{240}Pu	PuO_2	1.71×10^{-8}	2.90×10^{2}	5.76×10^{1}	3.80×10^{2}	2.47×10^{1}
^{241}Pu	PuO_2	1.71×10^{-8}	2.90×10^{2}	5.76×10^{1}	3.80×10^{2}	2.47×10^{1}
^{242}Pu	PuO_2	1.71×10^{-8}	2.90×10^{2}	5.76×10^{1}	3.80×10^{2}	2.47×10^{1}
^{241}Am	Am_2O_3	3.27×10^{-6}	2.90×10^{2}	5.76×10^{1}	3.80×10^{2}	2.47×10^{1}
^{243}Am	Am_2O_3	3.27×10^{-6}	2.90×10^{2}	5.76×10^{1}	3.80×10^{2}	2.47×10^{1}
^{242}Cm	Cm_2O_3	2.84×10^{-6}	2.90×10^{2}	5.76×10^{1}	3.80×10^{2}	2.47×10^{1}
^{243}Cm	Cm_2O_3	2.84×10^{-6}	2.90×10^{2}	5.76×10^{1}	3.80×10^{2}	2.47×10^{1}
^{244}Cm	Cm_2O_3	2.84×10^{-6}	2.90×10^{2}	5.76×10^{1}	3.80×10^{2}	2.47×10^{1}
^{249}Cf	$Cf(NO_3)_3$	3.49×10^{0}	3.00×10^{2}	5.96×10^{1}	3.90×10^{2}	2.54×10^{1}

[a]For sources, see note b, Table C.1.
[b]For sources, see note c, Table C.1.

Table C.12. Transport parameters used to calculate diffusion coefficients for waste (D_W) and concrete (D_C)

Nuclide	Self-diffusion coefficient D_s (m²/s)[a]	Transport parameters (dimensionless) for D_w: Geometry factor G	Distribution coefficient K	Retardation factor R	Waste diffusion coefficient D_W (m²/s)	Transport parameters (dimensionless) for D_C: Geometry factor G	Distribution coefficient K	Retardation factor R	Concrete diffusion coefficient D_C (m²/s)
^{3}H	9.31×10^{-9}	1.20×10^{0}	1.00×10^{0}	2.40×10^{0}	3.88×10^{-9}	2.50×10^{0}	1.00×10^{0}	5.00×10^{0}	1.86×10^{-9}
^{14}C	9.20×10^{-10}	9.80×10^{0}	5.50×10^{0}	6.37×10^{1}	1.44×10^{-11}	6.50×10^{1}	5.50×10^{0}	4.23×10^{2}	2.18×10^{-12}
^{26}Al	6.20×10^{-10}	5.00×10^{0}	1.00×10^{6}	5.00×10^{6}	1.24×10^{-16}	3.30×10^{1}	2.50×10^{1}	8.58×10^{2}	7.23×10^{-13}
^{36}Cl	2.03×10^{-9}	3.00×10^{0}	1.00×10^{0}	6.00×10^{0}	3.38×10^{10}	2.00×10^{1}	1.00×10^{0}	4.00×10^{1}	5.08×10^{-11}
^{40}K	1.96×10^{-9}	4.30×10^{0}	3.50×10^{1}	1.55×10^{2}	1.26×10^{-11}	2.90×10^{1}	6.90×10^{1}	2.03×10^{3}	9.66×10^{-13}
^{60}Co	7.30×10^{-10}	2.20×10^{0}	2.00×10^{7}	4.40×10^{7}	1.66×10^{-17}	1.40×10^{1}	7.60×10^{1}	1.08×10^{3}	6.77×10^{-13}
^{59}Ni	7.30×10^{-10}	2.20×10^{0}	3.20×10^{1}	7.26×10^{1}	1.01×10^{-11}	1.40×10^{1}	4.20×10^{1}	6.02×10^{2}	1.21×10^{-12}
^{63}Ni	7.30×10^{-10}	2.20×10^{0}	3.20×10^{1}	7.26×10^{1}	1.01×10^{-11}	1.40×10^{1}	4.20×10^{1}	6.02×10^{2}	1.21×10^{-12}
^{79}Se	1.06×10^{-9}	7.70×10^{0}	1.00×10^{0}	1.54×10^{1}	6.88×10^{-11}	5.20×10^{1}	1.00×10^{0}	1.04×10^{2}	1.02×10^{-11}
^{90}Sr	7.90×10^{-10}	1.50×10^{0}	4.40×10^{1}	6.75×10^{1}	1.17×10^{-11}	1.00×10^{1}	5.80×10^{1}	5.90×10^{2}	1.34×10^{-12}
^{94}Nb	4.84×10^{-10}	5.80×10^{1}	1.20×10^{2}	7.02×10^{3}	6.90×10^{-14}	3.90×10^{2}	1.60×10^{2}	6.28×10^{4}	7.71×10^{-15}
^{99}Tc	1.50×10^{-9}	1.60×10^{1}	6.50×10^{0}	1.20×10^{2}	1.25×10^{-11}	1.10×10^{2}	6.50×10^{0}	8.25×10^{2}	1.82×10^{-12}
^{113m}Cd	7.00×10^{-10}	1.50×10^{0}	2.00×10^{6}	3.00×10^{6}	2.33×10^{-16}	1.00×10^{1}	7.60×10^{1}	7.70×10^{2}	9.09×10^{-13}
^{121m}Sn	7.05×10^{-10}	2.20×10^{0}	5.80×10^{1}	1.30×10^{2}	5.43×10^{-12}	1.40×10^{1}	7.60×10^{1}	1.08×10^{3}	6.54×10^{-13}
^{126}Sn	7.05×10^{-10}	2.20×10^{0}	5.80×10^{1}	1.30×10^{2}	5.43×10^{-12}	1.40×10^{1}	7.60×10^{1}	1.08×10^{3}	6.54×10^{-13}
^{129}I	2.05×10^{-9}	3.00×10^{0}	1.00×10^{0}	6.00×10^{0}	3.42×10^{-10}	2.00×10^{1}	1.00×10^{0}	4.00×10^{1}	5.13×10^{-11}
^{137}Cs	2.06×10^{-9}	3.00×10^{0}	1.00×10^{2}	3.03×10^{2}	6.80×10^{-12}	2.00×10^{1}	2.00×10^{2}	4.02×10^{3}	5.12×10^{-13}
^{151}Sm	6.20×10^{-10}	3.90×10^{1}	1.90×10^{1}	7.80×10^{2}	7.95×10^{-13}	2.60×10^{2}	2.50×10^{1}	6.76×10^{3}	9.17×10^{-14}
^{152}Eu	6.20×10^{-10}	3.90×10^{1}	1.90×10^{1}	7.80×10^{2}	7.95×10^{-13}	2.60×10^{2}	2.50×10^{1}	6.76×10^{3}	9.17×10^{-14}
^{154}Eu	6.20×10^{-10}	3.90×10^{1}	1.90×10^{1}	7.80×10^{2}	7.95×10^{-13}	2.60×10^{2}	2.50×10^{1}	6.76×10^{3}	9.17×10^{-14}
^{155}Eu	6.20×10^{-10}	3.90×10^{1}	1.90×10^{1}	7.80×10^{2}	7.95×10^{-13}	2.60×10^{2}	2.50×10^{1}	6.76×10^{3}	9.17×10^{-14}
^{226}Ra	8.70×10^{-10}	2.10×10^{1}	1.00×10^{2}	2.12×10^{3}	4.10×10^{-13}	1.40×10^{2}	1.30×10^{2}	1.83×10^{4}	4.74×10^{-14}
^{229}Th	5.10×10^{-10}	5.80×10^{1}	2.70×10^{2}	1.57×10^{4}	3.24×10^{-14}	3.90×10^{2}	3.50×10^{2}	1.37×10^{5}	3.73×10^{-15}

Table C.12 (continued)

Nuclide	Self-diffusion coefficient D_s (m²/s)[a]	Transport parameters (dimensionless) for D_w: Geometry factor G	Distribution coefficient K	Retardation factor R	Waste diffusion coefficient D_w (m²/s)	Transport parameters (dimensionless) for D_c: Geometry factor G	Distribution coefficient K	Retardation factor R	Concrete diffusion coefficient D_c (m²/s)
^{230}Th	5.10×10^{-10}	5.80×10^{1}	2.70×10^{2}	1.57×10^{4}	3.24×10^{-14}	3.90×10^{2}	3.50×10^{2}	1.37×10^{5}	3.73×10^{-15}
^{232}Th	5.10×10^{-10}	5.80×10^{1}	2.70×10^{2}	1.57×10^{4}	3.24×10^{-14}	3.90×10^{2}	3.50×10^{2}	1.37×10^{5}	3.73×10^{-15}
^{232}U	5.07×10^{-10}	5.80×10^{1}	2.80×10^{2}	1.63×10^{4}	3.11×10^{-14}	3.90×10^{2}	3.70×10^{2}	1.45×10^{5}	3.50×10^{-15}
^{233}U	5.07×10^{-10}	5.80×10^{1}	2.80×10^{2}	1.63×10^{4}	3.11×10^{-14}	3.90×10^{2}	3.70×10^{2}	1.45×10^{5}	3.50×10^{-15}
^{234}U	5.07×10^{-10}	5.80×10^{1}	2.80×10^{2}	1.63×10^{4}	3.11×10^{-14}	3.90×10^{2}	3.70×10^{2}	1.45×10^{5}	3.50×10^{-15}
^{235}U	5.07×10^{-10}	5.80×10^{1}	2.80×10^{2}	1.63×10^{4}	3.11×10^{-14}	3.90×10^{2}	3.70×10^{2}	1.45×10^{5}	3.50×10^{-15}
^{236}U	5.07×10^{-10}	5.80×10^{1}	2.80×10^{2}	1.63×10^{4}	3.11×10^{-14}	3.90×10^{2}	3.70×10^{2}	1.45×10^{5}	3.50×10^{-15}
^{238}U	5.07×10^{-10}	5.80×10^{1}	2.80×10^{2}	1.63×10^{4}	3.11×10^{-14}	3.90×10^{2}	3.70×10^{2}	1.45×10^{5}	3.50×10^{-15}
^{237}Np	5.07×10^{-10}	5.80×10^{1}	2.80×10^{2}	1.63×10^{4}	3.11×10^{-14}	3.90×10^{2}	3.70×10^{2}	1.45×10^{5}	3.50×10^{-15}
^{238}Pu	5.07×10^{-10}	5.80×10^{1}	2.90×10^{2}	1.69×10^{4}	3.00×10^{-14}	3.90×10^{2}	3.80×10^{2}	1.49×10^{5}	3.41×10^{-15}
^{239}Pu	5.07×10^{-10}	5.80×10^{1}	2.90×10^{2}	1.69×10^{4}	3.00×10^{-14}	3.90×10^{2}	3.80×10^{2}	1.49×10^{5}	3.41×10^{-15}
^{240}Pu	5.07×10^{-10}	5.80×10^{1}	2.90×10^{2}	1.69×10^{4}	3.00×10^{-14}	3.90×10^{2}	3.80×10^{2}	1.49×10^{5}	3.41×10^{-15}
^{241}Pu	5.07×10^{-10}	5.80×10^{1}	2.90×10^{2}	1.69×10^{4}	3.00×10^{-14}	3.90×10^{2}	3.80×10^{2}	1.49×10^{5}	3.41×10^{-15}
^{242}Pu	5.07×10^{-10}	5.80×10^{1}	2.90×10^{2}	1.69×10^{4}	3.00×10^{-14}	3.90×10^{2}	3.80×10^{2}	1.49×10^{5}	3.41×10^{-15}
^{241}Am	6.20×10^{-10}	3.90×10^{1}	2.90×10^{2}	1.13×10^{4}	5.46×10^{-14}	2.60×10^{2}	3.80×10^{2}	9.91×10^{4}	6.26×10^{-15}
^{243}Am	6.20×10^{-10}	3.90×10^{1}	2.90×10^{2}	1.13×10^{4}	5.46×10^{-14}	2.60×10^{2}	3.80×10^{2}	9.91×10^{4}	6.26×10^{-15}
^{242}Cm	6.20×10^{-10}	3.90×10^{1}	2.90×10^{2}	1.13×10^{4}	5.46×10^{-14}	2.60×10^{2}	3.80×10^{2}	9.91×10^{4}	6.26×10^{-15}
^{243}Cm	6.20×10^{-10}	3.90×10^{1}	2.90×10^{2}	1.13×10^{4}	5.46×10^{-14}	2.60×10^{2}	3.80×10^{2}	9.91×10^{4}	6.26×10^{-15}
^{244}Cm	6.20×10^{-10}	3.90×10^{1}	2.90×10^{2}	1.13×10^{4}	5.46×10^{-14}	2.60×10^{2}	3.80×10^{2}	9.91×10^{4}	6.26×10^{-15}
^{249}Cf	6.20×10^{-10}	3.90×10^{1}	3.00×10^{2}	1.17×10^{4}	5.28×10^{-14}	2.60×10^{2}	3.90×10^{2}	1.02×10^{5}	6.10×10^{-15}

Note: D_w (or D_c) $= D_s/R$ where $R = G(1 + K)H^{-1}$. The term H is defined as the relative saturation of the pores with water. The pores are assumed to be full in the calculations shown in this table; that is, $H = 1.0$.

[a]*Sources:* D. G. Miller, *Estimation of Tracer Diffusion Coefficients of Ions in Aqueous Solution*, UCRL-5331, Sept. 7, 1982; C. J. Geankoplis, *Mass Transport Phenomena*, Holt, Rinehart and Winston, New York, 1972; F. Kepak, "Adsorption and Colloidal Properties of Radioactive Elements in Trace Concentrations," *Chemical Review* **71**(4), 1972; E. L. Cussler, *Diffusion—Mass Transfer in Fluid Systems*, Cambridge University Press, New York, 1984.

Table C.13. Inventory and uncertainty analysis data for key nuclides in Tumulus I

Nuclide	Formula	Molecular weight	Half-life[a] (year)	Solubility[b] (mol/L)	Waste K_d[c] (mL/g)	Inventory[d] (g/vault)	Diffusion coefficient[e] Waste (m^2/s)	Diffusion coefficient[e] Concrete (m^2/s)	Expected extent of values
^{3}H	T_2O	22	1.23×10^{1}	1.11×10^{2}	1.99×10^{-1}	1.42×10^{-6}	3.88×10^{-9}	1.86×10^{-9}	Probable
					1.99×10^{-2}	7.10×10^{-7}	7.76×10^{-10}	3.72×10^{-10}	Low
					1.99×10^{0}	2.13×10^{-6}	7.76×10^{-9}	3.72×10^{-9}	High
^{14}C	$BaCO_3$	199	5.73×10^{3}	1.11×10^{-4}	1.09×10^{0}	1.11×10^{-2}	1.44×10^{-11}	2.18×10^{-12}	Probable
					1.09×10^{-1}	5.56×10^{-3}	2.89×10^{-12}	4.36×10^{-13}	Low
					1.09×10^{1}	1.66×10^{-2}	2.89×10^{-11}	4.36×10^{-12}	High
^{90}Sr	$SrCO_3$	150	2.85×10^{1}	7.45×10^{-5}	8.74×10^{0}	1.38×10^{-4}	1.17×10^{-11}	1.34×10^{-12}	Probable
					8.74×10^{-1}	3.65×10^{-5}	2.34×10^{-12}	2.68×10^{-13}	Low
					8.74×10^{1}	3.01×10^{-4}	2.34×10^{-11}	2.68×10^{-12}	High
^{99}Tc	NH_4TcO_4	181	2.13×10^{5}	9.11×10^{-2}	1.29×10^{0}	1.11×10^{-1}	1.25×10^{-11}	1.82×10^{-12}	Probable
					1.29×10^{-1}	7.82×10^{-2}	2.50×10^{-12}	3.64×10^{-13}	Low
					1.29×10^{1}	1.50×10^{-1}	2.50×10^{-11}	3.64×10^{-12}	High
^{137}Cs	Cs_2CO_3	334	3.00×10^{1}	1.60×10^{1}	1.99×10^{1}	5.81×10^{-4}	6.80×10^{-12}	5.12×10^{-13}	Probable
					1.99×10^{0}	4.61×10^{-4}	1.36×10^{-12}	1.02×10^{-13}	Low
					1.99×10^{2}	7.70×10^{-4}	1.36×10^{-11}	1.02×10^{-12}	High
^{226}Ra	$RaSO_4$	322	1.60×10^{3}	6.21×10^{-8}	1.99×10^{1}	2.15×10^{-6}	4.10×10^{-13}	4.74×10^{-14}	Probable
					1.99×10^{0}	1.68×10^{-6}	8.20×10^{-14}	9.49×10^{-15}	Low
					1.99×10^{2}	2.86×10^{-6}	8.20×10^{-13}	9.49×10^{-14}	High
^{232}Th	ThO_2	264	1.41×10^{10}	7.57×10^{-8}	5.36×10^{1}	5.14×10^{0}	3.24×10^{-14}	3.73×10^{-15}	Probable
					5.36×10^{0}	3.31×10^{0}	6.49×10^{-15}	7.45×10^{-16}	Low
					5.36×10^{2}	6.43×10^{0}	6.49×10^{-14}	7.45×10^{-15}	High
^{233}U	UO_2	265	1.59×10^{5}	1.46×10^{-6}	5.56×10^{1}	5.14×10^{-2}	3.11×10^{-14}	3.50×10^{-15}	Probable
					5.56×10^{0}	5.14×10^{-3}	6.22×10^{-15}	7.01×10^{-16}	Low
					5.56×10^{2}	5.14×10^{-1}	6.22×10^{-14}	7.01×10^{-15}	High

Table C.13 (continued)

Nuclide	Formula	Molecular weight	Half-life[a] (year)	Solubility[b] (mol/L)	Waste K_d[c] (mL/g)	Inventory[d] (g/vault)	Diffusion coefficient[e] Waste (m^2/s)	Diffusion coefficient[e] Concrete (m^2/s)	Expected extent of values
^{238}U	UO_2	270	4.47×10^9	1.46×10^{-6}	5.56×10^1	6.87×10^2	3.11×10^{-14}	3.50×10^{-15}	Probable
					5.56×10^0	5.10×10^2	6.22×10^{-15}	7.01×10^{-16}	Low
					5.56×10^2	9.44×10^2	6.22×10^{-14}	7.01×10^{-15}	High
^{239}Pu	PuO_2	271	2.41×10^4	1.71×10^{-8}	5.76×10^1	7.37×10^{-3}	3.00×10^{-14}	3.41×10^{-15}	Probable
					5.76×10^0	7.37×10^{-4}	6.01×10^{-15}	6.82×10^{-16}	Low
					5.76×10^2	7.10×10^{-2}	6.01×10^{-14}	6.82×10^{-15}	High
^{241}Am	Am_2O_3	530	4.33×10^2	3.27×10^{-6}	5.76×10^1	1.22×10^{-4}	5.46×10^{-14}	6.26×10^{-15}	Probable
					5.76×10^0	1.22×10^{-5}	1.09×10^{-14}	1.25×10^{-15}	Low
					5.76×10^2	1.22×10^{-3}	1.09×10^{-13}	1.25×10^{-14}	High
^{243}Am	Am_2O_3	534	7.38×10^3	3.27×10^{-6}	5.76×10^1	4.74×10^{-5}	5.46×10^{-14}	6.26×10^{-15}	Probable
					5.76×10^0	6.01×10^{-6}	1.09×10^{-14}	1.25×10^{-15}	Low
					5.76×10^2	2.57×10^{-4}	1.09×10^{-13}	1.25×10^{-14}	High

Note: Inventory based on 197 vaults.

[a]*Sources:* General Electric Company, *Chart of the Nuclides*, Knolls Atomic Power Laboratory, Schenectady, N.Y., 1983; E. Browne and R. B. Firestone, *Table of Radioactive Isotopes*, ed. V. S. Shirley, John Wiley and Sons, Inc., New York, 1986.

[b]*Sources:* D. R. Lide, ed., *CRC Handbook of Chemistry and Physics*, 73rd ed., 1992; Freie Universität Berlin and Institut für Anorganische und Analytische Chemie, *Solubility and Speciation of Actinides in Salt Solutions and Migration Experiments of Intermediate Level Waste in Salt Formations*, FUB/FI 53132-415/85, 1986; M. Schweingruber, *Actinide Solubility in Deep Groundwaters—Estimates for Upper Limits Based on Chemical Equilibrium Calculations*, EIR-Bericht Nr. 507, December 1983; Agence Internationale de l'Energie Atomique, *Seminaire sur les Techniques d'Etude et les Methodes d'Evaluation des Sites en vue du Stockage Definitif Souterrain des Dechets Radioactifs*, IAEA-SR-104, February 1984.

[c]*Sources:* H. A. Friedman and A. D. Kelmers, *Laboratory Measurement of Radionuclide Sorption in Solid Waste Storage Area 6 Soil/Groundwater Systems*, ORNL-TM-10561, Martin Marietta Energy Systems, Inc., Oak Ridge Natl. Lab., June 1990; I. Neretnieks, "Diffusivities of Some Constituents in Compacted Wet Bentonite Clay and the Impact on Radionuclide Migration in the Buffer," *Nucl. Tech.* 71, 458–70 (1985).

[d]*Source:* R. Kenning, and L. Yong, *Evaluation of Uncertainty in the SWSA 6 Inventory Data*, Atlan-Tech, Inc., Roswell, Ga., February 1993.

[e]The apparent (effective or retarded) diffusion coefficient, D, is calculated using the self-diffusion coefficient, D_s, and the relationship $D = D_s/R$ where the retardation factor $R = G(1+K)(H^{-1})$. The G factor represents physical retardation effects. The factor K is a partition coefficient. The factor H represents the fraction of water saturation.

Table C.14. Inventory and uncertainty analysis data for key nuclides in Tumulus II

Nuclide	Formula	Molecular weight	Half-life (year)	Solubility (mol/L)	Waste K_d (mL/g)	Inventory (g/vault)	Diffusion coefficient[a] Waste (m^2/s)	Diffusion coefficient[a] Concrete (m^2/s)	Expected extent of values
^{3}H	T_2O	22	1.23×10^{1}	1.11×10^{2}	1.99×10^{-1}	7.54×10^{-7}	3.88×10^{-9}	1.86×10^{-9}	Probable
					1.99×10^{-2}	3.79×10^{-7}	7.76×10^{-10}	3.72×10^{-10}	Low
					1.99×10^{0}	1.14×10^{-6}	7.76×10^{-9}	3.72×10^{-9}	High
^{14}C	$BaCO_3$	199	5.73×10^{3}	1.11×10^{-4}	1.09×10^{0}	2.16×10^{-3}	1.44×10^{-11}	2.18×10^{-12}	Probable
					1.09×10^{-1}	1.08×10^{-3}	2.89×10^{-12}	4.36×10^{-13}	Low
					1.09×10^{1}	3.24×10^{-3}	2.89×10^{-11}	4.36×10^{-12}	High
^{90}Sr	$SrCO_3$	150	2.85×10^{1}	7.45×10^{-5}	8.74×10^{0}	1.10×10^{-4}	1.17×10^{-11}	1.34×10^{-12}	Probable
					8.74×10^{-1}	2.90×10^{-5}	2.34×10^{-12}	2.68×10^{-13}	Low
					8.74×10^{1}	2.39×10^{-4}	2.34×10^{-11}	2.68×10^{-12}	High
^{99}Tc	NH_4TcO_4	181	2.13×10^{5}	9.11×10^{-2}	1.29×10^{0}	6.30×10^{-2}	1.25×10^{-11}	1.82×10^{-12}	Probable
					1.29×10^{-1}	4.48×10^{-2}	2.50×10^{-12}	3.64×10^{-13}	Low
					1.29×10^{1}	8.50×10^{-2}	2.50×10^{-11}	3.64×10^{-12}	High
^{137}Cs	Cs_2CO_3	334	3.00×10^{1}	1.60×10^{1}	1.99×10^{1}	2.72×10^{-4}	6.80×10^{-12}	5.12×10^{-13}	Probable
					1.99×10^{0}	2.15×10^{-4}	1.36×10^{-12}	1.02×10^{-13}	Low
					1.99×10^{2}	3.60×10^{-4}	1.36×10^{-11}	1.02×10^{-12}	High
^{232}Th	ThO_2	264	1.41×10^{10}	7.57×10^{-8}	5.36×10^{1}	1.64×10^{1}	3.24×10^{-14}	3.73×10^{-15}	Probable
					5.36×10^{0}	1.15×10^{1}	6.49×10^{-15}	7.45×10^{-16}	Low
					5.36×10^{2}	1.91×10^{1}	6.49×10^{-14}	7.45×10^{-15}	High
^{233}U	UO_2	265	1.59×10^{5}	1.46×10^{-6}	5.56×10^{1}	2.44×10^{-2}	3.11×10^{-14}	3.50×10^{-15}	Probable
					5.56×10^{0}	2.44×10^{-3}	6.22×10^{-15}	7.01×10^{-16}	Low
					5.56×10^{2}	2.44×10^{-1}	6.22×10^{-14}	7.01×10^{-15}	High

Table C.14 (continued)

Nuclide	Formula	Molecular weight	Half-life (year)	Solubility (mol/L)	Waste K_d (mL/g)	Inventory (g/vault)	Diffusion coefficient[a] Waste (m^2/s)	Diffusion coefficient[a] Concrete (m^2/s)	Expected extent of values
^{238}U	UO_2	270	4.47×10^9	1.46×10^{-6}	5.56×10^1	9.91×10^1	3.11×10^{-14}	3.50×10^{-15}	Probable
					5.56×10^0	7.52×10^1	6.22×10^{-15}	7.01×10^{-16}	Low
					5.56×10^2	1.34×10^2	6.22×10^{-14}	7.01×10^{-15}	High
^{239}Pu	PuO_2	271	2.41×10^4	1.71×10^{-8}	5.76×10^1	3.81×10^{-3}	3.00×10^{-14}	3.41×10^{-15}	Probable
					5.76×10^0	3.81×10^{-4}	6.01×10^{-15}	6.82×10^{-16}	Low
					5.76×10^2	3.81×10^{-2}	6.01×10^{-14}	6.82×10^{-15}	High
^{241}Am	Am_2O_3	530	4.33×10^2	3.27×10^{-6}	5.76×10^1	1.39×10^{-4}	5.46×10^{-14}	6.26×10^{-15}	Probable
					5.76×10^0	1.39×10^{-5}	1.09×10^{-14}	1.25×10^{-15}	Low
					5.76×10^2	1.39×10^{-3}	1.09×10^{-13}	1.25×10^{-14}	High

Note: Inventory based on 220 vaults.
For sources, see notes a–d, Table C.13.
[a]See note e, Table C.13.

Table C.15. Inventory and uncertainty analysis data for key nuclides in the Intermediate Waste Management Facility

Nuclide	Formula	Molecular weight	Half-life (year)	Solubility (mol/L)	Waste K_d (mL/g)	Inventory (g/vault)	Diffusion coefficient[a] Waste (m^2/s)	Diffusion coefficient[a] Concrete (m^2/s)	Expected extent of values
^{3}H	T_2O	22	1.23×10^{1}	1.11×10^{2}	1.99×10^{-1}	3.77×10^{-6}	3.88×10^{-9}	1.86×10^{-9}	Probable
					1.99×10^{-2}	1.89×10^{-6}	7.76×10^{-10}	3.72×10^{-10}	Low
					1.99×10^{0}	5.66×10^{-6}	7.76×10^{-9}	3.72×10^{-9}	High
^{14}C	$BaCO_3$	199	5.73×10^{3}	1.11×10^{-4}	1.09×10^{0}	2.47×10^{-2}	1.44×10^{-11}	2.18×10^{-12}	Probable
					1.09×10^{-1}	1.23×10^{-2}	2.89×10^{-12}	4.36×10^{-13}	Low
					1.09×10^{1}	3.69×10^{-2}	2.89×10^{-11}	4.36×10^{-12}	High
^{36}Cl	KCl	75	3.01×10^{5}	4.61×10^{0}	1.99×10^{-1}	2.32×10^{-1}	3.38×10^{-10}	5.08×10^{-11}	Probable
					1.99×10^{-2}	1.79×10^{-1}	6.77×10^{-11}	1.02×10^{-11}	Low
					1.99×10^{0}	3.05×10^{-1}	6.77×10^{-10}	1.02×10^{-10}	High
^{90}Sr	$SrCO_3$	150	2.85×10^{1}	7.45×10^{-5}	8.74×10^{0}	1.64×10^{-4}	1.17×10^{-11}	1.34×10^{-12}	Probable
					8.74×10^{-1}	4.34×10^{-5}	2.34×10^{-12}	2.68×10^{-13}	Low
					8.74×10^{1}	3.57×10^{-4}	2.34×10^{-11}	2.68×10^{-12}	High
^{99}Tc	NH_4TcO_4	181	2.13×10^{5}	9.11×10^{-2}	1.29×10^{0}	6.19×10^{-2}	1.25×10^{-11}	1.82×10^{-12}	Probable
					1.29×10^{-1}	4.38×10^{-2}	2.50×10^{-12}	3.64×10^{-13}	Low
					1.29×10^{1}	8.34×10^{-2}	2.50×10^{-11}	3.64×10^{-12}	High
^{137}Cs	Cs_2CO_3	334	3.00×10^{1}	1.60×10^{1}	1.99×10^{1}	4.43×10^{-4}	6.80×10^{-12}	5.12×10^{-13}	Probable
					1.99×10^{0}	3.51×10^{-4}	1.36×10^{-12}	1.02×10^{-13}	Low
					1.99×10^{2}	5.88×10^{-4}	1.36×10^{-11}	1.02×10^{-12}	High
^{232}Th	ThO_2	264	1.41×10^{10}	7.57×10^{-8}	5.36×10^{1}	2.32×10^{0}	3.24×10^{-14}	3.73×10^{-15}	Probable
					5.36×10^{0}	1.63×10^{0}	6.49×10^{-15}	7.45×10^{-16}	Low
					5.36×10^{2}	2.69×10^{0}	6.49×10^{-14}	7.45×10^{-15}	High

Table C.15 (continued)

Nuclide	Formula	Molecular weight	Half-life (year)	Solubility (mol/L)	Waste K_d (mL/g)	Inventory (g/vault)	Diffusion coefficient[a] Waste (m^2/s)	Diffusion coefficient[a] Concrete (m^2/s)	Expected extent of values
^{233}U	UO_2	265	1.59×10^5	1.46×10^{-6}	5.56×10^1	6.83×10^{-2}	3.11×10^{-14}	3.50×10^{-15}	Probable
					5.56×10^0	6.83×10^{-3}	6.22×10^{-15}	7.01×10^{-16}	Low
					5.56×10^2	6.83×10^{-1}	6.22×10^{-14}	7.01×10^{-15}	High
^{238}U	UO_2	270	4.47×10^9	1.46×10^{-6}	5.56×10^1	1.23×10^3	3.11×10^{-14}	3.50×10^{-15}	Probable
					5.56×10^0	9.14×10^2	6.22×10^{-15}	7.01×10^{-16}	Low
					5.56×10^2	1.69×10^3	6.22×10^{-14}	7.01×10^{-15}	High
^{239}Pu	PuO_2	271	2.41×10^4	1.71×10^{-8}	5.76×10^1	5.34×10^{-3}	3.00×10^{-14}	3.41×10^{-15}	Probable
					5.76×10^0	5.34×10^{-4}	6.01×10^{-15}	6.82×10^{-16}	Low
					5.76×10^2	8.45×10^{-3}	6.01×10^{-14}	6.82×10^{-15}	High
^{241}Am	Am_2O_3	530	4.33×10^2	3.27×10^{-6}	5.76×10^1	1.39×10^{-5}	5.46×10^{-14}	6.26×10^{-15}	Probable
					5.76×10^0	6.76×10^{-6}	1.09×10^{-14}	1.25×10^{-15}	Low
					5.76×10^2	5.16×10^{-5}	1.09×10^{-13}	1.25×10^{-14}	High
^{243}Am	Am_2O_3	534	7.38×10^3	3.27×10^{-6}	5.76×10^1	9.35×10^{-5}	5.46×10^{-14}	6.26×10^{-15}	Probable
					5.76×10^0	2.82×10^{-5}	1.09×10^{-14}	1.25×10^{-15}	Low
					5.76×10^2	2.49×10^{-4}	1.09×10^{-13}	1.25×10^{-14}	High

Note: Inventory based on 140 vaults.
For sources, see notes a–d, Table C.13.
[a]See note e, Table C.13.

Table C.16. Inventory and uncertainty analysis data for key nuclides in low-range silos

Nuclide	Formula	Molecular weight	Half-life (year)	Solubility (mol/L)	Waste K_d (mL/g)	Inventory (g/silo)	Diffusion coefficient[a] Waste (m^2/s)	Diffusion coefficient[a] Concrete (m^2/s)	Expected extent of values
^{3}H	T_2O	22	1.23×10^{1}	1.11×10^{2}	1.99×10^{-1}	1.41×10^{-5}	3.88×10^{-9}	1.86×10^{-9}	Probable
					1.99×10^{-2}	7.85×10^{-6}	7.76×10^{-10}	3.72×10^{-10}	Low
					1.99×10^{0}	2.02×10^{-5}	7.76×10^{-9}	3.72×10^{-9}	High
^{14}C	$BaCO_3$	199	5.73×10^{3}	1.11×10^{-4}	1.09×10^{0}	2.16×10^{-1}	1.44×10^{-11}	2.18×10^{-12}	Probable
					1.09×10^{-1}	1.08×10^{-1}	2.89×10^{-12}	4.36×10^{-13}	Low
					1.09×10^{1}	3.23×10^{-1}	2.89×10^{-11}	4.36×10^{-12}	High
^{90}Sr	$SrCO_3$	150	2.85×10^{1}	7.45×10^{-5}	8.74×10^{0}	5.22×10^{-4}	1.17×10^{-11}	1.34×10^{-12}	Probable
					8.74×10^{-1}	1.08×10^{-4}	2.34×10^{-12}	2.68×10^{-13}	Low
					8.74×10^{1}	1.27×10^{-3}	2.34×10^{-11}	2.68×10^{-12}	High
^{99}Tc	NH_4TcO_4	181	2.13×10^{5}	9.11×10^{-2}	1.29×10^{0}	2.56×10^{0}	1.25×10^{-11}	1.82×10^{-12}	Probable
					1.29×10^{-1}	1.82×10^{0}	2.50×10^{-12}	3.64×10^{-13}	Low
					1.29×10^{1}	3.45×10^{0}	2.50×10^{-11}	3.64×10^{-12}	High
^{137}Cs	Cs_2CO_3	334	3.00×10^{1}	1.60×10^{1}	1.99×10^{1}	6.88×10^{-4}	6.80×10^{-12}	5.12×10^{-13}	Probable
					1.99×10^{0}	4.18×10^{-4}	1.36×10^{-12}	1.02×10^{-13}	Low
					1.99×10^{2}	9.61×10^{-4}	1.36×10^{-11}	1.02×10^{-12}	High
^{232}Th	ThO_2	264	1.41×10^{10}	7.57×10^{-8}	5.36×10^{1}	1.31×10^{2}	3.24×10^{-14}	3.73×10^{-15}	Probable
					5.36×10^{0}	1.15×10^{2}	6.49×10^{-15}	7.45×10^{-16}	Low
					5.36×10^{2}	1.45×10^{2}	6.49×10^{-14}	7.45×10^{-15}	High

Table C.16 (continued)

Nuclide	Formula	Molecular weight	Half-life (year)	Solubility (mol/L)	Waste K_d (mL/g)	Inventory (g/silo)	Diffusion coefficient[a] Waste (m^2/s)	Diffusion coefficient[a] Concrete (m^2/s)	Expected extent of values
^{233}U	UO_2	265	1.59×10^5	1.46×10^{-6}	5.56×10^1	3.79×10^{-2}	3.11×10^{-14}	3.50×10^{-15}	Probable
					5.56×10^0	3.79×10^{-3}	6.22×10^{-15}	7.01×10^{-16}	Low
					5.56×10^2	3.79×10^{-1}	6.22×10^{-14}	7.01×10^{-15}	High
^{238}U	UO_2	270	4.47×10^9	1.46×10^{-6}	5.56×10^1	5.43×10^3	3.11×10^{-14}	3.50×10^{-15}	Probable
					5.56×10^0	4.08×10^3	6.22×10^{-15}	7.01×10^{-16}	Low
					5.56×10^2	7.42×10^3	6.22×10^{-14}	7.01×10^{-15}	High
^{239}Pu	PuO_2	271	2.41×10^4	1.71×10^{-8}	5.76×10^1	7.44×10^{-3}	3.00×10^{-14}	3.41×10^{-15}	Probable
					5.76×10^0	7.44×10^{-4}	6.01×10^{-15}	6.82×10^{-16}	Low
					5.76×10^2	1.58×10^{-2}	6.01×10^{-14}	6.82×10^{-15}	High
^{241}Am	Am_2O_3	530	4.33×10^2	3.27×10^{-6}	5.76×10^1	1.07×10^{-4}	5.46×10^{-14}	6.26×10^{-15}	Probable
					5.76×10^0	1.63×10^{-5}	1.09×10^{-14}	1.25×10^{-15}	Low
					5.76×10^2	3.38×10^{-4}	1.09×10^{-13}	1.25×10^{-14}	High
^{243}Am	Am_2O_3	534	7.38×10^3	3.27×10^{-6}	5.76×10^1	7.23×10^{-4}	5.46×10^{-14}	6.26×10^{-15}	Probable
					5.76×10^0	7.23×10^{-5}	1.09×10^{-14}	1.25×10^{-15}	Low
					5.76×10^2	5.54×10^{-3}	1.09×10^{-13}	1.25×10^{-14}	High

Note: Inventory based on 75 silos.
For sources, see notes a–d, Table C.13.
[a]See note e, Table C.13.

Table C.17. Inventory and uncertainty analysis data for key nuclides in high-range silos

Nuclide	Formula	Molecular weight	Half-life (year)	Solubility (mol/L)	Waste K_d (mL/g)	Inventory (g/silo)	Diffusion coefficient[a] Waste (m^2/s)	Diffusion coefficient[a] Concrete (m^2/s)	Expected extent of values
^{3}H	T_2O	22	1.23×10^{1}	1.11×10^{2}	1.99×10^{-1}	3.14×10^{-5}	3.88×10^{-9}	1.86×10^{-9}	Probable
					1.99×10^{-2}	1.57×10^{-5}	7.76×10^{-10}	3.72×10^{-10}	Low
					1.99×10^{0}	4.71×10^{-5}	7.76×10^{-9}	3.72×10^{-9}	High
^{14}C	$BaCO_3$	199	5.73×10^{3}	1.11×10^{-4}	1.09×10^{0}	2.72×10^{-4}	1.44×10^{-11}	2.18×10^{-12}	Probable
					1.09×10^{-1}	1.36×10^{-4}	2.89×10^{-12}	4.36×10^{-13}	Low
					1.09×10^{1}	4.08×10^{-4}	2.89×10^{-11}	4.36×10^{-12}	High
^{90}Sr	$SrCO_3$	150	2.85×10^{1}	7.45×10^{-5}	8.74×10^{0}	7.80×10^{-2}	1.17×10^{-11}	1.34×10^{-12}	Probable
					8.74×10^{-1}	5.07×10^{-2}	2.34×10^{-12}	2.68×10^{-13}	Low
					8.74×10^{1}	1.34×10^{-1}	2.34×10^{-11}	2.68×10^{-12}	High
^{137}Cs	Cs_2CO_3	334	3.00×10^{1}	1.60×10^{1}	1.99×10^{1}	8.15×10^{-3}	6.80×10^{-12}	5.12×10^{-13}	Probable
					1.99×10^{0}	4.95×10^{-3}	1.36×10^{-12}	1.02×10^{-13}	Low
					1.99×10^{2}	1.14×10^{-2}	1.36×10^{-11}	1.02×10^{-12}	High
^{232}Th	ThO_2	264	1.41×10^{10}	7.57×10^{-8}	5.36×10^{1}	3.26×10^{1}	3.24×10^{-14}	3.73×10^{-15}	Probable
					5.36×10^{0}	2.79×10^{1}	6.49×10^{-15}	7.45×10^{-16}	Low
					5.36×10^{2}	3.62×10^{1}	6.49×10^{-14}	7.45×10^{-15}	High
^{238}U	UO_2	270	4.47×10^{9}	1.46×10^{-6}	5.56×10^{1}	9.91×10^{2}	3.11×10^{-14}	3.50×10^{-15}	Probable
					5.56×10^{0}	8.75×10^{2}	6.22×10^{-15}	7.01×10^{-16}	Low
					5.56×10^{2}	1.12×10^{3}	6.22×10^{-14}	7.01×10^{-15}	High

Table C.17 (continued)

Nuclide	Formula	Molecular weight	Half-life (year)	Solubility (mol/L)	Waste K_d (mL/g)	Inventory (g/silo)	Diffusion coefficient[a] Waste (m^2/s)	Diffusion coefficient[a] Concrete (m^2/s)	Expected extent of values
^{239}Pu	PuO_2	271	2.41×10^4	1.71×10^{-8}	5.76×10^1	7.31×10^{-3}	3.00×10^{-14}	3.41×10^{-15}	Probable
					5.76×10^0	7.31×10^{-4}	6.01×10^{-15}	6.82×10^{-16}	Low
					5.76×10^2	3.20×10^{-2}	6.01×10^{-14}	6.82×10^{-15}	High

Note: Inventory based on 33 silos.
For sources, see notes a–d, Table C.13.
[a]See note e, Table C.13.

Table C.18. Inventory and uncertainty analysis data for key nuclides in high-range wells

Nuclide	Formula	Molecular weight	Half-life (year)	Solubility (mol/L)	Waste K_d (mL/g)	Inventory (g/well)	Diffusion coefficient[a] Waste (m^2/s)	Diffusion coefficient[a] Concrete (m^2/s)	Expected extent of values
^{90}Sr	$SrCO_3$	150	2.85×10^{1}	7.45×10^{-5}	8.74×10^{0}	9.50×10^{-1}	1.17×10^{-11}	1.34×10^{-12}	Probable
					8.74×10^{-1}	6.42×10^{-1}	2.34×10^{-12}	2.68×10^{-13}	Low
					8.74×10^{1}	1.27×10^{0}	2.34×10^{-11}	2.68×10^{-12}	High
^{99}Tc	NH_4TcO_4	181	2.13×10^{5}	9.11×10^{-2}	1.29×10^{0}	4.37×10^{-1}	1.25×10^{-11}	1.82×10^{-12}	Probable
					1.29×10^{-1}	4.15×10^{-1}	2.50×10^{-12}	3.64×10^{-13}	Low
					1.29×10^{1}	4.59×10^{-1}	2.50×10^{-11}	3.64×10^{-12}	High
^{137}Cs	Cs_2CO_3	334	3.00×10^{1}	1.60×10^{1}	1.99×10^{1}	1.41×10^{0}	6.80×10^{-12}	5.12×10^{-13}	Probable
					1.99×10^{0}	1.28×10^{0}	1.36×10^{-12}	1.02×10^{-13}	Low
					1.99×10^{2}	1.62×10^{0}	1.36×10^{-11}	1.02×10^{-12}	High
^{152}Eu	Eu_2O_3	352	1.33×10^{1}	2.84×10^{-6}	3.78×10^{0}	5.74×10^{-2}	7.95×10^{-13}	9.17×10^{-14}	Probable
					3.78×10^{-1}	3.61×10^{-2}	1.59×10^{-13}	1.83×10^{-14}	Low
					3.78×10^{1}	8.48×10^{-2}	1.59×10^{-12}	1.83×10^{-13}	High
^{154}Eu	Eu_2O_3	356	8.80×10^{0}	2.84×10^{-6}	3.78×10^{0}	1.30×10^{-2}	7.95×10^{-13}	9.17×10^{-14}	Probable
					3.78×10^{-1}	8.16×10^{-3}	1.59×10^{-13}	1.83×10^{-14}	Low
					3.78×10^{0}	1.92×10^{-2}	1.59×10^{-12}	1.83×10^{-13}	High

Table C.18 (continued)

Nuclide	Formula	Molecular weight	Half-life (year)	Solubility (mol/L)	Waste K_d (mL/g)	Inventory (g/well)	Diffusion coefficient[a] Waste (m^2/s)	Diffusion coefficient[a] Concrete (m^2/s)	Expected extent of values
^{229}Th	ThO_2	261	7.34×10^3	7.57×10^{-8}	5.36×10^1	6.53×10^{-4}	3.24×10^{-14}	3.73×10^{-15}	Probable
					5.36×10^0	5.88×10^{-4}	6.49×10^{-15}	7.45×10^{-16}	Low
					5.36×10^2	7.18×10^{-4}	6.49×10^{-14}	7.45×10^{-15}	High
^{232}Th	ThO_2	264	1.41×10^{10}	7.57×10^{-8}	5.36×10^1	6.25×10^0	3.24×10^{-14}	3.73×10^{-15}	Probable
					5.36×10^0	5.62×10^0	6.49×10^{-15}	7.45×10^{-16}	Low
					5.36×10^2	6.87×10^0	6.49×10^{-14}	7.45×10^{-15}	High

Note: Inventory based on 12 wells.
For sources, see notes a–d, Table C.13.
[a]See note e, Table C.13.

Table C.19. Uncertainty analysis data for key nuclides in high-range wells in silos

Nuclide	Formula	Molecular weight	Half-life (year)	Solubility (mol/L)	Waste K_d (mL/g)	Inventory (g/silo)	Diffusion coefficient[a] Waste (m^2/s)	Diffusion coefficient[a] Concrete (m^2/s)	Expected extent of values
^{90}Sr	$SrCO_3$	150	2.85×10^{1}	7.45×10^{-5}	8.74×10^{0}	6.65×10^{0}	1.17×10^{-11}	1.34×10^{-12}	Probable
					8.74×10^{-1}	4.50×10^{0}	2.34×10^{-12}	2.68×10^{-13}	Low
					8.74×10^{1}	8.86×10^{0}	2.34×10^{-11}	2.68×10^{-12}	High
^{99}Tc	NH_4TcO_4	181	2.13×10^{5}	9.11×10^{-2}	1.29×10^{0}	3.06×10^{0}	1.25×10^{-11}	1.82×10^{-12}	Probable
					1.29×10^{-1}	2.91×10^{0}	2.50×10^{-12}	3.64×10^{-13}	Low
					1.29×10^{1}	3.21×10^{0}	2.50×10^{-11}	3.64×10^{-12}	High
^{137}Cs	Cs_2CO_3	334	3.00×10^{1}	1.60×10^{1}	1.99×10^{1}	9.87×10^{0}	6.80×10^{-12}	5.12×10^{-13}	Probable
					1.99×10^{0}	8.99×10^{0}	1.36×10^{-12}	1.02×10^{-13}	Low
					1.99×10^{2}	1.14×10^{1}	1.36×10^{-11}	1.02×10^{-12}	High
^{152}Eu	Eu_2O_3	352	1.33×10^{1}	2.84×10^{-6}	3.78×10^{0}	4.02×10^{-1}	7.95×10^{-13}	9.17×10^{-14}	Probable
					3.78×10^{-1}	2.53×10^{-1}	1.59×10^{-13}	1.83×10^{-14}	Low
					3.78×10^{1}	5.94×10^{-1}	1.59×10^{-12}	1.83×10^{-13}	High
^{154}Eu	Eu_2O_3	356	8.80×10^{0}	2.84×10^{-6}	3.78×10^{0}	9.13×10^{-2}	7.95×10^{-13}	9.17×10^{-14}	Probable
					3.78×10^{-1}	5.72×10^{-2}	1.59×10^{-13}	1.83×10^{-14}	Low
					3.78×10^{1}	1.34×10^{-1}	1.59×10^{-12}	1.83×10^{-13}	High
^{229}Th	ThO_2	261	7.34×10^{3}	7.57×10^{-8}	5.36×10^{1}	4.57×10^{-3}	3.24×10^{-14}	3.73×10^{-15}	Probable
					5.36×10^{0}	4.11×10^{-3}	6.49×10^{-15}	7.45×10^{-16}	Low
					5.36×10^{2}	5.03×10^{-3}	6.49×10^{-14}	7.45×10^{-15}	High
^{232}Th	ThO_2	264	1.41×10^{10}	7.57×10^{-8}	5.36×10^{1}	4.37×10^{1}	3.24×10^{-14}	3.73×10^{-15}	Probable
					5.36×10^{0}	3.93×10^{1}	6.49×10^{-15}	7.45×10^{-16}	Low
					5.36×10^{2}	4.81×10^{1}	6.49×10^{-14}	7.45×10^{-15}	High

Note: Inventory based on 6 silos with 7 wells in each silo for a total of 42 wells.
For sources, see notes a–d, Table C.13.
[a]See note e, Table C.13.

Table C.20. Inventory and uncertainty analysis data for key nuclides in fissile wells

Nuclide	Formula	Molecular weight	Half-life (year)	Solubility (mol/L)	Waste K_d (mL/g)	Inventory (g/well)	Diffusion coefficient[a] Waste (m^2/s)	Diffusion coefficient[a] Concrete (m^2/s)	Expected extent of values
^{137}Cs	Cs_2CO_3	334	3.00×10^{1}	1.60×10^{1}	1.99×10^{1}	4.43×10^{-1}	6.80×10^{-12}	5.12×10^{-13}	Probable
					1.99×10^{0}	2.69×10^{-1}	1.36×10^{-12}	1.02×10^{-13}	Low
					1.99×10^{2}	6.19×10^{-1}	1.36×10^{-11}	1.02×10^{-12}	High
^{235}U	UO_2	267	7.04×10^{8}	1.46×10^{-6}	5.56×10^{1}	4.05×10^{2}	3.11×10^{-14}	3.50×10^{-15}	Probable
					5.56×10^{0}	3.65×10^{2}	6.22×10^{-15}	7.01×10^{-16}	Low
					5.56×10^{2}	4.46×10^{2}	6.22×10^{-14}	7.01×10^{-15}	High
^{238}U	UO_2	270	4.47×10^{9}	1.46×10^{-6}	5.56×10^{1}	1.44×10^{4}	3.11×10^{-14}	3.50×10^{-15}	Probable
					5.56×10^{0}	1.29×10^{4}	6.22×10^{-15}	7.01×10^{-16}	Low
					5.56×10^{2}	1.58×10^{4}	6.22×10^{-14}	7.01×10^{-15}	High

Note: Inventory based on one well.
For sources, see notes a–d, Table C.13.
[a]See note e, Table C.13.

Table C.21. Inventory uncertainty analysis data for key nuclides in asbestos silos

Nuclide	Formula	Formula weight	Half-life (year)	Solubility (mol/L)	Waste K_d (mL/g)	Inventory (g/silo)	Diffusion coefficient[a] Waste (m^2/s)	Diffusion coefficient[a] Concrete (m^2/s)	Expected extent of values
^{3}H	T_2O	22	1.23×10^{1}	1.11×10^{2}	1.99×10^{-1}	4.71×10^{-7}	3.88×10^{-9}	1.86×10^{-9}	Probable
					1.99×10^{-2}	4.71×10^{-8}	7.76×10^{-10}	3.72×10^{-10}	Low
					1.99×10^{0}	4.71×10^{-6}	7.76×10^{-9}	3.72×10^{-9}	High
^{14}C	$BaCO_3$	199	5.73×10^{3}	1.11×10^{-4}	1.09×10^{0}	1.18×10^{-2}	1.44×10^{-11}	2.18×10^{-12}	Probable
					1.09×10^{-1}	5.92×10^{-3}	2.89×10^{-12}	4.36×10^{-13}	Low
					1.09×10^{1}	1.77×10^{-2}	2.89×10^{-11}	4.36×10^{-12}	High
^{90}Sr	$SrCO_3$	150	2.85×10^{1}	7.45×10^{-5}	8.74×10^{0}	3.14×10^{-5}	1.17×10^{-11}	1.34×10^{-12}	Probable
					8.74×10^{-1}	8.33×10^{-6}	2.34×10^{-12}	2.68×10^{-13}	Low
					8.74×10^{1}	6.86×10^{-5}	2.34×10^{-11}	2.68×10^{-12}	High
^{99}Tc	NH_4TcO_4	181	2.13×10^{5}	9.11×10^{-2}	1.29×10^{0}	5.47×10^{-3}	1.25×10^{-11}	1.82×10^{-12}	Probable
					1.29×10^{-1}	2.95×10^{-4}	2.50×10^{-12}	3.64×10^{-13}	Low
					1.29×10^{1}	1.47×10^{-2}	2.50×10^{-11}	3.64×10^{-12}	High
^{238}U	UO_2	270	4.47×10^{9}	1.46×10^{-6}	5.56×10^{1}	1.37×10^{3}	3.11×10^{-14}	3.50×10^{-15}	Probable
					5.56×10^{0}	1.02×10^{3}	6.22×10^{-15}	7.01×10^{-16}	Low
					5.56×10^{2}	1.89×10^{3}	6.22×10^{-14}	7.01×10^{-15}	High

Note: Inventory based on 11 silos.
For sources, see ntoes a–d, Table C.13.
[a]See note e, Table C.13.

Table C.22. Inventory and uncertainty analysis data for key nuclides in biological trenches

Nuclide	Formula	Molecular weight	Half-life (year)	Solubility (mol/L)	Waste K_d (mL/g)	Inventory (g/trench)	Diffusion coefficient[a] Waste (m^2/s)	Diffusion coefficient[a] Concrete (m^2/s)	Expected extent of values
^{3}H	T_2O	22	1.23×10^{1}	1.11×10^{2}	1.99×10^{-1}	1.87×10^{-7}	3.88×10^{-9}	1.86×10^{-9}	Probable
					1.99×10^{-2}	1.87×10^{-8}	7.76×10^{-10}	3.72×10^{-10}	Low
					1.99×10^{0}	1.87×10^{-6}	7.76×10^{-9}	3.72×10^{-9}	High
^{90}Sr	$SrCO_3$	150	2.85×10^{1}	7.45×10^{-5}	8.74×10^{0}	2.65×10^{-4}	1.17×10^{-11}	1.34×10^{-12}	Probable
					8.74×10^{-1}	1.92×10^{-4}	2.34×10^{-12}	2.68×10^{-13}	Low
					8.74×10^{1}	3.40×10^{-4}	2.34×10^{-11}	2.68×10^{-12}	High

Note: Inventory based on 5 trenches.
For sources, see notes a–d, Table C.13.
[a]See note e, Table C.13.

APPENDIX D

APPLICATION OF THE UNIFIED TRANSPORT MODEL, TUMSIM, AND WELSIM TO THE SOLID WASTE STORAGE AREA 6 PERFORMANCE ASSESSMENT

R. J. Luxmoore

APPENDIX D

APPLICATION OF THE UNIFIED TRANSPORT MODEL, TUMSIM, AND WELSIM TO THE SOLID WASTE STORAGE AREA 6 PERFORMANCE ASSESSMENT

D.1 UNIFIED TRANSPORT MODEL

The Unified Transport Model (UTM) is a water budget simulator that includes algorithms for interception storage, interception evaporation, infiltration, soil water drainage, soil evaporation, transpiration, and subsurface lateral flow (Fig. D.1). The code is documented in Patterson et al. (1974) and Huff et al. (1977b), and hydrologic simulations have been tested with data from Walker Branch watershed on the Oak Ridge Reservation (Huff et al. 1977a; Luxmoore and Huff 1989). The code operates with 15-min time steps during rainfall and otherwise hourly, to generate the water dynamics for up to seven soil-plant segments of a watershed. The lateral flow and drainage from each land segment can be assembled to generate streamflow simulations, but this option was not used in the present application.

The meteorological data needed for simulation with UTM are hourly precipitation, daily maximum and minimum air temperature, daily total solar radiation, daily average dew point temperature, and daily average wind speed. Records from Walker Branch Watershed and from the meteorological station at Oak Ridge Townsite have been compiled into the model format for application at sites in the vicinity of Oak Ridge National Laboratory. An evaluation of the data for the 1968–89 period showed that 1971 was a year with average precipitation (1372 mm/year), with 1968 being a dry year (933 mm/year) and 1973 a wet year (1895 mm/year). These three contrasting sets of data were selected for simulation to provide a range of hydrologic transport regimes. The data for the average year were used in most of the simulations. It was assumed that all chemicals leached from disposal unit sites are transported in drainage water, even if the volume was small. Limitations due to chemical solubility were determined in the SOURCE1 and SOURCE2 models.

Model applications were initialized by repeating simulations using the same weather data for a second year, with the simulated soil water values at the end of the first year being used to initiate the second simulation. The monthly water budget values from the end of the second year were used as the initial status of the landscape. Change in annual soil water storage was close to zero with this initialization procedure; thus, there was little or no influence of initial conditions on the simulated water budgets for the various stages of SWSA 6 operations.

The soils of SWSA 6 have been described and classified by Davis et al. (1987). Many of the profiles are shallow, being formed on weathered, interbedded shale and limestone (saprolite). Some alluvial soils occur along drainage ways in lower landscape positions of the burial ground. The hydraulic properties selected to represent these soils

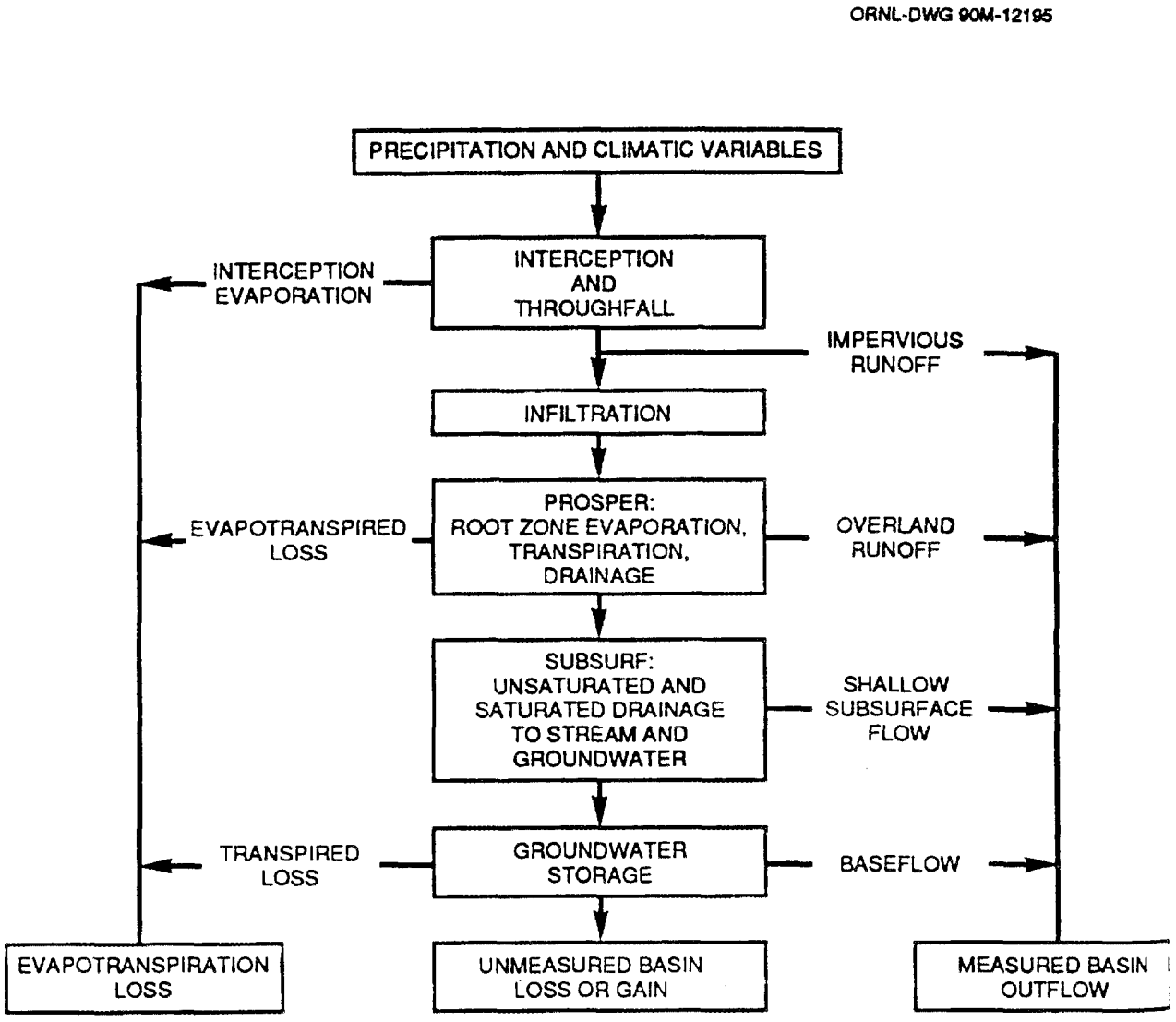

Fig. D.1. Hydrologic storage and flow components of the Unified Transport Model.

were derived from published sources reporting investigations conducted on SWSA 6 or from soils of the same geologic formation. A representative set of water retention data for SWSA 6 soil (Table D.1) showed total porosity varying in the upper 2 m (7 ft) of the profile from 0.390 to 0.476 m^3/m^3. Saturated hydraulic conductivity measurements showed a decrease with depth; values are about three orders of magnitude smaller at 3 to 4 m (10 to 13 ft) depth than at the surface. The water retention data were obtained from Luxmoore (1982) and Davis et al. (1987). Saturated conductivity data for the upper five soil layers shown in Table D.1 were obtained from Rothschild et al. (1984). The saturated hydraulic conductivity values for the bottom two layers were decreased from the values given by Rothschild et al. (1984) in an approximately exponential decrease such that the conductivity of the lowest layer was 5.8×10^{-9} m/s (0.5 mm/day). Simulations using the hydraulic properties listed in Table D.1 gave lateral flow and drainage results that agreed with the hydrologic framework outlined in Sect. 3.2.2. This framework projects that about 10% of subsurface flow will become recharge to aquifers, with the remainder generating lateral subsurface flow through a stormflow zone located in the upper 2 m (7 ft) of the soil profile.

In simulations involving a clay cap, the saturated conductivity of the second layer was reduced from 2.14×10^{-5} to 2.3×10^{-9} m/s. At a later stage in the simulations, soil macropores were included in the cap to represent the influence of cracks and channels through the material; this essentially negated any hydrologic impedance by the cap during the last 50 years of the closure period. Spatial variability of hydraulic properties in soil profiles similar to SWSA 6 have been determined for the surface soil (Wilson and Luxmoore 1988) and for the subsoil (Luxmoore et al. 1981; Wilson et al. 1989). These three studies showed lognormal frequency distributions for soil water flow rates and little or no spatial correlation between the measurement sites. For performance assessment purposes, spatial variability of soil properties in SWSA 6 was not included in the analysis. The one set of soil properties in Table D.1 was used. In the uncertainty analysis, however, the frequency distributions used for the hydraulic conductivity controlling recharge to groundwater were lognormal.

D.2 TUMSIM AND WELSIM

The TUMSIM and WELSIM codes provided annual time step calculations for the leaching of radionuclides from disposal units through the vadose zone to groundwater (recharge) and to surface water via lateral subsurface transport through the stormflow zone. The codes were an essential link between the leachate output from the SOURCE1 and SOURCE2 models and the input of radionuclide to groundwater needed in the USGS MOC aquifer simulations. The sequence of calculations used in both codes involved five main steps.

Table D.1. Volumetric soil water content at selected matric pressures and the saturated hydraulic conductivity of soil layers formed on saprolite

	Soil layer (cm)							
Matric pressure (−kPa)	0–30	30–60	60–100	100–150	150–200	200–300	300–400	400–500
0	0.467	0.419	0.455	0.456	0.390	0.390	0.390	0.390
1	0.472	0.410	0.432	0.448	0.384	0.384	0.384	0.384
2	0.468	0.403	0.418	0.440	0.378	0.378	0.378	0.378
3	0.466	0.397	0.410	0.433	0.373	0.373	0.373	0.373
4	0.463	0.392	0.402	0.429	0.369	0.369	0.369	0.369
5	0.462	0.388	0.396	0.425	0.366	0.366	0.366	0.366
10	0.452	0.369	0.372	0.406	0.352	0.352	0.352	0.352
15	0.439	0.352	0.354	0.389	0.342	0.342	0.342	0.342
18	0.430	0.346	0.347	0.380	0.336	0.336	0.366	0.366
33	0.370	0.310	0.330	0.350	0.330	0.330	0.330	0.330
100	0.355	0.300	0.305	0.325	0.305	0.305	0.305	0.305
200	0.340	0.285	0.295	0.315	0.295	0.295	0.295	0.295
400	0.310	0.270	0.275	0.295	0.275	0.275	0.275	0.275
800	0.250	0.250	0.250	0.270	0.250	0.250	0.250	0.250
1500	0.140	0.230	0.230	0.250	0.230	0.230	0.230	0.230
Saturated conductivity (m/s)	3.5×10^{-5}	2.14×10^{-5}	1.5×10^{-5}	9.8×10^{-6}	2.3×10^{-6}	5.8×10^{-7}	3.5×10^{-8}	5.8×10^{-9}

1. Calculation of radioactive decay for the total nuclide in the adsorbed and dissolved phases of the two vadose zone flow paths. The equation used has the form

$$\text{Nuclide } (t + 1) = \text{Nuclide } (t)\, e^{-\log 2.0/hl} \quad ,$$

which caused the nuclide quantity at time $(t + 1)$ to be diminished from the value at time (t) by a negative exponential that depended on the half-life (hl) of the particular nuclide (Table 3.7).

2. The annual chemical leachate flux from disposal units to the recharge and lateral flow paths (calculated by the SOURCE1 and SOURCE2 codes) was added to resident radionuclide in the two flow paths.

3. A new chemical equilibrium between the adsorbed and dissolved nuclide phases was calculated. The dissolved phase concentration (g/mL) was calculated by

$$\text{Dissolved Nuclide Concentration} = \frac{\text{Total Chemical (g)}}{\text{Volume Term (mL)}} \quad ,$$

where *Total Chemical* was the sum of the adsorbed, dissolved, and added leachate components, and the *Volume Term* was given by [water content at field capacity + annual flow volume + (K_d × Soil Volume × Bulk Density)].

These calculations accounted for chemical adsorption through the K_d (mL/g) term (Table 3.7). The soil volume used in the calculations was given by the area of the disposal unit site (increased as the number of disposal units increased) and the distance between the disposal unit site and the water table (recharge path) or the nearest receiving stream (lateral flow path). In the latter case, soil volume was arbitrarily reduced to 25% of its full value to account for convergence of subsurface lateral flow through the landscape (Table 3.5). This was a conservative assumption since reduced soil was available for adsorption, increasing the nuclide available for transport.

4. Chemical transport (g/year) was calculated as the product of the pathway water flux (mL/year, provided by the SOURCE1 and SOURCE2 models) and the dissolved nuclide concentration (g/mL) determined in step 3.

5. Following removal of dissolved nuclide in transport to groundwater and through the lateral flow path, a chemical mass budget was determined and a test for conservation of mass conducted.

The TUMSIM code was used for calculations for the Tumulus I, Tumulus II, and the Interim Waste Management Facility pads. Calculations were conducted on a per pad basis and not on a per cask basis in these cases. The WELSIM code was applicable to all other disposal units (silos, wells, trenches), and calculations were conducted on a disposal unit basis. The number of disposal units increased linearly with time, and the differing ages and numbers of disposal units were accounted for in the calculation procedure.

Simulations were conducted independently for 87 combinations of disposal unit sites and radionuclides. The essential aspects of the two codes are represented by steps 1 and 3 with appropriate bookkeeping for the various soil compartments and chemical fluxes.

D.3 REFERENCES

Davis, E. C., D. K. Solomon, R. B. Dreier, S. Y. Lee, P. M. Craig, A. D. Kelmers, and D. A. Lietzke 1987. *Summary of Environmental Characterization Activities at the Oak Ridge National Laboratory Solid Waste Storage Area Six, FY 1986 through 1987*, ORNL/RAP/LTR-87/68, Oak Ridge National Laboratory, Oak Ridge, Tenn.

Huff, D. D., G. S. Henderson, C. L. Begovich, R. J. Luxmoore, and J. R. Jones 1977a. "The Application of Analytic and Mechanistic Hydrologic Models to the Study of Walker Branch Watershed," pp. 741-63 in *Watershed Research in Eastern North America*, ed. D. L. Correll, Chesapeake Bay Center for Environmental Studies, Smithsonian Institution, Edgewater, Md.

Huff, D. D., R. J. Luxmoore, J. B. Mankin, and C. L. Begovich 1977b. *TEHM: A Terrestrial Ecosystem Hydrology Model*, ORNL/NSF/EATC-27, Oak Ridge National Laboratory, Oak Ridge, Tenn.

Luxmoore, R. J. 1982. *Physical Characteristics of Soils of the Southern Region: Fullerton and Sequoia Series*, ORNL-5868, Oak Ridge National Laboratory, Oak Ridge, Tenn.

Luxmoore, R. J., and D. D. Huff 1989. "Water," pp. 164-96 in *Analysis of Biogeochemical Cycling Processes in Walker Branch Watershed*, ed. D. W. Johnson and R. J. Van Hook, Springer-Verlag, New York.

Luxmoore, R. J., B. P. Spalding, and I. M. Munro 1981. "Areal Variation and Chemical Modification of Weathered Shale Infiltration Characteristics," *Soil Sci. Soc. Am. J.* 45, 687-91.

Patterson, M. R., J. K. Munro, D. E. Fields, R. D. Ellison, A. A. Brooks, and D. D. Huff 1974. *A User's Manual for the Fortran IV Version of the Wisconsin Hydrologic Transport Model*, ORNL-NSF-EATC-7, Oak Ridge National Laboratory, Oak Ridge, Tenn.

Rothschild, E. R., D. D. Huff, B. P. Spalding, S. Y. Lee, R. B. Clapp, D. A. Lietzke, R. G. Stansfield, N. D. Farrow, C. D. Farmer, and I. L. Munro 1984. *Characterization of Soils at Proposed Solid Waste Storage Area (SWSA) 7*, ORNL/TM-9326, Oak Ridge National Laboratory, Oak Ridge, Tenn.

Wilson, G. V., and R. J. Luxmoore 1988. "Infiltration, Macroporosity, and Mesoporosity Distributions on Two Forested Watersheds," *Soil Sci. Soc. Am. J.* 52, 329-35.

Wilson, G. V., J. M. Alfonsi, and P. M. Jardine 1989. "Spatial Variability of Saturated Hydraulic Conductivity of the Subsoil of Two Forested Watersheds," *Soil Sci. Soc. Am. J.* 53, 679–85.

APPENDIX E

THEORETICAL DESCRIPTION OF GROUNDWATER FLOW AND CONTAMINANT TRANSPORT: ASSUMPTIONS IN THE MATHEMATICAL MODEL OF RADIONUCLIDE TRANSPORT AT SOLID WASTE STORAGE AREA 6

M. W. Yambert

September 1993

APPENDIX E

THEORETICAL DESCRIPTION OF GROUNDWATER FLOW AND CONTAMINANT TRANSPORT: ASSUMPTIONS IN THE MATHEMATICAL MODEL OF RADIONUCLIDE TRANSPORT AT SOLID WASTE STORAGE AREA 6

E.1 INTRODUCTION

One of the central issues in modeling contaminant transport at SWSA 6 is the description of the velocity field. By using hydrogeological principles together with basic notions of fluid flow, one can theoretically determine the hydraulic head in an aquifer as the solution of the head equation (Bear 1979),

$$\frac{\partial}{\partial x}\left(K_x \frac{\partial h}{\partial x}\right) + \frac{\partial}{\partial y}\left(K_y \frac{\partial h}{\partial y}\right) = S_s \frac{\partial h}{\partial t} \qquad \text{(E.1)}$$

together with appropriate initial and boundary conditions. Here K_x and K_y are aquifer conductivities, and S_s is the specific storage. The solution of this equation may be constrained in several ways, principally by adjusting flow in and out of the system. In the best case, the computed head replicates the data-determined head shown in Fig. 4.3. These computations form the basis of the simulation of contaminated groundwater flow and provide our best estimates of radionuclide concentrations at compliance points. The actual concentration levels are simulated by numerically solving the usual contaminant transport equation,

$$D_x \frac{\partial^2 C}{\partial x^2} + D_{xy} \frac{\partial^2 C}{\partial x \partial y} + D_y \frac{\partial^2 C}{\partial y^2} = V_x \frac{\partial C}{\partial x} + V_y \frac{\partial C}{\partial y} + \frac{\partial C}{\partial t} + \lambda C , \qquad \text{(E.2)}$$

with appropriate initial and boundary conditions. The terms D_x, D_y, and D_{xy} are dispersion coefficients, and V_x, V_y are velocity components. The MOC code integrates this equation by way of a particle-tracking method along characteristic curves. This step can be completed only after the velocity field has been determined. The parameters that must be supplied are independent of those used in solving the head equation. Unfortunately, the lack of definitive data on contamination levels associated with the individual disposal sites precludes the possibility of tuning these parameters to such data.

The assumptions underlying this simulation are numerous; the principal ones are as follows. In the saturated groundwater domain at the SWSA 6 site (Fig. 4.2):

1. Darcy's Law is valid at all points in that the groundwater flow can be modeled as a single porous medium; unstressed flow is determined solely by hydraulic gradient,

and natural stresses such as recharge and discharge may be described as driving terms which are consistent with Darcy's Law.

2. The groundwater flow may be simulated as an areal flow (two-dimensional) of a given depth at each point in the domain.
3. Porosity and hydraulic conductivity are constant in time, and both are uniform over the entire site.
4. Transmissivities do not vary appreciably with changing aquifer depth.
5. The velocity field is not influenced by temperature, viscosity, or fluid density.
6. Ionic and molecular diffusions do not effectively influence dispersive flux.
7. Vertical variations in head and concentration are negligible; hence, a solute is uniformly distributed with respect to depth at any point in the simulation. (These are the consequences of assuming two-dimensional flow and transport.)
8. The hydraulic stresses on the aquifer are given solely by recharge and discharge to streams, drains, and White Oak Lake.
9. The aquifer at SWSA 6 may be modeled as homogeneous and anisotropic with respect to hydraulic conductivity and homogeneous and isotropic with respect to dispersivity.
10. The movement of each radionuclide is retarded in the porous medium by equilibrium-controlled sorption or ion exchange; the sorption-concentration may be described by a linear isotherm.
11. The mass decay of each radionuclide is exponential.
12. The major component of transport is advection (convection) due to the groundwater flow field, but existing, albeit unknown, heterogeneities in the aquifer may be modeled by the inclusion of a probabilistically based dispersion parameter.
13. The radionuclide solutes are independent in the sense that the concentration of one is not coupled to the concentration of another. Thus, the superposition of concentrations is valid.
14. The fractured, weather subsurface media can be modeled using an effective porous media model (Lee 1991).

The required velocities are obtained by solving the head equation subject to the constraint that the root-mean-square of the residuals between the computed and data-derived heads are minimal. This is an iterative process wherein the parameters and forcing terms are adjusted within reasonable limits. The USGS MOC code is used to solve the differential equation for head on a 40 × 52 set of block-centered nodes that covers all of the disposal units in question at SWSA 6. Given the yearly recharge rates supplied by the surface and shallow subsurface analysis in Sects. 4.2, a numerical solution for head was found by the code, and Darcy's Law provided the bulk velocities from which the seepage velocity vectors were deduced, assuming fixed porosity. The near steady-state groundwater velocity field for the area, shown in Fig. 4.4, implies that groundwater starting at any point in the simulation area evidently reaches a stream, drain, or White Oak Lake. (Thus, the simulation does not provide for excursion of contaminated groundwater under White Oak Lake or otherwise off-site.)

The maximum seepage velocity was computed to be approximately 0.7 m/day (3.0×10^{-5} ft/s). The actual solute transport rate is simulated at less than this maximum because of nominal retardation discussed below. The simulated transport of solutes was

accomplished following the velocity determination, and the groundwater concentration of each radionuclide from each respective disposal unit was simulated in accordance with the above description. No systematic effort was made to adjust the parameters in the contaminant transport runs. This was due solely to the absence of data mentioned above. Hence, the flow was adjusted with some care to the head distribution and recharge/discharge data, while the contaminant equation was simply supplied with values given in Tables E.1 and E.2.

E.2 CALIBRATION OF SWSA 6 FLOW MODEL

As previously described in Sect. 4.3, the modeled SWSA 6 water table surfaces were obtained via an iterative calibration process. Initially, measured head values taken from EBASCO (1992) were obtained. Kriging algorithms (Surfer 1990) were used to extrapolate the data to cover the area represented by the rectangular 40 × 52 grid used in the modeling analysis. The resultant initial water elevation surface and a calculated surface reflecting the proposed CERCLA caps (EBASCO 1992) were used as targets for the numerical solution of the flow equation. Velocity fields (EBASCO 1992) were also used as an aid in calibrating the initial and capped water tables. By adjusting various modeled parameters (see below) and recharge/leakance rates, and performing multiple model runs, we obtained solutions to the head equation that closely matched the initial (Fig. E.1) and capped (Fig. E.2) head surfaces. Figures E.3 and E.4 show the corresponding groundwater velocity fields for the initial and capped scenarios.

E.3 MODEL INPUT PARAMETER VALUES

Many of the parameter values used for the simulations were determined by simply using those calibrated at the Bear Creek test site. Others were adjusted by the iterative process, as described above. The essential parameters used in the SWSA 6 groundwater flow and transport simulations are given in Tables E.1 and E.2.

Table E.1. General model input parameters

Effective porosity	0.02
Longitudinal dispersivity	3.0 ft
Specific storage *	1.0×10^{-6}
Anisotropy (K_x/K_y)	3.0
Aquifer thickness	9.0 ft
Soil bulk density	1.35 g/mL
Simulation period	1000–4000 years

Table E.2. Distribution coefficients (K_d) and half-lives of isotopes

Isotope	K_d (mL/g)	Half-life (years)
^{14}C	0.2	5.73×10^3
^{36}Cl	0.2	3.01×10^5
^{3}H	0.2	1.23×10^1
^{152}Eu	3000.0	1.33×10^1
^{154}Eu	3000.0	8.80×10^0
^{137}Cs	3000.0	3.00×10^1
^{90}Sr	30.0	2.86×10
^{99}Tc	0.2	2.13×10^5
^{232}Th	40.0	1.41×10^{10}
^{229}Th	40.0	7.34×10^3
^{233}U	40.0	1.59×10^5
^{235}U	40.0	7.04×10^8
^{238}U	40.0	4.47×10^8
^{241}Am	40.0	4.33×10^2
^{243}Am	40.0	7.38×10^3
^{239}Pu	40.0	2.41×10^4
^{226}Ru	3000.0	1.60×10^3

E.4 MODELING ASSUMPTIONS

The assumptions made in the SWSA 6 analysis of groundwater flow and contaminant transport are as follows.

E.4.1 Recharge Values

Diffuse recharge rates used in the MOC analysis were assumed to be dependent on the type of ground cover and surface conditions. Each unique combination of these was modeled in MOC as a recharge class. Recharge rates for all classes were based on UTM

ORNL-DWG 94-5980

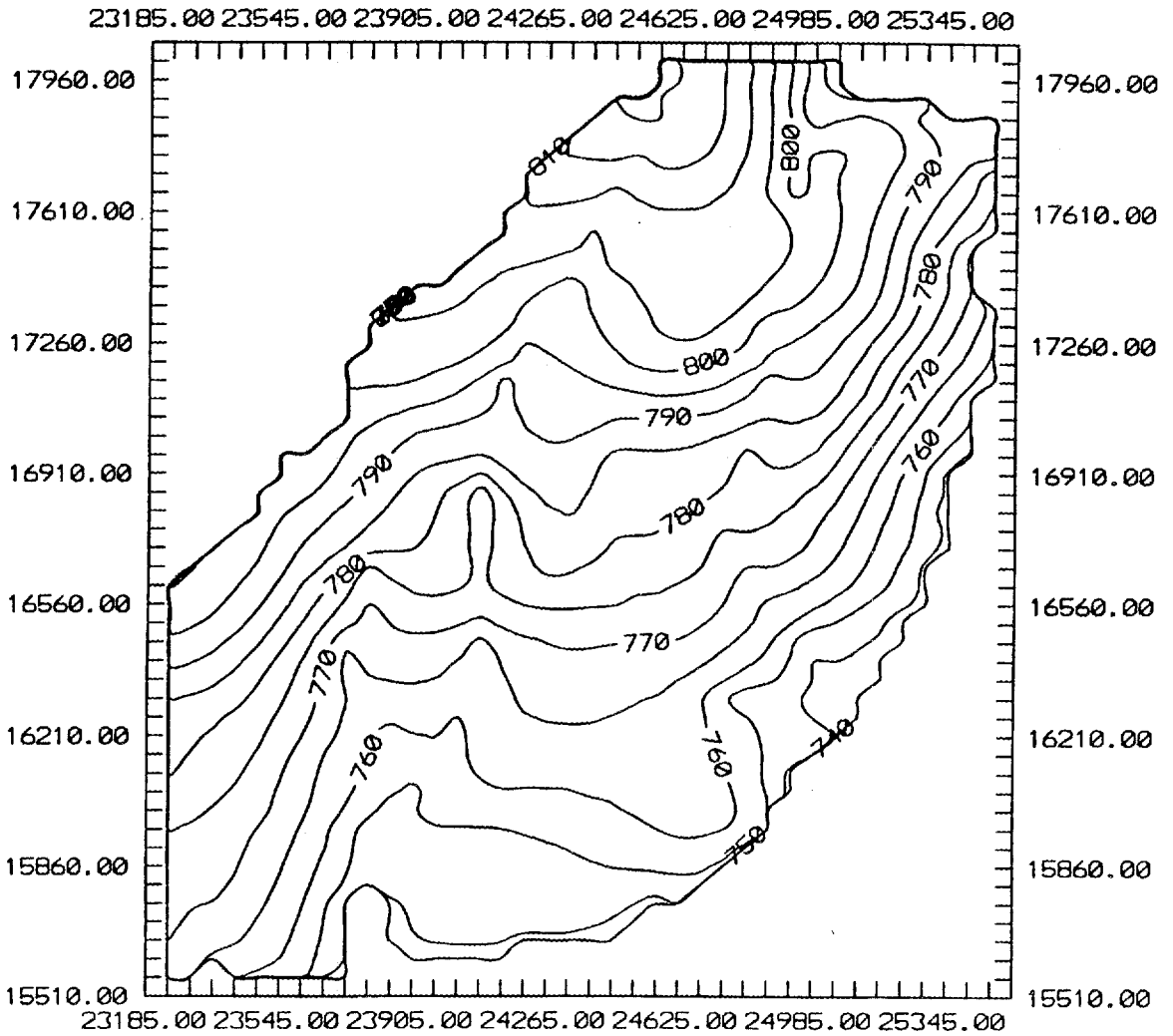

Fig. E.1. Calculated groundwater head elevations, t = 1.0 year, based on most probable input parameters.

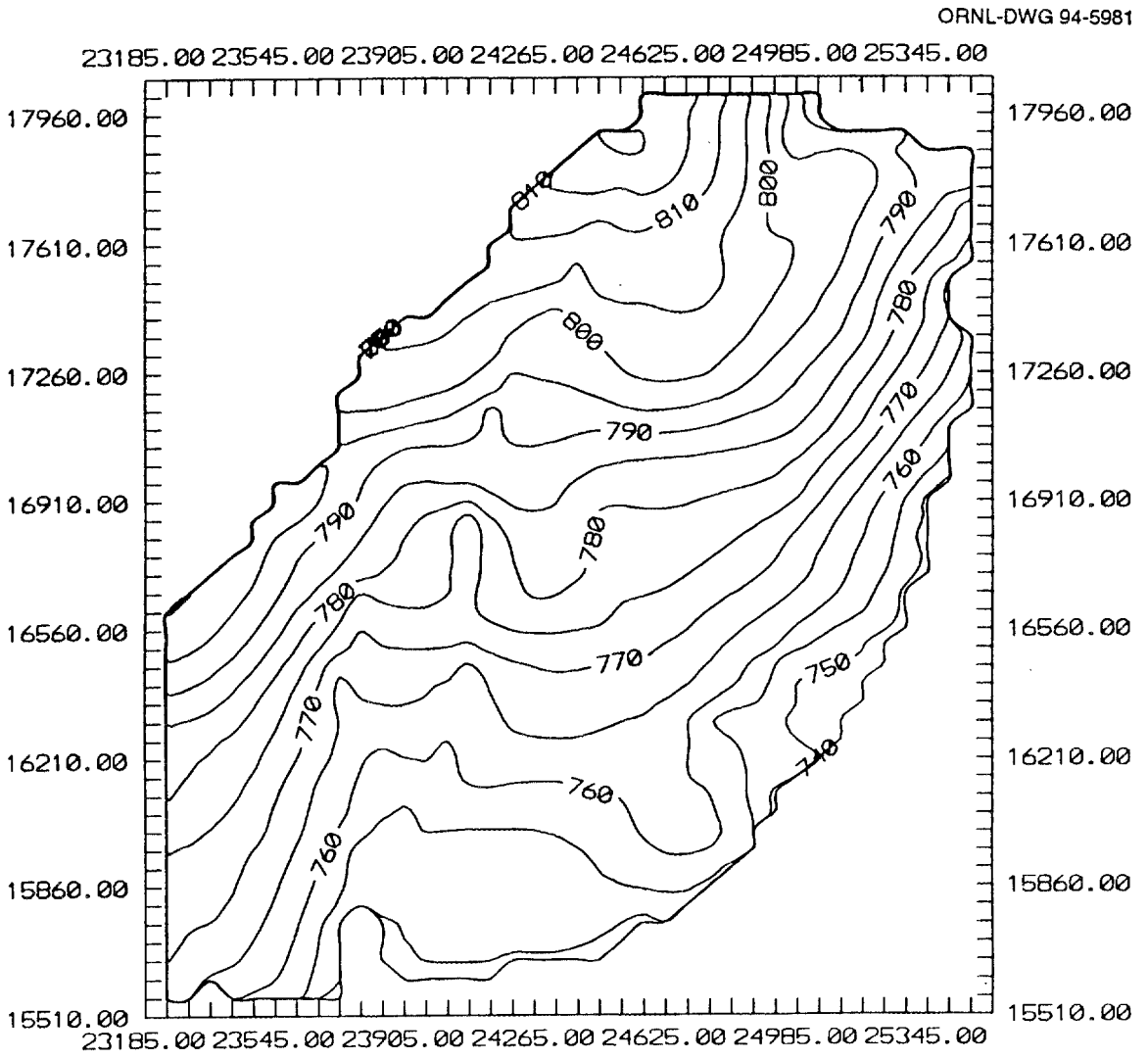

Fig. E.2. Calculated groundwater head elevations, t = 10.0 years, based on most probable input parameters.

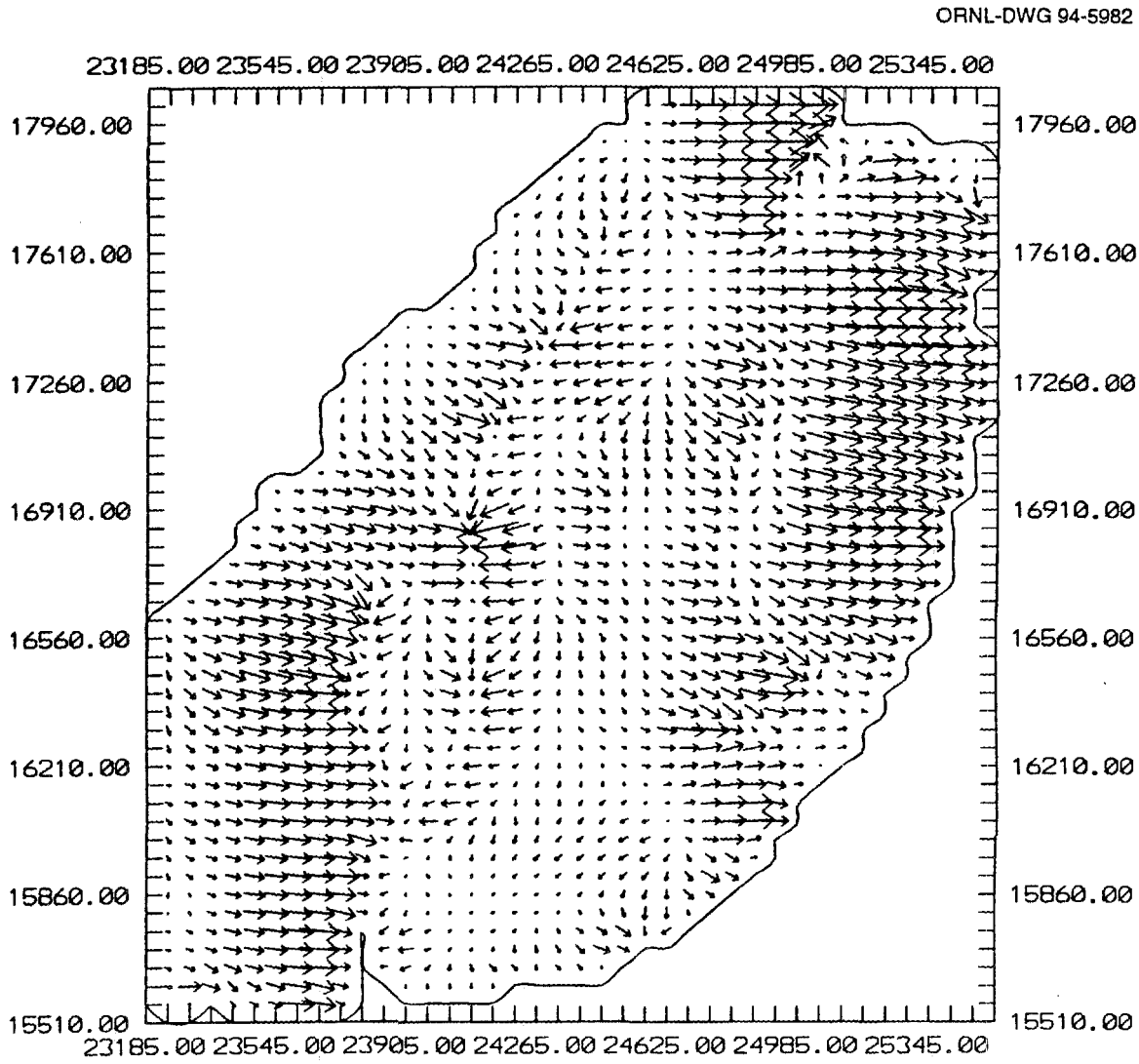

Fig. E.3. Calculated groundwater velocities, t = 1.0 year, based on most probable input parameters.

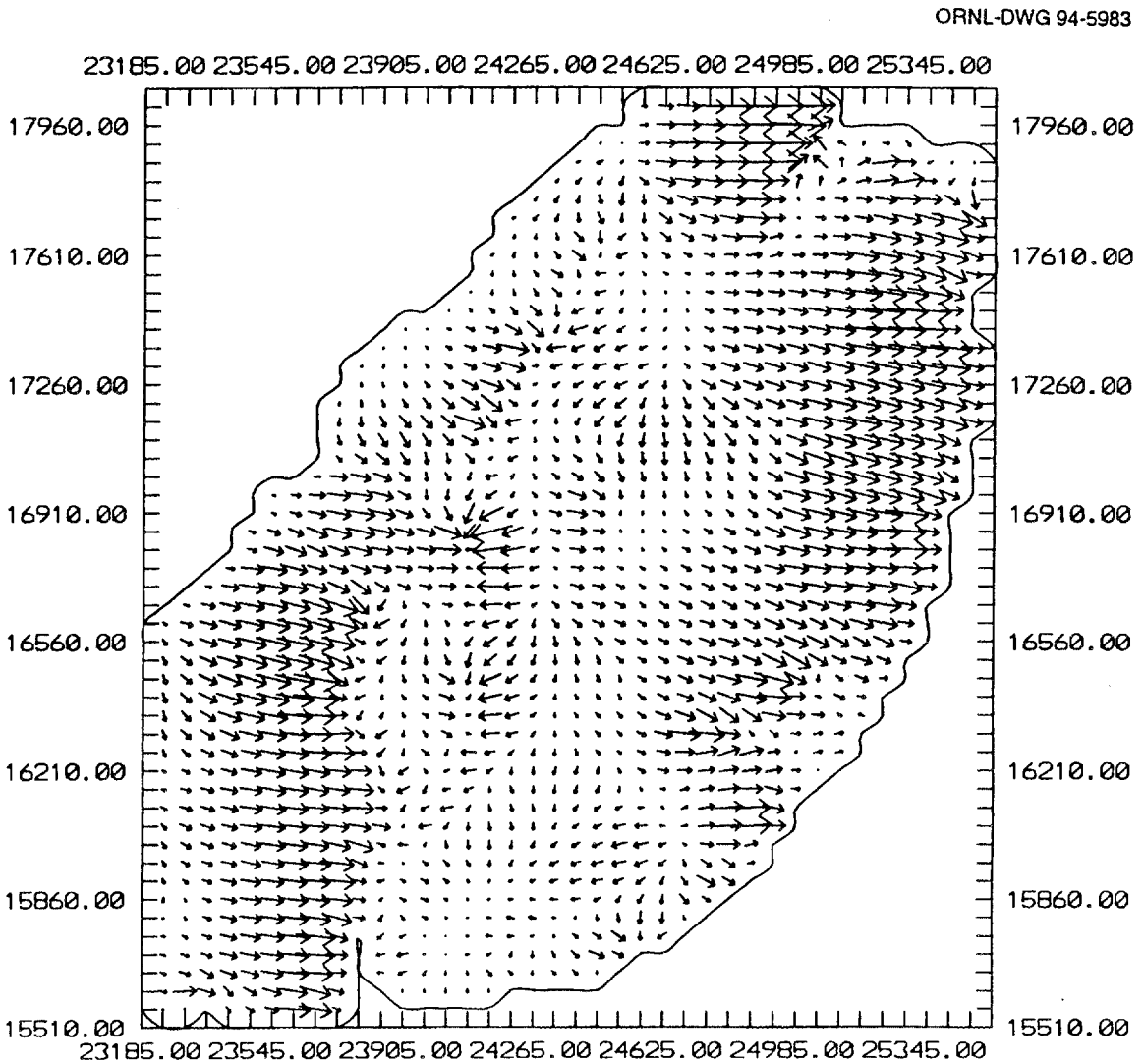

Fig. E.4. Calculated groundwater velocities, t = 10.0 years, based on most probable input parameters.

predictions (Sect. 4.2.1) From 1988 to 1996, three different classes—grassy, undisturbed, and forested surfaces; disturbed areas; and gravel areas—were assumed to be present. From 1997 to 2036 a fourth class was added to simulate the proposed CERCLA cap. In year 2037, it is assumed that the CERCLA caps will begin to deteriorate. This process is assumed to be a linear process over the next 10 years. After year 2047, all areas are modeled as mown grass with a leaking cap to year 2097 and undisturbed/forested for all years 2098 and beyond. Figure E.5 depicts the locations of the three original recharge classes and cap boundaries used in the MOC analysis. Recharge values corresponding to each of these class and time period combinations are listed in Table E.3.

E.4.2 Effects of Proposed CERCLA Remediation on Model Boundary Conditions

A number of physical features are addressed in the USGS MOC model through the used of specialized boundary conditions. These include water table divides (modeled using inactive or no-flow boundaries) and creeks and other surface water bodies (treated as constant head nodes by assigning large leakance values). Figure E.6 shows the locations at which specialized boundary conditions were initially applied. It is assumed that inclusion of CERCLA caps will cause most of the creek near the eastern edge of the model to run dry. Therefore, the constant head boundary conditions are removed during the time period in which the caps are in effect, 1997–2036 (Fig. E.7).

Table E.3. Diffuse recharge rates (mm/month) used in Solid Waste Storage Area 6 groundwater analysis

	Recharge class			
Time	Undisturbed/ forested	Disturbed	Gravel	Capped
1988–1996	14.5	10.7	15.2	NA
1997–2036	14.5	10.7	15.2	2.5
2037–2038	14.5	11.1	15.1	3.7
2038–2039	14.5	11.5	15.1	4.9
2039–2040	14.5	11.8	15.0	6.1
2040–2041	14.5	12.2	14.9	7.3
2041–2042	14.5	12.6	14.9	8.5
2042–2043	14.5	13.0	14.8	9.7
2043–2044	14.5	13.4	14.7	10.9
2044–2045	14.5	13.7	14.6	12.1
2045–2046	14.5	14.1	14.6	13.3
2046–2047	14.5	14.5	14.5	14.5
2047–	14.5	14.5	14.5	14.5

ORNL-DWG 94-5984

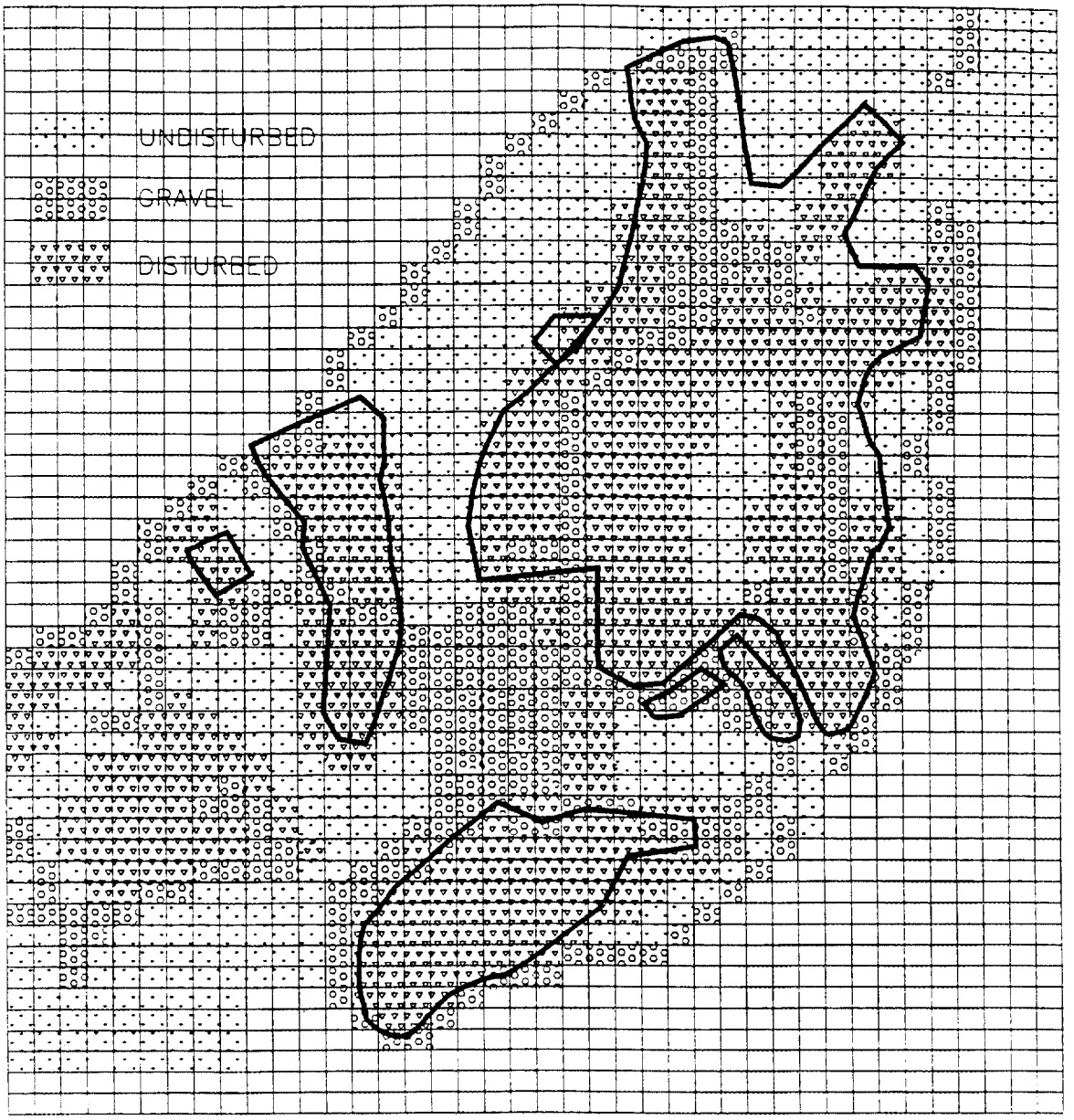

Fig. E.5. Locations of the three original recharge classes and cap boundaries used in the MOC analysis.

ORNL-DWG 94-5985

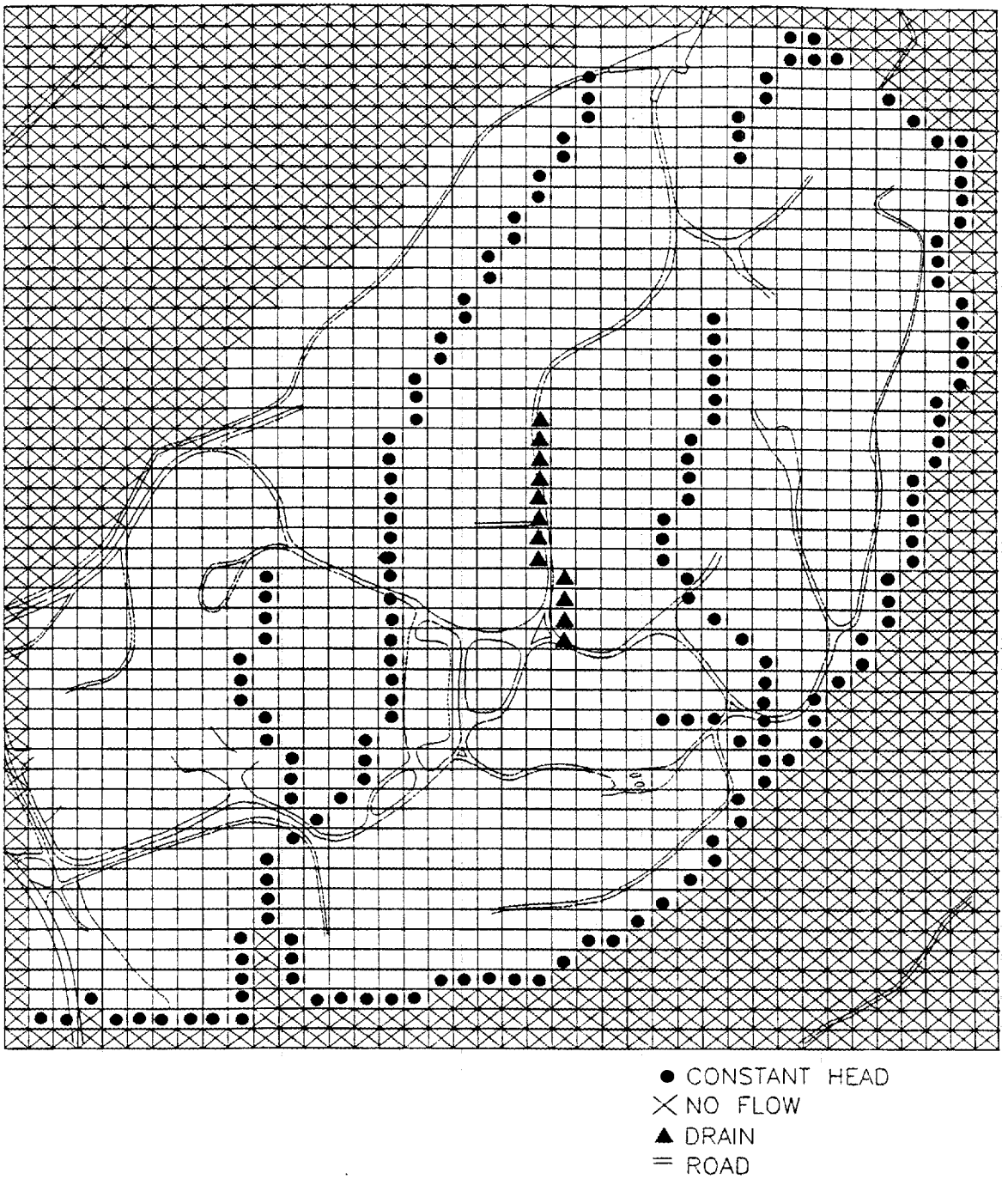

Fig. E.6. Initial locations for specialized boundary conditions.

ORNL-DWG 94-5986

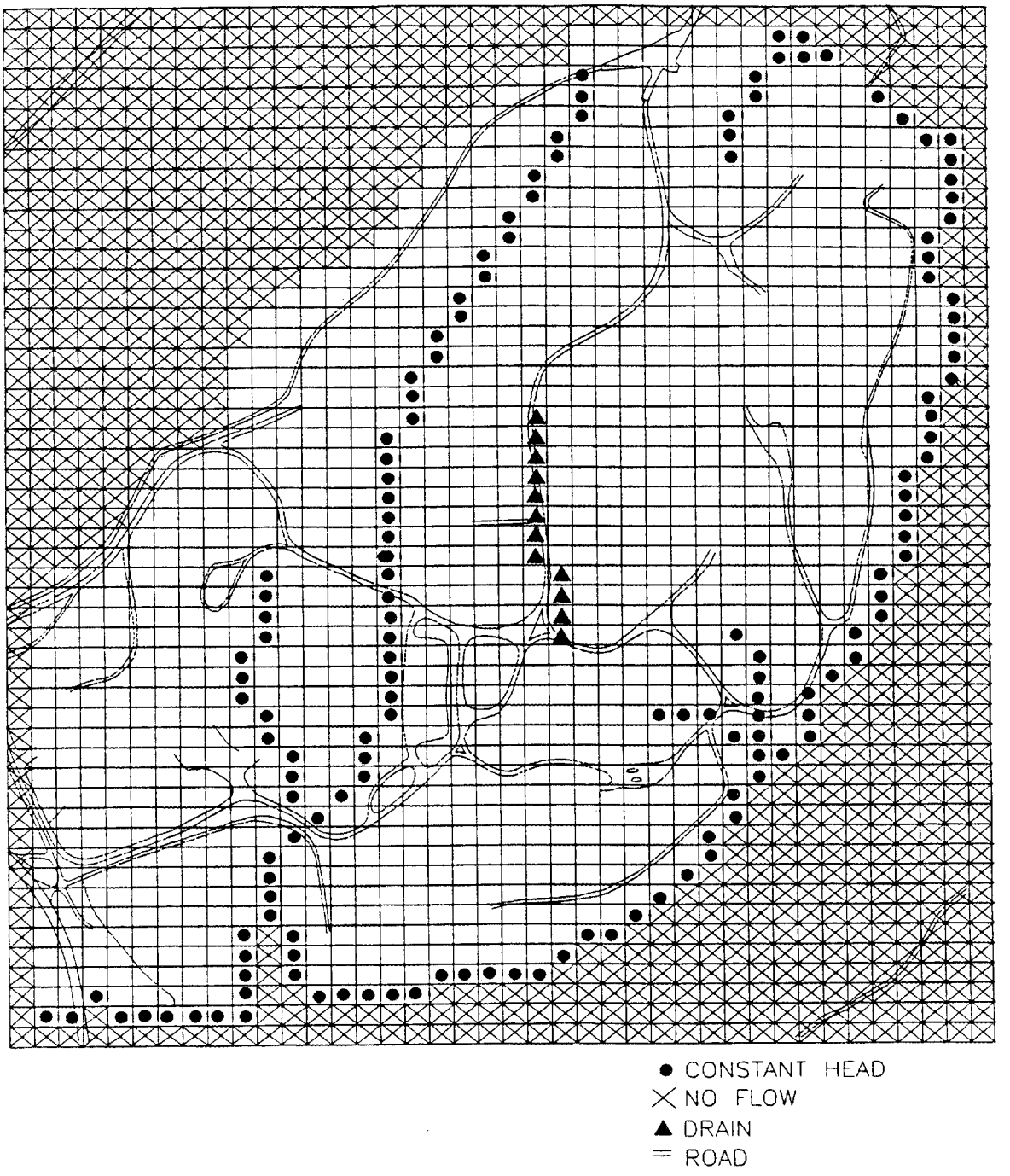

Fig. E.7. Locations for specialized boundary conditions for 1977–2036.

E.5 ANALYTICAL MODEL

As stated in Sect. 4.3, the use of the USGS MOC code was not feasible because of the extremely long simulation times required to model the transport of long-lived nuclides (^{232}Th and ^{238}U) through groundwater. Consequently, a simple, one-dimensional analytic model was developed to estimate transport of these nuclides. The one-dimensional forms of the equations for steady-state groundwater flow and contaminant transport used in the model are, respectively,

$$K\frac{d^2h}{dx^2} = 0 \tag{E.3}$$

and

$$D\frac{\partial^2 C}{\partial x^2} = V_r\frac{\partial C}{\partial x} + \frac{\partial C}{\partial t} + \lambda C \quad , \tag{E.4}$$

where

K	=	hydraulic conductivity (ft/s),
h	=	hydraulic head (ft),
x	=	distance (ft),
V	=	Darcy velocity (ft/s),
C	=	groundwater concentration (g/ft^3),
D	=	dispersion coefficient (ft^2/s),
V_r	=	retarded Darcy velocity (ft/s),
λ	=	decay constant (1/s),
t	=	time (s).

The solution to Eq. (E.3), used by the analytical model, gives

$$V = K\frac{dh}{dx} \quad . \tag{E.5}$$

The solution to Eq. (E.4) from a source of strength $C_o(t)$ is as follows:

$$C = \int_o^t C_o(t-\tau)\cdot\exp\frac{(V_rX)}{D}\cdot\frac{x}{2\sqrt{\pi D\tau^3}}\cdot\exp\left[\frac{-x^2}{4D\tau} - \left[(\lambda + \frac{V_r^2}{4D}\right]\tau\right]d\tau \quad , \tag{E.6}$$

with

$$V_r = \left[1 + \rho \frac{K_d}{\epsilon}\right]^{-1} \tag{E.7}$$

where

K_d	=	soil/water partitioning coefficient (ft^3/g),
ρ	=	soil density (g/ft^3),
ϵ	=	soil porosity.

The steps taken by the analytical code to determine contaminant concentration are as follows:

Step 1

Velocity values were calculated from Eq. (E.5) using head values at contaminant sources and compliance points, and distances based on the flow solutions generated by the USGS MOC code. Corresponding "retarded" velocities for use in Eq. (E.6) were then determined from Eq. (E.7).

Step 2

The source term function $C_o(t)$ in Eq. (E.6) was based on output from the TUMSIM and WELSIM codes (see Sect. 4.2.2). The TUMSIM and WELSIM runs generally covered simulation periods from 1000 years. In most cases, however, these simulations failed to show peak fluxes of the contaminants ^{232}Th and ^{238}U entering the groundwater. Furthermore, due to retardation effects [Eq. (E.7)], peak groundwater concentrations often occur at times much later than that of peak input. Since longer simulation periods were not practical with the TUMSIM and WELSIM codes, it was necessary to approximate the source term function for times greater than 1000 years and less than t_p, the time at which the disposal units' inventory was depleted. Assuming depletion due to radioactive decay and contaminant leaching, the following two cases were considered.

Case 1. For disposal units in which the TUMSIM/WELSIM leachate rates were constant or decreasing at $t = 1000$ years, a source of constant stength was assumed for $t > 1000$ years until the initial inventory was depleted. The remaining mass in a disposal unit was approximated by

$$M(t) = M_o \exp^{-\lambda(t - 1000)} - S_o - R(t-1000) \tag{E.8}$$

$$M'(t) = -\lambda M_o \exp^{-\lambda(t - 1000)} - R \quad . \tag{E.9}$$

Example plots of $M(t)$ and $M'(t)$ for a unit with decreasing leachate rate at $t = 1000$ years are given in Figs. E.8 and E.9.

Case 2. For disposal units in which the TUMSIM/WELSIM leachate rates were increasing at $t = 1000$ years, a linearly increasing source was assumed for $t > 1000$ years until the initial inventory was depleted. The approximations for the remaining mass in a disposal unit in this case were given by the following equations:

$$M(t) = M_o \exp^{-1000\lambda}\left[\exp^{-\lambda(t-1000)}\right] - \frac{b_1}{2}(t - 1000)^2 - R(t - 1000) - S_o + M_o \tag{E.10}$$

$$M'(t) = -\lambda M_o \exp^{-1000\lambda}\left[\exp^{-\lambda(t-1000)}\right] - b_1(t - 1000) - R \quad , \tag{E.11}$$

where

M	=	mass remaining at the disposal unit at time t (g),
M_o	=	initial mass in disposal unit (g),
S_o	=	mass removed by leaching from 0 to 1000 years (g),
R	=	leachate rate for $t > 1000$ years (g/year),
b_1	=	slope of leachate rate vs time for $t > 1000$ years (g/year^2).

Sample plots of $M(t)$ and $M'(t)$ for a unit with an increasing leachate rate at $t = 1000$ years are given in Figs. E.10 and E.11. The time at which the disposal unit's inventory was depleted, t_f, was estimated by applying Gaussian quadrature to Eqs. (E.8)-(E.11).

Step 3

Contaminant groundwater concentrations were calculated using the retarded velocities obtained from Step 1 and the modified source terms obtained from Step 2 as input to Eq. (E.6). The convolution interval from this equation was evaluated numerically using the trapezoidal rule. Concentrations were evaluated for a wide range of times, from which the peak groundwater concentration and associated time were obtained.

E.6 MODIFICATIONS TO THE USGS MOC (VERSION 3.0) CODE

The modeling of contaminant transport in groundwater for the SWSA 6 site was a complicated process involving long-term simulations with expansive multiple plumes as well as incorporation of site-specific details such as the effects of the proposed CERCLA caps on recharge rates and site geometry. Furthermore, the Latin hypercube (LHC) analysis (Sect. 4.6.1.4) required that multiple simulations be conducted for each radionuclide analyzed. Since the ability to perform these functions was beyond that of the USGS MOC Version 3.0 code, in-house modifications were necessary. The ORNL modifications are described in the following sections.

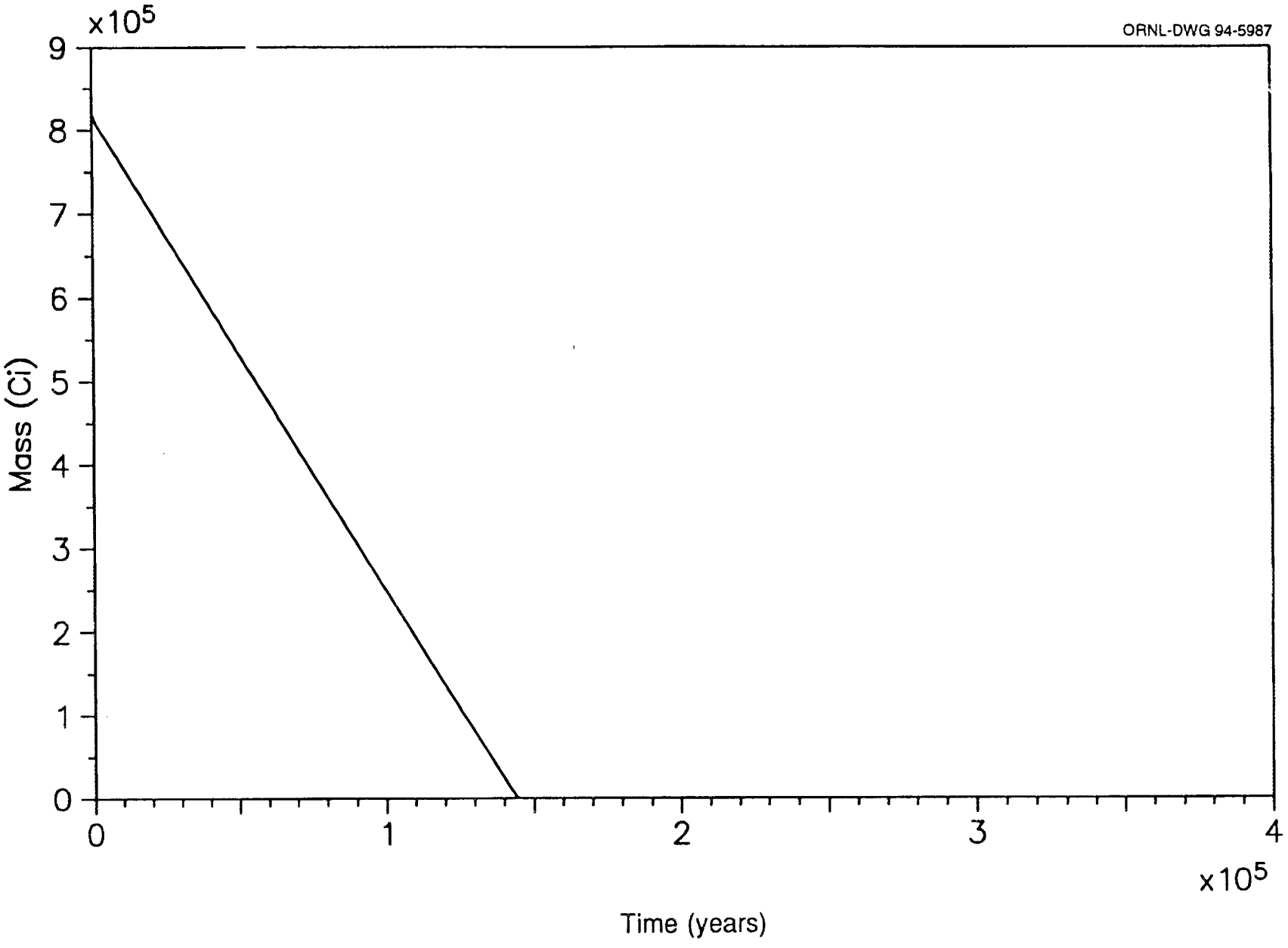

Fig. E.8. Mass of ^{238}U remaining in Interim Waste Management Facility vs time.

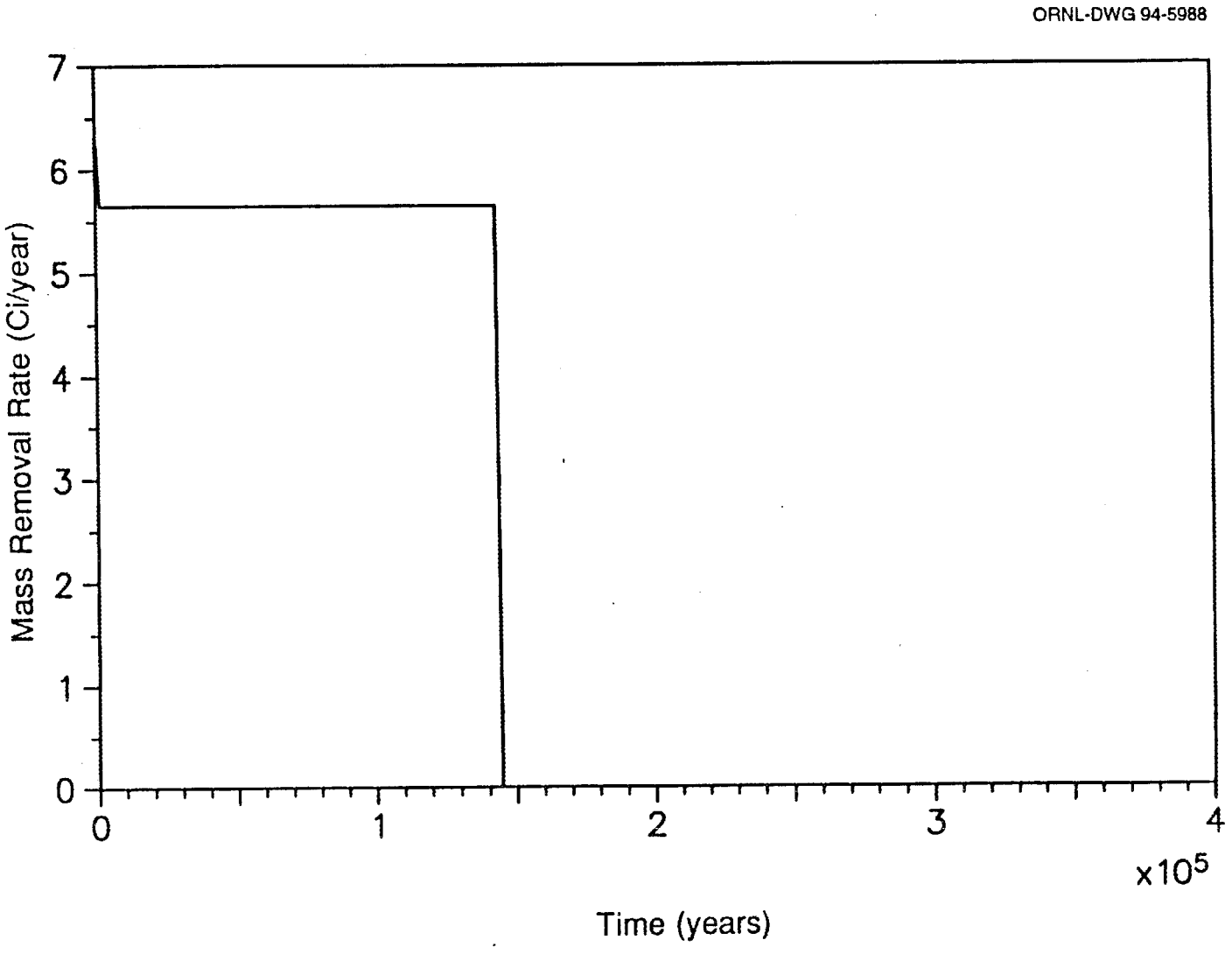

Fig. E.9. Mass removal rate of ^{238}U vs time at Interim Waste Management Facility.

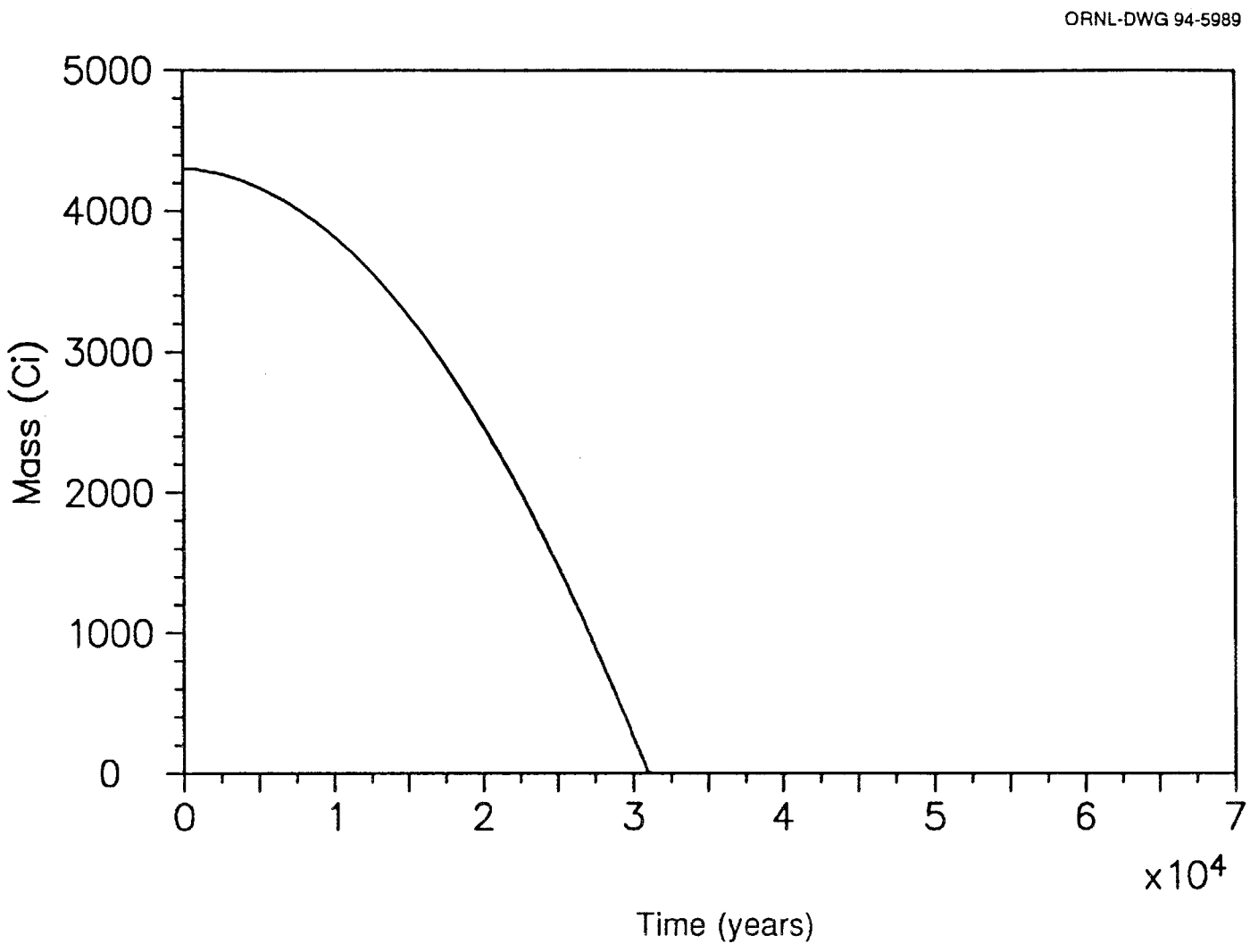

Fig. E.10. Mass of ^{238}U remaining in fissile wells vs time.

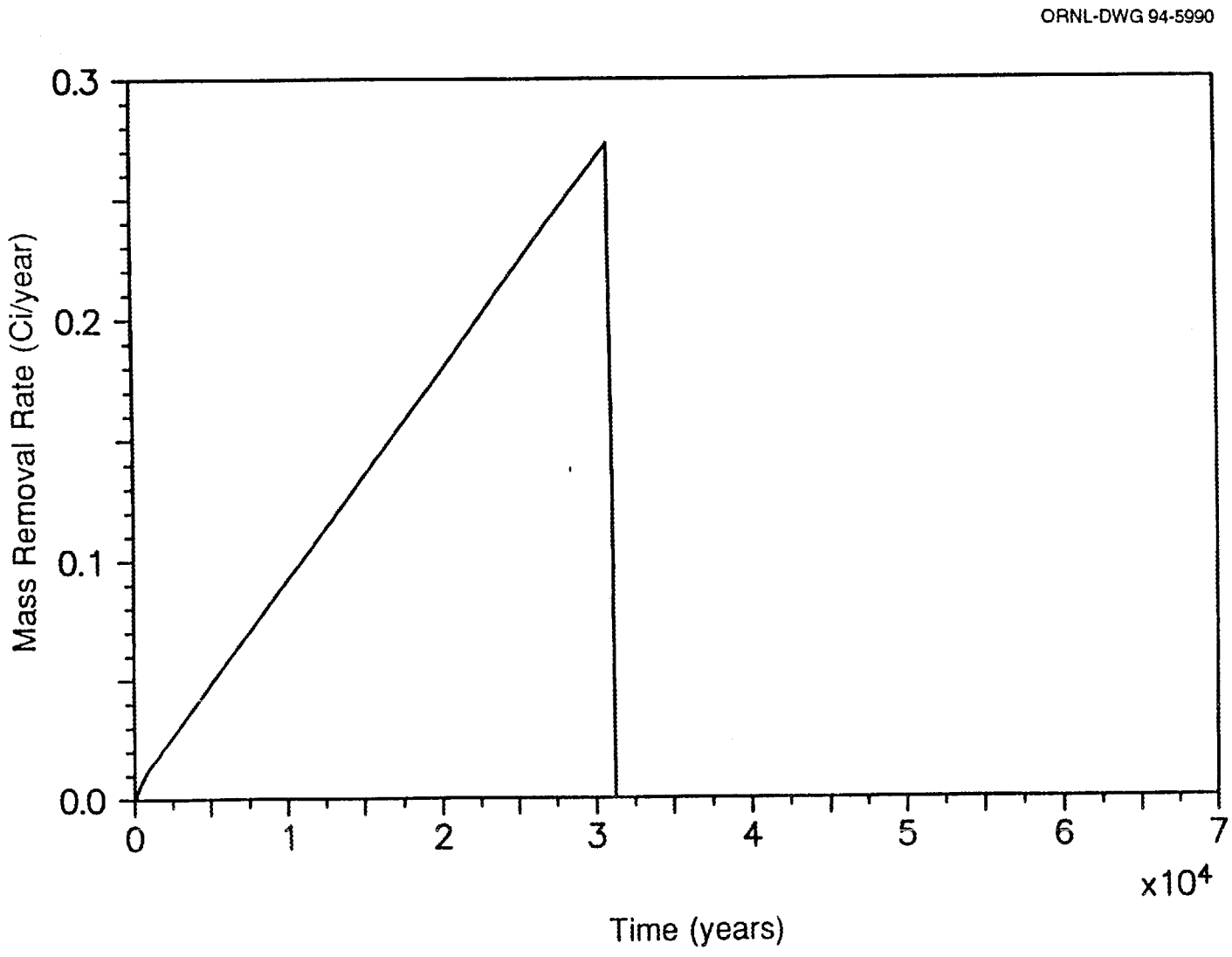

Fig. E.11. Mass removal rate of ^{238}U vs time at fissile wells.

E.6.1 Description of Code Modifications

The chief modifications made at ORNL to the USGS MOC 3.0 computer code can be summarized as follows:

1. Many of the array dimensions found in the original code were increased. This was done primarily to allow larger model grids (the grid size of the original MOC code was only 40 × 40) and more observation nodes (used for computing concentrations and fluxes at compliance points).
2. All floating-point and integer model inputs were converted to free format.
3. In order to simulate the effects of the proposed CERCLA caps, the ability to specify time-dependent locations for specialized model nodes and recharge values was added.
4. The LHC analyses described in Sect. 4.4 required modifications to enable runs using multiple parameter sets as input. Additional modifications were made for storing and summarizing the LHC results.
5. In addition to the original MOC input file, incorporation of items 3 and 4 above required the creation the following four additional input files:

   (a) a base recharge file, used to input time-dependent recharge values at model nodes;
   (b) a node ID input file, used to specify time-dependent locations of specialized model nodes such as no-flow boundaries, constant head locations, or contaminant sources;
   (c) source injection files, associated with each modeled disposal unit and containing time-dependent source strength values; and
   (d) the LHC parameter file, containing information required for performing LHC analyses, such as multiple sets of input parameters and associated control variables.

All of the above modifications were written in FORTRAN. The ORNL version of MOC USGS MOC/ORNL code was compiled and run on an HP 9000, series 730 workstation.

E.6.2 Code Verification

A number of checks were made to verify that the code modifications described in the previous section were performing as expected. The most significant of these are described briefly as follows.

First, to determine whether the code's treatment of time-dependent recharge values and special node locations was acceptable, calculated head surfaces and corresponding velocity fields for the "before" and "after" CERCLA cap scenarios were plotted. In the "after" cap scenario, head surfaces beneath the cap were expected to drop because of reduced recharge, and the creek located near the eastern edge of the model was assumed to run dry. Figures E.1 and E.2 show that the modeled results are consistant with these assumptions. Furthermore, velocity vectors in the area near the eastern creek (Figs. E.3 and E.4) also differ between the two scenarios.

The modifications made to enable MOC to perform LHC analyses were verified from deterministic model runs made using representative sets of input parameters from the LHC analysis. In all cases, results from the deterministic analysis matched those from the corresponding LHC sample.

E.6.3 Input Data Requirements for ORNL/USGS MOC Code

Detailed descriptions of the input information required by the modified MOC code are given in the following section. These descriptions identify the locations where additional records are needed relative to records found in the original USGS MOC main input file. For the purpose of reference, a listing of the input information required by the unmodified USGS MOC code is included as an attachment to this appendix.

Input Files Required:

Main Input File:	xxxx.in
LHC Parameter Input File:	xxxx.prm
Base Recharge Input File:	xxxx.rch
Node ID Input File:	xxxx.nod
Site Injection Files:	sitename.inj

Input File Requirements:

Main Input File: xxxx.in

Unless otherwise noted, all input cards for the main input files have been converted to free format. The following section lists the other modifications that have been made to the main input file.

Card	Parameters	
1.1	MX	First X node of transport subgrid.
	MY	First Y node of transport subgrid.
	MMX	Ending X node of transport subgrid.

	MMY	Ending Y node of transport subgrid.
1.2	XORIG	X coordinate corresponding to the lower left model node.
	YORIG	Y coordinate corresponding to the lower left model node.
2	The following parameters have been added to card 2:	
	IREACT	The reaction type specifier.
	NPNTPMP	Output scaling factor. If the current pumping period is a divisible by NPNTPMP, output for the pumping period is generated.
3	TINIT	TINIT is now read in months.
3.1	See Attachment.	
Data Set		Parameters
2	ICONCLASS	ICONCLASS inserted between REC and CNRECH. If ICONCLASS is other than 0, injection node concentrations are read from the corresponding site's ".inj" file (see description for the ".prm" file). If ICONCLASS = 0, injection node concentrations are set = CNRECH.
3.a.1	INPUT	If INPUT = 0, all blocks are set active. If INPUT = 1, the temporary array, VPRM, is read.

3.b	NY records of NX columns are read if the value for INPUT from 3.a above = 1.	
	VPRM	The temporary array, VPRM, used to indicate active and inactive blocks is read.
Data Set		Parameters
5	INPUT	If INPUT = 0, set all values in the base recharge array, BASERECH, = 1.0. If INPUT = 1, read values for the base recharge array from the ".rch" file.
	FCTR	Values for each element in the recharge array, RECH(i,j), are set equal to FCTR*BASERECH(i,j).
6	Data set 6 is no longer read.	
7	Data set 7 is now read from the ".nod" input file.	
10.b	Added the following parameters:	
	ITEMP 0: No changes to base recharge array, RECH, for the pumping period. 1: Read new base recharge array from the ".rch" file. Set RECH(i,j) = BASERECH(i,j)*FCTR. 2: Set RECH(i,j) = current value in BASERECH(i,j)*FCTR. 3: Set BASERECH(i,j) = 1.0. Set RECH(i,j) = BASERECH(i,j)*FCTR.	
	FCTR	New base recharge array factor.
	INEWNODE	Flag indicating whether new node ID information should be read for the current pumping period. If = 1, read new node ID information.

10.c	Added the following parameter:
ICONCLASS	If ICONCLASS is other than 0, injection node concentrations are read from the corresponding site's ".inj" file (see description for the ".prm" file). If ICONCLASS = 0, injection node concentrations are set = CNRECH.

LHC Parameter Input File: *xxxx.prm*

Unless otherwise noted, all input cards are free format.

Card		Parameters
1	NSAMPLES	The number of LHC iterations to perform. Set = 0 for deterministic case only.
2	NSIMYEARS	The number of simulation years run for each site's ".inj" file. This parameter should equal NPMP.
3	NSENSOUT	Number of intermediate iterations for which output is generated.
4	ISENSOUT(i)	For i = 1, NSENSOUT: intermediate iteration values for which standard MOC output files (.ddn, .hed, .sol, etc.) are written.
5	SENSFCTR(i)	For i = 1, 4: coefficients used to convert values for the LHC input parameters to units of ft/sec (conductivity), mL/g (K_d), percentage (porosity), and g/mL (density).

6	NRECHSITES	The number of locations for which concentration vs time ".inj" files are to be read.
7	NRECHSAMPLES(i)	For i = 1, NRECHSITES: The number of previous LHC samples used to generate each site's (".inj") concentration input file.
8	NRECHSITES records are read.	
	SITE(i)	For i = 1, NRECHSITES: The alphanumeric name corresponding to the prefix of the LHC concentration input file (".inj") for each site.
9	Parameter values for the current LHC iteration, a total of i = 1, NSAMPLES records are read.	
	SENSCOND(i)	Mean (deterministic) conductivity value.
	SENSDK(i)	Mean (deterministic) K_d value.
	SENSPOROS(i)	Mean (deterministic) porosity value.
	SENSRHOB(i)	Mean (deterministic) soil density value.

Card Set	Parameters
FCTR(i,j)	For j = 1, NRECHSITES, FCTR(i,j) is a value between 0 and 1 used by the code to determine which ".inj" file to use for the current LHC sample set. Concentrations at recharge nodes and injection wells are read from the ".inj" file for each pumping period. The code uses FCTR(i,j) and the value of NRECHSAMPLES(j) to calculate an integer value that determines which previous LHC concentration set to use for the current LHC simulation step.

LHC Base Recharge Input File: xxxx.rch

This file contains NP base recharge arrays.

Unless otherwise noted, all input cards are free format.

Card Set	Parameters	
1	TITLE	Alphanumeric identifier for the current base recharge array.
2	NY records are read	
	BASERECH(i,j)	For i = 1,NX, new values for the base recharge array, BASERECH(i,j), are read.

Card sets 1 and 2 are repeated for each pumping period in which a new base recharge array is required. (See data sets 5 and 10b from the previous section describing the revised ".in" file.)

Node Input File: xxxx.nod

This file contains NP base recharge arrays.

Unless otherwise noted, all input cards are free format.

Card Set	Parameters	
1	INPUT	If 0: All values in the node identification matrix are set equal to FCTR. Card set 2 is not read for the current pumping period. If 1: Values for the node identification matrix are read for the current pumping period and multiplied by the value of FCTR.

	FCTR	If INPUT = 1, values for the node identification matrix are multiplied by FCTR.
2	For j = 1, NY records are read if INPUT from card set 1 above = 1.	
	NODE(i,j)	For i = 1, NX, values for the node identification matrix, NODE(i,j) are read.
3	NCODES	The number of node identification codes to be specified for the current pumping period. (ICODE is not read for the initial pumping period.)
4	NCODES records are read	
	ICODE	For node IDs equal to ICODE, leakance is set equal to FCTR1.
	FCTR1	Leakance value at nodes whose IDs correspond to ICODE above.
	ICODESITE	If ICODESITE > 0, recharge concentration, CNRECH, at nodes whose IDs correspond to ICODE are set equal to the concentration read from the corresponding ".inj" file for the current pumping period.
	FCTR2	If ICODESITE = 0, recharge concentration, CNRECH(i,j), at nodes whose IDs correspond to ICODE are set equal to FCTR2.

Card sets 1–4 are repeated for each pumping period in which a new node ID matrix is needed (as determined by the value of INEWNODE in data set 10b of the model ".in" file.

Site Injection Files: sitename.inj

These files contain time-dependent values of mass flux for each modeled disposal site. For consistency, the time period on which these fluxes are based should match the value for pumping period, PINT.

Card	Parameters	
1	SENSCONC	Mass flux of pollutant from the disposal site (mass/time) for the current pumping period.

Card 1 is repeated for each pumping period.

E.7 REFERENCES

Bear, J. 1979. *Hydraulics of Groundwater*, McGraw-Hill, New York.

EBASCO (EBASCO Services Inc.) 1992. *OR-ERWM Program Design Critieria Studies: Results of 3DFEMWATER Modeling*, ER W6.01-002, Rev. 0, Environmental Consulting Engineers, Inc., Knoxville, Tenn., November 23.

Surfer 1990. Golden Software, Inc., Golden, Colo.

USGS MOC 1990. Computer code, with instructions in L. F. Knoikow and J. D. Bredehoeft, "Computer Model of Two-Dimensional Solute Transport and Dispersion in Ground Water," chap. C2, Book 7 of *Geological Survey Techniques of Water-Resources Investigations of the United States Geological Survey,* U.S. Department of the Interior, Washington, D.C., 1978.

Attachment III
Data Input Formats

Card	Column	Format	Variable	Definition
1	1–80	10A8	TITLE	Description of problem
2	1– 4	I4	NTIM	Maximum number of time steps in a pumping period (limit=100)*.
	5– 8	I4	NPMP	Number of pumping periods. Note that if NPMP>1, then data set 10 must be completed.
	9–12	I4	NX	Number of nodes in x direction (limit=20)*.
	13–16	I4	NY	Number of nodes in y direction (limit=20)*.
	17–20	I4	NPMAX	Maximum number of particles (limit=2000)*. (See eq 71.)
	21–24	I4	NPNT	Time-step interval for printing hydraulic and chemical output data.
	25–28	I4	NITP	Number of iteration parameters (usually 4≤NITP≤7).
	29–32	I4	NUMOBS	Number of observation points to be specified in a following data set (limit=5)*.
	33–36	I4	ITMAX	Maximum allowable number of iterations in ADIP (usually 100 ≤ITMAX≤200).
	37–40	I4	NREC	Number of pumping or injection wells to be specified in a following data set.
	41–44	I4	NPTPND	Initial number of particles per node (options=4, 5, 8, 9).
	45–48	I4	NCODES	Number of node identification codes to be specified in a following data set (limit=10)*.
	49–52	I4	NPNTMV	Particle movement interval (IMOV) for printing chemical output data. (Specify 0 to print only at end of time steps.)
	53–56	I4	NPNTVL	Option for printing computed velocities (0=do not print; 1=print for first time step; 2=print for all time steps).
	57–60	I4	NPNTD	Option for printing computed dispersion equation coefficients (option definition same as for NPNTVL).
	61–64	I4	NPDELC	Option for printing computed changes in concentration (0=do not print; 1=print).
	65–68	I4	NPNCHV	Option to punch velocity data (option definition same as for NPNTVL). When specified, program will punch on unit 7 the velocities at nodes.

*See footnotes at end of table.

Data input formats—Continued

Card	Columns	Format	Variable	Definition
3	1–5	G5.0	PINT	Pumping period in years.
	6–10	G5.0	TOL	Convergence criteria in ADIP (usually TOL=0.01).
	11–15	G5.0	POROS	Effective porosity.
	16–20	G5.0	BETA	Characteristic length, in feet (=longitudinal dispersivity).
	21–25	G5.0	S	Storage coefficient (set $S=0$ for steady flow problems).
	26–30	G5.0	TIMX	Time increment multiplier for transient flow problems. TIMX is disregarded if $S=0$.
	31–35	G5.0	TINIT	Size of initial time step in seconds. TINIT is disregarded if $S=0$.
	36–40	G5.0	XDEL	Width of finite-difference cell in x direction, in feet.
	41–45	G5.0	YDEL	Width in finite-difference cell in y direction, in feet.
	46–50	G5.0	DLTRAT	Ratio of transverse to longitudinal dispersivity.
	51–55	G5.0	CELDIS	Maximum cell distance per particle move (value between 0 and 1.0).
	56–60	G5.0	ANFCTR	Ratio of T_{xx} to T_{yy}.

Data set	Number of cards	Format	Variable	Definition
1	Value of NUMOBS (limit=5)*	2I2	IXOBS, IYOBS	x and y coordinates of observation points. This data set is eliminated if NUMOBS is specified as =0.
2	Value of NREC	2I2, 2G8.2	IX, IY, REC, CNRECH.	x and y coordinates of pumping (+) or injection (−) wells, rate in ft^3/s, and if an injection well, the concentration of injected water. This data set is eliminated if NREC=0.
3	a. 1			Parameter card[1] for transmissivity.
	b. Value of NY (limit=20)*	20G4.1	VPRM	Array for temporary storage of transmissivity data, in ft^2/s. For an anisotropic aquifer, read in values of T_{xx} and the program will adjust for anisotropy by multiplying T_{xx} by ANFCTR.
4	a. 1	I1, G10.0	INPUT, FCTR	Parameter card[1] for THCK.
	b. Value of NY (limit=20)*	20G3.0	THCK	Saturated thickness of aquifer, in feet.

* See footnotes at end of table.

ADDITIONAL INPUT FORMATS FOR DECAY, SORPTION, AND ION-EXCHANGE REACTIONS

Card 3.1 is inserted after card 3 if IREACT is not 0 or blank:

IREACT	Reaction	Parameters on card 3.1 in free format
-1	decay only	THALF
0	no reaction	do not insert card 3.1
1	linear sorption	DK, RHOB, THALF
2	Freundlich sorption	RHOB, EKF, XNF, THALF
3	Langmuir sorption	RHOB, EKL, CEC, THALF
4	monovalent exchange	RHOB, EK, CEC, CTOT, THALF
5	divanlent exchange	RHOB, EK, CEC, CTOT, THALF
6	mono-divalent exchange	RHOB, EK, CEC, CTOT, THALF
7	di-monovalent exchange	RHOB, EK, CEC, CTOT, THALF

Parameter	Definition
THALF	$t_{1/2}$ - Decay half-life, in seconds, T (if no decay, specify THALF=0.0)
RHOB	ρ_b - aquifer bulk density, mass of solid per unit volume of aquifer, ML^{-3}
DK	K_d - linear sorption distribution coefficient, L^3M^{-1}
EKF	K_f - Freundlich sorption coefficient, units depend on XNF
XNF	n - Freundlich sorption exponent, dimensionless
EKL	K_ℓ - Langmuir sorption coefficient, L^3M^{-1}
CEC	Q - Maximum sorption capacity or ion-exchange capacity, MM^{-1}
EK	K_m - Ion-exchange selectivity coefficient, dimensionless
CTOT	C_0 - Total solution concentration of two exchanging ions, equivalents/L^3

Data input formats—Continued

Data set	Number of cards	Format	Variable	Definition
8	a. 1	I1, G10.0	INPUT, FCTR	Parameter card† for WT.
	b. Value of NY (limit=20)*	20G4.0	WT	Initial water-table or potentiometric elevation, or constant head in stream or source bed, in feet.
9	a. 1	I1, G10.0	INPUT, FCTR	Parameter card† for CONC.
	b. Value of NY (limit=20)*	20G4.0	CONC	Initial concentration in aquifer.
10				This data set allows time step parameters, print options, and pumpage data to be revised for each pumping period of the simulation. Data set 10 is only used if NPMP >1. The sequence of cards in data set 10 must be repeated (NPMP −1) times (that is, data set 10 is required for each pumping period after the first).
	a. 1	I1	ICHK	Parameter to check whether any revisions are desired. Set ICHK=1 if data are to be revised, and then complete data set 10b and c. Set ICHK=0 if data are not to be revised for the next pumping period, and skip rest of data set 10.
	b. 1	10I4,3G5.0	NTIM, NPNT, NITP, ITMAX, NREC, NPNTMV, NPNTVL, NPNTD, NPDELC, NPNCHV, PINT, TIMX, TINIT	Thirteen parameters to be revised for next pumping period; the parameters were previously defined in the description of data cards 2 and 3. Only include this card if ICHK=1 in previous part a.
	c. Value of NREC	2I2, 2G8.2	IX, IY, REC, CNRECH	Revision of previously defined data set 2. Include part c only if ICHK=1 in previous part a and if NREC>0 in previous part b.

* These limits can be modified if necessary by changing the corresponding array dimensions in the COMMON statements of the program.

† The parameter card must be the first card of the indicated data set. It is used to specify whether the parameter is constant and uniform, and can be defined by one value, or whether it varies in space and must be defined at each node. If INPUT=0, the data set has a constant value, which is defined by FCTR. If INPUT=1, the data set is read from cards as described by part b. Then FCTR is a multiplication factor for the values read in the data set.

Table E.4. Groundwater concentration of nuclide: ^{3}H at observation nodes

Obs Node	Conc (uCi/L)	Time (Year)	Obs Node	Conc (uCi/L)	Time (Year)	Obs Node	Conc (uCi/L)	Time (Year)
1	7.8E-15	87.0	2	.0E+00	1000.0	3	3.1E-14	90.0
4	.0E+00	1000.0	5	.0E+00	1000.0	6	2.3E-16	81.0
7	9.6E-14	78.0	8	8.3E-14	62.0	9	2.5E-13	72.0
10	7.5E-14	88.0	11	2.8E-12	51.0	12	9.4E-13	75.0
13	7.6E-14	84.0	14	1.2E-11	43.0	15	1.6E-12	75.0
16	1.8E-13	66.0	17	1.0E-13	78.0	18	3.2E-10	43.0
19	1.8E-10	66.0	20	3.6E-12	77.0	21	3.0E-10	64.0
22	1.5E-06	64.0	23	8.2E-11	61.0	24	6.8E-09	57.0
25	6.2E-09	81.0	26	2.5E-08	75.0	27	1.5E-07	70.0
28	1.4E-06	77.0	29	4.5E-05	61.0	30	2.0E-06	75.0
31	2.4E-04	58.0	32	7.9E-05	58.0	33	2.3E-04	58.0
34	4.3E-04	60.0	35	1.1E-04	60.0	36	6.8E-04	61.0
37	4.1E-05	39.0	38	6.2E-05	63.0	39	3.2E-05	65.0
40	3.7E-05	47.0	41	3.9E-05	58.0	42	9.8E-05	64.0
43	1.9E-05	45.0	44	6.7E-06	61.0	45	2.5E-05	68.0
46	9.4E-06	70.0	47	3.7E-06	61.0	48	2.8E-05	17.0
49	8.5E-06	70.0	50	4.8E-07	62.0	51	1.9E-05	70.0
52	3.2E-06	60.0	53	2.6E-07	63.0	54	7.0E-07	75.0
55	7.8E-06	57.0	56	1.0E-07	65.0	57	7.4E-07	75.0
58	3.3E-06	58.0	59	3.0E-08	64.0	60	2.8E-07	76.0
61	1.0E-06	60.0	62	1.9E-07	15.0	63	9.0E-08	78.0
64	2.8E-08	67.0	65	4.4E-05	10.0	66	4.0E-08	56.0
67	1.4E-08	70.0	68	3.9E-05	25.0	69	6.5E-10	62.0
70	1.8E-08	68.0	71	3.3E-05	33.0	72	5.0E-11	37.0

Table E.4 (continued)

Obs Node	Conc (uCi/L)	Time (Year)	Obs Node	Conc (uCi/L)	Time (Year)	Obs Node	Conc (uCi/L)	Time (Year)
73	5.0E-09	72.0	74	1.7E-05	30.0	75	5.7E-14	18.0
76	5.4E-10	33.0	77	8.4E-10	74.0	78	9.4E-06	27.0
79	4.5E-12	29.0	80	5.4E-09	38.0	81	2.5E-10	75.0
82	5.7E-08	29.0	83	3.8E-10	24.0	84	1.8E-06	25.0
85	2.2E-09	8.0	86	2.2E-08	31.0	87	8.5E-09	33.0
88	1.1E-04	25.0	89	5.1E-09	25.0	90	4.0E-09	37.0
91	4.4E-06	29.0	92	1.2E-02	21.0	93	4.7E-07	13.0
94	9.3E-11	41.0	95	1.1E-03	24.0	96	3.6E-02	24.0
97	1.1E-05	18.0	98	3.6E-08	33.0	99	4.1E-01	23.0
100	9.9E-02	23.0	101	2.6E-06	17.0	102	3.8E-07	25.0
103	3.5E-01	28.0	104	6.1E-02	25.0	105	2.7E-07	9.0
106	6.1E-06	14.0	107	1.2E-05	14.0	108	7.2E-07	21.0
109	1.6E-09	57.0	110	2.1E-01	29.0	111	1.7E-03	33.0
112	8.0E-08	30.0	113	1.7E-08	31.0	114	6.5E-12	71.0
115	3.5E-02	36.0	116	3.6E-03	33.0	117	1.3E-08	71.0
118	1.0E-13	94.0	119	3.5E-02	36.0	120	1.8E-05	34.0
121	3.0E-08	57.0	122	2.6E-02	36.0	123	4.5E-06	35.0
124	1.9E-08	54.0	125	1.4E-03	45.0	126	2.2E-08	72.0
127	4.0E-03	44.0	128	5.2E-10	70.0	129	3.3E-03	43.0
130	1.2E-10	44.0	131	1.0E-03	45.0	132	1.9E-10	71.0
133	4.0E-05	47.0	134	4.4E-11	78.0	135	2.9E-06	45.0
136	3.5E-11	45.0	137	6.4E-08	34.0	138	1.0E-08	47.0
139	4.9E-08	73.0	140	3.2E-09	71.0	141	5.6E-09	87.0
142	6.4E-11	94.0	143	6.1E-09	78.0	144	4.4E-11	65.0
145	4.6E-12	65.0	146	1.9E-10	84.0	147	5.0E-09	84.0

Table E.4 (continued)

Obs Node	Conc (uCi/L)	Time (Year)	Obs Node	Conc (uCi/L)	Time (Year)	Obs Node	Conc (uCi/L)	Time (Year)
148	6.3E-09	84.0	149	4.2E-09	78.0	150	5.0E-10	91.0
151	1.5E-10	63.0	152	3.8E-12	65.0	153	3.0E-12	66.0
154	1.4E-12	91.0	155	1.1E-12	97.0	156	2.2E-12	84.0
157	2.0E-12	97.0	158	2.7E-15	159.0	159	2.0E-14	145.0
160	1.5E-11	63.0	161	6.8E-12	81.0	162	1.6E-11	62.0
163	2.4E-12	119.0	164	2.3E-12	120.0	165	2.4E-12	117.0
166	1.1E-01	29.0	167	1.9E-01	30.0	168	1.5E-01	30.0
169	1.2E-01	31.0	170	1.8E-05	34.0	171	5.5E-06	37.0
172	2.5E-06	47.0	173	1.3E-06	69.0	174	1.0E-04	52.0
175	1.1E-04	52.0	176	3.4E-06	62.0	177	9.3E-07	69.0
178	1.6E-07	74.0	179	4.2E-08	85.0	180	2.8E-08	86.0
181	4.5E-08	71.0	182	2.8E-10	72.0	183	5.2E-10	38.0
184	1.2E-09	69.0	185	8.2E-08	69.0	186	2.7E-08	69.0
187	6.0E-07	49.0	188	6.1E-07	62.0	189	2.4E-08	62.0
190	4.3E-07	13.0	191	1.5E-04	6.0	192	8.6E-08	60.0
193	2.9E-08	53.0	194	1.8E-08	54.0	195	4.7E-08	80.0
196	4.3E-08	81.0	197	2.1E-08	82.0	198	4.0E-06	62.0
199	5.8E-07	61.0	200	8.4E-08	56.0	201	2.0E-07	60.0
202	2.1E-06	59.0	203	1.2E-05	57.0	204	4.7E-05	54.0
205	9.8E-06	79.0	206	1.2E-05	73.0	207	2.9E-04	56.0
208	1.1E-03	57.0	209	4.9E-03	42.0	210	2.4E-03	53.0
211	8.0E-03	39.0	212	3.7E-03	42.0	213	9.3E-05	25.0
214	3.4E-05	55.0	215	1.3E-04	51.0	216	6.9E-05	59.0
217	4.8E-05	67.0	218	1.9E-05	42.0	219	1.2E-04	44.0
220	2.5E-03	45.0	221	4.9E-03	47.0	222	5.8E-03	49.0
223	2.4E-14	17.0	224	5.5E-14	38.0	225	1.0E-13	38.0

Table E.4 (continued)

Obs Node	Conc (uCi/L)	Time (Year)	Obs Node	Conc (uCi/L)	Time (Year)	Obs Node	Conc (uCi/L)	Time (Year)
226	1.0E-11	30.0	227	1.2E-09	25.0	228	3.6E-08	25.0
229	8.0E-08	24.0	230	2.0E-07	25.0	231	5.7E-09	28.0
232	6.6E-08	28.0	233	6.0E-07	28.0	234	6.5E-06	25.0
235	7.0E-05	26.0	236	2.1E-03	22.0	237	3.1E-02	22.0
238	2.1E-02	25.0	239	7.8E-03	27.0	240	7.4E-04	35.0
241	5.0E-05	43.0	242	1.4E-06	59.0	243	5.0E-08	74.0
244	4.2E-09	49.0	245	1.5E-09	76.0	246	1.6E-08	45.0
247	1.2E-07	43.0	248	7.8E-08	30.0	249	2.6E-05	37.0
250	1.4E-03	37.0	251	9.5E-03	37.0	252	3.2E-02	38.0
253	2.3E-09	75.0	254	2.8E-09	60.0	255	2.4E-09	59.0
256	5.2E-09	61.0	257	5.7E-10	66.0	258	1.3E-10	29.0
259	2.3E-09	30.0	260	8.2E-10	35.0	261	5.4E-10	34.0
262	1.8E-10	19.0	263	1.9E-11	19.0	264	8.4E-10	37.0
265	4.4E-09	37.0	266	9.9E-07	29.0	267	2.5E-04	26.0
268	2.0E-04	23.0	269	2.0E-04	26.0	270	1.8E-15	393.0
271	5.5E-05	33.0	272	4.3E-03	30.0	273	4.6E-03	37.0
274	6.1E-06	32.0	275	5.0E-05	39.0	276	1.6E-06	39.0
277	4.1E-05	53.0	278	1.8E-05	53.0	279	6.1E-06	51.0
280	2.0E-06	50.0	281	1.3E-07	66.0	282	6.4E-08	73.0
283	9.7E-09	66.0	284	4.7E-08	67.0	285	5.4E-08	66.0
286	1.8E-09	22.0	287	5.3E-08	26.0	288	1.5E-06	23.0
289	1.3E-05	24.0	290	8.7E-06	7.0	291	1.5E-06	5.0
292	2.5E-06	8.0	293	2.3E-06	9.0	294	3.3E-04	6.0
295	1.7E-04	13.0	296	2.0E-05	67.0	297	9.5E-04	35.0
298	1.7E-03	35.0	299	3.9E-03	30.0	300	2.8E-03	31.0
301	1.3E-05	57.0	302	1.9E-04	48.0	303	6.4E-04	52.0

Table E.4 (continued)

Obs Node	Conc (uCi/L)	Time (Year)	Obs Node	Conc (uCi/L)	Time (Year)	Obs Node	Conc (uCi/L)	Time (Year)
304	2.6E-03	43.0	305	1.3E-02	38.0	306	7.1E-02	30.0
307	4.3E-02	32.0	308	4.1E-02	30.0	309	2.0E-04	29.0
310	6.5E-05	36.0	311	4.3E-05	45.0	312	6.8E-02	26.0
313	1.2E-02	35.0	314	7.8E-04	58.0	315	8.0E-03	14.0
316	4.7E-02	23.0	317	9.8E-06	79.0	318	2.4E-12	53.0
319	1.8E-12	59.0	320	1.6E-12	61.0	321	2.9E-12	67.0
322	2.0E-12	73.0	323	5.1E-06	62.0	324	1.6E-05	53.0
325	1.9E-03	52.0	326	1.5E-03	53.0	327	1.2E-03	52.0
328	8.8E-04	54.0	329	5.4E-04	56.0	330	2.4E-04	53.0
331	1.4E-04	55.0	332	1.2E-04	55.0	333	2.7E-05	58.0
334	2.2E-06	58.0						

Table E.5. Groundwater concentration of nuclide: ^{14}C at observation nodes

Obs Node	Conc (uCi/L)	Time (Year)	Obs Node	Conc (uCi/L)	Time (Year)	Obs Node	Conc (uCi/L)	Time (Year)
1	3.3E-16	269.0	2	.0E+00	1000.0	3	1.4E-15	999.0
4	.0E+00	1000.0	5	.0E+00	1000.0	6	6.4E-16	1000.0
7	1.6E-15	902.0	8	1.6E-15	937.0	9	1.3E-15	999.0
10	1.6E-15	149.0	11	1.6E-15	981.0	12	1.5E-15	996.0
13	1.6E-15	260.0	14	1.2E-14	263.0	15	2.3E-15	260.0
16	1.6E-15	278.0	17	1.1E-15	280.0	18	3.4E-13	261.0
19	1.5E-12	261.0	20	1.8E-14	279.0	21	3.7E-11	256.0
22	1.5E-08	259.0	23	3.2E-13	296.0	24	1.8E-09	255.0
25	6.7E-11	283.0	26	3.8E-08	257.0	27	2.1E-10	285.0
28	2.6E-06	272.0	29	5.0E-08	73.0	30	1.7E-06	270.0
31	9.3E-08	75.0	32	1.2E-05	265.0	33	2.9E-08	65.0
34	2.0E-05	257.0	35	2.1E-08	76.0	36	1.9E-06	256.0
37	4.8E-07	259.0	38	1.6E-08	70.0	39	2.9E-05	260.0
40	3.5E-07	261.0	41	9.8E-09	72.0	42	6.2E-03	253.0
43	2.5E-07	272.0	44	2.4E-09	74.0	45	2.8E-02	250.0
46	5.7E-07	272.0	47	1.1E-09	286.0	48	2.5E-02	257.0
49	5.1E-07	274.0	50	1.0E-09	284.0	51	1.7E-02	252.0
52	2.6E-07	275.0	53	7.2E-10	286.0	54	1.8E-03	257.0
55	1.9E-07	279.0	56	2.6E-10	286.0	57	1.8E-03	257.0
58	1.0E-07	279.0	59	3.7E-10	248.0	60	1.1E-03	264.0
61	2.4E-08	282.0	62	9.6E-08	254.0	63	3.8E-04	265.0
64	4.1E-09	283.0	65	1.9E-05	252.0	66	7.1E-05	268.0
67	3.2E-09	65.0	68	2.7E-03	249.0	69	1.5E-06	289.0
70	1.6E-09	81.0	71	2.5E-03	252.0	72	3.3E-08	300.0
73	1.4E-09	87.0	74	1.6E-03	252.0	75	2.2E-12	121.0

Table E.5 (continued)

Obs Node	Conc (uCi/L)	Time (Year)	Obs Node	Conc (uCi/L)	Time (Year)	Obs Node	Conc (uCi/L)	Time (Year)
76	1.2E-08	304.0	77	2.8E-10	89.0	78	6.3E-04	249.0
79	1.0E-11	123.0	80	2.4E-08	121.0	81	1.0E-10	260.0
82	1.2E-05	249.0	83	2.4E-10	70.0	84	2.3E-06	116.0
85	1.9E-09	256.0	86	3.6E-06	250.0	87	2.0E-08	73.0
88	1.2E-04	111.0	89	1.2E-08	249.0	90	8.3E-07	256.0
91	1.5E-06	65.0	92	1.3E-02	109.0	93	7.2E-09	251.0
94	2.2E-08	259.0	95	9.1E-04	64.0	96	3.2E-02	109.0
97	3.1E-11	280.0	98	1.1E-08	260.0	99	3.1E-01	57.0
100	1.4E-01	113.0	101	3.4E-09	278.0	102	1.8E-10	267.0
103	2.9E-01	59.0	104	2.2E-01	109.0	105	2.0E-08	267.0
106	2.1E-06	266.0	107	2.7E-06	266.0	108	1.8E-08	279.0
109	6.8E-10	289.0	110	2.1E-01	63.0	111	2.2E-02	121.0
112	1.5E-05	275.0	113	7.4E-09	63.0	114	2.5E-09	292.0
115	4.3E-02	70.0	116	5.1E-03	126.0	117	6.5E-06	279.0
118	4.1E-11	287.0	119	5.4E-02	70.0	120	7.5E-07	142.0
121	6.7E-06	279.0	122	3.2E-02	70.0	123	1.5E-06	130.0
124	5.7E-06	270.0	125	2.9E-03	82.0	126	5.1E-06	267.0
127	7.6E-03	80.0	128	9.6E-08	265.0	129	6.4E-03	79.0
130	3.3E-08	272.0	131	1.9E-03	81.0	132	4.3E-08	272.0
133	2.8E-04	88.0	134	1.7E-08	279.0	135	1.0E-04	87.0
136	9.7E-10	289.0	137	1.1E-05	84.0	138	2.8E-07	97.0
139	5.7E-06	286.0	140	5.2E-07	269.0	141	1.4E-06	87.0
142	3.1E-08	100.0	143	6.1E-06	286.0	144	1.1E-09	104.0
145	4.3E-12	96.0	146	1.6E-08	292.0	147	3.9E-07	299.0
148	2.2E-06	292.0	149	1.8E-06	292.0	150	4.4E-07	299.0
151	1.3E-11	255.0	152	1.3E-11	91.0	153	1.7E-12	85.0

Table E.5 (continued)

Obs Node	Conc (uCi/L)	Time (Year)	Obs Node	Conc (uCi/L)	Time (Year)	Obs Node	Conc (uCi/L)	Time (Year)
154	3.9E-12	299.0	155	5.0E-12	305.0	156	3.5E-11	305.0
157	7.9E-11	305.0	158	1.2E-15	1000.0	159	1.7E-14	281.0
160	2.4E-11	87.0	161	8.0E-10	101.0	162	5.6E-10	102.0
163	2.0E-10	103.0	164	9.3E-13	266.0	165	1.3E-12	91.0
166	9.2E-02	67.0	167	1.2E-01	67.0	168	1.4E-01	67.0
169	1.3E-01	68.0	170	7.5E-07	142.0	171	8.1E-07	144.0
172	1.0E-06	145.0	173	6.7E-05	277.0	174	1.2E-03	270.0
175	5.8E-04	277.0	176	4.4E-05	277.0	177	3.3E-05	283.0
178	3.1E-05	282.0	179	3.2E-05	280.0	180	2.3E-05	281.0
181	2.0E-05	280.0	182	5.9E-08	269.0	183	9.5E-08	263.0
184	1.8E-07	264.0	185	1.5E-05	264.0	186	1.6E-08	296.0
187	1.3E-04	269.0	188	1.3E-09	286.0	189	7.0E-10	246.0
190	1.7E-07	253.0	191	5.2E-05	249.0	192	2.9E-04	268.0
193	4.0E-05	274.0	194	2.8E-05	281.0	195	2.1E-05	281.0
196	1.9E-05	282.0	197	7.7E-06	277.0	198	1.4E-06	69.0
199	7.8E-08	75.0	200	3.1E-08	60.0	201	4.6E-08	276.0
202	1.5E-07	269.0	203	2.3E-07	257.0	204	4.3E-07	275.0
205	1.5E-05	261.0	206	8.8E-06	268.0	207	2.5E-05	264.0
208	8.9E-05	257.0	209	5.3E-06	254.0	210	9.3E-04	249.0
211	1.4E-03	247.0	212	1.3E-02	245.0	213	3.5E-03	246.0
214	2.7E-05	251.0	215	1.1E-06	272.0	216	1.1E-06	272.0
217	3.2E-06	268.0	218	1.0E-06	270.0	219	2.8E-07	259.0
220	4.4E-07	55.0	221	9.3E-07	63.0	222	1.7E-06	61.0
223	3.8E-14	59.0	224	1.6E-14	57.0	225	2.9E-14	74.0
226	8.4E-12	65.0	227	7.7E-10	61.0	228	2.4E-08	57.0
229	5.3E-08	60.0	230	1.2E-07	57.0	231	4.4E-09	64.0

Table E.5 (continued)

Obs Node	Conc (uCi/L)	Time (Year)	Obs Node	Conc (uCi/L)	Time (Year)	Obs Node	Conc (uCi/L)	Time (Year)
232	4.8E-08	66.0	233	3.7E-07	64.0	234	3.9E-06	61.0
235	4.1E-05	62.0	236	1.6E-03	61.0	237	2.0E-02	60.0
238	1.6E-02	59.0	239	5.6E-03	65.0	240	3.8E-04	73.0
241	4.5E-05	79.0	242	5.1E-06	100.0	243	1.9E-08	243.0
244	3.7E-08	93.0	245	2.5E-08	74.0	246	7.4E-08	75.0
247	3.7E-07	86.0	248	1.1E-06	75.0	249	3.0E-04	81.0
250	4.1E-03	74.0	251	1.3E-02	73.0	252	4.2E-02	73.0
253	2.2E-06	288.0	254	2.9E-06	288.0	255	3.6E-06	287.0
256	3.4E-06	288.0	257	3.5E-07	287.0	258	5.0E-08	300.0
259	4.5E-09	300.0	260	7.4E-10	313.0	261	1.3E-10	319.0
262	2.3E-11	319.0	263	3.2E-12	326.0	264	1.6E-15	764.0
265	7.4E-10	52.0	266	1.3E-06	263.0	267	3.5E-04	253.0
268	7.0E-03	253.0	269	7.7E-03	250.0	270	1.6E-15	705.0
271	4.1E-05	58.0	272	5.6E-03	54.0	273	1.4E-01	250.0
274	2.5E-05	273.0	275	2.1E-06	144.0	276	1.4E-06	138.0
277	7.5E-05	53.0	278	2.6E-03	257.0	279	9.0E-04	262.0
280	3.3E-04	267.0	281	5.1E-05	267.0	282	4.3E-08	80.0
283	3.0E-09	86.0	284	1.0E-08	82.0	285	5.5E-09	85.0
286	1.4E-07	247.0	287	5.1E-06	246.0	288	7.9E-05	244.0
289	5.6E-04	245.0	290	5.5E-05	245.0	291	6.1E-07	246.0
292	5.4E-07	248.0	293	5.6E-07	249.0	294	8.2E-05	247.0
295	7.7E-02	248.0	296	3.1E-02	249.0	297	2.9E-02	254.0
298	2.1E-02	256.0	299	4.0E-02	253.0	300	1.2E-03	53.0
301	9.0E-06	256.0	302	3.4E-06	268.0	303	1.1E-05	262.0
304	2.6E-05	258.0	305	1.2E-04	251.0	306	8.7E-04	245.0
307	2.9E-05	55.0	308	3.5E-05	257.0	309	2.1E-06	253.0

Table E.5 (continued)

Obs Node	Conc (uCi/L)	Time (Year)	Obs Node	Conc (uCi/L)	Time (Year)	Obs Node	Conc (uCi/L)	Time (Year)
310	1.5E-06	266.0	311	2.1E-06	267.0	312	9.7E-04	246.0
313	3.2E-04	255.0	314	1.5E-04	254.0	315	6.8E-04	247.0
316	9.4E-04	247.0	317	1.5E-05	261.0	318	4.0E-16	74.0
319	1.5E-15	999.0	320	1.5E-15	988.0	321	1.1E-14	264.0
322	7.4E-15	259.0	323	4.0E-08	264.0	324	3.2E-08	261.0
325	2.6E-07	58.0	326	1.9E-07	61.0	327	1.6E-07	69.0
328	1.1E-07	70.0	329	8.1E-08	72.0	330	3.9E-08	73.0
331	3.2E-08	69.0	332	2.8E-08	69.0	333	6.2E-09	72.0
334	2.9E-09	283.0						

Table E.6. Groundwater concentration of nuclide: ^{36}Cl at observation nodes

Obs Node	Conc (uCi/L)	Time (Year)	Obs Node	Conc (uCi/L)	Time (Year)	Obs Node	Conc (uCi/L)	Time (Year)
1	2.3E-30	4000.0	2	.0E+00	4000.0	3	4.3E-30	3990.0
4	.0E+00	4000.0	5	.0E+00	4000.0	6	.0E+00	4000.0
7	3.7E-30	4000.0	8	.0E+00	4000.0	9	5.6E-30	3990.0
10	1.2E-29	4000.0	11	.0E+00	4000.0	12	1.4E-32	3997.0
13	1.2E-29	3997.0	14	.0E+00	4000.0	15	.0E+00	3483.0
16	1.1E-29	3997.0	17	6.4E-30	4000.0	18	2.9E-34	3999.0
19	.0E+00	3313.0	20	6.7E-30	3995.0	21	1.8E-32	3999.0
22	.0E+00	3008.0	23	3.0E-35	3160.0	24	3.8E-31	3990.0
25	.0E+00	3031.0	26	1.6E-31	3676.0	27	8.3E-35	3031.0
28	4.4E-28	3994.0	29	9.9E-33	3115.0	30	5.8E-26	3997.0
31	1.7E-33	2583.0	32	1.7E-25	3996.0	33	3.6E-33	2575.0
34	2.4E-40	519.0	35	5.9E-36	1829.0	36	6.1E-35	431.0
37	4.9E-35	1447.0	38	1.4E-35	1496.0	39	1.3E-32	702.0
40	1.1E-28	2841.0	41	1.0E-36	1208.0	42	1.3E-27	2168.0
43	4.3E-27	2837.0	44	9.0E-29	2454.0	45	2.2E-26	1814.0
46	3.5E-26	2866.0	47	2.5E-27	2849.0	48	7.1E-26	1315.0
49	2.0E-24	3763.0	50	3.1E-26	3710.0	51	1.6E-25	1063.0
52	3.2E-32	292.0	53	6.5E-24	2869.0	54	2.5E-20	3951.0
55	5.1E-31	271.0	56	9.3E-23	3773.0	57	4.8E-19	3998.0
58	3.8E-30	207.0	59	1.7E-21	2861.0	60	2.7E-18	3998.0
61	5.9E-28	247.0	62	3.6E-20	3752.0	63	6.3E-18	3963.0
64	8.6E-27	129.0	65	1.6E-19	3901.0	66	8.4E-18	4000.0
67	6.2E-25	110.0	68	2.5E-26	176.0	69	7.5E-18	2777.0
70	1.5E-23	103.0	71	7.4E-26	185.0	72	2.6E-16	61.0
73	8.2E-21	2268.0	74	3.1E-25	125.0	75	2.6E-14	29.0
76	2.8E-15	56.0	77	5.0E-23	113.0	78	1.0E-24	97.0

Table E.6 (continued)

Obs Node	Conc (uCi/L)	Time (Year)	Obs Node	Conc (uCi/L)	Time (Year)	Obs Node	Conc (uCi/L)	Time (Year)
79	1.2E-12	28.0	80	2.5E-14	52.0	81	2.3E-20	448.0
82	3.7E-24	102.0	83	1.0E-10	24.0	84	8.3E-13	52.0
85	4.9E-20	473.0	86	9.6E-24	98.0	87	3.7E-09	39.0
88	3.8E-11	43.0	89	7.4E-20	493.0	90	1.5E-21	483.0
91	1.2E-06	29.0	92	1.1E-09	44.0	93	1.8E-19	1294.0
94	1.6E-20	496.0	95	2.4E-04	24.0	96	4.8E-09	77.0
97	2.0E-19	1577.0	98	5.3E-18	1341.0	99	9.3E-02	23.0
100	6.0E-08	75.0	101	3.2E-19	2830.0	102	9.4E-18	1380.0
103	1.1E-01	28.0	104	2.1E-08	77.0	105	1.2E-17	2215.0
106	1.0E-17	3244.0	107	7.8E-18	2217.0	108	2.9E-19	514.0
109	2.3E-19	555.0	110	7.1E-02	29.0	111	3.4E-09	86.0
112	1.2E-17	1978.0	113	1.2E-20	252.0	114	9.6E-28	69.0
115	2.1E-02	36.0	116	1.0E-06	44.0	117	1.2E-17	1093.0
118	1.7E-26	97.0	119	2.0E-02	36.0	120	1.4E-08	48.0
121	1.2E-17	2219.0	122	1.6E-02	37.0	123	3.4E-06	55.0
124	1.2E-17	3192.0	125	1.2E-03	45.0	126	1.2E-17	2711.0
127	3.2E-03	44.0	128	1.2E-17	2971.0	129	2.0E-03	51.0
130	1.2E-17	3860.0	131	5.4E-04	45.0	132	1.2E-17	1255.0
133	1.9E-05	83.0	134	1.2E-17	1231.0	135	7.6E-06	87.0
136	1.2E-17	2333.0	137	1.0E-06	84.0	138	1.7E-08	91.0
139	1.2E-17	3795.0	140	1.2E-17	3568.0	141	1.5E-07	87.0
142	2.5E-09	94.0	143	1.2E-17	1540.0	144	1.3E-10	110.0
145	7.3E-12	65.0	146	5.2E-17	60.0	147	1.2E-17	2922.0

Table E.6 (continued)

Obs Node	Conc (uCi/L)	Time (Year)	Obs Node	Conc (uCi/L)	Time (Year)	Obs Node	Conc (uCi/L)	Time (Year)
148	1.2E-17	2500.0	149	1.2E-17	2610.0	150	1.2E-17	2515.0
151	3.3E-10	125.0	152	3.0E-11	135.0	153	4.0E-12	66.0
154	6.1E-13	65.0	155	9.0E-14	91.0	156	3.1E-14	69.0
157	5.1E-18	61.0	158	1.0E-14	136.0	159	7.0E-13	138.0
160	1.1E-10	133.0	161	7.2E-11	136.0	162	6.4E-11	130.0
163	2.6E-11	132.0	164	2.4E-11	136.0	165	2.4E-11	130.0
166	4.0E-02	37.0	167	6.6E-02	30.0	168	6.8E-02	34.0
169	5.4E-02	33.0	170	1.4E-08	48.0	171	7.2E-08	52.0
172	7.9E-09	58.0	173	1.7E-11	65.0	174	2.9E-14	62.0
175	2.7E-14	65.0	176	7.9E-15	69.0	177	1.3E-17	55.0
178	1.2E-17	1832.0	179	1.2E-17	2721.0	180	1.2E-17	3461.0
181	1.2E-17	3319.0	182	1.2E-17	3202.0	183	1.2E-17	2317.0
184	1.2E-17	2591.0	185	1.2E-17	2868.0	186	1.2E-17	1563.0
187	1.2E-17	1534.0	188	5.0E-27	2848.0	189	4.2E-21	3765.0
190	4.3E-20	3899.0	191	1.6E-19	3930.0	192	4.6E-19	3963.0
193	1.8E-20	3988.0	194	8.1E-21	3692.0	195	2.9E-20	3758.0
196	2.6E-20	3769.0	197	2.1E-20	3771.0	198	3.2E-21	3806.0
199	1.8E-24	93.0	200	2.2E-26	112.0	201	3.5E-28	137.0
202	2.6E-30	135.0	203	6.7E-32	79.0	204	2.4E-33	87.0
205	1.8E-32	2924.0	206	2.2E-40	1422.0	207	.0E+00	1029.0
208	.0E+00	621.0	209	.0E+00	519.0	210	3.3E-33	1060.0
211	1.1E-26	3993.0	212	1.0E-30	2459.0	213	9.4E-30	540.0
214	6.5E-30	616.0	215	1.2E-34	88.0	216	8.5E-35	85.0

Table E.6 (continued)

Obs Node	Conc (uCi/L)	Time (Year)	Obs Node	Conc (uCi/L)	Time (Year)	Obs Node	Conc (uCi/L)	Time (Year)
217	8.1E-34	460.0	218	3.1E-28	2739.0	219	3.1E-31	2579.0
220	6.5E-33	2575.0	221	1.7E-35	2740.0	222	1.1E-32	3125.0
223	6.9E-15	26.0	224	3.5E-15	38.0	225	1.4E-14	38.0
226	3.1E-12	30.0	227	3.1E-10	30.0	228	8.7E-09	25.0
229	1.7E-08	24.0	230	4.5E-08	25.0	231	1.5E-09	28.0
232	1.9E-08	28.0	233	1.7E-07	28.0	234	1.8E-06	28.0
235	1.8E-05	26.0	236	5.4E-04	26.0	237	7.7E-03	26.0
238	5.9E-03	28.0	239	2.2E-03	27.0	240	2.9E-04	35.0
241	3.1E-05	43.0	242	2.2E-06	61.0	243	3.6E-07	113.0
244	6.0E-09	57.0	245	7.9E-09	104.0	246	1.5E-08	88.0
247	1.4E-07	69.0	248	3.0E-07	75.0	249	2.3E-05	75.0
250	3.3E-04	74.0	251	3.6E-03	42.0	252	2.0E-02	38.0
253	6.3E-19	2519.0	254	3.7E-19	3764.0	255	5.8E-19	3129.0
256	5.4E-19	3134.0	257	9.1E-18	3062.0	258	1.0E-17	3107.0
259	1.2E-17	3091.0	260	1.1E-17	3244.0	261	1.2E-17	3020.0
262	1.2E-17	1315.0	263	1.2E-17	3409.0	264	1.2E-17	822.0
265	1.2E-17	625.0	266	1.2E-17	1673.0	267	1.2E-17	3193.0
268	1.2E-17	2768.0	269	1.2E-17	2071.0	270	2.0E-16	78.0
271	8.3E-17	81.0	272	3.0E-17	86.0	273	1.2E-17	3682.0
274	1.5E-15	51.0	275	2.0E-13	55.0	276	6.2E-11	62.0
277	1.2E-17	974.0	278	1.2E-17	3314.0	279	1.2E-17	2907.0
280	1.2E-17	1138.0	281	1.2E-17	3839.0	282	3.7E-19	3108.0
283	5.9E-22	78.0	284	3.9E-23	92.0	285	3.2E-23	94.0
286	3.5E-25	405.0	287	1.4E-25	357.0	288	6.9E-26	343.0
289	4.9E-26	328.0	290	1.6E-19	3560.0	291	9.2E-20	3145.0
292	8.8E-20	3890.0	293	8.9E-20	3149.0	294	1.7E-19	3893.0

Table E.6 (continued)

Obs Node	Conc (uCi/L)	Time (Year)	Obs Node	Conc (uCi/L)	Time (Year)	Obs Node	Conc (uCi/L)	Time (Year)
295	1.8E-25	1082.0	296	2.5E-23	3212.0	297	4.0E-26	494.0
298	2.6E-26	500.0	299	1.3E-26	506.0	300	7.3E-27	558.0
301	1.1E-28	705.0	302	.0E+00	145.0	303	.0E+00	215.0
304	.0E+00	375.0	305	.0E+00	1189.0	306	.0E+00	1679.0
307	.0E+00	1194.0	308	.0E+00	1190.0	309	.0E+00	1189.0
310	.0E+00	434.0	311	3.3E-35	451.0	312	.0E+00	1551.0
313	.0E+00	1733.0	314	.0E+00	2063.0	315	.0E+00	2431.0
316	.0E+00	2212.0	317	1.8E-32	2924.0	318	.0E+00	4000.0
319	.0E+00	4000.0	320	.0E+00	4000.0	321	.0E+00	3815.0
322	.0E+00	3600.0	323	.0E+00	3006.0	324	.0E+00	3008.0
325	4.6E-33	2555.0	326	3.2E-33	2576.0	327	2.9E-33	2576.0
328	3.1E-33	2577.0	329	3.2E-33	2565.0	330	5.9E-35	2359.0
331	3.6E-34	2458.0	332	4.2E-35	1488.0	333	5.2E-35	1187.0
334	1.6E-28	2459.0						

Table E.7. Groundwater concentration of nuclide: ^{90}Sr at observation nodes

Obs Node	Conc (uCi/L)	Time (Year)	Obs Node	Conc (uCi/L)	Time (Year)	Obs Node	Conc (uCi/L)	Time (Year)
1	3.1E-30	630.0	2	.0E+00	2000.0	3	1.9E-29	436.0
4	.0E+00	2000.0	5	.0E+00	2000.0	6	8.8E-31	517.0
7	2.0E-29	721.0	8	3.9E-26	478.0	9	1.1E-27	633.0
10	5.2E-30	605.0	11	4.2E-23	439.0	12	1.8E-26	459.0
13	3.7E-31	809.0	14	1.2E-21	215.0	15	3.6E-26	914.0
16	2.4E-31	1023.0	17	4.8E-32	973.0	18	8.6E-19	206.0
19	3.6E-19	361.0	20	7.7E-31	499.0	21	2.3E-24	1396.0
22	1.9E-14	327.0	23	1.0E-31	1223.0	24	1.3E-15	135.0
25	5.3E-31	472.0	26	4.3E-14	478.0	27	1.0E-28	684.0
28	1.0E-16	846.0	29	2.3E-25	645.0	30	9.4E-13	235.0
31	5.5E-23	371.0	32	5.5E-13	558.0	33	3.6E-19	289.0
34	6.7E-14	591.0	35	9.7E-17	289.0	36	6.7E-09	141.0
37	1.0E-13	423.0	38	1.1E-18	919.0	39	7.2E-12	240.0
40	4.2E-10	199.0	41	1.2E-13	441.0	42	5.9E-18	1055.0
43	4.0E-10	215.0	44	.0E+00	6.0	45	7.5E-12	378.0
46	5.7E-11	548.0	47	1.9E-12	361.0	48	6.4E-13	417.0
49	6.3E-08	285.0	50	1.8E-10	362.0	51	3.4E-14	311.0
52	1.9E-08	356.0	53	3.8E-11	361.0	54	2.7E-17	456.0
55	2.0E-12	468.0	56	2.2E-12	385.0	57	1.5E-18	236.0
58	9.8E-14	581.0	59	1.7E-13	468.0	60	2.3E-19	380.0
61	1.8E-14	573.0	62	7.2E-15	709.0	63	7.3E-20	659.0
64	3.4E-15	582.0	65	2.6E-11	177.0	66	5.4E-22	607.0
67	2.4E-19	317.0	68	2.9E-12	174.0	69	1.5E-24	394.0
70	5.6E-20	343.0	71	3.3E-14	228.0	72	7.8E-27	80.0
73	1.9E-22	400.0	74	2.4E-15	621.0	75	7.4E-23	379.0
76	.0E+00	4.0	77	1.9E-18	220.0	78	3.7E-15	389.0

Table E.7 (continued)

Obs Node	Conc (uCi/L)	Time (Year)	Obs Node	Conc (uCi/L)	Time (Year)	Obs Node	Conc (uCi/L)	Time (Year)
79	1.1E-21	174.0	80	3.4E-15	234.0	81	1.5E-15	209.0
82	3.2E-17	553.0	83	1.4E-18	357.0	84	1.0E-12	157.0
85	5.7E-13	173.0	86	4.9E-18	619.0	87	4.9E-15	245.0
88	9.1E-17	994.0	89	8.0E-15	498.0	90	5.0E-20	617.0
91	6.5E-12	146.0	92	1.0E-08	208.0	93	4.5E-14	260.0
94	8.3E-23	794.0	95	2.4E-14	675.0	96	1.4E-08	188.0
97	4.2E-14	347.0	98	1.1E-20	299.0	99	4.5E-08	184.0
100	2.0E-08	187.0	101	3.2E-14	410.0	102	1.4E-18	620.0
103	6.2E-09	99.0	104	1.6E-08	217.0	105	2.2E-12	156.0
106	2.5E-12	135.0	107	3.9E-13	278.0	108	5.2E-16	393.0
109	1.9E-20	1036.0	110	2.6E-10	224.0	111	6.9E-12	244.0
112	2.3E-18	759.0	113	3.0E-24	1126.0	114	3.5E-24	1062.0
115	3.2E-14	287.0	116	2.0E-14	175.0	117	4.3E-20	205.0
118	5.5E-28	1029.0	119	1.4E-14	318.0	120	2.6E-17	269.0
121	2.3E-22	661.0	122	9.7E-16	648.0	123	3.8E-19	454.0
124	2.7E-24	339.0	125	2.3E-19	555.0	126	2.9E-22	735.0
127	1.2E-17	347.0	128	2.1E-22	349.0	129	6.6E-18	421.0
130	1.7E-25	1013.0	131	4.8E-19	702.0	132	6.3E-21	264.0
133	5.9E-21	736.0	134	1.2E-18	222.0	135	1.8E-21	616.0
136	7.5E-21	220.0	137	1.2E-22	716.0	138	.0E+00	153.0
139	1.7E-24	193.0	140	2.5E-21	527.0	141	2.1E-23	619.0
142	.0E+00	238.0	143	2.8E-23	520.0	144	2.7E-27	685.0
145	1.5E-32	652.0	146	1.8E-28	737.0	147	4.6E-27	569.0
148	1.4E-25	826.0	149	1.5E-24	788.0	150	9.7E-26	580.0
151	6.0E-27	849.0	152	6.8E-29	697.0	153	.0E+00	1238.0

Table E.7 (continued)

Obs Node	Conc (uCi/L)	Time (Year)	Obs Node	Conc (uCi/L)	Time (Year)	Obs Node	Conc (uCi/L)	Time (Year)
154	1.2E-37	1957.0	155	7.1E-36	1110.0	156	3.4E-33	853.0
157	1.3E-32	730.0	158	.0E+00	799.0	159	2.4E-31	635.0
160	2.3E-29	798.0	161	5.2E-30	796.0	162	1.7E-30	851.0
163	1.8E-32	1009.0	164	1.2E-31	636.0	165	5.4E-32	713.0
166	1.0E-11	290.0	167	8.7E-12	263.0	168	6.6E-12	281.0
169	6.3E-12	291.0	170	2.6E-17	269.0	171	2.4E-20	269.0
172	1.1E-26	1438.0	173	1.9E-21	885.0	174	7.9E-17	604.0
175	5.2E-18	662.0	176	1.7E-19	496.0	177	2.7E-21	585.0
178	8.7E-21	666.0	179	4.5E-19	498.0	180	3.0E-21	338.0
181	6.3E-22	437.0	182	3.5E-18	207.0	183	3.5E-21	538.0
184	7.9E-21	430.0	185	2.5E-19	689.0	186	1.3E-21	225.0
187	6.8E-18	385.0	188	1.4E-10	377.0	189	1.3E-11	223.0
190	1.1E-14	774.0	191	1.3E-08	102.0	192	1.0E-19	668.0
193	2.0E-23	309.0	194	1.6E-22	348.0	195	9.9E-20	482.0
196	8.0E-20	649.0	197	3.4E-21	733.0	198	1.9E-30	68.0
199	2.0E-21	627.0	200	5.8E-21	433.0	201	1.1E-19	243.0
202	1.7E-17	312.0	203	8.6E-17	391.0	204	2.9E-19	528.0
205	1.2E-17	58.0	206	4.8E-12	195.0	207	1.9E-14	691.0
208	2.1E-11	383.0	209	1.6E-06	158.0	210	1.7E-09	124.0
211	1.4E-09	125.0	212	8.5E-10	162.0	213	7.9E-11	176.0
214	2.6E-20	1116.0	215	7.4E-17	181.0	216	5.0E-16	372.0
217	1.4E-14	310.0	218	1.4E-12	253.0	219	2.3E-14	431.0
220	1.5E-15	419.0	221	5.4E-15	411.0	222	3.3E-15	423.0

Table E.7 (continued)

Obs Node	Conc (uCi/L)	Time (Year)	Obs Node	Conc (uCi/L)	Time (Year)	Obs Node	Conc (uCi/L)	Time (Year)
223	2.0E-24	627.0	224	3.8E-23	434.0	225	1.1E-22	330.0
226	3.3E-26	1118.0	227	6.9E-18	290.0	228	1.3E-14	233.0
229	9.7E-15	223.0	230	1.1E-14	200.0	231	4.6E-17	217.0
232	2.5E-15	193.0	233	2.3E-14	223.0	234	1.6E-12	186.0
235	1.4E-11	185.0	236	4.0E-09	147.0	237	5.7E-08	146.0
238	3.3E-08	146.0	239	1.2E-09	325.0	240	.0E+00	2.0
241	.0E+00	3.0	242	.0E+00	4.0	243	.0E+00	9.0
244	2.4E-21	677.0	245	1.9E-20	607.0	246	3.8E-20	622.0
247	6.6E-18	763.0	248	4.1E-18	745.0	249	1.9E-16	651.0
250	6.8E-15	531.0	251	1.1E-14	520.0	252	4.7E-13	306.0
253	4.3E-24	393.0	254	2.3E-28	1693.0	255	6.9E-23	583.0
256	5.9E-22	482.0	257	1.0E-20	330.0	258	4.8E-19	279.0
259	5.7E-19	239.0	260	7.3E-16	197.0	261	8.3E-16	54.0
262	8.1E-17	333.0	263	.0E+00	3.0	264	6.1E-15	200.0
265	7.0E-17	394.0	266	2.5E-17	51.0	267	3.8E-12	167.0
268	7.4E-11	173.0	269	1.1E-10	173.0	270	.0E+00	1.0
271	5.6E-15	50.0	272	5.4E-11	173.0	273	4.0E-11	173.0
274	8.7E-15	214.0	275	.0E+00	3.0	276	1.7E-25	1378.0
277	.0E+00	1.0	278	3.8E-12	431.0	279	2.1E-14	224.0
280	1.0E-15	491.0	281	4.8E-21	835.0	282	2.3E-21	279.0
283	1.4E-20	285.0	284	4.3E-23	514.0	285	2.6E-22	654.0
286	8.8E-17	311.0	287	5.8E-14	316.0	288	1.2E-11	276.0
289	8.6E-10	289.0	290	2.3E-08	141.0	291	3.5E-09	138.0
292	2.8E-09	117.0	293	6.8E-11	333.0	294	3.1E-06	80.0
295	1.1E-11	286.0	296	1.5E-12	491.0	297	1.4E-11	388.0

Table E.7 (continued)

Obs Node	Conc (uCi/L)	Time (Year)	Obs Node	Conc (uCi/L)	Time (Year)	Obs Node	Conc (uCi/L)	Time (Year)
298	2.5E-11	325.0	299	8.1E-11	248.0	300	5.5E-16	57.0
301	5.0E-15	145.0	302	1.1E-16	181.0	303	2.7E-14	815.0
304	2.3E-21	1686.0	305	4.3E-12	785.0	306	1.6E-07	169.0
307	2.8E-08	169.0	308	1.4E-08	169.0	309	4.1E-11	208.0
310	2.0E-12	343.0	311	2.5E-15	705.0	312	2.7E-05	215.0
313	4.4E-08	251.0	314	2.8E-08	315.0	315	1.0E-05	363.0
316	1.5E-05	345.0	317	1.2E-17	58.0	318	.0E+00	21.0
319	2.2E-23	371.0	320	4.9E-24	365.0	321	4.1E-22	279.0
322	2.0E-22	407.0	323	4.2E-14	307.0	324	6.9E-16	458.0
325	1.6E-17	636.0	326	6.7E-18	278.0	327	1.6E-18	240.0
328	4.5E-20	486.0	329	1.5E-19	173.0	330	3.1E-16	173.0
331	2.8E-16	246.0	332	6.2E-17	766.0	333	3.0E-12	328.0
334	1.2E-19	74.0						

Table E.8. Groundwater concentration of nuclide: ^{99}Tc at observation nodes

Obs Node	Conc (uCi/L)	Time (Year)	Obs Node	Conc (uCi/L)	Time (Year)	Obs Node	Conc (uCi/L)	Time (Year)
1	1.0E-18	1953.0	2	.0E+00	2000.0	3	5.2E-18	1948.0
4	.0E+00	2000.0	5	.0E+00	2000.0	6	2.6E-18	2000.0
7	6.0E-18	1721.0	8	6.0E-18	1887.0	9	5.4E-18	1571.0
10	3.2E-22	311.0	11	6.0E-18	1696.0	12	6.1E-18	1484.0
13	3.1E-22	312.0	14	3.3E-18	1639.0	15	6.2E-18	1547.0
16	3.6E-22	344.0	17	3.2E-22	363.0	18	5.4E-18	1650.0
19	6.2E-18	1979.0	20	2.6E-19	656.0	21	1.4E-18	1617.0
22	6.2E-18	1577.0	23	5.4E-18	741.0	24	4.1E-18	1587.0
25	6.2E-18	1044.0	26	4.5E-18	259.0	27	6.2E-18	1476.0
28	1.5E-16	254.0	29	6.4E-18	1244.0	30	1.9E-14	250.0
31	1.6E-15	94.0	32	1.7E-12	248.0	33	2.2E-14	95.0
34	3.1E-10	248.0	35	2.0E-12	89.0	36	5.3E-08	258.0
37	1.6E-11	84.0	38	2.8E-10	87.0	39	1.4E-06	260.0
40	2.4E-08	85.0	41	1.1E-08	84.0	42	2.8E-04	253.0
43	5.8E-08	89.0	44	6.8E-11	54.0	45	1.3E-03	250.0
46	5.6E-07	90.0	47	7.0E-09	80.0	48	1.2E-03	257.0
49	2.9E-06	84.0	50	1.3E-04	87.0	51	7.4E-04	252.0
52	9.6E-07	92.0	53	2.9E-04	90.0	54	5.6E-05	257.0
55	6.3E-08	104.0	56	1.8E-04	97.0	57	6.8E-05	264.0
58	3.2E-08	103.0	59	1.1E-04	100.0	60	4.7E-05	264.0
61	7.7E-09	107.0	62	4.5E-06	97.0	63	1.6E-05	265.0
64	1.8E-10	113.0	65	1.8E-07	100.0	66	2.8E-06	268.0
67	8.7E-11	65.0	68	4.6E-06	249.0	69	6.4E-08	289.0
70	4.7E-11	81.0	71	4.3E-06	252.0	72	1.5E-09	300.0
73	3.8E-11	87.0	74	2.8E-06	252.0	75	2.5E-13	121.0
76	5.8E-10	304.0	77	7.9E-12	89.0	78	1.1E-06	249.0

Table E.8 (continued)

Obs Node	Conc (uCi/L)	Time (Year)	Obs Node	Conc (uCi/L)	Time (Year)	Obs Node	Conc (uCi/L)	Time (Year)
79	1.2E-12	123.0	80	2.5E-09	121.0	81	1.9E-12	88.0
82	2.0E-08	249.0	83	2.6E-11	120.0	84	2.5E-07	116.0
85	3.3E-12	256.0	86	6.1E-09	250.0	87	1.8E-10	73.0
88	1.3E-05	111.0	89	2.1E-11	249.0	90	1.4E-09	256.0
91	1.2E-08	65.0	92	1.4E-03	109.0	93	1.2E-11	251.0
94	3.7E-11	259.0	95	8.6E-06	64.0	96	3.4E-03	109.0
97	1.4E-12	280.0	98	1.8E-11	260.0	99	2.8E-03	57.0
100	6.5E-03	117.0	101	1.6E-10	278.0	102	9.2E-14	255.0
103	2.6E-03	59.0	104	8.4E-03	116.0	105	9.2E-10	267.0
106	9.4E-08	266.0	107	1.2E-07	266.0	108	8.6E-10	279.0
109	3.2E-11	289.0	110	2.2E-03	63.0	111	8.3E-04	121.0
112	7.0E-07	275.0	113	2.0E-10	63.0	114	1.2E-10	292.0
115	4.7E-04	70.0	116	2.1E-04	126.0	117	3.1E-07	279.0
118	1.9E-12	288.0	119	5.9E-04	70.0	120	2.8E-08	142.0
121	3.2E-07	279.0	122	3.4E-04	70.0	123	6.3E-08	130.0
124	2.6E-07	283.0	125	3.1E-05	82.0	126	2.4E-07	267.0
127	8.0E-05	80.0	128	4.4E-09	265.0	129	6.7E-05	79.0
130	1.5E-09	272.0	131	2.0E-05	81.0	132	2.0E-09	272.0
133	2.9E-06	88.0	134	5.8E-10	279.0	135	1.1E-06	87.0
136	1.3E-11	292.0	137	1.1E-07	84.0	138	2.8E-09	97.0
139	2.3E-07	268.0	140	2.4E-08	269.0	141	1.4E-08	87.0
142	3.2E-10	94.0	143	2.1E-07	292.0	144	7.9E-12	104.0
145	1.0E-13	305.0	146	4.9E-10	305.0	147	1.5E-08	305.0
148	6.3E-08	292.0	149	5.7E-08	299.0	150	1.5E-08	299.0
151	3.3E-13	255.0	152	1.4E-13	91.0	153	4.8E-14	306.0

Table E.8 (continued)

Obs Node	Conc (uCi/L)	Time (Year)	Obs Node	Conc (uCi/L)	Time (Year)	Obs Node	Conc (uCi/L)	Time (Year)
154	1.5E-13	312.0	155	2.0E-13	305.0	156	1.4E-12	305.0
157	2.8E-12	305.0	158	8.8E-18	273.0	159	4.3E-16	281.0
160	2.1E-13	87.0	161	7.8E-12	101.0	162	5.4E-12	102.0
163	1.9E-12	103.0	164	2.4E-14	266.0	165	2.4E-14	260.0
166	1.0E-03	67.0	167	1.3E-03	67.0	168	1.6E-03	67.0
169	1.4E-03	68.0	170	2.8E-08	142.0	171	3.2E-08	144.0
172	4.1E-08	145.0	173	2.8E-06	277.0	174	4.8E-05	270.0
175	2.2E-05	277.0	176	1.5E-06	284.0	177	9.7E-07	290.0
178	8.7E-07	282.0	179	9.8E-07	280.0	180	8.0E-07	286.0
181	5.6E-07	280.0	182	2.7E-09	269.0	183	4.4E-09	263.0
184	8.4E-09	264.0	185	6.9E-07	264.0	186	4.5E-10	309.0
187	6.0E-06	269.0	188	1.8E-05	86.0	189	1.1E-04	97.0
190	8.4E-07	88.0	191	3.2E-07	105.0	192	9.7E-06	268.0
193	1.3E-06	274.0	194	1.2E-06	281.0	195	9.9E-07	281.0
196	9.1E-07	282.0	197	3.5E-07	277.0	198	3.7E-08	69.0
199	2.3E-09	270.0	200	8.2E-10	60.0	201	2.1E-09	276.0
202	6.7E-09	269.0	203	1.0E-08	257.0	204	5.9E-09	256.0
205	5.7E-17	268.0	206	1.4E-14	264.0	207	1.8E-12	259.0
208	4.4E-10	257.0	209	1.3E-07	254.0	210	4.2E-05	249.0
211	6.5E-05	247.0	212	5.9E-04	245.0	213	1.6E-04	246.0
214	1.2E-06	251.0	215	1.5E-08	250.0	216	5.5E-09	250.0
217	1.4E-09	257.0	218	4.0E-09	91.0	219	5.7E-11	89.0
220	3.2E-13	92.0	221	1.0E-15	107.0	222	6.1E-18	1047.0
223	1.6E-15	115.0	224	1.4E-16	57.0	225	2.5E-16	74.0
226	7.5E-14	65.0	227	7.0E-12	62.0	228	2.2E-10	57.0

Table E.8 (continued)

Obs Node	Conc (uCi/L)	Time (Year)	Obs Node	Conc (uCi/L)	Time (Year)	Obs Node	Conc (uCi/L)	Time (Year)
229	5.7E-10	60.0	230	1.1E-09	57.0	231	4.8E-11	64.0
232	4.9E-10	66.0	233	3.9E-09	64.0	234	4.3E-08	60.0
235	4.4E-07	62.0	236	1.7E-05	61.0	237	2.1E-04	60.0
238	1.8E-04	59.0	239	5.8E-05	65.0	240	3.6E-06	73.0
241	4.0E-07	79.0	242	4.3E-08	100.0	243	4.8E-10	243.0
244	3.7E-10	93.0	245	2.5E-10	74.0	246	7.1E-10	75.0
247	3.1E-09	86.0	248	1.1E-08	69.0	249	3.1E-06	81.0
250	4.2E-05	74.0	251	1.3E-04	73.0	252	4.3E-04	73.0
253	1.0E-07	288.0	254	1.3E-07	288.0	255	1.6E-07	287.0
256	1.6E-07	288.0	257	1.5E-08	287.0	258	2.3E-09	300.0
259	2.0E-10	300.0	260	3.5E-11	313.0	261	6.1E-12	319.0
262	1.0E-12	319.0	263	1.5E-13	332.0	264	.0E+00	2.0
265	2.7E-11	289.0	266	6.6E-08	276.0	267	1.6E-05	254.0
268	3.3E-04	253.0	269	3.5E-04	250.0	270	.0E+00	.0
271	1.2E-06	58.0	272	1.6E-04	63.0	273	6.1E-03	250.0
274	1.4E-06	254.0	275	8.7E-08	144.0	276	5.6E-08	138.0
277	2.1E-06	53.0	278	1.2E-04	257.0	279	4.2E-05	262.0
280	1.5E-05	267.0	281	2.3E-06	274.0	282	1.2E-09	80.0
283	8.4E-11	79.0	284	2.7E-10	82.0	285	1.5E-10	85.0
286	2.3E-10	247.0	287	8.7E-09	246.0	288	1.4E-07	245.0
289	9.6E-07	245.0	290	9.5E-08	245.0	291	3.1E-07	89.0
292	2.1E-06	95.0	293	1.1E-06	96.0	294	1.5E-07	104.0
295	2.4E-03	255.0	296	1.3E-03	255.0	297	1.4E-03	254.0
298	9.9E-04	256.0	299	1.9E-03	253.0	300	3.2E-05	53.0
301	4.2E-07	259.0	302	8.7E-09	248.0	303	1.1E-10	262.0
304	3.7E-09	249.0	305	1.6E-09	249.0	306	4.2E-11	250.0

Table E.8 (continued)

Obs Node	Conc (uCi/L)	Time (Year)	Obs Node	Conc (uCi/L)	Time (Year)	Obs Node	Conc (uCi/L)	Time (Year)
307	9.5E-08	247.0	308	1.4E-08	247.0	309	6.6E-12	254.0
310	5.7E-10	253.0	311	7.6E-10	255.0	312	5.5E-10	249.0
313	2.5E-12	254.0	314	1.4E-14	259.0	315	8.6E-15	256.0
316	1.6E-12	253.0	317	5.7E-17	268.0	318	6.1E-18	1590.0
319	6.2E-18	1398.0	320	6.2E-18	1654.0	321	6.2E-18	1655.0
322	6.4E-18	1707.0	323	6.2E-18	1811.0	324	6.1E-18	1256.0
325	2.9E-14	98.0	326	3.0E-15	81.0	327	2.0E-14	85.0
328	2.3E-14	87.0	329	3.8E-14	92.0	330	4.9E-12	85.0
331	3.2E-12	88.0	332	3.6E-10	84.0	333	2.3E-08	84.0
334	1.5E-07	87.0						

Table E.9. Groundwater concentration of nuclide: ^{137}Cs at observation nodes

Obs Node	Conc (uCi/L)	Time (Year)	Obs Node	Conc (uCi/L)	Time (Year)	Obs Node	Conc (uCi/L)	Time (Year)
1	.0E+00	2000.0	2	.0E+00	2000.0	3	.0E+00	2000.0
4	.0E+00	2000.0	5	.0E+00	2000.0	6	.0E+00	2000.0
7	.0E+00	2000.0	8	.0E+00	2000.0	9	.0E+00	2000.0
10	.0E+00	2000.0	11	.0E+00	2000.0	12	.0E+00	2000.0
13	.0E+00	2000.0	14	.0E+00	2000.0	15	.0E+00	2000.0
16	.0E+00	2000.0	17	.0E+00	2000.0	18	.0E+00	87.0
19	.0E+00	296.0	20	.0E+00	2000.0	21	.0E+00	59.0
22	2.8E-31	462.0	23	.0E+00	2000.0	24	3.5E-32	57.0
25	.0E+00	2000.0	26	4.1E-30	462.0	27	.0E+00	2000.0
28	.0E+00	8.0	29	.0E+00	2000.0	30	4.2E-29	462.0
31	.0E+00	2000.0	32	.0E+00	25.0	33	.0E+00	130.0
34	4.8E-28	422.0	35	1.6E-34	496.0	36	1.2E-26	51.0
37	5.2E-24	153.0	38	.0E+00	153.0	39	.0E+00	2.0
40	1.6E-17	216.0	41	2.6E-32	392.0	42	.0E+00	2.0
43	1.2E-17	216.0	44	.0E+00	120.0	45	1.3E-25	422.0
46	1.5E-19	78.0	47	6.5E-32	391.0	48	1.2E-25	422.0
49	8.7E-17	216.0	50	8.5E-28	347.0	51	5.0E-26	422.0
52	.0E+00	2.0	53	1.8E-28	347.0	54	5.1E-32	464.0
55	4.6E-26	72.0	56	2.1E-29	347.0	57	3.0E-32	465.0
58	3.9E-33	10.0	59	5.7E-31	348.0	60	5.2E-33	465.0
61	.0E+00	15.0	62	2.8E-31	348.0	63	.0E+00	2000.0
64	.0E+00	123.0	65	.0E+00	2000.0	66	.0E+00	2000.0
67	.0E+00	2000.0	68	.0E+00	2000.0	69	.0E+00	2000.0
70	.0E+00	2000.0	71	.0E+00	2000.0	72	.0E+00	2000.0
73	.0E+00	2000.0	74	.0E+00	2000.0	75	.0E+00	2000.0
76	.0E+00	74.0	77	.0E+00	2000.0	78	.0E+00	2000.0

Table E.9 (continued)

Obs Node	Conc (uCi/L)	Time (Year)	Obs Node	Conc (uCi/L)	Time (Year)	Obs Node	Conc (uCi/L)	Time (Year)
79	4.1E-34	383.0	80	2.3E-24	299.0	81	.0E+00	2000.0
82	.0E+00	2000.0	83	.0E+00	45.0	84	5.9E-20	256.0
85	.0E+00	2000.0	86	.0E+00	2000.0	87	.0E+00	6.0
88	.0E+00	2.0	89	.0E+00	2000.0	90	.0E+00	2000.0
91	2.0E-19	210.0	92	1.3E-18	256.0	93	.0E+00	2000.0
94	.0E+00	2000.0	95	.0E+00	2.0	96	2.6E-18	252.0
97	.0E+00	2000.0	98	.0E+00	2000.0	99	3.6E-17	210.0
100	5.5E-18	265.0	101	.0E+00	2000.0	102	.0E+00	2000.0
103	1.3E-21	253.0	104	4.7E-18	266.0	105	.0E+00	297.0
106	.0E+00	2000.0	107	.0E+00	2000.0	108	.0E+00	2000.0
109	.0E+00	2000.0	110	2.3E-22	253.0	111	.0E+00	4.0
112	.0E+00	2000.0	113	.0E+00	2000.0	114	.0E+00	2000.0
115	3.8E-28	296.0	116	1.3E-25	309.0	117	.0E+00	2000.0
118	.0E+00	2000.0	119	3.1E-29	296.0	120	3.2E-27	309.0
121	.0E+00	2000.0	122	8.4E-31	297.0	123	1.6E-32	353.0
124	.0E+00	2000.0	125	.0E+00	2000.0	126	.0E+00	2000.0
127	.0E+00	2000.0	128	.0E+00	2000.0	129	.0E+00	2000.0
130	.0E+00	2000.0	131	.0E+00	2000.0	132	.0E+00	2000.0
133	.0E+00	2000.0	134	.0E+00	2000.0	135	.0E+00	2000.0
136	.0E+00	2000.0	137	.0E+00	2000.0	138	.0E+00	2000.0
139	.0E+00	2000.0	140	.0E+00	2000.0	141	.0E+00	2000.0
142	.0E+00	2000.0	143	.0E+00	2000.0	144	.0E+00	2000.0
145	.0E+00	2000.0	146	.0E+00	2000.0	147	.0E+00	2000.0
148	.0E+00	2000.0	149	.0E+00	2000.0	150	.0E+00	2000.0
151	.0E+00	2000.0	152	.0E+00	2000.0	153	.0E+00	2000.0
154	.0E+00	2000.0	155	.0E+00	2000.0	156	.0E+00	2000.0

Table E.9 (continued)

Obs Node	Conc (uCi/L)	Time (Year)	Obs Node	Conc (uCi/L)	Time (Year)	Obs Node	Conc (uCi/L)	Time (Year)
157	.0E+00	2000.0	158	.0E+00	2000.0	159	.0E+00	2000.0
160	.0E+00	2000.0	161	.0E+00	2000.0	162	.0E+00	2000.0
163	.0E+00	2000.0	164	.0E+00	2000.0	165	.0E+00	2000.0
166	1.6E-23	253.0	167	1.8E-23	253.0	168	1.9E-23	253.0
169	2.3E-24	253.0	170	3.2E-27	309.0	171	6.6E-32	352.0
172	.0E+00	2000.0	173	.0E+00	205.0	174	2.1E-28	422.0
175	1.7E-32	464.0	176	6.4E-34	495.0	177	.0E+00	2000.0
178	.0E+00	2000.0	179	.0E+00	2000.0	180	.0E+00	2000.0
181	.0E+00	2000.0	182	2.1E-35	119.0	183	.0E+00	2000.0
184	.0E+00	2000.0	185	.0E+00	2000.0	186	.0E+00	2000.0
187	.0E+00	2000.0	188	8.7E-28	347.0	189	7.8E-27	304.0
190	2.6E-30	347.0	191	1.1E-31	347.0	192	.0E+00	2000.0
193	.0E+00	2000.0	194	.0E+00	2000.0	195	.0E+00	2000.0
196	.0E+00	2000.0	197	.0E+00	2000.0	198	.0E+00	2000.0
199	.0E+00	2000.0	200	.0E+00	2000.0	201	.0E+00	157.0
202	.0E+00	101.0	203	1.0E-31	73.0	204	2.2E-23	249.0
205	1.9E-29	60.0	206	6.0E-25	420.0	207	.0E+00	3.0
208	5.0E-28	462.0	209	.0E+00	2.0	210	.0E+00	1.0
211	3.1E-17	339.0	212	4.9E-16	339.0	213	.0E+00	1.0
214	.0E+00	2.0	215	.0E+00	2.0	216	2.9E-18	205.0
217	9.3E-14	161.0	218	2.8E-18	205.0	219	6.3E-26	304.0
220	.0E+00	95.0	221	4.5E-34	558.0	222	1.6E-34	580.0
223	.0E+00	2000.0	224	.0E+00	2000.0	225	.0E+00	2000.0
226	.0E+00	135.0	227	.0E+00	44.0	228	2.9E-24	253.0
229	2.4E-24	253.0	230	2.4E-24	253.0	231	1.3E-28	296.0
232	4.8E-25	253.0	233	4.3E-24	253.0	234	2.7E-20	210.0

Table E.9 (continued)

Obs Node	Conc (uCi/L)	Time (Year)	Obs Node	Conc (uCi/L)	Time (Year)	Obs Node	Conc (uCi/L)	Time (Year)
235	2.4E-19	210.0	236	6.1E-15	167.0	237	8.9E-14	167.0
238	5.1E-14	167.0	239	.0E+00	1.0	240	.0E+00	2.0
241	.0E+00	4.0	242	.0E+00	43.0	243	.0E+00	147.0
244	.0E+00	2000.0	245	.0E+00	2000.0	246	.0E+00	2000.0
247	.0E+00	2000.0	248	.0E+00	2000.0	249	2.3E-30	296.0
250	8.7E-29	296.0	251	1.1E-28	296.0	252	4.8E-25	253.0
253	.0E+00	2000.0	254	.0E+00	2000.0	255	.0E+00	2000.0
256	.0E+00	2000.0	257	3.2E-34	439.0	258	1.3E-31	342.0
259	2.6E-31	342.0	260	.0E+00	2000.0	261	.0E+00	2000.0
262	.0E+00	2000.0	263	.0E+00	2000.0	264	.0E+00	118.0
265	.0E+00	10.0	266	4.3E-26	51.0	267	1.8E-18	339.0
268	3.6E-17	339.0	269	5.6E-17	339.0	270	.0E+00	1.0
271	6.7E-22	50.0	272	2.6E-17	339.0	273	1.9E-17	339.0
274	4.3E-23	380.0	275	.0E+00	18.0	276	.0E+00	223.0
277	.0E+00	1.0	278	3.3E-22	380.0	279	7.7E-27	422.0
280	2.6E-31	464.0	281	.0E+00	2000.0	282	.0E+00	2000.0
283	.0E+00	2000.0	284	.0E+00	2000.0	285	.0E+00	2000.0
286	.0E+00	2000.0	287	.0E+00	2000.0	288	.0E+00	2000.0
289	.0E+00	2000.0	290	.0E+00	97.0	291	.0E+00	10.0
292	5.3E-27	304.0	293	1.9E-26	304.0	294	7.6E-32	347.0
295	8.9E-22	380.0	296	2.3E-22	380.0	297	5.8E-23	380.0
298	.0E+00	2.0	299	8.9E-21	380.0	300	7.1E-25	57.0
301	4.8E-23	379.0	302	.0E+00	1.0	303	7.6E-14	161.0
304	2.9E-14	161.0	305	.0E+00	1.0	306	6.4E-15	337.0
307	1.1E-15	337.0	308	5.6E-16	337.0	309	1.6E-18	205.0
310	.0E+00	1.0	311	1.4E-13	161.0	312	9.8E-15	337.0

Table E.9 (continued)

Obs Node	Conc (uCi/L)	Time (Year)	Obs Node	Conc (uCi/L)	Time (Year)	Obs Node	Conc (uCi/L)	Time (Year)
313	.0E+00	1.0	314	5.8E-20	378.0	315	5.0E-15	337.0
316	7.7E-15	337.0	317	1.9E-29	60.0	318	.0E+00	2000.0
319	.0E+00	2000.0	320	.0E+00	2000.0	321	.0E+00	2000.0
322	.0E+00	2000.0	323	1.1E-30	462.0	324	1.4E-34	506.0
325	4.3E-31	347.0	326	3.5E-31	348.0	327	.0E+00	102.0
328	.0E+00	105.0	329	5.5E-32	347.0	330	4.7E-27	304.0
331	1.6E-30	347.0	332	.0E+00	67.0	333	2.6E-28	347.0
334	.0E+00	34.0						

Table E.10. Groundwater concentration of nuclide: ^{152}Eu at observation nodes

Obs Node	Conc (uCi/L)	Time (Year)	Obs Node	Conc (uCi/L)	Time (Year)	Obs Node	Conc (uCi/L)	Time (Year)
1	.0E+00	2000.0	2	.0E+00	2000.0	3	.0E+00	2000.0
4	.0E+00	2000.0	5	.0E+00	2000.0	6	.0E+00	2000.0
7	.0E+00	2000.0	8	.0E+00	2000.0	9	.0E+00	2000.0
10	.0E+00	2000.0	11	.0E+00	2000.0	12	.0E+00	2000.0
13	.0E+00	2000.0	14	.0E+00	2000.0	15	.0E+00	2000.0
16	.0E+00	2000.0	17	.0E+00	2000.0	18	.0E+00	2000.0
19	.0E+00	2000.0	20	.0E+00	2000.0	21	.0E+00	2000.0
22	.0E+00	2000.0	23	.0E+00	2000.0	24	.0E+00	2000.0
25	.0E+00	2000.0	26	.0E+00	2000.0	27	.0E+00	2000.0
28	.0E+00	2000.0	29	.0E+00	2000.0	30	.0E+00	2000.0
31	.0E+00	2000.0	32	.0E+00	2000.0	33	.0E+00	2000.0
34	.0E+00	2000.0	35	.0E+00	2000.0	36	.0E+00	2000.0
37	2.9E-27	58.0	38	.0E+00	2000.0	39	.0E+00	2000.0
40	1.6E-20	135.0	41	.0E+00	2000.0	42	.0E+00	2000.0
43	1.3E-20	133.0	44	.0E+00	2000.0	45	.0E+00	2000.0
46	7.4E-21	66.0	47	.0E+00	2000.0	48	.0E+00	2000.0
49	9.1E-20	135.0	50	7.6E-32	194.0	51	.0E+00	2000.0
52	.0E+00	2.0	53	1.6E-32	194.0	54	.0E+00	2000.0
55	2.7E-27	64.0	56	1.9E-33	191.0	57	.0E+00	2000.0
58	1.2E-33	10.0	59	.0E+00	2000.0	60	.0E+00	2000.0
61	.0E+00	21.0	62	.0E+00	2000.0	63	.0E+00	2000.0
64	.0E+00	2000.0	65	.0E+00	2000.0	66	.0E+00	2000.0
67	.0E+00	2000.0	68	.0E+00	2000.0	69	.0E+00	2000.0
70	.0E+00	2000.0	71	.0E+00	2000.0	72	.0E+00	2000.0
73	.0E+00	2000.0	74	.0E+00	2000.0	75	.0E+00	2000.0
76	.0E+00	2000.0	77	.0E+00	2000.0	78	.0E+00	2000.0

Table E.10 (continued)

Obs Node	Conc (uCi/L)	Time (Year)	Obs Node	Conc (uCi/L)	Time (Year)	Obs Node	Conc (uCi/L)	Time (Year)
79	.0E+00	2000.0	80	.0E+00	2000.0	81	.0E+00	2000.0
82	.0E+00	2000.0	83	.0E+00	2000.0	84	.0E+00	2000.0
85	.0E+00	2000.0	86	.0E+00	2000.0	87	.0E+00	2000.0
88	.0E+00	2000.0	89	.0E+00	2000.0	90	.0E+00	2000.0
91	.0E+00	2000.0	92	.0E+00	2000.0	93	.0E+00	2000.0
94	.0E+00	2000.0	95	.0E+00	2000.0	96	.0E+00	2000.0
97	.0E+00	2000.0	98	.0E+00	2000.0	99	.0E+00	2000.0
100	.0E+00	2000.0	101	.0E+00	2000.0	102	.0E+00	2000.0
103	.0E+00	2000.0	104	.0E+00	2000.0	105	.0E+00	2000.0
106	.0E+00	2000.0	107	.0E+00	2000.0	108	.0E+00	2000.0
109	.0E+00	2000.0	110	.0E+00	2000.0	111	.0E+00	2000.0
112	.0E+00	2000.0	113	.0E+00	2000.0	114	.0E+00	2000.0
115	.0E+00	2000.0	116	.0E+00	2000.0	117	.0E+00	2000.0
118	.0E+00	2000.0	119	.0E+00	2000.0	120	.0E+00	2000.0
121	.0E+00	2000.0	122	.0E+00	2000.0	123	.0E+00	2000.0
124	.0E+00	2000.0	125	.0E+00	2000.0	126	.0E+00	2000.0
127	.0E+00	2000.0	128	.0E+00	2000.0	129	.0E+00	2000.0
130	.0E+00	2000.0	131	.0E+00	2000.0	132	.0E+00	2000.0
133	.0E+00	2000.0	134	.0E+00	2000.0	135	.0E+00	2000.0
136	.0E+00	2000.0	137	.0E+00	2000.0	138	.0E+00	2000.0
139	.0E+00	2000.0	140	.0E+00	2000.0	141	.0E+00	2000.0
142	.0E+00	2000.0	143	.0E+00	2000.0	144	.0E+00	2000.0
145	.0E+00	2000.0	146	.0E+00	2000.0	147	.0E+00	2000.0
148	.0E+00	2000.0	149	.0E+00	2000.0	150	.0E+00	2000.0
151	.0E+00	2000.0	152	.0E+00	2000.0	153	.0E+00	2000.0
154	.0E+00	2000.0	155	.0E+00	2000.0	156	.0E+00	2000.0

Table E.10 (continued)

Obs Node	Conc (uCi/L)	Time (Year)	Obs Node	Conc (uCi/L)	Time (Year)	Obs Node	Conc (uCi/L)	Time (Year)
157	.0E+00	2000.0	158	.0E+00	2000.0	159	.0E+00	2000.0
160	.0E+00	2000.0	161	.0E+00	2000.0	162	.0E+00	2000.0
163	.0E+00	2000.0	164	.0E+00	2000.0	165	.0E+00	2000.0
166	.0E+00	2000.0	167	.0E+00	2000.0	168	.0E+00	2000.0
169	.0E+00	2000.0	170	.0E+00	2000.0	171	.0E+00	2000.0
172	.0E+00	2000.0	173	.0E+00	2000.0	174	.0E+00	2000.0
175	.0E+00	2000.0	176	.0E+00	2000.0	177	.0E+00	2000.0
178	.0E+00	2000.0	179	.0E+00	2000.0	180	.0E+00	2000.0
181	.0E+00	2000.0	182	.0E+00	2000.0	183	.0E+00	2000.0
184	.0E+00	2000.0	185	.0E+00	2000.0	186	.0E+00	2000.0
187	.0E+00	2000.0	188	7.8E-32	194.0	189	1.6E-30	174.0
190	2.8E-34	200.0	191	.0E+00	2000.0	192	.0E+00	2000.0
193	.0E+00	2000.0	194	.0E+00	2000.0	195	.0E+00	2000.0
196	.0E+00	2000.0	197	.0E+00	2000.0	198	.0E+00	2000.0
199	.0E+00	2000.0	200	.0E+00	2000.0	201	.0E+00	2000.0
202	.0E+00	2000.0	203	.0E+00	2000.0	204	.0E+00	129.0
205	.0E+00	2000.0	206	.0E+00	2000.0	207	.0E+00	2000.0
208	.0E+00	2000.0	209	.0E+00	2000.0	210	.0E+00	2000.0
211	.0E+00	2000.0	212	.0E+00	2000.0	213	.0E+00	2000.0
214	.0E+00	2000.0	215	.0E+00	2000.0	216	3.0E-34	242.0
217	2.7E-30	100.0	218	1.4E-25	83.0	219	1.3E-29	174.0
220	.0E+00	2000.0	221	.0E+00	2000.0	222	.0E+00	2000.0
223	.0E+00	2000.0	224	.0E+00	2000.0	225	.0E+00	2000.0
226	.0E+00	2000.0	227	.0E+00	2000.0	228	.0E+00	2000.0
229	.0E+00	2000.0	230	.0E+00	2000.0	231	.0E+00	2000.0
232	.0E+00	2000.0	233	.0E+00	2000.0	234	.0E+00	2000.0

Table E.10 (continued)

Obs Node	Conc (uCi/L)	Time (Year)	Obs Node	Conc (uCi/L)	Time (Year)	Obs Node	Conc (uCi/L)	Time (Year)
235	.0E+00	2000.0	236	.0E+00	2000.0	237	.0E+00	2000.0
238	.0E+00	2000.0	239	.0E+00	2000.0	240	.0E+00	2000.0
241	.0E+00	2000.0	242	.0E+00	2000.0	243	.0E+00	2000.0
244	.0E+00	2000.0	245	.0E+00	2000.0	246	.0E+00	2000.0
247	.0E+00	2000.0	248	.0E+00	2000.0	249	.0E+00	2000.0
250	.0E+00	2000.0	251	.0E+00	2000.0	252	.0E+00	2000.0
253	.0E+00	2000.0	254	.0E+00	2000.0	255	.0E+00	2000.0
256	.0E+00	2000.0	257	.0E+00	2000.0	258	.0E+00	2000.0
259	.0E+00	2000.0	260	.0E+00	2000.0	261	.0E+00	2000.0
262	.0E+00	2000.0	263	.0E+00	2000.0	264	.0E+00	2000.0
265	.0E+00	2000.0	266	.0E+00	2000.0	267	.0E+00	2000.0
268	.0E+00	2000.0	269	.0E+00	2000.0	270	.0E+00	2000.0
271	.0E+00	2000.0	272	.0E+00	2000.0	273	.0E+00	2000.0
274	.0E+00	2000.0	275	.0E+00	2000.0	276	.0E+00	2000.0
277	.0E+00	2000.0	278	.0E+00	2000.0	279	.0E+00	2000.0
280	.0E+00	2000.0	281	.0E+00	2000.0	282	.0E+00	2000.0
283	.0E+00	2000.0	284	.0E+00	2000.0	285	.0E+00	2000.0
286	.0E+00	2000.0	287	.0E+00	2000.0	288	.0E+00	2000.0
289	.0E+00	2000.0	290	.0E+00	2000.0	291	.0E+00	14.0
292	1.1E-30	174.0	293	3.9E-30	174.0	294	.0E+00	2000.0
295	.0E+00	2000.0	296	.0E+00	2000.0	297	.0E+00	2000.0
298	.0E+00	2000.0	299	.0E+00	2000.0	300	.0E+00	2000.0
301	.0E+00	2000.0	302	.0E+00	2000.0	303	.0E+00	2000.0
304	.0E+00	2000.0	305	.0E+00	2000.0	306	.0E+00	2000.0
307	.0E+00	2000.0	308	.0E+00	2000.0	309	.0E+00	2000.0
310	1.2E-29	173.0	311	2.8E-30	96.0	312	.0E+00	2000.0

Table E.10 (continued)

Obs Node	Conc (uCi/L)	Time (Year)	Obs Node	Conc (uCi/L)	Time (Year)	Obs Node	Conc (uCi/L)	Time (Year)
313	.0E+00	2000.0	314	.0E+00	2000.0	315	.0E+00	2000.0
316	.0E+00	2000.0	317	.0E+00	2000.0	318	.0E+00	2000.0
319	.0E+00	2000.0	320	.0E+00	2000.0	321	.0E+00	2000.0
322	.0E+00	2000.0	323	.0E+00	2000.0	324	.0E+00	2000.0
325	.0E+00	2000.0	326	.0E+00	2000.0	327	.0E+00	2000.0
328	.0E+00	2000.0	329	.0E+00	2000.0	330	9.4E-31	174.0
331	.0E+00	2000.0	332	.0E+00	103.0	333	2.4E-32	195.0
334	.0E+00	64.0						

Table E.11. Groundwater concentration of nuclide: ^{154}Eu at observation nodes

Obs Node	Conc (uCi/L)	Time (Year)	Obs Node	Conc (uCi/L)	Time (Year)	Obs Node	Conc (uCi/L)	Time (Year)
1	.0E+00	2000.0	2	.0E+00	2000.0	3	.0E+00	2000.0
4	.0E+00	2000.0	5	.0E+00	2000.0	6	.0E+00	2000.0
7	.0E+00	2000.0	8	.0E+00	2000.0	9	.0E+00	2000.0
10	.0E+00	2000.0	11	.0E+00	2000.0	12	.0E+00	2000.0
13	.0E+00	2000.0	14	.0E+00	2000.0	15	.0E+00	2000.0
16	.0E+00	2000.0	17	.0E+00	2000.0	18	.0E+00	2000.0
19	.0E+00	2000.0	20	.0E+00	2000.0	21	.0E+00	2000.0
22	.0E+00	2000.0	23	.0E+00	2000.0	24	.0E+00	2000.0
25	.0E+00	2000.0	26	.0E+00	2000.0	27	.0E+00	2000.0
28	.0E+00	2000.0	29	.0E+00	2000.0	30	.0E+00	2000.0
31	.0E+00	2000.0	32	.0E+00	2000.0	33	.0E+00	2000.0
34	.0E+00	2000.0	35	.0E+00	2000.0	36	.0E+00	2000.0
37	2.6E-29	58.0	38	.0E+00	2000.0	39	.0E+00	2000.0
40	6.7E-23	116.0	41	.0E+00	2000.0	42	.0E+00	2000.0
43	5.6E-23	115.0	44	.0E+00	2000.0	45	.0E+00	2000.0
46	6.9E-23	62.0	47	.0E+00	2000.0	48	.0E+00	2000.0
49	3.8E-22	116.0	50	1.4E-34	164.0	51	.0E+00	2000.0
52	.0E+00	2.0	53	.0E+00	2000.0	54	.0E+00	2000.0
55	2.2E-29	60.0	56	.0E+00	2000.0	57	.0E+00	2000.0
58	.0E+00	10.0	59	.0E+00	2000.0	60	.0E+00	2000.0
61	.0E+00	97.0	62	.0E+00	2000.0	63	.0E+00	2000.0
64	.0E+00	2000.0	65	.0E+00	2000.0	66	.0E+00	2000.0
67	.0E+00	2000.0	68	.0E+00	2000.0	69	.0E+00	2000.0
70	.0E+00	2000.0	71	.0E+00	2000.0	72	.0E+00	2000.0
73	.0E+00	2000.0	74	.0E+00	2000.0	75	.0E+00	2000.0
76	.0E+00	2000.0	77	.0E+00	2000.0	78	.0E+00	2000.0

Table E.11 (continued)

Obs Node	Conc (uCi/L)	Time (Year)	Obs Node	Conc (uCi/L)	Time (Year)	Obs Node	Conc (uCi/L)	Time (Year)
79	.0E+00	2000.0	80	.0E+00	2000.0	81	.0E+00	2000.0
82	.0E+00	2000.0	83	.0E+00	2000.0	84	.0E+00	2000.0
85	.0E+00	2000.0	86	.0E+00	2000.0	87	.0E+00	2000.0
88	.0E+00	2000.0	89	.0E+00	2000.0	90	.0E+00	2000.0
91	.0E+00	2000.0	92	.0E+00	2000.0	93	.0E+00	2000.0
94	.0E+00	2000.0	95	.0E+00	2000.0	96	.0E+00	2000.0
97	.0E+00	2000.0	98	.0E+00	2000.0	99	.0E+00	2000.0
100	.0E+00	2000.0	101	.0E+00	2000.0	102	.0E+00	2000.0
103	.0E+00	2000.0	104	.0E+00	2000.0	105	.0E+00	2000.0
106	.0E+00	2000.0	107	.0E+00	2000.0	108	.0E+00	2000.0
109	.0E+00	2000.0	110	.0E+00	2000.0	111	.0E+00	2000.0
112	.0E+00	2000.0	113	.0E+00	2000.0	114	.0E+00	2000.0
115	.0E+00	2000.0	116	.0E+00	2000.0	117	.0E+00	2000.0
118	.0E+00	2000.0	119	.0E+00	2000.0	120	.0E+00	2000.0
121	.0E+00	2000.0	122	.0E+00	2000.0	123	.0E+00	2000.0
124	.0E+00	2000.0	125	.0E+00	2000.0	126	.0E+00	2000.0
127	.0E+00	2000.0	128	.0E+00	2000.0	129	.0E+00	2000.0
130	.0E+00	2000.0	131	.0E+00	2000.0	132	.0E+00	2000.0
133	.0E+00	2000.0	134	.0E+00	2000.0	135	.0E+00	2000.0
136	.0E+00	2000.0	137	.0E+00	2000.0	138	.0E+00	2000.0
139	.0E+00	2000.0	140	.0E+00	2000.0	141	.0E+00	2000.0
142	.0E+00	2000.0	143	.0E+00	2000.0	144	.0E+00	2000.0
145	.0E+00	2000.0	146	.0E+00	2000.0	147	.0E+00	2000.0
148	.0E+00	2000.0	149	.0E+00	2000.0	150	.0E+00	2000.0
151	.0E+00	2000.0	152	.0E+00	2000.0	153	.0E+00	2000.0
154	.0E+00	2000.0	155	.0E+00	2000.0	156	.0E+00	2000.0

Table E.11 (continued)

Obs Node	Conc (uCi/L)	Time (Year)	Obs Node	Conc (uCi/L)	Time (Year)	Obs Node	Conc (uCi/L)	Time (Year)
157	.0E+00	2000.0	158	.0E+00	2000.0	159	.0E+00	2000.0
160	.0E+00	2000.0	161	.0E+00	2000.0	162	.0E+00	2000.0
163	.0E+00	2000.0	164	.0E+00	2000.0	165	.0E+00	2000.0
166	.0E+00	2000.0	167	.0E+00	2000.0	168	.0E+00	2000.0
169	.0E+00	2000.0	170	.0E+00	2000.0	171	.0E+00	2000.0
172	.0E+00	2000.0	173	.0E+00	2000.0	174	.0E+00	2000.0
175	.0E+00	2000.0	176	.0E+00	2000.0	177	.0E+00	2000.0
178	.0E+00	2000.0	179	.0E+00	2000.0	180	.0E+00	2000.0
181	.0E+00	2000.0	182	.0E+00	2000.0	183	.0E+00	2000.0
184	.0E+00	2000.0	185	.0E+00	2000.0	186	.0E+00	2000.0
187	.0E+00	2000.0	188	1.5E-34	173.0	189	2.8E-33	142.0
190	.0E+00	2000.0	191	.0E+00	2000.0	192	.0E+00	2000.0
193	.0E+00	2000.0	194	.0E+00	2000.0	195	.0E+00	2000.0
196	.0E+00	2000.0	197	.0E+00	2000.0	198	.0E+00	2000.0
199	.0E+00	2000.0	200	.0E+00	2000.0	201	.0E+00	2000.0
202	.0E+00	2000.0	203	.0E+00	2000.0	204	.0E+00	2000.0
205	.0E+00	2000.0	206	.0E+00	2000.0	207	.0E+00	2000.0
208	.0E+00	2000.0	209	.0E+00	2000.0	210	.0E+00	2000.0
211	.0E+00	2000.0	212	.0E+00	2000.0	213	.0E+00	2000.0
214	.0E+00	2000.0	215	.0E+00	2000.0	216	.0E+00	2000.0
217	1.2E-32	90.0	218	8.9E-28	72.0	219	2.4E-32	142.0
220	.0E+00	2000.0	221	.0E+00	2000.0	222	.0E+00	2000.0
223	.0E+00	2000.0	224	.0E+00	2000.0	225	.0E+00	2000.0
226	.0E+00	2000.0	227	.0E+00	2000.0	228	.0E+00	2000.0
229	.0E+00	2000.0	230	.0E+00	2000.0	231	.0E+00	2000.0
232	.0E+00	2000.0	233	.0E+00	2000.0	234	.0E+00	2000.0

Table E.11 (continued)

Obs Node	Conc (uCi/L)	Time (Year)	Obs Node	Conc (uCi/L)	Time (Year)	Obs Node	Conc (uCi/L)	Time (Year)
235	.0E+00	2000.0	236	.0E+00	2000.0	237	.0E+00	2000.0
238	.0E+00	2000.0	239	.0E+00	2000.0	240	.0E+00	2000.0
241	.0E+00	2000.0	242	.0E+00	2000.0	243	.0E+00	2000.0
244	.0E+00	2000.0	245	.0E+00	2000.0	246	.0E+00	2000.0
247	.0E+00	2000.0	248	.0E+00	2000.0	249	.0E+00	2000.0
250	.0E+00	2000.0	251	.0E+00	2000.0	252	.0E+00	2000.0
253	.0E+00	2000.0	254	.0E+00	2000.0	255	.0E+00	2000.0
256	.0E+00	2000.0	257	.0E+00	2000.0	258	.0E+00	2000.0
259	.0E+00	2000.0	260	.0E+00	2000.0	261	.0E+00	2000.0
262	.0E+00	2000.0	263	.0E+00	2000.0	264	.0E+00	2000.0
265	.0E+00	2000.0	266	.0E+00	2000.0	267	.0E+00	2000.0
268	.0E+00	2000.0	269	.0E+00	2000.0	270	.0E+00	2000.0
271	.0E+00	2000.0	272	.0E+00	2000.0	273	.0E+00	2000.0
274	.0E+00	2000.0	275	.0E+00	2000.0	276	.0E+00	2000.0
277	.0E+00	2000.0	278	.0E+00	2000.0	279	.0E+00	2000.0
280	.0E+00	2000.0	281	.0E+00	2000.0	282	.0E+00	2000.0
283	.0E+00	2000.0	284	.0E+00	2000.0	285	.0E+00	2000.0
286	.0E+00	2000.0	287	.0E+00	2000.0	288	.0E+00	2000.0
289	.0E+00	2000.0	290	.0E+00	2000.0	291	.0E+00	38.0
292	2.0E-33	144.0	293	7.2E-33	141.0	294	.0E+00	2000.0
295	.0E+00	2000.0	296	.0E+00	2000.0	297	.0E+00	2000.0
298	.0E+00	2000.0	299	.0E+00	2000.0	300	.0E+00	2000.0
301	.0E+00	2000.0	302	.0E+00	2000.0	303	.0E+00	2000.0
304	.0E+00	2000.0	305	.0E+00	2000.0	306	.0E+00	2000.0
307	.0E+00	2000.0	308	.0E+00	2000.0	309	.0E+00	2000.0
310	2.2E-32	140.0	311	1.3E-32	86.0	312	.0E+00	2000.0

Table E.11 (continued)

Obs Node	Conc (uCi/L)	Time (Year)	Obs Node	Conc (uCi/L)	Time (Year)	Obs Node	Conc (uCi/L)	Time (Year)
313	.0E+00	2000.0	314	.0E+00	2000.0	315	.0E+00	2000.0
316	.0E+00	2000.0	317	.0E+00	2000.0	318	.0E+00	2000.0
319	.0E+00	2000.0	320	.0E+00	2000.0	321	.0E+00	2000.0
322	.0E+00	2000.0	323	.0E+00	2000.0	324	.0E+00	2000.0
325	.0E+00	2000.0	326	.0E+00	2000.0	327	.0E+00	2000.0
328	.0E+00	2000.0	329	.0E+00	2000.0	330	1.7E-33	143.0
331	.0E+00	2000.0	332	.0E+00	2000.0	333	.0E+00	2000.0
334	.0E+00	134.0						

Table E.12. Groundwater concentration of nuclide: ^{226}Ra at observation nodes

Obs Node	Conc (uCi/L)	Time (Year)	Obs Node	Conc (uCi/L)	Time (Year)	Obs Node	Conc (uCi/L)	Time (Year)
1	.0E+00	5000.0	2	.0E+00	5000.0	3	.0E+00	5000.0
4	.0E+00	5000.0	5	.0E+00	5000.0	6	.0E+00	5000.0
7	.0E+00	5000.0	8	.0E+00	5000.0	9	.0E+00	5000.0
10	.0E+00	5000.0	11	.0E+00	5000.0	12	.0E+00	5000.0
13	.0E+00	5000.0	14	.0E+00	5000.0	15	.0E+00	5000.0
16	.0E+00	5000.0	17	.0E+00	5000.0	18	.0E+00	5000.0
19	.0E+00	5000.0	20	.0E+00	5000.0	21	.0E+00	5000.0
22	.0E+00	5000.0	23	.0E+00	5000.0	24	.0E+00	5000.0
25	.0E+00	5000.0	26	.0E+00	5000.0	27	.0E+00	5000.0
28	.0E+00	5000.0	29	.0E+00	5000.0	30	.0E+00	5000.0
31	.0E+00	5000.0	32	.0E+00	5000.0	33	.0E+00	5000.0
34	.0E+00	5000.0	35	.0E+00	5000.0	36	.0E+00	5000.0
37	.0E+00	5000.0	38	.0E+00	5000.0	39	.0E+00	5000.0
40	.0E+00	5000.0	41	.0E+00	5000.0	42	.0E+00	5000.0
43	.0E+00	5000.0	44	.0E+00	5000.0	45	.0E+00	5000.0
46	.0E+00	5000.0	47	.0E+00	5000.0	48	.0E+00	5000.0
49	.0E+00	5000.0	50	.0E+00	5000.0	51	.0E+00	5000.0
52	.0E+00	5000.0	53	.0E+00	5000.0	54	.0E+00	5000.0
55	.0E+00	5000.0	56	.0E+00	5000.0	57	.0E+00	5000.0
58	.0E+00	5000.0	59	.0E+00	5000.0	60	.0E+00	5000.0
61	.0E+00	5000.0	62	.0E+00	5000.0	63	.0E+00	5000.0
64	.0E+00	5000.0	65	.0E+00	5000.0	66	.0E+00	5000.0
67	.0E+00	5000.0	68	.0E+00	5000.0	69	.0E+00	5000.0
70	.0E+00	5000.0	71	.0E+00	5000.0	72	.0E+00	5000.0
73	.0E+00	5000.0	74	.0E+00	5000.0	75	.0E+00	5000.0
76	1.6E-32	5000.0	77	.0E+00	5000.0	78	.0E+00	5000.0

Table E.12 (continued)

Obs Node	Conc (uCi/L)	Time (Year)	Obs Node	Conc (uCi/L)	Time (Year)	Obs Node	Conc (uCi/L)	Time (Year)
79	.0E+00	3600.0	80	2.0E-27	5000.0	81	.0E+00	5000.0
82	.0E+00	5000.0	83	.0E+00	4128.0	84	8.9E-24	5000.0
85	.0E+00	5000.0	86	.0E+00	5000.0	87	6.8E-34	5000.0
88	1.8E-20	5000.0	89	.0E+00	5000.0	90	.0E+00	5000.0
91	.0E+00	5000.0	92	1.4E-17	5000.0	93	.0E+00	5000.0
94	.0E+00	5000.0	95	.0E+00	5000.0	96	.0E+00	2.0
97	.0E+00	5000.0	98	.0E+00	5000.0	99	.0E+00	5000.0
100	1.0E-15	5000.0	101	.0E+00	5000.0	102	.0E+00	5000.0
103	5.0E-33	5000.0	104	9.6E-16	5000.0	105	.0E+00	5000.0
106	.0E+00	5000.0	107	.0E+00	5000.0	108	.0E+00	5000.0
109	.0E+00	5000.0	110	3.2E-34	5000.0	111	.0E+00	9.0
112	.0E+00	5000.0	113	.0E+00	5000.0	114	.0E+00	5000.0
115	.0E+00	569.0	116	7.7E-22	5000.0	117	.0E+00	5000.0
118	.0E+00	5000.0	119	2.2E-31	5000.0	120	1.9E-23	5000.0
121	.0E+00	5000.0	122	2.4E-33	5000.0	123	2.2E-27	5000.0
124	.0E+00	5000.0	125	1.2E-31	5000.0	126	.0E+00	5000.0
127	.0E+00	5000.0	128	.0E+00	5000.0	129	.0E+00	5000.0
130	.0E+00	5000.0	131	.0E+00	5000.0	132	.0E+00	5000.0
133	.0E+00	5000.0	134	.0E+00	5000.0	135	.0E+00	5000.0
136	.0E+00	5000.0	137	.0E+00	5000.0	138	.0E+00	5000.0
139	.0E+00	5000.0	140	.0E+00	5000.0	141	.0E+00	5000.0
142	.0E+00	5000.0	143	.0E+00	5000.0	144	.0E+00	5000.0
145	.0E+00	5000.0	146	.0E+00	5000.0	147	.0E+00	5000.0
148	.0E+00	5000.0	149	.0E+00	5000.0	150	.0E+00	5000.0
151	.0E+00	5000.0	152	.0E+00	5000.0	153	.0E+00	5000.0
154	.0E+00	5000.0	155	.0E+00	5000.0	156	.0E+00	5000.0

Table E.12 (continued)

Obs Node	Conc (uCi/L)	Time (Year)	Obs Node	Conc (uCi/L)	Time (Year)	Obs Node	Conc (uCi/L)	Time (Year)
157	.0E+00	5000.0	158	.0E+00	5000.0	159	.0E+00	5000.0
160	.0E+00	5000.0	161	.0E+00	5000.0	162	.0E+00	5000.0
163	.0E+00	5000.0	164	.0E+00	5000.0	165	.0E+00	5000.0
166	.0E+00	5000.0	167	.0E+00	5000.0	168	.0E+00	5000.0
169	.0E+00	1877.0	170	1.9E-23	5000.0	171	9.1E-27	5000.0
172	.0E+00	412.0	173	.0E+00	1445.0	174	.0E+00	5000.0
175	.0E+00	5000.0	176	.0E+00	5000.0	177	.0E+00	5000.0
178	.0E+00	5000.0	179	.0E+00	5000.0	180	.0E+00	5000.0
181	.0E+00	5000.0	182	.0E+00	5000.0	183	.0E+00	5000.0
184	.0E+00	5000.0	185	.0E+00	5000.0	186	.0E+00	5000.0
187	.0E+00	5000.0	188	.0E+00	5000.0	189	.0E+00	5000.0
190	.0E+00	5000.0	191	.0E+00	5000.0	192	.0E+00	5000.0
193	.0E+00	5000.0	194	.0E+00	5000.0	195	.0E+00	5000.0
196	.0E+00	5000.0	197	.0E+00	5000.0	198	.0E+00	5000.0
199	.0E+00	5000.0	200	.0E+00	5000.0	201	.0E+00	5000.0
202	.0E+00	5000.0	203	.0E+00	5000.0	204	.0E+00	5000.0
205	.0E+00	5000.0	206	.0E+00	5000.0	207	.0E+00	5000.0
208	.0E+00	5000.0	209	.0E+00	5000.0	210	.0E+00	5000.0
211	.0E+00	5000.0	212	.0E+00	5000.0	213	.0E+00	5000.0
214	.0E+00	5000.0	215	.0E+00	5000.0	216	.0E+00	5000.0
217	.0E+00	5000.0	218	.0E+00	5000.0	219	.0E+00	5000.0
220	.0E+00	5000.0	221	.0E+00	5000.0	222	.0E+00	5000.0
223	.0E+00	5000.0	224	.0E+00	5000.0	225	.0E+00	5000.0
226	.0E+00	5000.0	227	.0E+00	5000.0	228	.0E+00	5000.0
229	.0E+00	5000.0	230	.0E+00	5000.0	231	.0E+00	5000.0
232	.0E+00	5000.0	233	.0E+00	5000.0	234	.0E+00	5000.0

Table E.12 (continued)

Obs Node	Conc (uCi/L)	Time (Year)	Obs Node	Conc (uCi/L)	Time (Year)	Obs Node	Conc (uCi/L)	Time (Year)
235	.0E+00	5000.0	236	.0E+00	5000.0	237	.0E+00	5000.0
238	.0E+00	5000.0	239	.0E+00	5000.0	240	.0E+00	5000.0
241	.0E+00	5000.0	242	.0E+00	5000.0	243	.0E+00	5000.0
244	.0E+00	5000.0	245	.0E+00	5000.0	246	.0E+00	5000.0
247	.0E+00	5000.0	248	.0E+00	5000.0	249	.0E+00	5000.0
250	.0E+00	5000.0	251	.0E+00	5000.0	252	.0E+00	5000.0
253	.0E+00	5000.0	254	.0E+00	5000.0	255	.0E+00	5000.0
256	.0E+00	5000.0	257	.0E+00	3866.0	258	5.7E-32	5000.0
259	2.1E-29	5000.0	260	.0E+00	599.0	261	.0E+00	670.0
262	.0E+00	649.0	263	3.4E-30	5000.0	264	.0E+00	396.0
265	1.3E-29	5000.0	266	1.2E-29	5000.0	267	2.1E-30	5000.0
268	1.0E-26	5000.0	269	6.8E-22	5000.0	270	4.0E-18	5000.0
271	1.8E-21	5000.0	272	6.3E-25	5000.0	273	1.6E-28	5000.0
274	.0E+00	287.0	275	.0E+00	292.0	276	.0E+00	353.0
277	5.3E-34	5000.0	278	.0E+00	5000.0	279	.0E+00	5000.0
280	.0E+00	5000.0	281	.0E+00	5000.0	282	.0E+00	5000.0
283	.0E+00	5000.0	284	.0E+00	5000.0	285	.0E+00	5000.0
286	.0E+00	5000.0	287	.0E+00	5000.0	288	.0E+00	5000.0
289	.0E+00	5000.0	290	.0E+00	5000.0	291	.0E+00	5000.0
292	.0E+00	5000.0	293	.0E+00	5000.0	294	.0E+00	5000.0
295	.0E+00	5000.0	296	.0E+00	5000.0	297	.0E+00	5000.0
298	.0E+00	5000.0	299	.0E+00	5000.0	300	.0E+00	5000.0
301	.0E+00	5000.0	302	.0E+00	5000.0	303	.0E+00	5000.0
304	.0E+00	5000.0	305	.0E+00	5000.0	306	.0E+00	5000.0
307	.0E+00	5000.0	308	.0E+00	5000.0	309	.0E+00	5000.0
310	.0E+00	5000.0	311	.0E+00	5000.0	312	.0E+00	5000.0

Table E.12 (continued)

Obs Node	Conc (uCi/L)	Time (Year)	Obs Node	Conc (uCi/L)	Time (Year)	Obs Node	Conc (uCi/L)	Time (Year)
313	.0E+00	5000.0	314	.0E+00	5000.0	315	.0E+00	5000.0
316	.0E+00	5000.0	317	.0E+00	5000.0	318	.0E+00	5000.0
319	.0E+00	5000.0	320	.0E+00	5000.0	321	.0E+00	5000.0
322	.0E+00	5000.0	323	.0E+00	5000.0	324	.0E+00	5000.0
325	.0E+00	5000.0	326	.0E+00	5000.0	327	.0E+00	5000.0
328	.0E+00	5000.0	329	.0E+00	5000.0	330	.0E+00	5000.0
331	.0E+00	5000.0	332	.0E+00	5000.0	333	.0E+00	5000.0
334	.0E+00	5000.0						

Table E.13. Groundwater concentration of nuclide: ^{229}Th at observation nodes

Obs Node	Conc (uCi/L)	Time (Year)	Obs Node	Conc (uCi/L)	Time (Year)	Obs Node	Conc (uCi/L)	Time (Year)
1	.0E+00	3000.0	2	.0E+00	3000.0	3	.0E+00	3000.0
4	.0E+00	3000.0	5	.0E+00	3000.0	6	.0E+00	3000.0
7	.0E+00	3000.0	8	.0E+00	3000.0	9	2.3E-35	2904.0
10	.0E+00	3000.0	11	.0E+00	3000.0	12	.0E+00	3000.0
13	.0E+00	3000.0	14	.0E+00	3000.0	15	.0E+00	1804.0
16	1.4E-33	2600.0	17	7.0E-33	2887.0	18	6.5E-34	2461.0
19	5.0E-30	2481.0	20	2.6E-31	2895.0	21	1.3E-32	2391.0
22	1.3E-25	2459.0	23	2.5E-29	2502.0	24	1.1E-34	1020.0
25	3.0E-27	2318.0	26	1.7E-30	2056.0	27	1.0E-24	2806.0
28	1.8E-26	2835.0	29	4.5E-22	2884.0	30	1.8E-25	3000.0
31	7.1E-19	1970.0	32	2.2E-24	3000.0	33	1.2E-17	2889.0
34	2.8E-31	972.0	35	4.2E-16	2758.0	36	8.4E-24	2861.0
37	3.4E-15	1419.0	38	2.8E-14	1986.0	39	1.2E-26	2556.0
40	2.5E-12	1434.0	41	1.3E-12	1533.0	42	.0E+00	692.0
43	3.2E-11	625.0	44	1.1E-24	96.0	45	.0E+00	808.0
46	9.9E-11	2497.0	47	8.9E-11	1602.0	48	.0E+00	992.0
49	4.2E-10	2551.0	50	2.2E-08	2324.0	51	.0E+00	1046.0
52	1.5E-10	2734.0	53	2.4E-08	2883.0	54	3.7E-32	2416.0
55	3.8E-12	2608.0	56	1.1E-08	2744.0	57	.0E+00	1912.0
58	8.6E-13	2518.0	59	6.5E-09	2858.0	60	.0E+00	1960.0
61	9.0E-35	10.0	62	3.0E-10	2509.0	63	8.9E-33	3000.0
64	1.5E-17	643.0	65	4.4E-13	2004.0	66	1.1E-32	2999.0
67	5.9E-17	2366.0	68	2.1E-14	2046.0	69	2.4E-33	3000.0
70	2.1E-18	1571.0	71	5.0E-17	2320.0	72	2.6E-35	2851.0
73	3.1E-19	2650.0	74	4.7E-18	1955.0	75	.0E+00	3000.0
76	.0E+00	3000.0	77	9.4E-20	2950.0	78	1.8E-21	1434.0

Table E.13 (continued)

Obs Node	Conc (uCi/L)	Time (Year)	Obs Node	Conc (uCi/L)	Time (Year)	Obs Node	Conc (uCi/L)	Time (Year)
79	.0E+00	3000.0	80	.0E+00	3000.0	81	3.8E-22	2176.0
82	8.1E-20	3000.0	83	.0E+00	3000.0	84	.0E+00	3000.0
85	1.5E-21	2877.0	86	2.3E-21	3000.0	87	.0E+00	3000.0
88	.0E+00	3000.0	89	4.6E-22	2885.0	90	4.0E-22	3000.0
91	.0E+00	3000.0	92	.0E+00	3000.0	93	.0E+00	438.0
94	4.4E-25	3000.0	95	.0E+00	3000.0	96	.0E+00	3000.0
97	1.0E-25	2883.0	98	1.2E-27	2437.0	99	.0E+00	3000.0
100	.0E+00	3000.0	101	2.3E-26	2961.0	102	3.2E-28	2444.0
103	.0E+00	3000.0	104	.0E+00	3000.0	105	1.3E-29	2900.0
106	.0E+00	1024.0	107	2.6E-29	2645.0	108	2.2E-28	3000.0
109	2.2E-29	3000.0	110	.0E+00	3000.0	111	.0E+00	3000.0
112	1.6E-31	2758.0	113	5.2E-31	3000.0	114	5.8E-32	3000.0
115	.0E+00	3000.0	116	.0E+00	3000.0	117	8.5E-37	2507.0
118	.0E+00	3000.0	119	.0E+00	3000.0	120	.0E+00	3000.0
121	.0E+00	3000.0	122	.0E+00	3000.0	123	.0E+00	3000.0
124	.0E+00	3000.0	125	.0E+00	3000.0	126	.0E+00	3000.0
127	.0E+00	3000.0	128	.0E+00	3000.0	129	.0E+00	3000.0
130	.0E+00	3000.0	131	.0E+00	3000.0	132	.0E+00	3000.0
133	.0E+00	3000.0	134	.0E+00	3000.0	135	.0E+00	3000.0
136	.0E+00	3000.0	137	.0E+00	3000.0	138	.0E+00	3000.0
139	.0E+00	3000.0	140	.0E+00	3000.0	141	.0E+00	3000.0
142	.0E+00	3000.0	143	.0E+00	3000.0	144	.0E+00	3000.0
145	.0E+00	3000.0	146	.0E+00	3000.0	147	.0E+00	3000.0
148	.0E+00	3000.0	149	.0E+00	3000.0	150	.0E+00	3000.0
151	.0E+00	3000.0	152	.0E+00	3000.0	153	.0E+00	3000.0
154	.0E+00	3000.0	155	.0E+00	3000.0	156	.0E+00	3000.0

Table E.13 (continued)

Obs Node	Conc (uCi/L)	Time (Year)	Obs Node	Conc (uCi/L)	Time (Year)	Obs Node	Conc (uCi/L)	Time (Year)
157	.0E+00	3000.0	158	.0E+00	3000.0	159	.0E+00	3000.0
160	.0E+00	3000.0	161	.0E+00	3000.0	162	.0E+00	3000.0
163	.0E+00	3000.0	164	.0E+00	3000.0	165	.0E+00	3000.0
166	.0E+00	3000.0	167	.0E+00	3000.0	168	.0E+00	3000.0
169	.0E+00	3000.0	170	.0E+00	3000.0	171	.0E+00	3000.0
172	.0E+00	3000.0	173	.0E+00	3000.0	174	.0E+00	3000.0
175	.0E+00	3000.0	176	.0E+00	3000.0	177	.0E+00	3000.0
178	.0E+00	3000.0	179	.0E+00	3000.0	180	.0E+00	3000.0
181	.0E+00	3000.0	182	.0E+00	3000.0	183	.0E+00	3000.0
184	.0E+00	3000.0	185	.0E+00	3000.0	186	.0E+00	3000.0
187	.0E+00	3000.0	188	4.0E-09	1971.0	189	9.0E-09	2691.0
190	1.4E-10	2916.0	191	3.7E-13	1695.0	192	5.9E-31	2960.0
193	1.4E-30	3000.0	194	3.2E-30	3000.0	195	7.3E-29	2861.0
196	3.0E-30	1447.0	197	5.7E-27	3000.0	198	2.8E-24	3000.0
199	1.1E-22	1841.0	200	5.6E-19	2861.0	201	1.1E-17	1557.0
202	2.2E-18	920.0	203	3.8E-16	2965.0	204	4.9E-16	2928.0
205	3.1E-25	3000.0	206	4.8E-24	3000.0	207	2.2E-24	2933.0
208	7.7E-30	884.0	209	8.0E-23	3000.0	210	3.5E-28	927.0
211	3.5E-22	3000.0	212	2.2E-21	3000.0	213	2.3E-20	2945.0
214	5.5E-20	3000.0	215	1.8E-17	3000.0	216	8.9E-16	3000.0
217	6.5E-14	2928.0	218	3.5E-13	2719.0	219	6.0E-15	2436.0
220	6.5E-17	2793.0	221	8.0E-20	2781.0	222	5.9E-24	1282.0
223	.0E+00	3000.0	224	.0E+00	3000.0	225	.0E+00	3000.0
226	.0E+00	3000.0	227	.0E+00	3000.0	228	.0E+00	3000.0
229	.0E+00	3000.0	230	.0E+00	3000.0	231	.0E+00	3000.0
232	.0E+00	3000.0	233	.0E+00	3000.0	234	.0E+00	3000.0

Table E.13 (continued)

Obs Node	Conc (uCi/L)	Time (Year)	Obs Node	Conc (uCi/L)	Time (Year)	Obs Node	Conc (uCi/L)	Time (Year)
235	.0E+00	3000.0	236	.0E+00	3000.0	237	.0E+00	3000.0
238	.0E+00	3000.0	239	.0E+00	3000.0	240	.0E+00	3000.0
241	.0E+00	3000.0	242	.0E+00	3000.0	243	.0E+00	3000.0
244	.0E+00	3000.0	245	.0E+00	3000.0	246	.0E+00	3000.0
247	.0E+00	3000.0	248	.0E+00	3000.0	249	.0E+00	3000.0
250	.0E+00	3000.0	251	.0E+00	3000.0	252	.0E+00	3000.0
253	2.6E-32	3000.0	254	7.9E-32	2831.0	255	3.7E-30	2957.0
256	3.4E-30	2860.0	257	9.3E-30	2724.0	258	4.0E-28	3000.0
259	.0E+00	673.0	260	1.7E-28	2711.0	261	7.7E-29	2692.0
262	1.6E-30	3000.0	263	3.2E-31	3000.0	264	1.3E-32	3000.0
265	1.7E-33	3000.0	266	.0E+00	3000.0	267	.0E+00	3000.0
268	.0E+00	3000.0	269	.0E+00	3000.0	270	.0E+00	3000.0
271	.0E+00	3000.0	272	.0E+00	3000.0	273	.0E+00	3000.0
274	.0E+00	3000.0	275	.0E+00	3000.0	276	.0E+00	3000.0
277	.0E+00	3000.0	278	.0E+00	3000.0	279	.0E+00	3000.0
280	.0E+00	3000.0	281	2.2E-33	3000.0	282	2.4E-25	2876.0
283	2.3E-23	2815.0	284	1.8E-20	2906.0	285	3.4E-19	3000.0
286	4.1E-15	3000.0	287	2.3E-13	2812.0	288	2.9E-13	2729.0
289	1.0E-13	2960.0	290	2.6E-13	2178.0	291	7.3E-13	1990.0
292	4.0E-11	1516.0	293	1.6E-10	2667.0	294	1.2E-13	1584.0
295	.0E+00	910.0	296	4.8E-28	2907.0	297	9.1E-29	2103.0
298	3.3E-28	1451.0	299	1.7E-23	2559.0	300	5.7E-22	3000.0
301	2.6E-21	2850.0	302	1.5E-17	2888.0	303	9.3E-18	3000.0
304	2.9E-18	3000.0	305	4.3E-19	3000.0	306	1.4E-23	704.0
307	8.0E-20	3000.0	308	2.0E-19	2931.0	309	6.2E-17	3000.0
310	3.9E-15	2032.0	311	1.7E-14	3000.0	312	4.0E-25	960.0

Table E.13 (continued)

Obs Node	Conc (uCi/L)	Time (Year)	Obs Node	Conc (uCi/L)	Time (Year)	Obs Node	Conc (uCi/L)	Time (Year)
313	1.0E-32	297.0	314	1.9E-23	2556.0	315	8.4E-24	3000.0
316	1.4E-36	120.0	317	3.1E-25	3000.0	318	.0E+00	3000.0
319	.0E+00	3000.0	320	.0E+00	3000.0	321	9.3E-33	2913.0
322	9.7E-33	2834.0	323	2.8E-25	2232.0	324	2.2E-26	1601.0
325	1.7E-20	503.0	326	5.6E-19	1028.0	327	1.8E-18	1560.0
328	4.1E-18	2015.0	329	8.4E-18	2308.0	330	5.8E-16	2308.0
331	6.7E-16	2610.0	332	4.6E-14	1518.0	333	1.8E-12	1081.0
334	1.3E-11	2002.0						

Table E.14. Groundwater concentration of nuclide: ^{232}Th at observation nodes

Obs Node	Conc (uCi/L)	Time (Year)	Obs Node	Conc (uCi/L)	Time (Year)	Obs Node	Conc (uCi/L)	Time (Year)
1	1.5E-22	9717.0	2	.0E+00	25000.0	3	1.3E-21	9110.0
4	.0E+00	25000.0	5	.0E+00	25000.0	6	5.5E-27	2862.0
7	3.4E-21	7621.0	8	6.7E-23	4130.0	9	2.0E-20	6941.0
10	5.5E-21	8155.0	11	8.8E-21	3774.0	12	1.7E-21	4812.0
13	2.9E-21	8290.0	14	1.6E-19	4120.0	15	1.0E-19	5500.0
16	7.4E-21	6877.0	17	8.6E-21	7090.0	18	7.3E-18	2016.0
19	4.0E-17	5802.0	20	3.1E-19	6972.0	21	6.7E-16	2969.0
22	3.9E-13	4670.0	23	2.0E-23	2598.0	24	4.1E-14	2824.0
25	2.0E-15	8683.0	26	5.0E-13	2850.0	27	5.2E-15	8285.0
28	6.0E-11	5733.0	29	6.8E-14	7312.0	30	6.7E-11	5465.0
31	1.2E-13	7589.0	32	3.1E-10	4577.0	33	1.0E-13	7318.0
34	3.6E-10	3014.0	35	8.2E-14	7842.0	36	1.7E-11	5717.0
37	1.2E-11	4004.0	38	8.1E-14	7846.0	39	1.9E-12	3215.0
40	7.6E-12	3904.0	41	6.3E-14	8495.0	42	8.6E-10	2492.0
43	5.0E-12	3950.0	44	4.4E-27	96.0	45	2.0E-09	3166.0
46	1.7E-11	5643.0	47	1.5E-12	1602.0	48	3.5E-09	3494.0
49	1.5E-11	5872.0	50	4.7E-10	3038.0	51	3.2E-09	4608.0
52	5.6E-12	6349.0	53	5.4E-10	3439.0	54	3.0E-10	6846.0
55	2.3E-12	7742.0	56	3.5E-10	4958.0	57	3.1E-10	7706.0
58	1.0E-12	7495.0	59	2.6E-10	5310.0	60	1.4E-10	7944.0
61	3.1E-13	8585.0	62	1.2E-11	5830.0	63	6.1E-11	8647.0
64	8.4E-14	8588.0	65	4.9E-15	2624.0	66	1.5E-11	9691.0
67	3.3E-15	11489.0	68	2.6E-15	4674.0	69	4.1E-13	13138.0
70	1.3E-15	11534.0	71	3.4E-16	6275.0	72	1.8E-14	15028.0
73	1.4E-16	7459.0	74	2.5E-16	6488.0	75	1.5E-18	3251.0
76	5.9E-15	15653.0	77	2.0E-17	8447.0	78	7.3E-17	7078.0

Table E.14 (continued)

Obs Node	Conc (uCi/L)	Time (Year)	Obs Node	Conc (uCi/L)	Time (Year)	Obs Node	Conc (uCi/L)	Time (Year)
79	2.9E-18	1602.0	80	9.3E-15	3275.0	81	3.1E-18	8851.0
82	3.4E-19	16245.0	83	2.2E-16	4234.0	84	1.2E-12	2460.0
85	2.9E-19	9583.0	86	1.7E-19	16344.0	87	2.9E-16	1044.0
88	2.0E-10	1356.0	89	6.4E-20	9505.0	90	8.8E-20	16888.0
91	7.9E-14	1488.0	92	1.8E-08	1263.0	93	2.6E-20	9938.0
94	1.0E-20	18537.0	95	2.2E-11	1350.0	96	3.6E-08	1250.0
97	6.5E-19	22883.0	98	9.9E-21	20708.0	99	7.5E-09	835.0
100	3.1E-08	1254.0	101	1.0E-16	23407.0	102	4.0E-18	21263.0
103	5.6E-09	1675.0	104	3.6E-08	2399.0	105	5.0E-16	3726.0
106	7.9E-14	3620.0	107	7.5E-14	3669.0	108	1.7E-15	22466.0
109	9.1E-17	24225.0	110	4.6E-09	1646.0	111	3.2E-09	3527.0
112	1.5E-12	24055.0	113	1.6E-25	807.0	114	4.1E-16	23536.0
115	1.2E-09	2983.0	116	6.4E-10	4182.0	117	7.9E-13	24647.0
118	5.4E-18	22867.0	119	1.0E-09	3454.0	120	3.1E-13	13496.0
121	2.0E-12	23460.0	122	6.0E-10	3457.0	123	2.3E-13	3693.0
124	1.6E-12	23127.0	125	6.8E-11	5396.0	126	8.8E-13	8225.0
127	2.2E-10	5133.0	128	1.6E-14	6804.0	129	1.8E-10	5008.0
130	4.3E-15	9078.0	131	6.6E-11	5307.0	132	8.6E-15	6906.0
133	9.6E-12	5429.0	134	5.5E-17	1373.0	135	3.1E-12	6373.0
136	4.3E-17	2134.0	137	2.5E-13	5873.0	138	1.1E-14	6970.0
139	1.3E-12	11301.0	140	8.4E-14	5305.0	141	3.0E-14	5269.0
142	1.1E-15	7483.0	143	1.9E-12	24702.0	144	5.0E-17	6949.0
145	6.3E-19	24644.0	146	5.8E-15	23571.0	147	1.6E-13	24672.0
148	6.8E-13	24686.0	149	5.6E-13	24705.0	150	1.7E-13	21499.0
151	1.3E-17	9142.0	152	3.8E-18	7666.0	153	2.2E-19	24877.0
154	1.6E-19	24778.0	155	1.3E-19	23598.0	156	2.8E-18	23595.0

Table E.14 (continued)

Obs Node	Conc (uCi/L)	Time (Year)	Obs Node	Conc (uCi/L)	Time (Year)	Obs Node	Conc (uCi/L)	Time (Year)
157	1.4E-17	24725.0	158	1.9E-22	10624.0	159	3.3E-20	10452.0
160	3.3E-17	10857.0	161	5.3E-17	10936.0	162	1.4E-23	2579.0
163	2.3E-20	6074.0	164	8.5E-19	8051.0	165	1.1E-18	8183.0
166	2.6E-09	3153.0	167	2.9E-09	3067.0	168	3.5E-09	2366.0
169	3.3E-09	2098.0	170	3.1E-13	13496.0	171	3.0E-13	11631.0
172	3.1E-13	12965.0	173	8.8E-16	1527.0	174	2.7E-10	24258.0
175	1.3E-10	24342.0	176	1.1E-11	21019.0	177	9.1E-12	22120.0
178	8.7E-12	23022.0	179	8.9E-12	22682.0	180	7.5E-12	19275.0
181	5.1E-12	14881.0	182	8.7E-15	6955.0	183	1.8E-14	7594.0
184	3.0E-14	5545.0	185	2.9E-12	7643.0	186	2.2E-16	992.0
187	2.8E-11	24141.0	188	7.3E-11	1971.0	189	2.9E-10	4905.0
190	2.8E-12	3265.0	191	3.3E-14	7603.0	192	6.6E-11	8393.0
193	9.4E-12	10580.0	194	8.7E-12	10596.0	195	6.6E-12	10610.0
196	5.7E-12	10832.0	197	1.5E-12	13178.0	198	1.2E-14	3335.0
199	1.1E-14	5388.0	200	1.6E-14	10722.0	201	1.2E-13	9672.0
202	7.4E-13	8208.0	203	2.6E-12	7001.0	204	7.0E-12	6887.0
205	2.3E-10	3942.0	206	3.0E-10	4830.0	207	7.8E-10	4388.0
208	1.4E-09	3283.0	209	4.4E-11	5326.0	210	9.3E-11	6464.0
211	1.8E-10	1697.0	212	1.5E-09	1346.0	213	4.3E-10	2474.0
214	2.5E-11	6213.0	215	2.2E-11	6137.0	216	2.1E-11	6182.0
217	7.2E-11	5101.0	218	9.7E-12	3702.0	219	6.3E-12	4683.0
220	3.0E-12	4952.0	221	3.5E-12	4934.0	222	2.5E-12	4923.0
223	8.7E-21	1731.0	224	6.5E-22	1234.0	225	2.0E-22	2594.0
226	1.4E-19	2598.0	227	1.4E-17	1439.0	228	5.1E-16	927.0
229	8.6E-16	1353.0	230	2.5E-15	1421.0	231	8.7E-17	1926.0
232	1.0E-15	1753.0	233	8.3E-15	1990.0	234	1.0E-13	2039.0

Table E.14 (continued)

Obs Node	Conc (uCi/L)	Time (Year)	Obs Node	Conc (uCi/L)	Time (Year)	Obs Node	Conc (uCi/L)	Time (Year)
235	8.4E-13	1741.0	236	2.8E-11	2016.0	237	3.2E-10	2016.0
238	2.7E-10	1668.0	239	1.2E-10	2661.0	240	1.4E-12	4882.0
241	.0E+00	3.0	242	.0E+00	4.0	243.0	E+00	5.0
244	8.5E-16	7503.0	245	7.4E-16	4287.0	246	1.4E-15	4374.0
247	8.1E-15	3938.0	248	1.7E-13	3227.0	249	1.1E-11	4400.0
250	1.2E-10	4206.0	251	4.3E-10	4032.0	252	1.4E-09	2891.0
253	7.2E-13	12973.0	254	1.0E-12	12894.0	255	1.2E-12	12785.0
256	1.2E-12	11813.0	257	1.5E-13	13895.0	258	2.2E-14	15019.0
259	2.8E-15	17170.0	260	5.2E-16	19412.0	261	8.8E-17	22618.0
262	1.6E-17	23746.0	263	1.6E-22	1001.0	264	.0E+00	4.0
265	.0E+00	3.0	266	5.5E-13	20847.0	267	6.4E-11	23553.0
268	1.2E-09	20709.0	269	1.0E-09	3133.0	270	2.0E-16	243.0
271	3.4E-20	50.0	272	5.4E-10	9486.0	273	2.4E-08	21958.0
274	6.8E-12	23729.0	275	2.4E-13	11690.0	276	4.3E-13	12885.0
277	.0E+00	1.0	278	5.4E-10	22010.0	279	2.1E-10	22824.0
280	7.3E-11	21546.0	281	6.6E-12	23771.0	282	1.9E-24	555.0
283	1.3E-16	6172.0	284	1.3E-15	6506.0	285	6.2E-16	7089.0
286	5.2E-16	11618.0	287	6.4E-15	3919.0	288	1.3E-14	4447.0
289	1.8E-14	4392.0	290	6.9E-15	3176.0	291	4.2E-14	3097.0
292	5.7E-13	1516.0	293	2.7E-12	2667.0	294	8.8E-15	7273.0
295	1.0E-08	3906.0	296	5.2E-09	5121.0	297	5.9E-09	5039.0
298	4.3E-09	5189.0	299	7.8E-09	2559.0	300	2.8E-12	4125.0
301	7.2E-12	6931.0	302	7.6E-11	5103.0	303	2.5E-10	4108.0
304	6.7E-10	3322.0	305	3.0E-09	2173.0	306	2.0E-08	1128.0
307	3.6E-10	3951.0	308	9.0E-10	3122.0	309	4.0E-11	1959.0
310	2.3E-11	3235.0	311	4.6E-11	4969.0	312	2.6E-08	896.0

Table E.14 (continued)

Obs Node	Conc (uCi/L)	Time (Year)	Obs Node	Conc (uCi/L)	Time (Year)	Obs Node	Conc (uCi/L)	Time (Year)
313	6.9E-09	2897.0	314	4.7E-09	2593.0	315	1.6E-08	1562.0
316	2.0E-08	1562.0	317	2.3E-10	3942.0	318	.0E+00	19.0
319	3.6E-21	3594.0	320	8.9E-21	3974.0	321	3.8E-19	4852.0
322	2.8E-19	5291.0	323	1.2E-12	4374.0	324	8.9E-13	4680.0
325	1.6E-12	5520.0	326	1.1E-12	5872.0	327	7.2E-13	6200.0
328	5.0E-13	6501.0	329	3.0E-13	6883.0	330	2.1E-13	7184.0
331	1.5E-13	7478.0	332	1.4E-13	7521.0	333	1.1E-13	7611.0
334	1.6E-14	2002.0						

Table E.15. Groundwater concentration of nuclide: ^{233}U at observation nodes

Obs Node	Conc (uCi/L)	Time (Year)	Obs Node	Conc (uCi/L)	Time (Year)	Obs Node	Conc (uCi/L)	Time (Year)
1	.0E+00	4165.0	2	.0E+00	5000.0	3	.0E+00	3509.0
4	.0E+00	5000.0	5	.0E+00	5000.0	6	.0E+00	5000.0
7	1.6E-36	3193.0	8	.0E+00	2973.0	9	8.3E-34	5000.0
10	.0E+00	3674.0	11	4.3E-34	2738.0	12	6.6E-33	5000.0
13	.0E+00	3861.0	14	4.1E-31	3893.0	15	2.7E-31	4963.0
16	4.7E-34	5000.0	17	3.8E-35	4991.0	18	3.5E-28	5000.0
19	2.9E-30	4714.0	20	2.0E-32	4890.0	21	9.5E-26	4950.0
22	4.5E-27	4854.0	23	5.7E-30	4899.0	24	3.8E-24	4727.0
25	8.7E-29	4539.0	26	5.7E-22	3629.0	27	6.7E-27	5000.0
28	2.0E-20	2812.0	29	6.7E-24	5000.0	30	2.1E-18	2143.0
31	4.3E-25	3675.0	32	8.5E-17	1748.0	33	.0E+00	813.0
34	1.3E-14	1228.0	35	2.1E-21	5000.0	36	2.1E-13	3336.0
37	2.7E-18	2161.0	38	7.2E-21	5000.0	39	5.1E-11	3215.0
40	6.3E-17	2338.0	41	9.4E-21	4861.0	42	2.0E-08	2492.0
43	1.7E-15	3969.0	44	1.1E-20	5000.0	45	3.8E-08	3166.0
46	9.5E-15	3429.0	47	5.1E-20	4925.0	48	7.9E-08	2387.0
49	9.7E-15	4310.0	50	3.8E-19	4926.0	51	7.1E-08	2394.0
52	9.1E-15	3526.0	53	3.8E-19	5000.0	54	5.7E-09	4632.0
55	7.0E-14	3490.0	56	2.5E-19	5000.0	57	5.8E-09	4385.0
58	6.9E-14	3795.0	59	2.0E-19	5000.0	60	2.6E-09	4623.0
61	5.4E-15	2700.0	62	2.9E-19	4971.0	63	1.0E-09	4908.0
64	7.4E-16	3053.0	65	8.9E-21	5000.0	66	1.5E-10	4156.0
67	3.6E-16	3490.0	68	9.1E-35	1116.0	69	1.2E-13	4251.0
70	5.2E-16	4573.0	71	6.4E-34	1234.0	72	5.6E-15	4189.0
73	2.8E-16	4864.0	74	1.3E-34	1384.0	75	2.7E-16	3251.0
76	1.6E-14	4189.0	77	9.4E-18	4019.0	78	4.1E-34	1427.0

Table E.15 (continued)

Obs Node	Conc (uCi/L)	Time (Year)	Obs Node	Conc (uCi/L)	Time (Year)	Obs Node	Conc (uCi/L)	Time (Year)
79	6.5E-16	1602.0	80	1.7E-12	3275.0	81	1.4E-18	5000.0
82	7.8E-32	1694.0	83	3.5E-14	4234.0	84	2.2E-10	1980.0
85	7.4E-22	2941.0	86	.0E+00	623.0	87	9.5E-13	2765.0
88	3.7E-08	1356.0	89	4.7E-23	2885.0	90	1.2E-22	5000.0
91	2.0E-10	1488.0	92	3.1E-06	1263.0	93	4.2E-20	4199.0
94	2.2E-28	1359.0	95	5.7E-08	1350.0	96	6.5E-06	1250.0
97	8.0E-18	4913.0	98	1.4E-19	4838.0	99	1.9E-05	835.0
100	1.8E-05	1937.0	101	2.0E-15	4588.0	102	1.3E-23	1489.0
103	1.4E-05	1675.0	104	3.1E-05	2399.0	105	1.2E-14	3726.0
106	2.1E-12	3620.0	107	2.0E-12	3669.0	108	1.1E-14	4754.0
109	5.1E-18	4299.0	110	1.2E-05	1646.0	111	2.8E-06	3527.0
112	8.6E-12	4429.0	113	4.6E-22	1019.0	114	3.7E-16	4717.0
115	3.2E-06	2983.0	116	5.7E-07	4182.0	117	3.5E-12	4721.0
118	1.1E-17	5000.0	119	2.6E-06	3454.0	120	5.4E-11	5000.0
121	8.3E-12	4641.0	122	1.5E-06	3457.0	123	2.4E-10	3693.0
124	8.0E-12	4899.0	125	1.3E-07	4289.0	126	1.7E-11	4904.0
127	5.1E-07	4910.0	128	3.4E-13	4908.0	129	4.4E-07	4828.0
130	6.4E-14	4650.0	131	1.2E-07	4200.0	132	1.6E-13	4692.0
133	1.1E-08	4558.0	134	1.9E-15	1373.0	135	1.2E-09	4361.0
136	1.1E-15	2020.0	137	5.3E-10	4843.0	138	7.0E-13	4447.0
139	2.2E-11	3980.0	140	1.4E-12	4198.0	141	3.3E-11	4162.0
142	.0E+00	207.0	143	3.8E-12	4776.0	144	9.4E-15	4535.0
145	7.5E-18	4718.0	146	1.3E-15	4752.0	147	1.0E-14	4746.0
148	5.4E-14	4760.0	149	4.3E-14	4860.0	150	5.1E-14	4894.0
151	4.4E-17	4824.0	152	8.7E-17	4576.0	153	4.5E-18	4951.0
154	5.5E-20	4852.0	155	5.7E-21	4737.0	156	7.5E-19	5000.0

Table E.15 (continued)

Obs Node	Conc (uCi/L)	Time (Year)	Obs Node	Conc (uCi/L)	Time (Year)	Obs Node	Conc (uCi/L)	Time (Year)
157	6.2E-22	2865.0	158	2.1E-23	2192.0	159	1.3E-21	2325.0
160	8.1E-17	4215.0	161	1.5E-16	4294.0	162	3.0E-19	2586.0
163	2.2E-17	4967.0	164	2.6E-17	4730.0	165	3.2E-17	4862.0
166	6.7E-06	3153.0	167	7.5E-06	3067.0	168	8.9E-06	2366.0
169	8.5E-06	2098.0	170	5.4E-11	5000.0	171	3.3E-11	4264.0
172	5.5E-13	3002.0	173	3.0E-14	1527.0	174	3.6E-09	4332.0
175	1.1E-09	4414.0	176	2.9E-11	4414.0	177	2.0E-11	4408.0
178	5.7E-12	4203.0	179	4.0E-11	4970.0	180	4.3E-11	4884.0
181	2.2E-11	4918.0	182	1.7E-13	4741.0	183	3.3E-13	4273.0
184	6.7E-13	4438.0	185	6.2E-11	4322.0	186	1.2E-14	992.0
187	3.6E-10	4215.0	188	1.5E-19	4747.0	189	5.1E-19	5000.0
190	8.2E-19	5000.0	191	2.9E-19	5000.0	192	9.6E-10	4869.0
193	1.3E-11	4854.0	194	1.1E-11	4944.0	195	6.6E-14	2861.0
196	5.3E-13	3083.0	197	2.6E-13	5000.0	198	1.2E-13	3335.0
199	2.0E-13	4281.0	200	5.3E-15	1866.0	201	1.5E-19	526.0
202	3.8E-13	4887.0	203	5.8E-13	3241.0	204	6.1E-13	3190.0
205	3.2E-21	4732.0	206	1.3E-19	4830.0	207	1.5E-17	3130.0
208	7.7E-16	3283.0	209	3.4E-12	2412.0	210	2.2E-09	1876.0
211	3.1E-09	1299.0	212	3.5E-08	984.0	213	1.1E-08	1367.0
214	1.0E-10	2892.0	215	1.0E-12	2226.0	216	4.7E-13	1943.0
217	7.4E-14	2887.0	218	6.5E-15	2435.0	219	2.2E-18	4857.0
220	2.3E-19	5000.0	221	1.6E-20	5000.0	222	1.4E-24	2700.0
223	4.9E-18	1651.0	224	2.0E-18	1234.0	225	2.8E-18	3701.0
226	3.7E-16	2598.0	227	3.7E-14	1439.0	228	1.3E-12	927.0
229	2.2E-12	1353.0	230	6.4E-12	1421.0	231	2.2E-13	1926.0
232	2.7E-12	1753.0	233	2.1E-11	1990.0	234	2.6E-10	2039.0

Table E.15 (continued)

Obs Node	Conc (uCi/L)	Time (Year)	Obs Node	Conc (uCi/L)	Time (Year)	Obs Node	Conc (uCi/L)	Time (Year)
235	2.2E-09	1741.0	236	7.2E-08	2016.0	237	8.3E-07	2016.0
238	7.1E-07	1668.0	239	3.0E-07	2661.0	240	3.3E-09	4882.0
241	.0E+00	3.0	242	.0E+00	4.0	243	.0E+00	6.0
244	1.0E-12	5000.0	245	1.9E-12	4287.0	246	3.8E-12	4374.0
247	2.2E-11	3938.0	248	4.4E-10	3227.0	249	2.8E-08	4400.0
250	3.1E-07	4206.0	251	1.1E-06	4032.0	252	3.5E-06	2891.0
253	3.4E-14	4743.0	254	4.0E-14	4395.0	255	2.0E-15	3090.0
256	4.7E-15	2957.0	257	3.6E-16	1617.0	258	4.7E-15	2108.0
259	2.1E-18	441.0	260	1.6E-29	96.0	261	5.5E-17	1116.0
262	6.1E-18	2601.0	263	4.6E-18	2150.0	264	.0E+00	4.0
265	.0E+00	3.0	266	7.9E-12	4242.0	267	1.4E-09	5000.0
268	2.7E-08	5000.0	269	2.5E-08	4240.0	270	5.7E-13	250.0
271	1.9E-18	50.0	272	1.3E-08	3951.0	273	5.6E-07	4246.0
274	5.4E-11	1654.0	275	.0E+00	3.0	276	5.4E-13	1815.0
277	.0E+00	1.0	278	1.2E-08	4298.0	279	4.2E-09	4763.0
280	1.4E-09	4941.0	281	9.0E-11	4952.0	282	4.5E-22	559.0
283	3.4E-16	3958.0	284	7.4E-15	4292.0	285	3.9E-15	4875.0
286	2.3E-17	4221.0	287	3.9E-18	4955.0	288	1.5E-17	4943.0
289	2.1E-19	5000.0	290	1.4E-18	4282.0	291	2.0E-18	4834.0
292	2.2E-18	4930.0	293	1.9E-18	5000.0	294	8.5E-19	5000.0
295	2.3E-07	1692.0	296	1.0E-07	1800.0	297	1.2E-07	2825.0
298	8.5E-08	2975.0	299	1.6E-07	2559.0	300	9.6E-11	3464.0
301	3.2E-11	3610.0	302	5.7E-13	1368.0	303	7.0E-15	2215.0
304	2.6E-13	1671.0	305	1.1E-13	1801.0	306	2.6E-15	2015.0
307	5.0E-12	1729.0	308	1.0E-12	1676.0	309	.0E+00	4.0
310	2.0E-15	2685.0	311	2.7E-14	2502.0	312	2.8E-14	2007.0

Table E.15 (continued)

Obs Node	Conc (uCi/L)	Time (Year)	Obs Node	Conc (uCi/L)	Time (Year)	Obs Node	Conc (uCi/L)	Time (Year)
313	1.3E-16	2858.0	314	2.0E-18	4770.0	315	1.5E-18	4870.0
316	8.1E-17	2655.0	317	3.2E-21	4732.0	318	.0E+00	1740.0
319	7.2E-33	4701.0	320	1.1E-32	5000.0	321	5.5E-31	5000.0
322	4.3E-31	4944.0	323	9.5E-27	4853.0	324	5.3E-28	2435.0
325	1.3E-19	5000.0	326	6.9E-20	5000.0	327	2.6E-20	5000.0
328	9.3E-22	5000.0	329	.0E+00	555.0	330	1.5E-20	5000.0
331	6.0E-21	5000.0	332	1.8E-20	4926.0	333	3.1E-20	5000.0
334	4.0E-20	5000.0						

Table E.16. Groundwater concentration of nuclide: ^{235}U at observation nodes

Obs Node	Conc (uCi/L)	Time (Year)	Obs Node	Conc (uCi/L)	Time (Year)	Obs Node	Conc (uCi/L)	Time (Year)
1	3.9E-36	3223.0	2	.0E+00	4000.0	3	2.2E-33	3968.0
4	.0E+00	4000.0	5	.0E+00	4000.0	6	1.9E-39	4000.0
7	2.2E-32	3897.0	8	5.4E-35	4000.0	9	1.5E-31	3986.0
10	6.7E-33	4000.0	11	1.2E-32	4000.0	12	6.0E-33	3868.0
13	1.4E-33	3862.0	14	9.1E-32	3598.0	15	1.1E-34	1504.0
16	8.3E-31	4000.0	17	5.1E-31	4000.0	18	9.1E-30	3568.0
19	1.5E-27	3979.0	20	2.9E-29	3783.0	21	4.8E-28	3521.0
22	9.5E-24	3566.0	23	4.2E-27	3792.0	24	2.5E-26	3489.0
25	1.0E-25	3432.0	26	7.7E-25	2424.0	27	2.2E-25	2641.0
28	3.5E-24	1301.0	29	2.0E-21	3843.0	30	1.1E-19	3551.0
31	4.6E-20	3825.0	32	1.1E-17	2954.0	33	1.5E-20	2092.0
34	7.6E-17	3014.0	35	8.1E-29	644.0	36	9.8E-16	2739.0
37	9.4E-13	1213.0	38	6.9E-20	2137.0	39	1.9E-16	3671.0
40	6.7E-11	2024.0	41	4.1E-17	3747.0	42	3.0E-16	3599.0
43	5.7E-09	1755.0	44	3.4E-16	3818.0	45	2.2E-17	3166.0
46	1.4E-08	1690.0	47	2.7E-15	3816.0	48	1.7E-17	3494.0
49	1.3E-08	2096.0	50	2.6E-14	3979.0	51	1.6E-17	3501.0
52	4.2E-09	1921.0	53	3.4E-14	3990.0	54	3.7E-20	3683.0
55	9.2E-10	2876.0	56	1.9E-14	3851.0	57	4.7E-21	3531.0
58	4.3E-10	3067.0	59	1.8E-14	3978.0	60	2.5E-21	3846.0
61	1.1E-10	3050.0	62	6.9E-14	3898.0	63	1.1E-21	3938.0
64	2.8E-11	3053.0	65	5.9E-16	4000.0	66	3.4E-22	4000.0
67	5.6E-14	3694.0	68	8.0E-17	3762.0	69	1.4E-24	3240.0
70	1.7E-14	3785.0	71	5.1E-19	4000.0	72	6.6E-26	3676.0
73	1.4E-16	4000.0	74	4.0E-20	3855.0	75	1.1E-34	2881.0
76	1.1E-25	3799.0	77	7.0E-19	2912.0	78	1.8E-19	3851.0

Table E.16 (continued)

Obs Node	Conc (uCi/L)	Time (Year)	Obs Node	Conc (uCi/L)	Time (Year)	Obs Node	Conc (uCi/L)	Time (Year)
79	2.5E-35	3203.0	80	2.2E-27	4000.0	81	3.2E-28	931.0
82	2.0E-21	4000.0	83	8.1E-39	2906.0	84	1.2E-27	4000.0
85	3.9E-21	3599.0	86	7.6E-22	3957.0	87	2.7E-40	2607.0
88	8.2E-29	3992.0	89	6.5E-22	3767.0	90	3.5E-22	3746.0
91	9.3E-38	4000.0	92	4.8E-29	4000.0	93	1.0E-22	3895.0
94	4.0E-24	4000.0	95	1.0E-38	3836.0	96	1.2E-30	3755.0
97	2.7E-25	4000.0	98	2.0E-24	4000.0	99	.0E+00	4000.0
100	3.5E-33	4000.0	101	1.2E-25	4000.0	102	1.2E-25	4000.0
103	.0E+00	3539.0	104	9.7E-36	3951.0	105	6.6E-29	4000.0
106	.0E+00	1024.0	107	8.5E-28	3668.0	108	1.5E-27	4000.0
109	7.3E-28	3880.0	110	.0E+00	4000.0	111	.0E+00	2822.0
112	3.5E-30	3240.0	113	7.5E-30	4000.0	114	2.7E-30	4000.0
115	.0E+00	3724.0	116	.0E+00	3033.0	117	8.8E-33	3906.0
118	1.0E-33	4000.0	119	.0E+00	3755.0	120	.0E+00	4000.0
121	1.7E-35	4000.0	122	.0E+00	4000.0	123	.0E+00	4000.0
124	9.1E-36	3844.0	125	.0E+00	4000.0	126	2.8E-39	4000.0
127	.0E+00	4000.0	128	.0E+00	4000.0	129	.0E+00	4000.0
130	.0E+00	4000.0	131	.0E+00	4000.0	132	.0E+00	4000.0
133	.0E+00	4000.0	134	.0E+00	4000.0	135	.0E+00	4000.0
136	.0E+00	4000.0	137	.0E+00	4000.0	138	.0E+00	4000.0
139	.0E+00	4000.0	140	.0E+00	4000.0	141	.0E+00	4000.0
142	.0E+00	4000.0	143	.0E+00	4000.0	144	.0E+00	4000.0
145	.0E+00	4000.0	146	.0E+00	4000.0	147	.0E+00	4000.0
148	.0E+00	4000.0	149	.0E+00	4000.0	150	.0E+00	4000.0
151	.0E+00	4000.0	152	.0E+00	4000.0	153	.0E+00	4000.0
154	.0E+00	4000.0	155	.0E+00	4000.0	156	.0E+00	4000.0

Table E.16 (continued)

Obs Node	Conc (uCi/L)	Time (Year)	Obs Node	Conc (uCi/L)	Time (Year)	Obs Node	Conc (uCi/L)	Time (Year)
157	.0E+00	4000.0	158	.0E+00	4000.0	159	.0E+00	4000.0
160	.0E+00	4000.0	161	.0E+00	4000.0	162	.0E+00	4000.0
163	.0E+00	4000.0	164	.0E+00	4000.0	165	.0E+00	4000.0
166	.0E+00	4000.0	167	.0E+00	4000.0	168	.0E+00	4000.0
169	.0E+00	4000.0	170	.0E+00	4000.0	171	.0E+00	4000.0
172	.0E+00	4000.0	173	.0E+00	4000.0	174	.0E+00	4000.0
175	.0E+00	4000.0	176	.0E+00	4000.0	177	.0E+00	4000.0
178	.0E+00	4000.0	179	.0E+00	4000.0	180	.0E+00	4000.0
181	.0E+00	4000.0	182	.0E+00	4000.0	183	.0E+00	4000.0
184	.0E+00	4000.0	185	.0E+00	4000.0	186	2.0E-38	3988.0
187	3.2E-35	4000.0	188	1.1E-14	3618.0	189	1.4E-13	3996.0
190	8.3E-14	3715.0	191	1.0E-13	3968.0	192	7.9E-22	3597.0
193	9.0E-22	3938.0	194	1.8E-21	3954.0	195	2.7E-20	3968.0
196	1.8E-20	3083.0	197	6.4E-20	3858.0	198	1.9E-17	3335.0
199	4.3E-18	2067.0	200	7.7E-15	2973.0	201	9.3E-13	3035.0
202	3.5E-14	1566.0	203	6.7E-12	1352.0	204	6.3E-11	1059.0
205	4.3E-21	3942.0	206	2.7E-19	3723.0	207	2.1E-17	3104.0
208	2.7E-16	2751.0	209	6.5E-18	905.0	210	7.4E-15	3934.0
211	4.3E-14	3934.0	212	7.4E-13	2472.0	213	1.2E-11	2945.0
214	1.4E-11	2850.0	215	6.2E-11	2445.0	216	7.9E-09	1341.0
217	7.7E-08	1122.0	218	2.5E-08	1328.0	219	2.8E-14	1536.0
220	2.9E-16	2793.0	221	3.6E-18	3143.0	222	1.9E-20	3901.0
223	2.0E-36	3071.0	224	7.6E-38	3341.0	225	4.9E-40	3444.0
226	.0E+00	3731.0	227	.0E+00	4000.0	228	.0E+00	4000.0
229	.0E+00	4000.0	230	.0E+00	4000.0	231	.0E+00	4000.0
232	.0E+00	4000.0	233	.0E+00	4000.0	234	.0E+00	4000.0

Table E.16 (continued)

Obs Node	Conc (uCi/L)	Time (Year)	Obs Node	Conc (uCi/L)	Time (Year)	Obs Node	Conc (uCi/L)	Time (Year)
235	.0E+00	4000.0	236	.0E+00	4000.0	237	.0E+00	4000.0
238	.0E+00	4000.0	239	.0E+00	4000.0	240	.0E+00	4000.0
241	.0E+00	4000.0	242	.0E+00	4000.0	243	.0E+00	4000.0
244	.0E+00	4000.0	245	.0E+00	4000.0	246	.0E+00	4000.0
247	.0E+00	4000.0	248	.0E+00	4000.0	249	.0E+00	4000.0
250	.0E+00	4000.0	251	.0E+00	4000.0	252	.0E+00	4000.0
253	2.0E-24	3174.0	254	8.7E-25	3089.0	255	1.5E-22	3929.0
256	4.3E-23	2860.0	257	1.4E-23	2947.0	258	3.8E-34	623.0
259	8.6E-36	583.0	260	7.7E-24	4000.0	261	1.2E-25	4000.0
262	5.6E-27	4000.0	263	1.4E-28	4000.0	264	1.5E-37	1496.0
265	7.4E-36	2638.0	266	7.7E-34	3950.0	267	9.3E-36	4000.0
268	8.6E-38	3561.0	269	1.1E-35	4000.0	270	1.6E-36	4000.0
271	5.8E-38	4000.0	272	2.8E-38	4000.0	273	.0E+00	4000.0
274	.0E+00	4000.0	275	.0E+00	4000.0	276	.0E+00	4000.0
277	8.6E-38	3852.0	278	.0E+00	2454.0	279	.0E+00	2352.0
280	8.8E-36	3973.0	281	2.7E-32	4000.0	282	6.5E-20	3984.0
283	9.3E-23	2012.0	284	5.6E-18	3768.0	285	3.6E-16	4000.0
286	2.6E-14	3539.0	287	4.0E-14	3919.0	288	3.3E-14	3836.0
289	5.3E-15	3835.0	290	3.4E-14	3734.0	291	9.3E-14	3176.0
292	2.9E-13	3312.0	293	2.0E-13	3601.0	294	5.8E-14	3806.0
295	7.0E-17	3906.0	296	2.6E-18	2907.0	297	2.7E-17	3665.0
298	4.3E-20	978.0	299	1.0E-13	3666.0	300	1.1E-12	3632.0
301	3.7E-12	3610.0	302	6.0E-10	1894.0	303	7.0E-10	1406.0
304	2.2E-10	1671.0	305	4.4E-12	2172.0	306	4.4E-15	3280.0
307	3.8E-13	3951.0	308	1.6E-12	3122.0	309	2.1E-11	1958.0
310	1.2E-09	1578.0	311	5.7E-08	950.0	312	6.0E-17	548.0

Table E.16 (continued)

Obs Node	Conc (uCi/L)	Time (Year)	Obs Node	Conc (uCi/L)	Time (Year)	Obs Node	Conc (uCi/L)	Time (Year)
313	6.9E-18	1751.0	314	9.9E-19	3342.0	315	4.5E-19	2656.0
316	2.4E-28	84.0	317	4.3E-21	3942.0	318	.0E+00	864.0
319	9.4E-34	3594.0	320	3.4E-33	3987.0	321	2.8E-31	3711.0
322	9.1E-31	4000.0	323	4.7E-23	3173.0	324	7.5E-23	4000.0
325	1.8E-16	2654.0	326	5.2E-17	3064.0	327	2.7E-17	3986.0
328	1.5E-17	3894.0	329	2.1E-19	2787.0	330	3.8E-19	2161.0
331	.0E+00	163.0	332	3.0E-19	2111.0	333	2.8E-16	3939.0
334	1.1E-15	3968.0						

Table E.17. Maximum groundwater concentration of nuclide: ^{238}U at 100 m from disposal units

Disposal Unit	Concentration (uCi/L)	Time (Year)
IWMF	2.1E-08	5920.0
Tumulus I	5.2E-07	6940.0
Tumulus II	7.4E-09	578.0
Low-activity silos (N)	5.9E-08	5980.0
Low-activity silos (S)	2.3E-07	6940.0
Fissile wells	8.9E-09	31500.0
Asbestos silos	6.2E-09	678.0
High-activity silos	8.9E-09	726.0

Table E.18. Groundwater concentration of nuclide: ^{239}Pu at observation nodes

Obs Node	Conc (uCi/L)	Time (Year)	Obs Node	Conc (uCi/L)	Time (Year)	Obs Node	Conc (uCi/L)	Time (Year)
1	1.6E-24	1968.0	2	.0E+00	3000.0	3	6.8E-22	3000.0
4	.0E+00	3000.0	5	.0E+00	3000.0	6	1.1E-24	2895.0
7	5.4E-21	2790.0	8	1.9E-20	3000.0	9	3.9E-20	2879.0
10	2.5E-21	3000.0	11	1.9E-18	3000.0	12	1.2E-19	2987.0
13	9.5E-22	3000.0	14	1.2E-17	2491.0	15	6.8E-18	3000.0
16	1.1E-21	2906.0	17	5.4E-22	3000.0	18	8.8E-16	2016.0
19	7.5E-16	3000.0	20	8.7E-25	1569.0	21	7.8E-14	2969.0
22	7.7E-12	2456.0	23	2.0E-20	2783.0	24	4.8E-12	2824.0
25	3.0E-31	640.0	26	5.8E-11	2850.0	27	3.0E-18	2944.0
28	1.1E-11	1119.0	29	2.1E-15	2884.0	30	3.1E-10	2941.0
31	1.2E-15	2997.0	32	6.7E-09	2954.0	33	3.4E-16	2890.0
34	3.1E-08	2957.0	35	7.2E-17	2902.0	36	1.2E-09	2396.0
37	1.1E-09	2897.0	38	4.5E-17	2940.0	39	6.9E-11	3000.0
40	7.0E-10	2797.0	41	2.7E-17	2960.0	42	2.4E-08	2492.0
43	3.7E-10	2843.0	44	9.5E-18	3000.0	45	3.2E-08	2059.0
46	1.9E-10	2972.0	47	5.8E-18	3000.0	48	9.4E-08	2387.0
49	9.5E-12	2641.0	50	1.4E-17	3000.0	51	8.4E-08	2394.0
52	1.4E-12	2676.0	53	4.1E-18	2899.0	54	1.1E-09	2818.0
55	2.1E-13	2462.0	56	8.2E-19	2926.0	57	5.0E-10	2424.0
58	8.9E-14	2980.0	59	2.6E-19	2870.0	60	2.5E-10	2984.0
61	6.5E-15	2700.0	62	2.4E-21	2602.0	63	8.2E-11	2831.0
64	6.9E-17	1946.0	65	6.9E-26	1831.0	66	1.5E-13	1942.0
67	5.5E-17	2383.0	68	5.3E-29	1548.0	69	2.5E-16	3000.0
70	1.2E-17	2650.0	71	8.4E-34	1234.0	72	1.6E-28	106.0
73	6.2E-18	2990.0	74	1.4E-34	1358.0	75	1.3E-16	2310.0
76	3.6E-15	3000.0	77	1.4E-18	2950.0	78	3.6E-34	1404.0

Table E.18 (continued)

Obs Node	Conc (uCi/L)	Time (Year)	Obs Node	Conc (uCi/L)	Time (Year)	Obs Node	Conc (uCi/L)	Time (Year)
79	5.7E-16	1602.0	80	1.2E-12	2645.0	81	7.5E-21	3000.0
82	9.5E-32	1694.0	83	1.0E-14	1215.0	84	2.0E-10	1978.0
85	1.2E-21	2941.0	86	.0E+00	916.0	87	3.9E-13	1044.0
88	3.6E-08	1356.0	89	4.6E-23	2885.0	90	2.7E-25	2908.0
91	9.6E-11	1488.0	92	3.0E-06	1263.0	93	4.5E-21	2994.0
94	2.8E-28	1359.0	95	2.8E-08	1350.0	96	6.3E-06	1250.0
97	4.4E-20	2645.0	98	1.8E-21	2995.0	99	9.4E-06	835.0
100	1.6E-05	1937.0	101	1.4E-18	2565.0	102	1.6E-23	1489.0
103	6.9E-06	1675.0	104	2.8E-05	2399.0	105	8.1E-15	2617.0
106	2.1E-13	2513.0	107	1.8E-13	2562.0	108	3.1E-22	1017.0
109	2.0E-21	2093.0	110	5.7E-06	1646.0	111	2.2E-06	2420.0
112	2.1E-13	3000.0	113	5.8E-22	1022.0	114	8.2E-19	3000.0
115	1.5E-06	2983.0	116	1.1E-07	1968.0	117	1.5E-14	3000.0
118	6.6E-20	3000.0	119	1.1E-06	2832.0	120	3.9E-11	1787.0
121	6.0E-14	3000.0	122	3.2E-07	2875.0	123	3.6E-11	2892.0
124	4.3E-15	1886.0	125	2.9E-10	2567.0	126	9.0E-13	2923.0
127	3.3E-08	2919.0	128	6.7E-14	2932.0	129	1.2E-08	2794.0
130	2.0E-15	3000.0	131	2.9E-10	3000.0	132	2.0E-14	2838.0
133	2.4E-11	2804.0	134	2.3E-15	1373.0	135	1.8E-12	3000.0
136	1.4E-15	1436.0	137	2.7E-12	2728.0	138	.0E+00	134.0
139	1.2E-11	2423.0	140	4.4E-13	2942.0	141	1.7E-14	1948.0
142	.0E+00	251.0	143	8.3E-14	2502.0	144	3.5E-17	2720.0
145	2.5E-21	2504.0	146	2.4E-18	2575.0	147	2.9E-17	3000.0
148	7.1E-17	3000.0	149	3.6E-17	3000.0	150	4.6E-16	2680.0
151	4.2E-36	262.0	152	5.9E-19	3000.0	153	2.7E-21	3000.0
154	3.0E-32	793.0	155	5.8E-23	3000.0	156	2.4E-22	3000.0

Table E.18 (continued)

Obs Node	Conc (uCi/L)	Time (Year)	Obs Node	Conc (uCi/L)	Time (Year)	Obs Node	Conc (uCi/L)	Time (Year)
157	8.6E-22	2876.0	158	9.6E-24	2192.0	159	5.2E-22	2307.0
160	3.8E-21	1409.0	161	1.6E-19	2534.0	162	1.7E-19	2579.0
163	2.8E-20	3000.0	164	1.3E-19	2516.0	165	2.2E-19	2669.0
166	3.1E-06	2930.0	167	3.5E-06	2210.0	168	4.2E-06	2366.0
169	4.1E-06	2098.0	170	3.9E-11	1787.0	171	1.1E-12	3000.0
172	1.8E-13	2159.0	173	3.6E-14	1527.0	174	2.5E-10	2118.0
175	6.0E-11	3000.0	176	1.8E-12	3000.0	177	6.7E-13	2194.0
178	3.1E-13	2961.0	179	8.0E-13	2865.0	180	6.9E-13	3000.0
181	4.8E-13	2222.0	182	1.3E-14	2527.0	183	1.2E-13	2934.0
184	1.8E-13	2932.0	185	3.8E-12	2581.0	186	1.5E-14	992.0
187	1.7E-11	2001.0	188	2.2E-17	3000.0	189	1.6E-19	2982.0
190	1.5E-22	2158.0	191	1.4E-31	984.0	192	1.2E-11	2918.0
193	6.7E-15	2858.0	194	9.0E-15	1740.0	195	7.5E-14	2861.0
196	2.3E-14	2108.0	197	2.3E-15	2995.0	198	5.0E-15	1128.0
199	1.2E-14	2067.0	200	6.4E-15	1866.0	201	1.7E-19	526.0
202	9.6E-17	921.0	203	1.8E-13	2966.0	204	1.0E-12	3000.0
205	1.8E-09	2835.0	206	3.9E-09	2941.0	207	1.4E-08	2402.0
208	1.4E-07	2751.0	209	4.7E-09	2739.0	210	3.4E-09	2088.0
211	6.0E-09	2015.0	212	4.4E-08	984.0	213	1.3E-08	1367.0
214	3.0E-10	2892.0	215	7.7E-11	2889.0	216	6.8E-11	2889.0
217	5.3E-11	1822.0	218	8.3E-10	2911.0	219	3.0E-10	2469.0
220	4.9E-11	2884.0	221	6.5E-11	2781.0	222	4.2E-11	2709.0
223	3.3E-18	1651.0	224	1.0E-18	1234.0	225	7.0E-19	2594.0
226	1.8E-16	2598.0	227	1.8E-14	1439.0	228	6.5E-13	927.0
229	1.1E-12	1353.0	230	3.1E-12	1421.0	231	1.1E-13	1926.0
232	1.3E-12	1753.0	233	1.0E-11	1990.0	234	1.3E-10	2039.0

Table E.18 (continued)

Obs Node	Conc (uCi/L)	Time (Year)	Obs Node	Conc (uCi/L)	Time (Year)	Obs Node	Conc (uCi/L)	Time (Year)
235	1.1E-09	1741.0	236	3.5E-08	2016.0	237	4.0E-07	1570.0
238	3.4E-07	1668.0	239	1.4E-07	2661.0	240	.0E+00	2.0
241	.0E+00	3.0	242	.0E+00	4.0	243	.0E+00	9.0
244	2.9E-14	3000.0	245	1.1E-13	2073.0	246	3.8E-13	2160.0
247	7.2E-12	2146.0	248	2.3E-11	2120.0	249	1.0E-09	2203.0
250	2.4E-08	2974.0	251	3.1E-07	2925.0	252	1.7E-06	2891.0
253	4.6E-17	2233.0	254	1.3E-15	2931.0	255	1.8E-15	2822.0
256	5.4E-15	2957.0	257	3.5E-16	1617.0	258	4.5E-15	2108.0
259	2.1E-18	441.0	260	1.6E-29	96.0	261	5.2E-17	1116.0
262	7.0E-18	2602.0	263	2.0E-18	2150.0	264	.0E+00	5.0
265	.0E+00	3.0	266	1.1E-20	52.0	267	1.5E-09	3000.0
268	2.9E-08	3000.0	269	2.7E-08	2105.0	270	4.8E-13	249.0
271	2.3E-18	50.0	272	1.5E-08	2844.0	273	5.4E-07	2032.0
274	6.5E-11	1654.0	275	.0E+00	3.0	276	4.8E-13	1815.0
277	.0E+00	1.0	278	1.0E-08	2777.0	279	3.2E-09	2898.0
280	4.0E-10	2727.0	281	5.5E-12	2738.0	282	3.1E-22	557.0
283	3.2E-18	1744.0	284	2.4E-16	2906.0	285	2.4E-16	2816.0
286	5.1E-20	2012.0	287	1.1E-24	1457.0	288	6.1E-28	814.0
289	8.0E-29	879.0	290	9.6E-32	558.0	291	4.0E-22	1990.0
292	1.9E-28	836.0	293	5.6E-29	966.0	294	2.9E-31	844.0
295	2.8E-07	1692.0	296	1.3E-07	1800.0	297	1.4E-07	1718.0
298	1.0E-07	2975.0	299	1.9E-07	2559.0	300	7.3E-15	279.0
301	3.8E-11	2991.0	302	1.5E-10	1894.0	303	1.4E-09	2861.0
304	7.4E-08	2853.0	305	3.5E-07	2173.0	306	2.5E-06	1128.0
307	9.0E-09	1382.0	308	6.8E-08	2931.0	309	4.9E-09	1959.0
310	2.4E-09	2688.0	311	1.3E-09	2929.0	312	3.2E-06	896.0

Table E.18 (continued)

Obs Node	Conc (uCi/L)	Time (Year)	Obs Node	Conc (uCi/L)	Time (Year)	Obs Node	Conc (uCi/L)	Time (Year)
313	8.1E-07	2897.0	314	5.5E-07	2593.0	315	1.9E-06	1562.0
316	2.5E-06	1562.0	317	1.8E-09	2835.0	318	.0E+00	34.0
319	4.2E-19	2487.0	320	9.5E-19	3000.0	321	2.6E-17	2528.0
322	2.4E-17	2834.0	323	2.3E-11	2232.0	324	1.8E-11	2841.0
325	3.3E-12	2654.0	326	1.7E-12	2956.0	327	3.1E-13	2879.0
328	2.8E-14	3000.0	329	1.5E-14	2968.0	330	1.6E-15	2908.0
331	5.4E-16	2902.0	332	2.5E-16	2940.0	333	1.3E-16	2992.0
334	2.4E-17	2908.0						

Table E.19. Groundwater concentration of nuclide: ^{241}Am at observation nodes

Obs Node	Conc (uCi/L)	Time (Year)	Obs Node	Conc (uCi/L)	Time (Year)	Obs Node	Conc (uCi/L)	Time (Year)
1	.0E+00	2000.0	2	.0E+00	2000.0	3	.0E+00	2000.0
4	.0E+00	2000.0	5	.0E+00	2000.0	6	.0E+00	2000.0
7	.0E+00	2000.0	8	.0E+00	2000.0	9	.0E+00	2000.0
10	.0E+00	2000.0	11	.0E+00	2000.0	12	.0E+00	2000.0
13	.0E+00	2000.0	14	2.2E-33	1844.0	15	.0E+00	2000.0
16	.0E+00	2000.0	17	.0E+00	2000.0	18	2.0E-31	1739.0
19	.0E+00	2000.0	20	.0E+00	2000.0	21	6.2E-29	1839.0
22	7.5E-32	1805.0	23	.0E+00	2000.0	24	2.1E-27	1651.0
25	.0E+00	2000.0	26	7.8E-27	826.0	27	7.8E-35	1838.0
28	7.1E-23	2000.0	29	.0E+00	1466.0	30	1.3E-19	1406.0
31	3.5E-30	1902.0	32	9.3E-18	1523.0	33	.0E+00	969.0
34	2.0E-15	1228.0	35	5.4E-30	2000.0	36	2.4E-21	52.0
37	.0E+00	96.0	38	2.1E-30	1985.0	39	.0E+00	2.0
40	5.2E-18	1690.0	41	2.4E-35	1054.0	42	1.5E-10	1385.0
43	9.6E-18	1755.0	44	3.9E-29	2000.0	45	6.7E-10	962.0
46	7.2E-18	1865.0	47	7.2E-29	2000.0	48	5.8E-10	1280.0
49	5.1E-18	1797.0	50	3.5E-28	1944.0	51	4.2E-10	1287.0
52	3.0E-18	1921.0	53	6.0E-29	1972.0	54	1.3E-12	1950.0
55	4.5E-17	1769.0	56	2.5E-29	2000.0	57	6.0E-13	2000.0
58	1.4E-17	1975.0	59	2.1E-29	1989.0	60	3.1E-13	1962.0
61	3.0E-20	777.0	62	.0E+00	944.0	63	4.2E-14	1960.0
64	6.8E-21	787.0	65	.0E+00	1066.0	66	5.7E-15	1942.0
67	4.5E-20	1276.0	68	.0E+00	1194.0	69	3.3E-18	2000.0
70	3.2E-21	1531.0	71	.0E+00	1395.0	72	2.7E-28	106.0
73	4.7E-21	1924.0	74	.0E+00	1640.0	75	4.8E-18	1729.0
76	.0E+00	4.0	77	2.0E-22	1805.0	78	.0E+00	1469.0

Table E.19 (continued)

Obs Node	Conc (uCi/L)	Time (Year)	Obs Node	Conc (uCi/L)	Time (Year)	Obs Node	Conc (uCi/L)	Time (Year)
79	4.5E-18	965.0	80	4.1E-14	530.0	81	5.5E-24	2000.0
82	8.0E-33	1672.0	83	2.0E-16	1064.0	84	1.7E-11	1900.0
85	3.7E-25	1834.0	86	.0E+00	1256.0	87	1.3E-14	878.0
88	8.4E-09	1356.0	89	3.8E-26	1890.0	90	3.5E-29	1947.0
91	1.3E-12	1488.0	92	8.4E-07	1263.0	93	1.2E-23	1985.0
94	4.9E-29	1304.0	95	5.2E-10	1194.0	96	1.8E-06	1250.0
97	3.5E-22	1714.0	98	2.7E-25	2000.0	99	3.6E-07	835.0
100	2.2E-06	1254.0	101	5.5E-21	1267.0	102	6.4E-24	1337.0
103	1.3E-07	1254.0	104	2.7E-06	1292.0	105	1.6E-16	1757.0
106	3.6E-16	1511.0	107	2.6E-16	1498.0	108	5.6E-22	1022.0
109	2.7E-23	1359.0	110	8.7E-08	1222.0	111	1.3E-08	1716.0
112	5.2E-16	1915.0	113	1.8E-22	1045.0	114	2.4E-22	1396.0
115	1.6E-09	1876.0	116	4.7E-09	1968.0	117	2.0E-17	2000.0
118	6.1E-23	2000.0	119	4.7E-10	1725.0	120	2.1E-12	1787.0
121	4.3E-17	1677.0	122	2.3E-10	1985.0	123	3.3E-13	1785.0
124	2.5E-16	1886.0	125	1.2E-14	1460.0	126	9.5E-16	1816.0
127	1.5E-12	1812.0	128	3.6E-16	1587.0	129	1.1E-12	1687.0
130	6.1E-18	2000.0	131	3.4E-13	1986.0	132	1.5E-16	1731.0
133	2.2E-15	2000.0	134	3.3E-16	1373.0	135	1.2E-15	1945.0
136	1.8E-16	1418.0	137	4.6E-16	1621.0	138	.0E+00	198.0
139	2.4E-26	257.0	140	2.1E-15	1984.0	141	1.7E-16	1948.0
142	.0E+00	307.0	143	6.5E-17	1455.0	144	2.5E-20	2000.0
145	2.1E-25	1982.0	146	9.9E-24	1041.0	147	3.2E-20	2000.0
148	1.7E-19	2000.0	149	2.0E-19	1458.0	150	9.0E-19	1573.0
151	.0E+00	264.0	152	4.8E-23	2000.0	153	2.1E-26	1630.0
154	7.3E-33	793.0	155	8.8E-27	2000.0	156	6.4E-26	1973.0

Table E.19 (continued)

Obs Node	Conc (uCi/L)	Time (Year)	Obs Node	Conc (uCi/L)	Time (Year)	Obs Node	Conc (uCi/L)	Time (Year)
157	2.1E-27	1146.0	158	6.9E-27	1725.0	159	1.1E-27	950.0
160	8.5E-23	1407.0	161	6.1E-23	2000.0	162	2.8E-23	2000.0
163	1.1E-23	1911.0	164	1.2E-23	1985.0	165	5.0E-24	1974.0
166	1.5E-08	1982.0	167	2.1E-08	1960.0	168	2.5E-08	1926.0
169	1.6E-08	1764.0	170	2.1E-12	1787.0	171	4.8E-15	1972.0
172	7.6E-15	1895.0	173	2.7E-15	1442.0	174	1.0E-12	1934.0
175	1.3E-13	2000.0	176	5.5E-15	2000.0	177	2.6E-16	2000.0
178	6.6E-16	1989.0	179	5.0E-16	1988.0	180	8.9E-16	2000.0
181	4.2E-16	2000.0	182	6.5E-19	356.0	183	3.5E-16	1994.0
184	9.8E-16	1110.0	185	9.8E-15	1474.0	186	2.5E-15	992.0
187	4.4E-13	1998.0	188	1.7E-27	1995.0	189	2.0E-28	2000.0
190	5.7E-31	1534.0	191	.0E+00	805.0	192	4.4E-14	1999.0
193	4.3E-16	1724.0	194	9.2E-16	1740.0	195	8.0E-16	1754.0
196	7.2E-16	861.0	197	2.0E-16	1084.0	198	6.7E-16	1128.0
199	2.5E-16	1953.0	200	2.5E-16	1866.0	201	6.4E-20	526.0
202	1.0E-28	77.0	203	4.8E-19	459.0	204	8.6E-15	1727.0
205	6.2E-24	971.0	206	1.0E-20	1064.0	207	1.2E-20	503.0
208	4.6E-29	13.0	209	.0E+00	2.0	210	1.0E-10	1404.0
211	6.2E-10	841.0	212	7.7E-09	691.0	213	1.2E-09	1367.0
214	3.2E-12	1785.0	215	5.1E-14	1782.0	216	2.3E-14	1781.0
217	3.8E-16	1780.0	218	2.4E-17	1328.0	219	6.8E-21	1536.0
220	1.4E-26	938.0	221	2.4E-26	1305.0	222	1.4E-26	2000.0
223	5.0E-20	1220.0	224	3.1E-20	1234.0	225	6.5E-21	843.0
226	2.0E-18	2000.0	227	4.7E-16	1248.0	228	2.2E-14	927.0
229	3.6E-14	899.0	230	5.6E-14	852.0	231	1.5E-15	1399.0
232	1.7E-14	1387.0	233	1.1E-13	1429.0	234	2.0E-12	912.0

Table E.19 (continued)

Obs Node	Conc (uCi/L)	Time (Year)	Obs Node	Conc (uCi/L)	Time (Year)	Obs Node	Conc (uCi/L)	Time (Year)
235	1.6E-11	1109.0	236	1.0E-09	885.0	237	1.3E-08	851.0
238	8.9E-09	698.0	239	1.8E-09	471.0	240	.0E+00	2.0
241	.0E+00	3.0	242	.0E+00	4.0	243	.0E+00	19.0
244	3.7E-17	2000.0	245	4.6E-16	1997.0	246	1.8E-15	1958.0
247	1.2E-13	1017.0	248	4.0E-14	993.0	249	3.6E-12	1992.0
250	6.7E-11	1992.0	251	1.6E-10	1818.0	252	3.5E-09	1784.0
253	3.8E-20	1074.0	254	2.5E-18	2000.0	255	7.4E-18	2000.0
256	1.7E-17	1850.0	257	8.2E-17	1578.0	258	7.8E-16	1513.0
259	2.0E-18	441.0	260	2.8E-29	96.0	261	2.4E-17	1116.0
262	5.5E-19	1995.0	263	1.2E-19	2000.0	264	.0E+00	6.0
265	.0E+00	3.0	266	8.2E-21	52.0	267	7.7E-11	1087.0
268	1.6E-09	1081.0	269	2.1E-09	832.0	270	3.0E-13	249.0
271	1.7E-18	50.0	272	8.1E-10	1366.0	273	5.2E-08	897.0
274	5.2E-12	1290.0	275	.0E+00	3.0	276	2.5E-14	1815.0
277	.0E+00	1.0	278	3.9E-10	1670.0	279	5.5E-11	1442.0
280	1.8E-12	1620.0	281	7.4E-15	1941.0	282	2.6E-19	1769.0
283	2.0E-19	1744.0	284	1.2E-18	2000.0	285	2.0E-19	1709.0
286	1.4E-21	1655.0	287	1.2E-21	1770.0	288	2.6E-23	2000.0
289	5.1E-24	1990.0	290	4.4E-35	493.0	291	2.2E-27	1233.0
292	1.7E-27	1396.0	293	1.8E-28	1406.0	294	.0E+00	660.0
295	1.6E-08	1441.0	296	5.9E-09	1800.0	297	7.4E-09	1718.0
298	6.1E-09	1559.0	299	1.0E-08	1452.0	300	3.7E-15	279.0
301	1.2E-13	584.0	302	6.6E-14	1334.0	303	.0E+00	3.0
304	2.0E-14	1468.0	305	7.2E-15	1586.0	306	1.9E-16	1823.0
307	9.6E-13	799.0	308	8.1E-14	1406.0	309	.0E+00	6.0
310	1.4E-16	1578.0	311	3.0E-16	1395.0	312	2.2E-15	1317.0

Table E.19 (continued)

Obs Node	Conc (uCi/L)	Time (Year)	Obs Node	Conc (uCi/L)	Time (Year)	Obs Node	Conc (uCi/L)	Time (Year)
313	6.9E-18	1979.0	314	4.8E-32	52.0	315	1.7E-20	2000.0
316	6.3E-18	1548.0	317	6.2E-24	971.0	318	.0E+00	2000.0
319	.0E+00	2000.0	320	.0E+00	2000.0	321	.0E+00	2000.0
322	.0E+00	2000.0	323	2.1E-33	936.0	324	4.6E-30	2000.0
325	.0E+00	400.0	326	.0E+00	405.0	327	.0E+00	552.0
328	.0E+00	646.0	329	.0E+00	736.0	330	9.5E-28	1973.0
331	9.6E-29	1943.0	332	3.4E-29	2000.0	333	2.5E-32	1219.0
334	7.3E-28	1970.0						

Table E.20. Groundwater concentration of nuclide: ^{243}Am at observation nodes

Obs Node	Conc (uCi/L)	Time (Year)	Obs Node	Conc (uCi/L)	Time (Year)	Obs Node	Conc (uCi/L)	Time (Year)
1	.0E+00	5000.0	2	.0E+00	5000.0	3	.0E+00	4292.0
4	.0E+00	5000.0	5	.0E+00	5000.0	6	.0E+00	5000.0
7	.0E+00	3736.0	8	.0E+00	4104.0	9	3.1E-34	5000.0
10	.0E+00	4781.0	11	.0E+00	2779.0	12	2.1E-33	4991.0
13	.0E+00	4968.0	14	1.7E-31	3893.0	15	9.0E-32	4963.0
16	2.1E-34	5000.0	17	1.3E-34	4991.0	18	1.4E-28	5000.0
19	1.7E-30	4714.0	20	1.0E-32	4890.0	21	3.7E-26	4950.0
22	4.3E-31	1805.0	23	2.3E-30	4899.0	24	1.5E-24	4727.0
25	3.5E-29	4437.0	26	1.6E-22	3629.0	27	6.1E-27	5000.0
28	6.4E-21	2812.0	29	3.1E-24	5000.0	30	7.1E-19	1833.0
31	2.0E-25	3538.0	32	3.5E-17	1523.0	33	.0E+00	969.0
34	4.7E-15	1228.0	35	1.6E-21	5000.0	36	1.0E-21	52.0
37	.0E+00	81.0	38	3.7E-21	5000.0	39	1.5E-11	3215.0
40	3.5E-17	2567.0	41	3.8E-21	5000.0	42	6.4E-09	2492.0
43	5.5E-16	3969.0	44	5.9E-21	5000.0	45	1.2E-08	3166.0
46	2.7E-15	3429.0	47	5.0E-20	4925.0	48	2.5E-08	2387.0
49	2.2E-15	4310.0	50	3.0E-19	5000.0	51	2.2E-08	2394.0
52	2.6E-15	3526.0	53	2.3E-19	4926.0	54	1.6E-09	3525.0
55	2.0E-14	3490.0	56	1.2E-19	5000.0	57	1.6E-09	4385.0
58	2.0E-14	3795.0	59	9.4E-20	5000.0	60	6.8E-10	4623.0
61	1.7E-15	2700.0	62	1.3E-19	4971.0	63	2.7E-10	4219.0
64	2.1E-16	3053.0	65	1.9E-21	5000.0	66	4.1E-11	4156.0
67	9.7E-17	3490.0	68	2.3E-35	1116.0	69	3.2E-14	4251.0
70	1.5E-16	4573.0	71	2.5E-34	1225.0	72	2.0E-17	4006.0
73	9.6E-17	4864.0	74	5.3E-36	1229.0	75	1.9E-19	2027.0
76	8.7E-18	4906.0	77	7.9E-18	4019.0	78	1.2E-35	1404.0

Table E.20 (continued)

Obs Node	Conc (uCi/L)	Time (Year)	Obs Node	Conc (uCi/L)	Time (Year)	Obs Node	Conc (uCi/L)	Time (Year)
79	1.5E-17	4655.0	80	4.0E-18	1283.0	81	1.5E-18	5000.0
82	2.7E-32	1679.0	83	5.7E-16	1215.0	84	1.3E-16	1017.0
85	1.8E-19	5000.0	86	.0E+00	916.0	87	2.3E-14	2765.0
88	1.3E-14	677.0	89	9.8E-21	4874.0	90	1.5E-23	4681.0
91	4.9E-12	1488.0	92	1.1E-12	700.0	93	1.7E-20	4199.0
94	1.3E-22	4974.0	95	1.4E-09	1350.0	96	3.8E-10	2357.0
97	1.5E-17	5000.0	98	5.1E-20	4838.0	99	5.0E-07	835.0
100	2.6E-07	1937.0	101	5.2E-16	4588.0	102	5.3E-24	1489.0
103	3.5E-07	1675.0	104	5.0E-07	2399.0	105	3.5E-15	3725.0
106	6.0E-13	3620.0	107	5.7E-13	3669.0	108	2.9E-15	4754.0
109	1.8E-18	4299.0	110	2.9E-07	1646.0	111	4.0E-08	3527.0
112	2.3E-12	4429.0	113	2.4E-22	1054.0	114	1.1E-16	4717.0
115	6.9E-08	2983.0	116	8.0E-09	3075.0	117	9.1E-13	4721.0
118	4.1E-18	5000.0	119	5.5E-08	3454.0	120	7.3E-13	5000.0
121	2.2E-12	4641.0	122	3.2E-08	3457.0	123	3.6E-12	3693.0
124	2.0E-12	4899.0	125	2.5E-09	4289.0	126	4.6E-12	4904.0
127	9.6E-09	4026.0	128	9.3E-14	4590.0	129	8.2E-09	4828.0
130	1.7E-14	4650.0	131	2.4E-09	4200.0	132	4.3E-14	4692.0
133	2.0E-10	4558.0	134	6.5E-16	1373.0	135	2.2E-11	4361.0
136	4.0E-16	1435.0	137	9.7E-12	4843.0	138	1.3E-14	4447.0
139	6.1E-12	3980.0	140	3.9E-13	4198.0	141	6.4E-13	4162.0
142	.0E+00	307.0	143	1.0E-12	4776.0	144	1.9E-16	4535.0
145	4.2E-19	4718.0	146	3.4E-16	4752.0	147	2.7E-15	4746.0
148	1.4E-14	4760.0	149	1.1E-14	4779.0	150	1.3E-14	4894.0
151	.0E+00	264.0	152	1.6E-17	4762.0	153	2.7E-19	4951.0
154	9.6E-21	4852.0	155	9.8E-21	5000.0	156	2.0E-19	4828.0

Table E.20 (continued)

Obs Node	Conc (uCi/L)	Time (Year)	Obs Node	Conc (uCi/L)	Time (Year)	Obs Node	Conc (uCi/L)	Time (Year)
157	4.9E-19	5000.0	158	4.4E-25	2192.0	159	1.4E-23	2325.0
160	2.7E-22	1409.0	161	7.5E-19	3641.0	162	8.6E-19	3686.0
163	4.8E-19	4322.0	164	5.4E-18	4730.0	165	7.2E-18	4862.0
166	1.5E-07	3153.0	167	1.7E-07	2210.0	168	2.1E-07	2366.0
169	2.0E-07	2098.0	170	7.3E-13	5000.0	171	4.2E-13	4264.0
172	6.8E-19	889.0	173	1.0E-14	1527.0	174	9.9E-10	4332.0
175	3.0E-10	4414.0	176	7.7E-12	4414.0	177	5.4E-12	4408.0
178	1.5E-12	4203.0	179	1.0E-11	4970.0	180	1.1E-11	4884.0
181	5.6E-12	4918.0	182	4.4E-14	4741.0	183	9.2E-14	4273.0
184	1.9E-13	4438.0	185	1.7E-11	4322.0	186	4.4E-15	992.0
187	1.0E-10	4215.0	188	1.5E-19	5000.0	189	2.4E-19	5000.0
190	3.8E-19	5000.0	191	8.1E-20	5000.0	192	2.5E-10	4869.0
193	3.3E-12	4854.0	194	2.7E-12	4944.0	195	2.0E-14	2861.0
196	1.6E-13	3083.0	197	6.5E-14	5000.0	198	3.7E-14	3335.0
199	5.4E-14	4281.0	200	1.8E-15	1866.0	201	5.1E-20	526.0
202	8.8E-14	4887.0	203	1.7E-13	3241.0	204	1.8E-13	3190.0
205	2.0E-21	4732.0	206	2.8E-19	4830.0	207	3.7E-17	4237.0
208	1.8E-29	13.0	209	1.0E-12	2412.0	210	7.2E-10	1876.0
211	1.1E-09	1299.0	212	1.3E-08	984.0	213	3.8E-09	1367.0
214	3.2E-11	2892.0	215	3.3E-13	2135.0	216	1.6E-13	1943.0
217	2.2E-14	2887.0	218	2.2E-15	3542.0	219	3.5E-19	2804.0
220	1.7E-19	5000.0	221	8.7E-21	5000.0	222	5.5E-25	2700.0
223	1.4E-19	1647.0	224	1.2E-19	3304.0	225	2.0E-19	3701.0
226	1.6E-17	2673.0	227	9.2E-16	1439.0	228	3.4E-14	927.0
229	5.6E-14	1353.0	230	1.6E-13	1421.0	231	5.4E-15	1926.0
232	6.5E-14	1753.0	233	5.1E-13	1990.0	234	6.3E-12	2039.0

Table E.20 (continued)

Obs Node	Conc (uCi/L)	Time (Year)	Obs Node	Conc (uCi/L)	Time (Year)	Obs Node	Conc (uCi/L)	Time (Year)
235	5.3E-11	1741.0	236	1.7E-09	2016.0	237	2.0E-08	1570.0
238	1.7E-08	1668.0	239	7.0E-09	2661.0	240	.0E+00	2.0
241	.0E+00	3.0	242	.0E+00	4.0	243	.0E+00	15.0
244	1.9E-14	5000.0	245	4.1E-14	4287.0	246	8.8E-14	4374.0
247	5.2E-13	3938.0	248	9.3E-12	3227.0	249	5.5E-10	4400.0
250	6.2E-09	4206.0	251	2.2E-08	4032.0	252	7.7E-08	2891.0
253	8.9E-15	4743.0	254	1.1E-14	4395.0	255	6.1E-16	3090.0
256	1.4E-15	2957.0	257	1.4E-16	4054.0	258	2.3E-17	4759.0
259	5.8E-19	5000.0	260	5.8E-24	499.0	261	2.0E-19	1116.0
262	8.2E-20	1606.0	263	6.6E-22	741.0	264	.0E+00	6.0
265	.0E+00	3.0	266	2.2E-12	4242.0	267	4.4E-10	5000.0
268	8.6E-09	5000.0	269	8.2E-09	4240.0	270	.0E+00	1.0
271	7.2E-19	50.0	272	4.2E-09	3951.0	273	1.8E-07	4246.0
274	1.8E-11	1654.0	275	.0E+00	3.0	276	2.1E-15	1815.0
277	.0E+00	1.0	278	3.6E-09	4298.0	279	1.2E-09	4763.0
280	3.8E-10	4941.0	281	2.3E-11	4952.0	282	2.5E-23	1008.0
283	9.5E-17	3958.0	284	2.0E-15	4292.0	285	1.0E-15	4875.0
286	1.8E-20	2007.0	287	2.2E-24	1457.0	288	7.1E-19	4943.0
289	2.4E-29	879.0	290	3.3E-19	4847.0	291	8.2E-19	4933.0
292	8.3E-19	5000.0	293	8.1E-19	4887.0	294	2.6E-19	5000.0
295	7.9E-08	1692.0	296	3.5E-08	1800.0	297	3.9E-08	1718.0
298	2.8E-08	1868.0	299	5.1E-08	2559.0	300	2.4E-11	3483.0
301	9.0E-12	2974.0	302	2.0E-13	1368.0	303	2.0E-15	2215.0
304	8.9E-14	1671.0	305	3.8E-14	1801.0	306	8.5E-16	2015.0
307	1.7E-12	1729.0	308	3.4E-13	1676.0	309	.0E+00	5.0
310	6.4E-16	2685.0	311	8.5E-15	2502.0	312	9.4E-15	2007.0

Table E.20 (continued)

Obs Node	Conc (uCi/L)	Time (Year)	Obs Node	Conc (uCi/L)	Time (Year)	Obs Node	Conc (uCi/L)	Time (Year)
313	7.4E-17	4273.0	314	1.1E-18	5000.0	315	9.7E-19	4870.0
316	7.1E-17	4703.0	317	2.0E-21	4732.0	318	.0E+00	2465.0
319	2.2E-33	4390.0	320	2.9E-33	5000.0	321	1.8E-31	5000.0
322	1.5E-31	4944.0	323	1.7E-27	4195.0	324	2.6E-28	2435.0
325	1.1E-19	5000.0	326	5.8E-20	5000.0	327	3.0E-20	5000.0
328	1.1E-20	5000.0	329	1.5E-21	5000.0	330	9.1E-21	5000.0
331	4.2E-21	5000.0	332	7.9E-21	4926.0	333	1.3E-20	5000.0
334	2.4E-20	5000.0						

APPENDIX F

PREDICTED AMOUNTS OF VARIOUS RADIONUCLIDES LEACHED FROM DISPOSAL UNITS IN SOLID WASTE STORAGE AREA 6

J. W. Nehls, Jr.
M. L. Tharp
M. W. Yambert

June 1993

Table F.1. Example of an input and output file for the leaching of ^{232}Th from Tumulus II[a]

Input data summary

Groundwater properties

Flux entering disposal unit
(cm/month)

January:	9.58×10^{0}	February:	8.56×10^{0}	March:	8.30×10^{0}
April:	5.77×10^{0}	May:	7.43×10^{0}	June:	6.70×10^{-1}
July:	2.00×10^{-1}	August:	2.50×10^{-1}	September:	1.60×10^{-1}
October:	1.00×10^{-1}	November:	7.00×10^{-2}	December:	6.86×10^{0}

Disposal unit area	3.56×10^{2} m^3
Total dissolved solids	3.49×10^{2} ppm
Groundwater temperature	1.50×10^{1} °C
Groundwater pH	6.75×10^{0}

Saturated hydraulic conductivity:	
Recharge	5.80×10^{-7} cm/s
Soil backfill	3.50×10^{-3} cm/s
Concrete	1.00×10^{-10} cm/s

Groundwater constituent concentrations:	
Ca^{2+}	2.10×10^{-3} mol/L
Cl^{-}	2.04×10^{-4} mol/L
CO_3^{2-}	1.00×10^{-3} mol/L
Mg^{2+}	5.21×10^{-4} mol/L
SO_4^{2-}	2.62×10^{-4} mol/L
O_2	1.63×10^{-4} mol/L

Constituent solubilities:	
$Ca(OH)_2$	2.00×10^{-2} mol/L
CO_3^{2-}	1.20×10^{-3} mol/L
Mg^{2+}	1.20×10^{-3} mol/L

Table F.1 (continued)

Concrete constituent concentrations:	
Calcium concentration in C-S-H system	1.75×10^{0} mol/L
Calcium concentration in pore fluid	2.00×10^{-2} mol/L
CaO content in cement	2.11×10^{0} mol/L
Free Cl^-	1.00×10^{-2} mol/L
Silica concentration in C-S-H system	7.10×10^{-1} mol/L
Concrete design specifications:	
Compressive strength at 28 days	3.52×10^{2} kg/cm^2
Poisson's ratio of concrete	1.50×10^{-1}
Modulus of elasticity of steel	2.04×10^{6} kg/cm^2
Yield strength of steel	4.22×10^{3} kg/cm^2
Modulus of subgrade reaction	1.41×10^{2} kg/cm^2
Young's modulus of elasticity	2.04×10^{5} kg/cm^2
Concrete water/cement ratio	4.00×10^{-1}
Concrete density	2.40×10^{0} g/cm^3
Concrete porosity	1.50×10^{-1}
Cement content	3.85×10^{2} kg/m^3
Initial pH	1.25×10^{1}
Diffusion coefficients in concrete:	
NaOH, KOH	2.12×10^{-11} m^2/s
$Ca(OH)_2$	1.82×10^{-11} m^2/s
Cl^-	5.08×10^{-11} m^2/s
CO_2	1.92×10^{-10} m^2/s
O_2	2.10×10^{-10} m^2/s
SO_4^{2-}	1.06×10^{-11} m^2/s
Tumulus design specifications:	
Layers of vaults	2
Number of vaults wide	10
Number of vaults long	11
Vault dimensions:	
Width	1.52×10^{0} m
Length	2.13×10^{0} m
Height	1.65×10^{0} m

Table F.1 (continued)

Concrete member thickness:	
Roof	1.78×10^{1} cm
Walls	1.78×10^{1} cm
Floor	1.78×10^{1} cm
Steel reinforcement radius:	
Roof	7.94×10^{-1} cm
Walls	6.35×10^{-1} cm
Floor	6.35×10^{-1} cm
Spacing of steel reinforcement:	
Roof	2.54×10^{1} cm
Walls	3.05×10^{1} cm
Floor	3.05×10^{1} cm
Concrete cover thickness on tension face:	
Roof:	
X-direction	7.77×10^{0} cm
Y-direction	9.37×10^{0} cm
Walls:	
Horizontal direction	8.26×10^{0} cm
Vertical direction	9.52×10^{0} cm
Floor:	
X-direction	5.08×10^{0} cm
Y-direction	6.35×10^{0} cm
Static load:	
Vault layer 1	3.65×10^{-1} kg/cm^2
Vault layer 2	7.10×10^{-1} kg/cm^2
Soil and waste properties:	
Earthen cover thickness	1.83×10^{0} m
Earthen cover density	1.76×10^{0} g/cm^2
Friction angle of waste backfill	4.00×10^{1} deg
Friction angle of soil backfill	3.00×10^{1} deg
Density of waste backfill	1.76×10^{0} g/cm^3
Density of soil backfill	1.76×10^{0} g/cm^3
Waste density	1.76×10^{0} g/cm^3
Average moisture content of waste	9.90×10^{-1}

Table F.1. (continued)

Concrete and waste package failure rates:	
Waste container:	
Start of failure	0 years
Time to complete failure	6.00×10^{1} years
Epoxy coating:	
Start of failure	0 years
Time to complete failure	2.00×10^{1} years

Nuclide-specific parameters

Nuclide	^{232}Th
Half-life	1.41×10^{1} years
Solubility	7.57×10^{-8} mol/L
Waste K_d	5.36×10^{1} ml/g
Diffusion coefficient	
Waste	3.24×10^{-14} m^2/s
Concrete	3.73×10^{-15} m^2/s
Initial inventory	1.64×10^{1} g

Output summary (leaching of ^{232}Th)

	Inventory[b]		Amount leached[c,d] (g/year)		
Year	Vault 1	Vault 2	Advection	Diffusion	Total
1	1.64×10^{1}	1.64×10^{1}	6.14×10^{-8}	0	6.14×10^{-8}
10	1.64×10^{1}	1.64×10^{1}	6.14×10^{-7}	0	6.14×10^{-7}
20	1.64×10^{1}	1.64×10^{1}	1.22×10^{-6}	0	8.97×10^{-7}
30	1.64×10^{1}	1.64×10^{1}	1.84×10^{-6}	0	8.97×10^{-7}
40	1.64×10^{1}	1.64×10^{1}	2.45×10^{-6}	0	8.97×10^{-7}
50	1.64×10^{1}	1.64×10^{1}	3.08×10^{-6}	0	8.97×10^{-7}
60	1.64×10^{1}	1.64×10^{1}	3.69×10^{-6}	0	8.97×10^{-7}
70	1.64×10^{1}	1.64×10^{1}	3.69×10^{-6}	0	8.97×10^{-7}
80	1.64×10^{1}	1.64×10^{1}	3.69×10^{-6}	0	8.97×10^{-7}
90	1.64×10^{1}	1.64×10^{1}	3.69×10^{-6}	0	8.97×10^{-7}
100	1.64×10^{1}	1.64×10^{1}	3.69×10^{-6}	0	9.97×10^{-7}
110	1.64×10^{1}	1.52×10^{1}	1.30×10^{-1}	0	6.81×10^{-2}
120	1.64×10^{1}	1.40×10^{1}	1.20×10^{-1}	0	6.81×10^{-2}
130	1.64×10^{1}	1.28×10^{1}	1.10×10^{-1}	0	6.81×10^{-2}
140	1.64×10^{1}	1.17×10^{1}	1.01×10^{-1}	0	6.81×10^{-2}

Table F.1 (continued)

Output summary: ^{232}Th (continued)

Year	Inventory[b] Vault 1	Inventory[b] Vault 2	Amount leached[c,d] (g/year) Advection	Diffusion	Total
150	1.64×10^{1}	1.08×10^{1}	9.28×10^{-2}	0	6.81×10^{-2}
160	1.64×10^{1}	9.89×10^{0}	8.51×10^{-2}	0	6.81×10^{-2}
170	1.64×10^{1}	9.08×10^{0}	7.81×10^{-2}	0	6.81×10^{-2}
180	1.64×10^{1}	7.64×10^{0}	1.32×10^{-1}	0	6.81×10^{-2}
190	1.64×10^{1}	6.43×10^{0}	1.11×10^{-1}	0	6.81×10^{-2}
200	1.64×10^{1}	5.42×10^{0}	9.40×10^{-2}	0	6.81×10^{-2}
210	1.64×10^{1}	4.56×10^{0}	7.91×10^{-2}	0	6.81×10^{-2}
220	1.64×10^{1}	3.84×10^{0}	6.67×10^{-2}	0	6.67×10^{-2}
230	1.64×10^{1}	3.23×10^{0}	5.61×10^{-2}	0	5.61×10^{-2}
240	1.64×10^{1}	2.72×10^{0}	4.72×10^{-2}	0	4.72×10^{-2}
250	1.64×10^{1}	2.29×10^{0}	3.98×10^{-2}	0	3.98×10^{-2}
260	1.64×10^{1}	1.93×10^{0}	3.34×10^{-2}	0	3.34×10^{-2}
270	1.64×10^{1}	1.62×10^{0}	2.81×10^{-2}	0	2.81×10^{-2}
280	1.64×10^{1}	1.37×10^{0}	2.38×10^{-2}	0	2.38×10^{-2}
290	1.64×10^{1}	1.15×10^{0}	2.00×10^{-2}	0	2.00×10^{-2}
300	1.64×10^{1}	9.68×10^{-1}	1.69×10^{-2}	0	1.69×10^{-2}
310	1.64×10^{1}	8.15×10^{-1}	1.42×10^{-2}	0	1.42×10^{-2}
320	1.64×10^{1}	6.86×10^{-1}	1.19×10^{-2}	0	1.19×10^{-2}
330	1.64×10^{1}	5.77×10^{-1}	1.00×10^{-2}	0	1.00×10^{-2}
340	1.64×10^{1}	4.86×10^{-1}	8.44×10^{-3}	0	8.44×10^{-3}
350	1.64×10^{1}	4.09×10^{-1}	7.11×10^{-3}	0	7.11×10^{-3}
360	1.64×10^{1}	3.45×10^{-1}	5.98×10^{-3}	0	5.98×10^{-3}
370	1.64×10^{1}	2.90×10^{-1}	5.04×10^{-3}	0	5.04×10^{-3}
380	1.64×10^{1}	2.44×10^{-1}	4.24×10^{-3}	0	4.24×10^{-3}
390	1.64×10^{1}	2.06×10^{-1}	3.57×10^{-3}	0	3.57×10^{-3}
400	1.64×10^{1}	1.73×10^{-1}	3.00×10^{-3}	0	3.00×10^{-2}
410	1.64×10^{1}	1.46×10^{-1}	2.53×10^{-3}	0	2.53×10^{-3}
420	1.64×10^{1}	1.23×10^{-1}	2.13×10^{-3}	0	2.13×10^{-3}
430	1.64×10^{1}	1.03×10^{-1}	1.79×10^{-3}	0	1.79×10^{-3}
440	1.64×10^{1}	8.69×10^{-2}	1.51×10^{-3}	0	1.51×10^{-3}
450	1.64×10^{1}	7.32×10^{-2}	1.27×10^{-3}	0	1.27×10^{-3}
460	1.64×10^{1}	6.16×10^{-2}	1.07×10^{-3}	0	1.07×10^{-3}

Output summary: ^{232}Th (continued)

Year	Inventory[b] Vault 1	Inventory[b] Vault 2	Amount leached[c,d] (g/year) Advection	Amount leached[c,d] (g/year) Diffusion	Amount leached[c,d] (g/year) Total
470	1.64×10^{1}	5.18×10^{-2}	9.00×10^{-4}	0	9.00×10^{-4}
480	1.64×10^{1}	4.36×10^{-2}	7.58×10^{-4}	0	7.58×10^{-4}
490	1.64×10^{1}	3.67×10^{-2}	6.38×10^{-4}	0	6.38×10^{-4}
500	1.64×10^{1}	3.09×10^{-2}	5.37×10^{-4}	0	5.37×10^{-4}
510	1.64×10^{1}	2.60×10^{-2}	4.52×10^{-4}	0	4.52×10^{-4}
520	1.64×10^{1}	2.19×10^{-2}	3.81×10^{-4}	0	3.81×10^{-4}
530	1.64×10^{1}	1.85×10^{-2}	3.20×10^{-4}	0	3.20×10^{-4}
540	1.64×10^{1}	1.55×10^{-2}	2.70×10^{-4}	0	2.70×10^{-4}
550	1.64×10^{1}	1.31×10^{-2}	2.27×10^{-4}	0	2.27×10^{-4}
560	1.64×10^{1}	1.10×10^{-2}	1.91×10^{-4}	0	1.91×10^{-4}
570	1.64×10^{1}	9.27×10^{-3}	1.61×10^{-4}	0	1.61×10^{-4}
580	1.64×10^{1}	7.80×10^{-3}	1.35×10^{-4}	0	1.35×10^{-4}
590	1.64×10^{1}	6.57×10^{-3}	1.14×10^{-4}	0	1.14×10^{-4}
600	1.64×10^{1}	5.53×10^{-3}	9.60×10^{-5}	0	9.60×10^{-5}
610	1.64×10^{1}	4.65×10^{-3}	8.08×10^{-5}	0	8.08×10^{-5}
620	1.64×10^{1}	3.92×10^{-3}	6.80×10^{-5}	0	6.80×10^{-5}
630	1.64×10^{1}	3.30×10^{-3}	5.73×10^{-5}	0	5.73×10^{-5}
640	1.64×10^{1}	2.78×10^{-3}	4.82×10^{-5}	0	4.82×10^{-5}
650	1.64×10^{1}	2.34×10^{-3}	4.06×10^{-5}	0	4.06×10^{-5}
660	1.64×10^{1}	1.97×10^{-3}	3.42×10^{-5}	0	3.42×10^{-5}
670	1.64×10^{1}	1.66×10^{-3}	2.88×10^{-5}	0	2.88×10^{-5}
680	1.64×10^{1}	1.39×10^{-3}	2.42×10^{-5}	0	2.42×10^{-5}
690	1.64×10^{1}	1.17×10^{-3}	2.04×10^{-5}	0	2.04×10^{-5}
700	1.64×10^{1}	9.88×10^{-4}	1.72×10^{-5}	0	1.72×10^{-5}
710	1.64×10^{1}	8.32×10^{-4}	1.44×10^{-5}	0	1.44×10^{-5}
720	1.64×10^{1}	7.00×10^{-4}	1.22×10^{-5}	0	1.22×10^{-4}
730	1.64×10^{1}	5.89×10^{-4}	1.02×10^{-5}	0	1.02×10^{-5}
740	1.64×10^{1}	4.96×10^{-4}	8.62×10^{-6}	0	8.62×10^{-6}
750	1.64×10^{1}	4.18×10^{-4}	7.26×10^{-6}	0	7.26×10^{-6}
760	1.64×10^{1}	3.52×10^{-4}	6.11×10^{-6}	0	6.11×10^{-6}
770	1.64×10^{1}	2.96×10^{-4}	5.14×10^{-6}	0	5.14×10^{-6}
780	1.64×10^{1}	2.49×10^{-4}	4.33×10^{-6}	1.40×10^{-45}	4.33×10^{-6}
790	1.64×10^{1}	2.10×10^{-4}	3.64×10^{-6}	4.20×10^{-45}	3.64×10^{-6}

Output summary: ^{232}Th (continued)

Year	Inventory[b] Vault 1	Inventory[b] Vault 2	Amount leached[c,d] (g/year) Advection	Amount leached[c,d] (g/year) Diffusion	Amount leached[c,d] (g/year) Total
800	1.64×10^{1}	1.77×10^{-4}	3.07×10^{-6}	8.41×10^{-45}	3.07×10^{-6}
810	1.64×10^{1}	149×10^{-4}	2.58×10^{-6}	2.24×10^{-44}	2.58×10^{-6}
820	1.64×10^{1}	1.25×10^{-4}	2.17×10^{-6}	5.18×10^{-44}	2.17×10^{-6}
830	1.64×10^{1}	1.05×10^{-4}	1.83×10^{-6}	1.19×10^{-43}	1.83×10^{-6}
840	1.64×10^{1}	8.87×10^{-5}	1.54×10^{-6}	2.66×10^{-43}	1.54×10^{-6}
850	1.64×10^{1}	7.47×10^{-5}	1.30×10^{-6}	5.86×10^{-43}	1.30×10^{-6}
860	1.64×10^{1}	6.29×10^{-5}	1.09×10^{-6}	1.26×10^{-42}	1.09×10^{-6}
870	1.64×10^{1}	5.29×10^{-5}	9.19×10^{-7}	2.64×10^{-42}	9.19×10^{-7}
880	1.64×10^{1}	4.45×10^{-5}	7.74×10^{-7}	5.43×10^{-42}	7.74×10^{-7}
890	1.64×10^{1}	3.75×10^{-5}	6.51×10^{-7}	1.10×10^{-41}	6.51×10^{-7}
900	1.64×10^{1}	3.16×10^{-5}	5.48×10^{-7}	2.17×10^{-41}	5.48×10^{-7}
910	1.64×10^{1}	2.66×10^{-5}	4.62×10^{-7}	4.21×10^{-41}	4.62×10^{-7}
920	1.64×10^{1}	2.24×10^{-5}	3.89×10^{-7}	8.04×10^{-41}	3.89×10^{-7}
930	1.64×10^{1}	1.88×10^{-5}	3.27×10^{-7}	1.51×10^{-40}	3.27×10^{-7}
940	1.64×10^{1}	1.59×10^{-5}	2.75×10^{-7}	2.78×10^{-40}	2.75×10^{-7}
950	1.64×10^{1}	1.33×10^{-5}	2.32×10^{-7}	5.04×10^{-40}	2.32×10^{-7}
960	1.64×10^{1}	1.12×10^{-5}	1.95×10^{-7}	9.00×10^{-40}	1.95×10^{-7}
970	1.64×10^{1}	9.46×10^{-6}	1.64×10^{-7}	1.58×10^{-39}	1.64×10^{-7}
980	1.64×10^{1}	7.96×10^{-6}	1.38×10^{-7}	2.74×10^{-39}	1.38×10^{-7}
990	1.64×10^{1}	6.70×10^{-6}	1.16×10^{-7}	4.68×10^{-39}	1.16×10^{-7}
1000	1.64×10^{1}	5.74×10^{-6}	0	0	0

The solubility constraints were exceeded.

[a]1000-year simulation length, 50-year output edit frequency.

[b]In the output summary Vault 1 represents an intact storage vault, and Vault 2 represents a cracked storage vault.

[c]Years in which the sum of the advective and diffusive leaching exceeds the total presented are constrained by the solubility limit (e.g., years 20–210) (see Sect. C.2.).

[d]Disposal unit failure is predicted at year 102. As a result, more water flows through the unit causing a higher release. The total release is constrained by the solubility limit (e.g., years 110–210) until the inventory is depleted to a level that allows a K_d controlled release.

Table F.2. Examples of an input and output file for the leaching of ^{137}Cs from high-range wells (7) in a silo[a]

Input data summary

Groundwater properties

Flux entering disposal unit
(cm/month)

January:	9.58×10^{0}	February:	8.56×10^{0}	March:	8.30×10^{0}
April:	5.77×10^{0}	May:	7.43×10^{0}	June:	6.70×10^{-1}
July:	2.00×10^{-1}	August:	2.50×10^{-1}	September:	1.60×10^{-1}
October:	1.00×10^{-1}	November:	7.00×10^{-2}	December:	6.86×10^{0}

Disposal unit area	1.00×10^{1} m^2
Total dissolved solids	3.49×10^{2} ppm
Groundwater temperature	1.50×10^{1} °C
Groundwater pH	6.75×10^{0}

Saturated hydraulic conductivity:	
Recharge	5.80×10^{-7} cm/s
Soil backfill	3.50×10^{-3} cm/s
Concrete	1.00×10^{-10} cm/s

Groundwater constituent concentrations:	
Ca^{2+}	2.10×10^{-3} mol/L
Cl^{-}	2.04×10^{-4} mol/L
CO_3^{2-}	1.00×10^{-3} mol/L
Mg^{2+}	5.21×10^{-4} mol/L
SO_4^{2-} (inside silo or well)	2.62×10^{-4} mol/L
SO_4^{2-} (outside silo or well)	2.62×10^{-4} mol/L
O_2	1.63×10^{-4} mol/L

Table F.2 (continued)

Constituent solubilities:	
$Ca(OH)_2$	2.00×10^{-2} mol/L
CO_3^{2-}	1.20×10^{-3} mol/L
Mg^{2+}	1.20×10^{-3} mol/L
Concrete constituent concentrations:	
Calcium concentration in C-S-H system	1.75×10^{0} mol/L
Calcium concentration in pore fluid	2.00×10^{-2} mol/L
CaO content in cement	2.11×10^{0} mol/L
Free Cl^-	1.00×10^{-2} mol/L
Silica concentration in C-S-H system	7.10×10^{-1} mol/L
Concrete design specifications:	
Compressive strength at 28 days	3.52×10^{2} kg/cm^2
Poisson's ratio of concrete	1.50×10^{-1}
Modulus of elasticity of steel	2.04×10^{6} kg/cm^2
Yield strength of steel	4.22×10^{3} kg/cm^2
Modulus of subgrade reaction	2.11×10^{1} kg/cm^2
Young's modulus of elasticity	2.04×10^{5} kg/cm^2
Concrete water/cement ratio	4.00×10^{-1}
Concrete density	2.40×10^{0} g/cm^3
Concrete porosity	1.50×10^{-1}
Cement content	3.85×10^{2} kg/m^3
Initial pH	1.26×10^{1}
Well steel properties:	
Steel density	7.80×10^{0} g/cm^3
Steel Poisson ratio	3.00×10^{-1}
Yield strength of steel wall	3.60×10^{4} lb/in.^{2}
Diffusion coefficients in concrete:	
NaOH, KOH	2.12×10^{-11} m^2/s
$Ca(OH)_2$	1.82×10^{-11} m^2/s
Cl^-	5.08×10^{-11} m^2/s
CO_2	1.92×10^{-10} m^2/s
O_2	2.10×10^{-10} m^2/s
SO_4^{2-}	1.06×10^{-11} m^2/s
Silo design specifications:	
Silo dimensions:	
Silo radius	2.64×10^{-1} m
Silo height	6.10×10^{0} m

Table F.2 (continued)

Concrete member thickness:	
Roof	3.05×10^{1} cm
Walls	1.90×10^{0} cm
Floor	3.05×10^{1} cm
Steel reinforcement radius:	
Roof	4.76×10^{-1} cm
Walls	0 cm
Floor	4.76×10^{-1} cm
Spacing of steel reinforcement:	
Roof	1.52×10^{1} cm
Walls	0 cm
Floor	1.52×10^{1} cm
Corrugated steel thickness:	
Compression face	1.52×10^{-1} cm
Tension face	1.52×10^{-1} cm
Concrete cover thickness on tension face:	
Roof:	
X-direction	1.48×10^{1} cm
Y-direction	1.48×10^{1} cm
Walls:	
Horizontal direction	0 cm
Vertical direction	0 cm
Floor:	
X-direction	1.48×10^{1} cm
Y-direction	1.48×10^{1} cm
Well design specifications:	
Well dimensions:	
Radius	2.92×10^{1} cm
Well height	6.10×10^{2} cm
Structural member thickness:	
Roof	3.05×10^{1} cm
Wall	7.62×10^{0} cm
Floor	3.05×10^{1} cm

Table F.2 (continued)

Concrete cover thickness on tension face:	
Roof:	
X-direction	0 cm
Y-direction	0 cm
Floor:	
X-direction	0 cm
Y-direction	0 cm
Static load	3.95×10^{-1} kg/cm^2
Soil and waste properties:	
Earthen cover thickness	1.83×10^{0} m
Earthen cover density	1.76×10^{0} g/cm^2
Friction angle of waste backfill	4.00×10^{1} deg
Friction angle of soil backfill	3.00×10^{1} deg
Density of waste backfill	1.76×10^{0} g/cm^3
Density of soil backfill	1.76×10^{0} g/cm^3
Waste density	1.76×10^{0} g/cm^3
Average moisture content of waste	9.90×10^{-1}
Concrete and steel failure rates:	
Epoxy coating:	
Start of failure	0 years
Time to complete failure	2.00×10^{1} years
Steel liner:	
Start of failure	0 years
Time to complete failure	5.00×10^{1} years
Well wall:	
Start of failure	0 years
Time to complete failure	7.50×10^{1} years

Nuclide-specific parameters

Nuclide	^{137}Cs
Half-life	3.00×10^{1} years
Solubility	1.60×10^{1} mol/L
Waste K_d	1.99×10^{1} ml/g
Diffusion coefficient	
Waste	6.80×10^{-12} m^2/s
Concrete	5.12×10^{-13} m^2/s
Initial inventory	1.41×10^{0} g

Table F.2 (continued)

Output summary (leaching of ^{137}Cs)				
		Annual amount leached (g/year)		
Year	Inventory of wells (g)	Advection	Diffusion	Total
1	1.38×10^{0}	9.51×10^{-8}	0	9.51×10^{-8}
10	1.12×10^{0}	7.72×10^{-7}	0	7.72×10^{-7}
20	8.88×10^{-1}	1.23×10^{-6}	1.59×10^{-36}	1.23×10^{-6}
30	7.05×10^{-1}	1.46×10^{-6}	7.31×10^{-26}	1.46×10^{-6}
40	5.60×10^{-1}	1.54×10^{-6}	1.42×10^{-20}	1.54×10^{-6}
50	4.44×10^{-1}	1.53×10^{-6}	1.92×10^{-17}	1.53×10^{-6}
60	3.52×10^{-1}	1.22×10^{-6}	1.82×10^{-15}	1.22×10^{-6}
70	2.80×10^{-1}	9.65×10^{-7}	4.31×10^{-14}	9.65×10^{-7}
80	1.45×10^{-1}	1.07×10^{-2}	3.03×10^{-13}	1.07×10^{-2}
90	5.70×10^{-2}	4.20×10^{-3}	8.42×10^{-13}	4.20×10^{-3}
100	2.24×10^{-2}	1.65×10^{-3}	1.57×10^{-12}	1.65×10^{-3}
110	8.76×10^{-3}	6.45×10^{-4}	2.20×10^{-12}	6.45×10^{-4}
120	3.44×10^{-3}	2.53×10^{-4}	2.47×10^{-12}	2.53×10^{-4}
130	1.35×10^{-3}	9.92×10^{-5}	2.36×10^{-12}	9.92×10^{-5}
140	5.28×10^{-4}	3.89×10^{-5}	1.97×10^{-12}	3.89×10^{-5}
150	2.07×10^{-4}	1.52×10^{-5}	1.49×10^{-12}	1.52×10^{-5}
160	8.11×10^{-5}	5.98×10^{-6}	1.03×10^{-12}	5.98×10^{-6}
170	3.18×10^{-5}	2.34×10^{-6}	6.69×10^{-13}	2.34×10^{-6}
180	1.25×10^{-5}	9.19×10^{-7}	4.09×10^{-13}	9.19×10^{-7}
190	4.90×10^{-6}	3.60×10^{-7}	2.38×10^{-13}	3.60×10^{-7}
200	1.92×10^{-6}	1.41×10^{-7}	1.33×10^{-13}	1.41×10^{-7}
210	7.52×10^{-7}	5.54×10^{-8}	7.18×10^{-14}	5.54×10^{-8}
220	2.95×10^{-7}	2.17×10^{-8}	3.76×10^{-14}	2.17×10^{-8}
230	1.16×10^{-7}	8.51×10^{-9}	1.91×10^{-14}	8.51×10^{-9}
240	4.53×10^{-8}	3.33×10^{-9}	9.55×10^{-15}	3.34×10^{-9}
250	1.78×10^{-8}	1.31×10^{-9}	4.67×10^{-15}	1.31×10^{-9}
260	6.97×10^{-9}	5.13×10^{-10}	2.24×10^{-15}	5.13×10^{-10}
270	2.73×10^{-9}	2.01×10^{-10}	1.06×10^{-15}	2.01×10^{-10}

Table F.2 (continued)

Year	Inventory of wells (g)	Annual amount leached (g/year) Advection	Diffusion	Total
280	1.07×10^{-9}	7.89×10^{-11}	4.93×10^{-16}	7.88×10^{-11}
290	4.20×10^{-10}	3.09×10^{-11}	2.27×10^{-16}	3.09×10^{-11}
300	1.65×10^{-10}	1.21×10^{-11}	1.03×10^{-16}	1.21×10^{-11}
310	6.45×10^{-11}	4.75×10^{-12}	4.65×10^{-17}	4.75×10^{-12}
320	2.53×10^{-11}	1.86×10^{-12}	2.08×10^{-17}	1.86×10^{-12}
330	9.92×10^{-12}	7.30×10^{-13}	9.18×10^{-18}	7.30×10^{-13}
340	3.89×10^{-12}	2.86×10^{-13}	4.03×10^{-18}	2.86×10^{-13}
350	1.52×10^{-12}	1.12×10^{-13}	1.76×10^{-18}	1.12×10^{-13}
360	5.98×10^{-13}	4.40×10^{-14}	7.62×10^{-19}	4.40×10^{-14}
370	2.34×10^{-13}	1.73×10^{-14}	3.29×10^{-19}	1.73×10^{-14}
380	9.19×10^{-14}	6.76×10^{-15}	1.41×10^{-19}	6.76×10^{-15}
390	3.60×10^{-14}	2.65×10^{-15}	6.01×10^{-20}	2.65×10^{-15}
400	1.41×10^{-14}	1.04×10^{-15}	2.55×10^{-20}	1.04×10^{-15}
410	5.54×10^{-15}	4.08×10^{-16}	1.08×10^{-20}	4.08×10^{-16}
420	2.17×10^{-15}	1.60×10^{-16}	4.54×10^{-21}	1.60×10^{-16}
430	8.51×10^{-16}	6.27×10^{-17}	1.91×10^{-21}	6.27×10^{-17}
440	3.34×10^{-16}	2.46×10^{-17}	7.97×10^{-22}	2.46×10^{-17}
450	1.31×10^{-16}	9.63×10^{-18}	3.32×10^{-22}	9.63×10^{-18}
460	5.13×10^{-17}	3.78×10^{-18}	1.38×10^{-22}	3.78×10^{-18}
470	2.01×10^{-17}	1.48×10^{-18}	5.73×10^{-23}	1.48×10^{-18}
480	7.88×10^{-18}	5.80×10^{-19}	2.37×10^{-23}	5.80×10^{-19}
490	3.09×10^{-18}	2.28×10^{-19}	9.77×10^{-24}	2.28×10^{-19}
500	1.21×10^{-18}	8.92×10^{-20}	4.02×10^{-24}	8.92×10^{-19}
510	4.75×10^{-19}	3.50×10^{-20}	1.65×10^{-24}	3.50×10^{-20}
520	1.86×10^{-19}	1.37×10^{-20}	6.77×10^{-24}	1.37×10^{-20}
530	7.30×10^{-20}	5.37×10^{-21}	2.77×10^{-25}	5.37×10^{-21}
540	2.86×10^{-20}	2.11×10^{-21}	1.13×10^{-25}	2.11×10^{-21}
550	1.12×10^{-20}	8.26×10^{-22}	4.61×10^{-26}	8.26×10^{-22}
560	4.40×10^{-21}	3.24×10^{-22}	1.88×10^{-26}	3.24×10^{-22}
570	1.72×10^{-21}	1.27×10^{-22}	7.63×10^{-27}	1.27×10^{-22}
580	6.76×10^{-22}	4.98×10^{-23}	3.10×10^{-27}	4.98×10^{-23}

Table F.2 (continued)

Year	Inventory of wells (g)	Annual amount leached (g/year) Advection	Diffusion	Total
590	2.65×10^{-22}	1.95×10^{-23}	1.26×10^{-27}	1.95×10^{-23}
600	1.04×10^{-22}	7.65×10^{-24}	5.09×10^{-28}	7.65×10^{-24}
610	4.07×10^{-23}	2.30×10^{-24}	2.06×10^{-28}	2.30×10^{-24}
620	1.60×10^{-23}	1.18×10^{-24}	8.31×10^{-29}	1.18×10^{-24}
630	6.26×10^{-24}	4.61×10^{-25}	3.35×10^{-29}	4.61×10^{-25}
640	2.45×10^{-24}	1.81×10^{-25}	1.35×10^{-29}	1.81×10^{-25}
650	9.62×10^{-25}	7.08×10^{-26}	5.44×10^{-30}	7.09×10^{-26}
660	3.77×10^{-25}	2.78×10^{-26}	2.19×10^{-30}	2.78×10^{-26}
670	1.48×10^{-25}	1.09×10^{-26}	8.80×10^{-31}	1.09×10^{-26}
680	5.80×10^{-26}	4.27×10^{-27}	3.54×10^{-31}	4.27×10^{-27}
690	2.27×10^{-26}	1.67×10^{-27}	1.42×10^{-31}	1.67×10^{-27}
700	8.91×10^{-27}	6.56×10^{-28}	5.69×10^{-32}	6.56×10^{-28}
710	3.49×10^{-27}	2.57×10^{-28}	2.28×10^{-32}	2.57×10^{-28}
720	1.37×10^{-27}	1.01×10^{-28}	9.13×10^{-33}	1.01×10^{-28}
730	5.37×10^{-28}	3.95×10^{-29}	3.65×10^{-33}	3.95×10^{-29}
740	2.10×10^{-28}	1.55×10^{-29}	1.46×10^{-33}	1.55×10^{-29}
750	8.25×10^{-29}	6.08×10^{-30}	5.84×10^{-34}	6.08×10^{-30}
760	3.23×10^{-29}	2.38×10^{-30}	2.33×10^{-34}	2.38×10^{-30}
770	1.27×10^{-29}	9.34×10^{-31}	9.31×10^{-35}	9.34×10^{-31}
780	4.97×10^{-30}	3.66×10^{-31}	3.71×10^{-35}	3.66×10^{-31}
790	1.95×10^{-30}	1.43×10^{-31}	1.48×10^{-35}	1.43×10^{-31}
800	7.64×10^{-31}	5.63×10^{-32}	5.90×10^{-36}	5.63×10^{-32}
810	2.99×10^{-31}	2.21×10^{-32}	2.35×10^{-36}	2.21×10^{-32}
820	1.17×10^{-31}	8.65×10^{-33}	9.36×10^{-37}	8.65×10^{-33}
830	4.60×10^{-32}	3.39×10^{-33}	3.73×10^{-37}	3.39×10^{-33}
840	1.80×10^{-32}	1.33×10^{-33}	1.48×10^{-37}	1.33×10^{-33}
850	7.07×10^{-33}	5.21×10^{-34}	5.89×10^{-38}	5.21×10^{-34}
860	2.77×10^{-33}	2.04×10^{-34}	2.34×10^{-38}	2.04×10^{-34}
870	1.09×10^{-33}	8.01×10^{-35}	9.31×10^{-39}	8.01×10^{-35}
880	4.26×10^{-34}	3.14×10^{-35}	3.70×10^{-39}	3.14×10^{-35}
890	1.67×10^{-34}	1.23×10^{-35}	1.47×10^{-39}	1.23×10^{-35}
900	6.55×10^{-35}	4.82×10^{-36}	5.83×10^{-40}	4.82×10^{-36}

Table F.2 (continued)

Year	Inventory of wells (g)	Annual amount leached (g/year)		
		Advection	Diffusion	Total
910	2.57×10^{-35}	1.89×10^{-36}	2.31×10^{-40}	1.89×10^{-36}
920	1.01×10^{-35}	7.41×10^{-37}	9.17×10^{-41}	7.41×10^{-37}
930	3.95×10^{-36}	2.91×10^{-37}	3.64×10^{-41}	2.91×10^{-37}
940	1.55×10^{-36}	1.14×10^{-37}	1.44×10^{-41}	1.14×10^{-37}
950	6.06×10^{-37}	4.47×10^{-38}	5.71×10^{-42}	4.47×10^{-38}
960	2.38×10^{-37}	1.75×10^{-38}	2.26×10^{-42}	1.75×10^{-38}
970	9.32×10^{-38}	6.86×10^{-39}	8.95×10^{-43}	6.86×10^{-39}
980	3.65×10^{-38}	2.69×10^{-39}	3.56×10^{-43}	2.69×10^{-39}
990	1.43×10^{-38}	1.05×10^{-39}	1.37×10^{-43}	1.05×10^{-39}
1000	5.61×10^{-39}	4.13×10^{-40}	5.04×10^{-44}	4.13×10^{-40}

The solubility constraints were not exceeded.

[a]1000-year simulation length, 50-year output edit frequency.

Table F.3. Examples of an input and output file for the leaching of ^{238}U from a high-range silo[a]

Input data summary

Groundwater properties

Flux entering disposal unit
(cm/month)

January:	9.58×10^{0}	February:	8.56×10^{0}	March:	8.30×10^{0}
April:	5.77×10^{0}	May:	7.43×10^{0}	June:	6.70×10^{-1}
July:	2.00×10^{-1}	August:	2.50×10^{-1}	September:	1.60×10^{-1}
October:	1.00×10^{-1}	November:	7.00×10^{-2}	December:	6.86×10^{0}

Disposal unit area	1.00×10^{1} m^2
Total dissolved solids	3.49×10^{2} ppm
Groundwater temperature	1.50×10^{1} °C
Groundwater pH	6.75×10^{0}
Saturated hydraulic conductivity:	
Recharge	5.80×10^{-7} cm/s
Soil backfill	3.50×10^{-3} cm/s
Concrete	1.00×10^{-10} cm/s
Groundwater constituent concentrations:	
Ca^{2}	2.10×10^{-3} mol/L
Cl^{-}	2.04×10^{-4} mol/L
CO_3^{2-}	1.00×10^{-3} mol/L
Mg^{2+}	5.21×10^{-4} mol/L
SO_4^{2-} (inside silo or well)	2.62×10^{-4} mol/L
SO_4^{2-} (outside silo or well)	2.62×10^{-4} mol/L
O_2	1.63×10^{-4} mol/L
Constituent solubilities:	
$Ca(OH)_2$	2.00×10^{-2} mol/L
CO_3^{2-}	1.20×10^{-3} mol/L
Mg^{2+}	1.20×10^{-3} mol/L

Table F.3 (continued)

Concrete constituent concentrations:	
Calcium concentration in C-S-H system	1.75×10^{0} mol/L
Calcium concentration in pore fluid	2.00×10^{-2} mol/L
CaO content in cement	2.11×10^{0} mol/L
Free Cl^-	1.00×10^{-2} mol/L
Silica concentration in C-S-H system	7.10×10^{-1} mol/L
Concrete design specifications:	
Compressive strength at 28 days	3.52×10^{2} kg/cm^2
Poisson's ratio of concrete	1.50×10^{-1}
Modulus of elasticity of steel	2.04×10^{6} kg/cm^2
Yield strength of steel	4.22×10^{3} kg/cm^2
Modulus of subgrade reaction	2.11×10^{1} kg/cm^2
Young's modulus of elasticity	2.04×10^{5} kg/cm^2
Concrete water/cement ratio	4.00×10^{-1}
Concrete density	2.40×10^{0} g/cm^3
Concrete porosity	1.50×10^{-1}
Cement content	3.85×10^{2} kg/m^3
Initial pH	1.26×10^{1}
Diffusion coefficients in concrete:	
NaOH, KOH	2.12×10^{-11} m^2/s
$Ca(OH)_2$	1.82×10^{-11} m^2/s
Cl^-	5.08×10^{-11} m^2/s
CO_2	1.92×10^{-10} m^2/s
O_2	2.10×10^{-10} m^2/s
SO_4^{2-}	1.06×10^{-11} m^2/s
Silo design specifications:	
Silo dimensions:	
Radius	1.30×10^{1} m
Height	6.10×10^{0} m
Concrete member thickness:	
Roof	3.05×10^{1} cm
Walls	1.52×10^{1} cm
Floor	3.05×10^{1} cm
Steel reinforcement radius:	
Roof	4.76×10^{-1} cm
Walls	0 cm
Floor	4.76×10^{-1} cm

Table F.3 (continued)

Spacing of steel reinforcement:	
Roof	1.52×10^{1} cm
Walls	0 cm
Floor	1.52×10^{1} cm
Corrugated steel thickness:	
Compression face	1.52×10^{-1} cm
Tension face	1.52×10^{-1} cm
Concrete cover thickness on tension face:	
Roof:	
X-direction	1.48×10^{1} cm
Y-direction	1.48×10^{1} cm
Walls:	
Horizontal direction	0 cm
Vertical direction	0 cm
Floor:	
X-direction	1.48×10^{1} cm
Y-direction	1.48×10^{1} cm
Static load	3.95×10^{-1} kg/cm^2
Soil and waste properties:	
Earthen cover thickness	1.83×10^{0} m
Earthen cover density	1.76×10^{0} g/cm^2
Friction angle of waste backfill	4.00×10^{1} deg
Friction angle of soil backfill	3.00×10^{1} deg
Density of waste backfill	1.76×10^{0} g/cm^3
Density of soil backfill	1.76×10^{0} g/cm^3
Waste density	1.76×10^{0} g/cm^3
Average moisture content of waste	9.90×10^{-1}
Concrete and steel failure rates:	
Epoxy coating:	
Start of failure	0 years
Time to complete failure	2.00×10^{1} years
Steel liner:	
Start of failure	0 years
Time to complete failure	5.00×10^{1} years

Table F.3 (continued)

Nuclide-specific parameters

Nuclide	^{238}U
Half-life	4.47×10^{9} years
Solubility	1.46×10^{-6} mol/L
Waste K_d	5.56×10^{1} ml/g
Diffusion coefficient	
Waste	3.11×10^{-14} m^2/s
Concrete	3.50×10^{-15} m^2/s
Initial inventory	9.91×10^{2} g

Output summary (leaching of ^{238}U)

Year	Inventory of silo (g)	Annual amount leached[b,c] (g/year) Advection	Diffusion	Total
1	9.91×10^{2}	5.19×10^{-6}	0	5.19×10^{-6}
10	9.91×10^{2}	5.19×10^{-5}	0	5.19×10^{-5}
20	9.91×10^{2}	1.04×10^{-4}	0	1.04×10^{-4}
30	9.91×10^{2}	1.56×10^{-4}	0	1.10×10^{-4}
40	9.91×10^{2}	2.08×10^{-4}	0	1.10×10^{-4}
50	9.91×10^{2}	2.60×10^{-4}	0	1.10×10^{-4}
60	9.91×10^{2}	2.60×10^{-4}	0	1.10×10^{-4}
70	9.91×10^{2}	2.60×10^{-4}	0	1.10×10^{-4}
80	9.91×10^{2}	2.60×10^{-4}	0	1.10×10^{-4}
90	9.91×10^{2}	2.60×10^{-4}	0	1.10×10^{-4}
100	9.91×10^{2}	2.60×10^{-4}	0	1.10×10^{-4}
110	9.91×10^{2}	2.60×10^{-4}	0	1.10×10^{-4}
120	9.91×10^{2}	2.60×10^{-4}	0	1.10×10^{-4}
130	9.91×10^{2}	2.60×10^{-4}	0	1.10×10^{-4}
140	9.91×10^{2}	2.60×10^{-4}	0	1.10×10^{-4}
150	9.91×10^{2}	2.60×10^{-4}	0	1.10×10^{-4}
160	9.91×10^{2}	2.60×10^{-4}	0	1.10×10^{-4}
170	9.91×10^{2}	2.60×10^{-4}	0	1.10×10^{-4}
180	9.91×10^{2}	2.60×10^{-4}	0	1.10×10^{-4}

Table F.3 (continued)

Year	Inventory of silo (g)	Annual amount leached[b,c] (g/year) Advection	Diffusion	Total
190	9.91×10^{2}	2.60×10^{-4}	0	1.10×10^{-4}
200	9.91×10^{2}	2.60×10^{-4}	0	1.10×10^{-4}
210	9.91×10^{2}	2.60×10^{-4}	0	1.10×10^{-4}
220	9.91×10^{2}	2.60×10^{-4}	0	1.10×10^{-4}
230	9.91×10^{2}	2.60×10^{-4}	0	1.10×10^{-4}
240	9.75×10^{2}	1.88×10^{1}	0	8.01×10^{0}
250	8.95×10^{2}	1.73×10^{1}	0	8.01×10^{0}
260	8.15×10^{2}	1.57×10^{1}	0	8.01×10^{0}
270	7.35×10^{2}	1.42×10^{1}	0	8.01×10^{0}
280	6.54×10^{2}	1.27×10^{1}	0	8.01×10^{0}
290	5.74×10^{2}	1.11×10^{1}	0	8.01×10^{0}
300	4.94×10^{2}	9.61×10^{0}	0	8.01×10^{0}
310	4.14×10^{2}	8.08×10^{0}	0	8.01×10^{0}
320	3.41×10^{2}	6.66×10^{0}	0	6.66×10^{0}
330	2.81×10^{2}	5.49×10^{0}	0	5.49×10^{0}
340	2.32×10^{2}	4.52×10^{0}	0	4.52×10^{0}
350	1.91×10^{2}	3.73×10^{0}	0	3.73×10^{0}
360	1.58×10^{2}	3.07×10^{0}	0	3.07×10^{0}
370	1.30×10^{2}	2.53×10^{0}	0	2.53×10^{0}
380	1.07×10^{2}	2.09×10^{0}	0	2.09×10^{0}
390	8.82×10^{1}	1.72×10^{0}	0	1.72×10^{0}
400	7.27×10^{1}	1.42×10^{0}	0	1.42×10^{0}
410	5.99×10^{1}	1.17×10^{0}	0	1.16×10^{0}
420	4.94×10^{1}	9.64×10^{-1}	0	9.64×10^{-1}
430	4.07×10^{1}	7.95×10^{-1}	0	7.95×10^{-1}
440	3.36×10^{1}	6.55×10^{-1}	0	6.55×10^{-1}
450	2.77×10^{1}	5.40×10^{-1}	0	5.40×10^{-1}
460	2.28×10^{1}	4.45×10^{-1}	0	4.45×10^{-1}
470	1.88×10^{1}	3.67×10^{-1}	0	3.67×10^{-1}
480	1.55×10^{1}	3.02×10^{-1}	0	3.02×10^{-1}
490	1.28×10^{1}	2.49×10^{-1}	0	2.49×10^{-1}

Table F.3 (continued)

Year	Inventory of silo (g)	Annual amount leached[b,c] (g/year) Advection	Diffusion	Total
500	1.05×10^{1}	2.05×10^{-1}	0	2.05×10^{-1}
510	8.68×10^{0}	1.69×10^{-1}	0	1.69×10^{-1}
520	7.15×10^{0}	1.40×10^{-1}	0	1.40×10^{-1}
530	5.90×10^{0}	1.15×10^{-1}	0	1.15×10^{-1}
540	4.86×10^{0}	9.48×10^{-2}	0	9.49×10^{-2}
550	4.01×10^{0}	7.82×10^{-2}	0	7.82×10^{-2}
560	3.30×10^{0}	6.44×10^{-2}	0	6.44×10^{-2}
570	2.72×10^{0}	5.31×10^{-2}	0	5.31×10^{-2}
580	2.24×10^{0}	4.38×10^{-2}	1.26×10^{-44}	4.38×10^{-2}
590	1.85×10^{0}	3.61×10^{-2}	3.36×10^{-44}	3.61×10^{-2}
600	1.52×10^{0}	2.98×10^{-2}	1.21×10^{-43}	2.98×10^{-2}
610	1.26×10^{0}	2.45×10^{-2}	4.15×10^{-43}	2.45×10^{-2}
620	1.04×10^{0}	2.02×10^{-2}	1.37×10^{-42}	2.02×10^{-2}
630	8.54×10^{-1}	1.67×10^{-2}	4.31×10^{-42}	1.67×10^{-2}
640	7.04×10^{-1}	1.37×10^{-2}	1.30×10^{-41}	1.37×10^{-2}
650	5.80×10^{-1}	1.13×10^{-2}	3.77×10^{-41}	1.13×10^{-2}
660	4.78×10^{-1}	9.33×10^{-3}	1.05×10^{-40}	9.33×10^{-3}
670	3.94×10^{-1}	7.69×10^{-3}	2.83×10^{-40}	7.69×10^{-3}
680	3.25×10^{-1}	6.34×10^{-3}	7.36×10^{-40}	6.34×10^{-3}
690	2.68×10^{-1}	5.23×10^{-3}	1.85×10^{-39}	5.23×10^{-3}
700	2.21×10^{-1}	4.31×10^{-3}	4.50×10^{-39}	4.31×10^{-3}
710	1.82×10^{-1}	3.55×10^{-3}	1.06×10^{-38}	3.55×10^{-3}
720	1.50×10^{-1}	2.93×10^{-3}	2.44×10^{-38}	2.93×10^{-3}
730	1.24×10^{-1}	2.41×10^{-3}	5.43×10^{-38}	2.41×10^{-3}
740	1.02×10^{-1}	1.99×10^{-3}	1.18×10^{-37}	1.99×10^{-3}
750	8.40×10^{-2}	1.64×10^{-3}	2.50×10^{-37}	1.64×10^{-3}
760	6.93×10^{-2}	1.35×10^{-3}	5.14×10^{-37}	1.35×10^{-3}
770	5.71×10^{-2}	1.11×10^{-3}	1.03×10^{-36}	1.11×10^{-3}
780	4.71×10^{-2}	9.18×10^{-4}	2.03×10^{-36}	9.18×10^{-4}
790	3.88×10^{-2}	7.57×10^{-4}	3.91×10^{-36}	7.57×10^{-4}
800	3.20×10^{-2}	6.24×10^{-4}	7.37×10^{-36}	6.24×10^{-4}

Table F.3 (continued)

Year	Inventory of silo (g)	Annual amount leachedb[b,c] (g/year) Advection	Diffusion	Total
810	2.64×10^{-2}	5.14×10^{-4}	1.36×10^{-35}	5.14×10^{-4}
820	2.17×10^{-2}	4.24×10^{-4}	2.46×10^{-35}	4.24×10^{-4}
830	1.79×10^{-2}	3.49×10^{-4}	4.37×10^{-35}	3.49×10^{-4}
840	1.48×10^{-2}	2.88×10^{-4}	7.62×10^{-35}	2.88×10^{-4}
850	1.22×10^{-2}	2.37×10^{-4}	1.31×10^{-34}	2.37×10^{-4}
860	1.00×10^{-2}	1.96×10^{-4}	2.20×10^{-34}	1.96×10^{-4}
870	8.27×10^{-3}	1.61×10^{-4}	3.64×10^{-34}	1.61×10^{-4}
880	6.81×10^{-3}	1.33×10^{-4}	5.93×10^{-34}	1.33×10^{-4}
890	5.62×10^{-3}	1.10×10^{-4}	9.52×10^{-34}	1.10×10^{-4}
900	4.63×10^{-3}	9.03×10^{-5}	1.50×10^{-33}	9.03×10^{-5}
910	3.82×10^{-3}	7.45×10^{-5}	2.35×10^{-33}	7.45×10^{-5}
920	3.15×10^{-3}	6.14×10^{-5}	3.61×10^{-33}	6.14×10^{-5}
930	2.59×10^{-3}	5.06×10^{-5}	5.47×10^{-33}	5.06×10^{-5}
940	2.14×10^{-3}	4.17×10^{-5}	8.19×10^{-33}	4.17×10^{-5}
950	1.76×10^{-3}	3.44×10^{-5}	1.21×10^{-32}	3.44×10^{-5}
960	1.45×10^{-3}	2.83×10^{-5}	1.77×10^{-32}	2.83×10^{-5}
970	1.20×10^{-3}	2.34×10^{-5}	2.55×10^{-32}	2.34×10^{-5}
980	9.87×10^{-4}	1.93×10^{-5}	3.64×10^{-32}	1.93×10^{-5}
990	8.13×10^{-4}	1.59×10^{-5}	5.13×10^{-32}	1.59×10^{-5}
1000	6.70×10^{-4}	1.31×10^{-5}	7.16×10^{-32}	1.31×10^{-5}

The solubility constraints were exceeded.

[a]1000-year simulation length, 50-year output edit frequency.

[b]Years in which the sum of advective and diffusive leaching exceeds the total presented are constrained by the solubility limit (e.g., years 30–310) (see Sect. C.2).

[c]Disposal unit failure is predicted at year 239. As a result, more water flows through the unit causing a higher release. The total release is constrained by the solubility limit (e.g., years 240–310) until the inventory is depeleted to a level that allows a K_d controlled release.

Table F.4. Example of an input and output file for the leaching of ^{137}Cs from Tumulus I

Input data summary

Groundwater properites

Flux entering disposal unit
(cm/month)

January:	9.58×10^{0}	February:	8.56×10^{0}	March:	8.30×10^{0}
April:	5.77×10^{0}	May:	7.43×10^{0}	June:	6.70×10^{-1}
July:	2.00×10^{-1}	August:	2.50×10^{-1}	September:	1.60×10^{-1}
October:	1.00×10^{-1}	November:	7.00×10^{-2}	December:	6.86×10^{0}

Disposal unit area	4.66×10^{2} m^2
Total dissolved solids	3.49×10^{2} ppm
Groundwater temperature	1.50×10^{1} °C
Groundwater pH	6.75×10^{0}
Saturated hydraulic conductivity:	
Recharge	5.80×10^{-7} cm/s
Soil backfill	3.50×10^{-3} cm/s
Concrete	1.00×10^{-10} cm/s
Groundwater constituent concentrations:	
Ca^{2+}	2.10×10^{-3} mol/L
Cl^{-}	2.04×10^{-4} mol/L
CO_3^{2-}	1.00×10^{-3} mol/L
Mg^{2+}	5.21×10^{-4} mol/L
SO_4^{2-}	2.62×10^{-4} mol/L
O_2	1.63×10^{-4} mol/L
Constituent solubilities:	
$Ca(OH)_2$	2.00×10^{-2} mol/L
CO_3^{2-}	1.20×10^{-3} mol/L
Mg^{2+}	1.20×10^{-3} mol/L
Concrete constituent concentrations:	
Calcium concentration in C-S-H system	1.75×10^{0} mol/L
Calcium concentration in pore fluid	2.00×10^{-2} mol/L
CaO content in cement	2.11×10^{0} mol/L
Free Cl^{-}	1.00×10^{-2} mol/L
Silica concentration in C-S-H system	7.10×10^{-1} mol/L

Table F.4 (continued)

Concrete design specifications	
Compressive strength at 28 Days	3.52×10^{2} kg/cm^2
Poisson's ratio of concrete	1.50×10^{-1}
Modulus of elasticity of steel	2.04×10^{6} kg/cm^2
Yield strength of steel	4.22×10^{3} kg/cm^2
Modulus of subgrade reaction	1.41×10^{2} kg/cm^2
Young's modulus of elasticity	2.04×10^{5} kg/cm^2
Concrete water/cement ratio	4.00×10^{-1}
Concrete density	2.40×10^{0} g/cm^3
Concrete porosity	1.50×10^{-1}
Cement content	3.85×10^{2} kg/m^3
Initial pH	1.25×10^{1}
Diffusion coefficients in concrete:	
NaOH, KOH	2.12×10^{-11} m^2/s
$Ca(OH)_2$	1.82×10^{-11} m^2/s
Cl^-	5.08×10^{-11} m^2/s
CO_2	1.92×10^{-10} m^2/s
O_2	2.10×10^{-10} m^2/s
SO_4^{2-}	1.06×10^{-11} m^2/s
Tumulus design specifications:	
Layers of vaults	2
Number of vaults wide	8
Number of vaults long	18
Vault dimensions:	
Width	1.52×10^{0} m
Length	2.13×10^{0} m
Height	1.65×10^{0} m
Concrete member thickness:	
Roof	1.78×10^{1} cm
Walls	1.78×10^{1} cm
Floor	1.78×10^{1} cm
Steel reinforcement radius:	
Roof	7.94×10^{-1} cm
Walls	6.35×10^{-1} cm
Floor	6.35×10^{-1} cm

Table F.4 (continued)

Spacing of steel reinforcement:	
Roof	2.54×10^1 cm
Walls	3.05×10^1 cm
Floor	3.05×10^1 cm
Concrete Cover Thickness on Tension Face	
Roof	
X-direction	7.77×10^0 cm
Y-direction	9.37×10^0 cm
Walls	
Horizontal direction	8.26×10^0 cm
Vertical direction	9.52×10^0 cm
Floor	
X-direction	5.08×10^0 cm
Y-direction	6.35×10^0 cm
Static load	
Vault layer 1	3.65×10^{-1} kg/cm^2
Vault layer 2	7.10×10^{-1} kg/cm^2
Soil and waste properties:	
Earthen cover thickness	1.83×10^0 m
Earthen cover density	1.76×10^0 g/cm^3
Friction angle of waste backfill	4.00×10^1 deg
Friction angle of soil backfill	3.00×10^1 deg
Density of waste backfill	1.76×10^0 g/cm^3
Density of soil backfill	1.76×10^0 g/cm^3
Waste density	1.76×10^0 g/cm^3
Average moisture content of waste	9.90×10^{-1}
Concrete and waste package failure rates:	
Waste container:	
Start of failure	0.00×10^0 years
Time to complete failure	6.00×10^1 years
Epoxy coating:	
Start of failure	0.00×10^0 years
Time to complete failure	2.00×10^1 years

Table F.4 (continued)

Nuclide	^{137}Cs
Half-life	3.00×10^{1} years
Solubility	1.60×10^{1} mol/L
Waste K_d	1.99×10^{1} ml/g
Diffusion coefficient	
Waste	6.80×10^{-12} m^2/s
Concrete	5.12×10^{-13} m^2/s
Initial inventory	5.81×10^{-4} g

Output summary (leaching of ^{137}Cs)

	Inventory[a] (g/vault)		Annual amount leached (g/year)		
Year	Vault 1	Vault 2	Advection	Diffusion	Total
1	5.68×10^{-4}	5.68×10^{-4}	5.63×10^{-12}	0.00×10^{0}	5.63×10^{-12}
10	4.61×10^{-4}	4.61×10^{-4}	4.57×10^{-11}	1.46×10^{-29}	4.57×10^{-11}
20	3.66×10^{-4}	3.66×10^{-4}	7.26×10^{-11}	2.66×10^{-18}	7.26×10^{-11}
30	2.90×10^{-4}	2.91×10^{-4}	8.64×10^{-11}	1.97×10^{-14}	8.64×10^{-11}
40	2.31×10^{-4}	2.31×10^{-4}	9.14×10^{-11}	1.84×10^{-12}	9.33×10^{-11}
50	1.83×10^{-4}	1.83×10^{-4}	9.07×10^{-11}	2.88×10^{-11}	1.20×10^{-10}
60	1.45×10^{-4}	1.45×10^{-4}	8.64×10^{-11}	1.80×10^{-10}	2.66×10^{-10}
70	1.15×10^{-4}	1.15×10^{-4}	6.86×10^{-11}	5.65×10^{-10}	6.33×10^{-10}
80	9.15×10^{-5}	9.15×10^{-5}	5.44×10^{-11}	1.28×10^{-9}	1.34×10^{-9}
90	7.26×10^{-5}	7.26×10^{-5}	4.32×10^{-11}	2.35×10^{-9}	2.39×10^{-9}
100	5.76×10^{-5}	5.76×10^{-5}	3.43×10^{-11}	3.69×10^{-9}	3.72×10^{-9}
110	4.57×10^{-5}	4.14×10^{-5}	4.63×10^{-7}	4.95×10^{-9}	4.68×10^{-7}
120	3.62×10^{-5}	2.94×10^{-5}	3.29×10^{-7}	6.05×10^{-9}	3.35×10^{-07}
130	2.87×10^{-5}	2.09×10^{-5}	2.33×10^{-7}	6.93×10^{-9}	2.40×10^{-07}
140	2.28×10^{-5}	1.48×10^{-5}	1.65×10^{-7}	7.54×10^{-9}	1.73×10^{-07}
150	1.80×10^{-5}	1.05×10^{-5}	1.17×10^{-7}	7.88×10^{-9}	1.25×10^{-07}
160	1.43×10^{-5}	7.42×10^{-6}	8.30×10^{-8}	7.97×10^{-9}	9.09×10^{-8}
170	1.13×10^{-5}	5.24×10^{-6}	5.86×10^{-8}	7.83×10^{-9}	6.64×10^{-8}

Table F.4 (continued)

Year	Inventory[a] (g/vault)		Annual amount leached (g/year)		
	Vault 1	Vault 2	Advection	Diffusion	Total
180	8.97×10^{-6}	3.30×10^{-6}	7.46×10^{-8}	4.01×10^{-9}	7.86×10^{-8}
190	7.12×10^{-6}	2.07×10^{-6}	4.68×10^{-8}	3.10×10^{-9}	4.99×10^{-8}
200	5.65×10^{-6}	1.29×10^{-6}	2.93×10^{-8}	2.35×10^{-9}	3.16×10^{-8}
210	4.48×10^{-6}	8.06×10^{-7}	1.82×10^{-8}	1.74×10^{-9}	2.00×10^{-8}
220	3.56×10^{-6}	5.00×10^{-7}	1.13×10^{-8}	1.27×10^{-9}	1.26×10^{-8}
230	2.82×10^{-6}	3.09×10^{-7}	7.01×10^{-9}	9.15×10^{-10}	7.93×10^{-9}
240	2.24×10^{-6}	1.91×10^{-7}	4.32×10^{-9}	6.48×10^{-10}	4.97×10^{-9}
250	1.78×10^{-6}	1.17×10^{-7}	2.65×10^{-9}	4.52×10^{-10}	3.10×10^{-9}
260	1.41×10^{-6}	7.13×10^{-8}	1.62×10^{-9}	3.12×10^{-10}	1.93×10^{-9}
270	1.12×10^{-6}	4.33×10^{-8}	9.82×10^{-10}	2.12×10^{-10}	1.19×10^{-9}
280	8.90×10^{-7}	2.61×10^{-8}	5.93×10^{-10}	1.43×10^{-10}	7.36×10^{-10}
290	7.06×10^{-7}	1.57×10^{-8}	3.56×10^{-10}	9.47×10^{-11}	4.51×10^{-10}
300	5.61×10^{-7}	9.35×10^{-9}	2.13×10^{-10}	6.22×10^{-11}	2.75×10^{-10}
310	4.45×10^{-7}	5.55×10^{-9}	1.26×10^{-10}	4.04×10^{-11}	1.67×10^{-10}
320	3.53×10^{-7}	3.27×10^{-9}	7.44×10^{-11}	2.59×10^{-11}	1.00×10^{-10}
330	2.80×10^{-7}	1.91×10^{-9}	4.36×10^{-11}	1.65×10^{-11}	6.01×10^{-11}
340	2.22×10^{-7}	1.11×10^{-9}	2.54×10^{-11}	1.04×10^{-11}	3.57×10^{-11}
350	1.77×10^{-7}	6.42×10^{-10}	1.47×10^{-11}	6.44×10^{-12}	2.11×10^{-11}
360	1.40×10^{-7}	3.68×10^{-10}	8.41×10^{-12}	3.96×10^{-12}	1.24×10^{-11}
370	1.11×10^{-7}	2.10×10^{-10}	4.79×10^{-12}	2.41×10^{-12}	7.20×10^{-12}
380	8.83×10^{-8}	1.18×10^{-10}	2.71×10^{-12}	1.46×10^{-12}	4.16×10^{-12}
390	7.01×10^{-8}	6.63×10^{-11}	1.52×10^{-12}	8.68×10^{-13}	2.39×10^{-12}

Table F.4 (continued)

Year	Inventory[a] (g/vault)		Annual amount leached (g/year)		
	Vault 1	Vault 2	Advection	Diffusion	Total
400	5.56×10^{-8}	3.69×10^{-11}	8.44×10^{-13}	5.12×10^{-13}	1.36×10^{-12}
410	4.41×10^{-8}	2.03×10^{-11}	4.66×10^{-13}	2.99×10^{-13}	7.65×10^{-13}
420	3.50×10^{-8}	1.11×10^{-11}	2.55×10^{-13}	1.73×10^{-13}	4.28×10^{-13}
430	2.78×10^{-8}	6.03×10^{-12}	1.38×10^{-13}	9.91×10^{-14}	2.38×10^{-13}
440	2.21×10^{-8}	3.24×10^{-12}	7.45×10^{-14}	5.61×10^{-14}	1.31×10^{-13}
450	1.75×10^{-8}	1.73×10^{-12}	3.98×10^{-14}	3.14×10^{-14}	7.12×10^{-14}
460	1.39×10^{-8}	9.14×10^{-13}	2.10×10^{-14}	1.74×10^{-14}	3.85×10^{-14}
470	1.10×10^{-8}	4.79×10^{-13}	1.10×10^{-14}	9.57×10^{-15}	2.06×10^{-14}
480	8.76×10^{-9}	2.49×10^{-13}	5.74×10^{-15}	5.20×10^{-15}	1.09×10^{-14}
490	6.95×10^{-9}	1.28×10^{-13}	2.95×10^{-15}	2.80×10^{-15}	5.75×10^{-15}
500	5.52×10^{-9}	6.52×10^{-14}	1.51×10^{-15}	1.49×10^{-15}	2.99×10^{-15}
510	4.38×10^{-9}	3.30×10^{-14}	7.62×10^{-16}	7.83×10^{-16}	1.54×10^{-15}
520	3.48×10^{-9}	1.65×10^{-14}	3.82×10^{-16}	4.08×10^{-16}	7.89×10^{-16}
530	2.76×10^{-9}	8.18×10^{-15}	1.89×10^{-16}	2.10×10^{-16}	3.99×10^{-16}
540	2.19×10^{-9}	4.01×10^{-15}	9.31×10^{-17}	1.07×10^{-16}	2.00×10^{-16}
550	1.74×10^{-9}	1.95×10^{-15}	4.53×10^{-17}	5.40×10^{-17}	9.93×10^{-17}
560	1.38×10^{-9}	9.40×10^{-16}	2.18×10^{-17}	2.70×10^{-17}	4.88×10^{-17}
570	1.09×10^{-9}	4.48×10^{-16}	1.04×10^{-17}	1.33×10^{-17}	2.37×10^{-17}
580	8.69×10^{-10}	2.12×10^{-16}	4.93×10^{-18}	6.50×10^{-18}	1.14×10^{-17}
590	6.90×10^{-10}	9.90×10^{-17}	2.31×10^{-18}	3.14×10^{-18}	5.45×10^{-18}
600	5.47×10^{-10}	4.58×10^{-17}	1.07×10^{-18}	1.50×10^{-18}	2.57×10^{-18}
610	4.34×10^{-10}	2.10×10^{-17}	4.90×10^{-19}	7.10×10^{-19}	1.20×10^{-18}

Table F.4 (continued)

Year	Inventory[a] (g/vault)		Annual amount leached (g/year)		
	Vault 1	Vault 2	Advection	Diffusion	Total
620	3.45×10^{-10}	9.52×10^{-18}	2.23×10^{-19}	3.32×10^{-19}	5.55×10^{-19}
630	2.74×10^{-10}	4.27×10^{-18}	1.00×10^{-19}	1.54×10^{-19}	2.54×10^{-19}
640	2.17×10^{-10}	1.90×10^{-18}	4.45×10^{-20}	7.03×10^{-20}	1.15×10^{-19}
650	1.72×10^{-10}	8.36×10^{-19}	1.96×10^{-20}	3.18×10^{-20}	5.14×10^{-20}
660	1.37×10^{-10}	3.64×10^{-19}	8.54×10^{-21}	1.42×10^{-20}	2.28×10^{-20}
670	1.09×10^{-10}	1.57×10^{-19}	3.68×10^{-21}	6.31×10^{-21}	9.99×10^{-21}
680	8.62×10^{-11}	6.68×10^{-20}	1.57×10^{-21}	2.76×10^{-21}	4.33×10^{-21}
690	6.84×10^{-11}	2.82×10^{-20}	6.64×10^{-22}	1.20×10^{-21}	1.86×10^{-21}
700	5.43×10^{-11}	1.18×10^{-20}	2.77×10^{-22}	5.12×10^{-22}	7.90×10^{-22}
710	4.31×10^{-11}	4.86×10^{-21}	1.15×10^{-22}	2.17×10^{-22}	3.32×10^{-22}
720	3.42×10^{-11}	1.99×10^{-21}	4.69×10^{-23}	9.09×10^{-23}	1.38×10^{-22}
730	2.72×10^{-11}	8.03×10^{-22}	1.90×10^{-23}	3.77×10^{-23}	5.67×10^{-23}
740	2.16×10^{-11}	3.21×10^{-22}	7.61×10^{-24}	1.54×10^{-23}	2.30×10^{-23}
750	1.71×10^{-11}	1.27×10^{-22}	3.01×10^{-24}	6.25×10^{-24}	9.26×10^{-24}
760	1.36×10^{-11}	4.98×10^{-23}	1.18×10^{-24}	2.50×10^{-24}	3.69×10^{-24}
770	1.08×10^{-11}	1.93×10^{-23}	4.58×10^{-25}	9.92×10^{-25}	1.45×10^{-24}
780	8.55×10^{-12}	7.39×10^{-24}	1.76×10^{-25}	3.88×10^{-25}	5.64×10^{-25}
790	6.79×10^{-12}	2.80×10^{-24}	6.67×10^{-26}	1.50×10^{-25}	2.17×10^{-25}
800	5.39×10^{-12}	1.05×10^{-24}	2.50×10^{-26}	5.76×10^{-26}	8.26×10^{-26}
810	4.28×10^{-12}	3.89×10^{-25}	9.28×10^{-27}	2.18×10^{-26}	3.11×10^{-26}
820	3.39×10^{-12}	1.43×10^{-25}	3.41×10^{-27}	8.16×10^{-27}	1.16×10^{-26}
830	2.69×10^{-12}	5.18×10^{-26}	1.24×10^{-27}	3.02×10^{-27}	4.26×10^{-27}
840	2.14×10^{-12}	1.86×10^{-26}	4.45×10^{-28}	1.11×10^{-27}	1.55×10^{-27}

Table F.4 (continued)

	Inventory[a] (g/vault)		Annual amount leached (g/year)		
Year	Vault 1	Vault 2	Advection	Diffusion	Total
850	1.70×10^{-12}	6.59×10^{-27}	1.58×10^{-28}	4.00×10^{-28}	5.58×10^{-28}
860	1.35×10^{-12}	2.31×10^{-27}	5.55×10^{-29}	1.43×10^{-28}	1.99×10^{-28}
870	1.07×10^{-12}	8.03×10^{-28}	1.93×10^{-29}	5.06×10^{-29}	6.99×10^{-29}
880	8.49×10^{-13}	2.76×10^{-28}	6.62×10^{-30}	1.77×10^{-29}	2.43×10^{-29}
890	6.74×10^{-13}	9.35×10^{-29}	2.25×10^{-30}	6.12×10^{-30}	8.37×10^{-30}
900	5.35×10^{-13}	3.14×10^{-29}	7.56×10^{-31}	2.09×10^{-30}	2.85×10^{-30}
910	4.24×10^{-13}	1.04×10^{-29}	2.51×10^{-31}	7.07×10^{-31}	9.58×10^{-31}
920	3.37×10^{-13}	3.42×10^{-30}	8.26×10^{-32}	2.36×10^{-31}	3.19×10^{-31}
930	2.67×10^{-13}	1.11×10^{-30}	2.68×10^{-32}	7.79×10^{-32}	1.05×10^{-31}
940	2.12×10^{-13}	3.56×10^{-31}	8.62×10^{-33}	2.54×10^{-32}	3.41×10^{-32}
950	1.68×10^{-13}	1.13×10^{-31}	2.74×10^{-33}	8.21×10^{-33}	1.09×10^{-32}
960	1.34×10^{-13}	3.55×10^{-32}	8.60×10^{-34}	2.62×10^{-33}	3.48×10^{-33}
970	1.06×10^{-13}	1.10×10^{-32}	2.67×10^{-34}	8.26×10^{-34}	1.09×10^{-33}
980	8.42×10^{-14}	3.38×10^{-33}	8.21×10^{-35}	2.58×10^{-34}	3.40×10^{-34}
990	6.68×10^{-14}	1.02×10^{-33}	2.49×10^{-35}	7.94×10^{-35}	1.04×10^{-34}
1000	5.30×10^{-14}	3.07×10^{-34}	7.48×10^{-36}	2.42×10^{-35}	3.17×10^{-35}

The solubility constraints were not exceeded.

[a]In the output summary, Vault 1 represents an intact waste storage vault, and Vault 2 represents a cracked waste storage vault.

Table F.5. Input data summary for a biological trench at Solid Waste Storage Area 6[a]

Input Data Summary

Groundwater properties

Flow entering trench
(cm/month)

January:	9.58×10^{0}	February:	8.56×10^{0}	March:	8.30×10^{0}
April:	5.77×10^{0}	May:	7.43×10^{0}	June:	6.70×10^{-1}
July:	2.00×10^{-1}	August:	2.50×10^{-1}	September:	1.60×10^{-1}
October:	1.00×10^{-1}	November:	7.00×10^{-2}	December	6.86×10^{0}

Disposal unit area	4.70×10^{1} m^3
Total dissolved solids	3.49×10^{2} mg/L
Groundwater temperature	1.50×10^{1} °C
Groundwater pH	6.75×10^{0}
Saturated hydraulic conductivity	
Recharge	5.80×10^{-7} cm/s
Soil backfill	3.50×10^{-3} cm/s
Concrete	3.50×10^{-3} cm/s
Groundwater constituent concentrations	
Ca^{2+}	2.10×10^{-3} mol/L
Cl^{-}	2.04×10^{-4} mol/L
CO_3^{2-}	1.00×10^{-3} mol/L
Mg^{2+}	5.21×10^{-4} mol/L
SO_4^{2-} (inside)	2.62×10^{-4} mol/L
SO_4^{2-} (outside)	2.62×10^{-4} mol/L
O_2	1.63×10^{-4} mol/L
Constituent solubilities	
$Ca(OH)_2$	2.00×10^{-2} mol/L
CO_3^{2-}	1.20×10^{-3} mol/L
Mg^{2+}	1.20×10^{-3} mol/L

Table F.5 (continued)

Properties of concrete	
Concrete constituent concentrations	
Calcium concentration in C-S-H system	1.75×10^{0} mol/L
Calcium concentration in pore fluid	2.00×10^{-2} mol/L
CaO content in cement	2.11×10^{0} mol/L
Free Cl^-	1.00×10^{-2} mol/L
Silica concentration in C-S-H system	7.10×10^{-1} mol/L
Concrete design specifications	
Compressive strength at 28 days	3.52×10^{2} kg/cm^2
Poisson's ratio of concrete	1.50×10^{-1}
Modulus of elasticity of steel	0.00×10^{0} kg/cm^2
Yield strength of steel	0.00×10^{0} kg/cm^2
Modulus of subgrade reaction	2.11×10^{1} kg/cm^2
Young's modulus of elasticity	0.00×10^{0} kg/cm^2
Concrete water/cement ratio	4.00×10^{-1}
Concrete density	2.40×10^{0} g/cm^3
Concrete porosity	1.50×10^{-1}
Cement content	3.85×10^{2} kg/m^3
Initial pH	1.26×10^{1}
Diffusion coefficients in concrete	
NaOH, KOH	2.12×10^{-11} m^2/s
$Ca(OH)_2$	1.82×10^{-11} m^2/s
Cl^-	5.08×10^{-11} m^2/s
CO_2	1.92×10^{-10} m^2/s
O_2	2.10×10^{-10} m^2/s
SO_4^{2-}	1.06×10^{-11} m^2/s
Trench design specifications[b]	
Trench dimensions	
Trench radius	4.98×10^{0} m
Trench height	5.20×10^{0} m
Concrete member thickness	
Roof	3.05×10^{1} cm
Walls	1.52×10^{1} cm
Floor	3.05×10^{1} cm

Table F.5 (continued)

Steel reinforcement radius	
Roof	0.00×10^0 cm
Walls	0.00×10^0 cm
Floor	0.00×10^0 cm
Spacing of steel reinforcement	
Roof	0.00×10^0 cm
Walls	0.00×10^0 cm
Floor	0.00×10^0 cm
Corrugated steel thickness	
Compression face	0.00×10^0 cm
Tension face	0.00×10^0 cm
Concrete cover thickness on tension face	
Roof	
X-direction	1.48×10^1 cm
Y-direction	1.48×10^1 cm
Walls	
Horizontal direction	0.00×10^0 cm
Vertical direction	0.00×10^0 cm
Floor	
X-direction	1.48×10^1 cm
Y-direction	1.48×10^1 cm

Soil and waste properties

Earthen cover thickness	1.83×10^0 m
Earthen cover density	1.76×10^0 g/cm^3
Friction angle of waste backfill	4.00×10^1 deg
Friction angle of soil backfill	3.00×10^1 deg
Density of waste backfill	1.76×10^0 g/cm^3
Density of soil backfill	1.76×10^0 g/cm^3
Waste density	1.76×10^0 g/cm^3
Average moisture content of waste	9.90×10^{-1}

Table F.5 (continued)

Concrete and steel failure rates

Epoxy coating	
Start of failure	0.00×10^{0} years
Time to complete failure	0.00×10^{0} years
Steel liner	
Start of failure	0.00×10^{0} years
Time to complete failure	0.00×10^{0} years

Nuclide-specific parameters

Nuclide	^{90}Sr
Half-life	2.85×10^{1} years
Solubility	7.45×10^{-5} mol/L
Waste K_d	8.74×10^{0} mL/g
Diffusion coefficient	
Waste	1.17×10^{-11} m^2/s
Concrete	1.34×10^{-12} m^2/s
Initial inventory	2.65×10^{-4} g

Output summary

		Annual amount leached (g/year)		
Year	Inventory (g)	Advection	Diffusion	Total
1	2.41×10^{-4}	1.80×10^{-5}	4.94×10^{-15}	1.80×10^{-5}
10	1.17×10^{-4}	4.33×10^{-8}	1.61×10^{-8}	5.94×10^{-8}
20	9.15×10^{-5}	3.38×10^{-8}	2.05×10^{-8}	5.42×10^{-8}
30	7.13×10^{-5}	2.63×10^{-8}	1.70×10^{-8}	4.34×10^{-8}
40	5.56×10^{-5}	2.05×10^{-8}	1.31×10^{-8}	3.37×10^{-8}
50	4.28×10^{-5}	3.85×10^{-7}	9.88×10^{-9}	3.95×10^{-7}
60	2.42×10^{-5}	1.20×10^{-6}	5.59×10^{-9}	1.21×10^{-6}
70	1.17×10^{-5}	5.82×10^{-7}	2.60×10^{-9}	5.84×10^{-7}
80	5.64×10^{-6}	2.81×10^{-7}	1.21×10^{-9}	2.82×10^{-7}
90	2.73×10^{-6}	1.36×10^{-7}	5.61×10^{-10}	1.36×10^{-7}
100	1.32×10^{-6}	6.55×10^{-8}	2.62×10^{-10}	6.58×10^{-8}
110	6.36×10^{-7}	3.17×10^{-8}	1.22×10^{-10}	3.18×10^{-8}

Table F.5 (continued)

Year	Inventory (g)	Annual amount leached (g/year) Advection	Diffusion	Total
120	3.07×10^{-7}	1.53×10^{-8}	5.72×10^{-11}	1.54×10^{-8}
130	1.48×10^{-7}	7.39×10^{-9}	2.68×10^{-11}	7.42×10^{-9}
140	7.17×10^{-8}	3.57×10^{-9}	1.26×10^{-11}	3.58×10^{-9}
150	3.47×10^{-8}	1.72×10^{-9}	5.93×10^{-12}	1.73×10^{-9}
160	1.67×10^{-8}	8.33×10^{-10}	2.79×10^{-12}	8.36×10^{-10}
170	8.09×10^{-9}	4.03×10^{-10}	1.32×10^{-12}	4.04×10^{-10}
180	3.91×10^{-9}	1.95×10^{-10}	6.21×10^{-13}	1.95×10^{-9}
190	1.89×10^{-9}	9.41×10^{-11}	2.93×10^{-13}	9.44×10^{-11}
200	9.13×10^{-10}	4.55×10^{-11}	1.39×10^{-13}	4.56×10^{-11}
210	4.41×10^{-10}	2.20×10^{-11}	6.57×10^{-14}	2.20×10^{-11}
220	2.13×10^{-10}	1.06×10^{-11}	3.11×10^{-14}	1.06×10^{-11}
230	1.03×10^{-10}	5.13×10^{-12}	1.48×10^{-14}	5.15×10^{-12}
240	4.98×10^{-11}	2.48×10^{-12}	7.00×10^{-15}	2.49×10^{-12}
250	2.41×10^{-11}	1.20×10^{-12}	3.33×10^{-15}	1.20×10^{-12}
260	1.16×10^{-11}	5.80×10^{-13}	1.58×10^{-15}	5.81×10^{-13}
270	5.63×10^{-12}	2.80×10^{-13}	7.51×10^{-16}	2.81×10^{-13}
280	2.72×10^{-12}	1.35×10^{-13}	3.57×10^{-16}	1.36×10^{-13}
290	1.32×10^{-12}	6.55×10^{-14}	1.70×10^{-16}	6.56×10^{-14}
300	6.36×10^{-13}	3.16×10^{-14}	8.10×10^{-17}	3.17×10^{-14}
310	3.07×10^{-13}	1.53×10^{-14}	3.86×10^{-17}	1.53×10^{-14}
320	1.49×10^{-13}	7.39×10^{-15}	1.84×10^{-17}	7.41×10^{-15}
330	7.18×10^{-14}	3.57×10^{-15}	8.76×10^{-18}	3.58×10^{-15}
340	3.47×10^{-14}	1.73×10^{-15}	4.18×10^{-18}	1.73×10^{-15}
350	1.68×10^{-14}	8.35×10^{-16}	1.99×10^{-18}	8.37×10^{-16}
360	8.12×10^{-15}	4.04×10^{-16}	9.51×10^{-19}	4.05×10^{-16}
370	3.92×10^{-16}	1.95×10^{-16}	4.54×10^{-19}	1.96×10^{-16}
380	1.90×10^{-15}	9.44×10^{-17}	2.17×10^{-19}	9.46×10^{-17}
390	9.17×10^{-16}	4.56×10^{-17}	1.04×10^{-19}	4.57×10^{-17}
400	4.43×10^{-16}	2.21×10^{-17}	4.95×10^{-20}	2.21×10^{-17}
410	2.14×10^{-16}	1.07×10^{-17}	2.37×10^{-20}	1.07×10^{-17}
420	1.04×10^{-16}	5.16×10^{-18}	1.13×10^{-20}	5.17×10^{-18}
430	5.01×10^{-17}	2.50×10^{-18}	5.41×10^{-21}	2.50×10^{-18}

Table F.5 (continued)

Year	Inventory (g)	Annual amount leached (g/year)		
		Advection	Diffusion	Total
440	2.42×10^{-17}	1.21×10^{-18}	2.59×10^{-21}	1.21×10^{-18}
450	1.17×10^{-17}	5.83×10^{-19}	1.24×10^{-21}	5.84×10^{-19}
460	5.67×10^{-18}	2.82×10^{-19}	5.93×10^{-22}	2.82×10^{-19}
470	2.74×10^{-18}	1.36×10^{-19}	2.84×10^{-22}	1.37×10^{-19}
480	1.32×10^{-18}	6.59×10^{-20}	1.36×10^{-22}	6.60×10^{-20}
490	6.40×10^{-19}	3.19×10^{-20}	6.51×10^{-23}	3.19×10^{-20}
500	3.10×10^{-19}	1.54×10^{-20}	3.12×10^{-23}	1.54×10^{-20}
510	1.50×10^{-19}	7.45×10^{-21}	1.49×10^{-23}	7.47×10^{-21}
520	7.24×10^{-20}	3.60×10^{-21}	7.16×10^{-24}	3.61×10^{-21}
530	3.50×10^{-20}	1.74×10^{-21}	3.43×10^{-24}	1.75×10^{-21}
540	1.69×10^{-20}	8.42×10^{-22}	1.64×10^{-24}	8.44×10^{-22}
550	8.19×10^{-21}	4.07×10^{-22}	7.88×10^{-25}	4.08×10^{-22}
560	3.96×10^{-21}	1.97×10^{-22}	3.78×10^{-25}	1.97×10^{-22}
570	1.91×10^{-21}	9.53×10^{-23}	1.81×10^{-25}	9.54×10^{-23}
580	9.26×10^{-22}	4.61×10^{-23}	8.69×10^{-26}	4.62×10^{-23}
590	4.48×10^{-22}	2.23×10^{-23}	4.17×10^{-26}	2.23×10^{-23}
600	2.16×10^{-22}	1.08×10^{-23}	2.00×10^{-26}	1.08×10^{-23}
610	1.05×10^{-22}	5.21×10^{-24}	9.59×10^{-27}	5.22×10^{-24}
620	5.06×10^{-23}	2.52×10^{-24}	4.60×10^{-27}	2.52×10^{-24}
630	2.45×10^{-23}	1.22×10^{-24}	2.21×10^{-27}	1.22×10^{-24}
640	1.18×10^{-23}	5.89×10^{-25}	1.06×10^{-27}	5.90×10^{-25}
650	5.72×10^{-24}	2.85×10^{-25}	5.09×10^{-28}	2.85×10^{-25}
660	2.77×10^{-24}	1.38×10^{-25}	2.44×10^{-28}	1.38×10^{-25}
670	1.34×10^{-24}	6.66×10^{-26}	1.17×10^{-28}	6.67×10^{-26}
680	6.47×10^{-25}	3.22×10^{-26}	5.63×10^{-29}	3.23×10^{-26}
690	3.13×10^{-25}	1.56×10^{-26}	2.71×10^{-29}	1.56×10^{-26}
700	1.51×10^{-25}	7.53×10^{-26}	1.30×10^{-29}	7.55×10^{-27}
710	7.32×10^{-26}	3.64×10^{-26}	6.24×10^{-30}	3.65×10^{-27}
720	3.54×10^{-26}	1.77×10^{-27}	3.00×10^{-30}	1.77×10^{-26}
730	1.71×10^{-26}	8.52×10^{-28}	1.44×10^{-30}	8.53×10^{-28}
740	8.29×10^{-26}	4.12×10^{-28}	6.92×10^{-31}	4.12×10^{-28}
750	4.00×10^{-27}	2.00×10^{-28}	3.32×10^{-31}	2.00×10^{-28}

Table F.5 (continued)

Year	Inventory (g)	Annual amount leached (g/year) Advection	Diffusion	Total
760	1.94×10^{-27}	9.64×10^{-29}	1.60×10^{-31}	9.66×10^{-29}
770	9.37×10^{-28}	4.67×10^{-29}	7.69×10^{-32}	4.67×10^{-29}
780	4.53×10^{-28}	2.26×10^{-29}	3.70×10^{-32}	2.26×10^{-28}
790	2.20×10^{-28}	1.10×10^{-29}	1.78×10^{-32}	1.10×10^{-29}
800	1.06×10^{-28}	5.28×10^{-30}	8.53×10^{-33}	5.29×10^{-30}
810	5.12×10^{-29}	2.56×10^{-30}	4.10×10^{-33}	2.56×10^{-30}
820	2.48×10^{-29}	1.23×10^{-30}	1.98×10^{-33}	1.23×10^{-30}
830	1.20×10^{-29}	5.97×10^{-31}	9.49×10^{-34}	5.98×10^{-31}
840	5.80×10^{-30}	2.89×10^{-31}	4.56×10^{-34}	2.89×10^{-31}
850	2.80×10^{-30}	1.40×10^{-31}	2.20×10^{-34}	1.40×10^{-31}
860	1.36×10^{-30}	6.75×10^{-32}	1.06×10^{-34}	6.76×10^{-32}
870	6.56×10^{-31}	3.27×10^{-32}	5.08×10^{-35}	3.27×10^{-32}
880	3.18×10^{-31}	1.58×10^{-32}	2.44×10^{-35}	1.59×10^{-32}
890	1.53×10^{-31}	7.63×10^{-33}	1.18×10^{-35}	7.64×10^{-33}
900	7.41×10^{-32}	3.70×10^{-33}	5.64×10^{-36}	3.70×10^{-33}
910	3.59×10^{-32}	1.79×10^{-33}	2.72×10^{-36}	1.79×10^{-33}
920	1.73×10^{-32}	8.63×10^{-34}	1.30×10^{-36}	8.66×10^{-34}
930	8.40×10^{-33}	4.18×10^{-34}	6.29×10^{-37}	4.19×10^{-34}
940	4.07×10^{-33}	2.02×10^{-34}	3.02×10^{-37}	2.02×10^{-34}
950	1.97×10^{-33}	9.78×10^{-35}	1.46×10^{-37}	9.79×10^{-35}
960	9.50×10^{-34}	4.72×10^{-35}	7.00×10^{-38}	4.73×10^{-35}
970	4.60×10^{-34}	2.29×10^{-35}	3.38×10^{-38}	2.29×10^{-35}
980	2.22×10^{-34}	1.10×10^{-35}	1.62×10^{-38}	1.10×10^{-35}
990	1.07×10^{-34}	5.34×10^{-36}	7.80×10^{-39}	5.36×10^{-36}
1000	5.20×10^{-35}	2.59×10^{-36}	3.76×10^{-39}	2.60×10^{-36}

The solubility constraints were not exceeded.

[a]1000-year simulation length, 50-year output edit frequency.
[b]Trench modeled as a right circular cylinder with equivalent surface area.

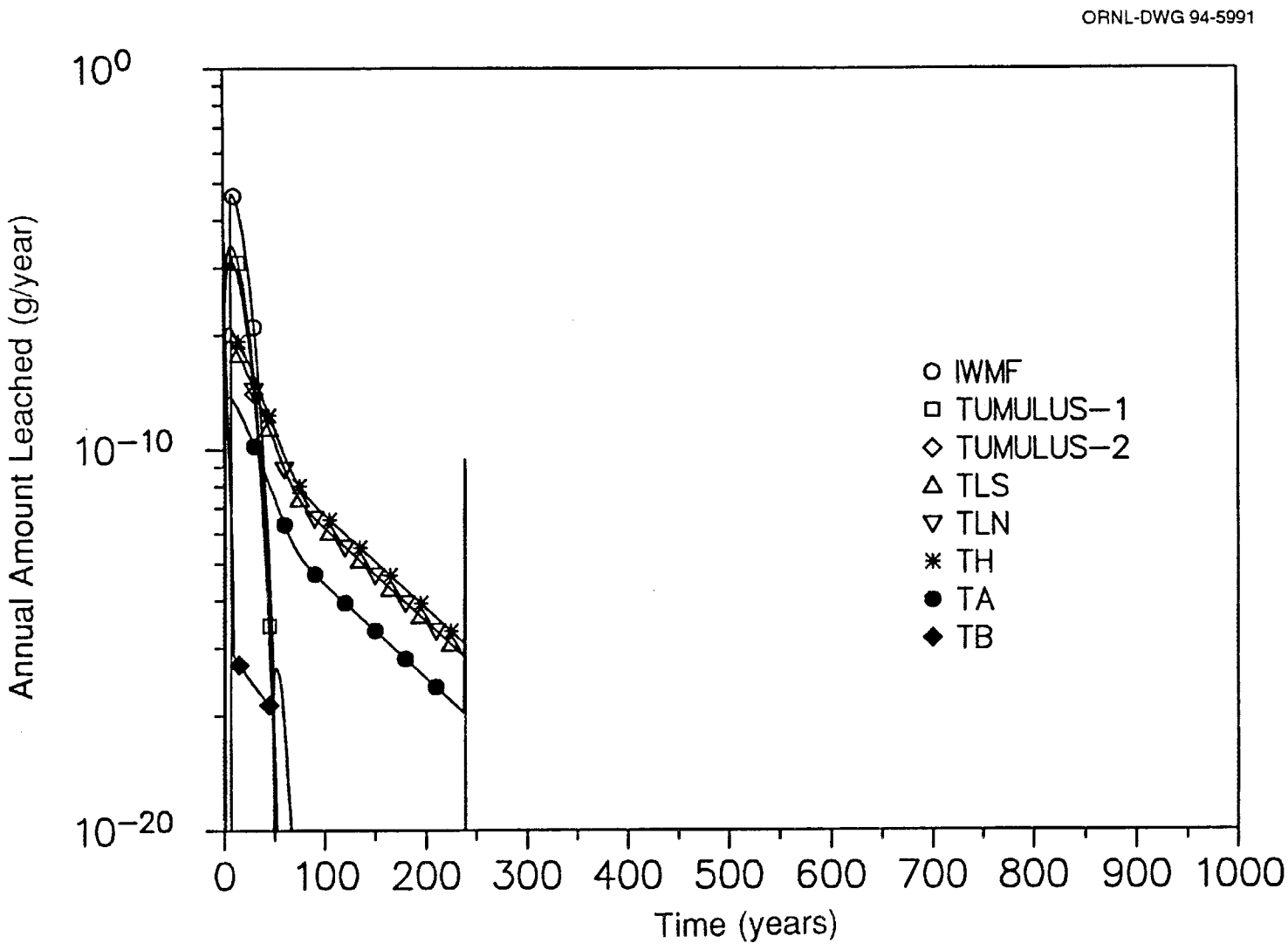

Fig. F.1. Calculated release rates of ^3H from SWSA 6 disposal sites.

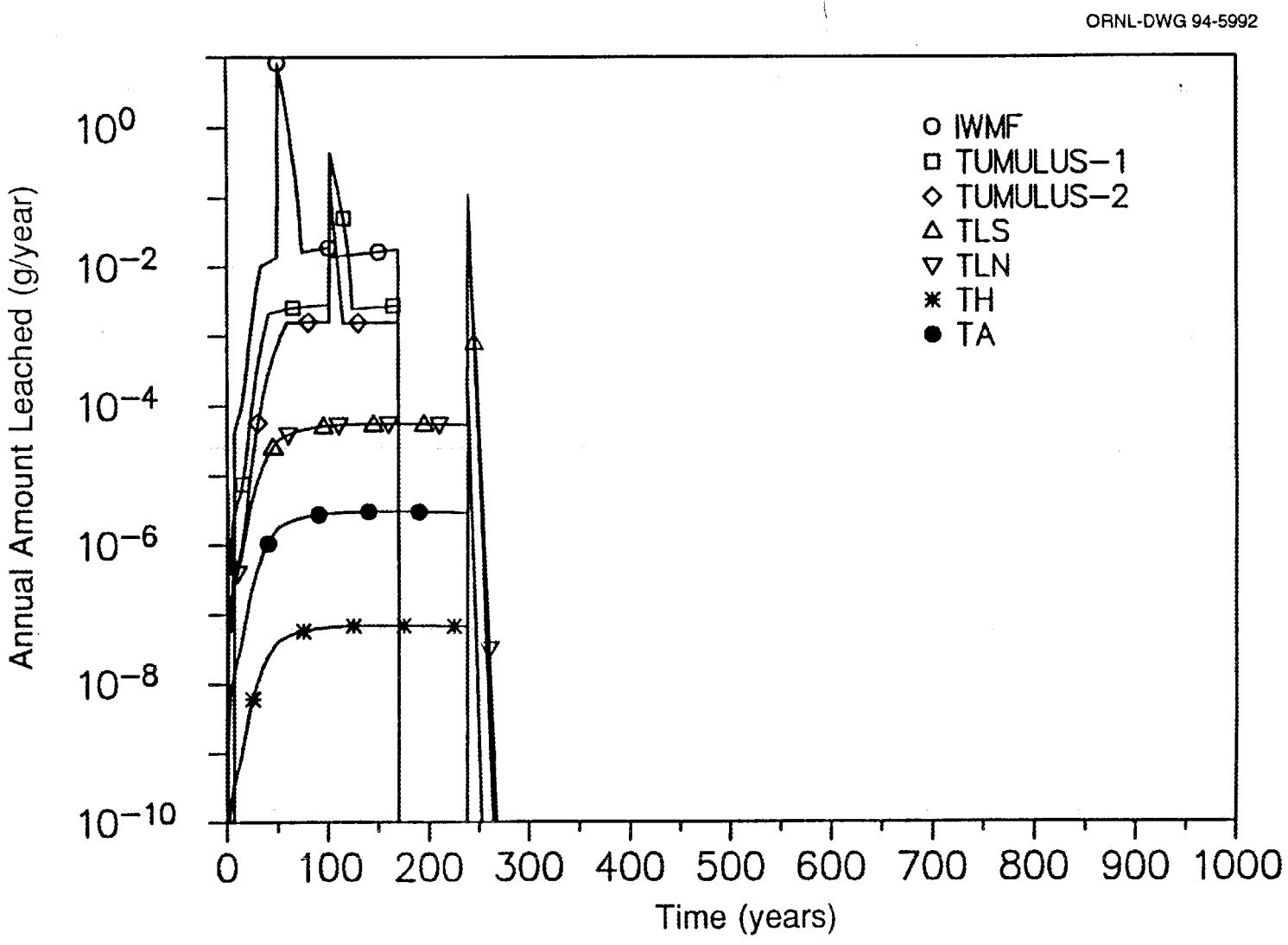

Fig. F.2. Calculated release rates of ^{14}C from SWSA 6 disposal sites.

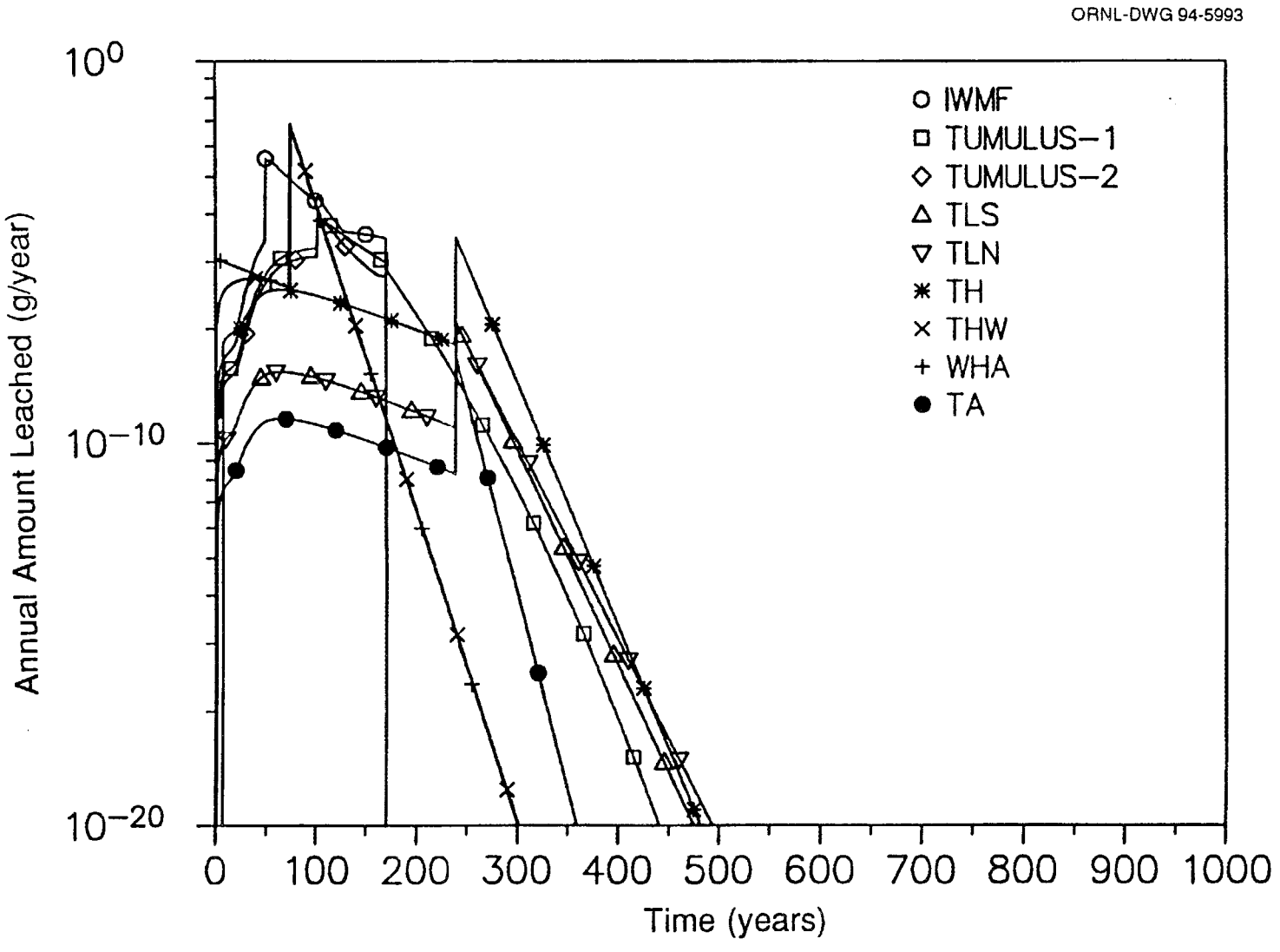

Fig. F.3. Calculated release rates of ^{90}Sr from SWSA 6 disposal sites.

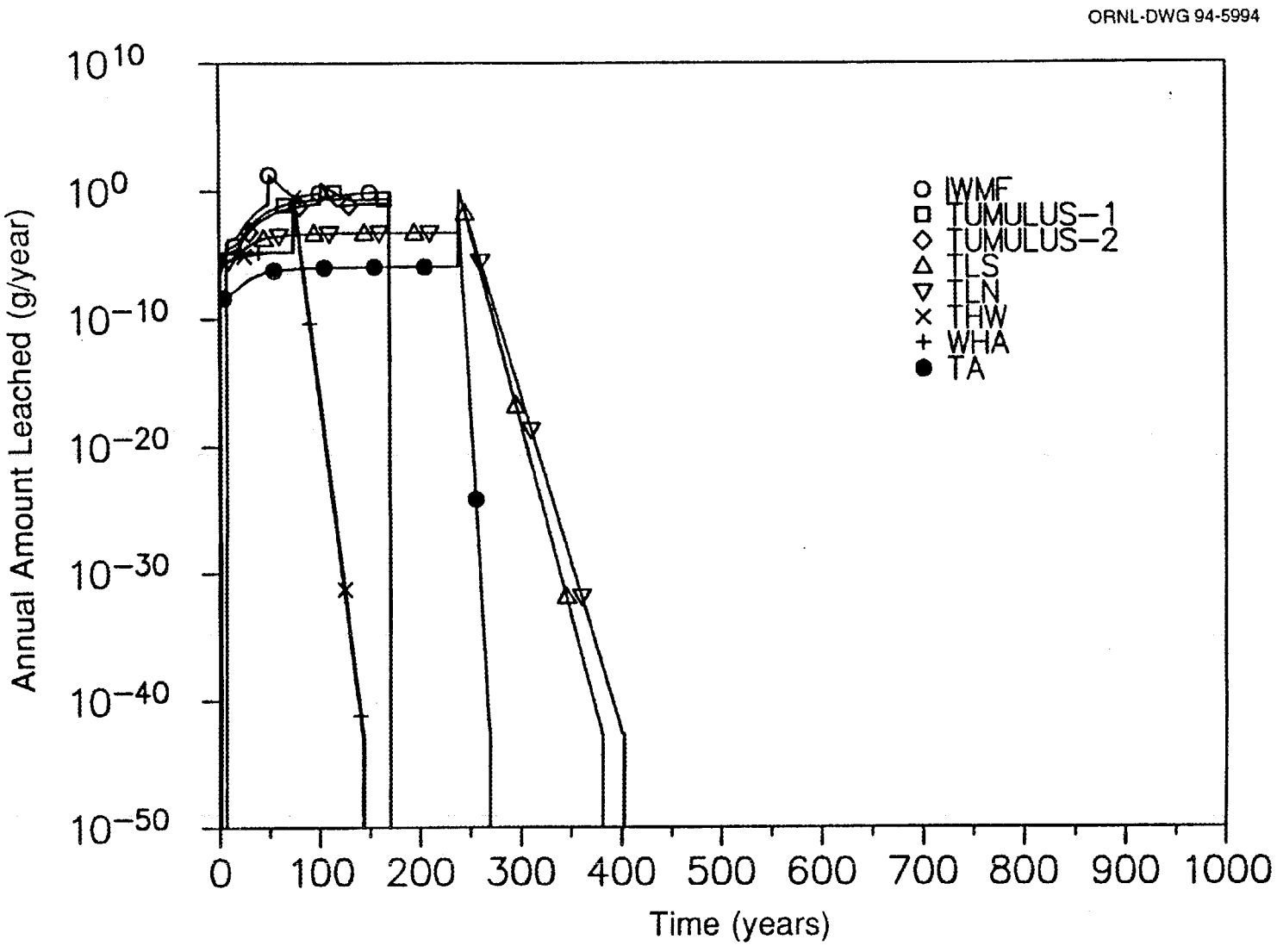

Fig. F.4. Calculated release rates of ^{99}Tc from SWSA 6 disposal sites.

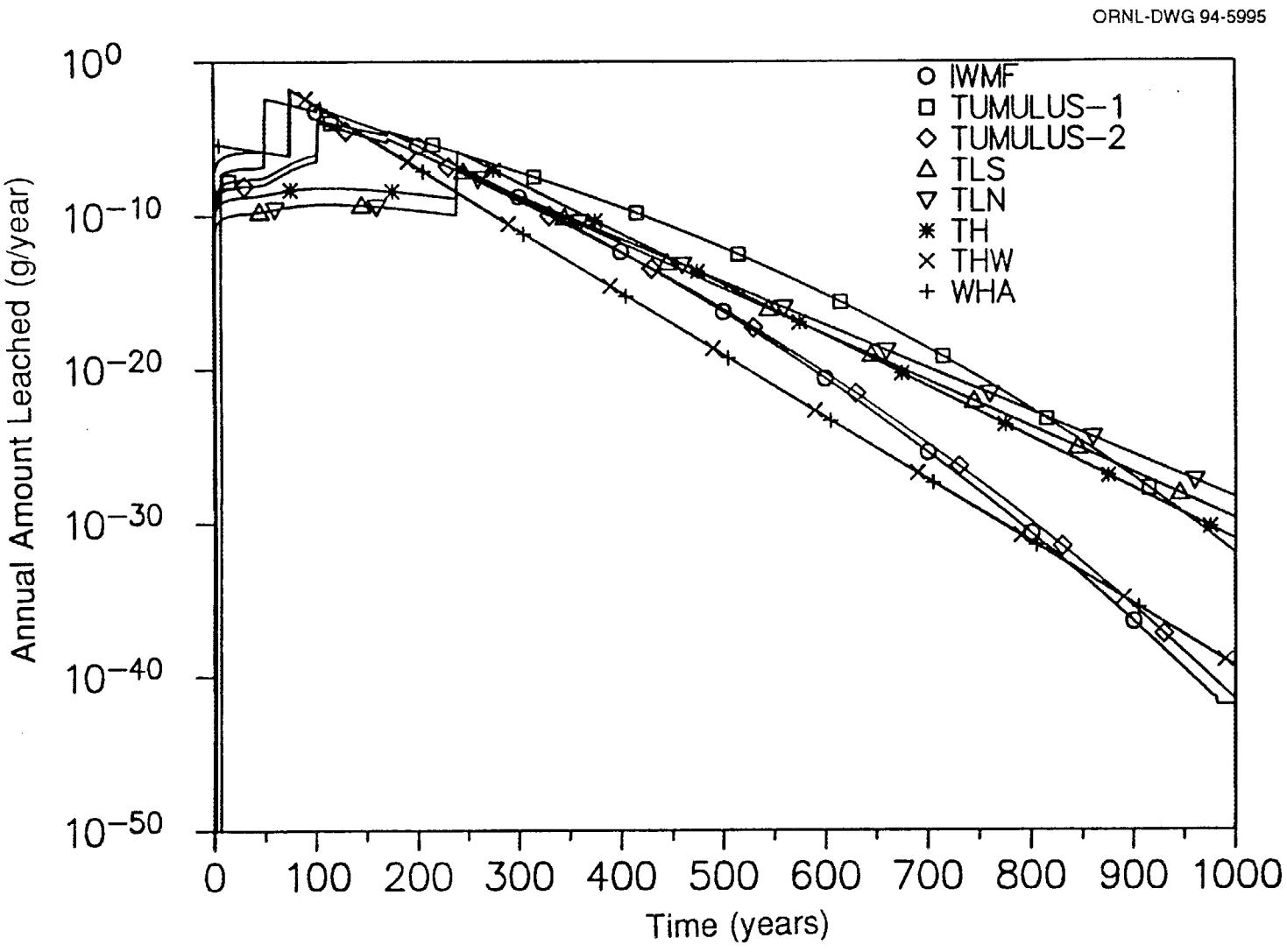

Fig. F.5. Calculated release rates of ^{137}Cs from SWSA 6 disposal sites.

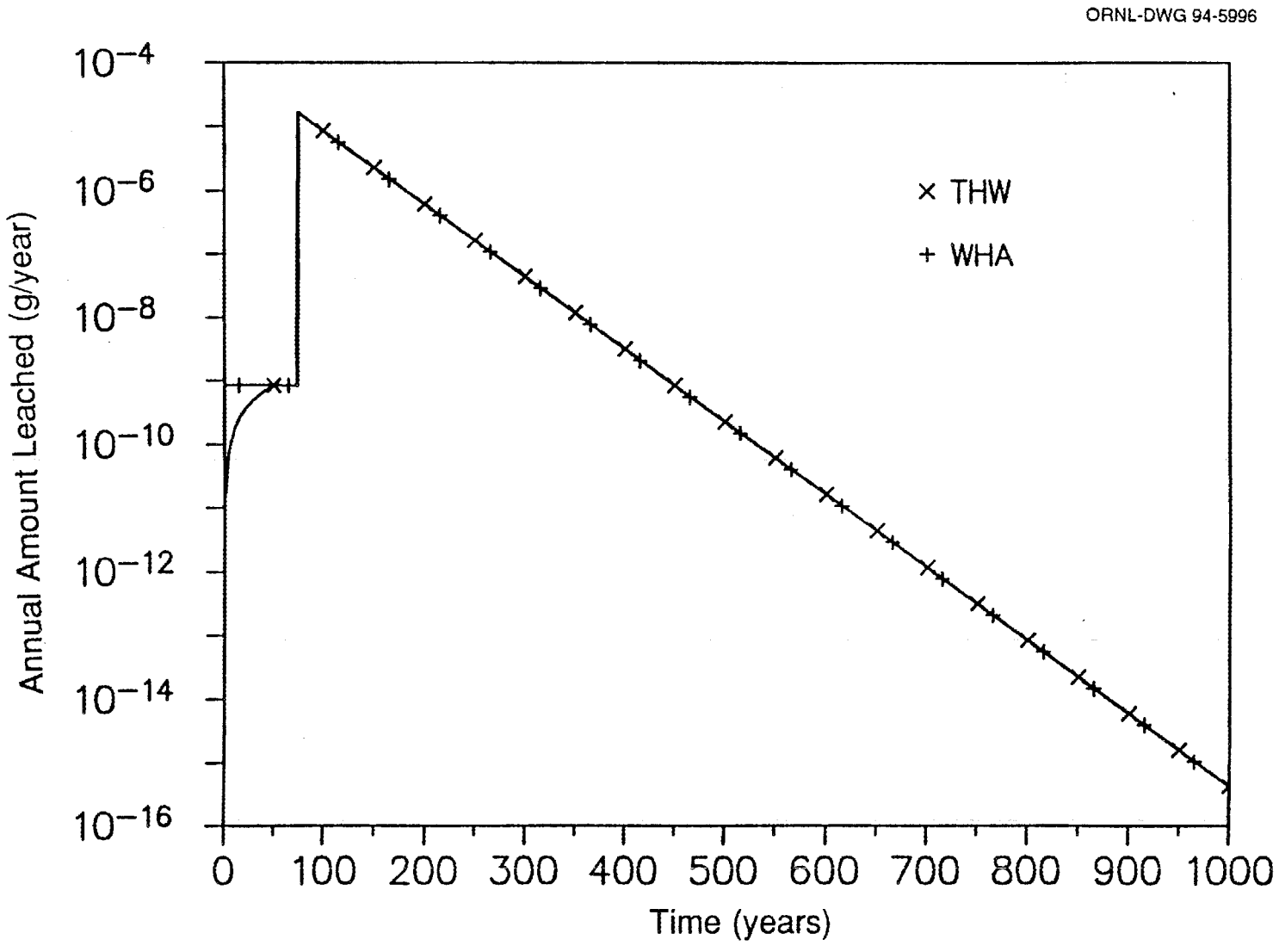

Fig. F.6. Calculated release rates of ^{229}Th from SWSA 6 disposal sites.

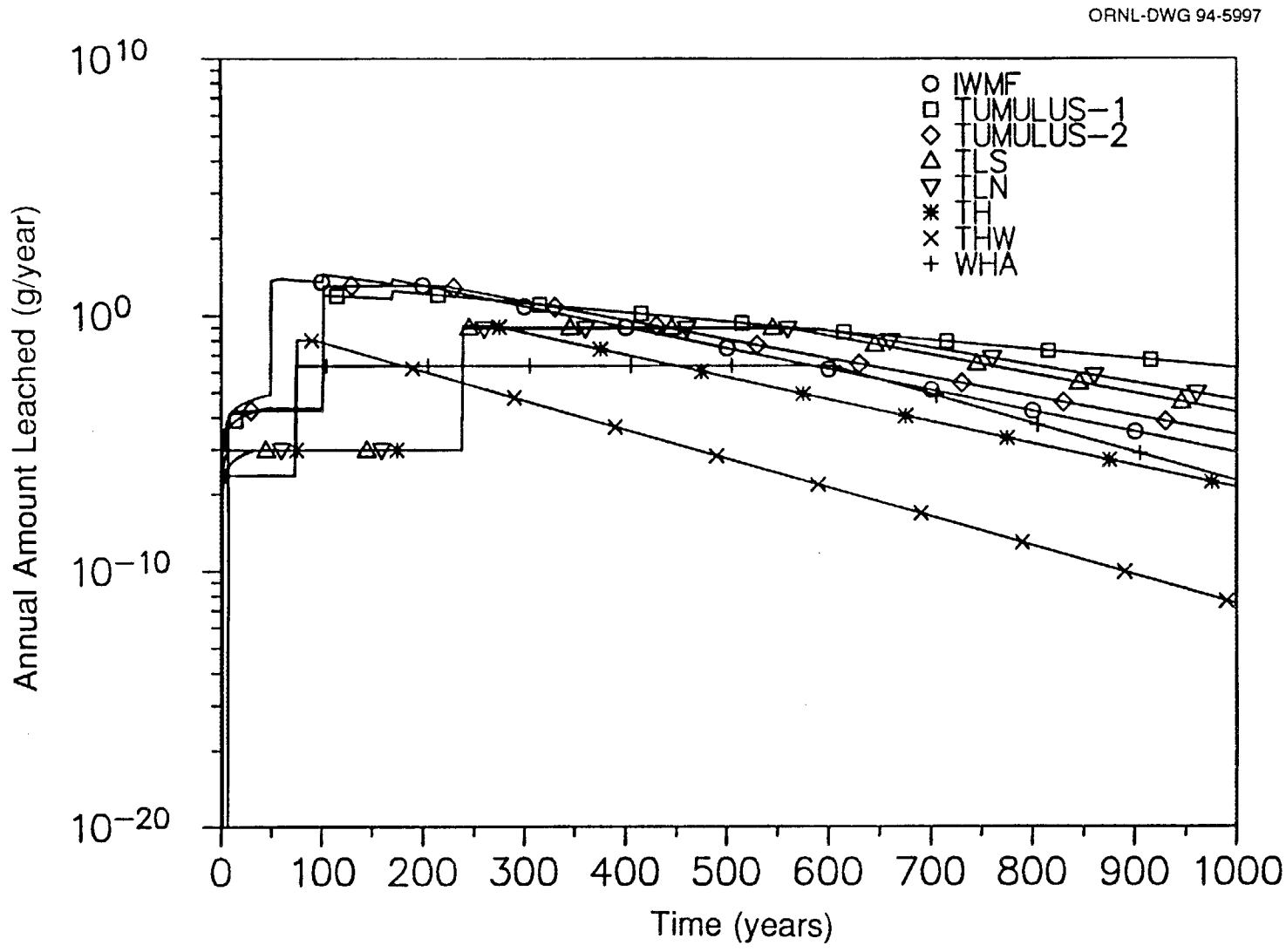

Fig. F.7. Calculated release rates of ^{232}Th from SWSA 6 disposal sites.

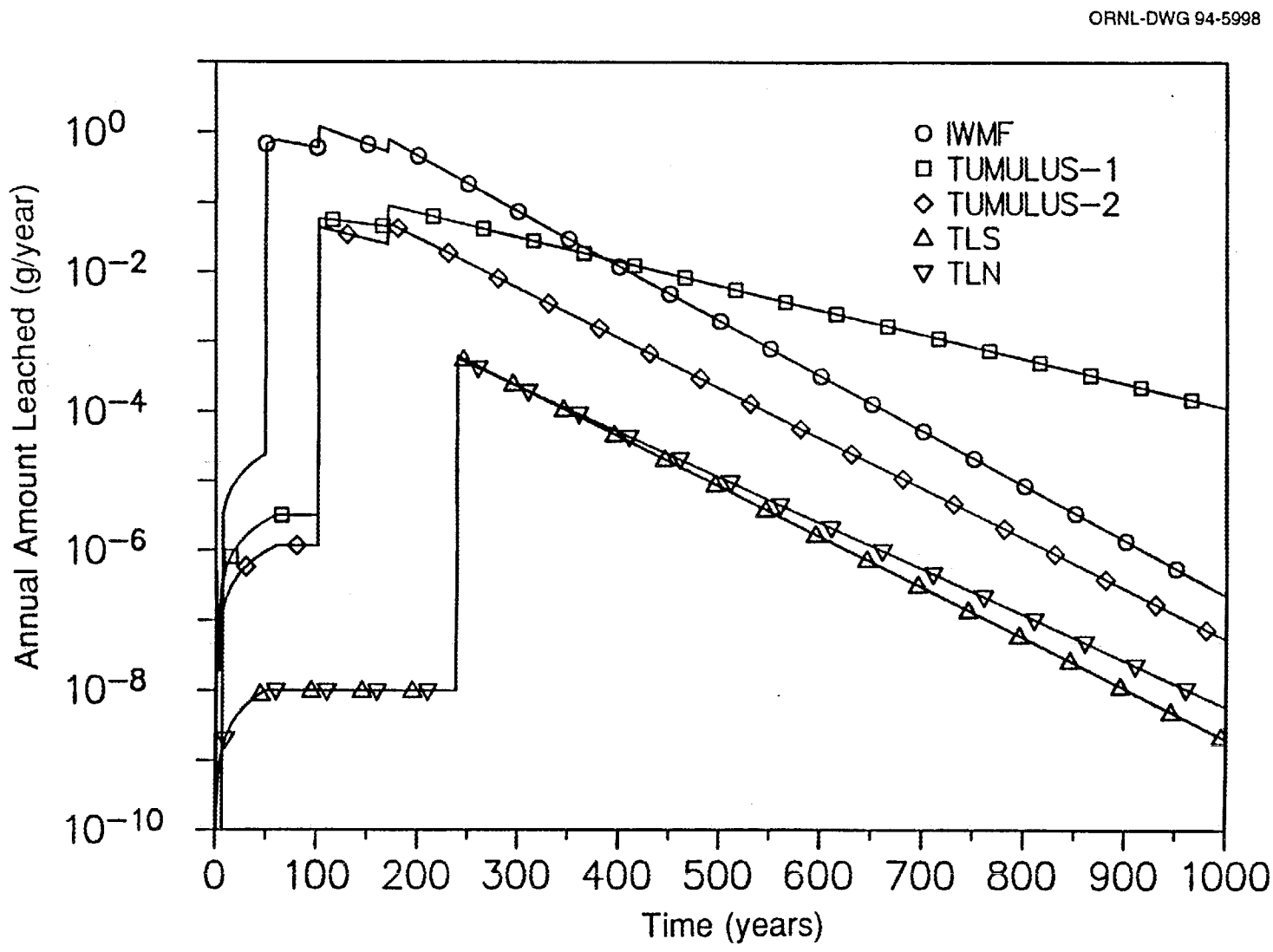

Fig. F.8. Calculated release rates of ^{233}U from SWSA 6 disposal sites.

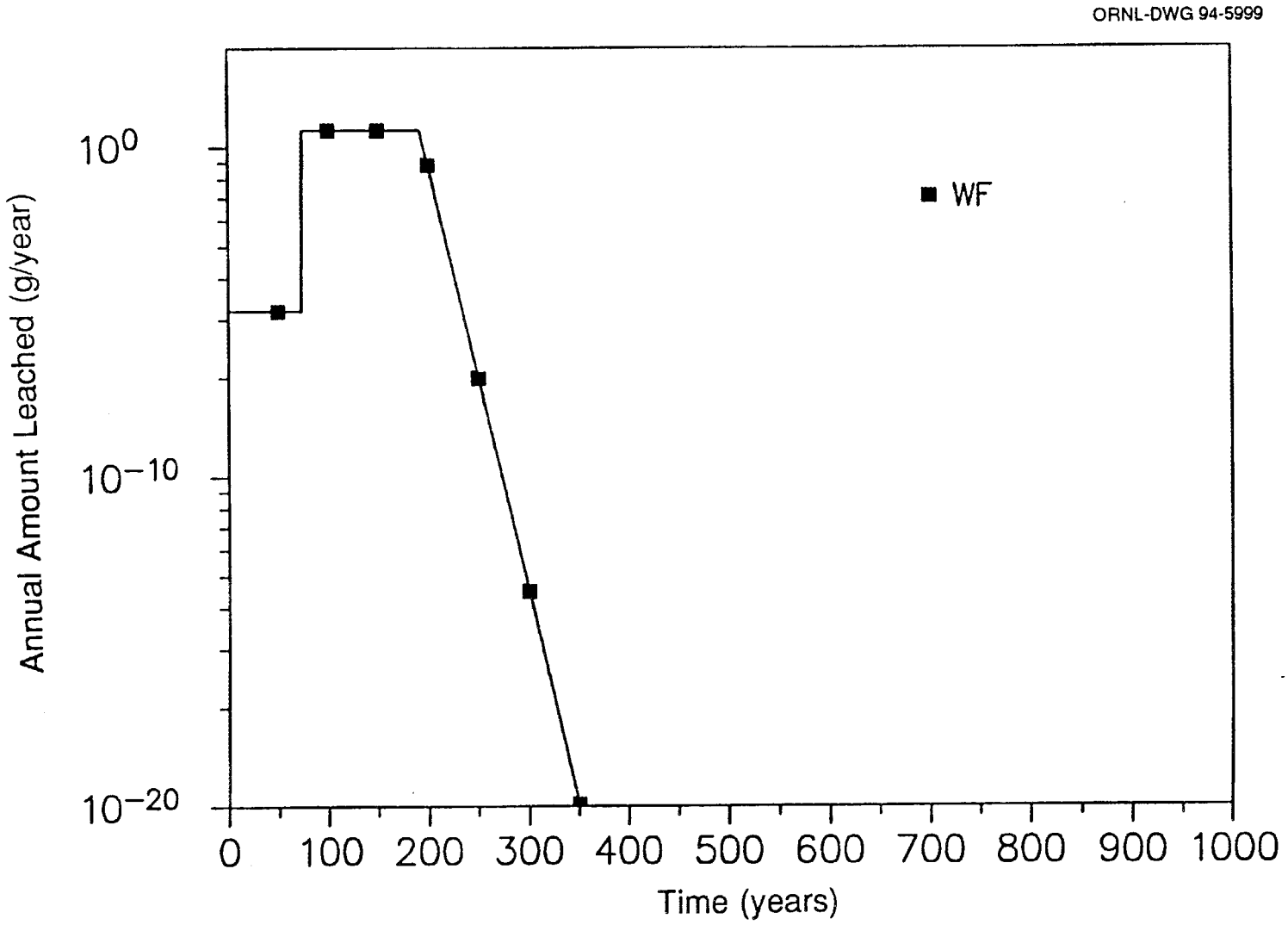

Fig. F.9. Calculated release rates of ^{235}U from SWSA 6 disposal sites.

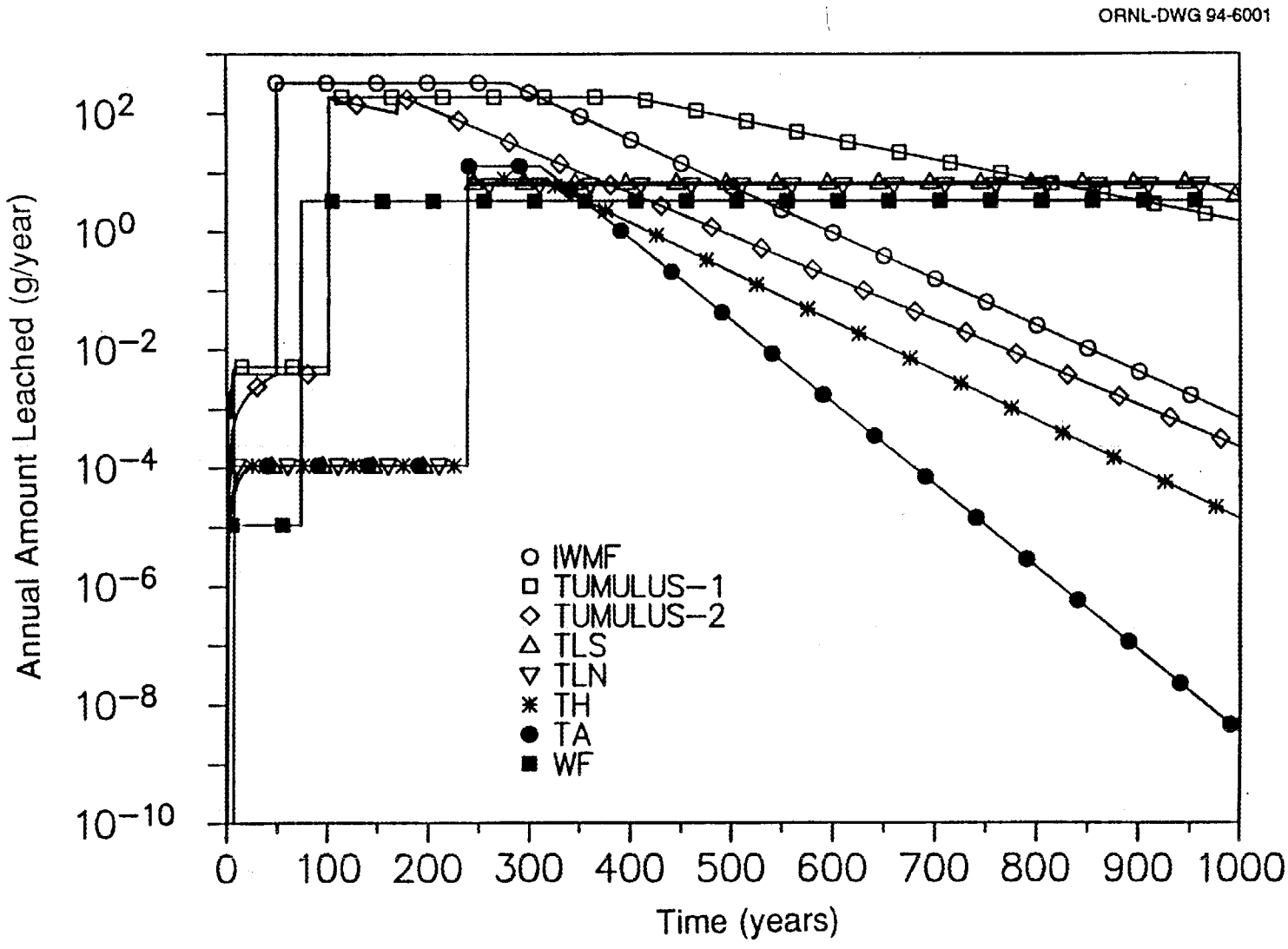

Fig. F.10. Calculated release rates of ^{238}U from SWSA 6 disposal sites.

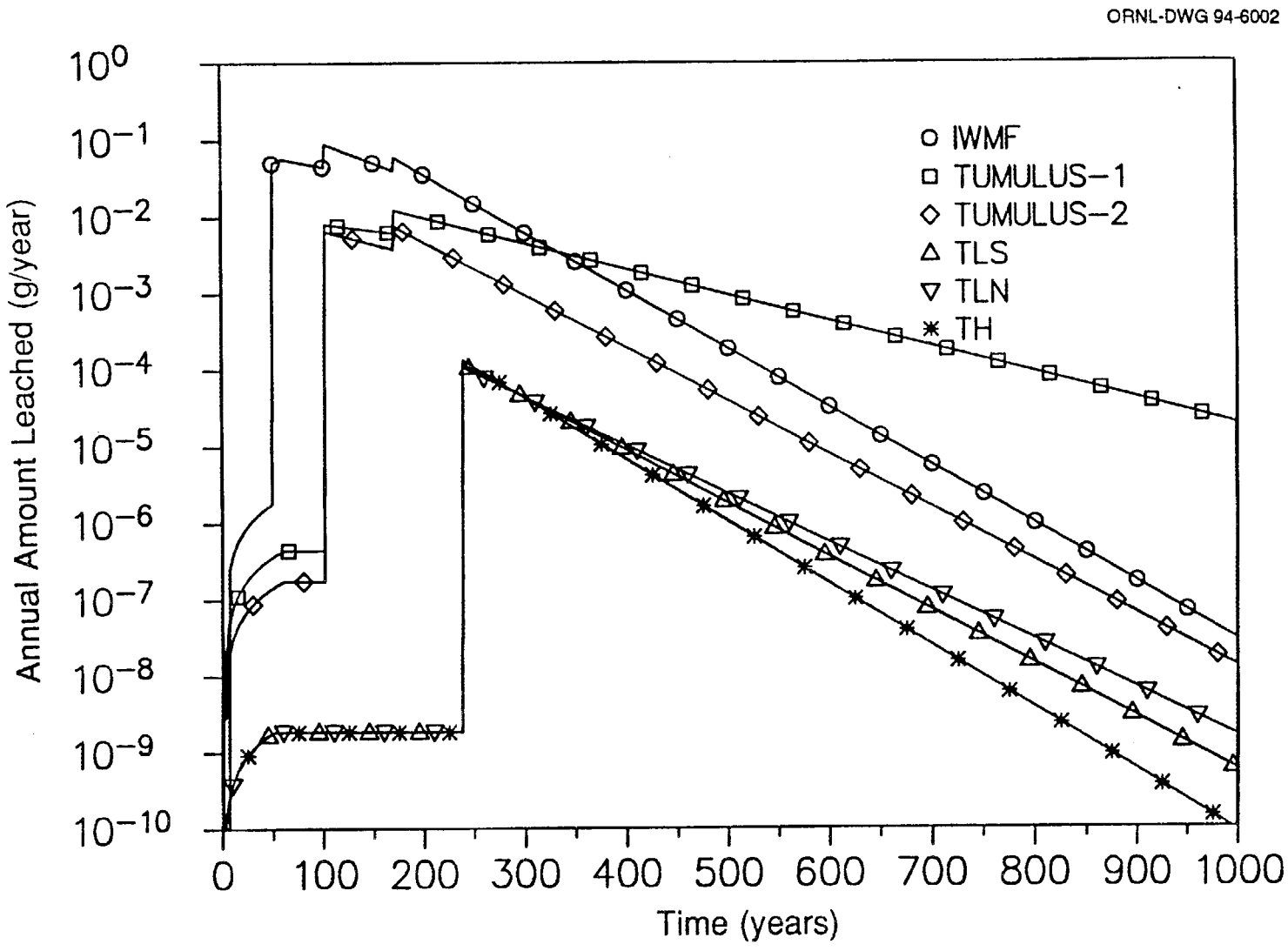

Fig. F.11. Calculated release rates of ^{239}Pu from SWSA 6 disposal sites.

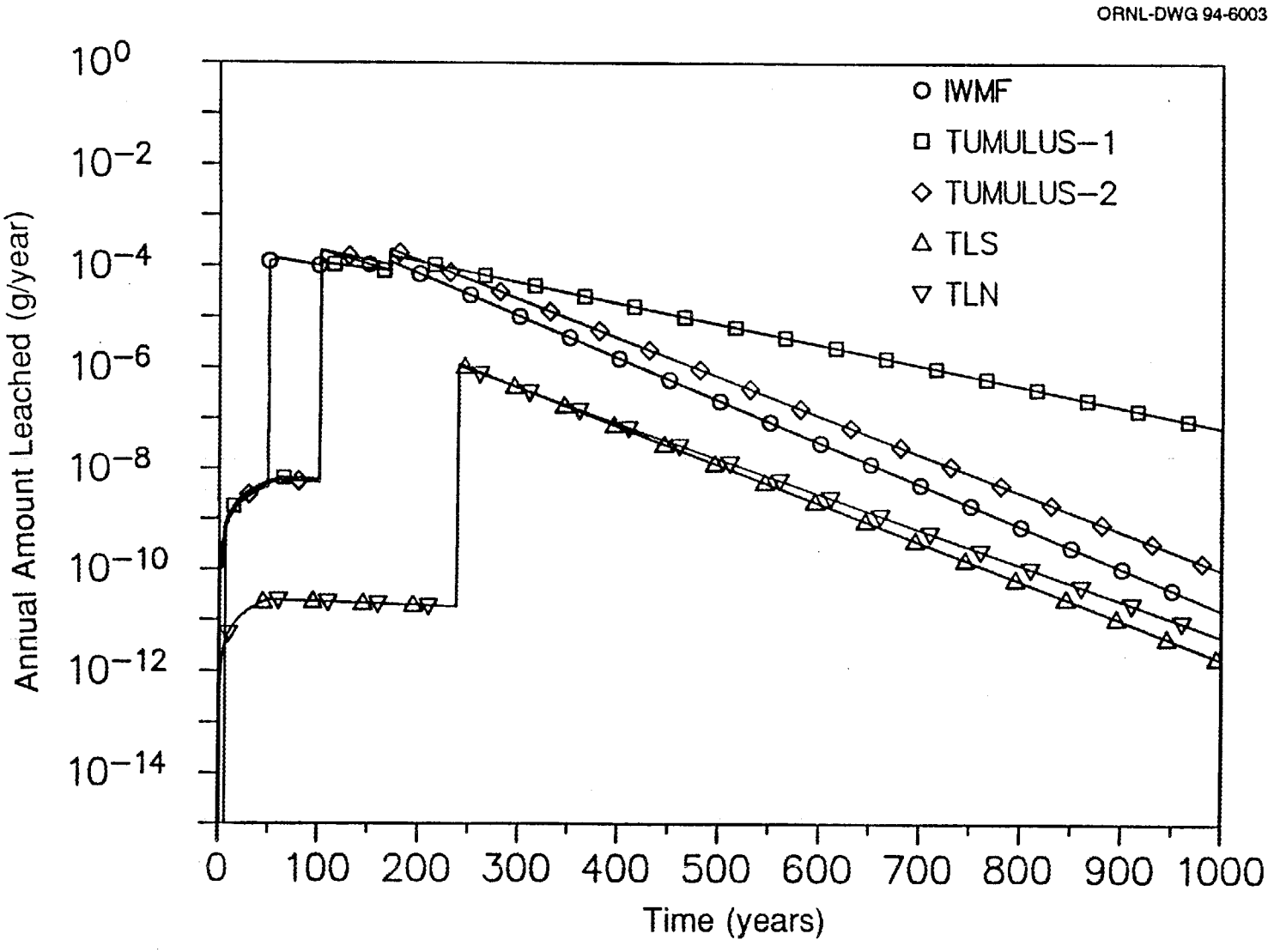

Fig. F.12. Calculated release rates of ^{241}Am from SWSA 6 disposal sites.

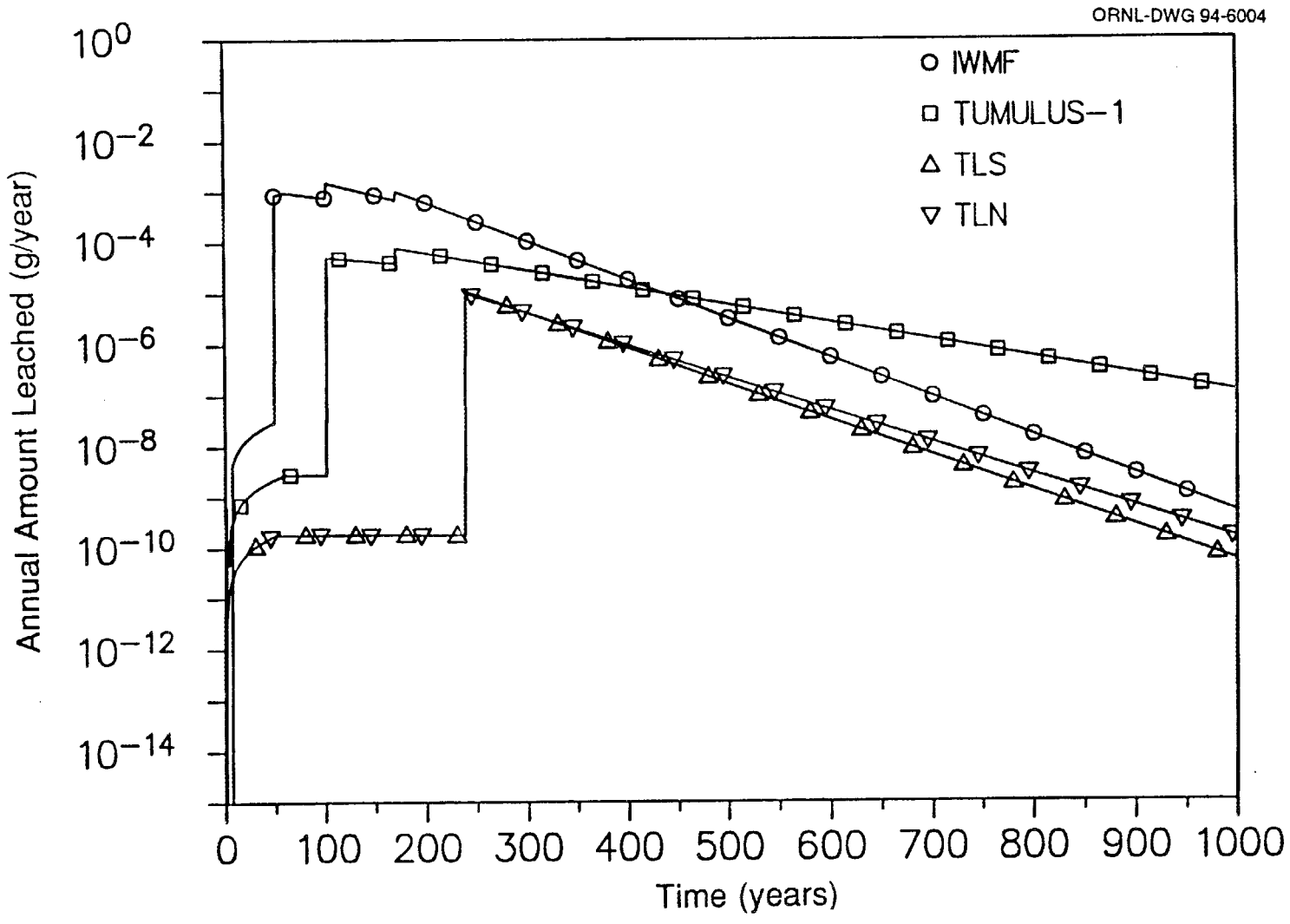

Fig. F.13. Calculated release rates of ^{243}Am from SWSA 6 disposal sites.

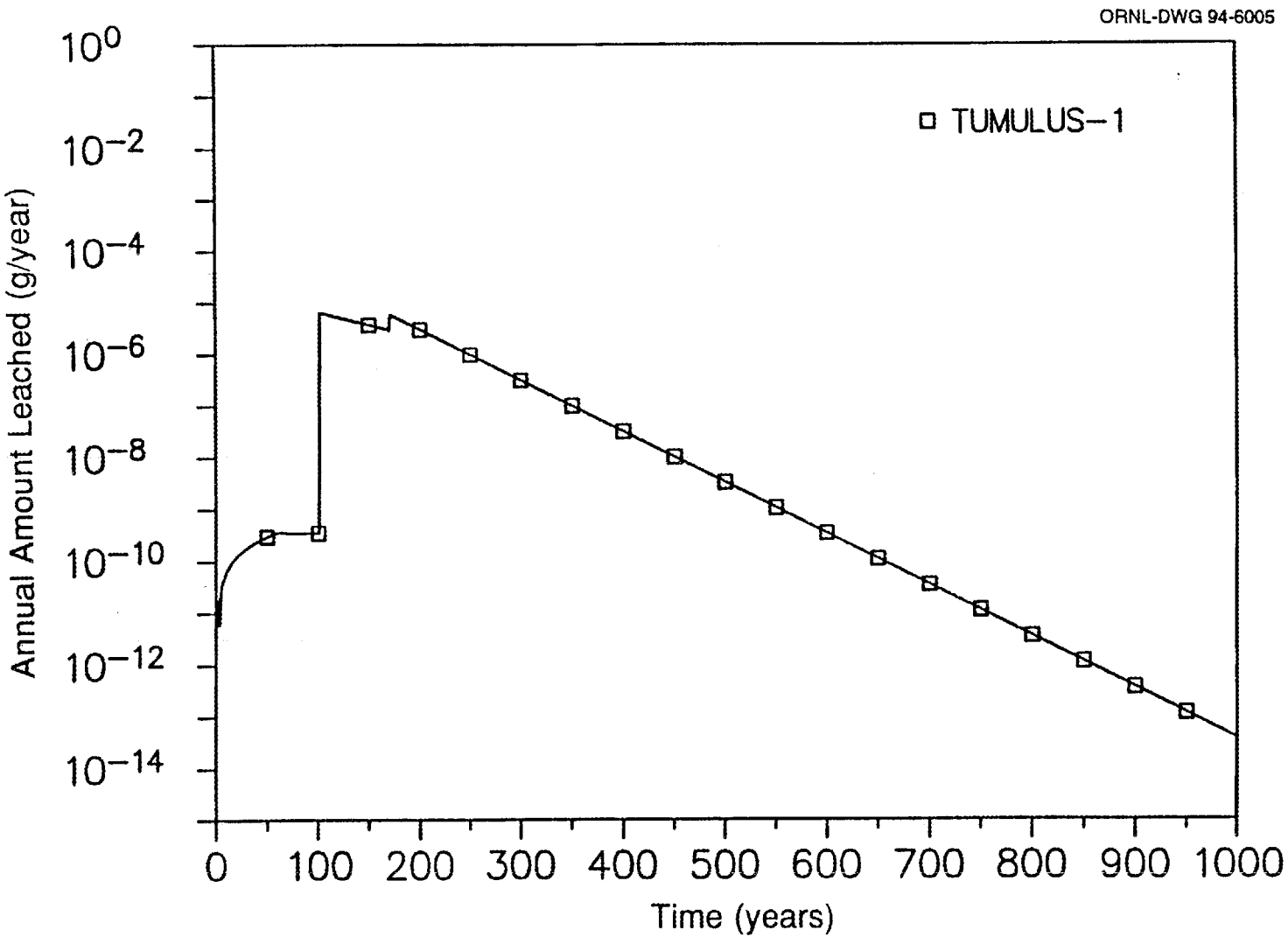

Fig. F.14. Calculated release rates of ^{226}Ra from SWSA 6 disposal sites.

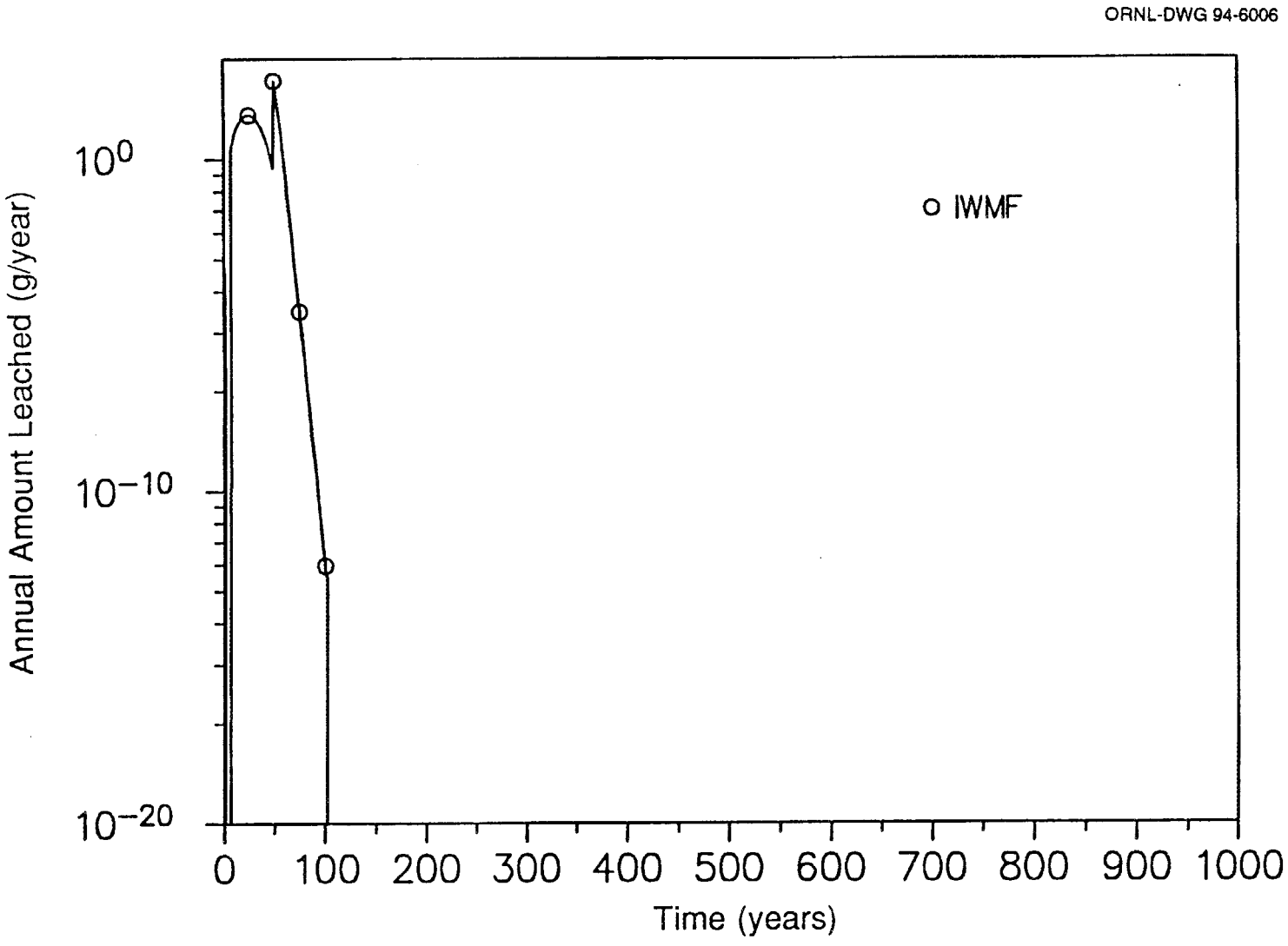

Fig. F.15. Calculated release rates of ^{136}Cs from SWSA 6 disposal sites.

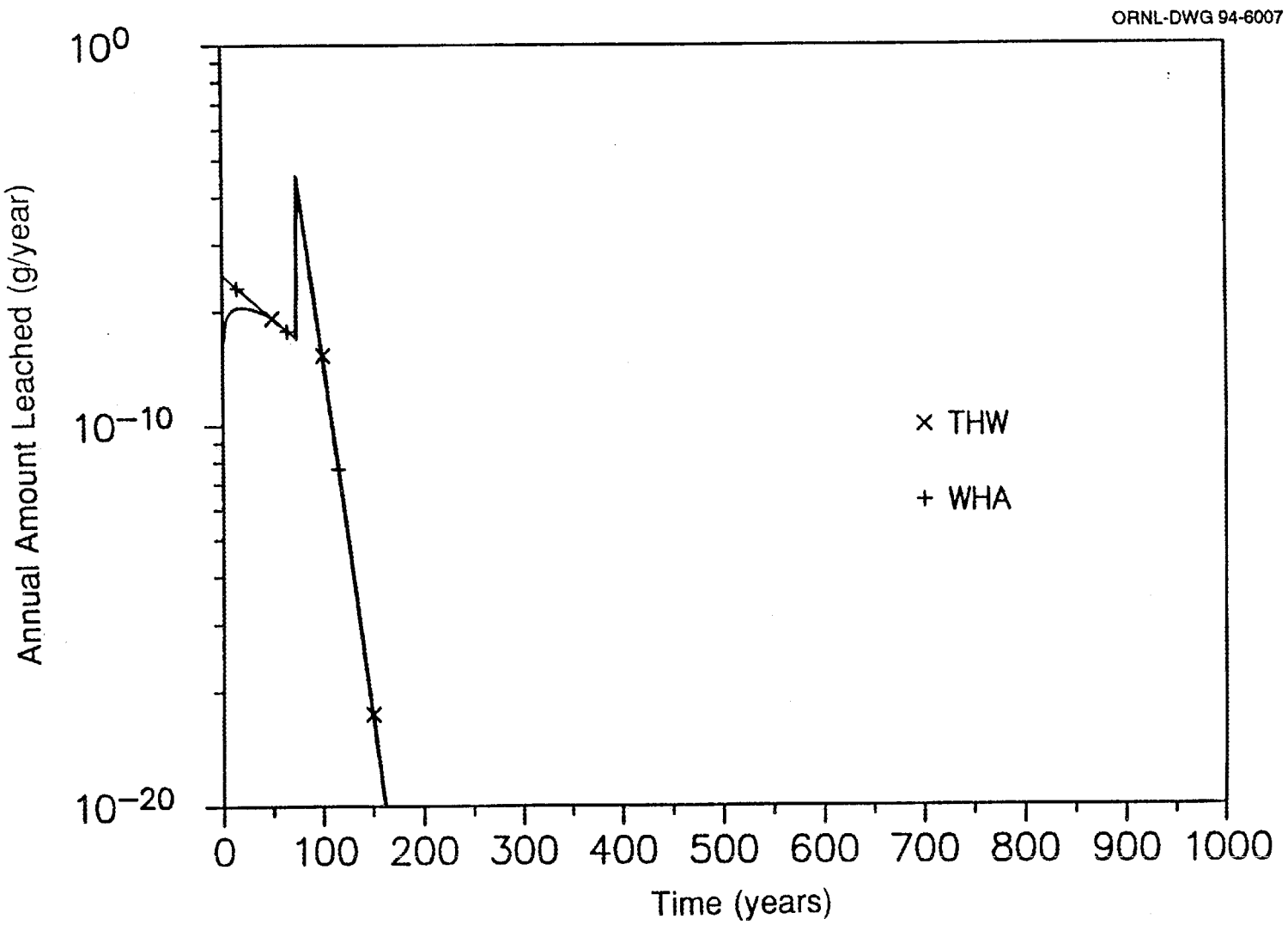

Fig. F.16. Calculated release rates of ^{152}Eu from SWSA 6 disposal sites.

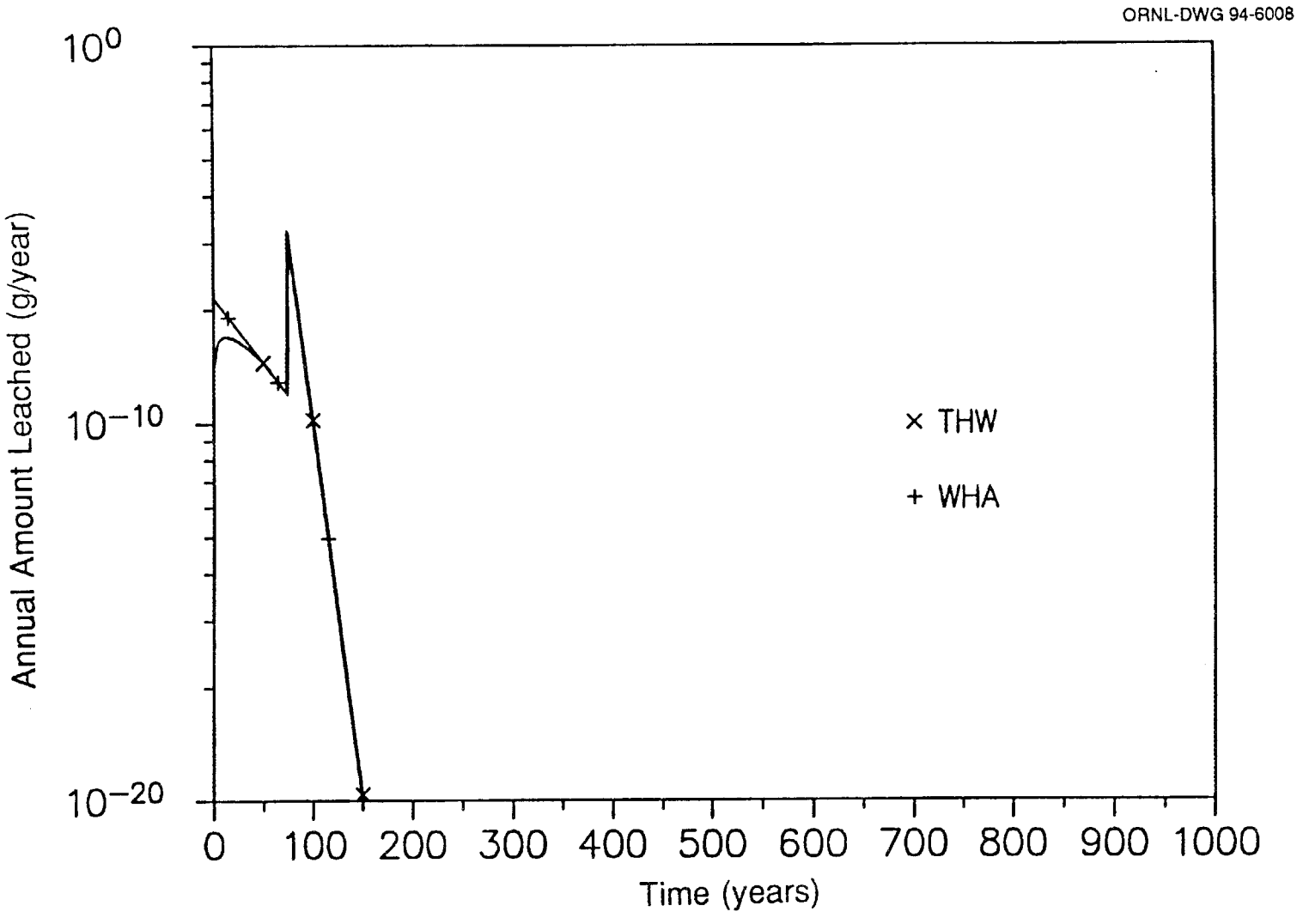

Fig. F.17. Calculated release rates of ^{154}Eu from SWSA 6 disposal sites.

APPENDIX G

DOSE ANALYSIS FOR OFF-SITE INDIVIDUALS AND INADVERTENT INTRUDERS

D. C. Kocher

September 1993

APPENDIX G

DOSE ANALYSIS FOR OFF-SITE INDIVIDUALS AND INADVERTENT INTRUDERS

G.1 INTRODUCTION

This appendix presents the models and data bases used to estimate radiation doses to members of the public per unit concentration of radionuclides in the environment following disposal of low-level waste in the different types of disposal units at the SWSA 6 facility. The dose analysis considers two groups of exposed individuals:

- *off-site individuals* (i.e., members of the public who reside outside the boundary of the disposal facility); and
- *inadvertent intruders* (i.e., individuals who come onto the disposal site following loss of active institutional control).

Off-site individuals may receive exposures from radionuclides that are transported beyond the facility boundary at any time after disposal. However, according to current Department of Energy (DOE) policy (DOE 1988a), inadvertent intrusion onto the disposal site is assumed to be precluded by active institutional controls for 100 years after disposal.

The performance assessment for low-level waste disposal units in the SWSA 6 facility assumes that transport of radionuclides in surface water and groundwater is the principal mechanism for removal of radionuclides from disposal units (see Sects. 4.2 and 4.3). Thus, off-site individuals are assumed to receive radiation doses primarily as a result of exposure to contaminated water.

The dose analysis for inadvertent intruders considers two types of exposure scenarios. The first involves direct intrusion into disposal units, and four different exposure scenarios involving direct intrusion are evaluated. The second type of scenario involves exposure to contaminated water obtained from a source within the facility boundary.

The following sections discuss the exposure scenarios and exposure pathways that are assumed for off-site individuals or inadvertent intruders and the models and parameter values that are used in calculating effective dose equivalents to off-site individuals or inadvertent intruders for each exposure pathway. For exposures of off-site individuals or inadvertent intruders to contaminated water, the results of the dose analyses are summarized in the form of effective dose equivalents per unit concentration of radionuclides in water. For exposures of inadvertent intruders resulting from direct intrusion into disposal units, the results are summarized in the form of effective dose

equivalents per unit concentration of radionuclides in disposal units at the time intrusion is assumed to occur.

G.2 RADIONUCLIDES OF IMPORTANCE TO DOSE ANALYSIS

As indicated in Appendix A, low-level waste intended for disposal in SWSA 6 contains a large number of radionuclides. However, not all of the radionuclides are potentially important in a dose analysis for off-site individuals or inadvertent intruders. Many radionuclides occur only in very low concentrations, and other radionuclides are sufficiently short-lived that they would decay to low levels either before off-site transport via water pathways could occur or before inadvertent intrusion onto the disposal site could occur at 100 years after disposal.

The radionuclides initially considered in the dose analysis for off-site individuals or inadvertent intruders are listed in Table G.1. The choice of radionuclides was based on those listed in Tables A.3–A.11 of Appendix A. However, only radionuclides in disposed waste with half-lives greater than about 5 years are potentially important because radionuclides with shorter half-lives could not possibly result in significant doses for either group of exposed individuals, due to the performance of engineered barriers in conjunction with radionuclide travel times in the environment and the imposition of active institutional controls for 100 years after disposal.

G.3 ASSUMED EXPOSURE SCENARIOS AND EXPOSURE PATHWAYS

This section describes the exposure scenarios and exposure pathways assumed in the dose analyses for off-site individuals and inadvertent intruders. The model equations and parameter values for each exposure pathway are presented in the following section.

G.3.1 Exposure Scenarios and Exposure Pathways for Off-Site Individuals

The performance assessment for disposal units at the SWSA 6 facility assumes that radionuclides are transported to locations beyond the facility boundary primarily via the surface water pathway and that all contaminated groundwater is discharged to the surface within the facility boundary (see Sects. 4.2 and 4.3). Off-site transport via the atmospheric pathway following suspension into the air of radionuclides in solid waste is believed to be relatively unimportant.

An individual residing outside the boundary of the disposal facility is assumed to use contaminated water for domestic and recreational purposes. The following pathways involving exposure to contaminated water are assumed to occur:

- direct ingestion of contaminated drinking water;
- ingestion of milk and meat from dairy and beef cattle that drink contaminated water; and
- external exposure while swimming in contaminated water.

Table G.1. Radionuclides considered in dose analysis for off-site individuals and inadvertent intruders

Nuclide[a]	Half-life[b,c]	Nuclide[a]	Half-life[b,c]
^{3}H	12.28 y	^{232}Th	1.405×10^{10} y
^{14}C	5730 y	^{228}Ra (1.0)	5.75 y
^{26}Al	7.2×10^{5} y	^{228}Ac (1.0)	6.13 h
^{36}Cl	3.01×10^{5} y	^{228}Th (1.0)	1.9132 y
^{40}K	1.277×10^{9} y	^{224}Ra (1.0)	3.62 d
^{60}Co	5.271 y	^{220}Rn (1.0)	55.61 s
^{63}Ni	100.1 y	^{212}Pb (1.0)	10.643 h
^{90}Sr	28.6 y	^{212}Bi (1.0)	60.55 m
^{90}Y (1.0)	64.1 h	^{208}Tl (0.3593)	3.053 m
^{99}Tc	2.13×10^{5} y	^{232}U[d]	72 y
^{113m}Cd	13.7 y	^{233}U	1.5952×10^{5} y
^{137}Cs	30.17 y	^{234}U	2.445×10^{5} y
^{137m}Ba (0.946)	2.552 m	^{235}U	7.038×10^{8} y
^{152}Eu	13.6 y	^{231}Th (1.0)	25.52 h
^{154}Eu	8.8 y	^{236}U	2.3415×10^{7} y
^{155}Eu	4.96 y	^{238}U	4.468×10^{9} y
^{210}Pb	22.26 y	^{234}Th (1.0)	24.10 d
^{210}Po (1.0)	138.378 d	^{234m}Pa (1.0)	1.17 m
^{226}Ra	1600 y	^{234}Pa (0.0016)	6.70 h
^{222}Rn (1.0)	3.8235 d	^{237}Np	2.14×10^{6} y
^{214}Pb (1.0)	26.8 m	^{233}Pa (1.0)	27.0 d
^{214}Bi (1.0)	19.9 m	^{238}Pu	87.75 y
^{229}Th	7.34×10^{3} y	^{239}Pu	24131 y
^{225}Ra (1.0)	14.8 d	^{240}Pu	6569 y
^{225}Ac (1.0)	10.0 d	^{242}Pu	3.758×10^{5} y
^{221}Fr (1.0)	4.8 m	^{241}Am	432.2 y
^{213}Bi (1.0)	45.65 m	^{243}Am	7.38×10^{3} y
^{209}Tl (0.0216)	2.20 m	^{239}Np (1.0)	2.355 d
^{230}Th	7.7×10^{4} y	^{243}Cm	28.5 y
		^{244}Cm	18.11 y
		^{249}Cf	350.6 y

[a]Indented entries are radiologically significant decay products of parent radionuclide listed. For each decay product, the branching fraction in the decay of the parent radionuclide is given in parentheses.

[b]Values from Kocher (1981).

[c]y = year; m = month; d = day.

[d]Entries for ^{228}Th, ^{224}Ra, ^{220}Rn, ^{212}Pb, ^{212}Bi, and ^{208}Tl decay products are listed following ^{232}Th.

Use of contaminated water by off-site individuals (as well as inadvertent intruders) for irrigation of food crops or pasture land is not considered, because rainfall is usually abundant in Oak Ridge and irrigation is not widely practiced at the present time.

G.3.2 Exposure Scenarios and Exposure Pathways for Inadvertent Intruders

In estimating doses to an inadvertent intruder following loss of active institutional control over the disposal facility, an intruder is assumed to establish a permanent homestead on the site at any time beyond 100 years after disposal. Furthermore, the intruder is assumed to have no prior knowledge of waste disposal activities at the facility. Inadvertent intruders are assumed to receive radiation exposures from use of contaminated water obtained from sources within the facility boundary and from direct intrusion into waste disposal units.

Exposure of inadvertent intruders to radionuclides in contaminated water is assumed to occur in conjunction with any of the scenarios involving direct intrusion into waste disposal units described below. For inadvertent intruders, the following exposure pathways involving use of contaminated water are assumed to occur:

- direct ingestion of contaminated drinking water; and
- ingestion of milk and meat from dairy and beef cattle that drink contaminated water.

Thus, inadvertent intruders are assumed to use contaminated water within the facility boundary for domestic purposes only. The two exposure pathways are the same as those for off-site individuals, and the dose analyses for inadvertent intruders and off-site individuals for each pathway would differ only in regard to the assumed concentrations of radionuclides in the source of water used by those individuals. The pathway involving external exposure while swimming in contaminated water, which was included in the dose analysis for off-site individuals, is not included in the dose analysis for inadvertent intruders because surface waters suitable for swimming are not found within the boundary of the disposal site.

For direct intrusion into the various disposal units after loss of institutional control, exposures are assumed to occur according to one of four different scenarios—the agriculture, resident, discovery, and post-drilling scenarios. In all scenarios, an intruder is assumed to establish a permanent homestead on the disposal site and to establish on-site sources of foodstuffs. The four exposure scenarios and their associated exposure pathways are described as follows.

In the agriculture scenario, an inadvertent intruder is assumed to construct a home directly on top of disposal units, and the foundation is assumed to extend into the units themselves. Radioactive wastes are assumed to be exhumed during construction of the foundation, and all wastes remaining in the disposal units at the time direct intrusion occurs are assumed to be indistinguishable from native soil. Some of the exhumed waste is assumed to be mixed with native soil in the intruder's vegetable garden, and the

following pathways involving exposure to radionuclides in the solid waste are assumed to occur:

- ingestion of vegetables grown in the contaminated garden soil;
- direct ingestion of contaminated soil from the garden in conjunction with vegetable intakes;
- external exposure to contaminated soil while working in the garden or residing in the home on top of the disposal units; and
- inhalation of radionuclides suspended into the air from contaminated soil while working in the garden or residing in the home.

In the resident scenario, an intruder also is assumed to dig a foundation for a home at the location of disposal units, as in the agriculture scenario described above, but is assumed to encounter an intact and impenetrable engineered barrier (e.g., reinforced concrete) on top of the disposal units. The intruder then is assumed to construct a home directly on top of the intact engineered barrier above the waste. Since the engineered barrier is assumed not to be breached during excavation, the only exposure pathway of concern for the resident scenario is external exposure to photon-emitting radionuclides in the waste during the time the intruder resides in the home on top of the disposal units. Because of the presence of an engineered barrier in the resident scenario, which provides considerable shielding, the external dose per unit concentration of radionuclides in disposed waste while residing in the home on top of disposal units will always be greater in the agriculture scenario than in the resident scenario. Therefore, the resident scenario is intended to be applied only when inadvertent intrusion onto the disposal site first occurs at 100 years after disposal and the engineered barriers presumably are intact, at which time the external dose from shorter-lived radionuclides in the waste could be considerably higher than the dose at later times when the engineered barrier has degraded and residence on top of exposed waste could occur but the concentrations of these radionuclides would be greatly reduced by radioactive decay.

In the discovery scenario, an intruder again is assumed to dig a foundation for a home at the location of disposal units and is assumed to encounter an intact and impenetrable engineered barrier (e.g., reinforced concrete) used in constructing the units, as in the resident scenario described above. However, shortly after encountering the engineered barrier, the intruder decides to abandon digging at that location and moves elsewhere. Since waste in the disposal units is not directly accessed during the excavation activities, due to the assumed impenetrability of the engineered barrier, the only exposure pathway for this scenario is external exposure to photon-emitting radionuclides in the disposal units during the time the intruder digs at that location. For a given thickness of an engineered barrier, the external dose per unit concentration of radionuclides will always be greater in the resident scenario than in the discovery scenario, due to the much longer exposure time for the resident scenario. However, some disposal units in the SWSA 6 facility are constructed with engineered barriers at the top which are considerably thicker than the engineered barriers at the sides. Therefore, the discovery scenario is intended to take into account that, in excavating at a disposal site, an intruder could approach disposal units from the side, rather than from the top, and the lesser exposure time in the discovery scenario could be compensated for by the reduced shielding at the side of

disposal units. The discovery scenario presumes that an intruder would not construct a home immediately beside engineered disposal units.

In the post-drilling scenario, direct intrusion into disposal units is assumed not to occur during construction of a home. Direct intrusion into disposal units during construction could be precluded by the presence of impenetrable engineered barriers, by burial of waste at depths greater than the normal depth of a foundation for a home, or by construction of a home at a location other than the location of disposal units. However, an intruder is assumed to access solid waste by drilling through a disposal unit (e.g., for the purpose of constructing a well for the intruder's domestic water supply). During drilling, a small volume of radioactive waste, which is assumed to be indistinguishable from native soil, is brought to the surface. All of the drilling waste is assumed to be mixed with native soil in the intruder's vegetable garden, and the following pathways involving exposure to radionuclides in the solid waste are assumed to occur:

- ingestion of vegetables grown in the contaminated garden soil;
- direct ingestion of contaminated soil from the garden in conjunction with vegetable intakes;
- external exposure to contaminated soil while working in the garden; and
- inhalation of radionuclides suspended into air from contaminated soil while working in the garden.

These pathways correspond to some of the pathways assumed for the agriculture scenario. However, in the post-drilling scenario, external and inhalation exposures while residing in the home are not considered, because all of the drilling waste is assumed to be mixed with soil in the vegetable garden.

G.4 DOSE CONVERSION FACTORS FOR INTERNAL AND EXTERNAL EXPOSURE

From the descriptions of the assumed exposure scenarios given above, doses to off-site individuals and inadvertent intruders are assumed to result from ingestion and inhalation of radionuclides and from external exposure to photons emitted by radionuclides in contaminated water, contaminated soil, or in the disposal units themselves. This section presents the factors that are used in the dose analysis to convert intakes of radionuclides via ingestion and inhalation to internal doses and to convert concentrations of radionuclides in water, soil, or disposal units to external dose rates.

The internal dose conversion factors for ingestion and inhalation of radionuclides are given in Tables G.2 and G.3, respectively. These dose conversion factors give 50-year committed effective dose equivalents per unit activity intake of each radionuclide. These values were developed by the International Commission on Radiological Protection and have been adopted by DOE in assessing radiation doses to the public (DOE 1988b).

Table G.2. Internal dose conversion factors for ingestion of radionuclides[a]

Nuclide[b]	f_1 [c]	Rem per μCi ingested	Nuclide[b]	f_1 [c]	Rem per μCi ingested
^{3}H	1.0	6.3×10^{-5}	^{232}Th	0.0002	2.8
^{14}C	1.0	2.1×10^{-3}	^{228}Ra	0.2	1.2
^{26}Al	0.01	1.3×10^{-2}	^{228}Th	0.0002	3.8×10^{-1}
^{36}Cl	1.0	3.0×10^{-3}	^{224}Ra	0.2	3.3×10^{-1}
^{40}K	1.0	1.9×10^{-2}	^{212}Pb	0.2	4.1×10^{-2}
^{60}Co	0.3	2.6×10^{-2}	^{232}U[d]	0.05	1.3
^{63}Ni	0.05	5.4×10^{-4}	^{233}U	0.05	2.7×10^{-1}
^{90}Sr	0.3	1.3×10^{-1}	^{234}U	0.05	2.6×10^{-1}
^{90}Y	0.0001	1.0×10^{-2}	^{235}U	0.05	2.5×10^{-1}
^{99}Tc	0.8	1.3×10^{-3}	^{236}U	0.05	2.5×10^{-1}
^{113m}Cd	0.05	1.5×10^{-1}	^{238}U	0.05	2.3×10^{-1}
^{137}Cs	1.0	5.0×10^{-2}	^{234}Th	0.0002	1.3×10^{-2}
^{152}Eu	0.001	6.0×10^{-3}	^{237}Np	0.001	3.9
^{154}Eu	0.001	9.1×10^{-3}	^{238}Pu	0.001	3.8
^{155}Eu	0.001	1.3×10^{-3}	^{239}Pu	0.001	4.3
^{210}Pb	0.2	5.1	^{240}Pu	0.001	4.3
^{210}Po	0.1	1.6	^{242}Pu	0.001	4.1
^{226}Ra	0.2	1.1	^{241}Am	0.001	4.5
^{229}Th	0.0002	3.5	^{243}Am	0.001	4.5
^{225}Ra	0.2	3.1×10^{-1}	^{243}Cm	0.001	2.9
^{225}Ac	0.001	9.5×10^{-2}	^{244}Cm	0.001	2.3
^{230}Th	0.0002	5.3×10^{-1}	^{249}Cf	0.001	4.6

[a]Values from DOE (1988b) give 50-year committed effective dose equivalent per unit activity ingested.

[b]Indented entries are radiologically significant decay products of the parent radionuclide listed.

[c]Fraction of ingested radionuclide absorbed into blood from gastrointestinal tract.

[d]Values for ^{228}Th, ^{224}Ra, and ^{212}Pb decay products are listed following ^{232}Th.

Table G.3. Internal dose conversion factors for inhalation of radionuclides[a]

Nuclide[b]	Clearance class[c]	Rem per μCi inhaled	Nuclide[b]	Clearance class[c]	Rem per μCi inhaled
^{3}H		6.3×10^{-5}	^{232}Th	Y	1.1×10^{3}
^{14}C[d]		2.1×10^{-3}	^{228}Th	Y	3.1×10^{2}
^{26}Al	D	7.9×10^{-2}	^{220}Rn[f]		
^{36}Cl	W	2.0×10^{-2}	^{232}U[g]	Y	6.7×10^{2}
^{40}K	D	1.2×10^{-2}	^{233}U	Y	1.3×10^{2}
^{60}Co	Y	1.5×10^{-1}	^{234}U	Y	1.3×10^{2}
^{63}Ni[e]	D	3.0×10^{-3}	^{235}U	Y	1.2×10^{2}
^{90}Sr	Y	1.3	^{236}U	Y	1.2×10^{2}
^{99}Tc	W	7.5×10^{-3}	^{238}U	Y	1.2×10^{2}
^{113m}Cd	D	1.4	^{237}Np	W	4.9×10^{2}
^{137}Cs	D	3.2×10^{-2}	^{238}Pu	W	4.6×10^{2}
^{152}Eu	W	2.2×10^{-1}	^{239}Pu	W	5.1×10^{2}
^{154}Eu	W	2.6×10^{-1}	^{240}Pu	W	5.1×10^{2}
^{155}Eu	W	3.9×10^{-2}	^{242}Pu	W	4.8×10^{2}
^{210}Pb	D	1.3×10^{1}	^{241}Am	W	5.2×10^{2}
^{210}Po	W	8.1	^{243}Am	W	5.2×10^{2}
^{226}Ra	W	7.9	^{243}Cm	W	3.5×10^{2}
^{222}Rn[f]			^{244}Cm	W	2.7×10^{2}
^{229}Th	Y	1.7×10^{3}	^{249}Cf	W	5.5×10^{2}
^{230}Th	Y	2.6×10^{2}			

[a]Values from DOE (1988b) give 50-year committed effective dose equivalent per unit activity inhaled.

[b]Indented entries are radiologically significant decay products of the parent radionuclide listed.

[c]Clearance from respiratory passages for radionuclides in particulate form in a matter of days (D), weeks (W), or years (Y).

[d]Radionuclide is assumed to be in organic form.

[e]Radionuclide is assumed to be in inorganic form.

[f]Inhalation doses from isotopes of radon and their short-lived decay products are estimated using the model described in Sect. G.5.2.1.

[g]Values for ^{228}Th and ^{220}Rn decay products are listed following ^{232}Th.

For some radionuclides, more than one dose conversion factor for ingestion or inhalation is given in the DOE compilation (DOE 1988b). If ingestion dose conversion factors are given for two GI-tract absorption fractions, the value for the higher absorption fraction is adopted in Table G.2, because radionuclides that are transported in water or through terrestrial food chains should be in relatively soluble form and more easily absorbed in the GI tract. In all cases, this choice gives the higher dose conversion factor (DOE 1988b). If inhalation dose conversion factors are given for more than one lung clearance class, the clearance class giving the highest dose conversion factor is adopted in Table G.3 for most radionuclides. The one exception is thorium, which is assumed to be Class Y because thorium in soil is expected to be highly insoluble (e.g., in oxide or hydroxide form). However, for the isotopes of thorium listed in the table, the dose conversion factors for the two clearance classes differ only by 30% or less (DOE 1988b).

The dose conversion factors for external exposure give external dose rates per unit concentration of radionuclides. These factors depend on the distribution of radionuclides in the source region, the amount of self-shielding provided by the source region, and the amount of shielding between the source region and the location of the exposed individual. Therefore, separate sets of dose conversion factors for external exposure are required for the assumed exposure pathways involving immersion in contaminated water while swimming, exposure to activity in contaminated soil while gardening, and exposure to activity in disposal units during indoor residence or during excavation at the site.

For external exposure to radionuclides while swimming in contaminated water, the radionuclides are assumed to be uniformly distributed throughout a source region of infinite extent (DOE 1988c). The external dose-rate conversion factors for immersion in contaminated water, which have been adopted by the DOE in assessing radiation doses to the public (DOE 1988c), are given in Table G.4. For radioactive decay chains, the dose-rate factor for each short-lived decay product takes into account the branching fraction in the decay of its parent radionuclide (Kocher 1981).

For external exposure to radionuclides in contaminated soil while gardening or in disposal units, either during indoor residence or during excavation near the units, the source region is assumed to be a uniformly contaminated slab of infinite lateral extent. Depending upon the exposure scenario, the slab is assumed to have either finite or infinite thickness, and the shielding provided by uncontaminated material between the source and receptor locations is taken into account. The idealized distributions of radionuclides in the source region assumed in the dose analysis probably are reasonable, because only about 1 m of soil-equivalent material between a source and a receptor location provides nearly complete shielding (Kocher and Sjoreen 1985).

In all calculations of external dose from radionuclides in contaminated garden soil or in disposal units, an exposed individual is assumed to be located at a distance of 1 m from the source region (DOE 1988c). In all cases, the shielding provided by 1 m of air is negligible compared with the shielding provided by the soil in the source region itself or by an engineered barrier.

For external exposure while working in the vegetable garden, the source region is assumed to be a slab extending from the ground surface to a depth of 15 cm, which is a typical thickness of a plowed layer. The external dose-rate conversion factors for this case are given in Table G.5. For external exposures while residing in the home on top of exposed waste, the source region is assumed to be a slab of essentially infinite thickness

Table G.4. External dose-rate conversion factors for immersion in contaminated water[a]

Nuclide[b]	Dose-rate factor (rem/y per μCi/L)	Nuclide[b]	Dose-rate factor (rem/y per μCi/L)
^{26}Al	3.1×10^{1}	^{232}Th	—
^{40}K	1.8	^{228}Ac	1.1×10^{1}
^{60}Co	2.8×10^{1}	^{212}Pb	1.7
^{137}Cs	—	^{212}Bi	2.1
^{137m}Ba	6.2	^{208}Tl	1.5×10^{1}
^{152}Eu	1.3×10^{1}	^{232}U[c]	—
^{154}Eu	1.4×10^{1}	^{235}U	1.7
^{155}Eu	6.7×10^{-1}	^{231}Th	1.4×10^{-1}
^{226}Ra	—	^{238}U	—
^{214}Pb	2.7	^{234}Th	9.1×10^{-2}
^{214}Bi	1.8×10^{1}	^{234m}Pa	1.3×10^{-1}
^{229}Th	9.9×10^{-1}	^{234}Pa	3.5×10^{-2}
^{225}Ra	8.6×10^{-2}	^{237}Np	2.7×10^{-1}
^{225}Ac	1.6×10^{-1}	^{233}Pa	2.4
^{221}Fr	3.5×10^{-1}	^{241}Am	2.3×10^{-1}
^{213}Bi	1.5	^{243}Am	6.1×10^{-1}
^{209}Tl	5.2×10^{-1}	^{239}Np	1.9
		^{243}Cm	1.4
		^{249}Cf	3.6

[a]Values from Appendix A.2 of DOE (1988c), and assuming branching fractions for radioactive decay chains from Kocher (1981), give the external effective dose-equivalent rate per unit activity concentration in water.

[b]Indented entries are radiologically significant decay products of the parent radionuclide listed.

[c]Values for ^{212}Pb, ^{212}Bi, and ^{208}Tl decay products are listed following ^{232}Th.

Table G.5. External dose-rate conversion factors for radionuclides uniformly distributed in 15 cm of surface soil[a]

Nuclide[b]	Dose-rate factor (rem/y per μCi/m^3)	Nuclide[b]	Dose-rate factor (rem/y per μCi/m^3)
^{26}Al	1.1×10^{-2}	^{232}Th	—
^{40}K	6.1×10^{-4}	^{228}Ac	3.8×10^{-3}
^{60}Co	1.0×10^{-2}	^{212}Pb	4.7×10^{-4}
^{137}Cs	—	^{212}Bi	7.5×10^{-4}
^{137m}Ba	2.4×10^{-3}	^{208}Tl	4.5×10^{-3}
^{152}Eu	4.6×10^{-3}	^{232}U[c]	—
^{154}Eu	5.0×10^{-3}	^{235}U	4.6×10^{-4}
^{155}Eu	1.1×10^{-4}	^{231}Th	2.6×10^{-5}
^{226}Ra	—	^{238}U	—
^{214}Pb	9.7×10^{-4}	^{234}Th	1.4×10^{-5}
^{214}Bi	6.0×10^{-3}	^{234m}Pa	4.7×10^{-5}
^{229}Th	2.0×10^{-4}	^{234}Pa	1.3×10^{-5}
^{225}Ra	1.1×10^{-5}	^{237}Np	5.0×10^{-5}
^{225}Ac	3.4×10^{-5}	^{233}Pa	7.9×10^{-4}
^{221}Fr	1.0×10^{-4}	^{241}Am	2.7×10^{-5}
^{213}Bi	5.8×10^{-4}	^{243}Am	7.8×10^{-5}
^{209}Tl	1.8×10^{-4}	^{239}Np	5.0×10^{-4}
		^{243}Cm	3.9×10^{-4}
		^{249}Cf	1.4×10^{-3}

[a]Values based on calculations for monoenergetic photon sources in Kocher and Sjoreen (1985) and radioactive decay data and branching fractions for radioactive decay chains in Kocher (1981) give the external effective dose-equivalent rate per unit activity concentration in soil at a distance of 1 m from the source region.

[b]Indented entries are radiologically significant decay products of the parent radionuclide listed.

[c]Values for ^{212}Pb, ^{212}Bi, and ^{208}Tl decay products are listed following ^{232}Th.

beginning at the ground surface, with no shielding assumed between the source region and the receptor location other than that provided by the soil in the source region (shielding provided by the walls of the home during indoor residence is taken into account by a parameter in the dose analysis itself). The external dose-rate conversion factors for this case are given in the column in Table G.6 labeled "No shielding."

For external exposure in the resident and discovery scenarios, the source region also is assumed to be a slab of infinite thickness; but a thickness of uncontaminated shielding material between the source and receptor locations, equivalent to either 15 cm or 30 cm of soil depending upon the disposal unit, is assumed to be provided by the impenetrable engineered barrier in the disposal units. The external dose-rate conversion factors for the two thicknesses of shielding are given in the last two columns in Table G.6.

The external dose-rate conversion factors in Tables G.5 and G.6 are obtained from calculations of absorbed dose rates in air for monoenergetic photon sources in soil (Kocher and Sjoreen 1985), the spectrum of photons emitted by each radionuclide (Kocher 1981), and the branching fractions in radioactive decay chains (Kocher 1981) assuming that all short-lived decay products are in secular equilibrium with the parent radionuclide. For all radionuclides, absorbed dose in air is converted to effective dose equivalent in an exposed individual by multiplying by a factor of 0.8. This is an excellent approximation for all photon energies above 0.1 MeV and provides a conservative overestimate of dose equivalent for lower photon energies.

G.5 MODELS AND PARAMETER VALUES FOR EXPOSURE PATHWAYS

This section presents the models used to calculate doses to off-site individuals and inadvertent intruders for the various exposure pathways involving use of contaminated water and direct intrusion into disposal units. In each case, the parameter values assumed in implementing the models also are presented. For each exposure pathway, the results are presented in summary tables which give effective dose equivalents per unit concentration of radionuclides in water or in the disposal units at the time the exposures are assumed to occur.

The parameter values selected for use in the models usually are intended to represent reasonable best estimates rather than worst-case values. This approach is reasonable when one considers the hypothetical nature of the assumed exposure scenarios, including the assumptions that exposures occur at the locations of greatest radionuclide concentrations.

G.5.1 Exposure Pathways for Radionuclides in Contaminated Water

Intakes of contaminated water by off-site individuals or inadvertent intruders are assumed to result from use of a contaminated source as a drinking water supply and from ingestion of milk and meat from dairy and beef cattle that drink the contaminated water. Off-site individuals also are assumed to receive external exposure from immersion in contaminated water while swimming, but this exposure pathway is not credible for inadvertent intruders on the disposal site.

Table G.6. External dose-rate conversion factors for radionuclides uniformly distributed in infinite thickness of soil[a]

Nuclide[b]	Dose-rate factor (rem/y per μCi/m^3)		
	No shielding	15-cm shielding	30-cm shielding
^{26}Al	1.4×10^{-2}	3.0×10^{-3}	9.4×10^{-4}
^{40}K	8.0×10^{-4}	1.9×10^{-4}	5.9×10^{-5}
^{60}Co	1.3×10^{-2}	2.9×10^{-3}	8.2×10^{-4}
^{137}Cs	—	—	—
^{137m}Ba	2.9×10^{-3}	4.5×10^{-4}	9.0×10^{-5}
^{152}Eu	5.6×10^{-3}	1.1×10^{-3}	2.8×10^{-4}
^{154}Eu	6.3×10^{-3}	1.2×10^{-3}	3.2×10^{-4}
^{155}Eu	1.1×10^{-4}	2.0×10^{-6}	5.7×10^{-8}
^{226}Ra	—	—	—
^{214}Pb	1.1×10^{-3}	1.1×10^{-4}	1.6×10^{-5}
^{214}Bi	7.7×10^{-3}	1.7×10^{-3}	5.2×10^{-4}
^{229}Th	2.0×10^{-4}	6.6×10^{-6}	3.7×10^{-7}
^{225}Ra	1.1×10^{-5}	—	—
^{225}Ac	3.5×10^{-5}	1.5×10^{-6}	1.1×10^{-7}
^{221}Fr	1.1×10^{-4}	6.3×10^{-6}	4.9×10^{-7}
^{213}Bi	6.6×10^{-4}	8.3×10^{-5}	1.4×10^{-5}
^{209}Tl	2.3×10^{-4}	4.9×10^{-5}	1.5×10^{-5}
^{232}Th	—	—	—
^{228}Ac	4.7×10^{-3}	8.7×10^{-4}	2.2×10^{-4}
^{212}Pb	5.0×10^{-4}	—	—
^{212}Bi	9.4×10^{-4}	1.8×10^{-4}	4.8×10^{-5}
^{208}Tl	6.1×10^{-3}	1.6×10^{-3}	6.0×10^{-4}
^{232}U[c]	—	—	—
^{235}U	4.8×10^{-4}	2.5×10^{-5}	1.6×10^{-6}
^{231}Th	2.6×10^{-5}	—	—
^{238}U	—	—	—
^{234}Th	1.4×10^{-5}	—	—
^{234m}Pa	5.7×10^{-5}	1.1×10^{-5}	2.7×10^{-6}
^{234}Pa	1.5×10^{-5}	2.8×10^{-6}	6.8×10^{-7}
^{237}Np	5.1×10^{-5}	1.1×10^{-6}	5.1×10^{-8}
^{233}Pa	8.7×10^{-4}	8.0×10^{-5}	9.9×10^{-6}
^{241}Am	2.7×10^{-5}	3.6×10^{-8}	—
^{243}Am	7.9×10^{-5}	6.0×10^{-7}	—
^{239}Np	5.3×10^{-4}	3.3×10^{-5}	3.0×10^{-6}

Table G.6 (continued)

Nuclide[b]	Dose-rate factor (rem/y per μCi/m^3)		
	No shielding	15-cm shielding	30-cm shielding
^{243}Cm	4.1×10^{-4}	2.5×10^{-5}	2.2×10^{-6}
^{249}Cf	1.5×10^{-3}	1.7×10^{-4}	2.3×10^{-5}

[a]Values based on calculations for monoenergetic photon sources in Kocher and Sjoreen (1985) and radioactive decay data and branching fractions for radioactive decay chains in Kocher (1981) give the external effective dose-equivalent rate per unit activity concentration in soil at a distance of 1 m from the source region and assumed thicknesses of shielding by soil-equivalent material between source and receptor locations.

[b]Indented entries are radiologically significant decay products of the parent radionuclide listed.

[c]Values for ^{212}Pb, ^{212}Bi, and ^{208}Tl decay products are listed following ^{232}Th.

Drinking Water Pathway. The annual committed effective dose equivalent (rem/year) from direct ingestion of radionuclide i in drinking water (w) is given by

$$H_{iw} = C_{iw} U_w D_i \ , \tag{G.1}$$

where

C_{iw} = concentration of radionuclide i in drinking water (μCi/L),
U_w = annual consumption of drinking water (L/year), and
D_i = dose conversion factor for ingestion of radionuclide i (rem/μCi ingested).

In implementing the model, a daily consumption of contaminated drinking water of 2 L (i.e., an annual consumption of 730 L) is assumed.

The model for estimating the dose from the drinking water pathway is summarized in Table G.7. The annual dose per unit concentration of a radionuclide in water is obtained by multiplying the assumed annual consumption of drinking water by the ingestion dose conversion factor given in Table G.2.

Milk and Meat Pathways. The annual committed effective dose equivalents (rem/year) from ingestion of radionuclide i in milk (m) and meat (f) are given by

$$H_{im} = C_{im} U_m D_i \ , \tag{G.2}$$

$$H_{if} = C_{if} U_f D_i \tag{G.3}$$

Table G.7. Annual effective dose equivalents from drinking water pathway per unit concentration of radionuclides in water[a]

Nuclide[b]	Annual dose (rem/y per μCi/L)	Nuclide[b]	Annual dose (rem/y per μCi/L)
^{3}H	4.6×10^{-2}	^{232}Th	2.0×10^{3}
^{14}C	1.5	^{228}Ra	8.8×10^{2}
^{26}Al	9.5	^{228}Th	2.8×10^{2}
^{36}Cl	2.2	^{224}Ra	2.4×10^{2}
^{40}K	1.4×10^{1}	^{212}Pb	3.0×10^{1}
^{60}Co	1.9×10^{1}	^{232}U[c]	9.5×10^{2}
^{63}Ni	3.9×10^{-1}	^{233}U	2.0×10^{2}
^{90}Sr	9.5×10^{1}	^{234}U	1.9×10^{2}
^{90}Y	7.3	^{235}U	1.8×10^{2}
^{99}Tc	9.5×10^{-1}	^{236}U	1.8×10^{2}
^{113m}Cd	1.1×10^{2}	^{238}U	1.7×10^{2}
^{137}Cs	3.7×10^{1}	^{234}Th	9.5
^{152}Eu	4.4	^{237}Np	2.8×10^{3}
^{154}Eu	6.6	^{238}Pu	2.8×10^{3}
^{155}Eu	9.5×10^{-1}	^{239}Pu	3.1×10^{3}
^{210}Pb	3.7×10^{3}	^{240}Pu	3.1×10^{3}
^{210}Po	1.2×10^{3}	^{242}Pu	3.0×10^{3}
^{226}Ra	8.0×10^{2}	^{241}Am	3.3×10^{3}
^{229}Th	2.6×10^{3}	^{243}Am	3.3×10^{3}
^{225}Ra	2.3×10^{2}	^{243}Cm	2.1×10^{3}
^{225}Ac	7.0×10^{1}	^{244}Cm	1.7×10^{3}
^{230}Th	3.9×10^{2}	^{249}Cf	3.4×10^{3}

[a]Values give 50-year committed effective dose equivalent from one year's intakes of drinking water.

[b]Indented entries are radiologically significant decay products of the parent radionuclide listed.

[c]Values for ^{228}Th, ^{224}Ra, and ^{212}Pb decay products are listed following ^{232}Th.

respectively, where

C_{im}	=	concentration of radionuclide i in milk (μCi/L),
C_{if}	=	concentration of radionuclide i in meat (μCi/kg),
U_m	=	annual consumption of milk (L/year),
U_f	=	annual consumption of meat (kg/year), and
D_i	=	dose conversion factor for ingestion of radionuclide i (rem/μCi ingested).

The dairy and beef cattle are assumed to drink only contaminated water, and the radionuclide concentrations in milk and meat are given by

$$C_{im} = C_{iw} Q_{wm} F_{im} , \tag{G.4}$$

$$C_{if} = C_{iw} Q_{wf} F_{if} , \tag{G.5}$$

respectively, where

C_{iw}	=	concentration of radionuclide i in drinking water (μCi/L),
Q_{wm}	=	daily consumption of drinking water by dairy cattle (L/d),
Q_{wf}	=	daily consumption of drinking water by beef cattle (L/d),
F_{im}	=	ratio of equilibrium concentration of radionuclide i in milk to daily intake by dairy cattle (μCi/L in milk per μCi/d intake), and
F_{if}	=	ratio of equilibrium concentration of radionuclide i in meat to daily intake by beef cattle (μCi/kg in meat per μCi/d intake).

In implementing the model, the assumed intake-to-milk transfer coefficients for dairy cattle and intake-to-meat transfer coefficients for beef cattle are given in Tables G.8 and G.9, respectively. The other parameter values assumed in the model are as follows: a daily consumption of water for dairy and beef cattle of 60 L and 50 L, respectively, and an annual consumption of milk and meat by an individual of 110 L and 90 kg, respectively (NRC 1977).

The models for estimating dose from the milk and meat pathways are summarized in Tables G.10 and G.11, respectively. The annual dose per unit concentration of a radionuclide in water for each pathway is based on the models and parameter values described above and the ingestion dose conversion factor given in Table G.2.

Table G.8. Elemental intake-to-milk transfer coefficients for dairy cattle

Element	F_m(d/L)[a]	Element	F_m(d/L)[a]
H	1.4×10^{-2}[b]	Eu	2.0×10^{-5}
C	1.5×10^{-2}[b]	Pb	2.5×10^{-4}
Al	2.0×10^{-4}	Po	3.5×10^{-4}
Cl	1.5×10^{-2}	Ra	4.5×10^{-4}
K	7.0×10^{-3}	Ac	2.0×10^{-5}
Co	2.0×10^{-3}	Th	5.0×10^{-6}
Ni	1.0×10^{-3}	U	6.0×10^{-4}
Sr	1.5×10^{-3}	Np	5.0×10^{-6}
Y	2.0×10^{-5}	Pu	1.0×10^{-7}
Tc	1.0×10^{-2}	Am	4.0×10^{-7}
Cd	1.0×10^{-3}	Cm	2.0×10^{-5}
Cs	7.0×10^{-3}	Cf	2.0×10^{-5}[c]

[a]Values from Fig. 2.24 of Baes et al. (1984), unless otherwise noted.
[b]Value from Table 4 of Ng (1982).
[c]Value from Table 7 of Ng et al. (1977).

Table G.9. Elemental intake-to-meat transfer coefficients for beef cattle

Element	F_f(d/kg)[a]	Element	F_f(d/kg)[a]
H	1.2×10^{-2}[b]	Eu	5.0×10^{-3}
C	3.1×10^{-2}[b]	Pb	3.0×10^{-4}
Al	1.5×10^{-3}	Po	9.5×10^{-5}
Cl	8.0×10^{-2}	Ra	2.5×10^{-4}
K	2.0×10^{-2}	Ac	2.5×10^{-5}
Co	2.0×10^{-2}	Th	6.0×10^{-6}
Ni	6.0×10^{-3}	U	2.0×10^{-4}
Sr	3.0×10^{-4}	Np	5.5×10^{-5}
Y	3.0×10^{-4}	Pu	5.0×10^{-7}
Tc	8.5×10^{-3}	Am	3.5×10^{-6}
Cd	5.5×10^{-4}	Cm	3.5×10^{-6}
Cs	2.0×10^{-2}	Cf	3.6×10^{-6}[c]

[a]Values from Fig. 2.25 of Baes et al. (1984), unless otherwise noted.
[b]Value from Table E-1 of NRC (1977).
[c]Value from Table 5.37 of Peterson (1983).

Table G.10. Annual effective dose equivalents from milk pathway per unit concentration of radionuclides in water[a]

Nuclide[b]	Annual dose (rem/y per μCi/L)	Nuclide[b]	Annual dose (rem/y per μCi/L)
^{3}H	5.8×10^{-3}	^{230}Th	1.7×10^{-2}
^{14}C	2.1×10^{-1}	^{232}Th	9.2×10^{-2}
^{26}Al	1.7×10^{-2}	^{228}Ra	3.6
^{36}Cl	3.0×10^{-1}	^{224}Ra	9.8×10^{-1}
^{40}K	8.8×10^{-1}	^{212}Pb	6.8×10^{-2}
^{60}Co	3.4×10^{-1}	^{232}U[c]	5.1
^{63}Ni	3.6×10^{-3}	^{233}U	1.1
^{90}Sr	1.3	^{234}U	1.0
^{99}Tc	8.6×10^{-2}	^{235}U	9.9×10^{-1}
^{113m}Cd	9.9×10^{-1}	^{236}U	9.9×10^{-1}
^{137}Cs	2.3	^{238}U	9.1×10^{-1}
^{152}Eu	7.9×10^{-4}	^{237}Np	1.3×10^{-1}
^{154}Eu	1.2×10^{-3}	^{238}Pu	2.5×10^{-3}
^{155}Eu	1.7×10^{-4}	^{239}Pu	2.8×10^{-3}
^{210}Pb	8.4	^{240}Pu	2.8×10^{-3}
^{210}Po	3.7	^{242}Pu	2.7×10^{-3}
^{226}Ra	3.3	^{241}Am	1.2×10^{-2}
^{229}Th	1.2×10^{-1}	^{243}Am	1.2×10^{-2}
^{225}Ra	9.2×10^{-1}	^{243}Cm	3.8×10^{-1}
^{225}Ac	1.3×10^{-2}	^{244}Cm	3.0×10^{-1}
		^{249}Cf	6.1×10^{-1}

[a]Values give 50-year committed effective dose equivalents from one year's intakes of milk.

[b]Indented entries are radiologically significant decay products of parent radionuclide listed.

[c]Values for ^{224}Ra and ^{212}Pb decay products are listed following ^{232}Th.

Table G.11. Annual effective dose equivalents from meat pathway per unit concentration of radionuclides in water[a]

Nuclide[b]	Annual dose (rem/y per μCi/L)	Nuclide[b]	Annual dose (rem/y per μCi/L)
^{3}H	3.4×10^{-3}	^{230}Th	1.4×10^{-2}
^{14}C	2.9×10^{-1}	^{232}Th	7.7×10^{-2}
^{26}Al	8.8×10^{-2}	^{228}Ra	1.4
^{36}Cl	1.1	^{224}Ra	3.7×10^{-1}
^{40}K	1.7	^{212}Pb	5.5×10^{-2}
^{60}Co	2.3	^{232}U[c]	1.2
^{63}Ni	1.5×10^{-2}	^{233}U	2.4×10^{-1}
^{90}Sr	1.8×10^{-1}	^{234}U	2.3×10^{-1}
^{90}Y	1.4×10^{-2}	^{235}U	2.3×10^{-1}
^{99}Tc	4.9×10^{-2}	^{236}U	2.3×10^{-1}
^{113m}Cd	3.7×10^{-1}	^{238}U	2.1×10^{-1}
^{137}Cs	4.5	^{237}Np	9.7×10^{-1}
^{152}Eu	1.4×10^{-1}	^{238}Pu	8.6×10^{-3}
^{154}Eu	2.0×10^{-1}	^{239}Pu	9.7×10^{-3}
^{155}Eu	2.9×10^{-2}	^{240}Pu	9.7×10^{-3}
^{210}Pb	6.9	^{242}Pu	9.2×10^{-3}
^{210}Po	6.8×10^{-1}	^{241}Am	7.1×10^{-2}
^{226}Ra	1.2	^{243}Am	7.1×10^{-2}
^{229}Th	9.5×10^{-2}	^{243}Cm	4.6×10^{-2}
^{225}Ra	3.5×10^{-1}	^{244}Cm	3.6×10^{-2}
^{225}Ac	1.1×10^{-2}	^{249}Cf	7.5×10^{-2}

[a]Values give 50-year committed effective dose equivalents from one year's intakes of milk.

[b]Indented entries are radiologically significant decay products of parent radionuclide listed.

[c]Values for ^{224}Ra and ^{212}Pb decay products are listed following ^{232}Th.

External Exposure Pathway. For external exposure (e) to contaminated water while swimming, the annual effective dose equivalent (rem/year) from radionuclide i is given by

$$H_{ie} = C_{iw} U_w D_{iw} , \tag{G.6}$$

where

C_{iw}	=	concentration of radionuclide i in water (μCi/L),
U_w	=	fraction of the year during which external exposure to contaminated water while swimming occurs, and
D_{iw}	=	dose conversion factor for external exposure to radionuclide i in water (rem/year per μCi/L).

In implementing the model, a fraction of the year during which exposure while swimming occurs of 0.01 (i.e., an exposure time of about 100 hours per year) is assumed (DOE 1988c).

The model for estimating dose from external exposure while swimming in contaminated water is summarized in Table G.12. The annual dose per unit concentration of a radionuclide in water is obtained by multiplying the assumed fraction of the year during which exposure occurs by the external dose-rate conversion factor given in Table G.4.

All Pathways. The annual doses to off-site individuals and inadvertent intruders per unit concentration of radionuclides in water from all exposure pathways are summarized in Tables G.13 and G.14, respectively. The dose to an inadvertent intruder is the sum of the doses from the drinking water, milk, and meat pathways summarized in Tables G.7, G.10, and G.11, respectively, and the dose to an off-site individual is the sum of the doses from the three ingestion pathways and the external dose while swimming summarized in Table G.12. On the basis of the models and parameter values assumed in this analysis, the drinking water pathway is more important than the milk, meat, and external exposure pathways for all radionuclides, and the dose per unit concentration of radionuclides in water usually is essentially the same for off-site individuals and inadvertent intruders.

G.5.2 Exposure Pathways for Direct Intrusion into Disposal Units

Exposures of inadvertent intruders resulting from direct intrusion into disposal units after loss of active institutional control are assumed to occur according to the agriculture, resident, discovery, or post-drilling scenarios. This section presents the models and parameter values used to estimate effective dose equivalents per unit concentration of radionuclides in disposal units for the different exposure pathways assumed for each exposure scenario.

Table G.12. Annual effective dose equivalents from external exposure while swimming per unit concentration of radionuclides in water

Nuclide[a]	Annual dose (rem/y per μCi/L)	Nuclide[a]	Annual dose (rem/y per μCi/L)
^{26}Al	3.1×10^{-1}	^{232}Th	—
^{40}K	1.8×10^{-2}	^{228}Ac	1.1×10^{-1}
^{60}Co	2.8×10^{-1}	^{212}Pb	1.7×10^{-2}
^{137}Cs	—	^{212}Bi	2.1×10^{-2}
^{137m}Ba	6.2×10^{-2}	^{208}Tl	1.5×10^{-1}
^{152}Eu	1.3×10^{-1}	^{232}U[b]	—
^{154}Eu	1.4×10^{-1}	^{235}U	1.7×10^{-2}
^{155}Eu	6.7×10^{-3}	^{231}Th	1.4×10^{-3}
^{226}Ra	—	^{238}U	—
^{214}Pb	2.7×10^{-2}	^{234}Th	9.1×10^{-4}
^{214}Bi	1.8×10^{-1}	^{234m}Pa	1.3×10^{-3}
^{229}Th	9.9×10^{-3}	^{234}Pa	3.5×10^{-4}
^{225}Ra	8.6×10^{-4}	^{237}Np	2.7×10^{-3}
^{225}Ac	1.6×10^{-3}	^{233}Pa	2.4×10^{-2}
^{221}Fr	3.5×10^{-3}	^{241}Am	2.3×10^{-3}
^{213}Bi	1.5×10^{-2}	^{243}Am	6.1×10^{-3}
^{209}Tl	5.2×10^{-3}	^{239}Np	1.9×10^{-2}
		^{243}Cm	1.4×10^{-2}
		^{249}Cf	3.6×10^{-2}

[a]Indented entries are radiologically significant decay products of parent radionuclide listed.
[b]Values for ^{212}Pb, ^{212}Bi, and ^{208}Tl decay products are listed following ^{232}Th.

Table G.13. Annual effective dose equivalents to off-site individuals per unit concentration of radionuclides in water from all exposure pathways[a]

Nuclide[b]	Annual dose (rem/y per μCi/L)	Nuclide[b]	Annual dose (rem/y per μCi/L)
^{3}H	5.5×10^{-2}	$^{232}Th + d$	3.4×10^{3}
^{14}C	2.0	$^{232}U + d$	1.5×10^{3}
^{26}Al	9.9	^{233}U	2.0×10^{2}
^{36}Cl	3.6	^{234}U	1.9×10^{2}
^{40}K	1.7×10^{1}	^{235}U	1.8×10^{2}
^{60}Co	2.2×10^{1}	^{236}U	1.8×10^{2}
^{63}Ni	4.1×10^{-1}	$^{238}U + d$	1.8×10^{2}
$^{90}Sr + d$	1.0×10^{2}	^{237}Np	2.8×10^{3}
^{99}Tc	1.1	^{238}Pu	2.8×10^{3}
^{113m}Cd	1.1×10^{2}	^{239}Pu	3.1×10^{3}
$^{137}Cs + d$	4.4×10^{1}	^{240}Pu	3.1×10^{3}
^{152}Eu	4.7	^{242}Pu	3.0×10^{3}
^{154}Eu	6.9	^{241}Am	3.3×10^{3}
^{155}Eu	9.9×10^{-1}	^{243}Am	3.3×10^{3}
$^{210}Pb + d$	4.9×10^{3}	^{243}Cm	2.1×10^{3}
$^{226}Ra + d$[c]	5.7×10^{3}	^{244}Cm	1.7×10^{3}
$^{229}Th + d$	2.9×10^{3}	^{249}Cf	3.4×10^{3}
^{230}Th	3.9×10^{2}		

[a]Values give sum of 50-year committed effective dose equivalents per unit concentration from one year's intakes of drinking water, milk, and meat given in Tables G.7, G.10, and G.11, respectively, and effective dose equivalent per unit concentration from one year's external exposure given in Table G.12.

[b]"d" denotes short-lived radioactive decay products that are assumed to be in secular equilibrium with the parent.

[c]Decay products include ^{210}Pb and its decay product, which are assumed to be in secular equilibrium with the parent.

Table G.14. Annual effective dose equivalents to inadvertent intruders per unit concentration of radionuclides in water from all exposure pathways[a]

Nuclide[b]	Annual dose (rem/y per μCi/L)	Nuclide[b]	Annual dose (rem/y per μCi/L)
^{3}H	5.5×10^{-2}	$^{232}Th + d$	3.4×10^{3}
^{14}C	2.0	$^{232}U + d$	1.5×10^{3}
^{26}Al	9.6	^{233}U	2.0×10^{2}
^{36}Cl	3.6	^{234}U	1.9×10^{2}
^{40}K	1.7×10^{1}	^{235}U	1.8×10^{2}
^{60}Co	2.2×10^{1}	^{236}U	1.8×10^{2}
^{63}Ni	4.1×10^{-1}	$^{238}U + d$	1.8×10^{2}
$^{90}Sr + d$	1.0×10^{2}	^{237}Np	2.8×10^{3}
^{99}Tc	1.1	^{238}Pu	2.8×10^{3}
^{113m}Cd	1.1×10^{2}	^{239}Pu	3.1×10^{3}
^{137}Cs	4.4×10^{1}	^{240}Pu	3.1×10^{3}
^{152}Eu	4.5	^{242}Pu	3.0×10^{3}
^{154}Eu	6.8	^{241}Am	3.3×10^{3}
^{155}Eu	9.8×10^{-1}	^{243}Am	3.3×10^{3}
$^{210}Pb + d$	4.9×10^{3}	^{243}Cm	2.1×10^{3}
$^{226}Ra + d$[c]	5.7×10^{3}	^{244}Cm	1.7×10^{3}
$^{229}Th + d$	2.9×10^{3}	^{249}Cf	3.4×10^{3}
^{230}Th	3.9×10^{2}		

[a]Values give sum of 50-year committed effective dose equivalents per unit concentration from one year's intakes of drinking water, milk, and meat given in Tables G.7, G.10, and G.11, respectively.

[b]"d" denotes short-lived radioactive decay products that are assumed to be in secular equilibrium with the parent.

[c]Decay products include ^{210}Pb and its decay product, which are assumed to be in secular equilibrium with the parent.

G.5.2.1 Agriculture Scenario

In the agriculture scenario, an inadvertent intruder is assumed to exhume waste from disposal units in digging a foundation for a home on top of the units, and some of the waste is then mixed with native soil in the intruder's vegetable garden. The pathways for chronic exposure assumed for this scenario include (1) ingestion of vegetables grown in contaminated soil, (2) direct ingestion of contaminated soil in conjunction with vegetable intakes, (3) external exposure to contaminated soil while working in the garden and during indoor residence on top of the disposal units, and (4) inhalation of suspended activity while working in the garden and during indoor residence.

Vegetable Pathway. The annual committed effective dose equivalent (rem/year) from ingestion of radionuclide i in vegetables (v) is given by

$$H_{iv} = C_{iv} U_v D_i \,, \tag{G.7}$$

where

C_{iv}	=	concentration of radionuclide i in vegetables (μCi/kg),
U_v	=	annual consumption of vegetables (kg/year), and
D_i	=	dose conversion factor for ingestion of radionuclide i (rem/μCi ingested).

Radionuclides are assumed to be transferred to vegetables via root uptake from the contaminated soil. Radionuclide concentrations in vegetables are given by

$$\begin{aligned} C_{iv} &= B_{iv} C_{is} / \rho_s \\ &= B_{iv} f_s C_{it} / \rho_s \,, \end{aligned} \tag{G.8}$$

where

B_{iv}	=	plant-to-soil concentration ratio for radionuclide i (μCi/kg wet weight in vegetation per μCi/kg dry weight in soil),
C_{is}	=	concentration of radionuclide i in soil in vegetable garden (μCi/m^3),
ρ_s	=	density of soil (kg/m^3),
C_{it}	=	concentration of radionuclide i in disposal units (μCi/m^3), and
f_s	=	dilution factor for mixing of exhumed waste from disposal units into soil in vegetable garden.

In implementing the model, the assumed plant-to-soil concentration ratios in vegetables are given in Table G.15. Although some site-specific data for these concentration ratios are available [e.g., see Garten et al. (1987)], measurements for the variety of radionuclides of concern to low-level waste disposal and for a variety of food crops are lacking. Therefore, the values adopted for use in this analysis were based almost entirely on published compilations and evaluations that are generic in nature. The adopted values for almost all elements were obtained from the evaluation of published

Table G.15. Elemental plant-to-soil concentration ratios in vegetables

Element	B_v[a]	Element	B_v[a]
H	4.8[b]	Eu	1.7×10^{-3}
C	5.6×10^{-1}[c]	Pb	3.9×10^{-3}
Al	2.8×10^{-4}	Po	1.7×10^{-4}
Cl	3.0×10^{1}	Ra	6.5×10^{-4}
K	2.4×10^{-1}	Ac	1.5×10^{-4}
Co	3.0×10^{-3}	Th	3.7×10^{-5}
Ni	2.6×10^{-2}	U	1.7×10^{-3}
Sr	1.1×10^{-1}	Np	4.3×10^{-3}
Y	2.6×10^{-3}	Pu	1.9×10^{-5}
Tc	6.5×10^{-1}	Am	1.1×10^{-4}
Cd	6.5×10^{-2}	Cm	6.5×10^{-6}
Cs	1.3×10^{-2}	Cf	6.5×10^{-6}[d]

[a]μCi/kg wet weight of vegetation per μCi/kg dry weight of soil; unless otherwise noted, values are based on concentration ratios on dry-weight basis of vegetation given in Fig. 2.2 of Baes et al. (1984) multiplied by factor of 0.43 to convert to fresh-weight basis of vegetation (Baes et al 1984).

[b]Value from Table E-1 of NRC (1977).

[c]Value from Sheppard et al. (1991) for carbonate form in acidic soil with low organic matter content; concentration ratio on dry-weight basis of vegetation is multiplied by factor of 0.43 to convert to fresh-weight basis of vegetation (Baes et al 1984).

[d]Value is assumed to be the same as value for Cm.

data by Baes et al. (1984). Although this approach clearly is judgmental for application to the Oak Ridge Reservation, selection of the concentration ratios primarily from a single source at least ensures some degree of consistency among the values for the different elements, because similar procedures presumably were used by the compilers in obtaining the ratios from published data.

Baes et al. (1984) give two sets of data for concentration ratios in vegetation—one for vegetative portions of food crops, which would apply to leafy vegetables, and the other for nonvegetative (reproductive) portions, which would apply to nonleafy vegetables. The values for nonvegetative portions of food crops were adopted for use in this analysis, because consumption of nonleafy vegetables generally is about an order of magnitude greater than consumption of leafy vegetables (Baes et al. 1984; Hamby 1992). The

reported concentration ratios on a dry-weight basis of nonleafy vegetation were converted to a fresh-weight basis by multiplying by a factor of 0.43, which represents the average conversion factor for all types of nonleafy vegetables (Baes et al. 1984). Taking into account the concentration ratios for leafy vegetables would not significantly change the adopted values in Table G.15, due to the relatively low consumption of leafy vegetables and the much higher fresh-weight to dry-weight ratio for leafy vegetables than for nonleafy vegetables (Peterson 1983).

The other parameter values assumed in the model for the vegetable pathway are as follows: a dilution factor for mixing of exhumed waste from the disposal units into native soil in the vegetable garden of 0.2 (Oztunali et al. 1981; NRC 1982; Napier et al. 1984), a soil density of 1,400 kg/m^3 (Baes and Sharp 1983), and an annual consumption of contaminated vegetables, including both leafy and nonleafy vegetables, by an individual of 90 kg. The dilution factor for mixing of exhumed waste with native soil in a vegetable garden is based on the reasonable assumption that no more than a relatively small fraction of the soil in the garden could be exhumed waste in order for the garden to be fertile. The assumed annual consumption of leafy and nonleafy vegetables from the garden is consistent with data obtained near the Savannah River Site (Hamby 1992), which should be reasonably representative of data for the Oak Ridge Reservation, and the assumption that half of an intruder's entire intakes of all vegetables would be obtained from the home garden. An assumption that an intruder's entire intakes of all vegetables would be obtained from the home garden is unreasonably conservative.

The model for estimating dose from the vegetable pathway is summarized in Table G.16. The annual dose per unit concentration of a radionuclide in exhumed waste from a disposal unit at the time intrusion occurs is based on the model and parameter values described above and the ingestion dose conversion factors given in Table G.2.

Soil Ingestion Pathway. The annual committed effective dose equivalent (rem per year) from direct ingestion of radionuclide i in contaminated soil (s) is given by

$$H_{is} = C_{is} U_s D_i \,, \tag{G.9}$$

where

C_{is}	=	concentration of radionuclide i in soil in vegetable garden (μCi/kg),
U_s	=	annual consumption of contaminated soil (kg/year), and
D_i	=	dose conversion factor for ingestion of radionuclide i (rem/μCi ingested).

Ingestion of contaminated soil is assumed to occur as a result of incomplete washing of vegetables from the garden before consumption. At humid sites with extensive vegetation, such as the Oak Ridge Reservation, direct ingestion of contaminated soil from sources other than the garden should be relatively unimportant for an average adult. Radionuclide concentrations in soil in the vegetable garden are given by

$$C_{is} = f_s C_{iv} / \rho_s \,, \tag{G.10}$$

Table G.16. Annual effective dose equivalents from vegetable pathway per unit concentration of radionuclides in exhumed waste for agriculture scenario[a]

Nuclide[b]	Annual dose (rem/y per μCi/m^3)	Nuclide[b]	Annual dose (rem/y per μCi/m^3)
^{3}H	3.9×10^{-6}	^{232}Th	1.3×10^{-6}
^{14}C	1.5×10^{-5}	^{228}Ra	1.0×10^{-5}
^{26}Al	4.7×10^{-8}	^{224}Ra	2.8×10^{-6}
^{36}Cl	1.2×10^{-3}	^{212}Pb	2.0×10^{-6}
^{40}K	5.9×10^{-5}	^{232}U[c]	2.9×10^{-5}
^{60}Co	1.0×10^{-6}	^{233}U	5.9×10^{-6}
^{63}Ni	1.8×10^{-7}	^{234}U	5.7×10^{-6}
^{90}Sr	1.8×10^{-4}	^{235}U	5.5×10^{-6}
^{99}Tc	1.1×10^{-5}	^{236}U	5.5×10^{-6}
^{113m}Cd	1.3×10^{-4}	^{238}U	5.0×10^{-6}
^{137}Cs	8.4×10^{-6}	^{237}Np	2.2×10^{-4}
^{152}Eu	1.3×10^{-7}	^{238}Pu	9.3×10^{-7}
^{154}Eu	2.0×10^{-7}	^{239}Pu	1.1×10^{-6}
^{155}Eu	2.9×10^{-8}	^{240}Pu	1.1×10^{-6}
^{210}Pb	2.6×10^{-4}	^{242}Pu	1.0×10^{-6}
^{226}Ra	9.2×10^{-6}	^{241}Am	6.4×10^{-6}
^{229}Th	1.7×10^{-6}	^{243}Am	6.4×10^{-6}
^{225}Ra	2.6×10^{-6}	^{243}Cm	2.4×10^{-7}
^{225}Ac	1.8×10^{-7}	^{244}Cm	1.9×10^{-7}
^{230}Th	2.5×10^{-7}	^{249}Cf	3.9×10^{-7}

[a]Values give 50-year committed effective dose equivalents from one year's intakes of vegetables.

[b]Indented entries are radiologically significant decay products of parent radionuclide listed.

[c]Values for ^{224}Ra and ^{212}Pb decay products are listed following ^{232}Th.

where

C_{it}	=	concentration of radionuclide i in disposal units (μCi/m^3),
f_s	=	dilution factor for mixing of exhumed waste from disposal units into soil in vegetable garden, and
ρ_s	=	density of soil (kg/m^3).

In implementing the model, a dilution factor for mixing of exhumed waste from the disposal units into native soil in the vegetable garden of 0.2 and a soil density of 1,400 kg/m^3 are assumed, as in the model for the vegetable pathway. A daily consumption of contaminated soil from the vegetable garden of 0.1 g (i.e., an annual consumption of 0.037 kg) also is assumed (EPA 1989).

The model for estimating dose from the soil ingestion pathway is summarized in Table G.17. The annual dose per unit concentration of a radionuclide in exhumed waste from a disposal unit at the time intrusion occurs is based on the model and parameter values described above and the ingestion dose conversion factors given in Table G.2.

External Exposure Pathways. For external exposure (e) to contaminated soil while working in the vegetable garden, the annual effective dose equivalent (rem/year) from radionuclide i is given by

$$H_{ie} = C_{is} U_s D_{is} , \tag{G.11}$$

where

C_{is}	=	concentration of radionuclide i in soil in vegetable garden (μCi/m^3),
U_s	=	fraction of the year during which external exposure to contaminated soil in vegetable garden occurs, and
D_{is}	=	dose conversion factor for external exposure to radionuclide i in garden soil (rem/year per μCi/m^3).

As in the models for the vegetable and soil ingestion pathways, the radionuclide concentrations in soil in the vegetable garden are given by

$$C_{is} = f_s C_{it} , \tag{G.12}$$

where

C_{it}	=	concentration of radionuclide i in disposal units (μCi/m^3), and
f_s	=	dilution factor for mixing of exhumed waste from disposal units into soil in vegetable garden.

In implementing the model, a dilution factor for mixing of exhumed waste from the disposal units into native soil in the vegetable garden of 0.2 is assumed, as in the models for the vegetable and soil ingestion pathways. The fraction of the year during which external exposure while working in the garden occurs is assumed to be 0.01 (Oztunali et al. 1981) (i.e., the assumed exposure time is about 100 h/year).

Table G.17. Annual effective dose equivalents from soil ingestion pathway per unit concentration of radionuclides in exhumed waste for agriculture scenario[a]

Nuclide[b]	Annual dose (rem/y per μCi/m^3)	Nuclide[b]	Annual dose (rem/y per μCi/m^3)
^{3}H	3.3×10^{-10}	^{232}Th	1.5×10^{-5}
^{14}C	1.1×10^{-8}	^{228}Ra	6.3×10^{-6}
^{26}Al	6.9×10^{-8}	^{228}Th	2.0×10^{-6}
^{36}Cl	1.6×10^{-8}	^{224}Ra	1.7×10^{-6}
^{40}K	1.0×10^{-7}	^{212}Pb	2.2×10^{-7}
^{60}Co	1.4×10^{-7}	^{232}U[c]	6.9×10^{-6}
^{63}Ni	2.9×10^{-9}	^{233}U	1.4×10^{-6}
^{90}Sr	6.9×10^{-7}	^{234}U	1.4×10^{-6}
^{90}Y	5.3×10^{-8}	^{235}U	1.3×10^{-6}
^{99}Tc	6.9×10^{-9}	^{236}U	1.3×10^{-6}
^{113m}Cd	7.9×10^{-7}	^{238}U	1.2×10^{-6}
^{137}Cs	2.6×10^{-7}	^{234}Th	6.9×10^{-8}
^{152}Eu	3.2×10^{-8}	^{237}Np	2.1×10^{-5}
^{154}Eu	4.8×10^{-8}	^{238}Pu	2.0×10^{-5}
^{155}Eu	6.9×10^{-9}	^{239}Pu	2.3×10^{-5}
^{210}Pb	2.7×10^{-5}	^{240}Pu	2.3×10^{-5}
^{210}Po	8.5×10^{-6}	^{242}Pu	2.2×10^{-5}
^{226}Ra	5.8×10^{-6}	^{241}Am	2.4×10^{-5}
^{229}Th	1.9×10^{-5}	^{243}Am	2.4×10^{-5}
^{225}Ra	1.6×10^{-6}	^{243}Cm	1.5×10^{-5}
^{225}Ac	5.0×10^{-7}	^{244}Cm	1.2×10^{-5}
^{230}Th	2.8×10^{-6}	^{249}Cf	2.4×10^{-5}

[a]Values give 50-year committed effective dose equivalents from one year's intakes of soil.
[b]Indented entries are radiologically significant decay products of parent radionuclide listed.
[c]Values for ^{228}Th, ^{224}Ra, and ^{212}Pb decay products are listed following ^{232}Th.

The model for estimating external dose while working in the garden is summarized in Table G.18. The annual dose per unit concentration of a radionuclide in exhumed waste in a disposal unit at the time intrusion occurs is based on the model and parameter values described above and the external dose-rate conversion factors given in Table G.5.

For external exposure to waste during indoor residence on top of the disposal units, the annual effective dose equivalent (rem/year) from radionuclide i is given by

$$H_{ie} = C_{it} U_t D_{it} S \ , \tag{G.13}$$

where

C_{it}	=	concentration of radionuclide i in disposal units (μCi/m^3),
U_t	=	fraction of the year during which external exposure to waste in disposal units during indoor residence occurs,
D_{it}	=	dose conversion factor for external exposure to radionuclide i in disposal units (rem/y per μCi/m^3), and
S	=	shielding factor for radionuclides during indoor residence.

The shielding factor takes into account the reduction in external dose provided by the walls and floor of the home.

In implementing the model, the fraction of the year during which exposure in the home is assumed to occur is 0.5 (Oztunali et al. 1981) (i.e., the assumed exposure time is about 4000 h per year). The exposure time could be as much as a factor of two higher, but the assumed exposure time is more reasonable for an average individual residing on the disposal site. A shielding factor from indoor residence of 0.7 is assumed for all radionuclides (NRC 1977).

The model for estimating external dose during indoor residence is summarized in Table G.19. The annual dose per unit concentration of a radionuclide in a disposal unit at the time intrusion occurs is based on the model and parameter values described above and the external dose-rate conversion factors given in the column in Table G.6 labeled "No shielding."

Inhalation Pathways. While working in the contaminated vegetable garden or residing in a home on top of disposal units, the annual committed effective dose equivalent (rem/year) from inhalation of radionuclide i suspended into air (a) in particulate form is given by

$$H_{ia} = C_{ia} f_a U_a D_i \ , \tag{G.14}$$

where

C_{ia}	=	concentration of radionuclide i in air (μCi/m^3),
f_a	=	fraction of the year during which inhalation exposure occurs,
U_a	=	annual air intake (m^3/year), and
D_i	=	dose conversion factor for inhalation of radionuclide i (rem/μCi inhaled).

Table G.18. Annual effective dose equivalents from external exposure while working in vegetable garden per unit concentration of radionuclides in exhumed waste for agriculture scenario

Nuclide[a]	Annual dose (rem/y per μCi/m^3)	Nuclide[a]	Annual dose (rem/y per μCi/m^3)
^{26}Al	2.2×10^{-5}	^{232}Th	—
^{40}K	1.2×10^{-6}	^{228}Ac	7.6×10^{-6}
^{60}Co	2.0×10^{-5}	^{212}Pb	9.4×10^{-7}
^{137}Cs	—	^{212}Bi	1.5×10^{-6}
^{137m}Ba	4.8×10^{-6}	^{208}Tl	9.0×10^{-6}
^{152}Eu	9.2×10^{-6}	^{232}U[b]	—
^{154}Eu	1.0×10^{-5}	^{235}U	9.2×10^{-7}
^{155}Eu	2.2×10^{-7}	^{231}Th	5.2×10^{-8}
^{226}Ra	—	^{238}U	—
^{214}Pb	1.9×10^{-6}	^{234}Th	2.8×10^{-8}
^{214}Bi	1.2×10^{-5}	^{234m}Pa	9.4×10^{-8}
^{229}Th	4.0×10^{-7}	^{234}Pa	2.6×10^{-8}
^{225}Ra	2.2×10^{-8}	^{237}Np	1.0×10^{-7}
^{225}Ac	6.8×10^{-8}	^{233}Pa	1.6×10^{-6}
^{221}Fr	2.0×10^{-7}	^{241}Am	5.4×10^{-8}
^{213}Bi	1.2×10^{-6}	^{243}Am	1.6×10^{-7}
^{209}Tl	3.6×10^{-7}	^{239}Np	1.0×10^{-6}
		^{243}Cm	7.8×10^{-7}
		^{249}Cf	2.8×10^{-6}

[a]Indented entries are radiologically significant decay products of parent radionuclide listed.
[b]Values for ^{212}Pb, ^{212}Bi, ^{208}Tl decay products are listed following ^{232}Th.

Concentrations of suspended radionuclides in particulate form in air are estimated using a mass-loading model (Anspaugh et al. 1975), which is based on observations of airborne concentrations of naturally occurring materials, such as uranium and thorium, relative to their concentrations in surface soils. In this model, airborne concentrations of radionuclides are given by

$$C_{ia} = C_{is} L_d / \rho_s \,, \tag{G.15}$$

Table G.19. Annual effective dose equivalents from external exposure during indoor residence per unit concentration of radionuclides in disposal units for agriculture scenario

Nuclide[a]	Annual dose (rem/y per μCi/m^3)	Nuclide[a]	Annual dose (rem/y per μCi/m^3)
^{26}Al	4.9×10^{-3}	^{232}Th	—
^{40}K	2.8×10^{-4}	^{228}Ac	1.6×10^{-3}
^{60}Co	4.6×10^{-3}	^{212}Pb	1.8×10^{-4}
^{137}Cs	—	^{212}Bi	3.3×10^{-4}
^{137m}Ba	1.0×10^{-3}	^{208}Tl	2.1×10^{-3}
^{152}Eu	2.0×10^{-3}	^{232}U[b]	—
^{154}Eu	2.2×10^{-3}	^{235}U	1.7×10^{-4}
^{155}Eu	3.9×10^{-5}	^{231}Th	9.1×10^{-6}
^{226}Ra	—	^{238}U	—
^{214}Pb	3.9×10^{-4}	^{234}Th	4.9×10^{-6}
^{214}Bi	2.7×10^{-3}	^{234m}Pa	2.0×10^{-5}
^{229}Th	7.0×10^{-5}	^{234}Pa	5.3×10^{-6}
^{225}Ra	3.9×10^{-6}	^{237}Np	1.8×10^{-5}
^{225}Ac	1.2×10^{-5}	^{233}Pa	3.0×10^{-4}
^{221}Fr	3.9×10^{-5}	^{241}Am	9.5×10^{-6}
^{212}Bi	2.3×10^{-4}	^{243}Am	2.8×10^{-5}
^{209}Tl	8.1×10^{-5}	^{239}Np	1.9×10^{-4}
		^{243}Cm	1.4×10^{-4}
		^{249}Cf	5.3×10^{-4}

[a]Indented entries are radiologically significant decay products of parent radionuclide listed.
[b]Values for ^{212}Pb, ^{212}Bi, and ^{208}Tl decay products are listed following ^{232}Th.

where

C_{is}	=	concentration of radionuclide i in surface soil (μCi/m^3),
L_a	=	atmospheric mass loading of surface soil (kg/m^3), and
ρ_s	=	density of soil (kg/m^3).

The mass-loading model described above is applied to all radionuclides except isotopes of radon and their short-lived decay products. The model for estimating inhalation doses due to radon released from contaminated soil or disposal units is described later in this section.

For inhalation exposure while working in the vegetable garden, the concentration of radionuclide i in soil again is given by

$$C_{is} = f_s C_{iu} , \tag{G.16}$$

where

C_{iu}	=	concentration of radionuclide i in disposal units (μCi/m^3), and
f_s	=	dilution factor for mixing of exhumed waste from disposal units into soil in vegetable garden.

In implementing the model, a dilution factor for mixing of exhumed waste from the disposal units into native soil in the garden of 0.2, a soil density of 1,400 kg/m^3, and a fraction of the year during which exposure while working in the garden occurs of 0.01 (about 100 hours per year) again are assumed, as in the model for external exposure while working in the garden. The annual air intake (breathing rate) is assumed to be 8,000 m^3 (NRC 1977). Finally, the atmospheric mass loading of contaminated soil while working in the garden is assumed to be 10^{-7} kg/m^3.

The assumed atmospheric mass loading of contaminated soil while working in the vegetable garden of 10^{-7} kg/m^3 is somewhat greater than the average background dust loading for nonurban areas in the United States of about 4×10^{-8} kg/m^3 (Anspaugh et al. 1975) and, furthermore, is in good agreement with an average dust loading of 6×10^{-8} kg/m^3 measured above two agricultural fields at the Savannah River Site (Shinn et al. 1982), where meteorological conditions and soil moisture levels should be similar to those on the Oak Ridge Reservation. The choice of an atmospheric mass loading for this exposure pathway is based on these data and the following considerations. Although some gardening activities presumably would increase atmospheric concentrations of suspended soil well above background levels, it probably is unreasonable to assume that the average concentration during all gardening activities would be much greater than the average background level in the United States. First, the average background level of suspended soil originating from the Oak Ridge Reservation should be substantially lower than the average level in the United States, because of the high annual precipitation, extensive vegetation, and low average wind speed at the site. Second, at any location, airborne concentrations of suspended surface soil consist of material originating from a wide area, not just from the particular location where inhalation exposures occur. Finally, the model assumes that all suspended soil particles are respirable. However, particularly during more vigorous gardening activities that could result in higher-than-average atmospheric mass

loadings, such as hoeing and tilling, some particles are likely to be too large to be respirable. Taking all of these factors into account, the choice of 10^{-7} kg/m^3 to represent the average mass loading during gardening activities on the Oak Ridge Reservation seems to be a reasonable assumption for this highly uncertain parameter.

The model for estimating inhalation dose while working in the garden is summarized in Table G.20. The annual dose per unit concentration of a radionuclide in exhumed waste in a disposal unit at the time intrusion occurs is based on the model and parameter values described above and the inhalation dose conversion factors given in Table G.3. Again, the results for isotopes of radon are estimated using a model described later in this section.

For inhalation exposures while residing in the home, the airborne concentration of radionuclide i is given by

$$C_{ia} = C_{it} L_a / \rho_s \,, \tag{G.17}$$

where

C_{it}	=	concentration of radionuclide i in disposal units (μCi/m^3),
L_a	=	mass loading of soil in the atmosphere (kg/m^3), and
ρ_s	=	density of soil (kg/m^3).

In implementing the model, a soil density of 1,400 kg/m^3, a fraction of the year during which exposure in the home occurs of 0.5 (i.e., about 4,000 hours per year), and an annual air intake of 8,000 m^3 again are assumed. The atmospheric mass loading of contaminated soil at the location of the home on top of disposal units is assumed to be 10^{-8} kg/m^3, which is approximately one-fourth of the average dust loading in the United States (Anspaugh et al. 1975). On the basis of the previous discussion of the atmospheric mass loading of contaminated soil while working in the vegetable garden, it seems unreasonable to assume that the mass loading of largely undisturbed surface soil on the Oak Ridge Reservation during indoor residence would be as high as the average dust loading in the United States. The assumption that the average mass loading at the disposal site is one-fourth of the average background level in the United States is intended to take into account the abundant precipitation, extensive vegetation, and low average wind speed at the disposal site, as well as the presence of uncontaminated soil suspended from other locations. In addition, the model for inhalation exposure indoors does not take into account the possibility that indoor concentrations of suspended soil particles may be somewhat less than the concentrations outdoors.

The model for estimating inhalation dose during indoor residence is summarized in Table G.21. The annual dose per unit concentration of a radionuclide in disposal units at the time intrusion occurs is based on the model and parameter values described above and the inhalation dose conversion factors given in Table G.3. The results for isotopes of radon are estimated using the model described below.

In this analysis, inhalation doses from isotopes of radon and their short-lived decay products while working in the vegetable garden containing contaminated soil or while residing in a home of top of exposed waste in disposal units are estimated using a natural

Table G.20. Annual effective dose equivalents from inhalation while working in vegetable garden per unit concentration of radionuclides in exhumed waste for agriculture scenario[a]

Nuclide[b]	Annual dose (rem/y per μCi/m^3)	Nuclide[b]	Annual dose (rem/y per μCi/m^3)
^{3}H	7.2×10^{-14}	^{232}Th	1.3×10^{-6}
^{14}C	2.4×10^{-12}	^{228}Th	3.5×10^{-7}
^{26}Al	9.0×10^{-11}	^{220}Rn	2.1×10^{-5}[c]
^{36}Cl	2.3×10^{-11}	^{232}U[d]	7.7×10^{-7}
^{40}K	1.4×10^{-11}	^{233}U	1.5×10^{-7}
^{60}Co	1.7×10^{-10}	^{234}U	1.5×10^{-7}
^{63}Ni	3.4×10^{-12}	^{235}U	1.4×10^{-7}
^{90}Sr	1.5×10^{-9}	^{236}U	1.4×10^{-7}
^{99}Tc	8.6×10^{-12}	^{238}U	1.4×10^{-7}
^{113m}Cd	1.6×10^{-9}	^{237}Np	5.6×10^{-7}
^{137}Cs	3.7×10^{-11}	^{238}Pu	5.3×10^{-7}
^{152}Eu	2.5×10^{-10}	^{239}Pu	5.8×10^{-7}
^{154}Eu	3.0×10^{-10}	^{240}Pu	5.8×10^{-7}
^{155}Eu	4.5×10^{-11}	^{242}Pu	5.5×10^{-7}
^{210}Pb	1.5×10^{-8}	^{241}Am	5.9×10^{-7}
^{210}Po	9.3×10^{-9}	^{243}Am	5.9×10^{-7}
^{226}Ra	9.0×10^{-9}	^{243}Cm	4.0×10^{-7}
^{222}Rn	1.3×10^{-4}[c]	^{244}Cm	3.1×10^{-7}
^{229}Th	2.0×10^{-6}	^{249}Cf	6.3×10^{-7}
^{230}Th	3.0×10^{-7}		

[a]Values give 50-year committed effective dose equivalents from one year's intakes of air.
[b]Indented entries are radiologically significant decay products of parent radionuclide listed.
[c]Value is normalized to unit concentration of parent radionuclide.
[d]Values for ^{228}Th and ^{220}Rn decay products are listed following ^{232}Th.

Table G.21. Annual effective dose equivalents from inhalation during indoor residence per unit concentration of radionuclides in disposal units for agriculture scenario[a]

Nuclide	Annual dose (rem/y per μCi/m^3)	Nuclide[b]	Annual dose (rem/y per μCi/m^3)
^{3}H	1.8×10^{-12}	^{232}Th	3.1×10^{-5}
^{14}C	6.0×10^{-11}	^{228}Th	8.9×10^{-6}
^{26}Al	2.3×10^{-9}	^{220}Rn	1.0×10^{-2}[c]
^{36}Cl	5.7×10^{-10}	^{232}U[d]	1.9×10^{-5}
^{40}K	3.4×10^{-10}	^{233}U	3.7×10^{-6}
^{60}Co	4.3×10^{-9}	^{234}U	3.7×10^{-6}
^{63}Ni	8.6×10^{-11}	^{235}U	3.4×10^{-6}
^{90}Sr	3.7×10^{-8}	^{236}U	3.4×10^{-6}
^{99}Tc	2.1×10^{-10}	^{238}U	3.4×10^{-6}
^{113m}Cd	4.0×10^{-8}	^{237}Np	1.4×10^{-5}
^{137}Cs	9.2×10^{-10}	^{238}Pu	1.3×10^{-5}
^{152}Eu	6.3×10^{-9}	^{239}Pu	1.5×10^{-5}
^{154}Eu	7.4×10^{-9}	^{240}Pu	1.5×10^{-5}
^{155}Eu	1.1×10^{-9}	^{242}Pu	1.4×10^{-5}
^{210}Pb	3.7×10^{-7}	^{241}Am	1.5×10^{-5}
^{210}Po	2.3×10^{-7}	^{243}Am	1.5×10^{-5}
^{226}Ra	2.3×10^{-7}	^{243}Cm	1.0×10^{-5}
^{222}Rn	1.2×10^{-1}[c]	^{244}Cm	7.7×10^{-6}
^{229}Th	4.9×10^{-5}	^{249}Cf	1.6×10^{-5}
^{230}Th	7.4×10^{-6}		

[a]Values give 50-year committed effective dose equivalents from one year's intakes of air.
[b]Indented entries are radiologically significant decay products of parent radionuclide listed.
[c]Value is normalized to unit concentration of parent radionuclide.
[d]Values for ^{228}Th and ^{220}Rn decay products are listed following ^{232}Th.

analog model. Specifically, known average doses from exposure to ^{222}Rn and ^{220}Rn both indoors and outdoors, which result from known average concentrations of their respective parent radionuclides ^{226}Ra and ^{232}Th in surface soil, are used to estimate doses from the radon isotopes per unit concentration of the parent radionuclides in disposed waste for the inhalation pathways of concern for the agriculture scenario. The analysis based on the natural analog model proceeds as follows.

The National Council on Radiation Protection and Measurements (NCRP 1987) has estimated that the average effective dose equivalent from exposure to radon in the United States is about 0.2 rem/year. This estimate evidently applies only to exposure to ^{222}Rn and its short-lived decay products in homes and, furthermore, assumes continuous residence indoors (NCRP 1987). The estimated dose from ^{222}Rn indoors results from an average concentration of the parent radionuclide ^{226}Ra in surface soil of about 0.6 pCi/g (NCRP 1984), which, for an average bulk density of soil of 1.4 g/cm^3 (Baes and Sharp 1983), corresponds to a concentration of 0.84 μCi/m^3. Therefore, for continuous residence indoors, the annual effective dose equivalent from exposure to ^{222}Rn and its short-lived decay products per unit concentration of ^{226}Ra in surface soil is estimated as:

^{222}Rn, continuous residence indoors -

$$(0.2 \text{ rem/year})/(0.84\ \mu\text{Ci/m}^3) = 0.24 \text{ rem/year per } \mu\text{Ci/m}^3.$$

The dose from ^{222}Rn during continuous residence indoors given above can be used to estimate the dose from inhalation during indoor residence in a home on top of exposed waste in disposal units containing ^{226}Ra by taking into account the fraction of the year during which residence in the home at the disposal site occurs. As described previously, this factor is assumed to be 0.5. Therefore, for inhalation exposure while residing in a home on top of exposed waste in disposal units, the annual effective dose equivalent from ^{222}Rn and its short-lived decay products per unit concentration of ^{226}Ra in the disposal units is estimated as:

^{222}Rn, indoor residence in agriculture scenario -

$$(0.24 \text{ rem/year per } \mu\text{Ci/m}^3)(0.5) = 0.12 \text{ rem/year per } \mu\text{Ci/m}^3.$$

This dose estimate is given in Table G.21.

The inhalation dose from ^{222}Rn while working in the vegetable garden contaminated with ^{226}Ra is estimated as follows. The United Nations Scientific Committee on the Effects of Atomic Radiation (UNSCEAR 1988) has estimated that, for continuous exposure, the average effective dose equivalent from outdoor ^{222}Rn would be about 28% of the average dose from indoor ^{222}Rn. Therefore, for continuous residence outdoors, the annual effective dose equivalent from exposure to ^{222}Rn and its short-lived decay products

per unit concentration of ^{226}Ra in surface soil is estimated from the previous result for continuous indoor residence as:

^{222}Rn, continuous residence outdoors -

(0.24 rem/year per $\mu Ci/m^3$)(0.28) = 0.067 rem/year per $\mu Ci/m^3$.

The dose from ^{222}Rn during continuous residence outdoors given above can be used to estimate the dose from inhalation while working in the vegetable garden containing ^{226}Ra by applying two corrections. The first is the fraction of the year that an intruder spends working in the vegetable garden, which is assumed to be 0.01. The second is the dilution factor for mixing of radionuclides in exhumed waste from disposal units into soil in the garden, which is assumed to be 0.2. Therefore, for inhalation exposure while working in the vegetable garden, the annual effective dose equivalent from ^{222}Rn and its short-lived decay products per unit concentration of ^{226}Ra in exhumed waste is estimated as:

^{222}Rn, residence in vegetable garden in agriculture scenario -

(0.067 rem/year per $\mu Ci/m^3$)(0.01)(0.2) = 1.3×10^{-4} rem/year per $\mu Ci/m^3$.

This dose estimate is given in Table G.20.

The dose estimates for inhalation exposure to ^{220}Rn and its short-lived decay products during indoor residence and while working in the vegetable garden are obtained from the data on average doses from ^{222}Rn both indoors and outdoors presented above and the following information. First, for continuous residence, the average dose from indoor ^{220}Rn is estimated to be about 14% of the average dose from indoor ^{222}Rn, and the average dose from outdoor ^{220}Rn is estimated to be about 26% of the average dose from outdoor ^{222}Rn (UNSCEAR 1988). Second, the estimated doses from ^{220}Rn result from an average concentration of the parent radionuclide ^{232}Th in surface soil of about 1 pCi/g (NCRP 1984) which, for an average bulk density of soil of 1.4 g/cm^3 (Baes and Sharp 1983), corresponds to a concentration of 1.4 $\mu Ci/m^3$.

Using the data on doses from ^{222}Rn for continuous residence indoors and outdoors presented previously, the data on doses from ^{220}Rn relative to the doses from ^{222}Rn and the average concentration of ^{232}Th in surface soil given above, and the assumptions in the agriculture scenario for the indoor residence time, the residence time while working in the vegetable garden, and the dilution factor for mixing of exhumed waste in garden soil, the following dose estimates for ^{220}Rn are obtained. For inhalation exposure while residing in a home on top of exposed waste in disposal units, the annual effective dose equivalent from ^{220}Rn and its short-lived decay products per unit concentration of ^{232}Th in the disposal units is estimated as:

^{220}Rn, indoor residence in agriculture scenario -

(0.2 rem/year)(0.14)(0.5)/(1.4 $\mu Ci/m^3$) = 0.010 rem/year per $\mu Ci/m^3$.

This dose estimate is given in Table G.21. For inhalation exposure while working in the vegetable garden, the annual effective dose equivalent from ^{220}Rn and its short-lived decay products per unit concentration of ^{232}Th in exhumed waste is estimated as:

^{220}Rn, residence in vegetable garden in agriculture scenario –

$$(0.2 \text{ rem/year})(0.28)(0.26)(0.01)(0.2)/(1.4\ \mu\text{Ci/m}^3) = 2.1 \times 10^{-5} \text{ rem/year per } \mu\text{Ci/m}^3.$$

This dose estimate is given in Table G.20. The dose estimates for ^{220}Rn during indoor residence and while working in the vegetable garden given above also apply to ^{220}Rn produced in the decay of ^{232}U.

All Pathways. For the agriculture scenario, the annual doses to an inadvertent intruder from all exposure pathways per unit concentration of radionuclides in disposal units at the time intrusion is assumed to occur are summarized in Table G.22. The total dose for each radionuclide is the sum of the doses from the vegetable, soil ingestion, external exposure, and inhalation pathways summarized in Tables G.16–G.21.

On the basis of the models and parameter values assumed in the dose analysis for the agriculture scenario, the most important exposure pathways depend on the particular radionuclide. For the fission and activation products and ^{210}Pb, the vegetable pathway is the most important, unless the radionuclide is a photon emitter in which case external exposure while residing in the home is the most important pathway. For ^{226}Ra, ^{232}Th, and ^{232}U, inhalation of radon and its short-lived decay products while residing in the home is the most important pathway. However, if the inhalation dose from radon is excluded, external exposure while residing in the home is the most important pathway for ^{226}Ra and the actinide radioelements when the isotope emits significant intensities of high-energy photons, but the vegetable and soil ingestion pathways and inhalation exposure while residing in the home usually are significant contributors to the total dose when the isotope is not a high-energy photon emitter. For many of the actinide radioelements, the soil ingestion pathway is more important than the vegetable pathway, due to the low plant-to-soil concentration ratios in vegetables assumed for most of these elements.

G.5.2.2 Resident Scenario

In the resident scenario, an inadvertent intruder is assumed to construct a home on top of disposal units, as in the agriculture scenario described in Sect. G.5.2.1. However, in digging the foundation, an intruder is assumed to encounter an intact engineered barrier above the waste that cannot be penetrated by normal excavation procedures. The home then is assumed to be located on top of the intact barrier, rather than on top of exposed waste as in the agriculture scenario. An intruder is assumed to receive a chronic external exposure while residing in the home on top of the disposal units, but ingestion exposures and inhalation exposures to radionuclides in particulate form are precluded by the intact engineered barrier. Inhalation of radon and its short-lived decay products during indoor residence also is assumed to be mitigated by the presence of an intact engineered barrier above the waste.

External exposure while residing in the home in the resident scenario is estimated using the model given in Eq. G.13. As in the agriculture scenario described previously,

Table G.22. Annual effective dose equivalents to inadvertent intruders per unit concentration of radionuclides in disposal units from all exposure pathways for agriculture scenario[a]

Nuclide[b]	Annual dose (rem/y per μCi/m^3)	Nuclide[b]	Annual dose (rem/y per μCi/m^3)
^{3}H	3.9×10^{-6}	^{232}Th + d[d]	4.3×10^{-3}
^{14}C	1.5×10^{-5}	^{220}Rn	1.0×10^{-2}[e]
^{26}Al	4.9×10^{-3}	^{232}U + d[d]	2.7×10^{-3}
^{36}Cl	1.2×10^{-3}	^{220}Rn	1.0×10^{-2}[e]
^{40}K	3.4×10^{-4}	^{233}U	1.1×10^{-5}
^{60}Co	4.6×10^{-3}	^{234}U	1.1×10^{-5}
^{63}Ni	1.8×10^{-7}	^{235}U + d	1.9×10^{-4}
^{90}Sr + d	1.8×10^{-4}	^{236}U	1.0×10^{-5}
^{99}Tc	1.1×10^{-5}	^{238}U + d	4.0×10^{-5}
^{113m}Cd	1.3×10^{-4}	^{237}Np + d	5.8×10^{-4}
^{137}Cs + d	1.0×10^{-3}	^{238}Pu	3.4×10^{-5}
^{152}Eu	2.0×10^{-3}	^{239}Pu	4.0×10^{-5}
^{154}Eu	2.2×10^{-3}	^{240}Pu	4.0×10^{-5}
^{155}Eu	3.9×10^{-5}	^{242}Pu	3.8×10^{-5}
^{210}Pb + d	3.0×10^{-4}	^{241}Am	5.6×10^{-5}
^{226}Ra + d[c,d]	3.4×10^{-3}	^{243}Am + d	2.7×10^{-4}
^{222}Rn	1.2×10^{-1}[e]	^{243}Cm	1.7×10^{-4}
^{229}Th + d	5.2×10^{-4}	^{244}Cm	2.0×10^{-5}
^{230}Th	1.1×10^{-5}	^{249}Cf	5.7×10^{-4}

[a]Values give sum of 50-year committed effective dose equivalents per unit concentration from one year's intakes of vegetables, soil, and air given in Tables G.16, G.17, and G.20, and G.21, respectively, and effective dose equivalents per unit concentration from one year's external exposure given in Tables G.18 and G.19.

[b]"d" denotes short-lived radioactive decay products that are assumed to be in secular equilibrium with the parent.

[c]Decay products include ^{210}Pb and its decay product.

[d]Dose from radon decay product is listed separately.

[e]Value is normalized to unit concentration of parent radionuclide.

the fraction of the year during which external exposure in the home occurs is assumed to be 0.5, and the shielding factor for all photon-emitting radionuclides during indoor residence is assumed to be 0.7. The dose conversion factor for each photon-emitting radionuclide is the external dose-equivalent rate per unit concentration in the disposal units taking into account the shielding provided by the source region and the engineered barrier on top of the disposal units. For the different types of disposal units in SWSA 6 that are constructed with engineered barriers (see Sects. 2.3.5 and 2.3.6), the shielding provided by the intact barrier on top of the disposal units is assumed to be equivalent to the shielding provided by a layer of soil of thickness 30 cm.

The model for estimating external dose in the resident scenario is summarized in Table G.23. The annual dose per unit concentration of a radionuclide in the disposal units at the time intrusion occurs is obtained from the assumed exposure time and shielding factor during indoor residence given above and the external dose-rate conversion factors given in the column in Table G.6 labeled "30-cm shielding."

G.5.2.3 Discovery Scenario

In the discovery scenario, an inadvertent intruder is assumed to encounter an intact and impenetrable engineered barrier in disposal units while digging a foundation for a home, as in the resident scenario described in Sect. G.5.2.2. However, the discovery scenario differs from the resident scenario in two respects. First, an intruder is assumed to receive an external exposure only for a short period of time while attempting to excavate at the disposal site (i.e., an intruder does not construct a home at the location of the disposal units). Second, an intruder is assumed to receive exposure while working at the side of disposal units, rather than on top of the units. As in the resident scenario, ingestion exposures and inhalation exposures to radionuclides in particulate form are precluded by the intact engineered barrier, and inhalation of radon and its short-lived decay products is assumed to be mitigated by the presence of an intact engineered barrier between the waste and the receptor location.

External exposure while digging next to disposal units in the discovery scenario is estimated using a model of the form given by Eq. G.11. The only parameters in the model are the time during which external exposure while excavating at the site occurs and the amount of shielding provided by the engineered barrier at the side of disposal units.

The choice of an exposure time for the discovery scenario is highly subjective. The time spent excavating at the disposal site probably would be at least 10 hours (i.e., about 0.1% of the time during a year) but is unlikely to exceed 100 h (about 1% of the time during a year) before an intruder would decide to abandon digging at the site and move elsewhere. In this analysis, an exposure time of 100 hours during a year is assumed, in order to provide a prudently conservative estimate of dose for this scenario.

For the different types of disposal units in SWSA 6 that are constructed with engineered barriers (see Sects. 2.3.5 and 2.3.6), the shielding provided by the intact barrier at the sides of the disposal units is assumed to be equivalent to the shielding provided by a layer of soil of thickness either 15 or 30 cm. However, doses for the discovery scenario need to be estimated only for disposal units with shielding at the sides equivalent to 15 cm of soil. For units with shielding at the sides equivalent to 30 cm of soil, the thickness of the engineered barrier at the top and sides is the same, and the dose from the resident

Table G.23. Annual effective dose equivalents to inadvertent intruders per unit concentration of radionuclides in disposal units for resident scenario[a]

Nuclide[b]	Annual dose (rem/y per μCi/m^3)	Nuclide[b]	Annual dose (rem/y per μCi/m^3)
^{26}Al	3.3×10^{-4}	^{232}Th + d	3.0×10^{-4}
^{40}K	2.1×10^{-5}	^{232}U + d	2.3×10^{-4}
^{60}Co	2.9×10^{-4}	^{235}U + d	5.6×10^{-7}
^{137}Cs + d	3.2×10^{-5}	^{238}U + d	1.2×10^{-6}
^{152}Eu	9.8×10^{-5}	^{237}Np + d	3.5×10^{-6}
^{154}Eu	1.1×10^{-4}	^{243}Am + d	1.1×10^{-6}
^{155}Eu	2.0×10^{-8}	^{243}Cm	7.7×10^{-7}
^{226}Ra + d	1.9×10^{-4}	^{249}Cf	8.1×10^{-6}
^{229}Th + d	1.0×10^{-5}		

[a]Values give effective dose equivalent per unit concentration from one year's external exposure, and are 35% of corresponding external dose-rate conversion factors for 30-cm shielding in Table G.6.

[b]"d" denotes short-lived radioactive decay products that are assumed to be in secular equilibrium with the parent.

scenario involving exposure for 50% of the time during the year would always be much greater than the dose from the discovery scenario involving exposure only for about 1% of the time during a year.

The model for estimating external dose in the discovery scenario is summarized in Table G.24. The annual dose per unit concentration of a radionuclide in the disposal units at the time intrusion occurs is obtained from the assumed exposure time given above and the external dose-rate conversion factors given in the column in Table G.6 labeled "15-cm shielding."

G.5.2.4 Post-Drilling Scenario

In the post-drilling scenario, an inadvertent intruder is assumed to drill through a disposal unit (e.g., for the purpose of constructing a well for a domestic water supply), and the entire amount of drilling waste is assumed to be mixed with native soil in the intruder's vegetable garden. The pathways for chronic exposure assumed for this scenario include (1) ingestion of vegetables grown in contaminated soil, (2) direct ingestion of contaminated soil in conjunction with vegetable intakes, (3) external exposure to contaminated soil while working in the garden, and (4) inhalation of suspended activity while working in the garden.

Table G.24. Effective dose equivalents to inadvertent intruders per unit concentration of radionuclides in disposal units for discovery scenario[a]

Nuclide[b]	Dose (rem per μCi/m^3)	Nuclide[b]	Dose (rem per μCi/m^3)
^{26}Al	3.0×10^{-5}	^{232}Th + d	2.7×10^{-5}
^{40}K	1.9×10^{-6}	^{232}U + d	1.8×10^{-5}
^{60}Co	2.9×10^{-5}	^{235}U + d	2.5×10^{-7}
^{137}Cs + d	4.5×10^{-6}	^{238}U + d	1.4×10^{-7}
^{152}Eu	1.1×10^{-5}	^{237}Np + d	8.1×10^{-7}
^{154}Eu	1.2×10^{-5}	^{241}Am	3.6×10^{-10}
^{155}Eu	2.0×10^{-8}	^{243}Am + d	3.4×10^{-7}
^{226}Ra + d	1.8×10^{-5}	^{243}Cm	7.7×10^{-7}
^{229}Th + d	1.5×10^{-6}	^{249}Cf	1.7×10^{-6}

[a]Values give effective dose equivalent per unit concentration from external exposure and are 1% of corresponding external dose-rate conversion factors for 15-cm shielding in Table G.6.

[b]"d" denotes short-lived radioactive decay products that are assumed to be in secular equilibrium with the parent.

The exposure pathways for the post-drilling scenario are similar to those for the agriculture scenario described in Sect. G.5.2.1. However, external and inhalation exposures during indoor residence do not occur in the post-drilling scenario, because all of the exhumed waste is assumed to be mixed with native soil in the vegetable garden and the intruder's home is not located on top of any disposal units. Therefore, the models given by Eqs. G.7 and G.8 for the vegetable pathway, Eqs. G.9 and G.10 for the soil ingestion pathway, Eqs. G.11 and G.12 for external exposure while working in the garden, and Eqs. G.14, G.15, and G.16 for inhalation exposure while working in the garden, as well as the natural analog model for estimating inhalation dose from exposure to radon while working in the garden, also apply to the post-drilling scenario.

In implementing the models for the different exposure pathways, most of the parameter values for the post-drilling scenario would be the same as the values assumed for the agriculture scenario. The only exception is the dilution factor for mixing of exhumed waste from a disposal unit with native soil in the vegetable garden, which is denoted by f_s for all radionuclides. For all exposure pathways in the post-drilling scenario, the dose per unit concentration of a radionuclide in a disposal unit is directly proportional to this dilution factor.

In the post-drilling scenario, the volume of contaminated drilling waste is assumed to be 0.5 m^3 (Kennedy et al. 1983), and this material is assumed to be uniformly mixed to a depth of 15 cm in a vegetable garden of area about 200 m^2. A garden of this size

reasonably could provide half of the entire yearly intake of all vegetables by an intruder, as assumed in this analysis. Therefore, the volume of soil in the garden into which the drilling waste is mixed is about 30 m^3, and the resulting dilution factor is about 0.02. The assumed dilution factor for the post-drilling scenario thus is a factor of ten less than the value 0.2 assumed for the agriculture scenario. Therefore, for any exposure pathway in the post-drilling scenario, the dose per unit concentration of a radionuclide in a disposal unit is a factor of ten less than the corresponding value for the same pathway in the agriculture scenario.

For the post-drilling scenario, the annual doses to an inadvertent intruder from all exposure pathways per unit concentration of radionuclides in disposal units at the time intrusion is assumed to occur, as obtained from the models and parameter values described above, is summarized in Table G.25. The total dose for each radionuclide is one-tenth of the sum of the doses from the vegetable, soil ingestion, external exposure, and inhalation pathways for the agriculture scenario given in Tables G.16, G.17, G.18, and G.20, respectively.

G.6 SUMMARY

This appendix has presented the models and data bases used in estimating effective dose equivalents to (1) off-site individuals and inadvertent intruders resulting from exposure to radionuclides in contaminated water and (2) inadvertent intruders resulting from direct intrusion into waste disposal units. In each case, particular exposure scenarios and associated exposure pathways have been assumed. For each exposure pathway, simple models for estimating dose have been developed, and doses per unit concentration of radionuclides in water or in disposal units have been estimated on the basis of assumed parameter values for the particular pathway models. In the absence of site-specific data, the assumed parameter values were based on generic data available in the literature.

For each exposure scenario, the doses per unit concentration of a radionuclide for each exposure pathway have been combined to obtain the total dose per unit concentration from all pathways. The following summary tables give the total dose per unit concentration of radionuclides at the time intrusion is assumed to occur for the different exposure scenarios:

- Table G.13, exposure of off-site individuals to radionuclides in contaminated water;
- Table G.14, exposure of inadvertent intruders to radionuclides in contaminated water;
- Table G.22, agriculture scenario for exposure of inadvertent intruders to radionuclides in disposal units;
- Table G.23, resident scenario for exposure of inadvertent intruders to radionuclides in disposal units;
- Table G.24, discovery scenario for exposure of inadvertent intruders to radionuclides in disposal units; and
- Table G.25, post-drilling scenario for exposure of inadvertent intruders to radionuclides in disposal units.

Table G.25. Annual effective dose equivalents to inadvertent intruders per unit concentration of radionuclides in exhumed waste from all exposure pathways for post-drilling scenario[a]

Nuclide[b]	Annual dose (rem/y per μCi/m^3)	Nuclide[b]	Annual dose (rem/y per μCi/m^3)
^{3}H	3.9×10^{-7}	^{232}Th + d[e]	6.2×10^{-6}
^{14}C	1.5×10^{-6}	^{220}Rn	2.1×10^{-6}[e]
^{26}Al	2.2×10^{-6}	^{232}U + d[e]	5.7×10^{-6}
^{36}Cl	1.2×10^{-4}	^{220}Rn	2.1×10^{-6}
^{40}K	6.0×10^{-6}	^{233}U	7.5×10^{-7}
^{60}Co	2.1×10^{-6}	^{234}U	7.3×10^{-7}
^{63}Ni	1.8×10^{-8}	^{235}U + d	7.9×10^{-7}
^{90}Sr + d	1.8×10^{-5}	^{236}U	6.9×10^{-7}
^{99}Tc	1.1×10^{-6}	^{238}U + d	6.6×10^{-7}
^{113m}Cd	1.3×10^{-5}	^{237}Np + d	2.4×10^{-5}
^{137}Cs + d	1.3×10^{-6}	^{238}Pu	2.1×10^{-6}
^{152}Eu	9.4×10^{-7}	^{239}Pu	2.5×10^{-6}
^{154}Eu	1.0×10^{-6}	^{240}Pu	2.5×10^{-6}
^{155}Eu	2.6×10^{-8}	^{242}Pu	2.4×10^{-6}
^{210}Pb + d	3.0×10^{-5}	^{241}Am	3.1×10^{-6}
^{226}Ra + d[c,d]	3.3×10^{-5}	^{243}Am + d	3.2×10^{-6}
^{222}Rn	1.3×10^{-5}[e]	^{243}Cm	1.6×10^{-6}
^{229}Th + d	3.0×10^{-6}	^{244}Cm	1.3×10^{-6}
^{230}Th	3.4×10^{-7}	^{249}Cf	2.8×10^{-6}

[a]Values give sum of 50-year committed effective dose equivalents per unit concentration from one year's intakes of vegetables, soil, and air and effective dose equivalents per unit concentration from one year's external exposure; values for each exposure pathway are one-tenth of values for agriculture scenario given in Tables G.16, G.17, and G.18, and G.20, respectively.

[b]"d" denotes short-lived radioactive decay products that are assumed to be in secular equilibrium with the parent.

[c]Decay products include ^{210}Pb and its decay product.

[d]Dose from radon decay product is listed separately.

[e]Value is normalized to unit concentration of parent radionuclide.

The dose analyses for each exposure scenario and exposure pathway were based on assumed model parameters, some of which are radionuclide- or element-specific and others of which are independent of radionuclide. The radionuclide- or element-specific parameter values are given in Tables G.2–G.6, G.8, G.9, and G.15. The parameter values that are independent of radionuclide are summarized in Table G.26.

For the four scenarios involving direct intrusion into disposal units, the radionuclide concentrations in the disposal units to which the doses obtained in this analysis are normalized are the concentrations at the time intrusion is assumed to occur, rather than the concentrations at the time of disposal. That is, the dose analyses for these scenarios presented in this appendix do not include any assumptions about the time after disposal at which intrusion occurs. Such assumptions are applied when the results of the intruder dose analyses are combined with the results of the performance assessments for the various types of disposal units, which yield predictions of the concentrations of radionuclides remaining in disposal units as a function of time after disposal.

Table G.26. Summary of radionuclide-independent parameter values used in dose analyses for off-site individuals and inadvertent intruders

Parameter description	Symbol	Parameter value
Consumption of contaminated drinking water –		
humans[a]	U_w	730 L/y
dairy cattle[a]	Q_{wm}	60 L/d
beef cattle[a]	Q_{wf}	50 L/d
Consumption of contaminated vegetables[b]	U_v	90 kg/y (fresh weight)
Density of soil[b]	ρ_s	1,400 kg/m^3
Dilution factor for mixing of exhumed waste with native soil in vegetable garden	f_s	0.2[c] 0.02[d]
Consumption of contaminated soil[b]	U_s	0.037 kg/y
Exposure times –		
swimming[e]	U_w	1%/y
working in garden[b]	U_s, f_a	1%/y
residing in home[f]	U_t, f_a	50%/y
excavating at disposal site[g]	U_s	100 h
Shielding factor for external exposure during indoor residence[f]	S	0.7
Air intake (breathing rate)[b]	U_a	8,000 m^3/y
Atmospheric mass loading of contaminated surface soil –	L_a	
working in garden[b]		10^{-7} kg/m^3
residing in home[c]		10^{-8} kg/m^3

[a]Parameter applies to exposure of off-site individuals and inadvertent intruders from use of contaminated groundwater or surface waters.
[b]Parameter applies to agriculture and post-drilling scenarios for inadvertent intruders.
[c]Parameter applies to agriculture scenario for inadvertent intruders.
[d]Parameter applies to post-drilling scenario for inadvertent intruders.
[e]Parameter applies to exposure of off-site individuals from use of contaminated surface waters.
[f]Parameter applies to agriculture and resident scenarios for inadvertent intruders.
[g]Parameter applies to discovery scenario for inadvertent intruders.

G.8. REFERENCES

Anspaugh, L. R., J. H. Shinn, P. L. Phelps, and N. C. Kennedy 1975. "Resuspension and Redistribution of Plutonium in Soils," *Health Physics* **29**, 571.

Baes, C. F. III, and R. D. Sharp 1983. "A Proposal for Estimation of Soil Leaching Constants for Use in Assessment Models," *Journal of Environmental Quality* **12**, 17.

Baes, C. F. III, R. D. Sharp, A. L. Sjoreen, and R. W. Shor 1984. *A Review and Analysis of Parameters for Assessing Transport of Environmentally Released Radionuclides Through Agriculture,* ORNL-5786, Oak Ridge National Laboratory, Oak Ridge, Tenn.

DOE (U.S. Department of Energy) 1988a. "Management of Low-Level Waste," Chap. III in *Radioactive Waste Management*, Order 5820.2A, DOE, Washington, D.C.

DOE (U.S. Department of Energy) 1988b. *Internal Dose Conversion Factors for Calculation of Dose to the Public*, DOE/EH-0071, DOE, Washington, D.C.

DOE (U.S. Department of Energy) 1988c. *External Dose-Rate Conversion Factors for Calculation of Dose to the Public*, DOE/EH-0070, DOE, Washington, D.C.

EPA (U.S. Environmental Protection Agency) 1989. *Risk Assessment Guidance for Superfund. Volume I. Human Health Evaluation Manual (Part A)*, EPA/540/1-89/002, EPA, Washington, D.C.

Garten, C. T., Jr., E. A. Boudietti, J. R. Traballea, R. L. Walker, and T. G. Scott 1987. "Field Studies on the Terrestrial Behavior of Actinide Elements in East Tennessee," p. 109 in *Environmental Research on Actinide Elements*, ed. by J. E. Pinder III, J. J. Alberts, K. W. McLeod, and R. G. Schreckhise, CONF-841142, U.S. Department of Energy.

Hamby, D. M. 1992. "Site-Specific Parameter Values for the Nuclear Regulatory Commission's Food Pathway Dose Model," *Health Physics* **62**, 136.

Kennedy, W. E., Jr., B. A. Napier, and J. K. Soldat 1983. "Advanced Disposal Systems for Transuranic Waste: Preliminary Disposal Criteria for Plutonium-239 at Hanford," *Nucl. Chem. Waste Manage.* **4**, 103.

Kocher, D. C. 1981. *Radioactive Decay Data Tables*, DOE/TIC-11026, U.S. Department of Energy, Washington, D.C.

Kocher, D. C., and A. L. Sjoreen 1985. "Dose-Rate Conversion Factors for Photon Emitters in Soil," *Health Physics* **48**, 193.

Napier, B. A., R. A. Peloquin, W. E. Kennedy, Jr., and S. M. Neuder 1984. *Intruder Dose Pathway Analysis for the Onsite Disposal of Radioactive Waste: The ONSITE/MAXI1 Computer Program*, NUREG/CR-3620, PNL-4054, Pacific Northwest Laboratory, Richland, Wash.

NCRP (National Council on Radiation Protection and Measurements) 1984. *Exposures from the Uranium Series with Emphasis on Radon and Its Daughters*, NCRP Report No. 77, NCRP, Bethesda, Md.

NCRP (National Council on Radiation Protection and Measurements) 1987. *Exposure of the Population in the United States and Canada from Natural Background Radiation*, NCRP Report No. 94, NCRP, Bethesda, Md.

Ng, Y. C. 1982. "A Review of Transfer Factors for Assessing the Dose from Radionuclides in Agricultural Products," *Nuclear Safety* **23**, 57.

Ng, Y. C., C. S. Colsher, D. J. Quinn, and S. E. Thompson 1977. *Transfer Coefficients for the Prediction of the Dose to Man via the Forage-Cow-Milk Pathway from Radionuclides Released to the Biosphere*, UCRL-51939, Lawrence Livermore Laboratory, Livermore, Calif.

NRC (U.S. Nuclear Regulatory Commission) 1977. *Regulatory Guide 1.109. Calculation of Annual Doses to Man from Routine Releases of Reactor Effluents for the Purpose of Evaluating Compliance with 10 CFR Part 50, Appendix I*, NRC, Washington, D.C.

NRC (U.S. Nuclear Regulatory Commission) 1982. *Final Environmental Impact Statement on 10 CFR Part 61 "Licensing Requirements for Land Disposal of Radioactive Waste"*, NUREG-0945, Vol. 1, NRC, Washington, D.C.

Oztunali, O. I., G. C. Re, P. M. Moskowitz, E. D. Picazo, and C. J. Pitt 1981. *Data Base for Radioactive Waste Management*, NUREG/CR-1759, Vol. 3, Dames and Moore, Inc., U.S. Nuclear Regulatory Commission, Washington, D.C.

Peterson, H. T., Jr. 1983. "Terrestrial and Aquatic Food Chain Pathways," Chap. 5 in *Radiological Assessment*, ed. J. E. Till and H. R. Meyer, NUREG/CR-3332, ORNL-5968, U.S. Nuclear Regulatory Commission and Oak Ridge National Laboratory, Washington, D. C.

Sheppard, M. I., S. C. Sheppard, and B. D. Amiro 1991. "Mobility and Plant Uptake of Inorganic ^{14}C and ^{14}C-Labelled PCB in Soils of High and Low Retention," *Health Physics* **61**, 481.

Shinn, J. H., D. N. Norman, and D. D. Gay 1982. "Plutonium Aerosol Fluxes and Pulmonary Exposure Rates During Resuspension from Bare Soils Near a Chemical Separation Facility," p. 1131 in *Precipitation Scavenging, Dry Deposition, and Resuspension*, Vol. 2, ed. by H. R. Pruppacher, R. G. Semonin, and W. G. N. Slinn, Elsevier Science Publishing Co., New York.

UNSCEAR (United Nations Scientific Committee on the Effects of Atomic Radiation) 1988. *Sources, Effects and Risks of Ionizing Radiation*, United Nations, New York.

APPENDIX H

SENSITIVITY AND UNCERTAINTY ANALYSIS

N. M. Larson
S. J. Norton
M. W. Yambert

APPENDIX H

SENSITIVITY AND UNCERTAINTY ANALYSIS

H.1 DEFINITIONS AND INTRODUCTION

This performance assessment is based on a linkage of models constructed to approximate chemical transport along the water pathways at SWSA 6. In this assessment, the radionuclide inventories are estimated, followed by modeled release and transport of the contaminants. Each stage in the modeling uses simplifying assumptions involving inexact parameters and variables. The influence of the uncertainty in model parameters on the predicted contaminant concentrations is typically estimated by means of a parameter variance study. Such a study was carried out here by Latin hypercube (LHC) sampling of the parameters, whose variability is assumed to be represented by appropriate probability distributions. The uncertainty in the model parameters associated with each stage contributes to an overall uncertainty in the final projected contaminant concentration and dose. The analysis was performed so that a random output from one stage (or model segment) becomes input for the next stage, while parameter variance is "inserted" at each stage by LHC sampling. In what follows, it is convenient to use the term "objective uncertainty" to refer to the uncertainty associated solely with parameter variability. However, an attempt is also made here to assess the subjective uncertainty associated with the assumptions used in the modeling. As seen below, this subjective assessment amounts to a "smearing" of the objective probability distribution—that is, of the contaminant probability distribution derived from the LHC analysis—which leads to an increase in the overall uncertainty associated with the estimated probability of compliance.

In assessing the performance of SWSA 6 far into the future, the approach here is to provide a "best estimate" of projected (or modeled) dose, accompanied by an estimate of the probability that the actual future dose is near the projected dose. More specifically, in terms of concentrations, if C denotes the (unknown) actual contaminant concentration, and C^* denotes the maximum allowable concentration associated with a dose limit, the analysis provides the probability of compliance, $P_c = \Pr(C \leq C^*)$. This is in contrast to a more definitive statement that $C \leq C^*$. If P_c is near 1, the results of the composite model suggest that $C \leq C^*$ and SWSA 6 is in compliance; a value of P_c near 0 suggests noncompliance.

The uncertainty associated with projected compliance or noncompliance, as used here, is directly associated with the value of $P_c = \Pr(C \leq C^*)$. If $P_c = 0.5$ then no confident conclusion can be drawn as to whether or not $C \leq C^*$; there is an "even chance" of compliance. If $P_c \approx 1$ or $P_c \approx 0$, then the analysis supplies a stronger statement as to whether C does or does not exceed C^*. A quantitative measure of uncertainty, borrowed from information theory, is the computable quantity (the "entropy")

$$U = -[P_c \log_2(P_c) + (1-P_c) \log_2(1-P_c)] \ . \qquad \text{(H.1)}$$

If $P_c = 0.5$, the uncertainty is at its maximum: $U = 1$. If $P_c = 0$ or $P_c = 1$, then $U = 0$. Thus, any feature of the SWSA 6 analysis that has the effect of driving P_c nearer to 0.5 is a feature which contributes to the uncertainty of the assertion that $C \leq C^*$ and that SWSA 6 is in compliance. (Recall that the dose is acceptable if and only if $C \leq C^*$.) With this approach, the determination of compliance or noncompliance is judged on a probability scale, and the uncertainty in the judgment is also scaled between 0 and 1. If $P_c = \Pr(C \leq C^*) = 1$, then the model predicts compliance, with no uncertainty ($U = 0$). If $P_c = \Pr(C \leq C^*) = 0$, then the model predicts noncompliance, again with no uncertainty. Realistically, since it is not possible to predict the long-term fate of contaminants without some uncertainty, the ultimate objective of the uncertainty analysis is to obtain a probability distribution for possible doses at compliance points at SWSA 6. For doses due to water consumption, the maximum allowable dose of radiation from a given radionuclide in water corresponds directly to a maximum allowable concentration of that radionuclide. Hence, the probability of compliance and the uncertainty associated with it are related to concentrations predicted by the modeling, and for any given probability of compliance, there corresponds a computable uncertainty (entropy) given by the above equation for U.

It is assumed that the actual concentration, C, of a given radionuclide at a given point in time and specified compliance point is a random-valued quantity. The maximum value of the (unknown) concentration over all time, starting at 1988, is assumed to be a random variable determined by a plethora of random and planned events, including inventory, weather and climate, concrete and steel durability, and future geologic and hydrologic events. Since some radionuclides (e.g., ^{238}U and ^{232}Th) have half-lives in the billions of years, some of the modeled predictions occur on a geological time scale. Hence, the random events that determine actual concentrations are virtually limitless in scope, and any model must be put in proper perspective with some evaluation of accompanying uncertainty beyond routine LHC analysis.

In summary, it is recognized that the model is not likely to produce a computed concentration without errors. The uncertainty associated with asserting that the actual C is in compliance ($C \leq C^*$) is assumed to come from two basic sources: (1) given that the model is an accurate representation of the transport process, the physical parameters are never known exactly; (2) the composite model may be flawed in the sense that it is not sufficiently specific to adequately describe the site and its details and, at the same time, is not sufficiently robust to describe the site for tens of thousands of years. These two sources of uncertainty are considered separately and in combination below.

H.2 UNCERTAINTY DUE TO PARAMETER VARIANCE

The composite transport model basically consists of six components (or stages): inventory, rainfall and infiltration, release, shallow subsurface, groundwater, and surface water. Thus, the uncertainty analysis involves the serial variation in concentrations from one stage to the next. The probability of compliance (POC) is computed at selected compliance points for each radionuclide using LHC sampling. The coupled sampling

procedure is illustrated in Fig. H.1. In each model component, 50 inputs from the preceding component are sampled simultaneously with all the relevant parameters in the given component. The result is a set of 50 time evolutions consisting of concentrations (or mass and volumetric flux) that serve as input to the next component. Thus, the output of the coupled system depicted in Fig. H.1 yields a sample of 50 concentrations in groundwater and surface water.

The finite number of samples used in LHC sampling is itself a source of some small statistical error. A 90% confidence bandwidth due to sampling variability is given as follows: Defining $d = 1.22/\sqrt{N}$, where N is the sample size, then

$$\hat{P}_c - d < P_c < \hat{P}_c + d \quad ,$$

where $\hat{P}_c$ is the POC derived from the composite model. With the sample size $N = 50$, $d = 1.22/\sqrt{50} = 0.17$. Again, this assumes that the sample concentrations are taken from an actual population of possible outcomes. This would be the case if the model is indeed an accurate representation of all the physical processes that will yield a future population of concentrations. Hence, this determination of the POC in terms of the computed $\hat{P}_c$ involves only variances in the input parameters and the combined (serial) effects propagating through the composite model. The more difficult determination of uncertainties due to perceived restrictive assumptions in the model is considered below. This component is subjective and cannot be defended beyond the fact that it is the opinion of an "expert."

H.3 UNCERTAINTY AND SUBJECTIVITY

The SWSA 6 analysis of potential dose to a future individual relies on the composite ("daisy chain") model, which effectively converts an initial mass of radionuclide into a dose of radioactivity under a plethora of assumed physical properties and consumer behavior. Each component of the model introduces additional uncertainties that should be accounted for. The composite uncertainty should be a measure of propagation of component uncertainties through the daisy chain. This overall uncertainty propagation can be expressed using standard probability rules, as shown later. The essential model components are

- determination of initial mass (inventory),
- determination of representative precipitation at SWSA 6 for tens of thousands of years,
- prediction of release rates for each site and each radionuclide,
- prediction of transport through the saturated groundwater system,
- prediction of transport to surface water from the shallow subsurface and groundwater discharge, and

ORNL-DWG 93M-15889

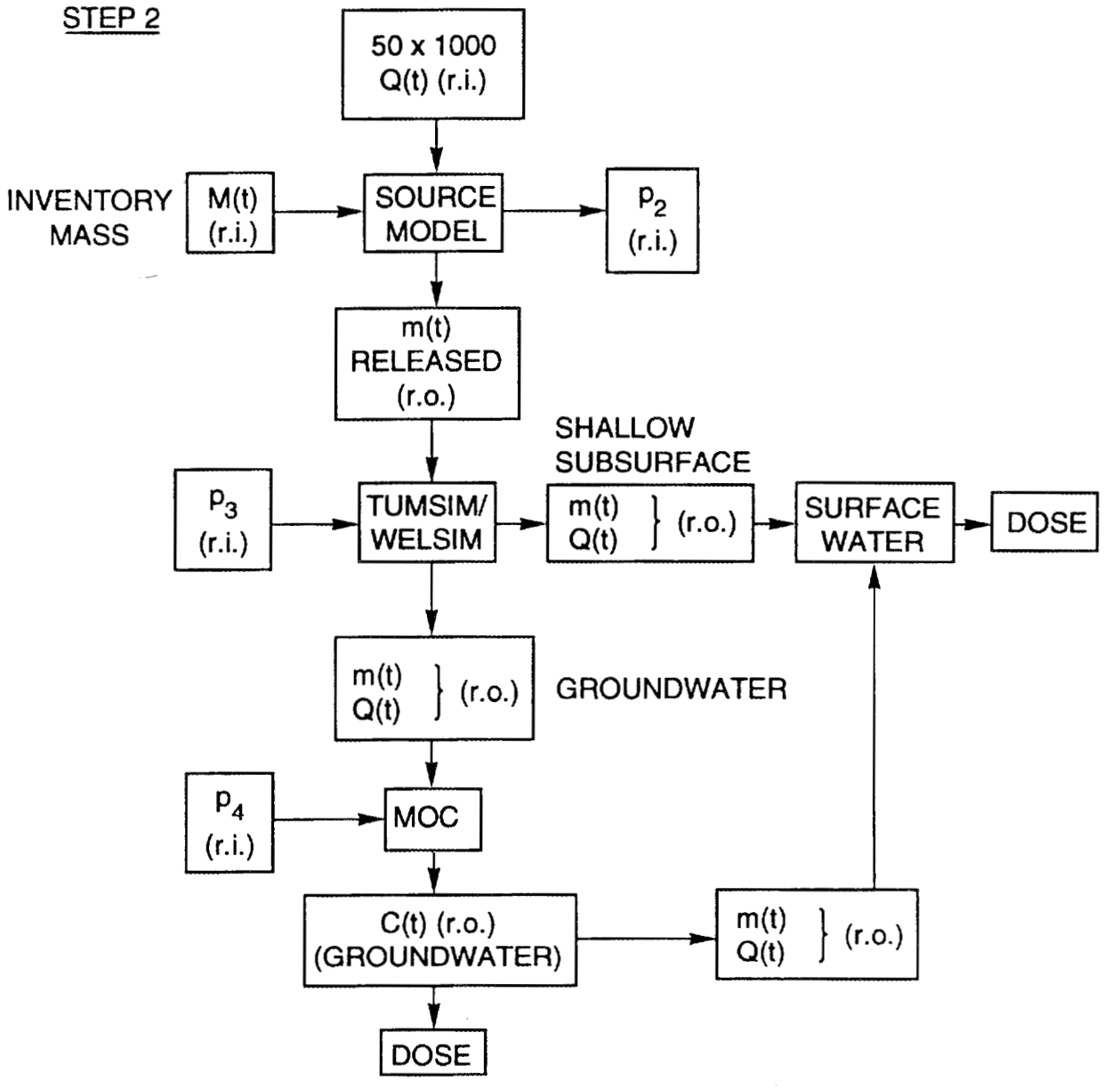

Fig. H.1. Coupled sampling procedure.

- prediction of doses based on future contaminant concentrations and presumed future consumer behavior.

Aside from variances in results due to inexact input parameters, a basic source of uncertainty at any stage in the modeling is the inadequacy of the model for representing the site and making long-range predictions. The uncertainty in the adequacy of the model is determined subjectively, since it is based on experience and is not measurable. In attempting to factor into the analysis subjective assessments, an attempt is made to keep these perceived sources of uncertainty separate. That is to say, it is useful to draw a distinction between "objective uncertainty" and "subjective uncertainty" in deriving the probability of compliance, where the former is associated solely with the propagation of parameter variance through the composite model. The objective uncertainty is expressed by the cumulative probability distributions (CDFs) derived from the LHC simulations. CDFs do not account for uncertainty associated with a judgment about the actual "validity" of the model. This is a subjective assessment best made by the model developer, or expert, who can express his or her confidence (or lack thereof) in the fundamental validity of each model segment. If expressed appropriately, this subjective judgment of confidence can then be incorporated into the uncertainty analysis with the result of modifying the objective LHC CDFs. The effect of incorporating subjectivity in this fashion is to smear the objective distributions somewhat, and hence to increase the uncertainty of compliance, as defined by Eq. (H.1).

To show where judgments of validity in a model may arise, it is useful to break down each component of the transport model into the elements listed in Table H.1. Sources of subjective uncertainty can occur for any of the reasons noted. All of these hierarchical elements may contribute to a greater or lesser extent to an overall subjective judgment about the validity of the model.

Table H.1. Sources of subjective uncertainty in the transport model

Element of modeling process	Course of uncertainty
Conceptual model	Incomplete understanding of all aspects of the transport process or uncertainty in underlying assumptions of the model
Mathematics/physics	Failure to adequately capture or express conceptual understanding in mathematical language
Numerical	Failure to formulate the mathematics in usable algorithms
Computer model	Failure to eliminate errors in resulting computer codes
Interpretation of results	Difficulty in interpreting results in terms of the conceptual model

Below we describe two possible approaches for incorporating the subjective expert's opinion about whether a model (or model component) is "valid," in a sense to be defined shortly. The first approach (Sect. H.3.1) employs a very simple, but crude weighting scheme that yields a lower bound on the probability of compliance. This approach requires a subjective assessment from each expert in the form of a single number between 0 and 1 that attempts to assign a weight to the validity of his or her model component. The second approach (Sect. H.3.2) attempts to incorporate expert opinion in a more rigorous fashion but requires a more quantitative expression of the model's validity from the expert, as explained below. This is the method used in the present analysis.

H.3.1 A Lower Bound for the Probability of Compliance

In the lower-bound approach, an expert assigned to a particular model segment is asked to provide a weight, w, with $0 \leq w \leq 1$, where the choice $w = 1$ means that his or her segment is (completely) valid in the sense that the expert has a significant degree of confidence in all elements of the model, as listed above. The weight $w = 0$ means that the expert has no confidence in one or more of the above elements. That is, $w = 0$ means that the model component is incapable of representing the physical system and is not suitable for prediction. Choosing w, with $0 \leq w \leq 1$, amounts to a subjective estimate of how relevant the model is in representing the physical system and making predictions. Or, the subjective weight, w, relates to the degree with which a model component is valid. The goal will be to incorporate the choice for w into the more standard "objective" uncertainty analysis of parameter variance based on LHC sampling. To this end, it is convenient to define w as the probability of validity:

$$w = \Pr(\text{model segment is valid}).$$

Each component in the model may also be assigned a validity weight, as follows:

w_1 = Pr(initial mass approximation is valid)

w_2 = Pr(hydrologic model is valid)

w_3 = Pr(contaminant release model is valid)

w_4 = Pr(transport to shallow subsurface and groundwater recharge model is valid)

w_5 = Pr(groundwater transport model is valid)

w_6 = Pr(consumer scenario is valid)

w_7 = Pr(dose calculation is valid)

For the purpose of identifying the "weakest link" in the model, it is reasonable to take the overall validity as the minimum:

$$w = \text{Minimum } \{w_1, w_2, w_3, w_4, w_5, w_6, w_7\}.$$

This weight will now be combined with the computational uncertainty estimates derived from the LHC sampling simulations.

Viewing C (contaminant concentration) as a random variable, the event $C \leq C^*$ occurs with a certain probability. This event can evidently happen in two ways:

$$C \leq C^* \text{ and (model is valid)}$$

or

$$C \leq C^* \text{ and (model is not valid).}$$

Let A and $\tilde{A}$ be events defined as follows:

A : Model segment is valid

$\tilde{A}$: Model segment is not valid

Note that the definition $w = \Pr(A)$ implies $\Pr(\tilde{A}) = 1 - w$. Then the event can be related to the probability that the composite model actually predicts $C \leq C^*$ by the formula for total probability:

$$\Pr(C \leq C^*) = \Pr(C \leq C^* | A)\Pr(A) + \Pr(C \leq C^* | \tilde{A})\Pr(\tilde{A}),$$

or

$$\Pr(C \leq C^*) = \Pr(C \leq C^* | A) \cdot w + \Pr(C \leq C^* | \tilde{A}) \cdot (1 - w). \qquad \text{(H.2)}$$

As a simple, commonsense check, notice that if $w = 1$, then $\Pr(C \leq C^*) = \Pr(C \leq C^* | A)$, which is to say that the sought result $\Pr(C \leq C^*)$ is given wholly by $\Pr(C \leq C^* | A)$. That is, $\Pr(C \leq C^*)$ can be determined *computationally* from an analysis of the model. (This is precisely the assumption when parameter propagation studies are solely used to determine uncertainty, e.g., via LHC sampling simulations.) If $w = 0$, then $\Pr(C \leq C^*) = \Pr(C \leq C^* | \tilde{A})$, which is to say that the desired quantity should be determined somehow with no regard for the model. Finally, since it is always true that $0 \leq \Pr(C \leq C^* | \tilde{A}) \leq 1$, Eq. (H.2) implies

$$\Pr(C \leq C^* | A) \cdot w \leq \Pr(C \leq C^*) \leq \Pr(C \leq C^* | \tilde{A}) \cdot w + 1 \cdot (1 - w).$$

The lower half of the inequality, namely $\Pr(C \leq C^* | A) \cdot w \leq \Pr(C \leq C^*)$, shows that a LHC sampling-derived value for $\Pr(C \leq C^* | A)$ and a subjective weight w, chosen for model validity, yield a lower bound for the probability of compliance.

H.3.2 An Alternative Approach to Uncertainty Biasing

This section describes a more rigorous method of incorporating subjective expert opinion into the analysis, one that requires more detailed information from the expert. This was the approach chosen for the current study.

To employ subjective information to modify the LHC CDFs using the rules of probability, an expert assigned to a particular model segment is queried as follows: "Under the assumption that the concentration predicted by the model is based on the true parameters, express your confidence in this value by drawing a confidence band about the predicted value." Using $\hat{C}$ and C to denote, respectively, the predicted and true contaminant concentrations associated with the model segment, one can then approximate the conditional probability distribution $P^{\text{Subj}}(C|\hat{C})$ from this confidence band. (Below, the symbol P will refer to a probability density function.) The modified distribution is then derived from the rule of total probability:

$$P(C) = \int P^{\text{Subj}}(C|\hat{C})P^{\text{MC}}(\hat{C})d\hat{C} \tag{H.3}$$

where $P^{MC}(\hat{C})$ is the LHC sampling-derived distribution. The above integration has the effect of broadening the original $P^{MC}(\hat{C})$, and hence, of increasing the uncertainty of compliance. Equation (H.3) shows how subjective information is used to modify the LHC sampling distribution in one model segment. In the propagation of probabilities through the daisy chain, subjective information can be incorporated at each stage. This process is described by the next three equations. Below, C^i_{in} represents the contaminant concentration entering the i-th stage, and C^i_{out} is the contaminant concentration predicted (or "output") from the i-th stage. The term C^i_{out} denotes the LHC sampling-derived ("objective") output probability from the i-th stage. Recall that the output concentration of one model component is used as the input for the next component, that is, $C^{i-1}_{\text{out}} = C^i_{\text{in}}$. This implies

$$P(C^i_{\text{in}}) = P(C^{i-1}_{\text{out}}) \ . \tag{H.4}$$

Now let $P^{MC}(\hat{C}^i_{out})\,|\,C^i_{in})$ denote the conditional probability distribution that expresses model uncertainty as estimated by the LHC sampling simulations for component i. Then the following relation shows how the contaminant probability density function predicted by the previous model component, $P(C^{i-1}_{\text{out}})$ [$= P(C^i_{\text{in}})$], is affected by parameter variability in the present component:

$$P(\hat{C}^i_{\text{out}}) = \int P^{\text{MC}}(\hat{C}^i_{\text{out}}|C^i_{\text{in}})P(C^i_{\text{in}})dC^i_{\text{in}} \ . \tag{H.5}$$

The next step is to modify the "objective" distribution, $P(C^i_{out})$, using the expert's subjective assessment about the "validity" of model segment i. This information is expressed by the conditional probability density function, $P^{\text{Subj}}(C^i_{\text{out}}|C^i_{\text{out}})$. This conditional distribution is constructed from the expert's opinion as follows: given the model prediction of $\hat{C}^i_{out}$ based on the LHC sampling simulation, a probability distribution (or confidence band) is drawn about this predicted value that expresses the expert's confidence in this value, and hence in the validity of the model. When this is done, the following relation

shows how the output (LHC sampling) distribution for the i-th segment, $P(\hat{C}^i_{out})$, is modified by the subjective uncertainty to yield the new output distribution for the i-th segment $P(C^i_{out})$:

$$P(C^i_{out}) = \int P^{Subj}(C^i_{out}|\hat{C}^i_{out})P(\hat{C}^i_{out})d\hat{C}^1_{out} . \tag{H.6}$$

This is merely a restatement of Eq. (H.3) for segment i.

The above equations define how the probability distribution of the i-th segment is derived from that of the previous segment. A sequence of such equations can then be linked together to obtain the probability distribution associated with the composite model, namely, the output distribution from the final segment, $P(C^N_{out})$, where N is the total number of segments. The composite distribution is then used to compute the probability of compliance, P_c, where

$$P_c = P_r(C \leq C^*) = \int_o^{C^*} P(C^N_{out})dC^N_{out} , \tag{H.7}$$

C^* being the compliance concentration. From this result, one can compute the compliance uncertainty defined by the entropy relation [Eq. (H.1)]. It can be shown that the effect of incorporating subjective information into the analysis in this way almost always results in an increase in uncertainty as defined by Eq. (H.1). (Exceptions can be found if the subjective probability distribution is significantly skewed in one direction—for example, to convey a judgment that the LHC sampling predictions are extremely conservative.) This can be seen by noting that subjective information tends to "smooth" the objective (LHC sampling) distribution function, with the result that the probability "density" is distributed more evenly above and below the compliance point C^*; this drives P_c toward 0.5 and hence U toward 1. In other words, if the LHC sampling-predicted compliance probability is initially far from 0.5, subjective information will tend to force it closer to 0.5; as a consequence, the addition of subjective information can *increase* the probability of compliance if it is initially below 0.5. The more important case, however, occurs when the LHC sampling analysis predicts compliance between 0.5 and 1.0. Here, additional subjective information will tend to decrease the probability of compliance and again push the uncertainty, U, closer to 1.

Under certain conditions, it is possible, and computationally convenient, to compute the overall (composite) objective and subjective probability distributions separately, and then to combine these composite distributions using a relation similar to Eq. (H.3). That is, one first performs the LHC sampling simulation on the composite model without incorporating subjective information at each stage. The individual subjective distributions are combined separately to form an overall subjective distribution. This is then used to modify the composite LHC sampling distribution according to Eq. (H.3). The separate computation of the objective and subjective distributions can be justified if Eqs. (H.5) and (H.6) are approximately convolution integrals. The latter assumption holds if the transport models are linear in the contaminant concentration (i.e., given that doubling the "input" contaminant concentration implies a doubling of the "output" concentration). Although a particular model segment may be highly nonlinear in the total flow field (e.g., groundwater transport), if the contaminant concentration itself represents a small perturbation of the total flow volume, it is reasonable to expect that the model will behave linearly in the

contaminant concentration to first order. With this assumption and an appropriate normalization of the concentration scales, Eqs. (H.5) and (H.6) can be expressed as convolution integrals. Then the composite probability distribution of an N-stage model may be written as

$$P_N = [P_{N-1}^{\mathrm{MC}} * P_{N-2}^{\mathrm{Subj}}] * [P_{N-2}^{\mathrm{MC}} * P_{N-2}^{\mathrm{Subj}}] * \ldots * [P_1^{\mathrm{MC}} * P_1^{\mathrm{Subj}}] , \tag{H.8}$$

where * denotes convolution, and the subscript indicates model segment. Since the convolution operation is commutative, the order of the convolutions can be rearranged to yield

$$P_N = P_{\mathrm{total}} = P_{\mathrm{total}}^{\mathrm{MC}} * P_{\mathrm{total}}^{\mathrm{Subj}} , \tag{H.9}$$

where

$$P_{\mathrm{total}}^{\mathrm{MC}} = P_{N-1}^{\mathrm{MC}} * P_{N-2}^{\mathrm{MC}} * \ldots * P_1^{\mathrm{MC}} , \tag{H.10}$$

and

$$P_{\mathrm{total}}^{\mathrm{Subj}} = P_{N-1}^{\mathrm{Subj}} * P_{N-2}^{\mathrm{Subj}} * \ldots * P_1^{\mathrm{Subj}} . \tag{H.11}$$

Here, Eq. (H.10) is computed by an LHC sampling simulation applied to the entire composite model, and Eq. (H.11) shows that the total subjective distribution can be estimated by convolving the individual (properly normalized) subjective distributions of the separate model segments.

H.4. COMPUTER PROGRAM

The methods presented in Sect. H.3.2, above, for incorporating subjective uncertainties with parametric uncertainties associated with the LHC analyses of the composite transport model are implemented through the use of a computer program. The code consists of approximately 300 lines written in FORTRAN. It is compiled and run on an HP 9000, Series 700 workstation. The code uses the following approximation to Eq. (H.3) to combine subjective information with modeled, "objective" results:

$$P(C_i) = P^{Subj}(C_i|\hat{C}_j) * P_j^{MC}(\hat{C}) \quad , \tag{H.12}$$

where

$P(C_i)$	=	probability that the actual concentration is in interval i,
$P^{Subj}(C_i \mid \hat{C}_j)$	=	subjective probability for a given model segment that the actual concentration, C, is in interval i given the modeled concentration, $\hat{C}$ is in interval j,
$P_j^{MC}(\hat{C})$	=	probability that the modeled concentration, $\hat{C}$, is in a given interval, j (originally this probability corresponds to the "objective", LHC analysis results).

The following section briefly described the steps used by the computer code.

Step 1

A concentration (or flux) range that encompasses all values generated by the LHC analysis for a given nuclide, as well as the associated compliance value, C^{lim}, is determined. This range is then divided into n unit-width intervals. While the actual number of intervals, n, is nuclide-specific, the values used in this analysis ranged from 20 to 60.

Step 2

For each of the five model segments, subjective probabilities are assigned for the n intervals, $P^{Subj}(C_i \mid \hat{C}_j)$. The code allows input of 11 subjective values, corresponding to $P^{Subj}(C_i|\hat{C}_{i-5})$ to $P^{Subj}(C_i|\hat{C}_{i+5})$. These probabilities are based on distributions provided by experts on the particular composite transport model segment. A "rest-of-the-world" probability, uniformly distributed over the remaining $(n-11)$ intervals, is also input.

Step 3

Once the intervals and subjective probabilities have been stored, initial values for $P_j^{MC}(\hat{C})$ based on the objective distributions obtained from the LHC analysis, are generated. These probabilities are simply the ratio of the number of objective values which fall within each interval and the total number of objective values (i.e., 50).

Step 4

Using the estimates for $P_j^{MC}(\hat{C})$, and the subjective probabilities for the first model segment, values for $P(C_i)$ are calculated for each interval using Eq. (H.12).

Step 5

The previous probabilities, $P_j^{MC}(\hat{C})$, are then replaced by the corresponding values of $P(C_i)$ calculated in Step 4.

Step 6

Using the updated values for $P_j^{MC}(\hat{C})$, and subjective probabilities $P^{Subj}(C_i|\hat{C}_j)$, for the next model segment, Steps 4 and 5 are repeated for each of the remaining model segments.

Steps 4 and 5 are then repeated for each of the remaining model segments. These values are then used with the subjective estimates for the next model segment and step 4 is repeated.

APPENDIX I

PERFORMANCE ASSESSMENT PEER REVIEW PANEL RECOMMENDATIONS

APPENDIX I

PERFORMANCE ASSESSMENT PEER REVIEW PANEL RECOMMENDATIONS

On March 19 and 20, 1993, a preliminary review of this performance assessment (PA) was conducted for the U.S. Department of Energy (DOE) Performance Assessment Peer Review Panel. The Peer Review Panel provided 32 recommendations to be considered in preparing this PA based on its review of the initial draft of this document, a site visit, and prepared presentations. In this appendix each recommendation is listed, and responses to the recommendations are provided. The responses identify how the recommendation was implemented in this performance assessment.

Recommendation 1

The Panel is very appreciative to DOE Oak Ridge Operations Office (ORO) and ORNL for their courteous reception, generous hospitality, and openness of discussion.

Response: No action requested.

Recommendation 2

The Panel commends ORNL for the quality and detail of the draft report and for the effective multi-disciplinary team approach taken. The draft report will provide a very sound basis for finalizing the performance assessment.

Response: No action requested.

Recommendation 3

ORNL is to be commended for the effort expended in interpretation of the PA results.

Response: No action requested.

Recommendation 4

The Panel commends ORNL for their efforts to calibrate groundwater models to conform to the understanding of the disposal site's hydrological behavior.

Response: No action requested.

Recommendation 5

The Panel also commends the waste management operations organization for beginning efforts to bring operations into compliance with the performance objectives of DOE Order 5820.2A.

Response: No action requested.

Recommendation 6

The Panel agrees that further analyses should be carried out beyond 500 years. The Panel suggests that, for technical completeness, the analysis be carried out to estimate the peak dose(s) and year(s) of occurrence. A tabulation of peak doses and years of occurrence would also be helpful. If the analysis is terminated at some arbitrary time, the trend in dose beyond that time should be discussed.

Response: The analyses have been extended beyond 500 years to the point of peak dose for every radionuclide considered in detail. An analytical model was used for ^{238}U to extend groundwater calculations to the point of peak dose because the computer code was not suited for extended computations in time without excessive roundoff error. Peak doses for uranium isotopes were also considered that included the effects of buildup of decay products at extraordinary long times. The tabulation of peak doses and years of occurrence is included in Sect. 4.

Recommendation 7

The Panel agrees that the conclusions drawn to date, from the draft PA, appear to be correct and appropriate.

Response: No action requested.

Recommendation 8

ORNL is encouraged to continue the critical examination of disposal records to develop an accurate inventory. This effort should be documented in the final PA report. The absence of significant quantities of potentially important radionuclides such as ^{129}I and ^{59}Ni should be explained.

Response: Critical examination of disposal records represent a significant effort in revising the PA. In 1990, ORNL conducted an internal review of approximately 17,000 hard copy disposal records and their equivalent data base files in the ORNL Solid Waste Information Management System (SWIMS). The most common errors were data base entry errors including incorrect activity (Ci), volume, and weight. Approximately 10% of the data base files contained one or more of these errors. These data base files have been corrected, and monthly audits of newly generated data are now performed to ensure the validity of disposal information and avoid further discrepancies.

In 1992, ORNL commissioned two independent reviews of the radiological source term data. The *SWSA 6 Performance Assessment Inventory Verification Study* was designed to investigate the data records that contain high concentrations of radionuclides that resulted in high dose estimates to inadvertent intruders in the draft PA. SWIMS records

sorted by radionuclide for each disposal unit were used to identify the specific disposal records that contained high concentrations of radionuclides. The hard copy records (Request for Storage or Disposal of Radioactive Solid Waste or Special Materials, Form UCN-2822; Log-in Data Sheet for Generators of LLW, Form UCN-16114) were reviewed to determine if there were any data entry or transcription errors and if the reported values by waste generators were reasonable and consistent. Anomalous or suspicious records were thoroughly investigated. Waste generators were interviewed to determine the appropriateness of waste characterization methods. The study revealed widespread difficulties with the current method of characterizing radioactive wastes. The most prevalent concerns expressed by the waste generators were in the dose-rate-to-curie conversion method for determining radioactivity in the waste and the practice of reporting multiple radionuclides in a 1:1 ratio. The general feeling was that the standard ORNL conversion factor overestimated the activity by a factor of 2 to 10.

The *Evaluation of Uncertainty in the SWSA 6 Inventory Data* (see Appendix A) was performed as a follow-up to the first study to determine the impact of the concerns identified by the waste generators. The objective of this study was to estimate the most probable activity and associated uncertainty for the key radionuclides that were evaluated in the SWSA 6 PA. The study was divided into two phases. In most cases, the majority of activity for the key radionuclides (from a dose perspective) was reported in a few disposal records. In the first phase, a sufficient number of records to account for a large percentage of the total activity for each key radionuclide in each disposal unit were selected for review. Waste generators were interviewed, and the disposal records (UCN-2822 and UCN-16114) were reviewed to ascertain (1) the method used by generators to determine the package activity (e.g., dose conversion factor estimation, calculation, assay, etc.); (2) the physical form of the waste packets; (3) the instrument used to perform the radiological survey of the waste; (4) the dose rate measured for the packets within the package; (5) the distance from the instrument to the packet; and (6) whether the generator assumed the packet contained multiple radionuclides. Based upon the above information, the activity probability distribution was determined, and the most probable activity and associated minimum and maximum activity (at the 95% confidence level) were determined for each key radionuclide in significant activity packages. In the second phase of the study, the activity was calculated for each radionuclide in the remaining packages that were not evaluated in phase one. For most radionuclides, a large number of disposal records accounted for a small percentage of the total activity. Thus, a thorough investigation of these records was not practical. The information acquired from phase one of facility-specific waste characterization methods was used to select the most appropriate methods to calculate the remaining most probable activity, minimum activity, and maximum activity. This determination was specific to each radionuclide in each disposal unit.

A final investigation examined some of the more exotic long half-lived fission and activation product radionuclides that were not evaluated during the development of the draft PA on SWSA 6. Primarily, these radionuclides are very low energy beta or x-ray emitters such as ^{59}Ni, ^{79}Se, ^{93}Zr, ^{94}Nb, ^{99}Tc, ^{113m}Cd, ^{121m}Sn, ^{126}Sn, ^{129}I, and ^{151}Sm that would be difficult to quantify with the routine analytical techniques typically used by generators for waste characterization. This required relying on engineering estimates for the quantities of these radionuclides relative to the quantities yielded for other, more common

radionuclides, that were analyzed in the revised PA. The predominant sources for isotopes in this category result from reactor and fuel/target reprocessing operations that yield both activation products and mixed fission products and from accelerator operations that produce mostly activation products. ORNL reactor operations have decreased dramatically during the last several years. Reactor operations at ORNL have been limited to the High Flux Isotope Reactor (HFIR), which restarted and has operated since late 1990. Target reprocessing during the same period has occurred at the Radiochemical Engineering Development Center (REDC) (Building 7920/7930) with the reprocessing of one HFIR target during 1991 and one Mark 42 target from Savannah River during 1992–1993. Large-scale accelerator operations are associated with activities in the Van De Graff accelerator facility, the Linear Electron Accelerator, the Solid State Accelerator Facility, and the Holifield Heavy Ion Accelerator.

A review of the liquid, solid, and gaseous radioactive wastes from these locations was performed using process knowledge of the operations to evaluate the potential for significant quantities of long-lived fission/activation products in waste streams. The results indicate that the production of long-lived fission/activation products relative to the production of other more common radionuclides appears to be very small. The impact of ^{59}Ni on the inadvertent intruder dose is less than half of that for ^{63}Ni, which had the lowest dose/unit concentration by far of any isotope considered in the assessment analysis. Since the dose impact of ^{59}Ni is much less than that of ^{63}Ni and the reported inventories of the latter produced no dose consequences during the assessment, the missing inventory of ^{59}Ni is considered to be nonproblematic. The fission yield of ^{129}I is approximately 17% of that for ^{137}Cs and would be produced in largest quantity, as indicated earlier, from reactor operation or fuel/target reprocessing. The half-life of ^{129}I, however, is such that the expected quantity of this isotope relative to ^{137}Cs inventory in the same waste stream is small. ORIGEN calculations of REDC target reprocessing confirm ^{129}I quantities to be on the order of 10^6 to 10^9 less than those for ^{137}Cs. Since the contribution from these waste streams to the total SWSA 6 ^{137}Cs inventory is relatively small, the potential impact upon the dose analysis performed in the PA from this long-lived radionuclide is not believed to be significant.

Recommendation 9

ORNL is encouraged to consider the degradation of concrete barriers and to consider advective transport as the PA is finalized.

Response: The conceptual and mathematical modeling methodology used in the SOURCE1 and SOURCE2 codes includes concrete degradation, cracking, structural failure, water flux partitioning, and advective and diffusive release of radionuclides. Concrete degradation was considered in terms of surface and bulk attack mechanisms. Surface attack was primarily due to sulfate attack. Bulk attack was primarily due to calcium hydroxide leaching. Corrosion of reinforcing steel was included. The models are described in greater detail in Appendix B.

Recommendation 10

ORNL is encouraged to pursue development of waste acceptance criteria and waste certification programs to provide confidence in future disposal inventories.

Response: Waste Acceptance Criteria development and the waste certification program are discussed in Sect. 2.3.

Recommendation 11

ORNL is encouraged to finalize the PA as soon as possible.

Response: This PA represents the effort to respond to this recommendation.

Recommendation 12

In the final PA, the relationship between RCRA closure and closure to meet DOE Order 5820.2A requirements should be discussed. The closure expected to be implemented must be discussed in detail. Describe how the modeling accounts for the effects and performance of caps installed at SWSA 6 as part of the RCRA activities.

Response: SWSA 6 is now being closed under the requirements of the Comprehensive Environmental Response, Compensation, and Liability Act (CERCLA). A discussion of the relationship between the CERCLA closure and closure to meet the requirements of DOE Order 5820.2A is included in Sects. 2 and 3. The approach to modeling the site with the concepts for closure that have been developed to date is included in Sect. 3. Closure plans for SWSA 6 are not complete at this time, and further development of the closure plan is expected. Should the closure plan represent a significant impact on the long-term performance of SWSA 6, the PA will be revised to address the impacts of closure.

Recommendation 13

Any other reviews of the PA (such as an internally commissioned review group or by an outside agency such as the National Academy of Sciences) should be discussed in the final report.

Response: Reviews of the PA are discussed in Sect. 1. The PA has been reviewed internally and by Rogers and Associates Engineering Corporation.

Recommendation 14

A summary discussion of the various studies which have contributed to the understanding of the site, as well as referencing the studies, would strengthen the document.

Response: Efforts towards understanding the geohydrologic characteristics of the Oak Ridge Reservation (ORR) including the Conasauga Group date back to 1951. The work over the intervening years has been evolutionary and led to the present level of understanding presented in this PA. A recent synthesis report (Solomon et al. 1992)

provides a comprehensive review and evaluation of the hydrologic framework attributed to SWSA 6. The essential features of this synthesis are presented in Sect. 2.1 and 3.2.

Recommendation 15

The final PA should contain a discussion of verification and validation of the computer codes NEWBOX and FLOWTHRU. These codes have been used to derive the source terms but have not been published.

Response: SOURCE1 and SOURCE2 are the codes that have been used for source term analyses in the PA. FLOWTHRU has been incorporated into these codes. Verification and validation of SOURCE1 and SOURCE2 are discussed in Sect. 3.4.7. Continued work towards verification of SOURCE1 and SOURCE2 is discussed in Sect. 4.9. Validation of these codes will be limited as a result of limited available data.

Recommendation 16

The Panel notes that it would be helpful to quantify and tabulate the potential dose impacts from the analysis of sensitivity.

Response: Additional analyses have been incorporated into the PA to further address the sensitivity and uncertainty of the results. These analyses are discussed in Sect. 4.7. Discussion of the dose impacts from the analysis of sensitivity and uncertainty is provided in Sect. 4.7.2.

Recommendation 17

The panel recognizes the complexity of the hydrogeology at SWSA 6 and the effect this has on the PA effort.

Response: No action requested.

Recommendation 18

In the site description section, include a discussion of the pre-existing groundwater contamination problems near the SWSA 6 facility and the potential impact on the long-term performance of that facility.

Response: As noted in Sects. 2.1 and 3, historical disposal operations in SWSA 6 have resulted in the contamination of groundwater and surface waters. The extent of this contamination is being addressed by RCRA/CERCLA investigations at SWSA 6. Environmental monitoring of SWSA 6 from waste disposal operations addressed by DOE Order 5820.2A will be masked by the release of contaminants from historical disposal operations. Contaminants released from historical operations are not expected to adversely impact the performance of the disposal units addressed by DOE Order 5820.2A.

Recommendation 19

The effect of surface and subsurface disturbance at SWSA 6 on lateral flow should be discussed; data presented to the Panel appear to be from an undisturbed forest site,

which may not be representative of SWSA 6. Discuss why decay of radionuclides during transport through the shallow subsurface is not accounted for by the model.

Response: Disturbance of the land as a result of facility operations has been accounted for in the modeling of the shallow subsurface by considering two main land types within the SWSA 6 facility. Disturbed surfaces were accounted for either as a disturbed grass surface with a low leaf area index (LAI = 2) or a disturbed gravel surface (LAI = 0.001) during the active sites period. The consolidation of the disturbed areas was taken into account by allowing an increase in the LAI to mown grass during the period of active institutional control and ultimately to forest cover in the times that follow (LAI = 4.9). The estimates for the LAI from disturbed surfaces were determined from field inspections of SWSA 6 in September 1992, and the appropriate surface for each waste site and its upslope mini-watershed were defined.

Decay of radionuclides during transport in the shallow subsurface has been incorporated into the TUMSIM and WELSIM codes. This addition to the modeling of site performance is described in Sect. 3.4.4.

Recommendation 20

In the final PA, there should be a discussion of how the individual radionuclide disposal units were modeled as viewed from the point of compliance (e.g., multiple point sources, extended sources, etc.) and how overlapping plumes from these disposal units have been taken into account when calculating the dose.

Response: Sect. 3.2 discusses how the disposal units were modeled, and further information is provided in Sect. 4.3 and Appendix E. Each disposal unit was considered as a point source within the model and was accounted for internally within the respective codes. Overlapping plumes from different types of disposal units were not encountered in the analysis because of the short transport distances between the disposal units and ephemeral streams where contaminants were discharged to surface water. Doses for groundwater were calculated using the maximum concentrations at the compliance points identified within the facility that were outside the 100-m (328-ft) buffer zone. Surface water doses were calculated based on the discharge of all contaminated waters over White Oak Dam. TUMSIM and WELSIM were prepared to ensure that mass of the contaminants discharged to surface water was conserved in the calculations.

Recommendation 21

There appears to be inconsistency in the K_d values used among different sections of the PA: source term, shallow subsurface flow, and groundwater transport.

Response: Consistency in K_d values has been corrected in this version of the PA as described in Sect. 3. The variation of values for an individual radionuclide that is apparent in the PA is the consequence of the different materials being evaluated. To the extent possible, selections of K_d values are based on field or experimental data in preference to literature values.

Recommendation 22

The Panel recommends that the potential future use of on-site surface waters as drinking water supplies be considered and discussed. Possible impacts from such use should be analyzed.

Response: A discussion of on-site surface waters is provided in Sect. 2.1.4. The available data clearly demonstrate that on-site surface waters are not suitable as potential drinking water supplies, and they are consequently not considered in the dose analysis. The dose analysis is performed using the discharge at White Oak Dam, which is immediately off-site.

Recommendation 23

The impacts of radioactive contaminant concentrations at or near Watts Bar Reservoir area should be considered and discussed.

Response: Watts Bar Reservoir has been contaminated from discharges from ORNL prior to the issuance of the Order and is presently part of the RCRA/CERCLA investigations being conducted on the ORR as part of the Environmental Restoration Program. Contaminant releases from SWSA 6 have an incidental contribution to the existing contamination, and any releases from SWSA 6 are discharged to White Oak Lake prior to being discharged to Watts Bar Reservoir. Doses have been calculated based on discharges to White Oak Lake. Doses cannot be reasonably expected to increase as a result of discharges from White Oak Creek to Watts Bar Lake where substantial additional dilution is provided by the Clinch River. The discharge from White Oak Dam averages 0.38 m^3/s (13.9 ft^3/s) while the average discharge of the Clinch River at the confluence with White Oak Creek is 4500 ft^3/s. This provides for a dilution factor of 0.0030 for all contaminants released from White Oak Creek.

Recommendation 24

In several of the appendices, too many significant figures were used. This implies more precision than is justified.

Response: Excessive precision in calculations has been corrected in the PA. In some cases, extra digits are presented to illustrate results in the sensitivity and uncertainty analysis.

Recommendation 25

ORNL is encouraged to consider the use of intruder barriers and passive intruder controls to provide reasonable assurance that the performance objectives of DOE Order 5820.2A will not be exceeded. The Panel agrees that development of restrictive waste acceptance criteria to limit disposed concentrations of long-lived radionuclides may be necessary for continued operations at SWSA 6. For those disposal units that cannot be brought into compliance with the performance objectives, operations should cease and closure proceed per DOE Order 5820.2A, III.3.j(1).

Response: As noted in Sect. 2.3, several types of disposal units are no longer being used for waste disposal in response to the findings of the draft PA. Sect. 4.8 discusses changes in operations made in response to the findings of this PA. Waste Acceptance Criteria and the waste certification program are discussed in Sect. 2.3. The implementation of the Waste Acceptance Criteria and waste certification program is ongoing as of the completion of this PA.

Recommendation 26

The Panel recommends that doses be calculated using intruder scenarios at the White Oak Creek and White Oak Lake areas. Intruder agriculture and, perhaps, intruder construction scenarios should be considered.

Response: White Oak Creek and White Oak Lake are outside of the 100-m (328-ft) buffer zone around each disposal unit and the SWSA 6 facility boundary. Wastes from SWSA 6 have not been disposed of outside of the site boundary and will not be disposed of outside the facility boundary. Consequently, intruder scenarios do not apply to either the lake or the creek in that there is no waste present as a result of the use of SWSA 6 as a disposal facility. Existing contamination in White Oak Lake and White Oak Creek are the result of historical liquid discharges from the main plant area and are properly being considered as part of the Environmental Restoration Program. White Oak Lake and White Oak Creek are considered in the analysis of the off-site dose to individuals, and the results show compliance with the performance objective for off-site exposure.

Recommendation 27

It would be helpful to tabulate all parameters used in the intruder scenarios.

Response: The requested table has been incorporated into Appendix G.

Recommendation 28

The Panel suggests considering the use of diet values published by Yang and Nelson of the Environmental Protection Agency ("An Estimation of Daily Food Usage Factors for Assessing Radionuclide Intakes in the U.S. Population," by Y. Y. Yang and C. B. Nelson, Health Physics, 50, 245-257) rather than the 1977 Nuclear Regulatory Commission data. Site-specific diet values, if properly justified, would also be acceptable.

Response: Dietary data published by Hamby (1992) have been used in the calculations for the PA. These data were derived from studies near the Savannah River Site and were deemed to be more applicable to the southern United States. These data are largely consistent with the data provided by Yang and Nelson.

Recommendation 29

The Panel suggests that the mass loading coefficient that was used for inhalation may be too high and that the ratio of indoor air to outdoor air that was used may be too low. ORNL is reminded that all parameters, assumptions, etc. should be justified.

Response: Revisions to the text in Appendix G and in Sect. 4.5 have been made in response to this recommendation.

Recommendation 30

Direct ingestion of soil should be discussed in the intruder analysis.

Response: Direct ingestion of soil is discussed in Appendix G and Sect. 4.5 in response to this recommendation.

Recommendation 31

Dismissal of pathways and/or scenarios should be justified.

Response: Revisions to the text in Sect. 3 have been made in response to this recommendation.

Recommendation 32

The Panel notes that summary Table 5.1 (page 5-2) does not agree with the discussion in paragraph 4.5.2.5 (page 4-53) with respect to the acute dose from the Tumulus, I, II, and IWMF. The table lists 4.6 mrem/year, and the text refers to "an order of magnitude" exceedance of the performance objective.

Response: Revisions to the text have been made to correct the typographical error noted in this recommendation.

INTERNAL DISTRIBUTION

1. T. J. Abraham
2. P. W. Adcock
3. J. K. Bailey
4. J. S. Baldwin
5. T. J. Blasing
6. B. Blaylock
7. C. R. Boston
8. J. B. Cannon
9. S. A. Carnes
10. E. D. Copenhaver
11. T. R. Curlee
12. A. H. Curtis, III
13. D. L. Daugherty
14. D. E. Fields
15. J. R. Forgy, Jr.
16. C. E. Frye
17. H. W. Godbee
18. D. F. Hall
19. F. J. Homan
20. R. J. Hydzik
21. A. S. Icenhour
22. R. H. Ketelle
23. D. C. Kocher
24. M. A. Kuliasha
25–29. D. W. Lee
30. R. R. Lee
31. R. J. Luxmoore
32. C. A. Manrod
33. B. C. McClelland
34. C. W. McGinn
35. L. E. McNeese
36. L. J. Mezga
37. S.-P. Miaou
38. J. R. Moline
39. R. V. O'Neil
40. R. M. Reed
41. D. E. Reichle
42. A. L. Rivera
43. P. S. Rohwer
44. T. F. Scanlon
45. R. B. Shelton
46. M. L. Socolof
47. W. P. Staub
48. M. M. Stevens
49. F. J. Sweeney
50. L. M. Tharp
51. J. R. Trabalka
52. M. W. Tull
53. J. C. Wang
54. M. W. Yambert
55. G. P. Zimmerman
56. ORNL Patent Office
57–58. Central Research Library
59. Document Reference Section
60–62. Laboratory Records

EXTERNAL DISTRIBUTION

63. Bill Adams, DOE-ORO, Federal Building, Oak Ridge, TN 37831
64. Mac Roddye, DOE-ORO, Federal Building, Oak Ridge, TN 37831
65. Larry Radcliffe, DOE-ORO, Federal Building, Oak Ridge, TN 37831
66. R. Shuman, Rogers & Associates, P.O. Box 330, Salt Lake City, UT 84110-0330
67. Doug Underwood, DOE-ORO, Federal Building, Oak Ridge, TN 37831
68. Dr. Helen Ingram, Director, Udall Center for Studies in Public Policy, University of Arizona, 803/811 East First Street, Tucson, AZ 85719
69. Calvin D. MacCracken, President, Calmac Manufacturing Corp., 101 West Sheffield Ave., P.O. Box 710, Englewood, NJ 07631
70. Jacquelin B. Shrago, Director, Office of Technology Transfer, 405 Kirkland Hall, Vanderbilt University, Nashville, TN 37240
71–81. Office of Scientific and Technical Information (OSTI), U.S. Department of Energy, P.O. Box 62, Oak Ridge, TN 37831
82. Office of the Assistant Manager of Energy Research and Development, DOE-ORO, P.O. Box 2008, Oak Ridge, TN 37831-6269